EXPLORATION GEOPHYSICS

EXPLORATION GEOPHYSICS

BY

J. J. JAKOSKY, Sc.D.

Consultant

LOS ANGELES 24
CALIFORNIA

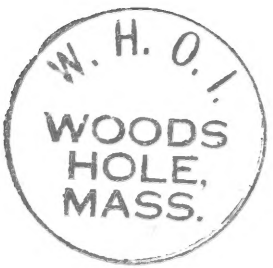

Second Edition
Second Impression

TRIJA PUBLISHING COMPANY
Gayley Avenue
Los Angeles 24, Calif.

PRINTED IN THE UNITED STATES OF AMERICA
TIMES-MIRROR PRESS

PREFACE TO SECOND EDITION

Ten years have passed since the manuscript for the first edition of *Exploration Geophysics* was prepared. During this period geophysical exploration has progressed from an interesting tool used by relatively few into a world-wide art recognized as a basic technique for subsurface exploration. A major portion of the oil fields discovered during the past decade can be credited wholly or in part to geophysics. The monetary value of these fields is many times the cost of the geophysical work which preceded their discovery. During this same period the professional status of the geophysicist has been established. His basic technical knowledge and mathematical training have been found to be essential spokes in the wheel of modern exploration. These spokes will carry more and more of the load as the exploration wheel revolves toward the problems of future development.

The phenomenal success record established by exploration geophysics is a tribute to the inventiveness, scientific ability, integrity, and perseverance of the personnel engaged in this work. Too much credit cannot be given to those men. They have built up the industry by their high professional standards. Coupled with these attributes are the good business judgment and fine public relationships of the administrators in the profession. By and large, the industry has had few subsidies. The advances in technique and improvements in instrumentation have been brought about largely by the ventured capital of private enterprise. Healthy competition within the industry has required that skillful use be made of allied technical advances in such fields as physics, electronics, transportation and communication.

In an effort to provide a text of broad scope which would be of greater service both to the student and to the practicing geophysicist and geologist, the 1940 edition of *Exploration Geophysics* has been revised. So many changes in technique and instrumentation have taken place since the book was first published that the revision has been a task very nearly equalling that of the original compilation. The major portion of the book has undergone complete rewriting, in order to include the important developments of the past decade. Every effort has been made to create a text which not only presents background and theory, but also shows in a practical manner how these fundamentals may be applied to the problems of exploration.

Our grateful thanks are extended to the consultants and the personnel of the many companies and institutions who have so generously contributed new material or collaborated in the revision and criticism of the manuscript. An attempt has been made in the list of *Contributors and Collaborators* to give recognition to these co-workers and to indicate the subject matter of their contributions. Without the help of these men, an up-to-date and comprehensive edition would scarcely have been possible. The author has reworked their data and manuscript material as was necessary to integrate it into the remainder of the text. In many cases this reworking has shifted the original emphasis, and the recognition accorded the various collaborators does not necessarily mean that they individually endorse the text as published. The final decision has rested with the author and is based upon his training and experience.

Special mention must be made of the work of Dart Wantland and Joshua Soske, who have given most freely of their time and energy. It is also a pleasure to acknowledge the work in the non-technical phases of the revision, particularly to Helen Murphy for her painstaking assistance in editing and compiling the manuscript and to Dorothy Stark who made the drawings and gave valuable aid during the compilation of the text and index. Clyde H. Wilson and Herbert Leifer contributed many helpful suggestions during reading of the manuscript.

Los Angeles 24, Calif.,
December, 1949.

J. J. JAKOSKY.

CONTRIBUTORS AND COLLABORATORS
Second Edition

Introduction: *CHAPTER I*

HELEN MURPHY, B.A., Los Angeles, Calif.
KATHARINE JAKOSKY, B.A., Los Angeles, Calif.
BLAKEMORE THOMAS, Ph.D., University of Kansas, Lawrence, Kans.
HOWARD PYLE, M.S., Continental Southern Oil Co., Los Angeles, Calif.

Geologic and Economic Background: *CHAPTER II*

CLYDE H. WILSON, M.S., International Geophysics, Los Angeles, Calif.
DART WANTLAND, M.S., U.S. Bureau of Reclamation, Denver, Colo.

Magnetic: *CHAPTER III*

DART WANTLAND, M.S., U.S. Bureau of Reclamation, Denver, Colo.

Airplane Operations:

E. A. ECKHARDT, Ph.D., Gulf Research and Development Corp., Pittsburgh, Pa.

Helicopter Operations:

HANS LUNDBERG, Sc.D., Lundberg Explorations, Ltd., Toronto, Ontario

Gravity: *CHAPTER IV*

DART WANTLAND, M.S., U.S. Bureau of Reclamation, Denver, Colo.

Gulf Underwater Gravimeter:

E. A. ECKHARDT, Ph.D., Gulf Research and Development Corp., Pittsburgh, Pa.

Diving Bell:

EUGENE W. FROWE, M.S., Robert H. Ray Co., Houston, Texas

Terrestrial Photogrammetric Mapping:

W. O. BAZHAW, B.S., Republic Exploration Co., Tulsa, Okla.

Seismic: *CHAPTER VII*

JOSHUA L. SOSKE, Ph.D., Geophysical Engineering Corp., Pasadena, Calif.

Propagation of Seismic Waves:

D. H. CLEWELL, Ph.D., and R. F. SIMON, Magnolia Petroleum Co., Dallas, Texas

Graphical Analogue Computer:

ROBERT B. MORAN, JR., B.S., William Miller Corp., Pasadena, Calif.

Instrumental Analysis: Filtering, Frequency:

JOHN J. JAKOSKY, JR., B.S., International Geophysics Co., Los Angeles, Calif.

Geovision:

JOHN OHMAN, EVA J. ZENTNER, Ph.D., and LUGARDA RIEBER, Geovision, Inc., New York, N. Y.

Mirragraph:

G. M. GROSJEAN, Western Electric Co., Inc., Los Angeles, Calif.

Explosives:

E. L. WATTS, B.S., Hercules Powder Co., San Francisco, Calif.

Drilling Equipment:

J. A. NOYES, B.S., Joy Manufacturing Co., Dallas, Texas

Air Shooting:

THOMAS C. POULTER, Ph.D., Stanford Research Institute, Calif.

Offshore Operations:

RAYMOND A. PETERSON, Ph.D., United Geophysical Co., Pasadena, Calif.

Radio Surveying Techniques:

ROBERT B. MORAN, JR., B.S., William Miller Corp., Pasadena, Calif.

Responsibility in Exploration:

B. W. BEEBE, Ph.D., Anderson-Prichard Oil Co., Oklahoma City, Okla.

Shallow Exploration:

DART WANTLAND, M.S., U.S. Bureau of Reclamation, Denver, Colo.

Chemical: *CHAPTER VIII*

LEO HORVITZ, Ph.D., Horvitz Research Laboratories, Houston, Texas

Radioactivity: *CHAPTER X*

HENRY FAUL, Ph.D., Research Associate, the Laboratory for Nuclear Science and Engineering, and the Department of Geology, Massachusetts Institute of Technology, Cambridge, Mass.

Bore Hole Investigations: *CHAPTER XI*

Electrical Logging and Sampling:

H. G. DOLL, Ph.D., ROGER HENQUET, M.S.,
MAURICE MARTIN, M.S., ANDRÉ POUPON, M.S.,
FRANCIS SEGESMAN, M.S., Schlumberger Well Surveying Co., Houston, Texas
JOHN C. STICK, JR., Lane-Wells Co., Los Angeles, Calif.

Radioactivity Logging:

R. E. FEARON, M.S., E. S. MARDOCK, A.B. (Chem.), and G. SWIFT, B.S., Well Surveys, Inc., Tulsa, Okla.

Production Problems: *CHAPTER XII*

JOHN JAKOSKY, JR., B.S., International Geophysics Co., Los Angeles, Calif.
N. VAN WINGEN, M.S., Petroleum Technologists, Inc., Montebello, Calif.

Land Tenure, Permit and Trespass Practices; Insurance and Patents: *CHAPTER XIII*

HOWARD PAINTER, LL.B., and THOMAS REYNOLDS, J.D., Reynolds, Painter, and Cherniss, Los Angeles, Calif.
WESTON BOURRET, E.M., Kennecott Copper Corp., Pasadena, Calif.

Insurance:

RALPH E. BRIDGES, Travelers Insurance Co., Los Angeles, Calif.

Patents:

HERBERT A. HUEBNER, A.B., Huebner, Beehler, Worrel, Herzig, and Caldwell, Los Angeles, Calif.
PAUL F. HAWLEY, Ph.D., Stanolind Oil and Gas Co., Tulsa, Okla.

Preface and Acknowledgments (First Edition)

The chief object of this book is to describe the fundamental theories, equipment and field techniques of the recognized exploratory geophysical methods, and to illustrate their application to problems of economic geology. The wide-spread use of geophysics has resulted in a voluminous quantity of domestic and foreign literature, in addition to some three thousand patents on geophysical methods, apparatus and allied equipment. The dynamic condition of the art has necessitated continual revision of the manuscript during the period of its preparation. As new and better techniques became accepted by the profession, their inclusion in the text relegated previously written material to a position of less importance. Constant revision of the manuscript has been necessary to keep abreast of developments.

A careful attempt has been made throughout the text to give full credit to the proper investigators for all original ideas and applications. It often is difficult to differentiate between original developments of one individual and developments that occur over a period of time, and which are due to the collaboration of many workers. Especially is this true in the field technique governing the application of the various exploratory methods and the development of the practical equipment.

An effort has been made to cite patent references whenever possible as well as literature references, because, due to the highly competitive nature of modern exploration geophysics, patent specifications oftentimes tend to be more authoritative than the reports in contemporary literature.

During final compilation of the manuscript, each chapter was submitted to reviewers who had extensive experience in the particular phases of geophysics treated in that chapter. In practically all cases, the reviewers reworked portions of the chapter or added new material. The present form of the book has been determined in large measure by the criticisms and additions supplied by these collaborators. In many cases where controversial views were held, all the reviewers naturally did not agree as to the relative advantage or disadvantage of certain methods or equipment and therefore did not subscribe to all statements of the text. In such cases, the author has attempted to present both views, and he must necessarily assume full responsibility for errors of omission, or over emphasis, of this controversial material.

Grateful acknowledgment is given to the various consulting geophysicists and officials of oil companies who so generously supplied certain material and assisted in the revision of the manuscript. The excellent cooperation of these collaborators and critics is one of the pleasant memories associated with the compilation of the text.

COLLABORATORS AND CRITICS (First Edition)

Geologic and Economic Background of Exploration Geophysics:

C. H. Wilson, M.S., International Geophysics Oil Co., Inc., Los Angeles, California.

H. W. Hoots, Ph.D., Consultant, Los Angeles, California.

Howard C. Pyle, M.S., Continental Southern, Los Angeles, California.

Magnetic:

C. H. Wilson, M.S., International Geophysics, Inc., Los Angeles, California.

Noel H. Stearn, Ph.D., W. C. McBride, Inc., St. Louis, Missouri.

V. G. Gabriel, Consultant, Sc.D., Los Angeles, California.

Gravity:

W. M. Rust, Jr., Ph.D., Humble Oil and Refining Co., Houston, Texas.

L. M. Mott-Smith, Ph.D., General Geophysical Co., Houston, Texas.

Paul Weaver, Gulf Oil Corporation, Houston, Texas.

L. F. Athy, Ph.D., Continental Oil Co., Ponca City, Oklahoma.

E. V. McCollum, M.S., E. V. McCollum and Co., Tulsa, Okla.

Donald C. Barton, Ph.D., Humble Oil and Ref. Co., Houston, Texas.

V. G. Gabriel, Sc.D., Los Angeles, California.

Seismic:

M. B. Widess, Ph.D., Standard Oil Co. of Indiana, Tulsa, Okla.

W. M. Rust, Jr., Ph.D., Humble Oil and Refining Co., Houston, Texas.

Beno Gutenberg, Ph.D., Professor of Geophysics, California Institute of Technology, Los Angeles, California.

L. F. Athy, Ph.D., Continental Oil Company, Ponca City, Oklahoma.

Henry Salvatori, M.S., Western Geophysical Company, Los Angeles, California.

N. A. Haskell, Ph.D., U. S. Smelting, Refining, and Manufacturing Co., Boston, Mass.

Frank Rieber, B.Sc., Frank Rieber, Inc., Los Angeles, California.

Wm. Miller, Miller Corporation, Pasadena, California.

Explosives:

A. R. Ely, B.Sc., in collaboration with A. E. Forster, E.M., H. E. Nash, B.Sc., and J. M. Martin, B.Sc., Hercules Powder Company, Wilmington, Delaware.

Drilling Exploration:

J. A. Noyes, S.B., Joy Manufacturing Co., Dallas, Texas.

Soil Analysis:

W. B. Lewis, Ph.D., Humble Oil and Refining Company, Houston, Texas.

Eugene McDermott, M.S., Geophysical Service, Inc., Dallas, Texas.

E. E. Rosaire, Ph.D., Subterrex, Houston, Texas.

Thermal Methods:

J. N. A. van den Bouwhuijsen, Ph.D., International Geophysics, Inc., Los Angeles, California.

Drill Hole Measurements:

E. G. Leonardon, M.S., Schlumberger Oil Well Surveying Corporation, Houston, Texas.

R. R. Henquet, E.M., Schlumberger Oil Well Surveying Corp., Los Angeles, California.

J. C. Stick, Jr., B.Sc., Lane-Wells Company, Los Angeles, California.

Physical Principles Applied to Production Problems:

Howard C. Pyle, M.S., Continental Southern Oil Co., Los Angeles, California.

Everett G. Trostel, M.S., DeGolyer and MacNaughton, Dallas, Texas.

Daniel F. Elam, B.Sc., Halliburton Oil Well Cementing Company, Duncan, Oklahoma.

Permit and Trespass Practices, and Insurance:

Howard Painter of Reynolds and Painter, Los Angeles, California.

History of Geophysics:

Katharine F. Jakosky, A.B., Los Angeles, California.

Special mention is made of the excellent work of Dr. Florence Ehrenkranz in checking the material included in the text, as well as her many original mathematical contributions and suggestions.

The original subject matter of this text is based upon lectures delivered at and a manuscript submitted to the faculty of the College of Mines and Engineering of the University of Arizona, in 1933. The author is indebted to Dean G. M. Butler and the faculty of that college for permission to use much of the material included in that manuscript.

J. J. Jakosky.

July, 1940.

CONTENTS

CHAPTER V

CHAPTER VI

CHAPTER VII

CHAPTER I

INTRODUCTION

Geophysics is a study of the physics of the earth with special reference to its physical properties, structure, and composition. It is commonly divided into two general branches. The first includes the subdivisions of the physical sciences such as electricity, magnetism, chemistry, heat, elasticity, etc., while the second branch pertains to the study of the three major components of the earth: solid (lithosphere), liquid (hydrosphere) and gas (atmosphere). The wide diversity of subject matter embraced in the field of geophysics may be more thoroughly appreciated by reference to Table 1.†

Exploration geophysics is the art of applying the physical sciences to the study of the structure and composition of those layers of the earth which are sufficiently shallow to be exploited by man. This book is primarily concerned with the application of geophysics to the outer portion of the earth's crust, especially in the solution of problems of structural and economic geology. This application may embrace practical engineering techniques at one extreme and the methods of mathematical physics at the other.

Exploration geophysics has evolved from the practical use of the knowledge accumulated by many investigators working independently in different parts of the world. Although it is a comparatively young science and until 25 years ago no authoritative English text on the subject had been compiled, vague indications of its beginnings may be said to exist in ancient Chinese and in medieval literature. For centuries the divining rod was the most common device used in the attempt to locate valuable substances concealed underground. The success of this method actually depended more upon the law of averages than on the psychic powers of the man with the hazel twig, who was certain to be right once in a while, particularly when looking for water. Commercial application was therefore rather limited, although, as one writer states, the divining rod has been used in the quest for "water, minerals, witches, criminals, Protestants, hidden treasure, lost animals, and the points of the compass."‡ Any exhaustive study of this method of exploration would properly belong to the field of psychology.

However, many of the fundamental laws and theories of present-day geophysics were developed by scientists of the past few centuries, most of whom probably had no thought of the direct application to economic geol-

† B. Gutenberg, "Geophysics as a Science," *Geophysics*, Vol. 2, July, 1937.
‡ A. S. Eve and D. A. Keys, *Applied Geophysics*, p. 7.

ogy. Due chiefly to stiff commercial competition, this branch of applied geophysics is a dynamic art continually changing and bristling with personalities. Many different methods are being used, and it is the purpose of this book to outline the fundamental theory and general application of these various exploratory methods.

The demand for metals in the latter part of the nineteenth century contributed much to the development of mining geophysics. The chief incentive to modern exploration geophysics, however, was the search for oil during the early years of the twentieth century. No longer can the geologist go forth to look for oil using only such signs as gas bubbles on water, petroleum seepage along creek beds, outcropping oil-bearing strata, or other surface evidence of subsurface oil accumulation. To these methods of finding oil have been added surface geology, cartography, micropaleontology, lithology, electrophysics, geophysics, and geochemistry.

Most underground structures can be diagnosed if detectable variations in these structures exist. Thus the four leading geophysical techniques relate to the four most common characteristics which can be determined from the surface: magnetism, density, electrical conductivity, and elasticity, which are investigated respectively by magnetic, gravitational, electrical, and seismic methods. Variations discovered by these methods are then assessed in geologic terms. Sometimes the desired results may be achieved indirectly: if the mineral being sought lacks properties detectable from the surface, another body associated with it and possessing these properties may be mapped.*

During the period of early petroleum production only six per cent of the wildcat wells were successfully completed as producers. An increased demand for oil and the inadequacy of the haphazard methods of the early "wildcatter" in meeting this demand forced the development of the new science of petroleum geology, and with it the effective tools of geophysical exploration so well adapted to the study of the remaining unexplored areas. Even with these aids, only about 21 per cent of the exploratory wells now drilled are completed as producers. During the entire life of the American petroleum industry an average of about 180,000 barrels of oil have been discovered for each dry hole drilled. During 1947, with geophysical exploration as the guide in a large portion of the wells drilled, discovery of oil was made at the rate of about 528,000 barrels for each dry hole. This increased efficiency must be credited to the better geophysical-geological techniques now in use.

Geophysical methods have been successful in the search for oil primarily because of their ability to determine the geologic structure of buried formations, mapping conditions which are favorable for the accumulation of oil or gas. Although each method is undergoing constant revision to improve its accuracy and broaden its field, several have had phenomenal success in

* For example, highly magnetic magnetite associated with gold in a placer, or a geologic structure related to ground water.

TABLE 1

MAJOR PROBLEMS OF GEOPHYSICS †

(a) General problems, (b) Applied problems.

	Solid Body	*Hydrosphere*	*Atmosphere*
Mechanics	(a) Forces and stresses; gradual and sudden movements; earthquakes, earthquake waves, elastic and viscous movements; tides; movements of the poles; figure; density; volcanism (belongs also in other sections and geochemistry); mechanical effects of ice, water, wind (b) Reduction of earthquake damage; seismic prospecting	(a) Tides, waves, currents; hydrology (b) Investigation and prediction of tides and currents for navigation and fisheries; hydrology; echo sounding	(a) Tides, waves including sound; currents (b) Weather forecasting
Gravitation	(a) Gravity; layering; pressure; isostasy; sedimentation (b) Use of pendulum, torsion balance, etc., in prospecting	(a) Layering; sedimentation	(a) Distribution of gases; layering
Electricity	(a) Electric currents and electric waves (b) Electric prospecting	(a) Electric phenomena	(a) Electric phenomena; ionosphere; aurora
Magnetism	(a) Earth's magnetism (b) Magnetic prospecting	(b) Compass; magnetic charts	
Optics		(a) Color and transparency of lakes, oceans	(a) Meteorological optics, halos, etc.; color of sky; polarization; turbidity; colors of clouds (b) Visibility for aviation
Composition of matter	(a) Composition of the earth; radioactivity; state of the interior	(a) Radioactivity of hydrosphere; salt content	(a) Composition of the atmosphere, ozone, etc.
Heat	(a) Temperature in the earth and its changes; crystallization and melting (b) Thermal prospecting	(a) Temperature in lakes, rivers and oceans; glaciers; icebergs; thermal currents	(a) Thermodynamics of the atmosphere; temperature; climates (include other factors) (b) Climatology

delineating subsurface features. The seismograph in particular has been successful in revealing hidden structures favorable for the occurrence of new oil and gas fields.

Whereas oil originally came entirely from shallow wells, it is now produced in wells which may be as deep as 13,000 feet. In 1946, 106 wells were drilled to depths in excess of 12,000 feet, bringing the total of deep wells in this class to 326. Of the 326 wells, 116 had found production at some level, 99 of these at a depth of more than 10,000 feet. The number of deep wells for 1946 was 66 per cent greater than that for 1945; deepest production during this year was obtained from a Louisiana well at 13,778 feet.‡ In 1947, the average for 154 exploratory holes in southern Louisiana

† Gutenberg, *Geophysics, loc. cit.*

‡ Ernestine Adams, "Deep exploratory wells on increase," *The Petroleum Engineer,* February, 1947.

alone was 10,178 feet.‡ The cost of the exploratory drilling to these deep-seated oil deposits is a prohibitive gamble without reliable data as to the existence of favorable geologic structure.

The estimated proved oil reserves in the United States are in excess of those known ten years ago, in spite of the fact that more petroleum has been produced than was previously assumed to exist. An estimated total of about 60,000 million barrels of oil have been discovered (1947), of which about 36,000 million barrels have been produced, leaving 24,000 million barrels in the ground as proved oil reserves.§ Of this reserve, the state of Texas has about 50 per cent, California 13 per cent, Oklahoma 4 per cent, Louisiana 6 per cent, and New Mexico 4 per cent (approximate figures), with the balance chiefly in Kansas, Wyoming, Illinois, Arkansas, and Pennsylvania. It is probable that many new fields will be found to augment this supply materially. Exploration geophysics has played an important part in the discoveries of the last 25 years, and it will be only by the improvement of present methods or the development of new methods that the recent rate of discovery can be maintained.

Each geophysical method has had its period of initial trial, followed by its peak commercial application over a period of a few years. As the areas amenable to a particular method have been studied and covered, the application or popularity of that method decreased and it was replaced by other methods. The succession of one method after another sometimes followed rapidly. At other times there has been considerable lapse of time between peak applications of various methods. Each method has had a limited period of maximum commercial activity, because it either eventually covered the most amenable areas, or else was succeeded by a newer technique having economic advantages.

HISTORY OF DEVELOPMENT

Magnetic Methods.—Probably the first geophysical instrument had its beginning in the discovery that a lodestone, or a piece of a certain kind of iron that has contacted a lodestone, will orient itself approximately in a north-south direction. Early Chinese literature indicates that this orientation property of lodestone or magnetized iron was known and utilized some time during the period from 2637 B.C. to 121 A.D. Peregrinus in 1269 discovered the "magnetic poles" and named them North and South. His investigations further proved that unlike poles attract and like poles repel each other. He also made the important discovery that fragments of broken magnets behaved as the original magnets. In 1492, on his voyage to America, Columbus noted that his compass deviated from astronomical north. Hartmann in 1544 discovered the inclination of the compass. In 1581, Robert Norman proved that magnetization of a steel needle had no effect upon its weight. This prepared the way for further studies of

‡ Frederic F. Lahee, "Statistics of exploratory drilling in 1947," *Geophysics*, June, 1948.
§ *Ibid*, p. 865.

magnetic inclination because it showed that the angle assumed by a magnetized needle was due to the inclination of the earth's magnetic field and not, as originally believed, to a mass which had been added during its magnetization.

William Gilbert, a physician and physicist contemporary of Queen Elizabeth of England, conducted various scientific investigations and experiments with magnets and magnetic bodies. His conception of the earth as a giant magnet was very advanced for his time. His book "De Magnete" was published in 1600.

In 1722 George Graham discovered that the orientation of the compass varies slightly throughout the day. Also, by the end of the 18th century it was known that the earth's total magnetic intensity varies laterally over its surface, and it became vaguely evident that there is some relationship between structural geology and the inclination of the earth's magnetic field. These observations were made by Baron von Humboldt, a German scientist and traveler, in 1798-1803. The diurnal variations in the intensity of the earth's magnetism were first noted by the French astronomer Dominique Arago in 1827. To Karl Friedrich Gauss, who carried out magnetic investigations in Göttingen in 1834, must be given credit for working out methods of measuring terrestrial magnetism. The electromagnetic unit of magnetic force is named for him.

As late as 1616, in *Magnetical Advertisements,* the compass was spoken of as "the most useful and admirable instrument of the whole world, yet blundering." In 1820, the English physicist Peter Barlow reported that "half the compasses of the British navy are mere lumber and should be destroyed." He built an improved one which remained in use until 1876, when the present type was adopted. As the compass has developed so have its uses.

Exploration geophysics probably had its beginning about 1640 when the compass was first used in the search for iron ores in Sweden. Theoretical aspects of the work were propounded in 1843 by Von Wrede, who suggested that local variations in the earth's field might be indicative of buried magnetic materials. Magnetic measurements were conducted in the Michigan iron district in 1873 by T. B. Brooks, in 1875 by H. Smock, and in 1899 by H. L. Smyth. Numerous measurements were made with these early, insensitive instruments. In 1879, Thalen published a detailed account of magnetic technique and results. Investigations on placer gold deposits were conducted in 1914 by Gibson, who carried out surveys in Butte and Shasta Counties in California, using a Thalen-Tiberg magnetometer. Hotchkiss used a dip needle for exploratory work over the iron ore deposits of Wisconsin in 1915.

Since the beginning of the century, numerous large scale geomagnetic* investigations have been made by various organizations throughout the

*The term *geomagnetics* as used here refers to the study of the magnetic properties of the crust or outer layers of the earth.

world. The purpose of the earlier investigations was to obtain information on the distribution of the earth's magnetism with particular reference to navigation problems, any geological conclusion being purely secondary. An impetus to practical geomagnetic investigations for exploration purposes was given by the construction of the Schmidt field magnetometer in 1915. This was the first rugged and portable instrument capable of detecting local magnetic anomalies of small magnitude.

Gravitational Methods.—The variation of gravity at different locations on the surface of the earth was discovered by Jean Richer in 1672, when he noted that a clock whose pendulum was calibrated to beat seconds in Paris lost about two and one-half minutes a day in Cayenne, French Guiana. It was known that the time of swing of a simple pendulum is a function of its length and the pull of gravity. Richer concluded that since the length had not altered, the variation in time must be due to the fact that the gravitational value in Cayenne differed from that in Paris. This explanation indicated that the gravitational attraction might be expected to vary at different locations on the earth and suggested a method of determining this variation, namely, the method of pendulum observations.

The first application of this method to a study of the shape of the earth was made by another Frenchman, Bouguer. Working on the measurement of a terrestrial arc, he led an expedition to Peru (1735-1743) during which he made original use of the invariable pendulum idea and achieved the first relative gravity measurements. His name designates corrections and anomalies employed in making such measurements today.†

The next important advance was the invention of the reversible pendulum by H. Kater in 1818. This type of pendulum is still employed for precision measurements of absolute gravity. The difficulty of calibrating a reversible pendulum accurately and the tediousness of the extreme precautions required in determinations of the absolute gravity led to the use of the so-called invariable pendulums. Invariable pendulums are suitable for determinations of the relative gravity at a large number of stations. This type of pendulum comprises a bob rigidly attached to a "massive" rod, in place of the "weightless" rod of the simple pendulum. The type of invariable pendulum most widely employed at present is patterned after that of the Austrian geodesist, von Sterneck.

Sir John Herschel, in a book published in 1833, suggested the first gravity meter wherein the relative displacements of a bob, suspended by a spring, would serve as a measure of the relative pull of the earth, i.e., the gravity, at various locations.

During the latter part of the 19th century and the early part of the present century, various gravity meters having an accuracy higher than that of the Herschel instrument were proposed. The Threlfall-Pollack gravity meter and the other meters proposed prior to 1918 were not widely used, due to the fact that their accuracy was even less than that of the pendulum.

† E. A. Eckhardt, "History of gravity methods of prospecting for oil," *Geophysics*, V, 3. pt. 1, July, 1940.

Ising in 1918 was probably the first investigator to propose a practical astatic gravity-meter design. The intensive development of gravity meters began during the years 1928-1930, when various American oil companies became interested in new geophysical instruments. At present there are several different types of gravity meters having an accuracy greater than 1 millidyne per gram, including a few with accuracy greater than 0.1 millidyne per gram. (Measurements to within 0.1 millidyne correspond to an accuracy of one ten-millionth of the total value of gravity.)

The attempt to determine how much the earth weighs led to a study of the force of gravity by Henry Cavendish, an 18th-century English chemist. Cavendish used the torsion balance, previously employed by Coulomb for studies of magnetic and electrical attraction, to measure the force of attraction between two masses. Further studies were pursued by Baron Roland von Eötvös, (1848-1919), who refined and applied the principles of the original Coulomb balance, primarily to the field of geodetic research. With the Eötvös instrument, geophysicists have been able to obtain concrete evidence of the variation of density with depth in the outer crust of the earth.

The characteristic feature of the Eötvös balance which renders it a practical and useful instrument for geophysical exploration is that, by placing two equal masses at different levels and by proper choice of instrumental constants, the balance may be made extremely sensitive to variations in the rate of change of gravity in a horizontal plane and to the curvature values. The double beam balance introduced by Eötvös in 1902 is essentially the same as the torsion balance employed at present. In addition to designing a practical field instrument, Eötvös investigated various fundamental principles of gravitational prospecting and applied his method to certain regions in Hungary. Schweydar modified the Eötvös balance by using a "Z-beam." Following him, Shaw and Lancaster Jones introduced a gradiometer which measured the gradient of gravity in a horizontal plane.

The application of gravity surveys as an aid in prospecting for petroleum was investigated in 1914 by E. de Golyer, who took an active part in subsequent exploration. The correlation of gravity variations and geology was due largely to Hugo V. Boeckh who, in 1917, gave geological reasons explaining why anticlines and domes, with cores of different density, produce gravity anomalies of magnitudes which are measurable by the Eötvös balance. He was probably the first to realize the general possibilities of such measurements in prospecting for oil. E. W. Shaw, about the same time, suggested the possibility of locating salt domes by gravity field studies. In 1918, Schweydar under the guidance of Boeckh made successful measurements over a German salt deposit. In 1920, de Golyer contracted for two balances to be built by F. Süss of Budapest, and in 1922, D. C. Barton went to Budapest to receive the instruments and instructions for their use. Barton occupied an important position in subsequent gravity work in the United States. The first commercial application of pendulum

equipment to oil prospecting was apparently made by the Marland Oil Company in Kansas and north-central Oklahoma (1925-26).† More recent developments are described later in the text.

Initial tests in 1922 over the Spindletop dome in Texas gave a definite gravity maximum, but subsequent work over various prospects gave indefinite results, until a survey of the Nash area in Texas showed a good anomaly. A well was drilled in 1924, proving the presence of the structure. Oil was found on the flank of this structure in 1926, probably the first oil pool to be discovered by geophysical methods in America. Large oil fields mapped by the torsion balance method which have now been developed include: Thomson (Rabbs Ridge), Sugarland, Tomball, Manvel, Dickinson, Hastings, Anahuac, Cedar Point, Fairbanks, Friendswood, Mykawa, Roanoke, Iowa, Gillis, and English Bayou. It is estimated that the total ultimate recovery from fields located by gravitational methods will exceed one billion barrels of oil.

Fig. 1. Gravimeter parties operating in the United States, 1938-1947 (E. A. Eckhardt, *Geophysics*, XIII, 4, Oct. 1948.)

As may be seen by Figure 1, the number of gravimeter parties reached a peak of 170 during 1945, declining to about 120 in 1947. Approximately one-quarter of the gravity work during that year was done in the coastal areas of Texas and Louisiana.‡ The geographical distribution of crews is illustrated in Figure 2.

Electrical Methods.—As early as 1720, Gray and Wheeler made electrical studies of rocks and tabulated their electrical conductivities. Watson, in 1746, discovered that the ground was a conductor and noted that current passed between electrodes imbedded in the ground at a separation of two miles acted erratically and in a different manner than when wire was used to complete the circuit.

The ore-finding problems of the mining industry led to the early study of electrical phenomena in relation to mineral deposits. Robert Fox in 1815

† E. A. Eckhardt, *ibid.*
‡ Eckhardt, *Geophysics*, XIII, 4, October, 1948.

and later Dr. Carl Barus in 1882 were convinced that the phenomenon of spontaneous polarization in rocks and minerals had possible application in locating ore bodies. Subsequent to the discovery by Fox, this phenomenon was studied by several investigators. The self-potential method used by Barus on the Comstock Lode in Nevada was essentially the same self-potential technique employed today. The first commercial use of the effects produced at the surface of the earth by spontaneous polarization as the

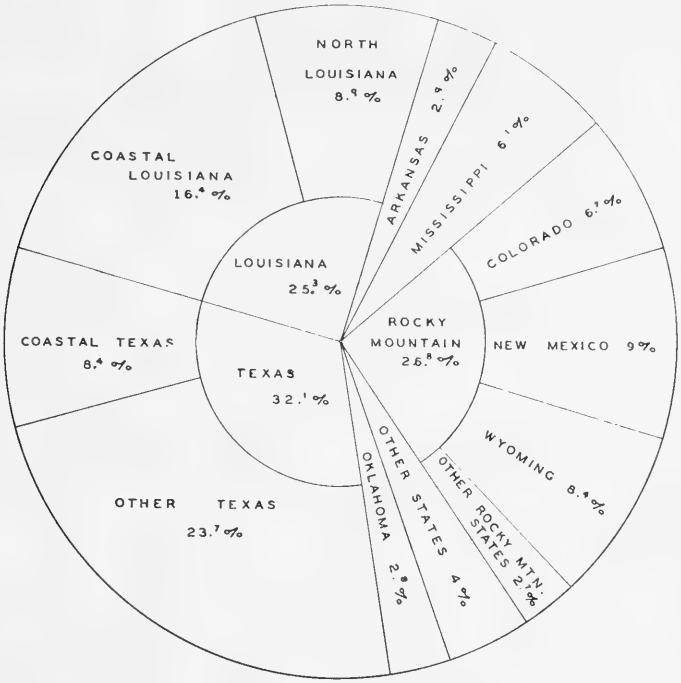

FIG. 2. Geographical distribution of gravity operations in the United States, 1947. (E. A. Eckhardt, *Geophysics,* XIII, 4, Oct. 1948.)

basis of a prospecting method was made by C. Schlumberger. Applied in 1913 at Bor, this technique resulted in what was probably the world's first geophysical discovery of a non-magnetic ore deposit. A published account of the results of these studies (deferred on account of World War I) appeared in 1920.

A second factor in the development of electrical methods was the general concept that subsurface bodies of relatively high conductivity should in some way affect conductivity measured between two points at the surface. Williams and Daft in 1897 attempted to determine differences in conductivity by an alternating current method which consisted in passing the current through the ground and observing the variations in the intensity of sound in a telephone receiver connected to two grounded electrodes. Professor James Fisher first experimented with electrical conductivity

devices in the Quincy Mine in Michigan in 1893, attempting to locate copper-bearing lodes. This was followed by the work of Osborn, who experimented with methods of mapping electric equipotential lines on the Mesabi iron range and in the Lake Superior copper areas.

At the beginning of the twentieth century, F. H. Brown carried out investigations and secured patents on a method wherein the resistance between two grounded points was measured. Several patents on modifications of this method were secured by Brown and McClatchey about 1900. Resistance measurements, as proposed by Brown, had a marked disadvantage: the ground in the immediate neighborhood of the electrodes exerts a large and undefinable effect on the measurements. In 1912 and 1913 C. Schlumberger proposed the direct current equipotential line method and Bergstrom the alternating current equipotential methods. The first significant proposal regarding the use of electromagnetic methods was made in 1913 by Schilowsky, who investigated the electromagnetic effects produced by subsurface anomalies when the ground was energized by alternating current.

Schlumberger's studies from 1912 to 1914 in the Calvados Silurian basin (France) probably constitute the first tectonic studies by geophysical methods using artificial fields of force. Additional studies of the French Sain-Bel and Serbian Bor ore deposits, carried out during the same period, showed that the qualitative concepts of locating ore deposits by their electrical conductivity had been transformed into an effective technique. Wenner's work about 1916 did much to simplify the calculation of resistivity data obtained by passing a current between two electrodes and measuring the potential between two auxiliary electrodes.

The concept of "apparent resistivity," which greatly simplified interpretation, was introduced in 1922 and led to the possibility of systematic geophysical studies over large areas. The first large scale petroleum survey was carried out by C. and M. Schlumberger in 1923, and led to the proving of the existence and the mapping of the Aricesti dome in the Rumanian plain.

Prior to the twentieth century, only a few isolated instances of successful application of geoelectrical methods for the discovery of commercially valuable ore bodies were recorded. With advancement in the art and greater utilization of metals, more attention was directed toward the discovery of ore bodies. The more obvious mineralized areas were approaching depletion, which furnished an incentive for the development of new means of detecting the presence of ore in unknown areas. The application of geophysical principles to mining problems reached its maximum during and immediately following World War I. Electrical methods were developed concurrently in France, Germany and Sweden, as well as in America, where men engaged in this work soon far surpassed previous accomplishments by perfecting highly specialized methods and equipment. Geophysical methods applied to mining have not resulted in any spectacular

developments, although a large number of smaller ore bodies, aggregating a most important economic value, have been located. In America there have been few major mineral discoveries since 1915, and in Europe none since 1850.

Recognition of the influence of subsurface structure on the current distribution at the earth's surface was followed by the use of electrical methods for structural mapping, with many successful applications to oil prospecting and civil engineering problems. Deep structural mapping by electrical methods has been most successful in the Permian basin of New Mexico and West Texas. There the geologic section comprises one to two thousand feet of recent depositional material, underlain with a salt and anhydrite section of variable thickness from a few feet to over a thousand feet. Beneath the anhydrite section lie the sandstones and limestones containing the petroliferous source beds. Commercial accumulations of petroleum occur in closed structures and stratigraphic traps.

The variable thickness of the anhydrite section has complicated successful application of seismic and gravitational methods, while the electrical methods have proved to be more applicable due to the large differences in electrical conductivity of the lithologic units constituting the section.

Electrical logging for determining the character and thickness of the strata penetrated by a drill hole was developed commercially by C. and M. Schlumberger in 1928. This technique with modifications has now become an accepted step in oil well drilling and structure correlation. In exploration work for mapping of subsurface structure the electrical logs are correlated between drill holes.

Popular interest in radio has focused attention on electrical methods of prospecting, and the rapid progress in radio communication has led to repeated attempts to locate ore bodies and oil by radio. To date, these methods have not been of commercial value, due to the poor penetrating power of high frequency currents and electromagnetic fields. Recent theories linking near-surface mineralization with deeper-seated petroleum deposits and structural conditions have revived interest in resistivity measurements for shallow stratigraphic studies. At the present time the economic usefulness in petroleum exploration of these shallow penetration methods is controversial.

Seismic Methods.—Perhaps the person most worthy of being called the first seismologist was John Michell. In 1761, Michell published a paper in which he stated that the motion of the ground produced by earthquakes was transmitted as elastic vibrations through the earth's crust. In the same memoir, Michell suggested that observations on the time of shock at several places would permit the determination of the place of origin of the earthquake. As early as 1855, a number of seismographs using electromagnetic recording had been constructed in Italy by Palmieri. Robert Mallet, the first investigator to suggest the term "seismology" and the discoverer of the refraction method, did much to create a widespread

interest in the study of earthquakes. In addition to his studies of natural earthquakes, Mallet in 1851 produced artificial earthquakes by exploding gunpowder and investigated the effects with a crude seismometer comprising a tray of mercury and a small telescope. He also suggested employing this method to study the earth's immense water-covered areas.

In 1888, A. Schmidt, on the basis of Mallet's work, suggested that time-distance graphs of artificial earthquake waves could be used to study the variation of velocity with depth.

One of the early papers (1889) which is of special interest is that of Fouque and Levy, describing certain experiments whereby they determined the velocity of seismic waves in various kinds of rocks. They used gunpowder and dynamite to create seismic waves in some of these experiments, while in others they utilized a large stamping machine weighing 100 tons. A dish of mercury served as their seismometer. Photographic registration on a moving plate was accomplished by focusing a concentrated beam of light on the surface of the mercury, from which it was reflected to the photographic plate. Telephonic communication was used in many of their experiments. Electrical firing of their explosive charge was accomplished by discharging a Leyden jar through a spark gap in proximity to gunpowder.

In the early part of the twentieth century, Belar, von dem Borne, Benndorf, Galitzin, and others suggested the use of artificial explosions for studying subsurface structure. Prince Boris Galitzin perfected the galvanometric seismometer with magnetic damping which bears his name. The results of Galitzin's investigations were published in a volume, *Seismometrie,* in 1911. A revised edition of Galitzin's work, translated into German, has become one of the classics of the science.

The Refraction Technique. L. P. Garrett, apparently the first to see the possibility of using refraction methods for locating salt domes, conducted investigations during the years 1905-1906 and made the first successful commercial application of refraction technique in 1923. Dr. L. Mintrop experimented with a mechanical seismograph during World War I. Working with Wiechert in Göttingen, he perfected his instrument and technique so that in 1919 he was able to secure a basic patent, later revoked, on the seismic method for determining subsurface structure. The first discovery of oil resulting from use of this method was on the Orchard Dome in Fort Bend County, Texas, by a crew of Mintrop's under the direction of Alexander Deussen, in 1924. This seemed, and later proved to be, an ideal method to use on the Gulf Coast in the search for shallow salt domes. There the rocks possess fairly uniform and low velocities which are in marked contrast with the high velocities of the intruding salt dome. The rapidity of this method and the positive character of its results surpassed those of earlier torsion balance methods. This method became obsolete as a leading exploration tool after about six years. However, as

stated by DeGolyer,† "the refraction technique in prospecting for salt domes in Coastal Texas and Louisiana is one of the most brilliant successes of applied geophysics in oil prospecting as well as the most clean-cut example of the life cycle of a technique." The refraction method in somewhat different form has been revived and used successfully in certain areas such as the Edwards Plateau and the Anadarko Basin, where reflections are erratic and difficult to obtain. Very deep subsurface structure can be mapped, although the procedure is somewhat expensive.

The Reflection Technique. The reflection method of seismic geophysics, developed almost entirely within the United States, was preceded by the studies of iceberg detection and measurement of ocean depths. Reginald Fessenden used it in 1914, and patented both refraction and reflection methods for use in locating geologic formations. Although Fessenden is

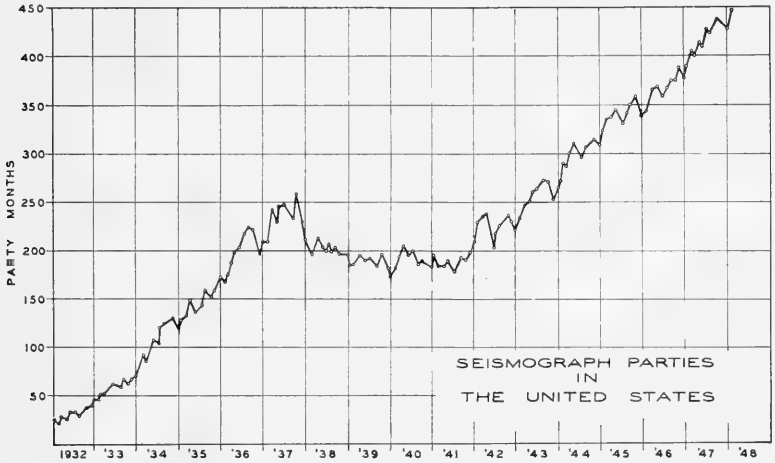

FIG. 3. Seismograph parties in the United States, 1932-1947. (E. A. Eckhardt, *ibid*, p. 530.)

usually credited as being the discoverer of the reflection method, J. C. Karcher, and others, notably E. A. Eckhardt and Burton McCollum, later improved the technique and made its application more practical. The first attempt to prove the applicability of this method was made in 1927 in Oklahoma. In 1928 drilling of a seismic high yielded a small producing well. The professionally accepted proof came in 1930 when three geophysical indications (seismic highs) found in the Seminole, Oklahoma, area were tested and yielded producing wells. Later the Edwards and the Chase areas in Oklahoma confirmed previous reflection predictions and definitely established the method. In 1929 the dip method of reflection shooting was developed. This seismic method today stands preeminently as the most successful and widely-used geophysical method for oil exploration. Of the $105,000,000 expended in 1947 for geophysical prospecting for oil within

† E. DeGolyer, "The Development of the Art of Prospecting," *The Guild of Brackett Lectures* (Princeton University Press).

the continental United States, seismograph operations accounted for some $90,000,000. Crews working in this country increased in number from four in 1929 to about 450 in 1947, as shown in Figure 3. It is interesting to note that about three-fourths of the seismograph work during the latter year was done in Texas, Louisiana, and Oklahoma, which states are credited with five-sixths of all the new oil pool reserves discovered in the United States in 1947, (Figure 4). Off-shore seismograph work accounted for one-sixth of the total for coastal Texas, and one-third for coastal Louisiana.† A great majority of all fields discovered during the past 15 years are wholly or in part due to seismic work.

FIG. 4. Geographical distribution of seismograph activity in the United States, 1947. (E. A. Eckhardt, *ibid.*)

Today, successful seismic prospecting is being carried to depths of 15,000 feet as routine procedure, and some surveys are being conducted to depths exceeding 25,000 feet.

CONTEMPORARY WORKERS AND PRESENT DEVELOPMENTS

Time and achievement must evaluate the improved methods being advocated and utilized today. This chapter, covering only the early history of development, is followed in later chapters by a record of current devel-

† E. A. Eckhardt, *Geophysics,* XIII, 4, Oct. 1948.

opment and research in the several methods of exploration geophysics. The contributions of many individuals to the progress and the enviable success achieved by these methods are recorded throughout the following text. More than 4,000 patents and literature references indicate the diversity of thought which has contributed to modern geophysics. Although geophysical prospecting techniques had their beginnings abroad, most of the important developments of the past twenty-five years have been made in the United States. It has been estimated that over 95 per cent of the world's geophysical work is being done by U. S. organizations.†

TRENDS IN DEVELOPMENT OF FUTURE METHODS

The generally dependable character of the geological data obtained by geophysical methods and the advantage of operating cost which these methods have over exploration by drilling or other direct exploration have established the worth of geophysics in evaluating prospective lands. Geophysical exploration will decline in scope, however, unless the resolving or detecting power of its methods is increased in proportion to the diminishing size and increased depth of the undiscovered deposits. This may be illustrated by a brief review of the several techniques that have been employed in the exploration for oil.

Early prospectors who located the first oil wells were guided entirely by the occurrence of surface seepages. Soon after the discovery of the first fields by this method and by even more haphazard prospecting, it became recognized that the occurrence of oil and gas is commonly limited to the structurally high parts of formations. The anticlinal or structural theory, advanced to explain this occurrence, soon became established as sound and of tremendous value in the search for oil. Throughout subsequent years geologists searched feverishly for favorable anticlines exposed at the surface, until the supply became largely exhausted.

Petroleum geologists later recognized the probable existence of additional favorable anticlines, hidden beneath extensive areas of shallow alluvium, or with poor surface exposures. The necessity for extending knowledge of structure into such areas led to pit-digging and trenching, a very old method of prospecting. As knowledge increased, it became apparent that suitable structural conditions may exist in the older strata unconformably underlying those exposed at the surface. To map such hidden structures, core drilling was introduced in Oklahoma in 1919. This method of exploration was new to the petroleum industry in this country. Core drilling gave the ultimate in exactness of data, but its application was limited by its high cost, with resultant restriction to relatively shallow depths. Core drilling was extended to most of the petroleum districts of the country and is still used in areas where structural relief is small, or where less direct methods are not effective.

The use of core drilling for structural mapping had made considerable

† E. A. Eckhardt, *ibid.*

progress in Oklahoma, Kansas, and some parts of the Gulf Coast, when it was abruptly superseded by the more rapid and economical reflection seismic method, introduced in 1927. However, during the past few years increasing use has been made of another type of drilling method, termed "slim-hole" drilling.

Direct exploratory methods, such as drilling, are a means of obtaining the most definite and irrefutable type of data. The information from such a direct method possesses three components that are most desirable: (1) direct determination of the structural conditions existing at a specific point or localized area, as contrasted to geophysical methods which involve measurements over areas of relatively large extent;* (2) specific information regarding the strata traversed by the bore hole, by means of cores or electrical logs; and (3) accurate depth measurements.

In present commercial usage, slim-hole drilling constitutes the drilling and electrical logging of a small diameter hole. Successful work of this type is being conducted to depths as great as 3,000 - 5,000 feet. The subsurface structure is determined by the correlation of the electrical logs from holes properly spaced in the area under investigation. Any desired portion of a hole may be cored to obtain samples for lithologic, paleontological, permeability and porosity studies and to determine the presence or absence of oil. Substitution of an electrical log for the complete core effects a saving which makes the method economically feasible in many areas, especially the Gulf Coast, where soft strata permit rapid drilling at low cost. There is a possibility of obtaining greater advantages and of effecting still further economy by the use of some form of electrical or mud-logging technique while drilling is in progress. Present commercial practice indicates that a 4½" hole is the minimum diameter if the drilling operation is to be followed by electrical logging. If a usable log could be obtained while drilling, the diameter of the hole could be reduced, with a material saving in drilling time and cost. Work now under way indicates that the logging-while-drilling techniques may be able to utilize holes of about 2 to 2½ inches in diameter. The limiting minimum diameter appears to be governed by the ability to circulate sufficient water or mud to clear the hole of cuttings.

Slim-hole drilling, with coring at desired intervals, may be combined with core analysis and orientation to produce an exploration procedure far surpassing in accuracy any technique in use today. If greater economy can be achieved in the drilling and logging technique, the cost of such work may become commercially feasible for general exploration. Considerable experimental work has already been done using slim-hole drilling as control, with holes spaced one to five miles apart, and other low-cost geophysical methods for structural mapping between holes. Successful develop-

* Reflection seismic work has a relatively good resolving power because its zone of measurement is small as compared to gravitational, magnetic, electrical, and other potential methods, which are decidedly "weighted" types of measurements involving zone of measurement of somewhat indefinite lateral extent and depth.

ment of such a combined technique would allow its application in many areas not amenable to the more common geophysical techniques.

The diversity of the electrical methods and the relative ease with which a measurable field of force may be established give these methods undeniable advantages over other potential type methods. However, electrical methods utilizing surface potential measurements have not had sufficiently definite results, due to the masking and disturbing effect of the near-surface materials on the potential distribution. Work during the past few years indicates that many of these near-surface effects can be minimized by a more direct type of measurement (such as the measurement of the magnetic field associated with the flow of current) instead of the indirect measurements dependent upon the surface distribution of potential. Proper utilization of this type of measurement may produce a method giving sufficient accuracy in many areas where other geophysical methods have not proven applicable.

Soil analysis, including the determination of both the hydrocarbon and mineralization content, has attracted much attention due to its ability to detect and measure diagnostic variables which appear to be directly associated with known oil and/or gas fields. Unless this method proves useful in directly determining the presence of oil, its value is limited, since its use adds little to the geological knowledge of the structure and stratigraphy of the area surveyed. The usual data must be treated from a statistical viewpoint to evaluate the areal distribution of hydrocarbons or minerals, after which allowance must be made for the effects of surface or near-surface conditions not necessarily related to the deeper existence of oil accumulation. Careful consideration must also be given ground water movements and their effect on the distribution of hydrocarbons and secondary mineralization at the surface of the earth. Present indications seem to point to the use of soil analysis methods for furnishing confirmatory evidence as an adjunct to the other exploratory methods capable of mapping structure directly and quantitatively.

Since 1943 there has been a rapid increase in the use and development of seismograph methods for exploring water-covered areas lying off the continental shores. The close relationship and geologic similarity over thousands of square miles of submerged off-shore lands to adjacent rich petroliferous land areas make it highly probable that very sizeable oil reserves await discovery and development. This and other factors have led to a vigorous program of off-shore exploration, and to the development of practical methods for drilling and producing prospects. Limited areas of interest off the California coast have been explored. However the major activity has been in the Gulf Coast region, off the shores of Louisiana and Texas.

Discovery of the Creole field in 1938 proved an incentive to the present campaign of exploration, leasing, and drilling which began about 1945.†

† Dean A. McGee, "Gulf Activity Spurred by Eleven Discoveries," *The Petroleum Engineer*, April, 1949.

Since that time more than 2,000,000 acres of submerged land off the coast of Louisiana have been leased, and eleven fields discovered. Early in 1949 about 30 active operations were under way, with 17 reflection seismographs in use. Some exploration was being done beyond the 27-marine mile boundary claimed by the state. It has been shown by seismic work that salt domes similar to those found on land extend at least this distance from the coast. Gravity data assembled by the U. S. Navy indicate the existence of salt domes as far as 75 miles from shore. In such cases the mechanical difficulties in exploring and drilling in these deeper waters must be added to the hazards caused by sea and weather conditions. The water in the open Gulf is often rough, and hurricanes may force the withdrawal of a crew.

However, since off-shore work indicates a density pattern similar to that found in the coastal land belt, as well as a thicker sedimentary section, it is believed that the total oil reserve in this area will exceed that on land. To meet the challenge of this assumption new methods and equipment will be developed to speed exploration, drilling, and production in this difficult and perhaps rewarding area. It is estimated that $70,000,000 per year is currently being spent on exploration in the tidelands area alone.

An interesting and popular reconnaissance technique has developed in the last few years as an outgrowth of submarine detection methods. In this method, a magnetometer is carried by an aircraft. It traces a continuous profile of relative magnetic intensity and gives a generalized picture of the area rather than the discrete information collected by ground surveys. It has the obvious advantages of large coverage and extreme rapidity. For example, an airborne magnetometer, carried by a plane flying at an altitude of 300 to 1,500 feet with a speed of about 125 miles per hour, can furnish data on an area of 1,000 to 10,000 square miles per month.† More than a quarter of a million square miles have been mapped by the airborne magnetometer since its first preliminary runs in 1941. This method will undoubtedly continue to grow in popularity, and will result in the reconnaissance mapping of extremely large areas over both land and water.

Exploration geophysics will continue to move forward. Increasing applications will be found for both instruments and fundamental techniques. Many of these developments will be employed in other lines of commercial endeavor and for military purposes. For instance, applications of seismic methods are being made to buildings and foundations, dam sites, etc., to determine their natural period of vibration as an aid in minimizing possible earthquake damage.

† Homer Jensen and E. F. Peterson, "Prospecting from the Air," *Scientific American*, Vol. 178, No. 1, pp. 24-26, January, 1948.

CHAPTER II

GEOLOGIC AND ECONOMIC BACKGROUND OF EXPLORATION GEOPHYSICS

Exploration for mineral resources, which are bountifully but always irregularly distributed within the earth's crust, has engaged the attention of man since earliest times,† and the art of mineral exploration has advanced step by step.‡. Formerly explorers searched for those mineral deposits whose presence was suggested or indicated by evidence at the surface of the ground. The present-day search is for mineral substances which are deeply buried below the earth's surface. Modern exploration methods have made it possible to discover these hidden deposits even though indicative surface outcrops are completely absent.*

The science and art of exploration has in general kept pace with the advance of civilization and the improvement in methods for refining and conserving mineral resources. Before the advent of geophysical exploration, the chief hope of maintaining a continuing supply of these necessary mineral resources was provided by improvements in exploitation and refining, which permitted increasingly greater recovery and utilization of the raw materials and minerals. The recent application of geophysical exploration methods on a world-wide scale, while in no way insuring a permanent supply of metals and oil, has resulted in a vast increase in estimated known reserves. Much more yet needs to be done to relieve the critical shortage of metals.

General Factors Governing Application and Choice of Geophysical Methods.—The application of geophysical methods to the various geological problems involved in the search for mineral resources** is governed primarily by two conditions: (1) the technical factors which are associated with mode of geologic occurrence and type of geologic structure, and (2) the economic factors pertaining to cost of operation.

Irrespective of the specific field of exploration in which it is proposed to do geophysical work, there are certain general considerations which

† T. A. Rickard, *Man and Metals*, 2 vols., Whittlesey House, McGraw-Hill, New York, 1932.

‡ A. J. Ellis, "The Divining Rod—A History of Water Witching," U.S.G.S. Water Supply Paper No. 416.

* An example of the successful culmination of modern exploratory effort is the recent discovery and production of oil from strata buried over 13,000 feet below the blanketing alluvium of the San Joaquin Valley, California. H. W. Hoots, "Additions to California Oil Reserves," *California Oil World*, April, 1939. See also the March, 1938 issue of the *Petroleum World*.

** The term *mineral resources* is used here to include any substance whose natural habitat is the earth's crust and whose beneficial exploitation requires the use of the various well-known mining, drilling, and engineering methods. Practically, the term includes metallic and non-metallic minerals, petroleum, and water.

will indicate, first, whether use of a geophysical method is technically justified and second, whether its use is economically sound. Technical justification depends primarily on the possibility of coordinating the known and/or probable subsurface geological conditions in any area with the data which can be supplied by a specific geophysical method. Some of the methods are uniquely applicable to certain geological and terrain conditions. The selection of a suitable method requires, therefore, a study of the theoretical applicability of the various methods to the specific problem.

Economic justification for the use of geophysics in any case is mainly to decrease the financial risk of subsequent exploration. Due to the complexity of geological conditions in different areas, however, strict standardization of cost is not possible in geophysical work. Generally, the cost can be evaluated only after proper study has been given the geological and other technical considerations. The interrelation of the cost factors and the technical factors may be expressed by defining the purpose of a geophysical survey as the securing of maximum geologic or subsurface information at minimum cost.

Theoretically, the applicability of geophysical methods of exploration may extend to any area in which the subsurface geological relations are obscure and where additional subsurface information may serve to reduce the financial risk or engineering hazard involved in future exploration. Practically, specific fields of application as well as the choice of proper methods to employ depend upon a great many considerations. Some of the more important may be listed as follows: (1) amount of surface and/or subsurface geological information already available, (2) local geology (probable type of structure, etc.), (3) purpose of survey, (4) depth of investigation required, (5) terrain conditions and geographic location, (6) theoretical applicability of specific methods, (7) cost of geophysical survey, (8) cost of alternative means of securing required information (core drilling, etc.), (9) local land ownership, and (10) geographic location of the area and available means of transportation. These various items are discussed in greater detail in following sections, which outline the specific applications of the several methods in the fields of petroleum geology, mining geology, civil engineering, and water supply engineering.

Classification of Exploration Methods.—In the following tabulation the various methods are listed in the generally recognized order of increasing resolving power†: i.e. their ability to obtain specific data diagnostic of subsurface conditions. The term *resolving power* relates only to the *general* use and applicability of the methods, because a method which usually has a relatively low resolving power might under *specific* favorable circumstances become a method of superior resolving power. For example, magnetic methods, while generally of low resolving power

† See also E. E. Rosaire, "On the Strategy and Tactics of Exploration for Petroleum," *Journal of the Society of Petroleum Geophysicists*, Vol. VI, No. 1, July, 1935, pp. 11-26.

Natural Field of Force	Artificial Field of Force
Geothermal	Electrical (inductive)
Magnetic	Electrical (conductive)
Gravitational	Electrical (magnetic)
Geochemical: surface soil or gas analysis	Seismic (refraction)
Radioactive	Seismic (reflection)
Electrical self-potential	Slim-hole drilling, with electrical logging
Slim-hole drilling with mud logging	
Core-hole drilling, with paleontological studies and core orientation	

for sedimentary structural investigations, achieve a high resolving power when applied to the location of highly magnetic subsurface bodies under shallow depth of cover.

Generally, the resolving power of the methods utilizing natural fields of force is less than that of methods in which the force field is artificially created and subject to control in direction, intensity, and effective depth range. It is characteristic of the group of methods utilizing a natural field that the field of force measured at the surface is the resultant or summation effect of near-surface irregularities and regional variations, as well as the effect of local geological structure concerning which information is desired. The practical difficulty of separating this composite effect into its component parts is a serious disadvantage of these methods. The methods utilizing artificial fields may also be subject to several component effects. In the case of the latter methods, however, the extraneous effects usually may be evaluated or minimized. This is done by properly selecting the points of application of the force fields. An important feature is the ability to control the effective depth range of the artificially-created force fields.

The technique of slim-hole drilling as now used commonly incorporates a subdivision of the electrical methods and/or the geochemical methods. It differs from other exploratory methods in that measurements are made in previously drilled deep core holes, rather than on the surface of the ground. Ordinary electrical logging comprises those methods utilizing electrical measurements in wells or holes drilled primarily for discovery and production of oil. Slim-hole drilling, on the other hand, employs the technique of making electrical measurements in small-diameter, low-cost holes drilled expressly for this purpose. In the electrical logging and slim-hole drilling techniques, the electrical measurements are ordinarily conducted after completion of drilling. The more recent techniques, however, obtain electrical and mud-logging data during the process of drilling.* Another recently developed method of recording subsurface data is that of constructing drilling-time logs which commonly reveal any important change in lithology by the change in the rate of drilling.

*See chapter on Drill Hole Investigations.

The geochemical method, as subsequently explained, holds promise of being able to detect petroleum accumulations directly, in contrast to the usual use of geophysics merely as a means of determining structures favorable for oil accumulation. For this reason, the geochemical method, although possibly of minor importance in its present stage of development, is potentially a method of higher detectability for oil deposits than other surface methods now in use.

The following classification shows the fundamental properties and relationships which form the basis for the various methods:

Method	*Field of Force*	*Physical or Chemical Property*
Magnetic	Earth's magnetic field	Magnetic permeability
Gravitational	Earth's gravitational field	Density
Electrical	Natural potential field	Spontaneous polarization
	Artificially created electric, electromagnetic, or magnetic field	Electrical conductivity or its reciprocal resistivity; path of current flow
Seismic	Artificially created seismic waves	The velocity of transmission and/or the frequency characteristics of seismic waves, as affected by density, elasticity, etc.
Radioactive	Radioactive radiation	Radioactivity, i.e., the emission of electrically charged particles from the nuclei of the atoms of radioactive materials
Geothermal	Earth temperature gradients	Thermal conductivity
Geochemical	Emanation of hydrocarbon vapors	Hydrocarbon content of the earth
	Ascending or descending aqueous solutions.	Mineral content of the earth

The fundamental principles and general procedure are essentially the same for all of the geophysical methods. All depend for their *modus operandi* upon the following basic facts. (1) The subsurface normally is composed of rock formations possessing certain differing physical properties. (2) Natural or artificially-created force fields within the subsurface are affected to different degrees by these differing physical properties. (3) The extent to which certain force fields are affected depends, among other factors, on the magnitude of the particular physical properties and on the sizes, masses, and arrangements of the subsurface rock materials. (4) The effects produced by the subsurface variations in physical properties upon certain force fields can be measured at the surface of the ground.** (5) The data obtained can be interpreted or translated into terms of prob-

** An exception is noted in electrical logging and slim-hole drilling wherein the measurements are made below the surface.

able geological structure. The basic procedure in all methods, therefore, consists in (a) measuring variations in force fields at the surface of the ground and (b) predicting, on the basis of knowledge of the influencing physical properties, the probable configuration of subsurface materials (geological structure) which might cause the measured effects.

As will be shown later in this chapter, the relationship of these various physical properties of the rock materials to problems of economic geology is usually the main factor dictating applicability and choice of methods for exploring any given area.

Technique of Applying a Geophysical Method.—In applying a geophysical method the mode of attack may be either direct or indirect. In the direct attack, the purpose of the geophysical measurements is to locate a subsurface body or geological condition by means of an anomaly which is directly associated with, and the direct result of, this body or condition. Examples of the direct method are the location of bodies of sulphide ore by means of their high electrical conductivity, the location of bedrock underneath fill material by the differences in electrical conductivity, the detection of a petroleum accumulation by an increased concentration of hydrocarbons in the soil, etc. In one type of the indirect mode of attack, the probable location of the desired subsurface deposits is inferred from the similarity of the geological structure, determined by the geophysical survey, to those structures known commonly to contain such deposits. An example of the indirect attack is the locating of a petroleum deposit by the detection of a subsurface structure or trap suitable for petroleum accumulation which, when drilled, may be found to contain petroleum. An example in mining exploration is the indirect location of placer gold associated with black sand concentrations by means of the magnetic anomalies produced by these black sands.

In mining exploration the direct method is of predominant importance, but there are many applications of the indirect type. A combination of both techniques, where possible, has produced the most satisfactory results in many cases.

The choice of a particular type of geophysical method is commonly dictated by existing conditions. The mapping of basic igneous dikes that intrude sedimentary formations is an example. For this particular problem, the use of magnetic methods combined with available surface geological data will usually give maximum information at minimum cost. In a majority of cases, however, the controlling factors are not so obvious, and judicious exploration may demand the use of more than one geophysical method.

Initial exploratory studies of a reconnaissance nature commonly are conducted to indicate, in a general way, the major geological features of probable importance. Further investigations may be carried out with a method of greater selectivity to obtain confirmatory and more detailed evidence in certain parts of the area. An example of this procedure in

mining exploration is the preliminary use of a magnetic survey to outline the plan location of certain magnetic dikes or ore-bearing mineral veins, followed by an electrical survey to determine the occurrence, location, and depth of sulphide mineralization in the veins, or associated with the dikes. A similar example in petroleum exploration is the common procedure of supplementing preliminary magnetic or gravimetric results by detailed seismic surveys.

Outline of an Exploration Program

A general exploration program can, with minor revisions, be applied to a wide variety of exploratory problems. The initial step for such a program in any given area, whether for ore deposits, petroleum, or other resources, should be a preliminary study of available geological literature pertaining to the region and to the specific area. This will be concerned principally with regional geology, manner of occurrence of ore or petroleum deposits, and the history of their discovery and exploitation in this and adjacent areas.

The second step is the securing of a temporary legal control and right-of-way on the land to be investigated. This may be of various forms. In mining, the common form is the bond and lease with option to purchase. In oil prospecting, however, the geophysical work occasionally is done with nothing but right-of-way permission to trespass on the property or permits to drill shot holes. Lease-holds may be obtained during or after completion of the survey and the discovery of favorable prospects.

The third step in this general program is the preliminary geological field study, undertaken for two purposes: (1) to determine to what extent geophysical methods will be required to secure information necessary for economical development of the property, and (2) to provide information which will determine the choice of geophysical methods and aid in subsequent interpretation of the geophysical data. Since the geophysical survey is to be conducted to gather geophysical data pertaining to matters such as structure and the location and depth of certain rock formations, it is essential that all available geological information from rock outcrops, drill holes, pits, and excavations, be correlated and appraised in advance of the more costly geophysical survey. By this means the geophysical survey may be planned to the best advantage, and the time and money spent may be materially reduced. In many cases, when diagnostic surface conditions prevail, the geological study alone will indicate the character and amount of geophysical work needed to complete the desired geological picture.

The preparation of preliminary maps is an important part of this third step in the exploration program. Topographic maps are of value for several reasons. (1) They aid in planning any exploration program and in interpreting surface geology. (2) They provide the topographic control essential to the interpretation of geophysical data obtained from areas of appreciable surface relief. (3) Topographic relief frequently is related to structure and is a further aid, therefore, in accomplishing the purpose of the survey:

namely, the determination of local subsurface conditions. In certain cases, the use of aerial photographs will be of much assistance and will be justified economically.† Careful and systematic inspection of air photos, particularly with a stereoscope, provides valuable clues to the dip of strata, the position of faults and critical rock ledges, and the location of native vegetation and crops which may impede geophysical work, as well as roads and trails. The use of aerial photography, however, is more readily justified for relatively extensive exploration in undeveloped areas and under difficult terrain conditions. Considerable discrimination is necessary at all times to insure that the economic value of the technical data secured justifies the expense. All preliminary maps should be prepared with due regard to their proposed use in conjunction with the planning of a survey and the plotting and interpretation of the geophysical results.

The fourth step in a general exploration program is the determination of the applicability of the various geophysical methods to the problem at hand, and the selection of one or more methods. (This step may, of course, be contemporaneous with preceding steps.) If the previously acquired geological information is comprehensive and requires for completion of the study only an extension of known surface features to greater depths, it is probable that the need of a detailed survey by a particular geophysical method in certain limited parts of the area will be clearly indicated. The choice of method commonly is controlled by the geological setting, the information desired, and the cost. Where the area is large and available geological information is meager, economic considerations may dictate a preliminary reconnaissance by one of the more rapid and less costly geophysical methods before certain parts of the area are selected for detailed survey by a more costly method.

The fifth step is the performance of the geophysical field work. This is an engineering as well as a scientific task. The engineering work of geophysical surveys has much in common with that of other land surveys requiring the compilation of a series of observations at designated locations. The taking of notes, the proper recording of station locations, and the plotting of stations and recorded data on maps are similar in all types of land surveys.

The tabulated geophysical measurements are next subjected to computations by means of appropriate formulas and corrections. The computed results should show the variations, if present, in some physical property of the subsurface such as magnetic permeability, electrical conductivity, or density; or they may show the depth and altitude of reflecting beds, elastic wave velocity, etc. Usually the computed results are plotted in a manner which lends itself readily to subsequent analysis and correlation with known geology and surface features.

The sixth step is the analysis and interpretation of the observed and recorded data. The interpretation consists primarily of translating the

† Report of symposium on "Aerial Geologizing." (Tech. Pub. No. 756, *A.I.M.E.*, 1936).

computed results into a graphic three-dimensional picture of the subsurface. Graphs, cross sections, contour maps, and vector diagrams are the usual means of illustrating these final results.

In field operation, it is desirable that the computation and interpretation of results proceed almost contemporaneously with the securing and recording of field data. Preliminary interpretations are used to guide the survey as it progresses and to expedite land acquisition and/or the performance of lease requirements, prior to completion of the survey.

The complete results of the geophysical survey should be contained in a final report, giving the location of the area, its geological setting, the relationship of the geology to the geophysical measurements, and the economic purpose of the survey.* The field work conducted should be covered in an appropriate degree of detail, depending on the function of the report. If it is to be presented to laymen who are not familiar with the fundamental principles of exploration, it is often best to discuss briefly the limitations of the work. On the other hand, if the report is being made to a group of engineers who have had experience with the type of measurements employed, much elementary detail may be omitted, and the report confined almost entirely to a discussion of the measurements made and the results obtained. Such a report is often the work of several men who may be conversant with special phases of the survey. Final and complete maps are included, together with an interpretation of the geophysical findings.

If the survey has been successful in gathering the desired information, recommendations usually will take one of three forms: (1) test drilling or mining, (2) abandonment of the venture or (3) holding the property for later development. The decision to abandon an enterprise is fully as important and oftentimes more important with regard to conservation of capital, than the decision to mine or drill. The history of mining and oil exploration clearly indicates that the greatest single factor causing loss of capital has been the common human trait of "not knowing when to stop."

The interpretation of the geophysical data is the most important step in the general exploration program. The technique of interpretation covers a wide range of procedures, from that relying predominantly on basic theory and rigid mathematical analysis, to that relying predominantly on empirical relationships. The latter are built up through extensive experience in actual field problems and are often supplemented by empirical data from small scale laboratory experiments. In most cases, successful interpretation includes both a mathematical and an empirical treatment of the field data, the relative predominance of one over the other usually being a function of the amount of diagnostic geological information available and the relative complexity of the subsurface structure. Pure mathematical analysis alone is seldom adequate, principally because of the many complex variations in the structure, configuration and composition of underground rocks. Successful

* The importance of final reports cannot be overemphasized. Professional men have found the ability to write clear and accurate reports a most important success factor.

interpretation usually is based on theoretical considerations tempered by experience gained during prior similar studies.

The interpretation of geophysical data is a highly involved task requiring ingenuity, imagination and adequate training in geology and physics. It is not uncommon for the task to be divided in such a manner that the observed and computed data are first translated into basic geologic terms by a geologist trained in the theories and methods of analyzing geophysical data and thoroughly familiar with the regional and local structural details of the areas under investigation. *Experience teaches that it is only by the intelligent correlation of geophysical data with all available geologic data that the greatest ultimate practical value of a geophysical survey can be realized.* At present, relatively few men are qualified by adequate training and experience to handle without assistance the many problems of geophysical interpretations.†.

GEOPHYSICAL METHODS IN PROSPECTING FOR PETROLEUM

General Field of Application.—The initial impetus to the development of geophysical exploration methods was provided by their demonstrated usefulness in the search for certain types of ore bodies. The greatest application, development, and utility of the methods, however, has been in the field of petroleum exploration rather than in mining.

Until the advent of geophysical methods, the search for and the discovery of new deposits of petroleum were accomplished by mapping of surface features, core drilling, and correlation of subsurface data made available from drilled wells. Exploration for possible oil-bearing structure was first extended to those areas in which surface evidence of one sort or another indicated the probability of subsurface oil accumulation. Such favorable surface signs included: (1) direct evidence of petroleum occurrence such as oil seeps, gas seeps, bituminous rocks or dikes, "paraffin dirt," asphalt pits, oil-impregnated shales, etc.; (2) exposed anticlinal folds and other structural features favorable for petroleum accumulation at depth; (3) topographic and physiographic evidence of favorable structure not otherwise reflected at the surface of the ground. Extensive search in the known oil-bearing provinces between 1860 and 1920 rapidly depleted the supply of favorable prospects apparent from the use of exploration methods then available. Subsurface information from drilled wells and exploratory core holes became increasingly important after 1915. Although still of indispensable value, these data took a subordinate place in aggressive exploration following the advent of successful geophysical methods in 1922. The need for new methods was pressing at that time, since the demand for large supplies of petroleum was increasing rapidly.

In many of the known oil-bearing provinces, large areas contiguous to

† "Round Table on Geophysical Education," *A.I.M.E., Geophysical Prospecting,* Tech. Pub. No. 950.

producing oil fields are masked by soil, alluvium, glacial deposits, sand dunes, or water which, to date, have prevented or seriously impeded the determination of deeper structure. Regional geological considerations of such areas may indicate the presence of probable petroleum source beds, and the possible existence of favorable traps for oil, below the concealing mantle of surface materials. Notable examples of such areas in the United States are the glacial drift-covered parts of Michigan, Indiana, Illinois, Missouri, Nebraska and Iowa, and the extensive alluvium-covered San Joaquin and Sacramento valleys in California.† In such regions, the possibility of additional future discoveries of petroleum rests largely on the application of improved techniques in geophysical exploration. Even in cases where structure of the surface formations can be mapped satisfactorily, the projection of exposed structure to the depths at which oil accumulation might be expected often introduces a high element of risk because of obvious structural asymmetry, or the possible occurrence of unconformities or appreciable variations in the thickness of subsurface beds.

Many known accumulations of petroleum occur in sand lenses and other types of stratigraphic traps not necessarily associated with closed anticlinal structures. The discovery of such stratigraphic traps is a difficult problem and not much help can be obtained from our current (1949) geophysical technique. Present methods of approach to this problem include: the application of such knowledge of the regional and local geologic history as is available; study of subsurface structure as determined by geophysical work or previously drilled wells in the area; slim-hole drilling; and geochemical surveys.

Geophysical exploration for petroleum structures consists primarily in locating and delineating those types of subsurface structure which experience has shown to be favorable for oil accumulation. The success of the methods to date may be measured, therefore, by the extent to which they have disclosed favorable subsurface structures for which geologic evidence was previously uncertain or lacking. By this criterion and the many prolific new fields so discovered, petroleum geophysics has become established as a necessity in most exploration programs.

Relative Utility and Importance of the Methods

Magnetic Methods

Magnetic methods have been widely employed in some areas for specific problems in oil exploration. Their greatest success has been in certain cases of uniquely favorable geological conditions wherein strong magnetic anomalies are directly associated with the oil-bearing structure. For instance, magnetic methods have been used successfully to map the trends of buried igneous ridges and other features of basement topography, which from previous experience are known to have, commonly, a definite relation to

† W. G. Osborn, (1) "Geological Complex of Iowa," *The Oil and Gas Journal,* May 13, 1937; (2) "Geologic Aspects of the Forest City Basin," *The Oil and Gas Journal,* January 5, 1939.

oil-bearing structures in the overlying sedimentary rocks. A noteworthy example is the Hobbs oil field of New Mexico, which occurs on a structure overlying a pronounced uplift in the basement rocks. The location of the discovery well of this field was based on the results of a magnetic survey. (See Figure 106.)

As an independent exploration technique, magnetic methods have several serious disadvantages, chief of which are (1) lack of depth control, (2) difficulty in separating the unrelated magnetic components due to near-surface materials from those which reflect the deeper structure, (3) difficulty in distinguishing between anomalies due to structural variation and those due to lithologic and mineralogic variations, (4) difficulty in relating the areal location of a magnetic anomaly to a definite location of the structure causing the anomaly. The two greatest deterrents to successful interpretation of magnetic data are: (a) the difficulty of specifying whether magnetic anomalies are due to structure or to depositional variations, and (b) the fact that even when the magnetic anomalies are structural in origin, there may be no definite relationship between the type of anomaly and the structure, e.g., subsurface structural "highs" may, in different geologic settings, be associated with either magnetic "highs" or magnetic "lows." These unfavorable factors arise in the use of magnetic methods in searching for favorable structure in sedimentary rocks, but are not present in many local problems of specific nature, such as the location of igneous dikes.

Compensating features in the use of magnetic methods are their relatively high speed and low cost. These are sufficiently pronounced to indicate a definite field of usefulness for magnetic reconnaissance, preliminary to further detailed studies by other methods. This is particularly true in areas where information is available on the controlling magnetic properties of the subsurface.

Gravitational Methods

In fundamental theory and in practical limitations the gravitational or gravimetric methods are quite similar to the magnetic methods. In general, however, the gravitational methods have been used more extensively and with greater success in mapping the relative topographic relief of the comparatively dense basement rocks. They are thus oftentimes valuable in locating associated structure in the overlying sedimentary formations, as well as in finding major structural features such as faults, contacts, etc., in the overlying sediments. The outstanding economic use of gravitational methods in the United States has been the locating of the deep, lower-density salt plugs which form the cores of the numerous salt domes in the Gulf Coast region.

Precisely as with magnetic methods, the chief deterrent to more general application of gravimetric methods is the difficulty of interpretation, particularly in the resolution of differential depth effects. However, the

relationship between structure and variations in gravity is commonly more definite than similar relationships between structure and the earth's magnetic field. For example, salt dome structures are usually associated with gravity minima, while ordinary domal or anticlinal structures are more often associated with gravity maxima. (The gravity maxima existing over certain shallow salt domes such as the Spindletop dome, the Nash dome, and a few others, constitute an exception to this rule.)

Use of gravitational methods for reconnaissance was formerly restricted by their limited applicability in areas outside the salt dome province and by the relatively high cost of torsion balance work. However, recent development and improvement of the gravimeter have resulted in wider use of this method both for preliminary reconnaissance and for detailed work.

Electrical Methods

The applicability of electrical methods in oil structure mapping is generally conditioned by limitations as to depth and their adaptation to local conditions, and by appreciable cost for moderate depth of exploration. Certain of the electrical techniques permit controlled variation of the current field, configuration and spacing of electrodes, etc., allowing a depth control which is not enjoyed by either magnetic or gravitational methods. Electrical methods may be successfully adapted to the requirements of both reconnaissance and detailed work in areas where the character of subsurface rocks is favorable for their operation. For reconnaissance work, the cost of electrical profiling is generally less than that of any other method, with the exception of the magnetic methods and the improved gravimeter methods. Reconnaissance electrical profiling consists in measuring lateral variations in resistivity, generally at a constant electrode spacing or depth, in order to obtain an indication of the location of hidden structural features. In detailed work a depth variable is obtained by varying the electrode spacing, which permits the mapping of underground structure by determining the depth and configuration of some electrically prominent member of the stratigraphic section.

Electrical methods employing depth control are generally comparable to the refraction seismic method in resolving power, but are inferior to the reflection seismic method. Although the cost of continuous electrical profiling to depths of about 4,000 feet is usually less than that for seismograph work, the low resolving power of electrical results restricts its adaptation in oil exploration.

The electrical methods commonly have distinct advantages in the mapping of near-surface features. In many cases, they can be used as a direct means of locating faults, principally because fault zones in general have a relatively high electrical conductivity.

Electrical logging of oil wells has assumed considerable importance in correlation work. This method measures the vertical variation in the electrical characteristics of the geologic section traversed by the drill hole. The

measurements are made in the drilled well, or while drilling, and are plotted as a continuous log. From a study and comparison of the logs of wells in an area it is generally possible: (1) to differentiate between beds of shale and sand, (2) to distinguish sands containing oil or gas from those carrying salt and fresh water, and (3) to make stratigraphic correlations and thus determine structure. These methods are discussed in detail in Chapter XI.

Seismic Methods

The seismic methods have proved generally the most applicable and uniformly successful of the various geophysical methods used in oil exploration. Two general types of seismic technique are employed: (1) refraction surveying and (2) reflection surveying.

The refraction seismic method has been used most extensively and successfully in the search for shallow salt domes in the Gulf Coast of Texas and Louisiana. The characteristic higher velocity of the salt core of the domes renders this type of structure readily amenable to refraction technique. In some regards, the general limitations of refraction technique are similar to those of electrical methods, particularly in that increasing depth results in rapidly increasing costs and loss in detectability.

A somewhat different form of refraction seismic work was developed shortly before World War II. It is characterized by exceptionally long distances (up to several miles) between the shot points and the geophones. Quite often two shooting trucks are used. It has been found that the depth to a refracting horizon, or refractor, can be determined along exploration lines at as many points as desired. Such a refractor (often more than one) can be mapped and correlations of its geologic position in the section established from drilled wells. This work can be carried to a depth of more than 12,000 feet without difficulty. The technique has been successfully used for mapping deep subsurface structure in the Edwards Plateau area of west Texas, in the Anadarko Basin north of the Amarillo buried granite ridge, in the West Texas Permian Basin, and elsewhere. It is somewhat more costly than the shallow refraction work mentioned above.

Reflection seismic surveys are currently the most popular and successful of the geophysical techniques used in exploration for oil structures. They have been employed in areas containing practically all types of geological structures important in oil exploration, and in most of the major oil-producing provinces of the world. They are of special value in mapping geological structure in sedimentary beds to depths of 15,000 feet. This is usually accomplished by one of three techniques: (a) by correlating corresponding reflections from the same formation over an area, (b) by computing isolated dips *(dip-shooting)* of the formations from which reflections are obtained, or (c) by continuous correlation of short interlocking profiles obtained from closely spaced shot points. The procedure is called *continuous profiling.*

The results of actual drilling have shown that the reflection seismic method has mapped oil structures with required accuracy to depths of approximately 15,000 feet, and current data indicate that reliable records are oftentimes obtained below that depth.

In common with the other methods, the reflection technique has inherent limitations which hinder or prevent its application in certain areas.† These limitations are especially pronounced: (1) in extensively faulted areas, (2) in steeply dipping areas, (3) in areas which are covered by thick layers of material having irregular velocities, such as usually encountered where there exist several hundred feet of alluvium, glacial till, deep weathering, etc., (4) in areas in which the reflecting properties of the subsurface formations are so mediocre that difficulty is encountered in recognizing corresponding reflections from the same formation throughout the area.

Choice of Methods for Particular Geologic Problems.—The general factors to be considered in selecting the proper geophysical methods for exploration have already been discussed briefly. Perhaps the most important factors to be considered in particular cases are the geological and terrain conditions of the area. Commercial accumulations of petroleum are always associated with extensive areas of sedimentary rocks, and with very few exceptions the oil-bearing rock is of sedimentary origin—most commonly porous sand, sandstone, limestone, or fractured shale. Accumulation of petroleum is governed by structural, stratigraphic, and lithologic conditions. The essential requirements are: (1) petroleum "source beds," (2) a porous and permeable reservoir rock such as sandstone to contain the oil and gas, (3) an impervious overlying bed or cap rock, such as shale, to prevent upward escape of the oil and gas, and (4) a favorable structural or stratigraphic trap for the accumulation of oil and gas. The selection of regions favorable for the first of these conditions is the responsibility of petroleum geology. In the search for conditions fulfilling the last requirement, we are dependent upon petroleum geophysics. The presence or absence of the second and the third requirements can be determined only by actual drilling.

The search for certain types of geologic features as favorable sites for new oil fields is governed entirely by knowledge of the manner of occurrence of oil in existing fields throughout the world, and an understanding of the geologic factors which control these occurrences. The general conditions affecting oil accumulations have become well established since the anticlinal theory‡ first achieved prominence some 80 years ago. Traps which cause accumulation of important oil deposits have been discussed by DeGolyer.§ "Geologically, the trap may be of structural, stratigraphic or chemical origin. If of structural origin, it may be the result of folding, of

† Report on symposium on "Seismograph Prospecting for Oil," A.I.M.E., *Geophysical Prospecting*, Tech. Pub. No. 1059, April, 1939.

‡ For additional information see W. H. Emmons, *The Geology of Petroleum* (McGraw-Hill, 1921).

§ E. DeGolyer, "The Development of the Art of Prospecting," *The Guild of Brackett Lectures* (Princeton Univ. Press).

faulting, of a combination of the two, of differential compaction of sediments over buried hills, of the intrusion of igneous rocks, or of the formation of salt domes. If of stratigraphic origin, it may be the result of the lensing out or shaling out of sands, of old shore lines, of the deposition of sands against old land masses, of the removal of sand by erosion and subsequent roofing by deposition of relatively impervious formations or of various combinations of stratigraphic processes. If of chemical origin, the trap may be the result of solution, of cementation, or of metamorphic alteration which may involve both processes."

The more common forms of oil-bearing structures are listed in Table 2.

TABLE 2

CLASSIFICATION OF OIL STRUCTURES WITH RESPECT TO APPLICATION OF GEOPHYSICAL METHODS

I. STRUCTURAL TRAPS
- A. *Folded Structures*
  1. Anticlines and domes
  2. Salt domes
  3. Domes or anticlines over igneous intrusions
  4. Domes or anticlines over buried ridges
     a. Folds due to uplift
     b. Folds due to differential compaction of sedimentary beds
  5. Noses
- B. *Homoclinal Structures*
  1. Homoclines cut by igneous dikes
  2. Outcropping homoclines sealed by paraffin or asphalt
  3. Homoclines sealed by local cementation of reservoir rock
- C. *Faulted Structures*
  1. Faulted anticlines
  2. Faulted homoclines

II. STRATIGRAPHIC TRAPS
- A. Unconformities
- B. Lateral variations in lithology (sand lenses)
- C. Lateral variations in porosity and permeability

III. MISCELLANEOUS
- A. Combinations of two or more of the above structural features
- B. Differential porosity on the flanks of folded structure
- C. Accumulation in faults, fissures, joints, etc.

Throughout the world there are certain areas or regions (generally sedimentary basins) in which major accumulations of oil occur and in which have been developed the major producing oil fields of the world. The petroleum accumulations (oil fields or districts) in each region are usually related genetically, and structural conditions in the various districts are often similar and typical of the region as a whole. Such regions are known as petroliferous provinces. Examples of petroliferous provinces in the United States are the Permian basin of southeastern New Mexico and the Gulf Coast province of Texas and Louisiana.†

† Walter A. Ver Wiebe, *Oil Fields in the United States* (McGraw-Hill, 1930).

Frequently some certain type or types of oil-bearing structure are characteristic of a particular province or of particular districts within a province. Even more frequently, the stratigraphic sequence and accompanying lithology within a province are characteristic of that province and serve to distinguish it from other provinces.

The topography and vegetation of a province have some influence upon the choice of a geophysical method. Because of the wide geographical distribution of the petroliferous provinces, there is usually a corresponding diversity in terrain conditions. In the Permian basin, high, flat, treeless plains are characteristic of practically the entire province. In the Gulf Coastal province, low marshy ground is characteristic of a large part of the area. In certain parts of California, and in many other regions, the rural terrain is characterized by high topographic relief and semi-desert conditions.

Some areas are too thickly populated or too intensely cultivated to permit the use of certain geophysical methods. In the selection of the geophysical methods that will be most appropriate and efficient for any one area, one must consider the theoretical applicability of the methods as related to various structural, stratigraphic, topographic, and cultural factors.

Extensive application and the comparative successes of the various geophysical methods throughout the world during the past 10 to 20 years provide useful criteria in the selection of methods best adapted to the geological conditions and to the specific problems under consideration.

The usual purpose of reconnaissance by means of magnetic or gravitational methods is to locate any prominent anomalies in the buried surface of the basement rocks and to detect by this means the possible occurrence of favorable structures in the overlying sedimentary rocks. Suggestive anomalies are subsequently detailed by methods more adapted to obtaining precise data as to the actual structure in the sedimentary section. Reconnaissance may be conducted for the purpose of determining directly the major structural character of the sedimentary rocks. Success in such reconnaissance by use of magnetic or gravitational methods requires the presence of appreciable stratigraphic variations in the magnetic or density properties of the sediments, and the absence of lateral variations which might be interpreted erroneously as evidence of subsurface structure. A favorable condition would be the presence in the subsurface section of a formation of abnormally high magnetic permeability or density, in which case structural highs are located by corresponding magnetic or gravitational anomalies. Ordinarily, no depth measurements are obtainable from these methods, and the proper solution of the problem may justify the additional cost of other methods supplying quantitative data.

Gravitational and magnetic methods are not adapted to all conditions, even as reconnaissance techniques. For example, the magnetic method clearly cannot be used to map the structure of deep beds in an area where

near-surface magnetic deposits (alluvium, lava flows, etc.) exist. Gravitational methods are greatly hampered in areas of near-surface lateral density variations and in areas of large topographic relief.

The relative applicability of the various geophysical methods in the location of folded structures often depends more on the geologic setting (stratigraphic and lithologic properties of a petroliferous province) than upon the type of structure. For example, the seismic reflection method has given excellent results in most of the petroliferous provinces of the United States. However, in some provinces the relative success of this method has been moderate to mediocre. Difficulty has been experienced (a) in areas of steep dips and faults, as in California, (b) in areas covered by thick surface deposits of alluvial gravel or glacial fill, as in certain parts of California, Iowa, Illinois, Michigan, and (c) in areas in which lithologic continuity is poor and formations of high elastic wave velocity intervene between the surface and the oil-bearing structure, as exemplified by the salt beds of parts of Kansas and the Permian basin and the highly indurated limestone which caps the Edwards Plateau area of Texas. In certain instances of such unfavorable near-surface conditions, the drilling of deep shot holes might improve the success of this method, but the increased costs usually are not justified. Areas of this type often may be more satisfactorily explored by long distance refraction work or by slim-hole drilling.

Certain areas and problems found to be difficult for reflection seismic work sometimes have proved amenable to continuous electrical profiling, the outstanding cases being the successful mapping of structure near the top of the San Andreas Lime and at the base of the salt in the Permian basin, and the mapping of faults in California and South Texas. Electrical methods have also been successful in mapping faults and folded structure beneath a mantle of 500 to 800 feet of unconsolidated alluvium in the San Joaquin valley of California, and have been employed to determine structure beneath the glacial drift in parts of Iowa, Illinois, and Michigan. A small amount of electrical work has been conducted in the Edwards Plateau area, with some evidence that the surface cover of Edwards limestone may not prevent the mapping of underground structure by this method. The usefulness of electrical methods in petroleum exploration appears to be confined to: (1) detecting the location of faults, (2) mapping of shallow structure, and (3) detailed structural mapping to depths of about 5000 feet in certain districts where underground stratigraphy is favorable.

Salt dome structure may be classed as a special case of folded structure. The outstanding early success of refraction seismic and gravitational methods was in the location of relatively shallow salt dome structure, and this still constitutes a special field of applicability of refraction seismic methods. Reflection seismic methods, however, are the first choice in modern exploration for *deep-seated* salt domes.

The discovery of homoclinal oil-bearing structures by geophysical methods generally has been only moderately successful. (It is of interest to

note that the usual type of stratigraphic trap is associated with homoclinal structure.) If such a structure is sealed by a fault or by an igneous dike, or other intrusive, the location of possible oil accumulations may be determined indirectly by locating the impounding fault, dike, or intrusive. Magnetic, electrical, gravitational, and seismic methods have been employed in fault location. However, direct location of faults in sedimentary sections *generally* is most economically accomplished by use of electrical methods. If the impounding structure is an igneous dike or other type of igneous intrusion, the magnetic, and in some cases the gravitational, methods are clearly the most applicable.

As indicated previously, the application of geophysical methods to the solution of the general problem of locating stratigraphic traps has not been very successful. Oil accumulation may occur in the up-dip edges of sand lenses and beds truncated by an unconformity on broad structural arches or plunging anticlinal noses. The reflection seismograph generally can reveal the location and depth of these features, but, except in cases of large divergence, can seldom provide an indication of the occurrence and location of the stratigraphic trap itself. Slim-hole drilling, although commonly expensive, offers the most positive method of exploring for such traps. Geochemistry or soil analysis may ultimately provide a direct method of locating oil-containing traps of this type. Stratigraphic traps are responsible for the East Texas field, the East Coalinga field, much of the accumulation in the Midway-Sunset, and many other important producing areas scattered throughout the United States. Accumulations of oil in traps frequently are extensive and profitably recoverable. The future of petroleum exploration depends to a large extent upon the development of methods to locate the stratigraphic traps that still remain hidden.

In predicting the future tasks of exploration geophysics, it may be assumed that the oil traps still to be found are similar to those known to contain accumulations. Hence, if present methods and future improvements in geophysical techniques are to be successful in the search for yet undiscovered accumulations of oil, they must be adapted to locating: (1) anticlinal structures of low relief, (2) structural closures against faults, and (3) stratigraphic traps, whether they be depositional sand lenses, unconformities, or lenticular zones of porosity resulting from chemical action.

Economics of Petroleum Geophysics. — Emphasis in the preceding sections has been placed mainly upon the geological considerations influencing choice of methods, with only brief reference to cost. Cost of geophysical surveys is mainly determined by: (1) equipment, the necessary operating personnel, and supplies, (2) quantity and quality of information required, and (3) terrain and other conditions affecting speed of operation. The amount of detail required is obviously a function of the amount of geological information already available, the complexity of the problem, and the general purpose of the survey. Speed of operation and coverage is

determined principally by the nature of the geophysical technique employed, terrain conditions, local land ownership, etc.

It is obvious from these factors that specific cost is a characteristic of individual surveys and that only an approximate general tabulation of relative costs can be made. Table 3 is such a tabulation, listing the methods in the order of increasing cost.

TABLE 3

APPROXIMATE COST OF GEOPHYSICAL PROSPECTING

Method	*Cost per month*[a] *1940*	*Cost per month*[b] *1949*
Magnetic	$ 500- 700	$ 1,000- 2,500[c]
Aerial magnetic		$ 6- 12 per profile mile[d]
Gravitational:		
Gravimeter	3,000- 5,000	3,500- 6,000[e]
Torsion balance	3,500- 4,500	2,000- 6,000
Marine gravity work		10,000-20,000[f]
Electrical:		
Self potential		1,000- 1,500
Resistivity	3,000- 5,000	4,000- 5,000
Equipotential		2,500- 3,000
Geochemical	3,000- 6,000	4,500- 6,000
Seismic		
Reflection	6,000-11,000	7,000-20,000[g]
Refraction	6,000-15,000	9,500-22,000
Shallow refraction		2,500- 4,000
Marine seismic work		20,000-75,000
Slim-hole drilling	.25-1.75/ft.	.50-3.00/ft.

[a] Data from the first edition of *Exploration Geophysics,* compiled in 1939-1940.

[b] Compiled from figures submitted by:
J. A. Sharpe, Frost Geophysical Corporation, Tulsa, Oklahoma.
E. J. Handley, Century Geophysical Corporation, Tulsa, Oklahoma.
William B. Heroy, Geotechnical Corporation, Dallas, Texas.
Raymond L. Sargent, geophysicist, Houston, Texas.
Leo Horvitz, Horvitz Research Laboratories, Houston, Texas.
E. V. McCollum, geophysicist, Tulsa, Oklahoma.
John Bible, Tidelands Exploration Company, Houston, Texas.
Henry Salvatori, Western Geophysical Company, Los Angeles, California.
H. Klaus, Klaus Exploration Company, Lubbock, Texas.
L. L. Nettleton, Gravity Meter Exploration Company, Houston, Texas.
John H. Wilson, Independent Exploration Company, Fort Worth, Texas.
Raymond A. Peterson, United Geophysical Company, Pasadena, California.
Dart Wantland, Bureau of Reclamation, Dept. of the Interior.

[c] Higher figure for marshy or difficult terrain.

[d] Excluding cost of photography or radio location.

[e] If helicopters are used, add $13,000-$18,000.

[f] Lower figure for inland waters.

[g] Higher figures include all "extras."

Rosaire† has presented an interesting summary of the various factors which are important in formulating and applying geophysical exploration programs. The economics of geophysical exploration is but one phase of the larger sphere of petroleum exploration economics, albeit an increasingly

† E. E. Rosaire, "On the Strategy and Tactics of Exploration for Petroleum," *Jour. Soc. Pet. Geoph.*, Vol. VI, No. 1, July, 1935; *Geophysics,* Vol. III, No. 1, Jan., 1938.

important one. The sole purpose of petroleum geophysics is to furnish preliminary information which can be used in the evaluation of prospective oil land. Current evaluation of oil land, however, may have alternative purposes: (1) discovery of prospects for immediate drilling, and (2) discovery of prospects suitable for maintenance of reserve. In the first class, search is for prospects which, by reason of location, shallow depth, and other factors, can be exploited rapidly and profitably in modern markets under modern proration requirements. Under maintenance of reserve, on the other hand, will fall prospects which because of greater depth, high drilling and production costs, poor location with reference to accessibility or markets, proration requirements, etc., are unsuitable for immediate exploration. These prospects are therefore considered as a future reserve on the assumption that increasing price due to diminishing supply will eventually allow them to be profitably produced.

Relationship between Supply and Demand

Periodically, the question of an adequate oil supply becomes of vital importance. At such times, the oil production in the United States exceeds the total discovery of new oil. Many and various factors contribute to this unfavorable condition, the most important being the complex relationship between exploration and the price of oil, which often is of a politico-economic and technological nature. The complexity of conditions may be illustrated by considering the period from 1938 to 1948.

During that time a major cause of the discouraging relationship between the production of oil and the discovery of new domestic fields was the type of controlled economy which prevailed. The petroleum industry in 1940 was the second largest in the United States, and probably the most outstanding example of an industry that had developed under private initiative, where open competition and a sane economy gave us world leadership. When this condition was suppressed by unfavorable legislation and regulations, initiative was stifled and aggressive exploration was inhibited. During the war period of controlled price ceilings for crude oil, profits were not sufficient to yield a return adequate to stimulate exploration in the high-risk areas. Wildcatting was suppressed, and much of the drilling was directed toward the proving-up of the more favorable prospects, and the extension of known producing areas. The inhibiting effect† of too low a price was particularly exaggerated after issuance of the "hold-the-line order" in April, 1943, which froze the price of oil at substantially a fixed level, while labor and material costs were allowed to advance. During this same period, exploration difficulties continually increased. Between 1943 and 1947 the average income from the sale of crude oil was approximately 35 cents less per barrel than the replacement cost of new oil. The industry as a whole avoided bankruptcy by the simple expedient

† *Report on the Cost of Finding, Developing, and Producing Crude Petroleum,* submitted to the Office of Price Administration by the National Crude Oil Industry Advisory Committee, February 11, 1946.

of operating chiefly on funds derived from the sale of crude oil obtained from producing properties discovered during the prior decade. A brief overall picture of the increased replacement costs for new oil during that period may be obtained from the data given below,† which show the relationship between the lease operating costs*, the drilling or development costs,** and the exploration costs.***

Year	*Development Costs*	*Operating Costs*	*Exploration Costs*	*Total Cost of New Oil*
1936	0.262	0.212	0.180	0.654
1937	0.274	0.213	0.145	0.632
1938	0.311	0.201	0.163	0.675
1939	0.295	0.191	0.360	0.846
1941	0.292	0.199	0.262	0.753
1942	0.311	0.218	0.415	0.947
1943	0.307	0.296	0.434	1.037
1944	0.308	0.383	0.907	1.598

During that decade the lease operating costs increased only about 17 per cent. There was an average increase of about 70 per cent in basic wages and other costs. Offsetting this increase in wages were two factors: an increase in production per man-hour, due to the installation of better field equipment as the producing fields became stabilized; and, secondly, greater production from wells as proration regulations were removed during the war emergency. Better operating efficiency therefore held the *lease operating costs* below a value which might be expected in view of the general price rises.

During this time the *development costs* increased approximately 80 per cent. This was nearly 10 per cent more than the average increase in basic wages and other costs and shows the normal increase due to: greater depth of wells, larger size of holes, heavier equipment, and the increase in the number of dry holes. The percentage of dry holes rose from 13.5 per cent to more than 27 per cent.

Exploration costs, however, increased more than 400 per cent. Wages in exploration work reflected the average increase in basic oil-field wages. Tending to offset increased labor and material costs were the many advances which had been made in geological and geophysical techniques. Nevertheless the *exploration costs* increased 30 times more than the *lease operating* costs, and over 6 times more than the *development* costs.

This greatly increased exploration cost was due chiefly to the decrease in effectiveness of both geological and geophysical techniques, as old areas were reworked and marginal areas extended.

† *Loc. cit.*

*Total operating costs divided by volume of production will disclose operating cost per barrel. *Ibid.*

**Total cost of oil wells completed each year, divided by volume of estimated oil reserves recoverable from such wells, approximates development cost per barrel on a replacement basis. *Ibid.*

***Total of finding costs, divided by the volume of new reserves discovered in the same year, approximates finding cost on a replacement basis.

Exploration techniques have followed cycles, each of which covered a period of relatively few years. The first technique utilized surface indications such as oil seeps. Then came the period of creekology, which ushered in the trend theory; then the reversion to surface indications, as geology and plane-table mapping were employed to find structural highs. During this time much wildcat drilling was being done. The wells were not too expensive due to their shallow depth.

Systematic core drilling techniques in slim-holes were introduced to work out structure covered by shallow overburden and unconformities. The relatively high cost of such exploratory drilling and the increased cost of deeper wildcat wells encouraged the use of geophysical methods to map the subsurface structure. Then came the peak periods and cycles of application of refraction seismic, torsion balance, magnetometer, reflection seismic, gravity meter, and some geochemical and electrical work, in the order listed. Slim-hole drilling with electrical logging was also developed.

Present Exploration Trends.—Today, for lack of better methods, as we continue our search for the subsurface structural highs, the trend in general is toward the ultra-refinement of present techniques, which comprises the careful re-evaluation of an area. This requires the use of more intensive geology, where possible, supplemented by two or more geophysical mthods. By correlation of the data from different geophysical methods, it often is possible to interpret some of the weaker anomalies, the significance of which is not apparent from the application of one single geophysical method. Obviously the cost of such work, necessitating the combination of independent techniques, must be high.

If it were not for the limitations imposed by economic considerations, it would be possible to continue along the present lines of endeavor with more and more intensive application of the combined geophysical and geological procedures. Such a program will of course find additional oil, but its use can result only in increasingly greater costs. Thus the law of diminishing returns enters the picture. Often the development of deeper structures is not overly attractive due to the greater cost of deep drilling, coupled with the fact that the deeper horizons generally have a smaller recovery per acre. The increased development and lease operating costs, together with the lower productivity, far too often make the exploitation of a deep-lying structure a risky marginal operation.

These conditions will probably furnish an impetus to the search for relatively shallow occurrences in new areas and for shallow stratigraphic traps and low closure structures in or adjacent to present producing areas. In the United States, the most important undeveloped regions remaining today are the covered or masked areas, complex fault accumulations, and the stratigraphic traps created by unconformities, pinch-outs, changes in porosity or sedimentation, and lensing. Nearly a third of the important oil fields in this country are of the stratigraphic type, and were discovered by

random drilling. This list includes, such important producing fields as the Midway-Sunset, Coalinga, and Kern River in California; Glen, Burbank, and Bristow-Slick in Oklahoma; the East Texas in Texas; the Smackover in Arkansas; perhaps the New Delhi in Louisiana, the Bradford in Pennsylvania, and Mush Creek in Wyoming. In addition, we have many smaller fields, such as the Cut Bank in Montana; and the shoestring pools of Kansas. Such a high frequency of blind discovery without the aid of geology and geophysics clearly indicates the importance of these stratigraphic accumulations. Since present exploration methods are not generally applicable to the detecting and mapping of stratigraphic traps, it is to be expected that unless some more effective technique of prospecting for them is developed very shortly, there will be a reversion to the wildcat drilling cycle of exploration. If this happens, much exploratory drilling will be done along stratigraphic trends, using less geology and geophysics, and depending primarily on actual drilling luck for success. In the past, such random drilling has been moderately successful in some areas and undoubtedly will find more oil in the future. Price increases for crude oil will stimulate this type of exploration. Such wildcat drilling, however, will not be as attractive as it was one or two decades ago, due to the greater cost of drilling and the limitations imposed by present laws and taxes on the financing of such operations.†

Comparison of Wells Located with and without Technical Evidence

The effectiveness of geophysics in petroleum exploration has been established by the past twenty-five years of intensive use. During 1947, geophysical work was solely responsible for the locations of wells which resulted in 165 producers and 615 dry holes. The combination of geophysics and geology together is credited with locating sites which yielded 134 producers and 405 dry holes. In this period there was a total of 6775 wells drilled.‡ This means that geophysics played a vital role in the location of about one-third of all the oil wells drilled in 1947, with a success record of about one producing well to each four wells drilled.

In the ten-year period from 1938 to 1947, inclusive, wells located by geophysics had a success record of 21 per cent. During this same period, the wells located on a non-technical basis had a success record of only 5.3 per cent. The technically-located wells were four times as successful as those drilled without technical advice. Considering these trends, it is within the bounds of realism to predict that probably fifty per cent of our new well locations in the next ten-year period will be based on geophysical work.

† J. J. Jakosky, "Whither Exploration," *A.A.P.G. Bulletin*, Vol. 31, No. 7, July, 1947.

‡ Frederic H. Lahee, "Exploratory Drilling in 1947," *A.A.P.G. Bull.*, Vol. 32, June, 1948, No. 6, pp. 851-868.

GEOPHYSICAL METHODS IN MINING

General Field of Application.—The application of geophysics to mining exploration may be divided into two general categories. First is its application to operating mines or previously mined areas where detailed studies are necessary. Second is its application to wider areas, where reconnaissance studies are conducted to delineate the areas of special interest, which then may be subjected to intensive investigation.

The largest application of mining geophysics has been to operating or previously worked properties. In detailed studies of such areas, mining exploration differs from petroleum exploration chiefly in the scale and complexity of the geological problems involved. Whereas in petroleum exploration the geophysicist deals with large areas and simple structures, in mining he is concerned with complex local structures of small areal extent, generally in more rugged terrain. Consequently, greater detail is necessary in the mining geophysical observations, and closer correlations are required between geophysical data, surface geology, and history of local ore occurrence. Usually, therefore, costs per acre for mining geophysical exploration are higher than those for petroleum exploration. Also, the relatively small size of the ore bodies imposes depth limitations on the various geophysical methods, and increases costs of surveys. The feasible exploration range on a given property may not even include the entire depth range which may be amenable to economic ore exploitation in any one mining district.

These factors have acted to delay a more general adoption of geophysics in mining as compared to petroleum exploration. Another significant factor, however, is that property lines and claim corners far too often are important legal limitations in a survey, and the problem of the geophysicist becomes one of locating an ore body within the confines of a particular property. Under such conditions, geophysical work for mining, is, in fact, usually a distress measure, resorted to as a last attempt to find ore and stave off shut-downs. With the required goal of locating commercial ore, it has little chance of achieving success, due simply to the fact that there are relatively few so-called "extensions" of ore bodies, or new bodies, in previously worked areas. However, when used in such areas as a means of evaluation and a guide for operational planning, geophysics can serve a most useful function. If a new ore body is indicated, continued mining can be projected. If not, an intelligent decision can be made as to when to discontinue operations, avoiding the useless expenditure of further capital. A wider appreciation of the value of geophysics in providing an answer to the question of "when to stop" would stimulate its application in the field of mining.

The complex geology of mining districts and the variable nature of mineral deposits offer an extensive and fertile field for the application of geophysical methods. The more prominent modes of mineral occurrence, particularly metal deposits, form abrupt discontinuities in local geology,

and the magnitude of the associated changes in physical properties of the rocks and ores may be correspondingly large. The electrical conductivity of a pyrite vein may be over a thousand times greater than that of the adjacent country rock. Such large differences in physical properties can often offset the adverse influence of structural complications, irregularities, and small size.

The second category of application, geophysical exploration over wider areas, has in the past few years become increasingly important.† In a survey of this type, the program must be directed primarily toward obtaining an overall regional picture, and at the lowest cost per property or per acre. It is thus more akin to petroleum geophysics. In many cases this can be accomplished by the following steps: (1) geological studies, with reference to structure, modes of ore occurrence, and mineralogical guides in the area; (2) reconnaissance geophysics, over the geologically favorable areas; then (3) detailed geological and, if applicable, detailed geophysical examination of the favorable zones; followed by (4) direct exploration, such as trenching, shaft, tunnel, or drill hole.

By proper planning, geologically-guided geophysical work may be applied as economically as haphazard prospecting or geologically-guided direct exploration. Quite often a comparison is made between the cost of a geological examination and a geophysical examination of a mining property. This comparison is not too enlightening, because geological work alone in the usual complex mining area is limited in its ability to predict the subsurface conditions. Dips and strikes of exposed rocks must be extended underground with extreme caution, in the usual folded and faulted area. As the experienced mining engineer and geologist also knows, geological prediction is greatly handicapped until enough development has been done to establish local habits of ore genesis and occurrence. Geological work then must be supplemented with direct exploration such as tunneling and drilling. The cost of such geological work and the necessary direct exploration usually is far greater, as to expenditure of both time and money, than geologically-guided geophysical work.

Whether geologically-guided direct exploration or geologically-guided geophysical reconnaissance is the better procedure will depend upon local conditions and the information desired. For instance, the cost of a single 300-foot drill hole is equivalent to the cost of a number of days of geophysical work. The drill hole may give detailed and specific information about conditions along the exact path traversed by the drill. On the other hand, the geophysical work may give general information over a relatively large area. Obviously, there can be no fixed rule as to which is the more expedient technique. In general, however, the geologically-guided geo-

† Hans Lundberg, "Mining Geophysics," *A.I.M.E., Min. & Met.*, Vol. 29, No. 494, pp. 88-92, February, 1948.

V. G. Gabriel, "Geophysical Prospecting—Its Part in American Mining," *Eng. and Min. Jnl.*, April, 1939.

physical work will be more economical during the reconnaissance stage while obtaining an overall picture of the area.

Some of the practical problems encountered in the various phases of mining geophysics may be described briefly as follows:

Metal Mining: locating of new ore bodies, extensions of old ore bodies; depths of oxidized zones; location and determination of general extent of sulphide deposits below oxidized cappings; determination of length and width of mineralized areas; extensions of partially exposed ore bodies; location of faulted segments of veins; delineation of ore shoots in veins, etc.

Non-Metallic Mining: determination of thickness of overburden; presence and location of faults and other structural features; extent of particular formations of rock masses; depth, size, and extent of gravel deposits; etc.

Depth of Application.—The depth to which reliable geophysical work may be conducted in the exploration for minerals is governed almost entirely by the size and configuration of the ore body and the physically measurable differences between the ore *in situ* and the country rocks. For instance, a medium-size massive sulphide ore deposit could produce a detectable gravitational anomaly (in an area where the necessary corrections may be made for topography and changes in formation) at depths of 700 to 1,000 feet. On the other hand, this same quantity of sulphide ore existing as a stringer of mineralization along a vein can seldom be detected by gravity work to a depth of even a hundred feet. However, such a long extended ore body could easily be detected by the electrical methods, which should be able to show its presence to depths of perhaps 400 feet. Generally speaking, mining geophysical work should seldom be attempted to depths exceeding 300 to 400 feet from the point of measurement. The use of geophysical studies should therefore be confined to these depths, unless there are very good reasons for believing that the local conditions are favorable enough to allow the work to be conducted to depths exceeding that range.

Even with this limitation, there are very large fields of application for geophysical work in mining exploration. In Canada, about 90 percent of the pre-Cambrian shield is covered with shallow water and overburden. In the United States and Mexico there are many hundreds of square miles covered with alluvial fill, lake beds, and other masking material, underneath which commercial mineralization may exist.

Choice of Methods for Particular Geologic Problems.—In general, the selection of geophysical methods for mining exploration is governed by considerations similar to those that influence the selection for petroleum exploration; namely, geological information available, type of mineral occurrence, resolving power of the geophysical method, etc. Magnetic, electrical, seismic, gravitational and thermal methods have been employed

successfully. The magnetic and electrical methods have enjoyed the greatest general application and success because of the relatively prominent variations in magnetic and electrical properties typical of the majority of types of ore and rock deposits commonly encountered. Complex geology and rough terrain usually hinder or prevent the application of seismic and gravitational methods. However, seismic methods have been used successfully in determining thickness of overburden and bedrock contours. Successful location of ledges of pyrite and other relatively heavy materials by means of the torsion balance and gravity meter has also been reported.† Rugged terrain characteristic of most mining areas is a specific deterrent to wider application of the torsion balance, because under these conditions extraneous near-surface anomalies are excessive.‡ Terrain and topographic corrections required are almost prohibitively laborious and time-consuming.

The magnetic or electrical effects produced at the surface by an ore body or a structure depend primarily upon: (1) the *difference* between the magnetic susceptibility or electrical conductivity of an ore body, or the structure, and the same property (susceptibility or conductivity) of the surrounding country rock; (2) the size, form, and orientation of the subsurface ore body or structure; and (3) the effective depth of the subsurface ore body or structure.

The complexity of geological conditions which exists in a majority of mining areas usually precludes the use of any one single geophysical method, if the most useful information is to be obtained. It is seldom that a clean-cut prediction of subsurface conditions can be made with the data from only one type of geophysical measurement, for it must be borne in mind that the resolving power of any one geophysical method is often low, while the complexity of subsurface conditions is high. Therefore, geophysical methods preferably should be chosen to give complementary data. For instance, the successful use of the magnetometer in reconnaissance exploration for the nickel-bearing ores in Canada is predicated upon the fact that pyrrhotite, a magnetic sulfide mineral, occurs with the nickel. There are, of course, many other conditions which can cause magnetic highs in that area, such as disseminated magnetite or intrusive basic rocks. To differentiate between the sulfide ore desired and some other magnetic condition, a traverse or two with one of the electrical methods will give the necessary complementary information. The self-potential method, when ground water conditions are correct, will detect sulfide bodies. If, therefore, a self-potential survey discloses an active electrical negative center over the same general area where a magnetic high was mapped, we can be fairly certain that this dual condition is caused by pyrrhotite ore. If,

† "Studies of Geophysical Methods, 1930," *Memoir 170,* p. 108 (Geological Survey, Canada Department of Mines, Ottawa, Canada).

V. E. Barnes, R. W. Mathis, and F. Romberg, "Gravity prospecting for lead and zinc, New Mexico," *Internat. Geol. Cong.,* 18th sess., 1948.

‡ P. W. George, "Experiments with Eötvös Torsion Balance in the Tri-State Zinc and Lead District," A.I.M.E. *Geophysical Prospecting,* 1929.

however, an active electrical center is not obtained over a magnetic high, the chances are that the magnetic work has merely mapped a basic igneous rock or a concentration of magnetite.

Two types of geophysical measurement often can be made during the same survey without an appreciable increase in cost. For example, magnetic and gravity measurements can be made at each station with an increased time for reading which adds about 20 per cent to the total cost. Complementary measurements allow more reliable interpretation, and in many cases actually result in a reduction in overall cost of the work by decreasing the detail which would be necessary if only one method were applied.

A complementary method which has received little attention, but which can be of considerable value, is the electrical logging of drill holes. Although diamond and core drills usually are not considered as geophysical equipment, their use often is closely related to the geophysical work. The function of geophysics is to show where subsurface anomalies exist. Drilling is a means of investigating these anomalies and of obtaining the most direct type of data at minimum cost. Information from such a direct method possesses three components which are most desirable: (1) direct determination of the structural conditions existing at a specific point or localized area; (2) specific information regarding the material traversed by the drill hole, by means of cores which may be examined or assayed; (3) accurate depth measurements. Electrical logging will greatly expand the range of this data. Prevalent in mining folklore are stories of ore bodies that have been missed a few inches by the drill hole. By means of electrical logging, the effective radius of the hole may be extended to from ten to fifteen feet, with reliable results. Electrical logging is extensivly employed in petroleum work; it provides a rapid, economical means for determining the depth and thickness of strata penetrated by the drill hole, and allows correlation of drill holes. Its use in mining exploration should prove to be of equal value.

The usual classification of ore deposits with respect to a consideration of geophysical methods comprises the genetic divisions: (1) mechanical concentration deposits, (2) chemical concentration deposits.†

TABLE 4

CLASSIFICATION OF ORE DEPOSITS WITH RESPECT TO THE APPLICATION OF GEOPHYSICAL METHODS

A. PLACER DEPOSITS

1. Gold Placers
   a. Eluvial placers
   b. Stream placers (alluvial)
   c. Bench or terrace placers
   d. Marine placers
   e. Buried stream placers
2. Placer deposits of other heavy minerals
3. Detrital deposits

† Waldemar Lindgren, *Mineral Deposits* (McGraw-Hill).

B. VEINS, LODES, AND DIKES (REGULAR DEPOSITS)
1. Lodes in which the valuable ore mineral has diagnostic physical properties, e.g., sulphide ore bodies having high electrical conductivity
2. Lodes in which the valuable ore minerals are genetically and structurally associated with minerals having diagnostic physical properties, e.g., auriferous pyrite veins containing electrically conductive pyrite
3. Gold-quartz veins
4. Pegmatite dikes
5. Lodes in which the ore mineral is a refractory type (non-magnetic, non-conductive, etc.), e.g., sphalerite veins

C. IRREGULAR CONCENTRATED DEPOSITS
1. Shear zones
2. Pipes and stocks
3. Replacement deposits
4. Contact-metamorphic deposits
5. Magmatic segregations

D. DISSEMINATED DEPOSITS
1. Disseminations in igneous rocks, e.g., "porphyry coppers"
2. Disseminations in sedimentary rocks

E. BEDDED DEPOSITS

Metallic
1. Gold-bearing conglomerates (South African)
2. Sedimentary iron ores
3. Residual deposits
4. Copper-bearing conglomerates and lavas

Non-Metallic
1. Sedimentary rocks
2. Saline residues
3. Residual deposits
4. Coal and lignite
5. Miscellaneous non-metallic deposits

However, in determining the applicability of geophysical methods, the form, size, and mineralogical content of an ore body are usually more important than its genesis. Table 4, while incomplete from a genetic viewpoint, illustrates all the common forms of ore or mineral deposits which normally need be considered in studying the applicability of geophysical methods.

Placer Deposits

Geophysical methods have been extensively and successfully employed in placer exploration.† Gold placers are the best known of this type of

† A. Gibson, "Magnetometric Determinations Applied to Placer Mining," *Eng. and Min. Jnl.* (1922), vol. 114.
K. C. Laylander, "Magnetometric Surveying as an Aid in Exploring Placer Ground," *Eng. and Min. Jnl.* (1926), vol. 121.
C. A. Heiland and W. H. Courtier, "Magnetometric Investigations of Gold Placer Deposits near Golden, Colorado." *A.I.M.E. Geophysical Prospecting* (1929.)
Dart Wantland, "Comparison of Geophysical Surveys and the Results of Operations at the Roscoe Placer of the Humphreys Gold Corporation, Jefferson County, Colorado," *Colorado School of Mines Quarterly*, Vol. 32, No. 1, January, 1937, pp. 87-118.
H. R. Joesting, "Magnetometer and Direct Current Resistivity Studies in Alaska," *A.I.M.E. Tech. Paper 1284*, February, 1941.

deposit and will serve as an example for the broad class of placer deposits. The purpose and utility of geophysical methods in gold placer exploration are usually twofold: (1) indirect location of gold concentrations, (2) determination of depth to and contour of the underlying bedrock.

No geophysical method can locate placer gold directly, in the normal concentrations usually found in placer deposits. In many placers, however, concentrations of "black sands" (magnetite, ilmenite, etc.) are associated with gold, thereby providing an indirect means for its location, for, under favorable conditions, these magnetic "black-sand" concentrations can be located by magnetic methods. However, such magnetic data are capable of a unique interpretation only when simple conditions prevail in the area. When the bedrock and the deeper basement complex have fairly uniform or low magnetic permeabilities, the magnetic studies will usually show the main concentrations of placer materials by magnetic "highs" superimposed over the regional average of the underlying rocks.

Such favorable conditions do not usually exist. Variations in thickness of the gravel will cause magnetic anomalies. These variations may be caused by irregular surface topography (which can be seen) and irregular bedrock contour (that can not be seen). Similarly, the unknown variations in bedrock permeability will produce anomalous magnetic variations. Most of these factors cannot be properly evaluated or recognized by geological and magnetic studies alone, so that much supplementary work is generally necessary.

Magnetic methods may also be employed for the various other types of placer deposits. They usually are not applicable, however, when the placer deposits are capped by lava flows—as is typically the case in the Sierra Nevada placers of California, in Australia, and in other parts of the world. In such cases, magnetic methods may sometimes be utilized for evaluating the thickness and extent of the lava flows, but they are seldom useful for locating "black-sand" concentrations.

Electrical and seismic methods have both been employed for determining the depth of bedrock in placer deposits; the former far more extensively than the latter. These methods usually furnish a reliable and rapid means of determining the thickness of gravels and the contour of the underlying bedrock. The electrical methods will also indicate important structural features in the bedrock, such as faults and dikes, as well as the subsurface distribution of water.

Determining bedrock depth and contour is an important part of the preliminary exploration of placer ground. Ordinarily, depth determinations are made over a grid work of stations or along sectional traverses. From these studies it is possible: (1) to plot bedrock contours, and thereby locate and trace stream channels in the bedrock, (2) to estimate yardage of gravel, overburden, etc., and (3) to determine suitable locations for mining and sluicing operations to take advantage of existing slope of bedrock. Electrical methods have been employed successfully in locating and tracing gold-bearing stream channels below lava caps.

Two criteria serve to indicate the subsurface location of such channels:† (1) the difference in electrical conductivity between the water-bearing gravels and the bedrock and (2) the lowest point in the bedrock profile.

Veins and Lodes

Magnetic and electrical methods have been employed extensively in exploration for commercial mineralization in veins and lodes, while gravimetric methods have been employed to a much lesser extent. A great variety of minerals and ores occur in the form of veins and lodes. Prominent in these classes are: (1) *sulphide veins* (usually intermixed sulphides of copper, iron, lead, zinc, etc.), (2) *gold-pyrite veins,* and (3) *gold-quartz veins.* Electrical methods are useful for locating all of these types of deposits, but are especially applicable for deposits of electrically conductive base metal sulphides (ores of chalcopyrite, pyrite, galena). In the latter cases, the methods are used to locate the vein directly or to outline shoots or other concentrations within the vein. A problem which is frequently encountered is the location of possible zones of primary sulphides or of secondary enrichment beneath oxidized cappings. The electrical methods have been especially useful for locating non-outcropping veins in areas adjacent to outcropping veins of known characteristics and for locating veins beneath coverings of alluvium, glacial till, tundra, etc. ‡

The use of electrical methods in prospecting for gold-bearing veins and lodes is an indirect process. Such deposits may be located indirectly by means of the occurrence of pyrite or other metallic sulphides in genetic association with the gold. Gold-quartz veins, under favorable conditions, may be located by reason of their poor electrical conductivity relative to the country rock.§

Igneous dikes: Ore bodies are found in association with igneous dikes only infrequently. However, because such dikes have a structural significance in many mineralized areas, their occurrence is mentioned here. Dikes of basic material may be located by magnetic methods due to their high content of minerals of large magnetic susceptibility. ††

Pegmatite dikes: Valuable ore and mineral concentrations are frequently associated with pegmatic dikes. Where such dikes have a sufficiently lower electrical conductivity than the country rocks, they may be located by electrical methods, as in the case of quartz veins. Magnetic methods are applicable when, as is frequently the case, magnetite or other magnetic material is an accessory mineral in the pegmatite. The literature of geophysical methods contains many descriptions of successful

† J. J. Jakosky and C. H. Wilson, "Geophysical Studies in Placer and Water Supply Problems," *A.I.M.E. Geophysical Prospecting, Tech. Pub. No. 515,* 1934.

‡ "Summary of Results from Geophysical Surveys at Various Properties," *A.I.M.E. Geophysical Prospecting,* 1932.

§ Folke H. Kihlstedt, "Electrical Methods in Prospecting for Gold," *A.I.M.E. Geophysical Prospecting,* 1934.

Sherwin F. Kelly, Theodor Zuschlag and Bela Low, "Discovering Gold-Quartz Veins Electrically," *Mining and Metallurgy,* June, 1934.

†† W. R. Johnson, Jr., G. R. MacCarthy, J. C. Campbell, and H. W. Straley, III, "Tracing a basic dike by geoelectrical and geomagnetic methods," A.I.M.E., *Geophysics,* 1940.

application of geophysical methods to the discovery and mapping of veins, lodes, and dikes. §

Irregularly Concentrated Deposits

Magnetic and electrical methods have found extensive application in prospecting for irregular ore deposits such as those found in shear zones, pipes and stocks, replacements, contact-metamorphic deposits, and magmatic segregations. †† Spontaneous polarization methods are particularly applicable to vertical pipe-like bodies of sulphide ore.* In cases where the pipe-like form of the ore bodies is the result of their deposition in shattered volcanic plugs, magnetic methods often may be used to locate the intrusive plug. ‡‡

Replacement ore bodies are of many types and are widely distributed in occurrence and varied in mineralogical assemblage. Replacement processes occur to a certain extent in all cases of ore deposition. Common types are replacement bodies of base metal sulphides. These are often accompanied by gold and silver values deposited in limestone by ascending solutions ** or by percolating meteoric waters.*** The forms of these replacement ore bodies are usually very irregular, depending, in many cases, upon the texture and other properties of the host rock. In certain cases, replacement in fairly flat dipping limestones has extended laterally for sufficient distances to result in a bedded form of deposit.

Electrical methods are preferred for locating the various types of replacement ore bodies which have a high electrical conductivity. Occasionally, however, this method has not been successful, as, for example, in the upper Mississippi Valley where there is a large percentage of poorly conductive sphalerite in the ores. †

Contact-metamorphic deposits frequently contain the ore minerals: magnetite and chalcopyrite. Magnetic methods have been used for direct location of the magnetite ores of contact deposits and for outlining the intrusive igneous rocks responsible for the ore deposition. Electrical methods are applicable when the conductive base metal sulphides are the prominent ore constituents.

Ore deposits resulting from *segregation and separation of ore minerals from magmas* during the processes of solidification are common in many parts of the world. The Sudbury Canada nickel ores are prominent in this group. The chief application of geophysical methods to this class of deposit consists in locating and outlining the igneous rock in which the segregation may have taken place. When such deposits have a high content of magnetite or metallic sulphides, they can sometimes be located directly by magnetic or electrical methods. ‡

Disseminated Deposits

The class of disseminated deposits covers many genetic occurrences. They are important chiefly to the extent that concentration or enrichment

§ *A.I.M.E. Geophysical Prospecting,* 1929, 1932, 1934.
A. B. Broughton Edge and T. H. Laby, *Geophysical Prospecting.* The Report of the Imperial Geophysical Experimental Survey (of Australia), Cambridge University Press, 1931.
†† Hans Lundberg, "Recent Results in Electrical Prospecting for Ore," *A.I.M.E. Geophysical Prospecting,* 1929.
* See Chapter V.
‡‡ Compare Lindgren, *loc. cit.,* pages 153 and 183.
** E.g., lead-silver ores of Park City, Utah.
*** E.g., lead-zinc ores of the Mississippi Valley.
† Hans Lundberg, *loc. cit.*
‡ Max Mason, "Geophysical Exploration for Ores," *A.I.M.E. Geophysical Prospecting,* 1929.

has taken place subsequent to original deposition. Important representatives of this class of deposit are the so-called "porphyry coppers." * In the typical "porphyry copper" deposit, primary mineralization consists of copper and iron sulphides widely distributed through a large mass of intrusive rock, generally monzonitic in character. Oxidation processes in the upper portion of this mass have removed a large part of the original metallic content and redeposited it at greater depth in the form of secondary enrichment. Electrical methods may be employed to locate such zones of secondary sulphide concentration. In addition, they may sometimes be employed to outline the lateral extent of low-grade primary mineralization.

Bedded Deposits

Bedded mineral deposits are probably of greater commercial importance than any other general class. These deposits are found in all parts of the world and include a wide range of metallic and non-metallic ores. The most prominent auriferous deposits belonging to this class are the well-known gold conglomerates of the Witwatersrand in South Africa. Important representatives of the base metal ores are the sedimentary iron and sulphide ores.

Bedded Deposits — Metallic

Gold-Bearing Conglomerates.—Magnetic methods have been extensively applied in prospecting for the gold-bearing conglomerates in the Witwatersrand and other areas of South Africa. In the Witwatersrand area alone, magnetic surveys have been conducted over several thousand square miles. † From the standpoint of geophysical exploration, the steeply dipping Witwatersrand conglomerates are similar to veins and lodes. Because of their steep dips and large lateral extents, the outcropping deposits have been called reefs. Even though magnetite is practically absent in the conglomerates, the magnetic methods have been useful in locating certain magnetic formations which are genetically and structurally associated with the gold series.‡

Sedimentary Iron Ores.—The use of magnetic methods in the exploration for iron ores may be either direct or indirect. Direct location of such ore deposits can be accomplished only when magnetite or other magnetic material is a constituent of the ore. Only certain iron ores are magnetic. (Compare Chapter III.) In particular, some of the ores of

---

* E.g., in Bingham, Utah, and Ely, Nevada.
F. M. Galbraith, "The Magnetometer as a Geological Instrument at Sudbury," *A.I.M.E. Trans.*, Vol. 164, pp. 98-103, 1946.

† Noel H. Stearn, "Geomagnetic Exploration in 1938," *Geophysics*, Vol. IV, No. 2, March, 1939.
A. Frose, R. McIntire, E. Papenfus, and O. Weiss, "The discovery and prospecting of a potential gold field near Odendaalsrust in the Orange Free State, Union of South Africa," *Chem., Met. Min. Soc. South Africa Jour.*, Vol. 47, pp. 107-141, 1946.

‡ R. Krahman, "The Geophysical Magnetometric Investigations on West Witwatersrand Areas," *Trans. Geol. Soc. of S. Africa*, Vol. 39, 1936.

the Lake Superior district contain sufficient magnetic materials to allow their direct detection by means of magnetic measurements. In the majority of cases, however, the ores do not differ sufficiently from the adjacent formations and hence an indirect means of locating favorable areas is used: viz., the mapping of structure in the iron-bearing formations.§

In general, the chief constituent of sedimentary iron ores is hematite; hence, the ores are often less magnetic than the adjacent iron formations from which they may have been derived. In the limonite and hematite ores of direct sedimentary origin, for example the Clinton iron ores, the magnetic methods ordinarily can only be applied indirectly: that is, to determine structural conditions associated with the ore occurrence.

Electrical and gravitational methods have also been used in some of the iron ore districts, particularly at Lake Superior, but to date they have had little utility in direct iron ore location.

Residual Deposits.—Residual iron ores are representative of this class of ore deposits. The deposits have various forms and composition and are generally the result of rock decay and weathering. Frequently the individual deposits are quite irregular, although occurrence and form are generally somewhat controlled by bedding in sedimentary rocks. Geophysical methods have not been applied very extensively or successfully to this class of deposit. In certain cases, it is probable that magnetic and electrical methods may be useful in determining structure related to these deposits.

Copper-Bearing Conglomerates and Lavas.—The Lake Superior copper ores are a unique occurrence and are mentioned here to illustrate the use of magnetic methods for the location of ore bodies occurring in lava flows. In one type of ore body in this district, native copper occurs in amygdaloidal basalt flows which dip from 20° to 40°. Magnetic methods have been used to trace: (1) the flows in which the copper ore is concentrated and (2) certain flows which bear structural and genetic relationships to the copper deposits.†

Bedded Deposits — Non-Metallic

Geophysical prospecting in the field of non-metallic mining has expanded greatly in the past few years. The general class of sedimentary, bedded deposits includes representatives of most of the valuable non-metallic deposits. Because many non-metallic minerals and ores extend through a broad genetic range, it is not possible to restrict them to a strict classification as to form or mode of occurrence. Phosphate deposits, by way of illustration, may occur in the following ways:‡ (1) marine con-

§ Noel H. Stearn, *loc. cit.*
C. O. Swanson, "Use of Magnetic Data in Michigan Iron Ranges," *A.I.M.E. Geophysical Prospecting*, 1934.
† N. H. Stearn, *loc. cit.*
‡ Lindgren, *loc. cit.*, p. 277.

cretionary beds; (2) disseminations in igneous rocks; (3) pegmatite dikes; (4) guano deposits; (5) replacements of limestone; (6) residual concretions. A summary of prior literature dealing with exploration for various non-metallic materials is contained in an early publication. §

Applications of geophysical methods in the non-metallic field are governed by the factors outlined for other mineral resources earlier in this chapter. For the sake of brevity, the following discussion will comprise a resume of applications to bedded and residual deposits. The applications are primarily of the indirect type, i.e., the mapping of structure associated with the occurrence of commercially valuable deposits. The location of faults, dikes, and folds and the determination of thickness of overburden constitute the important problems. For the solution of these problems, magnetic, electrical, seismic, and gravitational methods are all used.

Sedimentary Rocks.—Examples of sedimentary rocks or rock materials which are of commercial importance are limestone, sandstone, clay, sand, gravel, etc. Electrical methods are ordinarily the most applicable in exploration for deposits of these materials.

In addition to structural studies, it is possible in some cases to locate the various deposits directly by utilizing differences in electrical conductivity relative to adjacent rocks. The degree of alteration or weathering, which is often important in evaluating limestones and other rocks employed for building purposes, may be determined by electrical methods. Oftentimes, sand and gravel deposits may be located directly by electrical methods. †

Magnetic methods may be useful (1) for determinating structural conditions governing deposits of these types of rock materials and (2) for locating buried stream gravels having an appreciable content of magnetite.

Saline Residues.—Saline residues are accumulations of certain minerals which have been deposited as the result of evaporation in closed or partially closed basins. Some of the commercially important minerals or ores in this class are rock salt, gypsum, anhydrite, sodium nitrate, borax, and potash.

Under favorable conditions, distinctive physical properties may permit direct detection of these deposits. For example, salt, relative to some sedimentary rocks, has a low density, poor electrical conductivity and transmits seismic waves at a high velocity. These properties have been utilized in exploration for salt domes by gravitational, electrical, and refraction seismic methods, respectively. To date, however, utilization of these properties in the direct location of salt and other saline deposits has been extremely limited.

§ C. A. Heiland, "Geophysical Prospecting in the Non-Metallic Field," *A.I.M.E. Geophysical Prospecting*, 1934.

† M. King Hubbert, "Results of Earth Resistivity Survey on Various Geologic Structures in Illinois," *A.I.M.E. Geophysical Prospecting*, 1934.

Karl S. Kurtenacker, "Some Practical Applications of Resistivity Measurements to Highway Problems," *A.I.M.E. Geophysical Prospecting*, 1934.

S. N. Wilcox, "Sand and Gravel Prospecting by the Earth Resistivity Method," *Geophysics*, Vol. 9, No. 1, Jan., 1934.

Magnetic and electrical methods have been employed to a limited extent in determining local structural conditions. An example is the search for borax deposits in California. The magnetic and electrical work located faults and determined the subsurface distribution of lake bed sediments and buried lava flows that are genetically related to the accumulations of borax in the Mojave desert area.

Residual Deposits.—The most common non-metallic ores or rock materials which occur as residual deposits are clay, barite, phosphate, and bauxite. Geophysical methods have not been extensively applied to these deposits, but the field for indirect application of the methods is similar to that for other non-metallic resources. Stearn † has given an example of the indirect use of magnetic methods in the search for bauxite deposits in Arkansas.

Coal and Lignite.—Measurements have been conducted in different parts of the world to investigate the applicability of geophysical methods in exploration for coal deposits. Due to the variable chemical and physical properties of coal, as well as the variety of structural conditions associated with the deposits, its direct location by geophysical methods has not been very successful. In a few cases of shallow occurrence, experimental electrical surveys have directly indicated the presence of coal seams. ‡ Hawkins § reports generally unsatisfactory results in attempts to locate lignite directly by resistivity measurements.

The geophysical work that has been done in exploring for coal indicates that direct location of coal beds may be accomplished only under especially favorable conditions of coal composition and structural setting. Anthracite deposits in some cases exhibit high electrical conductivity relative to the surrounding sediments. Under such conditions, these deposits undoubtedly can be located directly by electrical methods. Similarly, the relatively poor conductivity of bituminous beds in certain areas suggests the possibility of locating such deposits by electrical methods.

The resistivity method has been successfully used to find the depth to a shallow coal seam (about 75 feet) in connection with a proposed strip mining operation. It very effectively supplemented more costly drill exploration.

In general, however, it may be concluded that the most successful applications of geophysics in coal exploration will be in the field of structural and stratigraphic determinations. Electrical, seismic, gravitational, and magnetic methods have all been tried. At the present time, electrical methods promise to be the most valuable.

---

† N. H. Stearn, *loc. cit.*

‡ Maurice Ewing, A. P. Crary, J. W. Peoples and J. A. Peoples, Jr., "Prospecting for Anthracite by the Earth-Resistivity Method," *A.I.M.E. Geophysical Prospecting, Tech. Pub.* 683.

§ R. H. Hawkins, "Application of Resistivity Methods to Northern Ontario Lignite Deposits," *A.I.M.E. Geophysical Prospecting*, 1934.

Miscellaneous Non-Metallic Deposits.—Various kinds of igneous rocks are used commercially in the form of building stones, road building materials, etc. Magnetic methods are usually the preferred choice in exploration for these materials because of the relatively high magnetic susceptibility of most igneous rocks. Electrical methods are useful also—particularly to outline the extents of the rock deposits, locate contacts, and give qualitative information regarding the amount of weathering or alteration.

In some cases, geophysical methods are useful in indirect exploration for gems and precious stones by reason of their genetic relationship to certain types of rocks or formations. Stearn † gives an example of the location of diamond-bearing peridotites by magnetic methods. Gems, semi-precious stones, and certain non-metallic minerals of industrial use occur in pegmatites. The possibility of locating a pegmatite dike by use of electrical methods has been mentioned in a preceding section.

GEOPHYSICAL METHODS IN WATER SUPPLY ENGINEERING

Engineering, economic, and geological problems arising in the general field of water supply are very extensive and can be discussed here only briefly. ‡ The sources of water are: (1) surface water in lakes, streams, rivers, etc., and (2) subsurface water (ground water). Control, conservation, storage, and use of surface water is accomplished by building dams and other engineering works. Similar utilization of ground water requires storage in subsurface basins and the drilling of wells in proper locations to produce water by natural flow (artesian wells) or by pumping wells. The original source of the ground water for which drilling exploration is conducted is run-off water and rainfall. The *available supply* of ground water in any area is therefore mainly determined by: amount of precipitation, character of topography, extent of water-sheds and drainage basins, etc.

Local accumulation of ground water, however, is controlled primarily by the geological factors of local structure, petrology, porosity, etc. Detailed geological information is essential to aid the engineer in the proper location of water wells. He should know the extent, thickness, depth, composition and relative position of water-bearing strata or subsurface basins, the depth to the ground water table, the location of buried stream channels, faults, dikes and other subsurface structural features. Oftentimes some of this information may be obtained by surface geological observations. In recent years, geophysical methods have been applied in an increasing extent to secure much of the subsurface geological information which is necessary for the intelligent direction of subsurface water-supply development.

Information concerning accumulation and distribution of ground water may be desired for several purposes: (1) to locate a supply suitable for domestic uses, irrigation, mining, or other purposes; (2) to determine ground water conditions insofar

† Noel H. Stearn, *loc. cit.*
‡ C. F. Tolman, *Ground Water* (McGraw-Hill Book Company, New York, 1938).

as they may affect engineering construction such as dams and drainage projects; (3) to determine the distribution of ground water insofar as it may affect conservation of crops or encroachment of sea water, etc. The geological and geophysical problems involved in these determinations are generally resolved into: (1) location of permanent water table or perched bodies of water; (2) location of subsurface structure favorable to accumulation, impounding, and storage of water; (3) location of boundaries between fresh and saline waters.

Geophysical methods as applied to the various problems of water supply are usually of the indirect type wherein structural conditions influencing ground water distribution are determined. In certain relatively simple problems, the contour of the water-table may be mapped directly and isolated accumulations of water may be located.* Structural conditions that most commonly influence accumulation and impounding of subsurface water are: (1) subsurface basins and channels in bedrock underlying unconsolidated porous materials; (2) subsurface structural barriers such as erosional relief in the bedrock, igneous dikes, etc.; (3) faults.

Choice of Methods.—Electrical, magnetic, and seismic methods have been used to secure structural information. Electrical methods are being used more extensively than the other methods and are generally applicable to most phases of the structural problem: viz., determination of depth of unconsolidated alluvium, etc., mapping bedrock contour, and location of faults. Magnetic methods are useful in cases in which impounding of subsurface water is caused by igneous dikes. Seismic work has been employed to map bedrock boundaries. Improvements are being made in the adaptation of seismic methods to shallow work and it is likely, therefore, that the use of these methods in problems of water supply will increase. †

The actual location of the ground-water table is important in determining favorable locations for wells and in evaluating conditions prior to construction of dams, tunnels, etc.** Electrical methods have been used successfully to locate water impounded above bedrock in quaternary gravels and alluvium and to map the upper boundary of ground water at greater depths in the more consolidated sedimentary rocks. ‡ Various investigators have employed the seismic method in the direct location of water tables. The method depends upon increase in velocity of the elastic wave with increase in water content.§

GEOPHYSICAL METHODS IN CIVIL ENGINEERING

The application of geophysical methods in civil engineering and construction work has increased rapidly in recent years because of the recognition of the importance of geological structure in all phases of

* See Chapter V.

† F. L. Partlo and Jerry H. Service, "Seismic Refraction Methods as Applied to Shallow Overburdens," *A.I.M.E. Geophysical Prospecting,* 1934.

** See following section on Geophysical Methods in Civil Engineering.

‡ J. J. Jakosky, C. H. Wilson and J. W. Daly, "Geophysical Examination of Meteor Crater, Arizona," *A.I.M.E. Geophysical Prospecting,* 1932.

J. J. Jakosky and C. H. Wilson, "Geophysical Study of Fort Peck Dam Site and Reservoir," technical report.

§ C. M. Tattam, "Application of Electrical Resistivity Prospecting to Ground Water Problems," *Colo. School of Mines Quarterly,* Vol. 32, No. 1, January, 1937.

engineering concerned with excavation of material or selection of sites for dams and other earth works. The geophysical methods and procedures employed, and the nature of information desired, are similar to those described in the preceding section. Literature dealing with engineering applications of geophysics is fairly extensive.† Electrical methods have been employed almost to the exclusion of the other methods, although application of seismic methods is increasing and magnetic methods are often useful for special structural problems.

Examination and Location of Dam Sites.—Excellent discussions of the relationship between geology and engineering for dams and reservoirs have been given in various publications.‡

In evaluating the location of a dam, five geological factors are of primary importance: (1) the depth of overburden or fill materials which must be removed, (2) the presence of faults or other structural defects which might constitute a failure or leakage hazard, (3) the elevation or height of the water table in the abutments and the reservoir rims, (4) the strength of the foundation rocks, and (5) the perviousness of the foundation rocks.

Ordinarily, surface geological work will not provide sufficient detailed information along these lines and in such cases proper geophysical work combined with a small amount of confirmatory core drilling will usually provide the needed information. This is particularly true of the first three factors enumerated above. Bedrock depth determinations by geophysical methods are relatively simple and inexpensive. The accuracy obtainable is well within the necessary limits, especially when occasional drill-holes are used for control.

The location of major faults in the vicinity of the dam site is of great importance, not only from the standpoint of possible movement along them which might endanger the dam, but also from the standpoint of leakage through the reservoir rocks. The location of faults from surface evidence is a well-known geological technique. However, important faults may be covered by alluvial material, and they must therefore be identified by geophysical methods.

Ground water conditions at dam sites are important chiefly from the standpoint of leakage. The depth to the water table in the dam abutments

† Irving B. Crosby and E. G. Leonardon, "Electrical Prospecting Applied to Foundation Problems," *A.I.M.E. Geophysical Prospecting, Tech. Pub., No. 131* (1928).
E. G. Leonardon and Sherwin F. Kelly, "Some Applications of Potential Methods to Structural Studies," *AI.M.E. Geophysical Prospecting, Tech. Pub. No. 115* (1928).
S. F. Kelly, "Engineering Uses for Geophysics," *Civil Engineering*, October, 1932.
G. G. Stipe and Sherwin F. Kelly, "Geophysical Methods Aid Construction Work," *Civil Engineering*, April, 1937.
Karl S. Kurtenacker, "Some Practical Applications of Resistivity Measurements to Highway Problems," *A.I.M.E. Geophysical Prospecting*, 1934.
E. G. Leonardon, "Electrical Exploration Applied to Geophysical Problems in Civil Engineering," *A.I.M.E. Geophysical Prospecting*, 1932.

‡ "Geology and Engineering for Dams and Reservoirs," *A.I.M.E. Geophysical Prospecting, Tech. Pub. 215.* (Papers and discussions presented at the New York Meeting, February, 1929.)
Douglas Clark, "Application of Geology to Civil Engineering," *California Journal of Mines and Geology*, Vol. 29, January and April, 1933, pp. 161-173.

and reservoir rims usually can be determined satisfactorily by electrical methods.

In regard to the strength and perviousness of the foundation rocks, geophysical work will often give useful information for correlation with surface evidence, core holes, and laboratory tests. In limestone regions, the foundation rocks may be characterized by solution channels and caves at certain horizons, and such conditions can often be detected by changes in the apparent resistivity or the subsurface current distribution.

Several examples are cited below to illustrate the need for detailed geological and geophysical work.†

At the location of the O'Shaughnessy dam on the Tuolumne River at the lower end of the Hetch Hetchy Valley in Tuolumne County, California, the depth of the stream gravels overlying the granite bedrock was found to be excessive, the maximum depth being 101 feet. Owing to this condition a greater amount of excavation was required and a higher dam built than was originally planned, which added greatly to the cost of the project.

At the site of the St. Francis dam near Saugus, Los Angeles County, mica schist occurs on the east slope of the canyon and conglomerate of the Sespe formation on the west side. The contact between the two formations is a fault which parallels the canyon on the west slope about 60 feet above its base. Within the fault zone there are numerous seams of clay gouge and fractures filled with gypsum. Furthermore, the conglomerate, where fractured, completely disintegrates when immersed in water. A commission investigating the failure of this dam concluded that it was due to disintegration of the fractured conglomerate.

During the construction of the Lafayette earth-fill dam in Contra Costa County, California, by the East Bay Municipal Utility District, difficulty was encountered because of the occurrence of plastic clay beneath the dam. The strata underlying the dam site include beds of clays and sands of the Orinda formation, dipping at high angles and overlain by alluvial fill from 71 to 91 feet thick, the bedrock in part being sandy clay. When the dam was completed to within 20 feet of its final height the crest of the dam sank vertically 24 feet, causing a movement of the downstream face. The clay below the dam readily absorbed water and became a soft mud which moved out under the weight of the dam. This condition made it necessary to complete the dam with a height of 40 feet less than that originally intended and with greatly flattened slopes.

The foregoing are typical examples of adverse conditions unexpectedly revealed after the expenditure of large sums had made relocations inexpedient but which would very probably have been disclosed by preliminary geological and geophysical surveys.

Electrical, seismic, and magnetic methods are now being widely used to secure the geological information outlined at the start of this section. This no doubt will result in less frequent failure of dams, and subsequent discovery of unfavorable geological conditions that might have been disclosed by preliminary geophysical surveys. Geophysical methods are being utilized by the Bureau of Reclamation, U. S. Army Corps of Engineers, Tennessee Valley Authority, by various Municipal Agencies such as the Metropolitan Water District of Southern California, and by private engineering agencies.*

† Douglas Clark, *loc. cit.*

* Typical examples of geophysical investigation of dam sites are given in the chapter on Electrical Methods.

Location of Reservoir Sites.—Several years ago the U. S. Federal Government constructed the Hondo reservoir near Roswell, New Mexico, in connection with an irrigation project at a cost of about $500,000. The rocks underlying the reservoir area consist of alternating beds of gypsum and limestone and the structure of the formation is that of a faulted and collapsed anticline, the fault traversing the center of the reservoir. Underground cavities caused by the dissolving out of the relatively soluble gypsum apparently caused the collapse of the structure and rendered the reservoir useless for water storage. Proper geophysical and geological examinations would probably have saved the wasted expenditures.

Selection of proper reservoir sites is, of course, closely allied to that of dam sites. The main geological factor to be considered in the selection of reservoir sites is the perviousness of the reservoir rims. Leakage hazards may consist of (1) faults or solution channels in the rim formation and (2) insufficient elevation or breadth of bedrock along the rims relative to the pool level of the proposed reservoir. In many cases, these problems may be readily solved by electrical, seismic, and magnetic methods.*

Highway Engineering.—Many of the subsurface geological problems which are encountered in the building of highways, railroads, aqueduct and pipe line routes, etc., may be solved by geophysical methods. Usually, the required depth of study is relatively shallow (less than 100 feet) and geophysical surveys can be conducted rapidly and economically. As in other phases of civil engineering, electrical methods are proving most applicable to these general problems.

Several fields of investigation may be listed in this general class of engineering: (1) quarries, (2) pipe line and aqueduct routes, (3) tunnel sites, (4) bridge foundations, (5) cut and fill determinations.

Application of geophysical prospecting to quarry deposits was discussed briefly in the earlier section devoted to non-metallic mining. Quarrying operations are carried on extensively as a part of most civil engineering and construction projects. Selection of suitable quarry sites is based upon the accessibility of the quarry deposit, cost of quarrying and crushing the rock, quality of the deposit, and extent of the deposit. The last three factors are partially dependent upon geological conditions which may be evaluated by geophysical methods. A problem common to all quarrying operations is the determination of the thickness of the overburden, and this is readily accomplished by electrical methods. The electrical resistivity method has been successfully used to determine the extent of quartzite deposits and the yardage of such rock present in the search for riprap for a number of dams in the Missouri River Basin. This work as supplemental to a limited amount of core drilling has reduced the cost of exploring these deposits. Electrical methods can be used also to locate certain kinds of quarry deposits such as gravel, igneous rocks, limestone, etc., and to afford qualitative information as to degree of weathering. The presence of solution channels and sink holes is sometimes

* Examples of electrical, seismic and magnetic work in examination of reservoir rims are given in later chapters.

important in selecting suitable limestone deposits for quarrying, and such defects are readily located by electrical methods in many cases.

Magnetic and electrical work can be advantageously used prior to excavation to locate faults, changes in formation, degree of weathering, etc., along pipe line and aqueduct routes. If the work requires tunnel construction, determination of thickness of overburden can be made in connection with the other geophysical studies.*

The problems of cut and fill in highway construction involve classification of material to be excavated. Electrical methods are of aid in this classification. Electrical surveys have a valuable application in problems of highway grade settlement in swamps. It is often possible to determine the depth to firm material at the bottom of the swamp and in some cases whether or not newly constructed fill is properly settled on a firm foundation.†

Application of electrical work in bridge construction problems is similar to that for dam sites: namely, the determination of depth to bedrock or to a material of proper characteristics to support piling.

Seismic studies have also proved valuable in work of this nature and increasing applications of these methods for determining the bearing capacity of soils ‡ and the natural period of vibration of foundations and dams may be expected.

---

* Extensive electrical work of this kind was employed by the Metropolitan Water District of Southern California in planning aqueduct routes from the Colorado River to the city of Los Angeles.

† Karl S. Kurtenacker, *loc. cit.*

‡ R. K. Bernhard, "Geophysical Study of Soil Dynamics," *A.I.M.E. Geophysical Prospecting*, Tech. Pub. 834, 1938. See also chapter on Seismic Methods.

CHAPTER III

MAGNETIC METHODS

Magnetic methods of prospecting are one of the oldest forms of applied geophysics. The mining compass, in 1640, was used to locate iron ore bodies, according to a Swedish document. Prior to this, however, possibly as early as 1000 B.C., two original observations had caused thoughtful men to study magnetism. They were: (1) the tendency of a piece of the natural magnetic mineral *magnetite* to orient itself in a particular direction when freely suspended, and (2) the ability of a larger piece of *magnetite* to pick up smaller pieces.

Magnetic methods utilize a natural field of force, viz., the earth's magnetic field. They are applicable in regions where the magnetic properties of rocks and formations have some known relationship to economic geology.

The magnetic fields associated with geologic bodies or geologic situations, which are investigated in magnetic prospecting, are superimposed on the terrestrial magnetic field. For example, in the vicinity of a sizable near-surface magnetic dike the local magnetic field would be increased appreciably. A magnetic measurement at a station is, therefore, the summation or integral effect of all the magnetic fields from magnetic bodies within effective distance of the instrument superimposed upon the earth's magnetic field. In a given case this might mean the magnetic contribution of the dike mentioned above; or perhaps the effect of a tobacco can in the instrument man's pocket; and the normal magnetic field of the earth at the observation point.

Since summation effects are always measured in magnetic prospecting, these methods lack, in considerable degree, what is called *depth control.* It is not possible, except in a rather limited number of cases, to determine accurately or uniquely the depth to a magnetic body or the depth from which a particular magnetic effect is coming.

Interpretation of magnetic data is based on the fact that the earth's normal magnetic field is uniform over areas of magnetically homogeneous composition, but is measurably distorted in regions or local areas of inhomogeneous composition. The amount and the shape of this distortion depend on the relative magnetic susceptibilities of the subsurface materials, and the relative sizes and configurations of the zones of such component materials. Most magnetic anomalies (distortions from the theoretically normal) are due to igneous rocks, magnetic iron ores, and to those sedimentary deposits which contain magnetite, derived from igneous rocks.

Field of Application.—In oil prospecting, geomagnetic surveys are of greatest value in reconnaissance and preliminary work. They can be conducted rapidly with a small personnel at a resultant low cost. Often, such magnetic studies are useful in evaluating large areas, such as geologic basins, to determine the best places for the application of other geophysical methods of better resolving power.

In petroleum exploration, magnetic work is of value as a detail tool, for determining the location of buried hills or ridges if they are composed of granites, gneisses, or schists, and in cases where there are buried intrusions of igneous or metamorphic rocks. Anticlines can be mapped if the magnetic basement members are uplifted together with the sedimentary beds or if some of the formations subject to folding are themselves magnetic. Salt domes and salt core anticlines can also be outlined magnetically, although other geophysical methods are often more suitable for finding such structures.

On fault problems, which relate to both oil and mining exploration, magnetic investigations are applicable where the basement rocks or magnetic members of the geologic column are displaced and in situations where a fault fissure itself may contain igneous sheets or magnetic material. Faulting and/or formation boundaries can be located by magnetic measurements where adjacent formations have different magnetic characteristics.

In the field of mining geophysics magnetic methods are used in preliminary explorations of mining regions and groups of claims, and for detailed studies of igneous intrusions, igneous dikes, and contact-metamorphic zones in relation to which various types of ore may occur. Iron ore deposits of magnetite and, in some cases, hematite, and also numerous forms of occurrences of sulphide ore bodies, where some mineral present is appreciably magnetic, can be successfully mapped.

In an indirect way magnetic work can be used to locate non-magnetic minerals if they are associated or deposited with magnetic ones such as magnetite, ilmenite or pyrrhotite. This applies to gold or platinum bearing placer deposits where magnetite is present.

Meteorites are often highly magnetic; they have been located and their craters studied by magnetic means. On a similar basis the magnetometer has been used to find buried guns, ammunition, pipe lines, etc., and, in one case, metal objects of historic value at Valley Forge.

Classification of Magnets.—In presenting the subject of magnetic prospecting on a quantitative basis, it is necessary to consider certain fundamental concepts, classifications and definitions that come under the physical phase of geomagnetics.

A magnet is defined as a body or substance capable of attracting iron. Gravitational attraction is not considered in this definition. Magnets are classified into two groups; *natural* and *artificial*. *Natural magnets* are minerals such as magnetite particularly (earliest known magnets) and a num-

ber of others, notably, ilmenite, pyrrhotite and chromite. *Artificial magnets* are bodies which can be made into magnets by bringing them into a strong magnetic field, or by stroking them with other magnets. Examples of such substances are steel and iron, and to a lesser degree nickel, and cobalt. Certain alloys of non-magnetic substances can acquire magnetism. For example, one such alloy consists of 26.5% manganese, 14.6% aluminum and 58.9% copper.

On the basis of their ability to retain their acquired magnetism, artificial magnets are likewise divided into two groups, namely; *permanent* and *temporary*. *Permanent magnets* are generally made of hard steel or steel alloy, and possess high retentivity or ability to keep their magnetism. Steels of this kind are selected for compass needles and the permanent magnetic parts of the systems of magnetic instruments. *Temporary magnets* are made of substances such as soft iron and certain alloys of iron which become magnetic when placed in a magnetic field, but which lose their magnetism upon removal from that field. Temporary magnets are said to have little retentivity.

Classification of Substances.—All substances may be classified magnetically according to their behavior in a magnetic field as *diamagnetic,* or *paramagnetic*. The basis for such a classification was established in 1845 by Faraday, who demonstrated that *all* materials are affected to some extent by a strong magnetic field.

Certain paramagnetic substances that have very pronounced magnetic properties are put in a special group known as *ferromagnetic*. These latter are of particular importance geophysically.

Diamagnetic materials show a mild response to a magnetic field and the effect is said to be *repellent*. Substances can be tested, in a simple manner, by suspending them in a magnetic field of suitable strength and form. This is illustrated in Figure 5 (after Loeb)† which shows that in a divergent magnetic field diamagnetic materials tend to move *from the stronger to the weaker* parts of the field. They are repelled or pushed away from the field.

When pieces of diamagnetic material, of oblong form, are placed in a *uniform* field, they try to set their long dimension *at right angles* to the lines of force of the field. As will be described in detail later, the magnetic force lines of the field diverge from such materials.

Typical of the diamagnetic materials are bismuth, copper, rock salt, anhydrite, etc.

Paramagnetic materials show a definite attraction to a magnetic field, and the effect is described as *attractive*. Under test conditions (Figure 5), paramagnetic substances move *from the weaker to the stronger* portions of a divergent field. Oblong pieces of this kind of material tend to place their long dimension *parallel* to the lines of force of a uniform magnetic

† L. B. Loeb, *Fundamentals of Electricity and Magnetism,* John Wiley, 1931, p. 224.

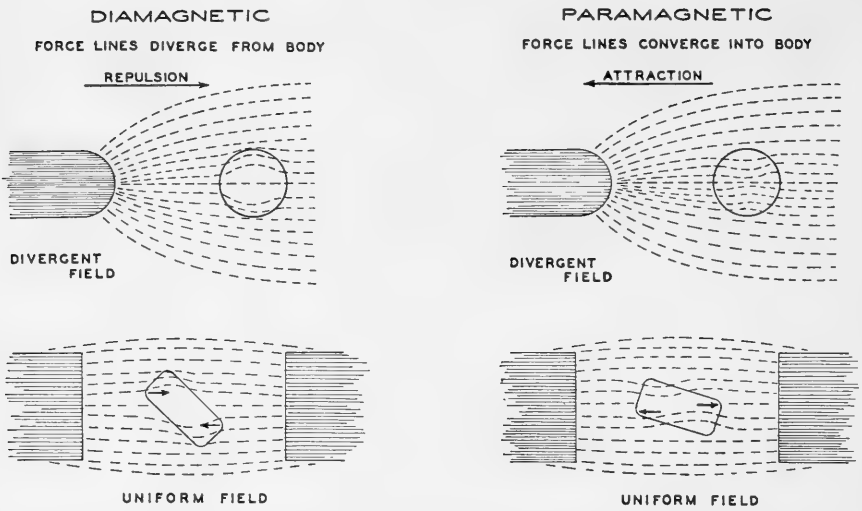

FIG. 5.—Showing the behavior of diamagnetic and paramagnetic bodies in a divergent and in a uniform magnetic field. Forces acting on bodies tend to cause rotation or movement, as shown by arrows. (After Loeb.)

field acting on them. The lines of the field converge into such bodies. Examples of paramagnetic materials are platinum, aluminum, and manganese.

Ferromagnetic materials show such pronounced paramagnetic reactions that few substances have been designated by this term, which means literally *magnetic like iron.* Test pieces of magnetite, steel, iron, nickel, or Huesler's alloy, for example, will show their ferromagnetic character by being strongly attracted into a divergent magnetic field or actively constrained to lie parallel to a uniform magnetic field, as shown in Figure 5.

Paramagnetic and diamagnetic reactions of test samples in magnetic fields are detectable, although feeble in comparison to the relatively strong force with which the earth's magnetic field acts on a steel (ferromagnetic) compass needle. Paramagnetic and diamagnetic characteristics of materials are also, in a sense, relative. It has been observed that if a substance is less magnetic that the medium surrounding it, it acts as a diamagnetic substance. For example, a ferric chloride solution (Fe_2Cl_6) is magnetic. A capsule filled with such a solution, if placed in a basin containing ferric chloride of a higher concentration (and hence more magnetic than the solution in the capsule) will act as though it were diamagnetic. If, however, the same capsule is placed in a basin of distilled water or of weaker ferric chloride solution, it will align itself with the force lines of a magnetic field and react as a magnetic substance.

Geomagnetically this experiment is significant. In northern Michigan, certain diabase dikes act as lenticular diamagnetic bodies, because of the

relatively more magnetic character of their surroundings. Diabase is ordinarily magnetic due to its magnetite content.

Some writers set up a slightly different magnetic classification of materials. In it the term *non-magnetic* is essentially synonymous with *diamagnetic,* as here used, and *magnetic* refers to both paramagnetic and ferromagnetic substances. Such terminology relates to the divergence of magnetic lines of force away from diamagnetic bodies* and their convergence into paramagnetic bodies. Certain materials *are* non-magnetic in the sense that lines of force do not easily penetrate them, and they cannot be made into magnets. A magnetic substance, however, attracts lines of magnetic force and in other respects acts like and may become a magnet. The system corresponds to popular usage and thought, for we ordinarily consider steel or iron as magnetic and wood and glass as non-magnetic.

The classification of magnets and magnetic substances or materials here presented can be summarized in the following table.

Magnetic Classification

Magnets	Bodies that attract iron
a. Natural magnets	Magnetite
b. Artificial magnets	Magnetized steel
(1) Permanent magnets	Compass needle
(2) Temporary magnets	Soft iron
Substances**	
a. Diamagnetic	Glass, rock salt
b. Paramagnetic	Manganese, pyrrhotite
(1) Ferromagnetic	Steel, magnetite, (with marked magnetic reactions)

MAGNETS AND MAGNETISM

Most magnets used in the instrument phase of magnetic prospecting are parts of the magnetic systems of field magnetometers or are necessary in the calibration of such instruments. These magnets are made of special types of steel. A number of substances, such as chromium, tungsten, nickel, cobalt, and the like, when added to iron in small yet critical percentages, greatly affect its magnetic properties. Thus an alloy containing up to 4% of nickel, tungsten, and cobalt, which has been quenched in cold water after having been heated to 850° C., produces magnets of high retentivity or great resistance to loss of magnetization.

The metallurgy of steels for magnetic systems is an important feature of instrument design; a balance must be made between a number of factors that relate to the composition of a particular steel, such as hardness, reten-

* This matter is treated in detail under the subject of magnetic permeability of materials.

** This classification is based on the findings of Faraday that *all* materials respond in one way or another to a magnetic field and therefore are diamagnetic or paramagnetic.

tivity, the effect of temperature on magnetic strength, and resistance to corrosion or oxidation.

In general, the Brinell hardness of a steel is somewhat proportional to its magnetic strength for a given volume. Therefore the use of hard steel would permit smaller magnetic systems to be made, which would be quite advantageous. However in building a magnetic system, the magnetic parts, as blades or in the form of a needle, for example, must be accurately shaped and machined to close tolerances. This precludes the use of extremely hard or brittle material. Also, resistance to corrosion in magnetic parts is of importance. Magnetic instruments are often used in tropical climates where moisture and fungus growths are extremely damaging to delicate equipment. The steel which shows the least loss of magnetic strength with increase in temperature (lowest magnetic coefficient of temperature) and the least loss of magnetization with time is the most desirable.

No artificial magnet, although it may be classed as permanent, will retain *all* the magnetism that can be initially induced in it. When a piece of steel is removed from its magnetizing field, a considerable portion of its magnetization is lost immediately. After that, the loss in magnetism is progressively slower, and a fairly long time, up to several months or more, is required for the magnet to acquire final magnetic stability.

The time of stabilization of a magnet can be shortened considerably by a series of treatments known as aging. This consists of subjecting a magnet, when in its final form (as a system, or as a calibrating magnet, for instance) to mild physical shock, vibration, and a number of cycles of temperature change. The magnetic strength of a properly aged magnet becomes very nearly constant. Although loss of magnetic strength with time cannot be completely halted, a well-aged magnet or magnetic system will not alter significantly under careful field use.

Properties of Magnets

The most simple type of magnet consists of a straight bar, and is known as a bar magnet. A consideration of magnets of this geometrical form conveniently sets up a quantitative basis for the analysis of the properties of magnets, magnetic materials and magnetic fields.

Magnetic Poles.—It has been found that there are small regions near the ends of a bar magnet where its magnetic properties seem to be concentrated. (See points N and S, Figures 6 and 9.) These localities are called *poles,* and they are situated at a distance of about 1/12 of the length of the bar from its ends. Their existence and approximate position can be demonstrated by the familiar experiment of dipping a bar magnet into a box of iron filings. A great number of the iron particles will attach themselves to the bar magnet at and near the poles, and there will be practically no attraction near the middle of the bar, as is illustrated in Figure 6.

If a bar magnet is suspended at its mid-point and left free to turn, (as is the case with a compass needle), one end of the magnet will always point toward the magnetic north pole. The pole at the north-seeking end of the magnet is arbitrarily called the *north pole* or *plus pole,* and is ordinarily marked with an N or +. The other end of the magnet is the *south pole* or *negative pole.*

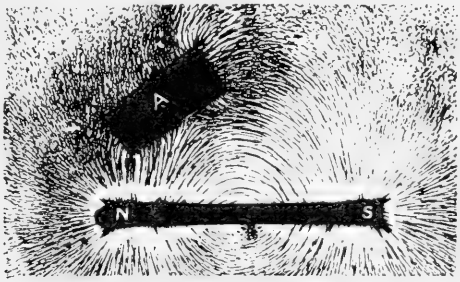

FIG. 6.—Photograph of iron filings illustrating the lines of force due to a bar magnet *N-S* and the distortion produced by a piece of iron *A*.

It is of interest that certain dike-type magnetic ore bodies exhibit polarity. Under ordinary conditions, in the northern hemisphere, they will have a south magnetic pole at their top, or nearest the surface. Polarity will also be exhibited by almost any iron body having considerable vertical height in comparison with its other dimensions. A tall steel filing cabinet or an iron stove will attract the N pole of a compass needle at its lower end, and repel the N pole at its upper end.

Law of Force between Magnetic Poles.—By experimenting with a form of torsion balance, Coulomb proved that the force *(F)* between two magnetic poles varies inversely as the square of the distance *(r)* between them.

It was also found that this force *(F)* is proportional to the product of the strength of the poles, *(m_1* and *m_2)*. This is expressed by:

$$F = \frac{1}{\mu} \frac{m_1 m_2}{r^2} \qquad (1)$$

$\frac{1}{\mu}$ is a constant depending upon the medium in which the poles are placed. μ = magnetic permeability. For air, $\mu = 1.0000004$ and it is, therefore, usually taken as = 1, where the poles are in air. Permeability is related to another magnetic quantity termed *susceptibility,* defined on page 76. The values for susceptibility are given in Table 5.

An important property of magnetic poles is the fact that those of *like sign repel* and of *unlike sign attract* each other. What we speak of as the *north* magnetic pole of the earth relates to its geographic position. Magnetically, it is a south pole. This is correct, since the north-seeking end of a compass points toward the (geographic) north, (i.e., unlike poles attract).

Equation 1 may be either positive or negative, depending on the sign of the product of the two poles involved. If the product is plus (two poles of like sign), the force is one of repulsion. If the product is negative (poles of unlike sign), the force is attractive.

The polarity in a bar magnet can be easily determined by bringing one end of it near the end of a compass needle, the polarity of which is known by its action in the earth's field, and noting whether that end of the compass is attracted or repelled.

Unit Magnetic Poles.—A system of units is established by defining a unit pole to be such as to make $F = 1$ in the first equation given. Hence a unit pole is one which when placed at a distance of 1 cm. from a similar pole will be acted upon with a force of one dyne.*

Fundamental Concept of Magnetized Matter.—Every positive pole has associated with it a negative pole of equal strength, and these two poles are always in the same piece of matter. It is impossible to have separate positive or negative magnets; hence, it is impossible to have a body charged with positive or negative magnetism as we may have one charged with electricity. A magnetized body of complex configuration may have any number of poles and at each pole there is, relatively, a charge of magnetism, but since the signs of the poles are opposite, the total charge is always zero.

Thus, the most fundamental piece of matter in considering magnetism from this point of view is a small body, (not carrying a single charge of magnetism), but carrying two equal and opposite charges at a certain distance apart. This leads to the concept of a line-magnet, which is an ideal bar magnet of infinitesimal width, finite length and with poles at the end-points of the line.

In the above case and in further mathematical developments, the *magnetic moment* of a magnet is taken as equal to the product of the pole strength and the distance between the poles. The symbol of magnetic moment is usually "M."

Magnetic Particle.—If we imagine the distance between poles to shrink until it is infinitesimal in length, then the magnet becomes what is known as a magnetic particle.

If $+m$ and $-m$ are the pole strengths involved and ds is the distance between them, the magnetic moment of one particle is $m\,ds$ or $M = mds$.

Two magnetic particles have the same effect if their moments are equal; length and strength of pole have no significance if considered separately.

Given two magnetic particles placed either side by side or end to end. In either case, the moment of the resulting magnet will be the same. (See Figure 7).

* The dyne, or unit of force, in the c.g.s. system, is a force that will impart to a gram mass an acceleration of 1 cm. per sec. per sec.

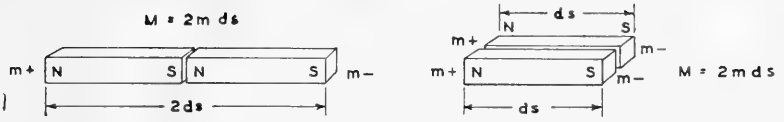

FIG. 7.—Two magnetic particles end to end, or side by side, have a moment $M = 2\ mds$.

If we place n similar magnetic particles end to end, the effect produced will be the same as a line magnet of length nds and $M = mnds$.

By experiment it has been found possible to produce two complete magnets by cutting any magnet between the poles; no matter where the cutting takes place, two magnets are produced. Furthermore, their relative strengths are proportional to their lengths.

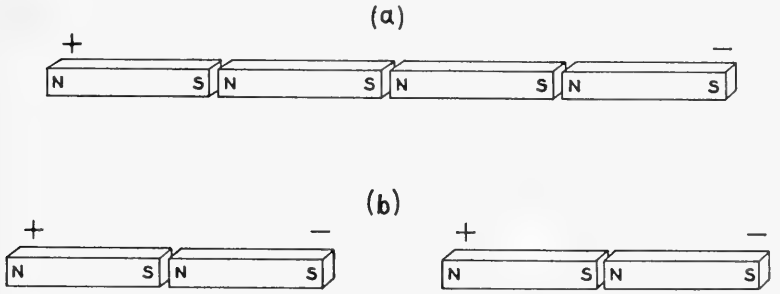

FIG. 8.—(a) n magnetic particles end to end produce a line magnet of length nds.
(b) Cutting a magnet between its poles makes two magnets.

Thus we see that a magnet must be considered as consisting of small magnetic particles. It is not necessary for mathematical analysis to consider these particles as molecules or even smaller than molecules. Any particle so small that the space occupied by it is infinitesimal may be considered as a magnetic particle.

Bar Magnet.—For most practical purposes, a bar magnet may be considered as a straight line magnet, with its magnetic poles located at points situated at a distance of 1/12 of the length of magnet from each end. These relationships are illustrated in Figure 9.

The longer a bar magnet is in comparison to its thickness, the nearer the poles are to its ends. Theoretically an infinitely thin magnet would show no magnetic effects at any place along it other than at the ends where the poles would be situated. Such a magnet is called a *simple magnet.*

Referring to Figure 9, if the physical length of the bar magnet L is 12 cm., the dimension *(l),* or one-half the distance separating the poles, would be 5 cm. The figure shows also that the two poles would be, in this

case, 10 cm. apart. With the dimensions of the bar magnet as given, for a pole strength of 5 c.g.s. units, the magnetic moment would be equal to 5 x 10 = 50 c.g.s. units. This follows from the definition of the magnetic moment, viz., pole strength times the distance between the theoretical poles. The formula for magnetic moment is

$$M = 2\ ml \qquad (2)$$

The exact position of the magnetic poles in a bar magnet *cannot* be located with precision, as such poles are small areas or regions. It is therefore customary to use formulae that involve measurements of distance taken from the center or middle line of a bar magnet, when one is used in calibrating instruments or in certain experiments which will be discussed later.

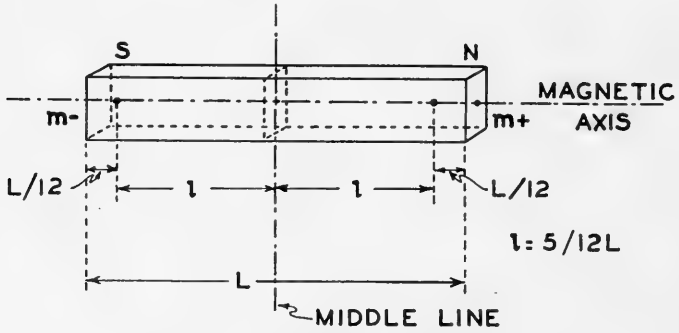

FIG. 9.—Diagram of a bar magnet.

Magnetic Axis.—The magnetic axis of a magnet, as is apparent from Figure 9, is usually defined as a line joining the poles. More strictly considered, the magnetic axis is a line drawn from the negative to the positive pole of a bar magnet, i.e., from south to north.

If a bar magnet is carefully and properly magnetized and is of symmetrical shape, the magnetic axis usually will coincide with the geometrical axis of the bar for its long dimension. In some bar magnets or magnetic needles the geometric axis and the magnetic axis are not identical. Allowance must be made for that fact, and suitable procedures adopted to overcome this defect, when making magnetic measurements.

Characteristics of Magnetic Fields

A magnetic field is defined as the zone surrounding a magnet or magnetic body, within which its influence can be traced or detected. According to this definition, the extent of a magnetic field, such as that surrounding a magnetic ore body for example, would depend on the sensitivity of the apparatus with which it was measured.

Field Strength.—The strength or intensity of a magnetic field is the force which it exerts on a magnetic body or a magnetic pole at some point in it. Quantitatively, the magnetic field intensity is the force in dynes with which it acts on a unit magnetic pole located at a given point. The conventional symbol for field strength is H.

If for a given field of intensity H, the force is represented by F and the pole strength by m, then:

$$F = \frac{1}{\mu} Hm \tag{3}$$

and

$$H = \frac{F}{\frac{1}{\mu} m} = \mu \frac{F}{m} \tag{4}$$

The quantity $\frac{1}{\mu}$ is a constant relating to the media involved as was discussed in Equation 1.

In this connection it is of interest to note that the earth's magnetic field has a strength (on the average) of about 0.6 dyne per unit magnetic pole, while the earth's gravitational field is considerably greater, being on the order of 1000 dynes. (The terminology here used is not necessarily preferred, as special names, viz., *gauss* and *gal*, respectively, are applied to strength units of magnetic and gravity fields.)

Lines of Force.—If an idealized pole is free in a magnetic field, it will move; the path described by it is called a *magnetic line of force*. The direction in which a free north (or+) pole moves, in a field, is the direction of the given line of force. A tangent to a line of force at any point gives the direction of the resultant magnetic field at that point.

For practical purposes, the lines of magnetic force can be traced by moving a small compass needle from place to place in the field and plotting its position and direction when at rest. The compass needle will orient itself so as to be tangent to the line of force at the test point. Also, the shape of a magnetic field can be clearly shown by the alignment of the lines formed when iron filings (which are minute magnets or compasses) are sprinkled into a magnetic field. Figure 6 illustrates the alignment where iron filings were sprinkled over a sheet of white cardboard (non-magnetic) underneath which was located a bar magnet.

Lines of force do not, in fact, exist. They are a convenient mental mechanism for visualizing and analyzing magnetic fields and will be so used.

Unit Magnetic Field.—By agreement in the c.g.s. system, a unit magnetic field has been defined as 1 line of force per square centimeter (the area taken at right angles to the force lines). It acts on a unit magnetic pole with a force of 1 dyne. A magnetic field of unit intensity is also said to have a strength of 1 gauss.*

*NOTE: In some old European literature a field of 1 gauss was one having 10 lines of force per square centimeter of section.

Therefore, the strength of a magnetic field and of a magnetic force is defined by its effect on a magnetic pole, usually a unit magnetic pole.

In a uniform magnetic field, the lines of force are parallel and the strength everywhere the same, and there are an equal number of such lines per unit perpendicular section. In a divergent field, as shown in Figure 5, the intensity varies from place to place; likewise the number of force lines passing through a square centimeter of the cross-section is different in different parts of the field.

Magnetic force is a vector quantity. Like other vector quantities, it can be completely defined in a specific case when (1) its magnitude is known, (2) its direction is shown by force lines and (3) its sense is stated as attractive or repulsive.

Magnetic field strength or intensity may be expressed in the following units, all of which are equal:

1. Dynes per unit pole
2. Gauss*
3. Lines of force per cm^2
4. Maxwells per cm^2

Lines of force from a unit magnetic pole.—In keeping with the convention that one line of force per square centimeter establishes a unit magnetic field, a unit magnetic pole is, by agreement, equivalent to 4π lines of force. This not too obvious statement can be demonstrated as follows:

1. The surface area of a sphere is $4\pi r^2$ where r is the radius of the sphere.

2. A sphere of unit radius or with $r = 1$ cm. has a surface area of 4π.

3. Inscribe such a unit radius around a unit magnetic pole m. (See Figure 10.)

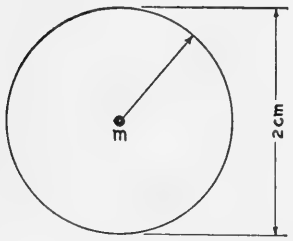

AREA = $4\pi r^2$ = $4\pi \cdot 1$ = 4π

FIG. 10.—Section through a sphere of unit radius inscribed about a unit magnetic pole m.

4. By definition, a unit magnetic pole is one which acts on a like pole with a force of one dyne when it is at a distance of 1 centimeter.

5. Another magnetic pole (of like sign to pole m of Figure 10) at any point on the surface of the unit sphere would be acted upon with a force of one dyne.

6. Likewise by definition, a magnetic field of unit strength (or with 1 line of force per square centimeter of section) acts on a unit magnetic pole in it with one dyne of force.

7. A unit magnetic field is therefore set up at every point on the surface of the unit sphere by pole m.

8. There are 4π square centimeters of surface area on the unit sphere.

* The term *oersted* is preferred by some in place of *gauss*, based on a 1930 ruling of the International Electro-technical Commission. The word *gauss* is, however, firmly established in geophysical literature by long usage, and will be used in this text.

Hence there must be 4π lines of force coming from pole m to provide one line for each of the 4π square centimeters of the surface of said unit sphere.

A magnetic pole of strength m would originate $m \cdot 4\pi$ lines of force. It would create a magnetic field of strength m at a distance of 1 centimeter. The above discussion introduces implicitly the concept of fractional parts of a line of force. In fact, the unit magnetic pole considered would generate 12.5664 lines of force, or 4π lines, using π as equal to 3.1416.

Another characteristic of magnetic fields that relates also to lines of force and their number per unit section is expressed in Equation 1. This equation indicates that magnetic force varies inversely as the square of the distance. Referring to the unit magnetic pole of Figure 10, if a sphere of 2 cm. radius were inscribed around it, the surface area of the sphere would

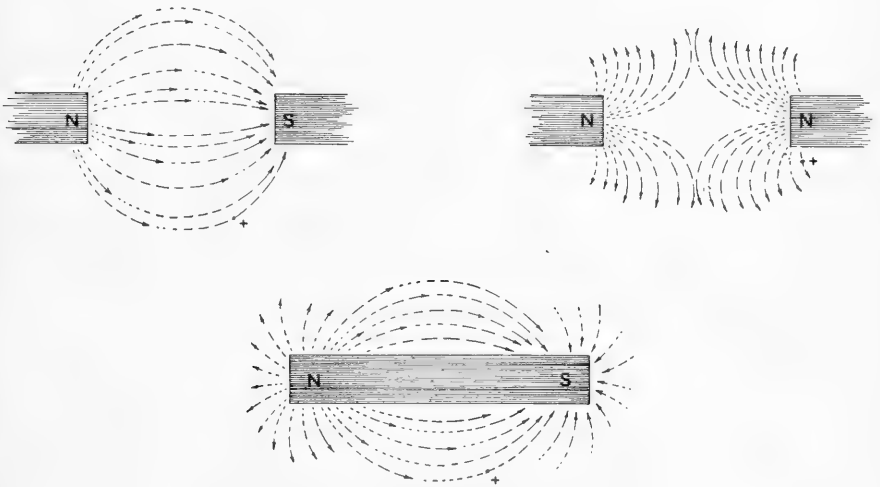

FIG. 11.—Examples of magnetic fields and lines of force.
NOTE: The arrows indicate the direction in which a free + pole would move.

be 16π (i.e. $4\pi \cdot 4$), or four times as great as in the case of the unit sphere.

With only 4π lines of force coming from the unit magnetic pole at the surface of the sphere of 2 cm. radius, there would be 0.25 of a line per square cm. A field of 0.25 line per square cm. is obviously only ¼ as strong as a field with 1 line per unit of section.

Using the relation of Equation 1: that $F = \frac{m_1 m_2}{r^2}$, in its application to the problem, m_1 and m_2 are unit poles. With m_1 fixed, and m_2 positioned first at a distance $r = 1$ cm., (or on the unit sphere) and second at a distance $r = 2$ cm. (or on the larger sphere):

For the first case: ($r = 1$ cm.) $\quad F = \frac{m_1 \cdot m_2}{r^2} = \frac{1 \cdot 1}{1} = 1 = H = 1$

For the 2nd case: ($r = 2$ cm.) $$F = \frac{m_1 \cdot m_2}{r^2} = \frac{1 \cdot 1}{4} = \frac{1}{4} = 0.25 = H = 0.25$$

These elementary mathematical relationships establish a basis for phases of the subjects that follow.

Magnetic lines of force in the vicinity of magnetic poles and around a bar magnet, as well as the direction in which a free (north) test pole would move, are summarized in Figure 11.

Magnetic Properties of Materials

Any *magnetic* substance, when placed in a magnetic field, will become magnetized or have magnetism induced in it. A bar magnet picking up iron filings or causing them to line up under the influence of its magnetic field illustrates this phenomenon. The iron filings become, by induction, little (temporary) magnets. Since the earth acts as a spherical magnet, a string of steel oil-well casing which has remained in the earth for some time will become magnetized. The top of the casing will acquire a south magnetic polarity, as evidenced by its ability to attract the north-seeking end of a compass.

Ferromagnetic, or paramagnetic, mineral deposits may also acquire magnetic polarity by induction in the magnetic field of the earth. Rocks magnetized in this manner can retain their magnetization for a long time even if displaced or overturned.

Magnetic Flux.—As noted above, when a magnetic body is put in a magnetic field, lines of force are induced in it. This condition is also described by saying that a *magnetic flux* is established in the body, or magnetic lines force their way into it. Flux generally is represented by the Greek letter ϕ.

Quantitatively, the amount of flux (or force lines) in a magnetizable body when it is in a magnetic field, divided by the end area A of the body, defines its flux density B. In equation form:

$$B = \frac{\phi}{A} \tag{5}$$

The end section of the body is taken at right angles to the flux lines.

Those substances in which flux is easy to establish acquire a high flux density for a given magnetizing field. Annealed iron is an example.

Permeability (relates to flux ϕ).—The magnetic permeability (μ) of a substance has been defined by Lord Kelvin as the ease with which a magnetic flux can be established in that material. Specifically, for a body placed within a uniform magnetic field, its permeability is defined as the ratio of the number of lines of force passing through a unit cross-section of the body to the number of force lines through a like cross-section in air.

$$\mu = \frac{\phi/A}{H} = \frac{B}{H} \tag{6}$$

The unit cross-sections in both cases are taken at right angles to the lines of force. These relationships are shown in Figure 12.

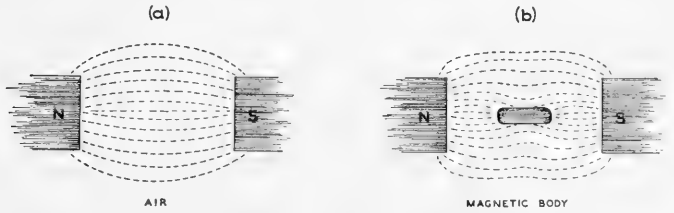

FIG. 12.—Illustration of magnetic permeability, showing lines of force in a magnetic field (a) in air, and (b) with a magnetic body in the field.

A magnetic body, such as iron, can be thought of as offering less resistance to the passage of lines of magnetic force than air, as depicted in Figure 12. The lines of force will therefore tend to concentrate in the medium of higher magnetic permeability, in order to take the path of least resistance.

Where a magnetic field is present in air, the flux per unit area $\left(\frac{\phi}{A} = B\right)$ and the strength of the field H are equal. Since $\mu = \frac{B}{H}$, μ for air $= 1$.

If the permeability of a material is less than that of air or its $\mu < 1$, the material is diamagnetic. Where a substance shows a permeability greater than air, viz., its $\mu > 1$, it is paramagnetic, and when $\mu >> 1$, it is termed ferromagnetic.

From Equation 6 it follows that:

$$B = \mu H \tag{7}$$

or flux density of a material in a magnetic field is its permeability times the field strength.

It also follows that:

$$H = \frac{B}{\mu} \tag{7a}$$

The magnetic field equals the flux density it establishes in a body divided by its permeability.

The quantity $1/\mu$ is the constant appearing in Equations 1 and 2.

Intensity of magnetization.—The intensity of magnetization of a magnet is a measure of its strength. More specifically, the intensity of magnetization I is the amount of magnetization possessed by a magnet.

It is pole strength per unit cross section of the magnet, taken at right angles to the direction of magnetization. In equation form:

$$I = \frac{m}{A} \tag{8}$$

where m = magnetic poles and A is end area.

The quantity I also equals magnetic moment per unit volume. This relation can be derived from Equation 8, by multiplying the numerator and the denominator of the second term by L', the distance between the poles of the magnet. mL' = magnetic moment M. AL' = volume of the magnet or V. Therefore

$$I = \frac{mL'}{AL'} = \frac{M}{V}$$

or

$$I = \frac{M}{V} \tag{9}$$

The strength of a magnet is conveniently represented by its magnetic moment per unit volume. Example: a magnet with a cross-section of 5 sq. cm. and a pole strength of 15 will have an intensity of magnetization of 3. Intensity of magnetization is also called polarization.

An iron bar or a bar of magnetic material, when placed in a magnetic field, becomes magnetized, a property which is known as magnetic susceptibility. Susceptibility, defined quantitatively, expresses the ratio of the intensity of magnetization acquired by a substance to the strength of the magnetizing field acting on the body. The letter k (or the Greek letter *kappa)* is used to denote susceptibility.

$$k = \frac{I}{H} \tag{10}$$

Equation 10 yields the following:

$$I = kH$$

and

$$H = \frac{I}{k}$$

Theoretically any material that has a magnetic susceptibility greater than zero will become a magnet when placed in a magnetic field in air.

A ferromagnetic or a paramagnetic substance in a magnetic field shows a susceptibility greater than zero. A cubic centimeter of such a substance has an appreciable magnetic moment. For a diamagnetic material the susceptibility is less than zero, or negative. In a magnetic field, a cubic centimeter of it will be magnetically weaker than its surroundings.

Volume and mass susceptibility.—The magnetic susceptibility of substances can be referred to either unit volume or unit mass. As defined,

intensity of magnetization of a body is its magnetic moment per cubic centimeter, or $I = M/V$ and volume susceptibility $k = I/H$, as given.

To express susceptibility in relation to the mass of a particular material, another term, specific magnetization Q, is introduced. Specific magnetization, for which the symbol X is sometimes used, stands in the same relation to mass susceptibility as does intensity of magnetization to volume susceptibility. Specific magnetization Q is magnetic moment per gram. With W = mass,

$$Q = \frac{M}{W} \tag{11}$$

$$\left.\begin{aligned} \text{and mass susceptibility } k' &= \frac{Q}{H} \\ \text{or } Q &= \frac{k'}{H} \end{aligned}\right\} \tag{12}$$

These are natural and logical units in the c.g.s. system for: volume magnetization I represents 1 cubic centimeter of a material that has 1 c.g.s. moment. Likewise, mass magnetization Q for a substance indicates that 1 gram of it has 1 c.g.s. moment.

Volume and mass magnetization are related in an apparently paradoxical manner which is shown as follows:

$$I = M/V = mL/AL = m/A \tag{13}$$

In this equation we have set pole separation as equal to L, the physical length of the magnet. This is true only in a theoretical magnet. Let d = density, and with the other symbols as previously given, we have

$$Q = M/W = M/Vd = M/ALd = mL/ALd = m/Ad \tag{14}$$

In words, intensity of magnetization is pole strength per unit area, and specific magnetization is pole strength per unit area times density. I and Q differ from each other only by the density factor.

If in the expression $Q = m/Ad$, both sides of the equation are multiplied by d, then $Qd = m/A$. However, as $m/A = I$, it is apparent that $Qd = I$. Since $I = kH$ and $Q = k'H$, *volume susceptibility equals mass susceptibility times density,* or

$$k = k'd \tag{15}$$

From similar analysis of the equation $Q = I/d$, *mass susceptibility equals volume susceptibility divided by density,* or

$$k' = k/d. \tag{15a}$$

The usual relations of mass, volume, and density are given in the definition of density. Density equals mass per unit volume; viz., $d = M/V$. Also, volume x density = mass (in symbols $W = V \cdot d$) and volume =

mass/density ($V = W/d$). That is, to get volume, mass is *divided* by density.

The seeming paradox referred to hinges on the equation in which it was shown that $k = k'd$. This signifies that, to obtain a volume magnetic susceptibility, a mass susceptibility is *multiplied* by the density. In like manner mass susceptibility equals volume susceptibility *divided* by density, as expressed in $k' = k/d$.

Relation between Permeability and Susceptibility.—The situation shown in Figure 12(b) brings out the way in which magnetic permeability μ and magnetic susceptibility k of a substance are related. When such a magnet, with cross-section A, is placed in a magnetic field H, it acquires a certain pole strength m by induction. The ratio of the pole strength and the cross-sectioned area is called the surface density of magnetization, or m/A, which expresses the number of magnetic poles per square centimeter.

The matter can be thought of in terms of magnetic force lines. The total flux (or lines of force) in the bar is the sum of the lines originally present, in the field H, and those arising from the m poles induced by the field H. It has been developed that a unit magnetic pole gives out 4π lines of force, so that the poles contribute $4\pi \frac{m}{A}$ lines. In equation form:

$$\sum \frac{\phi}{A} = H + 4\pi \frac{m}{A} \tag{16}$$

wherein $\sum \frac{\phi}{A}$ is total flux per unit area.

As defined $\frac{\phi}{A} = B$ or flux density and $\frac{m}{A} = I$ or intensity of magnetization. It can be written that

$$B = H + 4\pi I \tag{17}$$

If each side of this equation is divided by H, then

$$\frac{B}{H} = 1 + 4\pi \frac{I}{H}.$$

As shown in the earlier discussion $\frac{B}{H} = \mu$ and $\frac{I}{H} = k$. Therefore:

$$\text{permeability} = \mu = 1 + 4\pi k \tag{18}$$

$$\text{susceptibility} = k = \frac{\mu - 1}{4\pi} \tag{19}$$

Permeability describes the number of lines of force through a unit cross-section of a substance in relation to the number of lines of force through the same cross-section of air. *Susceptibility* describes how strong

a magnet a given magnetizing field will produce in a substance in relation to the strength of the magnetizing field applied.

It is apparent that these two magnetic properties relate to somewhat different aspects of the magnetic character of materials.

These matters have specific application in magnetic exploration. The magnetic strength and hence the detectability of a magnetic body, such as a magnetic dike, for instance, depend on its susceptibility and the contrast in susceptibility between it and the surrounding rock. See Figure 13.

FIG. 13.—Distortion of earth's field due to various materials: (a) non-magnetic material; (b) paramagnetic or ferromagnetic material having a susceptibility greater than the surrounding medium; (c) diamagnetic material, with a susceptibility less than the surrounding medium.

Magnetic Intensity Due to a Magnet

The operation of many magnetic instruments, and the calibration of Schmidt type magnetometers with auxiliary magnets, require the quantitative determination of the magnetic intensity at a measured distance from a simple bar magnet. There are three cases or positions of Gauss that adequately cover the usual situations. These are as follows:

Magnetic Force at a Point Due to a Bar Magnet:

Case I. Magnet end on, or Position I of Gauss. (See Figure 14.)

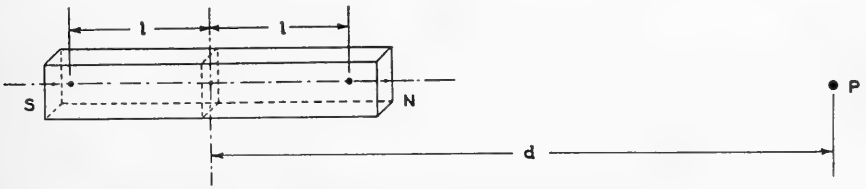

FIG. 14.—Magnetic force at a point due to a bar magnet: Position I of Gauss.

$$H_p = \frac{m}{(d-l)^2} - \frac{m}{(d+l)^2} = \frac{m\,(d^2+2ld+l^2) - m\,(d^2-2ld+l^2)}{(d^2-l^2)^2}$$

$$H_p = \frac{4\,m\,ld}{(d^2-l^2)^2} = \frac{2M\,d}{(d^2-l^2)^2} \qquad (20)$$

$$H_p = \frac{2M^*}{d^3} \tag{21}$$

Case II. Magnet broadside: Position II of Gauss. (See Figure 15.)

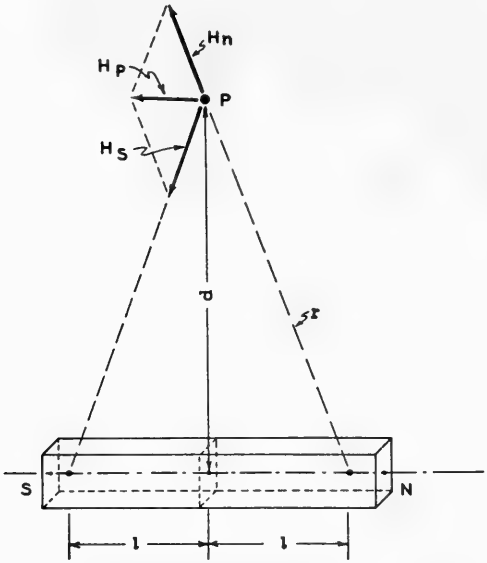

FIG. 15.—Magnetic force at a point due to a bar magnet: Position II of Gauss.

By the figure, from similar triangles,

$$\frac{H_p}{H_n} = \frac{2l}{r}; \quad H_p = \frac{H_n \cdot 2l}{r}; \quad \text{but } H_n = \frac{m}{r^2}$$

$$\text{Hence: } H_p = \frac{2ml}{r^3}: \quad \text{but } r = \sqrt{d^2 + l^2}$$

$$\text{so that } H_p = \frac{2ml}{(d^2 + l^2)^{3/2}} \tag{22}$$

As before, $M = 2ml$ and l may be neglected, hence:

$$H_p = \frac{M}{d^3} \tag{23}$$

Case III. Magnet in any position: Position III of Gauss. (See Figure 16.)

We can replace magnet NS by two magnets, one end on to P and the other perpendicular to the first. Then if the original magnet has a moment

* If small in comparison to d, l may be neglected.

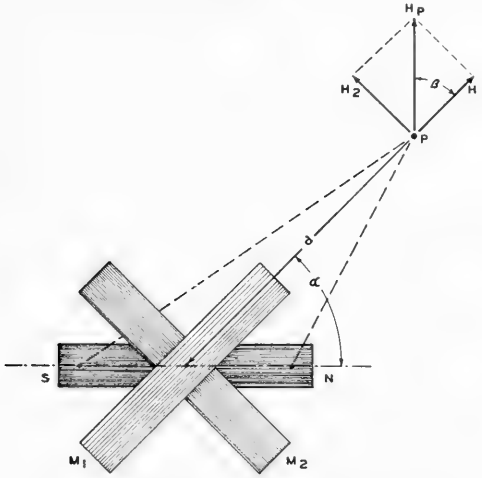

FIG. 16.—Magnetic force at a point due to a bar magnet in any position: Position III of Gauss.

M, the end-on magnet a moment M_1, and the broadside magnet a moment M_2,

$$M_1 = M \cos \alpha \qquad \text{and} \qquad M_2 = M \sin \alpha$$

This gives a combination of Cases I and II.

$$H_{1p} = \frac{2\,M \cos \alpha}{d^3} \text{ end on; and } H_{2p} = \frac{M \sin \alpha}{d^3} \qquad (24)$$

To calculate the magnitude and direction of the resulting force at P, it is necessary to determine the angle β:

$$\tan \beta = \frac{H_{2p}}{H_{1p}} = \frac{M \sin \alpha}{2M \cos \alpha} = \tfrac{1}{2} \tan \alpha \qquad (25)$$

Magnitude of Intensity, H_p

$$H^2{}_p = \frac{(2M \cos \alpha)^2}{(d^3)^2} + \frac{(M \sin \alpha)^2}{(d^3)^2} = \frac{4M^2 \cos^2 \alpha + M^2 \sin^2 \alpha}{d^6}$$

$$H_p = \frac{M}{d^3} \sqrt{4 \cos^2 \alpha + \sin^2 \alpha} \qquad (26)$$

Behavior of a Magnet in a Homogeneous Magnetic Field

In a homogeneous or uniform magnetic field, the field intensity is constant and always in the same direction.

A magnet free to turn in a horizontal plane will come to rest when its axis is aligned with the direction of the homogeneous magnetic field in

which it is placed. (See Figure 17.) NS represents a magnet placed at an angle α to the direction of the field, and of pole strength m.

Assuming a magnetic field of strength H, the N pole of the magnet experiences a force, $+Hm$, and the south pole a force, $-Hm$, the two forces giving rise to a couple whose turning moment is equal to either force multiplied by the perpendicular distance (AN) between them. $AN = NS \sin \alpha$; $NS = 2l$; and $M = 2\ ml$.

Therefore, the magnetic couple =

$$Hm\ (AN) = Hm\ (NS) \sin \alpha = MH \sin \alpha. \qquad (27)$$

This couple becomes zero when the magnet assumes a position parallel to H.

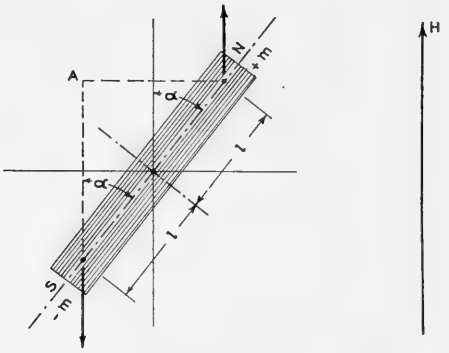

FIG. 17.—A magnet free to turn placed in a uniform magnetic field.

This expression for the couple acting on the needle consists of three parts: H, the disturbing field; α, which defines the position of the magnet; and m (NS), a characteristic of the magnet itself. This last quantity is the familiar *magnetic moment*, M, of the magnet.

In the case of an ideal magnet consisting of two poles, used in our previous consideration, the magnetic moment was defined as pole strength times distance between poles: or $2\ ml$. However, a definition of magnetic moment from the expression

$$\text{couple} = MH \sin \alpha \qquad (28)$$

does not depend on the idea of an ideal magnet. Any magnet may be suspended in a magnetic field, the couple required to maintain it in a given position measured, and its M, therefore, determined.

If the magnet is maintained at right angles to the magnetic field, $\alpha = 90°$ and the couple $= MH$. From this, another definition of the moment of a magnet can be written: the magnetic moment, M, is the couple required to maintain a magnet at right angles to a magnetic field of unit strength.

In Equation 28, when α is small (less than 3°), the value of the sine can be taken as the measure of the angle in radians, so that:

$$\text{couple} = MH\,\alpha \tag{29}$$

In the analyses to follow, l will represent the ½ length of magnet unless otherwise stated, or $M = 2\,ml$ and

$$\text{couple} = 2\,ml\,H\,\sin\,\alpha = MH\,\sin\,\alpha. \tag{28}$$

Behavior of a Magnetic Needle in Two Magnetic Fields

The conditions analyzed under the above heading cover the case of one of the pair of companion experiments performed in measuring the horizontal component of the earth's magnetic field. These experiments are described under the section on terrestrial magnetism.

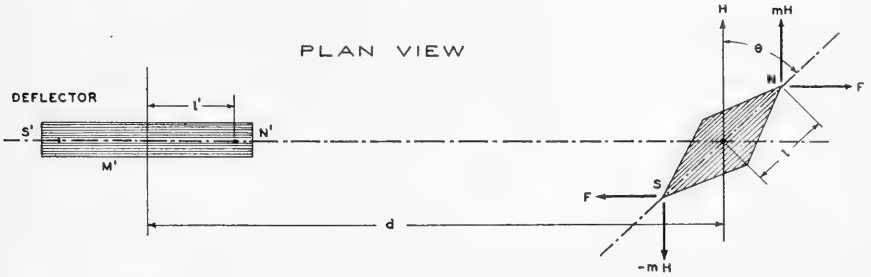

FIG. 18.—Behavior of a magnetic needle in two magnetic fields: Position I of Gauss.

Gauss Position I.—In the "end on" position, (Figure 18), the needle is considered to be very small, and we assume that the deflector magnet produces a uniform magnetic field, the field being the same at N, at S, and at the center of the needle, and of value H'.

The axis of the deflector magnet S'N' is perpendicular to the direction of the uniform field of intensity, H. The force acting on the magnetic needle from this homogeneous field is mH, m being the pole strength of the needle.

The value of the field intensity H' at the needle is due to the deflector:

$$H' = \frac{2M'}{d^3} \tag{20}$$

or if l' is fairly large in relation to d

$$H' = \frac{2M'd}{(d^2 - l'^2)^2} \tag{21}$$

The couple due to the field H:

$$\text{couple} = mHl\,\sin\,\theta + mHl\,\sin\,\theta = 2mlH\sin\theta.$$

The couple due to the deflector magnet:

$$\text{couple} = mH'2l\cos\theta$$

where θ is the angle between the direction of the homogeneous field H and the axis of the needle, after equilibrium has been established.

For equilibrium, the couples are equal, hence: $2mlH \sin\theta = 2mlH' \cos\theta$.

Substituting for H' gives: $2mlH \sin\theta = 2ml \dfrac{2M'\, d \cos\theta}{(d^2 - l'^2)^2}$

Eliminating $2ml$ from this equation and rearranging, we obtain:

$$\tan\theta = \frac{2M'd}{H\,(d^2 - l'^2)^2} \tag{30}$$

Note that l, the half length of the needle, does not enter the final equation.

A more simple form of the above, where l' is not involved, being small in comparison to d, is:

$$\tan\theta = \frac{2M'}{H\,d^3} \tag{31}$$

Example: assume the length of the deflector magnet of 10 cms. positioned at a distance of 80 cms. from the needle: $d^2 = 6400$ and $(l')^2 = 25$. The error involved in neglecting l' is about .4 of 1%, which is much less than the probable error in reading the deflection.

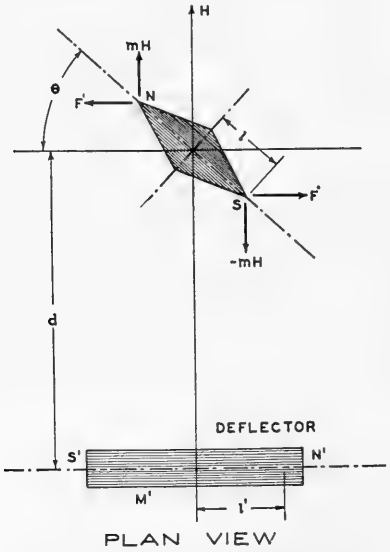

FIG. 19.—Behavior of a magnetic needle in two magnetic fields: Position II of Gauss.

Gauss Position II.—The same conditions are assumed in Figure 19 as in Figure 18. The needle is very small, with the deflector magnet, N'S',

exerting a uniform field H', and set perpendicular to homogeneous field H. This also is known as the "broadside" position.

The field due to the deflector magnet is H'.

$$H' = \frac{M'}{(d^2 + l'^2)^{3/2}} \tag{22}$$

or if l' is neglected $$H' = M'/d^3 \tag{23}$$

The force acting on the needle due to the homogeneous field is, as before, mH. The force acting on the needle from the deflector magnet is F'.

$$F' = mH' = mM'/(d^2 + l^2)^{3/2}$$

The couples acting on the needle from these two sources when in equilibrium as measured by the angle θ can be equated.

The couple due to the field $H = 2ml\ H \sin \theta$.

The couple due to the deflector magnet field $H' = 2mlH' \cos \theta$.

Equating these, after equilibrium has been established, gives:

$$2ml\ H \sin \theta = 2ml\ H' \cos \theta$$

Substituting for H' gives:

$$2ml\ H \sin \theta = 2ml\ M'/(d^2 + l^2)^{3/2} \cos \theta$$

As before, eliminating $2ml$ from this equation and rearranging:

$$\tan \theta = M'/H\ (d^2 + l^2)^{3/2} \tag{32}$$

Where l is small and therefore may be neglected, this equation becomes:

$$\tan \theta = M'/Hd^3 \tag{33}$$

Couples (or Action) Between Two Small Magnets

Case I—1st Position of Gauss.—This position is involved in the determination of the scale value of vertical intensity Schmidt-type magnetometers with auxiliary magnets.

As pictured in Figure 20, there are two short magnets, the deflector magnet S′-N′ of moment M' and the needle NS of moment M, pole strength m and length $2l$. In this situation the action of the earth's magnetic field is not considered. Simplifying assumptions as to uniformity of field set up by the deflector magnet as previously used are retained. α is the angle between the prolongation of the magnetic axis S′N′ of the deflector and the magnetic axis of the needle NS.

Using the more simple expressions which neglect the half length of the deflector magnet, the intensity of the field at the needle due to the deflector is:

$$H' = 2M'/d^3 \tag{21}$$

The force acting on the needle $F' = mH' = 2M'm/d^3$.

The couple acting on the needle is:

$$\frac{2M'm\,2\,l \sin a}{d^3} = \frac{2M'\,M \sin a}{d^3} \tag{34}$$

If a becomes 0°, or with both magnets in the same line, there is no couple acting since $\sin a = 0$.

If a becomes 90°, $\sin a = 1$ and the couple is a maximum. In this case,

$$\text{couple} = \frac{2M\,M'}{d^3} \tag{35}$$

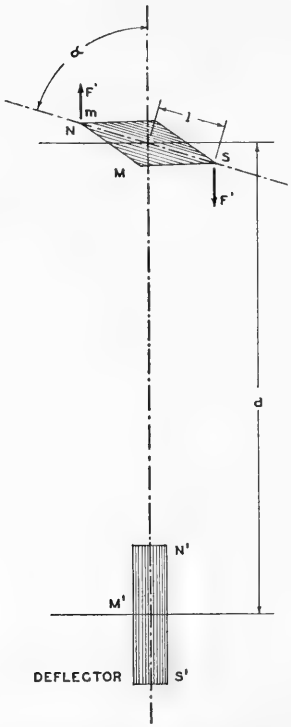

FIG. 20.—Action between two small magnets: Position I of Gauss, used in calibrating a vertical magnetometer.

Case II—2nd Position of Gauss.—This position is involved in the determination of the scale value of the *horizontal* intensity magnetometers with auxiliary magnets. (Figure 21.)

Under assumptions as made previously for Case I, except that α is measured from the horizontal (or parallel to S′ N′), the intensity of the magnetic field at the needle due to the deflector magnet is:

$$H' = M'/d^3 \tag{23}$$

and the force at the needle

$$F' = mH' = mM'/d^3$$

The couple acting on the needle is

$$\frac{2ml\ M'\ sin\ \alpha}{d^3} = \frac{MM'\ \sin\ \alpha}{d^3} \tag{36}$$

If $\alpha = 0°$, $\sin\ \alpha = 0$ and the couple $= 0$.

If $\alpha = 90°$, $\sin\ \alpha = 1$, and the couple is a maximum; then

$$\text{couple} = \frac{MM'}{d^3} \tag{37}$$

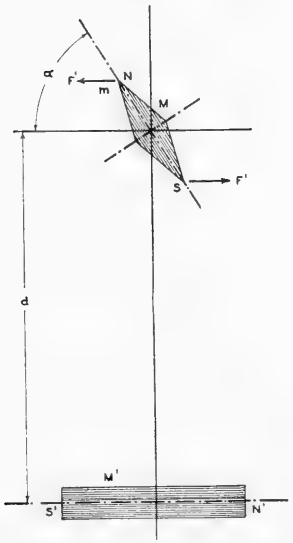

FIG. 21.—Action between two small magnets: Position II of Gauss used in calibrating a horizontal magnetometer.

Case III—3rd Position of Gauss.—The axis of rotation of the needle passes through the midpoint of the deflector, and is normal to it. (Figure 22.) This position is seldom used in calibration and therefore the develop-

ment of the formulae involved will be omitted. The relation is, however, similar to Gauss Position II, where at a maximum the couple is:

$$\text{couple} = MM'/d^3 \tag{37a}$$

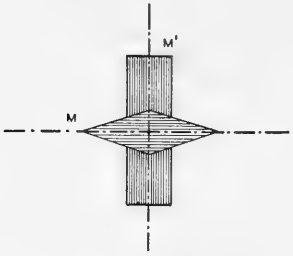

FIG. 22.—Two magnets in Position III of Gauss: where the magnetic needle is above the deflector magnet M'.

TERRESTRIAL MAGNETISM

The terrestrial phase of geomagnetics, or, to express it more simply, earth magnetism, utilizes the fundamentals of magnetism which have been presented. *The earth itself acts like a great spherical magnet.* In common with other magnets the earth has the power of attraction, exhibits polarity, and has a field of force. Except for its large size, which is not inherently a magnetic characteristic, the earth acts quite like any ordinary spherical magnet.

It is advantageous to take up geophysically pertinent features of earth magnetism before discussing the magnetic properties of rocks and formations in detail. This is because rock magnetization is considered to be caused largely by induction in the earth's magnetic field.

The general idea that the earth itself could be considered as a spherical magnet, and so treated, was developed some 350 years ago by Sir William Gilbert.* Gilbert carefully investigated the magnetic character of a sphere (or *terella*) turned out of magnetite, by placing small magnets mounted on pivots at various places on and around it. In his famous treatise *De Magnete* published in the year 1600, he wrote, "The earth is a great magnet."

Gilbert spent 18 years in the study of magnetism. The great value of his work lay in the fact that he thoroughly believed in the importance of experimentation. With his spherical loadstone he obtained a very good understanding of the distribution of the lines of force of the magnetic field of the earth, and their inclination or dip. He studied the change from zero dip at the equator to 90° dip at the poles and established that the rate of

* See Chapter I, page 5.

change of dip with latitude is more rapid near the equator than at the poles. From Gilbert's work, the basic concepts of geomagnetics were evolved.

Building on the discoveries of Gilbert and others, C. F. Gauss in 1832 put forward a general theory of earth magnetism. In it he presented a fairly accurate and quantitative idea of the nature and distribution of the magnetic field of the earth. Gauss developed a potential formula in terms of spherical harmonics to represent the facts of the earth's magnetism as then known. Based on the work of Gauss, the science of terrestrial magnetism has progressed steadily. It was, in fact, one of the first fields of international cooperation for the study of a world-embracing natural phenomenon.

The earth acts as a magnetized sphere surrounded and permeated by a magnetic field of strength of about 0.6 gauss. As a first approximation this field is so distributed at the surface and is of such an amount that it *could* arise from a short powerful bar magnet at the center of the earth. The moment of such a hypothetical magnet has been calculated and was found in 1922 to be some $8 \cdot 10^{25}$ c.g.s. units.

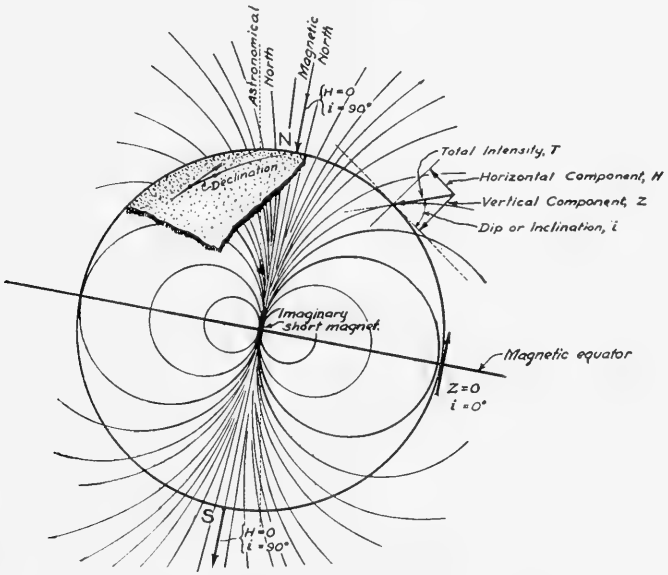

FIG. 23—Schematic diagram illustrating magnetic field produced by an imaginary bar magnet located at the earth's center.

The case under discussion is pictured in Figure 23 which shows an ideal earth and the magnetic field developed in it from a short bar magnet at its center.

Calculations indicate that the earth's field is most closely duplicated when the poles of the imaginary magnet, shown in Figure 23, are practically coincident. The magnetic poles, therefore, of the spherical magnetic earth

would be deep in the sphere and at practically the same distance from all points on the surface. This bears on the geometry of the earth's magnetic field as will appear subsequently.

The concept of a short bar magnet as the cause of the magnetic force in a magnetized spherical earth is useful in another respect. Modern investigations all point to the conclusion that earth magnetism is deep-seated, which would be the case with virtually coincident poles as assumed above.

From this generally accepted fact, it follows that the lines of force of the field must pass through the outer crust of the earth to reach the surface. The outer crust is made up of magnetically heterogeneous materials which cause distortions in the earth's magnetic field. Measurements at the surface have shown that extensive zones of rocks of different permeabilities and great areal extent, perhaps better described as tectonic features (mountain ranges, geologic basins, regional fault zones and the like), significantly warp the force lines from an ideal symmetrical shape. Such warping or distortion gives rise to magnetic anomalies* which will later be considered in detail.

In the foregoing nothing has been said as to the possible or probable causes of earth magnetism. There are a number of theories and assumptions to account for it, although the true cause of the deep-seated magnetization of the earth is not known.

Position of the Magnetic Poles.—As is well known, the earth, like any other spherical magnet, has magnetic poles. They are geometrically the two points of intersection of the earth's magnetic axis with the surface. Exploration has shown that they are regions of some miles in extent. They are, moreover, unique localities, for at the north magnetic pole the only compass direction is south and at the south magnetic pole the only direction is magnetic north. The magnetic poles of the earth are best defined as those places on the earth where the lines of force of the earth's magnetic field are essentially vertical.

Specifically the North magnetic pole was located in 1906 at latitude 71° 30′ north and longitude 97°40′ west, near the island of Boothia Phelix, in Northern Canada. Shackelford's south polar expedition established the South magnetic pole in 1909, at latitude 72°25′ south and longitude 155°-16′ east, or on the edge of South Victoria Land.

It is apparent that since the North and South magnetic poles are *not* symmetrically disposed, as evidenced by the locations given, a line joining them will not pass through the center of the earth, even allowing for the fact that the poles are regions and not points. A line joining the magnetic poles misses the earth's center by some 750 miles. This distortion of the

* Defined as a difference from an average value, for example, an increase in magnetic intensity in an area, markedly greater than would be normal for the latitude of the locality. Anomalies may be positive (increases), or negative (decreases), in relation to the average magnetic value.

earth's magnetic field shows quite definitely that the earth is not symmetrically or uniformly magnetized.

The Earth's Magnetic Field

Declination.—It is apparent that terrestrial magnetic measurements are, for practical purposes, confined to points on or near the earth's surface. A magnetic needle suspended so that it can turn freely about its center of balance (a compass, for example) will eventually come to rest with its magnetic axis directed along the lines of force of the earth's field. On this basis the magnetic field at a point of observation can be specified in part as follows.

The magnetic meridian at any such point is the vertical plane fixed by the direction of the magnetic lines of force. It is the direction assumed by a free magnetic needle when at rest. A compass is usually employed for determining the magnetic meridian or magnetic north line.

Magnetic declination is the angle between the astronomic meridian, or true north direction, and the magnetic meridian at the station of observation. It is measured in a horizontal plane and is designated as east or as west declination according as the magnetic meridian is east or west of true North. Declination is sometimes called *variation* or *variation of the compass.*

Inclination or Dip.—Magnetic inclination is the angle, measured in a vertical plane, which the lines of force make with the plane of the horizon at the point of measurement. It is called + if below the horizon and − if above it. A dip needle is an instrument closely similar to a compass, designed so that its needle can rotate in a vertical plane, and used to measure the inclination or dip angle.

Vectorial Representation.—At any point on the earth's surface, the magnetic field can be conveniently represented by a vector *(T)*. This vector starts at the point of observation and extends in the direction of the line of force of the field. Its vector length is proportional to the strength of the total intensity of the field. See Figure 24.

The total intensity can be resolved into two components in the plane of the magnetic meridian, namely, *H* or horizontal intensity, and the ver-

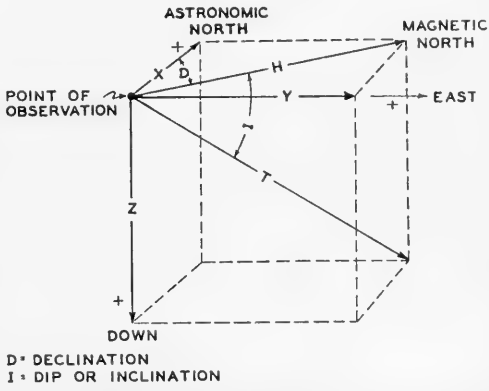

Fig. 24.—Vectorial representation of the earth's magnetic field at a point of observation.

tical intensity component Z. The former is effective on a compass or a horizontal magnetometer, and the latter on a vertical magnetometer or dip needle.

The horizontal intensity can be projected on the astronomic north direction, which amount is called X, and on the astronomic east direction, which amount is called Y. The angle between the magnetic meridian and the astronomic north is the declination D. The angle between the horizontal intensity vector (or a horizontal plane) and the total intensity vector is the dip (or inclination), symbol I.

The Magnetic Elements.—The quantities D, H and I are called the magnetic elements. The following formulae relating them to each other need no demonstration:

$$\left.\begin{aligned} &X = H\cos D\,; \quad Y = H\sin D\,; \quad Z = H\tan I = T\sin I \\ &H = \sqrt{X^2+Y^2} = T\cos I\,; \quad T = \sqrt{X^2+Y^2+Z^2} = \sqrt{H^2+Z^2} \\ &T = \frac{H}{\cos I}\,; \quad \tan I = \frac{Z}{H} = \frac{Z}{\sqrt{X^2+Y^2}}\,; \quad \tan D = \frac{Y}{X} \end{aligned}\right\} \quad (38)$$

The U. S. Coast and Geodetic Survey measures the magnetic elements at various stations throughout the United States. Three stations for Colorado are given below.

COLORADO

U. S. Government Magnetic Stations*

Pueblo: Lat. 38°14′ Lon. 104°38′
Survey 1899 as of 1-1-'25
Dec. 13°24′ E.I. 67°04′
$H = 0.2247$ gauss.

Fountain: Lat. 38°41′ Lon. 104°42′
Dec. 14°26′ E.I. 67°11′
$H = 0.2222$ gauss.

Canon City: Lat. 38°26′ Lon. 105°14′
Dec. 14°21′ E.I. 66°30′
$H = 0.2277$ gauss.

The horizontal intensity is recorded in gauss, 1 gauss being the strength of a magnetic field which acts on a unit magnetic pole with a force of 1 dyne. The unit more usual in the field surveys of geophysical prospecting is the gamma ($_\gamma$) or 1/100,000 of a gauss (10^{-5} gauss).

* From Government Magnetic Declination Tables and Isogonic Charts, C. & G. Survey 105, and 36th Ann. Serial Publication of U. S. Coast and Geodetic Survey, Results of Magnetic Survey in 1915-1926.

Measurement of D, H, and I.

Oscillations and Deflections.—To measure the horizontal magnetic intensity at a station, it is necessary to perform two experiments which require the use of a bar magnet of moment M, called the *deflector,* and a compass. In one experiment the quantity M/H is determined where H is the horizontal intensity of the earth's field at the point of observation. In the other experiment the quantity MH is found. This gives two simultaneous equations and two unknowns.

Deflection experiment: See Figure 25.

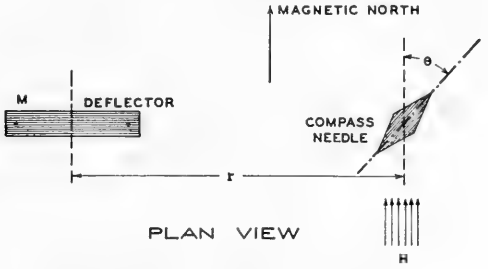

FIG. 25.—Set-up for deflection experiment to measure M/H.

Deflector magnet M

$r =$ cm. $H =$ earth's field, horizontal component.

$\theta =$ angle between magnetic N and compass needle at rest.

With such a setup $\dfrac{M}{H} = \frac{1}{2} r^3 \tan \theta$ (39)

Oscillations experiment: see Figure 26.

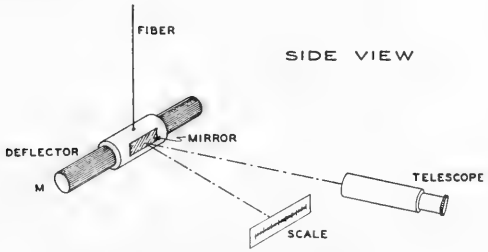

FIG. 26.—Set-up for oscillations experiment to measure MH.

Using the deflector magnet, from the previous experiment its period of oscillation T_o is determined when it is suspended on a fiber and swung in the earth's magnetic field. In this case,

$$T_o = 2\pi \sqrt{\frac{I_o}{MH}} \tag{40}$$

I_o equals the moment of inertia of the magnet which may be determined from its dimensions, as the magnet is of simple shape. Solving these two equations

$$H^2 = \frac{8\pi^2 I_o}{T_o^2 r^3 \tan\theta} \tag{41}$$

$$M^2 = \frac{2\pi^2 I_o r^3 \tan\theta}{T_o^2} \tag{42}$$

H can thus be found and M as well, if desired.

At the same station the declination can be obtained by measuring the angle between astronomic north, as determined by a solar or an observation on polaris, and the magnetic north. A specially-designed compass called a *declinometer* is used.

Also at the station, magnetic inclination, or dip, can be found with an accurate dip needle or dip circle. In this manner the three magnetic elements D, H, and I for a station are measured.

The instruments used by the Coast and Geodetic Survey for these purposes are of special design to insure accuracy of measurement. The procedure followed is somewhat more refined than that described here, in order to eliminate errors.† Some of the special instruments referred to are described in sections which follow.

Sine Galvanometers.—The sine galvanometer is an observatory instrument used for precision determinations of the absolute value of the horizontal intensity. The horizontal intensity is determined by the deflection method described above. The deflecting field in this case is produced by an electric current flowing in a coil of known dimensions. When current is passed through this coil, the suspended magnet is deflected from its free position in the magnetic meridian, through an angle which is dependent upon the ratio of the intensity of the field produced by the current in the coil and the horizontal component of the earth's magnetic field. Knowing the constants of the coil and the magnitude of the current, the horizontal intensity can be computed. Sine galvanometers for the determination of the horizontal intensity are described in detail by Barnett‡ and by Hazard.§ Figure 27 shows a photograph of a sine galvanometer designed and constructed by the Carnegie Institution of Washington for determining the magnetic horizontal intensity. The standard cells and electrical measuring appurtenances used when making observations with this sine galvanometer are mounted in a heat-insulated cabinet.

† D. L. Hazard, "Directions for Magnetic Measurements," *U. S. Coast and Geodetic Survey, Serial No. 166*, 3rd. Edition, 1930.

‡ S. J. Barnett, *Carnegie Institution of Washington, Publication 175*, pp. 373-394, Dec. 1921.

§ D. L. Hazard, *loc. cit.*, p. 38.

Compass-Variometers.—The Carnegie Institution of Washington has developed several compass-variometers capable of measuring relative values of the horizontal intensity. §

One type of compass variometer which has been used for measurement aboard ships is shown in Figure 28. Two disc-shaped magnets of equal magnetic moment are suspended independently one above the other. The distance between the two disc magnets is regulated by a graduated micrometer screw. A fine quartz-rod pointer, or index, is attached to each of the magnet supports. The pointer of the upper magnet is in the vertical plane through the magnetic axis of the upper magnet (a diameter of the disc), and the pointer of the lower magnet is in a vertical plane making an angle ψ with the magnetic axis of the lower magnet. (In general, the angle ψ is made 60°.)

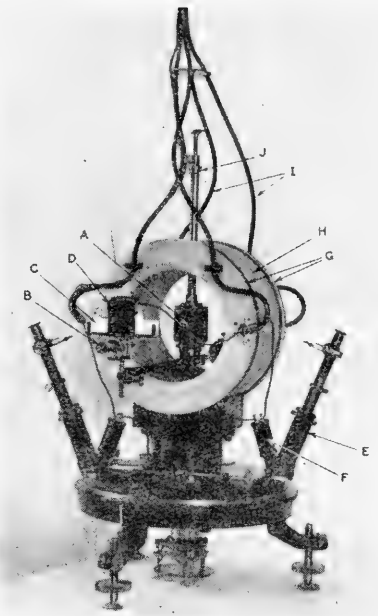

FIG. 27.—Carnegie Institution of Washington sine galvanometer. The international standard for determining magnetic horizontal intensity. A, suspended magnet; B, telescope; C, scale; D, lamp; E, circle microscopes; F, lamp; G, Helmholtz coils; H, marble cylinder; I, copper conductors to power supply; J, torsion wire housing. (Courtesy of U. S. Coast and Geodetic Survey.)

On looking down on the instrument through a lens one sees the quartz pointer of the lower support and an image of the pointer of the upper support reflected from a mirror which is mounted centrally with respect to the magnet system. The angle ψ between the two pointers is read off a graduated circle which is photographed on a glass plate mounted approximately in the plane of the reflecting mirror.

It may be shown that changes in the horizontal intensity are related to changes in the angle ψ by the equation

$$\Delta H = -\frac{DM}{57.3e^3} \sin \frac{\psi}{2} \cdot \Delta\psi$$

where

ΔH = change in horizontal intensity
D = instrumental constant
M = magnetic moment of either magnet
e = vertical distance between magnets
ψ = angle between two imaginary vertical planes passing through the magnetic axes of the two magnets

§ L. A. Bauer, W. J. Peters, and J. A. Fleming, "The Compass Variometer," *Carnegie Institution of Washington, Publication 175*, Vol. V, pp. 339-357.

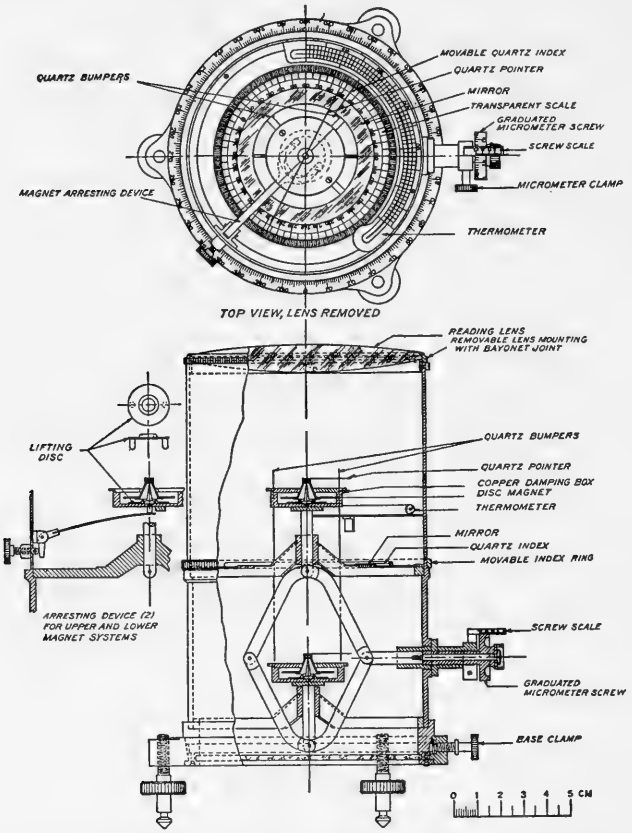

FIG. 28.—Horizontal and vertical sections of a C.I.W. compass-variometer (Bauer, Peters, and Fleming, Carnegie Institution of Washington, Publication 175, Vol. V.).

The usual method of measuring variations in H at different stations consists in keeping the distance e fixed and observing the changes in ψ. $\Delta\psi$ at any station will depend on the initial (base station) value of ψ and on the anomaly ΔH at the station. For a given variometer and given base station value of ψ, the value of $\Delta\psi$ at any station will depend only on the anomaly ΔH at that station.

It is evident that, for a given value of the magnetic moment M of the magnets, the sensitivity of the instrument depends on the value of ψ and of e. For $\psi = 60°$, $e = 6.5$ cm., the sensitivity (ΔH for $\Delta\psi = 1°$) is of the order of 75 gammas.

Inclination or Dip Determinations

Dip Circle.—The dip angle which the total intensity makes with the horizontal intensity is usually determined at magnetic stations by means

of an earth inductor; occasionally, however, a dip circle is employed. The dip circle comprises a magnetized needle, which is supported so that it is free to swing in a vertical plane, and a circle graduated in degrees. An axle passes through the center of gravity of the magnetized needle and terminates in small pivots which rest on pivot bearings. The angle of dip may be read directly off the vertical graduated circle which is concentric with the axis of rotation of the needle, provided this axis is perpendicular to the plane on the magnetic meridian. If the needle does not swing in the plane of the magnetic meridian, measurements must be made for two orientations of the instrument at right angles to each other. From these two readings, i_a and $i_{(90-a)}$, the true dip angle i can be calculated by the formula

$$\text{ctn}^2 i_a + \text{ctn}^2 i_{(90-a)} = \text{ctn}^2 i$$

Earth Inductors.—The earth inductor may be used to determine the inclination of the earth's magnetic field, any component of the earth's magnetic field, or the direction of the magnetic meridian.*

Various designs have been suggested. The operating principle of all of them, however, is essentially similar to that of a small dynamo. When a coil of wire is rotated in a magnetic field so as to cut magnetic lines of force, an E.M.F. is induced in the coil. The magnitude of the induced E.M.F. depends on the number of magnetic lines of force which are cut by the coil and may be expressed by an equation of the form:

$$E = \frac{2NHA}{\tau}$$

where

E = the average E.M.F. induced in the coil on rotating it through one-half turn.
N = the number of turns of wire in the coil.
H = component of the earth's magnetic field parallel to the axis of rotation of the coil.
A = area of the coil.
τ = time for one-half turn.

The induced E.M.F. creates a flow of current when the circuit is closed. The magnitude of this current is determined by the induced potential and the impedance of the coil and auxiliary circuit.

Evidently, when the plane of the coil is parallel to the magnetic field, no lines of magnetic force are cut, and the induced E.M.F. and current are zero. Hence, to determine the magnetic inclination with an earth inductor, it is only necessary to measure the angle of inclination of the brush assembly system making contact with the commutator of the coil when no current flows as the coil is rotated.

* For a detailed description of the theory of the standard earth inductor used for inclination measurements see N. E. Dorsey, "The Theory of the Earth Inductor as an Inclinometer," *Terr. Mag. 18* (1) pp. 1-37, 1937.

The inductor is usually mounted on a modified gimbal support so that the axis of rotation of the coil may be placed in any direction in space. The magnitude of the earth's total field, or any component of the total field, may be computed from the magnitude of the current induced in the coil and the constants of the instrument. The direction of the total field, or one of its components, may be ascertained by noting the inclination of the axis of rotation for zero current.

A photograph of the Wild pattern earth inductor employed by the United States Coast and Geodetic Survey is shown in Figure 29. The instrument comprises essentially a coil of copper wire wound on a cylindrical frame, a flexible shafting which is connected to the cylindrical frame, a commutator, a ring, and a graduated vertical circle which is rigidly attached to the ring. The cylindrical frame is supported by an axis (coil axis) that passes through a central diameter and rests in bearings in the ring. The axis of the ring (inclination axis) is perpendicular to the axis of the coil and is supported in a horizontal position on bearings in uprights attached to the alidade. The graduated vertical circle is parallel to the axis of the coil and concentric with the inclination axis.

The azimuth of the coil axis may be adjusted by turning the ring about the inclination axis, and the azimuth may be read by means of the

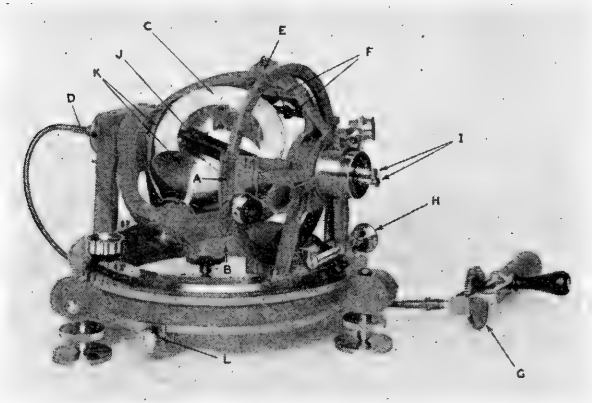

FIG. 29.—Wild pattern earth inductor. A, vertical circle; B, ring; C, coil; D, inclination axis; E, coil axis; F, brush assembly and commutator; G, hand-cranked gear drive; H, slow motion screw; I, binding posts; J, level; K, quarter sphere gears; L, horizontal circle clamp. (Courtesy of the U. S. Coast and Geodetic Survey.)

graduated vertical circle and comparator or microscope shown in the right hand portion of the figure. The coil may be rotated about its axis by means of the flexible shafting, which connects one end of the axis with a gear, and a hand crank.

The commutator consists of two brass half rings which surround the lower end of the axis of the coil. The half rings are connected to the ends of the wire of the coil but are insulated from the coil axis and from each other. The commutator brushes, one on each side of the axis of the coil, are attached to the large ring but are well insulated from it. They are so placed that commutation occurs when the plane of the coil is parallel to the inclination axis. The alternating current produced in the rotating coil by the induced E.M.F. is conveyed to the half rings of the commutator, taken off by the brushes as a direct current, and carried by the attached leads to the galvanometer.

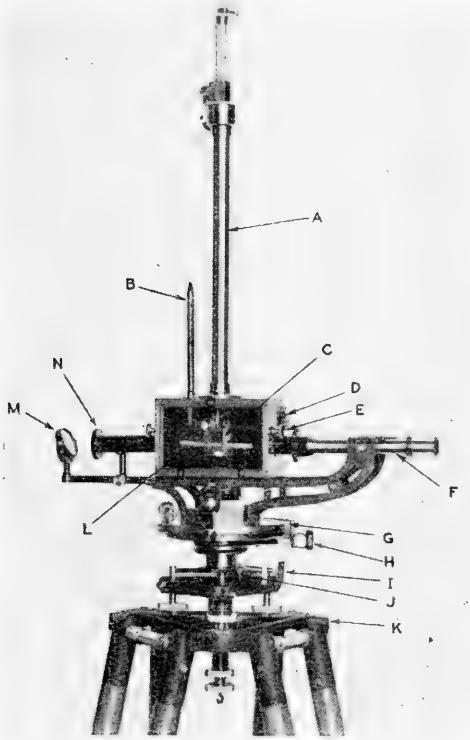

FIG. 30.—Field magnetometer set up for timing oscillations for horizontal intensity and observing declination: A, torsion tube; B, thermometer; C, stirrup (magnet holder); D, magnet arrester; E, control for auxiliary lens; F, telescope; G, horizontal circle; H, slow motion screw; I, lower motion clamp; J, slow motion screw; K, tripod head; L, magnet; M, mirror; N, iris diaphragm.

The operation of the instrument for dip determinations consists in placing the axis of the coil in the plane of the magnetic meridian and altering the inclination of the coil axis (by turning the ring) until a position is found where the galvanometer indicator stays at zero when the coil is

rotated. In this position, the axis of the coil is parallel to the resultant or total field of the earth, and the angle of inclination of the coil axis as measured on the vertical circle is the dip.

If only the *direction* of the earth's field is to be measured, any type of sensitive null-point galvanometer (string, loop, astatic, etc.) may be employed. If the *strength* or *intensity* of the field is to be determined, a ballistic galvanometer is usually employed. (If intensity measurements are based on the potential compensation principle, however, null-point galvanometers are again usable.)

Another type of *portable* earth indicator and galvanometer has been designed and constructed by the Carnegie Institution of Washington. The galvanometer is so designed that the arm carrying the telescope and scale can be folded and carried in the earth-inductor carrying case.† Peep sights and a compass attachment are sometimes provided for setting the earth inductor in the magnetic meridian. If the magnetic declination and the azimuth of a reference mark are known, the meridian setting may be made with the peep sights alone. Ordinarily, however, it is necessary to use the compass attachment. Various instruments have been developed for determining the magnetic declination. Generally, the magnetic declination is measured by two operations: (1) determining the true meridian by latitude observations at noon, if the longitude is known approximately; and (2) determining the magnetic meridian. One instrument for determining the magnetic meridian is illustrated in Figure 30, and is often referred to as a theodolite magnetometer. This instrument comprises a long hollow magnet suspended by a torsion fibre. A telescope and scale measure the angular deflection of the magnet system.

Special Devices for Determining the Magnetic Gradient, Intensity, and Meridian

Magnetic Gradiometer.—The magnetic gradient is measured by comparing the induced electromotive forces in two similar coils spaced apart with parallel axes of rotation and rotatable at the same speed.‡ If the magnetic field intensities perpendicular to the axes of rotation are different at the two coils, the relative magnitudes of the electromotive forces induced in the coils will depend on the relative magnitudes of the field intensities. The two coils of the gradiometer are mounted in a frame and are free to rotate about axes at right angles to the length of the frame. The ratio of the E.M.F.'s induced in the two coils is measured by connecting the coils to opposite arms of a Wheatstone bridge circuit. A sensitive galvanometer is employed for indicating the null-point.*

† Hazard, *loc. cit.*, pp. 80-93.

‡ J. Roman and T. C. Sermon, "A Magnetic Gradiometer," *A.I.M.E. Geophysical Prospecting*, 1934, pp. 373-388.

* For a derivation of the magnetic gradients as a function of the ratio of the induced E.M.F.'s, see Roman and Sermon, *loc. cit.*, pp. 381-384.

The principles embodied in instruments of this type open up many interesting applications and will become of more commercial importance as instrumental improvements are made. Instruments of this type practically eliminate the effects of diurnal and other magnetic variations for which corrections must be made when absolute or relative magnetic anomalies are observed.

Magnetic Balance for Intensity Measurements.—Various instruments have been proposed for accurate measurement of the earth's field. The various modifications of the dynamic type appear to be the most successful in elimination of fragile bearings and other friction supports that limit sensitivity and give difficulty in field use. A majority of the dynamic instruments utilize an electric means for accurate neutralization of the earth's field and for measuring the current required for neutralization. † Knowing this current and the constants of the instrument, the strength of the earth's field can be computed by use of fundamental formulas.

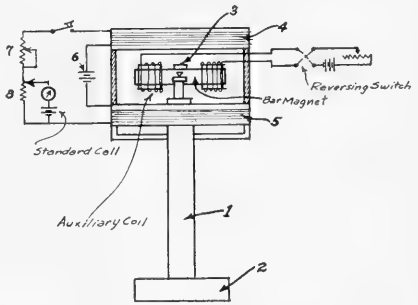

FIG. 31.—Balance for measurements of vertical component of earth's magnetic field. 1, support; 2, base; 3, mirror of optical system; 4, and 5, Helmholtz coils; 6, energizing battery; 7, rheostat; 8, potentiometer. (After Vacquier, U. S. Patent 2,151,627.)

Vacquier Balance for Absolute Measurements of the Vertical Intensity ‡

The operating principle of this instrument consists in neutralizing the vertical component of the earth's field by an opposing magnetic field created by an electrical current. The apparatus (Figure 31) comprises a magnet which is conveniently though not necessarily shaped as a bar and is supported for rotation about an axis very slightly above its center of gravity by means of knife-edges. The latter are made of quartz or other suitable material and rest on level quartz plates. (The plates are mounted on a standard which has a base.) In use, the axes of the knife-edges are aligned horizontally in a direction parallel to the magnetic meridian, so that only the vertical component will affect the magnet. If the magnet were not magnetized, it would assume a horizontal position (as shown) because of the small separation between the axis of rotation and the center of gravity. Under the influence of the earth's field, however, the magnet experiences a turning couple, the magnitude of which depends on the vertical component of the earth's field at that station. The angular deflection of the bar magnet is determined with the aid of a conventional optical system which consists of a small plane mirror affixed to the magnet and a lamp, lens, scale, etc.

The magnetic field for neutralizing the vertical intensity is obtained by means of a Helmholtz coil arrangement. The electrical energizing and measuring circuit comprises the Helmholtz coils, a battery, a rheostat, and a potentiometer. The applied field strength is altered by adjusting the resistance so as to bring the magnet to a standard position. Measurements are made, therefore, on the null or balancing principle.

† E. A. Johnson, "A Primary Standard for Measuring the Earth's Magnetic Vector," Jour. *Terrestrial Magnetism and Atmospheric Electricity*, Mar. 1939, Vol. 44, No. 1, pp. 29-42.

‡ Victor V. Vacquier, "Apparatus for and Method of Measuring the Terrestrial Magnetic Field," U. S. Patent 2,151,627. Issued Mar. 21, 1939.

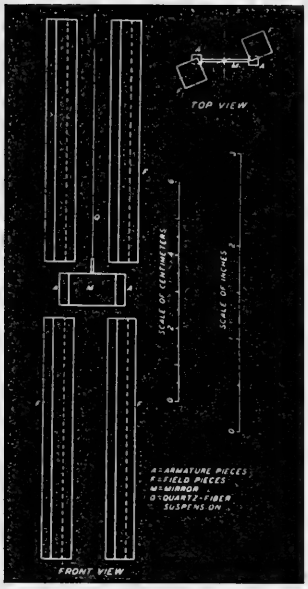

FIG. 32.—Schematic diagram of induction variometer. (McNish, *Rev. Sci. Ins.*, Sept. 1936, p. 338.)

The auxiliary electrical circuit shown in the right hand portion of Figure 31 provides a reversible magnetic field for reversing the direction of the induced magnetism of the bar magnet. This field is used to compensate the effect produced by a possible displacement of the center of gravity of the bar magnet due to warping, temperature effects, dust on the knife-edges, etc. The balance obtained by adjusting the current in the Helmholtz coils is the true balance if the scale deflection remains constant on reversing the induced magnetism of the bar magnet by means of the auxiliary magnetic field.

It is evident that the intensity of the applied field can be determined absolutely provided the instrumental constants are known.

Iron Induction Instruments. — The effects observed with iron-induction instruments are produced by magnetization induced in iron bars by the earth's field. The iron-induction instruments described below are used for determining the vertical component of the earth's field and the magnetic meridian.

Induction Variometer

The design of a recent type of induction variometer employed by the Carnegie Institution of Washington for vertical intensity measurements is illustrated schematically in Figure 32.† Four staves milled from a perminvar bar serve as field pieces.* These field pieces are mounted with their long axes vertical; hence, the induced magnetization in the direction of the long axes depends on the vertical component of the earth's field only. Two smaller pieces, milled from the same bar, serve as armature pieces. The latter are mounted symmetrically on two sides of a frame of brass to which a mirror is attached, the assembly being suspended by a quartz fibre. Variations of the magnetic fields associated with the induced magnetization of the field-pieces cause a rotation of the armature, and, as usual with suspension instruments, this rotation is restrained by the torsion of the suspension fibre. The angular deflection, which depends on the vertical component of the earth's field, is measured with the aid of a telescope by observing the deflection of a beam of light reflected from the mirror at-

† A. G. McNish, "An Induction-Variometer to Measure Magnetic Anomalies," *Rev. Sci. Ins.*, Vol. 7, 1936, pp. 336-338.

* Perminvar, which is an alloy of 45 per cent nickel, 25 per cent cobalt and 30 per cent iron, shows an extremely small hysteresis loss. A comparison of the magnetic properties of perminvar and other less highly magnetic alloys is given by G. W. Elamn, "Magnetic Alloys of Iron, Nickel and Cobalt," *Electrical Engineering*, Dec. 1, 1935, pp. 1292-1299.

tached to the armature. The variometer is calibrated by producing a known change of field with a Helmholtz coil arrangement.

Micromagnetometer

The *micromagnetometer*† originally was used to determine the magnetic meridian. Its operation depends on the induction produced by the earth's field in bars made of a magnetic alloy of high permeability. The bars are mounted end to end on a horizontal platform with a small air gap between them. A fine wire, which is free to vibrate, is stretched vertically between the two bars and energized with a 100 cycle alternating current. For most positions of the bars, the fine wire will vibrate under the action of the magnetic field produced by the induced magnetization of the magnetic bars. If, however, the bars are accurately perpendicular to the earth's field, the induction is zero and the wire will cease to vibrate. It is reported that the instrument will detect directional changes of less than 0.01 degrees.

The Magnetron as a Prospecting Instrument

A *magnetron* is a diode or thermionic tube having a straight axial cathode surrounded by a cylindrical anode.‡ Its proposed use as a magnetic prospecting instrument derives from the fact that in the presence of a magnetic field the electrons do not travel radially from the cathode to the anode. Instead, they spiral around the cathode in circular paths, and after a critical magnetic field intensity is reached, the electrons will return to the cathode without reaching the anode. At this field strength, the plate current will drop abruptly.

The procedure in operating the instrument consists in decreasing the plate voltage on the diode until a voltage is reached at which the current falls off rapidly. The plate voltage at which this occurs is related to the critical field strength H by the relation

$$H = \frac{6.72\sqrt{V}}{r}$$

where r is the radius of the anode. In practice, a compensation procedure is used, wherein the field to be measured is nullified by a known field produced by a Helmholtz coil arrangement.

The magnetron is affected only by the component of the earth's field which is parallel to its axis. Hence, the instrument theoretically may be used to measure any component of the earth's field by suitable orientation. The sensitivity of the tube may be increased through regeneration by passing the plate current through an additional solenoid. Interesting experimental results have been obtained by using magnetic alloy field pieces to increase the effective magnetic field.

Distribution of Earth Magnetism

The importance of and the need for accurate information on the distribution of the earth's magnetism became clear from the work of Gauss. He set up one of the first magnetic observatories in Göttingen (Germany) in 1832, and there developed suitable instruments for measuring variations

† F. Rieber, "A New Micromagnetometer," *A.I.M.E. Geophysical Prospecting,* 1929, pp. 409-415.
‡ A. W. Hull, *Phys. Rev.* 22 (Second Series), 1923, pp. 279-292
M. Rossiger, *Zeits. für Physik,* 43, 1927, pp. 480-488
M. Rossiger, *Zeits. für Instrumentenkunde,* 49, 1929, pp. 105-113.

in declination and horizontal intensity. Magnetic observatories have since been established in nearly every country. Ambronn† lists forty-eight in his book on geophysics published in 1928.

Magnetic surveys have been completed by various agencies. These surveys cover practically the entire world, both land and water areas, from latitudes 70° North to 60° South. They have been supplemented for high latitudes by the very important magnetic measurements of polar expeditions. In the last 40 years, particularly, improvements in methods of observation, coupled with an international comparison of instruments, have insured high accuracy of results.

Large scale magnetic studies in the United States have been made chiefly by the Coast and Geodetic Survey, a branch of the Department of Commerce which was established in 1843 and began magnetic work shortly thereafter. In 1899 that organization initiated a systematic magnetic survey of the entire country, which included the occupation of at least one station in every county, the stations being situated about 30 to 40 miles apart. This task was completed in 1915. Since then reoccupation of selected stations has been made to determine the changes in the earth's magnetic field.

The Department of Terrestrial Magnetism of the Carnegie Institution in Washington, D.C., was inaugurated in 1904 under the direction of Dr. L. A. Bauer. It has been active in completing the world magnetic survey. Magnetic measurements at sea were carried out successfully, first on the "Galileo", a chartered sailing vessel, and later on the "Carnegie", a sailing vessel with auxiliary steam power. It was especially built for magnetic studies and was so completely free of magnetic material as almost to eliminate the need for compass deviation corrections.

Magnetic Charts.—Contours of equal value of the magnetic elements can be drawn on the basis of Gauss' theory (of the distribution of earth magnetism) from the evaluation of the observational data for the entire earth. As displayed on special small scale maps, such contours are known as *isomagnetic lines*. Isomagnetic lines, as drawn, are purposely smoothed out and, insofar as is possible, do *not* take into account local magnetic disturbances, except as the latter may affect the measured values at a station used.

There are a number of different types of such magnetic maps, or charts, that cover the entire world, or in more detail, one country, as the United States, England, or France, for example.

These maps may show the following: *a.* lines of equal value of declination, called *isogonal lines; b.* contours of equal value of dip, known as *isoclines; c.* like lines of total value of magnetic intensity, which have no special name; *d.* contours of vertical intensity component (Figure 33); or *e.* contours of horizontal magnetic intensity.

Such special charts giving declination are widely used in air and sea navigation, and in land surveying. In general, however, isogonal maps have found little application in magnetic exploration, although they have been employed to some extent in the Lake Superior iron region.

Maps showing the variations of dip are of little use in detailed mag-

† R. Ambronn, Elements of Geophysics, McGraw-Hill, 1928 (translated by M. C. Cobb), page 71.

netic surveys, except to establish an area value of dip, where a dip needle was being used. In like manner, a map of nation-wide scope of the total magnetic intensity would be of limited use. It would serve as a general guide for work with one type of field instrument, the Hotchkiss Super-dip magnetometer. With this magnetometer, as will be explained, measurements of total magnetic intensity at stations are obtained.

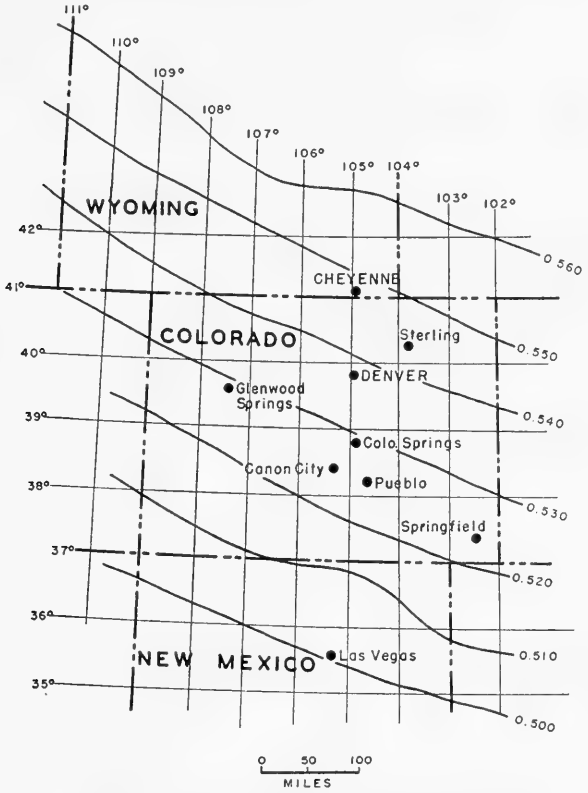

FIG. 33.—A portion of the chart for the United States showing contours of vertical magnetic intensity in c.g.s. units as of January 1, 1925. Such charts are used to find the latitude and longitude correction for magnetic field surveys.

The charts of vertical intensity and of horizontal intensity are, however, necessary in magnetic field work with vertical and horizontal magnetometers. From them the change in the magnetic force per mile for an area of a proposed survey is determined. This change, in gammas per mile, is applied as a latitude and a longitude correction, as will be shown later.

From careful measurements as above described at some 4300 stations in the United States, separate maps have been prepared showing the distribution of the three magnetic elements. A portion of the chart for the

distribution of magnetic vertical intensity is shown in Figure 33. The contours are made as smooth and regular as possible, in order to express the change in vertical intensity throughout the United States as a function of latitude and longitude only.

Latitude and Longitude Correction.—The contours show the value of vertical intensity in gauss. The change in gammas per mile north-south and east-west, used in field surveys with prospecting magnetometers is computed, for a given area, from such a map. This latitude and longitude correction (L. and L. correction) is for the central part of the state of Colorado 11.8 gammas per mile + to the north and 4.7 gammas per mile + to the east.* From a base station the change would be − to the south and − to the west. In the eastern part of the United States the contours of vertical magnetic intensity trend in a NE direction which makes the east-west gamma change per mile − to the east and + to the west.

A similar map for the variation in horizontal intensity is used to calculate the L. and L. correction, for field work with a horizontal magnetometer.

Time Variations.—The earth's magnetic field undergoes three *periodic* variations with time. These are known as secular, annual, and diurnal variations.

Secular variation is a change with a periodicity of about 960 years. Records of measurements of any of the magnetic elements do not extend far enough back to permit an accurate computation of secular change. It is known, however, that declination changed from 8° East in London in 1650 to 2° West in 1700, to a maximum of about 26° West in 1800 and then decreased to some 20° West by 1900. The inclination changed from about 70° to 75° to 71° to 64° at the above dates, respectively, at London. The rate of change is of the order of 2 minutes per year for declination. This change is ordinarily not of importance in magnetic surveys, except when a survey is being checked after a long period of years. For example, a line 1000 ft. long, run due north by compass from Boston in 1925 would have its north end 125 ft. farther west than a similar line run in 1785.

An annual change in the magnetic elements has been observed, having a periodicity of one year. The amplitude of the deviation for declination, in London, is about 2.25 minutes, with a maximum in an easterly direction in August and in a westerly direction in February. This annual variation for North America amounts to about 1 minute and may be considered negligible in general for the application of geomagnetics.

Diurnal variation is of importance in magnetic surveys and must be

* The latitude change in gammas per mile for a given area can be determined from the above chart (Figure 33) by scaling the distance in miles between contour lines and dividing that distance by the number of gammas between contours. For the north-south correction the distance is scaled in a north-south direction, and for the east-west correction the distance is scaled east-west.

corrected for. For a typical day based on an average of many days, the average variation in vertical intensity is shown in Figure 34.

The total variation covers a range of about 20 gammas. The type curve cannot be used for making daily variation correction in field surveys. A given day may be entirely different in the character of its variation.

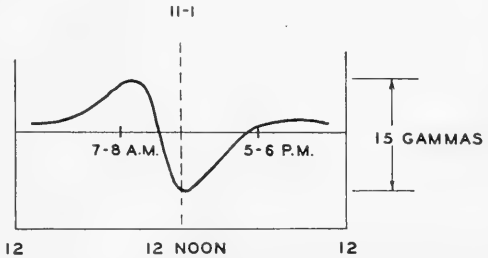

Fig. 34.—Graph of the average daily variation in vertical magnetic intensity. Useful in showing at what time of day the rate of change is the greatest, and hence, when base checks are most necessary.

In practice a reading at the base station is taken when it is first occupied; several times during the day the base is reoccupied and readings taken. Then, assuming the change to be linear between the times of readings, a daily variation or diurnal curve is plotted. From this curve a connection is made for each station read during the interval between readings at the base station. It is also possible to have a second magnetometer permanently at the base station for reading at intervals of ten to twenty minutes, or to use a continuously recording magnetometer, in order to obtain an accurate daily variation curve.

Magnetic Storms.—Magnetic storms are *aperiodic* and quite unpredictable variations in the earth's magnetic field. They are somewhat analogous to air pressure changes as evidenced on a barometer. Magnetic storms may occur very suddenly and cause such a rapid change in magnetic force (up to 500 gammas in less than one half hour) as to necessitate suspension of field operations.

Magnetic storms are of three types: (1) oscillatory, (2) sudden commencement and (3) bay type.

The *oscillatory* magnetic storm is evidenced by a pulsating variation which may be of the order of 10 gammas in horizontal intensity and of a periodicity of from 2 to 10 minutes. Such a pulsation may last about two hours and may take place on what is otherwise a magnetically quiet day. The back-and-forth magnetic pulsation would affect the other magnetic elements, as in the case of all magnetic storms, to some degree, perhaps to the extent of 5 minutes in declination.

The *sudden-commencement* type of magnetic storm is of importance in magnetic field work because it may cause large variations in a most erratic manner and in a very short time. Such magnetic storms appear to occur all over the world at approximately the same time, or within less than ten minutes. They may last a few hours or may even run for a day or more.

When severe, this type of storm may cause an abrupt and sudden change in magnetic force up to as much as 500 gammas in the vertical

intensity component in less than one-half hour. Such a storm would be apparent to the operator of a field magnetometer if he were taking readings at the time. A severe storm may show changes back and forth of the amount mentioned at 30 to 45-minute periods with a dying out or decrease in amplitude with time, but with the possibility that the storm will later come back at high intensity.

Any magnetic field work must quite obviously be suspended during a severe storm. Any stations taken would be unreliable, even though a base magnetometer were used to record daily variation. Fortunately such storms do not occur often; ordinarily not more than one or possibly two take place during the course of a field season.

The *bay* type of magnetic storm is a steady swell, a rise or fall in magnetic force, that may last for two to three hours. It may result in some 20 minutes change in declination, although the vertical and horizontal components of magnetic force are most affected. The bay type of storm usually repeats itself at about a 24-hour interval.

Under ordinary conditions, for field work in the United States it is possible to make arrangements with the nearest magnetic observatory to advise by wire collect of any significant magnetic disturbances. For the Western part of the country the observatory at Tucson, Arizona, is usually the nearest one. As a practical matter the usual base checks, or base instrument for obtaining daily variation, will show if an unusual condition exists. An erratic station, or stations, which do not fit into the contouring may be due to such disturbances.

MAGNETIC PROSPECTING INSTRUMENTS

The Compass.—The most familiar magnetic instrument is the compass. When pointing to the magnetic north, a compass needle aligns itself with the horizontal component of the earth's magnetic field at the point of observation. This property of magnets is utilized in magnetic instruments using magnetic needles; that is, a magnetic needle suspended and free to rotate will align itself with the direction of the lines of force of the magnetic field.

A small counterweight is necessary on a compass needle. For work in the northern hemisphere, it is placed on the south side of the pivot. This counterweight balances the needle by introducing a small moment of force due to gravity and causes the needle to swing in a horizontal plane. The resultant center of gravity is therefore shifted to the south side of the pivot. The need for this counterweight brings out the fact that the lines of force of the earth's magnetic field in most areas have an appreciable dip. The needle seeks to align itself with the direction of the earth's magnetic lines of force and would do so in so far as possible, rubbing on the compass case, were the counterweight not used.

Referring to Figure 35,* it will be seen that the north-seeking end of a compass needle at rest is acted upon by the total intensity force T. This force may be resolved into its horizontal component H and its vertical component Z. On the south-seeking end of the needle a similar condition exists, except that there is repulsion instead of attraction. The vertical components of both the attractive and the repulsive forces tend to rotate the needle in a vertical plane, about its pivot point. To counteract this moment, it is necessary to introduce an opposite and equal effect by using a small counterweight W. The magnitude of this counter moment is Wd. The distance d must therefore be adjusted when going from one area to another having an appreciable change in value of T. This same principle is utilized in the magnetic system of the vertical field magnetometer.

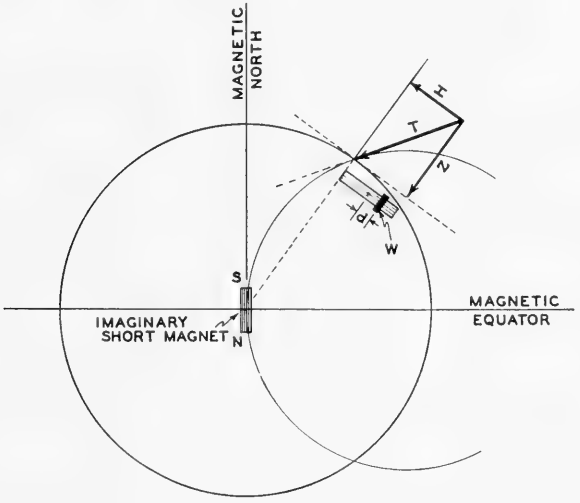

FIG. 35.—Diagram showing magnetic components in northern hemisphere.

When properly adjusted, a compass needle rotates in a horizontal plane and is acted upon *only* by the horizontal component of the earth's magnetic field; the torque due to the vertical magnetic component is balanced by the torque due to the counterweight and does not produce a rotative effect on the needle. For use in the southern hemisphere, the counterweight would be on the north side of the pivot.

The Wilson Attachment for a Brunton Compass

An attachment for a Brunton compass has been devised by Mr. John Wilson so that horizontal magnetic intensity can be measured. The attachment permits the determination of the absolute value of the horizontal

* See also Figure 24.

intensity of the earth's magnetic field with sufficient accuracy for certain kinds of geophysical work, though not for close or accurate magnetic investigations. It can be used where magnetic anomalies exceed 250 gammas. This instrument is of aid in tracing some types of dikes, the limits of intrusive bodies, and the investigation of iron ore deposits. The general precision of the instrument is comparable to the accuracy obtained by the Brunton in traverse survey work.

The Wilson attachment consists of a Brunton compass holder, and an arm graduated in millimeters. Slideable along the arm is a magnet holder,

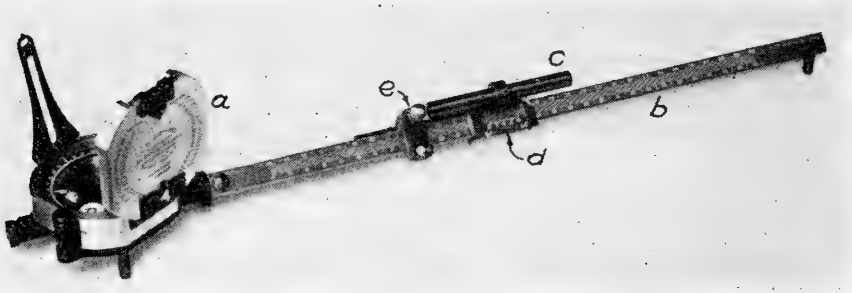

FIG. 36.—Wilson magnetometer attachment. *a*, Brunton compass; *b*, graduated arm; *c*, calibrated magnet; *d*, vernier scale; *e*, vernier adjustment knob with rack and pinion. (Courtesy of Wm. Ainsworth and Sons.)

equipped with a vernier reading device. (Figure 36.) The magnet holder is moved along the arm by a rack and pinion. The magnet arm makes an angle of 120° measured clockwise from the N. end of the compass box.

The instrument may be used on a flat board or a plane table, or mounted on a special tripod. At a station, the instrument is set up and leveled. The zero of the graduated circle of the compass is set at the index on the N. end of the compass box. The compass is then oriented to read zero. A small auxiliary magnet of known moment is placed in the magnet holder on the arm and brought up with its S. pole toward the compass until the compass needle reads exactly 30°. In this position the needle is perpendicular to the axis of the auxiliary magnet. The distance r on the extension arm is read with a vernier to the nearest tenth of a millimeter.

In this relationship the inverse cubes of the distances r are proportional to the horizontal intensities at a series of stations. The formula applicable when the instrument is so used is

$$H = \frac{4M}{r^3}\left[\frac{1}{1 - \frac{L^2}{2r^2} + \frac{L^4}{16r^4}}\right] \tag{43}$$

Where $H =$ horizontal magnetic intensity, in gammas,
$M =$ the magnetic moment of the auxiliary deflector magnet,
$r =$ the distance in cm. between the center of the auxiliary magnet and the compass needle, and
$L =$ the length of the auxiliary magnet.

Usually r is large in comparison to L, and the formula may be simplified.

$$H = \frac{4M}{r^3} \tag{44}$$

With the auxiliary magnet commonly used and reading r to 0.1 of a mm. it would *not* be possible to measure H closer than 25 to 50 gammas. Repeated measurements at any one station will usually show a departure of about 50 gammas from the mean value.†

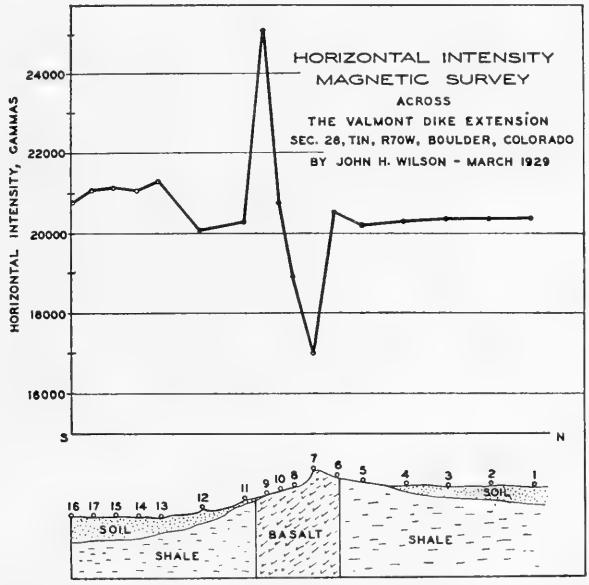

Fig. 37.—Horizontal intensity magnetic survey across the Valmont Dike Extension, Boulder County, Colorado. Survey made with Wilson attachment on a Brunton compass; after J. H. Wilson, 1929.

Figure 37 shows a magnetic traverse across a highly magnetic basalt dike, intruded between shale beds of weak magnetic properties.

Dip Needle Types of Instrument

The Dip Needle.—A dip needle is another simple magnetic instrument. Its center of gravity and center of rotation are at the same point. When in operation, the needle swings only in a vertical plane. Obviously such a needle, when aligned with the earth's magnetic field, measures minimum dip angle and its plane of rotation is in the magnetic meridian.

The dip instrument is read by suspending it vertically, and orienting it a few degrees to the right or the left of the magnetic meridian. The instrument is then slowly rotated through the magnetic meridian and the minimum angle noted. This is the dip angle.

† *A.A.P.G. Bull.*, Vol. 15, No. 11, pp. 1391-1398, Nov., 1931.

If a dip needle is oriented with its plane of rotation at right angles to the magnetic meridian, it will stand vertically. This is true because the horizontal component will be acting through the bearings, and only the vertical component of magnetic force will be effective in aligning the needle. Figure 38 shows a modern dip needle with a counterweight.

The dip needle can be used for geophysical surveys under certain conditions where relatively large anomalies exist. Its precision is about one-half that of the Wilson attachment for the Brunton compass. See Figure 38.

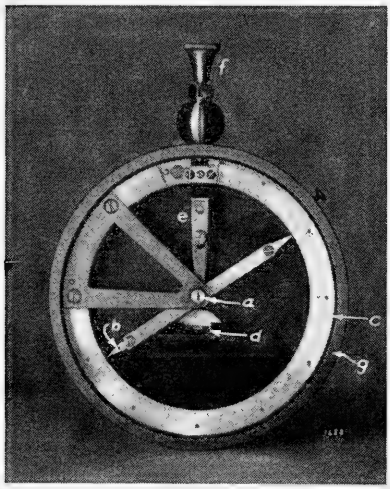

FIG. 38 — Dip Needle — Lake Superior Model; *a*, bearing support screw; *b*, counterweight; *c*, graduated arc; *d*, level; *e*, release finger; *f*, release button; *g*, non-magnetic case. (Courtesy of W. and L. E. Gurley.)

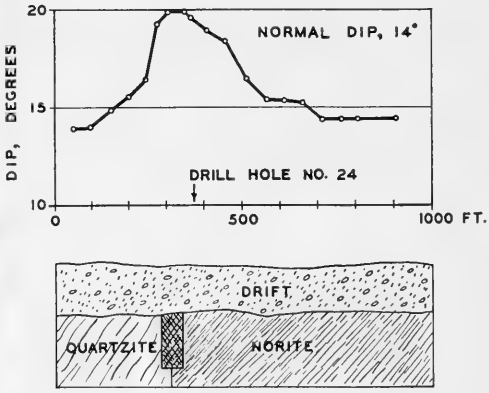

FIG. 39.—Dip needle traverse across nickeliferous ore body at Falconbridge, Sudbury District, Ontario, Canada; after Mason†.

Figure 39 illustrates a dip traverse across the Falconbridge magnetic ore-body. The main ore-body, about 30′ thick under 115′ of overburden, is located in the Sudbury District, Ontario, Canada.

Swedish Mining Compass.—This compass was probably the first "dip needle" employed in magnetic prospecting. At present, it is used widely in regions where the magnetic anomalies are very large and hence easily detected. Well-known regions of this type are the Lake Superior region in America and the Swedish iron ore districts. The Swedish mining compass consists essentially of a pillar which is mounted on the bottom of a cylindrical glass case and supports a needle point pivot.‡ The needle is free to move in a vertical and a horizontal plane. The rotation in the

† M. Mason, "Geophysical Exploration for Ores," *A.I.M.E. Geophysical Volume*, 1929, p. 30.
‡ Eugene Haanel, *On the Location and Examination of Magnetic Ore Deposits by Magnetometric Measurements* (Ottawa, 1904), pp. 65-66.

horizontal plane permits automatic alignment with the magnetic meridian. A counterweight is provided to compensate the effect due to the vertical intensity.

Because this mining compass is affected by the horizontal as well as the vertical intensity, its action is somewhat involved. In practice, the instrument is used for qualitative observations, and H and Z are not measured separately. Despite this limitation, it has been used extensively in prospecting and for preliminary magnetic surveying.

The modern dip needles commonly employed for reconnaissance surveys are more accurate than the Swedish mining compass.‡*

Thalen-Tiberg Magnetometer.—This instrument may be used to measure the horizontal intensity and the vertical intensity. In the former case, it functions as a deflection magnetometer and in the latter case as a magnetic balance. Essentially, the instrument consists of a magnetometer which is rotatable about a horizontal axis † and may be placed either in a horizontal or vertical plane. The magnetic needle system comprises a magnetized needle which carries a sliding weight and is pivoted at its center between two hardened steel bearings to permit free rotational movement. The needle can be adjusted to balance horizontally by altering the position of the sliding weight. A deflecting magnet of known magnetic moment is supported at any desired distance from the pivot by a fixed graduated horizontal arm. The instrument is supported on a light tripod, and means are provided for accurate leveling. The sensitivity of the instrument can be varied by altering the position of the center of gravity of the magnet system with respect to the axis of suspension.

The declination can be measured by orienting the instrument in the geographical meridian. For field intensity measurements, the operation of the instrument is essentially as follows. The deflecting magnet is attached to the horizontal arm; this arm is placed at right angles to the magnetic meridian and the magnetic needle is released. The needle deflects to an azimuth θ where the turning moment due to the magnet counterbalances that due to the earth's field. The deflection θ, the magnetic moment M_d of the deflecting magnet, and the distance r to the pivot can all be measured; hence, the horizontal component H of the earth's field can be calculated from the tangent formula, $H = 2M_d/r^3 \tan\theta$ (approx.). The horizontal intensity can also be calculated from the sine formula, $H = 2M_d/r^3 \sin\theta$ (approx.). The procedure in this case is to rotate the instrument about its vertical axis until the deflecting magnet and magnetized needle are mutually perpendicular and to observe the deflection θ of the needle as it returns to the meridian when the deflecting magnet is removed. Both the tangent and the sine methods yield the *total* horizontal field. The value of the magnetic *anomaly* is obtained by subtracting the normal field at the chosen base station from the field measured.

To measure anomalies in vertical intensity, the magnetometer is placed in a vertical plane at right angles to the magnetic meridian and is balanced so that it is horizontal in the normal earth's field. If the instrument is then set up at successive stations in the field to be surveyed, the tangents of the angles made by the magnetized

‡ N. H. Stearn, "The Dip Needle as a Geological Instrument," *A.I.M.E. Geophysical Prospecting*, 1929, pp. 345-363.

* If the suspension point coincided with the center of gravity, the instrument would be a *dip circle,* i.e., a device for measuring the *inclination* of the earth's field.

† The description given here follows Broughton Edge and Laby, *Geophysical Prospecting* (Cambr. Univ. Press, 1931), p. 182.

needle with the horizontal will be proportional to the vertical intensity *anomalies* at these stations.

The Thalen-Tiberg magnetometer is most useful in regions where the vertical intensity anomalies exceed 20 gammas.

In another type of magnetometer based on the compass principle, the opposing torque is supplied by the torsion of a helical spring instead of the field due to an auxiliary magnet. One of the earliest instruments of this type, the Dahlblom pocket magnetometer, comprises a compass mounted in a circular case, the latter being free to rotate about a horizontal axis. Because the magnetic needle system can swing in both a horizontal and a vertical plane, the magnetometer may be used to measure either the horizontal or the vertical intensity.† A magnetometer which is similar to the Dahlblom instrument, except that it measures the vertical intensity only, has also been proposed.‡

The Hotchkiss Superdip.—The Hotchkiss Superdip magnetometer combines in one instrument the functions of a dip needle and a magnetometer. Essentially, the superdip is an improved dip needle with adjustable sensitivity limited only by friction and other mechanical difficulties. The operating principles may best be explained by comparing the ordinary dip needle with the Hotchkiss Superdip.*

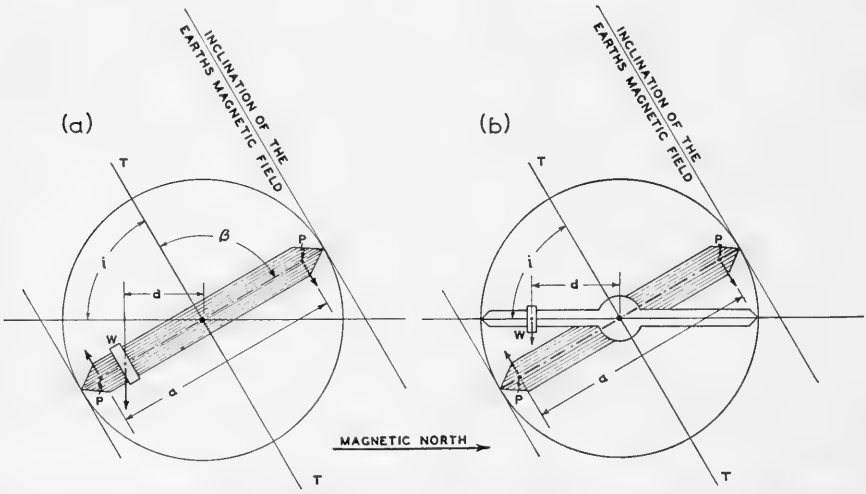

FIG. 40.—Sketches illustrating working principles of the ordinary dip needle *(a)* and the Superdip *(b)*. (After Stearn, *A.I.M.E. Geophysical Prospecting*, 1932.)

The action of the ordinary dip needle in measuring the intensity of the earth's field derives from the effect of the counterweight with which the needle is provided. (Figure 40.) When the instrument is oriented in the plane of the magnetic meridian, the counterweight serves to balance the magnetized needle at some fixed angle to the direction of the earth's

† E. Haanel, *On the Location and Examination of Magnetic Ore Deposits by Magnetometric Measurements* (Ottawa, 1904), pp. 99-106.

‡ C. A. Heiland, *Physics*, Vol. 3, pp. 18-22, July, 1932.

* N. H. Stearn, "Practical Geomagnetic Exploration with the Hotchkiss Superdip," *A.I.M.E. Geophysical Prospecting* (1932), pp. 169-197.

resultant field. That is, the magnet is acted on by two opposing couples and comes to rest in an azimuth where the couples are equal in magnitude. The magnetic couple (equal to the product of the magnetic moment M' of the needle times the sine of the angle β between M' and T) tends to rotate the needle in the direction of the earth's field, while the gravitational couple (equal to the product of the weight of the counterweight times d, its perpendicular distance from the center of gravity of the needle) opposes this rotation.

The equilibrium condition for a dip needle is given by the equation:

$$Wd = TM' \sin \beta \tag{45}$$

or

$$\frac{TM'}{W} = \frac{d}{\sin \beta}$$

where

Wd = couple due to the counterweight.
T = total earth's field.
M' = magnetic moment of needle.
β = angle between T and M'.

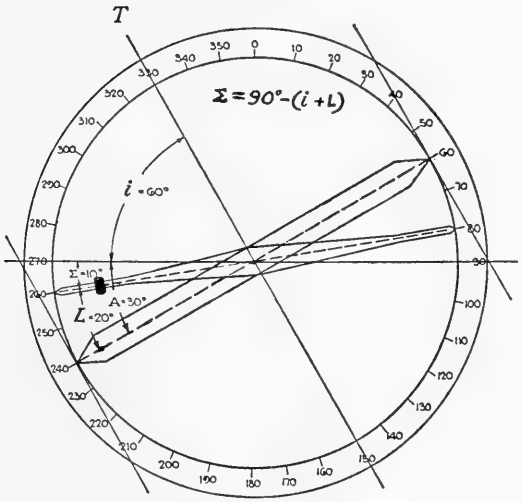

Fig. 41.—Setting of Hotchkiss Superdip. (After Stearn, *A.I.M.E. Geophysical Prospecting*, 1932.)

The characteristic feature of the Hotchkiss Superdip is that d and $\sin \beta$ are made to vary proportionately in such manner that d is a maximum when $\sin \beta$ is 1. This could be achieved in an ordinary needle only for the unusual case of inclination equal to 90°. It is accomplished in the Hotchkiss Superdip by an ingenious arrangement employing a duplex needle assembly which consists of an adjustable counterarm (provided

with a counterweight) frictionally pivoted with the magnetized needle. The theoretical sensitivity of the Superdip is determined almost entirely by the angle between the counterarm and the needle. (Figure 41.)

In practice, the limiting angle is established by the inclination of the earth's field. For example, if the inclination i of the earth's field is 60° the limiting angle A between the counterarm and the magnet would be 30° for maximum sensitivity, because in this position the counterarm is horizontal when the magnet is at right angles to the earth's field. Practically, however, maximum sensitivity is seldom desirable in field work, and the angle L which is actually set off is smaller than the limiting angle. The difference is called the sensitivity or Σ angle ($\Sigma = 90° - i - L$) and is adjustable to any desired degree of sensitivity.

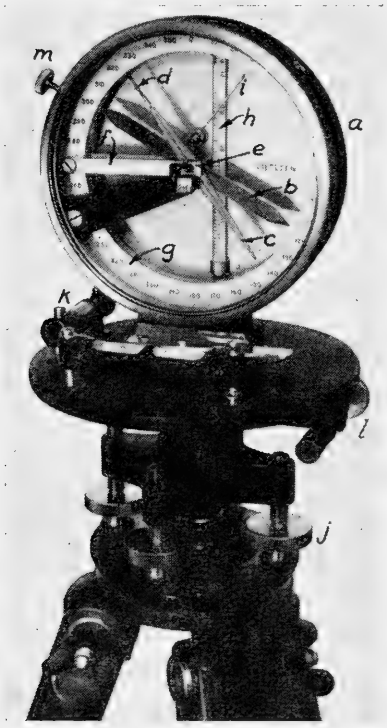

FIG. 42.—The Hotchkiss Superdip Magnetometer. *a*, non-magnetic case; *b*, magnet; *c*, counterarm; *d*, counterweight; *e*, pivot; *f*, release; *g*, scale circle; *h*, thermometer; *i*, adjustment finger; *j*, quadrature leveling screws; *k*, levels; *l*, azimuth adjustment; *m*, release screw.

A photographic view of the Hotchkiss Superdip is shown in Figure 42. The dust-tight cylindrical case is made of brass or aluminum and is mounted vertically. It is about 6 inches in diameter and 1½ inches thick and has a removable glass face. The swinging assembly which is mounted in the case consists of the magnet, counterarm, counterweight, and pivot, as well as a release device, scale circle, thermometer, and a mechanical adjustment finger. The instrument is mounted on a sturdy tripod which is equipped with quadrature leveling screws, two levels (at right angles), and vernier azimuth adjustment.

The magnetic system is a thin bar magnet made of tungsten-cobalt steel. The moving system swings in a vertical plane and is mounted on a pivot. The pivot is located at the center of gravity of the magnet and rolls on a pair of level jeweled knife-edges. The counterarm, which is attached to the same pivot, may be adjusted to any desired angular position with the axis of the magnet. The counterweight is placed on one end of the counterarm and is adjusted by varying its distance from the pivot.

The release device comprises two levers operated by a thumb screw, and is so designed that the swinging assembly may be raised from the horizontal

knife-edges and clamped against two centering pivot guides. The scale circle is graduated in degrees of arc so that the position of the magnet can be measured. The thermometer is mounted in the case to provide data for temperature corrections. A light wire arm, operated from the back of the case, moves the swinging assembly to its zero position. Orientation of the instrument in the field of the magnetic meridian is accomplished by means of an auxiliary compass which is placed on the tripod table. After proper orientation the compass is removed and the Superdip fastened to the tripod table.

Figure 43 is a graph of the practical working sensitivity of a typical Superdip. The curve marked $\Sigma = 0°$ is of interest. Theoretically it should coincide with the zero abscissa; its departure therefrom indicates the amount of the departure from infinite sensitivity introduced by the mechanical features of the instrument, including friction. Although the sensitivity curves for the various values of Σ are curved rather than straight, a simple linear coefficient of sensitivity is sufficiently accurate—e.g., 12½ gammas per scale division for a Σ of 1°.

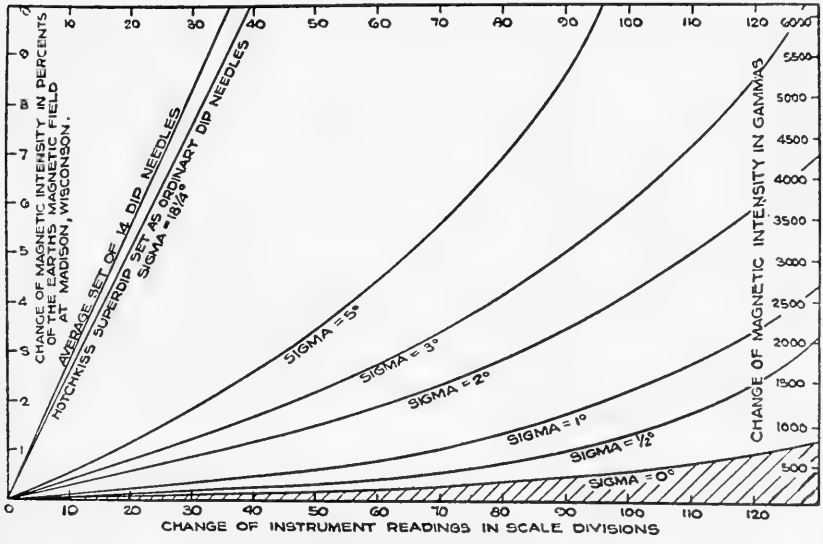

Fig. 43.—Sensitivity of Hotchkiss Superdip. (Stearn, *A.I.M.E. Geophysical Prospecting*, 1932.)

Preliminary Adjustment of Superdip Magnetometer in the Field

(1) The tripod table is leveled, and oriented by means of the compass.

(2) The counterarm is set parallel to the magnet, and the angle of inclination for the area is measured by using a small auxiliary scale.

(3) The counterarm is set at the desired sensitivity (sigma value).

(4) The counterweight is adjusted until the position of rest of the assembly is approximately at right angles to the magnetic inclination.

Each station reading of a Hotchkiss Superdip magnetometer involves the following steps:

(1) Set up the tripod and level the mounting plate.

(2) Place the compass on the mounting plate. Orient the plate in its proper relation to the earth's magnetic meridian, and clamp it.

(3) Remove the compass to a safe distance (20 feet or more) and mount the magnetometer.

(4) Move the north pole of the magnet to the zero position on the circular scale.

(5) Carefully lower the swinging assembly to the agate edges and note the end of the swing. (The reading taken is the position of the north pole of the magnet relative to the circular scale at the end of the swing.)

(6) Clamp the swinging assembly and record the reading, temperature, time, and location of the station.

Figure 43 also shows the average sensitivity of dip needles. This sensitivity is comparable to the Superdip, when $\Sigma = 18\frac{1}{4}°$. As the value of Σ is decreased, the sensitivity of the Superdip increases.

A profile run with a Superdip instrument is given in Figure 44. The line of profile was N 15° W, from a point two miles north of Amarillo, Texas, to the north line of Potter County in the same state. The Potter County fault and the Amarillo buried granite ridge were crossed. The Superdip was set with a value for Σ of about 2°, which gave a working sensitivity about 37 times that of an ordinary dip needle.†

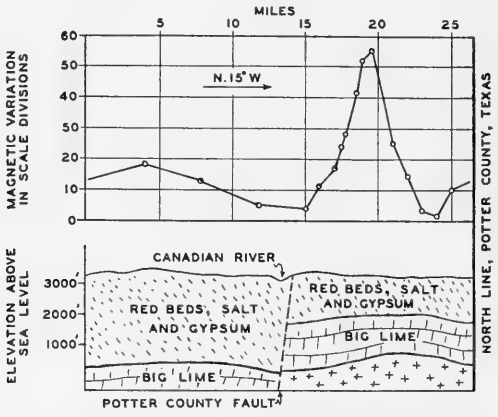

FIG. 44.—Magnetic profile with Hotchkiss Superdip Magnetometer across the Buried Granite Ridge in the Texas Panhandle. (After Stearn.)

Schmidt-type Field Magnetometers

The most widely used field magnetometers are those of the general type originally manufactured by the Askania Werke, of Berlin, Germany. It is significant that the beginning of the art of magnetic prospecting as practiced today dates from 1915 with the development, by Adolph Schmidt, of a portable magnetometer with which small magnetic anomalies could be measured rapidly.

† N. H. Stearn, *A.I.M.E. Geophysical Volume*, 1932, p. 189.

The following theory and description apply generally to all Schmidt-type field magnetometers, whether the Askania, made in Germany, the Ruska magnetometer made in Houston, Texas, or the Hilger and Watts magnetometer, made in England.

Two types of Askania-Schmidt field balance are available; one measures the vertical component of the earth's field and the other the horizontal component. In both instruments the mass distribution of the balance system is so arranged that the force exerted by gravity holds the magnetic system in such a position that it is acted upon chiefly by the desired component (vertical or horizontal) which is to be measured.†

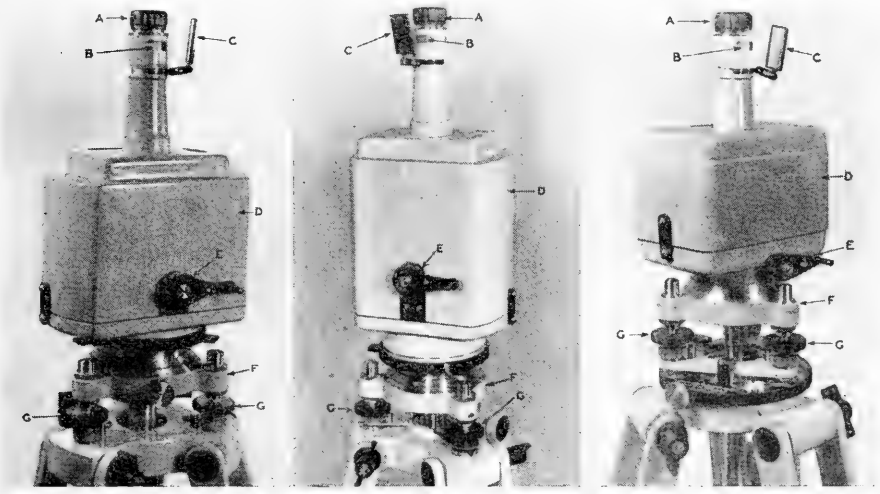

FIG. 45.—Views of the Ruska magnetometers: vertical component instrument, left; horizontal component instrument, center; and the Scout magnetometer, right. A, gauss eyepiece; b, window; C, mirror; D, case; E, clamp lever; F, tripod head; G, leveling screws. (Courtesy of the Ruska Instrument Corporation.)

Exterior views of late models of the Askania-Schmidt type magnetometers are shown in Figure 48.

Views of the Ruska magnetometers are shown in Figure 45. The standard vertical and horizontal component instruments can be adjusted for sensitivities of 10 gammas or more per scale division, with a total scale range of 120 divisions. The Scout vertical component magnetometer has a sensitivity of 25 gammas per division, and a scale range of 3000 gammas. This instrument is small and light-weight, and is designed primarily for reconnaissance and mining surveys.

The Hilger and Watts instruments are shown in Figure 46. The sensi-

† J. Wallace Joyce, *Manual on Geophysical Prospecting with the Magnetometer*, U. S. Bureau of Mines Publication (printed by the American Askania Corporation, Houston, Texas, 1937).

tivities are adjustable from 10 gammas or more per scale division, with a scale range of 40 divisions. The sensitivity is usually adjusted to a value of about 30 gammas per scale division.

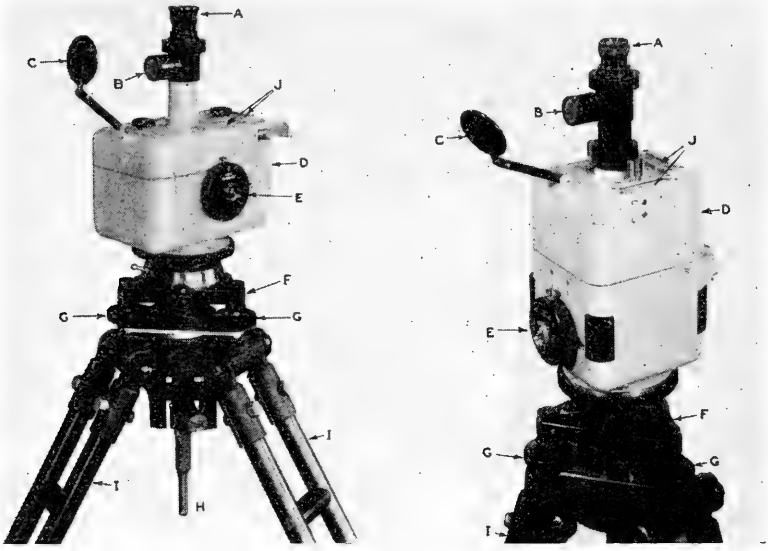

FIG. 46.—Hilger and Watts magnetometers. *Left,* vertical component instrument; *right,* horizontal component instrument. A, gauss eyepiece; B, light window; C, mirror; D, case; E, clamp lever; F, tripod head; G, leveling screws; H, auxiliary magnet; I, tripod; J, spirit levels. (Courtesy of Hilger and Watts, Ltd.)

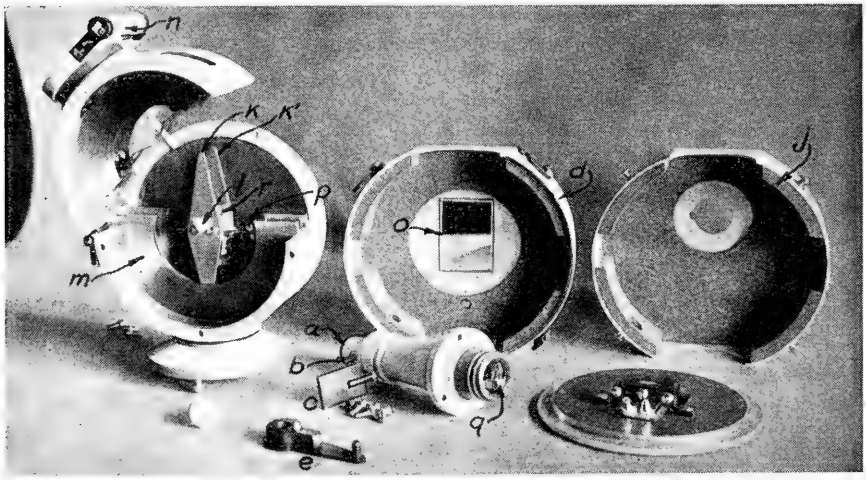

FIG. 47.—Interior view of Askania horizontal component field balance. *a,* gauss eyepiece; *b,* light window; *c,* mirror; *d,* instrument case; *e,* clamp lever; *j,* cork thermal insulation; *k* and *k',* magnetic system; *l,* quartz knife-edge; *m,* copper damping plates; *n,* level bubbles; *o,* door in case with mirror attached for reading thermometers; *p,* counterbalances; *q,* objective lens; *r,* mirror.

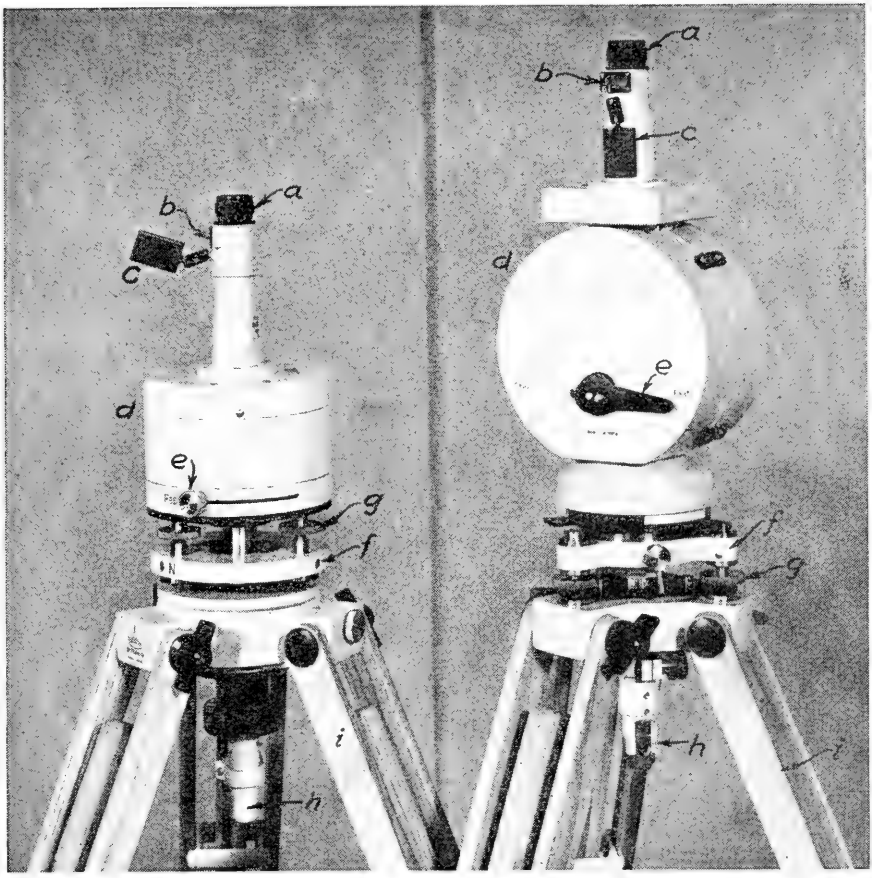

FIG. 48.—A, standard Askania magnetometer for measuring vertical or horizontal magnetic intensity; B, simplified Askania vertical magnetometer. *a*, gauss eyepiece; *b*, light window; *c*, mirror; *d*, instrument case; *e*, clamp lever; *f*, tripod head; *g*, leveling screws; *h*, auxiliary magnet holder; *i*, tripod legs.

Magnet System

The magnet system consists of two gold-plated, magnetized bars of tungsten or cobalt steel fastened together by a cube-shaped, structural member made of aluminum.† A view of two types of vertical and horizontal component magnetic systems is shown in Figure 49. A quartz knife-edge is fastened to the block at right angles to the long axes of the magnets. The quartz knife-edge rests on two semi-cylindrical quartz bearings and supports the moving system. An arresting system is provided to lift the quartz knife-edges from the cylindrical quartz bearings while the

† Erwin Roux, "Magnetic Balance for the Measurement of Intensities," U. S. Patent 1,976,636, Oct. 9, 1934.

instrument is being moved. This arrangement prevents "chipping" or other injury to the edges and also provides a means for resetting the system in the same place on the bearings. For transportation of the instrument, the magnet system must be clamped in the arrested position. Oscillations of the magnet system are dampened by eddy currents induced in copper plates (removable) placed near the poles of the magnets.

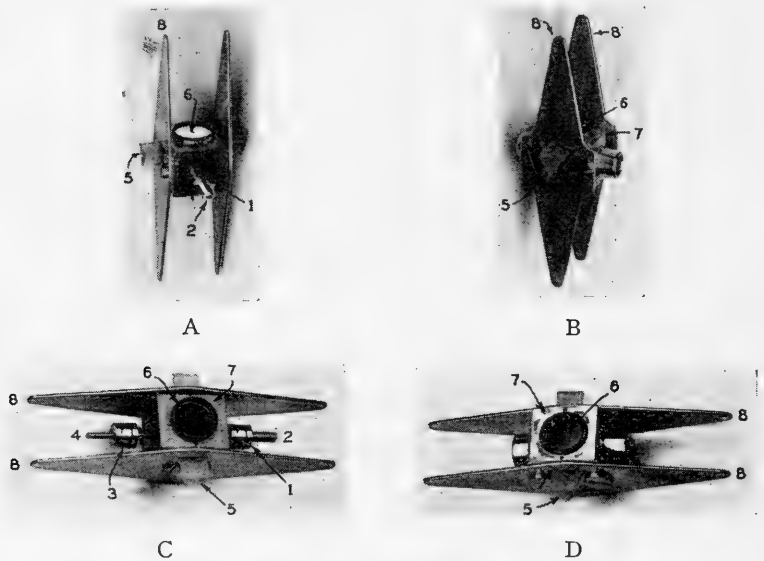

FIG. 49.—Magnetic systems of Askania magnetometers.

A—New-type, horizontal component, temperature-compensated system.
B—Uncompensated, horizontal component system.
C—New type vertical component, temperature-compensated system.
D—Uncompensated, vertical component system.

1—Temperature compensation weight.
2—Temperature compensation spindle (aluminum).
3—Latitude adjustment weight.
4—Latitude adjustment spindle (invar steel).
5—Quartz knife-edge.
6—Mirror.
7—Aluminum frame.
8—Magnets.

In order to provide for temperature corrections, two thermometers (having ranges of −15° to 24° C. and 17° to 55° C.) are fastened inside the case. The magnet system and thermometers are enclosed in a cork-lined, aluminum casing to minimize rapid temperature changes.

Small displacements of the magnet system from the horizontal are directly proportional to the vertical intensity. They are measured by means of a telescope with a gauss eyepiece using the optical arrangement shown in Figure 50. Sky light is reflected from a mirror, passes through a ground glass window in the side of the telescope and falls on a reflecting plate which deflects it downwardly so that it illuminates a scale. The scale is etched on a transparent glass plate situated at the focus point of the objective lens. (The latter is located vertically above the mirror attached to the magnet system.) The light transmitted through the scale plate

passes through the objective lens and is reflected back by the plane mirror fastened to the magnet system. Thus, two scales are seen superimposed in the eyepiece of the telescope; one is the direct and the other the reflected image. The difference in position of corresponding marks on these scales is a measure of the amount of the deflection of the magnet system.

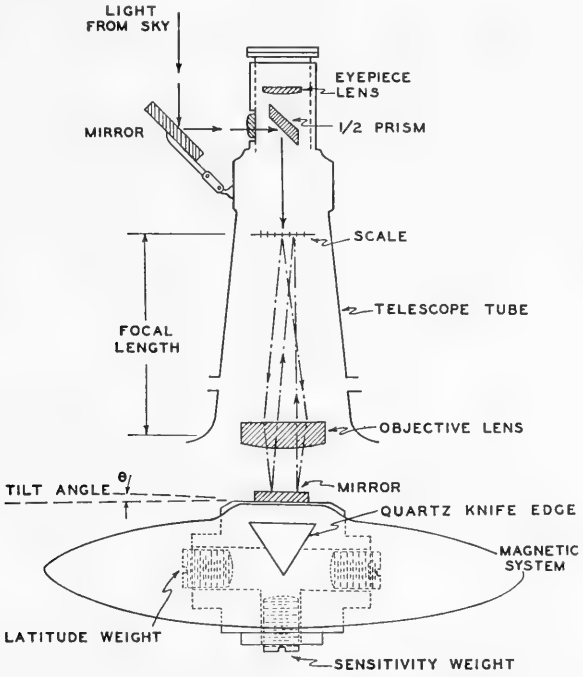

FIG. 50.—Optical system, vertical component magnetometer.

A vertical brass weight, supported on a threaded rod on the under side of the magnet system, affords a means of varying the sensitivity of the instrument. For ordinary subsurface structural investigations, the magnetic system of the vertical balance is usually adjusted for a sensitivity of about 10 to 30 gammas per scale division. The scale in one type of instrument is divided into 120 divisions; hence, the intensity range of the instrument is approximately 1200 to 3600 gammas. In areas of large magnetic disturbances, the sensitivity is decreased, with a resultant increase in total range of the instrument.

As shown in Figure 51, the magnetometer is clamped on a special adjustable wooden tripod, the graduated rotational head of which is leveled by means of a center bubble and three leveling screws. Fastened to the under side of the tripod head is an extension tube holder for an auxiliary magnet. A thumb screw clamps the auxiliary magnet at any desired dis-

tance from the magnetometer. (The distance may be read directly on a graduated scale etched on the magnet holder.)

Accessories consist of a compass which can be fitted into the tripod head for determination of the magnetic meridian, auxiliary magnets of various strengths, and small tools for adjusting and cleaning the instrument. Canvas cases are provided for carrying the magnetometer and the tripod.

Factors Affecting Magnetometer Readings

Orientation.—Orientation of the vertical component magnetometer must be such that the axis of rotation of the magnetic system is in the plane of the magnetic meridian and is horizontal. Orientation of the horizontal component magnetometer must be such that the axis of rotation of

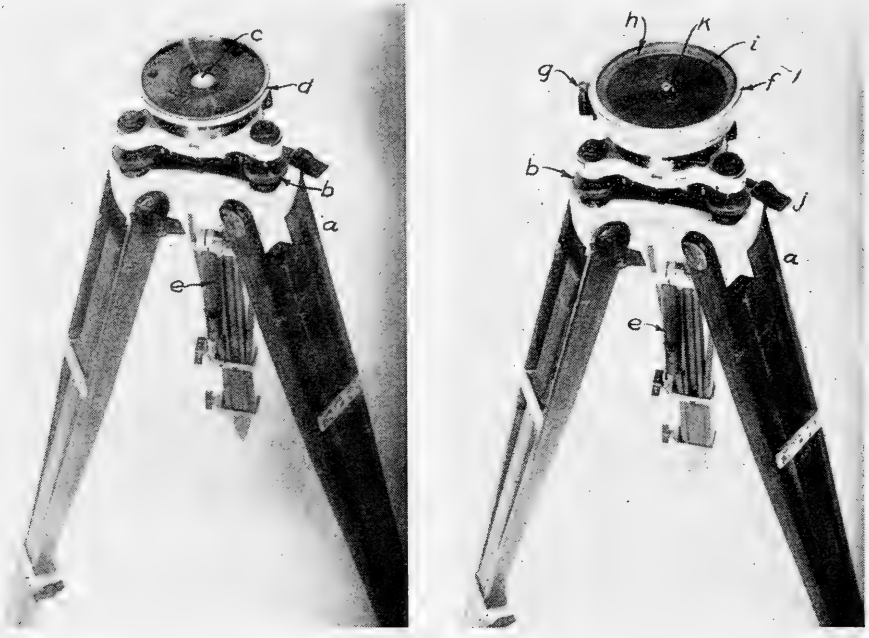

A B

FIG. 51.—Tripod leveling and orientation. *a*, tripod; *b*, level screws; *c*, level bubble; *d*, turntable; *e*, extension tube for auxiliary magnet; *f*, compass; *g*, compass needle clamp screw; *h*, graduated arc of 360°; *i*, compass needle; *j*, leg clamps; *k*, jewel support.

the magnetic system is perpendicular to the plane of the magnetic meridian and is also horizontal. The instrument is oriented indirectly as one of the steps in the initial set-up of the tripod; which consists of a turntable, adjustable auxiliary magnet holder, turntable stop-ring, turntable bearing, and leveling screws. The tripod head is also provided with three lugs to which are fastened three wooden tripod legs. The top of the turn-

table (Figure 51A) contains guide holes so that either the compass or the magnetometer may be placed in the same relative position on the turntable at a series of stations. In the center of the turntable is the level bubble used in preliminary leveling of the tripod head for initial orientation. The stop-ring is so adjusted that the turntable may be turned exactly 180° without reading the scale or compass, thereby facilitating check readings.

The turntable is oriented by placing the compass on it. (See Figure 51B.) Orientation of the instrument must be correct to within one-half degree of arc. This requires care and is one of the sources of errors militating against accuracy. Misalignment of the vertical instrument causes an error which is chiefly due to two factors: (a) a small portion of the horizontal magnetic component of the earth's field will act on the magnet system, and (b) the scale constant of the instrument will be altered. Misalignment of the horizontal instrument introduces a small portion of the vertical component which decreases the true reading. However, the sensitivity of the horizontal instrument is not affected by misalignment of a few degrees.

Leveling.—Initial leveling of the tripod head is accomplished by the level bubble. This leveling is sufficiently accurate for orientation of the turntable by the compass. After the orientation step is completed, the compass is removed from the turntable and the magnetometer is placed on it in the proper orientation for that station. The instrument is now accurately leveled by adjusting the three leveling screws on the tripod head and observing the two levels fastened to the magnetometer itself. The leveling should be accurate to within a half-division of the level bubbles (15 seconds of arc); under these conditions, errors due to incorrect leveling will be less than 0.1 of a scale division. If the leveling is changed by one division, due to clamping, unclamping, or rotation of the turntable, the instrument should be releveled and the reading repeated.

One prevalent cause of shifting of the instrument is due to improper placing of the tripod when first set up at the station. The tripod legs should make an angle of about 30° with the vertical and should be firmly pressed into the ground when initially set up. Apparent shifting of the instrument may be due to unequal expansion of the level glasses and supports when in the direct rays of the sun. The operator should stand between the instrument and the sun or employ an umbrella. Instruments at base stations should be shielded from direct sunlight and protected from wind and rain by suitable shelter.

Instrument Readings.—The optical system in the Askania magnetometers is shown in schematic form in Figure 50. Deflections are read by observing the relative displacement of two scale images. In the magnetometers manufactured prior to about 1935, the scale had 40 equal divisions,

and of these the 0, the 20, and the 40 division lines were longer and heavier than the others. This is illustrated in Figure 52.

FIG. 52.—Scale in old style magnetometers as it appears with system arrested.

In reading, the 20 mark, or center, of the reflected (moving) scale is used as an index on the stationary scale. This is shown in Figure 53(b). The tilt of the magnetic system at a station may be so great that the 20, or center index, is not on the stationary scale, in which case the 0 or the 40 index may be used, as in Figure 53(c). With these different indexes, the range of the scale is from − 20 to + 60 or a total of 80 scale divisions.

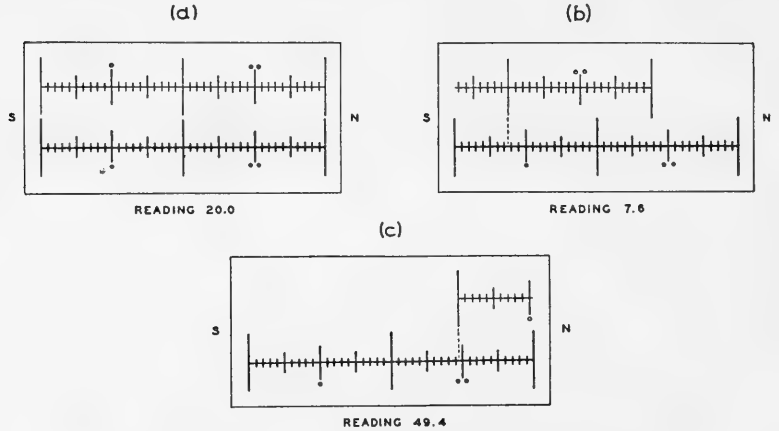

FIG. 53.—Examples of 3 scale readings of older type magnetometers. Upper scale is the moving scale. (Scales offset, to illustrate method of reading.)

The fixed and moving scales of Figure 53 show only the method of reading. In looking into the telescope of the magnetometer the two scales coincide closely. The moving scale appears to be superimposed on the fixed scale and seems to float along it as the system tilts.

When the magnetic system is at rest horizontally (zero tilt angle), the center of the scale, or 20 mark of the reflected scale, coincides with the center or 20 mark of the stationary scale. (See Figure 53a.) When reading the instrument, if the reflected (or moving) scale runs toward the north as marked on the outer case by an N, the tilt angle of the north end of the magnetic system is below a horizontal surface through the bearings on which the system rests. In this case (in the northern hemisphere) the reading is considered as plus or greater than 20. If the

moving scale runs toward the south end of the instrument, the tilt angle is above the horizontal and the reading is less than 20. The use of a reading of 20 for the horizontal position of the system or zero tilt angle is arbitrary. In each case the amount of a reading is so many scale divisions from 20, as shown in Figure 53.

In the optical system of the later models of magnetometers the scale has 60 divisions. Mounted to the side of this scale is a glass plate with 3 index lines. The double scale image is avoided, and by using the position of the index lines on the scale to measure the tilt angle, a range of 120 scale divisions is obtained.

In field work with the old style systems, the magnetic system is adjusted by means of the latitude adjustment screws at the ends of the aluminum block. In the new type systems, this adjustment is made by moving the weight on the latitude spindle. In both cases, the adjustment is made so that the instrument reads close to the 20 mark at the base station used in an area, when set up and the system released. This adjustment must be changed if a survey extends over an area so large that the normal increase or decrease of magnetic intensity causes the reflected scale to go out of view.

Theory of Operation of Vertical Magnetometer.—The magnetic system of the Askania vertical magnetometer is provided with three adjust-

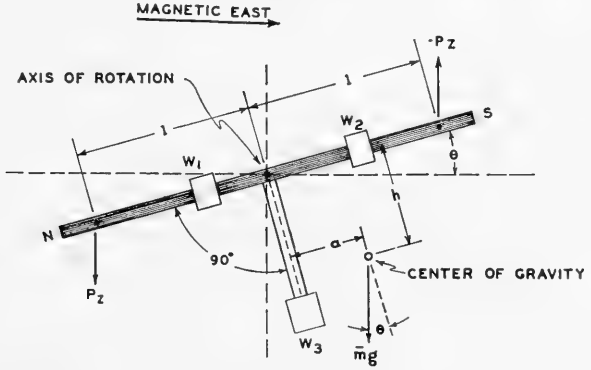

FIG. 54.—Diagram showing relationships of different parts of compensated magnetic system for the *vertical* magnetometer. Note that the center of gravity has been shifted away from the axis of rotation.

able counterweights or masses W_1, W_2, and W_3 as shown in Figure 54, illustrating the new-style, temperature-compensated system. The distribution of the mass of the magnetic blades and of the aluminum block in the older-style system, however, produced a like result, except that temperature compensation was not complete. The same theory applies to both systems.

The combined effect of these weights, or the mass distribution between

blocks and blades, is to position the center of gravity of the magnetic system at a point below and on the south (pole) side of the axis of rotation or knife edge.

m' = total mass of magnetic system in grams. (Note change in the meaning of m' as here used in relation to m as used previously for pole strength.)
g = acceleration due to gravity in cm. per sec. per sec.
$2l$ = distance between magnetic poles of system.
a = horizontal displacement and h = vertical displacement of center of gravity of the system from its axis of rotation, in cm., when $\theta = 0°$.
p = pole strength of system c.g.s. units.
$M = 2pl$ = magnetic moment of system.
Z = vertical component of the magnetic field, gammas.
$P_z = pZ$ = force on pole due to vertical component of earth's field.
θ = deflection angle of system.
W_1 = temperature coefficient adjustment weight.
W_2 = latitude adjustment weight.
W_3 = sensitivity adjustment weight.

The torque T_z on the magnet system due to the vertical magnetic component Z, is given by the equation:

$$T_z = (2pl)\ Z \cos\theta$$

However, $2pl = M$ = magnetic moment of the magnetic system from which we can write:

$$T_z = M\ Z \cos\theta \tag{46}$$

which is the torque due to the vertical component of the earth's magnetic field, when the magnetic system is oriented with its axis in the plane of the magnetic meridian, and horizontal.

The torque due to gravity T_g, opposes the magnetic torque T_z. The gravitational torque T_g may be expressed by

$$T_g = m'ga \cos\theta + m'gh \sin\theta \tag{46a}$$

When the magnetic moment equals the gravity moment, the system will come to equilibrium, and then $T_z = T_g$ or

$$MZ \cos\theta = m'ga \cos\theta + m'gh \sin\theta$$

from which may be derived

$$\tan\theta = \frac{MZ - m'ga}{m'gh} \tag{47}$$

To convert the angular deflection of the magnetic system into scale deflection it is seen that

$$\tan 2\theta = \frac{S - S_o}{f}$$

where θ = the angle of tilt of the system
S = scale reading corresponding to this deflection
S_o = scale reading corresponding to $\theta = 0°$, or when the axis of the system is horizontal.
f = the focal length of the objective lens of the telescope.

But, from trigonometry,

$$\tan 2\theta = \frac{2 \tan\theta}{1 - \tan^2\theta}$$

and since $\tan^2\theta$ is small compared to 1 (for small θ) the above can be written

$$\tan\theta = \frac{S - S_o}{2f}$$

since the design of the instrument is such that the maximum deflection angle is less than 2°, we can derive the relationship;

$$S - S_o = 2f\,\frac{MZ - m'ga}{m'gh} \tag{48}$$

If S_1 = the scale reading at one station and S_2 the scale reading at another station, corresponding to vertical intensity Z_1 and Z_2 respectively at the two stations, then

$$S_1 - S_2 = \frac{2fM\ (Z_1 - Z_2)}{m'gh}\ . \tag{49}$$

$$\text{If } E = \frac{m'gh}{2fM} \tag{50}$$

is called the scale value of the instrument then

$$Z_1 - Z_2 = E\ (S_1 - S_2), \tag{51}$$

or in words: the difference in vertical intensity at two stations is proportional to the difference in scale readings at the two stations. Further details are given in references†.

Theory of Operation of Horizontal Magnetometer.—The Schmidt-type horizontal component magnetometer is used to measure differences in the horizontal component of the earth's field at different stations. The same general arrangement of knife edge, blades, block and quartz bearings is used. The magnetic blades, however, stand vertically and the instrument is operated with the plane of rotation of the blades in the magnetic meridian.

Figure 55 shows the vector relationships of the various forces acting upon the moving system. The vertical component of the earth's field acts chiefly against the bearings and hence has a negligible rotational component at the small angles of tilt utilized in the measurements.

The magnetic component of the earth's field causes a torque, which may be expressed by the following equation:

$$T_m = 2Hpl\cos\theta - 2Zpl\sin\theta$$

but since $2pl = M$

$$T_m = MH\cos\theta - MZ\sin\theta \tag{52}$$

† O. C. Lester, "A Simple Derivation of the Working Equations of Magnetic Variometers for the Vertical and Horizontal Intensity." *A.A.P.G. Bull., Vol. 12*, p. 855, 1928.
C. A. Heiland and W. E. Pugh, "Theory and Experiments Concerning a New Compensated Magnetometer System," *A.I.M.E. Tech. Pub. 482*, July, 1932.
C. A. Heiland, "Theory of Adolf Schmidt's Horizontal Field Balance," *A.I.M.E. Geophysical Volume*, 1929, pp. 261-314.

The opposing gravitational torque is

$$T_g = m'ga \cos \theta + m'gh \sin \theta \qquad (52a)$$

At equilibrium, these two torques are equal and opposite, so by equating

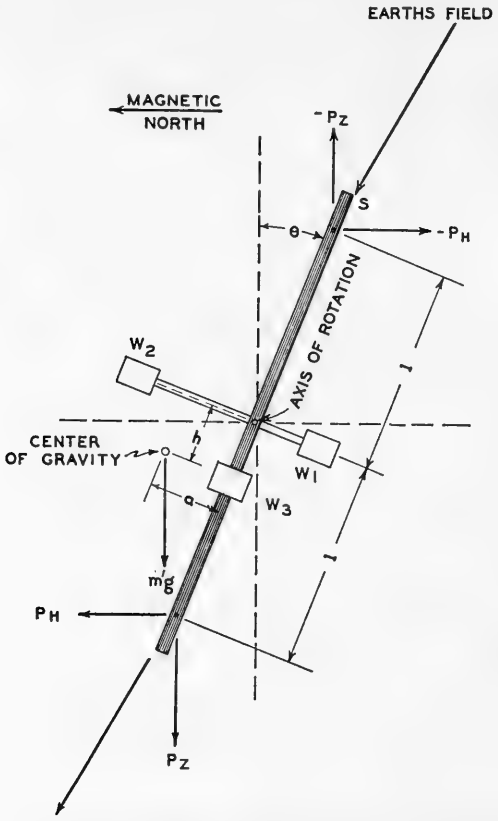

FIG. 55.—Diagram showing relationships of different parts of compensated magnetic system for *horizontal* magnetometer.

the two equations we determine that,

$$\tan \theta = \frac{MH - m'ga}{MZ + m'gh} \qquad (53)$$

m' = mass of the magnetic system in grams;
g = acceleration due to gravity in cm. per sec. per sec.
$2l$ = distance in centimeters between magnetic poles of the system;
a = the horizontal distance and
h = the vertical distance of the center of gravity of the system from the axis of rotation, in cm., when $\theta = 0°$.
P = pole strength of the system, c.g.s. units;
M = $2pl$ = magnetic moment of the system.
Z = vertical component of earth's magnetic field, gammas;
H = horizontal component of the earth's magnetic field, gammas;

P_Z = pZ = force on pole due to vertical component of earth's field.
P_H = pH = force on pole due to horizontal component of earth's field.
θ = deflection angle of the system.
W_1 = temperature coefficient adjustment weight.
W_2 = latitude adjustment weight.
W_3 = sensitivity adjustment weight.

Calibration of Schmidt-type Magnetometers

It is necessary to know two constants of the magnetometer used: namely, the *scale value, E,* and the temperature coefficient, T_c, to calculate the data from the field measurements.

Scale Value Determination.—The physical significance of the scale value has previously been given in terms of the mass and magnetic moment of the magnetic system, the gravity force acting, the focal length, and the vertical distance of the center of gravity from the center of rotation. (Equation 50.) It also may be defined as *the number of gammas of magnetic force necessary to deflect the magnetic system one scale division.* The scale value usually is determined by either of two methods; (1) using a calibrating coil, or (2) using auxiliary magnets.

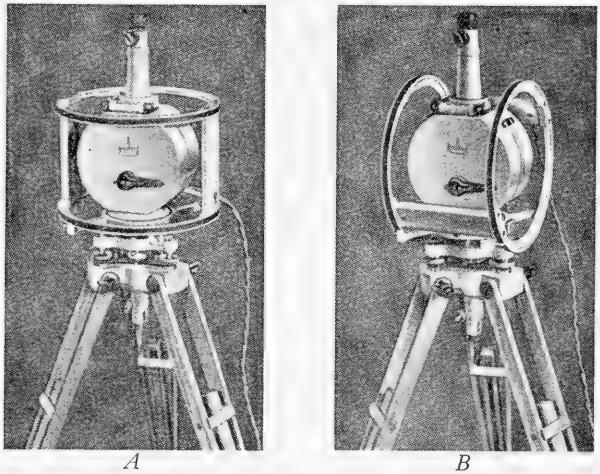

A *B*

FIG. 56.—*A,* vertical component magnetometer, and *B,* horizontal component magnetometer with calibration coil in position. (Courtesy American Askania Corp.)

Scale Value Using Calibrating Coil.—A magnetic field of known strength and direction can be created by passing a direct current through a coil of known constants. One special form is known as the Helmholtz coil. It utilizes the straight line magnetic field which exists between two identical coils, with their planes parallel and separated a distance about equal to their radius. Such a calibrating coil is shown in Figure 56. It is positioned on the instrument symmetrically to produce a straight line

magnetic field that is either (1) in a vertical direction when used on a vertical magnetometer, or (2) in a horizontal direction when applied to a horizontal magnetometer. The strength of the magnetic field is proportional to the current flowing in the coil. This current, measured in milliamperes, may be supplied by a small dry cell battery. The strength of the field may be varied by a rheostat, to give a multiplicity of points for calibration. A reversing switch is provided for changing the direction of the field.

The field intensity is a function of the current and the characteristics of the coils, and may be expressed by the relationship

$$F = IC = I\left[\frac{10\pi D^2 n}{\left(\frac{D^2}{4}+\frac{E^2}{4}\right)^{3/2}}\right] \tag{54}$$

where

F = field intensity, in gammas
C = coil constant
D = diameter of coils, centimeters
I = current, in milliamperes
n = number of turns in each coil
E = mean distance between coils, centimeters

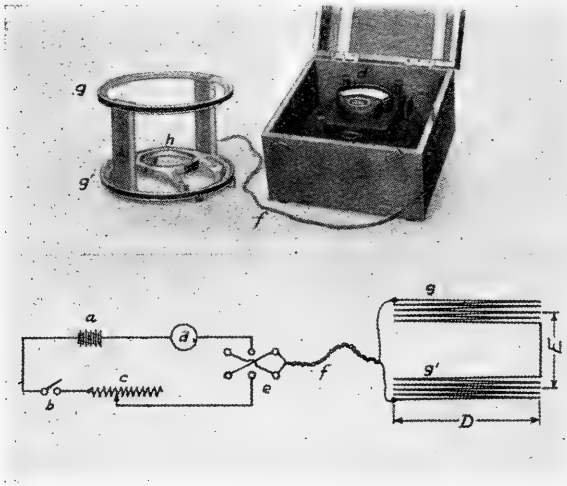

FIG. 57.—Helmholtz coil and diagram of connections. *a*, battery; *b*, switch; *c*, rheostat; *d*, milliammeter; *e*, reversing switch; *f*, twisted flexible connecting cord; *g* and *g'*, identical coils; *h*, coil holder bracket.

The diagram of connections is shown in Figure 57. Usually the coil constant C is supplied by the manufacturers. The coils are approximately 35 centimeters in diameter, and are spaced approximately 20 centimeters apart. A mounting bracket is fastened to the tripod turntable, and the coil system is placed on the bracket (Figure 56), with the coils in a horizontal position when calibrating a vertical component magnetometer

and in a vertical position with their axes parallel to the magnet system for calibration of a horizontal component magnetometer. The scale reading of the magnetometer may be brought to any desired value by using either the latitude adjustment screw or the auxiliary magnet. If the auxiliary magnet is employed, caution must be taken to avoid appreciable temperature changes during the calibration.

When calibrating a vertical magnetometer it is carefully leveled and oriented with the coils in position (Figure 56A). The scale reading and temperature are recorded when no current is flowing through the coils. The switch is then closed and the scale reading recorded with the value of current flowing through the coils. The direction of current flow is then reversed and the scale reading again recorded with the value of current. The circuit is opened and the zero or initial position of the scale checked. The scale value of the magnetometer may now be calculated by the relationship:

$$E = \frac{CI}{\frac{(S_0 - S_1) + (S_2 - S_0)}{2}} \text{ or } E = \frac{2CI}{S_2 - S_1} \qquad (55)$$

where E = scale value in gammas at the temperature of calibration, S_0 = scale reading for zero current, S_1 and S_2 = scale reading with current in first one and then the other direction.

If the values of $(S_0 - S_1)$ and $(S_2 - S_0)$ differ by more than a few per cent, the condition of the knife-edges should be carefully checked. A series of observations should be made with different values of current, when the north pole of the magnetometer is pointing east and then west. Any variation in deflection will be shown by irregularities in the calibration curves.

In calibration of a horizontal component magnetometer, the instrument is oriented in the magnetic meridian. As before, the values of initial and final scale readings, current, and temperature are recorded. The values are substituted in the preceding formulas and a series of tests conducted from which calibration curves may be drawn.

One typical calibrating coil has a constant of 173.2 gammas per milliampere. With the coil in place and no current flowing, a scale reading, S_0, is taken. With any given value of current I flowing, a second reading is taken: S_1. The scale value then would be:

$$E = \frac{173.2 \cdot I \text{ milliamps.}}{S_0 - S_1} \qquad (55a)$$

In practice, readings S_1 and S_2 are taken with the reversing switch in its two different positions, which changes the direction of the applied field. This procedure gives a larger range of readings. The scale value when this is done is:

$$E = \frac{2 \cdot 173.2 \cdot 1 \text{ milliamps.}}{S_2 - S_1} \qquad (55b)$$

which is the general formula. A number of different values of current should be used, to clearly establish the sensitivity-current relationship.

Example: Determination of the scale value of Askania Vertical Intensity Magnetometer No. 90493, using calibrating coil.

Scale readings

$S_1 = 42.3$

$S_0 = 27.2$

$S_2 = 11.9$

$S_2 - S_1 = 30.4$

Use Equation 55b above, with coil constant as given. Scale readings were at 1 milliampere of current.

In the example $2C = 346.4$

$$E = \frac{346.4 \cdot 1}{30.4} = 11.4 \text{ gammas / scale division.}$$

Slide rule accuracy is sufficient for these calculations. It is advisable to read the S_0 (or no-current value) in order to find if the differences $S_1 - S_0$ and $S_0 - S_2$ are approximately equal. If so, the instrument is functioning properly.

Before an instrument is taken into the field, it is advisable to calibrate it and thus check the scale value. In the course of field work it is also desirable to check the scale value at about 30- to 45-day intervals. In cases of unusual jolts to the instrument, or when latitude adjustments are necessary on the magnetic system, the scale value should be checked, as well as the temperature coefficient.

The scale value of an instrument is the inverse of its sensitivity. A large scale value indicates low sensitivity, while a small scale value shows high sensitivity.

After determining the scale value of the instrument with the Helmholtz coils, it is possible to determine or check the magnetic moments of the auxiliary magnets, by using the relationships given below.

Scale Value Using Auxiliary Magnets.—The second method of determining the scale value of a vertical component magnetometer consists in

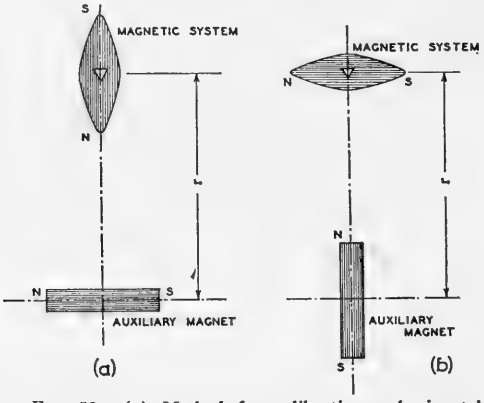

FIG. 58.—(a) Method for calibrating a horizontal component magnetometer. (b) Method for calibrating a vertical component magnetometer.

placing an auxiliary magnet of known moment at a measured distance directly below the instrument and observing the deflection of the scale. A special extension rod carrying a magnet holder may be used for setting the auxiliary magnet at any desired distance below the instrument. The extension rod is graduated in millimeters to give the distance between the center of the auxiliary magnet and the magnet system in the magnetometer.*

The magnetic force at a point r cm. along the magnetic axis from the center of such an auxiliary magnet is $2M/r^3$, where M is the magnetic moment of the magnet. To calibrate a vertical component instrument, it is

* Care is necessary to see that the distance as measured on the rod is correct. A check should be made with a meter stick or tape. Since the distance enters the calculation as a 3rd power it should be measured with the greatest accuracy practically possible.

set up and oriented, and the reading S_o is then taken, without the auxiliary magnet present. The latitude adjustment screws may need to be readjusted to bring the scale reading to approximately the mid-point. The auxiliary magnet of known moment is then placed in position, with the N. end up. (See Figure 58b.) The scale value E may then be calculated using the relationship:

$$E = \frac{2M}{r^3 (S_o - S_N)} \text{ (N. end up)} \qquad (56)$$

The auxiliary magnet may then be reversed, using the equation:

$$E = \frac{2M}{r^3 (S_S - S_o)} \text{ (S. end up)} \qquad (56a)$$

If desired, the calibration may be done merely by taking readings with the auxiliary magnet having the S, and then the N end up, in which case:

$$E = \frac{4M}{r^3 (S_S - S_N)} \qquad (57)$$

where S_S is the reading with S. end up, and S_N with the N. end up, for the auxiliary magnet.

The relationship between auxiliary magnet and magnetic system in calibrating the vertical component magnetometer is that of the first position of Gauss or the "end-on" position where the magnetic force is $2M/r^3$.

Examples: Determination of the scale value of vertical intensity magnetometer, using an auxiliary magnet of known moment $M = 500$ c.g.s., placed at a distance $r = 100$ cm. vertically below the instrument.

Scale readings

$S_S = 24.6$

$S_o = 20.0$

$S_N = 15.5$

$S_S - S_N = 9.1$

Using Equation 57 above:

$$E = \frac{2000 \cdot 100{,}000}{1{,}000{,}000 \cdot 9.1} = 21.97 \text{ gammas / scale division.}$$

Note: 1 gauss (*c.g.s.*) = 100,000 gammas. The figure 7 in the second decimal place has no particular significance except in connection with an average of a number of determinations. Scale values are ordinarily used to 0.1 of a gamma only; in this case the scale value would be 22.0.

For calibrating the horizontal magnetometer, the same procedure is applied except that the second position of Gauss, or "broad-side" position, is involved. The auxiliary magnet is set perpendicular to the magnetic axis of the magnetic system as shown in Figure 58a and the force $H = M/r^3$.

The scale value formula for the horizontal magnetometer is:

$$E = \frac{2M}{r^3 (S_S - S_N)} \qquad (58)$$

In this formula S_S = the reading with the auxiliary magnet horizontal and with its N. end toward the magnetic north. S_N = the reading with the S.

end of the auxiliary magnet toward the magnetic north. M = the moment in gammas of the known auxiliary magnet, and r = the distance between centers of the magnetic system and the auxiliary magnet.

When calibrating a magnetometer with a known auxiliary magnet, the situation is fundamentally similar to the use of a calibrating coil in that a field of known strength is applied to the instrument. The scale division deflection thus produced is determined. Calibrating coils are preferable to auxiliary magnets for establishing the scale value of a magnetometer in that they are free from temperature effects which change the moment of calibrating magnets, as well as gradual loss of moment with time.

Carrying out the same procedure on a horizontal intensity instrument, using the same auxiliary magnet at the same distance r, gave the following results:

Scale readings

$S_S = 22.3$

$S_o = 19.3$

$S_N = 16.3$

$S_S - S_N = 6.0$

Using Equation 58 as given:

$$E = \frac{1000 \cdot 100{,}000}{1{,}000{,}000 \cdot 6.0} = 16.66 \text{ gammas / scale division.}$$

The significance of S_S and S_N as symbols is changed as explained above.

Determination of the Moment of an Auxiliary Magnet.—It is a simple matter to determine the moment of an auxiliary or standard magnet, using either a vertical or a horizontal magnetometer, the scale value of which is accurately known. A series of deflection readings is taken, the magnet to be tested being placed at measured distances from the magnetic system of the magnetometer by means of the graduated extension tube and magnet holder. The procedure followed is in all respects similar to that just described for finding the scale value using an auxiliary magnet, except that Equations 57 and 58 are solved for the magnetic moment M of the magnet used. These formulae thus solved are:

For the vertical magnetometer:

$$M = \frac{E\, r^3\, (S_S - S_N)}{4} \tag{59}$$

For the horizontal magnetometer:

$$M = \frac{E\, r^3\, (S_S - S_N)}{2} \tag{59a}$$

Example: using vertical magnetometer No. 751414, scale value 9.9 gammas per scale division. To find the moment of a large standard magnet, the magnet is placed at a distance of 70 cm. beneath the instrument.

Scale readings

$S_S = 63.0$
$S_o = 15.6$
$S_N = 31.8$

$S_S - S_N = 94.8$

$r^3 = 343{,}000$; $E/4 = 2.48$
$M = 2.48 \cdot 343{,}000 \cdot 94.8 \cdot 10^{-5} = 806$ c.g.s.
A series of determinations are made in order to arrive at an average value for the moment M.

Standard magnets should be carefully handled and are usually carried in a padded box to prevent them from being jolted. They should, of course, be kept away from strong direct currents or powerful magnets. If more than one magnet is carried in the same case, they should be laid with their poles reversed to minimize their effect on each other.

The moment of an auxiliary magnet may be determined by using a standard magnet of known moment. The deflections of a magnetometer by magnets (of the same size) placed at the same distance from a magnetometer (with like poles up) are directly proportional to the moments of the two magnets.

If M_{st} = the magnetic moment of the standard magnet (which is known)

M_x = the magnetic moment of the unknown magnet

$(S_S - S_N)_{st}$ = the deflection produced by the standard magnet with its South and North ends up respectively, at a distance r cm.

$(S_S - S_N)_x$ = the deflection produced by the unknown magnet as above and at the same r distance.

The direct proportion is:

$$M_x : M_{st} = (S_S - S_N)_x : (S_S - S_N)_{st}$$

$$M_x = M_{st} \frac{(S_S - S_N)_x}{(S_S - S_N)_{st}} \qquad (60)$$

The magnetic moment of an auxiliary magnet may also be found by using a calibrating coil and a magnetometer. This is done by noting the deflection produced by the auxiliary magnet at a given distance and position from the instrument compared to the deflection produced by a given current flowing in the coil. The coil constant is an expression of the magnetic moment applied to the instrument by the coil. In the examples used, $C = 173.2$ c.g.s. per milliampere, expressed in gammas. A direct proportion would be involved.

Determination of Temperature Coefficient. — The temperature coefficient of a magnetometer is determined by placing the instrument in a heating box (or heating it by other suitable means) and observing the scale reading and temperature at about 5-minute intervals. If electrical heating is employed, the box must be non-inductively wound. Alternating current should be used with a tapped transformer and rheostat to control the amount of current and thus the rate of heating. Circulating water may be employed by providing a copper tube coil, through which hot or cold water can be circulated. The box should be provided with a detachable

cover with a hole in the center through which the telescope of the magnetometer protrudes. A small light on a rod inserted through another hole in the cover illuminates the thermometers, which are read through a small glass window in the cover. The mirror on the door in front of the thermometers can be held open at the proper angle by a peg inside the heating box.

While a temperature coefficient determination is being made, a second magnetometer should be read from time to time to keep track of the daily variation. A graph of scale reading versus temperature is drawn and the coefficient determined therefrom.

The temperature coefficient (T_c) is defined as: *the fraction of a scale division which the scale moves for a temperature change of 1 C.°:*

$T_c = S.D./C.°$ (where $S.D.$ = scale divisions).

As an example:

Time	*Reading S. D.*	*Temperature*
9:00	20.0	20.0°
9:05	19.8	21.0°
9:10	19.6	22.0°
9:15	19.3	23.0°
9:20	19.1	24.0°

A change of 0.9 S.D. for 4.0 C.° change in temperature shows a temperature coefficient of 0.225 S.D./1 C°.* If desired, the temperature coefficient may be expressed in gammas per degree, knowing the sensitivity (or scale value) of the instrument.

If a heating box is not available, the instrument can be placed in an oven (exercising due precaution), and carefully warmed, then set up and the readings, against fall in temperature, recorded. It is also possible during hot weather to place an instrument on a cake of ice to cool it and then observe the temperature change versus scale reading as the temperature rises. The use of "dry ice" for cooling a magnetometer is *not* recommended as it might easily produce excessive chilling, with resultant strains, of the metal, quartz and glass parts of the instrument.

Heating elements are sometimes made to the same dimensions as the plastic plug which screws into the bottom of the instrument. They can be built to use direct current from a small portable battery or from the battery of a car. In the latter case a long lead wire is provided, by means of which the magnetometer can be set up far enough from the car so that it will not affect the readings.

Temperature Effects.—The three chief effects on a magnetic system due to changes in temperature are: (a) changes in magnetic moment (decreasing moment with increasing temperatures); (b) unequal expansions of the component parts of the moving system with a resultant change in scale constant, variations in optical constants, and changes in gravitational moment accompanied by changes in scale value; (c) thermal and elastic lags of the component parts of the system.

It is the chief function of the heavy cork insulation of the case of the instrument to minimize temperature variations—particularly, rapid temperature fluctuations. Slow changes in temperature may be compen-

* It is seen that as the temperature rises the scale reading decreases. Some magnetic systems are over-compensated, and as temperature rises readings likewise increase.

sated by using a calibration curve which shows the correction for various changes in temperature. This curve is usually plotted with the temperature correction in gammas as ordinate and the change in temperature ($t—t_0$) in degrees Centigrade or Fahrenheit as abscissa. It is usually convenient to assume some mean temperature for the area under investigation and apply the appropriate correction factor for each reading. (As stated previously, thermometers are provided in the instrument so that the temperature may be read at the time of each magnetic reading.)

Certain instruments of recent design incorporate temperature compensation,† and the effects of moderate temperature variations are usually negligible with such equipment. In the temperature-compensated system, two threaded rods are employed; the rod on the north side of the axis is made of aluminum (see Figure 49) and carries the temperature-adjustment weight. The rod on the south side of the axis is made of invar steel and carries the latitude-adjustment weight. The thermal coefficient of the invar rod (carrying the latitude weight) is very small; hence, changes in the position of the latitude-adjustment weight with variations in temperature are extremely slight. Furthermore, the slight change in position of the latitude weight is largely compensated by the change in the position of the center of gravity of the aluminum rod.

Temperature changes greatly affect the scale readings when employing auxiliary magnets. This is caused by the following factors: (a) change in magnetic moment of the auxiliary magnet and (b) change in length of the magnet support which is fastened to the base of the turntable. For this reason, accurate measurements in an area must never be attempted with auxiliary magnets. Oftentimes, auxiliary magnets are employed to bring the scale of the instrument within view. This procedure is permissible where large magnetic anomalies are to be measured. In regions of small anomalies, the instrument must be opened and proper adjustment made by rotating the latitude-adjustment weight until a suitable position of the scale is observed.

Temperature Compensation of Magnetic Systems.—The mechanism of temperature compensation in the Askania magnetic systems is illustrated in Figure 54. As a magnet is heated it loses strength, with a resultant decrease in its magnetic moment. For a magnetometer set up at a station, at a given temperature a certain reading would be obtained. With an *increase* in temperature the magnet system would become weaker and therefore less strongly deflected by the magnetic force acting on it. This would result in less tilt angle of the system and a smaller scale reading.

As the temperature rises in a temperature-compensated system, however, the aluminum spindle carrying the weight W_1, which is on the north pole side of the system, expands and shifts the center of gravity of the

† Joyce, *loc. cit.*, p. 42.
C. A. Heiland and W. E. Pugh, "Theory and Experiments Concerning a New Compensated Magnetometer System," *A.I.M.E. Geophysical Prospecting*, Tech. Pub. 483, 1932.

system toward the knife edge, or axis of rotation, which causes a decrease in the pull of gravity on the system. This, in turn, counteracts the decrease in reading due to the lesser magnetic moment. When properly designed and adjusted, the temperature-compensated systems have zero temperature coefficients.

In these systems temperature changes do not affect the position of the weight W_2 on the latitude spindle in relation to the axis of rotation. The reason for this is that this spindle is made of invar metal which, for all practical purposes, has a negligible coefficient of expansion for changes in temperature.

In the earlier Askania systems an attempt was made to minimize temperature effects by controlling the relationship of the magnetic blades to the aluminum block to which they were attached. The knife edge, the latitude adjustment and sensitivity screws, and the resulting center of gravity of the system as a whole, were designed so as to compensate for temperature changes in the manner explained above. The compensation was, however, not complete.

Various means of temperature compensation for the old Askania systems have been proposed, utilizing the difference in the thermal coefficients of the different materials in the magnet system.†

With the new, or compensated, systems, it is still necessary to check the temperature coefficient from time to time to find out if it is truly zero. If it is not zero, the position of the weight W_1 on the temperature spindle, as shown in the figure previously referred to, can be adjusted and locked in position by its small set screw so as to bring the coefficient to zero.

The distance a between the center of gravity of the system and the axis of rotation (as shown in Figure 54) is 0.1 mm., measured along the magnetic axis of the system. The distance h or the displacement of the center of gravity below the axis of rotation is even smaller, being 0.08 mm. These minute distances are quite critical in affecting the temperature coefficient and scale value of a particular system. It is apparent therefore that a magnetometer, although it is a field instrument, must be handled with great care and protected from jolts and jars which might change the gravity center to rotation axis relationships. In cases where an instrument is accidentally dropped or jolted, the scale value and temperature coefficient should be checked. Magnetometers should also be kept away from strong magnets or high amperage direct current sources, as the magnetic moment of the system might be affected.

Temperature Correction.—Where the temperature coefficient of a magnetometer is *not* zero, a correction must be applied to the instrument readings. As will be seen later, in the section on the calculation of field notes, the readings at a series of stations are reduced to a common temperature. The reading at a station, in such a series, *after* the application of

† T. Koulomzine, "Temperature Compensation of Old Type Askania Magnetometers," *A.I.M.E. Mining Transactions,* pp. 133-136, Vol. 184, May, 1949.

the temperature correction is the theoretical reading that would have been obtained there if no temperature change had taken place.

The base temperature usually adopted in mild weather is 20° C. Using the temperature coefficient previously worked out in the example given, 0.225 S.D./ 1 C°, we can assume that at station 1 (of a set of stations) the magnetometer might read 21.3 S.D. at a temperature of 22.0° C. This temperature is 2.0° above the assumed base temperature of 20.0° C. Since the temperature has increased two degrees the instrument would read 2 x 0.225 S.D. *less* (or 0.46 S.D. less) than it would have read had the temperature remained at 20.0° C.

Therefore a correction of 0.46 scale divisions must be applied to the reading at station 1. Since the temperature was higher and the scale reading consequently less, the correction must be *added*. Inasmuch as the inherent sensitivity of the instrument is less than one-tenth scale division, the nearest tenth scale value is used; i.e., 0.5 in place of 0.46 scale divisions. The instrument reading, therefore, which would have been obtained at the 20.0° C. temperature is 21.3 + 0.5 or 21.8. This latter value would be used in calculating a set of field results.

If the temperature at station 1 had been 18.0° C., i.e., 2.0° less than the base temperature, the correction would be *subtracted*. The reading would be 22.3 at the 18.0° C. temperature. To reduce it to the 20° base, the calculation would be: 22.3° − 0.5° = 21.8°, which is the same as in the preceding case for the base temperature.

The temperature chosen for a base to which a set of readings is reduced is quite a matter of convenience. It is generally advisable, however, in order to avoid errors due to the wrong algebraic sign, to choose a temperature below or above that to be encountered during the work. The instrument readings at all stations of a set of readings must be reduced, or corrected, to those readings that theoretically would have been obtained if the ambient at some temperature had remained constant. If a fully compensated zero temperature coefficient system is used, obviously, temperature corrections are not required.

Magnetic Field Work

As stated previously, the normal values of the components of the earth's magnetic field vary over the surface of the earth. The vertical component of the earth's field varies from approximately *minus* 67,400 gammas at the south magnetic pole through zero at the magnetic equator to about *plus* 63,500 gammas at the north magnetic pole. The horizontal component has a maximum value of about 39,000 gammas at the equator and decreases to zero at each of the two poles. This variation of the magnetic field strength is usually unimportant where studies are confined to traverses of only a few miles length. In larger surveys, or when tying-in one survey with another at a different location, latitude corrections average from 10 to 12 gammas per mile for the vertical component and from 5 to 8 gammas per

mile for the horizontal component; the longitude corrections average 2 to 3 gammas per mile.

Due to the irregular distribution of the isodynamic lines along the earth's surface, the earth's normal field strength cannot be calculated theoretically from the latitude and longitude position, but must be obtained from maps of isodynamic lines. (See Figure 33.)

Latitude Corrections.—Calling d the distance measured perpendicular to the geographical latitude between two successive isodynamic lines differing in intensity by ΔZ or by ΔH, as the case may be, the corrections are:* vertical component $= \Delta\gamma_Z = \Delta Z/d$; horizontal component $= \Delta\gamma_H = \Delta H/d$. The vertical correction is to be subtracted from readings north of the base station in areas north of the magnetic equator or south of the base station in areas south of the magnetic equator. (The rule regarding signs derives from the fact that the magnetic intensity increases positively toward the north magnetic pole and negatively toward the south magnetic pole.) The horizontal correction is added to readings north of the base station in areas north of the magnetic equator or south of the base station in areas south of the magnetic equator. (This sign rule obtains because the horizontal intensity decreases toward the two poles.)

Usually it is convenient to employ a latitude correction curve, wherein distances measured perpendicular to the geographical latitude are plotted as abscissa and the calculated correction from the base station as ordinate.

Longitude Corrections.—Vertical component $= \Delta\gamma_Z = \Delta Z/d$; horizontal component $= \Delta\gamma_H = \Delta H/d$, where d is the distance measured perpendicular to the geographical longitude between two adjacent isodynamic lines differing in intensity by ΔZ or ΔH, as the case may be.

The longitude correction curves are plotted in the same manner as the latitude curves. The algebraic signs of the corrections depend on the magnetic declination in the area. For west declination areas, the corrections are added for all stations east of the base station. For east declination areas, the corrections are subtracted for all stations east of the base station. These corrections are generally quite small and often may be neglected in ordinary work. Latitude and longitude corrections can be combined into a single correction by using the magnetic north and south rather than the geographical north and south as the direction of measurement from the base station. Also, corrections for latitude and longitude are oftentimes included in the "regional gradient" in final interpretation. When the latter procedure is employed, the regional gradient is drawn in by inspection of the magnetic profiles, and anomalies are measured using the regional gradient as a reference line. This is illustrated in connection with Figure 112.

*Isodynamic lines on available charts are expressed in gauss. The rate per mile or kilometer must be reduced to gammas for use in field work.

Corrections for Daily Variations

Base Check Method

The irregular variations in the strength of the earth's magnetic field necessitate corrections for each of the various stations occupied during the course of a survey. These corrections are always the negative of the magnetic variations; e.g., if the magnetic intensity in the area *increases* at a certain time, the amount of increase will be *subtracted* from the magnetic reading made at that particular time. In general, the annual and secular variations are of interest in geomagnetic explorations only when surveys are conducted over a considerable period of time or when a lapse of several months occurs in extending or checking a given survey. The diurnal variations, however, are of considerable importance.

Corrections for magnetic variations during the progress of a survey are made by recording the variations of the magnetic intensity at one or more base stations. The ideal procedure is to employ a continuous recording magnetometer at the base station. This ideal procedure is approximated by setting up one instrument at a fixed station and taking intermittent readings. In many surveys where a separate instrument cannot be utilized for these fixed or base station measurements, results of lower (but often adequate) accuracy are obtained by readings made every hour or two at a central base station.

Intermittent Readings: Diurnal Variation.—In practice, intermittent readings of the diurnal variation frequently are made by setting up a magnetometer at a base station in the area under investigation and having an observer read the magnetic field strength at this station at intervals of 15 to 20 minutes. The readings should be started about an hour prior to the other field work and extend for a similar period of time beyond the other field measurements in order to establish general trends. Any variations in the field instruments are immediately apparent when check readings are taken at the base station. The two instruments must, of course, be mounted at a sufficiently large separation to insure that the mutual attraction between the two magnet systems is negligible.

If an extra instrument is not available for use as a base station magnetometer, usable results may be obtained by "checking-in" at the base station a number of times during the day. In this procedure, the operator returns to the base station at regular intervals and takes readings with his field magnetometer. These readings, when corrected for temperature changes, give a fair approximation of the diurnal variation. In this method, any change in instrument calibration will introduce an error which cannot be differentiated from diurnal variations.

An alternative field technique involves checking back on a previously occupied station rather than the base station. Occupy base station *A,* then stations, 1, 2, 3, 4 and back to *A*. Thus, corrected values for stations 1,

2, 3, and 4 are available for making any one of them usable as a check station. The survey might then proceed with stations 5, 6, 7, 8 and back to 4, etc. This saves time in difficult country.

Figure 59 shows corresponding curves obtained with a base station magnetometer and a field magnetometer "checked-in" at intervals of about two hours. The results are in fairly good agreement, with the exception of the time period between 1 P. M. and 3:15 P. M. Here the error would amount to about 4.5 gammas which may be sufficient to mask or distort a minor magnetic feature.

The graph (Figure 59) also shows that the diurnal variation fluctuated from +10 gammas at 7 A. M. to −14 gammas at 1:45 P. M., i.e., the variation had an amplitude of 24 gammas for that particular station and date.

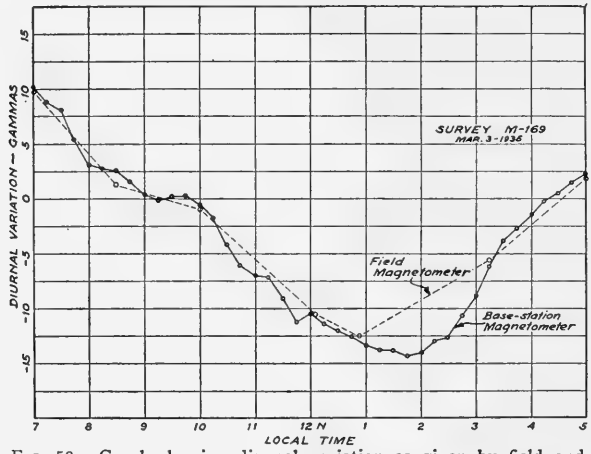

FIG. 59.—Graph showing diurnal variation as given by field and base station magnetometers.

The maximum magnetic variation due to structure in this area was about 10 to 15 gammas, i.e., approximately $\frac{2}{5}$ to $\frac{3}{5}$ the diurnal variation. It is evident, therefore, that in this case the diurnal variation had to be measured with the same accuracy as the anomalies.

In certain types of mining investigations where the magnetic anomalies are very large, the diurnal variation may oftentimes be neglected. However, magnetic storms are unpredictable and may cause variations of 50 to as much as 500 gammas. Generally speaking it is poor policy and false economy to omit the diurnal corrections.

Continuous Recording Magnetometers.—Practically all types of continuous recorders employ photographic recording on sensitized plates or paper. One type of instrument utilizing photographic recording on plates is illustrated in Figure 60. The magnetometer and the recording apparatus are both mounted in a cylindrical housing, which is supported on a tripod. The instrument is leveled and oriented in the same manner as

the standard field balance. The recording mechanism is located in the upper part of the cylindrical housing and comprises: plate holder, flash-light bulb, prism, moving plate holder, clock-drive mechanism. A removable brass plate carries the magnetic system which is similar to that of the standard magnetometer except that a prism is employed for deflecting the light beam instead of a mirror.

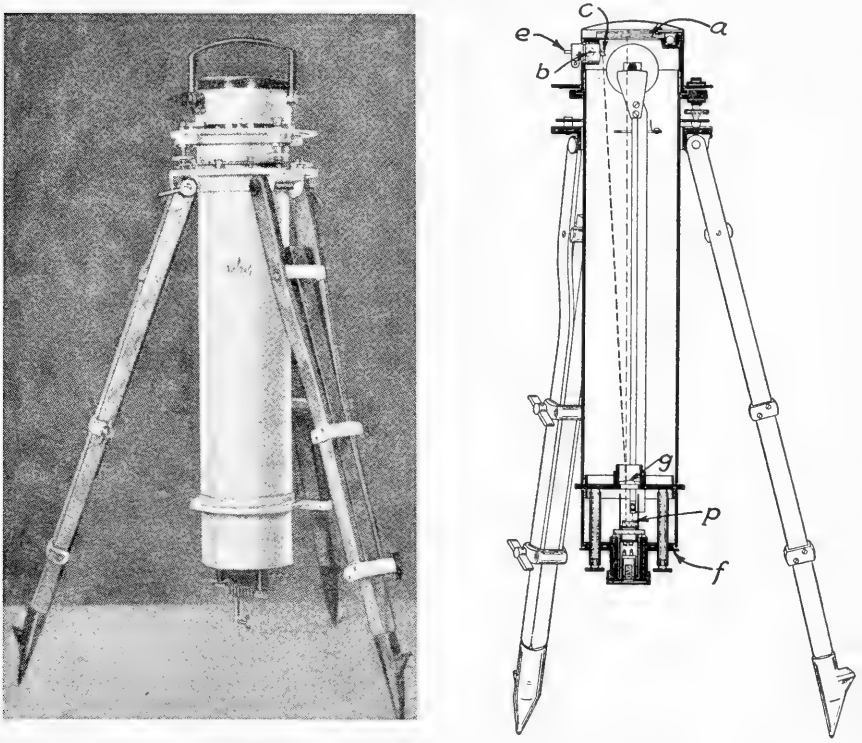

(A) (B)

FIG. 60.—Askania continuous recording magnetometer. *A*, exterior view; *B*, interior view. *a*, plate holder; *b*, flash-light bulb; *c*, prism; *e*, clock drive; *f*, support; *g*, lens; *p*, prism.

The light from the bulb passes through a diffusing glass and a diaphragm with a point aperture. The image of the aperture is projected on the photographic plate by means of the objective lens, the prism on the moving magnetic system, and the fixed mirror. The fixed mirror receives a portion of the light beam and reflects a continuously moving light spot in a plane perpendicular to the plane of vibration of the magnetic system. Like the fixed mirror which records the base-line, the counter-mirror is fixed to a pivot rotated from a clockwork by a long arm carrying a toothed segment. After the lapse of a given time interval, the toothed segment is thrown out of gear and returns to its starting position.

The photographic plates used with the magnetometer shown in Figure 60 are 45 mm. by 60 mm. and are read by means of a graduated plate. One millimeter of record equals 10 minutes time along the long axis of the plate and approximately 10 gammas along the field strength scale. (The latter is at right angles to the time axis or direction of movement of the plate.) A record obtained with a continuous recording instrument exhibits the minute variations which cannot be obtained with any type of intermittent reading method.

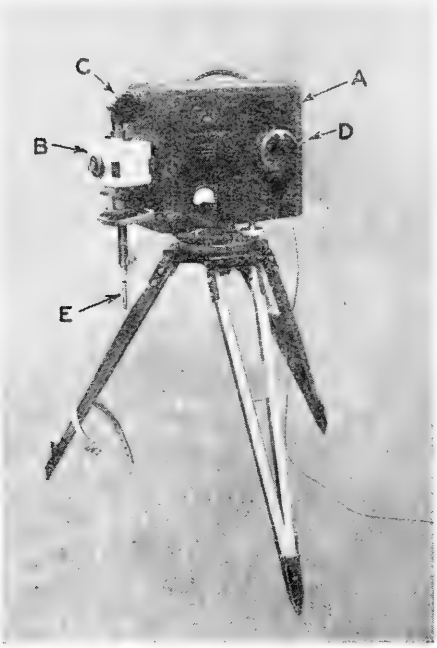

FIG. 61.—Hilger and Watts continuous recording magnetometer. The recording apparatus (A) may be used in conjunction with either a vertical (B) or a horizontal component magnetometer. The telescope of the magnetometer is exchanged for a reflecting head (C) which deflects the light beam into the recording apparatus. The total swing of the light beam is almost equal to the field of view of the magnetometer, with 1″ of record width equal to 10 scale divisions of the magnetometer. Accuracy of reading is about 0.1 scale division. (D) indicates drive mechanism and (E) auxiliary magnet.

The Hilger and Watts recording magnetometer utilizes either the vertical or the horizontal component magnetometers, which may be clamped to the recording instrument. A view of the instrument set up in the field is shown in Figure 61.

Correction for Auxiliary Magnets

In regions where the anomalies are large and precise measurements are not required, auxiliary magnets may be employed to extend the reading scale of the instrument. This makes it unnecessary to open the instrument and change the settings of the latitude screws. The preferred procedure for using auxiliary magnets is as follows. Observe the scale deflection at the station where the end of the scale has been almost reached, and record the reading. Choose an auxiliary magnet of suitable strength to bring the scale reading to the desired value. Record the new reading with the auxiliary magnet; record also the number or moment of the magnet used, and the reading on the extension rod. Then go back to one or two prior stations and repeat the procedure. The average difference in the two sets of readings at each of the stations is the auxiliary magnet correction in scale divisions for that particular setting of the auxiliary magnet. This correction will then be added or subtracted, as the case may be, for all readings employing the auxiliary magnet. A similar procedure will be useful if it becomes necessary

to change auxiliary magnets or the distance of a magnet on the extension rod.

If precise work involving an accuracy of 5 gammas or better is necessary, auxiliary magnets should not be employed for extending the scale of the instrument. At such times, the only procedure is to open the case of the instrument and adjust the latitude screw until the desired scale reading is obtained. The sensitivity adjustment should not be changed unless the work clearly shows the need for such a change. After shifting the scale reading by the latitude adjustment weight, repeat readings should be made at one or two prior stations to effect a proper tie-in of data.

Adjustment of Instrument Before Field Work

Latitude Adjustment.—This adjustment is accomplished by rotating the lateral screws until the zero point of the reflected scale is approximately at the middle of the scale.* In regions where the magnetic gradient is small, no other adjustment will be required to keep the scale in the field of vision. However, in regions where igneous rocks outcrop at or near the surface (e.g., in many mining regions), the magnetic anomalies are often large and show rapid variations. Under these conditions, it is often necessary to use auxiliary magnets to keep the scale within the field of vision. (The auxiliary magnets are so mounted that their effect on the magnetic system opposes that of the geologic anomaly).

Conditions of the Knife-Edge. — Sensitivity and accuracy of the instrument depend in large measure on the condition of the knife-edge. The operator must take every precaution, therefore, to protect the fragile quartz-edges on which the system pivots. The magnetic system must always be clamped, except during the time when a reading is being made. If the knife-edge is lowered upon the quartz bearings with a slow movement, and if the instrument is not jarred while the knife-edge is resting on the bearings, the edges and bearings should last as long as the instrument.

Special precautions must be taken to protect the instrument from dust and lint when the case is open for adjustment of the magnet system. The instrument should never be opened in windy or dusty places. A minute particle of grit between the knife-edge and the bearings will cause erratic readings and changes in sensitivity. Do not touch the fingers to the knife edges or the bearings. To do so deposits a film of organic matter that causes irregular operation of the balance. To remove such foreign material, the bearing surfaces should be wiped carefully, just prior to closing the instrument case, with a linen cloth dampened with pure ether or chloroform.

---

* In old-style magnetic systems the two latitude screws are on the ends of the block to which the magnetic blades are attached. In the compensated systems the latitude adjustment weight is on the small diameter spindle on the *south* end of the system.

Determination of the Scale Value.—Before conducting a magnetic survey, it is desirable to determine the scale value of the instrument. The differential magnetic intensity per scale division, generally expressed in gammas per scale division, is obtained by observing the deflection of the magnetic system produced by a magnet of known magnetic moment placed in one of two positions, and applying the required mathematical formulae involving the magnetic constants and the distances.

Instead of using a magnet of known magnetic moment, the scale value may also be determined with the aid of a Helmholtz coil arrangement, as discussed previously.

The steps outlined below illustrate the procedure at each station when using a vertical component Schmidt field balance after the instrument has been removed from the box and has acquired the temperature of the air.

(1) Remove all iron objects from the observer's person and from the immediate vicinity of the instrument. Place the carrying-box with its set of auxiliary magnets and other magnetic materials at a distance of 30 to 50 feet from the station.

(2) Set up and level the tripod. Carefully orient the tripod head at 270° on the compass, and clamp it. (With the tripod head oriented in this direction, the magnetometer will set in the head at right angles to the magnetic meridian.) Remove the compass to a safe distance from the instrument.

(3) Clamp the magnetometer on the turntable. Level the instrument accurately by means of the level screws.

(4) Release the magnetic system by means of the arresting device and note whether the reflected scale remains in the field of vision. If the instrument has been properly adjusted for latitude, the scale will be in view. If the scale is not in view and it disappears because of a large anomaly, employ an auxiliary magnet to bring it into the field of vision, recording which magnet is used and its position and distance.

(5) Read and record the scale reading. Revolve the instrument through 180°* and again read and record the position of the scale. Repeat these readings two or more times to obtain representative readings.

If instrumental trouble is not encountered, careful manipulation will give readings which check within one or two tenths of a scale division.†

(6) Read and note the temperature and time.

---

* Some tripods have an automatic reversing stop for this operation. Old-style tripods carry graduations in degrees on the lower and fixed portion of the tripod head and two index marks on the moving portion of the turntable or head. The appropriate index is used for the 180° reversal.

† Poor check readings may be due to the following causes: a. mis-orientation; b. misleveling of tripod; c. misleveling of the instrument when placed on the tripod; d. poor adjustment of the tripod or instrument levels; e. one quartz bearing, on which the knife edge rests, being higher than the other; f. chipped knife edge or bearing; g. dust or other foreign matter inside the instrument and on knife edge or bearings; h. improper releasing of system and letting it down on bearings too rapidly.

(7) Clamp the magnet system, remove instrument from the tripod and place in the carrying-box, and proceed to the next station.

Stray Magnetic Material

During a magnetic survey, the operator must always be on the alert to note the presence of any "tramp" iron which may cause erroneous anomalies. Iron or steel structures, pipe lines, culverts, railroads, direct current power lines (including street car lines with ground return circuits), junk piles, etc., are possible sources of error. A careful record of observed surface conditions should be kept, in order that the readings made in the neighborhood of such disturbances may be properly evaluated in the final interpretation of the magnetic data.

The operator should always remove personal articles which may be magnetic. Errors are oftentimes caused by wrist watches, notebooks with steel rings or backs, steel belt buckles (usually plated with the more expensive metals), iron arch supports in shoes or boots, steel-plated eyeglass frames, pocket-knives, Brunton compasses, fine wire in hat bands, zippers, cameras, metal pencils, buckles on shoes, metal buttons on clothing, etc. Horn-rimmed glasses can be obtained that are essentially non-magnetic.

For the best field results it is desirable for a magnetometer operator to develop his own standard routine practices in setting up and reading the instrument. Such practices include: remaining on the same side of the instrument when taking readings in both direct and reversed orientations; not walking around the tripod when it is set up more than is necessary; keeping a wrist watch the maximum distance from the instrument by placing the hands behind the back when taking readings; and keeping other persons at a distance while the instrument system is released.

Preferred Field Technique and Calculation of Field Notes

The following calculation of a sample set of field notes taken with a vertical magnetometer will illustrate one satisfactory procedure for field work. The form illustrated in Figure 64 was designed by Mr. John H. Wilson. Bound field notebooks of this form are available.*

The magnetometer is first set up at the base station with the tripod head properly oriented. The first reading is taken with the N end of the instrument in the magnetic east. Usually two readings are made (or more, if necessary) to obtain readings that check within 0.1 to 0.2 scale divisions. The two readings are entered in column 2 of the form under N. to E.

The instrument is then reversed 180°, using an index mark on the tripod, and a second set of readings is taken and recorded. Temperature and time are also recorded, as shown. The position of the base and subsequent stations must be known as to their location in a section, or on a control

* The form is used here through the courtesy of the Kendrick-Bellamy Co., Denver, Colo.

grid. Accuracy within 0.2 of a mile is sufficient for routine stations in oil structure surveys, which permits traversing by the speedometer of a car.

When an uncompensated magnetic system is used, it is necessary to wait at the base station for about one-half hour until the instrument has acquired the air temperature. In most magnetic work for oil structure, transportation is by automobile, and care must be used to prevent the magnetometer from receiving jolts which might knock the system out of adjustment or damage the knife edge and bearings.

Readings at subsequent stations are taken in turn, after the base station has been occupied. Each location is recorded in the note form and usually on a map of the area carried for that purpose. In the field it is necessary only to record the data required in columns 1, 2, and 3 of the form, and the location of the station. See sketch map (Figure 62) for location of stations in the survey notes (Figure 64).

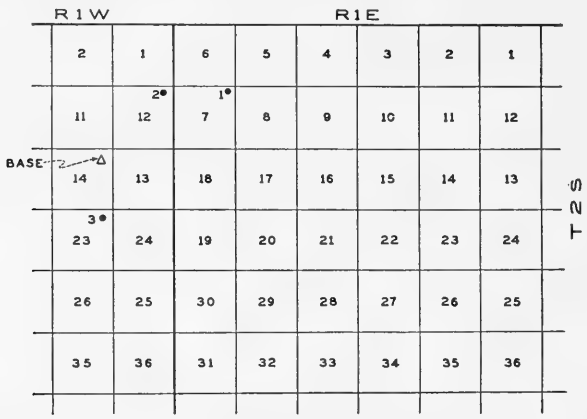

FIG. 62.—Sketch map showing location of stations used in set of field notes.

The first step in the calculation of field notes, with the form here used, is the correction of the reading due to temperature. In column 4, the recorded temperature, less 20° C., is set down. For the base station this is + 2.9°. The average reading is then figured from column 2 by taking the mean of readings with orientation of the instrument in the East and in the West positions. This is entered in column 6.

The heading of column 6 is *Mean Reading S.D.* For the base this is 20.1. The nearest 0.1 only is carried. This average is in scale divisions. The temperature correction is then applied by forming the sum of the figures in column 6 and in column 5, which gives, for column 7, the average reading corrected for temperature, in this case 21.0.

In the example given, if the temperature at the base had been 17.1° or 2.9° below the 20.0° base temperature, the operation of column 4 (or temperature − 20° C.) would have given −2.9 for the figure in column 4.

This would have made a temperature correction of −0.9 S.D., to have been applied to the average reading. This is correct in that a lower temperature would have increased the reading, necessitating the subtraction of a temperature correction to put the corrected reading on the 20° C. base.

In column 8 is recorded the corrected reading for the station, in gammas. This is obtained by multiplying the scale reading (as corrected for temperature) of column 7 by the scale value of the instrument. In this problem $E = 27.2$ gammas/$S.D.$ For the base station 21.0 x 27.2 = 572 gammas for column 8.

Concerning column 9, on certain stations of a survey the magnetic anomaly may be so great as to cause the scale to run out of view in either the plus or minus direction. When this occurs, place an auxiliary magnet of known moment directly under the instrument, by means of the holder and extension rod attached to the tripod. This magnet is set at a measured number of centimeters from the system. The magnet can be adjusted to bring the scale back into view so that a reading can be obtained.

The amount of the field thus added (or subtracted) is recorded in column 9, using the formula $F = 2M/r^3$ where F = field in gammas, M = moment of auxiliary magnet in gammas, and r = the distance in cm. from the magnetic system to the center of the auxiliary magnet. This procedure is not often necessary but can be applied for a few stations to save readjusting a system by means of the latitude screw. No auxiliary magnet was used in the sample notes.

The total amount of the daily variation in column 10 is determined by finding the difference in the reading at the base when it is first occupied and when it is occupied at the end of a series of stations. In this case 572 − 548 = 24 gammas, which is considered as minus because the reading at the base was less at the end of the run than at the beginning. The amount of this daily variation to be applied to each station may be determined from a graph with time plotted on one axis and total change on the other. See Figure 63.

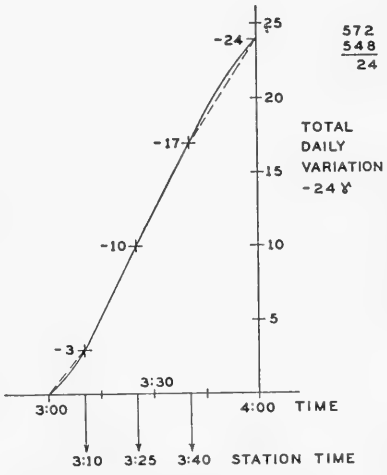

Fig. 63.—Graph showing a portion of the daily magnetic variation, from base checks, for sample set of notes.

It is assumed that the change in reading as shown by the base station checks is linear between points and represents the daily variation. This assumption is not strictly true, but, lacking a base station instrument with which to record the true daily variation, as is sometimes used, it is the procedure followed. For a large enough number of points, a smooth

AREA OBSERVER

1	2				3	4	5	6	7	8
	READINGS				Mean Time	Mean Temp. —20°C	Temp. Corr. S. D.	Mean Read. S. D.	Corr. Read. S. D.	Corr. Read. γ
	N. to E.		N. to W.							
	S. D.	Temp.	S. D.	Temp.						
						2	$4\times K_t$	2	6+5	7×E
Base	*20.0* *19.8*		*20.2* *20.4*	*22.9*	*3:00* *PM*	*+2.9*	*+0.9*	*20.1*	*21.0*	*572*
1	*22.2*		*22.4*	*22.0*	*3:10*	*+2.0*	*+0.6*	*22.3*	*22.9*	*622*
2	*25.3*		*25.5*	*21.8*	*3:25*	*+1.8*	*+0.5*	*25.4*	*25.9*	*705*
3	*26.0*		*26.2*	*21.5*	*3:40*	*+1.5*	*+0.5*	*26.1*	*26.6*	*723*
Base	*19.0* *18.8*		*19.1* *18.7*	*21.0*	*4:00*	*+1.0*	*+0.3*	*18.9*	*20.2*	*548*
	Next Day									
Base	*15.2* *15.0*		*15.0* *15.2*	*20.0*	*8:00* *AM*	*0*	*0*	*15.1*	*15.1*	*411*

(Courtesy of Kendrick-Bellamy Co., Denver, Colo.)

FIG. 64

curve may be drawn by inspection. If the time involved in a series of stations between occupation of the base is not too great, this assumption of linear change is not seriously in error on most days. It is good practice to reoccupy a base station about every hour during a day after the initial set-up thereon.

The latitude and longitude correction is entered in column 11. This correction removes the natural increase or decrease in the earth's field

DATE INSTRUMENT

9	10	11	12	13	14	15	16
Aux. Mag. Corr. γ	Diurn. Variat. γ	Long. & Latit. Corr. γ	Base Value γ	Sum Corr. γ	Vert. Int. Base=0 γ	Vert. Int. Base=X γ	Remarks, Location of Station Auxiliary Magnet Data
				9+10+ 11+12	8—13	14+X	
	0	*0*	*572*	*572*	*0*		*NE cor. Sec. 14 T2S R1W Base*
	−3	*+21*	*572*	*590*	*+32*		*NE cor. Sec. 7 T2S R1E*
	−10	*+17*	*572*	*579*	*+126*		*NE cor. Sec. 12 T2S R1W*
	−17	*−12*	*572*	*543*	*+180*		*NE cor. Sec. 23 T2S R1W*
	−24	*0*	*572*	*548*	*0*		*Base*
None Used			*Temperature Coefficient* $= K_t = (T_c) = 0.3$ *S.D./1°C.* *Scale Value* $= E = (\epsilon) = 27.2\ \gamma$*/S.D.*				
				L. & L. corr. = *11.8 γ/mi. + to N. and 4.7 γ/mi. + to E.*			
							γ = *gammas* *S.D.* = *Scale Divisions*

which is a function of the geographic location of the station, with reference to the base station used. It is applied on a mileage basis, and for the area here considered the earth's field increases 11.8 γ's per mile to the north (called + to the north, − to the south) and 4.7 γ's per mile to the east, (+ to the east, − to the west). + denotes an increase of the field and − a decrease.

The base station has, of course, zero L. and L. correction, (sometimes

called North and East correction). Station 1 is 1 mile N. and 2 miles E. This means 11.8 + (2 x 4.7) = +21.2 γ's; use 21 γ's. Station 2 is 1 mile N. and 1 mile E., or 11.8+ 4.7 = 16.5; use 17 γ's. Station 3 is 1 mile S. or −11.8 γ's; use −12 γ's.

It is a feature of this form that corrections are entered with their true signs. That is, if the daily variation decreases or is less, its sign in the form is −. Likewise, if the L. and L. correction represents an increase of the earth's field by virtue of a station being north of the base, the correction goes into the form as +. The correction is applied in the proper manner as a result of the operation of the form, as will be explained later.

In column 12 is entered the reading in γ's obtained at the base when first occupied; in this case it is 572, which is recorded in this column after each station and applied as a correction. It is subtracted from the reading at each station in the operation indicated in column 14.

In column 13, the corrections of columns 9, 10, 11, and 12 are added and set down as shown. Column 14 represents the operation column 8-13, that is, the station reading minus the sum of the corrections. The values for the stations, as shown in column 14, are the vertical intensity values with all corrections applied, assuming the base has a value of zero. They indicate how much higher or lower a station is, magnetically, than the base.

The diurnal and L. and L. corrections are properly applied in the operation of this form. Consider only the daily variation. This variation shows a decrease of 3 γ's for station 1. To eliminate this change and get the reading at station 1 on a basis of no daily variation, we would have to *add* to the reading at station 1 the amount of 3 gammas. This is actually what has been done, because in the operation of column 14 (considering the daily variation alone) the base value 572 was to be subtracted from the station value 622. We have subtracted from 622 a number three less than 572, or in effect we have added 3 gammas.

In like manner, considering only the L. and L. correction at station 1 of 21 γ's, the earth's field has increased 21 gammas at this station. To apply this correction properly and put station 1 on the same magnetic datum as the base, 21 gammas must be *subtracted* from the reading at station 1. This is done because we subtract from the 622 value for station 1 the base value 572 + 21 gammas. Considering L. and L. correction only, we take from 622 a higher number than 572, or 593.

To follow this through on another line: take the station reading for station 1 of 622 and add to it the 3 γ's of daily variation, which makes 625. From 625 subtract the 21 γ's of L. and L. change, leaving 604. From 604 take the base reading of 572 which leaves +32, the value previously obtained for station 1.

In column 15 the arbitrarily assumed value *(X)* assigned to the base is added to the values of vertical intensity obtained in column 14 relative to the base as zero. This value X is taken at a convenient figure for the

area and may be of such an amount as to eliminate negative magnetic values in contouring. The value X for the magnetic work in a given county for a survey base station may be set at 2000 γ's.

Such a base could be tied in magnetically, if desired, with a government magnetic station where the true and absolute value of vertical magnetic intensity is known. The absolute vertical intensity, however, is not necessary in much magnetic field work, as the values from field stations are obtained *relative* to a base. They represent the finer variations in the magnetic intensity which are of significance in geologic terms. This is the main difference between magnetic surveying for the purposes of applied geophysics and that carried on by the U.S. Coast and Geodetic Survey in measuring the total and absolute magnetic values at stations.

Station Spacing

A general rule for spacing of stations in magnetic or other geophysical surveys can be stated. Stations should be set sufficiently close together so that no important change in the quantity measured can occur without being shown in the results of the survey. In practice, this means for placer surveys stations from 5 to 25 feet apart; for dikes and ore bodies stations may be 25 to 50 or 100 feet apart, depending on the size of the body. For magnetic structural studies in connection with oil accumulation, from ¼ to 2-mile spacing may be used.* For serpentine plugs, with which oil is sometimes associated, as these features themselves are not large, ⅛ to ¼ mile stations are used. For faults and formation boundaries 100- to 300-foot spacing may be necessary.

It is customary when surveying traverses of stations to lay them out at right angles to the strike of the geologic feature involved. The most rapid change with distance normally occurs in such a direction for the magnetic effects. Lacking information on the strike, test traverses can be run to find the direction in which the most rapid change takes place. Regional strike is often an aid in choosing the proper traverse direction.

Plotting Magnetic Data.—The corrected data of a magnetic survey may be presented in a number of ways. Usually, however, the results are shown as: (1) magnetic profiles along traverse lines so chosen that the magnetic profiles may be correlated with known geological drill-hole or other data, or (2) isanomalic contour maps. In the first type of presentation, the data are usually plotted with the anomaly in gammas (or scale divisions) as ordinate and the traverse distance in feet or miles as abscissa. The second type of presentation (isanomalic contour map) is similar to the conventional topographic map; that is, the magnetic datum at each station is indicated on a plan view of the area at a point corresponding to the location of the station, and isanomalic magnetic contours are drawn

* This would depend on local conditions and on the type of survey, viz., reconnaissance or detail.

by inspection.* The small closed contours representing curves of greatest magnetic strength are usually shaded outwardly, and are termed magnetic "highs." The contours representing curves of lowest field strength are usually shaded inwardly, and are termed magnetic "lows." (Figure 65.)

Illustrations of magnetic anomaly profiles and isanomalic contour maps are given in the section dealing with results of surveys.

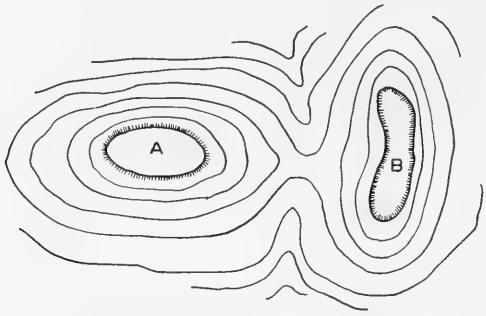

FIG. 65.—Method for representing *magnetic high* contours (A), and *magnetic low* contours (B).

"Normal" Values of the Earth's Intensity Components

Interpretation of magnetic anomaly curves is sometimes facilitated by knowing the "normal" intensity components in the area under investigation.

A precise definition of the normal intensities cannot be given. The procedure for arriving at the normal values for a given area is an approximation process. Consideration must be given the shapes of the anticipated geological features and their relative magnetic effects. In regions where large anomalies exist, the normal values are the intensity components measured at a station removed from the anomalous area.

Summary

Preliminary

In Laboratory

Determining temperature coefficient of instrument

Determining magnetic moments of auxiliary magnets

In Field

Adjusting for latitude

* In many surveys the method of least squares is applied before drawing final isanomalic contours. Barton † and Roman ‡ describe the application of this method to magnetic prospecting.

† D. C. Barton, "Control and Adjustment of Surveys with the Magnetometer or the Torsion Balance," *Bull. A.A.P.G.*, Vol. 13, 1929, pp. 1163-1183.

‡ I. Roman, "Least Squares in Practical Geophysics," *A.I.M.E. Geophysical Prospecting*, 1932, pp. 460-506.

Adjusting for sensitivity*
Checking scale value to determine gammas per scale division
Determining location of stations to allow best correlation with geology
Establishing base stations
Preliminary traverses: one traverse in a N-S direction to obtain maximum anomalies due to polarization

Field Work at Each Station

Setting up tripod at station
Leveling tripod
Orienting tripod head
Leveling instrument, after clamped to tripod head
Obtaining scale readings
Recording
Station number and map location
Scale readings
Temperature of instrument
Time of observation
Local conditions which may affect the reading

Corrections

Base reading to datum plane (for survey employing more than one instrument)

Latitude
Average for U. S.: 10-12 gammas per mile for vertical component
5-8 gammas per mile for horizontal component
When movement proceeds to the North
Subtracted for vertical component
Added for horizontal component

Longitude
Average for U. S.: 2 to 3 gammas per mile
When movement proceeds to the East
Subtracted for east declination areas
Added for west declination areas

Base station corrections
Diurnal and other variations in earth's field
Instrument variations (average of readings)

Temperature corrections
Correction for deflection due to use of auxiliary magnets

* May also be done in the laboratory.

Accuracy to Which the Work is Conducted
Depends upon anomalies in the region

Accuracy of Data Depends on
Errors in scale reading: 2 to 4 gammas
Temperature effects: 1 to 3 gammas
Diurnal variations: 2 to 5 gammas
Regional variation

Final Interpretation Includes
Checking scale value
Checking computations
Making corrections and converting readings to gammas
Correcting for regional gradient if necessary
Plotting of magnetic data
Correlating with areal and subsurface geology
Correlating with other geophysical work
Predicting probable subsurface conditions

Special Types of Magnetic Instruments

Kohlrausch Magnetometer.—The Kohlrausch magnetometer consists essentially of a circular, glass-covered case which houses a pivoted horizontal swinging magnetic needle.‡ The case is supported by a vertical rod which is coaxial with the pivot of the swinging needle. (Figure 66.) An auxiliary bar magnet is also supported by the vertical rod. The distance *d* between the bar magnet and the needle is adjustable, thereby controlling the sensitivity. The bar magnet may be rotated either clockwise or counterclockwise, the rotation to either side being limited by stops. The vertical rod is supported on a three-legged base which is provided with screws and a small bubble level so that the rod can be orientated in a vertical position.

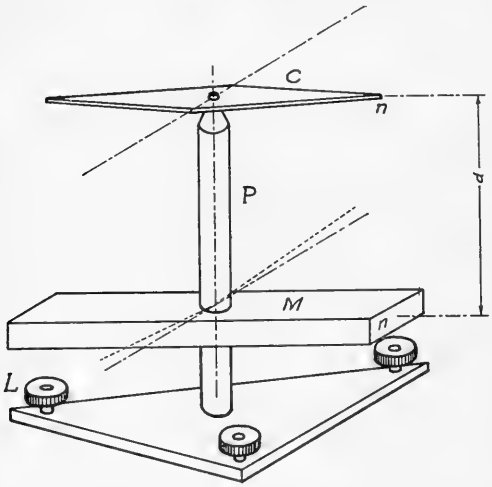

FIG. 66. — Kohlrausch magnetometer. *C*, pivoted magnetic needle; *P*, supporting pillar; *M*, bar magnet; *L*, leveling screws; *d*, sensitivity adjustment.

The magnetometer is first set up at a base station with the needle and magnet orientated in the direction of the magnetic meridian. The bar magnet is rotated until the compass needle is deflected 90° and one of the

‡ A. S. Eve and D. A. Keys, *Applied Geophysics* (Cambr. Univ. Press, 1938), pp. 31-35.

adjustable stops is clamped at this position to provide a reference mark. Next, the bar magnet is rotated in the opposite direction until the compass needle is again deflected through 90°, and the second adjustable stop is clamped at this position. The supplement θ of the mean value of the angle of rotation of the magnet is computed. The horizontal component H_0 of the earth's field at the base station and the horizontal component F of the field produced by the bar magnet are related by the equation

$$H_0 = F \cos \theta \tag{61}$$

The instrument is now moved to a new (field) station and leveled as before. If the horizontal intensity H at the field station is less than H_0 a rotation of the bar magnet to its stop will deflect the compass needle through an angle of magnitude $90° + \phi$. The components of H and F perpendicular to the plane of the resultant field are equal; that is,

$$H \cos \phi = F \cos (\theta + \phi) \tag{62}$$

On replacing F by $H_0/\cos \theta$ (Equation 61),

$$H = H_0(1 - \tan \theta \tan \phi) \tag{63}$$

Thus, if H_0 and θ are known for the base station, the relative variation in the horizontal intensity can be calculated by observing ϕ.

The angle ϕ in an ore-free district will vary only by one or two degrees; the variations over a magnetite deposit, however, may be considerable.

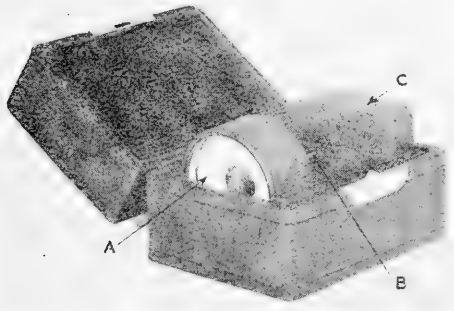

FIG. 67.—Gauss meter (A) with probe (B) and standard magnet (C). (Courtesy of General Electric Company.)

Gauss Meter.—An instrument has been designed for the purpose of tracing out high intensity magnetic force or flux lines and mapping their intensity.* This meter, illustrated in Figure 67, and shown diagramatically

* See p. 74.

in Figure 68, is a miniature magnetometer developed for measuring flux density and determining direction of flux in permanent magnets, electromagnetic coils, etc. It may be used for checking flux density and flux gradients in air gaps, and for measuring flux density in iron structures. The instrument comprises a very small magnet fastened to a delicately pointed shaft to which a pointer is attached. The deflecting torque of the pointer results from direct interaction between the flux under investigation and the small magnet.

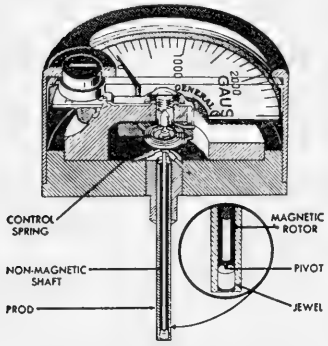

FIG. 68.—Sectional view of gauss meter. (Courtesy of General Electric Company.)

Flux density is measured by rotating the instrument case until maximum reading is obtained on the calibrated scale. This point is reached when the probe magnet flux is at a right angle to the flux being investigated, and the scale can be read directly in gauss. The probe diameter varies from .090 of an inch to as little as .052 of an inch.

To measure the flux density in the iron position of magnetic circuits, a small hole (0.09 inch in diameter) is drilled in the iron structure. If this hole is small in proportion to the iron, then

$$\text{Flux density} = H = \frac{1}{2}\left[1 - \frac{1}{\mu}\right] H_{hole} \qquad (64)$$

From known data on the BH curve of iron (Figure 73), flux density of the structure is easily computed. Thus, detailed information can be obtained about flux distribution in large and often irregularly-shaped iron structures used in generators and other large electric apparatus.†

Magnetic Properties of Rocks

The magnetic character of minerals and rocks and their geologic history govern the functioning of the magnetic methods. Magnetic susceptibility bears the same relation to magnetic field studies as does density to gravity studies. Susceptibility, however, is not as simple or as easily measured a physical property as density.

The magnetic susceptibility of a given rock or formation depends on a number of factors, some of which are not too well understood. These factors may be classed broadly as mineralogical and geological.

Mineralogical Factors.—Most substances react in a definite manner, some rather mildly, to a magnetic field. A few minerals, because of their marked magnetic properties, are set apart and called *ferromagnetic*. We will be largely concerned with these latter in discussing rock susceptibility.

In interpreting magnetic data it is assumed that the minerals, rocks and formations owe their magnetization to induction in the earth's magnetic field. In the north temperate zone this is a weak field of about 0.6 gauss

† General Electric Co., publication G.E.C.-238, Mar., 1938.

(60,000 gammas) strength. The earth's magnetic field, nevertheless, appears to be sufficient, coupled with the rather wide distribution of the ferromagnetic minerals, to account for and give rise to measurable and significant magnetic anomalies. These anomalies occur under quite a wide variety of geologic settings, and have patterns that can usually be recognized as having geologic causes and relationships.

The magnetic susceptibility of rocks usually is directly proportional to their content of ferromagnetic minerals. This rule applies to igneous, metamorphic, and sedimentary rocks.

The Ferromagnetic Minerals.—The key ferromagnetic minerals are: (1) magnetite, which is of the most importance; (2) ilmenite, of much importance but to a lesser extent than magnetite; (3) pyrrhotite; and (4) franklinite, which is definitely ferromagnetic but of least significance in magnetic mapping.

Typical values of magnetic susceptibility of these minerals, determined at magnetic fields of the same order as that of the earth, are given in the following table.

MAGNETIC SUSCEPTIBILITIES OF FERROMAGNETIC MINERALS

Mineral	*Volume susceptibility k*
1. Magnetite (Fe_3O_4)	$k = 0.032$ c.g.s.†
2. Ilmenite ($Fe\ Ti\ O_3$)	$k = 0.030$ c.g.s.‡
3. Pyrrhotite ($Fe_7\ S_6$)	$k = 0.028$ c.g.s.‡
4. Franklinite	$k = 0.0035$ c.g.s.‡

A study of the amount of magnetite and ilmenite present in rocks of different types has been made by N. H. Stearn.§ In general, it was found that the greater the percentage of these two minerals present in a particular rock, the higher its susceptibility. Stearn's work further indicates that the average sedimentary rock (which is considered to be 82% shale, 12% sandstone and 6% limestone) has a combined magnetite-ilmenite content of 0.09%. The average granite carries 2.03% and the average basalt 6.53% of these two ferromagnetic minerals.

Although average rocks are not encountered in the field, such generalizations are useful for an understanding of magnetic phenomena. Figures for the average sandstone show 0.83% of combined magnetite and ilmenite, and for the average igneous rock (composed of 65% granite and 35% basalt) 4.6%. From this, it appears that if all the magnetite and ilmenite in the earth's crust were distributed evenly, these two minerals would make up 2.95% of all rocks. The average shale and limestone do not carry sufficient magnetite or ilmenite to be magnetic.

It should not be assumed from this study of hypothetical average rocks of various kinds that shales may not be magnetic, for there are cases

† The susceptibility of magnetite varies considerably for different samples, with a range from 0.04 to 0.097 for pulverized samples. For solid magnetite values from 1 to 20 c.g.s. are of record.
‡ Pulverized samples.
§ N. H. Stearn, "A Background for the Application of Geomagnetics to Exploration," *A.I.M.E. Geophysical Prospecting Volume*, 1929, pp. 330-331.

of definitely magnetic shales. Likewise it should *not* be assumed that because a rock is intrusive (and therefore would show considerable magnetite ilmenite content on averages) it *is* necessarily magnetic. An intrusion covering over a square mile, which forms a considerable hill in Huerfano County, Colorado, is no more magnetic than the shales surrounding the area.

The high values of magnetic susceptibility of the ferromagnetic minerals, especially magnetite, contrast sharply with the susceptibilities of the more common minerals and rock types listed below.

MAGNETIC SUSCEPTIBILITIES OF CERTAIN MINERALS AND ROCKS

Minerals	*c.g.s. units*
Rock salt	$k = -0.000{,}0013$ to $-0.000{,}003$
Quartz	$k = -0.000{,}0014$ to $+0.000{,}0012$
Pyrite	$k = +0.000{,}0045$ to $0.000{,}120$
Limonite	$k = 0.000{,}057$ to $0.000{,}220$
Sphalerite	$k = 0.000{,}058$ (no data)
Hornblende	$k = 0.000{,}122$ (no data)
Rocks	
Anhydrite	$k = -0.000{,}010$ to $-0.000{,}001$
Limestone	$k = +0.000{,}0038$ (no data)
Granite	$k = 0.000{,}004$ to $0.000{,}650$
Sandstone	$k = 0.000{,}005$ to $0.000{,}0168$
Gneiss	$k = 0.000{,}008$ (no data)
Clay	$k = 0.000{,}020$ (no data)

Because of the range in the values of susceptibility for a given type of rock as shown in available tables, an attempt to group rocks and minerals strictly on a basis of their susceptibilities is beset with exceptions. This is evident in the case of the granite as given above. It is also evident that generally the ferromagnetic minerals are from 100 to 500 or more times higher in susceptibility than the great majority of other minerals or rocks. Even in the case of sedimentary rocks there usually exist sufficient contrasts in susceptibilities between formations to cause detectable and mapable magnetic anomalies.

These susceptibility contrasts are due to the content of the ferromagnetic minerals in a given rock or formation. Further evidence of this is furnished by the following examples. A specimen of sphalerite with an iron content (Fe_3O_4 magnetite) of 0.21% showed a susceptibility of 0.000001 c.g.s. units. Where the magnetite content was 14.69%, the susceptibility was 0.000519.

The magnetite content of shale samples gives the same general relationship. A shale with 0.4% of magnetite gave a susceptibility 4 times as great as a shale with 0.075% of magnetite. A granite-magnetite powder mixture tested in a magnetic field of 15 gauss showed that for a weight of magnetite of 2 units per 1000 the susceptibility was about 0.0003 c.g.s. For a similar mixture with 14 units of magnetite the susceptibility increased to about 0.002.

The Factor of Grain Size.—Measurements of the magnetic susceptibility of powdered samples of magnetite have shown that a decrease in the particle size greatly reduces the effective susceptibility. The use of crushed specimens is advantageous for study, and by preparing admixtures of magnetite dispersed in a non-magnetic material, a sample mixture is obtained

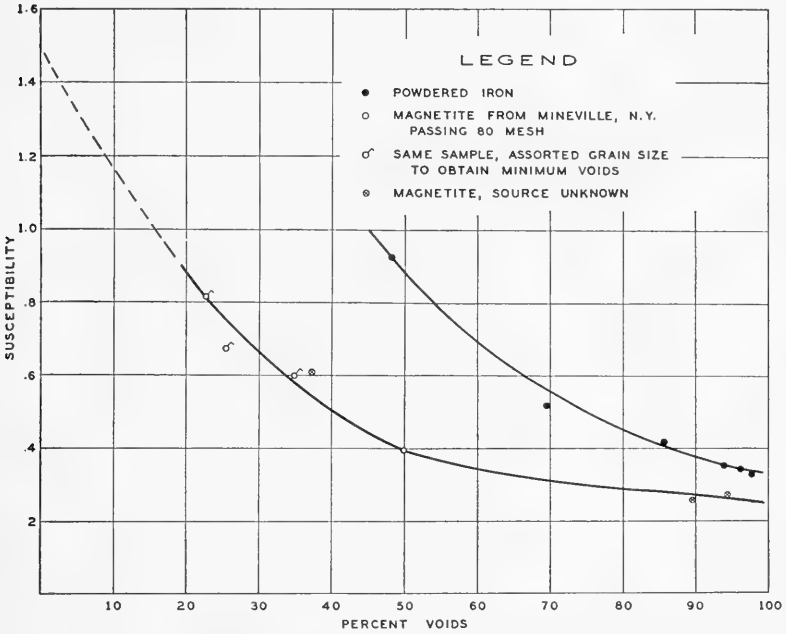

Fig. 69.—General range of variation of susceptibility of magnetite and iron powders with per cent voids in a field of 0.64 gauss. (L. B. Slichter, *A.I.M.E. Geophysical Prospecting,* 1929, p. 247.)

which approaches disseminations found in natural rocks. In a series of experiments the per cent of *voids* was varied from 23 per cent to nearly 100 per cent with a resulting marked decrease in magnetic susceptibility, as shown in Figure 69. In these tests, the iron and magnetite passed an 80-mesh sieve.

It appears that the susceptibility of magnetite powder with 90 per cent voids was about 0.26, and with 23 per cent voids 0.82, the latter being about the practical limit obtainable in preparing samples. Projecting the curve to zero voids, or the equivalent of solid magnetite, gave a value of 1.5, which is in general agreement with values of susceptibility for magnetite in solid form.

The findings discussed above correlate with the tabulated values of susceptibility. Those rocks in which the magnetite present is most widely dispersed show the lowest susceptibility.

Numerical Data on Magnetic Susceptibilities.—The usefulness of geomagnetic methods in obtaining information regarding subsurface conditions depends chiefly on the relative magnetic susceptibilities of the materials constituting the outermost portion of the earth's crust. Because in general rocks are mixtures of numerous mineral components, the effective susceptibilities depend on those of the individual constituents, and on the percentage of each constituent.

As a general rule, reliable magnetic anomalies cannot be measured by the usual field techniques of exploration geomagnetics unless the magnitude of the *difference* between the susceptibility of the anomalous geologic feature and the susceptibility of the surrounding media is equal to or greater than plus or minus 0.00015. If the susceptibility difference is positive, the anomalous subsurface feature usually possesses some ferromagnetic material. The *amount* of ferromagnetic materials which must be present is small due to the fact that a majority of the compounds of iron have very high susceptibilities. (See Figure 69.) The most familiar geologic feature possessing a *negative difference* with respect to surrounding media is a salt dome.

The magnetic susceptibilities of various materials which occur in the outer portion of the earth's crust are shown in Table 5.† Other values appear elsewhere in the literature.‡

† N. H. Stearn, "A Background for the Application of Geomagnetics to Exploration," *A.I.M.E. Geophysical Prospecting*, 1929, pp. 315-342.

‡ L. B. Slichter, *A.I.M.E. Geophysical Prospecting*, 1929, p. 343.

F. Stutzer, W. Gross and K. Borneman: "Ueber magnetische Eigenschaften der Zinkblende und einiger anderer Mineralien," *Metall und Erz* (1918) *15*, 1, quoted by L. B. Slichter, *A.I.M.E. Geophysical Prospecting*, 1929, p. 241.

TABLE 5.

MAGNETIC SUSCEPTIBILITY OF ROCKS AND MINERALS*

MAGNETIC MINERALS	*Susceptibility k (c.g.s. units)*			*Remarks*	*Reference***
Magnetite Crystals	6.3	to	24.0	Min. value is average of k parallel to 3 main crystal axes; Field (F)=2 gauss. Max. value parallel to binary axis, F = 1	b
Magnetite	0.04	to	2.0	Solid specimen (S) max. value at F = 1	a, b
Ilmenite	0.03	to	0.14	Pulverized sample (P) min. at F = 220 Max. at F = 1	c, f
Franklinite	0.036			No data on max.	d
Pyrrhotite	0.007	to	0.028	P. min. F = 220 Max. F = 0.6	d, e
Specularite	0.003	to	0.004	Specular Hematite P. min. F = 220 Max. F = 0.6	c
Chromite	0.002			No data on max. P. F = 220	f

TABLE 5—Continued.

MAJOR ROCK TYPES	*Susceptibility k (c.g.s. units)*			*Remarks*	*Reference***
Basic Effusives	0.001	to	0.004	Range of k covers 76% of 97 samples See graph figure	b
Basic Plutonics	>0.0001	to	<0.004	53 samples	b
Granites and allied rocks	>0.0001	to	<0.001	Range covers 83% of 74 samples	b
Gneisses, Schists and Slates	>0.0001	to	<0.001	Range covers 93% of 45 samples	b
Sedimentaries	>0.0001	to	<0.001	Range covers 92% of 48 samples	b
SPECIFIC ROCK TYPES					
Igneous Rocks					
Basalt	0.00068	to	0.0063	8 samples	f
Diabase	0.000078	to	0.0042	8 samples	f
Gabbro	0.00044	to	0.0041	6 samples	b, f
Granite	0.00003	to	0.0027	14 samples	f
Porphyry	0.000023	to	0.0005	11 samples	b, f
Metamorphic Rocks					
Serpentine	0.00025	to	0.014	2 samples	f
Slate	0.000039	to	0.0030	3 samples	f
Gneiss	0.00001	to	0.0020	2 samples	f
Schist	0.000026	to	0.00024	2 samples	b, f
Sedimentary Rocks					
Shale	0.00004	to	0.00005	3 samples	f
Clay	0.00002			1 sample	f
Sandstone	0.000005	to	0.000017	2 samples	f
Dolomite	0.0000009	to	0.000014	2 samples	d, f
Limestone	0.000004			1 sample	f
IRON ORES AND MINERALS					
Siderite	0.0001	to	0.0003	2 samples	f
Limonite	0.0001	to	0.0002	2 samples	f
Hematite	0.00004	to	0.0001	1 sample	f
Ankerite	0.00002	to	0.0001	2 samples	f
TYPICAL SULPHIDE MINERALS					
Arsenopyrite, Chalcopyrite, Chromite, Markasite, Pyrite	0.000005	to	0.0002	Many samples	f
DIAMAGNETIC MINERALS AND ROCKS					
Anhydrite and Gypsum	−0.0000011	to	−0.00001	1 or more samples	f
Quartz	−0.0000011	to	−0.0000012	1 or more samples	f
Sylvite	−0.0000009	to	−0.0000011	1 or more samples	f
Calcite	−0.0000006	to	−0.0000010	1 or more samples	f
Rock salt	−0.0000004	to	−0.0000013	1 or more samples	f

* See Equations 18 and 19 for the relationship between susceptibility and permeability.

**References for table of magnetic susceptibilities:

a. L. B. Slichter, *A.I.M.E. Geophysical Volume,* 1929, p. 242.
b. Ibid, *G.S.A. Special Paper No. 36,* 1942, p. 295.
c. N. H. Stearn, *A.I.M.E. Geophysical Volume,* 1929, p. 343.
d. Ambronn and Cobb, *Geophysics,* McGraw-Hill, 1928, p. 94.
e. L. B. Slichter, *ibid.,* p. 343.
f. C. A. Heiland, *Geophysical Exploration,* Prentice-Hall, 1940, pp. 310-314.

Figure 70 is a graphic classification of 317 samples of rock as to type and magnetic susceptibility.† A sufficient number of samples was tested for each of the 5 major rock types which were considered to make the susceptibility data representative and significant. The percentages of the samples of a given type of rock falling in a particular range of magnetic susceptibility are shown in the figure. The figure illustrates, for example,

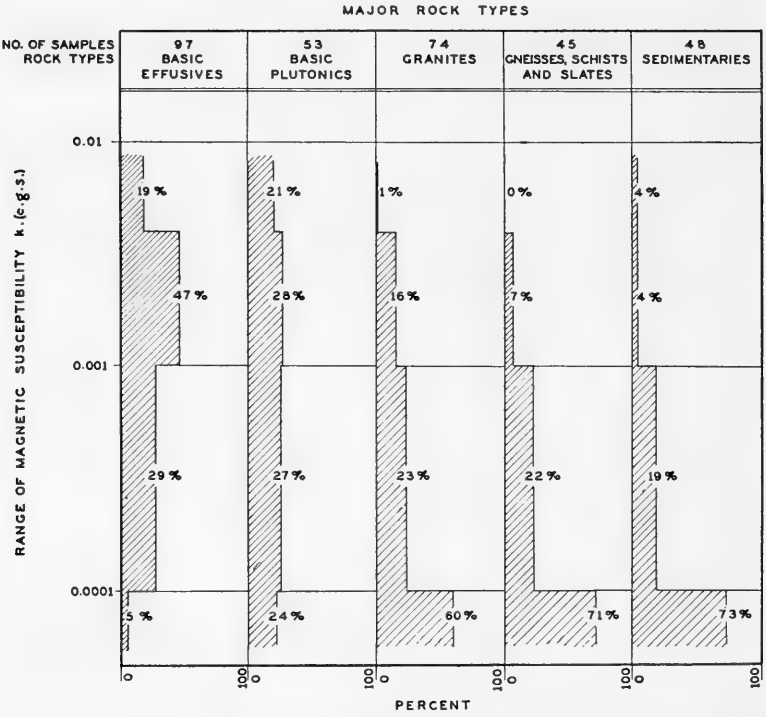

FIG. 70.—Graph showing the percentage of test samples of 5 major rock types having magnetic susceptibility ranges from $> 10^{-4}$ to $< 4\times10^{-3}$ c.g.s.

that of the 74 specimens of granite (and allied types of rock) whose magnetic susceptibility was measured, 60% had a susceptibility of less than 10^{-4} c.g.s. The remaining 40% of the samples was divided as follows: 23% in the susceptibility range of from 10^{-4} to 10^{-3}, 16% from 10^{-3} to 4×10^{-3}, and only 1% above this latter figure. The data from which this graph was constructed did not indicate how much above or below the 4×10^{-3} and the 10^{-4} values respectively the susceptibilities measured.

However, in planning magnetic surveys as applied to mining problems, it must be remembered that a conclusion which may be valid in one locality, on the basis of susceptibility contrasts, may not apply in another, although

† Based on data in Table 20-3, p. 296, *Handbook of Physical Constants; G.S.A. Special Paper No. 36*, section on Magnetic Properties of Rocks, by L. B. Slichter (January, 1942).

the same mineral may be present and conditions quite similar. Therefore the best procedure is to test samples of the mineral deposit where work is in view, covering not only the mineral or ore itself, but also the surrounding rock.

Geological Factors

There are a number of geological factors meriting consideration which will be discussed briefly. Any one of them might furnish a clue for an interpretation of a magnetic survey.

Thermal Effects.—A rigorous analysis of the effects of temperature on the magnetization of rock *in situ* is difficult, due to the many unknown variables. In general the permeability of magnetic materials increases continually with increase of temperature until a point known as the "temperature of recalescence" is reached.† After passing this temperature, the permeability decreases very rapidly, and within a few degrees of the recalescence temperature, ferromagnetic materials appear to lose their magnetic properties completely. The temperature at which magnetic materials become non-magnetic is also known as the *Curie point.* The Curie points for some ferromagnetic minerals are: magnetite‡ 515° C., pyrrhotite‡ 300° C., nickel§ 310° C., iron§ 690° C. to 870° C. These values for the Curie point have an important bearing on the question of the depth of the earth's crust at which magnetization of rocks can exist. It is estimated that due to increase of temperature with depth, permanent magnetization of rocks disappears below about 60,000 feet, or about 11.5 miles.††

It is not known if the same ferromagnetic body actually exists at temperatures beyond the Curie point, or whether another body with different structure and chemical properties has been formed. When a magnetic rock is heated until its magnetism disappears, and is then cooled, its magnetic property will reappear at a lower temperature than that at which it was lost.

Although in all probability not a strictly comparable case, the sun has a strong magnetic field notwithstanding its very high surface temperature of some 5900° C. Also, analysis of the distribution of the earth's magnetic field leads to the view that 52 per cent of its strength appears to originate in the core. As previously mentioned, however, below a depth of 60,000 feet magnetization of rocks would no longer exist due to the high temperatures. For this reason, the magnetic properties which appear to exist within the earth and the sun may be explained by assuming that they are due to an actual flow of electric current of high amperage.

Lightning.—Lightning may affect the local magnetization of exposed rocks. The large current intensities in lightning discharges (of the order of

† J. H. Jeans, *The Mathematical Theory of Electricity and Magnetism,* (Cambr. Univ. Press, 5th Ed.) p. 412.

‡ R. Ambronn, *Elements of Geophysics,* (McGraw-Hill, New York, 1928) p. 95.

§ S. G. Starling, *Electricity and Magnetism,* (Longhams, Green and Co., Ltd., 5th Ed. 1929) p. 287.

†† See also J. A. Fleming, *Terrestrial Magnetism and Electricity,* (McGraw-Hill, 1939) p. 321.

20,000 amperes) give rise to relatively strong magnetic fields. Hence, lightning discharges may offer an explanation for the irregular rock magnetization sometimes observed on exposed hill tops.

Stresses.—Forces such as are active in mountain building, faulting and folding affect the magnetization of rocks. Similar phenomena may be predicated on certain observed effects or reactions in rods or wires. For example, stretching a rod increases its intensity of magnetization in a weak field. A ferrous metal rod becomes magnetized when it is bent. There is a change in intensity of magnetization in certain substances with volume changes. These phenomena are examples of such reactions, and some of them may be duplicated by geologic processes. Some unusual magnetic anomalies which cannot be explained by differences in magnetic susceptibilities of known formations may possibly be due to such magneto-mechanical effects.

Structural Movements.—Geologic activity sufficient to cause disruptive deformation and overturning of deposits or dikes may often produce abnormal magnetizations. There are cases where north magnetic poles logically occur near the surface under conditions where south magnetic poles should be present. This is shown after a magnetic map has been contoured, when magnetic lows are found where magnetic highs would normally be expected to appear.

Disintegration.—Since trivalent iron is more magnetic than bivalent iron, it follows that magnetization will be much reduced when magnetite disintegrates to limonite or hematite.

Metamorphism.—The reverse of the above is evident in contact and dynamo metamorphic processes in sedimentaries and other rocks. The bivalent iron is changed to the trivalent form so that accumulations of magnetic rocks are often found near intrusive bodies.

Concentration.—Concentration of magnetic minerals has been shown to cause increase in magnetization in contact metamorphic zones and in the black sand accumulations of placer deposits. Such concentrations may take the form of dikes, fissure fillings, replacements, tabular veins, or irregular masses.

A study of the distribution of ferromagnetic minerals in one Keweenawan lava flow in Wisconsin indicates that the magnetic minerals show a concentration at definite horizons, or roughly parallel to definite planes. This may well account for the linear magnetic disturbances which occur parallel to the flows. As a consequence, any distortion or disruption of these planes would cause a concomitant change in the magnetic anomalies associated with them.

In sedimentary rocks the concentration of ferromagnetic minerals into definite horizons is also marked. In sandstone formations, magnetite-rich

beds may be intercalated with beds free from magnetite. In schists and gneisses the tendency to banding may cause a marked tabular distribution of ferromagnetic minerals.

Attitude of Tabular Concentrations.—The attitude (dip and strike) of tabular concentrations of magnetic materials is of importance, since it affects the type of magnetic anomaly produced. Certain ferromagnetic masses are sufficiently concentrated that the earth's magnetic field induces polarity in them, as has been indicated. In the northern hemisphere and under ordinary conditions, such induction in a tabular mass produces south polarity along the outcropping edge. There are, however, certain very limited attitudes which such a magnetic tabular concentration can assume in which its relation to the earth's magnetic field is such that the induced polarity in the outcropping edge will be north polarity. Specifically, if the magnetic bed strikes magnetic east-west and dips against the earth's magnetic field at an angle very slightly greater than the inclination of the earth's field, its outcrop will show north polarity. (See Figure 71.)

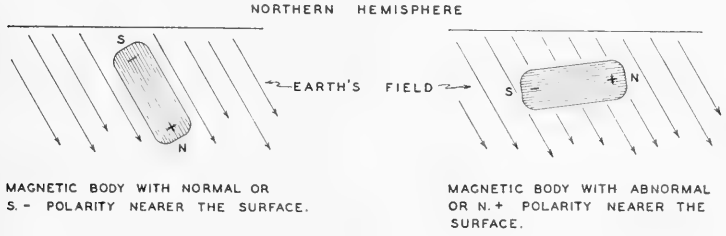

FIG. 71.—Showing the effect of the attitude of a tabular magnetic body on its induced polarity.

The actual occurrence of such induced north polarity is rare. In general, sharper distortions of the earth's magnetic field are made by steeply dipping magnetic formations, or those whose dip most closely approaches parallelism with that of the lines of force of the earth's magnetic field.

Topography.—The effects of topography are difficult to predict. It is certain, however, that variations in bed rock topography in a placer area would be a factor in determining the shape of the magnetic anomaly. Variation in bed rock depth alone would alter the magnetic effects arising from a given set of magnetic conditions.

The sub-outcrop of a magnetic orebody would show up in a considerably different manner if it were on a steep slope, at the top of a hill or ridge, or in a valley. In the case referred to, where the buried magnetic body lay on a steep slope, a magnetic traverse up the slope across the body would have quite different magnetic values for those stations below the body than for those above it.

Induced and Residual Magnetization

The magnetic character or magnetization of a rock may be considered as made up of two components: namely, the *induced* and the *residual* magnetization. The term *polarization* is sometimes used for magnetization. This can be illustrated by an imaginary case.

Given a magnetizable formation which has been subjected to the earth's magnetic field and has acquired magnetization and polarity by induction. The magnetization thus set up in the formation is the *induced* magnetization.

Due to tectonic forces, a portion of this magnetized formation might be overturned or even reversed end for end. In this new position, the earth's magnetic field would be acting on the overturned part to induce magnetization in it and even to reverse or reduce the direction and amount of the polarization originally set up. In time a change will be brought about, and a magnetization of different amount and direction would be present in the segment of the formation acted upon.

In most rocks there exists, to a greater or less degree, what is termed *residual* magnetization, or magnetization that resists removal or reversal. Residual magnetization in a body is that portion of its magnetization which is permanent or fixed. Such magnetization may be appreciable in magnitude and may not be in the same direction as the induced magnetization. It may even be in the opposite direction to the induced component.

Residual magnetization in rocks may account for reversed polarities in certain orebodies which have been displaced or overturned. In such rather rare cases a magnetic low may be found above an outcropping edge in latitudes where a magnetic high would be normal.

Certain simple tests can be made with a specimen of rock and a magnetometer to find out if there is any residual or remanent magnetization present, and the approximate proportions of induced and residual polarization. More elaborate tests are made by subjecting the specimen to a complete hysteresis cycle and recording data with which to plot the hysteresis curve for measuring induced and residual magnetization quantitatively.

Magnetic Hysteresis

The behavior of magnetic materials when subjected to cyclic changes of magnetizing fields presents some interesting phenomena.†

Consider a rod of magnetizable material in a demagnetized condition in a primary solenoid coil. A short secondary coil, surrounding the primary coil, is connected to a ballistic galvanometer. When a known current is passed suddenly through the primary coil, the throw of the galvanometer will be proportional to the flux density B in the specimen when the circuit is closed. When the circuit is broken, the galvanometer will move in the opposite direction. The magnitude of the galvanometer movement in the "make", in relation to the opposite direction of movement in the "break", permits the magnetic properties of the specimen to be measured.

† T. A. Ewing, *Magnetic Induction in Iron and Other Metals.*

With such apparatus the magnetizing current may be increased by steps to any desired amount, plus or minus, and at these various stages the value of the magnetizing field H, intensity of magnetization I, and flux density B can be determined.‡

The data thus obtained may be presented in two types of hysteresis curves. In one type, the IH curve, I is used as ordinate and H values for abscissa. In the other type or BH curve, B is the ordinate with H again as the abscissa.

With a ferromagnetic substance placed in the above-described apparatus, the magnetizing field is made to vary in small increments: proceeding from the zero value of H in Figure 72(a) to such positive value P as desired, and then back again to zero at point D. The current is then reversed and the necessary negative values are obtained, to P' and then again back to zero, point I. The intensity of magnetization, or the flux density B, of this substance as it varies with the field H is shown in a curve like that in Figure 72(a).

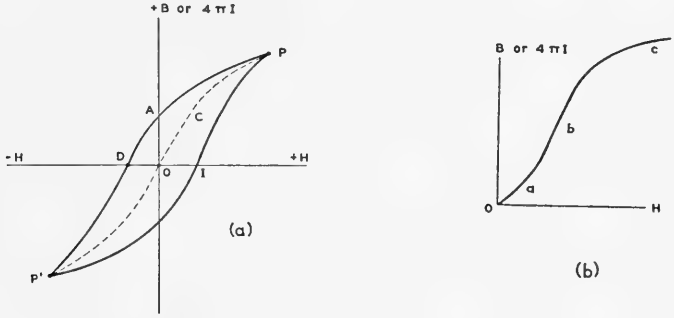

FIG. 72.—Typical hysteresis curve for a magnetizable material, showing variation of intensity of magnetization, or flux density B, vs. magnetizing field H.

There are three stages in the magnetization cycle. *The first* is the preliminary or initial magnetization stage. Here the value of H is small and a change therein produces only a very small change in B. Near the origin the curve is substantially a straight line and $\mu = B/H$ and is constant. This portion of the curve is represented at a in Figure 72(b).

The second or magnetization stage shows that the curve rises rapidly and a small change in H produces a large change in B. The permeability $\mu = B/H$ has its maximum value at the inflection point of the B-H curve in this stage. Note the portion b in Figure 72(b).

The third or saturation stage is reached when the curve becomes nearly horizontal, or where a large increase in H causes a relatively small increase in B. Here μ acquires quite low values, as may be seen by the portion c of the curve.

‡ Other procedures are often used for measuring these quantities; however this is one of the simplest.

Upon reducing the magnetizing field, after the third stage has been reached, the plotted curve follows along a different path than it traced as H was being increased. It is of note that during this reduction when H reaches zero, there is a certain amount of flux left in the specimen. This flux is designated as the *remanent magnetism.* See OA, Figure 72(a).

The phenomenon of the lagging behind of the flux density or magnetization as regards the intensity of the field is called *magnetic hysteresis.*†

Remanent Magnetism and Retentivity.—When there is remanent magnetism, it can be assumed that it is due to internal forces which cause the remaining flux (after the field has reached zero) to stay in the material. This characteristic, known as coercive force, is measured by OD of Figure 72(a). It is the force or coercive field necessary to reduce the flux in the specimen to zero. The usual symbol for coercive force is H_c. The reversed current portion of the hysteresis curve is shown in the third and fourth quadrants of Figure 72(a).

Retentivity defines the ability of a magnet to hold magnetism. Strictly speaking, it is the remanent magnetism of a substance, or *remanence,* in relation to the maximum magnetizing field. B_{rem} = remanent flux. Retentivity would be expressed by an equation thus:

$$\text{Retentivity} = \frac{B_{rem}}{H_{max}} \tag{65}$$

A high retentivity magnet steel is desirable for magnetic instrument systems.

The complete figure of variations of flux density or intensity of magnetization with field intensity is called the *hysteresis loop.* (Figure 72a.) The area formed by the loop is the energy in ergs per cubic centimeter per cycle involved in the operation.

In considering hysteresis curves, it is of note that the descending branch of the curve obtained with a reversed H is always above the ascending branch, hence the zero value of I or B is reached later in the cycle than the zero value of H.

If the field is removed after point A (Figure 72a) is reached, there will be a remaining magnetization equal to OA, and certainly the material is not demagnetized.

The only satisfactory way to demagnetize a specimen in hysteresis experiments is to take it repeatedly through cycles of continually decreasing range, ending with extremely small cycles (by alternating current).

TYPES OF HYSTERESIS

Figure 73 illustrates three typical hysteresis curves. (a.) The steep curve indicates a rapid increase of induction with magnetizing force. (b.) The area of the curve is small, indicative of the small amount of work necessary to reverse the magnetization. This iron will have a low hysteresis loss

† R. W. Hutchinson, "Advanced Text Book of Magnetism and Electricity," 1927, 2nd Edition, in two volumes, University Tutorial Press, Ltd., High St., New Oxford St., W. C., London.

when subjected to an alternating magnetic field, and would be suitable for transformer cores. (c.) The flatness of the curves and the large area is indicative of steel of high retentivity and coercive force which could be used in magnetic systems.

The coercive force of steel magnets increases with the carbon content. Tungsten, nickel and molybdenum also increase the coercive force in steel. Manganese reduces the magnetic properties of iron, and with 15.2% of Mn present the alloy is non-magnetic.

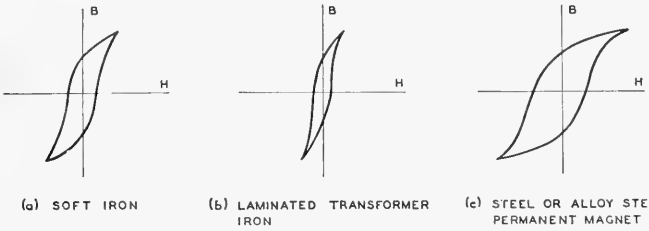

FIG. 73.—Hysteresis curves for three different types of magnets.

Measurement of Rock Magnetization

A number of methods have been developed for determining quantitatively the magnetic susceptibility of rocks. These are mainly laboratory procedures that require special apparatus. There are certain techniques, however, that can be used in the field, such as the one worked out by R. G. Paterson† for determining the susceptibility of rocks in place. These latter methods are particularly useful. A knowledge of the magnetic character of the different types of rock that may be involved in a given field problem is often of much importance in interpretation.

Test Tube Method.—One procedure for finding the relative susceptibility of a rock sample is called the *test tube method.* The instrument used comprises essentially a simple unifilar magnetometer consisting of a slender magnetic needle, about 10 inches long, which is attached at its center to a fine torsion fiber of about the same length. The less the stiffness of the torsion fiber, the greater the sensitivity. A suitable housing protects the fiber and needle from air currents, and a torsion head, to which the suspension fiber is attached at its upper end, permits the needle to be oriented. The instrument is equipped with a telescope and scale so that the deflections of the suspended system, to which a small mirror is fastened, can be accurately observed. In this respect it is similar to the familiar wall-type d'Arsonval laboratory galvanometer.

A base plate with leveling screws and small feet or a light tripod makes it possible to use this kind of test equipment in the field, although it is primarily a laboratory instrument. The essential features of the apparatus described above are shown in Figure 26.

With such a magnetometer, a susceptibility measurement is made by first placing a measured volume of pulverized sample of the rock under investigation in a test tube. The tube is then brought to within a few centimeters of one pole of the magnetic needle

† R. G. Paterson, "Determination of Magnetic Susceptibilities of Rocks in Situ," *A.I.M.E. Tech. Pub. No. 1298,* Feb., 1941.

and held at an accurately measured distance. The deflection caused by the test material is observed. This material is then removed and a like volume of some material of known magnetic susceptibility (preferably in the same test tube) is placed at the same position in respect to the needle. The deflection caused by the substance of known susceptibility is then observed. The comparison is a direct one. The deflections caused by exactly similar volumes of material, at exactly the same position and distance from the needle of the instrument, are directly proportional to their magnetic susceptibilities.

This can be seen as follows: $I = k\,H$; therefore, for a given H (e.g., the earth's field) the larger the k, the larger the I. But $B = H + 4\pi I$, and thus, the larger the k, the larger the B field, and the greater the field acting on the magnetometer needle. An example of such a determination follows a discussion of the standards of susceptibility with which test samples can be compared.

The horizontal component of the earth's magnetic field is the force which acts to orient the needle of a unifilar magnetometer of the form described when no magnetic samples are near by. It is, in effect, one type of compass. The sensitivity of such an instrument can be much increased if a bar magnet, of a strength sufficient to produce a field somewhat less than that of the earth's horizontal component, is placed below the magnetometer. The bar magnet is set in a horizontal position parallel to the needle and so oriented that its field opposes, and thus tends to compensate, the said horizontal component of the earth's field. In this way a smaller resultant or controlling field is acting on the needle. When a torsion fibre of small torsional coefficient is used, the system becomes responsive to the very small changes in the field created when samples of materials of different susceptibility are positioned near the needle.

Standards of Susceptibility.—In determining the magnetic susceptibility of test samples, standards of known value are needed. One of the most useful materials for this purpose is ferric chloride.

The mass susceptibility of a ferric chloride solution of known per cent may be calculated from the following formula†.

$$k\ (\text{mass}) = (\text{p}/100)\ \text{H} + (1 - \text{p}/100)\ \text{H}_\text{o} \qquad (66)$$

wherein $\text{H} = 90 \times 10^{-6}$ is the mass susceptibility of pure ferric chloride, H_o = the mass susceptibility of water or $-\ 0.79 \times 10^{-6}$, and p = percent iron chloride.

By this formula a solution of 46.45 percent iron chloride had a mass susceptibility of 41.38×10^{-6} c.g.s. Its density was 1.46, so that the volume susceptibility for this solution was 60.42×10^{-6} or 0.00006042 c.g.s. units. This figure was obtained by multiplying the mass susceptibility by the density. Iron chloride solutions of percentages of the order of the example cited make suitable standards for comparison measurements on rocks and minerals.

Such solutions should be carefully prepared and stored in a tightly-stoppered dark glass bottle for protection against changes caused by light and oxidization. A solution of such a high per cent (approaching 50%) of iron chloride is not entirely stable; some of the iron chloride may change to the ferrous form, altering the initial percentage value, and hence the susceptibility. A solution somewhat less than 50 per cent ferric chloride is about as high a concentration as will remain in a stable condition. It is desirable that the percentage and density of the solution be determined from time to time to guard against changes.

† *The Smithsonian Physical Tables,* 8th Edition, 1933, p. 475.

Field Magnetometer Method.—A direct comparison of similar volumes and shapes of material of known and unknown magnetic susceptibility can be made by using a field magnetometer. The procedure is essentially the same as that described under the test tube method.

For such measurements the magnetometer to be used is adjusted so that it has a high sensitivity. (This adjustment was given in detail in a preceding section.) An instrument of high sensitivity is necessary in order that a measurable response can be obtained from test samples and their equivalent volumes of standard susceptibility material. Where the construction of the particular magnetometer permits, its outer casing should be removed so that the sample can be brought as close to the magnetic system of the instrument as possible.

In one set of such tests an old-style Askania vertical intensity field magnetometer was used. It was adjusted so that one scale division movement of its magnetic system represented a change in magnetic field of 11.4×10^{-5} gauss. Such a sensitivity is about three times that usual for an instrument used in oil exploration field work. Before starting observations on the samples the instrument was carefully set up and its outer housing removed.

The first rock on which measurements were made was an oblong piece of amphibolite whose dimensions were 2.2 x 1.6 x 2.2 inches. It had smooth faces as it had been cut from a larger sample with a rock saw. This test sample was carefully placed on top of the magnetometer above the north pole of its magnetic system. In this position the face of the sample in contact with the instrument was 1.2 inches from the magnetic pole. A series of readings of the instrument scale was made, (1) with the sample in place and (2) with the sample removed, to determine the effect produced. Readings were taken with different faces of the sample in contact with the top of the instrument. It was found that the block of amphibolite caused an average change in scale reading of 12.0 scale divisions.

For the second part of the experiment an equal volume of iron chloride solution was put in a non-magnetic (copper) vessel of the same shape and size as the sample, and set in exactly the same place, on top of the magnetometer. With the box (1) in place and (2) removed, a number of readings were made which showed that the iron chloride gave an average scale deflection of 0.7 scale divisions.

To obtain a volume of standard susceptibility solution in an exactly similar form to the rock sample the following procedure was used. The cut sample of rock was put into the corner of the copper vessel and the remaining space in the container was filled with moulding clay. The rock was then removed and the space it had occupied was filled with the iron chloride solution.

The solution of iron chloride used in these tests was of 46.45%, and it had a volume susceptibility of 60.42×10^{-6} c.g.s., as calculated previously.

The magnetic susceptibility of the sample of amphibolite is related to

the above experimental data in a direct proportion: the deflection due to the rock sample is to the deflection caused by a like volume of iron chloride as the susceptibility of the sample is to the susceptibility of the iron chloride solution. In equation form:

$$12.0 : 0.7 = x : 60.42 \times 10^{-6}.$$

To solve:

$$12/0.7 \times 60.42 \times 10^{-6} = 1033 \times 10^{-6} \text{ c.g.s.}$$

The volume susceptibility of the particular sample of amphibolite rock is therefore 1033×10^{-6} or 0.001033 c.g.s. Such a value would indicate a highly magnetic material. Another amphibolite, which is described as fairly rich in magnetite, had a value of 1130×10^{-6}.

Among the rocks tested by this method, a specimen measuring 2.3 x 1.7 x 1.8 inches on a side, and from the same general area which was called paleozoic rock, was found to cause no deflection on the magnetometer. Its equivalent shape and volume of iron chloride solution gave a deflection of 0.3 scale divisions. From this somewhat negative result, it can be concluded that the paleozoic rock had a susceptibility less than the 60.42×10^{-6} of the solution. It follows, however, from these two isolated examples that in the general area where such paleozoics and amphibolites were involved any magnetic anomalies present would, in all probability, be associated with and arise from the amphibolites.

The Shape Factor in Test Samples.—The background for susceptibility measurements where a plane surface of a cut sample is placed near the pole of the system of a magnetometer has been given by J. G. Koenigsberger.† He applies the principle of the theory of electrical images to the magnetic case here involved.

The solution of the problem brings out the following facts: that the change in the magnetic field due to the presence of the test sample (as expressed in terms of instrument scale deflection) is (1) directly proportional to the susceptibility of the sample; (2) directly proportional to the pole strength of the system in the magnetometer; (3) inversely proportional to the square of the distance from the magnetic pole to the near face of the test specimen; and (4) dependent upon the shape factor and size of the specimen. In equation form: $\Delta D = \pi mkS/2r^2$, where ΔD is the change in magnetic field or the deflection of the instrument caused by the sample; m is the pole strength of the magnetic system of the magnetometer used; k is the susceptibility of the test sample, r the distance from the magnetic pole to the face of the sample, and S the shape-size factor.

The main point developed by Koenigsberger is that the above relation is true only for an infinite body and that for shaped samples of a relatively small thickness corrections relating to their dimensions are necessary. Experiments were conducted to determine the proper correction for a

† J. G. Koenigsberger, "Method for Measuring the Susceptibility of Rocks," *Terr. Mag. & Atmos. Elec.*, Vol. 34, p. 210, Sept. 1929.

shaped sample of a certain thickness in comparison to a sample of great thickness (theoretically of infinite thickness). A unifilar instrument was employed, with a needle 10 cm. long and 3 mm. in diameter. The deflections that should be obtained, on this magnetometer, for samples 1.2, 2.0, 3.0, and 6.0 cm. thickness were computed. The calculated deflections were compared to those actually obtained from cut samples of these thicknesses, and the results were found to agree within a few tenths of a scale division.

It was also found that a block of material 6 cm. thick gave very closely the same observed and computed deflection as one of (theoretically) infinite depth. The dimension of 6 cm. was therefore taken as a standard with a correction factor of 1. On this basis the sample 1.2 cm. thick had a factor of 0.68. This meant that a specimen of that thickness would produce a deflection of only 68 per cent of the deflection for the infinite case on which the theory of the method is based. In like manner the 2.0 cm. thickness and the 3 cm. thickness of test material gave correction factors of 0.85 and 0.93 respectively.

On a similar basis, by computation and testing with shaped samples the correction factor for the ratio of height and length was determined. From the preceding, it is evident that the samples should be cut to uniform shapes and sizes, preferably square and several inches on a side, in so far as possible.

These investigations also established the interesting fact that sometimes there appears to be a magnetic anisotropy in certain types of rocks, mainly crystalline schists. Such rocks show a maximum magnetic susceptibility when the magnetic lines of force of the induced image of the magnetic pole of the test instrument are parallel to the planes of rock schistocity. Where the force lines from the induced pole are at right angles to these planes the susceptibility is of a lesser amount. Gneissic granites also exhibit this characteristic.

Hyslop's Treatment of the Shape Factor.—In another technique,† the shape factor becomes the basis for a field method of determining the magnetic susceptibility of roughly shaped hand samples. In this method, the deflection of a Schmidt vertical intensity field magnetometer is noted when a test sample of rock is held close to one pole. Then by the application of the dimensions of the sample (end area and height) to a set of curves which relate dimensions and susceptibility, the latter may be estimated.

Separate sheets cover sample heights or thicknesses of 2, 4, 6 and 8 cm. Each graph sheet shows the variation in susceptibility for sample end sections of 2x2, 3x3, 4x4, 6x6, 7x7 and 8x8 cm.

An example will illustrate the use of these sets of curves. A piece of biotite granite was shaped roughly to a 3x3 cm. cross section and a height of 4 cm. Readings of the field magnetometer were made with the test block set over the pole in 8 different orientations, showing an average

† R. C. Hyslop, "A Field Method for Determining the Magnetic Susceptibility of Rocks," *A.I.M.E. Tech. Pub. 1285,* Feb. 1941.

deflection of 13.08 scale divisions. The sensitivity of the instrument was 15 x 10^{-5} c.g.s. units per scale division, which gave a figure of 196.3 gammas for the scale reading (15.0 x 13.08 = 196.3).

The graph for the 4 cm. height of sample was selected. On this graph the ordinate at 196.3 was traced upward to its intersection with the curve for the 3x3 cm. cross section and then across to the susceptibility axis. The value of susceptibility of 4200 x 10^{-6} was obtained.

The problem of finding a material of known susceptibility that could be conveniently cut into blocks of desired end section dimensions and height was solved by the use of mixtures of iron filings and moulding clay (plastocene). Five batches of clay with different percentages of iron filings thoroughly mixed gave a set of permanent susceptibility standards covering a wide range of values. The susceptibility of the clay-iron filings mixtures was determined by direct comparison with an iron chloride solution of known per cent.

A great number of instrument readings (about 2400) were required to build up the sets of curves of susceptibility vs. scale reading for the four thicknesses (heights) and the seven cross sections used.

Ambronn's Two Solenoid Method. — Several investigators† have devised various laboratory methods and equipment for determining rock susceptibilities by the use of solenoids. One operating principle may be described as follows.

Two identical solenoids are mounted symmetrically on either side of the lower magnet of an astatic magnetic system (Figure 74). An astatic system as here devised has two short magnets attached by a light rod. The system is suspended on a delicate torsion fibre. The magnets are placed with their poles reversed in respect to each other. Theoretically, and practically to a high degree, any changes in the horizontal magnetic field (earth's field) acting on the system would be neutralized and would not twist the suspended system of the instrument. This is because such a change would tend to turn the upper magnet in one direction and the lower magnet in the opposite direction, with the two torques acting upon each other through the rod attaching the two magnets. The solenoids are series-connected, near poles in opposition, and the system is carefully balanced by adjustment of the potentiometer until the magnetometer deflection is independent of the current flowing through the solenoids.

The test specimen *S* is now inserted in one solenoid. The specimen may be ground to size or pulverized and placed in a glass specimen tube. When current is passed through the coils, the different permeability of the specimen (compared to the air which previously filled the solenoid) upsets the magnetic balance of the solenoids and produces a deflection of the astatic magnetometer system. This magnetometer deflection is reduced to zero

† R. Ambronn, *Elements of Geophysics,* (Translated from the German by Margret Cobb), McGraw-Hill, 1928, p. 92.

by adjusting the potentiometer. The magnetic moment may be calculated from the change in potentiometer setting or ratio of current in the two coils and the constants of the apparatus. Knowing the magnetic moment of the specimen, the intensity of magnetization I may be calculated from the relation: I = magnetic moment per unit volume.

Another instrument for testing cores comprises a core suspended on a fibre and placed in a magnetic field. The core assumes an orientation indicating its direction of magnetization.†

An Improved Type of Two Solenoid Instrument.—An astatic susceptibility meter was developed and tested by R. C. Loring‡ in 1939, by means of which the complete hysteresis curve for a shaped rock sample could be determined. It is similar in design to the apparatus used by Ambronn, as shown in Figure 74, with one exception. In the Loring instrument one of the solenoids carries a secondary winding through which a measured current can be passed.

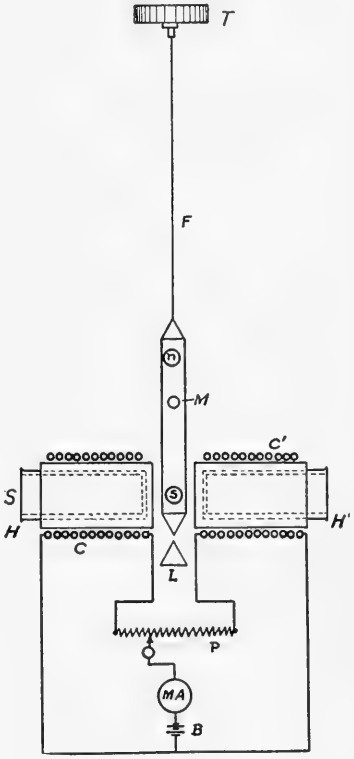

FIG. 74.—Method for determining magnetic susceptibility. *C* and *C'*, two identical solenoids with like poles opposing; *M*, mirror; *n* and *s*, astatic magnetic system; *T*, torque head; *F*, suspension fibre; *H* and *H'*, specimen holders, usually glass, in one of which is placed solid or pulverized specimen; *L*, leveling points; *P*, potentiometer; *MA*, milliampere meter; *B*, battery.

In operating this instrument it is necessary first to carefully adjust the position of the two solenoids, which are identical in size and shape. They are set so that with a certain current flowing through their primary winding no deflection is produced on the magnetic system of the instrument. With the current still flowing a test sample is then put in the solenoid (having the secondary winding) which will cause a deflection. This deflection is neutralized by setting a current in the auxiliary, or secondary, winding at such a value that, again, no deflection is obtained. The amount of such current, in milliamperes, required to neutralize the deflection is a measure of the induction in the test specimen resulting from the original current or field in the solenoids.

The above apparatus is quite versatile. For example, if a deflection is evident when a sample is placed in the solenoid that carries the two windings when *no* current is flowing, it would indicate that the sample had certain

† Randall Wright, U. S. Pat. 2,147,942, issued Feb. 21, 1939.

‡ Loring, R. C.; *The Design and Calibration of an Astatic Susceptibility Meter;* (unpublished) thesis for M.S. degree, Library, Colorado School of Mines, Golden, Colorado, May, 1939.

residual magnetization. The amount of such magnetization could be found by measuring the current in the solenoid needed to reduce the deflection to zero.

The magnetic moment of test samples of known volume can be determined quantitatively at given magnetizing fields. The latter are set up by a measured current in the primary windings of the two solenoids. The amount and direction of these fields can be controlled, permitting the hysteresis loop for a given test piece to be run. As indicated, the moment of a sample when in the solenoid is obtained in terms of the field, in the secondary winding, required to balance the magnetic system of the instrument to zero deflection.

From formulae previously given: $M = I\ V$; or magnetic moment of a sample M is its intensity of magnetization I times its volume V. The neutralizing or balancing field (in the secondary of the solenoid) is H. $H = 2Md/(d^2 - l^2)^2$. In this equation d equals the distance from the center of the sample to the magnet of the instrument, or system. The length of the test sample is $2l$. The value of H is found from the milliamperes of current in the secondary of the solenoid carrying the sample. The dimensions of the solenoid in length and turns of wire per centimeter are known.

Tests were run by Loring on a number of rocks of different types and on other materials. It was found, for example, in the case of a sample of granite, 2″ x 2.5″ x 5″, that there was no residual magnetization present. The magnetic susceptibility of this granite was constant at a value of 474 x 10^{-6} c.g.s. for fields up to 12 gauss. This would signify that the hysteresis loop had no area, but was represented by a straight line across the B-H graph at a constant slope; and such was the case when the data was plotted.

A sample of 50 per cent iron chloride solution, in a copper box, 2″ x 2″ x 5″ when tested in the instrument gave similar results. The hysteresis curve was a straight line of constant slope. This finding indicates the advantage of using iron chloride for standardization and comparison in these tests, as its susceptibility does not change in magnetic fields of different strength.

Two samples of basalt, one (1″ x 2″ x 3″) from an intrusive dike and the other (1.5″ x 2″ x 2.5″) from a flow, gave susceptibilities of 1420 x 10^{-6} and 1115 x 10^{-6} c.g.s. respectively. They both showed remanent magnetization of 0.01 gauss which was removed by a coercive force of 1.3 gauss.

A block of moulding clay 2″ x 2″ x 6″ in size, with which iron filings had been thoroughly mixed, exhibited a hysteresis loop that enclosed a sizable area and otherwise showed magnetic properties similar to a natural rock. This specimen had an initial remanent magnetization, before tests were run, of 2 gauss. The coercive force to obtain zero magnetization was 2.26 gauss. Some variation in susceptibility with magnetizing field was evident, but for a field of 0.9 gauss the susceptibility was 3500 x 10^{-6}.

The Alternating-Current Susceptibility Meter.—A high precision instrument having advantages as to ease and rapidity of operation, as well as a certain degree of portability, was perfected in 1932 by Wm. M. Barret.† It is known as a semi-portable alternating-current susceptimeter. The meter is a self-contained unit which can be conveniently used wherever 110-volt, 60-cycle current is available.

Barret's meter is a form of inductance bridge, with the usual four arms in which the condition of balance is indicated by a sensitive alternating-current galvanometer. At balance, or with no current passing through the galvanometer, the arms must be adjusted and balanced for capacitance, for inductance, and for resistance.

After such a balance of these three factors is obtained, a test sample in a suitable container is inserted in a test coil in one of the arms of the bridge, and the balance is disturbed. By altering a variable inductance in the arm with the test coil and sample, the balance can be restored. The added induction needed to restore the balance is a measure of the magnetic susceptibility of the sample. A calibration curve for the instrument is worked out so that the susceptibility of test specimens can be read directly in terms of inductance.

Samples to be tested are pulverized and put in glass tubes 2.7 cm. in diameter and 10 cm. long. Before making measurements the resistance balance of the bridge is established and adjusted if necessary, using 6-volt direct current. Following this the inductive and capacitative balance is obtained, and samples are tested with 60-cycle current.

The validity of susceptibility measurements made by the use of alternating current as compared to those found where direct current was used was critically examined by Barret. It was concluded, on the basis of tests, that the specific inductive capacity and the conductivity of test samples did not influence the results of susceptibility measurements when 60-cycle current was used. It was found that there were certain advantages to this form of instrument in the freedom from extraneous magnetic fields and the disturbances they might cause. Another feature is that measurements of susceptibility are independent of the magnetic history of the rock tested.

A bridge type of susceptibility meter, along similar lines, was developed by Barret in 1931.‡ It used direct current and had a very high sensitivity, as does the semi-portable instrument described above. With the earlier bridge a number of different procedures were possible for obtaining the susceptibility of samples. The minimum detectable variation in susceptibility, with the different techniques of operation, were from 0.0004450 to 0.0000331 c.g.s. It is apparent that bridge methods are most useful in measuring the small values of susceptibility found in sedimentary rocks.

† W. M. Barret, "A Semi-portable Alternating-Current Susceptibility Meter," *Physics*, Vol. 3, No. 3, pp. 149-154, Sept., 1932.

‡ W. M. Barret, "A Method for Determining Magnetic Susceptibility of Core Samples," *A.I.M.E. Tech. Pub. No. 394*, Feb., 1931.

Susceptibility Measurements of Rocks in Place.—A means of measuring the magnetic susceptibility of rocks in place was worked out by R. G. Paterson‡. It has the unique advantage that no samples need to be taken. The equipment required is small in size and light in weight so that rock exposures can be tested in the field where and when desired.

The principle underlying the method is the change caused in the inductance of a coil, carrying a current, when a paramagnetic or a diamagnetic substance comes into its magnetic field. The test coil is wound in the form of a circular disc, which is placed on a flat surface of the rock, susceptibility of which is to be measured. Only a part of the magnetic field from the coil penetrates the rock under test. The winding of the coil forms part of one arm of an alternating current inductance bridge so that the change in inductance in it, caused by the rock on which it lies, can be measured.

More accurately described, the test coil is 9.4 cm. in mean diameter, wound with 1000 turns of No. 31 enameled wire which occupies a slot 0.5 x 1.0 cm. in cross section. Its resistance is 139.1 ohms and its inductance 0.17995 henries.

The circuit used is the Owen bridge†, having the usual four arms with their impedances designated as Z_1, Z_2, Z_3 and Z_4. Of these Z_1 consists of the coil, as described above, which is connected by 8 feet of flexible 2-conductor lead and a 5000-ohm variable resistance. The arm Z_2 has a similar 5000-ohm variable resistance and a 0.13 microfarad condenser. The Z_3 arm carries an 0.06 microfarad condenser. A fixed value resistor of 5000 ohms makes up the Z_4 arm. A 500-cycle generator provides the necessary power, and the bridge balance is found by minimum sound with head phones and amplifier.

The inductance of the coil is first measured in air, and again measured when it is lying on the face of a rock under investigation. The difference of the two inductances is a measure of the magnetic susceptibility of the rock at that frequency. A calibration curve is used which gives the change in microhenries in terms of susceptibility, for a given field strength. The relation of change in coil inductance and susceptibility was determined by tests using solutions of different percentages of iron chloride.

This method of susceptibility measurement removes all question as to the possible change in the magnetic character of a specimen caused by shaping or pulverizing it. It affords an easy means for making a number of tests in the field at adjacent places on an outcrop. This greatly minimizes the inherent error of assuming that a given sample is representative.

There are two disadvantages to the method, one of which is the large size sample required for the test (unless it is used on a rock in place). The sample must have a relatively flat surface about twice the size of the coil, and a thickness about equal to 0.6 the coil dimension, in order to give the

‡ R. G. Paterson, "Determination of Magnetic Susceptibilities of Rocks in Situ," *A.I.M.E. Tech. Pub. 1298*, Feb., 1941.

† D. Owen, "A Bridge for the Measurement of Self-induction in Terms of Capacity and Resistance," *Proc. Phys. Soc.* (1915), Vol. 27, pp. 35-39.

necessary space factor for penetration of the magnetic flux. Another disadvantage lies in the use of relatively high frequency current which introduces a component due to the specific conductivity of the specimen. For instance, a sheet of any non-magnetic metal placed near the coil will cause a change in the inductance greater than the normal changes encountered due to susceptibility. For this reason it is not suitable for measuring the magnetic properties of highly conductive shales, slates or material from mineralized zones. The method works fairly consistently on those earth materials having a relatively high specific resistivity.

In the foregoing discussion of instruments and methods for the quantitative measurement of rock magnetization the objective has been to cover typical procedures. Preference has been given to those methods which could be employed conveniently in the field, in order to encourage such measurements. Limitations of space, in a work of this kind, do not permit the consideration of a number of other excellent and efficacious techniques for susceptibility measurements.

It is most advantageous to know the values of the magnetic susceptibility of typical rocks and formations that relate to a given magnetic problem. Such information minimizes one of the unknown factors often present in the interpretation of magnetic data.

The findings of W. H. Fenwick† in a study of induced and remanent magnetization of rocks are in point here. He shows that the remanent magnetization can have a decided effect on the character of a magnetic anomaly. It may result in either higher or lower values of vertical or horizontal intensities than are obtained if induced magnetization only is considered in an analysis.

THEORETICAL ANALYSIS OF MAGNETIC DATA

As stated previously, magnetic anomalies are produced chiefly by differences in the magnetic permeability of the rocks and formations comprising the earth's crust. In addition to the variation in permeability, remanent magnetism, such as is possessed by lodestone and a few other materials occurring in nature, may contribute to the anomalies. The problem of interpretation consists in inferring the position (or attitude), depth, configuration, and general character of the subsurface body or structure from the magnetic anomaly observed at the surface of the earth.

The usual treatment of magnetic data is almost exclusively empirical. Deductions and inferences are drawn in a qualitative manner from the sizes and configurations of the magnetic anomalies. (Compare p. 206.) However, the empirical treatment of magnetic data is based in part on a knowledge of the theoretical anomalies produced by certain inhomogeneities. Furthermore, a theoretical type of analysis is applicable in certain cases. Hence, it is advantageous to consider the theoretical procedure

† W. H. Fenwick, "Two Neglected Factors in the Interpretation of Magnetic Anomalies," Unpublished Thesis, Library, Colo. Sch. of Mines, Golden, Colo., 1938.

for inferring the subsurface structure from magnetic data obtained at the surface.

The theoretical procedure for deducing subsurface structure from magnetic data is: (1) to assume (a) a geologically plausible configuration of the subsurface formations and (b) probable values of the permeabilities (or susceptibilities); (2) to compute the magnetic effects which the assumed configuration (and permeabilities) would produce at the surface; (3) to compare the theoretical and observed results; (4) to modify the assumptions until a satisfactory agreement is obtained between the observed and theoretical data.

Three theoretical methods will be considered. The first method is used when the subsurface body has a small cross section relative to its length. The procedure followed in this method is to set up expressions for anomalies characteristic of a single pole, a vertical magnetic dipole and an inclined dipole, and to compare the theoretical results with the observed anomalies. This method is described in section A below.

The second method is used for calculating the magnetic anomalies produced by magnetized strata. The theoretical technique for obtaining the magnetic anomalies of magnetized strata may be subdivided into two separate methods. In one, use is made of a functional relation between the magnetic and gravitational effects of magnetic layers in order to obtain the unknown theoretical magnetic anomalies from known theoretical gravitational anomalies. In the other, it is postulated that the magnetic effects produced at the surface of the earth by the volume distribution of magnetization throughout the layers are approximately the same as those produced by surface distributions of magnetic charge located on the upper and lower faces and on vertical contacts of the layers. This method is described in section B below.

The third method is used to calculate the magnetic effects produced by uniformly magnetized geologic bodies having the shape of spheres, ellipsoids of revolution, etc. In the case of a uniformly magnetized sphere, the theoretical magnetic effects at the surface of the earth may be obtained by replacing the sphere by a bar magnet having a magnetic moment equivalent to that of the sphere. This method is described in section C below.

A. Anomalies Produced by Certain Ore Bodies and Igneous Intrusions.—Certain ore bodies and igneous intrusions which occur in the form of pipes, shoots, chimneys, etc., and have a small cross section relative to their length may be represented by single poles, provided their depth extent is large enough to warrant neglecting the effect of the accompanying magnetic pole at the lower end of the subsurface body.

1. Field Due to a Magnetic Pole

Assume that a pole of strength m exists at a depth d below the surface in a medium of permeability 1. The magnetic field at any point due to this pole may be calculated by computing the derivative of the magnetic poten-

tial. The potential at any point due to a magnetic pole of strength m may be defined as the work done in carrying a unit pole from infinity to the point in question. That is, the potential V may be defined by the equation:

$$V = -\int_{\infty}^{r} \frac{m}{r^2}\, dr = \frac{m}{r} \tag{67}$$

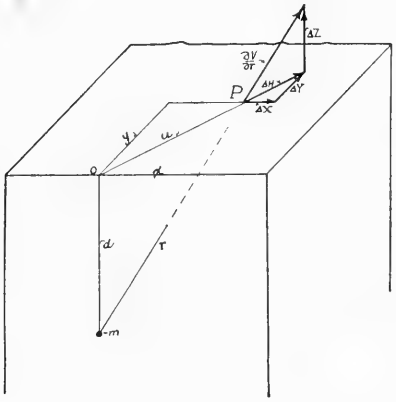

FIG. 75.—Field at P due to S pole of strength m located at a depth d.

The components of the magnetic field (Figure 75) at a point (x, y) due to a pole of strength m located at a depth d are:

$$\left.\begin{aligned} \Delta X &= -\frac{\partial V}{\partial x} = \frac{mx}{r^3} \\ \Delta Y &= -\frac{\partial V}{\partial y} = \frac{my}{r^3} \\ \Delta Z &= -\frac{\partial V}{\partial z} = \frac{md}{r^3} \end{aligned}\right\} \tag{68}$$

The horizontal component of the field due to the pole m is:

$$\Delta H = -\frac{\partial V}{\partial u} = \frac{mu}{r^3} \tag{69}$$

The actual shape of the curve obtained on plotting ΔH or ΔZ depends on the depth to the top of the ore body and the pole strength. Figure 76 shows the profiles in the x-direction ($y = 0$) when $d = -1$ and $m = -2$. For this case, Equations 68 and 69 for the vertical and horizontal intensity anomalies become

$$\Delta Z = \frac{md}{r^3} = \frac{md}{(d^2 + x^2)^{3/2}} = \frac{2}{(1 + x^2)^{3/2}} \tag{68a}$$

and

$$\Delta H = \Delta X = \frac{mx}{r^3} = -\frac{2x}{(1+x^2)^{3/2}} \qquad (69a)$$

An examination of the expression for ΔZ reveals that ΔZ is symmetrical with respect to the z-axis, has a maximum for $x = o$, i.e., directly over the pole and approaches the x-axis asymptotically. The expression (69a) for ΔH shows that ΔH is an odd function of x. (ΔH for negative values of x is equal to $-\Delta H$ for the corresponding positive values of x.) ΔH vanishes for $x = o$ and approaches the x-axis asymptotically for large positive or negative values of x.*

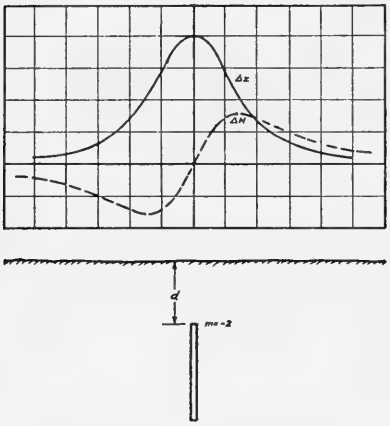

FIG. 76.—Vertical and horizontal intensity anomalies produced by an ore body equivalent in its magnetic effects to a single s pole of strength m located at a depth d.

Two "depth rules" are readily deduced from Equations 68 and 69.† (1) The horizontal distance u from a point directly over the pole to a point where ΔZ equals $\frac{1}{2}\Delta Z_{max}$ is approximately equal to $\frac{3}{4}$ the depth of the pole. (Tiberg depth rule.) (2) At a horizontal distance u equal to d, $\Delta Z = \frac{1}{3}\Delta Z_{max}$ (approximately). That is, the distance from the origin to a point at which ΔZ is approximately equal to $\frac{1}{3}\Delta Z_{max}$ is equal to the depth of the pole. (Haanel depth rule.)

An alternative method for obtaining an approximate value of thickness of the overburden is to draw the vector diagram of the total anomalies near the point of maximum vertical anomaly. ‡

The anomalies in the horizontal and vertical intensities are obtained by subtracting the normal values of the horizontal and vertical intensities in the area under investigation from the observed values. (Compare p. 156.) Corresponding values of the horizontal and vertical anomalies are then combined vectorially in order to obtain resultant vectors having the direction of the *total anomaly*. Since the resultant vector at any point is tangent to the line of force at that point, the resultant vectors near the point of maximum vertical intensity will intersect very nearly at the pole of the ore body. Figure 77 shows a diagram for the

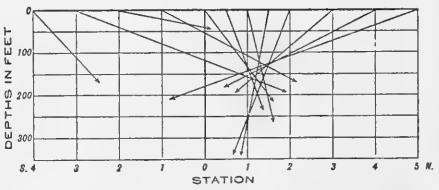

FIG. 77.—Vectors of resultant magnetic anomalies due to ore body. (Eve and Keys, *Canadian Memoir* 170, p. 39.)

* To draw the curves given in Figure 76, it is sufficient to assume four or five values of x and compute ΔZ and ΔH from Equations 68a and 69a.

† Compare C. A. Heiland, *A.I.M.E. Geophysical Prospecting*, 1932, p. 213.

‡ A. S. Eve and D. A. Keys, "Studies of Geophysical Methods," 1930, Department of Mines (Canada), *Memoir* 170, pp. 36-37.

resultant magnetic anomaly due to an ore body. In this case the vectors indicate that the pole is about 150 to 175 feet below the surface. This "depth" is of course an approximate value, because vector diagrams indicate a point near the center of attraction of the upper pole of the body and do not give the thickness of the overburden, which will always be less than that deduced from the diagram.

2. *Field Due to a Magnetic Dipole* †

If the depth extent of the subsurface magnetic feature (ore body, etc.) is too small to permit neglecting the magnetic effect of the pole on the deep end of the ore body, the total effect may be approximated by assuming that the ore body is equivalent to a magnetic dipole. (Figure 78.)

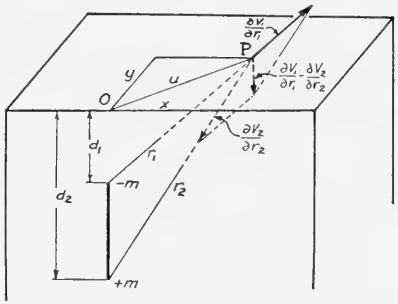

FIG. 78.—Field at P due to a vertical dipole.

The magnetic anomalies produced by a dipole are calculated by adding the effects of a south and a north pole vectorially. The application of Equations 68 and 69 to the poles $-m$ and $+m$ yields:

$$\Delta Z = -m\left(\frac{d_1}{r_1^3} - \frac{d_2}{r_2^3}\right) \tag{70}$$

and

$$\Delta H = -mu\left(\frac{1}{r_1^3} - \frac{1}{r_2^3}\right) \tag{71}$$

Sketches of the horizontal and vertical intensity anomalies produced by a vertical dipole are shown in Figure 79. The profiles in the x-direction are drawn for the case: $m = 2$, $d_1 = -1$, and $d_2 = -3$; that is

$$\Delta Z = 2\left[\frac{1}{(1+x^2)^{3/2}} - \frac{3}{(9+x^2)^{3/2}}\right]$$

$$\Delta H = -2x\left[\frac{1}{(1+x^2)^{3/2}} - \frac{1}{(9+x^2)^{3/2}}\right]$$

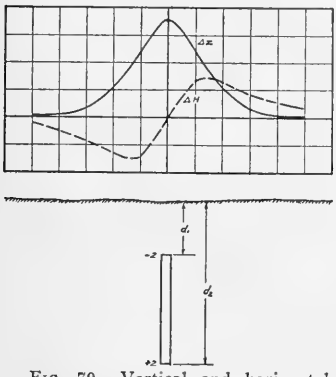

FIG. 79.—Vertical and horizontal intensity anomalies for an ore body which is magnetically equivalent to a vertical dipole.

An approximate depth rule for an ore body which is equivalent in its magnetic effects to a vertical dipole was given by Thalen in 1879. The rule may be stated as follows: The depth d_1 to the top of the ore body is equal approximately to 0.7 of the horizontal distance u from a point directly over the dipole to a point where $\Delta Z = 0$.

† H. Haalck, *Die Magnetischen Verfahren der Angewandten Geophysik* (Gebrüder Bornträger), Berlin, 1929.

A. Nippoldt, *Verwertung Magnetischer Messungen* (Springer), Berlin, 1930.

C. A. Heiland, Chapter on Magnetic Prospecting, pp. 136-139. *Terrestrial Magnetism and Electricity,* edited by J. A. Fleming (McGraw-Hill), 1939.

If the dipole is inclined (Figure 80), Equations 70 and 71 must be modified to include the cosine of the dip of the ore body and its length. It may be shown from an analysis similar to that given for the vertical

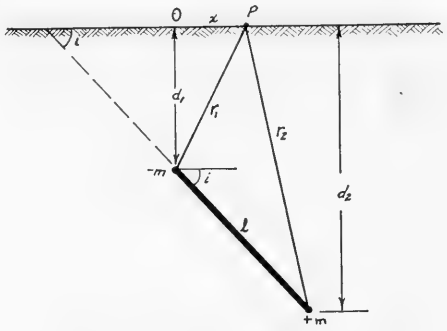

FIG. 80.—Sketch illustrating geometric relations of dip of ore body and vectors r_1 and r_2 to the point of observation P on an x traverse.

dipole that the expressions for the vertical and horizontal intensity anomalies along the x-axis are:

$$\Delta Z = -m\left[\frac{d_1}{{r_1}^3} - \frac{d_1 + l\sin i}{{r_2}^3}\right] \tag{72}$$

$$\Delta H = -m\left[\frac{x}{{r_1}^3} - \frac{x - l\cos i}{{r_2}^3}\right] \tag{73}$$

where d_1 is the depth to the top of the ore body; and $(d_1 + l\sin i) = d_2$ is the depth to the bottom of the ore body; r_1 and r_2 are the distances from the point of observation to top and bottom respectively; l is the length and

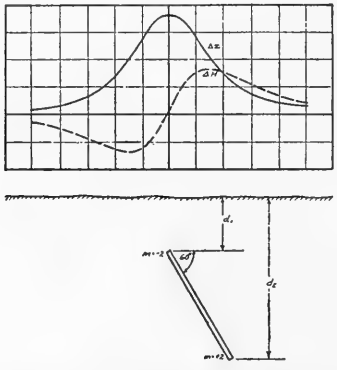

FIG. 81. — Vertical and horizontal intensity anomalies for an inclined doublet.

i the dip of the ore body; x is the distance from the origin to the point of observation.

Profiles of the horizontal and vertical intensity anomalies in the x-direction are shown in Figure 81. The curves were plotted for the case: $d_1 = -1$, $d_2 = -3$, $m = 2$, $i = 60°$, and $l = 2.305$; that is,

$$\Delta Z = +2\left\{\frac{1}{(x^2+1)^{3/2}} - \frac{3}{[9+(x-1.15)^2]^{3/2}}\right\} \tag{72a}$$

and

$$\Delta H = -2\left\{\frac{x}{(x^2+1)^{3/2}} - \frac{x-1.15}{[9+(x-1.15)^2]^{3/2}}\right\} \tag{73a}$$

3. *Anomalies Due to Long Narrow Dikes*

If the dike is approximately vertical, it is equivalent in its magnetic effects to a vertical magnetized "sheet" of finite thickness. Also, if the depth extent is sufficiently great that the effects due to the induced pole strength at the deep end may be neglected, the magnetic anomalies produced at the surface are essentially the same as would be produced by a linear distribution of magnetic charge. In particular, it may be shown that the maximum value of the vertical intensity anomaly is:†

$$\Delta Z_{\max} = \frac{2mb}{d} \tag{74}$$

where m is the magnetic pole strength per unit area, b the width of the dike, and d the depth to the effective linear distribution of magnetic charge. (d is, of course, somewhat greater than the distance from the surface to the top of the dike.)* The anomaly at a point P located at a distance x from the point of maximum anomaly along the line at right angles to the strike is:

$$\Delta Z_p = \frac{2mbd}{x^2+d^2} \tag{75}$$

If we choose the point P such that $\Delta Z = \frac{1}{2}\Delta Z_{\max}$ and combine the last two equations, we obtain

$$\frac{2mbd}{x^2+d^2} = \frac{mb}{d} \tag{76}$$

or

$$d = x$$

Thus the thickness of the overburden is equal approximately to the distance along the line perpendicular to the strike of the dike at which ΔZ is equal to $\frac{1}{2}\Delta Z_{\max}$.

† The method outlined here is described by D. A. Keys, "Determining Depth of Magnetic Ore Bodies," *A.I.M.E. Geophysical Prospecting*, Tech. Pub. 830, p. 5.

* Equation 74 which gives the maximum value of the vertical anomaly is essentially a particular application of the expression for the field due to a linear distribution of magnetic charge. (Compare p. 191.)

An alternative method for determining the approximate thickness of the overburden over a dike makes use of vector diagrams, as illustrated in connection with Figure 76.

B. Theoretical Anomalies Produced by Magnetic Strata.—Two methods may be employed to calculate the magnetic effects of two-dimensional bodies such as strata. In both methods it is assumed that the difference in susceptibilities between the anomalous body and the adjacent formation is such that *demagnetization effects** are negligible.

Method Utilizing Functional Relation Between Magnetic and Gravitational Anomalies

As a consequence of a theorem due to Poisson, it may be shown that the following relationships obtain between the magnetic and gravitational anomalies produced by two-dimensional bodies:†

$$\left.\begin{aligned} \Delta H &= \frac{\Delta k}{G\Delta\sigma}\left(H\frac{\partial^2 U}{\partial x^2}\sin\alpha + Z\frac{\partial^2 U}{\partial x\partial z}\right) \\ \Delta Z &= \frac{\Delta k}{G\Delta\sigma}\left(H\frac{\partial^2 U}{\partial x\partial z}\sin\alpha - Z\frac{\partial^2 U}{\partial x^2}\right) \end{aligned}\right\} \qquad (77)$$

where

Δk = susceptibility difference of the geologic body relative to the adjacent rock.
G = gravitational constant ($6.68 \cdot 10^{-8}$ c. g. s.)
$\Delta\sigma$ = density difference.
U = gravitational potential.
α = angle between geographical north and the west direction of strike.
H = horizontal component of earth's field.
Z = vertical component of earth's field.

The applicability of the ΔH and ΔZ formulas derives from the fact that the derivatives of the gravitational potential $\left(\frac{\partial^2 U}{\partial x^2}, \frac{\partial^2 U}{\partial x\partial z}\right)$ have been evaluated for numerous, two-dimensional geologic bodies. (Compare chapter on gravimetric methods.)

Method Utilizing Equivalence of Volume and Surface Distributions of Magnetic Charge

This method consists in calculating the magnetic effects of a uniformly magnetized formation in terms of its effective surface distribution of magnetic charge. This method postulates that the magnetic effects at the surface due to a volume distribution of magnetization throughout a stratum

* A discussion of demagnetization effects is given on p. 203 *et seq.*

† R. von Eötvös, "Bestimmung der Gradienten der Schwerekraft und ihrer Niveauflachen mit Hilfe der Drehwage," *XV. Allgemeine Konferenz der Intern. Erdmessung*, Budapest, 1906. See also W. P. Jenny, "Experimental Interpretation of Magnetic and Gravimetric Anomalies," *Terr. Mag.* 40 (No. 1) March 1935, pp. 71-78.

are approximately the same as those produced by surface distributions of magnetic charge located on the upper and lower faces of the stratum.

Before deriving the anomalies produced by two-dimensional geologic bodies, it will be convenient to describe: (a) the magnetic fields produced by linear distributions of charge and (b) the general expressions for the magnetic potential and magnetic field produced by surface distributions of charge.

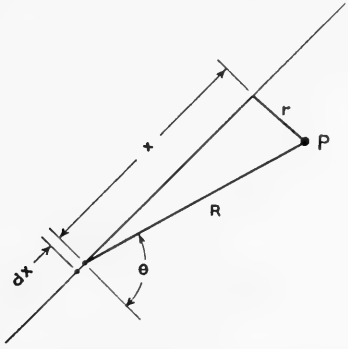

FIG. 82.—Sketch illustrating geometric relations between a linear distribution of magnetic charge in the direction x and an external point P.

Magnetic Fields Produced by Linear Distributions of Charge.—The magnetic field of force in the direction R due to element dx (Figure 82) is:

$$dF = \frac{m\,dx}{R^2}$$

where m equals the pole strength per unit length. The force dF is the vector sum of the components of dF_r in the direction normal to x and dF_x in the direction parallel to x.

But
$$dF_r = \frac{mr}{R^3}\,dx$$

Hence, the component in the direction r due to the whole line is

$$F_r = \int_{-\infty}^{\infty} \frac{mr}{R^3}\,dx = 2\int_0^{\infty} \frac{mr}{R^3}\,dx = 2mr\int_0^{\infty} \frac{dx}{(x^2+r^2)^{3/2}}$$

Let
$$x = r\tan\theta$$
$$dx = r\sec^2\theta\,d\theta$$
$$x^2 + r^2 = r^2\sec^2\theta$$

then
$$F_r = \frac{2\,m\,r}{r^2}\int_0^{\pi/2} \cos\theta\,d\theta = \frac{2m}{r} \qquad (78)$$

The component in the direction x is

$$F_x = \int_{-\infty}^{\infty} \frac{mx}{R^3}\, dx = 0 \,*$$

Hence, the resultant field for an infinite linear distribution of magnetic poles has the direction r and a magnitude $2m/r$.

The potential due to the linear distribution of charge is given by the equation

$$V = 2m \log r \qquad (79)**$$

Field Due to Two Parallel Linear Distributions of Equal Strength and Opposite Polarity (Figure 83)

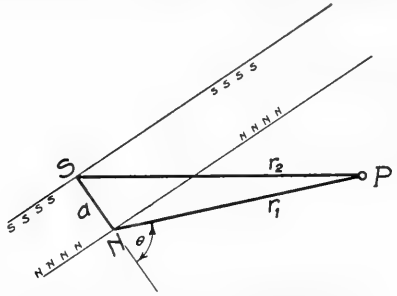

FIG. 83.—Sketch illustrating geometric relations between two parallel linear distributions and an external point P.

If the separation a of the two parallel lines is small compared to r, then the potential $V = V_1 + V_2 = 2m \log r_1 - 2m \log r_2$

$$= -2m \log \frac{r_2}{r_1} = -2m \log \left(\frac{r_1 + a \cos\theta}{r_1} \right)$$

$$= -2m \log \left(1 + \frac{a \cos\theta}{r_1} \right)$$

---

* To evaluate the integral $\int_{-\infty}^{\infty} \frac{mx}{R^3} dx = \int_{-\infty}^{\infty} \frac{mx\, dx}{(x^2 + r^2)^{3/2}}$

set

$$x = r \tan\theta$$

This yields

$$F_x = m \int_{-\pi/2}^{\pi/2} \frac{r \tan\theta\, r \sec^2\theta\, d\theta}{r^3 \sec^3\theta} = \frac{m}{r} \int_{-\pi/2}^{\pi/2} \sin\theta\, d\theta = 0$$

** It will be noticed that this expression for V makes V infinite at r equal to infinity. However, we are chiefly interested in the magnetic field, i.e., the derivative of the potential at a finite value of r, and this derivative always has a finite value.

where m is the pole strength per unit length. Since $\frac{a\cos\theta}{r_1}$ is small when a is small compared with r_1, the power series expansion of the logarithm gives $V = -2m\frac{a\cos\theta}{r_1}$ + terms of the order $\left(\frac{a}{r_1}\right)^2$ etc.
That is,

$$V = -2m\frac{a\cos\theta}{r_1}(\text{approx.}) \tag{80}$$

General Expressions for the Magnetic Potential and Field Produced by Surface Distributions of Charge.—The magnetic potential produced by a uniformly magnetized body at any external point P is given by the equation†

$$V = \iint \frac{I\cos\alpha}{r}\, dS$$

where r is the distance between P and the element of surface dS and α is the angle between the magnetization I and the outward normal at dS. For the cases to be considered, the magnetization is normal to the surface, i.e., $\alpha = 0$; hence,

$$V = \iint \frac{I\,dS}{r} \tag{81}$$

The magnetic field at P is obtained by taking the derivative of V. Differentiation of Equation 81 with respect to r yields:*

$$\Delta H_r = -\frac{\partial V}{\partial r} = -\frac{\partial}{\partial r}\iint\left(\frac{I\,dS}{r}\right) = \iint\frac{I\,dS}{r^2} \tag{82}$$

Equations 78 to 82 are the fundamental equations utilized in deriving the magnetic effects produced by two-dimensional geologic bodies.

Magnetic Anomalies Due to a Buried Contact of Two Very Thick Horizontal Layers Having Different Susceptibilities. — Assume that the materials A and B (Figure 84) are separated by a vertical plane, i.e., have a vertical contact, and that d is the thickness of layer C, k_1 susceptibility of layer A, k_2 susceptibility of layer B, k_3 susceptibility of layer C.

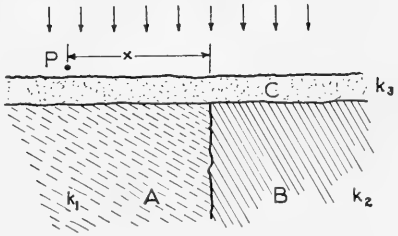

FIG. 84.—Buried contact of two thick layers.

On the upper surface of C there is a uniform distribution of magnetism of surface density $I_3 = k_3 Z$ units of pole per unit area.** This is south polarity or magnetism if C is paramagnetic and north polarity if C is

† J. H. Jeans, *Electricity and Magnetism*, 5th Edition, p. 374.
* In carrying out the differentiation with respect to r, the quantity IdS is held constant.
** Note that Z is the vertical component of the earth's field.

diamagnetic. On the lower surface of C the surface density of magnetism is $-I_3$. On the upper surface of A the density of magnetism is $I_1 = k_1 Z$ and along the upper surface of B it is $I_2 = k_2 Z$. This condition is equivalent to the following: Density I_3 on upper surface of C, density $I_1 - I_3$ on plane CA, density $I_2 - I_3$ on plane CB.*

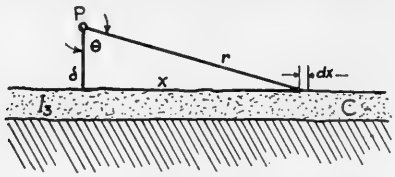

FIG. 85.—Sketch showing quantities which enter into the calculation of the effect of upper surface of C.

1. *Effect at P of Upper Surface of C (Figure 85).*** The magnetic field in the direction of r is computed by substituting $dx\,dy$ for dS in Equation 82; that is,

$$\Delta Z_r = \int_{-\infty}^{\infty} \int_{-\infty}^{\infty} \frac{I_3\,dx dy}{r^2}$$

If the height of the measuring instrument above the surface of the ground is designated by δ, the vertical component ΔZ_1 may be written

$$\Delta Z_1 = \int_{-\infty}^{\infty} \int_{-\infty}^{\infty} \frac{I_3 \cos\theta}{r^2}\,dx dy$$

$$= I_3\,\delta \int_{-\infty}^{\infty} \left[\int_{-\infty}^{\infty} \frac{dx}{[(x-x_1)^2 + (y-y_1)^2 + \delta^2]^{3/2}} \right] dy$$

To integrate the quantity within the brackets, set $(y-y_1)^2 + \delta^2 = a^2$ and introduce a variable ϕ defined by the relation $x = a \tan\phi$. Thus

$$\int_{-\infty}^{\infty} \frac{dx}{[(x-x_1)^2 + (y-y_1)^2 + \delta^2]^{3/2}} = \int_{-\infty}^{\infty} \frac{dx}{[(x-x_1)^2 + a^2]^{3/2}}$$

$$= \int_{-\pi/2}^{\pi/2} \frac{1}{a^2} \cos\phi\,d\phi = \frac{2}{a^2} = \frac{2}{(y-y_1)^2 + \delta^2}$$

$$\int_{-\infty}^{\infty} \int_{-\infty}^{\infty} \frac{I_3\,\delta}{[(x-x_1)^2 + (y-y_1)^2 + \delta^2]^{3/2}}\,dx dy = I_3\,\delta \int_{-\infty}^{\infty} \frac{2}{(y-y_1)^2 + \delta^2}\,dy$$

$$= \left[\frac{2I_3\,\delta}{\delta} \cdot \tan^{-1} \frac{y-y_1}{\delta} \right]_{-\infty}^{\infty} = 2\pi I_3$$

That is, the vertical component ΔZ_1 due to the magnetic density on the upper surface of C is $2\pi I_3$.

* This is an approximate treatment which does not hold strictly at the boundary AC and BC.

** For simplicity, the illustration shows a vertical section through a point P (x_1, y_1, δ).

2. *Effects of Surfaces BC and AC (Figure 86).*—The effects of surfaces BC and AC may be calculated as above. The vertical component of the field BC is:

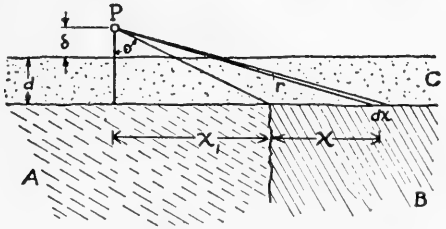

FIG. 86.—Sketch showing quantities which enter into the calculation of the effect of contact BC.

$$\Delta Z_2 = \int_0^\infty \int_{-\infty}^\infty \frac{(I_2 - I_3)\,(d+\delta)}{[(y-y_1)^2 + (x-x_1)^2 + (d+\delta)^2]^{3/2}}\,dx dy$$

In this case, it is simpler to integrate first with respect to y.

$$\int_{-\infty}^\infty \frac{dy}{[(y-y_1)^2 + (x-x_1)^2 + (d+\delta)^2]^{3/2}} = \frac{2}{(x-x_1)^2 + (d+\delta)^2}$$

Hence

$$\Delta Z_2 = 2(I_2 - I_3) \int_0^\infty \frac{d+\delta}{[(x-x_1)^2 + (d+\delta)^2]}\,dx$$

$$= 2(I_2 - I_3) \left[\tan^{-1} \frac{x-x_1}{d+\delta} \right]_0^\infty$$

or

$$\Delta Z_2 = 2(I_2 - I_3) \left(\frac{\pi}{2} + \tan^{-1} \frac{x_1}{d+\delta} \right)$$

The effect due to surface AC at P is obtained in similar fashion by integrating between x and ∞; this gives:

$$\Delta Z_3 = 2(I_1 - I_3) \left(\frac{\pi}{2} - \tan^{-1} \frac{x_1}{\delta + d} \right)$$

Hence, the total vertical anomaly (vertical component of the field due to induced magnetism) is:

$$\Delta Z = \Delta Z_1 + \Delta Z_2 + \Delta Z_3 = 2\pi I_3 + 2(I_1 - I_3) \left(\frac{\pi}{2} - \tan^{-1} \frac{x_1}{\delta + d} \right)$$

$$+ 2(I_2 - I_3) \left(\frac{\pi}{2} + \tan^{-1} \frac{x_1}{\delta + d} \right)$$

or

$$\Delta Z = 2I_1 \left(\frac{\pi}{2} - \tan^{-1} \frac{x_1}{\delta + d} \right) + 2I_2 \left(\frac{\pi}{2} + \tan^{-1} \frac{x_1}{\delta + d} \right) \qquad (83)$$

It is evident that ΔZ does not depend on I_3 but does depend on the layer thickness d. If the overlying formation consisted of a number of layers having different values of k, the effects would still cancel out. Figure 87 illustrates the vertical anomaly profiles for the case that I_2 is much greater than I_1. †

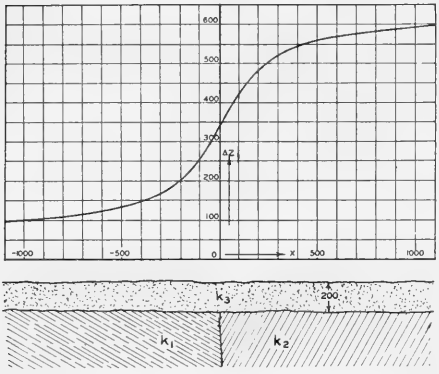

FIG. 87.—Anomaly due to buried contact of two thick layers. (Equation 83.)

Anomaly Due to Horizontal Component of Induction

If, as is generally the case, the earth's field is not vertical, the phenomenon would be the same as though two fields were present, i.e., a vertical field equal to the vertical component Z and a horizontal field equal to the horizontal component H. The calculations just made may be used to give the effect of the vertical field. The horizontal component, however, would produce an additional distribution of magnetism along the plane AB. (The effects produced by such a distribution will be considered in a later section.)

Thin Layer Terminating at a Distance d Below the Surface.—In this case there are two kinds of effects to be taken into account: the effect due to the end of the layer and the effect due to magnetization at right angles to the plane of the layer. (Figure 88.) We shall consider the end effect first. If I_1 is the intensity of magnetization parallel to the plane of the paper and normal to the end of the layer and t the thickness of the layer, the pole strength per unit length of the end of the layer is tI_1. If the layer is thin, the end effect is the same as that produced by a linear distribution of magnetic poles oriented at right angles to the plane of the paper. The potential due to such a distribution is given by Equation 79; that is,

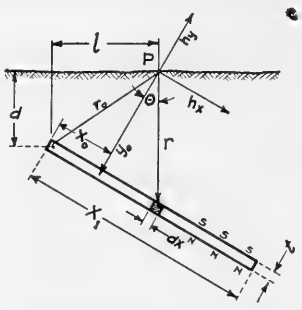

FIG. 88.—Sketch showing quantities which enter into the calculation of the potential due to magnetization at right angles to the surface of the layer.

$$V_1 = 2tI_1 \log r_0 = 2tI_1 \log (d^2 + l^2)^{\frac{1}{2}}$$

The vertical component of the anomaly at P is:

$$\frac{\partial V_1}{\partial d} = \frac{2tI_1 d}{d^2 + l^2} \qquad (84)^*$$

† See also L. B. Slichter, *A.I.M.E. Geophysical Prospecting*, 1929, p. 240.

* The field is expressed as the positive derivative of V in order to avoid carrying negative signs. Actually, the sign of the anomaly depends on the sign of I and this in turn depends on the orientation of the magnetic layer with respect to the earth's field.

The horizontal component at P is

$$\frac{\partial V_1}{\partial l} = \frac{2tI_1 l}{d^2 + l^2} \tag{84a}$$

The second effect (due to magnetization of the layer by the field at right angles to its surface) may be obtained as follows: Let I_2 and $-I_2$ be the densities of magnetic charge on the two surfaces of the layer. The potential at the point P due to a magnetized strip which is perpendicular to the plane of the paper and has a thickness t is

$$\frac{2tI_2 \cos\theta}{r}.$$

(Compare Equation 80.) The potential V_2 due to the magnetized *surface* may be obtained by integrating the potential due to the magnetized strip with respect to x; that is,

$$V_2 = \int_0^{x_1} \frac{2I_2 t \cos\theta}{r}\,dx = 2I_2 t \int_0^{x_1} \frac{y_0\,dx}{y_0^2 + (x - x_0)^2}$$

$$= 2I_2 t \left[\tan^{-1}\frac{x_0}{y_0} - \tan^{-1}\frac{x_0 - x_1}{y_0}\right]$$

The x and the y components of the magnetic field at P are:

$$\frac{\partial V_2}{\partial x_0} = 2I_2 t \left[\frac{y_0}{y_0^2 + x_0^2} - \frac{y_0}{y_0^2 + (x_0 - x_1)^2}\right]$$

and

$$\frac{\partial V_2}{\partial y_0} = 2I_2 t \left[-\frac{x_0}{y_0^2 + x_0^2} + \frac{x_0 - x_1}{y_0^2 + (x_0 - x_1)^2}\right]^*$$

SPECIAL CASE

Suppose that one end of the layer is very far removed from the earth's surface; that is, suppose that x_1 is very large. For this case, the equation given above for the potential due to cross magnetization reduces to

$$V_2 = 2I_2 t\left[\tan^{-1}\frac{x_0}{y_0} + \frac{\pi}{2}\right]$$

The x and y components of the anomaly due to the cross magnetization for this case are:

$$\frac{\partial V_2}{\partial y_0} = -2I_2 t \frac{x_0}{y_0^2 + x_0^2}$$

* This equation is obtained by differentiating V_2 with respect to y_0 under the integral sign and then integrating the resultant expression with respect to x_0 between the limits x_0 and x_1-x_0. In carrying out the integration use is made of the formula

$$\int \frac{2y_0^2\,dx}{[y_0^2 + (x - x_0)^2]^2} = \frac{x - x_0}{y_0^2 + (x - x_0)^2} + \int \frac{dx}{y_0^2 + (x - x_0)^2}$$

and

$$\frac{\partial V_2}{\partial x_0} = 2I_2 t \frac{y_0}{y_0^2 + x_0^2}$$

The vertical component of the anomaly is A_v = (y component) $\cos\theta$—(x component) $\sin\theta = h_y \cos\theta - h_x \sin\theta$ and the horizontal component is $A_h = h_y \sin\theta + h_x \cos\theta$. (Compare Figure 88.) Thus, for the cross magnetization:

$$A_{v_2} = \frac{\partial V_2}{\partial y_0}\cos\theta - \frac{\partial V_2}{\partial x_0}\sin\theta = -2I_2 t \frac{x_0\cos\theta + y_0\sin\theta}{x_0^2 + y_0^2}$$

But

$$y_0\sin\theta + x_0\cos\theta = l \quad \text{and} \quad x_0^2 + y_0^2 = r_0^2 = d^2 + l^2$$

$$\therefore A_{v_2} = -2I_2 t \frac{l}{d^2 + l^2} \tag{85}$$

Similarly

$$A_{h_2} = \frac{\partial V_2}{\partial y_0}\sin\theta + \frac{\partial V_2}{\partial x_0}\cos\theta = 2I_2 t\left(-\frac{x_0\sin\theta + y_0\cos\theta}{y_0^2 + x_0^2}\right)$$

But

$$y_0\cos\theta - x_0\sin\theta = d$$

$$\therefore A_{h_2} = \frac{2I_2 t d}{d^2 + l^2} \tag{85a}$$

The vertical and horizontal components of the anomaly due to the end effect have already been computed. In the new notation, the anomalies are

$$A_{v_1} = \frac{\partial V_1}{\partial d} = \frac{2tI_1 d}{d^2 + l^2} \tag{84}$$

and

$$A_{h_1} = \frac{\partial V_1}{\partial l} = \frac{2tlI_1}{d^2 + l^2} \tag{84a}$$

A comparison of Equation 84 (end effect) and Equation 85 (cross magnetization effect) shows that the horizontal component due to the end effect has the same form as the vertical component due to cross magnetization. Also, the horizontal component due to cross magnetization has the same form as the vertical component due to the end effect.

The relative magnitudes of the two effects depend on the orientation of the layer with respect to the magnetic field of the earth. For example,

if the surface of the layer were perpendicular to the total magnetic field of the earth, the end effect would be zero; on the other hand, if the surface of the layer were parallel to the total magnetic field, the end effect alone would be present. In the general case, both effects are present, and the magnitude of each depends on the components of the magnetic field. The end effect depends on I_1 (which is equal to the susceptibility k of the layer times the component of the magnetic field normal to the end of the layer), and the cross-magnetization effect depends upon I_2 (which is equal to k times the component of the magnetic field normal to the layer).*

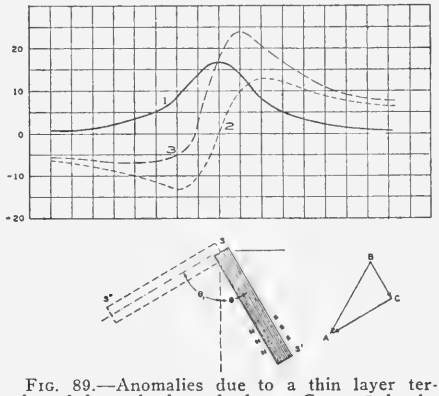

FIG. 89.—Anomalies due to a thin layer terminated by a horizontal plane. Curve 1 is the vertical component of the end effect (Equation 84); curve 2 is the vertical component due to magnetization of the layer by the field at right angles to its surface (Equation 85), and curve 3 is the resultant vertical anomaly.

The vertical anomalies due to the two effects are plotted in Figure 89 for the case that the layer makes an angle of about 32° with the vertical component of the earth's magnetic field. It should be emphasized that the end effect can be either positive or negative. That is, the sign, as well as the magnitude of this effect, depends upon the orientation of the layer. For example, if the layer in Figure 89 were horizontal ($\theta_1 = \pi/2$), the direction of the vertical component due to the end effect would be opposite to that of the vertical component of the earth's field; that is, the end effect would be negative. Thus, in some cases, *the presence of a magnetic low may indicate that a layer of strongly ferromagnetic material lies below the surface.* In general, the end of the layer does not lie directly under the maximum point of the magnetic anomaly, and the depth to the layer can be estimated only if its orientation relative to the earth's resultant field is taken into account.

Curves 1, 2 and 3 in Figure 89 also represent the horizontal anomalies. Curve 1 is the horizontal anomaly due to cross magnetization, curve 2 is the horizontal anomaly due to the end effect, and curve 3 is the total horizontal anomaly.

Effects Due to a Thick Layer.—Consider the effect produced at a point P (x_0y_0) by a magnetized strip which is perpendicular to the plane of the paper. (Figure 90.) The magnetized strip corresponds essentially to a linear distribution. Hence, the potential at an external point due to a magnetized strip of thickness dx is given by Equation 79; that is, $dV =$

* It is assumed here that the susceptibility of the surrounding medium is negligible.

$2I \log r\, dx$. The potential due to the entire surface between $x = x_1$ and $x = x_2$ is

$$V = 2\int_{x_1}^{x_2} I \log r\, dx = 2\int [I \log \{y_0^2 + (x - x_0)^2\}^{1/2}]\, dx$$

The x and y components of the magnetic force due to the surface layer at the point $(x_0 y_0)$ are

$$\left(\frac{\partial V}{\partial x_0}\right) = 2\int_{x_1}^{x_2} I \frac{\partial \log r}{\partial x_0}\, dx = 2I \int_{x_1}^{x_2} \frac{(x - x_0)\, dx}{y_0^2 + (x - x_0)^2}$$

$$= I \{\log [y_0^2 + (x_2 - x_0)^2] - \log [y_0^2 + (x_1 - x_0)^2]\} \qquad (86)$$

$$\left(\frac{\partial V}{\partial y_0}\right) = 2\int_{x_1}^{x_2} I \frac{\partial \log r}{\partial y_0}\, dx = 2I \int_{x_1}^{x_2} \frac{y_0\, dx}{y_0^2 + (x - x_0)^2}$$

$$= 2I \left[\tan^{-1} \frac{(x_2 - x_0)}{y_0} - \tan^{-1} \frac{(x_1 - x_0)}{y_0}\right] \qquad (87)$$

The vertical and horizontal components due to the end of the thick layer are given by the end effect equations for a thin layer. The total magnetic anomaly produced by a thick layer may be calculated by adding the effects produced by its surfaces and its end.

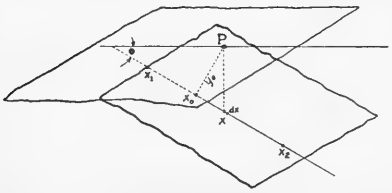

FIG. 90.—Sketch showing quantities which enter into the calculation of the magnetic potential produced by a thick layer at an external point P.

Special Cases

1. *Vertical Anomaly Near the End of a Thick Horizontal Layer.*—Assume that the upper surface of the layer is buried at a depth of 200 feet and that the layer is 1,000 feet thick. It will be convenient to consider separately the effects of the upper surface, the lower surface, and finally, the end of the layer. For a horizontal layer, the vertical anomalies produced by the surfaces are equal to the y_0 components. Hence, the vertical component due to the upper surface of the layer is:

$$\frac{\partial V}{\partial y_0} = 2I_1 \left[\tan^{-1} \frac{x_2 - x_0}{y_0} - \tan^{-1} \frac{x_1 - x_0}{y_0}\right]$$

If it is assumed that one end of the layer is vertical and the other end is very far removed from the region in which anomalies are being measured, the first quantity in the bracket approaches $\pi/2$. The second quantity in the bracket may be simplified by setting x_1 equal to zero. When these substitutions have been made, the last equation becomes:

$$\frac{\partial V}{\partial y_0} = 2I_1 \left[\frac{\pi}{2} + \tan^{-1} \frac{x_0}{y_0}\right]$$

where $y_0 = 200$ and $x_1 = 0$. Similarly the vertical anomaly due to the lower surface is

$$\frac{\partial V}{\partial y_0} = 2I_1 \left[\frac{\pi}{2} + \tan^{-1} \frac{x_0}{y_0} \right]$$

where $y_0 = 1200$ and $x_1 = 0$. The vertical component due to the end is equal to the horizontal component due to the surface. (Compare p. 198.) Thus, the vertical anomaly due to the end is

$$\frac{\partial V}{\partial x_0} = I_2 \left[\log \{y_0^2 + (x_0 - x_2)^2\} - \log \{y_0^2 + (x_0 - x_1)^2\} \right]$$

2. *Vertical Anomaly Due to a Thick Vertical Vein.*—The calculation of the vertical anomaly due to a thick vertical vein, the upper surface of which is located at a depth d below the surface, is essentially similar to that for a thick horizontal layer. First, the effect due to the upper surface of the layer is calculated. This may be assumed to be equivalent to the effect of a horizontal strip. Hence, the effect due to the surface of the layer is given by Equation 87; that is,

$$\frac{\partial V}{\partial y_0} = 2I_1 \left[\tan^{-1} \frac{x_2 - x_0}{y_0} - \tan^{-1} \frac{x_1 - x_0}{y_0} \right]$$

The effect due to the side of the layer is essentially the same as that due to a strip placed at right angles to the surface. Hence, the vertical component due to the side is given by Equation 86; that is,

$$\frac{\partial V}{\partial x_0} = I_2 \{\log [y_0^2 + (x_2 - x_0)^2] - \log [y_0^2 + (x_1 - x_0)^2]\}$$

If this equation is used for estimating the effects of each side of the layer separately, the following difficulty is encountered: When one end of the layer is assumed to be

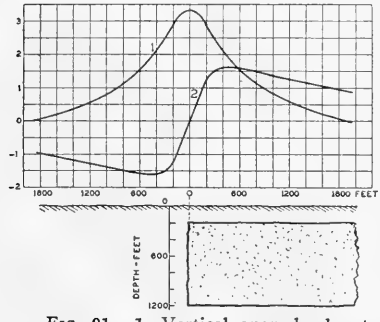

FIG. 91.—1, Vertical anomaly due to the magnetization of the side of a thick vertical layer. (Compare Equation 88.) 2. Horizontal anomaly. (Compare Equation 87.)

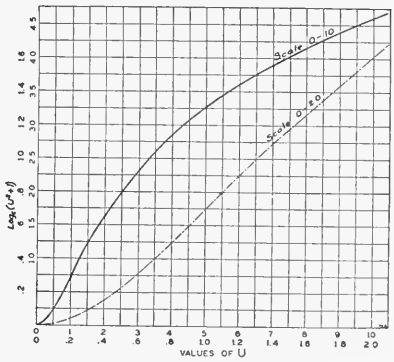

FIG. 92.—Auxiliary curve.

far away, the vertical anomaly due to one side becomes very large and positive, while the vertical anomaly due to the other side of the layer also becomes very large but negative. For this reason, it is necessary to add the effects due to the two sides before integrating Equation 86. A material simplification is achieved by assuming the other end of the layer removed to infinity as then the expression for the vertical anomaly

due to the side reduces to

$$\frac{\partial V}{\partial x_0} = I_2 \log \frac{y_0^2 + (x_1 - x_0)^2}{y_1^2 + (x_1 - x_0)^2} \tag{88}$$

where $y_1 = y_0 +$ the width of the layer.

The vertical anomaly due to the side of the thick vein is plotted in Figure 91 for an assumed negative value of I_2. (To simplify calculations, auxiliary curves are plotted in Figure 92.)

Effects Due to Surface Irregularities. (A Cliff.)—Consider the vertical anomaly in the neighborhood of a vertical cliff. (Figure 93.) The vertical component of the field along a line AA' is the resultant of the effects due to surfaces A, C, and B. The effect of surface A will be approximately constant, as the instrument is usually relatively close to the ground and the effects due to the edge are not apparent until the distance from the edge becomes comparable with the height of the instrument above ground. Surfaces C and B may be considered as strips and their effects calculated from the formulas already given.

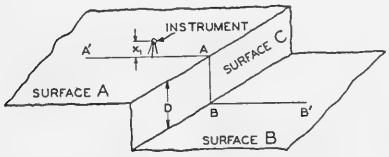

FIG. 93.—Surface irregularity. (A cliff.)

C. Magnetic Anomalies Produced by a Uniformly Magnetized Sphere.—The effect of induction in the earth's magnetic field for a sphere may be analyzed as follows:† Consider that the sphere has two volume densities of magnetic charge, $+\tau$ and $-\tau$, which coincide when there is no external field. (Figure 94.)‡ In the presence of a field, the sphere of positive charge is displaced relative to the sphere of negative charge in the direction of the field by a distance $00'$. As a consequence of this displacement the sphere becomes uniformly magnetized with an intensity of magnetization.

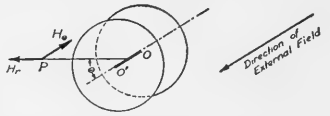

FIG. 94.—A uniformly magnetized sphere is equivalent to two spheres having equal and opposite densities of magnetic charge.

$$I = \tau \cdot \overline{00'} \tag{89}$$

It may be proved that the field at outside points due to a spherical distribution of magnetic charge is the same as that due to a single charge concentrated at the center of the sphere. Hence, the magnetic field at an external point P is the same as that produced by a dipole of magnetic moment:

$$M = 4/3\ (\pi R^3 \tau \cdot \overline{00'}) = 4/3\ (\pi R^3 I) \tag{90}$$

where R is the radius of the sphere.

† Compare Starling, *loc. cit.*, p. 142.
‡ Starling, *loc. cit.*, pp. 268, 269.

The field H' due to the magnetic moment M is shown by the broken lines of Figure 95. It is apparent that inside the sphere and in certain regions outside, the induced field H' opposes the earth's field (solid lines). The demagnetizing field H' is proportional to the moment of the magnetic dipole to which it is due, and this in turn is proportional to the intensity of magnetization. Hence, $H' = -NI$, where N is a constant. The "demagnetizing factor" N depends on the geometrical form of the magnetized body. It may be shown that for a sphere $N = 4/3\pi$. Therefore, if the total intensity of the earth's field is denoted by T, the effective field inside the sphere may be written: $T - 4/3\pi I$.

The intensity of magnetization is proportional to the effective field inside the sphere; that is,

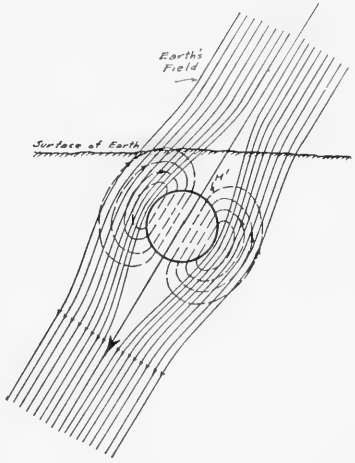

FIG. 95. — Diagram illustrating demagnetization effect: The field H' due to a uniformly magnetized sphere opposes the earth's field.

$$I = k\,(T - 4/3\,\pi I) \quad \text{or} \quad I = \frac{k\,T}{1 + 4/3\,k\pi} \tag{91}$$

where k is the susceptibility of the paramagnetic material constituting the sphere.

Equation 91 corresponds to the case that the susceptibility of the medium in which the sphere is imbedded is zero. If the susceptibility k_0 of the surrounding medium is not zero, the last equation becomes

$$I = \frac{(k - k_0)\,T}{1 + 4/3\pi\,(k - k_0)}$$

and

$$M = \frac{4/3\,\pi R^3\,(k - k_0)\,T}{1 + 4/3\pi\,(k - k_0)} \tag{92}$$

On introducing a new variable c defined by the equation

$$c \equiv \frac{4/3\,\pi R^3\,(k - k_0)}{1 + 4/3\pi\,(k - k_0)} \tag{93}$$

the expression for the magnetic moment M becomes

$$M = cT \tag{94}$$

The potential ΔV at an external point P due to the uniformly magnetized sphere is

$$\Delta V = \frac{M \cos\theta}{r^2} \tag{95}$$

where M is the magnetic moment of the sphere, r is the distance between the center of the sphere and the point P, and θ is the angle formed by r

and x. (Figure 96.)† The components of the magnetic field in the direction of increasing r and θ are (see p. 87, position III of Gauss).

$$\Delta H_r = \frac{2Mr}{r^3}$$
$$\Delta H_\theta = \frac{M\theta}{r^3} \qquad (96)$$

respectively, where M_r and M_θ are the components of M in the r and θ directions, respectively.

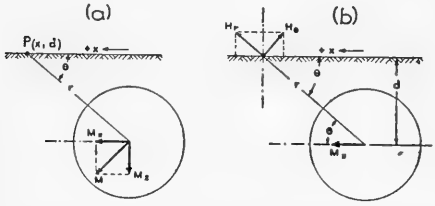

FIG. 96.
(a) Sketch illustrating method for resolving magnetic moment M into components M_x and M_z.
(b) Sketch illustrating method for determining horizontal and vertical magnetic anomalies due to magnetic moment M_x.

The horizontal and vertical components of the magnetic anomaly at a point P on the surface of the earth may be obtained by resolving the magnetic moment M of the sphere into the components M_x and M_z. (Figure 96(a).

The components of the field in the directions of increasing r and θ due to M_x are

$$(\Delta H_r)_x = \frac{2M_x \cos\theta}{r^3} = \frac{2M_x x}{r^4}$$

and

$$(\Delta H_\theta)_x = \frac{M_x \sin\theta}{r^3} = \frac{M_x d}{r^4}$$

The net x component $(\Delta H)_x$ of these fields is

$$(\Delta H)_x = \frac{2M_x x^2}{r^5} - \frac{M_x d^2}{r^5}$$

and the net z component $(\Delta Z)_x$ is

$$(\Delta Z)_x = \frac{2M_x xd}{r^5} + \frac{M_x xd}{r^5} = \frac{3M_x xd}{r^5}$$

In a similar manner it may be shown that the net x component $(\Delta H)_z$ of the fields due to M_z is

$$(\Delta H)_z = -\frac{3M_z xd}{r^5}$$

and the net z component $(\Delta Z)_z$ is

$$(\Delta Z)_z = \frac{M_z x^2}{r^5} - \frac{2M_z d^2}{r^5}$$

† Compare Starling, *loc. cit.*, p. 15.

The total x component ΔH due to M_x and M_z is

$$\Delta H = (\Delta H)_x + (\Delta H)_z = \frac{2M_x x^2}{r^5} - \frac{M_x d^2}{r^5} - \frac{3M_z xd}{r^5} \tag{97}$$

and the total z component ΔZ due to M_x and M_z is

$$\Delta Z = (\Delta Z)_x + (\Delta Z)_z = \frac{3M_x xd}{r^5} + \frac{M_z x^2}{r^5} - \frac{2M_z d^2}{r^5} \tag{98}$$

Equations 97 and 98 may be simplified by expressing the magnetic moments M_x and M_z in terms of the horizontal and vertical components H and Z of the earth's normal field. That is,

$$M_x = cH = cZ\,\frac{H}{Z}$$

and

$$M_z = cZ = cH\,\frac{Z}{H}$$

On substituting these values into Equations 97 and 98 and simplifying, one obtains †

$$\Delta H = \frac{cH}{r^5}\left(2x^2 - d^2 - 3xd\,\frac{Z}{H}\right) \tag{99}$$

$$\Delta Z = \frac{cZ}{r^5}\left(x^2 - 2d^2 + 3xd\,\frac{H}{Z}\right) \tag{100}$$

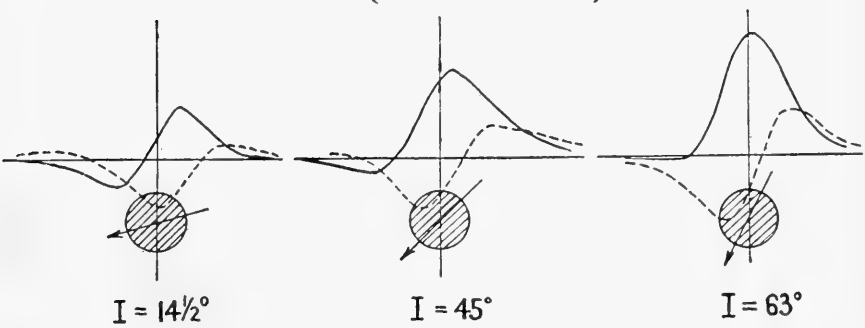

FIG. 97.—Sketches illustrating the anomalies produced by a uniformly magnetized sphere in regions of different inclination. (After Haalck, *Die Magnetischen Verfahren der Angewandten Geophysik.*)

Equations 99 and 100 show that the anomalies ΔH and ΔZ depend on the normal values H and Z. That is, the anomalies produced by a uniformly magnetized sphere depend on the normal value of the inclination of the earth's field in the region in which the subsurface sphere is located. The ΔH and ΔZ profiles for three values of the inclination are shown in Figure 97.‡

† Compare H. Haalck, "Die Magnetischen Methoden der Angewandten Geophysik," pp. 330-332. *Handbuch der Experimentalphysik*, edited by W. Wien and F. Harms. (Akademische Verlagsgesellschaft M.B.H., Leipzig 1930.) Vol. 25, part III.

‡ H. Haalck, *Die Magnetischen Verfahren der Angewandten Geophysik* (Gebrüder Bornträger, Berlin, 1927).

EMPIRICAL METHODS OF INTERPRETATION: CORRELATION WITH KNOWN GEOLOGY

In the practical application of magnetic measurements to the solution of subsurface problems of economic geology, theoretical calculations can be carried out only for relatively simple bodies, e.g., two-dimensional bodies, spheres, etc. However, the usual configurations of geologic bodies rarely produce the simple magnetic effects equivalent to those produced by simple geometric forms. The interpreter, therefore, must resort to other aids besides direct theory when solving his field problems. The three most effective aids are: first, and most important, adequate geologic or subsurface control; second, magnetic studies over known geologic conditions in the immediate area; and third, small scale model experiments.

The usual interpretative technique is almost exclusively empirical. Deductions and inferences are drawn qualitatively from the sizes, shapes, and configurations of the magnetic anomalies and are coordinated with the known regional and local geology.

In many problems where prior subsurface development work has been done, it is advantageous to carry out magnetic studies over known subsurface features or producing fields and utilize the results for interpretative control. For instance, in magnetic studies of the Sparta-Wilcox trend in central Louisiana, control studies were conducted over the Eola and Cheneyville structures, and the control used as a guide in interpretation. Similar studies have been employed in mapping the extension of the Kettleman structure in California. The magnetic results obtained over the Hobb's Field in Lea County, New Mexico (see Figure 106) have been used as interpretative control for numerous studies made in that area. The rapidity and low cost of magnetic work allows this type of interpretative control to be economically feasible. The combined reconnaissance and detail work in this type of study seldom cost more than 2½ to 5 cents per acre.

Model Experiments.—Model experiments are of value in determining the relationship between the directions of the magnetic vectors in space and the shape of a magnetic structure. The operating principle is to construct small-scale models having relative dimensions and geometric disposition similar to those assumed for the anomalous geologic bodies.

Experiments on model ore bodies have been reported by Hotchkiss, † Keys, ‡ and Jenny. §

Hotchkiss investigated the magnetic effects as a function of the dip and strike of model formations. One of the experimental arrangements consisted of a drawing board with a sheet of tin suspended by a wood frame from its side. The sheet was positioned at various distances from

† W. O. Hotchkiss, *Mineral Land Classification*, Wisconsin Geological and Natural History Survey Bulletin, No. 44, Madison, 1915, Ch. IV, "Magnetic Observations," pp. 112-126.
‡ D. A. Keys, *A.I.M.E. Geophysical Prospecting*, 1932, pp. 205-208.
§ W. P. Jenny, "Experimental Interpretation of Magnetic and Gravimetric Anomalies," *Terr. Mag.*, 40 (1), 1935, p. 72.

the board and at different angles of dip. The magnetic declination was measured with a compass at various positions along "traverses" parallel to the sides of a wood T square. The sheet could also be oriented at different strike angles with the magnetic field.

The Keys' experiment was a laboratory investigation of the magnetic effects of a "thin magnetized dike of limited length." † A. S. Eve, ‡ in collaboration with Keys and several other investigators, had carried out a survey over a portion of the Falconbridge ore body in which two sets of measurements were made with an Askania magnetometer, one set being made on the ground and the other on elevated platforms. The purpose of the survey was to determine the lower depth of the ore body from the differences in the anomalies at the two levels (ground and platform). The survey did not yield an accurate value of the lower depth, and the Keys' experiment was designed to verify the correctness of the method of interpretation used in the survey.

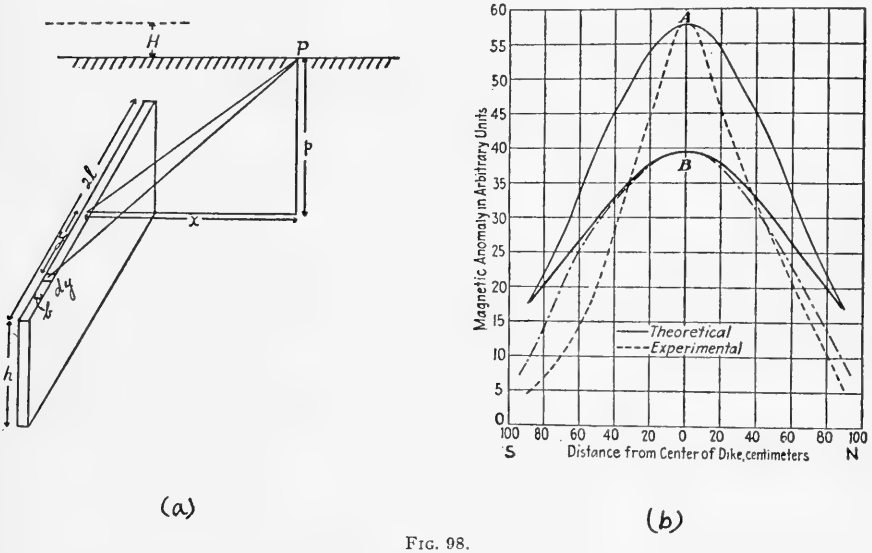

FIG. 98.

(a) Sketch of narrow magnetized dike of limited dimensions.
(b) Experimental and theoretical vertical magnetic anomalies at two different levels over a model magnetic dike. (Keys, *A.I.M.E. Geophysical Prospecting*, 1932, p. 206.)

A sheet of mild steel, which was approximately one-half inch thick, four feet high, and ten feet long, was supported vertically on its edge with its length perpendicular to the magnetic meridian. To magnetize the sheet ten turns of insulated copper wire were wound lengthwise around its center and a current of one ampere passed through the wire in a direction to make the upper edge a south pole. An Askania vertical variometer was

† D. A. Keys, *loc. cit.*
‡ A. S. Eve, "A Magnetic Method of Estimating the Height of Some Buried Magnetic Bodies," *A.I.M.E. Geophysical Prospecting*, 1932, pp. 200-205.

mounted on a platform so that the vertical distance between the needle of the instrument and the top of the steel plate was 88 cm. Measurements were made of the vertical anomalies at various points along a line parallel to the magnetic meridian through the center of the plate. A second set of measurements was then made along the same "traverse" with the needle 111 cm. above the top of the steel plate.

The results of the laboratory investigations are shown in Figure 98. In plotting these curves, the experimental readings were all multiplied by an arbitrary factor to facilitate the comparison of the theoretical and experimental results.

Readings are taken over the *center* of the dike at two levels separated by a vertical distance H, assuming two horizontal, linear distributions of magnetic charge (different polarity) of finite length separated by a distance h (cf. p. 191 and Figure 98a).

$$F_{\text{ground}} = \frac{2mp}{p^2}\int_0^{\tan^{-1} l/p} \cos\phi\, d\phi - \frac{2m\,(p+h)}{(p+h)^2}\int_0^{\tan^{-1} l/p + h} \cos\phi\, d\phi$$

$$= \frac{2m}{p}\sin\phi\Big|_0^{\tan^{-1} l/p} - \frac{2m}{(p+h)}\sin\phi\Big|_0^{\tan^{-1} l/p + h}$$

$$\left[\sin\left(\tan^{-1}\frac{l}{p}\right) = \frac{l}{(p^2+h^2)^{1/2}};\ \text{see Figure 98(a)}\right]$$

$$\text{Thus, } F_{\text{ground}} = \frac{2m}{p}\frac{l}{(p^2+l^2)^{1/2}} - \frac{2m}{(p+h)}\frac{l}{[(p+h)^2+l^2]^{1/2}}$$

$$= 2ml\left\{\frac{1}{p(p^2+l^2)^{1/2}} - \frac{1}{(p+h)\,[(p+h)^2+l^2]^{1/2}}\right\}$$

$$F_{\text{height H}} = \frac{2m\,(p+H)}{(p+H)^2}\int_0^{\tan^{-1} l/p + h} \cos\phi\, d\phi$$

$$- \frac{2m\,(p+h+H)}{(p+h+H)^2}\int_0^{\tan^{-1} l/p + h + H} \cos\phi\, d\phi$$

$$= 2ml\left\{\frac{1}{(p+H)\,[(p+H)^2+l^2]^{1/2}} - \frac{1}{(p+h+H)\,[(p+h+H)^2+l^2]^{1/2}}\right\}$$

Taking the ratio r of the readings (which are experimentally known) a relation can be obtained for the "height" h of the dike (i.e., the vertical distance between poles) in terms of known quantities.

$$\frac{F_{\text{ground}}}{F_H} = r = \text{experimentally known value}$$

$$r = \frac{\dfrac{1}{p(p^2+l^2)^{1/2}} - \dfrac{1}{(p+h)\,[(p+h)^2+l^2]^{1/2}}}{\dfrac{1}{(p+H)\,[(p+H)^2+l^2]^{1/2}} - \dfrac{1}{(p+h+H)\,[(p+h+H)^2+l^2]^{1/2}}}$$

where p = the depth to the top of the dike, l = one-half the length of the dike, and H = height above ground at which the record reading was taken.

In addition to investigations of model ore bodies, laboratory experiments have been carried out to determine the depth and geometric configuration of regional subsurface structural features. Figure 99 shows a schematic section of an apparatus devised by Jenny† which permits quantitative interpretation of vertical magnetic anomalies. Vertical bar magnets *1* are connected with counterweights *4* by means of ribbons *2* which pass over pulleys *3*. The displacements of the dip needles *5, 6, 7* produced by the magnets when they are all at the same level are compensated by counterweights (not shown) which are attached to the needles and by screws *8*. To determine depths, the bar magnets are displaced by means of the counterweights *4* so as to correspond to the assumed structure. For example, the positions of the bar magnets shown in Figure 99 would correspond to an anticline. Contours of equal depth may be obtained by studying several cross sections.

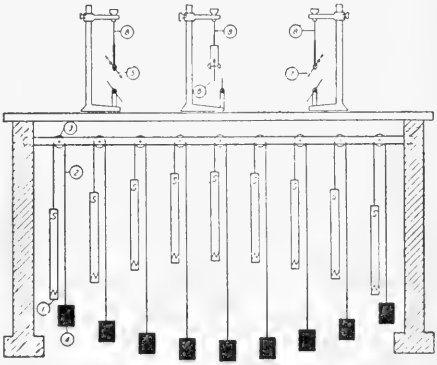

FIG. 99.—Schematic diagram of apparatus for experimental interpretation of magnetic and gravimetric anomalies. (Jenny, *Terr. Mag.* 40 (1), 1935, p. 72.)

The most flexible model arrangement for magnetic studies comprises a mixture of coarse iron filings and clean white sand placed in a large wooden tank, preferably about 8 feet in diameter and 2 feet high. The tank should be provided with a cover in order to exclude moisture and minimize rusting of the iron. The orientation of the tank with respect to the magnetic field can be varied by mounting it on a turntable. The latter should be placed on a wooden track with rollers so that it can be readily moved.

† W. P. Jenny, *loc. cit.*, p. 74.

The magnetic observations are made with the regular horizontal and vertical component magnetometers. The latter are mounted on a rigid platform above the movable tank. The "depth" of the magnetic body is simulated by varying the height of the magnetometers above the tank. Any desired shape and configuration of the body may be simulated by proper shaping of the sand-iron mixture.

The iron filings are preferably of the coarse type obtained from milling operations. Those employed by the author were obtained by milling a stack of laminated iron sheets across grain. (The iron sheets came from the core of an old power transformer.) The milling was done on a bias to give short cuttings. A mixture of sand and 10 to 30 per cent of filings, by weight, gives an easily handled material with sufficient magnetic permeability to allow sharp readings.

The movable tank arrangement with stationary magnetometer involves considerably more preparatory work than the use of a stationary tank or earth pit with a movable magnetometer. However, more accurate and rapid work may be done with the movable tank arrangement, because the magnetometer may be adjusted at the beginning of the experiment and not disturbed thereafter. Thus, the errors of misorientation, leveling, and other similar instrumental errors are avoided. The magnetometer is unclamped at the beginning of the experiment and readings are made thereafter without disturbing the instrument. A second magnetometer is employed for mapping the diurnal variations.

GEOMAGNETIC ANOMALIES

The outer crust of the earth comprises a magnetically heterogeneous assemblage of rocks which exists in the earth's magnetic field. Certain rocks exhibit the properties of magnets (induced or permanent) and superimpose their own magnetic fields on that of the earth. The superimposed fields are termed major, continental, regional, and local anomalies, depending on the scale of the geologic irregularities which produce them.

The major and continental magnetic anomalies may be defined as variations of the earth's magnetic field associated with major and continental irregularities (inhomogeneities of composition and/or structural distortions). Continental anomalies are negative in Europe and positive in North and South America. Major anomalies may show pronounced trends, such as a positive major trend paralleling the Rockies and the Andes and a negative major trend paralleling the Alpine chains.†

The regional anomalies cover smaller areas, one of the best known being in the Province of Kursk, Russia. Regional anomalies indicate the tectonics and the stratigraphic and the petrographic character of the upper portion of the rock zone. A basin that has strongly magnetic beds, such as

† W. P. Jenny, Abstract of paper delivered before the American Association of Petroleum Geologists, *Oil and Gas Journal*, April 11, 1940.

Illinois, is positive, and a basin that does not have strongly magnetic beds, such as West Texas, is negative. Uplifts that have a thick section of Ordovician limestones, such as the Ozarks, are negative because the flanks have magnetic shales and sands above the limestones. The Nemaha ridge is positive because the granite is sufficiently close to the surface to outweigh stratigraphic influences. ‡

Local anomalies, as the name implies, extend over relatively small areas. The magnetic intensity in these areas may occasionally reach a high value; for example, near Juneau, Alaska, a local magnetic pole produces an anomaly of sufficient magnitude to cause a dip needle to stand vertical.

Classification of Anomalies.—The geophysicist H. Haalck has given a very convenient classification of magnetic anomalies, dividing them into four classes.

Class 1 anomalies have a range of from 10,000 to 200,000 gammas of vertical magnetic intensity. Examples are rare, but probably the most famous one is the extremely large anomaly at Kursk, in Russia, already mentioned. An American example is the extensive magnetite deposit in Boulder County, Colorado.†

In such magnetic features the magnetic vertical intensity may be several times as great as the value of that component of the earth's magnetic field for the latitude of the locality. Such exceptionally great anomalies arise from large deposits of magnetite, often of economic importance.

Class 2 anomalies have values of from 1,000 to 10,000 gammas. They are generally due to extensive masses of volcanic or of crystalline rock rich in magnetite. The magnetic anomaly resulting from the Ralston Dike (basalt) in Jefferson County, Colorado is in this class§.

Class 3 anomalies are of from about 100 to 1000 gammas. They may be caused by masses of rock of the same kind that gives rise to Class 2 magnetic features, but carrying less magnetite. Also, they could be caused by less extensive bodies of magnetite-rich rock. Examples are numerous in the mining districts of the United States, Canada and Australia, from magnetic dikes and ore bodies, and the magnetite concentrations of certain placer deposits.

Class 4 anomalies include those up to 200 gammas. Haalck considers that these arise from sedimentary formations. The maximum figure should be perhaps 300 gammas.

The magnitude of a magnetic anomaly is an important factor in arriving at a conception of its cause. Another valuable guide in interpretation is the general geology of an area and the type of geologic structure that might reasonably be expected to occur in it. To use a somewhat exaggerated example, it would not be geologically sound to interpret a 20,000-gamma magnetic high, if found in eastern Colorado, as representing an anticlinal structure favorable for the accumulation of oil and gas. The magnetic anomaly associated with the large Ft. Morgan anticline in that area is only 600 gammas.

‡ W. P. Jenny, *loc. cit.*

† Heiland, Henderson & Malkovsky; U. S. Bureau of Mines, *Tech. Paper 439,* pp. 41-49, 1929. Covers geophysical surveys at Caribou, Colorado.

§ W. S. Levings, "A magnetic survey of the Ralston Dike, Jefferson County, Colo.," *Quarterly,* Colo. School of Mines, Vol. 27, No. 3, 1932.

Although not suggested by Haalck, a Class 5 for anomalies of about 100 gammas or less, some of which arise from serpentine plugs such as occur in Bastrop County, Texas, might be set up. This could also include the small negative anomalies (50 gammas or less) due to salt domes.

Magnetic Bodies That Can Be Treated As Bar Magnets Or As Magnetic Poles.—In certain cases the cause of a magnetic anomaly can, by implication, be treated as if it were a single magnetic pole. This assumption is sufficiently valid to be of use in interpretation for certain magnetic igneous dikes and tabular magnetic ore bodies.

Pole Depth Calculation.—Where the above assumptions are justified, the depth to the negative pole, which under normal conditions in the northern hemisphere will be nearest the surface, may be made as follows. The positive, or lower, pole is assumed to be at infinity (see Figure 100).

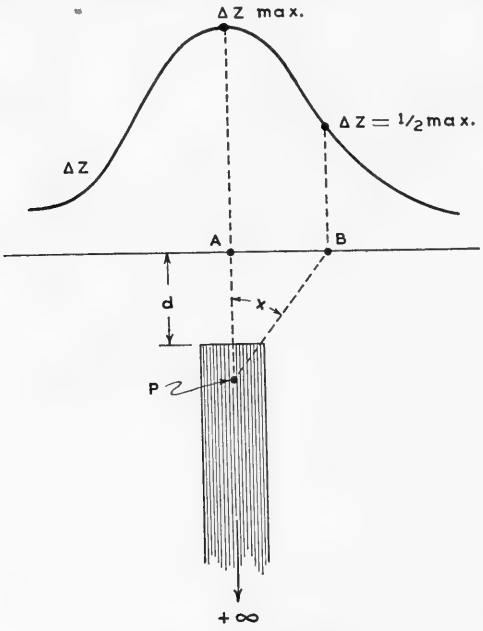

Fig. 100.—Vertical intensity anomaly curve, for calculation of pole depth.

The magnetic force at point A, or $\Delta Z_A = m/d^2$; (pole strength m divided by the distance squared.)

The magnetic force at B, designated F_B, is by the same formula total force acting in the direction BP divided by the square of the distance involved. This total force at B is designated as ΔT_B.

$$F_B = m/(BP)^2 = \frac{m}{\left(\frac{d}{\cos x}\right)^2} = \frac{m}{d^2}\cos^2 x = \Delta T_B \qquad (101)$$

since $\cos x = d/BP$, $BP = d/\cos x$.

The vertical magnetic intensity at B, or $\Delta Z_B = \Delta T_B \cos x$, which is obtained by projecting the force ΔT_B into the vertical direction.

$$\text{Hence: } \Delta Z_B = \Delta T_B \cos x = \frac{m}{d^2} \cos^3 x, \tag{102}$$

and since $\Delta Z_A = m/d^2$ we have

$$\Delta Z_B = \Delta Z_A \cos^3 x \text{ or } \cos^3 x = \frac{\Delta Z_B}{\Delta Z_A} \tag{103}$$

By the original assumption of the problem $\Delta Z_B = \frac{1}{2} \Delta Z_A$.

For this condition, $\cos^3 x = \frac{\frac{1}{2} \Delta Z_A}{\Delta Z_A} = \frac{1}{2}$ and $\cos x = \sqrt[3]{\frac{1}{2}} = 0.7937$ and $x = 37° 28'$

$$\left.\begin{aligned} &\text{This gives: } d = AB \cot x = 1.305\, AB = \frac{4}{3} AB \\ &\text{or } AB = \frac{3}{4} d \end{aligned}\right\} \tag{104}$$

In this equation d equals the depth to the pole.
AB is the distance in feet on the graph between the abscissa at A, the point of maximum vertical intensity, and B, the point of $\frac{1}{2}$ maximum vertical intensity.

If B had been selected at $1/3\ \Delta Z$ maximum $\cos x = \sqrt[3]{\frac{1}{3}}$ and $d = 0.962\ AB$. This formula is sometimes used, as are several others which are available. (cf. p. 186.)

By these formulae, the depth to the *pole* is found, not the depth to the top of the ore body. The ΔZ values of the curve represent the anomaly or vertical intensity values as measured, from which the average vertical intensity has been subtracted.

It is therefore necessary in surveying features which can be treated in this manner to take readings at a sufficient number of stations away from the influence of the dike or ore body, in order to insure a correct average base value for the vertical intensity of the locality. These base readings should also be taken at stations located in various directions from the body under study. An incorrect average vertical intensity subtracted from all readings would tend to increase or decrease the depth d as calculated.

Type Curves. — Formulae have been given in the previous sections whereby we may calculate the theoretical, or type, curves of ΔZ and ΔH for magnetic poles at assumed depths and for bar magnet type situations where both poles are considered. These are shown in Figures 76 and 79. It is of note that these curves are symmetrical, which is characteristic of *vertical* magnet-like tabular bodies. The cases referred to assume rod-like bodies. Sheet bodies with infinite extent, at right angles to the sections taken across them, also give symmetrical curves. The formulae by which theoretical cases of this kind can be calculated have also been presented.

It is of note that dip in the assumed tabular or magnet-like body expresses itself, in part, by lack of symmetry. This is illustrated in Figure 81. Other effects of dip will be treated in another section.

Calculation and construction of these curves are useful tools in interpretation. This procedure is valid only to the extent that the geologic conditions or the shape of the magnetic ore body permit such simplification.

Magnetic Disturbance Vectors.—Where both vertical and horizontal intensity measurements have been taken along a traverse crossing a magnetic feature which can be treated as a pole, it is possible to plot the disturbance

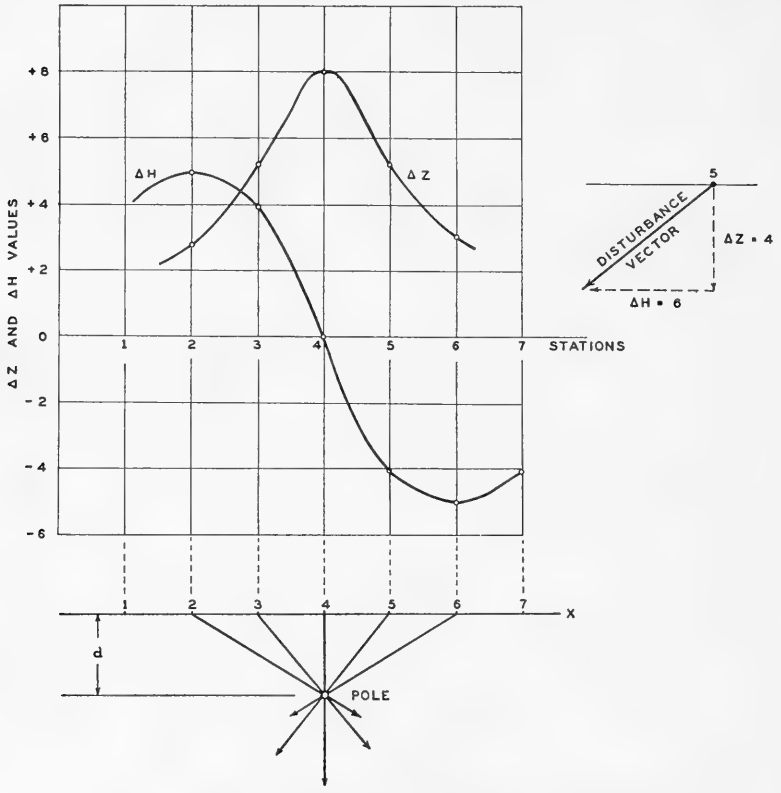

Fig. 101.—Magnetic disturbance vectors for pole depth determination.

vectors. The procedure is as follows: After subtracting the local average of Z and of H from the field observations, the curves of ΔZ and ΔH are plotted in a graph, the spacing of the stations being shown to proper scale, as abscissae. (See Figure 101.) On a line parallel to and below the line of abscissae the stations are plotted.

At a station on the lower x axis of the figure, the amount of ΔZ for that station is plotted downward, using some convenient scale. The amount of the ΔH for the station is plotted at the same scale, to the left if the ΔH is negative and to the right where the ΔH value is positive. The ΔH is plotted,

to express it more specifically, toward the pole. The resultant of the ΔZ and the ΔH forms the disturbance vector. See separate plot for station 5 of the figure.

An example of the application of this procedure is given in Figure 77, a traverse at the Falconbridge pyrrhotite deposit, in the Sudbury Basin of Ontario, Canada.

Depth Finding by Magnetic Triangulation.—N. H. Stearn presents a somewhat different solution for finding the depth to a magnetic pole. The procedure is termed *magnetic triangulation*. It is based, like the preceding method, on the use of magnetic vectors, and is particularly well suited to field measurements obtained with the Hotchkiss Superdip magnetometer. Figure 102 illustrates the method.

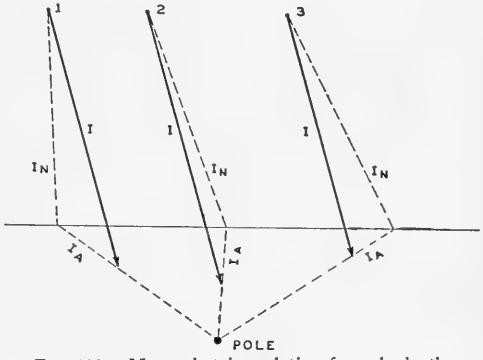

FIG. 102.—Magnetic triangulation for pole depth; Stearn's method.

As is shown in Figure 102, the vector I represents by its *length* the total magnetic intensity at a station as determined with a Superdip instrument. The same vector I represents by the *angle* at which it is plotted the direction of the said total intensity. This vector is resolved into two components: I_N and I_A. Component I_N is the normal or average total intensity for the area as given by its plotted length, and it is plotted at the normal (average) inclination angle for the locality. The average (or normal) would be the amount and the direction of the magnetic intensity for the local area at some distance from the magnetic feature involved.

The vectorial difference of I and I_N is the anomaly vector I_A. The vectors I_A represent the components of abnormality required to produce the resultant magnetic intensity and direction I†. The locus of intersection of the extended components of the anomaly vector I_A for a line of stations locates the position of the anomalous force or pole. The depth to the pole can thus be obtained graphically as shown on Figure 103 for a traverse across a peridotite plug.

The inclination of magnetic force at a series of stations can be obtained using the Superdip instrument as a dip needle. With it the total magnetic force can be measured at the same stations when it is operated as a magnetometer. The depth to the pole in the figure noted is about 500 feet below the top of the peridotite plug as determined by drilling.

These vectors tend to intersect (in a theoretical case) at loci around the pole, the depth of which can be found in terms of the distance scale on the x axis.

† N. H. Stearn, *A.I.M.E. Geophysical Volume*, 1932.

The procedure is useful in approximating the pole depth in cases in which the geological and geophysical situation permits a pole assumption. The pole is, of course, some distance below the top of such an ore body. In a bar magnet, as has been shown, the pole is 1/12 of the magnet length from the end. How far the pole would be below the top of an ore body depends upon many variables, only a few of which can be evaluated.

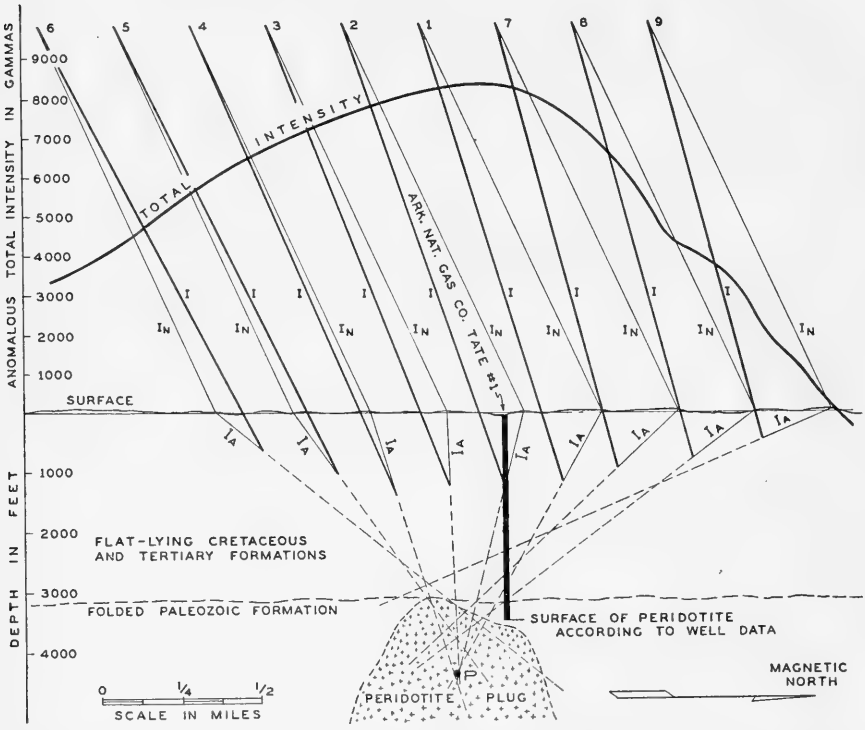

FIG. 103.—Magnetic depth-finding profile and section across a peridotite plug near Rison, Arkansas. I, recorded magnitude and direction of magnetic intensity; I_N, magnitude and direction of normal component of magnetic intensity; I_A, magnitude and direction of anomalous component of magnetic intensity. (After Stearn, *A.I.M.E. Geophysical Volume*, 1932, p. 197.)

To apply the 1/2 and 1/3 maximum rules previously set forth, tests on some vertical intensity profiles were made by Dart Wantland over magnetite concentrations at the A. E. Humphrey placer at Roscoe, Colorado. It was found that they apparently did *not* apply. In this case the depth to bed rock was known. It is inferred from this that the rich magnetite concentrations of this placer did not act geophysically like magnetic poles.

Three Factors Affecting the Symmetry of Anomaly Curves.—Three factors which can be evaluated qualitatively affect the shape of anomaly curves of the vertical and horizontal magnetic intensity, as shown by

traverses across dike-type magnetic bodies. These factors are: (a) the angle of inclination of the earth's magnetic field; (b) the dip of the magnetic body; and (c) the strike of the magnetic body.

The effect of changes in the inclination of the earth's field are shown by three curves after Haalck as given in Figure 97. They picture the cases for three different latitudes. If the spheres shown can be considered as roughly representing the magnetic cores of anticlines, one explanation of the shift of the position on the ground between a magnetic high and a structural high is apparent. Such a shift is often encountered in field exploration. An example of this is found in the Hobbs oil field. (See Figure 104.)

The general effect of dip on the symmetry of magnetic anomaly curves has been considered. In addition it is significant that changes in the dip, or in the strike, of a magnetic tabular body may cause a considerable shift of the point of maximum vertical intensity in relation to the point on the surface directly above the magnetic pole. The magnetic maximum may be moved either north or south of the surface point above the pole, depending on conditions.

Variation in the dip and/or the strike may also bring about differences in the amount of the maximum or the minimum value of horizontal magnetic intensity. In the interpretation of magnetic surveys on ore bodies and dikes for the location of test drill holes, to establish the position of such bodies, these factors must be weighed.

The type case for a fault where rocks of high magnetic susceptibility are brought closer to the surface on the upthrow side is given in Figure 86. The effect of the fault causing an increase in vertical magnetic force where more magnetic material is near the surface is the same as the effect of two formations which are in contact, one being of higher susceptibility. The latter case shows an increase in magnetic intensity for those stations above the high-susceptibility material.

Where the formation boundary or the fault is covered with overburden, it is not possible by study of the anomaly curve alone to distinguish between effects caused by movement along a fault plane and those caused by contact of two different materials. Secondary magnetite developed in and along a fault zone often will produce an appreciable anomaly. However, in a case of this kind the magnetite would give an anomaly curve of the same general kind as a magnetic dike, or a maximum in vertical intensity in the vicinity of the fault, rather than the smooth rise to higher values from left to right shown in Figure 87. These considerations again bring out the necessity of geologic thinking in interpretation.

That disturbance vectors are tangents to magnetic lines of force is illustrated by Figure 104 showing these two quantities.

Magnetic vector studies† have been made of the oil-producing states. The vectors indicate the intensity and the direction in space of the magnetic

† W. P. Jenny, "Magnetic Vector Study of Regional and Local Geologic Structure in Principal Oil States," *Geophysics*, Vol. 3, 1932.

lines of force due to the first 15,000 feet of the subsurface. These studies point out the areas of interest for magnetic surveys, the size of anomalies to be expected, and the area to be covered.

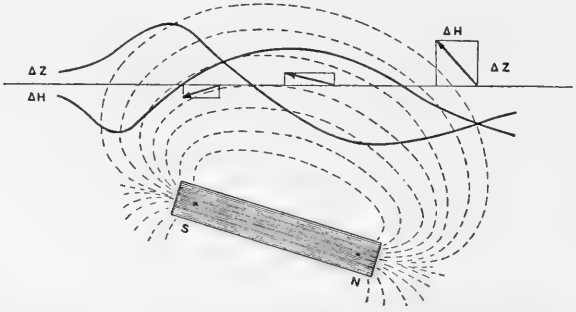

FIG. 104.—Showing the magnetic lines of force and the disturbance vectors based on them for a dipping ore body. The earth's magnetic field is not considered in this figure.

Magnetic Anomalies Associated with the Larger Geological Features

The vertical magnetometer has been widely used in the United States in the search for oil structures. Many anticlinal structures are situated over ridges of buried granite or metamorphic rock; over these structures the metamorphic rocks are nearer to the surface. Such granite and metamorphic basement rocks are usually (though not always) more magnetic than overlying sediments and cause an increase in magnetic intensity.

J. H. Wilson† writes as follows: "In interpreting the results of a magnetic survey in terms of structure, one would want to know that the basement rocks were uniform in character and that the possible producing horizons were conformable to the surface of the basement rocks. If this can be assured or assumed, then the magnetometer can be expected to give a faithful representation of structural conditions in the producing horizons.

"The more unconformities between the basement rocks and the producing horizons, then the less likely are the magnetic results to correspond to the structure of the producing horizons. In practice, one usually makes a survey over a known structure or oil field and compares the results obtained to those obtained in an adjacent area of unknown structure.

"In the absence of information as to character of the basement rocks or results over known structures, one may apply the following criteria to investigate the possible relation of an anomaly to structure:

1. Do the magnetic results indicate a structure of the general type that you would expect from geological considerations of the area?
2. Is the elongation of the magnetic anomaly in the direction of the dominant structural trend of the area?
3. Is the regularity of the isogams (lines of equal intensity) such as to suggest that the forces are derived from considerable depth?"

With a clue to the probable shape of the structure, and an idea of the magnetic properties of the rocks, it is possible to compute the theoretical

† J. H. Wilson, *Mines Magazine*, November, 1928.

anomalies for a series of structures which would give the results obtained from the field measurements, and to select from this series the structure that seemed most likely from the geological standpoint.

W. P. Jenny,† in discussing geological and physical problems in the interpretation of regional and local anomalies, states a simplification that is often valuable: "The geological interpretation of regional and local anomalies is based on the fact that the rocks which constitute the outer crust of the earth vary greatly in their magnetic susceptibility. The average magnetic susceptibility of basic igneous rocks and of some magnetite-bearing crystalline schists is generally assumed to be from 10 to 100 times stronger than the average susceptibility of sedimentary deposits, granites, and the majority of metamorphosed rocks (according to H. Reich, 1930)."

However, it is fundamentally wrong to assume that the magnetic anomalies are almost exclusively due to the igneous rocks. In most oil regions, the igneous or basement rocks are buried at depths ranging from 3,000 to over 20,000 feet. Since the magnetic effect of local structures is about inversely proportional to the square of their depth, any small magnetic variation in the near surface sedimentary rocks may produce anomalies comparable to the larger magnetic effect of the basement rocks.

A discussion of the importance of the sedimentary beds and their magnetic effects has been given by Weiss‡ who writes: "The application of the magnetic method in the Witwatersrand area has met with considerable success, especially in the locating of Post Karoo dykes and in determining the approximate location of the sub-outcrop of three strongly magnetic shale beds in the lower Witwatersrand system: the Water Tower shales, contorted beds, and West Rand Shales. By means of these magnetic key-beds, it is possible to delineate indirectly the zone of the approximate position of the main reef. The above three magnetic markers can be detected even if they are covered with 1,000 to 2,000 feet of younger sediments, and consequently the magnetic method is of great value in prospecting areas where Karoo beds and dolomite rest unconformably on the Witwatersrand system."

A further discussion of the magnetic effects of sedimentary beds has been presented by Lynton,†† who says: "General conditions for the use of magnetic geophysical methods in California are good, as there is marked variation in the magnetic susceptibility of the sedimentary rocks of economic interest. In Tertiary rocks, the magnetic susceptibility varies from 14×10^{-6} in the Sagus of the Upper Pliocene to 412×10^{-6} in the vivianitic sandstone of the McKittrick group of the Pliocene. This variation is sufficient to give a definite magnetic contrast at several horizons. *Magnetic marker beds,* such as this vivianitic sandstone, beds of volcanic tuff, and interbedded basaltic flows, extending throughout considerable areas, have been found, which are sufficiently thick and magnetic to cause anomalies of several hundred gammas at surface exposures and recognizable indications under deeper cover."

Rieber§ brings out that: "Certain strata in the more recent fresh-water deposits of the Tulare Series in the San Joaquin Valley, California, which contain material only slightly more magnetic than the adjacent strata, show sufficient magnetic anomalies in the vicinity of known faults and folds to give promise of extensive usefulness of magnetometer surveys in the exploration for oil."

---

† W. P. Jenny, *The Science of Petroleum,* Vol. 1, Oxford University Press, 1938.

‡ O. Weiss, "The Application and Limitation of Geophysical Prospecting Methods in the Witwatersrand Area", Jnl. Chem., Met. and Min. Society of S. Africa, Vol. 34, pp. 321-361, 1934.

†† F. D. Lynton, "Some Results of Magnetometer Surveys in California," *A.A.P.G. Bull.,* Vol. 15, pp. 1351-1370, 1931.

§ F. Rieber, "A New Micro-Magnetometer," *A.I.M.E. Geophysical Volume,* 1929, pp. 401-415.

To quote again from Jenny§: "The basic ideas prevalent in former years, that the magnetic effect is due almost exclusively to the chemical properties or the tectonic dislocations of the basement rocks underlying the oil areas, has led to many misinterpretations and has in many places discouraged magnetic prospecting, first, because under this assumption the station net was laid out on too wide a scale, and therefore would not permit the location of anomalies due to shallow local influence, and secondly, because the field measurements were not sufficiently accurate. Magnetic anomalies may be produced by lateral variation in the ferruginous content of a sedimentary bed, by lateral differentiations of igneous rocks, by thickening or thinning, or by the normal dip of a certain magnetic horizon. Besides these anomalies of a petrographic or stratigraphic origin, magnetic anomalies may be due to structural features. A magnetic shale bed may be brought closer to the surface on the up-throw side of a fault. Practically, non-magnetic dolomites may be uplifted along an anticlinal axis and thus displace stronger magnetic shales and sandstones. A nephelite syenite plug may intrude into much less magnetic sedimentary beds, or old igneous ridges may be covered by sedimentary deposits of much smaller magnetic susceptibility."

The following simplification is often valid: if the magnetic results in an area are picturing basement topography and the sedimentary members above the basement are conformable thereto, magnetic highs and lows should correspond with structural highs and lows. (See Figure 105A.) If, on the

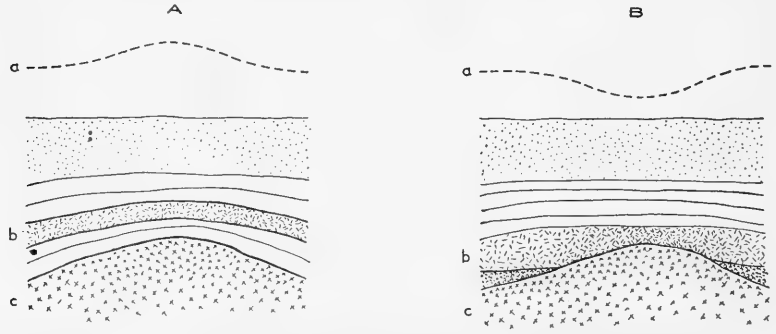

FIG. 105.—*A* shows magnetic high (a) over a magnetic sediment (b) lying conformable to a magnetic basement high (c). *B* shows magnetic low (a) over a magnetic sediment (b), thinning over a basement high (c) of low magnetic effect.

other hand, the basement is relatively non-magnetic or uniform in its magnetic effects, the magnetometer results may show merely the relative thickening or thinning of the overlying sedimentary section, or of the more magnetic members thereof. Magnetic highs then may correspond to structural lows and magnetic lows to structural highs, as shown in Figure 105B.

Oftentimes it is difficult to determine which of these two conditions exists. Previous exploration in a nearby geologically similar area may furnish a clue. Another geophysical method may supply the necessary data. For instance, the area in the immediate region of the magnetic anomaly might be checked with the reflection seismograph to map the structure of the sediments. Another somewhat less certain guide would be to determine

§ W. P. Jenny, *op. cit.*

the magnetic susceptibility of cores, if available, for a well in the area. If highly magnetic sedimentary beds were indicated and the basement was considered to be at great depth, a sedimentary picture would be suggested. A third means, though still less reliable, would be the application of pole depth rules to the magnetic anomaly, to determine whether the depth to the pole would indicate it lay in the basement or in the sedimentary section above. A combination of magnetic and gravity measurements may give a clue to the probable depth of the basement rock.

An example of a magnetic low associated with a known structural high is furnished by the Garber Oil Field, in Garfield County, Oklahoma. The Garber Field lies on the southern extension of the Nemaha granite ridge, which runs approximately north-south across the center of the state of Kansas and into Oklahoma. Drilling at Garber indicates a relatively thin section of the Arbuckle limestone (1,250 feet) on top of the pre-Cambrian granite of the ridge. The Arbuckle is practically non-magnetic, and has been lifted about 2000 feet in this anticline. In this general area it is normally overlain by up to 6000 feet of highly ferruginous shales and sandstones.

The magnetic low shown at the Garber field could be explained on the assumption that the granite, which is relatively non-magnetic, protrudes through strongly magnetic sediments and possibly some schists, which have thus been cut out.†

The Hobbs Oil Field, of Lea County in southeastern New Mexico, is a case in which there was fair agreement between a magnetic high and a structural high. (See Figure 105.)

The field was originally discovered as the result of magnetic work in 1926, and checked by a traverse of torsion balance stations. The discovery well (1928) was located in the center of the magnetic high, which fortunately was sufficiently "on structure" to give a small producer.‡ Figure 106 shows the magnetic contours and the final structure contours based on well logs obtained as the field was developed.§ In this case there is a shift of about 8,000 feet between the center of the structural high and the center of the magnetic high produced presumably by the basement rock. The field includes approximately 6,000 acres and 143 producing wells. Two oil producing zones exist: the Bowers sand at a depth of 3,170 to 3,225 feet; and the white lime, a white or crystalline lime of Permian age occurring at a depth of about 4,000 to 4,200 feet. The sedimentary series has a magnetic permeability of approximately one, and the basement granite has a relatively high magnetic permeability. The topography is flat, and the surface has a southeast slope of about 10 feet to the mile. The surface formation is caliche, and there are no outcrops.

† D. Wantland, "Magnetic Interpretation," *Geophysics*, Vol. 9, No. 1, Jan., 1944, pp. 47-59.

‡ C. B. Carpenter and H. B. Hill, "Petroleum Engineering Report, Big Spring and Other Fields in West Texas and Southeastern New Mexico," *Dept. of Interior, R.I. 3316*, Nov., 1936.

§ A somewhat similar figure is shown in a pamphlet entitled "Mapping Geological Structure with the Magnetometric Methods," published by William M. Barrett, Inc., Shreveport, Louisiana.

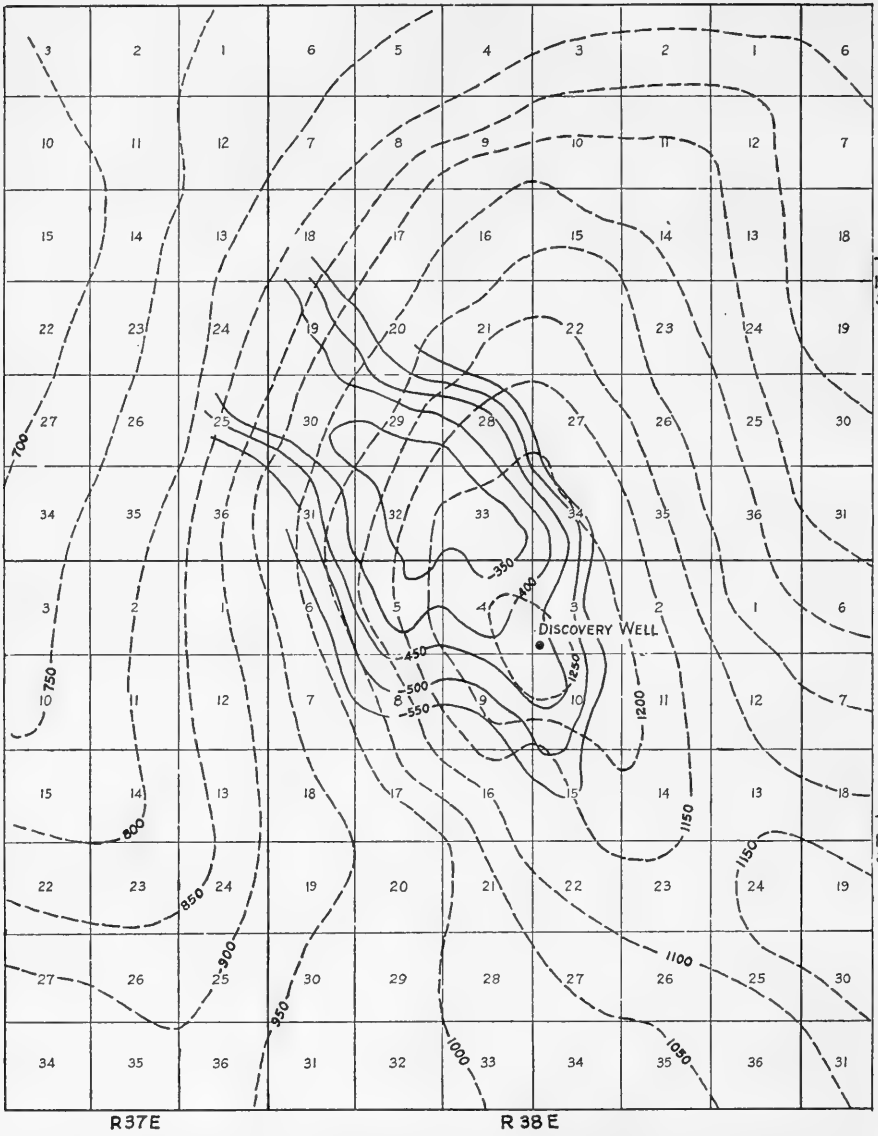

FIG. 106.—Magnetic contours and structure contours of Hobbs' Oil Field, Lea County, New Mexico. Structural contours (solid lines) after R. S. Christie, *A.I.M.E. Petroleum Tech.* 1932; magnetic contours (dotted lines) after H. T. Morley, Stanolind Oil and Gas Company.

The basement is vaguely assumed to lie at a depth of about 10,000 feet. The field is indicated magnetically by a pronounced maximum in the southwesterly part and a pronounced minimum in the northwesterly portion of the area surveyed. The high point of the producing structure is shifted about

1½ miles northwest of the magnetic high, making it apparent that the magnetometer was not faithfully recording the sedimentary structural high.

Geophysical afterthought strongly suggests that the magnetic high is due to induced polarity in a deep (basement) anticlinal ridge which lies below the producing structure. The small structural relief (about 250 feet) and the uplift of the shallower sedimentary beds probably do not enter into the magnetic picture. It is of interest that the geophysical exploration described led to the discovery of this important oil field.

The magnetic survey of the Nocona field, in northern Montague County, Texas, is another example of the application of the magnetometer in locating oil structure by mapping basement topography. The magnetic closure is small, about 30 to 50 gammas, and the magnetic high is shifted with respect to the structural high. The northern extension of the field was developed, however, as a result of a magnetic survey.†

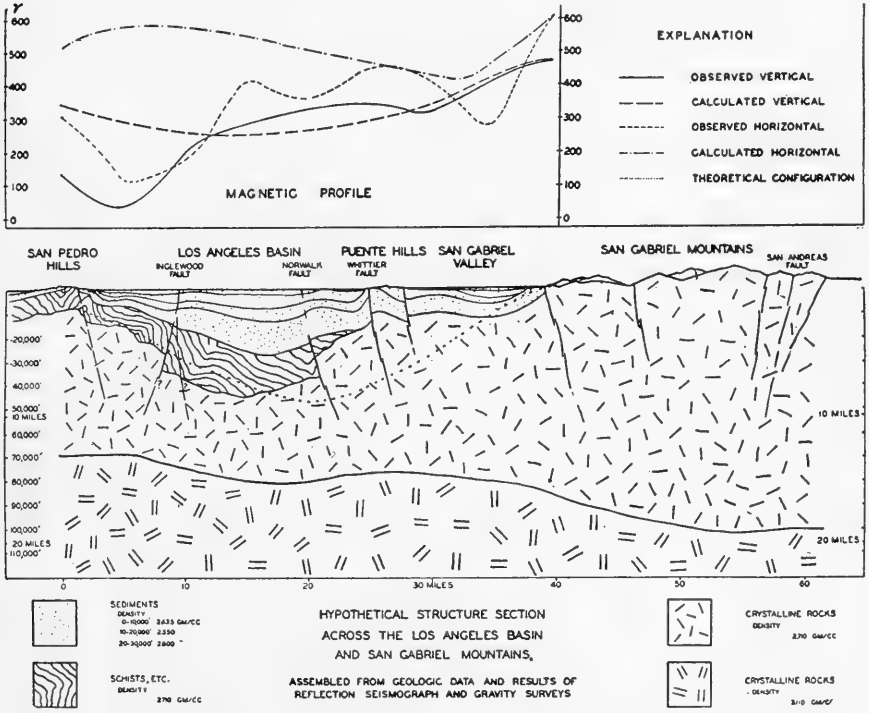

FIG. 107.—Illustration of regional survey in the Los Angeles Basin. (After Uhrig and Schafer, *Gerland's Beiträge zur Geophysik.*)

Regional Surveys.—Magnetic investigations of a deep-seated regional structure usually necessitate a careful interpretation based on comparisons of the observed and calculated (theoretical) values of the vertical and horizontal components along traverse lines. Figure 107 shows an in-

† C. A. Heiland, *Geophysical Exploration*, p. 429, Prentice-Hall, Inc.

vestigation of this type across the Los Angeles Basin.† This basin is a broad syncline with an axial trend northwest to southeast and is about 75 miles long and 25 miles wide. The geologic section shown in the figure is based on geologic, drill, seismic, and gravity data. It is predicted that this structural basin reaches a depth of over 40,000 feet at its deepest point. The granitic basement rocks are overlain by about 15,000 feet of schists and other non-crystalline metamorphic rocks, which are probably of Franciscan age. Overlying the metamorphosed rocks is a section of about 25,000 feet of soft sandstones and shales of marine origin, chiefly of Tertiary age. Shallow alluvial deposits form the surface covering. High angle faults of considerable displacement trend in a general northwest and southeast direction.

The magnetic investigations were conducted along a 45 mile traverse and comprised: (a) vertical component measurements at intervals of ¼ to ½ mile and (b) horizontal component measurements at intervals of from 3 to 4 miles.

The magnetic work failed to show the positions of the large faults which traverse the basin parallel to its major axis. At the shallower depths, the materials on both sides of the faults have about the same permeability; hence, they show no definite anomalies at their contacts. The computations for the calculated vertical and horizontal components were made by assuming that the contact between the overlying materials and the granite is an inclined smooth surface. The air, sediments, and metamorphics were given a weighted susceptibility of about $40 \cdot 10^{-6}$ c.g.s. units while the granite was assigned a value of $1012 \cdot 10^{-6}$ units.‡ It was assumed also that the field strength was 50,000 gammas and that the direction of the field made an angle of 30° with the vertical. The general agreement between the theoretical calculated configuration and the assumed configuration (as based on drill hole and geologic control, supplemented by seismic and gravity work) is fairly typical of the results which may be expected in a complex problem of this type.

Mapping Contacts by Magnetic Methods.—The contact between two materials of different magnetic permeabilities is readily disclosed by magnetic studies provided their difference in permeability is sufficient to produce a measurable anomaly. An application of magnetic work in contact mapping is shown in Figure 108. The high magnetic permeability of the serpentine gives rise to the large anomaly at the contact between the lime schist and the serpentine at the right end of the traverse and the short abrupt anomaly at the left end of the traverse. Due to the relatively small difference in permeability between the quartz mica schist and the altered zone of garnetized schist, and between the altered zone and the lime schist, there are no appreciable magnetic anomalies or change in trend produced

† L. F. Uhrig and S. Schafer, "Observed and Calculated Values of the Magnetic Intensity over a Major Geologic Structure," *Gerland's Beiträge zur Geophysik*, vol. 49, pp. 129-139, 1937.
‡ J. L. Soske, Unpublished Doctor's Thesis, Calif. Inst. of Tech., Pasadena, California.

at their gradational contacts. The effect of the high permeability of the granite basement rocks is shown by the gradual rise in the magnetic trend starting at about station 118 and extending to the left of the figure.

The profile also shows the magnetic high produced by an intrusive serpentine dike (at the left of the traverse). (Direct location of the dike

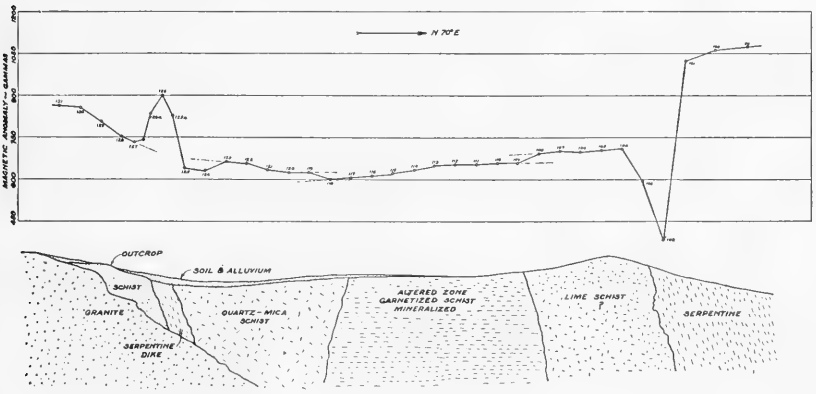

FIG. 108.—Magnetic profile over contacts of lime schist and serpentines.

could not be made by surface geology because of the covering of 50 feet of soil and alluvium fill.)

Magnetic Anomalies Over Steeply Dipping Structures.— In regions containing steeply dipping structures, the crest of the deeper sedimentary structure is usually over the crest of the uplift in the basement rocks. The magnetic anomaly is caused by the high magnetic permeability of the igneous basement rock. The overlying sediments usually have a relatively minor effect on the anomaly.

The peak of the magnetic vertical intensity often is shifted laterally due to the inclination of the earth's field. The amount of shift depends upon many factors, including depth to the basement rocks, relative permeabilities, inclination of the earth's field, etc. This effect is illustrated schematically in Figure 109.

In other cases, the magnetic and the subsurface structural features may be displaced when: (1) the igneous core is not in conformity

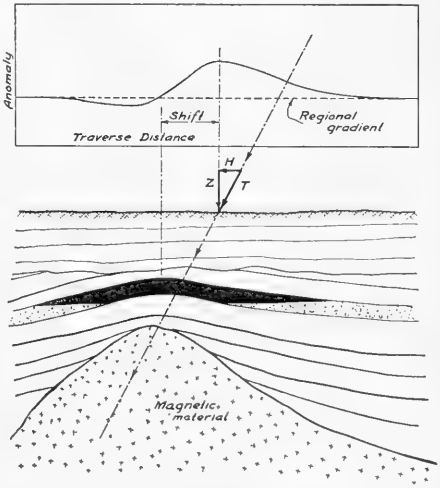

FIG. 109.—Diagram illustrating displacement of the peak of the magnetic anomaly with reference to the crest of the structure.

with the overlying sedimentaries (such as may be caused by differential compaction or distortion of the sedimentaries due to lateral thrust), (2) basement rocks are not of uniform magnetic properties, as may be caused by rocks of different composition or a buried hill of igneous and sedimentary rocks, or (3) the structural axis of the sedimentary structure shifts with depth.

Mapping Faults and Volcanic Formations.—The magnetic method may sometimes be employed to map the locations of faults in the sedimentary rocks. Ordinarily the magnetic location of such faults is contingent upon: (1) concentration of magnetic mineralization along the fault or, (2) displacement by the fault of the subsurface bed or beds which exert the controlling influence on the magnetic field at the surface.

The magnetic effect or anomaly mapped is chiefly a function of the difference in depths to the controlling magnetic beds on adjacent sides of the fault; i.e., the higher magnetic intensity occurs over the upthrow side of the fault. The plan location of the magnetic anomaly with reference to the fault is subject to the same considerations regarding displacement discussed in the preceding example. Ordinarily, however, this displacement is slight, due to the usually moderate depth to the controlling magnetic feature.

An example of magnetic work over an irregularly-shaped laccolithic mass at moderate depth (about 1500 feet) is given by Malamphy.† The results obtained from the magnetic and gravitational studies are shown in Figure 110. The magnetic inclination in this area is only 20° and has a reversed polarity with respect to that existing in the northern hemisphere.

The gravity gradients were calculated by the method described by Barton.‡ The theoretical and observed gravity gradient profiles are substantially in agreement.

The theoretical and observed magnetic profiles do not agree very well. According to Malamphy, the observed and theoretical magnetic and gravity gradient data can all be consistent only if the laccolithic mass possesses "magnetic properties in excess of those that normally would be induced by the earth's magnetic field alone."

The gravitational and magnetic anomalies are due chiefly to the igneous intrusions of the diabase, and to a minor extent, to the crystalline basement rocks.

Magnetic Anomalies Produced by Upper Magnetic Beds of Variable Thickness.—The magnetic anomalies produced by magnetic sedimentary beds or lava flows which overlie a substantially non-magnetic or diamagnetic basement depend on the depth to the contact with the under-

† Mark C. Malamphy, "Geophysical-Geological Study of the Sao Pedro Area, Brazil," *A.I.M.E. Geophysical Prospecting*, Tech. Pub. 696, 1936.

‡ D. C. Barton, "Eötvös Torsion Balance Method of Mapping Geologic Structure," *A.I.M.E. Geophysical Prospecting*, 1929, p. 429.

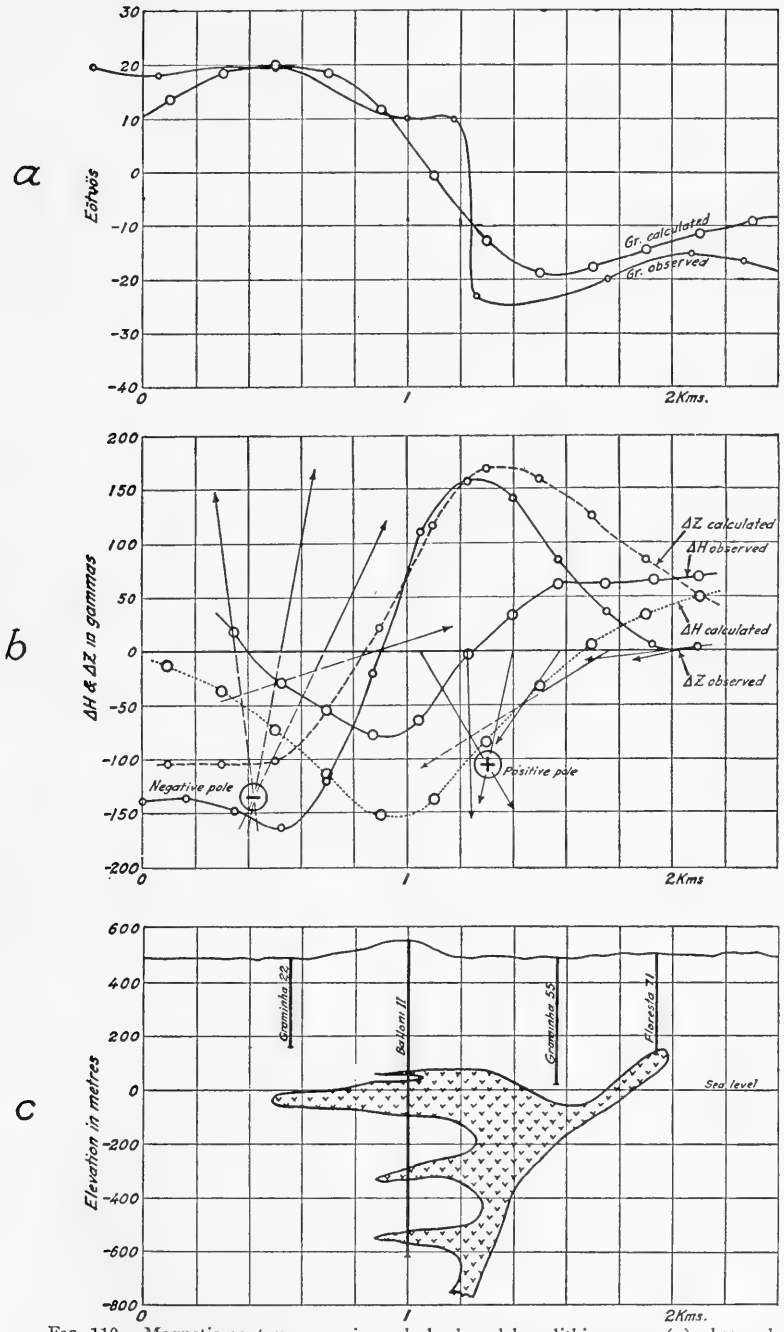

FIG. 110.—Magnetic contours over irregularly-shaped laccolithic mass. (*a*) observed and (*b*) calculated anomalies over intrusive mass of predicted shape shown in (*c*). (Malamphy, *A.I.M.E. Geophysical Prospecting*, Tech. Pub. 696.)

lying rocks. Thus, if the magnetic beds overlie a synclinal or old erosional low feature, a magnetic high will be produced, as illustrated in Figure 111A, due to the greater thickness of the magnetic material over the deeper contact. When the upper magnetic beds overlie a buried hill or other feature of relatively low permeability, as in Figure 111B, a magnetic low will result due to the lesser thickness of magnetic material over the basement high. (A supplemental geophysical method (such as electrical or seismic)

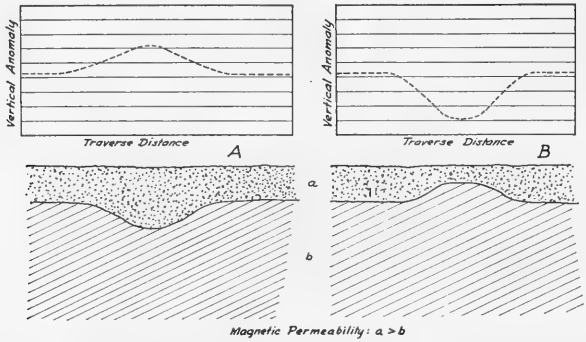

FIG. 111— *A*, magnetic high associated with increased thickness of shallow magnetic beds, and *B*, magnetic low associated with decreased thickness of shallow magnetic beds.

capable of indicating variations of thickness in the upper layer may be employed in problems of this type. Interpretation would then be based upon both types of data.)

Placer Deposits.—In a majority of placers the greatest concentration will be on the bedrock. Occasionally, the best values occur on a false bedrock ("hardpan" or conglomerate) which overlies the bedrock. The placer material is composed chiefly of the magnetic black sands and the other heavier materials, including the gold values. The magnetometer may be employed to locate the areas of magnetic high, which will be the zones of concentration of the placer material. Because the gold is found adjacent to the bedrock or false bedrock, it is important to know the depths to the bedrock and the thickness of the fill material. This may be accomplished by electrical or shallow refraction seismic methods.

Figure 112 shows a typical cross-section of a placer from a geophysical survey conducted in Trinity County, California. The largest concentration of placer material was indicated by the magnetic high, mapped with a vertical component Askania magnetometer. With the magnetometric method the complete outline of the old stream bed was obtained, together with the thickness of the lower gravels and the overlying clay and sand fill. With this information the necessary depth of test pits and drill holes was easily determined, and test locations recommended.

Another simple magnetic survey is illustrated by the contour results of a survey of a placer property in Pinal County, Arizona.† (Figure 113.) The general regional

† J. J. Jakosky and C. H. Wilson, "Geophysical Studies in Placer and Water-Supply Problems," *A.I.M.E. Geophysical Prospecting*, Tech. Pub. 515, 1933.

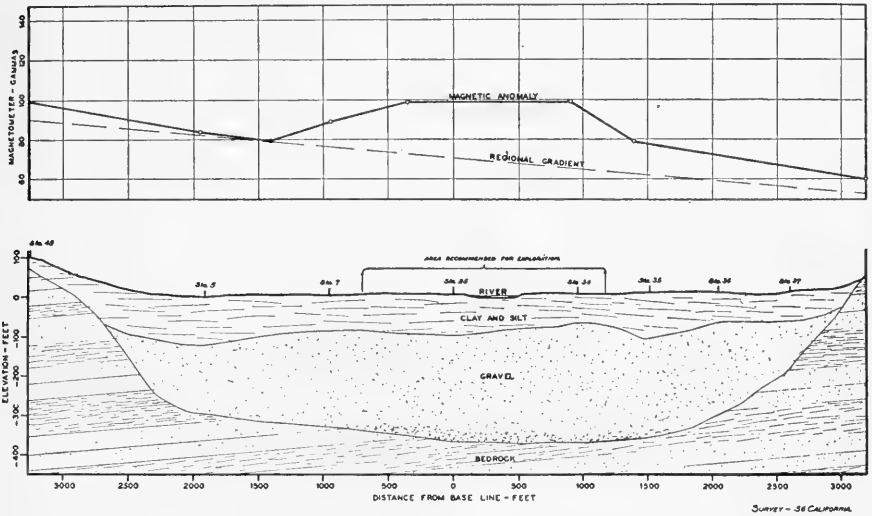

FIG. 112.—Magnetic traverse across a simple placer concentration in an old stream bed, in Trinity County, California. (Jakosky, *Arizona Mining Journal*, Aug. 1931.)

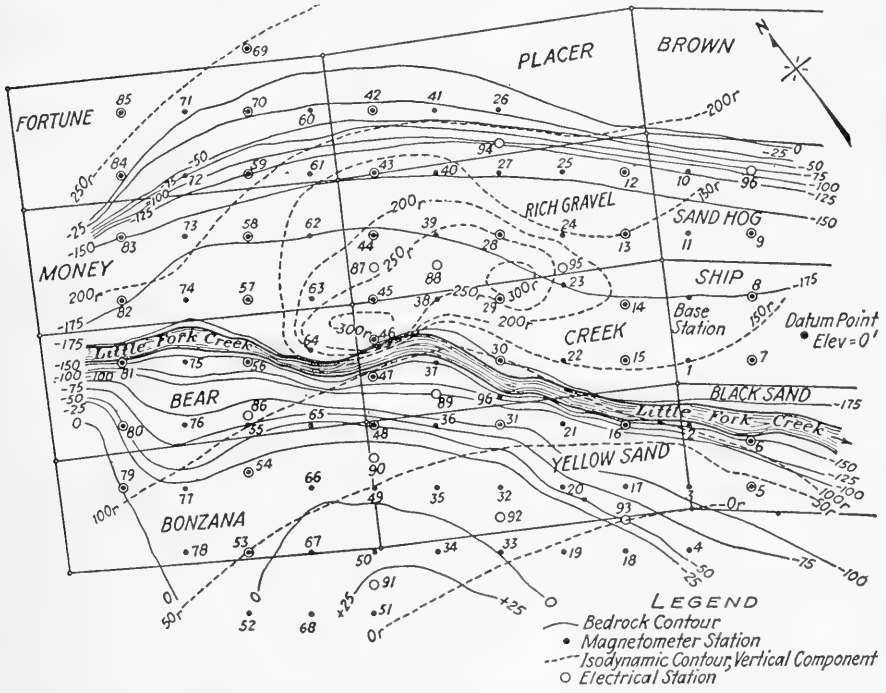

FIG. 113.—Magnetic and geological contours on a gold placer property in Pinal County, Arizona. (Magnetic contours dotted curves and geoelectrical bedrock contours solid curves.) (Jakosky and Wilson, *A.I.M.E. Geophysical Prospecting*, Tech. Pub. 515.)

gradient extended in a northwest-southeast direction. The concentration of placer materials is well shown by the magnetic highs.* The magnetic conditions in this particular area are almost ideal for application and interpretation of magnetometer studies.

A magnetic survey was carried out at the Roscoe Placer of the Humphreys Gold Corporation, on Clear Creek, Jefferson County, Colorado.† The rather tortuous course of the deepest portion of the old stream channel was traced by magnetic mapping of the concentrations of black sand, which carried the best gold values. It was found that magnetic lows were associated with areas of shallow bed rock or local bed rock ridges. The results of the magnetic work and resistivity determinations for bed rock depth were critically tested as bed rock was exposed in the course of operations.

H. R. Joesting‡ describes results of a number of magnetic and resistivity surveys on placer deposits in Alaska (1939-1940). When supported by geologic and mineral-

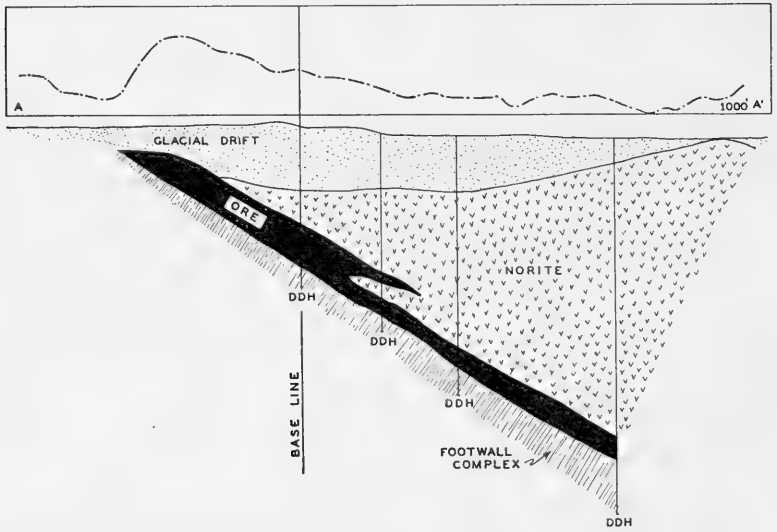

FIG. 114.—Geological cross section AA' with magnetic profile. (After Galbraith, *A.I.M.E. Geophysics Volume 164*, 1945.)

ogical data, the magnetic method was valuable in preliminary prospecting for about half of the gold placers in the interior of Alaska. Magnetic work was most useful where the placer ground contained appreciable amounts of magnetite concentrated in pay streaks. It was of no value where the placers carried little or no magnetite, as would be expected, or where large bed rock anomalies were present. While the magnetic method did not permit an evaluation of placer ground in all cases, it often obviated much costly drilling and shaft sinking in barren areas. The depth and areal distribution of permanently frozen ground and of thawed unconsolidated deposits were determined successfully by the direct current resistivity method, as part of the program of investigation.

* In the application of magnetic measurements to placer gold location, the interpretation must be made from the viewpoint that the magnetic methods are not locating the gold itself, but only the placer magnetic materials with which the gold is associated.

† D. Wantland, "A Comparison of Geophysical Surveys and the Results of Operations at the Roscoe Placer of the Humphreys Gold Corporation, Jefferson County, Colo.", *Colorado School of Mines Quarterly*, Vol. 32, No. 1, Jan., 1937, pp. 87-115.

‡ H. R. Joesting, "Magnetometer and Direct Current Resistivity Studies in Alaska", *A.I.M.E. Tech. Paper 1284*, Feb., 1941.

Another example of a regional magnetic survey was the work which led to the westward extension of the Rand† in South Africa. Vertical component magnetometers were used to map the sub-outcrop of a metamorphosed ferruginous shale formation buried under approximately 2,000 feet of unconformable dolomite. The buried formation was comprised of quartzites, slates, shales, some volcanics, and the gold-bearing conglomerates. The slates are magnetic, and their stratigraphic relation to the main gold-bearing reef is well established. Mapping the magnetic anomaly associated with the slate, therefore, served to locate the desired reef which carries the gold values. As a result of this work, it is estimated that the potential gold reserves of the Rand have been increased about 15 per cent.

A further example of regional magnetic work was that conducted by the International and the Falconbridge Nickel Companies in the Sudbury District, Ontario, Canada.‡ (Figure 114.) The ore is massive nickel and copper sulphides, with sufficient pyrrhotite to make it magnetic. The surface covering is chiefly glacial outwash, at depths varying from 50 to 300 feet. After completion of the reconnaissance work, electrical methods were used to check the magnetic anomalies, where detailed work was deemed advisable. The subsequent exploration results have established the success of this type of exploration technique as applied to that area.

Ilmenite, Pyrrhotite and Nickel Ore Deposits.—Ilmenite deposits have been located by magnetic methods by Gillson†† and Keys.§ Also, certain nickel-ore bodies which contain pyrrhotite have been located by magnetic investigations.‡‡

THE MOBILE MAGNETOMETER

The airborne or mobile magnetometer is the most recent development in magnetic measuring instruments applicable to prospecting.§§ The term may be applied in a general way to two types of surveying procedures. In one, the measurements are made at an elevation above ground sufficient to minimize the local surface effects and to emphasize the broader regional features. Work of this type is usually done from high-speed airplanes flying at elevations of from 500 to 5,000 feet. In the second type of survey,

† H. Krahmann, "Magnetometer Observations on the West Rand", *Journal, Chemical, Metallurgical, and Mining Society of South Africa,* March, 1936.

‡ F. Galbraith, "The Magnetometer as a Geological Instrument at Sudbury", *A.I.M.E. Geophysics Volume 164,* 1945, pp. 98-106.

†† J. L. Gillson, "Genesis of the Ilmenite Deposits of St. Urbain County, Charlevoix, Quebec," *Economic Geology,* Vol. 27, Sept.-Oct. 1932, pp. 554-577.

§ F. W. Lee, "Results of Some Magnetic Measurements on Dikes . . . in the Sudbury Dist. Ontario, Canada," U. S. Bureau of Mines, Tech. Paper No. 510, 1932.

‡‡ Lee, *loc. cit.*

L. B. Slichter, "Certain Aspects of Mag. Surveying," *A.I.M.E. Geophysical Prospecting,* 1929, pp. 238-260.

§§ M. Grotewahl, "Bericht über die Versuchsfahrt des Bidlingsmaier'schen Doppelkompasses mit dem Luftschiff *Graf Zeppelin," Terrestrial Magnetism and Atmospheric Electricity,* Vol. 35, pp. 226-229 (1930).

C. A. Heiland, "Geophysical mapping from the air: its possibilities and advantages", *Engineering and Mining Journal,* Vol. 136, pp. 609-610 (1935).

K. Ramsayer, "Die Anderung magnetischer Störgebiete mit der Höhe und ihr Einfluss auf die Flugnavigation", *Beiträge zur angewandten Geophysik,* Vol. 9, pp. 65-97, (1941).

E. A. Eckhardt, "Airborne Magnetometer", *Petróleo Interamericano,* Vol. 4, No. 8, pp. 52-58, August, 1946.

E. A. Eckhardt, "Airborne magnetometer: new geophysical tool overcomes jungle, mountains, swamps, desert, and water", *Oil and Gas Journal,* Vol. 45, No. 5, pp. 78-79, 91-92, June 8, 1946.

A. A. Logachev, "The development and applications of airborne magnetometers in the U. S. S. R.", *Geophysics,* Vol. 11, pp. 135-147 (1946). Also in *Petroleum Engineer,* Vol. 17, No. 10, July 1, 1946.

Homer Jensen, "Flying magnetometer: tool of aerial exploration", *World Petroleum,* Vol. 19, No. 3, pp. 84-87, March, 1948.

the measurements are made at lower elevations to give more emphasis to the local features, which are superimposed on the deeper-lying regional effects. Work of this type usually is done from automobile, motorship, or helicopter. Each type of survey fulfills a need and serves a useful purpose in the exploration picture.

The stationary-type magnetometer was one of the first instruments used in exploration geophysics. It has remained unchanged in basic principle for nearly two decades. Various research projects have been devoted to the development of an improved mobile-type magnetometer, and many instruments have been proposed. The most successful is the "flux-gate" type which operates due to the sensitivity of saturated core devices to superposed or ambient magnetic fields. These magnetic sensitive devices have no moving parts and hence are inherently independent of the disturbances caused by acceleration. They are therefore ideal for mobile operation. The development of the high permeability core materials has made possible the high sensitivity of the flux-gate type instruments. For use on the ground, it has few advantages over the conventional magnetometer.

The magnetization curve of many ferromagnetic materials is non-linear (Figure 72), and coils having such iron cores change their effective alternating current reactance when a unidirectional magnetic field is impressed on the field set up by an alternating current flowing in the coil. This change in effective reactance also results in a distortion of the alternating current wave form. For ordinary iron core materials, the unidirectional field must be quite intense, but for certain high-permeability alloys, the earth's field is of sufficient intensity (.6 gauss) to induce a magnetization which is an appreciable part of the total saturation. A coil with such a core will be sensitive to small changes in field intensity and becomes the heart of a flux-gate magnetometer by operating the core in the saturation region at the sharp knee in the B-H curve.

Schematically,† as may be seen by referring to Figure 115, the sensing element has a magnetic core that comprises essentially two thin strips of Mumetal, a high-permeability alloy, wound with identical windings through which an alternating sine wave exciting current is passed. This exciting current is indicated at A and A'. The two strips of Mumetal are joined together at each end to make a closed magnetic circuit. The two windings are connected so as to make the alternating fields additive around the closed core circuit. However, an external ambient field applied along the axis of the core aids the exciting field in one strip and opposes the field in the other strip. During the period that the ambient and the exciting fields are additive, the total flux is increased and the saturation point is

---

† James R. Balsley, Jr., "The airborne magnetometer", U. S. Department of the Interior, *Geophysical Investigations, Preliminary Report 3*, 1946.
Gary Muffly, "The airborne magnetometer", *Geophysics*, Vol. 11, pp. 321-334, 1946.
E. P. Felch, W. J. Means, T. Slonczewski, L. G. Parratt, L. H. Rumbaugh, and A. J. Tickner, "Airborne magnetometers", *Electrical Engineering*, Vol. 66, pp. 680-685, 1947.
John E. Quaile, "Airborne submarine detector equipment", *Military Engineer*, Vol. 39, No. 258, pp. 166-167, April, 1947.

reached earlier in the excitation cycle. During the period that the ambient field opposes the excitation flux, the total flux is decreased and saturation is reached at a later period in the excitation cycle. The difference in time between the maximum fields in each strip creates a phase lag and distortion of the wave shape. This unbalance creates a small resultant peak voltage, as shown by the wave shapes at *B*. The magnitude of these induced pulses is fairly proportional to the impressed ambient field.

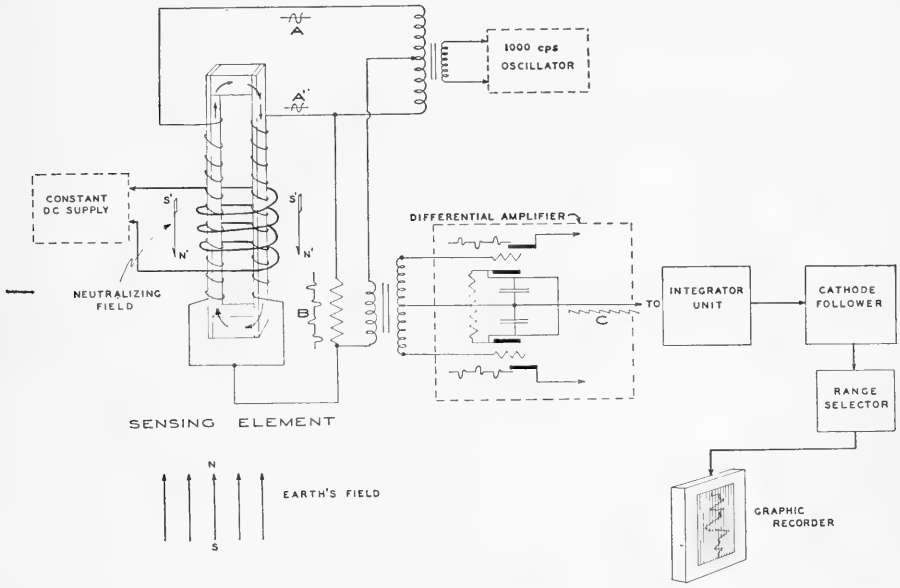

FIG. 115.—Schematic diagram of airborne magnetometer.

The pulses are applied to a differential amplifier which is equipped with a filter network for eliminating undesirable harmonics and background noise. The output from the differential amplifier is composed of unidirectional pulses as indicated at *C*. These pulses are applied to the input of an infinite impedance detector in the integrator unit. In the integrator unit the series of short unidirectional pulses are converted into a direct current voltage which is proportional to the energy content of the individual pulses. Thus a relatively pure direct current voltage is derived from the integrator unit and is in turn applied to the input of a cathode follower unit. This unit activates the DC graphic recorder which furnishes the data desired as a continuous record of the magnetic field intensity acting on the detector unit.

Around and coaxial with the core is a secondary winding, which in effect serves as a Helmholtz coil arrangement. Any desired portion of the ambient field acting on the core may be neutralized, and the flux regulated to allow operation at the desired magnetic saturation of the core. This

neutralizing current is supplied from a storage battery, through a constant impedance network, to maintain the current at a constant value. The polarity of this neutralizing field is opposite to the ambient field, as indicated by the arrows S′N′.

The recorder is provided with a range switch, with suitable steps, whereby full scale reading may cover values from a few hundred to many thousand gammas, with a readable sensitivity of better than 1 to a few gammas, depending on the scale range.

The magnetometer may be calibrated by using a Helmholtz coil to set up a magnetic field of specific intensity around the detector unit. Every range scale of the instrument may be calibrated in this way.

Orientation

The flux-gate magnetometer must be maintained at a constant average orientation throughout a series of readings, so as not to introduce undesirable variations by changes in any component of the earth's magnetic field. Gyroscopic orientation alone has been utilized in some instruments, but does not possess the necessary accuracy in orientation. The most successful form of orientation involves some type of servo-control, sometimes working in conjunction with gyroscopic control, whereby the magnetometer is maintained in proper orientation by means of a pair of auxiliary elements similar in type to the magnetometer itself.† Two of such elements mounted at right angles to each other define a plane. When the plane of the two elements is parallel to the magnetic horizon, a zero field is impressed and a zero control signal exists. With the magnetometer mounted normal to the plane of the two control elements, it is oriented parallel to the field and will give an accurate measurement. When the plane is tilted and departs from its correct alignment, the actuating current to the servo-motors is proportional to the sine of the angle of misalignment. The element may be rotated about either axis of the gimbal by one of the servo-motors, each of which is supplied with an actuating current of proper sense to restore that detector element into parallelism with the magnetic horizon. Two amplifiers and their controlling magnetic elements are required.

The sensitivity of an airborne magnetometer depends on the inherent sensitivity of the measuring device when used on a perfectly stable platform and also very much on the magnetic noise level. This arises in part from the lack of perfection in the stability of the platform and from the fixed and variable effects arising from the permanent and induced magnetization of the aircraft itself. Under the most favorable conditions of use, the flux-gate type instrument affords a sensitivity of better than one gamma and on the average the data are reliable to one or two gammas. This sensitivity is better than that available with any type of instrument commonly used for prospecting on the ground.

† R. D. Wyckoff, "The Gulf airborne magnetometer," *Geophysics,* Vol. 13, pp. 182-208, 1948. Victor Vacquier, R. F. Simons, and A. W. Hull, "A magnetic airborne detector employing magnetically controlled gyroscopic stabilization," *Review of Scientific Instruments,* Vol. 18, pp. 483-487, 1947.

In one type of instrument measuring the vertical component of the total intensity, the "sensing element" is mounted so that its axis of sensitivity lies normally in the vertical plane. The sensing element is kept vertical by a gyroscope which in turn is stabilized in order to minimize errors normally caused by the precession of the gyro. With the vertical orientation, the greatest error per unit of deviation from the vertical occurs when the deviation takes place along the magnetic meridian and the minimum error when the deviation is normal to the plane of the magnetic meridian.

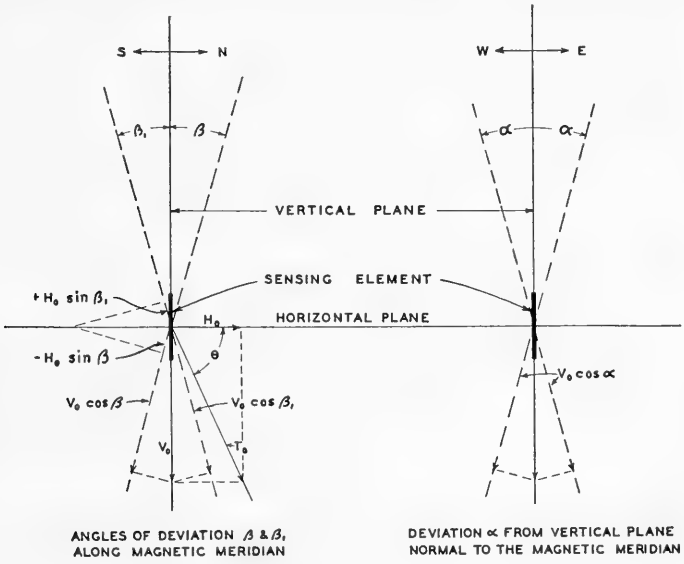

FIG. 116.—(a) Angles of deviation β and β_1 along magnetic meridian; (b), deviation α from vertical plane normal to the magnetic meridian. (Courtesy of Hans Lundberg.)

Referring to Figure 116,

Let $\theta =$ Angle of "dip" of total magnetic field intensity vector
$T_0 =$ Total magnetic field intensity vector
$V_0 =$ Vertical component of T_0
$H_0 =$ Horizontal component of T_0
$\beta =$ Deviation of sensing element from the vertical plane along magnetic meridian *North*
$\beta_1 =$ Deviation of sensing element from the vertical plane along magnetic meridian *South*
$\alpha =$ Deviation of sensing element from the vertical plane *normal* to the magnetic meridian.
$V =$ Magnetic field intensity acting on the sensing element
$V_0 = T_0 \sin \theta$
$H_0 = T_0 \cos \theta$
$V = V_0 = T_0 \sin \theta$ when the axis of sensitivity of the sensing element lies in the vertical plane.

For the deviation β:

$$V = V_o \cos \beta - H_o \sin \beta$$

For the deviation β_1:

$$V = V_o \cos \beta_1 + H_o \sin \beta_1$$

For the deviation α: (H_o is perpendicular to the diagram and thus does not enter into V):

$$V = V_o \cos \alpha$$

The % error made in measurement due to the misalignment angle can be represented as

$$\% \text{ error} = \frac{V_o - V}{V_o} \cdot 100$$

The ratio $\frac{V_o - V}{V_n}$: (for $\beta = \beta_1 = \alpha$)

For β:

$$\frac{V_o - V}{V_o} = \frac{V_o (1 - \cos \beta) + H_o \sin \beta}{V_o} = T_o \frac{\sin \theta (1 - \cos \beta) + \cos \theta \sin \beta}{T_o \sin \theta}$$

$$= (1 - \cos \beta) + \cot \theta \sin \beta$$

For β_1:

$$\frac{V_o - V}{V_o} = \frac{V_o (1 - \cos \beta) - H_o \sin \beta}{V_o} = (1 - \cos \beta) - \cot \theta \sin \beta$$

For α:

$$\frac{V_o - V}{V_o} = \frac{V_o (1 - \cos \beta)}{V_o} = (1 - \cos \beta)$$

For very small angle β, cos β is very nearly 1 and sin β is very small. However, as a table of functions will show, cos β is much closer to 1 than sin β is to zero.

A good approximation, then, for % error in the three cases is:

For β: % error $\cong$ (cot θ sin β) · 100

For β_1: % error $\cong -$ (cot θ sin β) · 100

For α: % error $\cong 0$

We see, then, that the greatest misalignment error arises from the introduction of a component H_o along the axis of sensitivity. In the case of East-West misalignment (Figure 116), H_o acts normal to the plane of misalignment and does not become a factor. Thus the minimum error is for condition *(b.)* of Figure 116.

It may be further noted that, by compensating for H_0 by superimposing a magnetic field of a predetermined attitude at the location of the sensing element, the term $H_0 \sin \beta$ would be reduced to a minimum, thus improving the apparent response of the detecting unit as well as the reliability.

It is now apparent that there is excellent reason for designing airborne magnetometers to measure the total intensity.

Referring to Figure 116, the sensing element in this case is oriented differently—such that its axis lies in the direction of the total intensity T_0. For case *(a)* or *(b)*, i.e., misalignment β in any direction from the vertical plane, the magnetic field intensity T acting on the sensing element is

$$T = T_0 \cos \beta$$

$\therefore$ the % error due to a misalignment β in any direction is

$$\% \text{ error} = \frac{T_0 - T}{T_0} \cdot 100 = (1 - \cos \beta) \cdot 100$$

Thus the error from misalignment in any direction of the instrument oriented along T_0 is the same as the minimum error (special case of E-W misalignment) for the vertically oriented instrument. For example, a misalignment of one degree causes an error of

$$(1 - \cos 1^\circ) \cdot 100 < 0.015\%.$$

This property is unique with respect to the direction of the total intensity, and since the measuring element will be unavoidably deflected through small angles of arbitrary orientation as a result of the motion of the aircraft, the alignment along the total intensity vector is the most favorable one possible.

Airplane Operations

Magnetometer operations with high speed aircraft unavoidably involve both substantial investments and high operating costs. It is only the low unit cost (cost per magnetometer profile mile) which makes this kind of large scale operation economical. The economy rapidly vanishes with decreasing size of the areas to be surveyed or when much idle time intervenes between surveys. It is therefore likely that mining and oil companies will conduct airborne magnetometer operations only if they have large areas to be surveyed.†

† Alvin W. Knoerr, "The airborne magnetometer: a new aid to geophysics", *Engineering and Mining Journal*, Vol. 147, No. 6, pp. 70-75, June, 1946.

Gordon B. Nicholson, "Airborne magnetometer expedites geophysical surveys", *Oil Weekly*, Vol. 122, No. 1, pp. 29-32, June 3, 1946.

"Seven groups to search Bahamas for petroleum", *World Petroleum*, Vol. 17, No. 11, pp. 44-46, Oct., 1946.

Ray L. Dudley, "Flying magnetometer completing 80,000-square mile survey", *World Oil*, Vol. 127, No. 7, pp. 247-251, Nov., 1947.

Warren W. Burns, "Modern exploratory tools being used in five-company Bahama oil search", *Oil and Gas Jnl.*, Vol. 46, No. 27, pp. 38-42, 129, Nov. 8, 1947.

James Affleck, "Aeromagnetometer profile flown from Venezuela to Texas", *World Oil*, Vol. 128, No. 3, pp. 223-224, 227-228, July, 1948.

Sylvain Pirson and Lloyal O. Bacon, "Airborne magnetometer survey in Central Pennsylvania", *Penn. State College Bull.*, Vol. 42, No. 10, March 5, 1948.

The measuring elements have been mounted in blisters on the wing tips, in a special tail extension referred to as a *stinger,* or in a bomb-like structure, called a *bird,* which is trailed beneath and behind the aircraft at the end of a cable (Figure 117). In all cases the purpose is to get the measuring element as far as possible from the disturbing magnetic masses (chiefly engines) of the aircraft. No plane is available in which the full inherent sensitivity of the instrument can be realized from an installation

(Courtesy of Gulf Research and Development Co.)

FIG. 117.—Magnetometer bird, trailing airplane.

in the plane itself, and in only very few types will the result be satisfactory after elaborate means have been provided for compensating both the fixed and variable magnetization of the aircraft structure. The navigation equipment and the magnetometer electronic controls and amplifiers, together with the recorder, are mounted in the passenger compartment (Figure 118). The equipment is usually installed in line with the wings to give better stability for operator comfort.

A continuous record is obtained of the magnetic intensity along the flight path of the airplane. To make this record usable, the position of the plane, that is, vertical projection on ground and elevation above ground, must be accurately known for each point on the magnetometer graph. The elevation may be obtained by use of a radio altimeter and may be continuously recorded on a photographic film. In some cases where contact flying may be employed, the position is obtained by photographing the ground beneath, using a slit camera in which the speed of a continuous film is so synchronized that the image and film are instantaneously relatively

stationary. The magnetometer, altimeter and ground photographs are marked periodically with fiducials to indicate corresponding points on the records. The strip photographs are compared to photo-mosaics of the area flown and the flight path is transferred from the flight strip photographs to the mosaic.

The photographic method of positioning is not usable over water, desert or other areas of featureless terrain. In such cases radio methods which

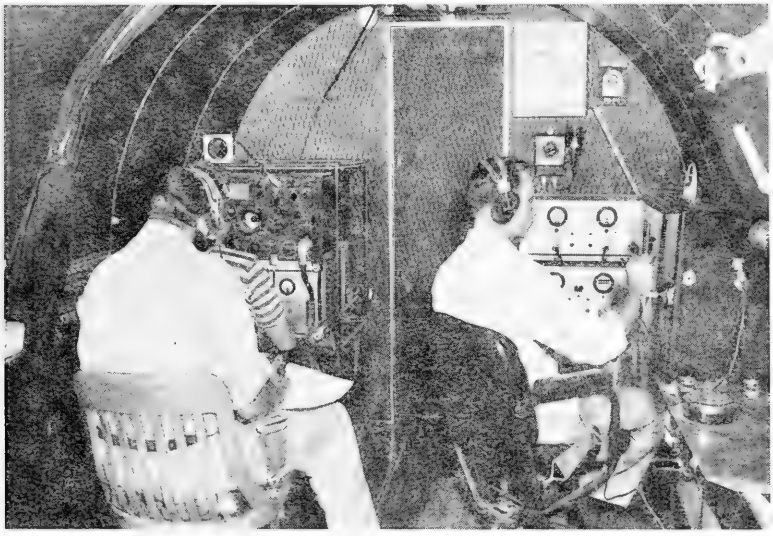

FIG. 118. — Magnetometer installation in DC-3 plane. (Left) — Shoran navigation equipment. (Right)—magnetometer electronics and continuous recorder. (Courtesy of Gulf Research and Development Company.)

involve the measurement of distances of the plane from two or more fixed ground stations are used. What is measured is essentially the transit time of a radio-pulse from the aircraft to a ground station and back to the plane. In determining distance in this way, the instrument time-lags must be taken into account. One radio system of this kind is known as Shoran. In this system the Shoran dials are photographed, which provides the position information when properly correlated with the magnetometer and altimeter records.

The Shoran method can often be used advantageously for position determination in areas in which the photographic method is perfectly feasible. Exceptions are where the flying is done at low levels, in which case the distance range of Shoran would be too limited, and in cases where suitable sites for ground Shoran stations are not accessible.

It is quite obvious that, to take full advantage of the magnetometer record, the corresponding positions must be quite accurately known. In

general, the determining of position with sufficient accuracy is more difficult than obtaining a satisfactory magnetometer record.†

When the photographic method of position determination is used, a base map is made from the photo-mosaic to which the position and magnetic data are readily transferred. The map may then be contoured and will show the distribution of the total magnetic intensity at the flight level above ground, projected onto the ground.

When the radio method of positioning is used, air photographs, though still useful, are not required. The map may then be prepared to a suitable scale and all points will be defined with respect to the positions of the

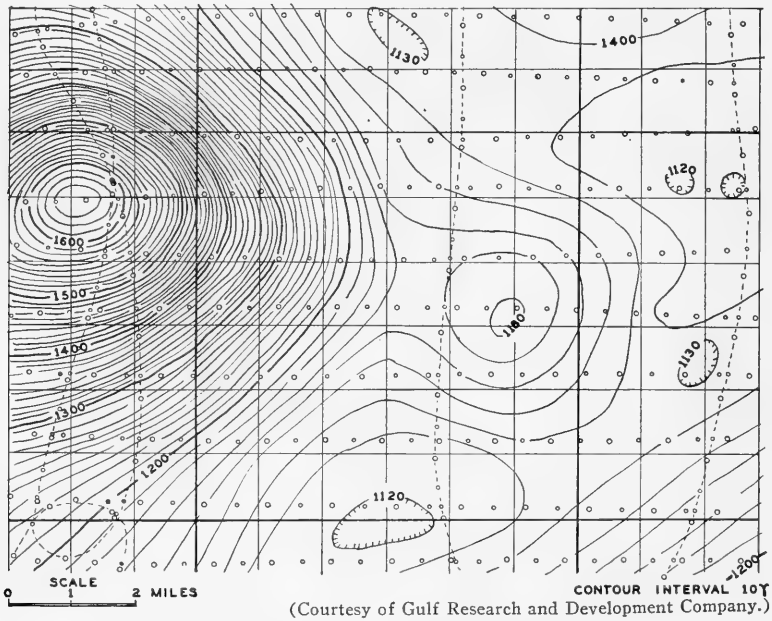

(Courtesy of Gulf Research and Development Company.)

Fig. 119.—Portion of an aeromagnetic map, New Mexico.

Shoran stations on the ground. On the other hand, by first plotting the ground station positions on any available base map of the area, the magnetic data may be directly transferred to the base map. Figure 119 is a small portion of an aeromagnetic map showing total intensity over an area in New Mexico.

The available literature on the interpretation of magnetic anomalies deals largely with anomalies in the vertical or horizontal intensity. This is because these components have been the most easily, and therefore the most commonly, measured elements. The usual airborne magnetometer records the variations in the total intensity. The available interpretation literature is

† Homer Jensen and J. R. Balsley, Jr., "Controlling plane position in aerial magnetic surveying", *Engineering and Mining Journal*, Vol. 147, No. 8, pp. 94-95, 153-154, August, 1946.

therefore not directly usable. However, the modification required is not difficult and can be readily worked out as needed.

The airborne magnetometer has placed control of the vertical dimension at the disposal of the geophysicist, and suitable exploitation of this advantage can be valuable in many ways.†

It is estimated that to date (1949) well over a half million miles of magnetic profile have been recorded in the air. The speed and low unit cost at which surveys can be made, especially in areas where work on the ground would be slow and difficult, are advantages at present available only with the airborne magnetometer.

Helicopter Operations

The helicopter-borne magnetometer has been developed along principles somewhat different from those of the magnetometer carried in fast-flying fixed-wing airplanes.‡ It is designed to outline local and detail anomalies of the magnetic field. Detail is advantageous particularly in exploring and prospecting for orebodies.

As an aircraft ascends from the ground, the distance from the magnetic ore-bearing structures and orebodies increases, and the magnetic intensity therefore decreases rapidly. § The details are lost even faster. As described previously, two sharp magnetic highs may merge into one if the intensity is recorded at an altitude somewhat comparable to the distance between the bodies. In such a case, a drill hole placed on the apparent maximum anomaly would penetrate the ground between the orebodies, never intersecting either of them.

The helicopter-borne magnetometer was built with the idea of duplicating as much as possible the results of magnetic surveys on the ground. This duplication has been achieved remarkably well, as indicated by Figure 120. The helicopter has proven most satisfactory for the mapping of local areas. As early as 1921 experiments had been made with captive balloons, but these were found to be cumbersome, and completely unmanageable in wooded terrain. The helicopter is an exceedingly maneuverable aircraft; it may be landed in a small clearing not more than 50 feet square; equipped

† A. A. Logatchev, "An experimental application of the aeromagnetic survey to the determination of depths in magnetic masses", materials of the Central Geological and Prospecting Institute, *Geophysics,* Fascicle 8, pp. 35-38, 1940. In Russian.

R. E. Gebhardt, "Investigation of height of local magnetic anomaly at Port Snettisham, southeastern Alaska", *Terrestrial Magnetism and Atmospheric Electricity,* Vol. 46, pp. 451-454, 1941.

"Aeromagnetic survey at three levels over Benson mines, St. Lawrence County, New York", U. S. Geological Survey, *Geophysical Investigations, Preliminary Map No. 2,* 1946.

Irwin Roman, "The resolving power of magnetic observations", *A.I.M.E. Tech. Pub.* 2097, Nov., 1946.

‡ "Employ helicopter for first time to explore remote mining regions", Skillings' *Mining Review,* Vol. 35, No. 12, July 6, 1946.

"Employ helicopter for geophysical surveying", *Eng. and Min. Jnl.,* Vol. 147, No. 8, August, 1946.

Hans Lundberg, "Magnetic surveys with helicopters", *Bull. Inst. of Min. and Met.,* No. 488, pp. 21-27, July, 1947.

Hans Lundberg, "Mining geophysics", *Min. and Met.,* Vol. 28, No. 482, Feb., 1947.

Hans Lundberg, "Results obtained by the helicopter-borne magnetometer", Canadian Institute of Mining and Metallurgy, *Transactions,* Vol. 50, pp. 392-400, 1947.

§ Hugo E. Kuehn and Guy E. Dent, "Comparative study of magnetic surveys of Worcester County, Maryland, made on the ground and from airplane observations", U. S. Bureau of Mines *Report of Investigations* 4070, May, 1947.

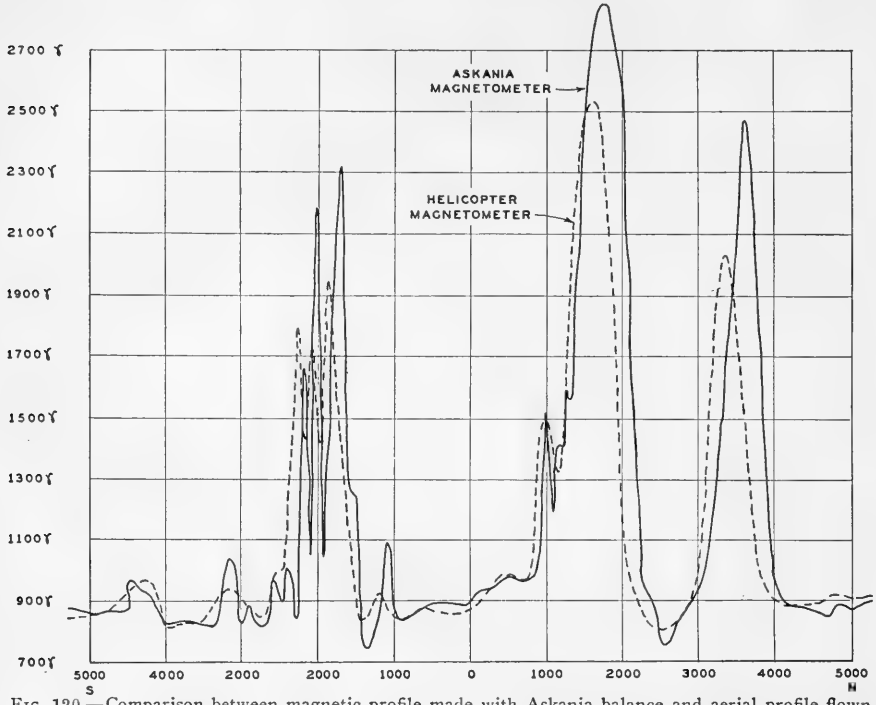

FIG. 120.—Comparison between magnetic profile made with Askania balance and aerial profile flown 150 feet above surface. (Courtesy of Lundberg Explorations, Limited.)

with floats, it may even be landed in a swamp, on thin ice, on water, or in soft snow. (Figure 121.) It can be kept still in the air or hovering over a given point at a given altitude; it may ascend and descend vertically, flying sideways and even backwards at the will of the pilot. It flies forward at any speed up to 100 m.p.h. It can be kept flying at any useful altitude from a few feet to several thousand feet above the ground and can be flown close to the ground with perfect safety. In clear, bare areas the survey flights may be performed a few feet above the ground, and in forest areas flights are made at a few feet above the tallest trees, or 100 to 150 feet above the ground. With the helicopter it is possible to mark a point of reference by using a small parachute-like marker which may be draped over a tree or laid out over the ground. This can be accomplished from the helicopter without touching the ground.

FIG. 121.—Helicopter equipped with floats, for mapping water-covered areas. (Courtesy of Lundberg Explorations, Limited.)

A drawback is the limited load capacity of the helicopter, as well as the rather cramped space for mounting instruments. The operating base must be close to the area to be mapped. The helicopter-borne magnetometer must be very light, but since it is generally flown close to the ground the need for great sensitivity becomes of less importance than in magnetometers flown at higher altitudes.

Installation in Helicopter.—The detecting unit is suspended forward five feet from the helicopter by means of a cantilever type of boom. The length of the boom is adjusted so that mechanical vibrations originating in the helicopter may be reduced to a minimum at the shock-mounted detecting unit.

The electronic section and the recorder are mounted in a common cabinet which is located alongside the instrument panel in the helicopter.

FIG. 122.—Helicopter installation: (right) amplifier recorder installed in control compartment, and (left) close-up view of equipment. (a) instrument panel, (b) amplifier, (c) ink recorder. (Courtesy of Lundberg Explorations, Limited.)

(Figure 122.) The detecting unit is electrically connected to the electronic section by means of a shielded multi-conductor cable.

Navigation and Mapping at Low Elevations.—The magnetic data would be quite useless without correlation of the geographic and topographic features. Aerial photographs are most useful for this purpose, as well as in planning a survey. However, a good topographic map may be sufficient.

On the map or photograph, course lines at suitable intervals are laid out, to be followed by the helicopter pilot. The altitude is decided upon after studying the topographic relief and taking into consideration the geological conditions as well as the geometrical dimensions of the magnetic features.

After each day, or flight, the records are transcribed into proper scale using an automatic transcriber. The results after transcription are then plotted on the map in proper scale and contours of isointensity are drawn, as in magnetic surveys on the ground.

Shipborne Magnetometer

For small areas the shipborne magnetometer has proven an economical and accurate reconnaissance method.† A standard airborne magnetometer is used with the magnetically-sensitive detector mounted in a watertight housing or *fish,* and towed behind the ship to minimize the ship's magnetic effects. With this arrangement the speed of the ship is slow enough to use inexpensive means for determining the ship's position. Radar can be effectively employed if suitable targets are available for ranging. Another method involves the use of buoys anchored at strategic points in the area and surveyed-in by conventional means. With the buoys in position, the ship runs from one buoy to another at a uniform rate of speed. By knowing the course, speed, and time, the ship's position can be determined readily. If the ship is equipped with a gyroscopic compass with automatic steering, its course is accurately and easily maintained. To further simplify navigation, a course recorder is available which continuously records the ship's heading.

Magnetic surveys in the Gulf Coast have shown that salt domes, which are the oil producers in this area, have only small anomalies associated with them. Since the magnetic anomaly of a structure varies as the square or higher power of the distance to the point where the measurements are made, it is important that the magnetometer be as close to the structure as possible. For this reason the shipborne magnetometer has a distinct advantage over the airborne magnetometer. If a structure located at a depth of 1,000 feet gives an anomaly of 10 gammas at the surface, the same anomaly mapped when flying at 1,000 feet altitude would be about 2.5 gammas.

MAGNETIC METHODS

UNITED STATES PATENTS

400,661 Issued Apr. 2, 1889. Adolphus Gipperich. "Apparatus for Determining Electric or Magnetic Forces."

961,298 Issued June 14, 1910. Dell W. Jewell. "Prospector's Needle."

1,574,350 Issued Feb. 23, 1926. J. B. Johnson. "Electrical Testing."

1,675,121 Issued June 26, 1928. Burton McCollum. "Method and Apparatus for Studying Geologic Contours."

1,676,619 Issued July 10, 1928. Burton McCollum. "Method and Apparatus for Studying Geologic Contours."

1,724,495 Issued Aug. 13, 1929. Burton McCollum. "Method and Apparatus for Determining the Slope of Subsurface Rock Boundaries."

1,724,720 Issued Aug. 13, 1929. Burton McCollum. "Method and Apparatus for Studying Subsurface Contours."

† Eugene Frowe, "A total field magnetometer for mobile operation", *Geophysics,* Vol. 13, pp. 209-214, 1948.

1,748,659 Issued Feb. 25, 1930. Karl Sundberg. "Method and Apparatus for Magnetic Prospecting."
1,792,639 Issued Feb. 17, 1931. H. N. Herrick. "Method and Apparatus for Determining the Direction of the Dip and Strike of the Earth's Strata."
1,819,797 Issued Aug. 18, 1931. Seizo Shimizu. "Magnetometer."
1,863,415 Issued June 14, 1932. Frank Rieber. "Magnetometer."
1,895,373 Issued Jan. 24, 1933. Ernest Bruche. "Apparatus for Measuring Magnetic Fields."
1,909,619 Issued May 16, 1933. Henry N. Herrick. "Measuring Instrument."
1,943,850 Issued Jan. 16, 1934. Orley H. Truman. "Magnetometer."
1,976,636 Issued Oct. 9, 1934. Erwin Roux. "Magnetic Balance for the Measurement of Intensities."
2,010,245 Issued Aug. 6, 1935. Erwin Roux. "Magnetic Balance."
2,104,752 Issued Jan. 11, 1938. H. N. Herrick and E. D. Lynton. "Method and Means for Determining Magnetic Polarity."
2,149,717 Issued Mar. 7, 1939. J. M. Pearson. "Method and Apparatus for Calibrating Magnetometers."
2,151,627 Issued Mar. 21, 1939. V. V. Vacquier. "Apparatus for and Method of Measuring the Terrestrial Magnetic Field."
2,196,314 Issued April 9, 1940. R. E. Lee. "Method of Measuring the Inherent Terrestrial Magnetism of the Earth's Crust."
2,246,259 Issued June 17, 1941. L. Machts. "Apparatus for Making Geophysical or other Measurements."
2,252,059 Issued Aug. 12, 1941. G. Barth. "Method and a Device for Determining the Magnitude of Magnetic Fields."
2,261,030 Issued Oct. 28, 1941. W. P. Jenny. "Micromagnetic Prospecting Device."
2,331,617 Issued Oct. 12, 1943. D. W. Moore, Jr. "Magnetic Field Responsive Device."
2,334,593 Issued Nov. 16, 1943. R. D. Wyckoff. "Apparatus for Measuring Magnetic Fields."
2,335,117 Issued Nov. 23, 1943. E. P. Harrison. "Magnetic Surveying Apparatus."
2,358,027 C. J. Penther and F. B. Rolfson.
2,374,166 Issued Apr. 24, 1945. L. F. Beach and J. C. Purves. "Magnetic Field Responsive Device."
2,376,883 Issued May 29, 1945. A. S. Riggs and H. H. Thompson. "Dynamic Earth Inductor Compass."
2,378,014 Issued June 12, 1945. P. P. Horni. "Methods of Determining the Effective Range of Magnetic Detectors."
2,379,716 Issued July 3, 1945. A. W. Hull. "Magnetic Field Gradient Meter."
2,383,459 Issued Aug. 28, 1945. L. F. Beach. "Indicator for Magnetic Fields."
2,383,460 Issued Aug. 28, 1945. J. C. Purves and L. F. Beach. "Magnetic Field Responsive Device."
2,383,461 Issued Aug. 28, 1945. O. E. Esval, R. S. Curry, C. F. Fragola, and L. F. Beach. "Flux Valve Compass System."
2,384,819 Issued Sept. 18, 1945. M. C. Depp. "Flux Valve."
2,389,146 Issued Nov. 20, 1945. C. F. Fragola, M. C. Depp, and R. S. Curry, Jr. "Flux Valve."
Re. 22,699 Issued Nov. 27, 1945. A. A. Stuart, Jr. "Magnetic Compass."
2,390,051 Issued Dec. 4, 1945. G. Barth. "Means for Measuring Magnetic Fields."
2,393,974 Issued Feb. 5, 1946. R. S. Curry, Jr. "Gyro Flux Valve Compass System."
2,403,347 Issued July 2, 1946. M. C. Depp and C. F. Fragola. "Flux Valve."
2,403,669 Issued July 9, 1946. E. J. Martin and C. E. Grinstead. "Inductor Compass."
2,404,806 Issued July 30, 1946. H. A. D. Lindsey. "Submarine Detector."
2,406,870 Issued Sept. 3, 1946. V. V. Vacquier. "Apparatus for Responding to Magnetic Fields."
2,407,202 Issued Sept. 3, 1946. V. V. Vacquier. "Apparatus for Responding to Magnetic Fields."
2,410,039 Issued Oct. 29, 1946. L. F. Beach. "Magnetic Field Responsive Device."
2,412,046 Issued Dec. 3, 1946. S. C. Hoare. "Resonant Circuit Saturable Core Measurement Apparatus."
2,414,448 Issued Jan. 21, 1947. L. F. Carter. "Gyro-Magnetic Compass System."
2,414,654 Issued Jan. 21, 1947. F. W. Meredith. "Flux Valve."

2,415,808 Issued Feb. 18, 1947. O. E. Buckley. "Detection of Large Magnetic Bodies."
2,418,553 Issued April 8, 1947. E. M. Irwin. "Flux Measuring System."
2,420,580 Issued May 13, 1947. L. L. Antes. "Magnetometer."
2,424,562 Issued July 29, 1947. C. F. Fragola. "Gyro Flux-Valve Compass System."
2,424,772 Issued July 29, 1947. F. Rieber. "System for Detecting Magnetic Masses."
2,425,180 Issued Aug. 5, 1947. C. H. Fay. "Magnetic Field Measurements."
2,426,470 Issued Aug. 26, 1947. A. T. Sinks. "Remote-Indicating Magnetic-Compass System."
2,426,622 Issued Sept. 2, 1947. A. G. Laird and T. Slonczewski. "Magnetic Field Detector."
2,427,014 Issued Sept. 9, 1947. W. J. Means. "Orienting Device."
2,427,654 Issued Sept. 23, 1947. L. F. Beach. "Remote-Reading Flux-Valve Compass System."
2,427,666 Issued Sept. 23, 1947. E. P. Felch, Jr. and T. Slonczewski. "Magnetic Field Strength Indicator."
2,428,014 Issued Sept. 30, 1947. R. S. Curry and C. F. Fragola. "Concentric-Core Flux Valve."
2,428,346 Issued Sept. 30, 1947. W. G. White. "Magnetic Compass."
2,431,319 Issued Nov. 25, 1947. W. B. Ellwood. "Magnetic Firing Device."
2,432,514 Issued Dec. 16, 1947. M. C. Depp and C. F. Fragola. "Adjustable Flux Valve."
2,434,324 Issued Jan. 13, 1948. H. Lehde. "Earth Inductor Compass."
2,435,276 Issued Feb. 3, 1948. E. L. Holmes. "Magnetic Field Indicating Means."
2,436,039 Issued Feb. 17, 1948. C. H. Fay. "Magnetic-Field Gradient Measurement."
2,436,394 Issued Feb. 24, 1948. W. P. Maltby and R. H. Park. "Magnetic Detector."
2,437,132 Issued Mar. 2, 1948. A. T. Sinks. "Remote Indicating Compass."
2,437,374 Issued Mar. 9, 1948. R. E. Burroughs. "Magnetic Field Measuring Device."
2,437,506 Issued Mar. 9, 1948. L. P. Crossman. "Repeater Compass."
2,437,692 Issued Mar. 16, 1948. E. W. Hart. "Magnetic Compass."
2,438,372 Issued Mar. 23, 1948. L. I. Mendelsohn. "Precision Magnetometer."
2,438,964 Issued Apr. 6, 1948. D. H. Cunningham and H. Belar. "Magnetic Field Detector."
2,440,503 Issued Apr. 27, 1948. C. H. Fay. "Magnetic Gradiometer."
2,441,269 Issued May 11, 1948. H. E. Hartig. "Electron Discharge Compass System."
2,442,732 Issued June 1, 1948. J. H. Rubenstein. "Magnetometer."
2,443,595 Issued June 22, 1948. F. D. Braddon. "Deviation Correcting Means for Magnetic Devices."
2,444,290 Issued June 29, 1948. C. E. Granqvist. "Earth Induction Compass."
2,444,669 Issued July 6, 1948. J. C. Pollard and C. F. Sellers. "Support for Submerged Area Surveying."
2,446,568 Issued Aug. 10, 1948. L. Wolfe. "Magnetic Compass."
2,447,496 Issued Aug. 24, 1948. M. C. Depp, R. S. Curry, Jr., and C. F. Fragola. "Flux Valve System and Method of Operation."
2,447,849 Issued Aug. 24, 1948. C. H. Fay. "Magnetometer."
2,447,880 Issued Aug. 24, 1948. J. D. Seaver. "Magnetometer."
2,448,613 Issued Sept. 7, 1948. F. G. Merrill. "Magnetic Detector."
2,451,819 Issued Oct. 19, 1948. A. Frosch. "Induction Magnetometer."

CHAPTER IV

GRAVITATIONAL METHODS

Prospecting by gravitational methods is the technique of measuring the gravitational field at the earth's surface and utilizing the data thus obtained to predict the subsurface structure. Gravitational methods are analogous to magnetic methods in that quantitative investigations are made of a natural field of force. The magnetic and gravitational methods are also analogous in their fundamental relationships, as will be seen during the development of the theory.

The physical property of the subsurface materials which produces the significant or diagnostic gravitational anomalies is *density*. It is necessary that the effects caused by the changes in density of the subsurface materials be of sufficient magnitude to manifest themselves over near-surface, topographic, and regional effects.

The three chief types of instruments available for gravity measurements are the pendulum, the torsion-balance and the gravity-meter or gravimeter. The following table gives their general operating characteristics.

Instrument	*Quantity Measured*	*How Measured*
Pendulum	Absolute vertical component of gravity	Time required for a given number of oscillations of the pendulum system.
Torsion balance	The gravity gradient along a horizontal plane, and the differential curvature of gravity equipotential surfaces	Angular movement of a beam system supported by a torsion wire.
Gravity meter		
(a) Stabilized type	Relative vertical component of gravity	Extremely high magnification to measure the vertical movement of a spring weighted system. Lineal displacement.
(b) Labilized type	Relative vertical component of gravity	Moderately high magnification to read null-point. Nonlineal displacement.

Gravity methods may be compared with magnetic methods, as is shown in the following tabulation.

Comparisons of Gravity and Magnetic Methods

Item	*Gravity*	*Magnetic*
Strength of field	1000 dynes (approximately)	0.6 gauss (dynes), average
Basic variation	Minimum at the equator; maximum at poles	Vertical component minimum at equator, maximum at poles. Horizontal component maximum at equator, minimum at poles

Comparisons of Gravity and Magnetic Methods (Continued)

Item	*Gravity*	*Magnetic*
Basic variation (Cont'd)	Change in north-south direction only is of significance	Change in north-south direction and in east-west direction must be considered
Absolute determinations	Difficult to measure total gravity with high accuracy	Comparatively simple to measure the magnetic elements
Underlying physical property of rocks and formations	Density. Very easy to measure, direct correlation with mineralogical and geological character	Susceptibility and permeability not readily determinable. Subtle relations with geologic conditions
The force itself	Attraction always. There is no repulsion, negative gravity or polarity	Attraction or repulsion. Polarity of subsurface bodies and magnets must be considered
Effects of terrain and/or topography	Important critically and affects accuracy in torsion balance work. Of less importance in pendulum and gravimeter operations.	Not too important, but difficult to evaluate
Cost of equipment	In general rather costly	Cost moderate
Personnel requirements	Requires field crew of several men	One man can operate effectively, two men efficiently
Speed of field work	Slow in pendulum and torsion balance; a few stations per day, due to nature of the measurements. Rapid in gravimeter surveys, 20 to 30 stations per day	Rapid; high output per unit per field day, averaging 25 to 40 stations per day
Applicability	In general limited to geologic studies for petroleum exploration. Some mining applications	Applicable to both petroleum and mining problems

Fundamental Principles and Phenomena

The Force of Gravity.—Gravity may be defined as the mutual attractive force between masses tending to draw them toward each other. The word "gravity" comes from the Latin *"gravis,"* meaning heavy. The law of universal gravitation, first clearly stated by Sir Isaac Newton, is expressed by the following familiar equation:

$$F = -G\frac{m_1 m_2}{r^2} \qquad (1)$$

F = the force of attraction in dynes between two masses, m_1 and m_2, being *proportional* to their product and *inversely proportional* to the square of their distance apart (r) in cm. multiplied by a constant G. The minus sign indicates that the direction of F is back toward m_1 along r. When $m_1 = m_2 = r = 1$, $|F| = G$. The best value for the constant of gravitation†, is $G =$

† P. R. Heyl, "A Redetermination of the Constant of Gravitation," Bureau of Standards *Journal of Research*, Vol. 5, Dec., 1930.

$66.7 \cdot 10^{-9}$ cm.^{3} g^{-1} sec^{-2} $\pm$ 0.005. $|F|$ means the absolute magnitude of F.

The law of gravitation is unique in its wide application. It applies alike to the motions of the heavenly bodies and of discrete particles of matter so minute that their dimensions can usually be disregarded. The gravitational force of attraction acts continuously along a direct line connecting the centers of gravity of masses and is independent of the nature of the material involved. According to exhaustive experiments‡ it is also independent of the temperature of the material considered.

It is not possible to screen off the force of gravity by the interposition of material between bodies. If such *were* the case, the portion of the earth's mass away from the sun would be less strongly attracted than that facing it. No such change in gravity appears to exist. A mass in Australia attracts a mass in London as if the earth were not interposed between them. This law of universal gravitational attraction is one of the broadest and most fundamental physical laws.

In verifying his conclusions concerning gravity, Newton realized that it was not possible for him appreciably to change the distance of a body from the earth's center in relation to the earth's radius of approximately 4,000 miles. Further, the attractional force between two bodies of ordinary size on the surface of the earth is very small and difficult to measure. Assuming an attractional force between bodies, according to the law expressed in Equation 1, it has been shown that a sphere which is homogeneous, or which can be considered as made up of homogeneous shells, such as the earth, will attract an outside body as though its mass were concentrated at its center.

Proof of Newton's Law From the Motion of the Moon. — Newton turned for proof of his law to the motion of the moon around the earth. The earth's radius is approximately 4,000 miles. At the surface of the earth a body is attracted as if the mass of the earth were concentrated at its center, and the acceleration of a falling body due to gravity averages 32.2 feet per second^2, $(= g)$. The average distance of the earth to the moon is about 240,000 miles, or 60 times the earth's radius.

With the above facts, we can determine the gravitational attraction of the earth on a body at the distance of the moon.

$$\left| F_1 \right| = G \frac{M_e m}{(60r)^2} = ma$$

$$\left| F_2 \right| = G \frac{M_e m}{r^2} = mg$$

$$\left| \frac{F_1}{F_2} \right| = \frac{a}{g} = \frac{1}{(60)^2}$$

‡ J. H. Poynting, and P. Phillips, *Proc. Roy. Soc.*, Vol. 76A, p. 445.

$$a = g/(60)^2 = \frac{32.2}{(60)^2} = 0.00894 \text{ ft./sec.}^2$$

where

F_1 = gravitational force of the earth on a mass m at the distance of the moon
F_2 = gravitational force of the earth on a mass m on the surface of the earth
g = acceleration of a body m due to gravity on the earth's surface
a = general acceleration of a body m, not on the earth's surface, due to the earth's attraction
M_e = mass of the earth

Since the moon stays in its orbit, we can conclude that the centrifugal force due to its movement around the earth just balances the attractional force calculated above. Hence, $ma = mU^2/R$, where U is the velocity of travel of the moon around the earth and R is the radius of the moon's path. R = 240,000 mi. = 1,267,200,000 feet. The period of revolution (T) of the moon around the earth = 27 days, 8 hours = 2,361,600 seconds.

$$U = \frac{2\pi R}{T}; \quad U^2 = \frac{4\pi^2 R^2}{T^2};$$

$$a = \frac{4\pi^2 R}{T^2} \tag{2}$$

$$a = \frac{4 \cdot (3.14)^2 \cdot 1{,}267{,}200{,}000}{(2{,}361{,}600)^2} = 0.00896 \text{ ft/sec}^2$$

This is in close agreement with 0.00894, considering the approximate values used, and gives evidence of the validity of the law of gravitation.

Determination of the Gravitational Constant G.—The value of the "universal constant of gravitation" G was determined by H. Cavendish in 1798. To find G it is necessary to measure, with extreme accuracy, the force F (as given in Equation 1), in a set-up where m_1, m_2, and r are known. The Cavendish torsion balance designed for this purpose (Figure 123) consisted of a light bar six feet long, $(2l)$, with two lead balls, (m_1, m_2), two inches in diameter, attached to its ends. The bar was suspended at its center by a fine wire attached by a short stem to which was fastened a small mirror for observing the deflection of a light beam. By oscillating the moving system comprising the rod and its two balls, the time required for a number of oscillations may be measured accurately. The moment of inertia of the system may be calculated, and from this value and the time of oscillation, the coefficient of torsion of the torsion wire (τ) may be readily calculated.

Two lead spheres M_1 and M_2, 12 inches in diameter, were placed at an accurately measured distance (r) about 9 inches from the balls on the ends of the bar. The position of the spheres could be changed relative to the small balls, as shown by positions 1 and 2 of the figure. The deflection caused by the spheres was read with the aid of the telescope and scale set at a distance D from the mirror.

A deflection ϕ of the bar produces a corresponding angle of reflection (2ϕ) of the light from the mirror. Prior to placing the two large masses M_1 and M_2 in position, the undeflected position of the torsion balance was n_0. After placing M_1 and M_2 in position, the deflection ϕ of the bar corresponds to a scale reading of $n_1 - n_0$. The deflecting torque due to the attraction (since two sets of masses are acting) will be approximately equal to $2Fl$. The resisting torque of the wire for a deflection ϕ is equal to $-\tau\phi$,

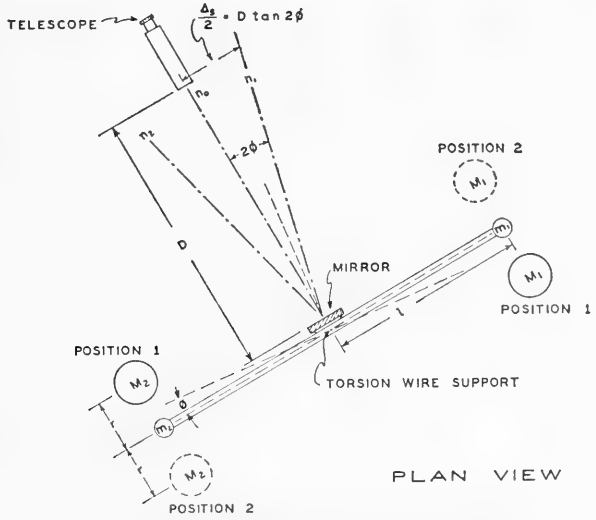

FIG. 123.—Sketch of general equipment used by Cavendish for determining the gravitational constant G.

the minus sign denoting that the direction of the torque is opposite to the deflection ϕ. At equilibrium, $-\tau\phi = 2Fl$. Attracting force

$$F = -G\frac{Mm}{r^2}$$

Hence,

$$2Fl = -G\frac{2M\,ml}{r^2} = -\tau\phi \tag{3}$$

The scale reading for the undeflected position of the beam is n_o, for a deflection ϕ in position 1, n_1, and for a deflection ϕ in position 2, n_2. Let $n_1 - n_o = \Delta s/2$.

$$\text{Then } \tan 2\phi = \frac{\Delta s/2}{D} = \frac{\Delta s}{2D}\text{, and for small angles } 2\phi = \frac{\Delta s}{2D}$$

For the total deflection or 2ϕ:

$$2(\tau\phi) = 2\left(\frac{G\,2M\,ml}{r^2}\right)$$

$$\frac{\tau\,\Delta s}{2D} = \frac{G\,4M\,ml}{r^2}$$

$$G = \frac{\tau \Delta s r^2}{8 D M m l} \text{ in terms of known quantities.} \qquad (4)$$

Cavendish's value for G = 66.579 • 10^{-9}.

Use of the Gravitational Constant to Weigh the Earth.—The force of gravity per unit mass *(g)* on the surface of the earth (neglecting for the moment the effect of the earth's rotation) is merely a special case of Newton's general law of gravitational attraction, as given by Equation 1. If we substitute $g = |F|$ in that equation, mass of the earth $(M) = m_1$; 1 gram at the earth's surface $= m_2$; and the radius of the earth $R = r$, it follows that:

$$g = G \frac{M \cdot 1}{R^2} = G \frac{M}{R^2} \qquad (5)$$

In the above equation g is the magnitude of the pull or force exerted by the earth on a gram of mass at its surface. As measured by means of a pendulum (to be described later) the force g is approximately 980 dynes; the value of G is 66.7 • 10^{-9}, and the radius of the earth is some 4,000 miles or 6.37 • 10^8 cm. With this data the earth can be weighed, i.e., the equation solved for its mass M, giving a value of 6.14 x 10^{27} grams.

The mean density of the earth can also be derived from the above data, since density equals mass divided by volume. If the earth is considered as a sphere, its volume would be $4/3\ \pi R^3$.

$$\text{Density} = \frac{6.14 \cdot 10^{27}}{\frac{4}{3} \cdot \pi (6.37 \cdot 10^8)^3} = 5.32 = \text{mean density.}$$

This value for mean density indicates a high density for the core of the earth, as the density of rocks in general at the surface is about 2.7 to 2.8.

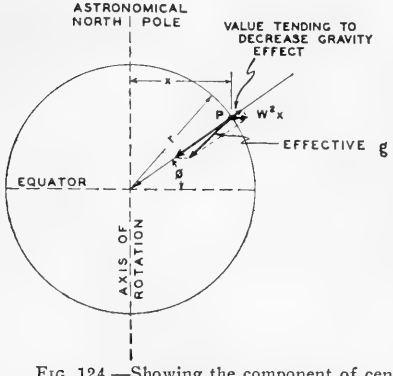

FIG. 124.—Showing the component of centrifugal force, due to the earth's rotation, which acts in a direction opposite to gravitational attraction. ϕ = latitude; r = earth's radius; x = radius of gyration of a point on the earth's surface.

The Effect of the Earth's Rotation on Gravity.—The effective force of gravity at the earth's surface is the resultant of the attractional effect of the earth's mass *less* a component acting in the opposite direction. This component is due to the centrifugal force created by the earth's rotation. Centrifugal force is expressed by angular velocity squared (symbol ω^2) times radius of gyration x. The radius of gyration of a point on the earth's surface is the perpendicular distance from the point to the axis of rotation of the earth (x of Figure 124). It is apparent that the centrifugal force component will be a maximum at the equator and zero at

the poles, because at the poles the value of x is zero. At the equator the component of centrifugal force opposing the attractional force of gravity is 3.39 cm/sec.^{2}, which is an appreciable amount in the refined measurements necessary for gravity exploration. The force of gravity therefore varies with latitude.

The Variation of Gravity with Latitude.†—Assume the earth to be a sphere with radius r, as shown in Figure 124, upon which the force of gravitational attraction A is the same at all points on the surface. At a point at latitude ϕ, g_ϕ the resultant of the attraction *(A)*, and the centrifugal force *(c)* is found as follows: at the equator, centrifugal force $c_e = \omega^2 r$.* The centrifugal force at the pole $c_p = 0$. If g_e = gravity at the equator, and g_p = gravity at the pole, then:

$$g_e = A - c_e \tag{6}$$

$$g_p = A - c_p = A \tag{7}$$

$$g_p - g_e = c_e \tag{8}$$

In latitude ϕ, $x = r \cos \phi$, and the centrifugal force in latitude ϕ (symbol c_ϕ) is:

$$c_\phi = \omega^2 \text{ r} \cos \phi = c_e \cos \phi \tag{9}$$

since $c_e = \omega^2 r$. The component of c_ϕ opposed directly to gravity A is $c_\phi \cos \phi$ (along the radius r) where $c_\phi \cos \phi = c_e \cos^2 \phi$, so that:

$$g_\phi = A - c_e \cos^2 \phi \tag{10}$$

Substituting in Equation 10 the value of A in Equation 6:

$$\begin{aligned} g_\phi &= g_e + c_e - c_e \cos^2 \phi \\ &= g_e + c_e \,(1\text{-}\cos^2 \phi) \\ &= g_e + c_e \sin^2 \phi \\ &= g_e + (g_p - g_e) \sin^2 \phi \end{aligned} \tag{10a}$$

† In the following, "g" and "c" refer to gravitational and centrifugal force, respectively, per unit mass. The symbols are generally used to denote the accelerations of a mass due to the respective forces, the forces themselves being mg and mc. For unit m, the forces and acceleration are equal. (See page 255.)

* Centrifugal force for a unit mass particle at the earth's surface at the equator is U^2/r, where r is the equatorial radius and U the velocity of the particle or the distance it moves, divided by the time involved. For such a particle the distance covered in one day is $2\pi r$ (the circumference of the earth). The time of rotation of the earth (T) is 24 hours = 86,400 seconds. From the above: $U = 2 \pi r/T$, and $U^2 = 4 \pi^2 r^2 / T^2$; centrifugal force is $4 \pi^2 r/T^2$, and in terms of angular velocity ω it is $\omega^2 r$.

Dividing both sides of the equation by g_e gives

$$\frac{g_\phi}{g_e} = 1 + \frac{g_p - g_e}{g_e} \sin^2 \phi$$

$$g_\phi = g_e (1 + \frac{g_p - g_e \sin^2 \phi)}{g_e}$$

The above may be written

$$g_\phi = g_e (1 + B \sin^2 \phi) \qquad (11)$$

The quantity symbolized by B in formulae is known as the gravitational flattening. It will be considered later in connection with gravity measurements and geodesy. B is the difference between the polar and the equatorial gravity, divided by the equatorial gravity.

Helmert in 1884 published a formula for the g_0, or sea level, value of gravity, as follows:

$$g_0 = 978.000 \ (1 + 0.005310 \sin^2 \phi) \qquad (12)$$

In 1901 he gave a more accurate form:†

$$g_0 = 978.046 \ (1 + 0.005320 \sin^2 \phi - 0.000007 \sin^2 2\phi) \qquad (13)$$

From these formulae or others of similar type‡ the *theoretical value* of gravity reduced to sea level may be calculated for a given latitude (ϕ).

The variation in the force of gravity between the equator and the poles is shown in the following table as determined from Berroth's†† formula

of $g = 978.046 \ (1 + 0.005296 \sin^2 \phi - 0.000007 \sin^2 2\phi)$: (14)

TABLE 6.

VALUE OF THE FORCE OF GRAVITY FOR VARIOUS LATITUDES.§

Latitude	*g. Dynes*
0	978.046
10	978.203
20	978.652
30	979.337
40	980.178
45	980.628
50	981.078
60	981.930
70	982.623
80	983.073
90	983.223

† F. R. Helmert, "Die Schwerkraft und die Messenverteilung der Erde", *Encyklopadie der mathematischen Weissenschaften,* Band VI, Teill, Heft 7, B. G. Taubner, Leipzig, 1906-1925, pp. 85-177.

‡ G. L. Hosmer, *Geodesy,* 2nd Edition, Chapter on Gravity Measurements, John Wiley & Sons.

†† A. Berroth, Gerland's *Beitrage zur Geophysik,* Vol. 14, 215-57, 1916.

§ This table of gravity values for different latitudes forms the basis for the latitude correction necessary in gravity field work. This correction is analogous to the latitude and longitude correction in magnetic exploration.

Units in Gravity Measurements.—Newton's second law of motion states that $F = ma$, or force equals mass times acceleration. Acceleration is the increase in velocity per unit of time, viz., cm./sec./sec.

A force per unit mass, therefore, is equal to the acceleration. Hence, the force of gravity may be expressed in units of force: dynes per unit mass; e.g., dynes/gram. It may likewise be stated in units of acceleration; e.g., cm./sec./sec.

The force of gravity at a station may be, say, 980.112 dynes, or 980.112 dynes/gram. With equal accuracy it could be stated that the gravity at the station was 980.112 cm./sec.^{2}, which is in terms of acceleration. These two forms of expression are numerically equal but convey a slightly different physical meaning.

A special name *gal* has been given to the gravity units of acceleration, (after Galileo). 1 gal = 1 cm./sec./sec. The 1/1000 part of a gal, or milligal, (mg.) is commonly used in gravity prospecting. 1 mg. = 0.001 gal or 0.001 cm./sec.^{2}

The previously considered Equation 5, ($g = G \cdot M \cdot 1/R^2$, symbols as given) is based on the assumption that the earth is a homogeneous stationary isolated sphere. Such a sphere would exert a radial attractional force on objects at its surface and the force per unit mass would be the same at all points on the surface. Actually, the earth is neither homogeneous, stationary, isolated, nor spherical. The result is that the force of gravity per unit mass varies, both in direction and in magnitude, from place to place and from time to time. Furthermore, data on gravitational anomalies furnish information about the deviation of the earth from a homogeneous, stationary, isolated sphere. Interpretation of the field measurements made in gravity surveying is based upon these variations or gravitational anomalies.*

Factors Causing Variations in Gravity.—The earth's deviation from a sphere derives from two factors: (a) the topographical features, i.e., the local phenomena of valleys, hills and mountains; and (b) the oblate spheroid shape resulting from its rotation. This second factor introduces a variation in the force of gravity which is a function of latitude. This variation and the effect of the centrifugal force of rotation are usually lumped together and called a "latitude, or north-south correction." From a knowledge of the mean shape of the earth and its speed of rotation about its axis, the latitude correction may be calculated mathematically; the correction amounts to about $1/194 \cdot \sin^2$ (latitude).

Another variation in gravity is caused by the differences in density of the materials of the earth. This phenomenon furnishes the physical basis of the gravitational methods of prospecting. Thus, a structure that

* At present, as far as geophysical prospecting is concerned, the fact that the earth is not isolated is of little importance. The attractions of the sun and the moon and the effects of the tides caused by them introduce changes in gravity which are smaller than the errors in observations. These latter are the time variations in gravity.

is denser than the average material of the earth's crust in its neighborhood exerts a greater force on a unit mass than would have been exerted if the structure had been absent. The magnitude of this gravitational anomaly is dependent upon the density, geometric configuration, depth, and location of the structure with reference to the point at which the effect of the structure is measured.

Reduction of Gravity Values to Sea Level Datum.—In order to compare absolute values of gravity, such as are obtained from pendulum observations, and to use them for geodetic purposes it is necessary that they be reduced to sea level as a datum. The reduction, or correction, is made up of two parts. The first part corrects for the *decrease* in gravity due to the height (or elevation) of the field station above sea level. It is called the elevation correction, or *free air* correction. The second part takes into consideration the *increase* in gravity, at a station, resulting from the mass of the material between it and the sea level datum. It is called the *Bouguer*† *correction.*

Elevation Correction.—The correction for elevation is derived from the law of gravitation (Equation 1) that attraction varies inversely as the square of the distance. Where g_0 = sea level gravity and g = observed gravity, with H = station elevation above sea level (or elevation difference) and R = the radius of the earth, it can be stated that:

$$\frac{g_0}{g} = \frac{(R+H)^2}{R^2} = \left(1 + \frac{2H}{R} + \frac{H^2}{R^2}\right) \tag{15}$$

For most exploration purposes the higher powers may be neglected, and the equation may be reduced to the more simple form:

$$g_0 = g\,(1 + 2H/R) \tag{16}$$

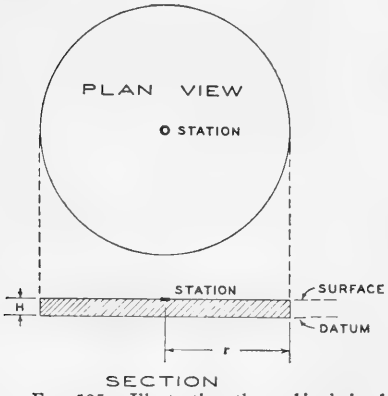

FIG. 125.—Illustrating the cylindrical form assumed for the material between the station and datum in calculating the Bouguer correction. r, radius and H, height of the cylinder.

The elevation correction is based on the assumption that no mass other than "free air" exists between the station and the datum. The constant for the elevation correction is 0.3086 milligals per meter or 0.09406 milligals per foot. After correction for elevation, gravity values are known as *free air gravities* and are given the symbol (g_0).

Bouguer Correction.—The correction for the effect of the mass of material between the station and datum can be derived by assuming some easily

† P. Bouguer, See Chapter I, p. 6.

calculatable shape. The most convenient shape mathematically is a flat cylinder or disc of material (similar to a large grindstone) as illustrated in Figure 125. The gravity station is assumed to be located at the center of the top surface of the cylinder. The height H of the cylinder is small in comparison to its radius. The radius may be considered as infinite, so that the correction takes into consideration *all* the material from the station elevation to datum.

According to Helmert† the attraction of a mass of this shape on a 1 gram mass at the station location is:

$$\Delta g = 2\pi G\ d \cdot H \tag{17}$$

wherein Δg = the gravity effect of the cylindrical mass; G = the gravitational constant; d = the density of the material in the cylinder, and H = the height of the station above the datum or thickness of the cylinder.

As previously given in Equation 5, the attraction of the earth on the same unit gram at the station is:

$$g = G\,M \cdot 1/R^2 = G\ 4/3\pi R^3\ \sigma/R^2 = G\ 4/3\pi R\sigma \tag{5}$$

(In the above M and R are the mass and the radius of the earth, respectively, and σ is its mean density. G is the gravitational constant.)

Dividing Equation 17 by Equation 5 and solving for Δg gives:

$$\frac{\Delta g}{g} = \frac{2\pi G\,d\,H}{G\ 4/3\ \pi\ R\ \sigma}\ ;\ \Delta g = g\,3/2\,\frac{d}{\sigma} \cdot \frac{H}{R} \tag{18}$$

This correction amounts to 0.04185 dH milligals per meter, or 0.0127 dH milligals per foot.

Application of Corrections.—The elevation correction and the Bouguer correction are of opposite algebraic sign. They are usually combined for convenience, and applied to observed gravity values, together with a terrain correction, which latter will be considered in the section on gravimeters. (See p. 404.) After correcting for elevation, Bouguer effect and (if necessary) for variations in terrain around the station, the gravity values are given the symbol g''_0 and are generally called *Bouguer* gravities.

A gravity value as measured at any given station can be reduced to the datum by making the elevation correction. This corrected value is the one which would have been obtained if the original reading had been made at the datum.* It represents the observed value of gravity plus the elevation effect, but does *not* consider the column of material between the datum and the surface.

† Helmert, *loc. cit.*

* Gravity at datum is greater than at the ground surface (when datum is below the station, as is generally the case). Gravity at a point nearer the center of the earth (datum) is greater (less R distance, Equation 5) than at the surface. The elevation correction is therefore plus and is *added* to the observed gravity.

At the time the station was occupied and gravity observed, the cylinder of material from the station down to datum contributed its effect to the observed value. This contribution is calculated in the Bouguer reduction and must be *subtracted* from the value of gravity at the datum plane, corrected for elevation only.

When thus corrected for *both* elevation and Bouguer effect, the g''_0 gravities are those that would have been obtained had the station been at the datum location.

Gravity Anomalies

The absolute gravity anomaly (which also reflects the major subsurface conditions to a certain degree) can be calculated by subtracting from the Bouguer gravity value the theoretical value of gravity for the latitude of the station. The theoretical value of gravity can be computed by use of Equation 14. Such theoretical values are usually designated as γ_0. After the subtraction is made for a given station, the resulting gravity anomaly value is symbolized $\Delta g''_0$ and is known as a *Bouguer gravity anomaly*. In brief, the absolute gravity anomaly at a station is the corrected observed gravity less the theoretical gravity for the station.

The sizes of certain pendulum gravity anomalies ($\Delta g''_0$ values) in the state of Colorado are as follows:†

PENDULUM GRAVITY ANOMALIES

	Station	*Anomaly*	*Conditions*	*Location*
1	Denver	−0.016	In center of Denver Basin	1
2	Colorado Springs	−0.007	On axis deep syncline	75 miles S of 1
3	Pike's Peak	+0.021	On uplifted mass	10 miles W of 2
4	Idaho Springs	+0.022	Uplifted area	30 miles W of 1
5	Boulder	−0.013	In basin, with minor nearby fold	30 miles NW of 1
6	Lafayette	−0.020	In Denver Basin local faulting	15 miles NNW of 1
7	Brighton	−0.006	In Denver Basin	20 miles N of 1

Gravitational Field of the Earth.—As a consequence of the inverse square law (Equation 1), there exists a physical quantity described as the gravitational potential which is analogous to the magnetic potential. The *gravitational potential* at a point is defined as the work required to move a unit mass from that point to a point infinitely distant. Gravitational potential is thus a scalar quantity.*

A *level surface* is a gravitational equipotential surface. It is a surface such that no work is done against gravity when a mass is moved between

† J. H. Wilson, *Mines Magazine*, August, 1928: Article on Pendulum Apparatus. D. White, "Gravity Observations from the Standpoint of Local Geology," *Bull. G. S. A.*, Vol. 35, 1924.

* An alternative definition of potential may be stated as follows: The gravitational potential at any point is that quantity whose rate of change in the direction of gravity is the force of gravity at that point.

two points on it. (A level surface is not necessarily a horizontal surface.) Because the potential is constant on a level or equipotential surface it is impossible for equipotential surfaces corresponding to different values of potential to intersect, for the two surfaces would have the same values of the potential at the points of intersection and hence the same values at all other points on the surfaces.

A level or equipotential surface has the following very important property: The force of gravity is perpendicular to the surface at every point.** Hence, if a line is drawn at a point (or points) which is normal to the equipotential surface through the point (or points) selected, the direction of the force of gravity will be along this line, as shown in Figure 153. Such a line is called a *vertical line*. Ordinarily, over distances which are not too large, the vertical lines will be practically straight.

Gravitational Prospecting and the Science of Geodesy. — The science of geodesy deals with measurements of large areas of the earth's surface by triangulation and astronomical observations. One department of geodesy comprises the study of the figure of the earth. This branch investigates deviations from homogeneity of segments of the earth's crust which have a large areal extent and thickness.† The main problem in gravitational prospecting, on the other hand, concerns the deviation from homogeneity of relatively small portions of the near-surface crust of the earth. However, the methods of geodesy are instructive because similar principles of measurement are applied.

In geodetic terminology, the term *sea level* applies to the equipotential surface that most nearly coincides with the average level of the ocean. This surface is called the *geoid*. The determination of the shape of the geoid involves a combination of surveying, astronomy, and gravitational methods.

Geodetic latitude and longitude determinations at a point involve a determination of the direction of the plumb line at that point. The direction of the plumb line may be greatly affected by the presence of large bodies of abnormal density near the point of measurement. If the body is denser than the surrounding material, it will exert an unduly large force of attraction on the plumb bob and cause the plumb line to deflect toward it. Differences in latitude or longitude due to this effect are usually only a few seconds of arc. Although these differences generally do not exceed ten seconds, except in mountainous areas, they are occasionally quite large. For example, between the north and south coasts of Puerto Rico the anomalous deflection of the plumb line produced by local inhomogeneities if not taken into account would lead to an error in distance of about 1 part in 50. This example is sufficient to show that the effects of

**The mean surface of a body of water such as an ocean is a portion of a gravitational equipotential surface.

† National Research Council, *Physics of the Earth II; The Figure of the Earth*, Washington, D.C.

local inhomogeneities may be great enough to cause considerable difficulty in geodetic measurements.

A Geodetic Use of Gravity Values.—The flattening or degree of departure from the spherical form of the earth can be computed from absolute gravity values. This is of importance geodetically in order to find the best assumed shape for the earth to produce maps with a minimum of distortion. The compression, or flattening, of the earth can be calculated from Clairaut's theorem as follows:

$$\frac{a-b}{a} = 5/2\,\frac{c_e}{g_e} - \frac{g_p - g_e}{g_e} \qquad (19)$$

In the equation b = the length of the earth's polar axis and a = the length of the equatorial axis (assuming that the equatorial section is circular, or that the earth is a 2-axial ellipsoid), g = gravity and subscripts p and e designate pole and equator respectively; i.e., c_e = equatorial centrifugal force.

The second term in the right hand side of the equation is the gravitational flattening previously mentioned.

Clairaut's theorem states that the difference in polar and equatorial axes divided by the polar axis is equal to 5/2 the centrifugal force at the equator, divided by the force of gravity at the equator, less the gravitational flattening. Since these quantities related by the equation can be measured or calculated, the shape of the earth can be determined.

From a careful study of gravity values in all parts of the world, the following value for axial difference ratio has been established:

$$\left(\frac{a-b}{a}\right) = \frac{1}{298.3} \pm 0.7 \text{ meter}$$

Isostasy

If the shape of a mountain or valley or any other topographical feature and the densities of the materials composing the feature and surrounding it are known, it is possible to compute the effect of the topographical feature on the gravitational field. It is found, however, that for large features, the effects so computed are generally much greater than the measured effect. The discrepancy in most cases is far in excess of the probable variations due to inaccuracy of data or calculations. This fact forms the experimental basis of the hypothesis of *isostasy* or *isostatic compensation.*‡

According to this hypothesis the apparent excess of matter represented by a hill or the apparent deficiency of matter represented by a valley or an ocean basin is compensated by underlying materials. Thus, beneath each hill there is somewhere sufficient material of lower density to compensate for the hill so that in reality there is little, if any, real excess of matter. Quite generally, the hypothesis of isostatic compensation

‡ William Bowie, *Isostasy* (E. P. Dutton Co., 1927); "Isostatic Investigations, etc." *U. S. Coast and Geodetic Spec. Pub.* Dept. of Commerce, 99, Serial 246, 1924.

postulates that the amount of material standing upon a unit area will be the same regardless of whether it is under highlands or lowlands, continents or ocean depths. The unit area, of course, cannot be taken indefinitely small; also, the state of isostasy is not perfect. In general, a circle 100 miles in radius is large enough to serve as a unit area, and frequently a much smaller circle may be used.

Two theories have been advanced as an explanation of the phenomenon of isostasy. One of these, published by J. H. Pratt in 1856, holds that there is a definite depth of compensation. The material constituting the outermost layers of the earth's crust is assumed to be less dense than the material below these layers. As a result, the total mass standing on any unit area is substantially the same. This hypothesis lends itself more readily to computation than the subsequently described theory. Topographical computations give 60 miles as an average depth of compensation.

Another theory published by Sir George Biddell Airy in 1855 is somewhat more in accord with geological theories. According to the Airy theory, blocks of the earth's crust are floating in a relatively dense plastic material, usually called magma or sima. The excess of mass corresponding to high blocks is compensated for by a displacement of the denser plastic magma or sima. Thus, blocks of crust containing excess mass produce a greater displacement of the magma than blocks containing a "normal" amount of mass. Calculations on this theory give an average depth of about 30 miles for the lighter crusts. This depth is, of course, less under the oceans and more under the continents and highlands.

Isostatic Method of Determining the Figure of the Earth.—In one method of determining the figure of the earth, the deflections of the plumb line are used to determine the ellipsoid which best fits a relatively small region. If it is desired to make the region representative of the earth as a whole, it is necessary to correct the deflections for the visible surface topography and its isostatic compensation. This isostatic method was applied by Hayford to observations extending over the United States, and the figure of the earth deduced by him was adopted in 1924 by the International Geodetic and Geophysical Union as the best available figure of the earth as a whole. The ellipsoid thus determined is known as the International Ellipsoid of Reference. The semi-major axis (or equatorial radius) equals 6,378,388 meters and the ellipticity is equal to 1/297. The mass of the ellipsoid, assuming a mean density of 5.527, is $5.988 \cdot 10^{21}$ metric tons. Later measurements of the deflection of the plumb line in Europe gave isostatic results which are substantially in agreement with Hayford's. Observations on the value of gravity discussed in the next section in general support the conclusions regarding isostasy.

"Normal" Variation of Acceleration Due to Gravity.—If it is assumed that the earth is an ellipsoid of revolution revolving about an axis of symmetry with a constant angular velocity and that the surface of the ellipsoid is a gravitational equipotential surface, it can be shown that the value of gravity at any point on the surface is given by the expression:

$$g_\phi = g_E (1 + a \sin^2 \phi - b \sin^2 2\phi) \qquad (20)$$

where g_ϕ is the value of gravity at sea level in geographic latitude ϕ, g_E is the value of gravity at the equator, and a and b are constants which depend upon the gravity at the equator, the angular velocity of rotation, and the departure of the shape of the earth from a true ellipsoid. The constant b is small and may be taken as 0.000007. This leaves two coefficients g_E and a. A commonly accepted value of g_E is 978.039 cm./sec.^{2}

and a commonly accepted value of a is 0.005294. On substituting these values into Equation 20, one obtains

$$g_\phi = 978.039\ (1 + 0.005294 \sin^2 \phi - 0.000007 \sin^2 \phi) \qquad (21)^*$$

In general, it is not possible to make gravitational measurements on the surface of the ellipsoid corresponding to sea level. If the height of the point of observation above the level surface is h, the value of gravity is obtained by adding a correction proportional to h to the observed value of gravity. The factor by which h must be multiplied amounts to a variation of gravity of about seven one hundred millionth of the total value of gravity for each foot of elevation. This correction for h may be the "free air correction" or the Bouguer correction, as described.

Stokes showed as early as 1849 that it was possible by gravitational observations to determine not only the flattening of the terrestrial ellipsoid, but also the deviation of the geoid from this assumed ellipsoid. When the suggestion was first made, it seemed to be of speculative interest only because it required that gravity be observed at intervals over the entire globe including the sea. No practical method existed for observing the value of gravity at sea at that time. An interesting method for carrying out observations at sea was devised later by Hecker. In this method the boiling point of water and the height of the mercury barometer are determined simultaneously. Because the atmospheric pressure governs both the boiling point of water and the height of a column of liquid of given density, the boiling point and fluid height data may be used to determine the density of the mercury which is proportional to the value of gravity. Recently, a much more accurate method has been developed by Vening Meinesz. By an arrangement of three pendulums the effect of the motion of the vessel is decreased. By using this apparatus in submarines submerged deeply enough to avoid most of the surface motion, it has been possible to make gravity determinations on the ocean floor.†

If there were no irregularities on the surface of the earth, the water would stand at a uniform depth over the whole earth. The plumb line at all places would be normal to the spheroid and the value of gravity would be the same for all points having the same latitude, and would increase uniformly north and south of the equator. Actually, the surface of the earth is not a regular mathematical surface but is quite irregular. However, it is found that the surfaces of the oceans and the imaginary sea levels continued under land areas approximate the surface of the spheroid which would exist if there were no irregularities. For any large area the plumb line will, on an average, be normal to the spheroid and the values of gravity after applying a correction for the elevation of the station above sea level will be very nearly the same.

---

* This formula is sometimes referred to as the Bowie Formula, Number 2.

† F. A. Vening Meinesz, "Projet d'un nouvel appareil pendulaire," *Bulletin Geodesique* Nr. 5, 1925; "Theory and Practice of Pendulum Observations at Sea," *Publiet Netherl. Geod. Comm.* 1929.

W. Heiskanen. *Handbuch der Geophysik* (Gutenberg) Vol. I, p. 765-780.

Geodesists have made searching investigations to determine the causes of the deviation from normal of the plumb line and the variation of gravity along parallels of latitude. It was readily realized that the land masses above sea level and the deficiencies in density due to water in ocean basins as compared with equal volumes of surface rock would cause irregularities. But even after corrections are applied for the effects of these excesses and deficiencies of mass, there are anomalies. The causes of these irregularities must lie in the outer portion of the earth because stations only short distances apart are affected differently. Consequently the causes of these effects must lie at depths comparable to the distances between the stations. In other words, there must be abnormal densities of materials in the outer portion of the earth. These abnormal densities at relatively shallow depths are the variables of interest in gravitational surveying.

Geodesists have made computations on the theory that at some depth below sea level the pressure for a unit area is the same, i.e., does not depend on the density of the rocks near the earth's surface. The computations have confirmed this assumption of isostasy to a remarkable degree. Thus, it has been shown that at least a greater portion of the abnormal densities occurs in the outer 60 miles of the earth. By these isostatic computations the anomalies in the goedetic data have been reduced to from 1/7 to 1/10 of what they would have been if there were no such compensation as the theory of isostasy postulates. These small residual anomalies are believed to be caused by rapid changes in density of the materials at a shallow depth and therefore are properly the object of investigations in applied science, because the variations in density producing these anomalies are caused by the juxtaposition of the different rocks close enough to the surface to interest the geophysicist and geologist.

DENSITIES OF MATERIALS

The applicability of the gravitational methods depends on the existence of detectable *differences* in density between a subsurface body and the surrounding medium. The density in grams per cubic centimeter of some of the materials found in the earth's crust are given in Table 7. The table affords only a general survey. Densities of materials in a particular region are preferably obtained from measurements made on samples taken from that region.

In a majority of petroliferous areas the density increases with depth. The increase in the Gulf Coast of the United States is 0.07 per thousand feet to depths of about 8,000 feet.† In applying gravimetric work to locate possible oil structures, it has been found that superimposed upon this general increase of density with depth, there are local variations that may be greater or less than the normal values. For instance, a decrease in density is found: (1) if a massive salt series is present at considerable depth; (2)

† D. C. Barton, "Gravitational Methods of Prospecting," *The Science of Petroleum* (Oxford Univ. Press, 1938), Vol. I, p. 374.

if a large thickness of diatomaceous shale is present at considerable depth; and (3) if a thick section of limestone or anhydrite overlies a thick section of sands, shales, clay marls or other poorly consolidated materials.

TABLE 7.

DENSITIES OF VARIOUS CONSTITUENTS OF THE EARTH'S CRUST †

TYPE OF MATERIAL	*Normal Range*	*Mean*
Igneous Rocks		
Pyroxenite	3.10 - 3.32	3.23
Peridotite	3.15 - 3.28	3.23
Gabbro	2.85 - 3.12	2.98
Norite	2.72 - 3.02	2.98
Diabase	2.80 - 3.11	2.97
Diorite	2.72 - 2.96	2.84
Quartz Diorite	2.68 - 2.96	2.81
Syenite	2.63 - 2.90	2.76
Granodiorite	2.67 - 2.79	2.72
Anorthosite	2.64 - 2.92	2.73
Granite	2.52 - 2.81	2.67
Extrusive Rocks		
Basalt	2.7 - 3.3	3.0
Lava	2.8 - 3.0	2.9
Andesite	2.4 - 2.8	2.6
Dacite	2.4 - 2.8	2.6
Trachyte	2.4 - 2.8	2.6
Phonolite	2.5 - 2.7	2.6
Rhyolite	2.4 - 2.7	2.55
Vitrophyre	2.4 - 2.5	2.45
Obsidian	2.2 - 2.4	2.3
Metamorphic Rocks		
Amphibolite	2.9 - 3.0	2.95
Phyllite	2.7 - 2.8	2.75
Gneiss	2.6 - 3.0	2.8
Slate	2.7 - 2.9	2.8
Marble	2.6 - 2.9	2.75
Graywacke	2.6 - 2.7	2.65
Schist	2.4 - 2.9	2.65
Serpentine	2.4 - 2.8	2.6
Quartzite	2.5 - 2.6	2.55
Rock Forming Minerals (Salic Minerals)*		
Zircon	4.0 - 4.9	4.45
Corundum	3.9 - 4.0	3.95
Anorthite	2.7 - 2.8	2.75
Albite	2.6 - 2.7	2.65
Nepheline	2.6 - 2.7	2.65
Quartz	2.5 - 2.7	2.6
Orthoclase	2.5 - 2.6	2.55
Leucite	2.5 - 2.5	2.5
(Femic Minerals)**		
Hematite	4.9 - 5.3	5.1
Magnetite	5.0 - 5.2	5.1
Ilmenite	4.4 - 4.9	4.65
Hypersthene	3.3 - 3.5	3.4

† The data given here represent typical averages. Wide variations may occur.
* Mnemonic for *siliceous, aluminous.*
** Mnemonic for *ferric* or *ferrous magnesian.*

TABLE 7. (Continued)

TYPE OF MATERIAL	Normal Range	Mean
Rock Forming Minerals (Femic Minerals)**		
Olivine	3.3 - 3.4	3.35
Diopside	3.2 - 3.4	3.3
Apatite	3.2 - 3.3	3.25
Typical Sulphide Minerals		
Cinnabar	8.0 - 8.2	8.1
Galena	7.4 - 7.6	7.5
Bismuthinite	6.6 - 6.7	6.65
Arsenopyrite	6.0 - 6.2	6.1
Chalcocite	5.5 - 5.8	5.65
Bornite	4.9 - 5.4	5.15
Pyrite	4.9 - 5.2	5.05
Marcasite	4.7 - 4.9	4.8
Molybdenite	4.4 - 4.8	4.6
Pyrrhotite	4.5 - 4.6	4.55
Stibnite	4.5 - 4.6	4.55
Sphalerite	3.5 - 4.0	3.75
Realgar	3.4 - 3.6	3.5
Typical Oxides		
Cassiterite	6.8 - 7.0	6.9
Cuprite	5.7 - 6.0	5.85
Specular Hematite	5.1 - 5.3	5.2
Franklinite	5.1 - 5.2	5.15
Chromite	4.3 - 4.6	4.45
Limonite	3.6 - 4.0	3.8
Spinel	3.5 - 4.1	3.8
Chalcedony	2.6 - 2.6	2.6
Bauxite	2.0 - 2.6	2.3
Opal	1.9 - 2.3	2.1
Miscellaneous Minerals		
Uraninite (Pitchblende)	8.0 - 9.7	8.35
Barite	4.3 - 4.6	4.45
Garnite	3.2 - 4.3	3.75
Pyroxene	2.8 - 3.7	3.25
Hornblende	3.0 - 3.3	3.15
Fluorite	3.1 - 3.2	3.15
Biotite	2.7 - 3.2	2.95
Muscovite	2.8 - 3.0	2.95
Oligioclase	2.6 - 2.7	2.65
Microcline	2.5 - 2.6	2.55
Native Elements		
Gold	15.6 - 19.3	
Platinum	14 - 19	
Silver	10.1 - 11.1	
Copper	8.8 - 8.9	
Iron	7.3 - 7.8	
Sulphur	1.9 - 2.1	
Miscellaneous		
Coal, hard	1.4 - 1.8	
Coal, soft	1.2 - 1.5	
Water	1.0	
Ice	0.88 - 0.92	
Petroleum	0.6 - 0.9	

**Mnemonic for *ferric* or *ferrous magnesian.*

Sedimentary Rocks and Near-surface materials[1]	*Bulk Dry Density* (B_d)	*Bulk Density Water Saturated*	*Porosity Range Per Cent* (P)[2]
Anhydrite	2.9	.....	.....[3]
Cap Rock	2.6	.....	.....[4]
Siltstone	2.3 - 2.47	2.47 - 2.54	7.4 - 15.4[8]
Gypsum	2.2 - 2.6	.....	.....
Rock Salt	2.1 - 2.4	.....	.....
Dolomite	2.04 - 2.54	2.28 - 2.65	6.2 - 8.6
Sands and Clays	2.5	.....	.....[5]
Sands and Clays	2.0 - 2.2	.....	.....[7]
Sands and Clays	1.7 - 2.2	.....	.....[9]
Mudstone	1.90 - 2.28	2.19 - 2.42	13.9 - 28.6
Sylvite	1.9 - 2.0	.....	.....
Chalk	1.8 - 2.6	.....	.....
Glacial Drift	1.8	.....	.....
Limestones	1.74 - 2.76	2.12 - 2.72	0.0 - 37.6[8]
Sandstones	1.60 - 2.68	1.99 - 2.77	0.0 - 51.3
Carnallite	1.6 - 1.7	.....	.....
Shales	1.56 - 3.17	1.92 - 3.21	2.5 - 36.3
Alluvium	1.5 - 1.6	2.0	42.3 - 43.3
Sands	1.4 - 1.8	1.9 - 2.1	30.2 - 48.4
Gravels	1.4 - 2.2	1.7 - 2.4	20.2 - 37.7
Clays	1.3 - 2.4	1.63 - 2.47	36.6 - 62.9
Silts	1.2 - 1.8	1.8 - 2.2	31.4 - 53.6
Soils	1.0 - 2.0	1.5 - 2.4	40 - 50
Marl	2.25 - 2.60	.....	.....
Marl	0.98	1.59	60.6
Diatomaceous Shale	0.9 - 1.1	.....	.....[10]
Loess	0.75 - 1.60	1.4 - 1.93	20.0 - 69.4[11]

[1] Values listed in table represent averages.
[2] Relationships: P (%) = 100 (1 −Bd/Sg), wherein P = total porosity; Bd = bulk density or apparent density of the dry sample; Sg = the specific gravity of the mineral grains in the sample.
[3] No data available.
[4] From salt domes.
[5] At 7,000 feet, Texas-Louisiana Gulf Coast.
[6] More complete data under tabular headings on earth materials is given in *Handbook of Physical Constants, G. S. A. Special Paper No. 36,* January, 1942, p. 14.
[7] At shallow depth, Texas-Louisiana Gulf Coast.
[8] Items listed in the plural represent density determinations averaged from many samples.
[9] Pleistocene, Texas-Louisiana Gulf Coast.
[10] San Joaquin Valley, California.
[11] *Loess,* plural.

Quantities Measured in Gravity Prospecting.—An analysis of the variations of the residual $\Delta g''_0$ values allows predictions to be made of subsurface conditions. Detailed discussions of various type of gravity surveys are given later in this chapter. The following brief analysis of over-simplified type conditions is intended merely to illustrate the general application of gravity theory to the prediction of subsurface conditions.

(a) $\Delta g''_0$ Profiles.

The value of the force of gravity at a station or series of stations can be measured with an accuracy of better than 0.001 dyne. As has also been discussed, when the theoretical value of the force of gravity for the latitude of a station has been subtracted from the observed gravity and the necessary corrections made for local conditions, the residual quantity is the gravity anomaly or $\Delta g''_0$ value.

A profile of $\Delta g''_0$ gravity values for a series of closely-spaced stations

across a granite ridge would show a gravity maximum over the crest of the ridge. The general shape of the $\Delta g''_o$ curve would correspond to the shape of the (heavy or more dense) subsurface ridge. This is shown in Figure 126.

Across a syncline the $\Delta g''_o$ curve follows the shape of the syncline, with a gravity minimum over the synclinal axis. In like manner, a fault which

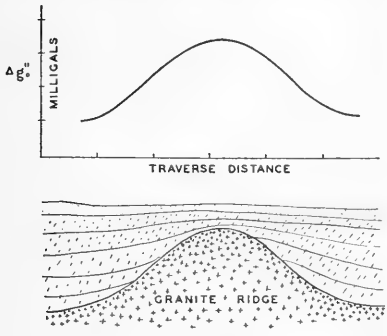

FIG. 126.—$\Delta g''o$ profile across a granite ridge; maximum gravity values over crest of ridge.

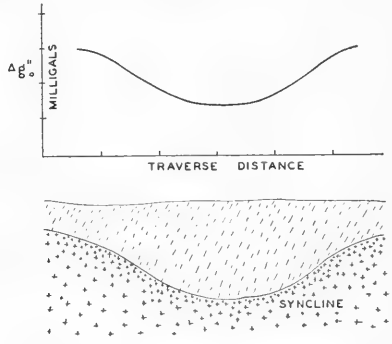

FIG. 127.—$\Delta g''o$ profile across a syncline; minimum value of gravity on synclinal axis.

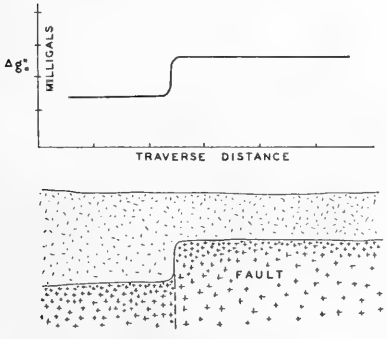

FIG. 128.—$\Delta g''o$ profile across a fault. Gravity values follow outline of subsurface heavy mass.

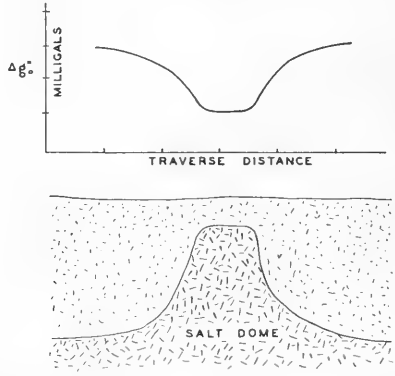

FIG. 129.—$\Delta g''o$ profile across a salt dome which has no cap. This geologic feature shows as a gravity minimum.

brings a dense rock closer to the surface, on the up-throw side, would show a profile of $\Delta g''_o$ that follows the shape of the dense basement rock quite closely. These situations are illustrated in Figures 127 and 128.

A salt dome, which is composed of salt with a density of about 2.2 in a host rock which usually has a density of 2.4 or more, would create a local deficit in gravity force and would show as a gravity minimum on the $\Delta g''_o$ curve. See Figure 129. The case here considered is for a salt dome without a heavy caprock, which sometimes modifies the overall effect, as will be described later.

(b) Gradient of Gravity

Consider the $\Delta g''_0$ for the granite ridge (Figure 126), which is also the case for an anticline. As is brought out in Figure 130, the slope of this curve at various points is a measure of the gradient of gravity at the points. At point A of Figure 130, forming the quotient dg/dx gives a numerical value for the rate of change of gravity force, or the gradient of gravity, at point A. The gradient at A can be assigned a direction, namely, toward increasing values of gravity, or what in this case amounts to the same thing, toward the crest of the granite ridge.

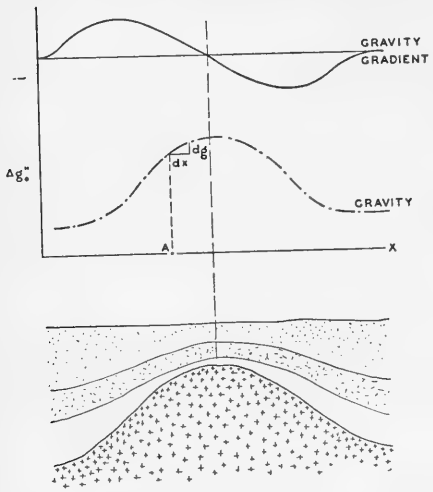

FIG. 130.—The gradient at point A equals dg/dx, or the rate of change of gravity with respect to distance x.

At the point of the maximum value of $\Delta g''_0$ the gradient (rate of change) would be zero. The direction of the gradient reverses as the ridge is crossed.

An analogy to the gradient of a function, such as gravity, is the reading of the speedometer of a traveling automobile at a given instant. If the momentary speed was 50 miles per hour, that value represents a function: namely, the velocity or distance divided by time. The torsion balance measures, at each station, the rate of change of gravity, or $\Delta g''_0$/distance.

The gravity gradient may be represented by a vector, plotted with the station at its origin. Torsion balance measurements give the gradient in two components: the north-south and the east-west gravity gradients at each station. These two vector quantities are used to plot the resultant, or total gradient. The total gradient may be plotted as a vector at the map position of the station, to show the magnitude and direction of the total gravity gradient.

The north vector* is the rate of change of gravity in the north direction. The east vector is the component of the horizontal gradient of gravity in that direction. By combining these two vectors to obtain their vector sum, the resultant is a vector whose length represents the total horizontal gradient, and whose *ori-*

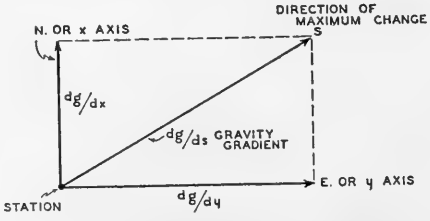

FIG. 131.—A plot of the N-S and E-W components of gravity gradient, showing dg/ds, or resultant gradient of gravity.

* In a given case the components might of course be south and west, respectively.

entation indicates the direction in which the horizontal rate of change of gravity is a maximum. (Figure 131).

Differences in gravity at two points can be determined by taking the average gradient between these points and multiplying it by the distance separating them, as will be shown in detail in a later section.

Absolute Gravity Measurements

The pendulum is essentially an instrument for the measurement of the absolute value of gravity. It has been employed chiefly by the various governmental and other agencies engaged in establishing absolute values of gravity for use in certain scientific and geodetic investigations. However, the pendulum has been used in oil exploration, especially by the Gulf Oil Corporation, which made many thousand observations during the period from 1930 to 1935. After that date their pendulum equipment was replaced by the more rapid and more accurate gravity-meter.

The Place of the Pendulum in Exploration.—The gravity pendulum has certain unique advantages in exploration. For sub-sea work it was first mounted in a submarine by the Dutch scientist, Dr. F. A. Vening Meinesz, in 1923.† Gravity observations at sea are of value in geophysical prospecting, on a reconnaissance basis. They also aid in elucidating the broad geological theories of continents and ocean basins, of mountain building and of the structure of island arcs.

The Vening Meinesz pendulum gravity apparatus was initially designed for observations on unstable bases or on board ship where the roll and pitch were less than 5 degrees. It was later adapted for use in underwater craft. Readings are taken with the submarine submerged to 50 feet or more, where stability may actually be greater than on a surface vessel. The equipment developed by Meinesz carries 3 working pendulums 0.25 meter long and is mounted on a specially-designed frame suspended in gimbals. Oscillations of the pendulum supports are transmitted to two other pendulums and thus measured. All recording is photographic. The use of a portable crystal chronograph will give the time of a ½-hour swing of the pendulums to 0.005 second. The accuracy of sea gravity measurements (in 1936) was from 1 to 5 milligals.

From 1923 to 1938 some 21 marine pendulum gravity surveys were made which involved a total of 1200 stations. The first such work relating to this country was conducted in 1928 by Dr. Meinesz in the submarine S-21, under the auspices of the Navy Department and the Carnegie Institution.††

Hess‡ brings out, in connection with such marine gravity measurements,

† M. Ewing, "Marine Gravimetric Methods and Surveys," *Am. Phil. Soc., Proc.* Vol. 79, No. 1: pp. 47-70, April 21, 1938.

†† See J. J. Hoskinson, "Gravity at Sea by Pendulum Observations," *A. I. M. E. Tech. Pub. No. 955*, 7 pages, February, 1938.

‡ H. H. Hess, "Gravity Anomalies and Island Arc Structure with Particular Reference to the West Indies," *Am. Phil. Soc. Proc.*, Vol. 79, No. 1, pp. 71-96, April 21, 1938.

that the discovery of large negative anomalies in the vicinity of island arcs is probably the most important contribution of the century in regard to the nature of mountain building. Such negative anomalies are in the form of a relatively narrow strip, or belt, about 90 miles wide, and up to 5,000 miles long in the case of the East Indies. The gravity anomaly in such a strip may be over −150 milligals with a maximum of −300 milligals, which is greater than anomalies known on the continents.

The strong negative anomaly belt lies, in most cases, on the outer (or convex) side of the main island arc, either approximately over the axis of a long narrow ocean deep or a little to one side thereof. This belt is bordered on each side by belts of positive gravity anomalies which generally coincide with topographic swells (geanticlines) in the ocean floor. The inner swell commonly emerges to form the main island arc.

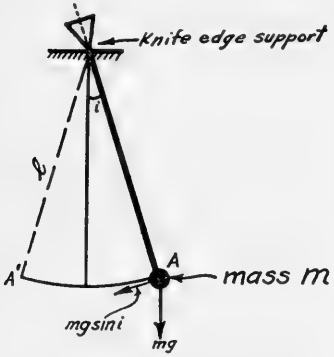

FIG. 132.—Simple pendulum. (mg is the force of gravity acting vertically downward. The force tending to move the mass m along the arc AA' is $mg \sin i$.)

It is concluded that such belts of negative anomalies represent abnormal mass distribution in the earth's crust below the strip. They may indicate a downward buckling of the earth's crust into a vertical isoclinical fold with upsqueezed zones flanking them, one of which may form an island arc or chain. Mountain building experiments tend to confirm these ideas.

Simple Pendulum.—A simple pendulum consists of a small, heavy mass suspended by a theoretically massless, perfectly flexible, string of unvarying length. Obviously, such an object does not exist but it offers a simple theoretical basis for the discussion of more complicated pendulums. As shown in Figure 132, the downward force on the bob is mg, where g is the acceleration due to gravity and m is the mass of the bob. The component of this force acting perpendicular to the string is $mg \sin i$, where i is the angle between the string and the vertical. The acceleration of the mass is $l\frac{d^2i}{dt^2}$ where l is the length of the string. Hence, from Newton's second law of motion,

$$ml\frac{d^2i}{dt^2} = -mg\sin i \quad \text{or} \quad \frac{d^2i}{dt^2} + \frac{g}{l}\sin i = 0$$

The solution of this equation is a periodic function with period T, where T is the time for the pendulum to swing from A to A' and back to A; where points A and A' represent the highest points of the swing.* T is

* In some of the literature the half period (time to swing from A to A') is referred to rather than the time for a complete oscillation.

a function of l, g, and the azimuthal angle from which the pendulum was initially set into oscillation. It is given by the formula:

$$T = 2\pi \sqrt{\frac{l}{g}} \left[1 + (\tfrac{1}{2})^2 \sin^2 \frac{i_0}{2} + (1.3/2.4)^2 \sin^4 \frac{i_0}{2} + \cdots\right] \quad (22)$$

where i_0 is the angle made by the string with the vertical at the start of the oscillations. For small amplitudes the period formula becomes

$$T_0 = 2\pi \sqrt{\frac{l}{g}} \quad (23)$$

Compound Pendulum: Reversible Type

A compound pendulum is a rigid body of any shape suspended by a horizontal axis and swinging through a small angle with negligible friction. Figure 133a shows a vertical section through the center of mass C and perpendicular to the axis of suspension S. The gravitational moment tending to rotate the pendulum about S is $mgh_1 \sin i$. The acceleration is $\frac{d^2i}{dt^2}$. Hence, from Newton's second law of motion

$$I_s \frac{d^2i}{dt^2} = -h_1 mg \sin i$$

where I_s is the moment of inertia about the axis through S and m is the mass of the pendulum. This equation of motion for a compound pendulum

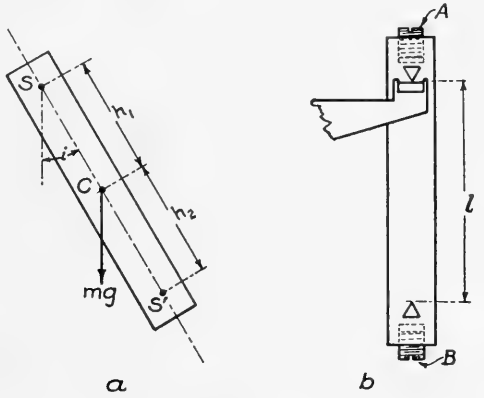

FIG. 133.—Schematic diagrams of reversible type, compound pendulum.

is similar to that for a simple pendulum. Hence, for small values of i the solution is a periodic function with period T_1, where

$$T_1 = 2\pi \sqrt{\frac{I_s}{mh_1 g}}$$

A comparison of this expression with the corresponding expression for a simple pendulum (Equation 23) shows that the compound pendulum is

equivalent to a simple pendulum of length l_1 where $l_1 = \frac{I_s}{mh_1}$. Hence, a compound pendulum may be used to determine the absolute value of g provided the equivalent length l_1 can be evaluated.

To determine the equivalent length l_1, use is made of the fact that to every point of suspension S there corresponds another point S', known as the center of oscillation, which has the property that the period of vibration about it is the same as the period of vibration about S. The proof that there is such a center of oscillation is readily shown by using a well known relation between the moment of inertia I_c about an axis through the center of mass C and the moment of inertia I_s about a parallel axis through S. That is,

$$I_s = I_c + mh_1^2 \quad \text{or} \quad I_s = mk^2 + mh_1^2$$

where k is the radius of gyration about the center of mass. If one substitutes the latter value for I_s into the expression for the period one obtains

$$T_1 = 2\pi\sqrt{\frac{mk^2 + mh_1^2}{mh_1 g}} \quad \text{or} \quad T_1 = 2\pi\sqrt{\left(\frac{k^2}{h_1} + h_1\right)\frac{1}{g}}$$

Hence, the length l_1 of the equivalent simple pendulum may be written in the form

$$l_1 = \frac{k^2}{h_1} + h_1$$

In the same manner it may be shown that the period of vibration about a parallel axis through another point such as S' on a line through S_c extended is

$$T_2 = 2\pi\sqrt{\left(\frac{k^2}{h_2} + h_2\right)\frac{1}{g}}$$

where h_2 is the distance between parallel axes through S' and C. The length l_2 of the equivalent simple pendulum for this case is

$$l_2 = \frac{k^2}{h_2} + h_2$$

For $l_1 = l_2$ the periods of vibration about the two axes S and S' will be the same. This condition may be written in the form

$$l = l_1 = l_2 = \frac{k^2}{h_1} + h_1 = \frac{k^2}{h_2} + h_2$$

On elimination of k, this condition becomes

$$l = h_1 + h_2$$

which is the relation sought.

The principle of the practical method advanced by Kater for determining the distance l between a point of suspension S and the corresponding center of oscillation S' will be evident from Figure 133b. The procedure consists simply in adjusting the two weights A and B until the period of vibration is the same when the pendulum is caused to vibrate first about S and then about S'. (An alternative design applicable in certain cases employs only one movable weight mounted between S and S'.) When the periods about S and S' have been made equal, the distance between the two parallel axes of suspension through S and S' is equal to the length of the equivalent simple pendulum. This distance can be measured with considerable accuracy and from it and the measured period of the pendulum, the value of g can be computed. Thus, the Kater pendulum can be used for absolute determinations of g in terms of measurable distances and times.

The absolute value of the force of gravity may be determined at a permanent base station by observing the period of oscillation of a pendulum under carefully controlled conditions to insure the greatest possible accuracy. A concrete pier in the pendulum room of the U.S. Coast and Geodetic Survey at Washington, D.C., is the official gravity base station for the United States. The value of gravity at this base station is 980.112 dynes. Absolute determinations, because of the elaborate precautions which must be taken to insure accuracy, require considerable time and patience.

Limitations of Commercial Pendulums

About two hours' time is required for making a station reading with the pendulum. This time requirement is greater than that usually necessary to carry out a gravimeter observation. Furthermore, according to Barton† the best commercially purchasable pendulums have a probable error of ± 0.5 milligals. It is this large probable error which limits the use of pendulums in geophysical prospecting to surveys of regional features or abnormally large anomalies. The gravitational anomalies characteristic of structures associated with oil deposits may be less than 1.5 milligals. Hence, measurements of the relative value of g in oil exploration work require a more sensitive type of instrument than the pendulum. The more sensitive instruments commonly employed to determine the relative value of g are: (a) gravity meters, or gravimeters, for direct determination of the relative value of g and (b) the torsion balance and, to a smaller extent, the gradiometer for indirect determinations.‡

Accuracy of Measurements

The accuracy of absolute gravity measurements with the reversible pendulum depends chiefly upon three factors: (1) measurement of length, (2) accuracy with which the center of gravity is placed on the line joining

† D. C. Barton, "Gravitational Methods of Prospecting," Science of Petroleum, Vol. I, Oxford Univ. Press, 1938.

‡ M. K. Hubbert and Frank A. Melton, "Gravity Anomalies and Petroleum Exploration by the Gravitational Pendulum," *A.A.P.G.*, Vol. 12, No. 9, 1928, pp. 889-898.

the two axes and the parallelism of the two axes, and (3) degree of perfection with which friction is eliminated. In use, the accuracy is chiefly dependent upon the accuracy of time measurement. The most accurate measurements of the absolute value of g are believed to be those of Kühnen and Furtwängler at Potsdam in 1898-1904 which had a probable error of three parts in a million.† Such accuracy of measurement cannot be achieved in field measurements and recourse generally is had to relative gravity measurements.

The Determination of the Relative Force of Gravity with a Pendulum

For small amplitudes of swing and when using the same pendulum for determining the relative force of gravity at various stations, a simple relationship exists. The period of vibration (T) of a given pendulum of length (l) varies with the value of the force of gravity (g) at the station, in accordance with Equation 23.

$$T = 2\pi \sqrt{\frac{l}{g}}$$

in which T = seconds; l = cm.; g = dynes/mass = cm./sec^2.

$$g = \frac{4\, l\pi^2}{T^2} \tag{24}$$

Comparative Gravity Measurements. — Relative determinations of gravity are made by first calibrating the pendulum by observing its period of oscillation at the Washington gravity base or some other base where the absolute value of gravity has been determined, and then observing the period of the same pendulum at the various field stations where readings are to be made. The value of gravity at the base and at each field station is inversely proportional to the square of the period of oscillation of the pendulum at the two stations; where subscript b = base and n = new station, with other symbols as already defined,

$$g_b = \frac{4\,\pi^2 l}{T_b{}^2}\,;\, g_n = \frac{4\,\pi^2 l}{T_n{}^2}$$

$$\frac{g_b}{g_n} = \frac{T_n{}^2}{T_b{}^2} \text{ or } g_n = \frac{g_b\, T_b{}^2}{T_n{}^2} \tag{25}$$

Comparative determinations are largely used in geodetic work. They can be made with an accuracy ± 0.0004 dynes or better, and more rapidly than absolute determinations.

Development of Gravity Work in the United States.—Active interest in gravity determinations by pendulum began in 1873 under the United

† *Handbuch der Geophysik*, Vol. 1, p. 753

States Coast and Geodetic Survey.† Between that date and 1890, many observations were made with heavy pendulums about a meter long of the Kater (K), Repsold (R), Pierce (P), and other types. (See Figure 134.) The results of these determinations were not of sufficient accuracy to be of value in modern investigations of gravity and isotasy.

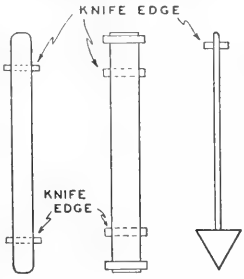

FIG. 134.—Sketch of the Pierce (P), Repsold (R), and Kater (K) pendulums. The Pierce and Repsold are reversible pendulums.

In 1891, the Mendenhall invariable ½-second (¼ meter) pendulum apparatus was designed. This equipment provided an air-tight case in which to swing the pendulum under reduced air pressure, to minimize air friction. An accurate chronometer was substituted for the clocks previously used to measure the period of vibration. These changes increased the accuracy of the measurements and lowered the time required for observation. Other improvements in the design of the government pendulum apparatus have been made since that date. By 1909, 47 stations had been occupied.

The period 1909-1930 saw some 230 stations established and the development of an interferometer method of determining the flexure of the pendulum support. After 1920, wireless time signals broadcast from the

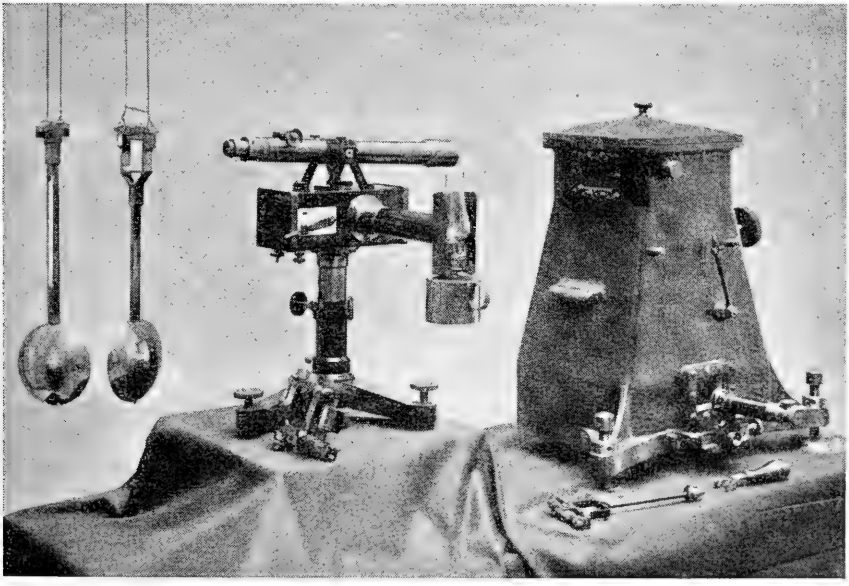

FIG. 135.—Pendulum prospecting equipment typical of the late 1920's. Left to right Two invar pendulums; light source for photographic recording; pendulum case. (Courtesy of L. F. Athy.)

† C. H. Swick, "Modern Methods for Measuring the Intensity of Gravity," *U. S. Coast and Geodetic Survey, Special Publication No. 69*, 1921.

U.S. Naval Observatory at Annapolis, Maryland, were used to calibrate chronometer rates at the field stations. A new type pendulum was also introduced made of invar, (a nickel-steel alloy of 1 part Ni and 2 parts Fe),

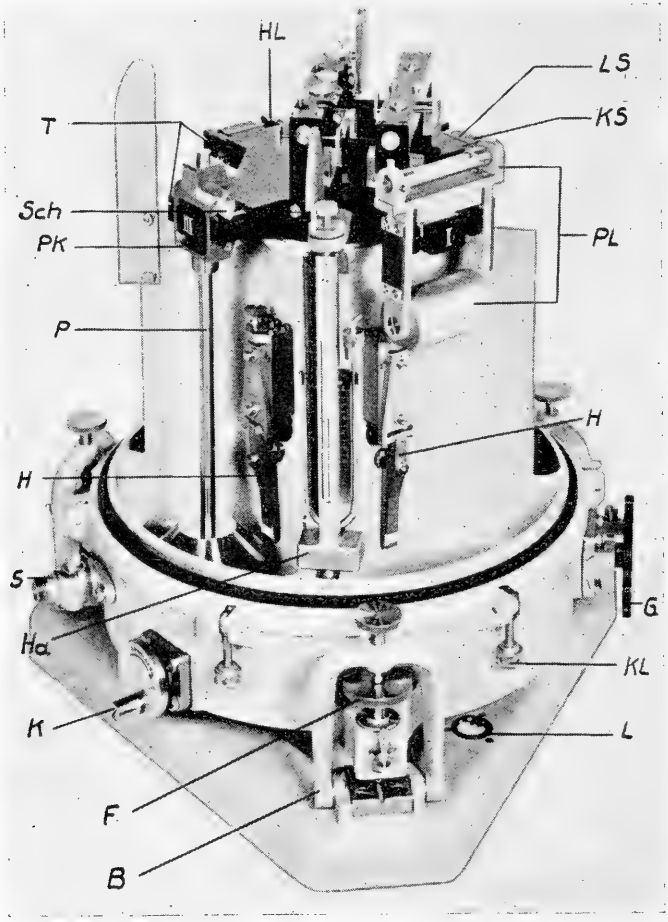

FIG. 136.—Base plate with pendulum tripod. (Courtesy of the Askania Corporation.)

F—level screw
B—holding stirrup for level screw
KL—swing bolt for hood
S—evacuation petcock
KS—headpiece of pendulum tripod
LS—agate bearing in head piece
P—pendulum
PK—pendulum head
Sch—pendulum wedge
PL—pendulum level
K—crank for releasing and clamping
HL—bearings in the arresting device
G—amplitude limiting device
H—adjusting lever for the amplitude limiting device
Ha—holder with thermometer and barometer

having a coefficient of expansion about 1/15 as much as the bronze previously used. Pendulum gravity field equipment is shown in Figures 135, 136, 137, and 138.

Apparatus

Relative gravity measurements are usually effected with the aid of a so-called invariable type compound pendulum. The pendulum as used in geophysical applications consists of two or more bobs or masses, supported by knife-edges and having lengths such that they swing in synchronism.* The bobs are released simultaneously so that their horizontal components of reaction on the support are of opposite phase and cancel each other. This minimizes the tendency of the system to sway upon its support.

Early Pendulum Prospecting Equipment.—Figure 135 shows pendulum prospecting equipment which was typical in the late 1920's. The two pendulums shown at the left of the figure are made of invar.

Von Sterneck-Askania 4-Pendulum Apparatus.—The Von Sterneck type of 4-pendulum apparatus is illustrated in Figures 136, 137, and 138. The apparatus consists of a pendulum base frame; tripod; 4 pendulums; and pendulum hood. The base frame fits into the tripod which also accommodates the pendulum and the hood.

The tripod contains all the equipment necessary for clamping; setting the pendulum into oscillation; adjusting the amplitude, etc. On the tripod is mounted an optical bridge which reflects the light coming from the point of observation via the four pendulum mirrors.

The pendulum tripod is supported by 3 level screws which rest on the base frame and are used for leveling and locking the apparatus. A disk is provided for starting the oscillation of one, two, or all four of the pendulums. A crank facilitates the releasing and clamping of the pendulums. The pendulums are supported by agate bearings and each pendulum swings in a separate chamber. (Figure 136.) The pendulum bridge consists of 6 prisms, each of which can be turned and tilted for adjusting purposes.

The pendulums are made of invar material and are gold-plated for protection against corrosion. (Figure 137.)

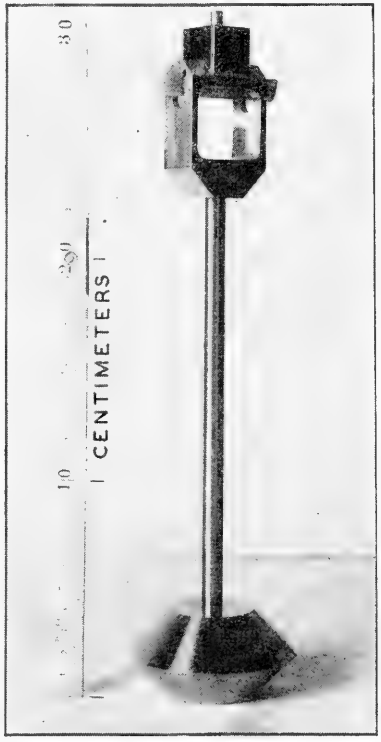

FIG. 137.—Von Sterneck type invariable pendulum. (Courtesy of the Askania Corporation.)

* A pendulum comprising two bobs is also described as a 2-pendulum apparatus; a pendulum comprising three bobs as a 3-pendulum apparatus, etc.

The wedge is made of quartz and is mounted in the pendulum head.

The metal mirror which is located in the pendulum head is ground in such a way that errors due to displacements of the plane of the mirror are minimized. The pendulum hood which covers the tripod and all its accessories is so mounted that a close air-tight fit is assured. Two windows are provided to read the thermometer and barometer and to permit the light ray to travel from the point of observation to the optical bridge and return.

Two levels, having a sensitivity of 10 sec. per division, are mounted so that they can be conveniently lowered to the agate bearings, the exact level position of which they control. Two heavy handles are provided for carrying the instrument.

During transport, the holder for the thermometer and barometer is carried in a box. Suitable means are provided so that the barometer will not be damaged while in transport, even if the mercury should be subject to considerable movement.

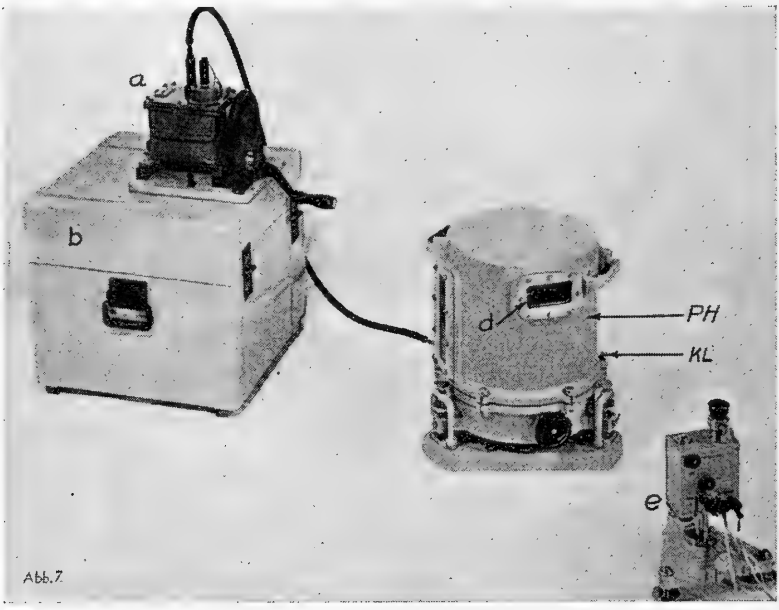

FIG. 138.—Askania 4-pendulum apparatus ready for operation.

a—oil pump
b—instrument box
PH—pendulum housing
d—observation window
e—observation equipment
KL—locking screw

GENERAL OUTLINE OF PROCEDURE AT EACH STATION FOR PENDULUM OBSERVATIONS

1. Selecting a Station

To obtain a high accuracy of the pendulum observation (about 1 milligal) it is necessary to select a place free from vibrations, preferably with a hard rock or cement

base, and not subject to large temperature fluctuations. Sufficient space must be provided for the setting up of the coincidence apparatus. (See p. 281.)

2. *Setting-up and Leveling of the Askania Equipment*

After the proper spot for the station has been located, the base frame is set on the ground, oriented, leveled and grouted with plaster-of-Paris in order to furnish a firm connection between base and ground. The pendulum apparatus is then mounted on the frame with the window facing the observation equipment. The level screws F and the pendulum levels PL (Figure 136) permit accurate leveling of the plane of the bearings. (Such leveling is necessary to prevent the pendulums from slipping off the bearings during oscillations, which last several hours.)

3. *Precautions to be Followed in Suspending the Pendulums*

In order to suspend the pendulums freely, it is first necessary to move the selector disk and the oscillation knob to the fixed stop. The operator should wear gloves when handling the pendulums in order to minimize temperature variations due to handling and deposition of oily films.

4. *Control of the Light Path and of the Amplitudes*

Before placing the hood over the apparatus, the observation equipment must be adjusted and the light path checked. Also, the magnitude of the oscillations is controlled and corrected, if necessary. The proper operation of the selector disk and oscillation knob is checked as well as the proper fitting of the hood.

The pendulum hood is fastened to the tripod base by means of 6 swing bolts. The equipment is then ready for evacuation of the air in the pendulum chamber.

5. *Evacuating the Apparatus*

For convenience, the oil pump is mounted on the shipping box (Figure 138) and the hose is fastened to the apparatus. The manufacturers recommend reducing the pressure to about 5 mm. of mercury and then admitting sufficient air to raise the pressure to about 10 mm. of mercury. By following this procedure, the danger of dew formation is practically eliminated.

6. *Adjustment of the Selector Disk: Oscillating the Pendulums*

The pendulums are lowered so that the wedge touches the bearings. (This should only be done when the oscillation knob touches the fixed stop. Also, the selector disk should be operated only when the knob is in this position.)

The various marked positions of the knob permit oscillating one, two, or all four of the pendulums at any desired amplitude.

Brown Pendulum

The current model Brown pendulum apparatus (Figure 139) consists of a standard invar quarter-meter pendulum housed in an evacuated chamber. The

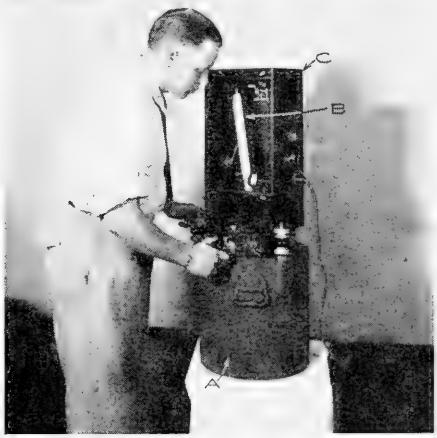

FIG. 139.—Brown gravity apparatus, with front cover removed. A, base chamber or vacuum case; B, photoelectric recording device; C, control case with cover removed. (Courtesy of U. S. Coast and Geodetic Survey.)

pendulum (Figure 140) is supported by agate knife edges, swinging on agate planes. Essential equipment used with this pendulum apparatus includes a chronograph, a radio receiver, and photoelectric and power amplifiers.

The chronograph records simultaneously both the pendulum beats and mean-time seconds (U.S. Naval Observatory time signals). Light pulses, controlled by the pendulum beats, are picked up by the photoelectric cell and amplified to operate a chronograph pen, using a relay. The time signals are received by radio, amplified, and then fed to a second chronograph pen. Both pens are adjusted to follow the same track, with one pen moving to the left and the other to the right. A micrometer-microscope is used to scale the chronograph records to 1/1000 of one second.

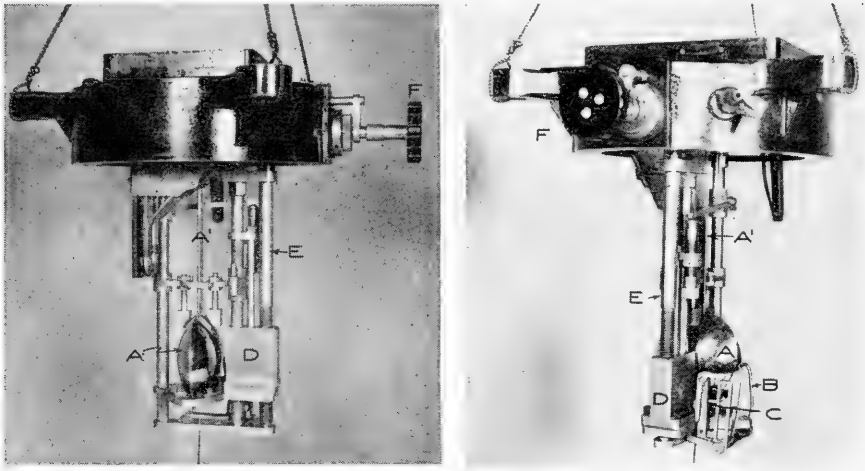

FIG. 140.—Brown gravity apparatus. A, pendulum (swing is parallel to plane of paper); A', pendulum support arm; B, lever for starting oscillation; C, release mechanism; D, pendulum clamp; E, clamp screw; F, clamp knob. (Courtesy of U. S. Coast and Geodetic Survey.)

The number of beats during the observations (which last for six hours) is determined, as is the time interval. The error in the latter is less than 0.005 second, using as control the time signals of the U.S. Naval Observatory.

The time periods of the pendulums are then corrected for pressure, temperature, and amplitude of oscillation, as well as for the slight motion of the supporting framework caused by the swinging of the pendulum. A specially designed interferometer is used to measure this movement caused by elastic yielding of the support, in units of wave lengths of monochromatic light. The instrument operates from batteries, charged in the field by a gasoline-driven generator.†

† U. S. Coast and Geodetic Survey, *Special Publication No. 233*, 1943.

Pendulum gravity apparatus, as indicated in Figures 135 to 140 inclusive, usually consists of the following essential parts:

1. One or more pendulums.
2. An air-tight receiver surrounding a suitably constructed base on which the pendulums are swung, under reduced air pressure.
3. A flash box and/or light source and telescope for observing pendulum vibration in measuring the period of oscillation.
4. One or more chronometers of high accuracy, and the necessary radio equipment for receiving standard time signals.
5. One or more chronographs. These consist of a cylindrical drum, rotated by a clock-work mechanism carrying a roll of paper on which a stylus marks the beats of a chronometer. They are used for checking rates and comparing the accuracy of chronometers.
6. An interferometer, or other device, for measuring the movement of the receiver caused by the oscillation of the pendulum.
7. Thermometers, installed in the receiver.
8. A manometer to measure air pressure in the pendulum housing.
9. An air pump for evacuating the receiver.

Field Measurements

The basic problem in pendulum gravity measurements is to determine, with the necessary accuracy, the period of vibration of a pendulum set up at each field station. The descriptions given relate, more particularly, to the Mendenhall apparatus (Figure 135), and serve to outline the general field technique and the necessary corrections. Instrumental developments in the years just prior to World War II (particularly the use of two-way radio between base and field stations) have simplified field operations and improved the accuracy of pendulum gravity measurements.

Timing.—Accuracy in gravity observations requires precise measurement of the period of the pendulum. Hourly time signals are sent out by the U.S. Navy stations at Annapolis on 4390, 9425, and 12630 kilocycles. Any sensitive short-wave receiver may be employed for receiving the time signals.

The Method of Coincidences.—In pendulum equipment where a flash box is used, two small mirrors catch the beam of light from the flash box and reflect it. One of the mirrors is attached to the support on which the pendulum swings and the other to the head of the pendulum itself.

With the pendulum at rest and the shutter of the flash box open, the beam of light, as seen through the telescope on top of the flash box, appears as two bright lines which coincide. When the pendulum is set in motion the reflected image or line from one mirror moves, while that from the fixed mirror remains stationary.

The shutter of the flash box is opened for a brief instant by an electromagnet actuated by the seconds beats of a chronometer. An observer look-

ing through the telescope sees, at each successive opening of the shutter, that the moving image changes its position relative to the fixed image. This shift takes place because the period of the pendulum is just slightly more or less than the time between the openings of the shutter.

Under these conditions, with the shutter openings representing seconds beats of the chronometer, and the pendulum likewise swinging with a very slightly different (less or more) time interval, there will be recurring intervals when the image lines will *coincide*. By carefully watching the flashes, noting the chronometer reading when a coincidence of the lines takes place, and at a later time again noting and recording the chronometer reading for another coincidence, the time interval in seconds between coincidences can be measured.

In the interval between two successive coincidences a standardized ½-second (period) pendulum will have made one more or one less than twice as many oscillations as the chronometer has beat seconds. Between any two coincidences, the number of pendulum oscillations is twice the number of seconds *(s)* plus or minus the number of coincidence intervals *(n)*. The time, or period, of one oscillation *(T)* is:

$$T = \frac{s}{2s \pm n} \tag{26}$$

the plus or minus being used when the pendulum has a period which is less or more, respectively, than its standardized ½-second value. The smaller or greater value of the period is, in turn, dependent on the local effect upon g, as can be seen from $T = 2\pi\sqrt{l/g}$.

This can be illustrated by an example. A coincidence might be recorded at 10:00 A.M. for a given observation. It would be noted as $10^h\ 00^m\ 00^s$. (h = hours, m = minutes and s = seconds). The time of the next coincidence might be $10^h\ 03^m\ 01^s$, or a coincidence interval of $03^m\ 01^s = 181$ seconds.

$$T = \frac{181}{361 - 1} = 0.50138 + \text{seconds.}$$

In the above example, the local effect was such as to decrease g, which in turn increased the period (T). Experimentally, the procedure was to compare the pendulum swings with the seconds beats of the chronometer, noting that the number of oscillations was less by one than twice the number of seconds. This implies a T greater than standard (½-second), which in turn denotes a decreased g.

An error in noting the exact time of the coincidence produces a relatively small error in the period, as the time interval between about 10 coincidences is recorded. For this reason the method is almost independent of observational errors.

The field procedure for determining the relative gravity by pendulum methods, in certain types of equipment, is based on the use of two or more pendulum instruments. The beats of the pendulum at a base station are transmitted by portable radio transmitter to the field station. There they

are recorded photographically on a strip of film on which is also recorded the beats of the pendulum at the field station.

If the times of swing (half periods) of the base pendulum and the field pendulum are exactly the same, the marks on the film which correspond to the beats of the two pendulums will coincide or lie on a straight line. If the times of swing are not exactly the same, the marks will be displaced with respect to one another. After a certain number of vibrations of the base pendulum, the marks due to the two pendulums will again coincide. This forms a coincidence, as in the case discussed previously. The number of oscillations of the base pendulum (which, in effect, functions like the chronometer previously considered) can be read directly from the photographic film.

Corrections.—A number of corrections must be applied to the period of oscillation of a pendulum. Corrections are made for the following effects: (1) infinitesimal arc of swing, (2) temperature, (3) pressure, (4) true sidereal time, (5) inflexible support.

As the details of determining and applying these corrections vary considerably with different pendulum apparatus they will not be presented. However the order of magnitude of the above corrections will show their relative importance.

Arc of swing. An error of 0.4 mm. in observing the initial arc of swing of the pendulum, or of 0.8 mm. in observing the final arc, produces an error of 0.001 dyne in the computed value of g. These figures apply to the Coast and Geodetic equipment shown in Figure 135.

Temperature. In the same equipment an error of 0.6° C. in temperature with bronze pendulums and of 0.9° C. with invar pendulums makes an error of 0.001 dyne in g.

Pressure. An error of 3 mm. of mercury column in the mean pressure inside the receiver may cause, as in the above cases, 0.001 error in g. This figure applies to invar pendulums.

Chronometer rate. The rate at which the chronometer used to determine the period gains or loses per 24 hours must be considered. Accuracy in timing is in fact the crux of pendulum gravity measurements. An error of 0.04 sec. in the observed daily rate of the chronometer, reduced to sidereal time, may bring about an error of 0.001 in gravity value calculated.

Flexure of the pendulum support. Observations with pendulums show that practically all so-called "rigid" supports have a certain flexibility. When a pendulum swings it communicates motion to the receiver in which it is housed and to the support, causing them to oscillate. This oscillation in turn affects the observed period of the pendulum.

Flexure of the support can be measured by an apparatus operating on the principle of the interferometer. This device consists of a lamp and lens properly set up to furnish a beam of sodium or other monochromatic light. A glass plate is arranged so as to separate the beam into two parts, one transmitted and the other reflected by the plate. Two mirrors are provided, one in the path of each beam, and a telescope for observing the resulting image. One of the mirrors is mounted on the pendulum receiver and the other on an independent support in front of it. When the different parts of

this apparatus are properly adjusted, dark and light bands will appear in the field of the telescope, due to interference of the sodium light waves of the two beams.

The slight motion imparted to the case by the swinging pendulum shifts the mirror on the case, making a small variation in the length of the path of one of the beams. This causes the interference bands to shift back and forth. The amount of the shift may be measured by a scale in the field of the telescope. The movement of the edges of a band divided by the width of the band (in scale divisions) gives the movement of the receiver in units of band width.

Tests with pendulums swung on supports of different degrees of flexibility will show the relation between the movement of "fringe" bands and the resulting error in the period of the pendulum. Experiments indicated that for the above-described equipment a movement equal to the width of 1 band produced a change of 173 in T in units of the 7th decimal place. This constant was determined with a pendulum swinging through a 5 mm. arc on the scale. All flexure observations are reduced to this arc before correcting T for flexure of the support.

The correction to the period is $D \cdot 173$, where D = the displacement in fringe bands per 5 mm. of arc. It develops that an error of 0.014 fringe of sodium light in observing flexure may cause an error of 0.001 in the value of g.

Flexure of the support is found in some types of apparatus by observing the oscillation acquired by a special pendulum in a separate place on the supporting framework. When a run is started this flexure-measuring pendulum is at rest. It is set in motion by the vibration of the working pendulum of the equipment. Flexure and the correction for it can be determined in terms of the period of swing imparted to the special pendulum.

To insure a rigid support for the base chamber, a hole about 10 inches in diameter and 12 inches deep is dug at each station. Plaster of Paris is placed in the hole and wetted with water. When the proper consistency has been obtained, the base chamber is set into the plaster and leveled with the small universal level bubble in the base. Most plasters will set rigidly within about thirty minutes. At permanent stations, concrete piers are recommended as a support for the apparatus. A thin layer of plaster of Paris is used to bond the base to the pier.

Example.—A certain set of pendulum observations made in 1901 on the island of Sumatra showed the first coincidence recorded at 9h 59m 03s and the final one at 16h 54m 46s, covering a total time of 6h 55m 43s, or 24,943 seconds. The approximate length of a coincidence interval was 181 seconds.

The number of coincidence intervals was verified by dividing 24,943 seconds by 181, which gave 137.9. As the number of coincidences must be a whole number, 138 was indicated. The true length of the coincidence interval (24,943 s./138) was 180.75 seconds.

The uncorrected period = 0.501386 sec., which shows the accuracy of the method. To this figure the following corrections were applied:

Uncorrected Period	0.5013869	
Corrections		
Arc	−5	
Temperature	−436	
Pressure	+9	
Rate (Chronometer)	+128	
Flexure	−6	
Corrected Period	0.5013559	seconds

As previously described, the value of gravity can be found, for the above field station, by comparing the period of the particular pendulum used with its period at

some base station where the value of gravity is known, such as at Washington, D.C. This assumes that no change has taken place in the pendulum between readings at the different stations.

TORSION BALANCE METHOD OF GRAVITY PROSPECTING

The torsion balance measures the gravity gradient in a horizontal plane and the curvature quantity or horizontal directive tendency (H.D.T.) directly.

This instrument was introduced into the United States in 1922 and from that time until about 1940 was very widely used in reconnaissance and detailed gravimetric work in the American oil industry. At the peaks of its popularity, from 1928 to 1930 and from 1934 to 1936 inclusive, not less than 125 instruments were engaged in exploration for oil each year.

Partial or total credit is given to the torsion balance for the discovery in the Gulf Coast area of seventy-nine oil fields and salt domes up to the beginning of 1938. † The addition in oil reserves which should be credited entirely to the torsion balance probably amounts to 1,027,500,000 barrels. (The pendulum and gravimeter should be given credit in the same area for the discovery of 108,000,000 barrels of oil, during that same period.) After the year 1938, the gravity-meter almost completely superseded the torsion balance and should be credited with practically all of the subsequent gravimetric discoveries.

The Eötvös Unit.—The gradient of gravity as measured by a torsion balance is defined as *the rate of change of the force of gravity per centimeter,* in a horizontal direction. It is measured in Eötvös units, (named for the Hungarian physicist, Roland von Eötvös); symbol E, $1\ E = 1 \cdot 10^{-9}$ dynes per cm. Maximum gradient is implied in speaking of the gradient, or the dg/ds of Figure 131. A gradient of gravity of 1 E indicates an increase in the intensity of gravity per centimeter (in a *horizontal* direction) in the amount of $1 \cdot 10^{-9}$ dynes. This is a rather small quantity.

An Eötvös unit is about 1 millionth of a millionth (10^{-12}) of the average value of the force of gravity ($\backsim 10^{+3}$ dynes). Such a small quantity is difficult to comprehend. As an example, it has been calculated that if a piece of wire weighing 1 gram were stretched out to encircle the earth 25 times and 1 centimeter of the stretched wire were cut, the segment would weigh $1 \cdot 10^{-12}$ grams. This weight is in the order of the magnitude of the forces measured by the Eötvös torsion balance.

Relation of Gravity Gradient to Subsurface Geology.—The gradient of gravity, as was seen from the $\Delta g''_0$ curve for the anticline or granite

† V. G. Gabriel, "Probable Discovery Rates in the Gulf Coast Area," *Oil Weekly*, Vol. 95, No. 1, Sept. 11, 1939.

ridge in Figure 126, is related to subsurface configuration of materials of different densities. Specifically, the gradient reflects the shape and slope of the contrast surface of light versus heavy material at depth, i.e., the granite against the sediments in the illustration. A plan view of the distribution of the gravity gradients in vector form for a traverse across a granite ridge is shown in Figure 141. The gradient arrows across a syncline and across a fault appear in Figures 142 and 143.

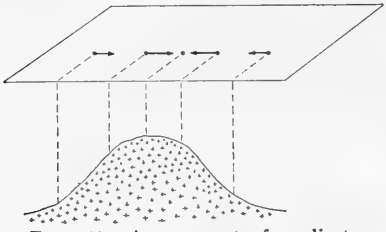

FIG. 141.—Arrangement of gradient arrows for torsion balance traverse across a granite ridge. Note zero gradient at crest of ridge.

In the case of a salt dome, as illustrated in Figure 144, the gradients radiate outward toward the relatively heavy sediments surrounding the dome. If, as is often the case, the salt dome has a heavy cap rock, the direction of the gradient arrows may be controlled by it; they may then be reversed, and converge to a point over the center of gravity of the salt plug and cap rock. As indicated in Figure 145, at stations well removed

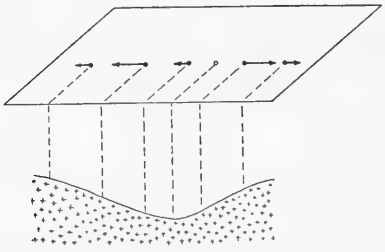

FIG. 142.—Showing distribution of gradients of gravity across a syncline. Gradient arrow is like a dip symbol, pointing up-dip.

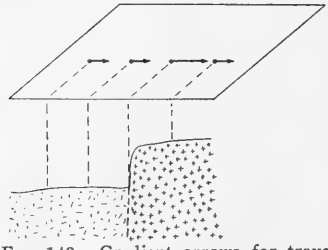

FIG. 143.—Gradient arrows for traverse across a fault. The gradient shows a maximum value for the station over the fault. At this position, the maximum rate in change of gravity occurs.

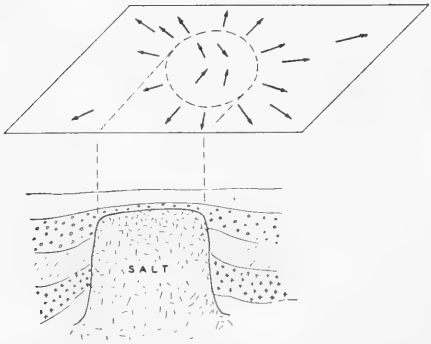

FIG. 144.—Gradient arrows radiating out from the crest of a simple salt dome. They point toward the relatively dense sediments surrounding the dome.

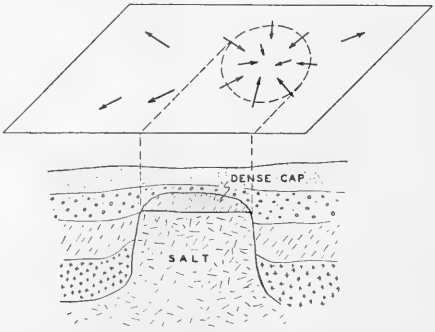

FIG. 145.—Gradients over a salt dome with a dense cap rock. Above and near the dome, the gradients are directed to the center of the dome due to the controlling influence of the cap rock. At a distance from the dome, the gradients reverse and point to the more dense surrounding sediments.

from the dome the influence of the shallow dense cap may become ineffective; the gradients may reverse and be directed away from the dome because of the influence of the deep-seated, lighter salt. For stations immediately above the dome itself, in both cases, the gradients may be weak and erratic as indicated in the figures.

As illustrated in the preceding simplified examples, the gradient points toward the higher structural position of a subsurface heavy mass. The length of the gradient vectors is directly proportional to the slope of the subsurface heavy mass or, more definitely, to the slope of the contact plane of heavy and light material in the subsurface. It is also proportional to the density contrast between heavy and light material on the two sides of this contact plane.

Two hypothetical cases will yield no gradient: (1) where there is no slope to a density contrast plane in the subsurface, and (2) where there is no density contrast in the section of rock below the surface, even though the beds might have a slope.

Curvature Quantity or R - line Value.—The torsion balance measures another feature relating to the configuration of subsurface masses called the *curvature quantity or R - line value.* It is known to the British as the H.D.T. or horizontal directive tendency.† The R-line value, as will be shown, reflects curvature conditions of equipotential surfaces of gravity.

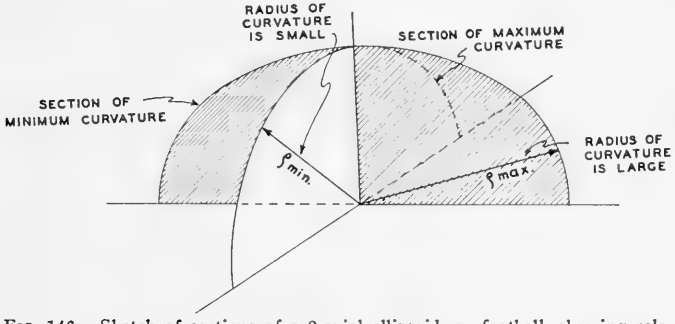

FIG. 146.—Sketch of sections of a 2-axial ellipsoid, or football, showing relation of curvature and radius of curvature ρ of sections, taken at right angles to each other.

ρ_{max} = maximum radius of curvature = section of minimum curvature.

ρ_{min} = minimum radius of curvature = section of maximum curvature.

The latter may be illustrated by a two-axial ellipsoid, such as a football. The curvature of the section through the long axis of the football is small. The curvature of such a section is inversely proportional to the radius of curvature (ρ). The section referred to, therefore, has a large curvature radius. This is shown in Figure 146.

The curvature of the section of the ellipsoid taken along a mid-perpendicular at right angles to its long axis is large, and its radius of curvature

† Edge and Laby, *Geophysical Prospecting,* Cambridge Univ. Press, 1931.

correspondingly small. We may represent by the length of a line the difference in curvature between such sections; namely, the sections of maximum and minimum curvature.

The R-line value, or curvature quantity, as determined by the torsion balance is, specifically, the amount of the difference in curvature of the sections of maximum and of minimum curvature of the gravity equipotential surface through the center of gravity of the instrument at the station of observation. *Equipotential surfaces of gravity follow the outline and configuration of subsurface heavy masses.*

The general equation for the R-line value is:

$$R = g\left(\frac{1}{\rho \text{ min.}} - \frac{1}{\rho \text{ max.}}\right) \tag{27}$$

R = R-line value; g = gravity; ρ = radius of curvature of gravity equipotential surface; min. = minimum; max. = maximum.

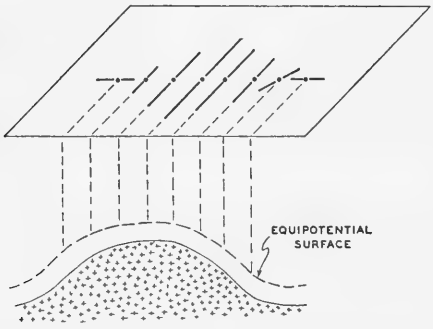

FIG. 147.—Distribution of the R-line value for a traverse across an anticline. Note that R-line is maximum at crest of anticline and lies parallel to its axis, and for stations in the adjacent syncline the R-line is rotated by 90°.

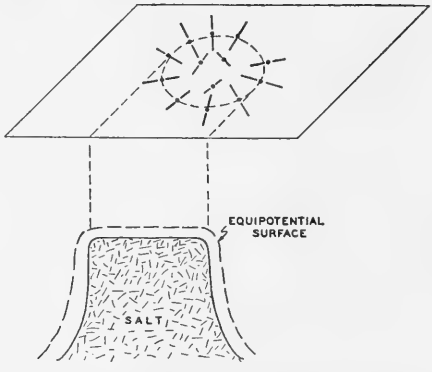

FIG. 148.—R-line values from torsion balance measurements over a salt dome: maximum R-line for stations above the edges of the dome; weak erratic curvature quantity values for stations above the dome itself.

The distribution and character of the curvature quantity or R-line value for torsion balance traverses across a number of typical structural situations are illustrated in Figures 147, 148, and 149. Figure 147 shows the case for an anticline flanked by two adjacent synclines.

Where stations are above the anticlinal portion of the structure, the R-line value parallels the strike of the subsurface heavy mass.

Where the station is above the syncline, the R-line lies in a direction at right angles to the strike (of the adjacent anticline). This reversal by 90° in the R-line is one means of determining the change from an anticlinal to a synclinal shape of the equipotential surfaces of gravity conformable with the subsurface mass. The maximum value of the curvature quantity is over the crest of the anticline.

Around the edges of a salt dome, as given in Figure 148, the R-line values radiate outward and are, in general, at right angles to the surface trace of the edge. Stations located in the vicinity of the trace show large values, but stations situated above the dome itself and inside the edge trace are usually small and indeterminate in direction. This is logical, since the top of a salt dome is, in general, rather flat with little curvature difference for different sections of the equipotential surfaces conformable to it. The edge stations, however, express the sharp difference in curvature between the more or less flat top of the dome and its very steep sides, resulting in a large curvature quantity.

The presence of a dense cap rock over a salt dome may not necessarily alter the diagnostic characteristics of the curvature quantities considered above. The R-line values express differences in the curvature of the equipotential surfaces of gravity which follow the outlines and shape of subsurface geologic structures, such as anticlines, domes, etc. More strictly considered, the equipotential surfaces reproduce with subdued outlines the density contrast surfaces or planes due to the structures.

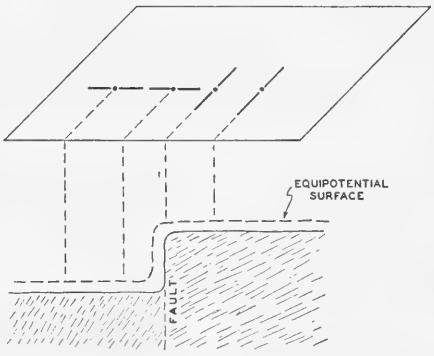

FIG. 149.—R-line values for stations across a fault. The presence of the fault is indicated by a rotation of 90° in the direction of the R-line quantity.

The above points may be further illustrated by a traverse of R-line values across a fault, Figure 149. The position of the fault is indicated by a 90° change in direction of the R-line. Such a reversal indicates that for stations above the down-throw side the equipotential surfaces are warped down (synclinal conditions), while for stations over the upthrow side, these surfaces are warped up (anticlinal conditions or with R-lines parallel to the strike).

The R-line value, like the gradient, is given in two components from torsion balance measurements. The resultant curvature quantity from the north-south and the east-west components is plotted with its *center* at the station on final maps, as shown in Figures 147 to 149 inclusive. The unit in which differential curvature is measured is $1 \cdot 10^{-12}$ radians per centimeter, which expresses the second term in the right hand side of Equation 27. This quantity is multiplied by g, which is approximately 10^3 c.g.s in magnitude, so that R-line values come out in units of 10^{-9}. This is numerically, though not dimensionally, the same as the Eötvös unit. The R-line quantities are plotted therefore in numerical equivalents of Eötvös units.

The gradient and the curvature quantities illustrated in Figures 141 to 149 serve as a background of basic type cases. Actually, such simplified structures are seldom encountered, and the regional effects may mask or

greatly modify the results. The map showing the gradient and curvature values over an anticline in northern Mexico is given in Figure 150 as a summary example.

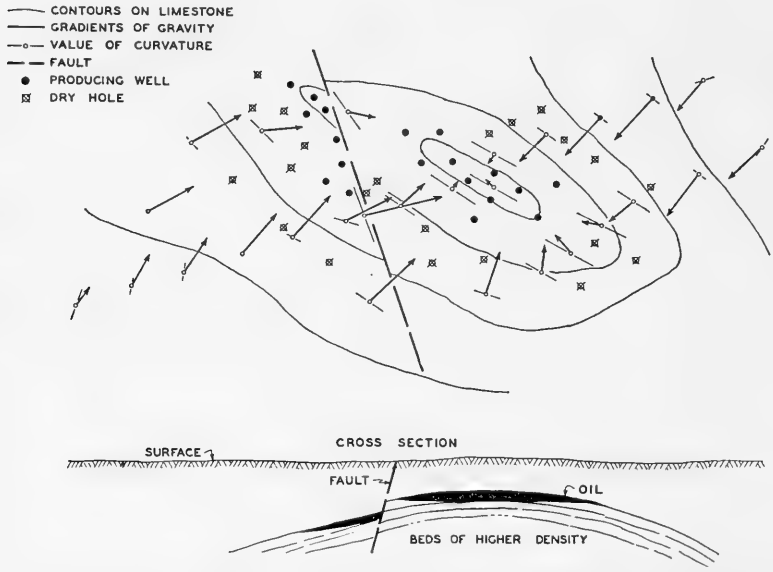

FIG. 150.—Gravity gradient and curvature values over an anticline in northern Mexico. (Courtesy of the American Askania Corporation.)

Density Determinations.—The importance of density of rocks and formations and of density contrast surfaces has been brought out in the preceding section. The density of any material is defined as its mass divided by its volume. One common method of determining relative densities, in the laboratory, is to weigh the sample first in air, and then in water to find its volume. The difference in weight in air and in water gives the weight of the volume of water displaced, hence the volume. (1 cubic centimeter of water weighs 1 gram.)

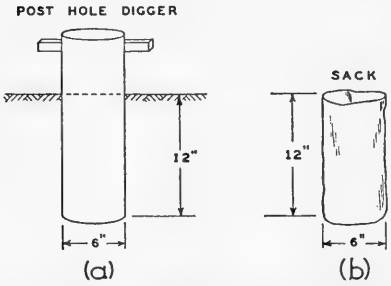

FIG. 151.—(a) Metal cylinder with handle, used in taking sample of soil for density determination. (b) Cloth sack used to find volume of material.

To apply the terrain correction necessary at a torsion balance station, the density of the surface material must be determined or estimated with fair accuracy. The equipment used in one very simple method of measuring density of the surface material in the field is shown in Figure 151.

A light steel cylinder or tube, about 18 inches long and 6 inches in diameter, fitted at its top end with a handle-bar, is turned and pushed into the ground to a depth of

about 1 foot. The core is removed from the cylinder and put into a container, or on a small sheet of canvas. The bottom of the hole is leveled, and small rocks removed. This material is added to the core, and the total material removed from the hole is weighed.

The volume of the hole is measured by putting into it a thin cloth sack of slightly larger diameter and of cylindrical shape. The sack is filled to the level of the original ground surface with glass beads or small marbles (about ¼-inch diameter) or other constant-volume, light-weight material. The volume of the material required to fill the sack is then measured, in cubic centimeters. The density of the surface layer is calculated by dividing the weight (grams) by the volume (cubic centimeters).

At the risk of generalization it may be said that most sedimentary formations have been deposited in fairly large basins and their density remains substantially constant, if undisturbed, for considerable distances laterally. This makes the assumption of uniform density of beds and the continuity of density contact surfaces, or surfaces of density contrast, valid to a useful degree, giving a basis for interpreting gravity results.

It is not implied that lateral changes in density may not give rise to gravity anomalies, for such are of record. However, they are the exception rather than the rule. In fact, if the density of the underlying materials is *not* reasonably uniform (as may be the case in glacial drift, which changes character very rapidly in short distances and in which boulders of various sizes may be present) the measured values of gravity gradient and curvature may be erratic and entirely useless.

Essential Features of the Torsion Balance

Whenever the gravitational field is warped or distorted, the values of gravity at neighboring points on the surface of the earth differ both in magnitude and direction. Thus, if two small masses at different elevations are supported at opposite ends of a beam which is suspended by a torsion wire, the equipotential surfaces passing through the two small masses will not be parallel and the magnitudes of the force of gravity acting on the two masses will not be the same. The nonparallelism of the two equipotential surfaces through the two masses and the difference in the forces of gravity acting on the masses create a rotational torque which acts on the suspended system. The torsion balance is an instrument for measuring this rotational torque. In principle, the torsion balance is simple. However, due to the extreme precision of measurement required, it is a complex and highly refined instrument.

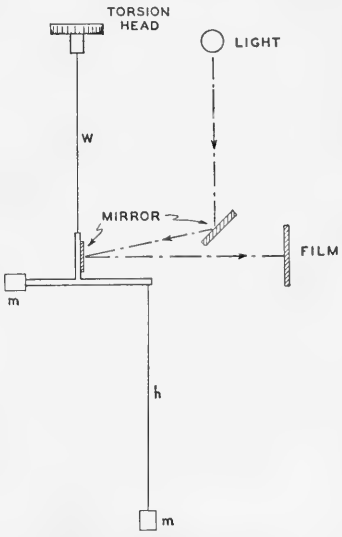

Fig. 152.—Schematic representation of Eötvös torsion balance.

A schematic representation of an Eötvös

torsion balance is shown in Figure 152. W is a calibrated torsion wire of very small diameter, terminating in a support carrying a small mirror and an aluminum bar of negligible mass. A small weight is fastened to one end of the bar, and a similar weight is suspended from a fine wire on the other end. The angular deflection of the suspended system is measured with the aid of a telescope by observing the shift of a scale image reflected by the mirror. The torque T required to rotate the swinging system (balance beam, weights, and mirror) through an angular deflection θ, with a torsion constant of τ, is

$$T = \tau\theta.$$

The working equation of the torsion balance will be determined therefore by an expression for T in terms of the parameters measured at a particular station and the instrumental constants of the balance.

The gravity force which turns the beam against the torsional resistance of the wire may be divided into two parts, viz.:

1. The force arising from the curvature of the equipotential surface passing through the center of gravity of the balance beam, called the *curvature quantity,* and

2. The force arising from the convergence of the equipotential surfaces passing through the hanging weight mass and through the mass on the end of the beam. This is called the *gradient of gravity.*

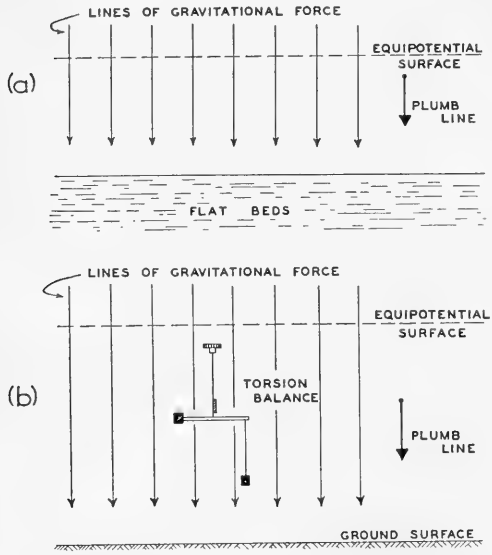

FIG. 153.—(a) Illustrating conditions of lines of force of gravity and an equipotential surface at right angles to it, for flat uniform beds in a local area. (b) Torsion balance placed in such a field experiences no twisting force. Direction of force lines shown by plumb line.

Curvature of Lines of Force of Gravity.—Consider the direction of the lines of force of gravity for a restricted portion of the earth's surface where there is no discontinuity in density in the subsurface and where the beds making up the geological section are flat. In such an ideal case, the direction and intensity of the lines of gravitational force would be the same at each of a series of closely spaced points across such an area. The lines of force would be parallel to each other and their direction would be shown by the direction of a plumb line. (See Figure 153a.) No forces would act to produce a twist on a torsion balance placed in such a force

field, as indicated in Figure 153b. An equipotential surface which would lie at right angles to the gravity force lines would be flat and horizontal.

If a mass of high density, such as a granite ridge, is introduced into the gravity force field pictured in Figure 153, an anomaly is created and the direction of the lines of force of gravity will be deflected very slightly toward this heavier mass. This will cause a curvature or distortion in the lines of force of gravity, as shown in Figure 154.

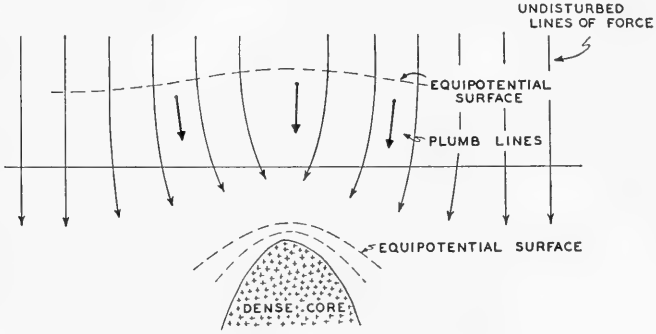

FIG. 154.—Showing the effect of a heavy subsurface mass which causes a deflection of the lines of force of gravity toward it and the arching of gravity equipotential surfaces over it.

A plumb line would show this deflection if we were able to measure the very minute change in direction thus caused. An equipotential surface which is everywhere at right angles to the direction of gravity force would be arched up above the heavy subsurface mass. These conditions are illus-

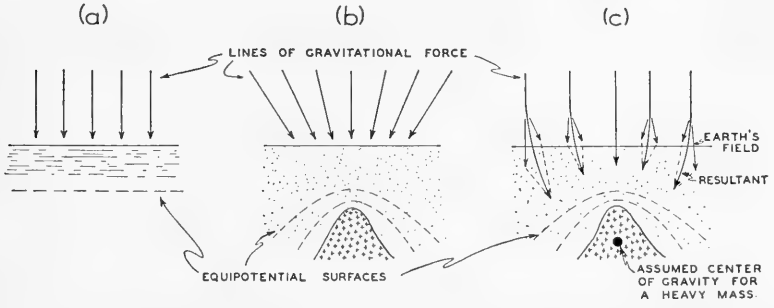

FIG. 155.—(a) Force lines of gravity over a homogeneous uniform density area; (b) force lines created by heavy subsurface mass only (theoretical case); (c) the resultant direction of the lines of force of gravity where a dense mass is introduced into the earth's field. Equipotential surfaces are given in each case.

trated again in the three parts of Figure 155 which show (a) the lines of force for an area where uniform conditions prevail; (b) the lines of force which would exist if the mass only were effective and (c) the resultant or deflected force lines, as caused by the combined attraction of the heavier mass and the center of gravity of the earth.

A torsion balance placed in a distorted force field will be deflected and twisted by the gravity forces acting on it, as illustrated in Figure 156. It will be understood that the curvatures of forces and equipotential surfaces are greatly exaggerated in the illustrations. The actual curvatures are extremely small, on the order of 10^{-12} radians per centimeter.

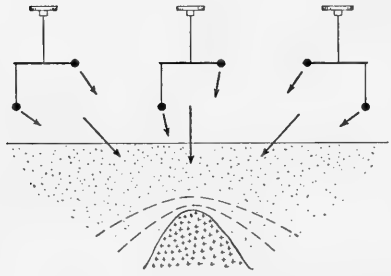

FIG. 156.—Showing the deflection of a torsion system by the curvature of the lines of force of gravity where a heavy mass is present in the subsurface.

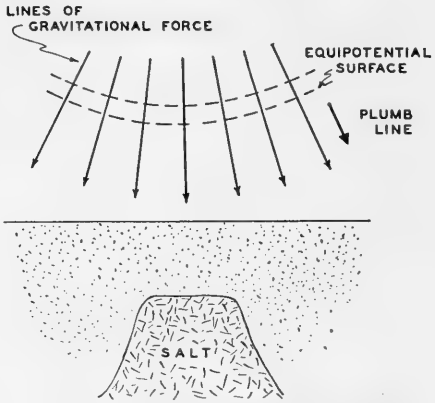

FIG. 157.—Illustrating the effects on lines of force of gravity and equipotential surfaces above a salt dome.

A mass of low density below the surface, such as a salt dome, would create a dispersion of the force field or a warping in the direction of the lines of force of gravity as illustrated in Figure 157. Such a low density area produces a sag in the equipotential surfaces above it. A plumb line at a station over a salt dome would be deflected toward the more dense sediments surrounding the dome.

Gravitational Potential and Equipotential Surfaces.—To understand the forces acting on a torsion balance, it is necessary to examine the nature of the potential function of the gravity field and, in more detail, the concept of equipotential surfaces of gravity. If we consider the space around a sphere of mass m, a mathematical function can be set up, called the *potential function,* which expresses the gravity potential for every point in this space.

Referring to Figure 158, the force on a unit particle at P_1, due to the spherical mass, is $F = -G\frac{m}{r_1^2}$, where the minus sign denotes that the force is in the negative r_1 direction, or is toward m.

The difference of potential between two points in a field is defined as the negative of the work done *by the field* in carrying the particle between the points. Physically, this means that a particle in a force field (force of gravity, in this case) will move from a point of higher to a point of lower potential. The potential is such that the magnitude of its space rate of

change, or gradient, at a point is the force which would act on a unit particle at this point. (To find the force on other than a unit particle, the force on a unit particle must be multiplied by the magnitude of the particle.)

To denote the direction of the force, it must be recalled that the particle will move from higher to lower potential. Thus if the gradient of the potential, in the positive r direction, is positive, the potential must be increasing in that direction. However the force is directed in the opposite direction, and the conclusion is that a minus sign is necessary. Consideration will show this to be true for all types of conservative fields (those which have a potential), be the force attractive or repulsive.

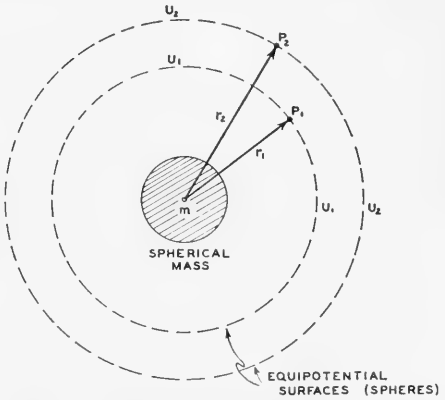

FIG. 158.—Showing equipotential surfaces U_1 and U_2 surrounding spherical mass m. P_1 and P_2 are points on surfaces U_1 and U_2 respectively.

Thus

$$F = -\frac{\partial U}{\partial r} \tag{28}$$

If, of course, the gradient is measured in the negative r direction, the minus signs will cancel.

From 28,

$$U = -\int F\,dr \tag{29}$$

It is apparent that U will not be uniquely determined to the extent of a constant of integration. However if the potential at infinity is arbitrarily set at zero, the potential at a point may be completely defined.

We are most concerned, however, with differences of potential. This has already been defined (ΔU) as the negative of the work done by the field in moving a particle between the points. That is, if the field has done work in moving a particle, it must, by conservation of energy, be at a lower potential at the final point. Its potential for doing work on a particle at this new point must have decreased.

Mathematically, in moving a particle from P_1 to P_2 (Figure 158) the field does work

$$W_{P_1P_2} = \int_{r_1}^{r_2} F\,dr = G\int_{r_1}^{r_2} \frac{-m}{r^2}\,dr = Gm\left(\frac{1}{r_2} - \frac{1}{r_1}\right) \tag{30}$$

a negative quantity.

The difference of potential

$$\Delta U = U_{P_2} - U_{P_1} = -W = Gm\left(\frac{1}{r_1} - \frac{1}{r_2}\right) \tag{31}$$

a positive quantity.

It is thus apparent that P_2 (at radius r_2) is at a higher potential than P_1 (at radius r_1). If the opposite were true, a particle in going from a higher to a lower potential would move away from the earth rather than toward it.

If now, point P_2 is considered as removed to infinity and $U_{P_2} = 0$, then

$$U_{P_1} = -G\frac{m}{r_1} \tag{32}$$

It is thus possible to define the gravitational potential at a point P_1 as

$$U_{P_1} = -\int_{\infty}^{r_1} F\,dr \tag{33}$$

or, in words, the potential at P_1 is the negative of the work done by the field in moving a particle from infinity to the point P_1.

Equipotential surfaces can be drawn about the spherical mass m (Figure 158). They are obviously spheres (the loci of all points a distance r from m). Likewise the equipotential surfaces arising from cylindrical masses are cylindrical in shape and coaxial with the cylindrical mass.

Equipotential surfaces can converge, but they do not touch each other, as such contact would represent one point having two different values of potential, which is not possible. Such surfaces follow the contours of heavy (dense) masses or configurations in smooth, gently-curved shapes.

Equipotential surfaces in the earth's gravitational field, as the term implies, are surfaces having at every point thereon the same value of gravity potential. They are also called *level* or *niveau* surfaces. Equipotential surfaces are *not* planes of equal gravity force, as they relate to a function of m/r, while gravity force is a function of m/r^2. The surface of a lake or other still body of water is an equipotential surface. Such surfaces are everywhere perpendicular to the direction of the force of gravity.

The equation for a level surface may be written as: $\frac{dU}{ds} = 0$ where s is a direction *in* the surface; or the equation may be written as U = a constant.

It also follows from the above that equipotential surfaces are arched over anticlines, since they are at all points perpendicular to the direction of the force of gravity. No work is involved in moving a unit mass from one point to another in an equipotential surface.

Potential difference between two points in a field has been logically and physically defined as the negative of the work done by the field in moving a particle between the points. A field doing negative work in moving a particle implies that work has been done against the field by outside forces. In such a situation the potential difference is positive (the negative of negative work) and the final point is at a higher potential than the initial. This is physically sound, since work has been done against the field by outside forces, and its potential for doing work on a particle at the final point has been increased. This situation corresponds to moving a mass away from the earth. Outside forces must do work (lifting) : the potential of the final point is greater, since the earth's gravitational field will return the work in moving the particle back to the earth's surface.

The difference in potential may thus be equivalently considered as the *positive* of the work done by *outside forces* against the field in moving the particle between the points. Mathematically, the equivalence can be seen as follows:

The outside force (F_o) necessary is equal but opposite to the gravitational field ($F_o = + G\frac{m}{r^2}$), thus making one sign change from our original definition. But ΔU is the positive of the work done by these outside forces, thus making the second sign change. The mathematical formulae remain identical. Care must be exercised to use one or the other definition consistently.

Finally it has been stated that the potential is such that $F = -\frac{\partial U}{\partial r}$; gravitational force per unit mass along r equals the negative space derivative of the potential.

$$U = -G\frac{m}{r} \quad \text{and} \quad \frac{\partial U}{\partial r} = G\frac{m}{r^2}$$

$$F = -\frac{\partial U}{\partial r} = -G\frac{m}{r^2}$$

consistent with our original definition. m denotes the mass creating the field.

Figure 159 illustrates a short section taken between two equipotential surfaces over an anticline, showing their convergence.

The gravity potential on the surface $AB = U_2$, and on the surface CD below it is U_1. The distance separating the surfaces from A to C = h_1, and between B and D = h_2. The mean gravity force along AC is g_1, and the mean gravity force along BD is g_2. Such a pair of equipotential surfaces might pass through the upper and the lower weights of a torsion balance. It is assumed that g varies along an equipotential surface such that g_1 and g_2 are not equal. However the variation of g between surfaces U_1 and U_2 along a given h (plumb line direction) is slight and the mean value practically constant.

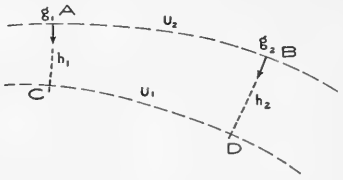

FIG. 159.—A short section taken between two equipotential surfaces over an anticline, showing their convergence. g_1 is the mean gravity force along AC, and g_2 is the mean gravity force along BD. h_1 and h_2 are the distances separating surface U_2 and lower equipotential surface U_1 at points A and B respectively.

If we move a unit mass from C to A against g_1 the work done = $g_1 \cdot h_1$. If we move a unit mass from D to B, the work done = $g_2 \cdot h_2$. The difference in potential between AC and BD = $U_2 - U_1$ and is a constant. Then:

$$g_1 h_1 = g_2 h_2 = \Delta U \tag{34}$$

From this it follows that as h_1 is less than h_2, g_1 must be greater than g_2.

This is an important concept in torsion balance work and indicates that while the *gravity potential* is *equal* at every point on an equipotential surface, the *gravity force* will be *different* at different points. This further shows that the gravity force on an

equipotential surface is inversely proportional to the distance separating adjacent equipotential surfaces. In other words, the greater the gravity force, the closer together are the equipotential surfaces.

Since it has been illustrated previously that the force of gravity is greatest over the crest of an anticline, it follows that equipotential surfaces are closer together over the crest of an anticline, than over the flanks and the adjacent synclines. It also follows from the above that it takes two equipotential surfaces to define the gravity *force* at a point.

Referring to Figure 159, $g_1 = \frac{\Delta U}{h_1}$ or $g_2 = \frac{\Delta U}{h_2}$

where only the magnitude of the gravity force is considered.

The gravity force g could, of course, be determined without two such surfaces if the potential were a simple enough function to be expressed mathematically. It would then only be necessary to differentiate U with respect to the direction h.

For $+h$ measured upward $g = -\frac{\partial U}{\partial h}$

For $+h$ measured downward $g = +\frac{\partial U}{\partial h}$

In both cases the direction of g is indicated in the sign ($\mp h$ direction respectively).

Field Instruments.—In the United States use has been made chiefly of three types of Askania torsion balance and two types of Süss-Rybar torsion balance. The instruments are usually designed either for visual observation or photographic recording. The accuracy of the instruments is of the order of 1 to 3 Eötvös units. (1 Eötvös unit $= 10^{-9}$ cm./sec^2.)

To conserve space, the discussion of field instruments given here will be limited to a description of the Eötvös-Askania torsion balances.*

Large Torsion Balance

A vertical cross section of the large type instrument is shown in Figure 160. The torsion balance proper, with its two suspension systems, is mounted in the upper part of the instrument. The torsion wires are made of specially treated platinum-iridium and have a diameter of 0.04 mm. and an approximate length of 56 cm. Each torsion wire is held tightly by clamps. The upper end is fastened to a torsion head, and the lower end to a small vertical rod attached to a balance beam and carrying a small mirror for photographic recording of the position of rest or equilibrium of the beam. One end of each beam carries a gold weight of about 42 g.; the other end has a small hook from which a lead weight of the same mass as the gold weight is suspended by a thin brass wire some 60 cm. or so in length. To minimize temperature fluctuations, the suspension systems are enclosed in three casings which are insulated from one another. The pro-

* For a description of the Rybar instrument the reader may refer to the catalogue of the Süss-Rybar manufacturing concern. A description of a gradiometer and the operating technique to be used with it may be obtained from L. Oertling, Ltd., London.

tective tubes containing the lower weights are unscrewed and packed separately for transport, as are also the weights and the brass suspension wires. The torsion wires and the balance beams remain in the instrument during transport; the balance beams can be locked by turning the milled knobs on the short side of the casing.

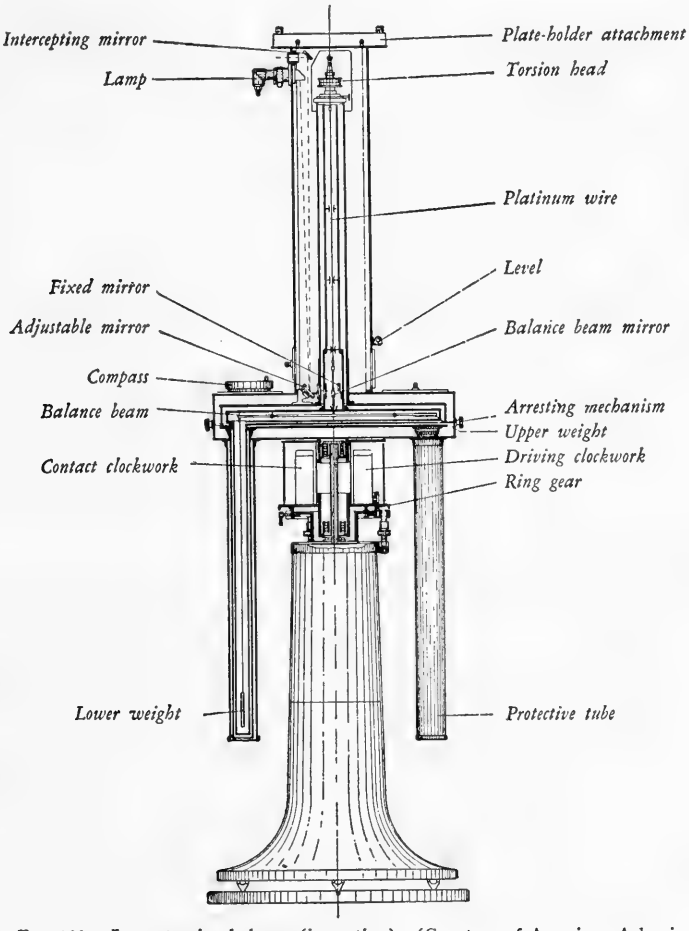

FIG. 160.—Large torsion balance (in section). (Courtesy of American Askania Corporation.)

A compass is mounted on the lid of the outer casing and is used for setting the upper part and the stops in the central portion of the instrument in the meridian. The upper part of the instrument can be set into an exactly vertical position by means of two tubular levels. The torsion heads permit micrometric twisting, raising, lowering and lateral shifting of the torsion wires and hence of the balance beams.

The base of the instrument consists of two parts, placed one within the other. The central section, which contains the clockwork mechanism, is screwed to the base. This section has three leveling screws for setting the instrument accurately in a vertical position. The lower part of the central section contains a plug contact for supplying current to the contact mechanism from a 4- to 6-volt battery, the latter being located under the center of the torsion balance. An azimuth ring is provided which has several adjustable stops for arresting the rotation of the instrument in different azimuths. Stops are provided for three, four, and five symmetrical positions of the torsion balance.

The contact mechanism is a precision clockwork which once an hour closes a contact and lights the electric lamps at the top of the instrument for making the photographic exposure. After the contact is opened, the upper part of the instrument is rotated to the next stop by means of a mechanical transmission gear between the contact clock and the driving mechanism.

The driving mechanism is mounted opposite the contact mechanism in the central portion of the instrument. A gear of the driving mechanism which meshes with the ring gear of the azimuth ring in the central portion of the instrument causes the upper section to rotate quietly and steadily until a lever in the driving mechanism runs against the next stop. The upper section of the instrument can be set free to rotate by using a control lever to disengage a friction clutch between the bevel pinion of the driving mechanism and the ring gear. The clockwork and driving mechanism are shielded from dust and damage by a cylindrical casing. The top plate of the central section carries a plug-in contact for electrical connection between the contact clock and the top of the instrument.

Current is supplied to the exposure lamps by a cable connected to the battery. The brightness of each lamp may be adjusted separately by use of rheostats. The light from the exposure lamps passes through a pinhole diaphragm, a prism, and then vertically downward to an adjustable mirror inclined at an angle of about 45°; the beam of light is reflected horizontally from the inclined mirror, passes through an achromatic lens to the mirror on the stem of the balance beam, and is again reflected on to a photographic plate in the plate-holder attachment at the top of the balance. The plate holder is mounted in a slide on rollers and can be moved across a slit in the base of the plate-holder attachment at a speed of 3.5 mm. per hour.

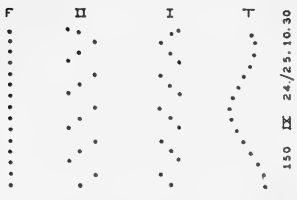

FIG. 161.—Record taken with the large torsion balance in 3 positions (repeated 4 times).

F—fixed points, i.e., spots of light reflected from fixed mirror.
II—second balance beam.
I—first balance beam.
T—temperature points, i.e., spots of light reflected from mirror attached to thermometric device (bimetallic strip).

Light is also reflected to the photographic plate from two additional mirrors, one for each balance, which are mounted within the innermost casing. One of these mirrors is

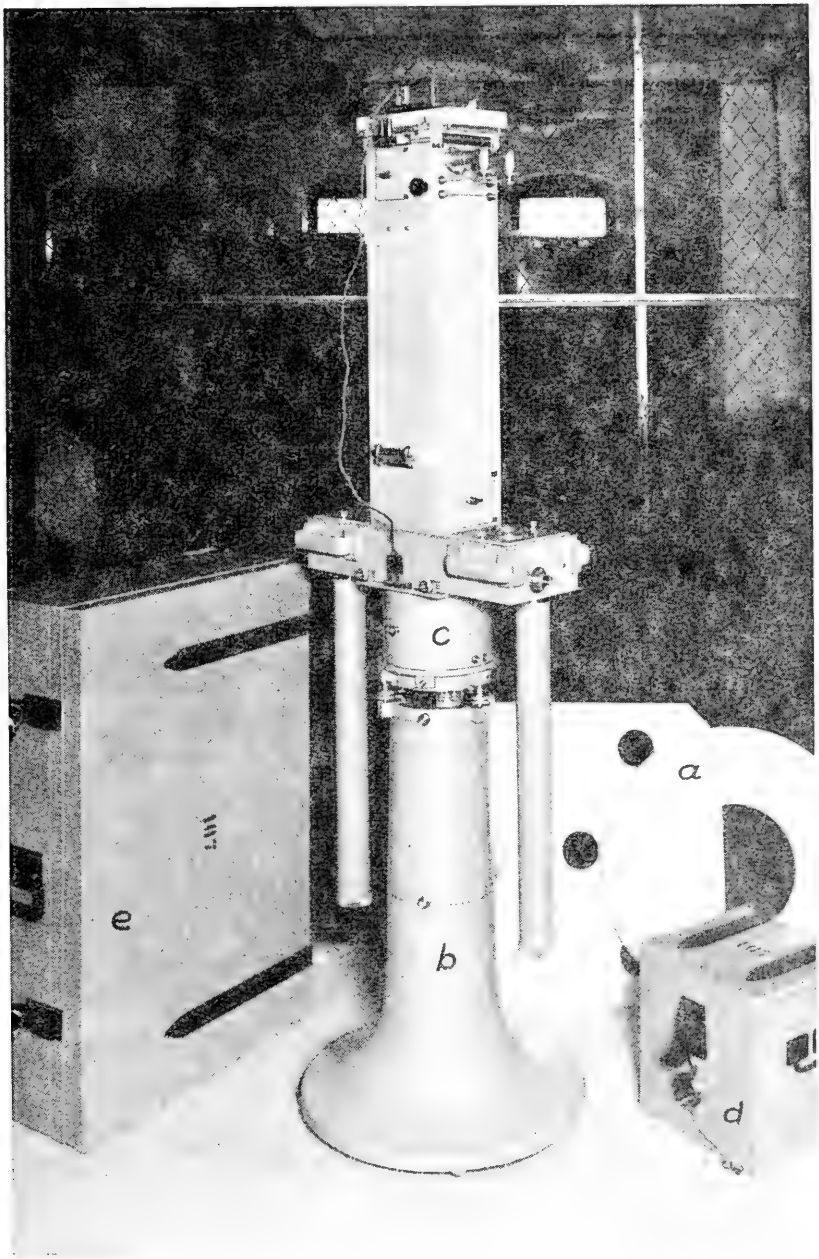

FIG. 162.—Exterior view of large torsion balance. (Courtesy of American Askania Corporation.)

a—Aluminum base plate
b—Pedestal
c—Turntable
d—Carrying case for turntable
e—Carrying case for balance

attached to a bimetallic strip for recording the temperature. (A one-half mm. displacement of the spot of light represents a temperature variation of about 1°C.) The other mirror is fixed, and the spots of light reflected by it are used as fiducial marks in measuring the displacements of the spots of light reflected from the two balance mirrors. A copy of a photographic record obtained with this balance is shown in Figure 161. The start of the plate is at the bottom of the figure. The instrument is turned until the first stop is reached. Then it is manually turned and oriented, using the compass until the north direction coincides with this stop and the regular runs comprising three dots are recorded.

The time required for the beam to come to rest in any azimuth, i.e., the observation period, is approximately 60 minutes. Thus the time required to obtain data for one station, i.e., readings in 3 azimuths, is 3 hours. (Actually, it is common practice to have a repeated observation at the first azimuth to obtain better accuracy so that the total time per station is 4 hours.)

The overall height of the large torsion balance is 183 cm. (72 in.), and its weight when set up for measurement is about 130 pounds. An exterior view of the balance is shown in Figure 162.

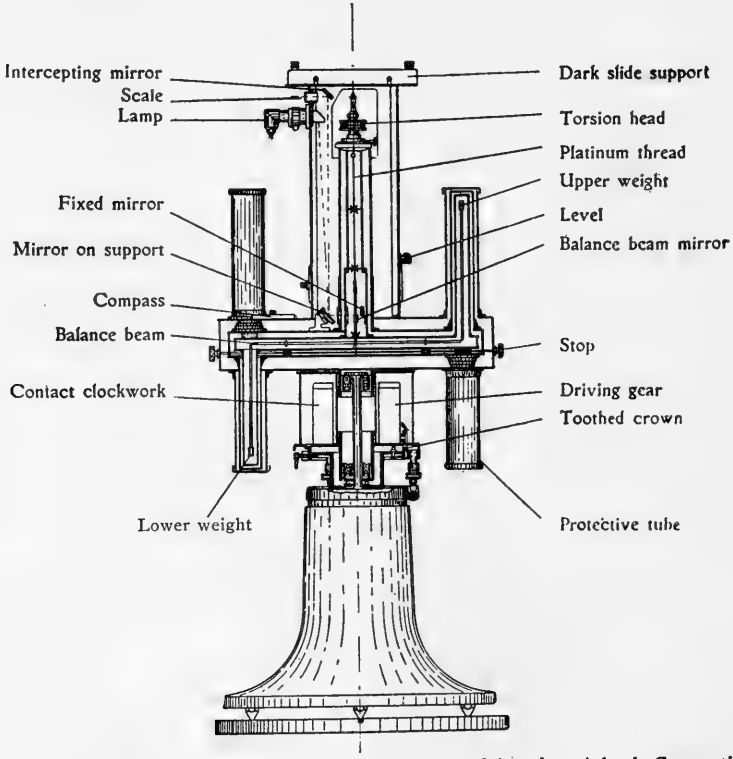

FIG. 163.—Z-beam torsion balance (in section). (Courtesy of American Askania Corporation.)

The sensitivity of the balance is about 0.46 Eötvös units per 0.1 of a scale division of the graduated plate.

Z-Beam Torsion Balance

In the Z-beam torsion balance (Figure 163) the end portions of each of the balance beams are bent so as to form right angles, and the weights are rigidly attached to the extremities of the vertical parts. With one weight above the balance beam and the other below it, the center of gravity of the suspension system is about 2 cm. above the beam. The small equal weights have a mass of about 22 g. and the distance between them h is 45 cm.

The base and central section are identical with those of the large torsion balance, except that the base consists of one piece. The overall height of the Z-beam torsion balance, however, is only 120 cm. (47 in.) and its weight when set up is 104 pounds.

The observation period or time for the balance beam to come to rest is 40 minutes. The sensitivity is about 0.6 Eötvös units per 0.1 of a scale division of the graduated plate.

The Z-beam torsion balance has been used for investigations of geologic structure and tectonic problems, and for locating salt domes, anticlines, and faults.

Torsion Balance with Inclined Beams

The central section and base of this instrument are similar to those of the large torsion balance and the Z-beam torsion balance except that the upper plate of the central section is designed to correspond with the base of the upper section. The center of gravity of the suspension system is 90 cm. above the base plate. The overall height of the inclined balance is 126 cm. (50 in.), and its weight when set up is 82 pounds.

An exterior view of the instrument is shown in Figure 164. The upper section of the inclined beam balance differs fundamentally from that of the large and Z-beam balances. It comprises a central casing for the optical system and two casings for the balance beams. Each of the balance casings can be removed independently of the other. The balance casings are double-walled as a protection against temperature changes, and each contains a torsion wire and torsion head in addition to the inclined balance beam. The torsion wire is 260 mm. long. The small masses weigh 40 g. each, the horizontal distance between them is 20 cm. and the vertical distance is 30 cm. The prism support is connected to the balance beam by a bifilar suspension which prevents the axial oscil-

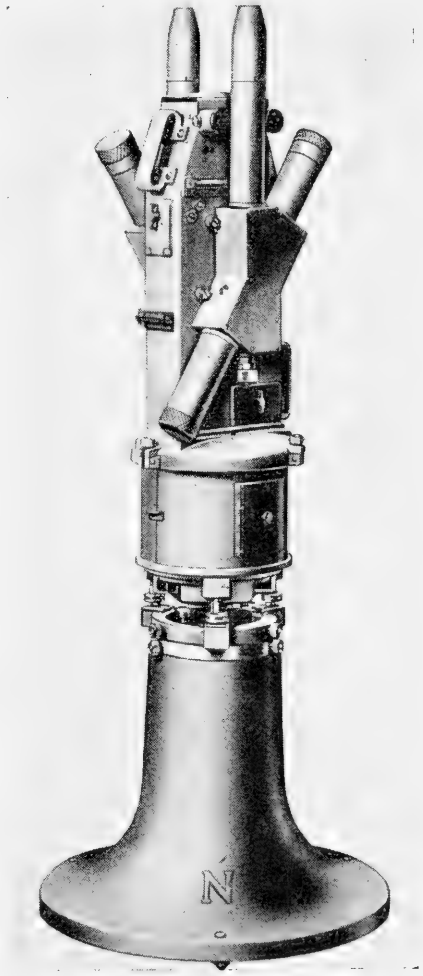

FIG. 164.—Torsion balance with inclined beams. (Courtesy of American Askania Corporation.)

lations of the balance beam from being transmitted to the suspension prism. The balance beam can be locked by turning a knob.

The balance beam can be viewed through a glass window by removing the screw caps at the ends of the tube. The torsion head is provided with a horizontal slide and a fine vertical and azimuth adjustment. In addition, the height adjustment screw is hollow which permits a considerable increase in the length of the torsion wire without a corresponding increase in the overall height of the instrument.

To decrease the observation time, tungsten wires having a torsion coefficient of $\tau = 1.2$ c. g. s. units are used. The sensitivity is 0.1 Eötvös units per 0.1 scale division of the graduated plate.

Torsion Balance Theory

Forces Acting on the Torsion Balance Due to the Gradient of Gravity.—A small section taken between two converging equipotential surfaces is shown in Figure 165, where U_2 is the gravity potential on the upper surface and U_1 that on the lower surface. g' and g are the values of the force of gravity on the U_2 surface at two points separated by the distance ds. As previously shown g' is greater than g; (see Figure 159 and Equation 34).

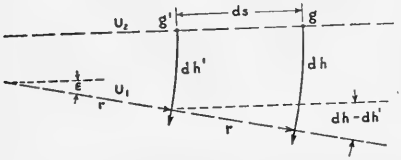

FIG. 165—Showing the curvature of the lines of force of gravity and two equipotential surfaces U_2 and U_1 which converge at the angle ϵ. g and g' = gravity force along dh and dh', and dh and dh' = the distance between the surfaces measured vertically down at these two points. r = radius of curvature of the gravity force lines.

The angle of convergence between the two surfaces, for the section taken, is ϵ, and r is the radius of curvature of the *lines of force of gravity*. The surfaces are spaced apart the amount dh' and dh at the points g' and g respectively. The distance ds is in a horizontal direction. h is measured vertically downward.

It is a general proposition that $g = -dU/dz$, which indicates that the force of gravity is the maximum potential gradient in the vertical direction. (dh is the vertical direction, along a line of force of gravity, which defines that direction or the direction of a plumb line, while the minus sign indicates that the force of gravity, or potential gradient, is directed toward decreasing potential.)

It then follows, that the difference in potential between equipotential surfaces, such as those of Figure 165, is $dU = +g\ dh$ since dh is measured in $-z$ direction. Applying this to points g' and g, it follows that dU (at g') $= g'\ dh'$, and dU (at g) $= g\ dh$. As noted, the value of dU (or ΔU) is everywhere the same between two adjacent equipotential surfaces so that

$$g'\ dh' = g\ dh$$

and

$$g'/g = dh/dh' \qquad (35)$$

We are, however, concerned with the curvature of the lines of force of gravity *from* the vertical. From Figure 165, the gravity force g' equals g plus the rate of change of gravity in the direction s (along the equipotential

surface) times the distance ds, where a uniform change is assumed. In equation form:

$$g' = g + dg/ds \cdot ds \tag{36}$$

With angles measured in radians, as illustrated in Figure 166, $dh = r\,d\epsilon$ (in general). If $d\epsilon$ has a definite value, then $dh = r\epsilon$. Applying this to Figure 165:

$$ds \cdot \epsilon = dh - dh' \tag{37}$$

In general, as seen from Figure 165, for any pair of equipotential surfaces $\epsilon \cdot r = dh$, where r is the radius of curvature of the lines of force of gravity as indicated.

The three previous equations (35, 36 and 37) establish the following:

$$g\,dh = g'\,dh' = (g + dg/ds \cdot ds)\,(dh - \epsilon\,ds) \tag{38}$$

It can also be demonstrated that

$$dg/ds = g/r \tag{39}$$

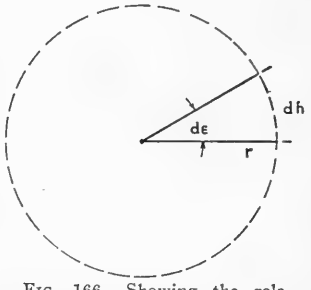

FIG. 166.—Showing the relation of the length of arc dh, angle $d\epsilon$ and radius r of a circle in radians.

Equation 39 above sets forth that the gradient of gravity dg/ds equals the force of gravity g (considered in general) times the curvature of the lines of force of gravity (curvature is $1/r$, where r equals the radius of curvature).

The intermediate steps in this derivation are as follows. The gradient of gravity along ds, assuming ds in a horizontal direction, is by definition dg/ds.

$$g' = g + \frac{dg}{ds}\,ds;\ \epsilon\,ds = dh - dh';\ ds = \frac{dh - dh'}{\epsilon}$$

$$\frac{g' - g}{ds} = \frac{dg}{ds} = \frac{g' - g}{\frac{dh - dh'}{\epsilon}} = \frac{\epsilon\,(g' - g)}{dh - dh'}$$

$$\text{Since}\quad \frac{g'}{g} = \frac{dh}{dh'};\quad dh = \frac{g'\,dh'}{g}$$

Therefore,

$$\frac{\epsilon\,(g' - g)}{\frac{g'\,dh'}{g} - dh'} = \frac{dg}{ds} = \frac{\epsilon\,(g' - g)}{\frac{g'\,dh' - g\,dh'}{g}} = \frac{\epsilon\,(g' - g)\,g}{(g' - g)\,dh'}$$

$$\frac{dg}{ds} = \frac{\epsilon\,g}{dh'}.$$

Using the more general dh for dh';

$$\frac{dg}{ds} = \frac{\epsilon\,g}{dh}\quad ;\ \epsilon = \frac{dg}{ds}\,\frac{dh}{g} \tag{40}$$

dh in general also equals $r' \cdot \epsilon$ so that:

$$\frac{\epsilon g}{r \epsilon} = \frac{dg}{ds} = \frac{g}{r}$$

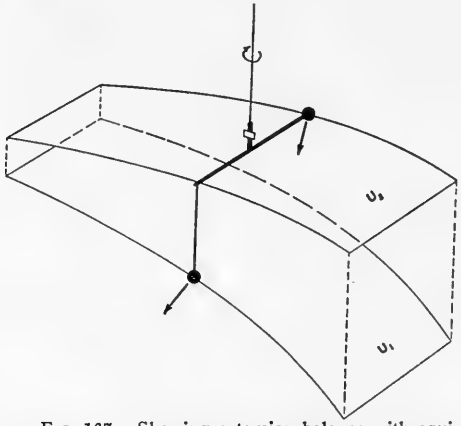

FIG. 167.—Showing a torsion balance with equipotential surfaces U_2 and U_1 which pass through the upper and lower weights respectively.

Moment Due to Gradient Forces.—The application of the above considerations to a torsion balance is brought out in Figures 167 and 168. They show equipotential surface U_2 passing through the upper weight on

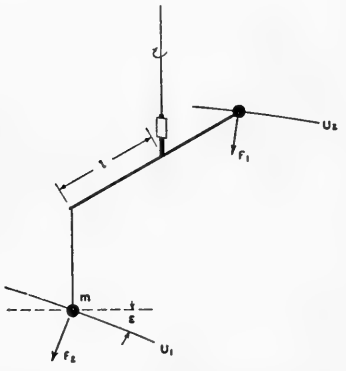

FIG. 168.—Showing the difference in direction of the gravity forces at the upper and lower weights of a torsion balance for the condition shown in Figure 167. ϵ is the angle of convergence of the equipotential surfaces U_2 and U_1.

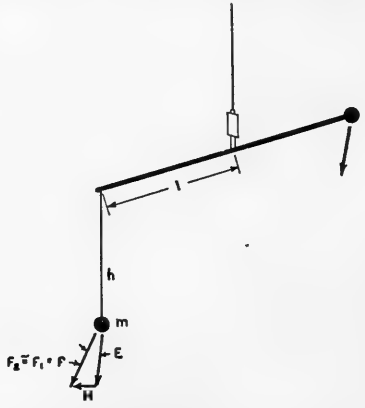

FIG. 169.—Illustrating the horizontal component of gravity force H tending to twist a torsion balance.

the end of the balance beam, and the equipotential surface U_1 through the lower, or hanging weight.

The *direction* of the gravity forces is not the same at the two weights. Because of this, as is shown in Figure 169, a horizontal component of force

H is produced which tends to twist the beam and which is the resultant of the two forces designated as f_1 and f_2 in the figure.

Where l = the half length of the balance beam, the moment of force M_1 is given by:

$$M_1 = lH \tag{41}$$

Since f_1 and f_2 are approximately equal, the subscripts may be dropped and the symbol f used for either of them.

The angle between f_1 and f_2 is ϵ, as they are perpendicular to the equipotential surfaces U_2 and U_1 which converge at that angle. Referring to Figure 169, it is seen that

$$f = m\ g \tag{42}$$

and that the horizontal projection H is approximately

$$H = mg\ \epsilon \tag{43}$$

From the figure also:

$$M_1 = l\ mg\ \epsilon \tag{44}$$

From Equation 40 which refers to the convergence angle of equipotential surfaces ϵ, if we let $h = dh$; then

$$\epsilon = h/g \cdot dg/ds$$

If this value of ϵ is substituted in the equation for M_1, that quantity can be written thus:

$$M_1 = l\ mg\ h/g \cdot dg/ds = l\ mh\ dg/ds \tag{45}$$

We assume that the maximum horizontal gradient of gravity is in the direction s and that this direction is at right angles to the beam. Also, it is assumed that for the position of the beam under consideration its hanging weight end makes the angle ϕ with the astronomic north direction x, and that y represents the east direction, as shown in Figure 170 in plan view.

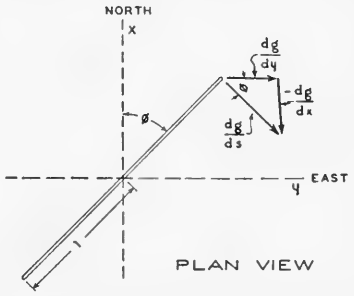

FIG. 170.—Plan view of forces due to the gradient of gravity acting on a torsion balance beam.

This figure illustrates the nature of the rate of change of gravity in the direction s, or that

$$dg/ds = dg/dy \cos \phi - dg/dx \sin \phi \tag{46}$$

Since,

$$\frac{dg}{dy} = \frac{dg}{ds}\cos\phi \qquad \text{and} \quad \frac{-dg}{dx} = \frac{dg}{ds}\sin\phi$$

$$\frac{dg}{dy}\cos\phi = \frac{dg}{ds}\cos^2\phi$$

$$\frac{-dg}{dx}\sin\phi = \frac{dg}{ds}\sin^2\phi$$

Therefore:

$$\frac{dg}{dy}\cos\phi - \frac{dg}{dx}\sin\phi = \frac{dg}{ds}(\cos^2\phi + \sin^2\phi) = \frac{dg}{ds}$$

The gravity g is itself a gradient of a potential, as $g = dU/dz$; where $+z$ is the downward vertical direction heretofore indicated as h. The gravity gradient in the s direction is then the second derivative of the potential, viz.,

$$\frac{dg}{ds} = \frac{\partial^2 U}{\partial z\,\partial s}$$

where $g = +\dfrac{\partial U}{\partial z}$,

and further:

$$\frac{dg}{ds} = \frac{\partial^2 U}{\partial y\,\partial z}\cos\phi - \frac{\partial^2 U}{\partial x\,\partial z}\sin\phi \tag{47}$$

Using the following notation for the above partial derivatives

$$\frac{\partial^2 U}{\partial y\,\partial z} = U_{yz}$$

and

$$\frac{\partial^2 U}{\partial x \partial z} = U_{xz}$$

The gradient moment $M_1 = mlh\ [U_{yz}\cos\phi - U_{xz}\sin\phi]$ (48)

is part of the fundamental equation of the torsion balance. The torsion balance (with a hanging weight) furnishes, therefore, in any given azimuth ϕ, the North-South component of the gradient U_{xz} and the East-West component of the gradient U_{yz}.

Units of Measurement.—The unit of measurement of the gradient of gravity is the Eötvös Unit, as previously defined. The value of gravity force is about 1000 dynes, or gals, and it varies in total between the equator and the poles from 978+ to 983, approximately. An Eötvös unit repre-

sents an increase of about 1×10^{-12} part of the value of gravity force. The usual size of gradients measured in field exploration ranges, on the average, from about 5 to 35 Eötvös units.

The angle ϵ is the difference in the direction of gravity at two points, one *dh cm.* above the other. Taking the sensitivity of the torsion balance as $1 \cdot 10^{-9}$ c.g.s. and *dh* as the distance between the upper and lower weights = 60 cm., it follows that the divergence of equipotential surfaces which can be measured with the instrument is of the order of 1/100,000 of a sec. of arc.

$$\epsilon = \frac{dh}{g} \cdot \frac{dg}{ds} \; ; \; \epsilon = \frac{60}{1000} \cdot 1 \cdot 10^{-9} = 6 \cdot 10^{-2} \cdot 10^{-9} = 6 \cdot 10^{-11}$$

ϵ is in radians; 1 sec. $= 4.8 \cdot 10^{-6}$ radians.

$$\epsilon = \frac{6 \cdot 10^{-11}}{4.8 \cdot 10^{-6}} \cong 1 \cdot 10^{-5} \text{ sec. or } \frac{1}{100{,}000} \text{ of a sec.}$$

Forces Acting on the Torsion Balance Due to the Curvature of Equipotential Surfaces

Equipotential surfaces, of gravitational potential are characterized by their curvature. A torsion balance is acted upon by components of the gravity forces existing in a horizontal plane which touches a curved equipotential surface, as shown in Figure 171.

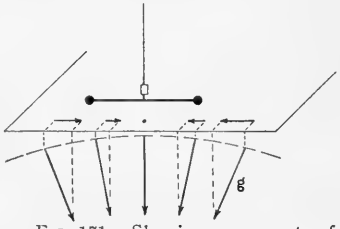

FIG. 171.—Showing components of gravity forces in a horizontal plane, containing a torsion balance beam, which touches a curved equipotential surface.

There is no restriction on the shape of an equipotential surface. However, within the small portions of such a surface occupied by a torsion balance, it is assumed that a linear variation of gravity with distance exists, and that the shape of the surface can be completely represented by two radii of curvature in two directions at right angles to each other. These two radii have the property of representing the maximum and minimum possible radius of curvature.

A curvature of an equipotential surface is designated as positive if the center of curvature is toward the earth's center from the surface, and negative if the surface is convex toward the earth. This corresponds to the general case of an anticline and a syncline respectively.

When the torsion balance curvature effects for certain types of subsurface mass configurations are computed, the curvatures may change along a traverse, from positive to negative. This represents a reversal of direction by 90° for the direction of the plotted R-line value (see Figures 147 to 149).

The curved equipotential surfaces arising from local subsurface structures (such as an anticline) are superimposed on the larger equipotential surfaces of the general gravitational field of the earth. Hence, although the

curvature of an equipotential surface due to a local structure may be negative, the curvature of the total resulting surface may still remain positive. This is analogous to the curvature effects on lines of force of gravity from local heavy masses in the subsurface when added to the direction of lines of force of the earth's field, as in Figure 155. We are entitled to consider the level surfaces from local subsurface structures and their curvature by themselves, however, or as though their effect were *not* superimposed on the general gravitational field, because we subtract the influence of the latter in the "normal value" correction from the torsion balance field readings.

Two vertical sections (I and II) through a *spherical* equipotential surface and the *horizontal* projections of gravity force in a horizontal plane touching the surface at one point are shown in Figure 172. The actual curvature radii are, of course, much larger than those illustrated. For the gravitational field of the earth these radii of curvature are of the order of the earth's radius, or some 4,000 miles.

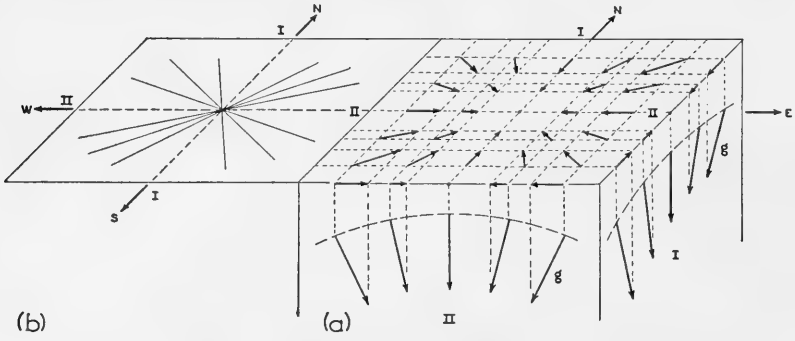

FIG. 172.—Showing vertical sections I and II taken at right angles to each other through a spherical equipotential surface, and the projections of the gravity forces acting in a horizontal plane which touches the equipotential surface at one point. Part B gives the direction of the resultants of the components of force in the horizontal plane which are straight lines converging toward the center.

In sections I and II we have principal curvatures which are at right angles to each other, and in this case equal. The resultant horizontal forces for any part of the horizontal plane are obtained by combining the components of sections parallel to section I and sections parallel to section II, and then forming the resultants.

Connecting the directions of these resultants gives the horizontal projections of the lines of force. These are straight lines which converge toward the center of the figure, as shown in part b, Figure 172. There would be no turning forces acting on a simple horizontal beam torsion balance (with no hanging weight) suspended in such a field. The forces would be acting along the beam in any orientation thereof.

Figure 173 is similar to Figure 172 with the important exception that section I in the N-S direction has a *smaller* curvature than section II in

the E-W direction. The curvature radius is large for section I. The sections are at right angles to each other as before. Point for point, the horizontal projections of gravity forces from section II are *larger* than those from section I. Constructing the plan view of the resultant forces at points on the horizontal surface touching this elliptical equipotential surface, in the same manner as in Figure 172, it is seen that the lines of force, or the direction of the resultants, do not converge on or point to the center of the figure. They are now parabolas. (See part b, Figure 173.)

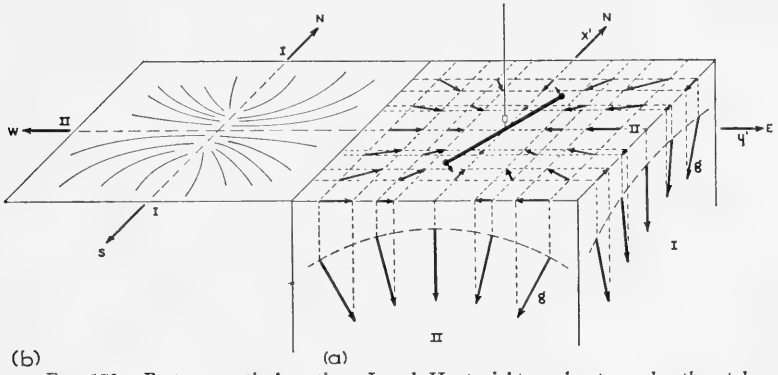

FIG. 173.—Part a: vertical sections I and II at right angles to each other taken through an elliptical equipotential surface, and the projections of gravity force in a horizontal plane which touches the surface at one point. Section II has a greater curvature than section I, hence larger projection components. Part b: lines of force in the horizontal plane (direction of the resultants of the projection components) which in this case are parabolas and do not converge to the center of the figure.

When a simple horizontal-beam torsion balance is brought into such a force field, it is evident that there *are* small horizontal forces tending to twist the beam into the direction of the smallest curvature. Hence, such a torsion balance will measure the deviation of the equipotential surface from the spherical shape.

In Figure 173, x' is designated as the N-S direction along section I, and y' the E-W direction along section II. From this figure it is seen that the *horizontal* component of the gravity force along section I, in the x' direction and denoted by $g_{x'}$, increases outward from the center. In a similar manner along section II, the E-W component $g_{y'}$, increases outward along the line of the section from the center, considering magnitudes only. It is assumed that this change in $g_{x'}$ and $g_{y'}$ is uniform along x' and y' respectively in the small area occupied by the torsion balance. The rate of change is clearly *not* the same for $g_{x'}$ and for $g_{y'}$ in the case pictured, but both changes are at a uniform rate.

The N-S horizontal gravity component $g_{x'} = -\dfrac{\partial U}{\partial x'}$

and the E-W horizontal gravity component $g_{y'} = -\dfrac{\partial U}{\partial y'}$

Minus signs denote forces in negative x' and y' directions respectively, for points of positive x' and y' coordinate values, and vice-versa. This goes back to the idea pre-

sented previously that the rate of change of gravity potential U in a given direction equals the force in the opposite direction (note that the directions x' and y' are in the horizontal touching plane and not in the equipotential surface).

The rates of change of g_x' in the x' direction and that of g_y' in the y' direction are given by the following expressions:

$$\frac{\partial g_x'}{\partial x'} \text{ and } \frac{\partial g_x'}{\partial y'}$$

also

$$\frac{\partial g_x'}{\partial x'} = -\frac{\partial^2 U}{\partial x'^2} \text{ and } \frac{\partial g_y'}{\partial y'} = -\frac{\partial^2 U}{\partial y'^2}$$

Heretofore we have considered only conditions along the directions of principal curvature x' and y' of Figure 173. It is also assumed that, for the small area occupied by the torsion balance, the rate of change of g_x' in the y' direction and the rate of change of g_y' in the x' direction are also uniform. In words, the rate of change of the N-S horizontal gravity component is uniform in the E-W direction and that of the E-W component is uniform in the N-S direction.

On this basis, establishing the center of the horizontal touching plane of Figure 173 as the center of coordinates, the values of g_x' and of g_y' for points in this plane whose coordinates are distances x' and y' can be found. For example, take a point A with coordinates x', y'; the value of the N-S horizontal component at point A, or

$$(g_x')_A = \frac{\partial g_x'}{\partial x'} \cdot x' + \frac{\partial g_x'}{\partial y'} \cdot y' \tag{49}$$

In words again, this means that the value of the N-S horizontal component at a point A is the rate of change of this component in the N-S direction times the x' coordinate of the point, plus the rate of change of this horizontal component in the E-W direction times the y' coordinate of the point. In like manner

$$(g_y')_A = \frac{\partial g_y'}{\partial x'} \cdot x' + \frac{\partial g_y'}{\partial y'} \cdot y' \tag{50}$$

The resultant horizontal gravity component at point A (Figure 174) which might be one of those pictured in Figure 173 would be, introducing second derivatives, the vector sum of

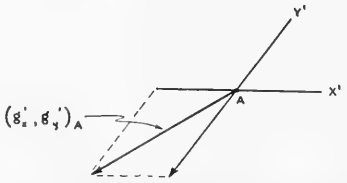

FIG. 174.—The resultant of horizontal gravity components at a point in the horizontal plane touching an equipotential surface. Point designated as A.

$$(g_x', g_y')_A = -\left\{\frac{\partial^2 U}{\partial x'^2} \cdot x' + \frac{\partial^2 U}{\partial x' \partial y'} \cdot y' + \frac{\partial^2 U}{\partial y' \partial x'} \cdot x' + \frac{\partial^2 U}{\partial y'^2} \cdot y'\right\} \tag{51}$$

Where x' and y' are positive, the minus sign indicates a resultant in the negative direction. This is the general equation for the change of the two horizontal gravity components in the horizontal plane, assuming the change may be considered as linear or uniform.

Along the x' *axis* there is no change in $g_{y'}$ and along the y' *axis* no change in $g_{x'}$. Hence, the value of $g_{x'}$ at some point x' along the x axis is:

$$g_{x'} = \frac{\partial g_{x'}}{\partial x'} \cdot x' = \frac{-\partial^2 U}{\partial x^2} \cdot x' \tag{52}$$

and for $g_{y'}$ at some point y' along the y' axis:

$$g_{y'} = \frac{\partial g_{y'}}{\partial y'} \cdot y' = \frac{-\partial^2 U}{\partial y'^2} \cdot y' \tag{53}$$

For these axes: $\dfrac{\partial^2 U}{\partial x' \partial y'} = \dfrac{\partial^2 U}{\partial y' \partial x'} = 0$ and drops out of Equation 51.

Equations 52 and 53 apply only to their respective axes.

To consider the special case of points on an axis:

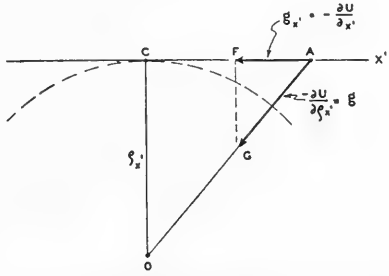

FIG. 175.—A section along the x' axis direction of an equipotential surface for which ρ_x = the radius of curvature.

Figure 175 shows a section along the x' axis. AO is approximately equal to $CO = \rho_{x'}$ = the radius of curvature of the equipotential surface in the x' direction.

$$\frac{g}{\rho_{x'}} = \frac{g_{x'}}{x'}$$

By similar triangles $\dfrac{AG}{AO} = \dfrac{AF}{AC} = \dfrac{g}{\rho_{x'}} = \dfrac{g_{x'}}{x'}$; $AC = x'$;

$g_{x'} = -\dfrac{\partial U}{\partial x'}$, the minus sign indicating the negative x' direction.

Substituting $g_{x'}$ from Equation 52 in the above:

$$\frac{g}{\rho_{x'}} = \frac{g_{x'}}{x'} = \frac{\dfrac{\partial g_{x'}}{\partial x'} \cdot x'}{x'} = \frac{\partial g_{x'}}{\partial x'} = \frac{-\partial^2 U}{\partial x'^2}$$

$$\frac{g}{\rho_{x'}} = \frac{-\partial^2 U}{\partial x'^2}$$

In like manner for the y' section

$$\frac{g}{\rho_{y'}} = -\frac{\partial^2 U}{\partial y'^2}$$

Since curvature $= \frac{1}{\rho}$ where $\rho =$ radius of curvature:

$$\frac{1}{\rho_{x'}} = \frac{-1}{g}\frac{\partial^2 U}{\partial x'^2} \quad \text{and} \quad \frac{1}{\rho_{y'}} = -\frac{1}{g}\frac{\partial^2 U}{\partial y'^2} \tag{54}$$

The difference in these curvatures or the "R" line value is

$$R = g\left(\frac{1}{\rho_{y'}} - \frac{1}{\rho_{x'}}\right) = \left(\frac{\partial^2 U}{\partial x'^2} - \frac{\partial^2 U}{\partial y'^2}\right) = \left(\frac{\partial g_{y'}}{\partial y'} - \frac{\partial g_{x'}}{\partial x'}\right) \tag{55}$$

$$\text{where } g_{y'} = -\frac{\partial U}{\partial y'}$$

$$g_{x'} = -\frac{\partial U}{\partial x'}$$

which is the deviation of the equipotential surface from the spherical shape

($\rho_{y'} = \rho_{\min}$, and $\rho_{x'} = \rho_{\max}$, while for a sphere $\rho_{y'} = \rho_{x'}$ and $R = 0$).

If ρ_2 and ρ_1 are used in place of $\rho_{x'}$ and $\rho_{y'}$ as representing the principal radii of curvature:

$$R = g\left(\frac{1}{\rho_1} - \frac{1}{\rho_2}\right) = \left(\frac{\partial^2 U}{\partial x'^2} - \frac{\partial^2 U}{\partial y'^2}\right) \tag{56}$$

Relation of the directions x' and y' to astronomic directions x and y or N-S and E-W:

We heretofore have designated x' and y' as the N-S and E-W directions. Actually the x' and y' directions are those of maximum and minimum curvature of subsurface equipotential surfaces and are not necessarily in the astronomic N-S and E-W. The strike of a subsurface anticline or the strike of the section of minimum curvature of the equipotential surfaces arising from such a feature will deviate from the north by an angle designated as λ.

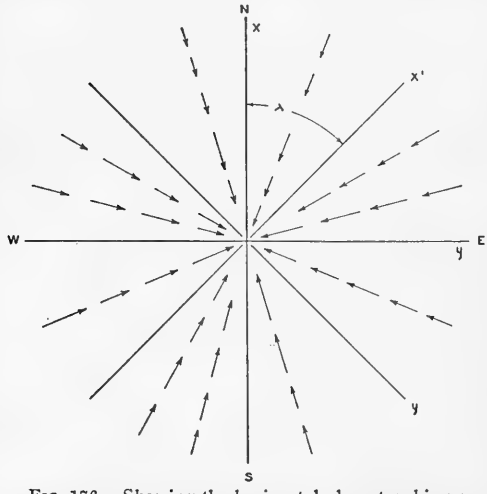

FIG. 176.—Showing the horizontal plane touching an elliptical equipotential surface at one point and the gravity components in the plane. The angle λ is the angle between the x' direction, or the section of minimum curvature of the surface and the astronomic north.

Figure 176 shows the horizontal plane touching an elliptical equipotential surface and the horizontal components of gravity force acting in this plane, together with the astronomic directions x or N-S, and y or E-W. The direction x' lies as before in the section of minimum curvature of the equipotential surface and the y' direction is at right angles thereto. The angle λ as indicated can be defined as the angle that the x' direction (or direction of the section of minimum curvature) makes with the astronomic north. It is measured in degrees clockwise from the true north.

From torsion balance measure-

ments the instrument is oriented and field data on gravity forces acting are measured with respect to the x and y (or the astronomic north-south and east-west) directions. For this reason, it is necessary to transform the horizontal gravity components $g_{x'}$ and $g_{y'}$ into gravity components g_x and g_y, using the angle λ between these two coordinate systems.

After several transformations, which are omitted, Equation 55 becomes

$$\frac{\partial^2 U}{\partial x^2} - \frac{\partial^2 U}{\partial y^2} = g\left(\frac{1}{\rho_{y'}} - \frac{1}{\rho_{x'}}\right) \cos 2\lambda \tag{57}$$

and

$$\tan 2\lambda = \frac{2\,\dfrac{\partial^2 U}{\partial x\,\partial y}}{\dfrac{\partial^2 U}{\partial x^2} - \dfrac{\partial^2 U}{\partial y^2}} \tag{58}$$

The quantity $\dfrac{\partial^2 U}{\partial x\,\partial y}$ occurred previously following Equation 53. In the x' and y' system of coordinates this quantity, which represents the N-S gradient of the E-W horizontal gravity component, was zero; however, in the x, y system it has a finite value.

Using the shorter form of notation

$$\tan 2\lambda = -\frac{2\,U_{xy}}{U_\Delta} \tag{59}$$

where $U_{xy} = -\dfrac{\partial^2 U}{\partial x\,\partial y}$, and $2\,U_{xy}$ is the E-W component of the curvature quantity; U_Δ is the N-S component of that quantity.

The magnitude of the curvature quantity or R-line value and the angle 2λ may be obtained graphically, as shown in Figure 177. In equation form, it is:

$$|\,R\,| = \sqrt{(2U_{xy})^2 + (-U_\Delta)^2} \tag{60}$$

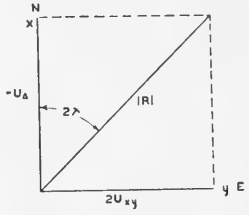

FIG. 177.—Graphical representation of the R-line quantity, as obtained from plotting its components. Note that the U_Δ component plots — to the north. The angle 2λ is shown as measured clockwise from the true north.

Moment Due to Curvature Forces.—In this discussion of the action of forces due to curvature conditions of equipotential surfaces, a simple type of beam is considered. It is assumed that the form of the torsion balance has been modified, and the masses m are placed on the ends of the horizontal beam. For a z-beam this would be equivalent to moving the upper mass down a distance of $h/2$ and moving the lower mass up a like distance. This is the same as considering the action of horizontal gravity components in a horizontal plane acting through the center of gravity of the beam or suspended system. Such a physical beam system is called a curvature variometer and with it the curvature quantity *only* can be measured. The horizontal components of gravity force arising from the curvature of equipotential surfaces act on the horizontal part of the beam of a torsion balance.

Figure 173 indicates that when such a modified form of beam is placed in a horizontal plane touching an elliptical equipotential surface, forces act to twist the beam into the direction of the section of minimum curvature. Figure 178 shows in plan view this type of beam placed in the force field pictured in Figure 176. The angle which the beam makes with the north direction is called ϕ, and its angle with the x' (or minimum curvature) direction is μ; l = the ½ length of the beam. In Figure 178 the beam is at rest, the gravity force components being balanced by the torsion in the suspension wire.

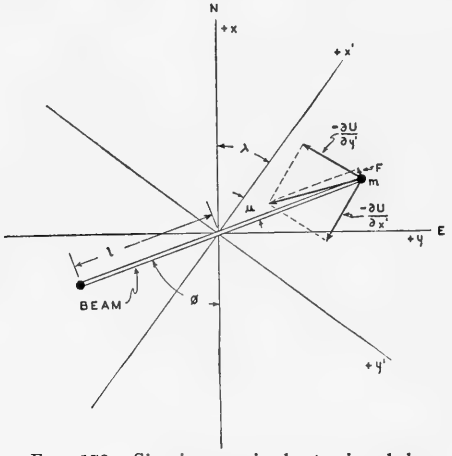

FIG. 178.—Showing a simple torsion balance beam (no hanging weight) placed in a horizontal plane touching an elliptical equipotential surface at one point. Gravity force components tend to twist the beam into the direction of the section of the surface of minimum curvature of x'.

As seen from Figure 178, a horizontal component of force F acting at right angles to the beam is produced, which is the resultant of $\frac{-\partial U}{\partial x'}$ and $\frac{-\partial U}{\partial y'}$. Since a similar force F acts on both ends of the beam and in opposite directions, the curvature moment M_2 is given by:

$$M_2 = 2mlF \tag{61}$$

The force F is derived by transforming the values of g_x' and g_y' in the x', y' system of coordinates into a system which makes the angle μ with the x', y' system. This latter has its x-direction along the beam and its y-direction at right angles to the beam.

$$F = g_y' \cos\mu - g_x' \sin\mu$$

or

$$F = -\frac{\partial U}{\partial y'} \cos\mu - \frac{-\partial U}{\partial x'} \sin\mu \tag{62}$$

from Figure 179. Since $g_y' = \frac{-\partial U}{\partial y'}$ and $g_x' = \frac{-\partial U}{\partial x'}$, the value of F may be written for positive x' and y',

$$F = \frac{\partial^2 U}{\partial x'^2} \cdot x' \sin \mu - \frac{\partial^2 U}{\partial y'^2} \cdot y' \cos \mu \tag{63}$$

using $\cos (90^\circ - \mu) = \sin \mu$ and Equations 52 and 53.

From Figure 179 it is seen that the coordinates of m, namely x' and y', are given by $x' = l \cos \mu$ and $y' = l \sin \mu$. Substituting these values and the value of F from Equation 63 into Equation 61 gives:

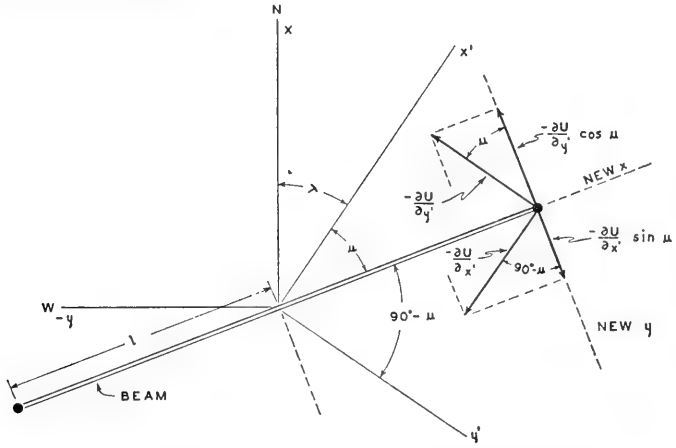

FIG. 179.—Showing force components acting on a simple torsion balance beam as in Figure 178, but with new system of coordinates with x axis along the beam and y axis at right angles to it. The beam makes the angle μ with the x' or minimum curvature direction of the equipotential surface.

$$M_2 = 2ml \left(\frac{\partial^2 U}{\partial x'^2} \cdot l \cos \mu \sin \mu - \frac{\partial^2 U}{\partial y'^2} l \sin \mu \cos \mu \right)$$

$$M_2 = ml^2\, 2 \sin \mu \cos \mu \left(\frac{\partial^2 U}{\partial x'^2} - \frac{\partial^2 U}{\partial y'^2} \right)$$

$(\sin 2A = 2 \sin A \cos A)$

$$M_2 = ml^2 \sin 2\mu \left(\frac{\partial^2 U}{\partial x'^2} - \frac{\partial^2 U}{\partial y'^2} \right)$$

$2l^2m = I$ the moment of inertia of the beam; hence,

$$M_2 = \frac{1}{2} I \sin 2\mu \left(\frac{\partial^2 U}{\partial x'^2} - \frac{\partial^2 U}{\partial y'^2} \right) \tag{64}$$

From Figure 179, substituting for the angle μ its equal, the angle $(\phi - \lambda)$ in Equation 64 and noting that

$$\sin (A + B) = \sin A \cos B - \cos A \sin B$$

$$M_2 = I \left(\tfrac{1}{2} \sin 2\phi \cos 2\lambda - \tfrac{1}{2} \cos 2\phi \sin 2\lambda \right) \left(\frac{\partial^2 U}{\partial x'^2} - \frac{\partial^2 U}{\partial y'^2} \right) \tag{65}$$

Combining Equations 55 and 57 gives

$$g\left(\frac{1}{\rho_y'}-\frac{1}{\rho_x'}\right)=\left(\frac{\partial^2 U}{\partial x'^2}-\frac{\partial^2 U}{\partial y'^2}\right)=\left(\frac{\partial^2 U}{\partial x^2}-\frac{\partial^2 U}{\partial y^2}\right)\frac{1}{\cos 2\lambda} \tag{66}$$

Substituting the last term in Equation 66 into Equation 65 produces:

$$M_2 = I\left(\frac{\partial^2 U}{\partial x^2}-\frac{\partial^2 U}{\partial y^2}\right)\ (\tfrac{1}{2}\sin 2\phi - \tfrac{1}{2}\cos 2\phi \tan 2\lambda) \tag{67}$$

From Equation 58,

$$\tan 2\lambda = \frac{\dfrac{2\,\partial^2 U}{\partial x\,\partial y}}{\left(\dfrac{\partial^2 U}{\partial x^2}-\dfrac{\partial^2 U}{\partial y^2}\right)}$$

Therefore:

$$M_2 = I\left[\left(\frac{\partial^2 U}{\partial x^2}-\frac{\partial^2 U}{\partial y^2}\right)\tfrac{1}{2}\sin 2\phi - \tfrac{1}{2}\cos 2\phi\, 2\frac{\partial^2 U}{\partial x\,\partial y}\right]$$

$$M_2 = \tfrac{1}{2} I\left[\left(\frac{\partial^2 U}{\partial x^2}-\frac{\partial^2 U}{\partial y^2}\right)\sin 2\phi - \cos 2\phi\, 2\frac{\partial^2 U}{\partial x\,\partial y}\right] \tag{68}$$

Using abbreviated notation:

$$\left(\frac{\partial^2 U}{\partial x^2}-\frac{\partial^2 U}{\partial y^2}\right)=U_\Delta \text{ and } 2\frac{\partial^2 U}{\partial x\partial y}=-2\,U_{xy}$$

$$M_2 = \tfrac{1}{2} I\,(U_\Delta \sin 2\phi + 2U_{xy}\cos 2\phi) \tag{69}$$

The above is the second part of the fundamental equation of the torsion balance. The torsion balance, therefore, measures two components of the curvature quantity (the N-S component and the E-W component) and gives the angle λ which is the direction of the section of minimum curvature of the equipotential surface with the north direction.

Units of Measurement of Curvature Values.—The unit of measurement for the differential curvature, $\left(\frac{1}{\rho_1}-\frac{1}{\rho_2}\right)$, strictly speaking, would be in units of 1×10^{-12} radians per cm. The significance of this magnitude lies in its indication of the *difference* in curvature of the two principal sections of the equipotential surface, at right angles to each other. The R line value used and plotted, however, is gravity (g) times this difference in curvature or $R = g\left(\frac{1}{\rho_1}-\frac{1}{\rho_2}\right)$ (see Equations 56 and 57). R is measured in Eötvös units in terms of 1×10^{-9} dynes, since

$$R=\left(\frac{\partial^2 U}{\partial x'^2}-\frac{\partial^2 U}{\partial y'^2}\right)\ ;\quad R = 10^3\,(10^{-12}) = 10^{-9}$$

The value of g is about 1000 or 10^3 dynes; g times the differential curvature in units of 10^{-12} gives R in units of 10^{-9}. Since the field measurements of R are not accurate within a few per cent, the numerical value of R in Eötvös units (or 1×10^{-9} dynes) is used.

The values of curvature for R actually measured in the field commonly range from 5 to 50 Eötvös units. Large values of R are much more common than large values of the gradient.

A torsion balance with a hanging weight is acted upon by two moments of force, M_1 and M_2. The rest position of the balance system represents a balance between these moments and the resistance to twist of the torsion wire in the instrument. Since the torsion coefficient of this wire is known, a means is thus available for measuring these moments.

M_1 arises from the forces acting on the instrument due to the gradient of gravity and is composed of a N-S component U_{xz} and an E-W component U_{yz}. M_2 arises from the forces acting on the instrument due to the curvature conditions of the equipotential surface of gravity passing through the center of gravity of the instrument. The curvature quantity is also made up of two components, namely U_Δ (the N-S component) and $2U_{xy}$ (the E-W component).

COMPUTATION OF GRAVITY DATA FROM TORSION BALANCE RECORDS

Methods of Observing Deflections of the Beam.—In the torsion balance with a hanging weight, the sum of the gradient moment M_1 and the curvature moment M_2 is balanced by the twist of the torsion wire at equilibrium. With τ = the torsion coefficient of the torsion wire and α = the angle of deflection of the beam, when equilibrium has been reached, we have

$$\tau\alpha = M_1 + M_2$$

The deflection can be measured by a telescope and graduated scale, utilizing the mirror on the stem of the balance beam. This system is shown in Figure 180. The distance f (focal length of the telescope lens) is in scale divisions.

With no forces acting on the torsion balance there would be no deflection. A reading of n_0 represents this *torsionless* position of the beam. If a deflection angle α of the beam is observed, the change in scale reading corresponds to the double angle or 2α, designated by a scale reading of n. Where $D = f$:

$$n - n_0 = 2\,\alpha\,D \tag{71}$$

A second method of observing balance beam deflections is to place a lens of focal length f in front of the balance beam mirror. A source of light and a photographic plate are both set at the distance of the focal length from the lens, as is shown in Figure 181.

In the photographic recording balance a dot is made on the photographic plate to record the rest position of the beam, as has been previously shown. (Figures 161 and 183.) A fixed mirror in the optical system of the instrument deflects a portion of the light beam, to give a fixed spot, or

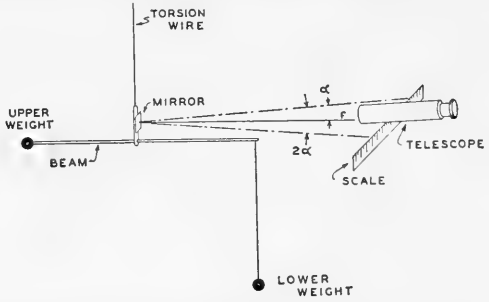

FIG. 180.—Optical system for measuring the deflection of a torsion balance beam. f= focal length of lens expressed in scale divisions.

reference mark, on the sensitized plate. This occurs simultaneously with the recording of the deflection.

The distance n from the fixed dot to the dot representing the deflected position of the beam is measured on the photographic plate with an accurately-made glass scaling-plate. The scaling plate is graduated in ½ mm. divisions. The torsionless position of the balance (which has special significance, as will be shown) or the position of the beam when it is *not* deflected would have a distance n_0 scale divisions from the fixed dot on the photo plate. In photographic recording the scaling plate is substituted for the scale used in visual observation of beam deflections.

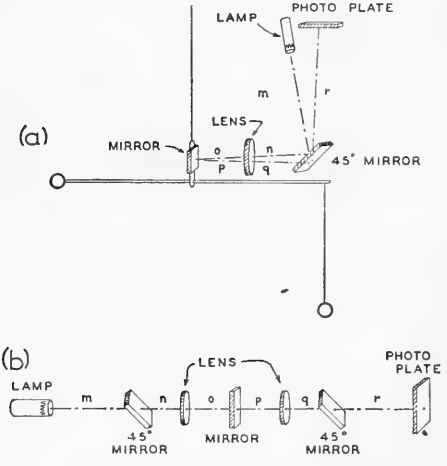

FIG. 181.—Part (a), optical arrangements in a torsion balance for photographic recording of beam deflections. Part (b) shows simplified diagram of the relation between light, lens and plate. f = focal length of lens, expressed in scale divisions.

If, then, the distance of the dot representing a beam deflection a is given by the distance of n scale divisions as scaled from the fixed or reference dot of the photographic plate, and if f is expressed in ½ mm. scale divisions, it follows that:

$$n - n_0 = 2\,a\,f \qquad (72)$$

In the Z-beam torsion balance, as indicated in Figure 181, the balance mirror is set at an angle of 45° to the axis of the beam.

The light ray, when the balance beam is deflected, reflects from this mirror to another mirror on the side of the tube that houses the torsion wire. This brings in a double reflection so that for the Z-beam balance, we have

$$n - n_0 = 4\ a\ f \tag{73}$$

NOTE: The n_0 value or torsionless position is *not* shown as an actual dot on the photographic record. It is obtained by calculation, and is used as a reference point from which to figure beam deflections. However, it *could theoretically* be represented by a dot at scale position n_0 on the photo plate.

Fundamental Equation of the Torsion Balance

Combining Equations 70 and 72 gives:

$$n - n_0 = \frac{2f\ (M_1 + M_2)}{\tau} \tag{74}$$

Substituting in this equation the final values for M_1 and M_2 developed in Equations 48 and 69, we have *the fundamental equation for a single beam torsion balance*† as:

$$n - n_0 = \frac{fI}{\tau}\sin 2\phi\ U_\Delta + \frac{fI}{\tau}\cos 2\phi\ 2U_{xy} + \frac{2fmlh}{\tau}\cos\phi U_{yz} - \frac{2fmlh}{\tau}\sin\phi U_{xz} \tag{75}$$

Definitions of the terms in the equation are listed in Table 8. Where these quantities have definite dimensions, those given are for Askania Balance No. 529, a Z-beam instrument and a fairly early model of that type.

TABLE 8.

SYMBOLS IN FUNDAMENTAL EQUATIONS

n = the scale reading representing the rest position of the balance beam in ½ mm. scale divisions.

n_o = the torsionless position of the balance beam (or undeflected position). A calculated scale reading value. *This quantity is an unknown in the equation* (1).

f = the focal length of the lens in the optical system, in ½ mm. scale divisions. For photographic recording this is 46 cm. (or 920 ½-mm. divisions) in the Z-beam instrument.

I = the moment of inertia of the suspended system = 18,586.

τ = the torsion coefficient of the torsion wire = 0.597. It represents the force necessary to twist the wire through a given angle.

ϕ = the angle of orientation of the beam box in degrees from the north. In effect, it is the orientation of the beam.

U_Δ = the N-S component of the curvature quantity (2).

$2U_{xy}$ = the E-W component of the curvature quantity (3)
These two quantities are unknowns.

m = the mass on the ends of the beam: 12.0 gr. on the upper end of the Z-beam and 10.6 gr. on the lower end. "m" enters the formula as the sum of these masses or 22.6 gr.

† Some of the original torsion balances had only the one beam.

TABLE 8 (Continued)

l = the ½ length of the beam (horizontal portion) = 20 cm.
h = distance between upper and lower masses: 21.8 cm. from beam to upper mass and 17.6 cm. from beam to lower mass. *"h"* enters the formula as the sum of these two values, or 39.4 cm.
U_{yz} = the E-W component of the gradient (4).
U_{xz} = the N-S component of the gradient (5).

Numbers (1) to (5) denote the five unknowns.

The quantities $\frac{fI}{\tau} = a$ and $\frac{2fmlh}{\tau} = b$ are set up as instrument constants, in which form they apply to an optical system where the double angle (2α) of deflection was measured (see Equation 72). Where the angle is 4α (see Equation 73), these constants would be $\frac{fI}{\tau} = a$ and $\frac{4fmlh}{\tau} = b$, which applies to the Z-beam instrument considered.

The general equation is thus simplified to:

$$n - n_o = a\ (\sin 2\phi U_\Delta + \cos 2\phi\ 2U_{xy}) + b\ (\cos \phi\ U_{yz} - \sin \phi\ U_{xz}) \tag{76}$$

The curvature components are functions of 2ϕ, and the gradient components of ϕ only.

Solution of the Fundamental Equation.—In Equation 76 there are 5 unknowns; namely, the torsionless position of the balance and the 4 components of the gravity quantities. These 5 unknowns may be obtained by setting the instrument in 5 azimuths or with ϕ successively 0°, 72°, 144°, 216°, and 288°, allowing the beam to come to rest, and taking readings. As it takes 40 minutes to take one reading, 3 hours and 20 minutes are required for the minimum number of readings.

With $\phi = 0°$ or North, Equation 76 would be:

$$n_1 - n_o = 2a\ U_{xy} + bU_{yz} \tag{77}$$

With $\phi = 72°$

$$n^2 - n_o = a \sin 36°\ U_\Delta - 2a \cos 36°\ U_{xy} + b \cos 72°\ U_{yz} - b \sin 72°\ U_{xz} \tag{78}$$

and in like manner for the other azimuths equations of similar form result. Setting up these 5 simultaneous equations and solving them for the gravity components, we have:

$$n_o = \frac{n_1 + n_2 + n_3 + n_4 + n_5}{5} \tag{79}$$

where the subscript for the scale reading n represents the azimuth of orientation starting with $\phi = 0° = 1$, $\phi = 72° = 2$.....etc.

The result of this solution of these 5 equations gives:

$$\left.\begin{aligned} U_{xz} &= \frac{1}{b}\ [A(n_5 - n_2) + B(n_4 - n_3)] \\ U_{yz} &= \frac{1}{b}\ [F(n_5 + n_2 - 2n_1) - E(n_4 + n_3 - 2n_1)] \\ U_\Delta &= \frac{1}{a}\ [B(n_5 - n_2) - A(n_4 - n_3)] \\ 2U_{xy} &= \frac{1}{a}\ [E(n_5 + n_2 - 2n_1) - F(n_4 + n_3 - 2n_1)] \end{aligned}\right\} \tag{80}$$

where

$$\left.\begin{aligned} A &= \frac{\sin 72^\circ}{2 - \cos 72^\circ - \cos 36^\circ} = 0.38042 \\ B &= \frac{\sin 36^\circ}{2 - \cos 72^\circ - \cos 36^\circ} = 0.23511 \\ E &= \frac{1 - \cos 36^\circ}{5(\cos 72^\circ - \cos 36^\circ)} = 0.32361 \\ F &= \frac{1 - \cos 72^\circ}{5(\cos 72^\circ - \cos 36^\circ)} = 0.12361 \end{aligned}\right\} \quad (81)$$

Double Beam Torsion Balance. — In order to shorten the time required to take all the readings necessary at a station, the double beam torsion balance was developed. In it are two similar but separate and independent torsion balance systems side by side, reversed 180° as regards their hanging weight ends. (See Figure 182.)

With this instrument, readings are taken in three symmetrically-spaced azimuths, or orientations, 0°, 120° and 240° from the north. At one setting of the instrument, data for the solution of two of the set of simultaneous equations are obtained. Two dots representing deflections of the beams are laid down on the photographic plate.

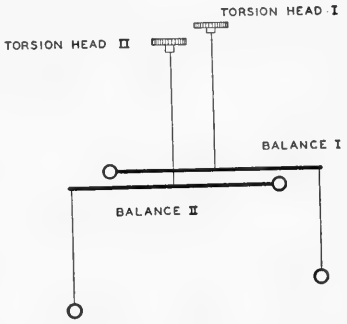

FIG. 182.—Diagram of double beams in a torsion balance. Beams are reversed in respect to hanging weight ends.

A sixth unknown, namely, the torsionless position of the second balance, has been introduced which requires the solution of 6 equations. The necessary information can be obtained with 3 readings or orientations, requiring only 2 hours. It is the usual practice to take two check readings on the first two orientations, making the time per station 3 hours and 20 minutes. 3 to 4 stations can be taken in 24 hours, more if the instrument is moved at night.

With the single prime (′) representing balance I and the double prime (″) balance II, the formulae for a double beam instrument may be set up using Equation 76. Two equations are obtained at each orientation. Balance II is read in azimuths 0°, 120°, and 240° successively for orientation positions 1, 2 and 3, while balance I is read in azimuths 180°, 300° and 60°. The following equations are thus obtained:

Position I

$\phi' = 180^\circ$

(Balance I) $n'_1 - n'_o = 2a'U_{xy} - b'U_{yz}$ (82)

$\phi' = 0^\circ$

(Balance II) $n''_1 - n''_o = 2a''U_{xy} + b''U_{yz}$ (83)

Position 2

$$\left.\begin{aligned}
&\phi' = 300^\circ \\
&\text{(Balance I)} \\
&n'_2 - n'_o = -a' \sin 60^\circ U_\Delta - 2a' \cos 60^\circ U_{xy} + b' \sin 60^\circ U_{xz} + b' \cos 60^\circ U_{yz} \\
&\phi'' = 120^\circ \\
&\text{(Balance II)} \\
&n''_2 - n''_o = -a'' \sin 60^\circ U_\Delta - 2a'' \cos 60^\circ U_{xy} - b'' \sin 60^\circ U_{xz} - b'' \cos 60^\circ U_{yz}
\end{aligned}\right\} \quad (84)$$

Position 3

$$\left.\begin{aligned}
&\phi' = 60^\circ \\
&\text{(Balance I)} \\
&n'_3 - n'_o = a' \sin 60^\circ U_\Delta - 2a' \cos 60^\circ U_{xy} - b' \sin 60^\circ U_{xz} + b' \cos 60^\circ U_{yz} \\
&\phi'' = 240^\circ \\
&\text{(Balance II)} \\
&n''_3 - n''_o = a'' \sin 60^\circ U_\Delta - 2a'' \cos 60^\circ U_{xy} + b'' \sin 60^\circ U_{xz} - b'' \cos 60^\circ U_{yz}
\end{aligned}\right\} \quad (85)$$

Two of the unknowns can be found by forming the arithmetic mean of the deflections as indicated:

$$n'_o = \frac{n'_1 + n'_2 + n'_3}{3} \quad \text{and} \quad n''_o = \frac{n''_1 + n''_2 + n''_3}{3} \qquad (86)$$

$$\left.\begin{aligned}
&\text{Calling } n'_1 - n'_o = \Delta'_1;\ n'_2 - n'_o = \Delta'_2;\ n'_3 - n'_o = \Delta'_3 \\
&n''_1 - n''_o = \Delta''_1;\ n''_2 - n''_o = \Delta''_2;\ n''_3 - n''_o = \Delta''_3
\end{aligned}\right\} \quad (87)$$

Solution of the simultaneous equations for the gravity values can be accomplished by using either Δ_1 and Δ_3, or Δ_2 and Δ_3. The most simple and usable set of equations, however, results from the Δ_1 and Δ_2 values and is as follows:

$$\left.\begin{aligned}
U_{xz} &= O(\Delta'_2 - \Delta'_3) - S(\Delta''_2 - \Delta''_3) \\
U_{yz} &= P(\Delta'_2 + \Delta'_3) - S(\Delta''_2 + \Delta''_3) \\
U_\Delta &= -Q(\Delta'_2 - \Delta'_3) + T(\Delta''_2 - \Delta''_3) \\
2U_{xy} &= -R(\Delta'_2 + \Delta'_3) + T(\Delta''_2 + \Delta''_3)
\end{aligned}\right\} \quad (88)$$

Instrument Constants.—In Equation 88 the values O, P, Q, R, S, and T are instrument constants which combine the constants a and b from both balances. The relations involved are:

$$\left.\begin{aligned}
O &= \frac{a''}{3\,(a'b'' + a''b')} & P &= O \cdot \sqrt{3} \\
Q &= \frac{b''}{3\,(a'b'' + a''b')} & R &= Q \cdot \sqrt{3} \\
S &= \frac{a'}{a''} & T &= \frac{b'}{b''}
\end{aligned}\right\} \quad (89)$$

The constants S and T are close to 1, and are so used, where the wires in the two balances have torsional coefficients of nearly the same value. The constants for Askania instrument No. 529, in 1930, were:

$$O = 2.61;\ P = 4.52;\ Q = -5.07;\ R = -8.78;\ S = 1.0206;\ \text{and}\ T = 1.0073.$$

This will serve to show the magnitude of these constants expressed in Eötvös units or 1×10^{-9} c.g.s. At the date on which the above constants were figured, the values of a and b and the torsional coefficient τ of the two balances were:

Balance I: $a' = 0.0573$; $b' = 0.1098$; $\tau = 0.597$
Balance II: $a'' = 0.0561$; $b'' = 0.1090$; $\tau = 0.600$

When a torsion wire is broken and has to be replaced, or if the physical dimensions of the instrument are altered, these constants have to be recalculated.

Reading Torsion Balance Plates.—Figure 183 represents a photographic plate obtained with a standard double beam torsion balance with readings taken in 3 azimuths. The plates are usually 6½ × 9 cm. and are sensitized with a high speed emulsion. Where the daily temperatures are high, a special tropical emulsion may be used which will not be adversely affected by warm developing solutions.

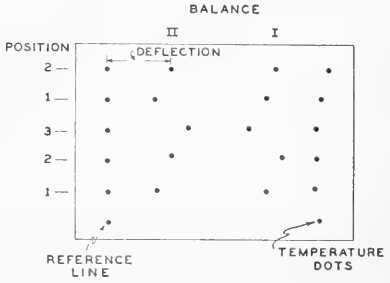

FIG. 183.—Torsion balance photographic plate.

There are four sets of dots on such a plate. Those on the left (Figure 183) form a straight line. They are laid down on the plate by the light ray from the fixed mirror to form a reference line. From this line of dots, scale readings n_1, n_2, and n_3, corresponding to the position of rest of the beam, are obtained for its orientation in azimuth or positions 1, 2, and 3. The values are read by placing the special glass scaling plate, graduated in ½ mm. divisions, over the photographic plate, and reading the scale divisions to tenths. The zero line of the scaling plate is carefully set on the dots of the reference line and the distance is scaled to the dot for a given rest position of the balance in each orientation.

In Figure 183, the second line of dots shows the rest positions for balance II in its orientation positions 1, 2, and 3, with check readings, or dots, for the first two of these positions. The third line of dots gives the rest positions of balance I. The fourth line shows temperature change by means of a metal spring thermometer which operates a mirror in the optical system of balance I.

Where the temperature dots shift to the right an increase of temperature is indicated. If the shift is erratic, the station should be repeated. In the sample calculation given later, no temperature correction has been used, although some organizations make temperature corrections in torsion balance surveys. Temperature change affects the torsional coefficient of the torsion wire and also causes a shift in the rest position of the beam. Torsion wires are carefully selected and heat-treated before they are used, to

eliminate the necessity for temperature correction under ordinary conditions.

It will be noticed that in Figure 183 an extra dot appears at the bottom of the row in the reference dot line. When the instrument is set up and ready for operation in the field, it is oriented in position 3, and the beam released. The lights are then turned on by turning the timing clock. These extra spots are photographed while the beams are swinging, and therefore they do not produce a dot. The instrument then moves itself around into position 1 (N-S). Forty minutes elapse while the beams quiet down and come to rest before the lights again come on and the four dots for position 1 are photographed. This extra reference line dot serves to orient the plate, being placed in the lower left-hand corner when the plate is read or scaled.

Field Procedure.—The organization of the torsion balance field parties depends on many factors both technical and economic. In the early days of torsion balance prospecting in America, two-instrument parties having a crew of 6 to 8 men were common. At the present time, a one-instrument party may comprise: 1 observer, 1 surveyor, and 2 helpers; a two-instrument party may comprise: 1 or 2 observers, 1 surveyor, and 3 helpers. A large, four-instrument party may include a total of 9 to 14 men.

Testing of Instrument

Prior to taking a torsion balance into the field, the instrument should be adjusted, checked and its constants determined. The work can best be done at the laboratory where adequate equipment and shop facilities are available.

Transportation of Instrument

The method of transportation to the area under investigation and from station to station depends on many factors: notably, climate, topography, the character of the roads and trails, surface conditions, and to some extent, the number of men and instruments in the party. On marshy ground, boats, canoes or marsh buggies may be used. On dry lands having relatively good roads and trails, the torsion balance is transported either in a trailer provided with a torsion balance shelter or in a passenger car or light truck equipped for this purpose.

Choice of Site

The choice of the instrument site depends both on its preliminary location on the map to suit the general balance net to be used in the area under investigation and on its topographic details. The topographic details must be such that observations made with the instrument will be of value for predicting underground structure and ore bodies. The properties which the site should have in order to minimize the topographic effects on the gradient and curvature values are summarized on p. 332.

The area under and immediately adjacent the instrument is leveled to within one-half of a centimeter for a radius of at least one and one-half meters. (Figure 184.)

Surveying

The choice of method of surveying depends on the topography and on the accuracy of data desired. In areas of rugged topography, surveying may be carried along 16 azimuths and as far as 250 meters from the instrument. In many surveys, 8 azimuths and distances of from 70 to 100 meters are sufficient. (However, in areas of relatively mild topography, it is common practice not to carry the surveying for topographic details beyond 30 to 40 meters from the balance.)

FIG. 184.—Initial leveling of station site in immediate vicinity of the instrument. *a*, stadia rod equipped with level bubble for leveling; *b*, portions of collapsible house for instrument.

The manner in which the stations are laid out depends on the type of subsurface structures expected in the area under investigation. For average reconnaissance work, the stations are placed from one-half to one-quarter of a mile apart. For detailed work, the station separation may be considerably less than one-quarter of a mile. The lines of stations are usually run in a manner to conform as far as possible to the roads and trails present in the area under investigation without altering to a large degree the station net agreed upon before starting the survey.

Instrument Set-Up

After arriving at the leveled station site, which should be well marked by a surveying crew in advance, the observer drives three wood or steel stakes into the ground so that their tops are in the same horizontal plane. The height of the stakes, as projected from the ground, should always be of the same standard value. After the stakes have been leveled carefully with a hand level, the aluminum base plate is laid upon them with its north groove pointing north. The next step is to set up the hut,

FIG. 185.—Final set-up of torsion-balance station. *a*, collapsible house; *b*, snub-lines to hold structure against wind.

which is a portable shelter consisting usually of a light wood frame covered inside and outside with thin plywood. The space between the plywood layers and frame is filled with a heat insulating material. (Figure 185.) After the hut has been set up, the torsion balance is placed on the aluminum base plate. The turntable is then placed on the pedestal and clamped in position. Next, the upper part of the balance is placed on the turntable, and the turntable is leveled and oriented.

After a new photographic plate has been inserted and the electric light connections and the performance of the electrical contact mechanism checked, the instrument is left on the station site to record automatically. (If a visual torsion balance is used, the observer reads the instrument and rotates it into the next position at certain fixed intervals until a satisfactory series of readings has been obtained.)

The instrument is usually kept at each station long enough to have a repeated observation and check reading in one azimuth at least.

Number of Stations Occupied Per Day

The number of stations occupied per day depends on several factors, such as type of instrument used and its condition, topography, climate, precision desired in the observations, and the number of men in the crew. Under ordinary conditions, a four-instrument crew can occupy 12 to 14 stations a day. The daily average of a two-instrument party may be 6 or 7 stations. A one-instrument party consisting of two men generally will occupy 2 or 3 stations per day at most.

Field Computations and Graphs

It is common practice to compute the observations pertaining to the evaluation of the gradient and curvature values at the field headquarters, preferably on the same day in which the observations were obtained. The computation and plotting of the results are done under the supervision of the party chief. After the data obtained in a day's work have been computed, the graphs and computed data usually are sent to a home office immediately for compilation into the work maps.

Computing the Torsion-Balance Data.—The following example outlines the calculations necessary in computing the uncorrected gravity components. The data from the photographic plate is processed through a form sheet to systematize calculations and minimize errors.

On page 329 are given readings from the plate for station No. 3 of a survey on the Wild Horse Park structure, Pueblo County, Colorado, April 21, 1930. Torsion Balance No. 529, previously referred to, was used.

Prime (′) refers to balance I and (″) to balance II. The left hand column 1, 2, 3, refer to orientation positions. The plate readings for the positions of rest of the balance n′ and n″ are entered opposite the orientation positions to which they refer. For example, for balance I, orientation position 1, the scale reading of the dot was 96.3; for position 2, 96.0, etc.

Area: WILD HORSE PARK STA. 3 Obs. BROWN Asst. MANHART & WALTERS

Time 1st point: 9:00 A. M. 4-21 19 30 Final Pos'n balance _____

Time last point: _____ M. _____ 19 __ No. of fixed points BAL. I 7; BAL. II 10

BALANCE I

Position		N'	N'6	Δ'1	Δ'2	Δ'3
	1	96.3				
	2	96.0	93.9		+2.1	
	3	89.5	93.6			-4.1
	1	95.2	93.3	+1.9		
	2	95.2	92.9		+2.3	
	3	88.3				
	1					
	2					
	3					
	1					
	2					
	3					
			MEAN Δ's	+1.9	+2.2	-4.1

$A' = \Delta'_2 - \Delta'_3$ +6.3 $B' = \Delta'_2 + \Delta'_3$ -1.9

A'-A''	+8.5	+2.62	+22.3	Ux
A'+A''	+4.1	-5.07	-20.8	

BALANCE II

	N''	N''6	Δ''1	Δ''2	Δ''3
1	65.3				
2	73.5	71.3		+2.2	
3	75.0	70.6			+4.4
1	64.0	70.4	-6.4		
2	72.3	70.1		+2.2	
3	74.0	69.8			+4.2
1	63.0	69.6	-6.1		
2	71.5	69.3		+2.2	
3	73.5				
1					
2					
3					
	MEAN Δ's		-6.5	+2.2	+4.4

$A'' = \Delta''_2 - \Delta''_3$ -2.2 $B'' = \Delta''_2 + \Delta''_3$ +6.6

B'-B''	-8.5	4.52	-38.7	Uy
B'+B''	+4.7	-8.79	-41.3	2Uxy

	Observed Result	Negative Corrections: Latitude	Terrain	Topography	Final Result
Ux	+22.3	+7.8	+5.6		+8.4
Uy	-38.7		-21.1		-17.6
UΔ	-20.8	+6.4	+2.0		-29.2
2Uxy	-41.3		-3.0		-34.3
				R	49.0
				2λ	308°
				λ	154°

Remarks: Light failed, balance 5 after 6 points.

Plate read by: WALTERS

Plate checked by: BROWN

The value of $n_o = \frac{n_1 + n_2 + n_3}{3}$. From the first three readings this balance is 93.9 and is entered in the n'_o column opposite orientation position 2.

The next n_o value, 93.6 is $\frac{n_2 + n_3 + n_1}{3}$ and is entered opposite position 3, the n_1 being the check reading for orientation 1 or the 4th dot on the plate for balance *I*. The third n_o value used $\left(\frac{n_3 + n_1 + n_2}{3}\right)$ in a similar manner and equals 93.3. The change in the n_o values is largely due to temperature. This method of handling the n_o partly compensates for temperature change.

$\Delta_1 = n_1 - n_o$, $\Delta_2 = n_2 - n_o$, $\Delta_3 = n_3 - n_o$, as indicated by Equation 87. A check is obtained on the accuracy of a station, as the sum of $\Delta_1 + \Delta_2 + \Delta_3$ should equal zero.

Forming A' and B' and A'' and B'', and determining their sums and differences carries out the operations indicated in Equation 88. (Note that Δ_2 and Δ_3 only are used). The instrument constants O, P, $-Q$ and $-R$ appear in the form. S and T are omitted.

The observed results of the 4 gravity components, shown in the lower left of the plate form above, represent uncorrected values. In order to obtain gravity values more closely related to subsurface conditions, these values must be corrected for the "normal value" of the gradient and curvature (planetary correction) and for the irregularities of the terrain surrounding the station. These matters will be considered in detail.

Reduction of Observations.—The gradient and differential curvature values given by the torsion balance are the vector sums of the effects of all the irregular mass distributions in the vicinity of the instrument which are sufficiently large to affect it. † These effects may be classified into three types: geologic, topographic and latitude. The geologic effects are those due to structural anomalies. The latitude effects are produced by the normal variation of gravity with latitude. The topographic effects, which are frequently of the same order of magnitude as the structural effects, are produced by irregularities in the distribution of mass due to hills and valleys and smaller mounds and depressions in the vicinity of the torsion balance.

Hence, before structural anomalies can be deduced from the torsion balance data, it is necessary to correct the values observed at each station for topographic and latitude effects.

Latitude or Planetary Corrections

The variation of *gravity* with latitude is given by Equation 3. That is

$$g_\phi = 978.039\ (1 + 0.0053 \sin^2 \phi - 0.000007 \sin^2 2\phi) \qquad (20)$$

The variation of the *gravity gradient* with latitude can be obtained by differentiating Equation 20 with respect to x and y respectively.

Because the parallels of latitude are circles, gravity does not vary from east to west. That is, $\frac{\partial g}{\partial y} = U_{yz} = 0$. Also, $\frac{\partial g}{\partial x} = U_{xz}$ is approximately equal to $\frac{1}{R}\frac{\partial g}{\partial \phi}$ where ϕ is the latitude of the area under investigation and

† D. C. Barton, "Eötvös Torsion Balance Method of Mapping Geologic Structure," *A.I.M.E. Geophysical Prospecting*, 1929, pp. 431-433.

R is the radius of the earth at the equator. Hence,

$$\frac{\partial g}{\partial x} = U_{xz} = \frac{1}{R}\frac{\partial}{\partial \phi}\left[978.039\,(1 + 0.0053 \sin^2 \phi - 0.000007 \sin^2 2\phi)\right]$$

$$= \frac{1}{6.38 \cdot 10^8}\left[978.039\,(0.0053 \sin 2\phi)\right] \quad \text{(approximately)}$$

$$= 8.15 \sin 2\phi \cdot 10^{-9} \quad \text{(approximately)} \qquad (90)$$

The planetary correction for the curvature is given by the formula:*

$$U_\Delta = 5.15\,E\,(1 + \cos 2\phi) \cdot 10^{-9} \qquad (91)$$

Graphs showing the latitude effects are given in Figure 186.

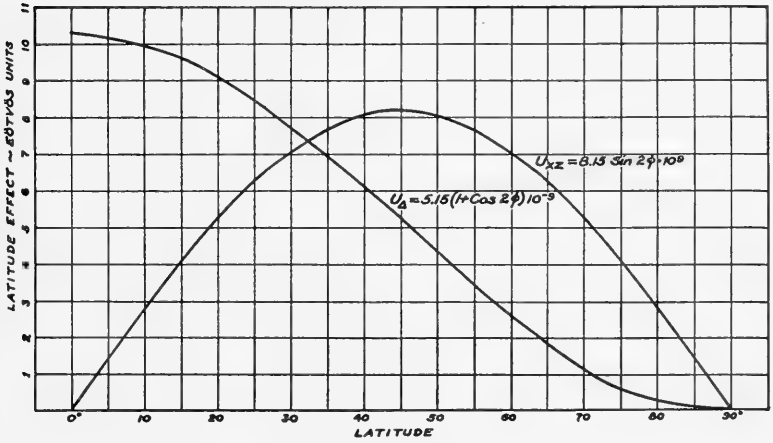

FIG. 186.—Effects of latitude on quantities measured by the torsion balance. (Courtesy of E. V. McCollum.)

Topographic Corrections

The magnitude of the topographic correction to be applied to the gravity gradient depends on several factors. For example, the correction for a small mass, say a boulder, would depend on: the horizontal distance and the vertical distance of the boulder from the torsion balance, the dimensions of the boulder, and its density relative to that of the surrounding media. The effect of the small mass on the gravity gradient is a maximum if the mass is situated within a space angle of 40° to 60° below or above the horizontal plane through the balance, and the effect is substantially zero when the small mass is either vertically below or level with the balance.

Except in very refined work, the effect on the gradient is negligible for irregularities of mass located within ±5° of the horizontal plane through

* Compare also, H. Shaw and E. Lancaster Jones, "The Theory and Practical Employment of the Eötvös Torsion Balance," *Mining Magazine*, July, 1927.

the balance. Furthermore, the effect varies inversely as the cube of the distance of the mass from the balance.*

As a consequence of the topographic effects on the gradient outlined above, it is not practical to use the torsion balance in rugged areas for determinations of gravity gradients due to structure, unless the gradients due to the structures under investigation are very large.

The effect of a small mass on the differential curvature value approaches its maximum value within 10° of the horizontal plane through the center of gravity of the balance. Hence, it is difficult even in regions of moderate relief to choose station sites such that the effect of topography will not be excessively great. From a practical viewpoint, therefore, the differential curvature is of negligible value for predicting structure in areas where the topography is even mildly rugged.

It is common practice to classify topographic corrections as terrain and cartographic corrections respectively, and to apply somewhat different theoretical assumptions and field methods for the evaluation of the two types. The term terrain corrections, as used here, connotes corrections for effects due to irregularities in topography which are present over a circular area having the balance at its center and a radius equal to 100 meters. Cartographic corrections refer to corrections due to topographic irregularities located at distances greater than 100 meters from the balance. As applied to field methods for evaluating these effects, this classification is not rigid because identical field methods frequently may be applied for evaluating effects due to excesses and deficiencies of mass located at distances from the balance of 3 to 300 meters.**

Analytical treatments of topographic and cartographic corrections have been given by von Eötvös, Schweydar, Numerov, Nikiforov, Lancaster Jones, Heiland, Ansel and others. Graphical treatments have been given by Numerov, Jung, Haalck and others. Also, a detailed description of the type corrections utilized in the Imperial Geophysical Experimental Survey is given by Broughton Edge and Laby.

Corrections for mass irregularities located at distances from the balance greater than 100 meters are computed most conveniently by graphical methods. Corrections for topographic or terrain effects, i.e., excesses or deficiencies of mass situated at distances of less than a hundred meters, are computed conveniently in many cases by the Schweydar analytical method.

* The practical significance of these facts in regard to field work may be stated as follows: Whenever feasible, the site chosen for the torsion balance station should be such that all appreciable mass irregularities are situated at moderate distances from the balance and within ±5° of the horizontal plane through the balance. Furthermore, if the balance were set up on an extensive hill sloping uniformly 1°, the effect of the slope on the gravity gradient would be approximately 14 Eötvös units, the precise value depending on the mean density of the topographic feature. Hence, because the gradients due to structure generally are of the order of 7 to 25 Eötvös units, it is preferable to choose station sites where the inclination of the ground is less than 1°.

** It is of some interest to note that many investigators classify the corrections due to topographic irregularities into three types: terrain (up to 100 feet from the site), topographic (from 100 to 1000 feet), and cartographic (over 1000 feet).

The application of this method requires that the area surrounding the station site be surveyed in such manner that the levels are known accurately for eight points on each of several circles having points on the vertical line through the station site as centers and radii of 1.5, 3, 5, 10, 20, 30, 40, 50, 70 and 100 meters respectively, the eight points for each circle being located in eight directions and separated by an angular distance of 45°.*

In his first paper Schweydar † expresses the heights on the various circles having the station as center in terms of a Fourier series as follows:

$$z_n = a_n + b_n \sin \alpha + c_n \cos \alpha + d_n \sin 2\alpha + e_n \cos 2\alpha + \ldots \tag{92}$$

where z_n is the difference in height between the station and a point on circle n, and a_n, b_n, c_n, etc. are coefficients.

$$\left.\begin{aligned} b_n &= \frac{1}{\pi}\int_{-\pi}^{\pi} z_n \sin \alpha \, d\alpha \\ c_n &= \frac{1}{\pi}\int_{-\pi}^{\pi} z_n \cos \alpha \, d\alpha \\ d_n &= \frac{1}{\pi}\int_{-\pi}^{\pi} z_n \sin 2\alpha \, d\alpha \\ e_n &= \frac{1}{\pi}\int_{-\pi}^{\pi} z_n \cos 2\alpha \, d\alpha \end{aligned}\right\} \tag{93}$$

Let**

(r, α) = the polar coordinates of an element of the terrain material referred to the station and the north direction.
σ = the density of the material.
h = the height of the center of gravity of the balance above the station site.
z = the height of the element of terrain above the station site.

The gradient in the x direction due to the element of terrain is***

$$\frac{\partial^2 U}{\partial x \partial z} = 3G\sigma \frac{r^2 \cos \alpha \, (h - z) \, d\alpha \, dr \, dz}{[r^2 + (h - z)^2]^{5/2}} \tag{94}$$

* In irregular country, the leveling is done in 16 azimuths instead of 8.

† W. Schweydar, *Zeit. für Geophysik*, Vol. 1, pp. 81-89 (1924).

** See also Broughton Edge and Laby, *loc. cit.* p. 309.

*** In the following potential discussions the magnitude of the gravity force in a direction r is $g = \frac{\partial U}{\partial r}$. The development of potential theory presented early in the chapter used a center of coordinates at the mass (m) producing the field, and thus the gravity force was given as $g = -\frac{\partial U}{\partial r}$, where the minus sign denoted the direction back toward m. In balance work theory, the center of coordinates is usually taken at the balance (above the mass) and the $+z$ axis is directed downward. If it is remembered that the force is one of attraction and thus the direction is toward m, the sign convention may be dispensed with, the gravity forces being considered as their magnitudes only.

where G is the gravitational constant. (G equals 6.68×10^{-8} in the centimeter-gram-second system of units.) The total gradient in the x direction due to the terrain is

$$\frac{\partial^2 U}{\partial x \partial z} = 3G\sigma \int_0^z \int_0^r \int_{-\pi}^{\pi} \frac{r^2 \cos \alpha \, (h - z)}{[r^2 + (h - z)^2]^{5/2}} \, d\alpha \, dr \, dz$$

Because $\frac{z^2 - 2hz}{r^2 + h^2}$ is small, only a small error is introduced by writing the expression for the gradient in the form

$$\frac{\partial^2 U}{\partial x \partial z} = 3G\sigma \int_0^r \int_{-\pi}^{\pi} \frac{r^2 \cos \alpha \, (hz_{nr} - \tfrac{1}{2} z_{nr}^2)}{(r^2 + h^2)^{5/2}} \, d\alpha \, dr$$

where z_{nr} is the value of z for a circle of radius r. Also, if the differences in height are small, the term $\frac{1}{2} z_{nr}^2$ is small relative to hz_{nr}, and the expression for the gradient $\frac{\partial^2 U}{\partial x \partial z}$ becomes

$$\frac{\partial^2 U}{\partial x \partial z} = 3G\sigma \int_0^r \frac{r^2 h \int_{-\pi}^{\pi} z_{nr} \cos \alpha \, d\alpha \, dr}{(r^2 + h^2)^{5/2}}$$

or

$$\frac{\partial^2 U}{\partial x \partial z} = 3\pi c_n G\sigma \int_0^r \frac{r^2 h}{(r^2 + h^2)^{5/2}} \, dr \qquad (95)$$

In similar manner, it can be shown that c_n is the only Fourier coefficient that must be known to determine $\frac{\partial^2 U}{\partial y \partial z}$ and that d_n and e_n are the only Fourier coefficients that must be known to determine the curvature quantity.

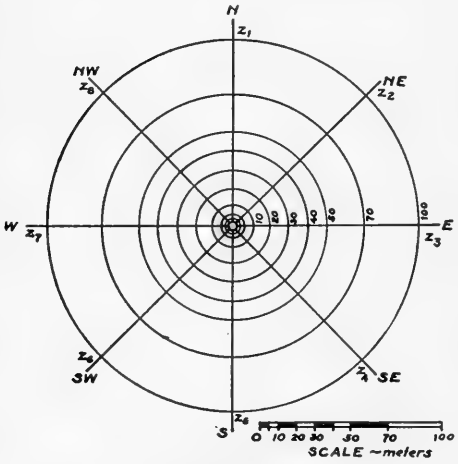

FIG. 187.—Layout for terrain leveling. (After Schweydar, *Zeitschrift für Geophysik.*)

In practical field work, it is impossible to specify z as a continuous function of α. Instead, Schweydar utilized 8 azimuths (0°, 45°, 90°, etc.). (For very rugged terrain, 16 or more azimuths may be used.) If the leveling is done in eight azimuths (0°, 45°, etc.) and if the differences in height on any circle are designated as z_1, z_2, z_3, etc. (Figure 187), substitution in the Fourier equation (92) yields:

$$\left.\begin{aligned} 4b_n &= \frac{1}{\sqrt{2}}(z_2 - z_6 + z_4 - z_8) + z_3 - z_7 \\ 4c_n &= \frac{1}{\sqrt{2}}(z_2 - z_6 - z_4 + z_8) + z_1 - z_5 \\ 4d_n &= z_2 - z_4 + z_6 - z_8 \\ 4e_n &= z_1 - z_3 + z_5 - z_7 \end{aligned}\right\} \qquad (96)$$

Schweydar now makes the assumption that the variations in height from one circle to the next in any given azimuth are proportional to the radial distances from the station. The values of the integral expressions for $\frac{\partial^2 U}{\partial x \partial z}$, $\frac{\partial^2 U}{\partial y \partial z}$, etc., obtained on this assumption are as follows:

$$\left.\begin{aligned} \frac{\partial^2 U}{\partial x \partial z} &= (K_1 c_1 + K_2 c_2 + \cdots) \\ \frac{\partial^2 U}{\partial y \partial z} &= (K_1 b_1 + K_2 b_2 + \cdots) \\ 2\frac{\partial^2 U}{\partial x \partial y} &= (L_1 d_1 + L_2 d_2 + \cdots) \\ \frac{\partial^2 U}{\partial y^2} - \frac{\partial^2 U}{\partial x^2} &= -(L_1 e_1 + L_2 e_2 + \cdots) \end{aligned}\right\} \qquad (97)$$

where c_1, b_1, d_1, e_1, refer to the first circle, c_2, b_2, . . . etc., refer to the second circle, and so on, and the K's and L's are constants which depend only on the values of h and the values of the successive radii.

Schweydar computed the terrain effects for h equal to 90 centimeters. In his second paper† he gives a more rigorous treatment for the evaluation of terrain effects without neglecting the z^2 term.

For the evaluation of cartographic effects, contour lines based on reasonably detailed general topographic surveys are used chiefly. There are other methods, however, which are sometimes applied for the evaluation both of terrain and cartographic corrections.

Numerov,‡ for example, devised a convenient graphical method for the determination of gradients due to topographical features by assuming that the value of r is large (over 33 meters) and by computing the effect due to a prism of mean height z_1, the cross section of which is included between radii r_n and r_{n+1} which are in azimuths Q_m and Q_{m+1}. The principle of this method is to divide the area surrounding the station into zones such that the quantity $\left(\frac{1}{2r_n^2} - \frac{1}{2r_{n+1}^2}\right)(\cos Q_{mh} - \cos Q_m)$ is constant. The application of the method is described by Broughton Edge and Laby. (*loc. cit.*)

† W. Schweydar, *Zeit für Geophysik*, Vol. 2, pp. 17-23 (1927).
‡ B. Numerov, *Zeit für Geophysik*, Vol. 1, pp. 367-371 (1925); Vol. 4, pp. 117-134 (1928).

The topographic or terrain correction is, in effect, a process of mathematically leveling the surface of the ground around the torsion balance station. As has been demonstrated in the preceding discussion, this is accomplished by dividing the terrain into a number of sectors, computing the effect of each, and adding them together.

The effects depend on the differences in elevation between points in the terrain and the instrument station. It is assumed, with usable validity, that the elevation differences may be expressed by a Fourier series and that the local terrain varies uniformly from point to point.

In making the terrain correction, there is a practical limit as to the number of points at which observations (rod readings) can be taken. Also, the average height of segments of the terrain is used in calculating the effects. It is apparent, therefore, that any terrain or topographic correction is an approximation and accurate only to the degree that a particular terrain fits the assumptions made.

Field Operation, Surveying the Station Site.—After proper leveling of the terrain, a transit is set up at the station where the torsion balance is to be placed. The astronomic north direction is set off with the transit, using its compass needle with the proper allowance for magnetic declination.

A light rope or steel tape 50 meters long is used, and on it the out-distances where rod readings are to be taken are marked. These distances are specific in the terrain correction developed by Schweydar (used in the example), and the coefficients in the form given are based on them. These distances are 1.5, 3, 5, 10, 20, 30, 40, 50 meters. Occasionally, readings are made to distances of 70 and 100 meters if extreme accuracy or rough terrain indicates.

The tape is laid out in the north azimuth. Rod readings, with the transit telescope used as a level, are taken at the marked distances. The rod readings at each out-distance are elevation differences from the height of instrument and are entered in the form by the instrument man. Such elevation differences are a requirement of the sample form given.*

After the 8 rod readings in the north azimuth are completed, the procedure is repeated for the seven remaining azimuths, oriented 45° apart, as indicated in Figure 187.

A convenient form of rod, shown in Figure 188, is so designed that elevation differences may be read directly. This rod is graduated in centimeters (and decimeters) to read both ways from a zero point located 125 centimeters from the bottom of the rod. The rod has an adjustable foot which can be locked in place with a wing nut and bolt, so that the zero

* The sample terrain correction computation, using the form as given, indicates that the summation of the terrain effects is multiplied by the quantity ½ density ($\delta/2$). This factor has a plus sign as applied to the two gradient components and to the east-west curvature quantity. It is negative for the north-south curvature correction.

If direct metric rod readings, rather than height differences, are used, the ½ density multiplying factor must be reversed in sign in each case. This can be demonstrated by running through calculations using height differences and direct rod readings.

mark on the rod can be set at the H.I. (or height of instrument) of the surveying instrument used.

The divisions of the rod below the zero point are painted red, indicating positive elevation differences, and the divisions above the zero mark are painted black, indicating negative elevation differences. These elevation differences are entered in the form with the corresponding sign on the basis noted, as *plus* where the ground rises and as *minus* where it is lower than at the instrument station. In order to obtain a proper value for the density of the soil at the station, this quantity is measured by the methods previously described. A terrain can be surveyed in something less than half an hour by an energetic crew.

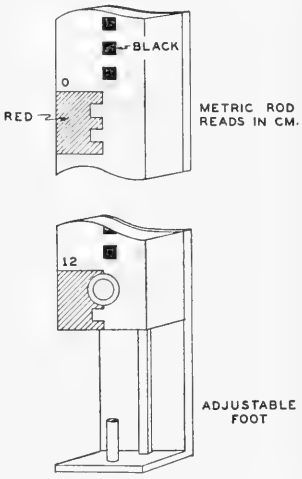

FIG. 188.—Showing a convenient form of metric rod for terrain correction survey. Rod has an adjustable foot so that the height of the instrument can be set at the zero on the rod.

Computations

The differences in elevation measured on the 8 points of each circle (or out-distance) are labeled Z and given a subscript indicating the azimuth on which they were taken, in accordance with the system of numbering shown in Figure 187. For example, Z_1 is the elevation difference in north azimuth, Z_2 the difference in the N. 45° E. azimuth, Z_3 that in the east azimuth, etc., with the Z values referring to a circle of given radius being considered together.

In the terrain computation, the coefficient b indicates the effect of the terrain on the east-west gradient or U_{yz}. As shown in the equation following, Z_3 is positive and Z_7 negative, and Z_2, Z_4, Z_6 and Z_8 enter the computation proportionately to the sin of 45° (0.707). (See also Equation 96.)

Since Z_1 and Z_5 are height differences in the north and south azimuths respectively (directly north or south of the torsion balance), they will have no effect and do not enter the equation.

$$(\approx U_{yz}) : b = 0.707\ (Z_2 + Z_4 - Z_6 - Z_8) + Z_3 - Z_7 \qquad (98)$$

The coefficient c gives the terrain effect on the north-south gradient, and therefore Z_1 is positive and Z_5 negative. Z_2, Z_8, Z_4 and Z_6 enter in proportion to the sin 45°. Z_3 and Z_7 do not affect the north-south gradient.

$$(\approx U_{xz}) : c = 0.707\ (Z_2 + Z_8 - Z_4 - Z_6) + Z_1 - Z_5 \qquad (99)$$

In a similar manner the terrain effects for the curvature values relate

to elevation differences on given azimuths as shown by the following equations:

$$(\approx U_{xy}) : d = Z_2 - Z_4 + Z_6 - Z_8 \qquad (100)$$

$$(\approx U_{\Delta}) : e = Z_1 - Z_3 + Z_5 - Z_7 \qquad (101)$$

It is apparent that elevation differences in the azimuths 1, 3, 5, and 7, or north, east, south and west, do not affect the east-west curvature quantity.

The coefficients *b, c, d,* and *e* are computed for every circle (or out-distance where rod readings are taken). They are given subscripts relating to the circle involved; for example, b_1 represents the correction effect for the first or 1.5 meter circle, and b_2 that for the out-distance of the second or 3 m., etc.

The operations indicated in Equations 98 to 101 result in a numerical value for *b, c, d,* and *e* for a given circle. For example, the amount of b_1 might be + 1.4 for the 1.5 meter ring, and for e_1 for the same out-distance the value might be −7. (See sample computation sheet.)

As gravity effects are inversely proportional, in general, to the inverse square of the distance, it follows that elevation differences on the circles nearer the station will exert more influence than will those which are farther away. This is "weighted" by proper constants for the *b, c, d* and *e* values.

As shown by the terrain correction form, the value for b_1 above (representing the 1.5 zone) is multiplied by the factor 0.59. For the 3-meter ring the factor is 0.161, and for 5 meters it is .0577. These factors are the same for the north-south and for the east-west gradient effects. A different set of factors applies to the curvature quantities with a value of 0.8255 for the 1.5 band, 0.49 for the 3-meter, and 0.3357 for the 5-meter zones, etc., as indicated on the form. Both the north-south and the east-west curvature effects take the same set of factors. These factors are the values *K* referred to in Equation 97 and are valid for a torsion balance positioned with its center of gravity 90 centimeters above the ground surface.

The terrain effects on the curvature quantities are considerably greater than on the gradients, as indicated by factors of 0.8255 for the 1.5 meter zone on the curvature and 0.59 for the gradient. This means that the curvature quantities are influenced more by terrain effects than are the gradients. This fact must be considered during interpretation of the results.

An example illustrating the preceding discussion on the terrain correction is given in the sample calculation on page 339. To save space, this correction is not complete, as the corrections should be carried out until the effects from the farther rings are small with respect to the curvature effects. The corrections are in Eötvös units, and from the sample terrain correction sheet are entered on the plate calculation form, in the box at the lower left.

AREA X STA. 1 OBSERVER JOHN DOE ASST. R. ROE

	1.5	3	5	10	20	30	40	50	70	100
N 1	-7	-14	-25	-43						
NE 2	-4	-9	-13	-22						
E 3	+2	+4	+8	+7						
SE 4	+8	+18	+24	+39						
S 5	+10	+20	+39	+56						
SW 6	+4	+4	+17	+38						
W 7	-2	-2	0	-6						
NW 8	-5	-16	-21	-38						
A 2-6	-8	-13	-30	-60						
B 8-4	-13	-34	-45	-77						
C A+B	-21	-47	-75	-137						
D A-B	+5	+21	+15	+17						
E .707C	-14.7	-32.9	-52.5	-95.9						
F .707D	+3.5	+14.7	+10.5	+11.9						
G 1-5	-17	-34	-64	-99						
H 3-7	+4	+6	+8	+13						
c G+E	-13.7	-66.9	-116.5	-194.9						
b H+F	+7.5	+20.7	+18.5	+24.9						
K	0.59	0.161	0.05975	0.0205	.00465	.0011675	.0004675	0.0003	0.0002	
$c' = K_1 \cdot C$	-18.7	-10.7	-7.0	-3.9						
$b' = K_1 \cdot b$	+4.4	+3.5	+1.1	+0.5						
I 2-4	-12	-27	-37	-61						
J 6-8	+9	+20	+38	+76						
K 1-3	-9	-18	-33	-50						
L 5-7	+12	+22	+39	+62						
d I+J	-3	-7	+1	+15						
c K+L	+3	+4	+6	+12						
K_2	0.8255	0.4905	0.33575	0.2110	.08925	.036705	.020125	.01715	0.0154	
$d' = K_2 \cdot d$	-2.5	-3.4	+0.3	+3.2						
$e' = K_2 \cdot e$	+2.4	+2.0	+2.0	+2.5						

Set zero on rod at H.I. Where ground rises rod readings are below this zero and go into form as +; where ground falls the opposite is true.

Date 4/2/37
H.I.
H.P.
Elev.
Sp. Gr. (6) = 2.0
$\frac{6}{2} = 1.0$

Sum		Corr.	
-40.3	+ 6/2	-40.3	Kx
+9.5	+ 6/2	+9.5	Ky

Sum		Corr.	
-2.4	+ 6/2	-2.4	Kx4
+8.9	- 6/2	-8.9	Kd

Sample Terrain Calculation

Plotting Corrected Torsion Balance Results.—After the observed results at a station have been corrected for the normal value and terrain (and for topography, if necessary), the final results are plotted on a map showing the stations of the survey. The conventional method of plotting is as follows: a cross is drawn through the station parallel to the N-S and E-W astronomic coordinates of the map. A suitable scale for the gradient and curvature values is chosen, usually 1 mm. = 1 Eötvös unit. The amount of the N-S gradient U_{xz} is plotted on the N-S axis, to the N. if positive (+) and to the S. if negative (−). The E-W gradient U_{yz} is plotted on the E-W axis to the E. if (+) and to the W. if (−). (See Figure 189.) The resultant of these two components represents the magnitude and direction of the gradient.

$$\text{The total gradient } \frac{dg}{ds} = \sqrt{(U_{xz})^2 + (U_{yz})^2}$$

Using the values from station 3 at Wild Horse Park, previously presented, the plotted gradient would be as shown in Figure 190. From this station the (corrected) final value of $U_{xz} = +8.9$ E., and $U_{yz} = -17.6$ E.

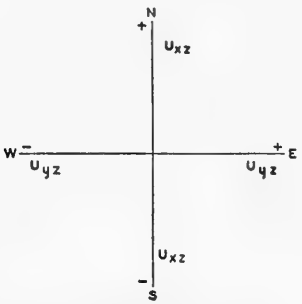

Fig. 189.—Plotting gradient of gravity.

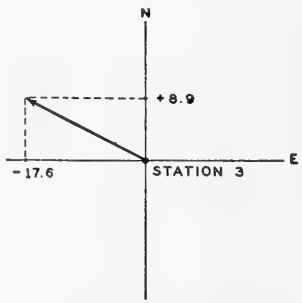

Fig. 190.—Gravity gradient at Station 3, Wild Horse Park, Pueblo County, Colorado. Scale: 1 mm. = 1 E.

In plotting the curvature quantity or R-line value, it is necessary to determine first the magnitude of R, representing the deviation of the equipotential surface from the spherical shape, and second the angle λ which gives the direction of the section of minimum curvature of this surface from the north. From equations,

$$|R| = \sqrt{(U_\Delta)^2 + (2U_{xy})^2} \quad \text{and} \quad \tan 2\lambda = \frac{2U_{xy}}{-U_\Delta}$$

A second small cross is drawn showing the N-S and E-W directions. (See Figure 191.) On this pair of axes, using the same scale as for the gradient values, the amount U_Δ is plotted to the N. if (−), and to the S. if (+). The amount of $2U_{xy}$ is plotted to the E. if (+) and to the W. if (−). The

magnitude of the R vector is the resultant of these two components, symbol $|R|$.

The angle 2λ is measured from the north, clockwise to the plotted R-line, and recorded. In Figure 192, the values for stations 3 for the R-line

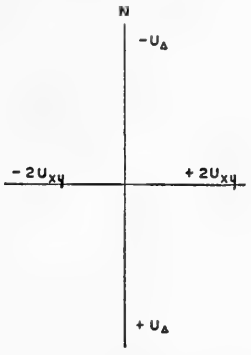

FIG. 191.—Plotting curvature value, R.

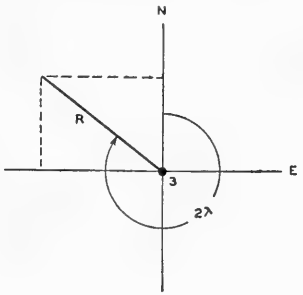

FIG. 192.—Curvature quantity: R-line value at Station 3, Wild Horse Park. Magnitude of R = 49.0, the angle 2λ = 308° and λ = 154°.

are plotted; the components of curvature quantity are $U_\Delta = -29.2$ E. and for 2 U_{xy} = —39.3. After the magnitude of the R-line and the angle λ have been determined, the R-line is divided into two equal parts by the station and plotted at the angle λ from the N. In the case of Station 3, this would be a length of 24.5 on each side of the station as center and at an angle of 154°. (See Figure 193.)

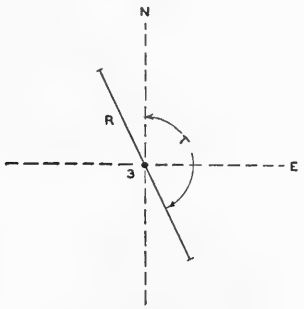

FIG. 193.—Plotting of curvature quantity.

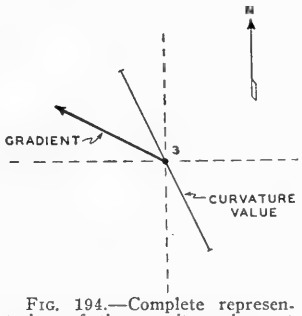

FIG. 194.—Complete representation of the gravity values at Station 3. Scale 1 mm. = 1 E.

The final form of the gradient and curvature values to be shown on the map is illustrated in Figure 194.

The Gradiometer.—The gradiometer is essentially a modified torsion balance so constructed that the torsion wire is acted on by a gradient torque only. The beam system of the gradiometer is shown schematically in Figure 195. Three small masses

are mounted at equidistant intervals (0°, 120°, 240°). Two of the masses m_2 and m_3 are supported on a light aluminum ring and a third mass m_1 is supported by a light aluminum rod above the level of the others. The mass m_2 is very approximately equal to m_3, and the combined mass of m_1 and the rod to which it is attached is equal to m_2 or m_3. †

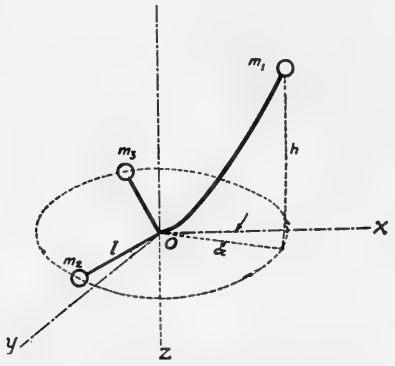

FIG. 195.—Diagrammatic sketch of the beam system of the gradiometer.

The derivation of the fundamental equation of the gradiometer is similar to the derivation of the fundamental equation of the torsion balance. The origin of coordinates is taken at the center of the beam system. The x, y, and z axes are directed toward the north, the east, and vertically downwards respectively. (Figure 195.) The direction of the arm of the gradiometer which carries the upper mass m_1 makes an angle α with the x direction. As in the case of the torsion balance, the gravity components at a point near the origin are

$$\left.\begin{aligned} g_x &= U_{xx}x + U_{xy}y + U_{xz}z \\ g_y &= U_{xy}x + U_{yy}y + U_{yz}z \\ g_z &= g + U_{xz}x + U_{yz}y + U_{zz}z \end{aligned}\right\} \tag{102}$$

The g_x and g_y components of gravity acting on each mass produce a torque T about the z axis given by

$$T = (xg_y - yg_x)\, m \tag{103}$$

Substituting the values of g_y and g_x from the system of equations (102) yields

$$T = [x^2U_{xy} + xyU_{yy} + xzU_{yz} - yxU_{xx} - y^2U_{xy} - yzU_{xz}]\, m$$

or

$$T = [\,(x^2 - y^2)U_{xy} + xyU_{\Delta} + xzU_{yz} - yzU_{xz}]\, m \tag{104}$$

For the upper mass, $x = l\cos\alpha$, $y = l\sin\alpha$, and $z = -h$

For the lower masses, $x = l\cos(\alpha + 120°)$, $y = l\sin(\alpha + 120°)$, and $z = 0$

and $x = l\cos(\alpha + 240°)$, $y = l\sin(\alpha + 240°)$, and $z = 0$

respectively.

The value of the turning moment due to the circular beam and spokes is zero. Hence, the *total* torque acting at the three masses is:

$$\begin{aligned} T = {} & m\{l^2[\cos^2\alpha - \sin^2\alpha]\,U_{xy} + l^2\sin\alpha\cos\alpha\,U_{\Delta} - lh\cos\alpha\,U_{yz} + lh\sin\alpha\,U_{xz}\} \\ & + m\{l^2[\cos^2(\alpha+120°) - \sin^2(\alpha+120°)]\,U_{xy} + l^2\sin(\alpha+120°)\cos(\alpha+120°)\,U_{\Delta}\} \\ & + m\{l^2[\cos^2(\alpha+240°) - \sin^2(\alpha+240°)]\,U_{xy} + l^2\sin(\alpha+240°)\cos(\alpha+240°)\,U_{\Delta}\} \end{aligned}$$

or

$$\begin{aligned} T = {} & ml^2U_{xy}[\cos 2\alpha + \cos(2\alpha+240°) + \cos(2\alpha+480°)] \\ & + \tfrac{1}{2}\,ml^2U_{\Delta}[\sin 2\alpha + \sin(2\alpha+240°) + \sin(2\alpha+480°)] \\ & - mhl\,[U_{yz}\cos\alpha - U_{xz}\sin\alpha] \end{aligned} \tag{105}$$

But the coefficients of U_{xy} and U_{Δ} are zero as is readily verified by expansion.

† Compare also A. Broughton Edge and Laby, *Geophysical Prospecting* (Cambr. Univ. Press, 1931), p. 139, pp. 299-300.

Hence Equation 105 reduces to

$$T = -mhl\ (U_{yz} \cos \alpha - U_{xz} \sin \alpha) \tag{106}$$

Introducing the relation

$$T = \tau\theta$$

where θ is the angular deflection and τ the torsion constant of the torsion wire, Equation 106 may be written in the form:

$$\theta = -\frac{mhl}{\tau}\ (U_{yz} \cos \alpha - U_{xz} \sin \alpha) \tag{107}$$

Replacing θ by its value in terms of the scale readings n_a and n_0 and the distance f (expressed in scale divisions) between scale and mirror

$$\theta = \frac{n_a - n_0}{2f} \tag{108}$$

Hence, the fundamental equation of the gradiometer becomes:

$$n_a - n_0 = -\frac{2fhml}{\tau}(U_{yz} \cos \alpha - U_{xz} \sin \alpha) \tag{109}$$

This equation states that the gradiometer deflection in any azimuth α is directly proportional to the horizontal gravity gradient ($U_{yz} \cos \alpha - U_{xz} \sin \alpha$). (cf. derivation for torsion balance, page 308, noting the one difference that h was measured down and $z = +h$; thus the difference in sign.)

Interpretation of Gravity Gradient and Curvature Data

The technique of interpreting gravity gradient and curvature data is complex and cannot be described in a standardized "step-by-step" method. Every survey involves a large number of variable factors, each contributing its effect to the gravity value measurable at the surface of the earth.

Generally, the first step in the interpretation consists in plotting the gravity gradient and curvature values on a map or on two separate maps. In some cases, these maps can be used to interpret the data directly. In other cases, field gradient and curvature maps alone are inadequate and it is necessary to draw isanomalic contours and profiles and utilize the isanomalic curves in the interpretation.

Curvature maps have a somewhat limited application in extended structural surveys for oil, because curvature values are influenced by topographic irregularities to a larger degree than the gravity gradients. In many reconnaissance surveys the curvature values are neither computed nor plotted.

The relationship between the gradient of gravity and the curvature quantity, as measured by the torsion balance, and the configuration of subsurface heavy masses has been discussed. Certain examples were presented in Figures 141 to 150 inclusive. Although these examples were simplified and quite elementary, they form the background for the interpretation of torsion balance results.

In like manner, the profiles of gravity anomaly (Δg) over similar subsurface structures, as shown in Figures 126 to 129, are fundamental.

Both of these sets of type figures are pertinent in relation to interpretation, and it is suggested that they be restudied at this time.

Torsion Balance Traverse Across an Anticline.—A plan view of a traverse of stations across an anticline showing the gradient and the curvature values is given in Figure 196a. (Note: the stations are set in a straight line, but in the figure they are staggered, so that each individual gradient arrow may be seen.)

The hypothetical structure depicted is a symmetrical anticline. The gradient arrows point up the dip on the flanks of the structure and show a zero value at the crest. The curvature quantity, in contrast to this, exhibits a maximum at the crest of the anticline, where its direction is parallel to the strike of the structure, and changes in direction by 90° where the station is off structure in the adjacent syncline. For stations in the syncline the magnitude of the curvature value is less than at the top of the anticline. These diagnostic variations in gradient and curvature quantities can be shown best by profiles.

The magnitude of the gradient of gravity at a station expresses the amount of the density difference between light and heavy subsurface masses. It also expresses the degree of slope of the subsurface density contrast surface. Gradients are maximum over steep slopes (steep-sided anticlines) and approach minimum where subsurface features are nearly flat. Gradient arrows are analogous to geologic dip symbols, except that they point up-dip.

Profiles of Gradient.—The values of the gradient of gravity along a traverse can be shown in the form of a profile. (Figure 196b.) The gradient at a station is projected onto the line of profile, and the amount of the projection is plotted as an ordinate at the station location. A certain direction for the gradient is chosen as representing a plus value, and for gradients in the opposite direction the ordinate is designated as minus and so plotted. The gradient changes sign when an anticline is crossed by the line of profile, as shown in Figure 196b.

The ordinates on gradient profiles designated as $\delta\ gr/\delta s$ represent the rate of change of the gradient (symbol gr.) in respect to the profile direction s as indicated in the figure.

Profiles of Curvature Quantity.—Profiles of curvature quantity are made in a somewhat similar manner to the gradient profiles. A form of projection is used to determine the amount of the ordinate at a station. This amount is based on the formula:

$$U_\Delta = |R| \cos 2\,\Psi \tag{110}$$

In the above $|R|$ is the magnitude of the R-line value at the station, and

Ψ is the angle which the R-line makes with the profile line. An example of a curvature quantity profile is given in Figure 197 for the anticline shown in Figure 196.

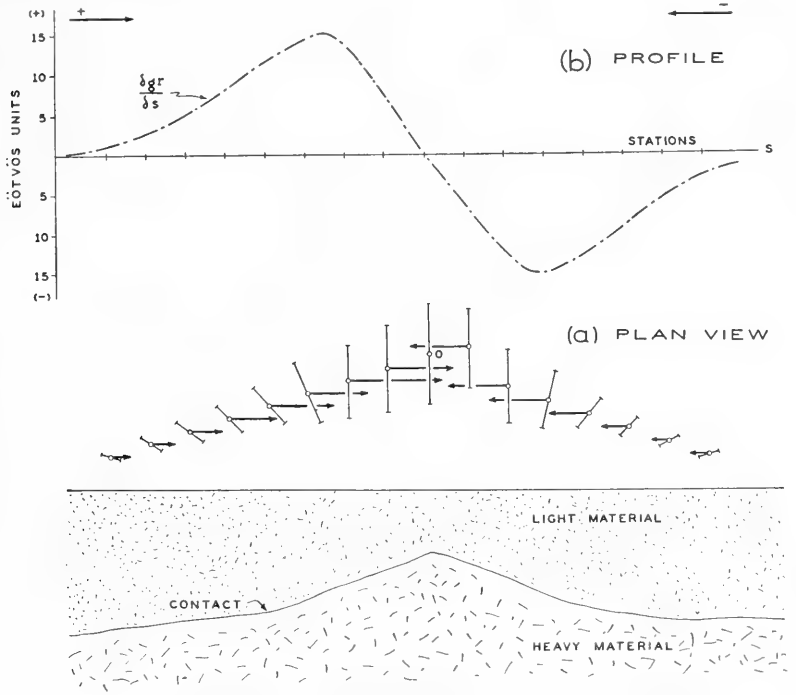

FIG. 196.—Traverse of torsion balance stations across a symmetrical anticline. (a) Plan view of gradient and curvature values at stations. (b) Profile of gradient of gravity.

Note: In (a) the stations are plotted on a curved traverse to permit showing their relative gradient lengths without overlapping. Actually, the stations lie along a straight line traverse.

A special form of projection is necessary, since where the curvatures of equipotential surfaces change from plus to minus from over an anticline to the neighboring syncline the direction of the R-line changes by 90°. A simple projection onto a profile line would not show such a variation.

The values of the quantities plotted in the profile of Figure 197 are presented in Table 9. The table shows that the sign of the ordinate is considered as negative where the stations are above the top of the structure (anticlinal form of gravity equipotential surfaces). The sign is positive where the stations are under the influence of synclinal conditions. Figure 197 is plotted on this basis, and shows that the sign of the curvature quantity changes between those stations where the direction of the R-line changes by 90°. As is expected, the maximum value of the curvature quantity is over the crest of the structure.

TABLE 9.

DATA FOR PLOTTING PROFILE OF FIGURE 197.

Station	Ψ	2Ψ	$\cos 2\Psi$	$\lvert R\rvert$	*Plot*
1	0°	0°	+1	3	+ 3
2	0°	0°	+1	3	+ 3
3	45°	90°	0	5	0
4	90°	180°	−1	7	− 7
5	90°	180°	−1	12	−12
6	90°	180°	−1	15	−15
7	90°	180°	−1	12	−12
8	90°	180°	−1	7	− 7
9	45°	90°	0	5	0
10	0°	0°	+1	3	+ 3
11	0°	0°	+1	3	+ 3

Some published examples of curvature quantity profiles have the plotting in reverse from that described, with the maximum plus values over the structural crest. This would be graphically equivalent to rotating the R-line profile (in Figure 197) 180° about the profile axis.

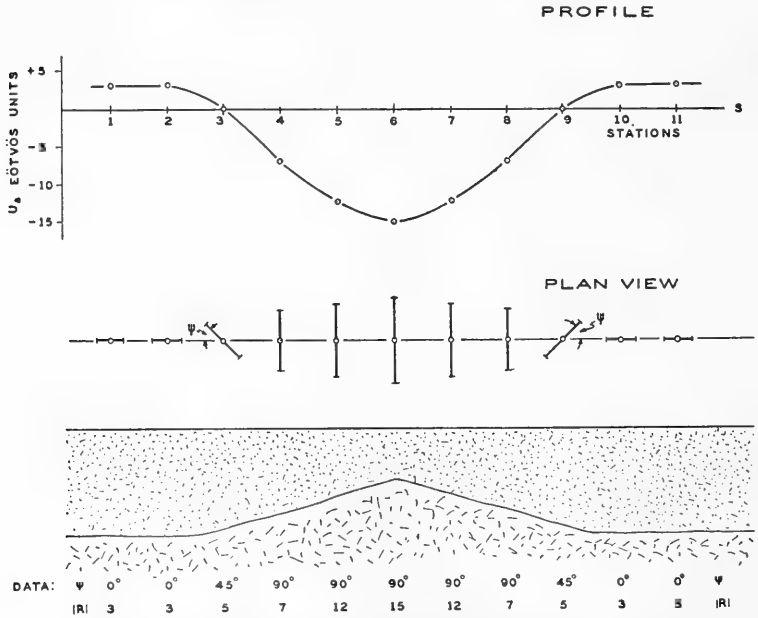

FIG. 197.—Profile of curvature quantity (R-line value) across an anticline. Data is shown for angle Ψ of R-line with line of profile and for $|R|$, the magnitude of the R-line value in Eötvös units, (E).

The magnitude of the curvature quantity at a given station is proportional to the gravity value at the station and to the amount of the *difference* in the curvature of equipotential surfaces as they reflect subsurface conditions. This is expressed in Equation 27. For this reason the largest R-line

values are at the crests of anticlines and over the edges of salt domes where the curvature contrasts are maximum. The gravity value as it relates to curvature quantities is a function of the degree of density contrast present in the subsurface.

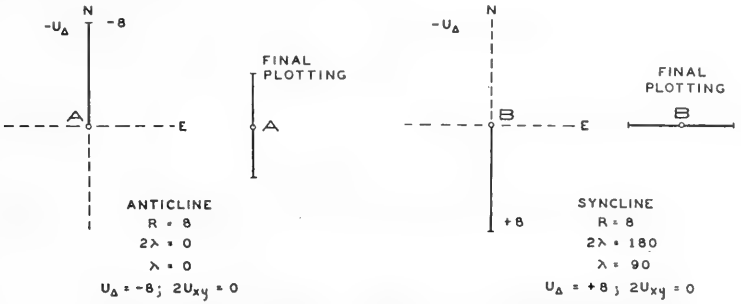

FIG. 198.—Plotting the R-line value for two stations, Station A taken over an anticline and Station B over a syncline. This shows the change in direction by 90° of the R-line value in the two cases.

The reversal of the direction of the R-line by 90° is a point of importance, as it furnishes a criterion as to whether a station is above the anticlinal portion of a structure or above the synclinal portion. Take, for example, two stations A and B, the first over an anticline and the second over a syncline with the following values for the U_Δ quantities.

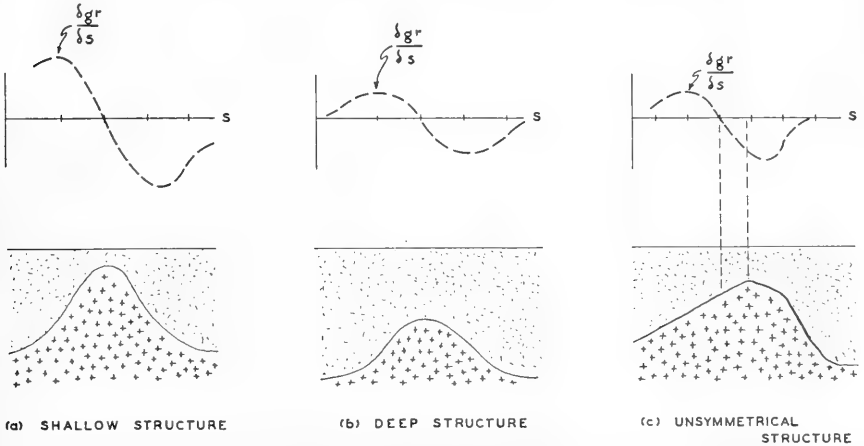

FIG. 199.—Illustrating the effect of (a) a shallow structure, (b) a deep structure, and (c) an unsymmetrical structure, on the amplitude and shape of profiles of the gradient of gravity.

For station A the $U_\Delta = -8$ E. and for station B the $U_\Delta = +8$ E. For both stations it is assumed that the $2U_{xy}$ values $= 0$. As demonstrated in Figure 198 (A) and (B), the reversal by 90° in the direction of the R-line value takes place.

As illustrated by Figure 199 (a) and (b), symmetrical subsurface

features yield symmetrical gradient profiles. The deeper structures give gradients of smaller values. Lack of symmetry in a subsurface structure is manifested by a greater amplitude to the gradient profile on the steep dip side of the subsurface feature and by a shift of the zero in the gradient toward the gentle dip side of the structure. (See Figure 199c.)

It has been shown in Figures 196 and 197 that curvature values are parallel to the strike of subsurface heavy masses when stations are above these masses. The R-line values however are at right angles to the strike when stations are away from uplifted portions of such heavy masses. This idea can be better expressed by saying that R-line values parallel the strike when the curvature of the equipotential surfaces, conforming to subsurface heavy features, is positive. They are perpendicular to the strike when the equipotential surfaces are negative, as discussed on page 288.

General Rules of Interpretation.—As illustrated in Figure 196, the gravity gradients point toward the highest elevation of the heavy masses or structures in the subsurface. The maximum gradient usually corresponds to the steepest outline of these masses (or of the boundary surface of light and heavy masses). Zero points of gradients, or points where their direction changes 180°, are places where the effect of the left side of a heavy mass equals that of the right side, i.e., usually above the center of the mass. However, localities of maxima in gradient or of zero points may shift considerably over the deeper heavy masses, and also over unsymmetrical masses. (See Figure 199, a, b, and c.)

Theoretically the curvature values would be zero above a flat density contrast surface as far as the contribution of that feature itself is concerned. In fact the outlines of heavy masses that are *level* for considerable distances have no effect on $\Delta g''_0$, gradient, or curvature values.

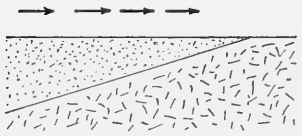

Fig. 200.—Theoretical case for a flat density contrast surface with uniform dip. No R-line value results from this type of feature, considered alone; gradients only are caused, as indicated.

If a density contrast surface is flat, but has a dip as in a monocline, it would produce a gradient and a change in the value of $\Delta g''_0$, but theoretically it would still not influence the curvature quantity. This situation is pictured in Figure 200.

Regional Effects.—The measured value of the gradient and the curvature quantity at a torsion balance station or a series of such stations is the sum of all the gravitational effects acting on the instrument. It will include the local terrain, the distant topography and even such items as buried boulders near the station site. It will be influenced by the configuration of shallow density contrast surfaces and also of deep ones, possibly a number of thousands of feet deep.

The deep density contrasts may represent regional effects such as the slope of the flank of a buried granite ridge or the floor of a basin. Where regional effects are strong, the local structural features may be obscured

and can be evaluated only after removing the regional gravity influences, that is, correcting for the regional gradient. This matter is illustrated schematically in Figure 201.

One way of determining the regional effect is to find the average value by taking the sum of the gradients recorded at all stations and dividing by the number of stations. This can be done in components and gives an average for the north-south gradient and also for the east-west gradient. The average is then subtracted from each station to obtain the residual value for it. The residual values may show features not apparent in the original plotting.

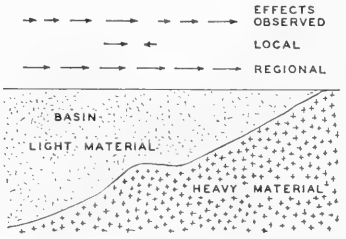

FIG. 201.—Sketch of local structure on the flank of a basin and the regional and local effects on the gradient of gravity along a traverse line. The observed gradient which is the sum of the regional and the local effects is shown.

This process has an inherent error in it, since the average figure obtained and applied as the regional correction is not the true regional. The error lies in the fact that each station entering the average has to a varying degree a portion of local anomaly value in it as well as the regional effect. However, as a means of approximating the regional value it is often useful.

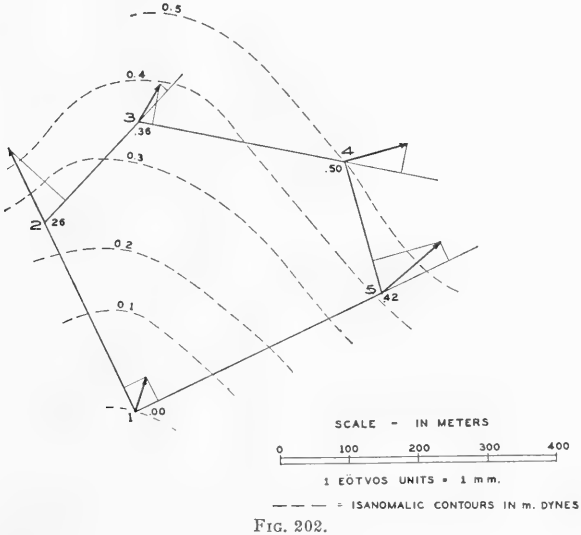

FIG. 202.

The drawing of contours in torsion balance surveys is based on the selection of stations through which a suitable closed traverse will be passed, and on the computation of differences in gravity value between these stations and an arbitrarily selected base station. The procedure may be

explained by referring to Figure 202 and its accompanying legend. A closed traverse is passed through stations 1, 2, 3, 4 and 5, station 1 being chosen as the base station. At each station, a vector is constructed which has a length proportional to the magnitude of the observed gradient at that station and a direction parallel to the direction of the observed gradient. Next, the gradient vector at each station is projected on the closed traverse and the magnitude of the component along the traverse is computed. (Component vectors having the same direction as that in which the traverse is traced are taken as positive, and those having the opposite direction are taken as negative.) The next step is to determine average values of the components by adding components corresponding to two adjacent stations and dividing by two. For example, the average value of the components corresponding to stations 1 and 2 is $\frac{4+16}{2}$, 4 being the component of the gradient at station 1 along the traverse (1, 2) and 16 the component at station 2 along the same traverse.

Computing the average value of the gradient component along a particular direction (specifically, the direction connecting two stations in the closed traverse) is equivalent to assuming that the gradient or change of gravity per unit length is uniform along the line connecting the stations. With this simplifying assumption, the difference in gravity values between two such stations can be readily computed merely by multiplying the average gradient component by the distance between the two stations. Thus, in Figure 202, it is assumed that the gravity anomaly at station 1 (base station) is zero. The anomaly at station 2 is equal to the distance between stations 1 and 2 times the average gradient component = 30,000 cm. • 10*E*/cm. = 300,000 *E*.

It is now necessary to adjust the gravity differences for error in closure. For zero error in closure, the sum of the differences in gravity (column 5) between the stations in a complete cycle of the closed traverse would be equal to the anomaly of the base station—zero in our example. However there is an error in closure of 180,000 Eötvös units or .18 milligals. The error is positive, and to correct for it the *fraction* of the total error corresponding to the probable error made between each set of two stations must be subtracted from the difference in gravity between the particular set of two stations. Any error made in difference of gravity between stations is proportional to the distance between the stations, since the gradient of gravity between them has been assumed constant.

Thus the fraction of the total error to be applied as a correction to the gravity difference between two stations must be proportional to the distance between them. This fraction can now be seen to be the ratio of the distance between any two stations to the total distance of the closed traverse. The correction for station 2 is $-\frac{30,000}{140,000}$ • 180,000 = —40,000 (approximately). The corrected difference, therefore is 300,000 — 40,000 = 260,000 *E*.

The sum of the corrected differences (column 6) should now be zero, since the closure error has been corrected. Had the exact corrections for each station been used rather than the approximations (e.g., exact correction for station 2 is 38,570), the closure error would have been entirely corrected. As it is, an error of 10,000 Eötvös units or .01 milligals allows accuracy which is quite sufficient for normal work.

The differences in columns 5 and 6 are, of course, relative to the base station (1). Column 7 is the sum of the corrected differences—converted into milligals—up to each particular station relative to the base station (proceeding consistently along the closed traverse from the base station).

TABLE 10

APPROXIMATE METHOD FOR DRAWING GENERAL ISANOMALIC CONTOURS IN RECONNAISSANCE SURVEY

1	2	3	4	5	6	7
Gravity Gradients in E.U.	Station No.	Distances in cm.	Average Gravity Gradient	Difference in Gravity Eotvos Units	Corrected Difference Eotvos Units	Accumulated anomalies in m. gals.
7	1	30000	$\frac{4+16}{2}=+10$	+300000	+260000	0
16	2	20000	$\frac{5+7}{2}=+6$	+120000	+100000	+.26
8	3	30000	$\frac{2.5+10}{2}=+6$	+180000	+140000	+.36
12	4	20000	$-\frac{0-6}{2}=-3$	−60000	−80000	+.50
14	5	40000	$\frac{-5-13}{5-13}=-9$	−360000	−410000	+.42
7	1					+.01
				+180000	+10000	

After adjusting the magnitudes of the gravitational anomalies at the traverse stations, the remaining stations plotted on the map are tied into the traverse. Various methods are employed. An approximate method for tieing in a station not too distant from the closed traverse already drawn is to connect this station with a neighboring station on the closed traverse by a straight line and to compute an average gradient component as before.

Finally, the stations of equal gravitational anomaly are connected by continuous curves. (Dotted curves of Figure 202.) The isanomalic contour intervals are usually made from 0.1 to 0.5 of a milligal; however, smaller or larger intervals are not uncommon.

An alternative method for converting a gradient map into a contour map is summarized in Figure 203.

In detailed reconnaissance surveys, one of several elaborate schemes based on an application of the method of least squares to torsion balance data may be used. An illustration of the application of least squares to torsion balance data is given by Roman. †

Detailed Interpretation

Detailed surveys require a more precise evaluation of data than reconnaissance surveys. For example, detailed interpretation generally requires the compiling and drawing of additional profiles and maps and the comparison of the experimental data obtained in the area under investigation with theoretical results obtained by computing the effects produced by various simple geometrical forms and simplified geological structures. Moreover, the final interpretation requires the application of quantitative or graphical and short-cut methods, or a combination thereof, in order to combine the data obtained with the torsion balance and the geological possibilities as derived from a detailed study of regional and local geology.

† I. Roman, "Least Squares in Practical Geophysics," *A.I.M.E. Geophysical Prospecting*, 1932 p. 460.

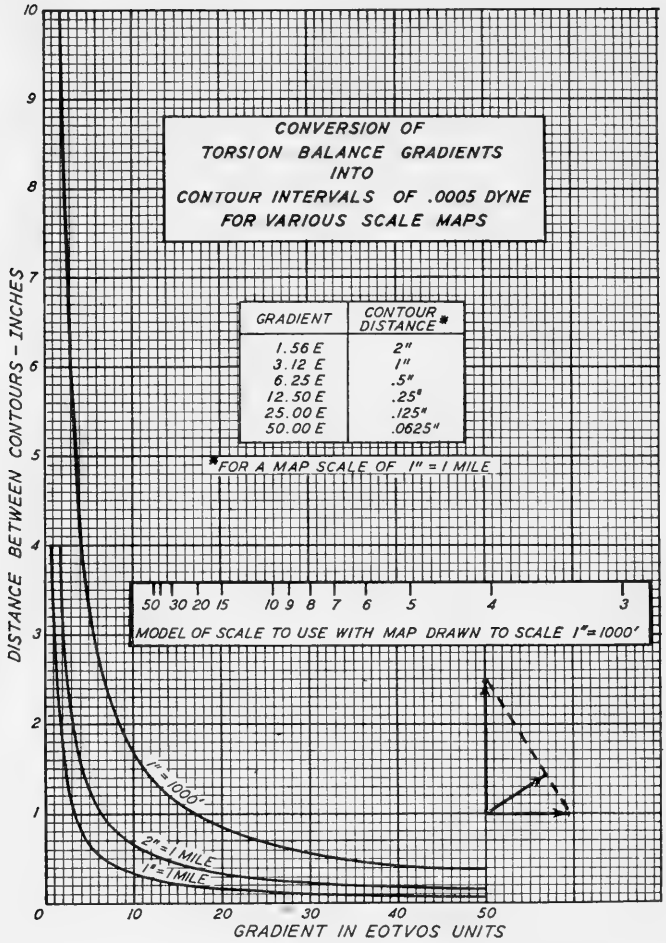

FIG. 203.—Conversion of torsion balance gradients into contour interval of 0.0005 dynes for various scale maps. To construct new curve, measure number of inches on particular map being used. Multiply this number by values in right hand side of above tabulated values, and plot against those on left hand side of table.

If so desired, a scale may be constructed from the curve which gives distance between contours but is graduated in terms of gradient units. (Courtesy of E. V. McCollum.)

Effects Produced by Simple Geometrical Forms and Structures. —A great number of petroliferous structures resemble approximately some one of the simple bodies shown in Figure 204. A horizontal layer of infinite extent alters the absolute value of gravity, but produces no effect on the relative gravity, the gradient, or the differential curvature. Hence, the presence of such an infinite layer tangent to the top or bottom of one of the basic forms will not affect the observed anomalies; i.e., the "equiva-

lent forms" of Figure 204 produce anomalies which are identical with those of the corresponding basic or primary forms.

The gradient and differential curvature anomalies produced by certain simple structures are shown in Figure 205 where the curves are drawn for the case that the structures are denser than the surrounding media. (If the anomalous geologic structures are less dense, the anomalies will have the same form but will be inverted.)

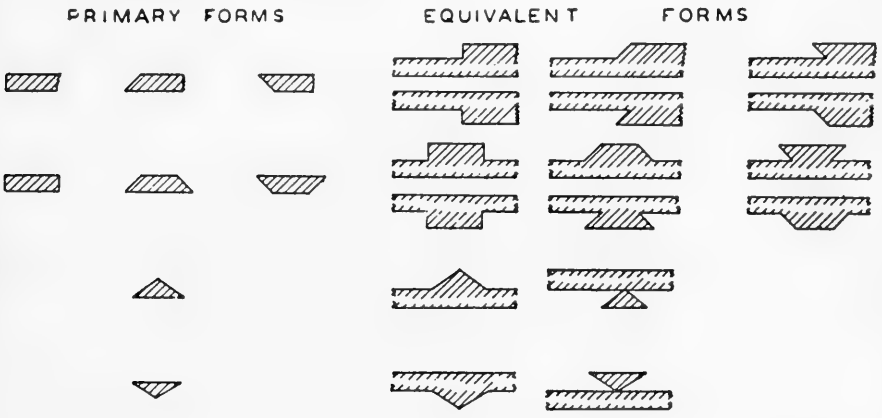

FIG. 204.—Simple geometric forms which correspond to many common types of geologic structure. (Barton, *The Science of Petroleum.*)

Convenient rules of thumb for determining the approximate depth to the top of the geologic structure are given by the following two relations: (1) for fairly symmetrical anomalies, e.g., type A, the horizontal distance

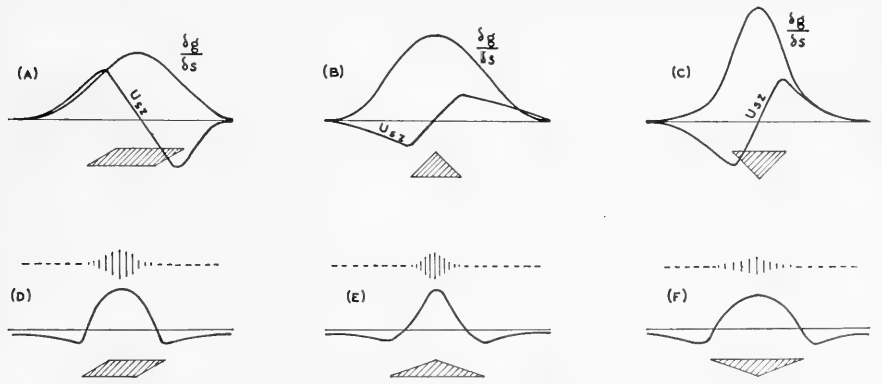

FIG. 205.—Anomalies produced by bodies of simple geometric form.

A. Relative gravity and gradient profiles for a plate-like prism.
B. Relative gravity and gradient profiles for a prism of triangular cross section, apex up.
C. Relative gravity and gradient profiles for prism of triangular cross section, apex down.
D. Differential curvature profile for horizontal plate-like prism.
E. Differential curvature profile for prism of triangular cross section, apex up.
F. Differential curvature profile for prism of triangular cross section, apex down.
(Barton, *The Science of Petroleum.*)

between two points at which the gradient is one-half the maximum gradient is equal to twice the depth to the top of the body; (2) for anomalies of the type B and C, the horizontal distance between the two points having the greatest absolute values of the gradient is equal to twice the depth to the top of the geologic body. For anomalies of the type B, rule (1) is used either with the right hand portion or the left hand portion of the anomaly.

Formulas for Computing Effects of Simple Forms.—The derivations of the analytical expression for anomalies associated with geologic bodies of simple geometric form utilize the same potential theory used in the solution of magnetostatic and electrostatic problems. The characteristic feature of the potential theory as employed in gravitational exploration work is that three types of quantities are evaluated: (1) the first derivative of the potential, i.e., the component of gravity in a particular direction; (2) second derivatives of the form U_{xx}, i.e., the rate of change of the x component in the x direction; (3) second derivatives of the form U_{yx}, i.e., the rate of change of the x component in the y direction.

The total gravitational effect of any mass is the algebraic sum, or integral, of the individual effects of its constituent elements. The elements usually employed are particles of mass, i.e., point elements, or thin cylindrical masses, i.e., line elements.†

The gravitational potential due to a particle of mass m (point element) at a point P located at a distance r from m follows directly from the definition of the potential. That is,

$$U = \int_r^\infty G \frac{m}{r^2}\, dr = \frac{Gm}{r} \tag{111}$$

where G is the gravitational constant ($6.68 \cdot 10^{-8}$ c.g.s. units.) The effect of this potential is to produce a differential curvature and gravity gradient at the torsion balance which may be computed as follows:

$$\frac{\partial U}{\partial x} = -Gm \frac{x}{r^3}$$

and

$$\frac{\partial^2 U}{\partial x^2} = U_{xx} = 3Gm \frac{x^2}{r^5} - G \frac{m}{r^3}$$

Similarly

$$\left.\begin{aligned} U_{yy} &= 3Gm \frac{y^2}{r^5} - G \frac{m}{r^3} \\ \text{and} \\ U_{yy} - U_{xx} &= 3Gm \frac{(y^2 - x^2)}{r^2} \end{aligned}\right\} \tag{112}$$

† See footnote (***) page 333.

Also

$$U_{yz} = \frac{3Gmyz}{r^5}$$

and

$$U_{zx} = \frac{3Gmzx}{r^5} \qquad (113)$$

A line element is equivalent to a thin cylinder of uniform cross section and density (Figure 206). The cross section of the line element PN will be designated by δ and its density by σ. 0 is the center of the balance.

The equations for the Eötvös effects in this case are:†

$$\left.\begin{aligned}
\frac{\partial^2 U}{\partial y^2} - \frac{\partial^2 U}{\partial x^2} &= 3G\sigma\delta\,(b^2 - a^2)\int_0^c \frac{dc}{r^5} = G\sigma\delta\,\frac{b^2 - a^2}{(b^2 + a^2)^2}\left(\frac{3c}{r} - \frac{c^3}{r^3}\right) \\
\frac{\partial^2 U}{\partial x \partial y} &= 3G\sigma\delta ab\int_0^c \frac{dc}{r^5} = G\sigma\delta\,\frac{ab}{(b^2 + a^2)^2}\left(\frac{3c}{r} - \frac{c^3}{r^3}\right) \\
\frac{\partial^2 U}{\partial x \partial z} &= 3G\sigma\delta a\int_0^c \frac{cdc}{r^5} = G\sigma a\delta\left[\frac{1}{(b^2 + a^2)^{3/2}} - \frac{1}{r^3}\right] \\
\frac{\partial^2 U}{\partial y \partial z} &= 3G\sigma\delta b\int_0^c \frac{cdc}{r^5} = G\sigma b\delta\left[\frac{1}{(b^2 + a^2)^{3/2}} - \frac{1}{r^3}\right]
\end{aligned}\right\} \qquad (114)$$

Utilizing the above formulas for point and line elements, it is possible to derive the Eötvös gravity effects: (a) for structures bounded by plane surfaces, e.g., infinite layers of finite rectangular cross section, semi-infinite layer with sloping edge, etc., and (b) for various irregular structures which can be represented, approximately, as the sum of several regular bodies.

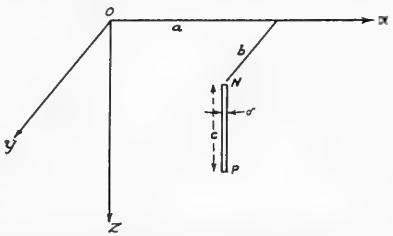

FIG. 206.—Coordinates of attracting line element NP referred to center of balance 0.

The more usable formulas for the gradient and the differential curvature anomalies produced by different types of bodies in different orientations are given below.* In these formulas, G is the gravitational constant and σ

† E. Lancaster Jones, "Computation of Eötvös Gravity Effects," *A.I.M.E. Geophysical Prospecting*, 1929, pp. 506-509.

* The summary of formulas given here is taken from D. C. Barton, "Calculations in the Interpretation of Observations with the Eötvös Torsion Balance," *A.I.M.E. Geophysical Prospecting*, 1929, pp. 481-486. The derivations of the formulas are given by Lancaster Jones in the article cited above, pp. 517-529.

is the relative density of the block, i.e., $\sigma = \sigma_1 - \sigma_2$ where σ_1 is the density of the block and σ_2 that of the medium in which the block lies.

(a) Infinite horizontal slab (Figure 207) bounded by $x = x_1$ and $+\infty$, $y = \pm\infty$, $z = z_1$ and z_2 $(z_2 > z_1)$.

$$U_{xz} = G\sigma \log_e \frac{x_1^2 + z_2^2}{x_1^2 + z_1^2} \tag{115}$$

$$U_\Delta = -2G\sigma \left(\tan^{-1} \frac{z_2}{x_1} - \tan^{-1} \frac{z_1}{x_1} \right) \tag{116}$$

$$U_{yz} = U_{xy} = 0$$

(b) Infinite horizontal slab bounded by an inclined face

$$U_{xz} = G\sigma \left[\sin^2 \phi \log_e \frac{x_2^2 + z_2^2}{x_1^2 + z_1^2} - (\theta_2 - \theta_1) \sin 2\phi \right] \tag{117}$$

$$U_\Delta = -G\sigma \left[\tfrac{1}{2} \sin 2\phi \log_e \frac{x_2^2 + z_2^2}{x_1^2 + z_1^2} + 2(\theta_2 - \theta_1) \sin^2 \phi \right] \tag{118}$$

$$U_{yz} = U_{xy} = 0$$

(c) Infinite horizontal prism with vertical faces bounded by $x = x_1$ and x_2, $y = \pm\infty$, $z = z_1$ and z_2.

$$U_{xz} = G\sigma \log_e \left(\frac{x_1^2 + z_2^2}{x_1^2 + z_1^2} \cdot \frac{x_2^2 + z_1^2}{x_2^2 + z_2^2} \right) \tag{119}$$

$$U_\Delta = -2G\sigma \left(\tan^{-1} \frac{z_2}{x_1} + \tan^{-1} \frac{z_1}{x_2} - \tan^{-1} \frac{z_1}{x_1} - \tan^{-1} \frac{z_2}{x_2} \right) \tag{120}$$

$$U_{yz} = U_{xy} = 0$$

(d) Infinite horizontal prism with inclined faces

$$U_{xz} = G\sigma \left[\sin^2 \phi_1 \log_e \frac{x_2^2 + z_2^2}{x_1^2 + z_1^2} - \sin^2 \phi_2 \log_e \frac{x_4^2 + z_2^2}{x_3^2 + z_1^2} - (\theta_2 - \theta_1) \sin 2\phi_1 + (\theta_4 - \theta_3) \sin 2\phi_2 \right] \tag{121}$$

$$U_\Delta = -G\sigma \left[\tfrac{1}{2} \sin 2\phi_1 \log_e \frac{x_2^2 + z_2^2}{x_1^2 + z_1^2} - \tfrac{1}{2} \sin 2\phi_2 \log_e \frac{x_4^2 + z_2^2}{x_3^2 + z_1^2} + 2(\theta_2 - \theta_1) \sin^2 \phi_1 - 2(\theta_4 - \theta_3) \sin^2 \phi_2 \right] \tag{122}$$

$$U_{yz} = U_{xy} = 0$$

(e) Finite rectangular prism with vertical and horizontal faces parallel to the axes, bounded by $x = x_1$ and x_2, $y = y_1$ and $-y_1$ (y_2), $z = z_1$ and z_2.

$$U_{xz} = G\sigma \left[\log_e \frac{\sqrt{x_1^2 + y^2 + z_1^2} + y}{\sqrt{x_1^2 + y^2 + z_1^2} - y} \cdot \frac{\sqrt{x_1^2 + y^2 + z_2^2} - y}{\sqrt{x_1^2 + y^2 + z_2^2} + y} \right.$$
$$\left. + \log_e \frac{\sqrt{x_2^2 + y^2 + z_1^2} - y}{\sqrt{x_2^2 + y^2 + z_1^2} + y} \cdot \frac{\sqrt{x_2^2 + y^2 + z_2^2} + y}{\sqrt{x_2^2 + y^2 + z_2^2} - y} \right] \quad (123)$$

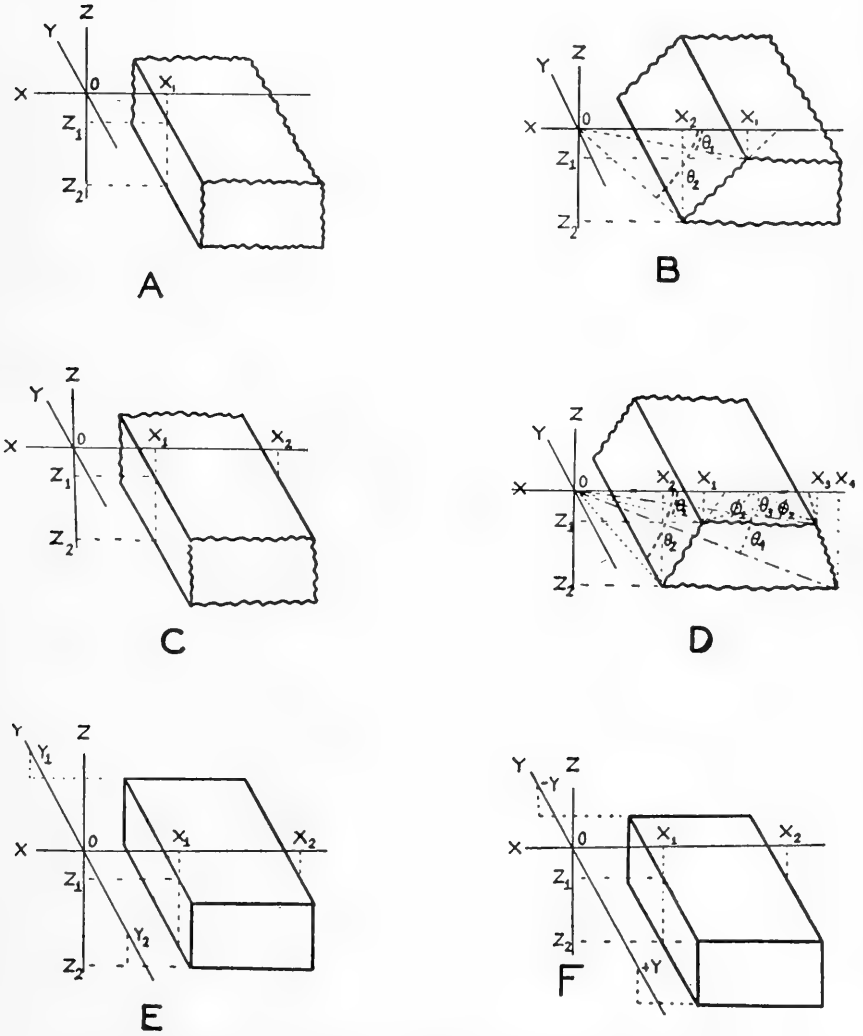

FIG. 207.—Relations of blocks and slabs to coordinate axes. Origin 0 coincides with the center of the torsion balance. (Barton, *A.I.M.E. Geophysical Prospecting*, 1929.)

$$U_\Delta = 2G\sigma\left[\tan^{-1}\frac{yz_2}{x_2\sqrt{x_2^2+y^2+z_2^2}}-\tan^{-1}\frac{x_2z_2}{y\sqrt{x_2^2+y^2+z_2^2}}\right.$$
$$-\tan^{-1}\frac{yz_1}{x_2\sqrt{x_2^2+y^2+z_1^2}}+\tan^{-1}\frac{x_2z_1}{y\sqrt{x_2^2+y^2+z_1^2}}$$
$$+\tan^{-1}\frac{yz_1}{x_1\sqrt{x_1^2+y^2+z_1^2}}-\tan^{-1}\frac{x_1z_1}{y\sqrt{x_1^2+y^2+z_1^2}}$$
$$\left.-\tan^{-1}\frac{yz_2}{x_1\sqrt{x_1^2+y^2+z_2^2}}+\tan^{-1}\frac{x_1z_2}{y\sqrt{x_1^2+y^2+z_2^2}}\right] \quad (124)$$

$$U_{xy} = U_{yz} = 0$$

(f) Same as (e) except $y = y_1$ and y_2 where $|y_2| \neq |y_1|$

$$U_{xz} = G\sigma\left[\log_e\frac{\sqrt{x_1^2+y_1^2+z_1^2}+y_1}{\sqrt{x_1^2+y_2^2+z_1^2}+y_2}\cdot\frac{\sqrt{x_1^2+y_2^2+z_2^2}+y_2}{\sqrt{x_1^2+y_1^2+z_2^2}+y_1}\right.$$
$$\left.+\log_e\frac{\sqrt{x_2^2+y_2^2+z_1^2}+y_2}{\sqrt{x_2^2+y_1^2+z_1^2}+y_1}\cdot\frac{\sqrt{x_2^2+y_1^2+z_2^2}+y_1}{\sqrt{x_2^2+y_2^2+z_2^2}+y_2}\right] \quad (125)$$

U_{yz} obtained from U_{xz} *by* interchanging x and y

$$U_{xy} = G\sigma\left[\log_e\frac{\sqrt{x_1^2+y_1^2+z_1^2}+z_1}{\sqrt{x_1^2+y_1^2+z_2^2}+z_2}\cdot\frac{\sqrt{x_1^2+y_2^2+z_2^2}+z_2}{\sqrt{x_1^2+y_2^2+z_1^2}+z_1}\right.$$
$$\left.+\log_e\frac{\sqrt{x_2^2+y_1^2+z_2^2}+z_2}{\sqrt{x_2^2+y_1^2+z_1^2}+z_1}\cdot\frac{\sqrt{x_2^2+y_2^2+z_1^2}+z_1}{\sqrt{x_2^2+y_2^2+z_2^2}+z_2}\right] \quad (126)$$

$$U_\Delta = -G\sigma\left[\tan^{-1}\frac{y_2z_2}{x_2\sqrt{x_2^2+y_2^2+z_2^2}}-\tan^{-1}\frac{x_2z_2}{y_2\sqrt{x_2^2+y_2^2+z_2^2}}\right.$$
$$+\tan^{-1}\frac{y_1z_1}{x_2\sqrt{x_2^2+y_1^2+z_1^2}}-\tan^{-1}\frac{x_2z_1}{y_1\sqrt{x_2^2+y_1^2+z_1^2}}$$
$$+\tan^{-1}\frac{y_2z_1}{x_1\sqrt{x_1^2+y_2^2+z_1^2}}-\tan^{-1}\frac{x_1z_1}{y_2\sqrt{x_1^2+y_2^2+z_1^2}}$$
$$+\tan^{-1}\frac{y_1z_2}{x_1\sqrt{x_1^2+y_1^2+z_2^2}}-\tan^{-1}\frac{x_1z_2}{y_1\sqrt{x_1^2+y_1^2+z_2^2}}$$
$$-\tan^{-1}\frac{y_1z_1}{x_1\sqrt{x_1^2+y_1^2+z_1^2}}+\tan^{-1}\frac{x_1z_1}{y_1\sqrt{x_1^2+y_1^2+z_1^2}}$$
$$-\tan^{-1}\frac{y_2z_2}{x_1\sqrt{x_1^2+y_2^2+z_2^2}}+\tan^{-1}\frac{x_1z_2}{y_2\sqrt{x_1^2+y_2^2+z_2^2}}$$
$$-\tan^{-1}\frac{y_1z_2}{x_2\sqrt{x_2^2+y_1^2+z_2^2}}+\tan^{-1}\frac{x_2z_2}{y_1\sqrt{x_2^2+y_1^2+z_2^2}}$$
$$\left.-\tan^{-1}\frac{y_2z_1}{x_2\sqrt{x_2^2+y_2^2+z_1^2}}+\tan^{-1}\frac{x_2z_1}{y_2\sqrt{x_2^2+y_2^2+z_1^2}}\right] \quad (127)$$

One of the simple formulas not included in the above list is that for a sloping plane: namely,

$$U_{xz} = 2G\pi\sigma m \quad \text{(approximately)} \qquad (128)$$

where m = slope.

This formula is accurate for gentle dips and is quite useful in computing terrain effects as well as subsurface effects.

Mathematical Treatment of Geologic Structures and Ore Bodies. —To calculate the gravitational effects of actual geologic structures and ore bodies, it usually is necessary to consider the structures as composed of a series of simple bodies for which formulas of the type 115 to 128 are available and not too complicated. The gravity effects are calculated for each of the constituent simple bodies and then summed up to get the effect

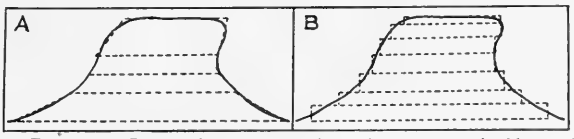

FIG. 208.—Schematic representation of a structural ridge. *A* shows approximation by four prisms, *B* by seven prisms. (Barton, *A.I.M.E. Geophysical Prospecting*, 1929.)

of the whole body. For example, in certain cases, an irregular ridge may be represented by four prisms (Figure 208A) or by seven rectangular prisms (Figure 208B), and the gravity effects of the ridge can be computed as the sum of the effects of the prisms.

The calculations are obviously quite lengthy.† For example, suppose the structure is split into several infinite horizontal prisms. Each evaluation of the appropriate formula would give the gradient for a single rectangular block at a single station. The minimum number of points to determine, approximately, a limited section of profile such as shown in Figure 209 would be five. Good accuracy would require at least nine points. For the differential curvature curve, seven points would be the minimum and thirteen, or more, preferable. To obtain the gradient profile corresponding to Figure 208A, Equation 121 would have to be calculated at least 20 and preferably 36 times; to obtain the differential curvature, Equation 122 would have to be calculated 28 and preferably 52 times.

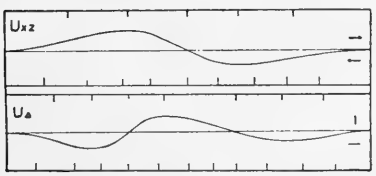

FIG. 209.—General type of gradient and differential curvature profiles produced by structural ridges. (Barton, *A.I.M.E. Geophysical Prospecting*, 1929.)

Quantitative Methods: Trial and Error Calculations.—Actually, the geophysicist is interested in the inverse problem of that described above: namely, it is desired to infer from the observed data, the form, dimensions,

† Barton, *loc. cit.*

and depth to the structure which gives the observed gravity effects. The quantitative, and very rarely used, procedure is as follows:† A tentative cross section as suggested by visual inspection of the results is sketched. This tentative structure is split into blocks, as shown in Figure 208, and the gravity effects are calculated block by block. The calculated anomalies are then compared with the observed anomalies. In order to make the observed and computed anomalies agree, it usually will be necessary to add and subtract blocks from the cross section and repeat the calculations for each addition or subtraction. This procedure is extremely tedious; for example, 3 months of steady calculations of this sort were required to obtain a satisfactory structural picture of the Hoskins Mound Salt Dome, Brazoria County, Texas. The time element, therefore, precludes any appreciable practical use of these interpretative methods.

Short-Cut Methods.†—The most extensive development of these methods has been done by Karl Jung ‡ who has devised formulas and graphical methods for the recognition of certain simple bodies and the determination of their depths and dimensions. Jung utilizes the abscissas of the numerical maxima and minima of the gradient and differential curvature profiles. With the exception of the sphere, the geologic bodies covered by the Jung formulas and graphical methods are assumed: (a) to be infinite at right angles to the vertical plane of the cross section, (b) to have a cross section of simple geometric shape, (c) to be homogeneous in density, and (d) to be surrounded by a homogeneous medium. The methods, therefore, have two obvious limitations: (1) In general, the abscissa of the point of maximum gradient or differential curvature cannot be determined with great accuracy. (2) Most geologic structures and ore bodies cannot be treated as infinite at right angles to the plane of the section; also, their gravity effects do not correspond to those of bodies having a simple geometric cross section.

Graphical Methods.—These methods utilize sets of standard graphs, each graph representing a vertical section along a line of symmetry. In constructing these graphs, formulas of the type 115 to 128 are employed. For example, graphs are based on formulas 119 and 121 when infinite prisms are used as the building blocks and on formulas 123 and 124 when finite prisms are used. In one convenient standard set, the following relations are assumed. Depth to top: depth to bottom: length of each prism $= a : b : c$, where the ratio $a : b$ is retained constant and c is varied.†† Graphs constructed according to this formula correspond to anticlines. (A complete discussion of the graphical method is given by Barton in the article cited.)

† Barton, *loc. cit.*

‡ Karl Jung, "Die Bestimmung von Lage und Ausdehnung einfacher Massenformen unter Verwendung von Gradient und Krümmung's Grösse," *Zeit. für Geophysik*, 1927, Vol. 3, p. 257.

†† D. C. Barton, *loc. cit.*

EXAMPLES OF TORSION BALANCE SURVEYS

Salt Domes.—A major salt dome usually produces a large, clearly defined density anomaly. Salt domes in the Gulf Coast usually comprise a frustrum of a cone of salt capped by a cylinder or thimble-like mass of lime rock-anhydrite-gypsum, intruded into 20,000 to 30,000 feet of Tertiary and Cretaceous sands and clays. † The diameter of the top of the salt core is usually between 1 and 3 miles; the height of the salt core above its base is 3 to 6 miles; and the difference between the densities of the salt and the surrounding beds range from 0 to +0.2 grams per cubic centimeter at the surface to − 0.5 grams per cubic centimeter (estimated) at a depth of 20,000 feet. The vertical thickness of the cap is usually between 200 and 500 feet, but on a few domes it varies between 900 and 1000 feet. The difference between the density of the cap and the surrounding sediments is + 0.5 to + 0.7 grams per cubic centimeter.

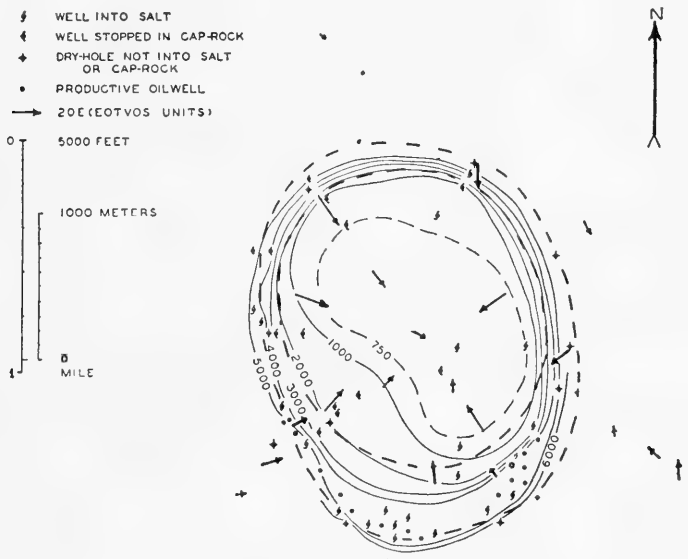

Fig. 210.—Gravity maximum over a shallow salt dome (Nash dome) located in the Gulf Coast, Brazoria and Fort Bend Counties, Texas. (Barton, *A.I.M.E. Geophysical Prospecting*, 1929.)

A characteristic shallow salt dome in the Gulf Coast produces a composite anomaly consisting of a small maximum within a large minimum. The cap, due to its relatively large positive density, produces a gravity maximum. The amplitude of the maximum, which is of the general order of 0.6 milligals, is large relative to the regional variations of gravity. Also, the maximum lies directly above the top of the dome and is only slightly wider than the cap.

† D. C. Barton, "Gravitational Methods of Prospecting," *Science of Petroleum*, Vol. I, pp. 374-375.

The lower half of the salt core, due to its relatively lower density, produces a gravity minimum. The amplitude of the minimum depends on the diameter of the salt core and the downward flare of the flanks. In the Gulf Coast it usually varies between 2.5 and 3.5 milligals, but may reach 7.0 milligals. The values of the gradients of these salt dome minima are of the same general magnitude as those of regional features. Hence, the center of the minimum may be shifted considerably. Most shallow domes show both the maximum and the minimum; one or the other, however, may be too small to be detected.

A deep salt dome produces a gravity minimum similar to that produced by the lower half of a shallow salt dome. The gravity anomaly produced by the cap of a deep dome is not detectible.

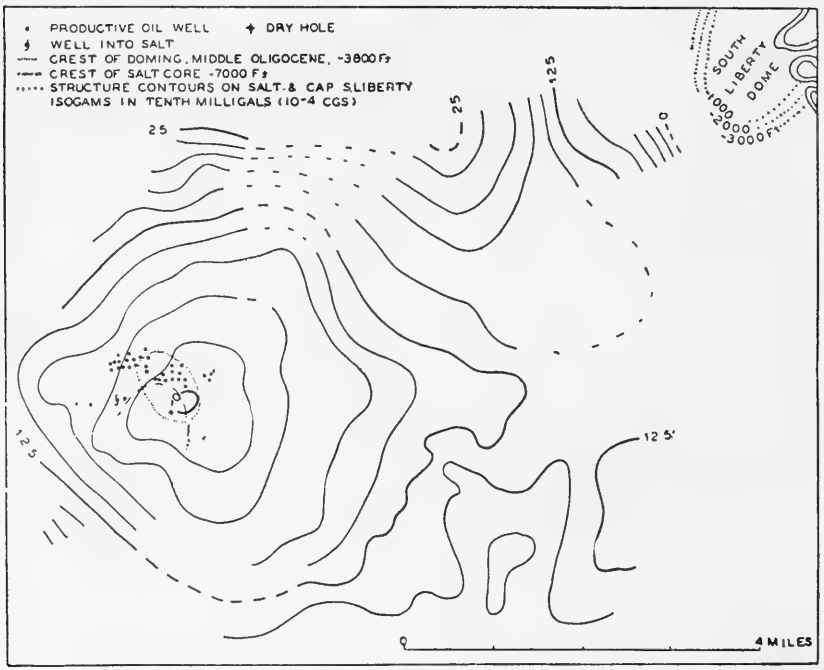

Fig. 211.—Isogams of Esperson salt dome minima. (Barton, *The Science of Petroleum.*)

Figures 210 and 211 show the gravity maximum of a shallow salt dome and the minima of a deep dome respectively. In Figure 210, the gradient arrows are superimposed on the structural contours on the top of the cap-salt. The Nash dome is of particular interest as the first Gulf Coast salt dome to be discovered by geophysical methods. It was predicted from the gradient arrows shown. The two heavy dashed lines are 500—900 feet and 4,000—5,000 feet contours on the cap-salt predicted prior to any drilling. The convergent gradient arrows well away from the dome are presumably due to a large minimum to the west, north, and east rather than to the Nash dome.

Figure 211 shows isogams due to (a) the minimum of a deep salt dome, Esperson, the top of whose salt core lies at a depth of 7,000 feet; (b) part of the minimum around a shallow dome, South Liberty, Texas, the top of whose cap is less than 320 feet

from the surface; (c) the maximum ridge between the two minima. The shift of the center of the minimum eastward from the crest of the dome is presumed to be due to asymmetry of the salt mass.

Other excellent examples of gravity surveys on salt domes are given by Eby and Clark.†

Anticlines.—A map showing the gradient and curvature values over an anticline in northern Mexico is given in Figure 150. This is a very good example which also shows the effect of a fault cutting the structure.

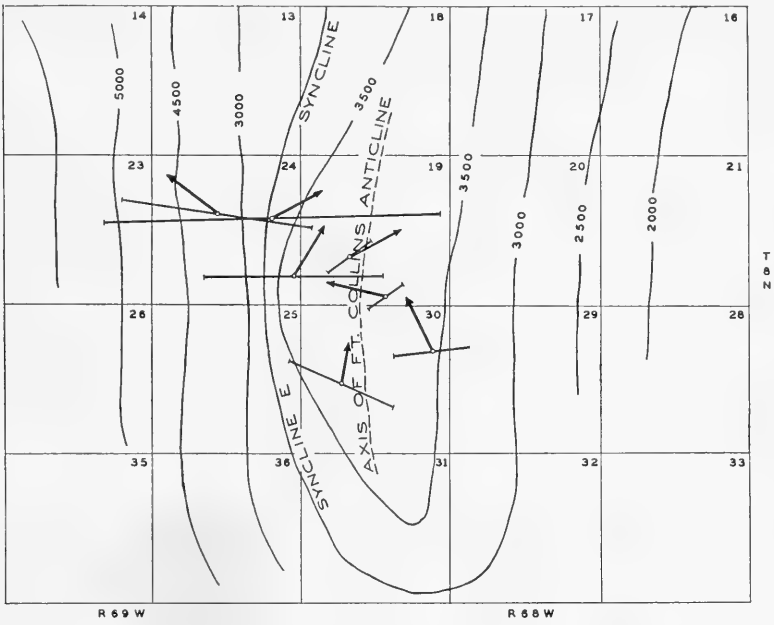

Fig. 212.—Torsion Balance Survey across the Ft. Collins Anticline, Larimer County, Colorado, October, 1928, under the direction of J. H. Wilson. Contours on the Hygene member of the Pierre shale are taken from U.S.G.S. *Bulletin* 796 B.

A torsion balance survey of the Fort Collins Oil Field, in Larimer County, Colorado, is shown in Figure 212. The gradient and curvature values are plotted on a structural contour map made on the Hygene member of the Pierre shale, as published in *Bulletin 796 B* of the United States Geological Survey.

Strong curvature values are indicated by the considerable length of the R-line values, which lie in a direction at approximately right angles to the anticlinal axis of the structure. This is believed to indicate that they are under the influence of a strong regional effect related to the uplift of the mountains not far to the west.‡

† J. B. Eby and R. P. Clark, *A.A.P.G. Bull. 19 (3)*, pp. 356-377, March, 1935.
‡ J. H. Wilson, *Colorado School of Mines Magazine*, Oct., 1928.

An anticline or buried ridge of limestone overlain by shale, with a relief of about 375 feet, is illustrated in Figure 213. The top of the ridge is at a depth of 1500 feet. The structure is not symmetrical, as the right flank is steeper than the left.

The gradient and curvature profiles shown are warped by the asymmetry of the ridge. The zero point of the gradient and the maximum value of the curvature do not lie immediately above the point of the ridge which is structurally highest. They are shifted slightly to the left, down the gentler slope of the structure. The amount of the shift of the gravity gradient minimum is proportional to the difference in the slopes of the two flanks.‡

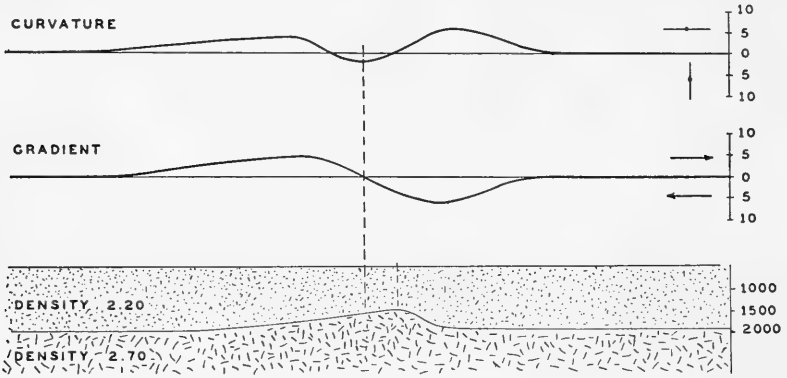

Fig. 213.—Curvature and gradient profiles across a buried limestone ridge. The example illustrates the shift in gradient minimum in relation to the high point of the structure which is asymmetrical. (Afer Barton.)

Faults.—An example of the effect of the famous Luling fault is shown by a survey made by the Rycade Oil Corporation.† Results are given in Figure 214. The change in direction of the R-line value as the fault is crossed is illustrated.

Regional Effects. — Separation of the extended regional gravity effects from those arising from smaller localized geologic structures is shown in a torsion balance survey of the Fox Hills Oil Fields, of Oklahoma.†† The gradients at the survey staions are given in Figure 215, which also shows regional gravity contours (isogams) tied to a U.S. Coast and Geodetic pendulum station.

Indications of the structure at the Fox oil field are only indifferently visible in this figure, but are suggested by the small size of the gradient arrows and their tendency to show a local reversal about 1.5 miles southwest of the town of Fox. The general NNE trend of the gradients and the general increase in the value of gravity in that direction, as indicated by the gravity contours, are the effects of the Arbuckle Mountains lying

‡ D. C. Barton, A.I.M.E. *Geophysical Prospecting*, 1929, p. 439.
† D. C. Barton, *loc. cit.*, *p.*. 451.
†† D. C. Barton, *loc. cit.*, p. 456.

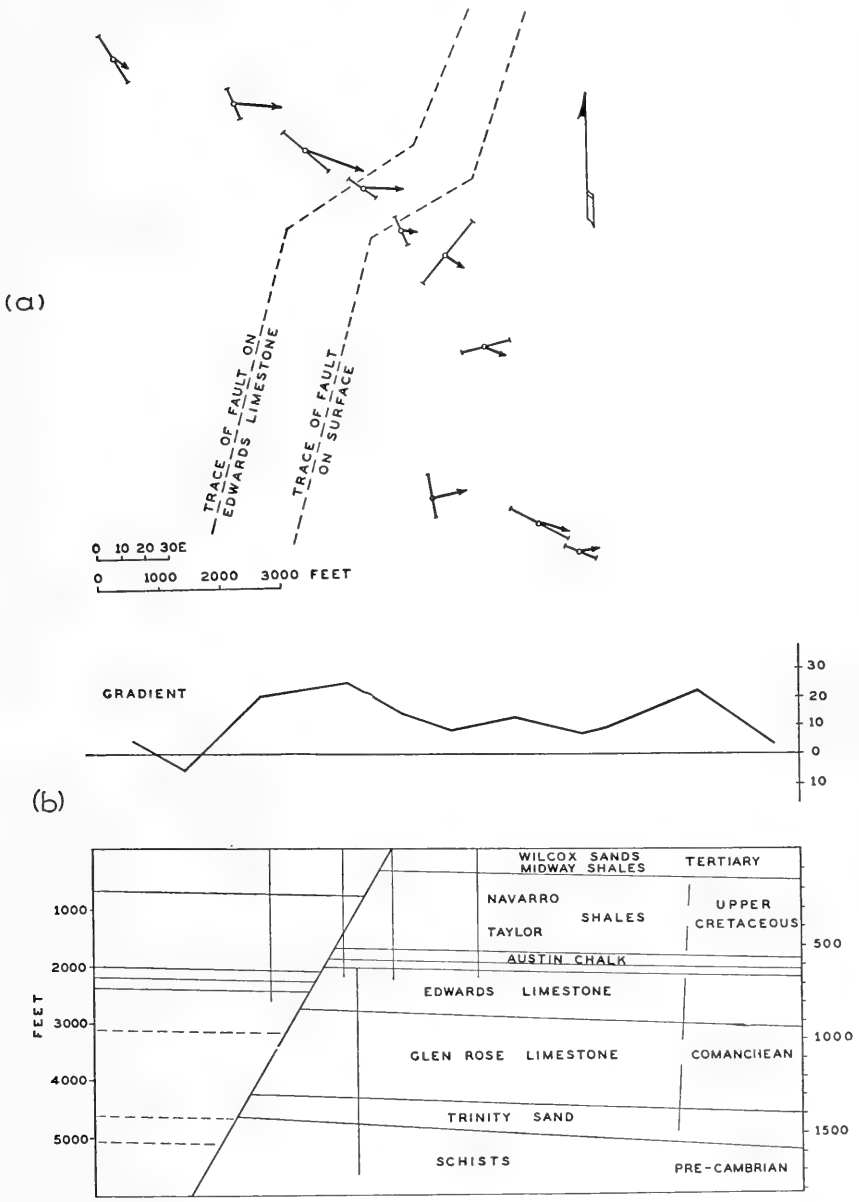

FIG. 214.—(a) Plan view of traverse of torsion balance stations across the Luling Fault, Texas. The surface trace of the fault and its trace on the Edwards Limestone at about 2000 feet depth are shown. (b) Geologic section and gradient profile along survey line. (After Barton.)

not far to the east and the northeast, and of the buried southwest slope of the Arbuckle mass.

The analysis of the torsion balance data consisted in the calculation of the difference in the value of gravity between each pair of adjacent stations and the least square adjustment of these values for the 68 stations

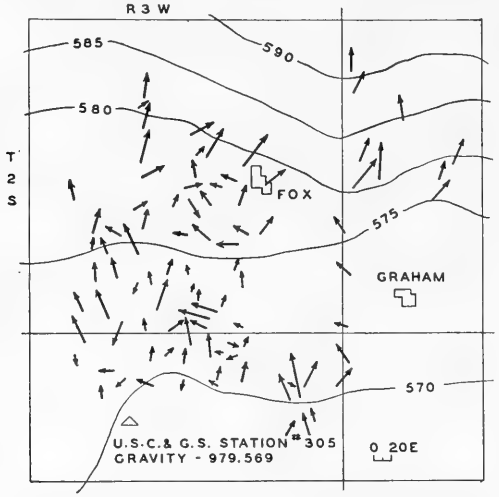

FIG. 215.—Torsion balance survey of the Fox Hills Oil Fields, Oklahoma, showing gradient values. Regional gravity contours (isogams) based on a pendulum gravity station are given. (After Barton.)

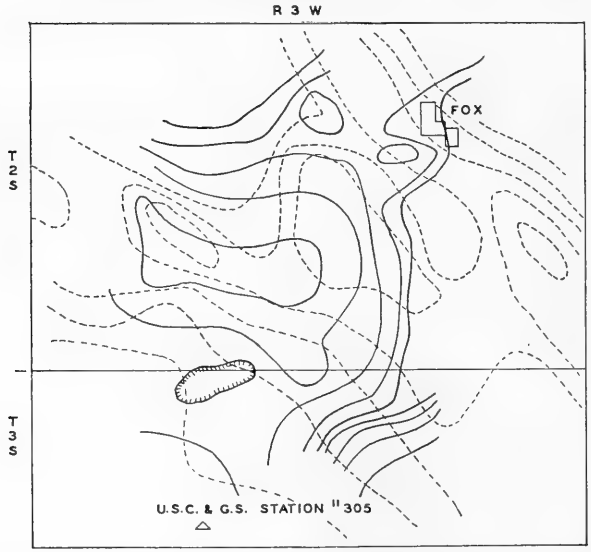

FIG. 216.—Anomalous isogams over the Fox Hills Oil Fields, Oklahoma, after correcting for regional gradient. Generalized subsurface contours shown by broken lines. (After Barton.)

lying S.W. of Fox, and a linear adjustment of values on closed traverses to the N. and W. and S.W. of Fox. The survey was tied into the Busby pendulum station of the U.S. Coast and Geodetic Survey (No. 305), which made it possible to give absolute gravity values to these isogams.

The study gave a value for the regional gradient to be applied to the results pictured in Figure 215. With this regional correction applied, the anomalous isogams are shown in Figure 216, which represents the more local structure of the Fox oil field. The anomalous isogams are superimposed on the generalized structure contour map of the area. (Amerada Petroleum Corporation).

If this had been a wildcat prospect, according to Barton, and acreage had been taken on the basis of the latter map from torsion balance results, a considerable part of the acreage would have been within the area proven to be productive. The slight shift of the anomalous isogams to the southwest from the subsurface structure is probably due to an error in the estimation of the magnitude of the regional gradient due to the Arbuckle mass. The type of analysis made at Fox was warranted by the very complete net of stations. Although here the torsion balance demonstrated ability to map structure showing rather faint gravity effects, such weak indications of structure should not be relied upon in reconnaissance work.

EXPLORATION WITH THE GRAVIMETER

The history of gravity measurements, like that of other exploration techniques, is characterized by cycles. The first stage in such a cycle is the development of the instrument or method. This is followed by the evaluation of its usefulness, its application to hitherto unsolved problems, its peak period of activity, and, eventually, the exhaustion of its possibilities. A resumé of the early history of gravity measurements is given in Chapter I.

The torsion balance was the first gravity instrument to be applied extensively in exploration for structures containing oil (1917-1937). Successful as this method proved to be, there were many advantages to be gained if relative gravity measurements could be made more quickly and with high accuracy. An instrument was needed which would obviate the necessity of laboriously converting gradient values, with their more complex interpretation, to the equivalent direct gravity force values.

About 1935 a number of direct gravity measuring instruments were developed having the necessary accuracy and speed of operation. These developments initiated a wave of gravimeter exploration which has continued to the present time (1949) and is just beginning to show signs of decrease. Thus the torsion balance was replaced by a new geophysical tool, which, if history repeats, will some day itself be superseded.

The next phase in gravity measurement work is not currently apparent. It is possible that, like the magnetometer, the gravimeter will become air-

borne, opening up wide new fields of application. Improved and less costly underwater gravimeters would likewise find wide application to geophysical exploration of the continental shelf area, which awaits more effective procedures and should contain rich rewards for the adventurous.

COMPARISON OF GRAVIMETER METHOD AND TORSION BALANCE METHOD

The modern gravimeter is superior to the torsion balance in regard to the rapidity with which a survey can be carried out. Under normal conditions, a crew using one gravimeter occupies 12 to 20 stations per day, whereas the usual two-instrument torsion balance crew occupies 6 or 7 stations per day. As a consequence of this factor, a gravimeter survey generally is much cheaper than a torsion balance survey.

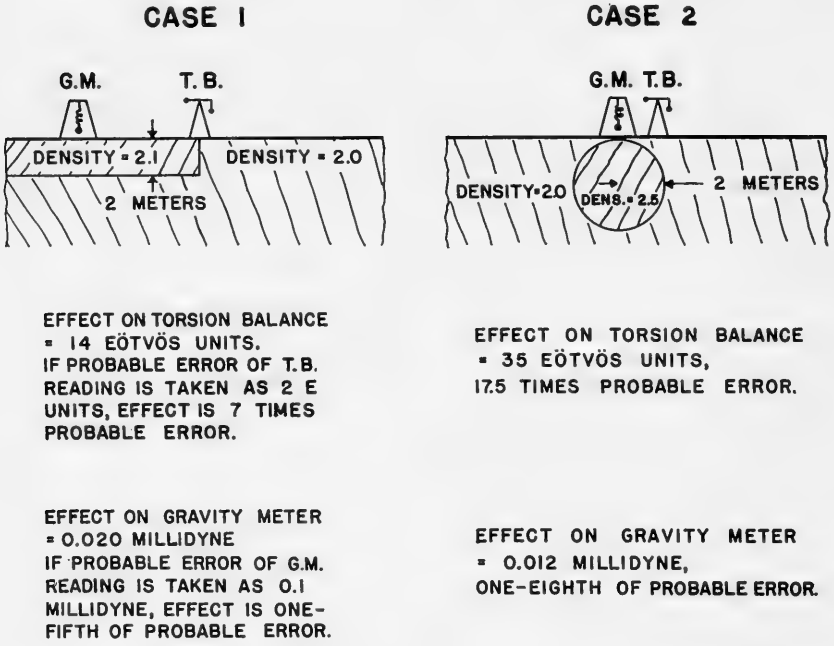

FIG. 217.—Comparison of the effect of disturbing masses on the gravimeter and on the torsion balance. (L. M. Mott-Smith, *Geophysics.*)

The accuracy of gravity maps obtained with the torsion balance is influenced more by the character of the terrain than those obtained with gravimeters. In regions where there is considerable relief or irregular surface materials, the use of a gravimeter is preferable. Thus, a distant mass which produces comparable effects on the two instruments, say one Eötvös unit on the torsion balance and one-tenth millidyne on the meter, will produce a considerably greater effect on the balance than on the meter when close to the two instruments.† This is illustrated in Figure 217 which gives two examples of the effect of local disturbances on the two instruments. Case 1 illustrates the effect of a thin layer which is located at or near the surface and has a greater density than the normal soil. This layer is assumed to begin as shown and extend

† L. M. Mott-Smith, "Gravitational Surveying with the Gravity Meter," *Geophysics*, Vol. II, No. 1, pp. 30-32.

forward, backward, and to the left for a considerable distance. Both the gravimeter (G.M.) and the torsion balance (T.B.) are placed at the least favorable position for each. The greatest effect on the meter occurs when it is directly over the bed and far removed from the edge; the greatest effect (maximum gradient) is experienced by the T.B. when it is set up over the edge as shown. The calculated effects, which are summarized in Fig. 217, show that the gradient effect is large, being about seven times the probable error of the T.B.; while the relative gravity effect is altogether negligible.

Case 2 deals with a boulder, which for simplicity has been taken as a sphere located just below the surface. The calculated effects corresponding to the least favorable positions of the two instruments are summarized in Fig. 217. They show again, that in terms of the probable errors of the instruments, the effect on the balance is considerably greater than on the meter. These calculations indicate that the gravimeter should be capable of obtaining usable results in regions where shallow irregularities of density would make torsion balance work practically worthless.

The Gravimeter

The gravimeter is an instrument with which relative values of the force of gravity can be measured directly. It is similar to a field magnetometer in many respects. Gravity values obtained with the gravity meter are relative only to some base station of the survey and, as in measurements of the magnetic intensity, changes in value only need to be considered. Latitude corrections and base checks for daily variation, which with the gravity meter are purely instrumental matters, are handled in much the same way as in magnetic surveying.

Direct determinations of the relative gravity with a gravimeter or gravity meter consist in "weighing" the same object with very great precision at several stations. The weight of an object at any location on the earth's surface is equal to the force of attraction exerted by the earth on the object. That is, the weight is equal to the product of the mass m of the object, which remains the same at all locations, and the acceleration g due to gravity. The acceleration g varies with the density of the materials comprising the outer crust of the earth. Hence, the weight of a constant mass m at any station is affected by the nature of the subsurface materials. For example, the value of g is greater at stations where the subsurface material is relatively dense. The observed changes in weight are very small, being of the order of one part in ten million of the total value of gravity.

The Gravimeter as a Weighing Device.—Since the gravimeter is essentially a very sensitive form of scales, its accuracy may be made extremely high. To illustrate this degree of accuracy, it will be recalled that 0.1 of a milligal is 1 part in ten million of the total force of gravity. L. L. Nettleton† has put this matter into understandable terms along the following line. In a spring-type gravimeter, a mass is suspended on a spring. If the mass were such that it would stretch the spring to a length of 30 centimeters, the accuracy of measurement necessary to detect a dif-

† L. L. Nettleton, "Geophysical Prospecting for Oil," McGraw-Hill, 1930, p. 31.

ference of 1 part in ten million would represent a movement of the mass (or an increase in the length of the spring) by only $30 \cdot 10^{-7}$ cm.

Such a small movement is not easy to detect, and is extremely difficult to incorporate into a repetitive, reproducible measurement. By various arrangements to magnify extremely small motions, as is brought out in the descriptions of gravimeters, the problem is solved for practical purposes.

Instrumental Problems in Gravimeter Construction

Many instrumental difficulties were encountered in the development of the gravimeter. The chief problem was measurement of the minute displacement of the mass produced by a change in the gravitational force of attraction. The measurement must be made with an accuracy of about one ten-millionth of an inch. Several systems have been developed which possess the required sensitivity. The most satisfactory method employs a compound spring system which is mechanically equivalent to a simple spring of very large extension. Compound spring systems increase the displacement some ten to one hundred times that of a practicable simple spring. A sensitive optical system, working in conjunction with the compound spring, constitutes the essential means for measuring the displacement to the required accuracy.

Another difficulty encountered in the gravimeter development was the variation in the displacement of the spring system due to changes in temperature. This variation is caused primarily by: (a) thermal expansion and (b) changes in the elasticity of the spring material. The first effect is large due to the high coefficients of expansion of the materials most commonly used for springs. For example, a steel spring may increase in length from one-half to two parts in ten thousand per degree centigrade rise in temperature. Thus exposure of a gravimeter having a steel spring to ordinary temperature variations would result in displacements due to temperature variations which would be very large in comparison to those due to gravity. Temperature effects have been minimized by a number of methods, chief of which may be mentioned: (1) compensation by use of bimetallic materials similar to those employed in the new temperature-compensated magnetic systems, (2) maintenance of constant temperature by use of electric thermostats, (3) utilization of spring materials having a very low temperature coefficient. Usually, all three of these methods are employed. The most effective control, however, is the use of a well-insulated cabinet provided with accurate thermostatic control. Such equipment can maintain the temperature constant within one-hundredth to one five-hundredth centigrade degree.

The most troublesome difficulty to be overcome was the imperfect elasticity exhibited by all elastic materials. This imperfection appears in two distinct manners termed *creep* and *elastic-after-effect* or *elastic lag*. Creep is simply a gradual yielding of any "solid" material when under load. This effect is usually negligible in ordinary engineering applications but must be

considered for precise work, as it may in unseasoned common steel springs cause an increase in length of twenty parts in ten million per hour. Elastic lag inhibits the rapid return of a spring to its original length after a displacement. The gradual return of a spring to its original condition depends on the amount of displacement and the length of time it has been displaced. Elastic lag, if present to an appreciable extent, impairs the accuracy because its effects are unpredictable.

The limitations of the gravimeter are due almost exclusively to the limitations of available spring materials. In addition to the preceding problems there are numerous secondary ones. The calibration of the instrument must not be affected by jars or vibration such as encountered in average field operations. Also, the damping of the elastic system should be as nearly aperiodic as possible, consistent with sensitivity. Unless this is done the system will be affected unduly by disturbances, such as might be caused by a passing automobile which sets the system into oscillations that persist for an extended period of time. Under these conditions, observation would be impossible if disturbances are frequent. Average vibration of the ground usually will not cause appreciable unrest of a properly designed elastic system; however, near the ocean, the pounding of the waves does produce a quite noticeable unrest of the elastic system.

Classifications of Gravimeters

The gravimeters used in geophysical prospecting may be classified into two types: static and astatic instruments. The simplest type of static gravimeter comprises a heavy mass M rigidly attached to an elastic spring. Some form of amplification system is employed, often optical, whereby slight displacements of the mass may be measured. The operative technique may be summarized briefly as follows. The equilibrium extension, or compression, of the spring supporting the weight is determined at a base station, and the reading recorded. The meter is then moved to one of the field stations and the equilibrium extension, or compression, at this station is recorded. A comparison of the two readings, after making the necessary corrections, gives the relative gravity of the field station as compared to the base station.

Astatic gravimeters employ an auxiliary restoring force opposite in sign and approximately equal in magnitude to the elastic restoring force. In general, therefore, the mass M or bob of an astatic gravimeter is subject to three reactions: (1) the pull of gravity, (2) the elastic restoring force of a spring, and (3) an astatizing or labilizing force which acts in the same direction as gravity and has a magnitude nearly, but not quite, the same as the elastic restoring force of the spring.

For small displacements, the force due to gravity tending to displace the mass is $A(g - g_0)$ where g is the gravity value at the point of reading and g_0 is the value at a base station; the elastic force is $-Bx$, where x is the displacement of the mass from the position occupied at the base station; and

the astatizing force is Cx. Hence, the resulting force on the mass when it is in equilibrium is:

$$A(g - g_0) - (B - C)x = 0$$

The displacement is:

$$x = \frac{A}{B - C}(g - g_0)$$

It is evident from the last relation that if C can be made approximately equal to B, the sensitivity, $A/(B-C)$, can be increased to any desired value. Naturally, this involves many instrumental difficulties.

It is interesting to notice that if Dd^2x/dt^2 is the force required to produce an acceleration of d^2x/dt^2, the equation for small motions, neglecting the effect of damping, is

$$D\frac{d^2x}{dt^2} = A(g - g_0) - (B - C)x$$

which has the solution

$$x = \frac{A}{B - C}(g - g_0) + A_0 \sin(2\pi t/T)$$

where

A_0 = a constant which depends on initial conditions

and

$$T = 2\pi\sqrt{\frac{D}{B - C}} = \text{period of oscillation about the new equilibrium position.}$$

The last relation shows that the sensitivity is proportional to the square of the period; that is, $1/(B-C)$, and hence $A/(B-C)$, is proportional to T^2.

A second classification of gravimeter types depends upon the method of reading the change in gravity. In scale reading instruments, an indicator of some kind moves across a graduated scale. In null reading instruments, an opposing force is applied to return the mass to a standard reference position and the amount of this force is measured on a scale based on prior calibration of the instrument.

Operating Principles of Various Gravimeters

The particular instruments described in the following pages illustrate representative types. The list is not intended to be exhaustive, but merely illustrative of the general trend of design.

Hartley Gravimeter.—The Hartley instrument, illustrated in Figure 218, is one of the simplest types of gravimeters.† In this instrument, displacements of the mass M due to variations in gravity are compensated by changing the pull of the spring S_2 so that the mirror D will show the

† A. B. Bryan, "Gravimeter Design and Operation," *Geophysics*, Vol. II, No. 4, pp. 302-308.

reflected image of the lamp L at some fixed position. The main spring S_1 supports the mass M. The cross member AB is hinged at A with a flexible metal strip, or Galitzin hinge, which permits the end B to move up and down, with movement of M. The movement of B causes the small mirror D which bridges the gap to tilt from side to side. Adjustment of the instrument is accomplished by returning the reflected image to a previously chosen reference line in the eyepiece E, by turning the divided head H.

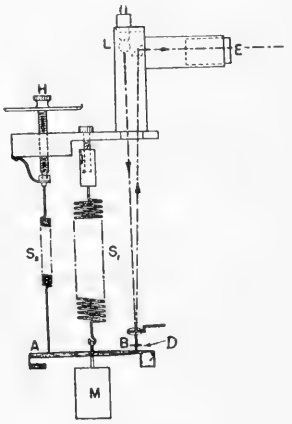

FIG. 218.—Diagrammatic sketch of Hartley type gravimeter. (Bryan, *Geophysics.*)

The Hartley meter employs no astatizing force, depending instead on mechanical and optical magnification of the displacement of the beam for its sensitivity. A movement of the mass of 10^{-5} mm. results in a movement of 0.6 mm. at the eyepiece. The meter employs a thermostat to keep the temperature constant to within 0.01°C. The instrument is highly damped and relatively insensitive to leveling. The mechanism is in an airtight container, with the clamps and screw H working through mercury seals.

Truman Gravimeter.—This instrument is illustrated in Figure 219. An approximately triangular framework A is hinged at N by flexible metal strips.† The spring S_1 supports the mass M which is attached to the outer end of the framework. A second spring S_2, which is attached to the lower end of the framework at B, pulls directly upward almost through the hinge line. This spring acts to increase the sensitivity of the instrument. By adjusting the tension of S_2 for a given position of B, the moving system approaches unstable equilibrium with increased sensitivity. A third very small spring (not shown in the sketch) is attached to the frame and works in parallel with S_1.

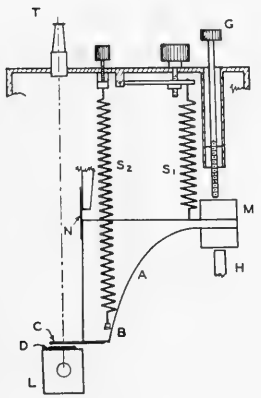

FIG. 219.—Diagrammatic sketch of Truman type gravimeter.

An optical system T is focused from above on a reference line C attached to the frame. Readings are made by observing the lateral motions of this reference line corresponding to vertical motions of M. A lamp L shining through a ground glass D illuminates the reference line or scale. Means are provided to damp the motion of the moving system electromagnetically and to clamp it.* Also, provision is made for the frame to

† A. B. Bryan, *loc. cit.*

* The instrument usually is either undamped or else damped electromagnetically.

carry a small rider of known weight which is used in calibrating the meter. A clamp screw *G* locks the system. The temperature of the case in which the meter is mounted is controlled accurately. The behavior of the commercial type meter is indicated by Table 11, which is a summary of data for five closed loops. Loop *B*, for example, involved a total of 20 miles of line, 6 gravity stations, a maximum gravity difference of 200 units between the highest and the lowest station, and an error in closing of 2.6 units. (The closure error, or the amount by which the algebraic sum of the gravity differences around a closed loop differs from zero, is a measure of the combined effects of: (1) uncompensated instrumental errors such as creep, elastic-after-effect, temperature changes, pressure variations, etc.; (2) inaccuracies in reading of the instrument; and (3) errors due to variations in calibration on scale value.)

TABLE 11 †

SAMPLE GRAVITY DATA OBTAINED WITH TRUMAN GRAVIMETER

Loop	Total Miles	Total Stations	Max. Gravity Difference in 10^{-4} C.G.S. Units *	Closure Error 10^{-4} C.G.S. Units
A	18	6	208	2.3
B	20	6	200	2.6
C	33	30	208	1.9
D	50	31	514	4.7
E	22	16	270	1.7

Hoyt Gravimeter. ‡—A schematic vertical section of this instrument is shown in Figure 220. The instrument was developed by the Gulf Oil Corporation§ as the result of research begun in 1933. It is unastatized and a mass is supported on a helical ribbon spring, thus retaining the simplicity of a spring balance. The advantage of this design is that gravity force changes are translated into rotation of the suspended mass.

The gravimeter consists primarily of a helical spring formed of steel or of other suitable elastic material. The helical spring is suspended at one end from a fixed support through an adjustable hanger 72 which allows the spring to assume freely a vertical position. The other end of the spring 64 is joined to another helical spring by means of a post 82. The post is provided with a collar 83 which carries a spider 84, which in turn carries a narrow-rimmed annular weight 85 concentric with the axis of the helix. The spring and weight combination hangs freely. The weight of the annulus 85 changes in accordance with the force of gravity at the location where the apparatus is set up. This change in weight produces

† Bryan, *Geophysics, loc. cit.*

* The unit employed is 0.1 millidyne or approximately 1/10,000,000 of the total value of gravity.

‡ Archer Hoyt, "Gravimeter," U. S. Patent 2,131,737, issued Oct. 4, 1938. (Assignor to the Gulf Research and Development Company.)

§ R. D. Wyckoff, "The Gulf Gravimeter", *Geophysics*, Vol. 7, No. 1, Jan., 1941, pp. 13-33.

a greater or less pull on the spring, as the case may be, and this causes an angular deflection of the lower end of the spring.

The angular deflection is observed with the aid of the lens 96 attached to the lower portion of the post 82 and additional optical apparatus including a source of light, scale and two totally reflecting prisms.

With an optical lever arm 22 inches long and using the 4th multiple reflection (although 6 are visible), a displacement of the index of 0.001 inch (corresponding to 0.1 milligal of force) can easily be read, with the microscope. The instrument can be quickly adjusted for the magnitude of gravity in an area, without affecting the calibration, by means of a torsion head from which the system is suspended.

The scale constant is 100 divisions per milligal on the 4th reflection, and readings to 0.05 mg. or better are possible under ordinary field conditions. Tests have shown a probable error for any one station of 0.02 mg.

In the Hoyt gravimeter the direction of instrument drift (or creep of the spring) can be controlled by adjusting the mass to the proper value. This adjustment is made so the meter is operating near the reversal point. A typical meter showed a drift over a 30-day period of only about 0.3 mg. in 24 hours.

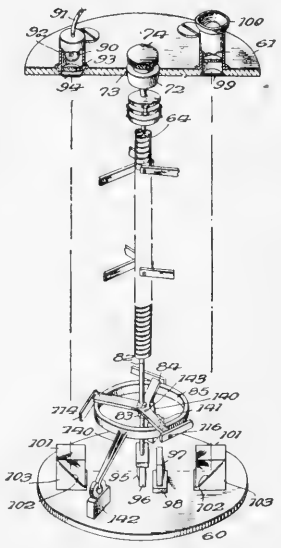

Fig. 220—Hoyt Gravimeter—schematic vertical section. (Hoyt, U. S. Patent 2,131,737.)

Electromagnetic damping is applied by a metallic vane (attached to the mass) moving through the air gap of a permanent magnet. Leveling is a critical feature of spring suspension arrangements because, when released, the system is essentially a plumb bob. In this case the system was made less sensitive to leveling by tapering the spring at the point of suspension to compensate for the bending of the spring caused by its being off level. Such bending is converted, in part, into rotation. Two 10-second spirit levels set at right angles are provided with special leveling screws which operate in an oil bath and are therefore dust free. As expressed in terms of level arc causing a 0.1 mg. change in reading, the meters varied from 10 to 60 seconds, so that the 10-second levels were sufficiently delicate.

The meter is clamped by means of 3 ball-tipped clamping arms actuated by a control shaft and gear train and engaging 3 lugs on the moving mass. The instrument is suspended in a heater shell surrounded by insulating material covered with thin aluminum. Temperature is controlled by a thermostat and the heater elements are supplied by a 12-volt battery. Temperature can be held constant to 0.02 C.° in field operations.

When an observation is made, the meter is removed from the field truck and set on three stakes driven into the ground. Usually 40 to 50 stations a mile apart can be made in an 8-hour day by an observer and one helper. An exterior view of the instrument is shown in Figure 221.

FIG. 221.—Gulf gravimeter, showing yoke (near center of gravity for support during transportation), carrying handles, leveling screws, and dust cover, which is removed. An operator is shown making final adjustments. The weight of the instrument proper is 25 lbs. The complete equipment weighs 95 lbs., while the battery and control equipment weigh from 45 to 85 lbs.

Thyssen Gravimeter.†—The principle of this meter will be evident from a consideration of Figure 222. Mass M, which is made of platinum and weighs approximately 20 grams, is fastened to one end of the quartz beam B. This beam is supported by a knife-edge K. At the other end of the beam is a spring S (of relatively small weight compared to M) fastened at its lower end to a micrometer screw J. The spring is enclosed within a closely fitted metal tube which in turn is enclosed in an insulating medium. Vertically above the knife edge there is supported an adjustable astatizing weight A. By suitable adjustment of this weight the astatizing force can be made to approach the spring force. Ordinarily, the astatizing mass is adjusted to give a period of from 6 to 10 seconds. The end of the mass carries a small scale which is read by means of a microscope and prism P

† A. Schleusener, "Messungen mit Transportablen Statischen Schweremessern," *Zeitschrift für Geophysik*, Vol. 9, 1934, p. 369.

St. v. Thyssen, "Ueber die Wirkungsweise von einigen Federgravimetern," *Zeitschrift für Geophysik*, Vol. 15, 1939, p. 121.

—an arrangement which gives an optical magnification of 60. The meter has very little damping. The spring material and construction, and the material and length of the tube surrounding the spring, are so chosen that the temperature effect is very small. In normal operation the entire meter is enclosed in a thermally insulated box, but usually without thermostat control. The instrument is very sensitive to level; consequently, in practice, two nearly identical units are employed with opposite orientation, i.e., with masses mounted at approximately the same level but on opposite sides of co-axial knife-edges. This expedient is employed in several other meters which are sensitive to level.

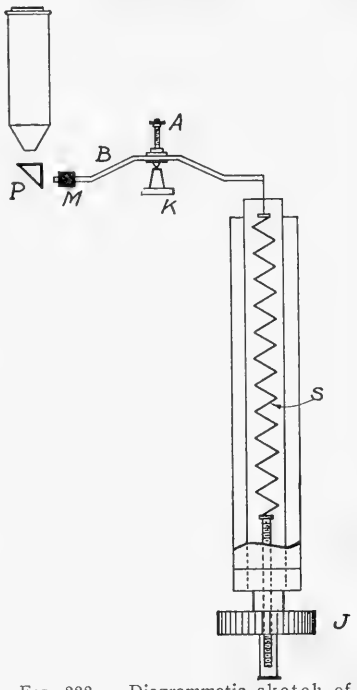

FIG. 222. — Diagrammatic sketch of Thyssen gravimeter. (*Zeitschrift für Geophysik.*)

"Zero Length" Spring Gravimeter. —Another gravimeter utilizes a "zero length" spring.† Figure 223 shows a diagram of the essential part of the meter. The spring S is so wound that its elongation is equal to the distance between the points where it is attached; that is, if one defines the initial length as the actual physical length minus the elongation, this type of spring has zero initial length.

The weight W is fixed to the arm DC which is pivoted at D. The spring S is attached to the arm at the point C and to the frame at the point F vertically above the pivot D. The distances a and b are about 45 cm. and the weight W about 2.5 kg.

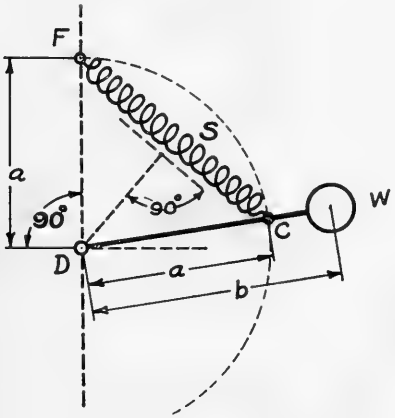

FIG. 223.—Diagrammatic sketch of spring gravimeter. (After La Coste, *Physics.*)

The period of the spring can be given almost any desired value by choosing a spring material which has an appropriate constant. For periods of about one minute the system tends to become unstable and hence very sensitive to variations in the torque exerted by the weight.

The meter is damped and employs an additional spring in order to return the mass to its standard position mak-

† L. J. B. La Coste, Jr., "A New Type of Long Period Vertical Seismograph." *Physics,* Vol. 5, 1934, p. 178.

ing the instrument a null reading type. The instrument is compensated for small changes in temperature.

Wright Gravimeter.‡—The Wright meter (Figure 224) comprises primarily two helical elastic springs which taper from opposite ends toward a common center portion to which is attached a relatively short aluminum rod. The rod carries a weight at its outer end and a mirror at or adjacent its inner end on the axis of the two helical springs. The helical springs are attached at their outer ends to a frame 12 which is rotatably mounted. The frame, together with the springs, may be rotated by means of a shaft extension terminating in a knurled head 14. Clamps are provided for preventing serious vibrations of the springs during transportation. Also, to minimize temperature variations within the case, and hence changes in the elastic constants of the spring, the case is thermally insulated by use of several outer casings.

The operating procedure may be summarized as follows. At a given location (base station) the frame and springs are rotated by means of the knurled head 14 until the aluminum rod and weight W are in an approximately horizontal position (standard reference position). The standard position of rest is determined by means of an autocollimating telescope sighted on the mirror M. The reference angle is read off the graduated circle 15 attached to the axis of rotation of the frame 12. The difference in the readings of the graduated circle for the two horizontal positions of the aluminum arm is a measure of the elastic deformation set up in the springs by the mechanical torque exerted by this arm in response to the gravity pull on weight W. The instrument is then moved to another location (field station) and the procedure repeated. The relative difference in the readings of the horizontal positions at the field station as referred to that at the base station is a measure of the relative gravity at the field station.

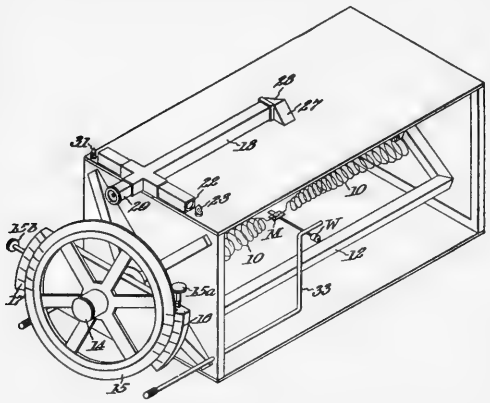

FIG. 224.—View of the Wright gravimeter. (U. S. Patent 1,579,273.) 10, helical elastic springs; W, mass; M, mirror; 12, supporting frame of helical springs; 14, adjustment knob; 15, graduated circle; 16 and 17, vernier scales; 18, autocollimating telescope; 23, light; 27, totally reflecting prism.

Boliden Gravimeter.†—This instrument is a static type wherein the

‡ F. E. Wright, U. S. Patent 1,579,273.

† H. Hedstrom, "A New Gravimeter for Ore Prospecting," *A.I.M.E. Geophysical Prospecting*, Tech. Pub. 953, pp. 12-15 (Feb., 1938).

determination of the relative gravity is based on a change in capacity produced by a vertical displacement of a spring-supported plate.

A schematic section of the gravimeter is shown in Figure 225. The movable body is suspended by the plate springs F which are attached to the cross piece of the support E. The top of the movable member forms one plate of a parallel plate condenser, the other plate of which is fixed to a thick steel disc A by an electric insulator B. The contact C connects the condenser with the oscillatory circuit of an ultramicrometer coupling which registers minute variations in capacity between the two plates. The function of the lower plates (the returning plates) is to provide a means for returning the movable body to the zero (base station) position. This is accomplished by applying a potential to one of the plates, thus causing the movable plate to be displaced due to the electrostatic forces produced by the potential difference between the plates.

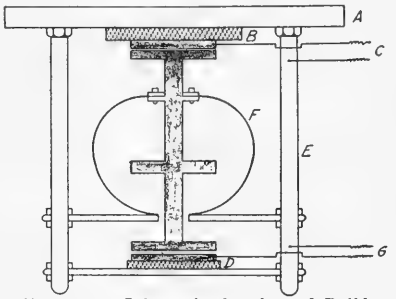

FIG. 225.—Schematic drawing of Boliden gravimeter. (After Hedstrom, *A.I.M.E. Geophysical Prospecting*, Tech. Pub. 953, p. 13.)

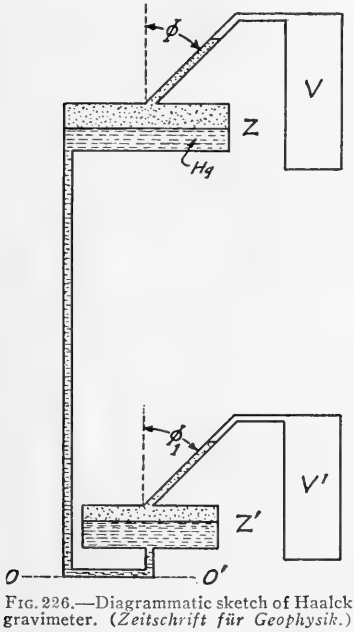

FIG. 226.—Diagrammatic sketch of Haalck gravimeter. (*Zeitschrift für Geophysik.*)

The ultramicrometer coupling is designed so that variations in the anode current caused by changes in the capacity between the two plates are registered on a milliammeter. To accomplish this, the plates are connected to the grid circuit of an oscillating tube. By choosing the instrument constants such that the plate separation of the condenser is 0.002 cm. and the coupling sensitivity 10 ma. per cm., a gravimeter sensitivity of 0.01 milligal may be obtained. An instrumental sensitivity between 0.01 and 0.05 milligal is claimed.

Haalck Gravimeter. †—The Haalck meter is a static meter using a sealed volume of gas as the elastic medium. A schematic representation of the meter is shown in Figure 226. The long vertical tube and the lower portions of the two containers Z and Z' are filled with mercury. The upper portion of each of the containers Z and Z' and a portion of the tubes above them are filled with a light fluid, such as toluol. When the value of gravity varies, the density of the mercury column varies correspondingly. Also, the volumes of gas in the two chambers V and

† H. Haalck, "Ein Statischer Schwerkraftsmesser," *Zeitschrift für Geophysik*, Vol. 7, 1931, p. 95; Vol. 8, 1932, pp. 17 and 197; Vol. 9, 1933, pp. 81 and 285.

V' vary in such manner that the total net gas pressure on the ends of the fluid column is equal to the weight of the fluid. By making the ratio of the area of the containers Z and Z' to the area of the capillary tubes containing the toluol very large, the displacement of the liquid in the capillary tubes can be made many times the displacement of the mercury in the containers so that a high sensitivity can be obtained by readings of the toluol menisci. Furthermore, if the proper choice of volumes is made the temperature effect can be somewhat decreased, but at best, the meter is quite sensitive to temperature and is usually used in an ice bath. The instrument is highly damped and has been used with considerable success for coarse work on ship board.

Astatic Hydraulic Gravimeter. ‡—This instrument is an astatic type which utilizes the flow of liquid as an astatizing means. The meter comprises a specially shaped container connected to a vertical spring and a fluid system whereby, upon lengthening of the spring, fluid flows into the mass, thus increasing its weight and further lengthening the spring. A schematic view of one form of the meter is shown in Figure 227. The tube system is completely filled with the fluid and the containers 4 and 13 are partially filled. Stops 8 and 9 on the scale 10 define the limits within which the balance can move.

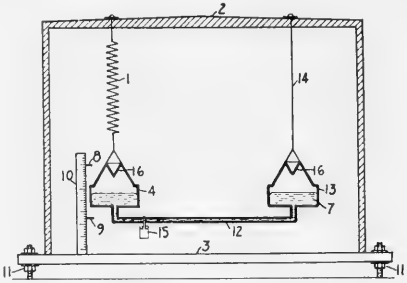

Fig. 227.—Schematic view of the astatic hydraulic gravimeter. (Evjen, U. S. Patent 2,117,471.)

The operation of the instrument may be summarized as follows. The gravimeter is leveled by means of the leveling screws so that the liquid in the container or pan 4 is at the same level as in the container 13. Any increase in the value of the force of gravity acting on the mass of the pan 4 will cause the pan to move downward, thereby stretching the spring 1. The liquid in the pan 4, however, will tend to remain at the same level as in the container 13, so that a certain amount of liquid will flow into the pan 4 from 13 through the tube system 12. The resulting increase in the quantity of liquid in pan 4 will cause a further stretching of the spring 1 and accentuate the downward movement of 4. A decrease in the value of gravity will cause a reverse process to take place. It is claimed that the instrument is capable of high precision provided it is leveled with very great accuracy.

Mott-Smith Gravimeter. †—This instrument is an astatic meter employing an auxiliary quartz fiber as a labilizing spring to effect a further movement of the "weight" after it is initially moved by gravity.

The component parts of the meter are shown schematically in Figure 228. A T-shaped frame 3 having arms 4 is rigidly attached to a casing by means of a clamp 2. A torsion fiber 5, which is about 1½ inches long and about 0.002 inches in diameter, carries a weight arm 7, which, in turn, is connected to the labilizing fiber 8. The latter is connected to the T-frame 3

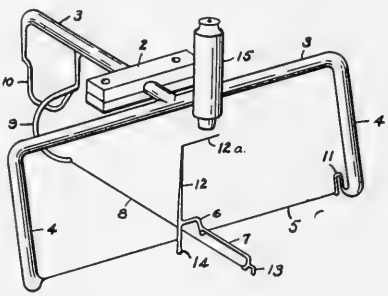

Fig. 228.—Perspective view of the Mott-Smith gravimeter. (Mott-Smith, U. S. Patent 2,130,648.)

‡ H. M. Evjen, "Gravimeter," U. S. Patent 2,117,471, issued May 17, 1938. (Assignor to Shell Development Company.)

† L. Mott-Smith, "Torsion Gravimeter," U. S. Patent 2,130,648, issued Sept. 20, 1938.

through two springs 9 and 10. The weight arm 7 is fixed and normally extends in a substantially horizontal position from the torsion fiber 5.

The center of gravity of the suspended system, which includes the arm 7, its extension 13, pointer 12, and counterweight 14, is placed as nearly as possible at the same level as the torsion fiber 5 by adjusting the counterweight 14. The substantially-horizontal equilibrium position of the weight

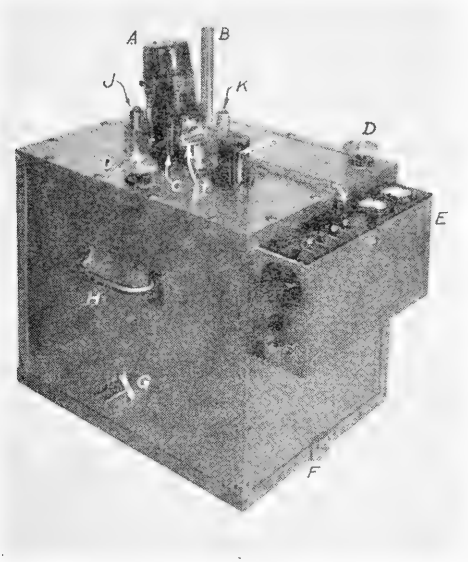

FIG. 228a.—Exterior view of Mott-Smith gravity meter.
(Courtesy of Mott-Smith Corporation.)

A—Bath stirring motor
B—Thermometer housing
C—Observing microscope housing
D—Leveling screws
E—Electric control panel for thermostat
F—Foot mounting bracket
G—Truck mounting bracket
H—Carrying handle
I—Reading light
J—Thermometer reading microscope
K—Thermometer reading light

arm 7 is adjusted by adding or removing quartz by fusion, or by bending the extension 13.

Operation of the instrument is as follows: The weight arm is adjusted at a base station until it is in a substantially horizontal position and the position of the pointer arm 12a attached to the pointer 12 is observed with the aid of the microscope 15. In this position, the auxiliary fiber 8 passes through the center of gravity of the suspended system and hence exerts no torque on it. The instrument is then moved to another station. If the acceleration due to gravity is greater at this station, the weight arm 7 will be pulled downwardly against the resistance of the torsion fiber 5; at the same time the fiber 8 exerts a torque on the suspended system, tending to

TABLE 12

CLOSURE DATA, ILLUSTRATING ACCURACY OF MOTT-SMITH GRAVIMETER†

Total Gravity Difference (millidynes)	Number of Differences in Loop	Error of Closure (millidynes)
17.07	4	0.19
15.20	3	0.26
14.90	4	0.11
15.65	5	0.03
6.05	4	0.05
8.67	3	0.23
6.48	3	0.16
8.16	4	0.04

displace it still further. The total displacement of the pointer arm 12a is then measured by means of the microscope 15.

An exterior view of the Mott-Smith gravity meter is shown in Figure 228a. The instrument is capable of measuring the force of gravity with an accuracy of 0.1 millidyne or better. To achieve this accuracy, it is necessary to observe various precautions. The casing must be air-tight and contain a drying agent to keep the air inside at a constant density. Also, it is necessary that the temperature within the case be kept constant to within about 0.001° C. The latter requirement is fulfilled by immersing the casing and level (not shown) in a water bath whose temperature is controlled by a mercury-toluene thermostat element.

The accuracy of the instrument is indicated by Table 12, which is a summary of closure data for eight loops. The first column gives the total numerical change in gravity around the loop, i.e., the sum of the differences added without regard to sign; the second column gives the number of observed differences which were added together to form the loop; the third column gives the error of closure. The probable error of closure was 0.11 millidyne, the average error 0.13 and the largest error 0.26 millidyne.

Portable Gravimeter.—An extremely portable meter has been developed‡ which utilizes a modified quartz mechanism similar to that illustrated in Figure 228. The entire mechanism is housed in a sealed steel chamber about 3 inches in diameter and 6 inches long. Micrometer screws, acting through sealed copper bellows, actuate the null-point setting. The steel chamber is housed in a 3½-inch Dewar glass flask for thermal insulation. Due to the high thermal efficiency of the Dewar flask, coupled with the temperature compensation incorporated into the mechanism, the temperature effects are small and gradual, and may be treated as a drift in the readings.

† Mott-Smith, *Geophysics*, Jan. 1937, p. 29.
‡ V. J. Meyer, Atlas Exploration Company.

The carrying case is provided with shoulder straps (Figure 229). In use, the meter rests on a small aluminum tripod, as shown in Figure 229a. The weight of the complete equipment is approximately 15 pounds. Meters of this type are extremely useful for oil reconnaissance and mining surveys.

FIG. 229.—Light weight portable meter for general oil reconnaissance and mining surveys. (Courtesy of International Geophysics Company.)

Electric Gauge Type Gravimeters.—Electric gauge type gravimeters offer several advantages. The ratio of the displacement of the indicator to the displacement under measurement can be made as high as 100,000 without introducing frictional effects, such as hysteresis or sticking. Also, the gauge permits measurements of very high accuracy and allows remote reading or recording.

The electric gauge may utilize any one of the sensitive electric measuring devices.†

† C. M. Hathaway and E. S. Lee, "The Electric Gauge," *Mechanical Engineering*, Sept. 1937.

FIG. 229a.—Field procedure for reading portable meters. (A) carrying case and cover; (B) gravity meter; (C) tripod. (Courtesy of International Geophysics Company.)

One method is illustrated by the Boliden gravimeter previously described. Because the total capacity is usually small, measurements are generally made at high frequency, which is most conveniently supplied by a small vacuum tube oscillator. In general, electric gauging methods utilize bridge-type circuits. The circuit is simple, comprising the conventional four-arm alternating-current bridge. In one arm is placed the capacity or the inductance whose value is changed by the movement of the gravity-meter system.

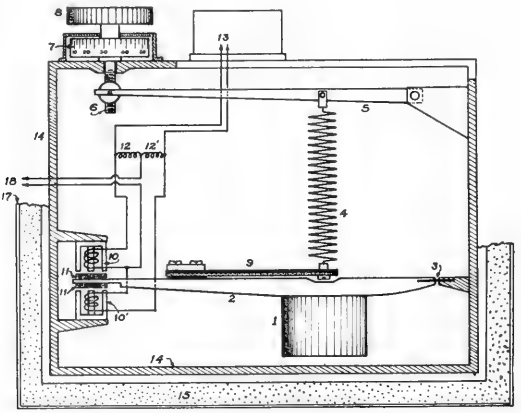

FIG. 230.—Electric gauge, bridge-type gravimeter. 1, mass; 2, suspension lever; 3, spring hinge; 4, suspension spring; 5, spring lever; 6, adjustment screw; 7, adjustment scale; 8, adjustment knob; 9, bimetallic temperature compensation lever; 10 and 10′, electric gauge heads, differential type; 11 and 11′, armatures; 12 and 12′, reactor coils; 13, alternating current vacuum tube voltmeter; 14, cast aluminum case; 15, thermal insulation; 17, polished duraluminum case; 18, leads to alternating current supply. (Courtesy International Geophysics, Inc.)

Sufficient sensitivity and output can generally be obtained with one or two stages of vacuum-tube amplification.

An electric gauge, bridge-type gravimeter is indicated schematically in Figure 230. The displacement of the mass 1 causes a displacement of a suspension lever 2 to the end of which is attached a light arm composed of a magnetic material. Movement of the magnetic arm between the pole pieces of the electromagnet varies the current through the reactors 12 and 12′, thereby producing a deflection of the voltmeter 13.

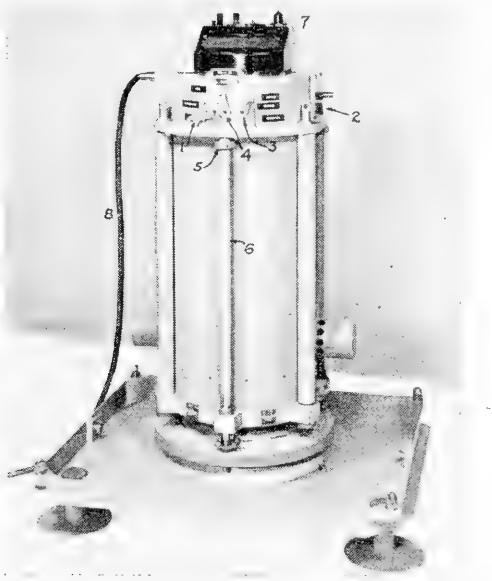

FIG. 231.—Exterior view of the Graf-Askania mechanical-electrical gravity meter. 1, arresting clamp; 2, scale range adjustment; 3, calibration weight; 4, spring adjustment; 5, leveling screw knob; 6, leveling screw shaft; 7, microammeter; 8, cable to storage battery. (Courtesy of the Askania Corporation.)

In another electric gauge-type gravimeter, determinations of the relative gravity are based on electrical measurements which show the change in length of a vertical spring to the lower end of which is attached a mass M.† Measurements of the relative gravity are made on a microammeter (without amplifier) or on a reading drum. The sensitivity of the instrument can be modified within a fairly wide range; for field investigations, 3 to 6 scale divisions of the microammeter are made to correspond to 1 millidyne. A double thermostat is provided which, however, is used only when the apparatus is moved between two observation stations far apart from each other. No temperature control is necessary for local investigations.

In one American modification of this method, the electric measuring device utilizes a change in impedance as a measure of the movement of the mass. In this system, a medium frequency alternating current is passed through a differential coil system, and any movement of M causes a change in impedance, with resultant unbalance of an alternating current, bridge measuring circuit.

† A. Graf, "Ein neuer statischer Schweremesser zur Messung und Registrierung lokaler und Zeitlicher Schwereänderungen," *Zeit. für Geophysik*, No. 14, Vol. 5/6, 1938, pp. 153-172.

An exterior view of the Askania meter is shown in Figure 231. The spring system and the electrical measuring device are contained inside a thick-walled, air-tight housing. All of the levers are so connected that they can be operated from outside the housing. The levers include: the arresting lever for the mass (left side of Figure 231), a drum for changing the measuring range (right side of Figure 231), a device for supporting a standard weight, and an arrangement for moving the spring. The last two devices are employed only occasionally and are not usually necessary for taking measurements. Levels with 60 second graduations are mounted inside the case and can be observed from above through a glass window. The leveling screws on the lower part of the instrument can be adjusted from the top of the instrument so that it is possible to view the inside graduated levels while making adjustments. Inside the main housing there is a triple-walled soft metal casing which holds a thermostat. The thermostat requires 20 to 25 watts for a temperature rise of 10°. The current source for operating the gravity meter is a 12-volt storage battery.

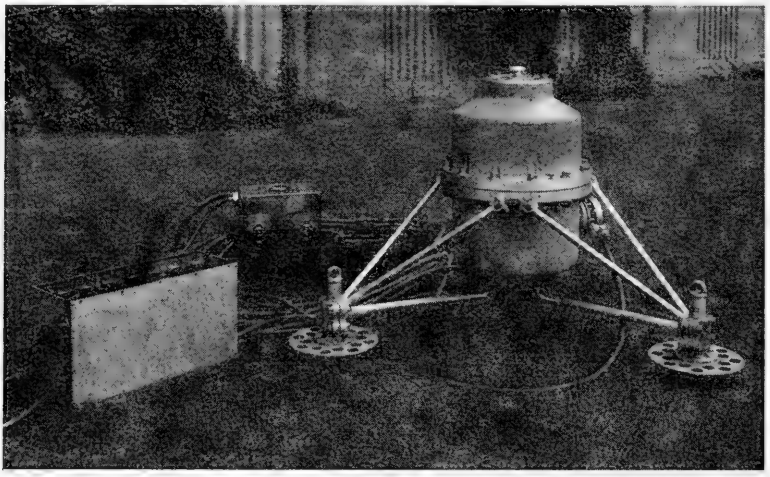

FIG. 232.—Gulf underwater gravimeter sealed with all control equipment necessary to operate. (Courtesy of Gulf Research and Development Company.)

The Gulf Underwater Gravimeter

The problem of geophysical exploration of the continental shelf brought about the development of an underwater gravimeter.† It is an adaptation of the standard Gulf gravimeter, described in the preceding section, and is illustrated in Figures 232 and 233. Measurements may be made in water to a depth of several hundred feet. The meter is lowered to the bottom by means of a cable and hoist operated by the engine of the small power-boat used in such work. The complete meter weighs 300 pounds in air but only 25 to 30 pounds when submerged. About 350 pounds of lead weights are often added to increase the stability of the apparatus. The working parts of the instrument are encased in a pressure housing, made of aluminum alloy, which will withstand a 700-foot head of water.

† T. B. Pepper, "The Gulf Underwater Gravimeter," *Geophysics*, Vol. 7, No. 1, Jan. 1941, pp. 34-44.

With an underwater gravimeter the operations of leveling, of releasing and clamping the system, and taking readings (all so simple on land) must be accomplished by remote control, from a vessel at the surface. Leveling is done by a dual motor-driven precision gimbal arrangement in which a single revolution of the motor equals 3 seconds of arc.

To ascertain when the instrument is level, the regular pair of levels of the meter is used in combination with 2 photo-voltaic cells for each level vial. The level vials are illuminated and a photo cell is set over each end and connected in parallel with a 25-0-25 micro-ammeter. When the micro-ammeter indicates a balance, the instrument

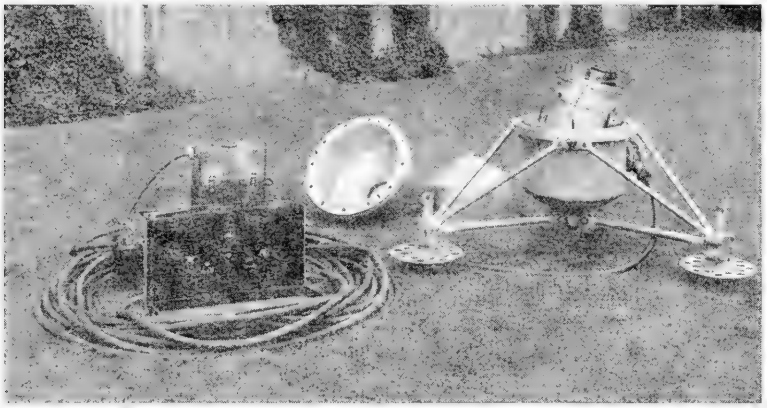

FIG. 233.—Gulf underwater gravimeter with the top half of the pressure housing removed, showing the leveling mechanism. (Courtesy of Gulf Research and Development Company.)

is level (to a sensitivity of 3 seconds of arc per micro-ampere) for the azimuth of the particular level involved.

The moving system is clamped by a permanent magnet motor working the arresting mechanism through a gear box. A warning light on the operator's control panel shows red when the meter is unclamped and green when it is securely locked. The readings are taken photographically on 35 mm. film. Records are read with a micrometer slide comparator with an accuracy of about 0.2 mg. Corrections are made for film shrinkage if necessary.

As in the case of land operations, thermostatic heat control is provided. A special alarm system gives warning if the housing is leaking water. A maximum of 17 stations has been made in a day, but 6 is an average run. As shown by field checks, the accuracy of observations was better than 0.1 milligal.

Diving Bell

A diving bell so designed as to accommodate both a gravimeter and an observer has been found useful in making gravity observations on rivers, lakes, and the ocean floor at depths of from 8 to 70 feet.† This bell is shown

† E. W. Frowe, "A Diving Bell for Underwater Gravimeter Operation," *Geophysics*, Vol. 21, No. 1, Jan. 1947, pp. 1-12.

in Figures 234 and 235. The fact that gravity data from adjacent land and water-covered areas can be contoured smoothly indicates that the underwater readings are reliable.

The use of the diving bell is advantageous in that the conventional land-type gravity meters may be employed. This is of importance for the surveying of limited areas involving short-term operations. For extended underwater operations, however, it is generally preferable to utilize the remote-controlled underwater-type meter.

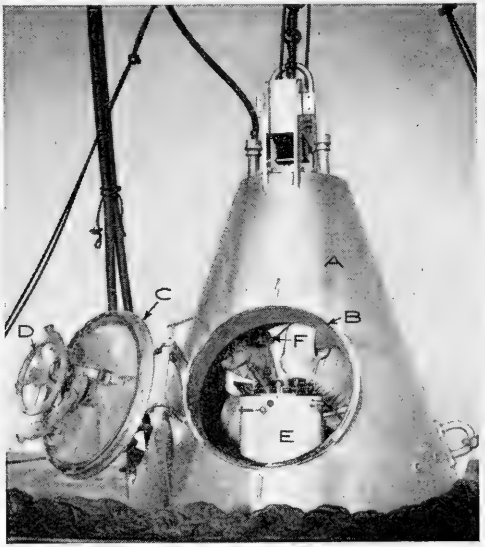

FIG. 234.—Diving bell for underwater gravity operations. A, diving bell; B, hatch; C, hatch cover; D, locking mechanism, operatable inside and outside; E, gravity meter; F, head phones and microphone for communication to attendant on deck. (Courtesy of Robert H. Ray Company.)

The remotely operated gravity meter has several advantages over the diving bell, which may be summarized as follows:— (1) The weight of the equipment handled is greatly reduced. The diving bell weighs about 4,000 pounds, while the remote gravity meter housing, with meter, weighs about 600 pounds. (2) Danger to personnel is eliminated with the remote meter. Insurance for the operator of the diving bell is an expensive item. (3) Better readings are obtainable with the remote meter in mud-covered areas, since the gravity meter is not accompanied by an instrument man whose every motion affects the level of the meter. Reading in a mud-bottom area is closely akin to reading in a very soft swamp where the observer literally has to hold his breath while taking a reading. (4) When the remote meter is read electronically, it is possible to use electronic averaging circuits when disturbed conditions are present. It has been found

that in the Gulf Coast area the ocean bottom is rarely still, and there is usually some motion of the scale indicator, which may make reading difficult. The electronic averaging circuits are of considerable value under these conditions.

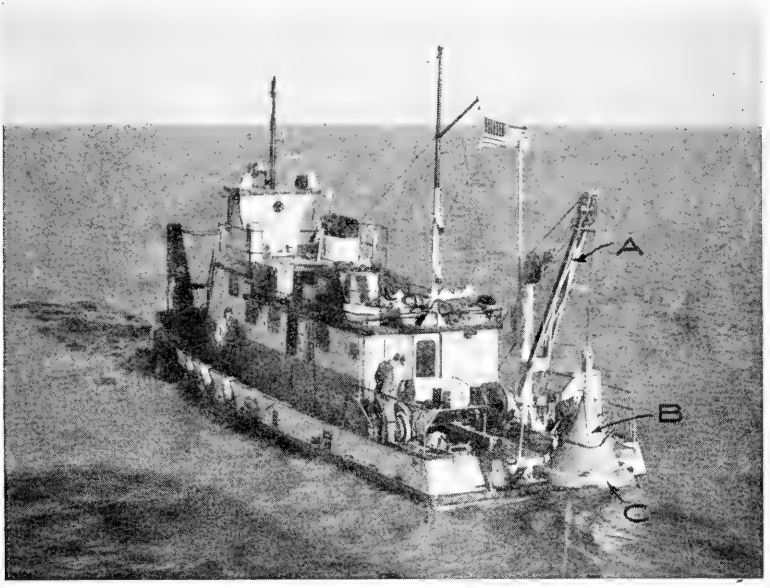

FIG. 235.—Diving bell in elevated position, when under way between stations. A, "A" frame hoist; B, diving bell, with large extended base C for better stability in areas with soft bottoms. (Courtesy of Union Oil Company of California.)

Calibration of Gravimeters

A gravimeter must be calibrated so that the change in the acceleration of gravity can be determined from the measured displacement of the mass. This may be done by several methods. One method, which is applicable for practically all types of gravity meters, consists in measuring the variation of gravity as a function of height or elevation. Such calibration measurements may be carried out conveniently in any tall building.*

Less simple is the calibration of an instrument by observations made at stations whose gravity differences have previously been measured accurately with pendulums or torsion balance.

Certain meters, for example, the Thyssen instrument described on page 376, may be calibrated conveniently by adding small weights. The sensitivity, or number of milligrams required to produce one scale deflection is obtained directly from a graph of scale divisions versus load (in milli-

* See, for example, "Gulf gravimeter tests in Empire State Building, Washington Monument, and Pittsburgh Cathedral of Learning," Report in National Research Council, Transactions of American Geophysical Union, Vol. I, Washington, July, 1938

grams). Certain other meters of proper design may be calibrated by the "tilt" method. Tilting the instrument decreases the effective value of gravity by a factor equal to the cosine of the angle of tilt. Hence, an indication of the sensitivity may be obtained by observing the scale deflections for various angles of tilt.

In all cases, it is desirable to provide a means by which calibration can be carried out in the field because changes in sensitivity may occur during the course of time. (Compare p. 371.) For instance, when dealing with a delicately balanced elastic system, small changes in geometry caused by relative motion of supports, or by readjustment to compensate for creep or large changes of gravity, may cause bothersome changes in calibration.

The calibration of gravimeters by taking measurements at different heights in tall buildings makes use of the change in gravity with elevation as expressed in the constant used in the "free air" reduction, (page 256). The constant, worked out by Helmert in 1910, is 0.3086 milligals per meter or 0.09406 milligals per foot, and carries a minus sign to indicate a lower force of gravity at a higher elevation. The vertical gradient of gravity has a slight variation which was investigated by Hammer.† It was concluded that the figure cited is accurate for all calibration purposes.

The calibration of a gravity meter is basically similar to the calibration of a magnetometer prior to field work. It is necessary to know the value of the change in gravity represented by one scale division (for direct reading instruments) or dial division (for null point instruments). This value is usually expressed as a constant k. As an example, for the Brown Gravimeter No. 21, (July, 1942), the k value was 0.0352 milligals per scale point. The term *scale point* is often used instead of *scale division,* in gravimeter work.

In certain meters the effect of barometric pressure must be considered. The moving mass in the instrument is buoyed up by the air in the case. If the case is not hermetically sealed, the buoyancy of the air will be a function of the barometer reading. By taking a series of readings at the same station, and varying the pressure within the case, the barometric correction may be determined. During field work with such meters it is necessary to take a barometer reading at each station. A barometer of the necessary accuracy is carried in the field truck for that purpose. Instruments with sealed cases do not require a barometric or air-pressure correction.

Temperature Effects. — Temperature changes have an appreciable effect on instrument readings. It is usual to protect the instrument from temperature changes by carefully-constructed housings or casings which maintain the working parts of the meter at a constant temperature. Temperature is held constant to about 0.2 of a centigrade degree by thermostat-controlled heating elements.

Power for these elements is usually supplied by a storage battery and the meter is kept under a constant temperature day and night during a

† S. Hammer, "Investigation of the Vertical Gradient of Gravity," *Trans. Amer. Geophys. Union;* Nat. Research Council, Wash., D.C., Part I, pp. 72-82, Aug. 1930.

survey. If the heat is turned off during long moves or discontinuance of work, a sufficient time (usually 24 hours) is allowed for the instrument to stabilize after it is again heated prior to new field work.

In other meters, sufficient thermal insulation is provided to make the temperature changes gradual, and then their effects are corrected for by the drift curve. One make of gravity meter is placed in a large Dewar flask or thermos bottle which serves as an excellent heat barrier.

Leveling.—Accurate levels are provided so that when a gravimeter is set up on its tripod or base plate it can be carefully leveled. The matter of tripods is covered in more detail in the section on field work.

Orientation.—Accurate orientation of a gravimeter is not ordinarily necessary, at least to the extent that a special operation is required for that purpose, as with the magnetometer. In routine field station set-ups the gravimeter is placed on its tripod with approximately the same orientation at each station.

With certain older-type instruments, a slightly different reading was obtained depending on the direction (north, east, south or west) in which the field truck was headed when a reading was being taken. In such a case the amount of the correction, which is only a scale point or two, is found by trial and applied when calculating the field notes.

Latitude Adjustment.—As has been noted, the normal value of gravity force varies uniformly with latitude. From the equator to the poles, the total gravitational change due to latitude is about 5.2 gals; (see Table 6, p. 254.) For a gravimeter with a scale value or scale constant of a fraction of a milligal per scale point, this change would represent a very large range in scale reading.

To provide for this change, gravimeters have a means of adjustment so that the scale is in view for work in a given area. If operations are shifted to another area at appreciably different latitude, for instance between South Texas and Colorado, the scale must be re-set for the new locality. This adjustment is similar to the latitude adjustment to bring the scale of a magnetometer in view when moving from one area to another.

Base Station Gravity Value.—The values of gravity at the various field stations shown on the final maps are relative to the main base station of the survey. An arbitrary value in milligals is assigned to this base station. This value should be selected at a convenient figure, usually large enough so there will not be negative values in the gravity contours (isogams).

The assuming of an arbitrary base station value in gravity work is comparable to using an assumed value of magnetic intensity at the magnetic base station. If desired, gravity data can be tied into pendulum gravity stations, just as magnetic data can be tied into total values of magnetic force at magnetic bench marks. This may be accomplished by

giving the base station its true gravity value, rather than some arbitrary value.

Station Elevations and Surveying.—Station elevations are run with an accuracy of 0.2 to 0.5 of a foot. The accuracy with which the elevations are determined is one of the chief factors governing the overall accuracy of the gravity work. One foot of elevation represents 0.09406 milligals in free air correction, which is a detectable quantity with modern gravimeters. Where high precision of final gravity values is desired, accuracy of this order is necessary. Accurate level instruments are preferred for determining elevations, especially where large areas are to be surveyed. For some distances a transit may be used almost as successfully. Alidade and plane table usually sacrifice some accuracy in running elevations, but are more convenient for plotting station locations and field contouring.

A survey unit usually comprises a field surveyor and his rodman, with a field car and driver. The car should be equipped with all necessary supplies (flagging, stakes, drinking water, etc.).

A land man or party chief usually secures the necessary permits for station settings from local land owners, and establishes land lines and map locations for the stations. Establishing stations and running the elevations is often a limiting factor of crew production. Two survey units with conventional level equipment usually are required to keep up with one gravity-meter crew.

The surveyor selects the location of stations judiciously so that they may be conveniently occupied by the field truck, preferably in places that are more or less flat. In areas of moderate topography, terrain survey and correction is not needed in gravimeter work as it is with the torsion balance.

TERRESTRIAL PHOTOGRAMMETRIC MAPPING

The mapping of the gravitational field in an area is as much dependent upon precise elevation measurements as upon the accuracy of the gravity measurements. Also the personnel and time required for the surveying usually exceed that required for the gravity measurements. For these reasons, surveying techniques are of special importance. One recent development which is becoming more widely used is photogrammetric mapping.

The science of terrestrial photogrammetry has been known for the past fifty years, but until recently its use has been confined principally to European countries. The fundamental work on this subject was done in Germany by S. Finsterwalder at the beginning of this century and was further developed by his son.†

The European method made use of an instrument known as the "photo-theodolite", which permitted surveying and mapping from ground positions by means of the resulting photographs taken of rod stations or other points under investigation. The standard field procedure for terrestrial photogrammetric mapping using the photo-theodolite consisted of taking shots of photographs from either end of a carefully measured base line. By identifying common points in the photographs taken from these two instrument

† Personal communication to W. O. Bazhaw, April 25, 1949, from Friedrich Breyer regarding completion of this development by R. Finsterwalder.

positions, and by recording the interior horizontal angles measured from the base line to the point in question, the distance to the point could be determined by simple triangulation. Knowing the distance, and by measuring the vertical angles directly from the photographs, it was possible to compute the elevation differences between the instrument and points under observation. This method has the advantage of obtaining elevations of inaccessible points, such as rugged coast lines, mountainous terrain, etc., but involves considerable work for both field and office personnel. The method is also subject to certain errors in visual readings made in the field.

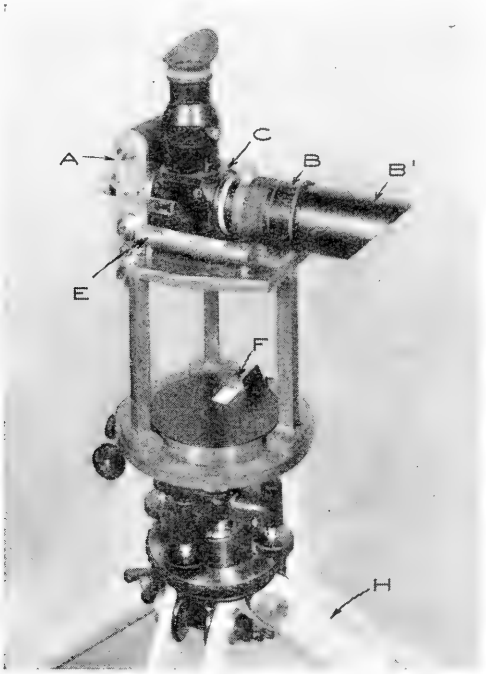

FIG. 236.—Topographic camera. A, 35 mm. camera; B, telephoto lens; B', sunshade; C, reflex housing; D, eyepiece; E, level bubble; F, compass; G, transit head; H, tripod. (Courtesy of Republic Exploration Company.)

With the recent American development of the *topographic camera*‡, shown in Figure 236, all visual readings in the field, as well as the measured base line, are completely eliminated. Both the horizontal and the vertical control data are combined on the same film-frame with all the speed, accuracy, and dependability that can be achieved with the photographic method of recording. Thus all of the data needed for the determination of distance, direction, and elevation difference between the instrument and rod point are obtained on one picture with one shot (Figure 237). The resultant field data are therefore free of the human element in reading and recording.

Fundamental Theory and Mathematical Relationships.—Referring to Figure 238, the *HI* line is the level line to which the instrument has been adjusted. This is the line numbered 50, as shown in the photograph.

‡ *World Oil*, January, 1948; *Oil and Gas Journal*, Nov. 22, 1947; *World Petroleum*, November, 1947; *Photogrammetric Engineering*, March, 1949. Patent applied for.

The position of the datum or top target above or below this 50 line is shown as H in the photograph. The interval between the top and bottom target is shown as i and is the interval measured in millimeters directly on the film. Let R represent the number of feet between the top and bottom targets; then the elevation difference is given as follows:

$$\Delta E = H/i \cdot R$$

The quantities H and i are both measured directly on the film negative to the nearest 0.01 mm. R is a constant depending upon the rod construction. From this it can be seen that the elevation difference is independent of the lens focal length, as well as of the distance between instrument and rod.

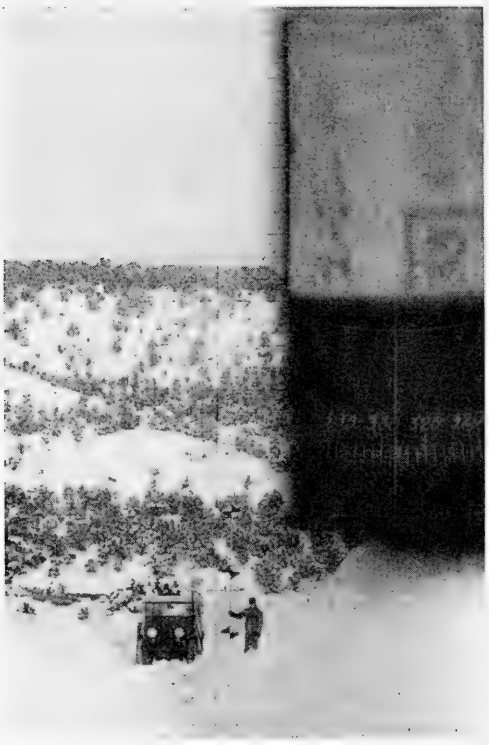

FIG. 237.—Typical photographic record showing distance, direction, and elevation difference between the instrument and the rod, and general terrain conditions. (Courtesy of Republic Exploration Company.)

The distance from instrument to rod is given as a function of the lens focal length (f), calibration constant (k), target spacing (R), and image size (i) as follows:

$$D = \frac{f \cdot k \cdot R}{i}$$

Since the instrument is leveled for all shots, the plane of the film is parallel to the plane of the rod, resulting in true elevation differences and map distances, regardless of

the vertical angle involved in the field work, without the need for secondary corrections of any kind.

Although the instrument is always level in operation, the lens used takes in a field of view of ten degrees vertical angle range, thereby permitting operation over relatively rough terrain.

Instrumentation and General Constructional Details of Equipment.—The topographic camera, as shown in Figure 236, consists of a 35 mm. camera with telephoto lens and reflex housing, all rigidly mounted on a specially-constructed head

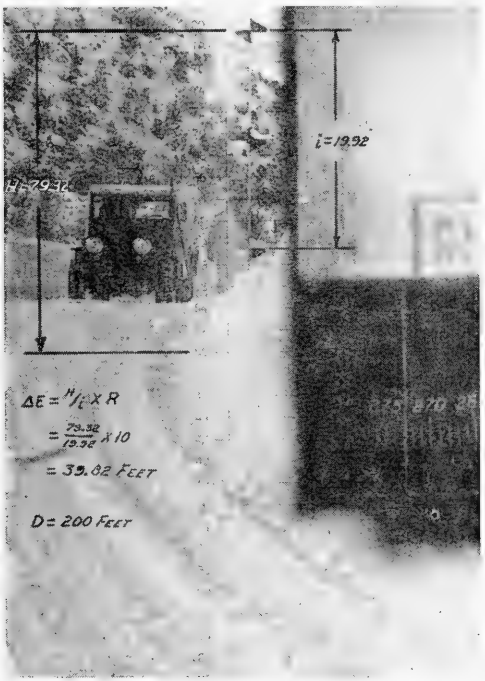

Fig. 238.—Method of reading photogrammetric record, showing elevation values H, fixed target distance i, and direction angle. (Courtesy of Republic Exploration Company.)

similar in appearance to a standard transit head. The mount is constructed in such a manner that no vertical angles can be turned with the objective lens. A sensitive level bubble is mounted on the right side of the reflex housing, and the instrument line-of-sight is adjusted parallel with the level position of this bubble. The adjustment is easily accomplished by means of the eyepiece mounted on the back of the camera box which permits viewing the image brought in by the objective lens and focused in the plane of the mil scale lines which are located in the plane of the film. By sighting on a Philadelphia rod, the instrument is adjusted by the standard two-peg method as used in the adjustment of a transit or other conventional surveying instrument. After adjustment is made, the eyepiece is covered and is not used again in regular field work, except to check adjustment at periodic intervals.

An auxiliary lens and prism system mounted on the left side of the reflex housing

projects an image of a portion of the azimuth compass card onto the film, thereby incorporating this data onto the same film-frame with the rod image.

The rod is of the fixed-target type, as shown in Figure 237. The fixed target interval serves to calibrate the scale of the resulting picture at the particular distance the rod is held from the instrument, thereby permitting vertical scaling of the film from the level reference line to the datum target in terms of feet of elevation difference per millimeter of film interval. The target material is chosen for certain desirable photographic properties, and yields good results regardless of field lighting conditions. Each rod has three targets, any two of which must be visible in the picture in order to determine distance, except on very short shots, in which case any one of the targets will give usable results.

Instrumentation for Reading Data.—All readings and measurements are made at the field office directly from the film negatives, using a reading device known as the *conversion projector,* shown in Figure 239. The film is loaded into the projector proper, which is located just below the screen and inside the main instrument case. The image is projected onto the back surface of the screen by means of double reflections from two front-surfaced mirrors.

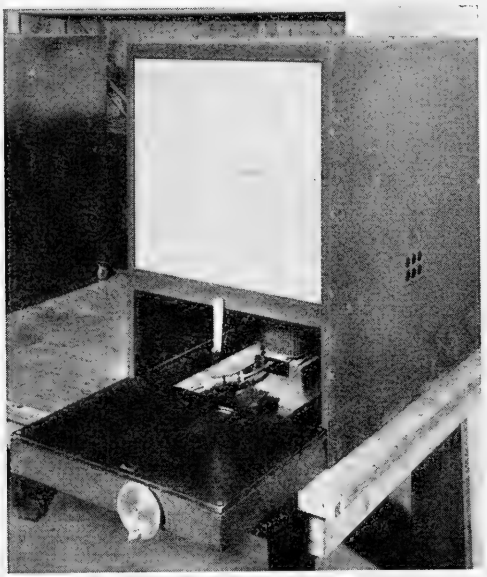

FIG. 239.—Conversion projector for measuring elevation and distance values. (Courtesy of Republic Exploration Company.)

The projector and the lower mirror are moved horizontally as a unit on a track by means of the small crank located on the lower right side of the case. Reference lines are drawn on the screen; the top line is the index or zero line. The remainder of the lines are used only to read the target intervals directly for short shots from about 20 to 400 feet distance. For longer distances, the readings are taken from a horizontal graduated dial contained in the housing to which the small crank is attached. In operation, the frame under study is positioned in the projector with the image of the top target on or very near the screen index line. The screen itself is then moved up or down slightly by means of the zero adjusting lever until the screen index line centers

the top target. The small hand crank is then turned counter-clockwise until the first mil scale line (white numbered line on the film) is brought into coincidence with the screen index line. This interval is read under the front dial index, added to the mil scale line value, and recorded in the notes under the *H* column. The projector is moved still further in the same direction until the index line centers the bottom target; then the conversion factor and distance are both read under the rear horizontal dial index and recorded in the *F* and *Distance* columns, respectively. Vertical angle measurements are made in this manner to within 6 seconds of arc, and distances are read to the nearest 10 feet. The azimuth or magnetic direction scale is read directly on the screen to the nearest 15 minutes of horizontal angle.

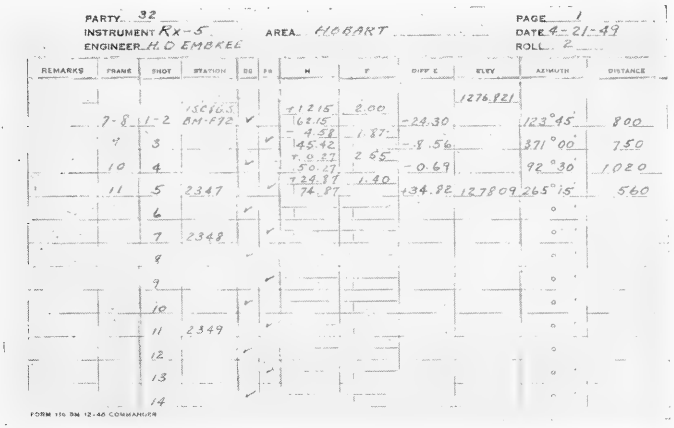

FIG. 240.—Calculation sheet for photogrammetric mapping.

Figure 240 shows a sample of engineer's notes which have been partially completed with office readings and calculations. The instrument man in the field fills only the columns marked *Shot* and *Station*, and places a check in the *BS* or *FS* column. The remainder of the columns are filled in with readings and calculations made by the office computer. Since the instrument is adjusted to the number 50 mil scale line, it is necessary to subtract 50.0 from all *H* readings, as shown in the sample calculations. The remainder is then multiplied by the factor in the *F* column and entered in the *Diff. E.* column, with due regard to algebraic sign for this elevation difference.

General Operational Procedure.—The instrument man levels his instrument, sights on the rod, and snaps the picture. Where transportation and visibility do not limit the speed of the survey to any great extent, it is possible to run between forty and eighty stations set at half-mile intervals in one day of operation. The accuracy which can be expected is given by the vertical closure formula in feet which applies to this method, $\pm 0.20\sqrt{\text{miles of traverse}}$. Length of shots should not be over one-fourth mile.

Experience has shown that there are three simple requirements for obtaining the above accuracy with the camera. First, the instrument must be in good adjustment; second, the instrument must be level at the instant the picture is taken; and third, the rodmen must be absolutely certain of exact take-off and tie-in points within each closed traverse run.

After the shots have been taken in the field, the film may be processed in the local field office. The readings are taken from the negative by the field computer. All spur lines are double-run on the film to check possible reading errors.

Applications and Economic Value.—In addition to engineering information, the film provides a visual check on the geological outcrops in connection with studies of surface geology and also shows the need for terrain corrections in connection with gravity surveys.

One instrument man with two rodmen, each with a car, can do the work which normally requires two transit men, each with rodman and car. Not only is the volume of work increased, but often the accuracy is improved. The camera has some operating advantages over the surveying instrument. For example, heat wave effects cannot be detected on the film, partly because of the short exposure time as compared with the low frequency of these effects, and partly because the film possesses a certain selective sensitivity to certain portions of the visible spectrum.

A further increase in speed is effected by the virtual elimination of re-runs in the field, since the film can be reviewed in the office at any time without the costly procedure of sending men, cars and equipment back to the field when a mis-tie occurs in a traverse.

A few days training is required to learn the operation of the field and office instruments. An elementary knowledge of photography is helpful, but is not a prerequisite. The simplicity of operation enables junior engineering personnel to handle the field work and permits checking and supervision of each step by senior personnel from a central office location.

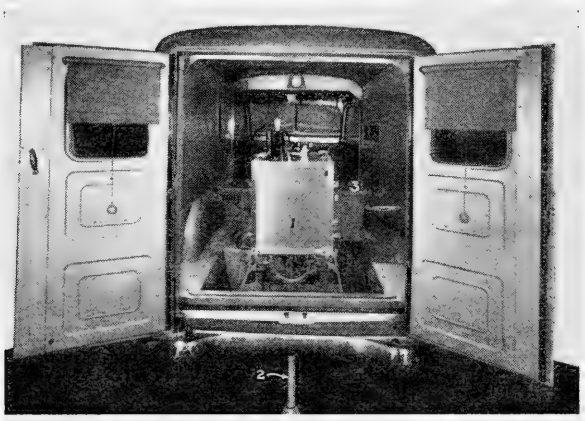

FIG. 241.—(1) Gravimeter on tripod in truck, with (2) extension leg resting on ground, (3) battery box for thermostat and motor battery. (L. M. and F. W. Mott-Smith, *The Petroleum Engineer.*)

Field Procedure. — The heavier semi-portable gravimeters are usually transported in a light closed panel truck. While making a measurement the instrument must rest on a firm base. For this purpose it is supported on a sturdy tripod arrangement inside the truck. When a measurement is to be made, the extension support is lowered to the ground through a hole in the floor of the truck. Figure 241 shows the instrument on such a tripod ready for a measurement. This method is advantageous in that the meter, and the operator, may be protected from inclement weather.

The lighter instruments may be transported in a jeep or light field

car. The instrument is carried in a shock-resistant cradle. When a reading is to be made, a small instrument tripod is placed upon the ground. The table of the tripod is leveled with a level bubble. The gravity meter is then lifted from its cradle, placed upon the tripod, and carefully leveled by means of the level bubbles on the meter.

The general field procedure* with direct gravity instruments of the pendulum or gravimeter type is similar to that with a magnetometer. The initial step for a field survey is the lay-out of a set of station locations in the area to be explored. The location of stations is done by a field surveying party. Each station is marked with a flag or stake for easy discovery and preferably located along roads or trails. The stations may be arranged in checkerboard fashion, or placed along traverse lines, etc., depending upon the nature of the problem. Each station is plotted on a field map or recorded by proper survey notes. For most reconnaissance work one station per mile is sufficient. In areas where more detail is needed as many as ten stations to the mile may be required. Occasionally when making a detailed survey in areas where abrupt changes are present, a closer spacing may be advisable. The optimum spacing of stations is governed by local conditions. The surveyors run relative elevations on all of the stations, and if necessary plot topographic contours. The survey work proceeds simultaneously with the gravity survey, with the surveyors working sufficiently ahead of the instrument party to prevent delays in finding stations.

The instrument is first set up at a chosen base station and adjusted for the area. A measurement is then taken, followed after a short interval by a second observation to guard against mistakes and to allow averaging of results to increase the accuracy. This procedure is then repeated at successive stations. After five to ten stations have been occupied the instrument is returned to the base station for a check observation. Usually the next step is to make a subsidiary base station of one of the new stations conveniently located for further expansion of the survey. This is accomplished by taking a second or repeat observation at the desired new base station. Each base station is simply a field station whose gravity value relative to another base has been made more certain by being occupied or measured at least twice. The survey then proceeds in the same manner from the new base, check readings now being taken at this base. In this way the area is gradually covered with a series of bases and ordinary stations. The use of subsidiary base stations avoids long trips back to the main base for check readings.

During the field work, a computer at the field office calculates the prior

* Personal communication from L. M. and F. W. Mott-Smith. Compare L. M. and F. W. Mott-Smith, *The Petroleum Engineer*, July, 1939. A major portion of this section is essentially a description of the general technique employed by the Mott-Smith Corporation and summarizes the important aspects of tested field procedure.

day's work and builds up the gravity anomaly map. The usual process of computation is as follows: (a) The instrument scale readings are first converted into milligals by using a calibration curve; (b) the drift curve is then obtained by plotting the value of gravity against the time at which the reading was taken. Figure 242 shows a drift curve representing the work of an average day. Analysis of the drift curves gives considerable information on the progress of the work during day. It also serves as a partial check on instrument operation and is used to compute the differences in the gravity between the several stations.

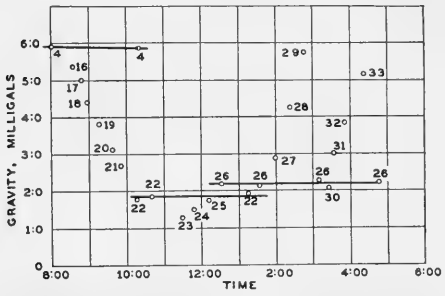

FIG. 242.—Drift curve for consecutive reading of stations. (L. M. and F. W. Mott-Smith, *The Petroleum Engineer.*)

On this particular day the operator first occupied base number 4 at 8:00 A.M. and made an observation. He then occupied stations 16 to 22 and returned to the initial base number 4 for a check reading at 10:20 A.M. If the instrument were perfect, he would have obtained exactly the same reading. Actually, due to slight instrumental inaccuracy or drift in the two hour and twenty minute interval, a reading was obtained which was 0.05 milligal less than the first reading. The instrument was then returned to station number 22, thus securing a second observation at this station and establishing it as a new base. Four new stations were then observed and a check reading at the new base taken. Station 26 was then established as a base and finally seven new stations were observed, with two check readings at base 26. It will be noted that on this particular day the instrument was set up 25 times, 18 new stations were determined, and two new bases established.

The difference in the gravity between the various bases and stations is taken directly from the drift curve. Small discrepancies between the various observations at a base are allowed for by drawing a mean straight line through the points. This procedure involves the assumption that the instrument drifted at a constant rate between observations. In usual field work the drift is fairly constant, although erratic results occur occasionally due to peculiarities of gravity instruments when subjected to rough handling, etc. However, experience has shown that this method is sufficiently accurate for practical purposes. The gravity difference in milligals between each station and the base to which it is referred is taken from the plot by measuring vertically between the drift lines.

Knowing the difference in gravity between each station and one of the bases, and the differences between bases, the gravity difference between all stations and bases and the main base can at once be obtained by simple arithmetic. At the start of the survey the main base in each area is given an

arbitrary gravity value, preferably chosen great enough so that none of the station values are negative, to avoid the inconvenience of carrying negative numbers. In all gravimeter work the absolute value of the acceleration of gravity is not obtained, because the instrument is capable only of giving the difference in gravity between two stations. Usually, however, this is not a disadvantage because interpretation is based upon the variations or anomalies in gravity exactly as is done in the interpretation of magnetic anomalies. If absolute gravity values are desired, the gravimeter survey must be supplemented with a pendulum gravity measurement at one or more of the base stations.

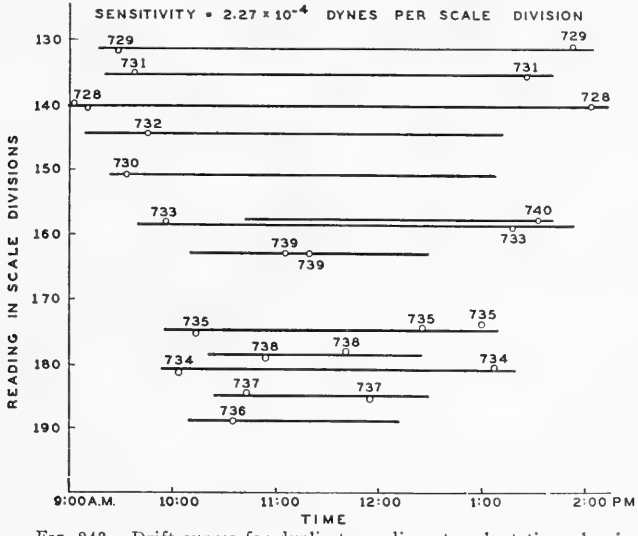

FIG. 243.—Drift curves for duplicate reading at each station, showing readings taken at 13 stations. (Bryan, *Geophysics.*)

An alternative procedure, which is not as rapid as that outlined above, consists in occupying each station at least twice during the day. When this procedure is used, the drift curve plot is similar to that shown in Figure 243.† For the case shown, the drift lines are practically horizontal, indicating that on that particular day the drift was very small and gratifyingly uniform. The gravity anomalies or differences between the various stations are obtained, as before, from the vertical interval on the plot.

After the gravity measurements at each station have been obtained, they should be subjected to two corrections: (a) elevation and (b) latitude

When corrected and reduced thereby to a suitable datum, the gravity values are placed on a final map and usually contoured at a contour interval best suited to show the variations. Following the above steps interpretation can proceed.

† A. B. Bryan, "Gravimeter Design and Operation," *Geophysics*, October, 1934, Vol. 2, No. 4, pp. 301-308.

Corrections Applied to Relative Gravity Measurements

Reduction to Datum.—The corrections applied to gravimeter measurements at a series of field stations are the same as those already considered in the reduction of pendulum gravity data (p. 256 to 258). The derivation of the constants used was given in that section. The reduction to datum, to review the matter briefly, consists of two parts: the free air correction or straight elevation correction, and the Bouguer correction which takes into account the density of the material between the station and the datum. The two are ordinarily combined, and the proper constant can be calculated on the basis that the elevation correction is at the rate of −0.09406 milligals per foot and the Bouguer correction is $+0.0127 \cdot d$ milligals per foot (d = density of the material from the surface to the datum chosen.) The equivalent figures in the metric system are −0.3086 milligals per meter for the elevation effect and $+0.04815 \cdot d$ milligals per meter for the Bouguer effect.

As an example, the combined correction factor for a density of 1.8 is 0.07109 milligals per foot (the sign is −), and for a density of 2.0 it is 0.06854 in like units. For a density of 2.2 the value is 0.06599. The value of density is usually assumed from density determinations of surface samples, with a judgment factor added. This assumed density then represents the value from the surface to the datum.

The datum is set at some convenient elevation below the survey base, or at the elevation of the base itself, if desired. It is quite an arbitrary matter, under the control of the person responsible for survey interpretation. A difference in the selection of a datum elevation merely represents a raising or lowering of all final map values of a survey.

As with corrections in magnetic surveys, the effect involved and the manner in which it is applied as a correction must be thought out carefully. Corrected gravity values represent the readings which would be obtained with the meter if it were set on the datum. The gravity at a higher elevation is less, due to elevation only, and the reading at such an elevated station has in it a contribution caused by the effect of the mass of material between the surface and the datum.

The above can be shown by an example. If we assume a gravimeter reading, corrected for drift and converted to milligals, at station X of a survey as 53.8 milligals, and the station elevation at 6295 feet, with a datum elevation (for convenience) at 6195, the necessary calculations are quite simple. Let us assume also that the density is 2.0.

The elevation difference, station to datum, is 100 feet. The elevation correction equals $100 \cdot 0.09406$ milligals per foot, or 9.4 mg. Therefore the station value 53.8 plus 9.4 gives 63.2 mg. for the value of station X on the datum, elevation only considered. This is the so-called "free gravity" value.

The Bouguer effect is $0.01276 \cdot 2 = 0.02552$ mg./ft. and 100 feet times this constant gives 2.6 mg. The meter reading of 63.2, on datum and cor-

rected for elevation only, still has in it this 2.6 mg., due to the 100 feet of material from the surface to the datum.

We therefore subtract the 2.6 from the 63.2, which gives 60.6 for the final corrected, on datum, value of the gravity at station X.

This pair of effects can be handled in one step by using the combined constant, which for a density of 2.0 is 0.06854 mg./ft. For 100 feet it amounts to 6.854 or 6.9. It follows that 53.8 plus 6.9 = 60.7, which checks within 0.1 mg. The above may appear elementary, and so it is, but if corrections are not handled properly, incorrect calculations are obviously the result.

Latitude Correction.—The correction for latitude is introduced to compensate for the change in gravity with latitude. This change is approximately a milligal per mile, increasing toward the poles of the earth.

With the accuracy attained in modern gravimeters, it is necessary that the value for the latitude correction be calculated for a survey area and carefully applied. The amount of the correction can be found by calculating the value of gravity, using suitable formulae such as No. 21. The distance in miles between the northern and southern boundaries is figured and divided into the difference in gravity, as determined by calculation at the north and the south extremes of the survey area.

For example, a certain survey in Russell County, Kansas, covered territory lying between latitude 38° 45′ and 39° 00′. The change was 1.3 milligals per mile. As applied, the latitude correction is handled in the same manner as the north-south correction in magnetic field work, increasing toward the north. There is no east-west correction in gravimeter work, in which respect it is more simple than the torsion balance method.

For a station a given distance north of a survey base, the gravity value is the per mile rate times the number of miles. Stations to the south of a base have a lower value of gravity due to this latitude change.

Topographic Correction.—The effect of minor topographic irregularities on the relative gravity is small and may often be neglected. In areas of rugged relief, however, certain corrections pertaining to topographic irregularities are usually made. Hammer† gives a comprehensive study of the method of terrain corrections for gravimeter surveys.

With the high accuracy of gravimeters and their increasing use in more rugged areas, topographic corrections are becoming more important. Hubbert‡ has recently published an article on gravitational terrain effects of two-dimensional features, presenting typical cases. For example, the effect of a slope of a certain degree or of a cliff of a certain height on a station at a given distance from the feature is shown. Hubbert's data can be readily applied in the field to determine how far a gravimeter station

† S. Hammer, "Terrain Corrections for Gravimeter Stations," *Geophysics,* Vol. IV, No. 3, July 1939.

‡ M. K. Hubbert, "Gravitational Terrain Effects of Two-Dimensional Topographic Features," *Geophysics,* Vol. XIII, No. 2, April 1948.

should be set from a certain terrain feature to render its effect negligible. This suggests that a judicious choice of station sites is advisable in rougher areas such as are often encountered in mining work. It is fortunately true, however, that in a great many gravimeter surveys no topographic corrections are required. In this respect the gravimeter is superior to the torsion balance, with which terrain is often a limiting factor.

Zone Chart Method of Terrain Correction.—A method for calculating the effect of rough terrain was presented by S. Hammer in 1939.† This method permits the contribution of the terrain to the gravity value measured at a station to be evaluated quantitatively to a relative accuracy of 0.1 milligal, which accuracy is necessary to utilize the high precision of modern gravimeters.

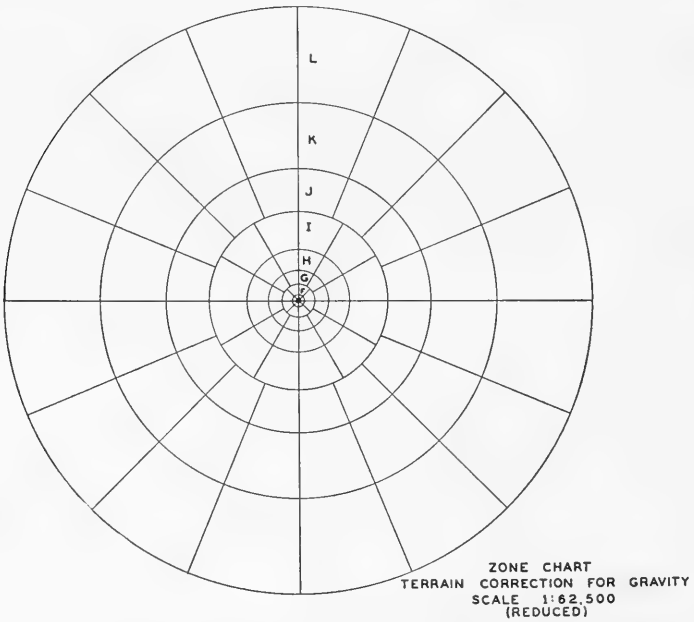

Fig. 244.—Zone chart for use in evaluating terrain corrections at gravity stations. (*Geophysics*, Vol. IV, No. 3, July, 1939, p. 188.)

Zone charts are easy to construct and use. An example of one, to the scale of 1 : 62500, is shown in Figure 244. A topographic map, or some form of terrain survey, around the gravity station or stations to be corrected is necessary. The chart is drawn in ink on a transparent sheet to the same scale as the topographic map, on which the gravity stations are plotted. The chart is laid on the map with its center at the station being studied.

A zone chart divides the terrain surrounding the station into circular zones or rings of a certain width, and these zones are, in turn, divided

† S. Hammer, *ibid*, p. 194.

into compartments or segments by radial lines from the center of the chart. Stated briefly, the gravity effect of the terrain in each of these segments is determined, and the sum thereof is the terrain correction.

The circular zones are designated as B, C, D, etc. (B, C, D and E toc small and M too large to be shown.) They have inner and outer radii of a definite length as, for example, 6.56 feet (2 meters) and 54.6 feet respectively for zone B. The radii of the boundaries of zone C are 54.6 feet and 175 feet, and in like manner for the other zones. Zone M covers the rings of terrain from 48,356 feet to 71,996 feet (or approximately 9.2 to 13.5 miles). It is not often used, as the difference in elevation relative to the station must be over 300 feet to produce an appreciable terrain effect at such a great distance.

The compartments or segments in each circular zone are equal in size. There are 4 of them in zone B and 6 in zones C and D. The number increases progressively to 16 for the J to M zones.

The zone chart is placed on the topographic map and centered at the station to be corrected. The average elevation of the area within a segment is determined by studying the contours visible through the chart. The elevation of the station is subtracted without regard to sign from the average segment elevation which established the average height of the segment. The area of a compartment in zone B is 2300 square feet, or the equivalent of a square section of terrain about 48 feet on a side. Its average elevation, as shown by surface contours, might be, for example, 4250 feet. For a station elevation of 4228, the average height of the segment would equal 4250 − 4228, or 22 feet.

Complete terrain correction tables (Tables 13 and 14)† have been prepared which list the gravity effect for a segment in a given zone in terms of its average height in feet above or below the station. For the example cited, where the average elevation difference was +22 feet, the table shows that for a compartment in the B zone a height of 21 to 24 feet produces a gravity effect of 0.08 milligals.

The complete terrain correction is obtained by adding together the individual gravity effects from all compartments in all zones where the elevation difference is great enough to be effective. Often a terrain correction can be made in from ½ to 1 hour per station. The tables are based on a density of 2.0. The total terrain correction must therefore be multiplied by ½ of the density which is assumed for the local area, unless it is 2.0; i.e., multiplied by the ratio of the density to the value 2.

The terrain correction tables are calculated by the formula for the gravitational attraction (Δg) of a vertical hollow cylinder (which is in effect a ring of the terrain) of height (h) at a point on the axis of the

† S. Hammer, *op. cit.* A similar but condensed table is given in L. L. Nettleton's "Geophysical Prospecting for Oil," McGraw-Hill, 1940, p. 145.

TABLE 13

TERRAIN CORRECTION TABLES FOR GRAVITY †

Each zone is a circular ring of given radii (in feet) divided into 4, 6, 8, 12, or 16 compartments of arbitrary azimuth. "h" is the mean topographic elevation in feet (without regard to sign) in each compartment with respect to the elevation of the station. The tables give the correction "T" for each compartment due to undulations of the terrain in units of 1/100 mg. for density (σ) = 2.0. This correction, when applied to Bouguer anomaly values which have been calculated with the simple Bouguer correction, is always positive.

Zone B 4 compartments 6.56 to 54.6*		Zone C 6 compartments 54.6 to 175		Zone D 6 compartments 175 to 558		Zone E 8 compartments 558 to 1280		Zone F 8 compartments 1280 to 2936		Zone G 12 compartments 2936 to 5018	
$\pm h$ (ft.)	T	$\pm h$ (ft.)	T	$\pm h$ (ft.)	T	$\pm h$ (ft.)	T	$\pm h$ (ft.)	T	$\pm h$ (ft.)	T
0 to 1.1	0	0 to 4.3	0	0 to 7.7	0	0 to 18	0	0 to 27	0	0 to 58	0
1.1– 1.9	0.1	4.3– 7.5	0.1	7.7– 13.4	0.1	18– 30	0.1	27– 46	0.1	58– 100	0.1
1.9– 2.5	0.2	7.5– 9.7	0.2	13.4– 17.3	0.2	30– 39	0.2	46– 60	0.2	100– 129	0.2
2.5– 2.9	0.3	9.7– 11.5	0.3	17.3– 20.5	0.3	39– 47	0.3	60– 71	0.3	129– 153	0.3
2.9– 3.4	0.4	11.5– 13.1	0.4	20.5– 23.2	0.4	47– 53	0.4	71– 80	0.4	153– 173	0.4
3.4– 3.7	0.5	13.1– 14.5	0.5	23.2– 25.7	0.5	53– 58	0.5	80– 88	0.5	173– 191	0.5
3.7– 7	1	14.5– 24	1	25.7– 43	1	58– 97	1	88–146	1	191– 317	1
7 – 9	2	24 – 32	2	43 – 56	2	97–126	2	146–189	2	317– 410	2
9 –12	3	32 – 39	3	56 – 66	3	126–148	3	189–224	3	410– 486	3
12 –14	4	39 – 45	4	66 – 76	4	148–170	4	224–255	4	486– 552	4
14 –16	5	45 – 51	5	76 – 84	5	170–189	5	255–282	5	552– 611	5
16 –19	6	51 – 57	6	84 – 92	6	189–206	6	282–308	6	611– 666	6
19 –21	7	57 – 63	7	92 –100	7	206–222	7	308–331	7	666– 716	7
21 –24	8	63 – 68	8	100 –107	8	222–238	8	331–353	8	716– 764	8
24 –27	9	68 – 74	9	107 –114	9	238–252	9	353–374	9	764– 809	9
27 –30	10	74 – 80	10	114 –120	10	252–266	10	374–394	10	809– 852	10
		80 – 86	11	120 –127	11	266–280	11	394–413	11	852– 894	11
		86 – 91	12	127 –133	12	280–293	12	413–431	12	894– 933	12
		91 – 97	13	133 –140	13	293–306	13	431–449	13	933– 972	13
		97 –104	14	140 –146	14	306–318	14	449–466	14	972–1009	14
		104 –110	15	146 –152	15	318–331	15	466–483	15	1009–1046	15

* Radii of the zone in feet.

† From *Geophysics*, Vol. 4, No. 3, July, 1939, p. 190.

TABLE 14

FOR PRECISE EVALUATION OF TERRAIN CORRECTIONS AT GRAVITY STATIONS*

Zone H 12 compartments 5018 to 8578		Zone I 12 compartments 8578 to 14,662		Zone J 16 compartments 14,662 to 21,826		Zone K 16 compartments 21,826 to 32,490		Zone L 16 compartments 32,490 to 48,365		Zone M 16 compartments 48,365 to 71,996	
$\pm h$ (ft.)	T	$\pm h$ (ft.)	T	$\pm h$ (ft.)	T	$\pm h$ (ft.)	T	$\pm h$ (ft.)	T	$\pm h$ (ft.)	T
0 to 75	0	0 to 99	0	0 to 167	0	0 to 204	0	0 to 249	0	0 to 304	0
75– 131	0.1	99– 171	0.1	167– 290	0.1	204– 354	0.1	249– 431	0.1	304– 526	0.1
131– 169	0.2	171– 220	0.2	290– 374	0.2	354– 457	0.2	431– 557	0.2	526– 680	0.2
169– 200	0.3	220– 261	0.3	374– 443	0.3	457– 540	0.3	557– 659	0.3	680– 804	0.3
200– 226	0.4	261– 296	0.4	443– 502	0.4	540– 613	0.4	659– 747	0.4	804– 912	0.4
226– 250	0.5	296– 327	0.5	502– 555	0.5	613– 677	0.5	747– 826	0.5	912–1008	0.5
250– 414	1	327– 540	1	555– 918	1	677–1119	1	826–1365	1	1008–1665	1
414– 535	2	540– 698	2	918–1185	2	1119–1445	2	1365–1763	2	1665–2150	2
535– 633	3	698– 827	3	1185–1403	3	1445–1711	3	1763–2086	3	2150–2545	3
633– 719	4	827– 938	4	1403–1592	4	1711–1941	4	2086–2366	4	2545–2886	4
719– 796	5	938–1038	5	1592–1762	5	1941–2146	5	2366–2617	5	2886–3191	5
796– 866	6	1038–1129	6	1762–1917	6	2146–2335	6	2617–2846	6	3191–3470	6
866– 931	7	1129–1213	7	1917–2060	7	2335–2509	7	2846–3058	7	3470–3728	7
931– 992	8	1213–1292	8	2060–2195	8	2509–2672	8	3058–3257	8	3728–3970	8
992–1050	9	1292–1367	9	2195–2322	9	2672–2826	9	3257–3444	9	3970–4198	9
1050–1105	10	1367–1438	10	2322–2443	10	2826–2973	10	3444–3622	10	4198–4414	10
1105–1158	11	1438–1506	11	2443–2558	11						
1158–1209	12	1506–1571	12	2558–2669	12						
1209–1257	13	1571–1634	13	2669–2776	13						
1257–1305	14	1634–1694	14	2776–2879	14						
1305–1350	15	1694–1753	15	2879–2978	15						

* From *Geophysics*, Vol. 4, No. 3, July, 1939, p. 191.

cylinder and in the plane through one end. This formula where r_1 and r_2 are the inner and outer radii of the cylinder is:

$$\Delta g = -2\pi G d \left[r_2 - r_1 + \sqrt{r_1^2 + h^2} - \sqrt{r_2^2 + h^2} \right] \qquad (129)$$

In the above, G = the gravitational constant and d = the density.

The tables do not give the correction for zone A, the area within 6.56 feet (2 meters) radius around the station. This is because only exceptional terrain conditions would give significant effects in this small area, or the terrain could be controlled by leveling it, as in torsion balance work. In practically all cases, a sufficiently level spot can be found on which to set a gravimeter. A terrain effect of 0.01 mg. (for $d = 2.0$) within zone A requires a slope of 27½°, which establishes a practical working limit for slope in locating stations in the field.

The terrain correction supplements the Bouguer correction described in the section on pendulum gravity corrections (p. 257). It has been shown that the Bouguer and the elevation corrections taken together reduced the gravity observations to what they would be if the gravimeter had been on the datum plane established for the survey.

The Bouguer correction intentionally treats the section of material between the ground surface at the station and the datum as if it were a flat circular slab of infinite radius bounded by two plane surfaces. These surfaces are a horizontal plane through the station and the horizontal datum plane. This assumption makes no allowance for any hills or hollows in the ground and therefore, so to speak, ignores the terrain. All depressions are treated as if they were filled up with material of a certain assumed density and hills are not considered. This is a valid process where the terrain is essentially flat. The terrain correction measures the gravity effect of existing undulations of the top surface of the slab, thereby determining the error inherent in the Bouguer correction and correcting for it.

The Bouguer correction, as applied, is always too great in those cases where either hills or depressions affect a gravity station. Gravimeter readings due to the presence of a hill or a valley are less than they would be if these terrain features were absent. The Bouguer correction therefore, by over-correcting, gives reduced (on datum) gravity values that are too small.

This can be explained as follows. A hill adjacent to a gravity station places a mass of material above the station and gives rise to a gravity component opposed to the downward gravity force. This results in a lower gravity value than would exist if the hill were not present, as is assumed in the Bouguer correction. The actual gravity effect of the hill (which tends to decrease the effective gravity) is shown by the terrain tables, and hence is added to the reduced gravity value in order to correct it. The Bouguer correction applied on the basis of no hill being present was, obviously, an over-correction of the reading or gravity value obtained.

A valley next to a station acts in the same manner. It represents a deficit in attractive force due to the absence of earth material in it. A gravimeter would give a lower reading in this case than if the valley were filled (as assumed in the Bouguer correction) instead of being occupied by air. The meter reading has been reduced as if the ground were flat. The terrain calculation shows the amount of over-correction and, by adding it to the gravity value, rectifies the error.

The above explains why the average height of a segment of terrain is calculated without regard to sign. Although the statement appears contradictory, it is true that hills and valleys act in a similar manner in their effect on a gravimeter.

Density Profiles.—The Bouguer correction as applied in gravity surveys, as has been brought out, deals with the effect of all of the material from the ground surface to the datum plane. For a given station the amount of this correction in milligals equals the factor 0.0127 • density • the distance in feet between the stations and the datum. In equation form, correction $= 0.0127 \cdot d \cdot$ distance in feet.

It can be shown that for a distance of 100 feet from station to datum an error in the assumed density of 0.1 would give an error of approximately 0.13 milligal. The value used for the density is considered to apply to the entire slab of material from the station down to the datum. Unless density determinations from drill cuttings for the geologic section to the datum are available, surface sample density values plus a factor of judgment are our only guides as to what the assumed density should be.

However a method has been outlined by L. L. Nettleton† whereby the effective, in place, density of a section of earth materials can be determined. The procedure is not complicated. A special traverse of gravimeter stations is run across a topographic feature, either a hill or a valley. The observations are corrected for latitude and for elevation in the usual manner. The resulting free air gravity values are plotted on a cross-section showing the elevations of the stations. These gravity observations (corrected for latitude and elevation only) will show a certain agreement with the topography across which they were taken. They will reflect the effects of the hill or the valley.

The next step is to complete the reduction of these free air gravity values by applying the Bouguer correction, using a number of different assumed values for the density factor. The Bouguer gravity values corrected at the different densities are also plotted on the section. The graph will show that the Bouguer gravities will still reflect the topographic feature if the density chosen was too small. The graph will likewise show that where the density selected is too great the observations will be over-corrected. It will exhibit a decrease in the plotted graph across a hill.

† L. L. Nettleton, "Determination of Density for Reduction of Gravimeter Observations," *Geophysics*, Vol. 4, No. 3, July, 1939, pp. 176-183.
L. L. Nettleton, "Geophysical Prospecting for Oil," McGraw-Hill, New York, 1940

The proper density for the area is that density which yields a minimum correlation with the topography. Ordinarily a rather definite selection can be made of the density which gives reduced gravity values showing a straight line on the graph of the profile. The method is quite advantageous in arriving at the best density figure to use in the Bouguer correction. It effectively weighs the topography of a feature so tested, and the density thus obtained can be used in the Bouguer reduction for an entire area.

Accuracy of Data *

The value of a gravity map depends largely on its accuracy. Various types of tests have been made to determine this accuracy. Aside from mistakes such as misreading the scale or error of computation, the error arises from three principal causes. The first is erratic fluctuations in the instrument reading from such causes as temperature fluctuation, elastic-after-effect, effect of jars, and the like. The second is inaccuracy of the calibration curve. The third is errors in making the latitude or elevation corrections due to inaccuracy of surveying or use of an incorrect elevation correction constant.

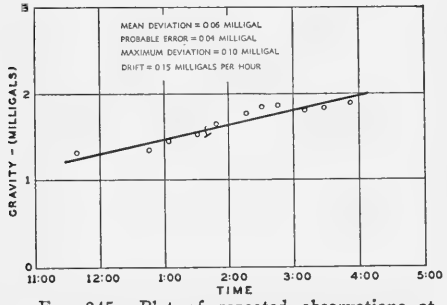

FIG. 245.—Plot of repeated observations at the base station. (L. M. and F. W. Mott-Smith, *The Petroleum Engineer.*)

The magnitude of the first type of error may readily be determined by noting the deviations of a succession of observations at the same station. In making such a test it is evidently necessary to simulate closely actual field conditions. The procedure, accordingly, is to occupy a station and make an observation in the manner customarily employed in the normal field work. The instrument is then transported in its truck a distance of one mile and returned to the same station. Here a second standard observation is made. A series of eleven such observations plotted as a drift curve are shown in Figure 245.‡ These data were treated as follows for the computation of the probable error of a single occupation of a station. The best straight line is first passed through the observed values. This may be readily done by a trial and error method or by the usual least square procedure. The deviations of the observed values from the drift line are then computed, and finally the probable error is obtained by the standard procedure of multiplying the square root of the average square deviation by the factor 0.67. In this test the mean deviation is found to be 0.06 milligal and the probable error of a single observation 0.04 milligal. The largest

* The method of determining accuracy has been supplied largely by L. M. and F. W. Mott-Smith in a personal communication.

‡ L. M. and F. W. Mott-Smith, "Advancements in the Use of the Gravimeter in Oil Exploration," *The Petroleum Engineer,* July, 1939, pp. 85-97.

deviation from the drift line occurred at the second trial and is 0.10 milligal. This accuracy is somewhat better than necessary for obtaining useful gravity maps.

The error caused by inaccuracy of calibration can partially be tested by determining the error of closure of closed loops of gravity differences. If the scale readings are converted into gravity values by means of an incorrect calibration curve, which might be the case if the sensitivity of the instrument changed during the course of a survey, errors of closure will appear. There is, however, also the possibility that an initially incorrect calibration might give proper closure, and yet all the measurements might be too large or too small by a constant percentage. This possibility may be detected in several ways. One method is to make observations at different known elevations in a building. (Compare p. 389.) Another is to check the gravimeter against gravity differences known from pendulum observations. Gravimeters are considered satisfactory if such tests indicate calibration errors of less than two per cent.

Errors caused by incorrect latitude and elevation corrections can be reduced to practically negligible proportions by surveying with sufficient accuracy and by taking care to use the proper elevation correction constant. It is practicable to establish the latitude of each station to within about one-twentieth of a mile. Thus the error in the latitude correction is about five hundredths of a milligal. It is also perfectly feasible to require closure of level line loops to within one foot, so that the error from incorrect elevation is not greater than about seven-hundredths of a milligal.

Sample Field Notes.—The various corrections applied to gravity meter readings are shown in the sample set of field notes on pages 412 and 413. The forms employed for field notes differ with each organization. Those illustrated here use two separate sheets. One of these is termed the *Gravity Computation Sheet,* and is used to record instrument observations and related data. The other, called the *Correction Sheet,* provides for the necessary corrections, which are summed up and the final correction transferred to the computation sheet.

The gravity computation sheet has 15 columns, the first three showing station number, time of observation, and instrument reading, in that order. The first reading at the base station in the sample set is 5-1360. The 5 refers to line five of a set of 10 lines in the moving scale of the meter used (Brown Gravity Meter No. 21). The position of this line on the fixed scale is 1360 scale points, or scale divisions.

The scale of this instrument is not quite linear, and the necessary calibration is achieved by adding a weight to the moving system, to determine the difference in scale divisions it causes. In this case, at the start of the survey, addition of the weight made a difference of 610 scale points. This calibration was made again at the end of the day's run, at which time there was a difference in reading of 600 scale points.

The instrument constant k, in milligals per scale point, is obtained by dividing a factor 21.3 (which relates the amount of the calibrating mass, the mass of the suspended system and the force of gravity) by the scale point deflection caused by adding the calibrating weight. See note, upper left of form.

For the scale range in the survey under consideration, the value of k is 0.0352 milligals per scale division. This figure was determined by taking an average deflection, from two tests, of 605 scale divisions and applying it to the factor 21.3, as shown at the bottom of the form. This procedure is similar to that used in finding the scale value of a magnetometer by applying a magnetic field of known amount to the instrument and observing the deflection. Here, by adding a small mass, a force of a given number of milligals (21.3) is applied to the gravimeter, causing 605 scale points deflection.

Columns 4 to 7 inclusive provide for instrumental corrections. Column 4 gives the direction, or azimuth, in which the meter truck is oriented at a station, and column 5 shows the correction for that orientation in scale divisions. The barometer reading is recorded in column 6, and the air

GRAVITY-METER SURVEY

GRAVITY COMPUTATION SHEET

Date JULY 23, 1942

m/M.G = 21.30 milligals calibration

Gravimeter No. 21

Computer P. I. B.

1 Sta. No.	2 Time	3 Instr. Rdng.	4 Scale Corrections Orientn Azm	5 Cor	6 Buoyancy Pres	7 Corr	8 Corr Rdng 3+5+7	9 Base Grph val	10 Scpts Diff 8-9	11 Mg/ sc. pt	12 Grav Diff mgls	13 Obs. Grav mgls	14 Adj.	15 Adj. Grav
BASE	2:20	5-1360	S	0	29.26	+87	1447	—	—	0.0352	00	100	52.40	152.40
BASE		5-1970	CALIBRATION			MASS ON				"	6105.	D.DIFF.		
1	2:40	5-1365	N	0	29.24	+81	1446	1446	00	"	00	100	52.65	152.40
2	4:45	5-1445	NW	-1	29.24	+81	1525	1439	+86	"	3.03	103.03	49.68	152.71
3	5:00	5-1415	W	-2	29.21	+71	1484	1438	+46	"	1.62	101.62	50.02	151.64
4	5:15	5-1420	N	0	29.23	+77	1497	1437	+60	"	2.11	102.11	49.88	151.99
BASE	5:40	5-1355	S	0	29.24	+81	1436	—		"	—			
5	6:00	5-1345	N	0	29.19	+64	1409	1433	-24	"	-0.84	99.16	52.77	151.93
6	6:13	5-1345	N	0	29.15	+50	1395	1432	-37	"	-1.30	98.70	51.85	150.55
BASE	6:35	5-1355	S	0	29.22	+74	1429	—			—			
BASE		5-1955	CALIBRATION MASS ON								600	S. D.	DIFF.	
						$K = \frac{21.30}{605} = .0352$								

GRAVITY-METER SURVEY

CORRECTION SHEET Date JULY 23, 1942

Gravimeter No. 21 Computer O. W.

1	2	3	4	5	6	7	8	9	10	11	12	13	14	15
		F-Air & Bouguer					Terrain							
Sta. No.	Elev.	F-Air Corr.	Den.	Boug.	Comb.	Zone B	Zone C	Zone D	Zone E	Total	Lat. Corr.	Total Corr.	Reg. Cor.	Totl. Adj.
BASE	1767.0		2.0		52.40					(miles) N-S 0	0			52.40
1	1770.3				52.65					0	0			52.65
2	1722.0				49.35					+0.25	+0.33			49.68
3	1725.0				49.50					+0.40	+0.52			50.02
4	1725.7				49.55					+0.25	+0.33			49.88
5	1778.3				53.10					-0.25	-0.33			52.77
6	1774.4				52.70					-0.65	-0.85			51.85
combined constant density = 2.0 used as 0.0683														
latitude corr = 1.3 milligals/mile + to N. Datum = 1000														

pressure or buoyancy correction is listed in column 7. The amount of the correction for a given air pressure is obtained from a table which has been previously worked out by tests on the particular instrument used. When the meter is not housed in a hermetically sealed case, variations in air pressure are important.

The instrumental corrections are added and applied to the reading of column 3, and the result recorded in column 8, which gives the corrected reading at the station in scale points.

The base graph value of column 9 represents the reading that would have been obtained at the base at a given time. It is found from the base graph, or drift curve, for the time at which the station was taken.

The base graph is plotted from base station check readings as shown in Figure 245 and gives the instrument reading, at the base, versus time. Instrument drift with a gravimeter, as noted, is purely an instrumental phenomenon, as there is no detectable daily variation in gravity force. A tidal variation of gravity, relating to the position of the sun and the moon, is just slightly below the range of operation accuracy of gravimeters and usually is neglected.

Column 11 gives the difference in reading at the station relative to the base and is obtained by subtracting the base graph value from the corrected station reading (column 8 minus column 9).

The instrument constant k shown in column 11 is applied to the gravity differences, in scale points, of column 10, and the result or gravity differ-

ences at the stations, in milligals, is given in column 12. The operation is column 10 times k.

The arbitrary gravity value assigned to the base station was 100 milligals. This value is used in column 13 by adding to it the figures in column 12. (Column 12 plus 100 mg.).

In column 14 the total corrections, noted as adjustments from the correction sheet referred to, are shown. Their application gives the final map value for the field stations in milligals relative to the survey base which is of record in column 15. The similarity of the above procedures to those in magnetic field work is obvious.

The *correction sheet* also has 15 columns, although not all of them are ordinarily used. Station number and elevation are entered in columns 1 and 2. Space is provided in columns 3, 4, 5, and 6 to calculate the free air and the Bouguer corrections separately, as is sometimes done.

In the set of notes given here, these two corrections are combined as represented in the constant 0.0683 milligals per foot, using an assumed density of 2.0 for the material between the station and the datum. The datum of the survey was set, for convenience, at an elevation of 1000 feet.

In column 6 is shown the combined correction, obtained from multiplying the combined constant by the number of feet from the station to the datum. For station 1 this was 767 feet · 0.0683, or 52.40 milligals.

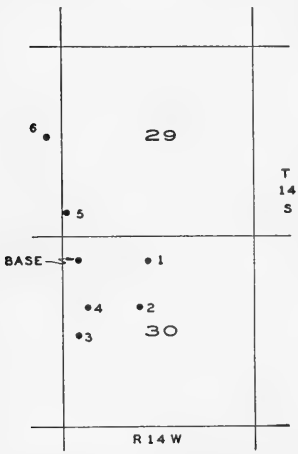

FIG. 246.—Locations of gravity meter stations for sample calculations.

Terrain corrections for the effect of certain zones at given out-distances from the station can be entered in columns 7 to 10. In the survey treated, the local terrain was rather flat and no terrain correction was needed.

The use of column 11, in these notes, is slightly changed from its heading as given. It represents the sum of the terrain zone effects. As used in the notes under consideration, the distances in fractions of a mile north or south of the base are listed. Station 2, for example, was 0.25 of a mile *south* of the base, as indicated on the map of the locations of the stations, Figure 246.

The latitude correction comes in column 12 and is at the rate of 1.3 milligals per mile in the present instance. It was determined by calculation for the latitude of the survey area, namely 38° 45′ and 39° 00′ north (see page 253). At station 2 the latitude correction is 0.33 milligals (0.25 · 1.3).

The latitude correction is applied in a proper manner in the operation of the form. At station 2, for instance, the latitude correction is plus 0.33 milligals (station 2 is 0.25 miles *south* of the base, where gravity is there-

fore less). The 0.33 enters the sum of the corrections indicated in column 15 as total adjustment, and is transferred to the computation sheet. It is there applied, or added, as a correction and in this way the value at station 2 has been increased by the necessary 0.33 milligals. The latitude correction for station 5, which is a like distance north of the base, shows a −0.33 in column 12.

If a regional correction is used, it can be set down in column 14. It is added or subtracted, as the case may be, and goes in as a part of the total adjustment of the last column.

The calculation of gravity meter notes is not difficult, but checking is necessary, and errors of multiplication, addition and subtraction must be guarded against, as in any operation involving numerous figures. Slide rule accuracy is sufficient for certain steps, which saves considerable time. Tables for certain operations can be constructed, such as for latitude correction or the conversion from scale points to milligals.

Interpretation of Relative Gravity Data (Contours and Profiles.)—The values of the relative gravity, after the necessary corrections, are plotted as isanomalic contours or as profiles. The isanomalic contours plotted in direct gravity work are lines of equal value of gravity anomaly referred to some point in the area, usually the main base station, where the anomaly is assigned some arbitrary value. The contour interval generally used is one-half to two milligals.*

Corrections for Regional Gravity Effects

The gravity observation at a station is the measurement of a summation effect—i.e., the resultant of all gravitational attractions or effects within the range of the gravity instrument. The factors which contribute to this summation effect are both physical and geological, and include (1) the station elevation, (2) the local terrain, (3) the more distant topography, (4) the normal value of the earth's gravitational field, (5) the density and distribution of the near-surface materials around the station, and (6) the deeper geological structure, both local and regional.

The procedure followed in calculating quantitatively the gravity effect of several of these components has been given in preceding sections. When the contribution of a particular component can be calculated, it may be applied as a correction to the station gravity value and thus removed as one of the variables. Such correction simplifies interpretation. Terrain effects are handled in this manner. As another example, the Bouguer gravity anomaly values at a set of field stations are more interpretable than the raw or uncorrected gravity values. The Bouguer values have been reduced to datum, which considers not only the elevation and the Bouguer effect, but also the earth's normal gravity field, and if necessary the local terrain and the more distant topography. This is the usual calcu-

*Illustrations of isanomalic contours are shown in the section entitled "Petroleum Surveys."

lation procedure in a gravity survey, and in itself provides a considerable simplification.

After correcting for the first five effects listed above, it is often necessary to consider the sixth, which in many cases can be separated into two parts, namely, the regional and the local or residual gravity components. In exploratory geophysics we are interested primarily in the residual gravity values and, to obtain a picture wherein they stand out more clearly, it is necessary to remove the masking effect of the regional gravity.

This separation is accomplished by constructing a residual gravity map, showing only the gravitational field due to local structure. The residual values are obtained by removing the regional gravity effects from the Bouguer station values. To express this mathematically,†

$$\Delta g = g(o) - \overline{g}(r) \tag{130}$$

where Δg is the residual gravity value,
$g(o)$ is the station gravity value, and
$\overline{g}(r)$ is the *average* gravity value for the area within a radius of r from the point where the station value $g(o)$ was obtained.

The average gravity value may be expressed by

$$\overline{g}(r) = \frac{1}{2\pi}\int_0^{2\pi} g(r, \theta)\, d\theta \tag{131}$$

which may be considered as the average value obtained at a series of reading points around a circle of radius r, with the station $g(o)$ as its center, in increments of $d\theta$.

In general, an integrable form of $g(r, \theta)$ is not known, and a close approximation may be had by obtaining the arithmetical average at a finite number of stations located on the circumference of the circle. This average, for a series of n points, may be expressed by the relationship†

$$\overline{g}(r) = [g_1(r) + g_2(r) + g_3(r) + \ldots g_n(r)]/n \tag{132}$$

The value of n may be any whole number. The resultant residual gravity Δg may be positive, zero, or negative, depending upon the relative gravity value of the point under study compared to the regional or background value of $\overline{g}(r)$.

Average Value Method.—The number and position of the points on a map at which gravity values are selected to find the regional, or average, value to be applied at a station can be varied to suit the problem at hand. These points may be chosen at an equal spacing on a circle of given radius

† W. R. Griffin, "Residual Gravity in Theory and Practice," *Geophysics*, Vol. XIV, No. 1, January, 1949.
† W. R. Griffin, *loc. cit.*

around the station to be corrected. The points may also be taken on the corners of a square ($n = 4$), a hexagon ($n = 6$), or a decagon ($n = 10$), etc. The dimensions of these figures may be varied. Figure 247 shows a conventional gravity survey map by Griffin, covering the South Houston Field and the adjacent area, and contoured at an interval of 0.2 millidyne.

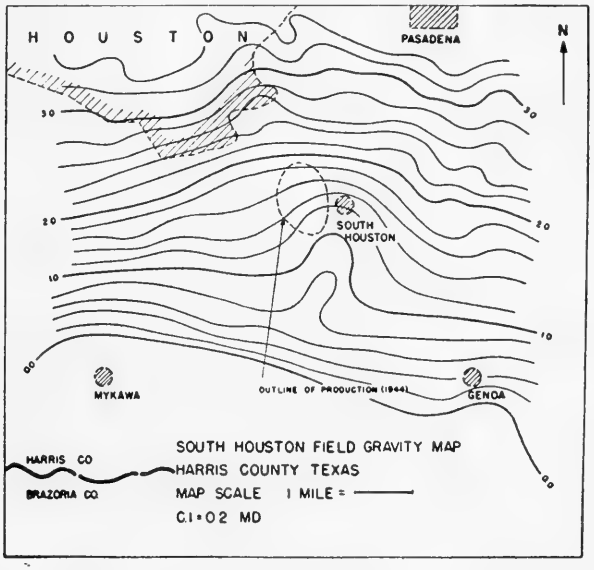

Fig. 247.—Conventional gravity map of South Houston field and adjacent area. Contour interval 0.2 millidyne. (W. R. Griffin, *Geophysics*, Vol. 14, No. 1, Jan., 1949.)

Figure 248, covering the same locality, illustrates the procedure under consideration. On this map is superimposed an octagon net which was used to calculate the average gravity value or regional effect, applicable at the center point of the net. Each octagon in the net permits 8 gravity map points to be averaged for the radius or outdistance selected.

It was found that the maximum variation from averaging 4 points (using a square) as against 8 points (using an octagon) was about 0.05 millidynes. In another test case, the difference between averaging 4 points (square) and 10 points (decagon) around the station was 0.10 millidynes. The number of points to be averaged usually is not a critical factor in calculating the regional correction.

Although the geometric pattern which controls the number of points averaged may not be critical, the dimensions of the figure are quite important. In the first test case, if the outer radius of the square (or 4-point

figure) was 1 inch, the maximum residual gravity value* was found to be 0.3 millidynes. Plot maps of approximately one inch to the mile were used. In the second case, for a decagon of 1.5 inches radius (1.5 mile), the maximum residual of gravity was −0.6 millidynes. For a 3-inch radius (3 miles) for the decagon, it was −1.51 millidynes.

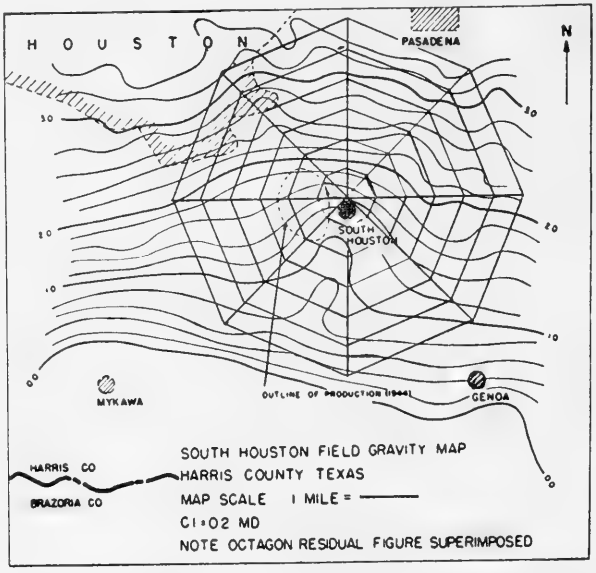

Fig. 248.—Superposition of family of concentric octagons, as applied to Figure 247. (W. R. Griffin, *Geophysics*, Vol. 14, No. 1, Jan., 1949.)

These variations in the maximum residual gravity value illustrate the importance of choosing the proper dimensions for the distribution figure. A cut-and-try procedure may be necessary to obtain what appears to be the most reasonable value. The decision as to the number and spacing of the map locations at which regional gravity calculations or averages are to be made usually is not a major factor in the final results. It is of about equal importance with the number of gravity values entering into the average.

The particular geometric figure selected for the number and the distribution of gravity values may be drawn to scale on a transparent sheet, as indicated in Figure 248. This sheet may be positioned at different points on the original gravity map of the area, and the point value of gravity may be read from the contours which will be visible through the overlay sheet.

* The residual (gravity) value at a station is the Bouguer gravity at the station *corrected* for the regional effect. Therefore for a set of stations corrected for regional gravity the maximum residual value would depend as to amount and sign on the particular regional correction applied.

These values of gravity are added, and then divided by the number of points read to obtain an average (or regional) value. This value can be ascertained for as many specific map locations as are deemed necessary, or for each survey station if desired.

The observed gravity values are corrected by the average regional values to obtain the residual or anomaly quantity. These latter values are put on a new map of the area and contoured at an interval best suited to express the resulting variation in the residual gravity.

The above procedure is rigorous only in so far as the numerical averaging itself is concerned. Tests can be made to select the best number of gravity values to be averaged and their distribution, as well as the map

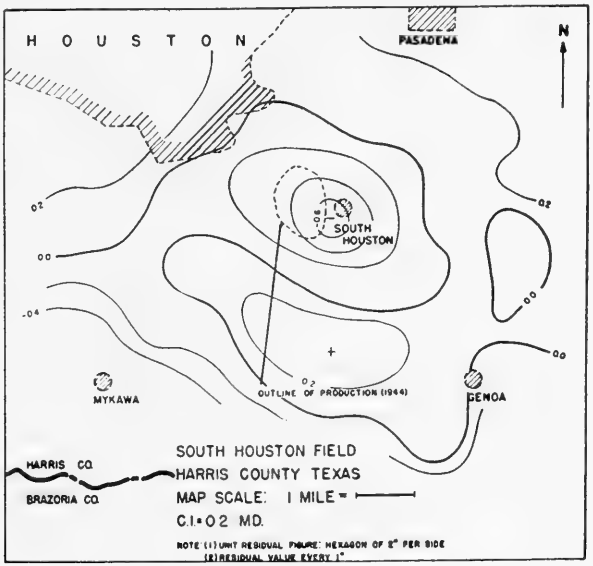

Fig. 249.—Residual gravity map of South Houston field using (1) unit residual figure: hexagon of 2 inches per side; (2) residual value every 1 inch; (3) contour interval, 0.2 millidyne. (W. R. Griffin, *Geophysics*, Vol. 14, No. 1, Jan., 1949.)

spacing of the locations where the regional gravity values are to be determined. Griffin found that it was safe to include gravity values within a 5-mile radius around a point where the regional effect was to be found. Beyond that distance the presence of neighboring subsurface bodies may alter the result. This finding applied to a salt dome area.

Two residual gravity maps for the South Houston area are given in Figures 249 and 250. In Figure 249, average or regional gravity values were calculated, using a hexagon as the unit residual figure. Its dimensions were 2 inches, or approximately 2 miles on a side. Regional correction values were determined at points 1 inch (1 mile) apart over the area.

In Figure 250, the sides of the hexagon were 3 inches to the same map scale, and as in the previous case average values were calculated for points at a 1-inch spacing. The two residual gravity (or local anomaly) maps show certain differences, relating, however, more to details than to the overall picture. They verify the earlier statement that the details of the residual anomaly are influenced chiefly by the choice of dimensions of the figure used.

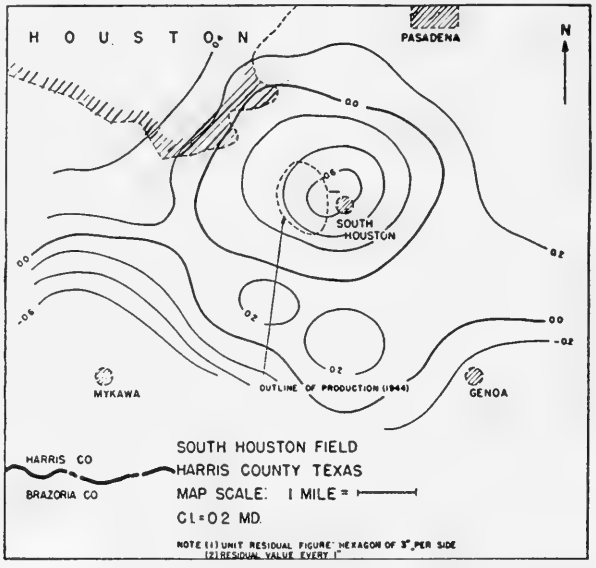

Fig. 250.—Residual gravity map of South Houston field using (1) unit residual figure: hexagon of 3 inches per side; (2) residual value every 1 inch; (3) contour interval, 0.2 millidyne. (W. R. Griffin, *Geophysics,* Vol. 14, No. 1, Jan., 1949.)

Smooth Contour Method.—One technique for differentiating between the regional and the residual anomaly is a visual inspection procedure and consists of drawing "smooth" gravity contour lines on the survey map, in a manner and at a contour interval which appears to best represent the regional gravity picture. After such a contour map of the regional gravity has been prepared, the departure or difference between the observed gravity contours and the regional contours is determined. If the "smooth" contours are substantially correct, these departures are the residual values for the points chosen, and become the local anomaly gravity values. The data should then be transferred to another map and contoured. Both the regional and the residual contour maps should be kept, for later restudy.

In the preparation of the "smooth" contour regional gravity map, the direction and spacing of the contours can be guided, in part, by the configuration of the contours of the original survey for those portions of the

area which are considered to be outside the local gravity anomaly. Judgment must be exercised in selecting the limits of the area which is held to be uninfluenced by the local anomaly. If too large an area is included, beyond the local feature under study, other adjacent subsurface anomalies may influence the observed gravity values, and hence the contours. For example, in areas where anticlinal structures are narrow, such a feature might be a nearby anticline; or in a salt dome region, a neighboring dome. If too small an area is used, the regional effect will not be properly shown.

No rigid rules can be set up to govern the drawing of such contours, as each case must be judged on its merits. The general size and dimensions of structures which are geologically reasonable in a locality will serve as a guide to the probable extent of a local gravity anomaly. On this basis, the width of the area outside the local anomaly and not influenced by it could be assumed with fair safety to be roughly equal to that of the anomaly itself.

It is apparent that the personal equation and the experience of the interpreter will play a large part in the application of the "smooth" contour method. The character and usefulness of the local anomaly obtained would thus depend to a considerable degree on the skill and judgment of the author of the "smooth" or hypothetical regional gravity map. The method is quite simple and has considerable merit. It does not take an undue amount of time, and in many cases a more elaborate analysis of gravity data is not justified.

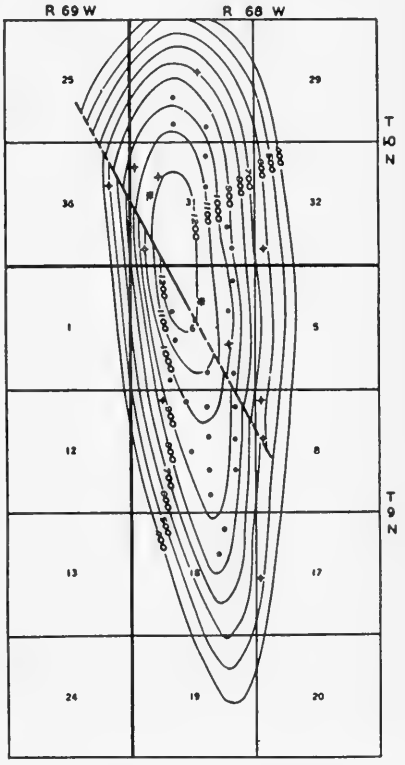

FIG. 251.—Wellington Oil Field, Larimer County, Colorado, subsurface structural map contoured on Muddy Sand. (J. H. Wilson, *Geophysics*, Vol. 6, No. 3, July, 1941.)

Profile Method.—A third way of finding the regional gravity in an area makes use of profiles of average gravity along section lines in the locality investigated, and is therefore adapted to sectionized country.† In unsectionized regions an arbitrary grid pattern would be selected.

In this profile method, the regional gravity effect is expressed in milligals per mile, as determined from the profiles, in the north-south and in the east-west directions. The amount of

† J. H. Wilson, "Gravity Meter Survey of the Wellington Field, Larimer County, Colorado", *Geophysics*, Vol. 6, No. 3, July, 1941, pp. 264-269.

the regional correction to be applied at a field survey station is found in the same way as the latitude and longitude correction in magnetic survey work; namely, at a given rate per mile, for the required number of miles.

The above procedure was successfully applied at the Wellington Field in Colorado. This field was selected for an experimental gravity study in 1940, as it was a typical mountain fold, situated on the west flank of the Denver Basin. It is an anticline about 5 miles long, with a closure of some 800 feet as shown by contours on the Muddy Sand (Figure 251). This

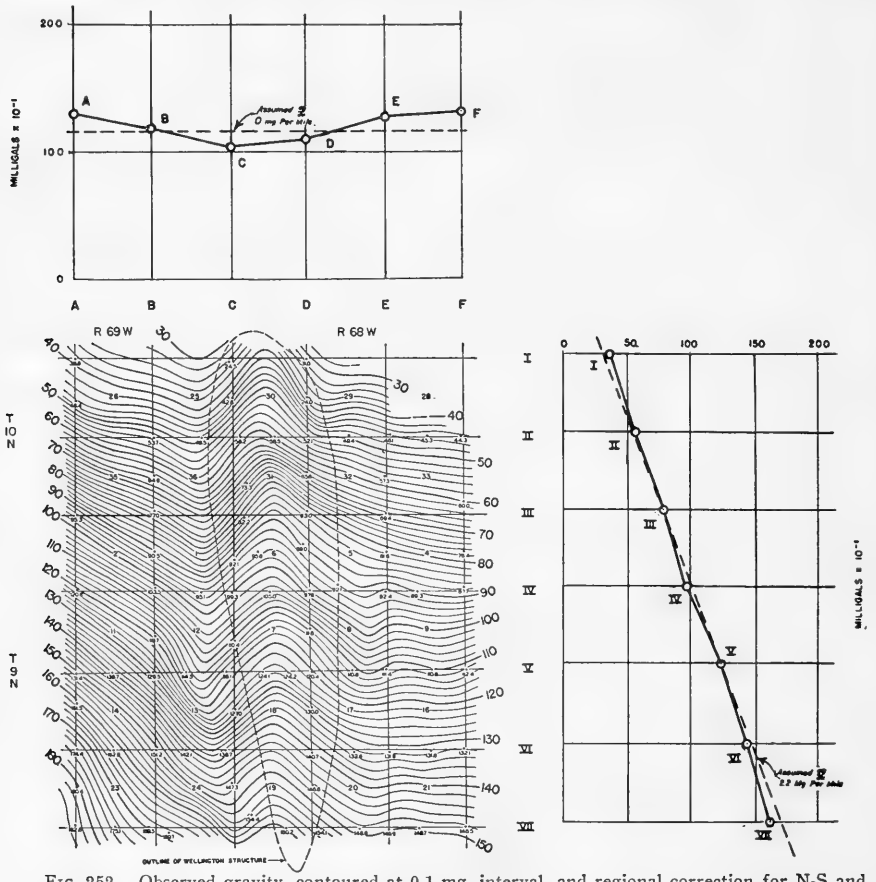

FIG. 252.—Observed gravity, contoured at 0.1 mg. interval, and regional correction for N-S and E-W profiles, Wellington Field, Larimer County, Colorado. (After J. H. Wilson, *Geophysics*, Vol. 6, No. 3, July, 1941.)

horizon is at a depth of approximately 4250 feet on the top of the structure. The field is cut by a fault running in a northwest-southeast direction.

The results of the gravimeter survey of the Wellington Field are given in Figure 252, in which gravity values relative to a base station have been contoured in 0.1 milligal units. The gravity stations have been corrected

for elevation, Bouguer effect and latitude as usual, but no regional correction has been applied. The map shows the outline of the Wellington Oil Field as traced by the lowest closing structural contour of the preceding figure.

It is apparent from the observed gravity map that the exact location and shape of the Wellington Anticline is masked to a large extent by the regional effect. The anticline is expressed by a persistent flexure or wrinkle in the observed gravity contours. This flexure appears to run from north to south across the survey area. The values also show a steady increase in gravity force toward the south or toward a known large regional gravity maximum. The Wellington structure lies on the north flank of this regional gravity feature. The regional gravity effect is superimposed upon and tends to mask the local gravity anomaly arising from the smaller (oil field) subsurface structure.

To evaluate the regional effect, averages were taken at equally spaced stations (section corners) across the map, along the north-south and the east-west section lines. Contour values were used where stations were missing at the regular spacing. These average values were plotted in profiles, as shown in Figure 252. If desired, straight line approximations may be used, as shown by the dotted lines. In some cases, curved line smoothing of the profiles is advantageous. The profiles indicated that the regional gravity in this area increased to the south at the rate of 2.2 milligals per mile. The east-west component of the regional effect was zero.

The resulting residual gravity map, after the above regional effect had been subtracted at each station, is presented in Figure 253. It reveals a closed local gravity anomaly which is in good general agreement, as to shape, size, position, and the strike of its axis, with the known Wellington Anticline disclosed by drilling. It is noteworthy that the highest closing gravity contour is very nearly in the same position as the highest closing structural contour. This example shows the advantage of correcting for the regional gravity effect.

As evidenced by the examples given, it is apparent that local gravity anomalies are related to local subsurface structures, and that the regional gravity effects express the larger scale regional subsurface conditions. It has been shown that often the regional effect can be approximated and applied as a correction to permit the residual anomalies of gravity to depict more clearly the local subsurface features.

It should be recognized that a lateral change in the density of subsurface formations or in the basement rocks can also give rise to a gravity anomaly. Such a lithologic density variation may or may not be meaningful in terms of local gravity anomalies or structures. Wilson† notes that the marked increase in gravity southward from the vicinity of the Wellington Field agrees with a large regional gravity maximum. This maximum, on the

† J. H. Wilson, *loc. cit.*

basis of the known geology of the area, is thought to relate to density variations in the basement rock.

It follows from the above that if a gravity anomaly of regional significance can be caused by a density change in the basement or in the subsurface section, so can a local gravity anomaly be caused in the same manner. The difference, in general, between regional and local gravity features or

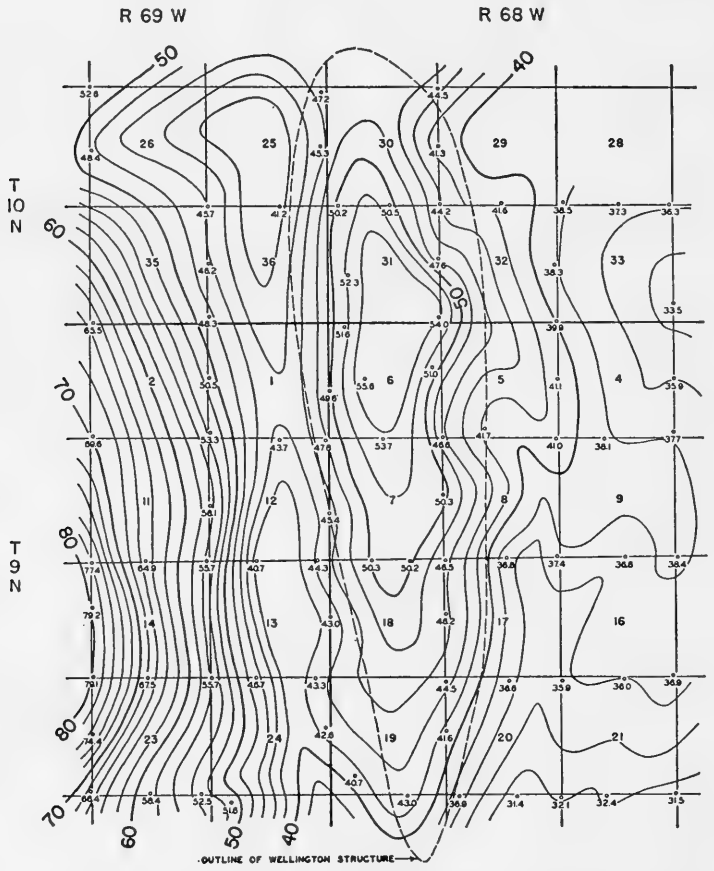

Fig. 253.—Adjusted gravity contoured at 0.2 mg. interval. Regional gradient of 2.2 mg. per mile south has been subtracted from observed gravity, Wellington Field, Larimer County, Colorado. (J. H. Wilson, *Geophysics*, Vol. 6, No. 3, July, 1941.)

structural features is largely a matter of size and areal extent. There is no reason, geologically, why density changes in shallow beds should not cause local gravity anomalies. This possibility should be kept in mind during interpretation of data in areas where there is a geological basis for expecting such subsurface lateral changes.

Mining Surveys

Anomalies Over Assumed Bodies.—Theoretical gravity anomalies over hypothetical bodies of rectangular cross section are shown in Figures 254, 255, and 256.† In all three cases it is assumed that the body has a density one unit greater than that of the surrounding medium; that is, denoting the density of the medium by σ, that of the body is $\sigma + 1$. A density

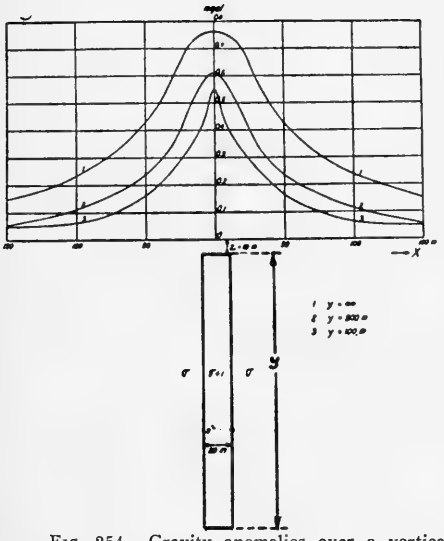

Fig. 254.—Gravity anomalies over a vertical body. (Hedstrom, *A.I.M.E. Geophysical Prospecting*, Tech. Pub. 953.)

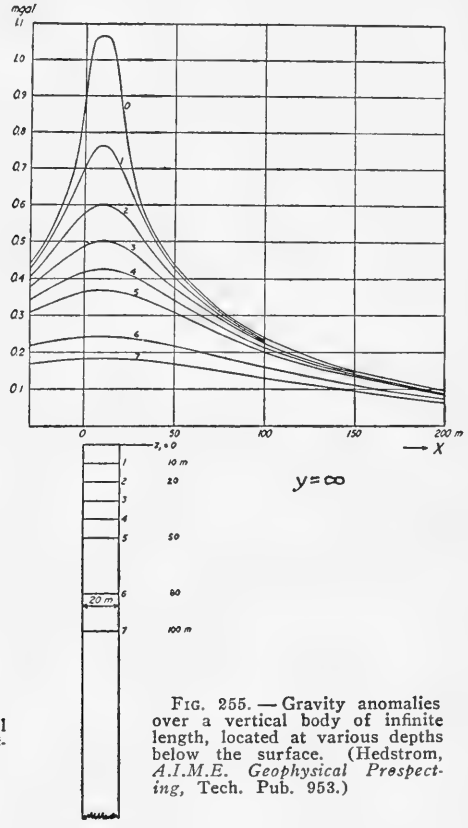

Fig. 255. — Gravity anomalies over a vertical body of infinite length, located at various depths below the surface. (Hedstrom, *A.I.M.E. Geophysical Prospecting*, Tech. Pub. 953.)

difference other than one unit would alter the amplitude but not the shape of the curves. In the case of a negative density difference, e.g., minus one unit, the anomalies will be inverted. Figure 254 shows the theoretical gravity anomalies over a vertical body whose length is ∞, 200 and 100 meters respectively. Figure 255 shows the theoretical gravity anomalies corresponding to a vertical body of "infinite" length, located at various depths below the surface. Figure 256 illustrates the theoretical anomalies corresponding to various dips for ore bodies of "infinite" length.

† H. Hedstrom, "A New Gravimeter for Ore Prospecting," *A.I.M.E. Geophysical Prospecting*, Tech. Pub. 953, 1938.

Figure 257 shows the gravity anomalies produced by step blocks located at various depths below the surface. The curves are drawn for the case that the density of the structure is greater than that of the surrounding medium.

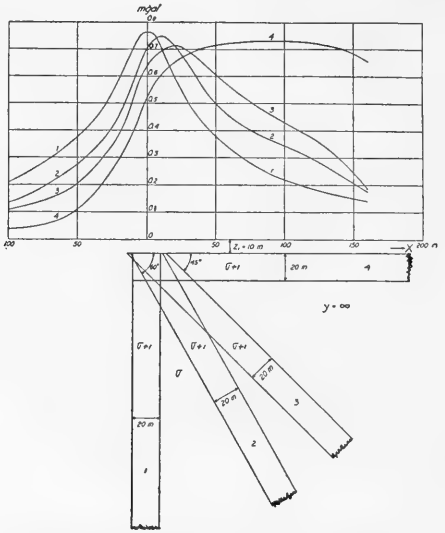

FIG. 256.—Gravity anomalies over bodies of different dips. (Hedstrom, *A.I.M.E. Geophysical Prospecting*, Tech. Pub. 953.)

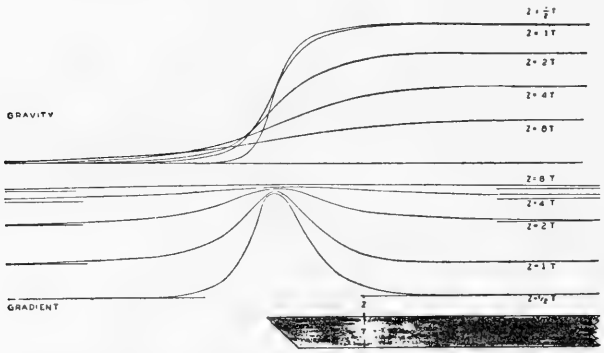

FIG. 257.—Relative gravity profiles for an infinite step block of thickness T, located at depths equal to $T/2$, T, $2T$, $4T$ and $8T$ below the surface. (Barton, *The Science of Petroleum*, Vol. I.)

Gravimeter Surveys over Ore Bodies.—The gravity anomaly over a large ore deposit in the Skellefte district is shown in Figure 258. The sulfide ore deposit, which had been previously disclosed by geoelectrical prospecting, consists of three parallel lenticular veins, dipping steeply to the north. One vein has a thickness of about 10 m. and the other two a thick-

ness of some 3 to 4 m. The uncorrected (primary) curve shows an effect of the contact with the schist. The reduced curve, which includes a correction for the effect of the contact on the assumption that the difference in density between the schist and leptite is 0.2, shows indications of two ore zones.*

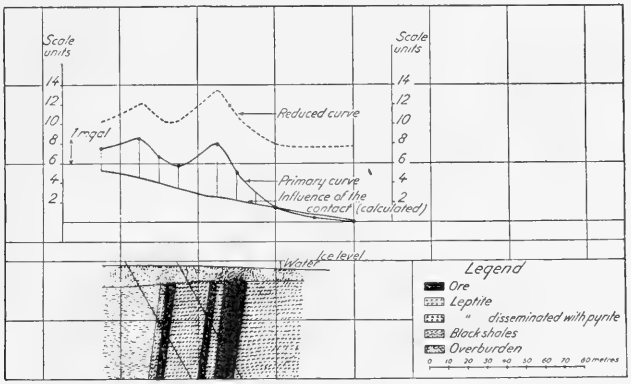

FIG. 258.—Gravity anomaly over a pyrite deposit located under a lake in the Skellefte district, Sweden. (Hedstrom, *A.I.M.E. Geophysical Prospecting*, Tech. Pub. 953.)

Petroleum Surveys †

Gravimeter Surveys over Salt Domes.—Figure 259 shows an example of a survey conducted with a gravimeter in the vicinity of Houston, Texas. The survey was made in nine working days, included 169 stations, and covered an area of approximately 100 square miles.

The area covered during the survey includes the Pierce Junction and the Mykawa oil fields. The Pierce Junction field is a piercement type dome having a substantially vertical salt plug approximately one mile in diameter. The cap rock overlying the plug is about 250 feet in thickness, and this in turn is covered with about 700 feet of recent material. The top of the salt is approximately 950 feet below the surface. The salt plug has a lower density than the surrounding rock, and its presence causes a gravity low or minimum. The gravity picture is complicated by the presence of a regional change of gravity, with the values increasing toward the south against the latitude gradient. Further complications are introduced by the neighboring gravity minimum due to the Mykawa field toward the southeast. The diagnostic gravity feature is a large so-called minimum nose, clearly indicated by several contours. This feature results when the gravity minimum caused by the salt plug is superposed on the regional or lateral change of gravity. A study of the contours shows that the decrease in gravity due to the dome is about two milligals and its effect is noticeable

* Note that the gravimeter did not "resolve" or differentiate between the two southern veins.

† L. M. and F. W. Mott-Smith, personal communication; also, see "Advancements in the Use of the Gravimeter, in Oil Exploration," *The Petroleum Engineer*, July 1939, pp. 85-97.

at a distance of about three miles from the center. There is also a small positive gravity effect superposed on the large minimum, appearing as a maximum of four-tenths of a milligal near the center of the dome. This feature, no doubt, is caused by the shallow denser cap rock. The gravity

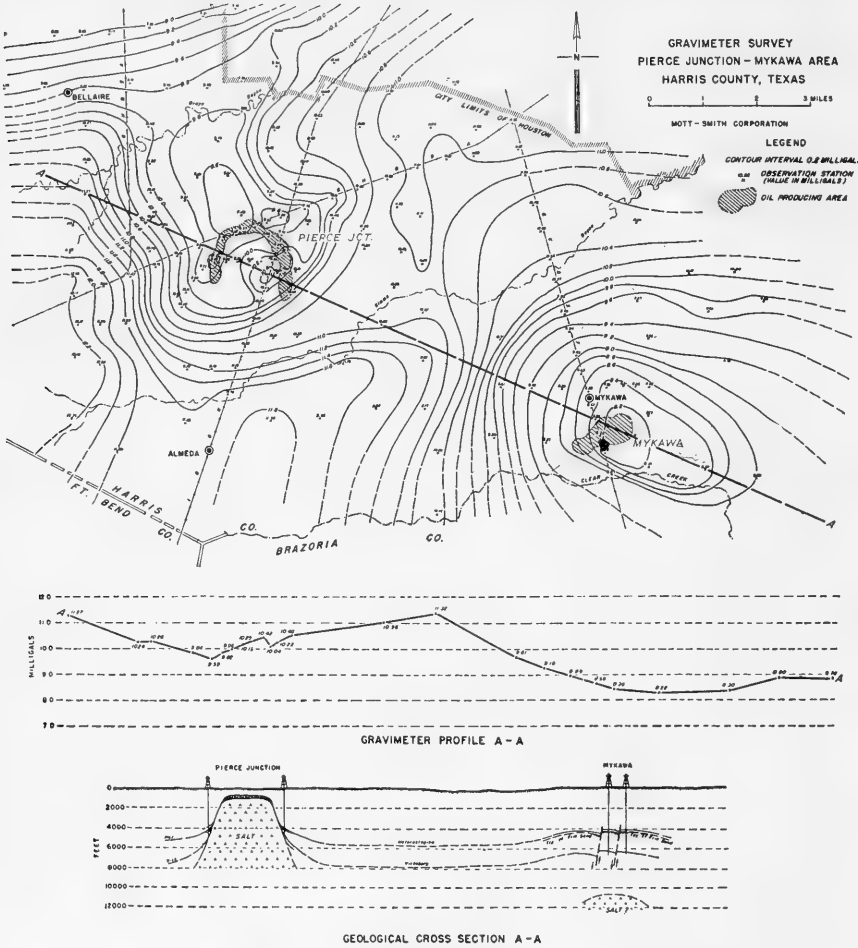

FIG. 259.—Pierce-Mykawa gravimeter survey. (L. M. and F. W. Mott-Smith, *Personal Communication.*)

maximum is somewhat displaced from the actual position of the cap rock as outlined by the producing area at the periphery of the dome. The displacement is principally caused by the regional gravity change and can be corrected for by applying corrections for regional change.* It can be seen, however, that even without correction, the gravity contours indicate the

*In using gravity work for detailing such structures, corrections for regional change are made whenever it is large enough to be important.

presence of the structure with sufficient accuracy for reconnaissance purposes.

The Mykawa field is on an uplift supposedly produced by a deeply buried salt mass. If this supposition is correct, the salt mass must lie at a depth greater than that of the deepest well which was drilled to 7,350 feet without hitting the salt. The Mykawa production comes from sands at depths of 4100 to 4900 feet.

The gravity minimum extends over a considerable area. In fact, it extends considerably beyond the limits of this survey in a southeasterly direction. The field is somewhat displaced from the center of the minimum, but such displacement could have been predicted by noting that the value of gravity drops toward the minimum much more rapidly on the northwest than on the southeast. This condition is produced by a salt mass of such vertical section that the center of gravity of the salt is not directly below its highest point. The center of the minimum is of course very nearly above the center of gravity, while the top of the uplifted beds is above the highest point. From a study of the exact shape of such a minimum it is possible to make a good estimate of the location most favorable for finding production.

Gravimeter Survey over Sedimentary Structures.—An interesting example of the way in which a gravimeter survey reveals subsurface geologic structure as related to the search for petroleum and of some of the geologic factors which enter the interpretation has been given by L. H. Boyd.† This example illustrates how in three cases gravity maxima were associated with structural highs, while in a fourth case a gravity *minimum* reflected a structural high, all in the same general area.

Boyd presents the results of gravimetric work along the Kettleman Hills-Lost Hills trend on the west side of the San Joaquin Valley in California. Figure 260 shows the gravity contours for the area, at an interval of 0.50 milligals, based on station values reduced to datum by correcting for geodetic position, for elevation and for the Bouguer effect. For the latter two, the constant 0.069 milligals per foot was applied, which assumes a density of 2.0 for the surface sediments. For the first, or latitude correction, the international formula for gravity of the U. S. Coast and Geodetic Survey was employed.

In the northwest part of the gravity map (Figure 260) there is an elongated closed gravity maximum, the axis of which runs in a northwest-southeast direction through T. 22 S. R. 18 E. This prominent gravity high correlates with the structural closure on Kettleman North Dome, as expressed by subsurface contours given in Figure 261. The agreement is quite striking in respect to width and alignment between gravity and structural features.

† L. H. Boyd, "Gravity Meter Survey of the Kettleman Hills-Lost Hills Trend, California," *Geophysics*, Vol. XI, No. 2, April, 1946, pp. 121-128.

The center of the top closing contour of this gravity maximum is about 2 miles west of the southeast corner of T. 22 S. R. 18 E. To the northwest the gravity axis follows a course of roughly N. 45° W. parallel to the subsurface strike of the dome. Southeast of the gravity high point,

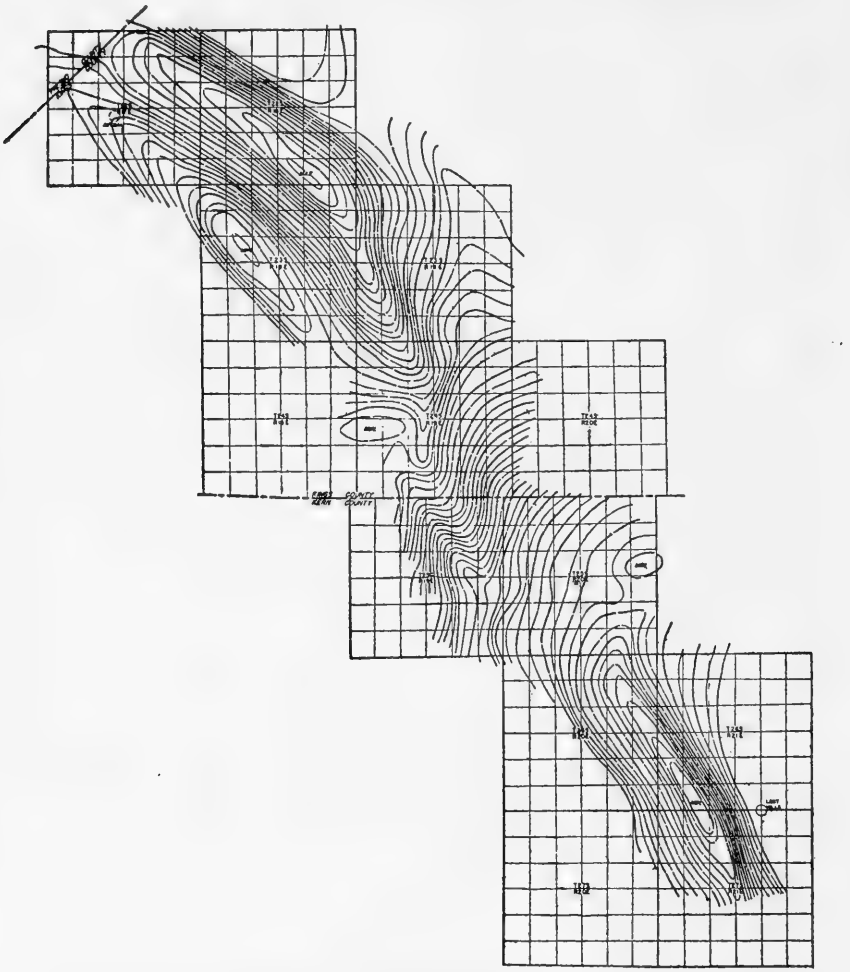

Fig. 260.—Gravity survey, Kettleman Hills-Lost Hills Area, California. Contours of observed gravity; contour interval 0.5 mg. (*Geophysics*, Vol. XI, No. 2, April, 1946, p. 122.)

however, the direction of the contours and the gravitational axis is roughly S. 20° E. There is a significant flattening of the gravity gradient along the crest in this direction for a distance of approximately 5 miles.

The second gravity anomaly of importance is the steep maximum nosing which covers the next 4 or 5 miles along the axial trend and southeast of

the flattening noted. The location of this second anomaly correlates with the position of the Kettleman middle dome, as also appears from the structural contours in Figure 261. The flattening in the gravity contours reflects the saddle between the two domes.

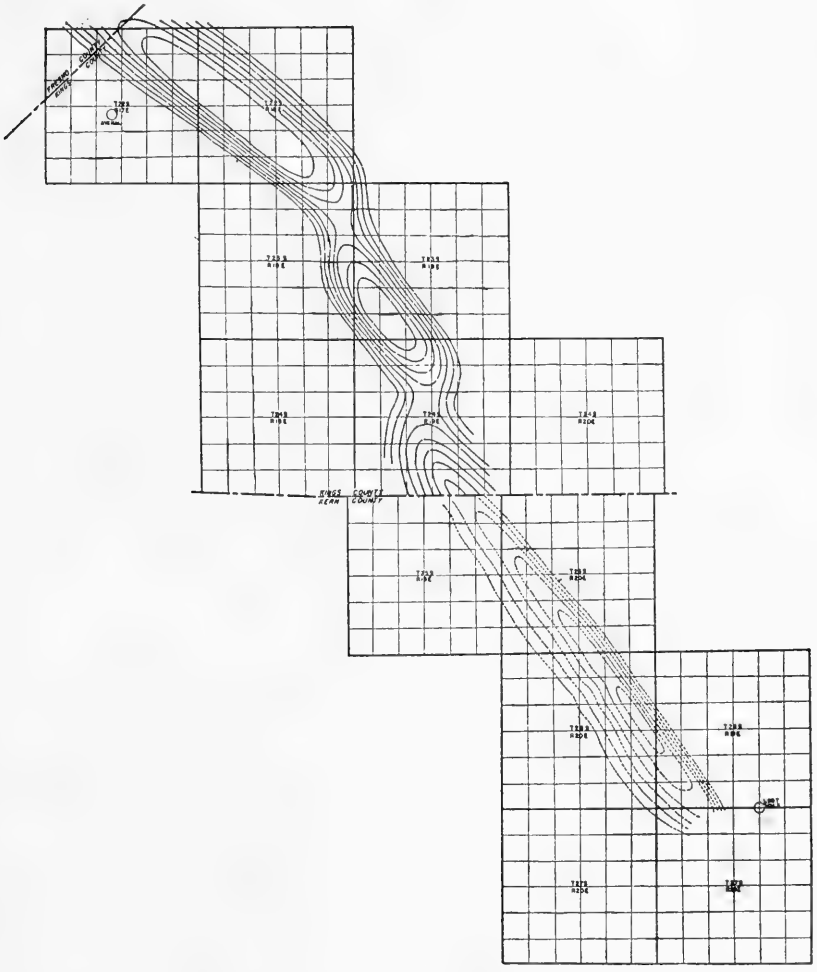

FIG. 261.—Subsurface contours for comparison with residual gravity of Figure 262. Contours in Kettleman Hills Area (north of Kings-Kern County line) after Uren (California Div. of Mines, *Bull. 118*, Part One, p. 45), contour interval 500 feet; in Lost Hills Area, on top of Temblor, after Follansbee (California Div. of Mines, *Bull. 118*, Part Three, p. 495), contour interval 1000 feet. (*Geophysics*, Vol. XI, No. 2, April, 1946, p. 125.)

Continuing along the gravity ridge (from the second gravity anomaly) the strike changes to a south direction, and the gradient again flattens near the center of T. 25 S. R. 19 E. A third gravity anomaly (which is similar to the second one) is expressed by a steep maximum gravity nosing.

This nosing begins after the decrease in gradient just referred to and continues on a strike of about S. 45° E.

As might be expected, the third anomaly coincides almost exactly with the Kettleman south dome. Also, as was true in the first instance, the flattening in the gravity gradient between the second and the third gravity features is in the structural saddle between the middle and south domes.

Continuing still further along the structural trend, we find that conditions change beyond the end of the third gravity anomaly. The one to one correlation of gravity and structural highs which carried through three townships no longer holds. There is a zone of decreased gravity gradient in T. 26 S. R. 20 E. which farther to the southeast (along the axis) develops into a very pronounced and elongated gravity minimum. This rather narrow gravity depression extends into T. 27 S. R. 21 E. and fits extremely well with the Lost Hills anticline.

The close agreement between these gravity expressions and subsurface geologic features (or oil fields) is even more strikingly illustrated by reference to Figure 262, which shows the *residual* gravity anomalies in the area surveyed at a 0.50 milligal contour spacing. To obtain them, the reduced gravity station values of Figure 260 are freed from the effect of the regional gravity gradient. This gradient (as shown by Figure 260) is a decrease in gravity from the northwest to the southeast along the entire trend. The amount of the regional correction to be applied at each station is determined by a special analysis of the gravity data.

The positions of the 4 residual gravity anomalies (as presented in Figure 262) fit quite closely the 3 Kettleman domes and the Lost Hills anticline. In the cases of the middle and south domes the residual anomalies show considerable gravity closure, which reflects like structural closure in these two features. The residual gravity contours bring out certain details not readily apparent from regionally uncorrected results of Figure 260. For example, the subsurface structural divides between the domes, which cause a flattening in the gradient, are shown as true saddles by the residual gravity contours.

No doubt there is a geological reason to explain the sudden change from a gravity maximum representing a structural high at the south dome to a gravity minimum representing a structural high at the Lost Hills. This transition takes place over a distance of but a few miles, and it cannot logically be a mere perversity of nature to plague geophysicists. An examination of the stratigraphy of the locality yields a reasonable answer.

The geologic section at the Lost Hills shows a considerable thickness of the (Miocene) Reef Ridge shales, which are punky and diatomaceous and from samples show an average density of 0.9. They are about 900 feet thick over the northern part of the Lost Hills structure, and their thickness increases somewhat to the south. The steep flanks of this anticline cause a large thickness of these relatively light shales to be present vertically below

either flank. Such light material is probably sufficient to account for the Lost Hills gravity minimum.

The same Reef Ridge formation farther to the north as found over the Kettleman Hills area is appreciably thinner, as only from 600 to 800 feet

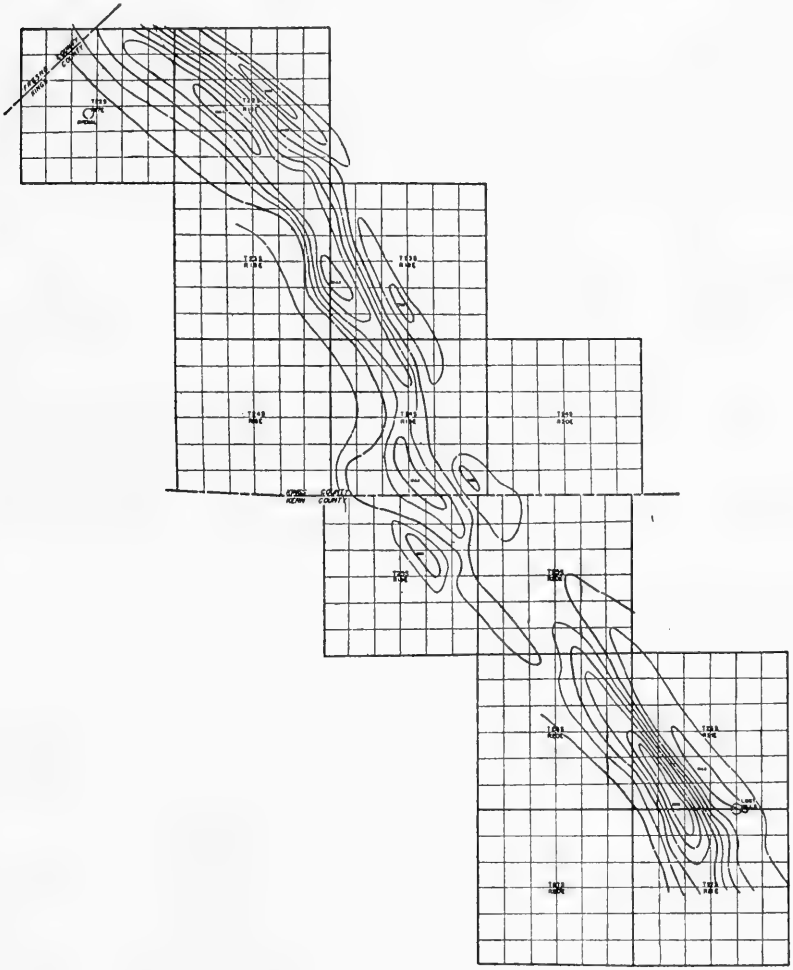

FIG. 262.—Residual gravity, Lost Hills-Kettleman Hills Area, California. Contour interval 0.5 mg. (*Geophysics*, Vol. XI, No. 2, April, 1946, p. 124.)

of it are present. Moreover it is here composed of harder shales, clays and sands than at the Lost Hills locality.

The formation below the Reef Ridge is the McClure Shale. It is relatively hard and dense, both at the Lost Hills and at the Kettleman Hills. It would appear to influence the gravity picture only to the extent that it

is somewhat thicker in the north, 1200 to 2000 feet, than at the Lost Hills, where it is from 1200 to 1400 feet in thickness.

The outstanding density variation in the area studied is the lightness of the Reef Ridge beds at Lost Hills. The gravity anomalies would indicate a probable transition within the Reef Ridge formation from the Lost Hills northward to the Kettleman Hills north dome. There is also a distinct possibility that the light diatomaceous material deposited at the Lost Hills was not present farther north along the trend.

GRAVITATIONAL METHODS

UNITED STATES PATENTS

1,796,150 Issued Mar. 10, 1931. Richard Hamer. "Gravity-Determining Device."
1,829,876 Issued Nov. 3, 1931. Stefan Rybar. "Eötvös Torsion Balance."
1,843,342 Issued Feb. 2, 1932. Ernest L. Jones and Herman Shaw. "Torsion Balance and the Like."
1,858,384 Issued May 17, 1932. Josef Andre. "Pendulum Apparatus."
1,861,229 Issued May 31, 1932. Ludwig Blau. "Torsion Balance."
1,868,010 Issued July 19, 1932. Hans Haalck. "Torsion Balance."
1,888,976 Issued Nov. 29, 1932. Ludwig W. Blau. "Apparatus for Measuring Relative Values of Gravity."
1,927,150 Issued Sept. 19, 1933. Alfred Berroth. "Measuring Instrument for Investigating Gravitation."
1,951,226 Issued Mar. 13, 1934. Peter Irving Wold. "Measurement of Gravitational Forces."
1,963,252 Issued June 19, 1934. Orley H. Truman. "Optical Torsion Balance."
1,975,516 Issued Oct. 2, 1934. Alexander McLean Nicolson. "Gravity Indicator."
1,987,786 Issued Jan. 15, 1935. Otto Meisser. "Pendulum for Gravity Determination."
1,988,508 Issued Jan. 22, 1935. Desiderius Pekar and Stefan Rybar. "Eötvös Balance."
1,988,527 Issued Jan. 22, 1935. Orley H. Truman. "Gravity Meter."
1,995,305 Issued Mar. 26, 1935. Harvey C. Hayes. "Method and Apparatus for Determining the Force of Gravity."
1,998,345 Issued April 16, 1935. Orley H. Truman. "Gravity Meter with Compensator."
2,000,948 Issued May 14, 1935. Harvey C. Hayes. "Apparatus for Determining the Force of Gravity."
2,032,381 Issued Mar. 3, 1936. Paul P. Stoutenburgh. "Method and Apparatus for Determining the Force of Gravity."
2,044,079 Issued June 16, 1936. John C. Karcher. "Apparatus for Determining Subsurface Tectonics of the Earth."
2,077,390 Issued April 20, 1937. Ludwig W. Blau. "Frequency Comparing Device for Determining the Force of Gravity."
2,080,062 Issued May 11, 1937. Henry Rainbow. "Torsion Balance."
2,089,164 Issued Aug. 3, 1937. Hermann Imhof. "Suspension for Eötvös Balance."
2,089,745 Issued Aug. 10, 1937. Anton Graf. "Gravity Instrument."
2,090,713 Issued Aug. 24, 1937. Harold A. Wilson. "Gravity Measuring Device."
2,097,156 Issued Oct. 26, 1937. F. Holweck. "Gravity Pendulum."
2,105,146 Issued Jan. 11, 1938. Hans Haalck. "Gravitation Measuring Instrument."
2,137,963 Issued Nov. 22, 1938. C. A. Heiland. "Gravimeter."
2,148,678 Issued Feb. 28, 1939. L. W. Blau and A. B. Bryan. "Apparatus for Comparing a Plurality of Oscillatory Systems."
2,149,953 Issued March 7, 1939. A. K. Birnbaum. "Automatic Leveler for Gravity Measuring Instruments."
2,150,405 Issued March 14, 1939. S. A. Scherbatskoy. "Gravity Meter."
2,159,082 Issued May 23, 1939. Kenneth Hartley. "Apparatus for Making Gravity Measurements."
2,179,892 Issued Nov. 14, 1939. A. R. Lindblad. "Apparatus for Determining Gravity."
2,182,298 Issued Dec. 5, 1939. Johan D. Malmqvist. "Method of Measuring Gravity."

2,183,115 Issued Dec. 12, 1939. F. G. Boucher. "Multiple Gravity Meter."
2,185,582 Issued Jan. 2, 1940. L. W. Blau. "Multiple Component Gravity Balance."
2,190,959 Issued Feb. 20, 1940. Stephen Baron von Thyssen-Bornemisza. "Gravity Measuring Instrument."
2,203,293 Issued June 4, 1940. Hart Brown. "Force Measuring Device."
2,209,140 I. Rybar.
2,217,123 Issued Oct. 8, 1940. J. D. Malmqvist. "Apparatus for Determining the Alterations of the Horizontal Components of the Force of Gravity."
2,217,361 Issued Oct. 8, 1940. H. M. Evjen and D. S. Muzzey, Jr. "Gravity Measuring Instrument."
2,218,140 Issued Oct. 15, 1940. F. E. Wright and J. L. England. "Gravity Torsion Balance."
2,220,199 Issued Nov. 5, 1940. J. L. Bible and R. H. Ray. "Clamping Device for Force Responsive Element."
2,221,480 Issued Nov. 12, 1940. G. A. Ising. "Gravity Measurements."
2,225,566 Issued Dec. 17, 1940. J. McD. Ide. "Gravity Meter."
2,225,582 Issued Dec. 17, 1940. J. L. Bible. "Gravity Meter Clamp."
2,232,177 Issued Feb. 18, 1941. J. McD. Ide. "Optical System."
2,239,049 Issued April 22, 1941. T. S. Morris. "Gravity Meter."
2,243,746—2,243,750, inclusive. Issued May 27, 1941. D. H. Clewell. "Gravity Meter."
2,253,472 Issued Aug. 19, 1941. T. B. Pepper. "Apparatus for Submarine Geophysical Prospecting."
2,255,876 Issued Sept. 16, 1941. D. H. Clewell and H. A. Maeder. "Gravity Meter."
2,258,613 Issued Oct. 14, 1941. F. M. Kannensteine and F. M. Floyd. "Measuring Instrument."
2,262,165 Issued Nov. 11, 1941. D. H. Clewell. "Gravity Meter."
2,263,096 Issued Nov. 18, 1941. J. A. Marchand. "Gravity Measuring Instrument."
2,264,342 Issued Dec. 2, 1941. D. Silverman and J. L. Bible. "Geophysical Instrument Mounting."
2,265,011 Issued Dec. 2, 1941. Sidney Siegel. "Sensitive Device for Measuring Forces."
2,277,505 Issued March 24, 1942. C. H. Barker and K. Q. Robert. "Carrying Device for Geophysical Instrument."
2,277,509 Issued March 24, 1942. D. H. Clewell. "Gravity Meter."
2,279,261 Issued April 7, 1942. J. M. Crawford and H. R. Prescott. "Torsion Gravimeter."
2,281,001 Issued April 28, 1942. D. H. Clewell. "Gravity Meter."
2,290,354 Issued July 21, 1942. R. H. Ray. "Geophysical Instrument Mounting."
2,290,740 Issued July 21, 1942. D. H. Clewell. "Gravity Meter."
2,291,628 Issued Aug. 4, 1942. G. A. Ising. "Apparatus for Relative Gravity Measurements."
2,293,437 Issued Aug. 18, 1942. L. J. B. LaCoste and A. Romberg. "Force Measuring Device."
2,294,201—2,294,202. Issued Aug. 25, 1942. T. B. Pepper. "Apparatus for Submarine Geophysical Prospecting."
2,295,026 Issued Sept. 8, 1942. H. Brown and J. H. Martin. "Force Measuring Device."
2,296,330 Issued Sept. 22, 1942. L. W. Blau. "Gravity Balance."
2,301,396 Issued Nov. 10, 1942. A. Graf. "Gravity Meter."
2,303,845 Issued Dec. 1, 1942. S. Krasnow. "Apparatus for the Measurement of Gravity."
2,304,191 Issued Dec. 8, 1942. L. M. Mott-Smith. "Gravity Meter."
2,304,324 Issued Dec. 8, 1942. P. S. Williams. "Gravity Meter."
2,304,737 Issued Dec. 8, 1942. H. A. Maeder. "Mass Clamp for Gravity Meters."
2,304,748 Issued Dec. 8, 1942. D. H. Clewell. "Gravity Meter."
2,307,917 Issued Jan. 12, 1943. D. H. Clewell. "Gravity Meter."
2,311,771 Issued Feb. 23, 1943. G. Norgaard. "Apparatus for Measuring Gravity."
2,316,915 Issued April 20, 1943. O. H. Truman. "Apparatus for Amplifying and Measuring Small Displacements."
2,318,665 Issued May 11, 1943. F. G. Boucher. "Measuring Device."
2,319,940 Issued May 25, 1943. W. A. Marrison. "Gravitational Force Measuring Apparatus."

2,322,615 Issued June 22, 1943. F. G. Boucher. "Leveling Device."
2,322,681 Issued June 22, 1943. H. M. Zenor. "Condenser Gravity Meter."
2,325,005 Issued July 20, 1943. D. H. Clewell. "Gravity Meter."
2,327,692 Issued Aug. 24, 1943. L. L. Antes. "Gravity Meter."
2,327,697 Issued Aug. 24, 1943. F. G. Boucher. "Gravity Meter."
2,331,904 Issued Oct. 19, 1943. G. V. A. Gustafsson and J. D. Malmqvist. "Geophysical Instrument."
2,337,152 Issued Dec. 21, 1943. D. H. Clewell. "Gravity Meter."
2,338,811 Issued Jan. 11, 1944. A. F. Hasbrook. "Level Indicator."
2,341,323 Issued Feb. 8, 1944. J. M. Ide. "Gravity Meter."
2,346,593 A. R. Lindblad and J. D. Malmqvist.
2,347,702 H. B. Maris.
2,349,404 D. W. Blair and F. G. Boucher.
2,351,955 A. Graf.
2,355,421 D. H. Clewell and H. A. Maeder.
2,356,206 F. G. Boucher.
2,357,356 O. S. Petty.
2,357,822 A. F. Hasbrook.
2,362,135 Issued Nov. 7, 1944. P. H. James. "Leveling Device for Gravimeters."
2,362,872 Issued Nov. 14, 1944. L. T. Weagle. "Spirit Level."
2,367,126 Issued Jan. 9, 1945. P. H. James. "Gravimeter Null Indicator."
2,369,802 Issued Feb. 20, 1945. G. V. Rylsky. "Liquid Level."
2,372,252 Issued March 27, 1945. D. H. Clewell. "Pilot for Gravity Meters."
2,377,889 Issued June 12, 1945. L. J. B. LaCoste and A. Romberg. "Force Measuring Instrument."
2,383,966 Issued Sept. 4, 1945. A. F. Hasbrook. "Geophysical Prospecting Apparatus."
2,383,997 Issued Sept. 4, 1945. R. C. Sweet. "Gravity Meter."
2,384,586 Issued Sept. 11, 1945. F. J. Allgeo. "Level."
2,384,739 Issued Sept. 11, 1945. A. F. Hasbrook. "Geophysical Prospecting Apparatus."
2,385,424 Issued Sept. 25, 1945. C. L. Shue and F. J. Allgeo. "Level."
2,389,866 Issued Nov. 27, 1945. M. E. Moore. "Apparatus for Making Gravity Measurements."
2,402,666 Issued June 25, 1946. A. Raspet. "Helical Spring."
2,404,786 Issued July 30, 1946. L. G. Bostwick and J. H. King. "Electromechanical Device."
2,417,392 Issued March 11, 1947. R. Craig and R. Q. Boyer. "Torsion Balance."
2,418,786 Issued April 8, 1947. F. H. Nadig and J. L. Bohn. "Hydraulic Inferometer."
2,432,875 Issued Dec. 16, 1947. E. Flint. "Level Indicating Device."
2,438,758 Issued March 30, 1948. C. C. Leach. "Liquid Column Level."
2,441,166—2,441,167 Issued May 11, 1948. A. Raspet. "Helical Spring."
2,444,669 Issued July 6, 1948. J. C. Pollard and C. F. Sellers. "Support for Submerged Area Surveying."
2,446,325 Issued Aug. 3, 1948. W. H. Gille. "Leveling Support."

CHAPTER FIVE

ELECTRICAL METHODS

Electrical prospecting is the technique of measuring certain properties of electrical fields of force and then utilizing such data to predict the subsurface deposits or structures. Usually, the electrical methods depend for their operation upon the effects produced at the surface of the earth by the flow of an electric current through subsurface formations.

There are several methods by which the electric field may be created. Natural electrochemically-generated ground currents create a field which may be utilized, as in the so-called self-potential method. More commonly, artificial means are employed wherein an electric current is conductively or inductively caused to flow in the portion of the subsurface to be investigated. Electric field properties which may be measured include: potential distribution at the earth's surface, ratio of surface potential to energizing current, phase shift, electromagnetic field strength and direction, distortion of wave front and polarization effects.

Often, the electrical properties of rocks will vary to a different degree than the other physical properties, and then the electrical methods may be of advantage under conditions where other methods cannot be employed successfully. Also, they may be utilized to obtain data which will supplement the data given by other methods. Conversely, electrical methods will not give useful data when the electrical properties of the subsurface are not sufficiently different to create detectable or measurable differences in the electric field.

ELECTRICAL PROPERTIES OF ROCKS

The magnitude and the distribution of current flow in the subsurface depend upon the effective *resistivity,* or its reciprocal, conductivity, of the subsurface materials. The resistivity of a material is defined as the resistance in ohms between opposite faces of a unit cube of the material. The units of resistivity commonly employed are the ohm-centimeter and the ohm-meter.† The corresponding conductivity units are the mho/centimeter and the mho/meter. Different rocks exhibit marked differences in resistivities, and in a great majority of rocks, a variation in electrical resistivity will be accompanied by a discernible variation in lithology.

The flow of an electric current in non-metallic rocks is chiefly *electro-*

† Compare S. F. Kelly, "A Uniform Expression for Resistivity," *A.I.M.E. Geophysical Prospecting,* 1932, pp. 141-143.

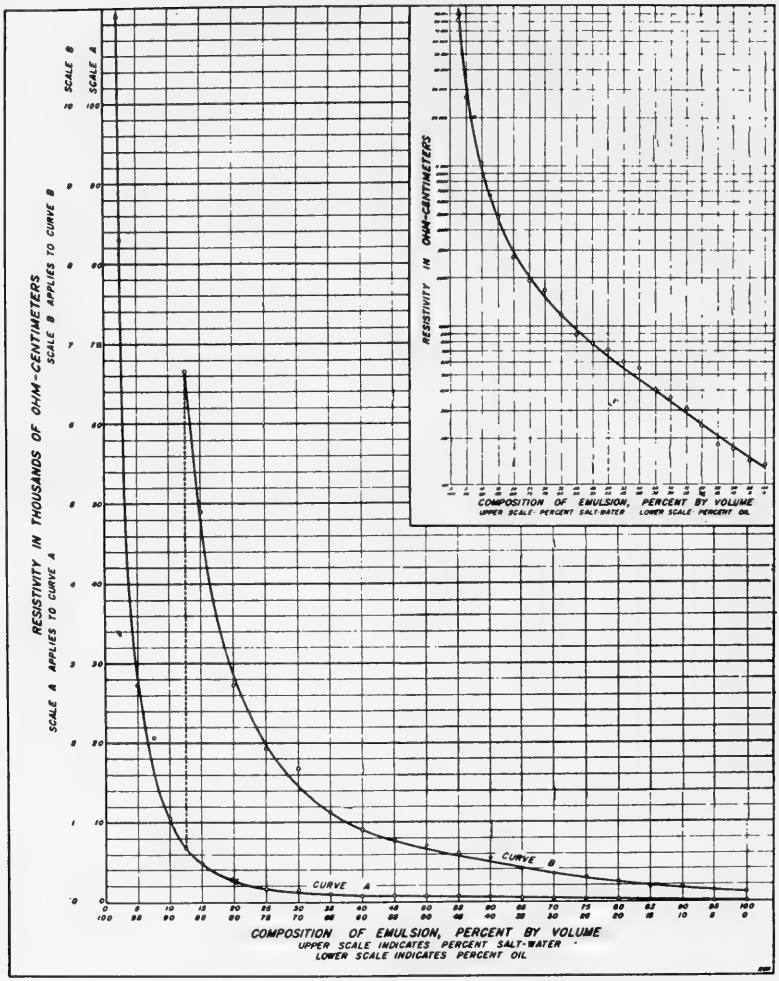

FIG. 263.—Resistivities plotted against oil-water compositions. Curve *B* is a more detailed plot of the lower part of curve *A*. The insert shows curve *A* drawn with a logarithmic ordinate scale. (Jakosky and Hopper, *Geophysics.*)

lytic. Practically all rocks are porous † and contain moisture, and it is due to this moisture that rocks are fair conductors despite the fact that their constituent minerals (quartz, feldspar, etc.) are poor conductors, or even excellent insulators.

Laboratory studies of both petroliferous and non-petroliferous rocks have shown that for high values of moisture content, the conductivity

† A report on sand porosity studies is given by C. S. Slichter, "Theoretical Investigation of the Motion of Ground Waters," U. S. Geol. Survey, 19th Annual Report, Part 2, 1897-1898. See also L. C. Uren, *Petroleum Production Engineering* (Oil Field Exploitation) (McGraw-Hill, 1939) p. 5.

approaches the conductivity of the absorbed electrolyte (moisture), while for very low values of moisture content the resistivity values are high and are governed by the properties of the rock materials. †

The decrease in resistivity with increased moisture content is of special significance with regard to the possible use of electrical methods in the

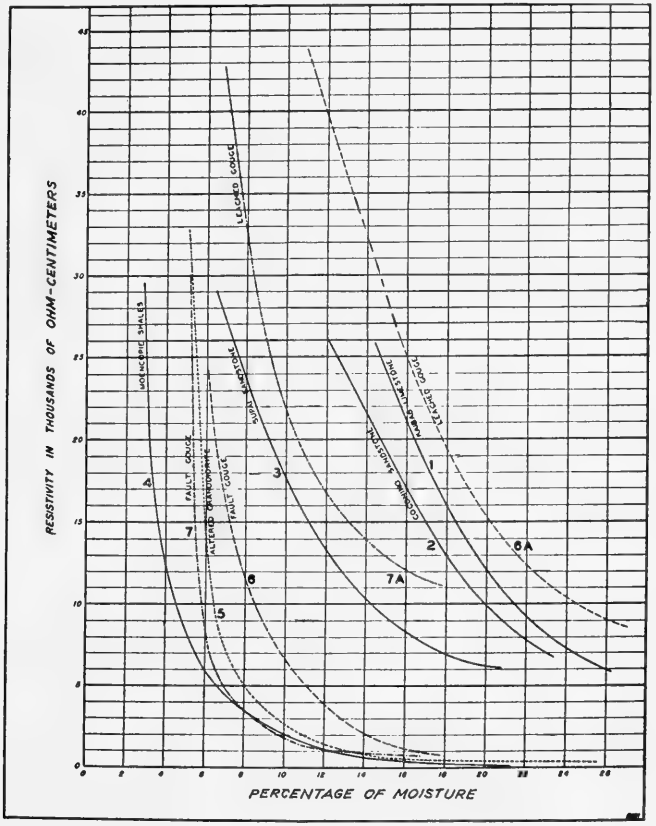

FIG. 264.—Resistivities plotted against moisture percentages for various rocks. (Jakosky and Hopper, *Geophysics.*)

direct location of petroliferous rocks. Crude oil is an almost perfect insulator against electrical current; hence, it might be expected that a porous rock containing oil would have a very high resistivity. However, practically all oil reservoir rocks contain both oil and water in their pores,‡ and the presence of dissolved salts in this water tends to lower the resistivity of the rock.

† J. J. Jakosky and R. H. Hopper, "The Effect of Moisture on the Direct Current Resistivities of Oil Sands and Rocks," *Geophysics*, Vol. 2, No. 1, pp. 33-35, 1937.

‡ H. C. Pyle and T. H. Jones, "Quantitive Determination of the Connate-Water Content of Oil Sands," *Oil and Gas Journal*, Nov. 12, 1936. Paper delivered at 17th annual meeting, American Petroleum Institute, Los Angeles.

Representative graphs of experimental values of the resistivities of emulsions of oil and water as a function of the percentage of water content are shown in Figure 263. Similar graphs for rocks impregnated with various percentages of moisture are shown in Figure 264.

Magnitudes of the Resistivities.—The electrical constants of rocks may be obtained by *laboratory* measurements, using rock specimens,

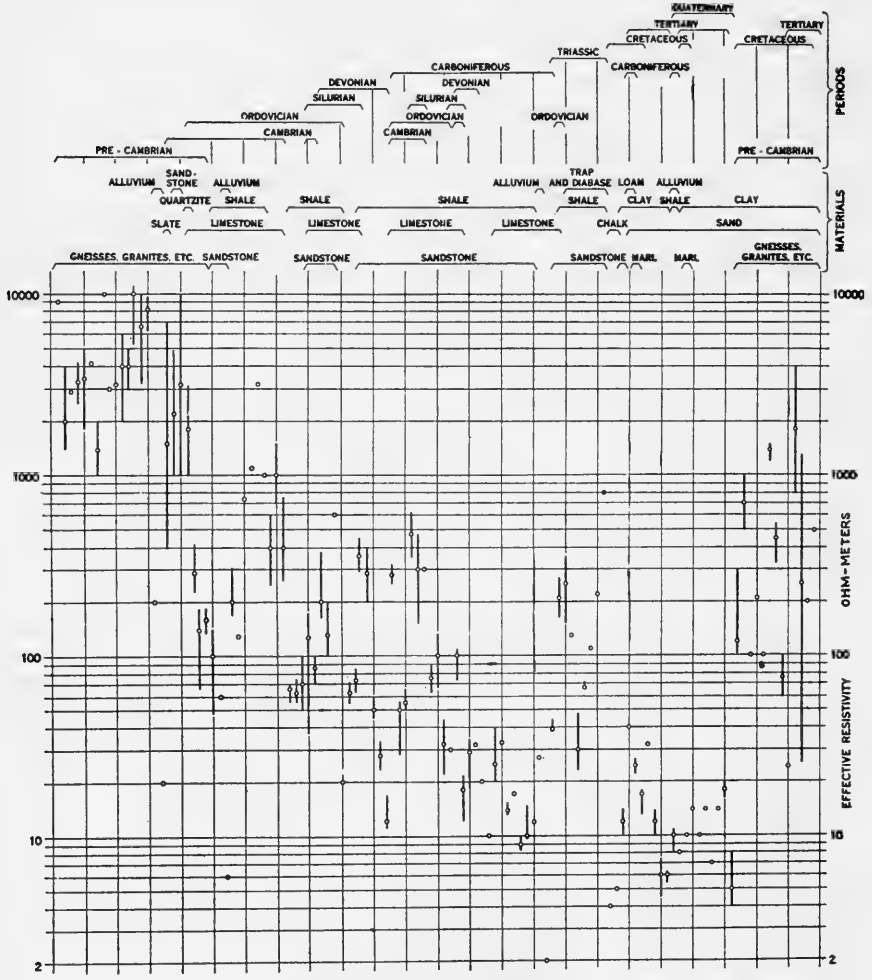

The heavy lines indicate the range of effective resistivities for tests in which measurements were made in several subsections or exploring wires; the mean effective resistivities are indicated by circles. Isolated circles indicate effective resistivities where only one measurement was made

The sequence in which the various types of materials are listed is not necessarily the time sequence in which these materials occur in the geological structures, although the oldest materials are, in general, on the left

The overburden is not indicated except in a few cases where material thicknesses of alluvium are present

"Limestone" as used in connection with silurian and earlier formations includes, in many cases, dolomites as well

FIG. 265.—Correlation of effective resistivities with geological periods and materials. (R. H. Card, "Earth Resistivity and Geological Structure," *Electrical Engineering*, Nov. 1935, p. 1156.)

and by *field* measurements in which average resistivities of subsurface materials and outcrops are measured in place.

The electrical resistivities of earth materials vary within very wide limits. For example, the resistivity of certain metallic elements is about 10^{-6} ohm-centimeters and the resistivity of certain igneous and metamorphic rocks is greater than 10^{7} ohm-centimeters.

The accompanying tables list some resistivity values obtained in field explorations in the United States and Canada and resistivity values for laboratory samples. Figure 265 is a graphical correlation of effective resistivities of earth materials of different geological periods.

TABLE 15

RESISTIVITIES OF MATERIALS FOUND IN THE OUTER CRUST OF THE EARTH

Igneous and Metamorphic Rocks	*Resistivity ohm-cm*
Basalt	2×10^{6}
Crystalline rock of normal physical character (igneous, gneiss, schist)	2×10^{4} - 2×10^{6}
Diabase	2×10^{3} - 2×10^{6}
Diorite	5×10^{6}
Gabbro	1×10^{4} - 1.5×10^{6}
Gneiss	2×10^{4} - 3.4×10^{6}
Granite	3×10^{4} - $>10^{6}$
Lava	1.2×10^{4} - 5×10^{6}
Marble	1×10^{4} - 1×10^{7}
Meteoric iron	1×10^{-6} - 3×10^{-6}
Porphyry	6×10^{3} - 1.5×10^{6}
Quartzite	1×10^{3} - 2×10^{7}
Schist	5×10^{2} - 1×10^{6}
Serpentine	2×10^{4} - 3×10^{5}
Syenite	1×10^{4} - 10^{7}
Trachyte	1×10^{3} - 1×10^{7}
Trap Rock	1.5×10^{4} - 3×10^{5}

Sedimentary Rocks	*Resistivity ohm-cm*
Alluvium and Silt	2.5×10^{3} - 1.5×10^{5}
Clay-Shales	4×10^{-2} - 9×10^{4}
Clay	5×10^{2} - 1.5×10^{5}
Glacial sediments	8×10^{-2} - 9.5×10^{5}
Conglomerate	2.5×10^{3} - 1.5×10^{6}
Consolidated sedimentary rocks (slates, shales, sandstones, limestones, etc.)	1×10^{3} - 5×10^{4}
Graywacke	2×10^{5} - 10^{6}
Limestone	6×10^{3} - 5×10^{7}
Loams	1×10^{3} - 4.5×10^{4}
Marls	0.5×10^{2} - 7×10^{3}
Sand	9.5×10^{1} - 5×10^{5}
Sandstone	3×10^{3} - 1×10^{7}
Shales	8×10^{2} - 1×10^{6}

TABLE 15 (Continued)

RESISTIVITIES OF MATERIALS FOUND IN THE OUTER CRUST OF THE EARTH

Minerals and Ores	*Resistivity ohm-cm*
Slate	6×10^{4} - 8×10^{4}
Soil	2×10^{2} - 1×10^{3}
Unconsolidated and recent formations (marls, clays, sands, alluvial deposits, etc.)	5×10^{1} - 1×10^{4}
Anhydrite	10^{5} - 10^{7}
Arsenopyrite	2×10^{1}
Bornite	0.5 - 5×10^{1}
Calcite	$>10^{7}$
Chalcocite	0.1 - 6×10^{1}
Chalcopyrite	1.5×10^{-2} - 3.5×10^{1}
Chalcopyrite-Hematite	5.5
Chalcopyrite-Sphalerite	1
Chalcopyrite-Pyrrhotite	<0.1
Chromite	1×10^{3} - 2×10^{3}
Coal (Bituminous)	6×10^{1} - 10^{7}
Coal (Anthracite)	1×10^{2} - 2×10^{7}
Coal (Lignite)	9×10^{2} - 2×10^{4}
Cobalt Iron	5×10^{-2}
Copper	1.5×10^{-6} - 1.5×10^{-1}
Copper-Iron	0.7
Covellite	<0.1
Cuprite	3×10^{4}
Diamond	1×10^{14}
Galena	3×10^{-3} - 2×10^{1}
Galena-Sphalerite	$6 - 10^{4}$
Graphite	8×10^{-4} - 6
Hematite	5×10^{4} - 10^{7}
Hematite (specular)	0.4
Limonite	1×10^{5} - 1×10^{7}
Magnetite	0.6 - 5×10^{3}
Marcasite	1 - 3.5×10^{2}
Meteoric iron (oxidized)	$>10^{3}$
Mica	9×10^{4} - 9×10^{7}
Molybdenite	0.1 - 5×10^{1}
Nickel	1×10^{-5} - 1.5×10^{-1}
Nickel-Cobalt	5×10^{-2} - 6×10^{-1}
Pyrite	5×10^{-2} - 1×10^{-4}
Pyrite-Chalcopyrite	<0.1
Pyrite-Pyrrhotite	<0.1
Pyrolusite-Psilomelane (mixed)	0.5
Pyrrhotite	5×10^{-2} - 5.0
Quartz	$>10^{7}$
Rock Salt	3×10^{3} - $>10^{7}$
Serpentine	2×10^{4} - 3×10^{5}
Siderite	7×10^{3}
Sphalerite	1.5×10^{2} - 1.5×10^{6}
Stibnite	$>10^{5}$
Sulphur	$>10^{7}$
Wulframite	1×10^{3} - 1×10^{7}

CLASSIFICATION OF METHODS

The electrical methods are more diversified than any of the other geophysical methods, and a rigid classification is difficult. The following classification is one which corresponds best to field practice.

(1) ***Conductive Methods***

These include all methods in which both the energizing and the measuring electrodes make direct contact with the ground. The energizing current may be direct or alternating. Two types may be enumerated:

(a) *Methods Applicable Under Steady State Conditions.*

These include the self-potential method, the direct current and low frequency alternating current equipotential line methods, and the various modifications of the resistivity methods. The characteristic feature of these methods is that the diagnostic variable, resistivity, for example, is determined under conditions such that steady state relationships exist, and the typical alternating current phenomena (real and imaginary components, phase differences, etc.) need not be considered in the interpretation of the data.

(b) *Methods Applicable Under Moving Field Conditions.*

These include all methods which employ alternating or variable current of sufficiently high frequency to produce significant inductive phenomena. Analysis of the data obtained with these methods must take into account such variables as phase shift, polarization ellipse, impedance (instead of resistivity), redistribution of current caused by inductive effects, etc. All methods employing medium and high frequency alternating currents and transient currents fall within this classification. The typical medium frequency alternating current methods are those in which frequencies ranging from about 50 to 500 cycles per second are employed. The typical high frequency methods employ alternating currents having frequencies from a few thousand cycles per second to the radio frequencies.

(2) ***Electromagnetic Methods***

This group includes those methods wherein the properties of the magnetic field associated with the flow of an electric current are utilized. Two groups are distinguished:

(a) *Methods Employing Conductive Energizing Means.*

In these methods, direct or alternating current is passed into the ground between two electrodes, and its subsurface distribution is studied by means of the magnetic field associated with the flow of current. If medium or high frequency alternating current is utilized, a direction-finding or search coil with appropriate amplifying and phase compensating apparatus may be employed. If direct current or low frequency alternating current is used for energizing the ground, various forms of variometers, magnetometers, etc., may be used for measuring the magnetic field associated with this flow of current.

(b) *Methods Employing Electromagnetic Energizing Means.*

The characteristic feature of this group is that an alternating current is induced in subsurface bodies by passing high or medium frequency alternating current through an energizing coil or loop mounted on the surface of the earth and oriented, usually, in a horizontal or vertical position. Studies of the subsurface distribution of current may be made by different means: such as, search coils and surface electrodes.

SPONTANEOUS POLARIZATION OR SELF-POTENTIAL METHOD

This method utilizes the natural flow of current in the earth. The general subsurface distribution of the natural earth current is determined from studies made of the lines of equipotential at the surface of the ground. From this information, and a knowledge of the geology of the district, predictions can be made regarding the presence of an oxidizing ore body at depth. This method is one of the simplest, and perhaps the oldest, geophysical process utilizing electrical phenomena. In recent years, the spontaneous polarization method has been used to locate corroding pipe lines and other extended metal structures in contact with the earth.†

OPERATING PRINCIPLE

The method operates on the fundamental premise that an ore body undergoing oxidation is a source of electric current. Water seeping downward from the surface carries absorbed oxygen. Such water coming in contact with a sulfide ore body creates, as a result of the oxidizing process, a natural large-scale galvanic cell, with the top or upper portion of the ore as the positive pole and with the weak acid formed in the oxidation process as the electrolyte. The potential differences at the surface of the earth resulting from the chemical activity of the ore body vary with the electrolytic properties, the size and configuration of the ore body, and with the depth of the body below the surface. In some cases this potential difference may be as great as 500 to 1000 millivolts. The electric current flow is usually downward within the ore body, and then outward and upward through the surrounding earth. The return currents spread outward for considerable distances, due to the relatively high resistance of the earth. At the surface of the earth, the current flow is toward a point, usually above the ore body, which is called the "negative center."

The negative center may be found by measurements over the surface of the ground: (1) by locating points at the same potential; (2) by measuring the earth potentials at regularly spaced intervals and drawing the equipotential contours; (3) by obtaining potential profiles in a direction across the ore body.

In the theoretically ideal case of a vertical cylindrical ore body surrounded by a homogeneous medium having a uniform distribution of moisture or subsurface water, the *equipotential curves** measured on the surface of the earth would be a set of concentric circles and the center of the circles would be the negative center.

---

† H. C. Hayes, "Electrical Prospecting," U. S. Patents No. 2,368,217 and 2,368,218, Jan. 30, 1945.

* An equipotential curve or an equipotential is a curve such that every point on it is at the same potential.

In practical cases, the negative center is directly over the ore body only if the topography of the region under investigation is relatively flat. (Compare Figures 266 and 270.)

An interesting theory proposed by Kelly* in explanation of the cause of self-polarization involves the pH content (measure of acidity) of surface solutions in comparison to solutions at depth. In laboratory experiments and field tests in South America, Kelly found experimental evidence that differences in potential are largely due to differences in pH between solutions at near surface and depth. The field tests were carried out on a sulphide body of short vertical extent and results showed a pH of about 2 (highly acidic) of the waters bathing the apex and a pH of about 8 (slightly basic) of the waters issuing from the bottom.

This evidence has not disproved the statement that oxidation can be the cause of spontaneous polarization, since oxidation increases the acidity of the near-surface waters. However, it does indicate that the difference of pH is a possible cause for spontaneous polarization potentials.

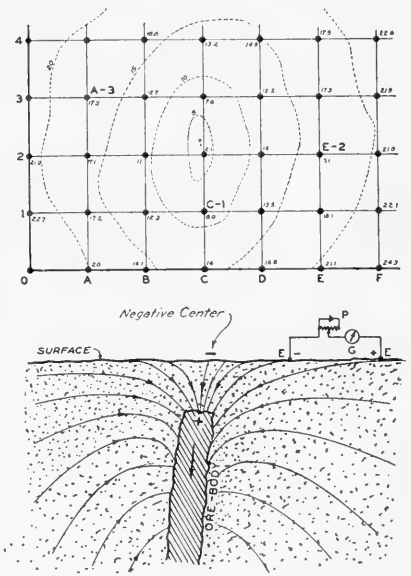

FIG. 266.—Equipotentials and negative center over a vertical ore body.

Additional evidence which may tend to support the theory is found in measurements over deposits of graphite and pegmatite, both totally lacking in sulphides, yielding high spontaneous polarization potentials. In such cases, the postulated low pH near the surface could arise from humic acids or carbonic acid from rain water taking up carbon dioxide from the atmosphere and vegetable matter.

FIELD EQUIPMENT AND PROCEDURE

Location of Points of Equal Surface Potential.—The apparatus for this work comprises: (a) indicating meter or galvanometer, (b) electrodes for making contact with the earth, and (c) two insulated cables, one about twenty feet and the other about two hundred fifty feet in length.

Galvanometer.—Various types of sensitive direct current galvanometers may be employed. The galvanometer should be of rugged construction and have a sensitivity of 0.25 to 2 microamperes per readable unit of scale. The resistance of the indicating meter should be 1000 ohms, or

* S. F. Kelly, personal communication, May 3, 1949.

higher, in order to minimize the effects of the contact resistance between the probe electrodes and the earth.

A number of commercial galvanometers are available for this work. It is preferable to employ a rugged pivotless instrument of the pointer type with the coil suspended between taut bronze ribbons. The suspension type instruments must be properly leveled while readings are made.

Electrodes.—The simplest ground contact would consist of a metal rod driven into the earth. This type of contact is unsuitable because of electrochemical effects. Due to the dissolved salts present in the ground, the moist earth acts as an electrolyte and a potential difference is created between the metal electrode and the earth. The magnitude of the electrochemical potentials depends on the metal constituting the electrodes, the concentration of the electrolyte, and the temperature of the electrodes. For instance, temperature differences between electrodes may create potentials of considerable magnitude when one electrode is in the hot sun and the other electrode in the shade.

Non-Polarizing Electrodes

One type of electrode whose potential is not appreciably affected by the chemical properties of the soil consists of a metallic electrode immersed in a supersaturated solution of one of its metallic salts, the solution being contained in a semi-permeable or porous cup that is in contact with the earth. This type of electrode is described in detail on p. 520.

Testing Electrodes in the Field.—During field work, the non-polarizing electrodes should be tested occasionally by immersing both of them in a single earthenware or glass container and observing the difference in potential with the aid of a galvanometer or a potentiometer. This difference in potential should be less than one millivolt if chemically pure materials have been used. While not in use, the electrodes should be kept immersed in a non-metallic jar (glass or glazed earthen ware) containing the same strength solution as in the porous cups. Distilled water should be used for mixing all solutions, if possible. In field work it may be difficult to obtain pure water, and should it be necessary to use water containing appreciable quantities of dissolved minerals, care must be taken to keep the solutions in both electrodes the same. This may be accomplished by emptying both cells into a large container and refilling with the mixed solution once or twice a day. Any difference in potential between the two cells must be compensated by adding or subtracting from the field reading. The compensation may be positive or negative depending upon the relative polarity of the electrodes and the field readings.

Field Procedure for Locating Equipotential Lines

In surveying an area, an arbitrary starting point, say station 1, is selected. The meter and tripod are set up near this station and connected by a short length of wire to the non-polarizing electrode buried at the sta-

tion. The other electrode, which is connected to the meter by the long length of insulated wire, is contacted with the earth's surface at a point approximately 100 to 200 feet from the first electrode. The polarity and magnitude of the potential difference between the electrodes are noted, and the electrode is then moved to another location. If the reading is lower, the movement has been in the right direction; the electrode is then moved to various locations until a point is found where no potential difference exists. This point is now marked with a suitable stake and constitutes the second station on the equipotential curve. The galvanometer and its electrode (which were at station 1) are now moved to the new location (station 2) and the process repeated to find another equipotential station. By continuing this procedure, the equipotential stations will eventually close in

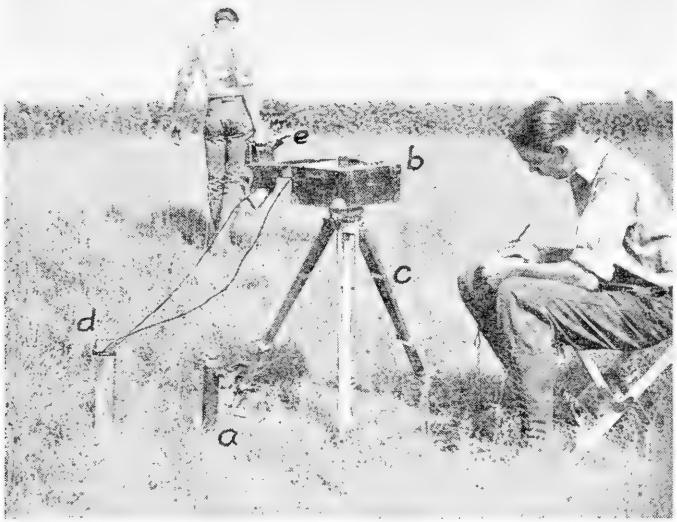

FIG. 267.—Photographic view of equipment for measuring earth potentials. *a*, non-polarizing electrode; *b*, potentiometer; *c*, tripod; *d*, anchor stake; *e*, reel.

on the first arbitrarily selected point. This completes one group of equipotential stations and a line drawn through these points is an equipotential curve. Another arbitrary starting point is selected about 100 feet inside the curve and the steps outlined above are repeated, thereby locating another group of equipotential stations. On continuing this procedure, the enclosures will become smaller in size; the smallest enclosure, theoretically a point, is the negative center. The various stations are now located on a suitable map, prepared from data obtained by an alidade and plane table survey, and are connected by closed lines so as to form equipotential curves. The various curves will be concentric with the negative center as their origin.

Field work of this type is relatively slow, both as regards tracing out the points of equipotential, and the time required for surveying-in the equipotential stations with their irregular locations. However, if the field work is carefully done, the method often is more accurate than that described in the following section.

Measurements of Earth Potentials at Regularly Spaced Intervals.— The equipment required for the direct measurement of potentials is somewhat more involved than that described for locating points of equipotential. It comprises a potentiometer, two non-polarizing electrodes, and a long insulated flexible connecting wire which is wound on a reel to facilitate handling. A photographic view of the complete equipment and operators is shown in Figure 267.

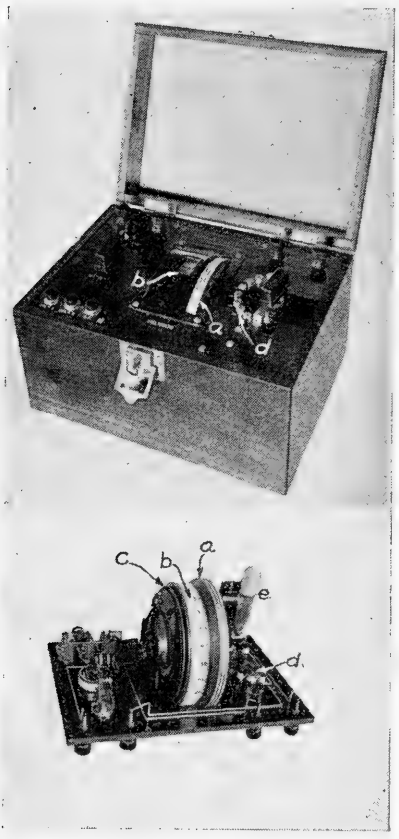

FIG. 268.—Interior and exterior views of potentiometer showing: *a*, control dial; *b*, calibrated scale; *c*, variable and *d*, fixed resistors; and *e*, standard cell.

The direct current potentiometer should have a range of 0 to 1000 millivolts. A double-pole double-throw switch is provided for reversing the input. The entire apparatus should be mounted in a hardwood or metal waterproofed box equipped with suitable carrying straps. A short, sturdy tripod for the potentiometer and a camp stool for the operator facilitates the field work.

Direct Current Potentiometer.— The potentiometer is a basic instrument used in many types of quantitative direct current measurements. The theory of the potentiometer is given in any standard text on general physics or electricity. Constant potentials of any value within the range of the instrument may be obtained by proper combination of a dial or drum setting, which controls a variable resistor and a tap switch. Photographic views of the exterior and interior of a potentiometer are shown in Figure 268.

Field Procedure for Potential Measurements

The measurements are conducted to determine the relative potential and polarity between certain pre-selected stations in the area. Usually, the

first step consists in surveying two base lines at right angles to each other (lines 0F and 04 in Figure 266) and then surveying two series of regularly spaced traverse lines, each series being parallel to one of the base lines. Their intersections form a grid-work of stations. A satisfactory field procedure consists in setting up the potentiometer at a station on one of the base lines and measuring the difference in potential between that reference point and other points along a traverse line which passes through the station and is parallel to the other base line. (To connect the potentiometer with the distant base line, it is convenient to use a reel containing about 1000 feet of insulated wire.)

Upon completion of the traverse line the wire is disconnected from the instrument and anchor stake and is wound up by the reelman as he returns to the instrument. The instrument is then carried to the next station, set up, and the potential measured between the new base station and the previous station. The reel is now moved along the new traverse and the procedure repeated. Should the work extend over a distance greater than 1000 feet, the potentials between the various base stations should be checked once or twice daily, so that corrections can be made for marked potential fluctuations.

An average lineman, who handles the reel and digs holes (to a depth of 3″ to 6″) for the non-polarizing electrode, usually can contact from 10 to 15 stations, at one hundred foot intervals, per hour. Slightly greater speed is obtained by having an assistant dig the electrode holes.

Sources of Error

Considerable potential variations will oftentimes occur in an area due to natural earth currents, rains, changes in temperature (especially in regions where the nights are cool and the mid-days hot), and freezing and thawing weather. Additional potential variations caused by industrial or mining operations will be found in many localities, and these are usually the most common source of error in obtaining accurate field data.

Earth Currents.—The phenomenon designated as "earth currents" is due to a great variety of causes. The potential difference between two grounded electrodes consists of several components; some change with time relatively slowly, and others fluctuate rapidly and irregularly. The earth potential components of preponderantly direct-current character include: the electrode potentials already described;* potentials due to oxidizing ore bodies; a regional gradient in the area which amounts, according to place and time of year, to some 10 to 100 millivolts per kilometer.

* The electrode potential variations are, of course, minimized when non-polarizing electrodes are used.

In addition to these more or less steady components, various fluctuating potentials occur. Earth currents have strong diurnal variations, magnetic storm fluctuations, and other variations with a period longer than one day.† Figure 269 shows a comparison of the variations in earth currents, magnetic activity, and sunspot numbers over a period of several years.‡ The curves are necessarily "smoothed out"; that is, monthly, daily, and hourly variations that would give the curves a saw-toothed character are not shown. Hourly earth-current records are shown by Gish.§

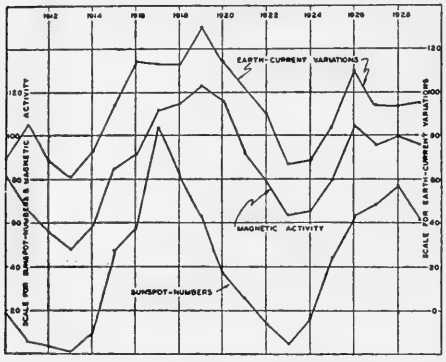

FIG. 269.—Comparison of variations in earth currents, magnetic activity, and sunspot numbers. (Rooney, "Earth Currents," *Terrestrial Magnetism and Electricity.*)

The errors due to varying earth currents are minimized by employing relatively short separations between the measuring electrodes. In average areas, the effects of varying earth currents are of minor importance at separations less than 500 feet.

Traverses Across Vein Conductors.—The self-potential method can often be employed to advantage in studying veins and parallel vein systems undergoing oxidation by running traverses across the area at right angles to the vein system. Work of this type is much more rapid than the equipotential studies previously outlined. For this work, a potentiometer, reel, and non-polarizing electrode system are employed. Readings are made at suitable intervals along the traverse line. Plots may be made of the differences in potential between the stations as ordinates and the traverse distances as abscissas. Due to the change in the direction of current flow above the oxidizing ore body, the potential curve has a minimum value above the negative center. Non-symmetry of the curve about the negative center may be caused by a dipping ore body, differences in the electrical conductivity of the rock on each side of the vein system, variations in ground water elevation and distribution, or the regional gradient. These variables must be evaluated by proper geologic control and measurement technique.

† W. J. Rooney, "Earth Current Variations with Periods Longer than One Day," *Terr. Mag.* 42, No. 2, p. 166, June, 1937.

‡ W. J. Rooney, "Earth Currents," p. 291 *Terrestrial Magnetism and Electricity* (Edited by J. A. Fleming) (McGraw-Hill, 1939.)

§ O. H. Gish, "Electrical Messages from the Earth, their Reception and Interpretation," *Journal of the Washington Academy of Sciences,* Vol. 26, No. 7, July 15, 1936.

INTERPRETATION OF SPONTANEOUS POLARIZATION STUDIES

The field work involved in spontaneous polarization measurements is relatively simple, yet its interpretation is oftentimes complicated due to several factors. In some cases, it is of interest to compare observed potential data with theoretical potential profiles.† Final interpretation should give careful consideration to: (1) effects of topography, (2) geological and structural conditions, (3) spurious earth currents, (4) ore occurrence in the district, and (5) regional gradient.

In areas where rugged topography prevails, interpretation is usually complicated by an irregular distribution of surface potentials. In many cases, the negative center will be shifted, with a resultant shift in the predicted location of the oxidizing ore zone. This effect is apparent when the topographic contour map of the area is studied in conjunction with the potential map. As a general rule, the negative center in fault studies will be shifted toward the hanging-wall side of the ore body.

Interpretation should never be attempted without proper geological control. Areal maps should be drawn to the same scales as the geophysical potential contours. Contacts of different materials containing ground waters of different chemical properties often give rise to earth potentials which may not be related to ore occurrence. In addition, different geological formations usually possess different electrical conductivities; hence, they cause a distortion of the normal regional ground currents with a resultant redistribution of the surface potentials. Fault zones filled with wet clay gouges, or other conducting materials, cause severe distortion of the surface potentials.

The effects of topography and different materials may best be seen by reference to Figure 270 which shows the surface potentials existing over a pyrite vein formation in Arizona. The sulfides exist at a depth of approximately 45 feet. A general cross section of the vein is shown in the upper portion of the figure. The mineralization occurs at the contact of the limestone and a monzonite intrusion. The limestone has an electrical resistivity of 85,000 ohm-cm. while the monzonite has a value of 30,000 to 50,000 ohm-cm. As shown on the plan view, the mineralization is localized between two cross faults. The faults are filled with a clay gouge material which when wet has a very low resistivity, approximately 8,000 ohm-cm. Laboratory measurements of the pyrite vein material gave values of 200 to 6,000 ohm-cm. The equipotential lines are shown dotted in the plan view in the lower portion of the figure. It will be noted that the current flow was concentrated chiefly between the faults in the lower resistance monzonite. The negative center was found to be approximately 40 feet to the east of the actual vein itself.

† Theoretical potential profiles produced by (1) a polarized rod and (2) a polarized sheet are discussed by Broughton Edge and Laby, *Geophysical Prospecting* (Cambr. Univ. Press, 1931), pp. 243-246.

The self-potential method is capable of furnishing important data, provided the interpretation is made with due regard to ore occurrence in that particular district. Final utilization of the survey results is accomplished by subsequent drilling or other direct exploration to ascertain the commercial value of the ore. There is no known physical relationship between galvanic currents or surface potentials and the economic value of the mineralization.

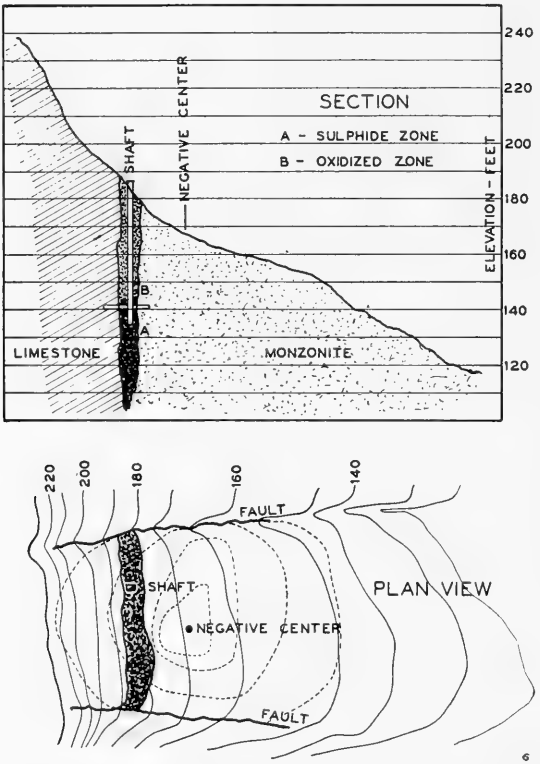

Fig. 270.—Sketch illustrating the displacement of the negative center with respect to the top of the ore body. Equipotential lines, dotted; topographic contours, solid.

In regions where the water table is considerably below the surface and where the upper near-surface material is highly resistant (as is the case in many desert areas), the magnitude of the galvanic currents which penetrate the highly resistant overlying materials may be too small to create a measurable potential difference at the surface. Under such conditions, the self-potential method will not give interpretable results. Also, application of the self-potential method in certain localities will quickly show that many persistent earth potentials are present which are not related to mineralized areas or ore occurrence.

Artificial conductors such as car rails, pipe lines (especially those extending from the surface to underground workings), etc., are all possible, and usually probable sources of earth currents. In areas where mining operations are in progress and direct current is used for power, difficulty will usually be met due to leakage and "ground-return" power circuits. Oftentimes, these leakage currents are encountered at distances of a mile or more from the mine and cause erratic self-potential data. In one case, failure to correct for leakage currents led to an erroneous conclusion. (Fortunately, the error was disclosed on checking the area by resistivity measurements prior to development of the "indication.")

Various methods have been proposed for interpreting self-potential field data, all making certain simplifying assumptions. Stern based a method on formulas derived from assuming the ore body to be a polarized bar.† Heiland assumed a vertically polarized sphere in his method.‡ DeWitte§ provided a method based on the theory for surface distribution of potentials worked out by Petrovsky.††

DeWitte's method provided interpretation for location, depth and dip of the ore body making use of an equipotential line pattern. The ore body is assumed to be a polarized sphere, and for the theory, an image of this body is assumed to be located symmetrically above the horizontal boundary (surface of the earth). The unique points of this theory involve determining a positive maximum of potential, as well as a negative minimum, and the "mid-value" point of potential. The value of the angle of dip is then determined from theoretical curves, while the depth is determined from the curve involving various angles of dip. A final set of curves readily yields the vertical projection of the center of the ore body.

FIELD RESULTS

Surveys of Sulphide Ore Bodies.—A well known self-potential survey is that made by Schlumberger in 1913 on the Sain-Bel ore body.‡‡ (Figure 271.) The potential difference between the negative center and a distant point of the surrounding terrain is of the order of 220 millivolts. The hatched area represents a cross section of the ore body at a depth of about 300 feet. It will be noted that the equipotential curves outline the area of mineralization quite accurately. The dotted profiles show the variation of the potential in the transverse direction across the ore body. At *A* there was located a negative center which was later proved to lie over a lens of fine pyrite.

† W. Stern, *A.I.M.E. Transactions,* Vol. 164, 1945, p. 189.
‡ C. A. Heiland, *Geophysical Exploration,* p. 673, Prentice Hall, New York, N. Y.
§ L. DeWitte, "A New Method of Interpretation of Self-potential Field Data," *Geophysics,* Vol. XIII, No. 4, October, 1948, pp. 600-608.
†† A. Petrovsky, *Philosophical Magazine* 5 (1928), pp. 334, 914, 927.
‡‡ C. Schlumberger, *Etude de la Prospection Electrique du Sous-Sol.* (Gauthier-Villars, Paris 1920).

Self-potential surveys of sulphide ore bodies have also been described by Kelly,‡ Mason § and others.††

Another example of the application of the spontaneous polarization method to a geophysical study is provided in Figure 272, representing pro-

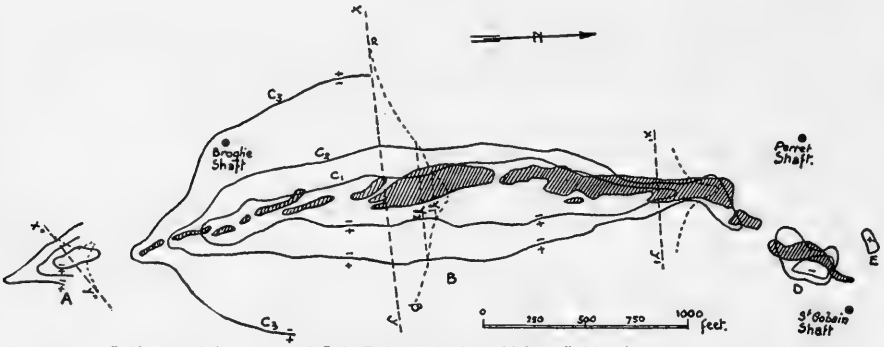

FIG. 271.—Self-potential survey of Sain-Bel ore body. (After Schlumberger, *Etude de la prospection Electrique du Sous-Sol.*)

files over one tunnel of an abandoned nickel prospect near Winesap, Chelan County, Washington. The discussion and interpretation† was made by Patty and Kelly in 1946.

Surveys Over Anthracite Coal Deposits.—Anthracite coal quite frequently shows the phenomenon of spontaneous polarization. It is found that a *positive* instead of a negative center occurs over the upper part of the anthracite beds. The potentials encountered are usually much smaller than those found over sulphide ores.

Corrosion Surveys.—The oxidation of pipe lines is an important commercial problem which has been the object of numerous investigations.‡‡ The types of corrosion that may affect a buried metallic conductor may be enumerated as follows:§§

1. Soil corrosiveness. The conductor is attacked by the surrounding soil.
2. Autogalvanic corrosion. If a metallic conductor connects two regions of the

‡ S. F. Kelly, *Engineering and Mining Journal*, Vol. 114, Oct. 7 and Oct. 14, 1922.
§ M. Mason, "Geophysical Exploration for Ores," *A.I.M.E. Geophysical Prospecting*, 1929, p. 27.
†† Broughton Edge and Laby, *Geophysical Prospecting*, pp. 81-84, 98-100.
† E. N. Patty and S. F. Kelly, "A Geological and Geophysical Study of the Chelan Nickel Deposit," *A.I.M.E. Tech. Pub.* 1953.
‡‡ F. N. Speller, *Corrosion Causes and Prevention* (McGraw-Hill, 1935).
O. P. Watts, "Electrochemical Theory of Corrosion," *Trans. Electrochem. Soc.*, Vol. 64, pp. 125-153, 1933.
T. G. Elliott, R. J. Sarjant, and W. Cullen, "Special Alloy Steels As Applied to Chemical Engineering," *J. Soc. Chem. Ind.*, Vol. 51, pp. 502-531, 1932.
Scott Ewing, "Electrical Methods for Estimating the Corrosiveness of Soils," *Amer. Gas Assoc. Monthly*, Vol. 14, pp. 356-360, 1932.
W. G. Heltzel, "The Maintenance of Oil Pipe Lines," *Proc. Amer. Petroleum Inst.*, Vol. 14, pp. 168-191, 1933.
G. N. Scott, "Report of A.P.I. Research Associate to the Committee on Corrosion of Pipe Lines," *Proc. Amer. Petroleum Inst.*, Vol. 14, pp. 204-220, 1933.
J. M. Pearson, "The Value of Soil-Survey Methods," *Oil and Gas Journal*, Nov. 18, 1938, p. 100.
§§ C. and M. Schlumberger and E. G. Leonardon, "Location and Study of Pipe Line Corrosion by Surface Electrical Measurements," *A.I.M.E. Geophysical Prospecting*, Tech. Pub. 476 (1932).

ground in which the electrolytes have a different composition, an electric current will be generated, and certain zones of the conductor will be oxidized.

3. Electrolytic corrosion. Stray currents, due to power lines for example, may enter the conductor in certain sections and leave it in others, thus causing oxidation in certain zones.

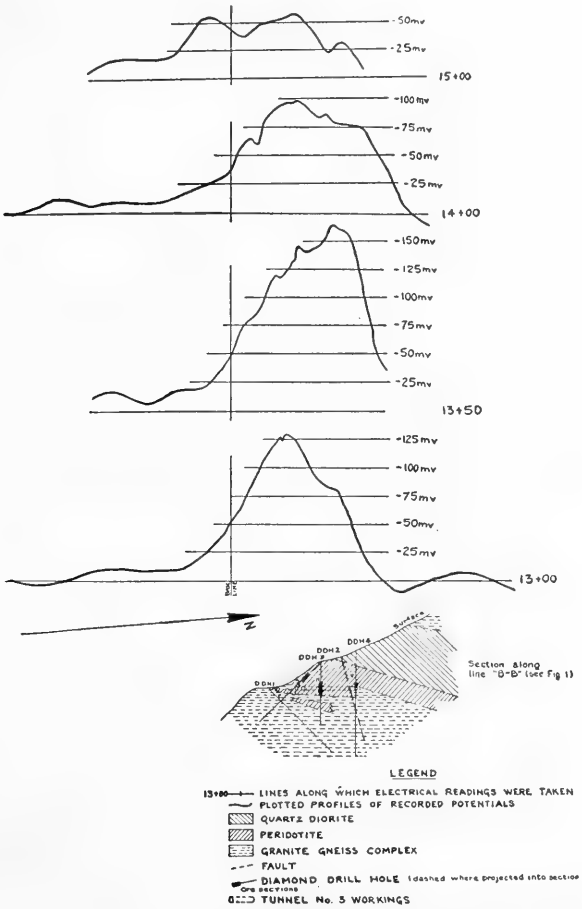

FIG. 272.—Spontaneous polarization profiles and drill data at Tunnel No. 3, Chelan Nickel Prospect. (Drill data courtesy of U. S. Bureau of Mines.) (*A.I.M.E. Tech. Pub.* 1953.)

The effects produced at the surface due to autogalvanic and electrolytic corrosion are entirely analogous to the effects produced by oxidizing ore bodies. Hence, spontaneous polarization methods may be employed to locate the corrosive regions.

Utilization of Telluric Currents

In contrast to phenomena of limited areal extent (some man-made, such as streetcar and power lines, and others due to local electrochemical

effects and conductive ore bodies) are the differences of potentials caused by currents covering large areas, in fact the entire earth.

The use of these natural earth currents,† or *telluric* currents,‡ in geophysical prospecting has so far been meager,§ since investigations of the phenomena have themselves been very limited, although knowledge of their existence is far from recent.

These currents circulate about the earth in large "sheets" covering vast sections of the earth's surface; generally they consist of four huge current whorls covering the whole globe. Between two points, the component of the difference of potential arising from telluric current is approximately proportional to the separation of the points. However the telluric field at a given point varies so in intensity and direction (particularly during the daylight hours) that the daily average field is probably zero. Over shorter periods of time (of the order of an hour) definite facts can be established; for example, the field has two maxima and two minima per day, and its average direction is generally that of the magnetic meridian for the middle latitudes while almost perpendicular to the magnetic meridian for lower latitudes.

That telluric currents do flow in such large sheets and that telluric phenomena between distant points are interrelated is demonstrated by simultaneous recordings made by crews at widely separated points on the earth—for example, southern France and Madagascar.††

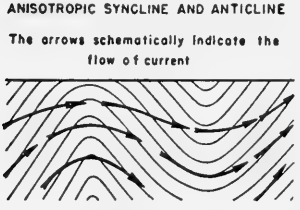

FIG. 273.—Flow of the telluric current in an anisotropic folded ground. (*Geophysics*, Vol. XIII, No. 3, July, 1948, p. 401.)

Problems to which telluric currents may possibly be applied are, in general, those anomalies which cause a horizontally flowing current to be disturbed. A salt dome will deflect the current, since the salt plug is nonconductive. This upward deflection of the telluric current causes a concentration of current near the surface, with a resultant higher telluric potential vector over the salt dome. Folded formations, which are generally anisotropic, will show an increased telluric vector at the peak of an anticlinal or domic structure (Figure 273), since the current tends to flow along the bedding planes rather than perpendicular to them. Faults are detectable if the resistivities, size and positions of the beds cause a concentration of the current along the fault.

---

† R. S. Dahlberg, Jr., "An Investigation of Natural Earth Currents," *Geophysics*, Vol. X, No. 4, October, 1945.

‡ E. Boissonnas and E. G. Leonardon, "Geophysical Exploration by Telluric Currents," *Geophysics*, Vol. XIII, No. 3, July, 1948, pp. 387-403.

§ M. Schlumberger, "Method and Apparatus for Electrical Underground Prospecting," U. S. Patents No. 2,240,520, May 6, 1941, and 2,284,990, June 2, 1942.
J. A. Marchand, "Geophysical Prospecting," U. S. Patent No. 2,263,097, Nov. 18, 1941.

†† Boissonnas and Leonardon, *loc. cit.*

EQUIPOTENTIAL POINT AND LINE METHODS

In equipotential point and line methods, artificially created potential fields are utilized. In favorable cases, the use of these methods permits mapping subsurface deposits of anomalous conductivity, such as a highly conductive ore body in a less conductive formation.

OPERATING PRINCIPLE

When an electric potential is applied between two points, or between two parallel line conductors, on the surface of the ground, an electric current will flow. The potential distribution produced by flow of electric current in a homogeneous medium can be readily calculated. (See Figure 285.) Where the ground is not homogeneous, the potential distribution will not follow the pattern calculated for the homogeneous medium. Hence, it is always possible, at least theoretically, to detect the presence of an inhomogeneity by comparing the measured potential distribution with the theoretical distribution for a homogeneous medium.

In practice the usual procedure is to note any deviation of the potential distribution from a regular pattern and to attribute this to subsurface inhomogeneities, without recourse to comparison of theoretical and observed distributions — a form of visual interpretation qualitative in nature.

The most practical type of energizing current is direct current or low frequency alternating current. From a theoretical viewpoint, the concept of equipotential lines in the case where alternating fields are used has significance only with reference to mean effective values of the potential. However, for low frequencies the field distribution is represented with sufficient accuracy by the D.C. field distribution.

When the frequency is not sufficiently low, appreciable phase shifts will occur. The phase shifts are produced by the inductive effects of the alternating field in the conductive materials, e.g., the ground, mineral bodies, *et al,* lying within the area investigated. When alternating current potential profiles are to be determined in regions of high conductivity where appreciable phase shifts occur, use is made of some form of phase compensator, as described later.

D.C. galvanometers and potentiometers or A.C. galvanometers and vacuum tube voltmeters may be used with direct current or low frequency alternating current, respectively, for determining the lines of equipotential. If audio-detecting means (usually headphones with vacuum tube amplification) are used, the frequency should only be high enough to give a clear cut signal, because the effective depth of penetration decreases as the frequency increases. Frequencies from 100 to 500 cycles are often employed for work of this type.

The potential methods are chiefly useful for general reconnaissance purposes. In simple cases, such as sulphide lodes extending to within 50

feet or so of the surface, these methods will locate the conducting bodies with sufficient accuracy for practical purposes.† For deeper deposits, electrical methods of better resolving power are necessary.

FIELD PROCEDURE AND APPARATUS

Direct Current Method.—The energizing electrodes are positioned to include the area under investigation. Sufficient current is caused to flow between the electrodes to create a measurable potential field. After this field has been created, the field investigations are quite similar to those made in the spontaneous potential method. In the previously described self-potential method, only one datum is necessary at each point of measurement: namely, the value of the natural earth field. In the D.C. equipotential line method, two data should be obtained: namely, (a) the undisturbed natural earth field and (b) the resultant field due to the natural earth current and the artificial current. The readings of (a) are employed for correcting the values of (b).

Power may be supplied to the energizing electrodes by a gasoline-driven, direct current generator. The generator should have an output of 1500 to 2000 watts and a voltage up to 220 volts for extensive surveys. The contact resistance in the energizing circuit should be minimized by use of large extended electrodes.* Because of the losses by polarization and electrolysis or contact potentials adjacent the electrodes, a larger power supply is necessary when employing direct current than when employing alternating current. The power is constant throughout a series of readings, or else the data are reduced to potential per unit current.

Alternating Current Audio Method.—The methods employing A.C. are more common in field practice than those employing D.C. for several reasons:

(a) increased portability of the movable circuit, consisting of metallic electrodes, headphones, and an amplifier;
(b) absence of non-polarizing electrodes which are difficult to handle;
(c) decreased power of generator necessary when vacuum tube amplification is used.

The equipment used in the A.C. audio-frequency potential methods comprises essentially: two power electrodes; insulated connecting wire on reels; power source for energizing the ground; two search electrodes or "probes"; amplifier; headphones, or other balance indicating instruments; and flexible, rubber-insulated connecting cables.

Electrodes.—The multipoint electrodes commonly employed in the energizing circuit are described on page 522. The probe electrodes are preferably made of duralumin and have a diameter of ½ inch and a length

† Compare, also, Broughton Edge and Laby, *Geophysical Prospecting*, p. 43.

* The electrodes are described in detail on p. 522, *et seq.*

of 3 feet. They are pointed at the ground end and provided with an insulated handle for the operator.

Power Sources.—Portable gasoline-engine driven alternators are commonly used as a power source. The alternator should develop from 250 to 1000 watts output at a frequency well up in the audio range, preferably from 100 to 500 cycles per second. The load voltage output of the alternator should have a value of 100 to 200, or a suitable output transformer should be employed to allow proper impedance matching between the alternator and the load.

Amplifiers. — A two- or three-stage transformer-coupled, audio-frequency amplifier may be used. It should be well shielded electromagnetically and electrostatically. The amplifier should be rugged, portable and non-microphonic. Plate supply may be small "B" batteries, and "A" batteries may be used to heat the filaments of dry-cell tubes. The design of the amplifier follows that of conventional audio-frequency equipment.

Headphones.—The headphones should be a light-weight, rugged type and should be provided with rubber cushions to minimize extraneous interfering noise, such as that due to the wind.

A.C. Methods Based on Comparison of In-Phase Current Components. — Equipotentials are obtained in a manner analogous to that used in the D.C. method. The points of equipotential are traced out on the surface of the ground by moving one probing electrode until a minimum of sound is detected in the headphones.*

The A.C. Potential Ratio Method.—The principle of the A.C. potential ratio method developed by Broughton Edge † may be illustrated by reference to Figure 274. The method consists essentially in employing a bridge circuit which makes contact with the ground at three points *A, B, C,* the point *B* being chosen such that *AB* equals *BC*. Each of the two ratio arms *AO* and *CO* contain a condenser and resistance connected in series.

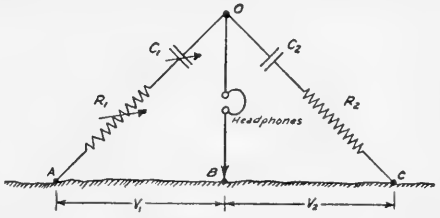

FIG. 274.—Alternating current bridge method, with ratio bridge.

An audio frequency alternating current (about 500 cycles per second) is passed through the ground between distant earthed conductors. This arrangement is used to compare the potential drops V_1 and V_2 between

* If the frequency of the alternating current is not sufficiently low, the investigation must take into account the phase relation between the energizing current and the potential field at the surface of the ground. Zuschlag has proposed a method wherein an alternating electric or electromagnetic ground field is created, and measurements are then made to determine the ratio between the electric potentials or the electromagnetic fields at desired points in the area under investigation.

† Broughton Edge and Laby, *loc. cit.*, p. 50.

the pairs of contacts AB and BC and also to determine the difference in phase angle between them.

When in complete balance, i.e., no sound in headphones,

$$\frac{V_2}{V_1} = \frac{R_2 \sin \tan^{-1} \frac{R_1}{X_1}}{R_1 \sin \tan^{-1} \frac{R_2}{X_2}}$$

where R_1 and R_2 are the resistances and X_1 and X_2 are the capacitative reactances of the two arms of the bridge; also,

$$\theta_2 - \theta_1 = \tan^{-1} \frac{R_2}{X_2} - \tan^{-1} \frac{R_1}{X_1}$$

where $\theta_2 - \theta_1$ is the difference in phase angle between V_2 and V_1. This difference is positive when V_2 leads V_1 and vice versa.

In applying this method, it is essential that the earth at contact B be intermediate in potential with respect to contacts A and C. Observations are usually made along straight line traverses. From data obtained with this bridge both potential and phase variations can be plotted.

A.C. Method Utilizing Three or More Current Electrodes.—In this method, several current electrodes are used and the strengths of the currents in each circuit are made to vary in a predetermined manner. † When three power electrodes are used, the total current I_1, which enters the earth through a common power electrode, will be distributed in the subsurface so that currents of magnitude I_2 and I_3, respectively, reach the other two power electrodes. The ratio of the currents I_2 and I_3 is varied by varying the effective impedance of each branch circuit.

The characteristic and important advantage claimed for the method is that the depth of maximum current density in the ground depends on the ratio $\frac{I_2}{I_3}$. Hence, because the potential difference is a function of the ratio $\frac{I_2}{I_3}$ and because the ratio $\frac{I_2}{I_3}$ can be varied so as to penetrate to any preassigned depth, the measured potential difference theoretically can be made to correspond to a current penetration to any desired depth.

Method Employing Commutated Current.‡—Serious limitations of the D.C. methods outlined above are the errors introduced by undesired earth potentials and the necessity of employing non-polarizing electrodes which are difficult to handle, except under favorable terrain conditions. Marked disadvantages of the audio-frequency A.C. methods are their poor penetrating power and the indefiniteness of the minima detected with

† H. M. Evjen, "Electrical Method of Geophysical Exploration," U. S. Patent 2,169,685; issued Aug. 15, 1939. U. S. Patent 2,172,557; issued Sept. 12, 1939.

‡ H. M. Evjen, "Apparatus for Making Geophysical Explorations," U. S. Patents No. 2,314,873, Mar. 30, 1943, and 2,342,626, Feb. 29, 1944.

D. S. Muzzey, Jr. and R. D. W. Miller, "Apparatus for Electrical Exploration," U. S. Patent No. 2,363,987, Nov. 28, 1944.

D. H. Clewell, "Geological Exploration System," U. S. Patent No. 2,454,911, Nov. 30, 1948.

headphones when working in conducting regions where marked out-of-phase conditions are encountered. These limitations are minimized by using the very low frequencies developed by commutated direct current.

A schematic diagram of a circuit employing commutated currents is shown in Figure 275. The commutator *C* is connected to a direct current generator or to a bank of heavy duty batteries *B*. One lead from the commutator is connected to one of the power electrodes *A;* the other commutator lead is series-connected to the second power electrode *A'* through a current meter *I* and through the field coil of a galvanometer *G*. (The galvanometer should have a fairly long period, 2 to 5 seconds, to give smooth operation.) The two search electrodes are connected to the movable coil of the galvanometer. The current is reversed periodically by the commutator, which is connected by suitable gears or belt drive to the generator.

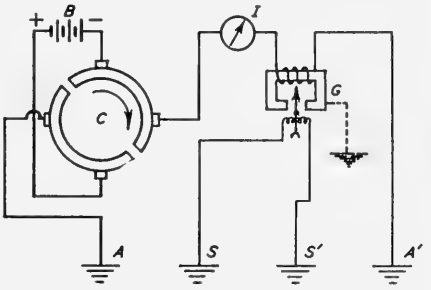

FIG. 275.—Circuit employing commutated direct current for mapping potential profiles.

The chief disadvantage of this method is the necessity of connecting the galvanometer field coil with the power supply, because this requires handling extra wires during the field operations. From the viewpoint of apparatus design, another undesirable feature is introduced: namely, the necessity of insulating the moving or potential coil of the galvanometer from the effects of the field coil. This is a marked disadvantage, because it is difficult to prevent electrostatic and electromagnetic coupling between the two circuits.

Usually frequencies of from 5 to 10 cycles/sec. are employed. These frequencies are sufficiently high that earth current variations, which ordinarily have a frequency of less than 1 cycle/sec. will not affect the readings. Also, the frequencies are sufficiently low to preclude appreciable phase shift phenomena. A direct current, direct-coupled amplifier may be employed for greater sensitivity; however, this is seldom necessary. Ordinary iron electrodes are used for all contacts.

A method of electrical prospecting using alternating current of rectangular or other non-sinusoidal wave form is described by West† (page 551.) The null method, in which the detected electromotive force is balanced against an adjustable electromotive force of a standard oscillator, is used to determine changes in wave form caused by anomalous subsurface structure.

Low Frequency Voltmeter Method.—For shallow investigations the most satisfactory form of apparatus for alternating current work com-

† S. S. West, "Electrical Prospecting with Non-sinusoidal Alternating Currents," *Geophysics*, Vol. III, No. 4, October, 1938, pp. 306-314.

prises: (1) low frequency (25 cycle) gasoline-driven alternator, (2) ordinary iron electrodes for both the energizing and the measuring circuits, and (3) one or two stages of audio-frequency amplification feeding a vacuum tube voltmeter.

This type of apparatus, while more complicated than the simple D.C. galvanometer method, eliminates the errors and difficulties due to earth currents and electrode-contact phenomena. For shallow investigations, the frequency is low enough to avoid bothersome inductive effects and phase-shift phenomena. In addition, no electrical connection need be employed between the energizing circuit or power supply and the detecting or measuring circuit.

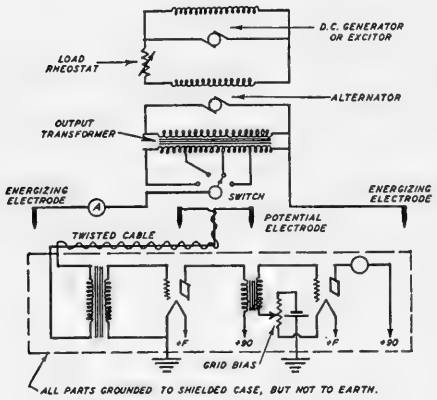

FIG. 276.—Low frequency voltmeter method.

The complete apparatus is illustrated in Figure 276. The alternator for supplying power may be of conventional design, with an output of about 1000 watts at 110 volts. The output is controlled by the rheostat in the excitor circuit. The gasoline engine should preferably be of the standard 2-cycle type which is made of cast iron and has water-bath cooling. The light-weight, high-speed, air-cooled engines, frequently advocated because of their portability, usually are not satisfactory for continuous, heavy duty work. An output transformer must be employed for proper matching of the load impedance, which varies over very wide limits, due to variations in stake resistance.

The vacuum tube voltmeter consists of one stage of 25-cycle amplification and a rectifying tube or detector which functions as a vacuum tube voltmeter. A grid-bias control is provided for proper initial adjustment of the meter. Details of vacuum tube voltmeter design and theory are given in many texts,† and excellent meters are available on the market.

INTERPRETATION OF EQUIPOTENTIAL DATA

Simple calculations suffice for converting the field readings into usable data. Usually, the only corrections necessary are those for natural earth potentials (when using the D.C. methods) and instrumental or meter characteristics. The stations occupied during the survey are plotted accurately on a map, preferably with alidade and plane table while the survey is in progress. The equipotential lines are plotted later by drawing in the best-fitting contours.

† J. H. Morecroft, *Principles of Radio Communication* (John Wiley & Sons, 1927).
A. Hund, *Phenomena in High-Frequency Systems* (McGraw-Hill, 1936).
F. E. Terman, *Measurements in Radio Engineering* (McGraw-Hill, 1935).

A map which shows surface topography and areal geology is necessary for final interpretation of the electrical data. This map should be drawn to the same scale as the equipotential contour map.*

The interpretation is largely empirical in character and must be based on previous experience with the method and knowledge of the local geology. Usually, it is relatively simple to make a qualitative interpretation of the results by outlining the indicated conductive zones and determining by inspection which of them are best defined and are in best accord with the geologic possibilities. In general, potential data alone will not permit determinations of the depth of the conductive body, its strike, length, or width. Usually, shallow deposits give narrow and pronounced potential peaks, while the deeper lying bodies produce broader and less pronounced peaks. The steepness and the width of the peak are thus oftentimes an index as to the depth of the body.

Various modifications of the general field technique may be employed to suit special conditions. If an ore body is partly accessible, one of the energizing electrodes may be connected to the ore body, thereby making the potential of the surface of its conductive portion the same as that of the energizing electrode. The shape of the ore body may then be inferred from the equipotentials observed at the surface of the earth. Another modification takes advantage of the anisotropy of sedimentary rocks. The dip and strike of formations may be indicated from the increased conductivity in the direction of bedding planes. †

Model Experiments.—The interpretative techniques of the equipotential point and line methods may be facilitated by experiments with small scale models or test tanks. The tanks usually are filled with layers of different conductive materials, such as moist sand, clay, etc.; or they are filled with a weak electrolytic solution (such as soluble salt added to fresh water) in which are immersed model ore bodies made of a conductive material. The model may conveniently be made by forming a block of wood into the desired shape and covering it with a layer of 20 to 24 gauge sheet copper, with joints soldered.

Laboratory model experiments are of value because they show the type of anomalies which would be obtained under the simple conditions selected for the experimental work. However, because actual geological conditions are usually quite complex, the application of model results to the solution of field problems is valid only to the extent that the conditions pertaining to the laboratory work exist in the field.

* Generally the potential irregularities produced by topographic features are evaluated empirically, although in certain cases these anomalies can be computed by making a sufficient number of simplifying assumptions.

† E. G. Leonardon and S. F. Kelly, "Some Applications of Potential Methods to Structural Studies," *A.I.M.E. Geophysical Prospecting*, 1929, pp. 180 to 186.

C. and M. Schlumberger and E. G. Leonardon, "Electrical Measurements in Anisotropic Media," *A.I.M.E. Geophysical Prospecting*, 1934, pp. 159-181.

FIELD RESULTS

A number of equipotential surveys for the location of ore have been described by Lundberg † and by Broughton Edge and Laby. ‡ The sur-

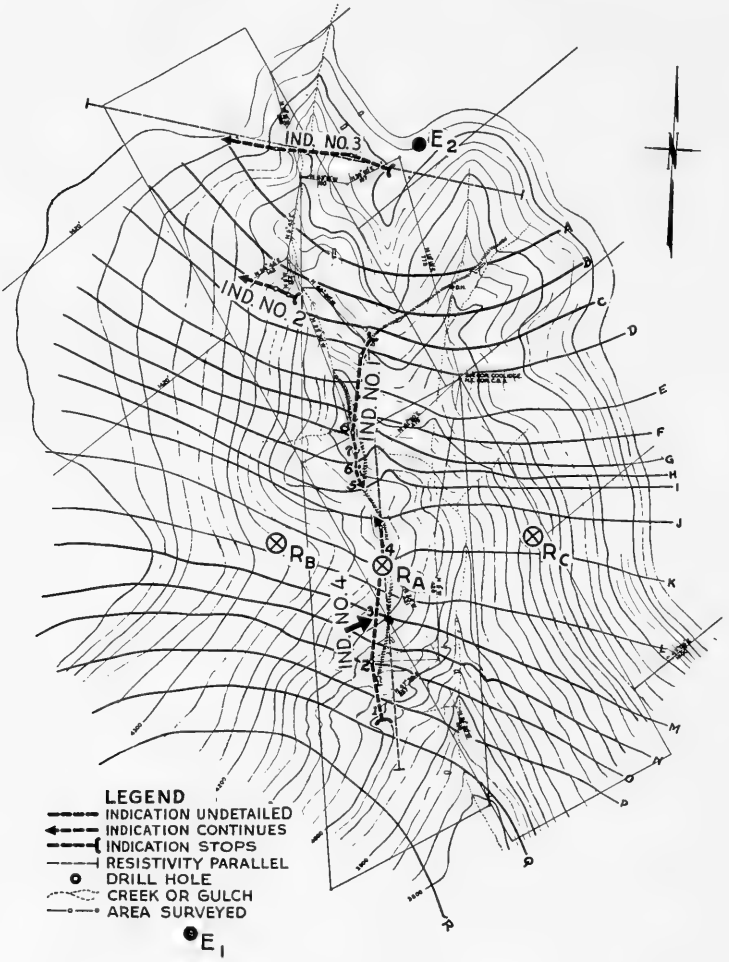

FIG. 277.—Results obtained in an alternating current equipotential line survey in Pinal County, Arizona.

veys of the latter investigators (with one exception) were made in the eastern part of Australia (Queensland, New South Wales, Victoria and Tasmania).

Figure 277 shows the results obtained in an alternating-current equi-

† Hans Lundberg, "Recent Results in Electrical Prospecting for Ore," *A.I.M.E. Geophysical Prospecting*, 1929, p. 105, p. 110, pp. 120-122.

‡ A. Broughton Edge and Laby, *loc. cit.*, pp. 74, 83, 86, 92-94, 111, 116, 122.

potential survey in Pinal County, Arizona. The ground was energized with a 25-cycle gasoline-driven alternator. The iron power electrodes were positioned at locations E_1 and E_2. The lines of equipotential were traced with two probing electrodes connected to the voltmeter type of equipment illustrated in Figure 276.

The topography in this area is moderately rough. The formations are well exposed and the surface contacts can be traced easily. Within the area covered by the survey are rocks of diabase, hornblende porphyry, and quartzite schist. The area is cut by numerous faults, and the ore usually occurs in the north-south fault or fracture system. The ore is associated with quartz, which fills the fractures. The ore is galena accompanied by sphalerite, tetrahedrite, chalcopyrite, and bornite. The chalcopyrite and bornite are usually found in the diabase close to the fracture zones. The galena ore is an excellent electrical conductor.

The location of the fractured mineralized zones was known from geological and exploratory work. The chief purpose of the equipotential studies was to ascertain the zones of high electrical conductivity, because it was predicted that the best commercial values would be found in such zones.

Three types of electrical studies were conducted: (1) equipotential, (2) high frequency inductive, and (3) resistivity. The high frequency studies were conducted first, and the "indications" followed the main fracture system. The strongest effects were obtained between stations 1 to 8. The electrodes E_1 and E_2 for energizing the ground for the equipotential studies were located so as to allow the current path to include the main fracture system. The lines of equipotential A to R showed their maximum deviation from the normal along contours G to L, in the vicinity of stations 4 to 8. The anomalies in the contours may be seen best by holding the book so the plane of Fig. 277 is level with the eye and sighting along the contours.

Because both the high frequency and the equipotential methods are "indicative" only, it was decided to obtain more detailed information regarding the probable depth of the mineralized area by use of resistivity-depth studies. The centers of three resistivity-depth stations were located at R_B, R_A and R_C, with the lines oriented parallel to the fracture zone (approximately in a north-south direction). Subsequent drilling established the existence of a good grade commercial ore zone at a depth of approximately 400 feet.

RESISTIVITY METHODS

The resistivity methods allow quantitative electrical data to be obtained from the field measurements. Calculations may be made of the average resistivity of the portion of the subsurface included in the measurements. The methods have a greater resolving power than the regular potential

methods,* because the field work can be conducted so as to introduce a depth variable which relates the electrical data obtained at the surface with the variation of effective resistivity with depth.

Operating Principles

The field procedure employed in resistivity determinations consists in passing a measured current through a selected portion of the earth and measuring the potential drop, or some other electrical quantity associated with this flow of current. This is usually accomplished by passing the current between energizing electrodes placed at two selected points and measuring the potential difference between two or more auxiliary electrodes placed at other points in the area under investigation. For convenience in the interpretative analysis, all the electrodes are usually placed in a straight line. From the observed values of the current and potential, the apparent resistivity of the material included within the zone of measurement can be calculated for any given electrode configuration.

The effective depth of measurement is governed, to a considerable extent, by the spacings of the various electrodes involved in the measurements and by the relative resistivities of the various geologic strata included in the measurement. In a particular area it is necessary to evaluate the effective depth of measurement empirically, using whatever is known of the local geology as a control.

Generally, the subsurface is heterogeneous and the potential distribution at the surface of the ground is affected by the size, shape, composition, and relative positions of the subsurface rock masses. Because these are the elements of geologic study, the geoelectrical problem is to infer the subsurface geology from the surface measurements of electrical quantities. Interfering factors are always present. These include natural ground currents, polarization phenomena, uneven topography, and non-structural near-surface resistivity variations. The effect of such factors must be evaluated or minimized by proper technique in the field work or in the interpretation.

Resistivity investigations as usually conducted may be divided into two general classifications: (1) studies wherein the specific subsurface conditions are to be deduced; (2) studies wherein relative subsurface conditions at one locality (station) are to be compared with the conditions existing at another locality.

In (1), the field work and the interpretative technique must be so conducted that deductions may be made regarding the configuration, mass, distribution, and depths of the materials which constitute the subsurface. Analysis of the data is based on relationships derived for certain relatively simple conditions. The interpretative technique includes the following

* Potential surface methods include all summation potential methods, such as the magnetic, gravitational, and the self-potential and equipotential line methods.

steps: (a) deriving theoretical curves for various assumed subsurface conditions; (b) comparing the theoretical curves with the actual field curves; (c) inferring from an evaluation of all available data the combination of assumed subsurface conditions which would produce electrical anomalies that approximate the observed anomalies. The field procedure and interpretative technique of these methods are applicable for relatively simple subsurface conditions only.

In (2), a quite different type of field procedure and interpretative technique is employed. The field work is conducted primarily to obtain general resistivity-depth relationships from which a characteristic or type curve may be obtained for some sequence of subsurface conditions, whatever they may be. If approximately similar subsurface conditions exist at two localities in a given area, the type curves will generally exhibit recognizable similarities; if the geological conditions are different, the type curves will generally show variations which may be correlated with the geological variations. This type of analysis may be applied best in areas where lateral variations in geology are restricted largely to changes in the depth to certain characteristic beds or "markers." Due to the complexity of beds forming a sedimentary series, deep structural investigations may be handled more successfully by this method than by method (1).

Derivation of Fundamental Formulas

Ohm's Law.—The elementary and familiar form for Ohm's law is

$$I = \frac{E}{R} \quad \text{or} \quad R = \frac{E}{I}$$

where I = current in amperes
E = electromotive force in volts
R = resistance in ohms

For a conductor (such as a wire)

$$R = \rho \frac{L}{A}$$

where A = cross-sectional area
L = length
ρ = resistivity or the resistance of a cube of unit length.

By combining these two equations, it is evident that

$$E = \rho \frac{LI}{A} \quad \text{or} \quad I = \frac{EA}{\rho L}$$

The application of Ohm's law to the measurement of the electrical resistance of a wire is illustrated in Figure 278, wherein the current is measured by the ammeter I and the voltage by the voltmeter E.

The last equation is the starting point for determining the laws gov-

erning the current distribution in an infinite or semi-infinite conductor. Let E represent the potential difference between two points at which the potentials are V_1 and V_2; then

$$E = V_2 - V_1$$

Also, the elementary Ohm's law becomes

$$I = \frac{(V_2 - V_1)\,A}{\rho L} \tag{1}$$

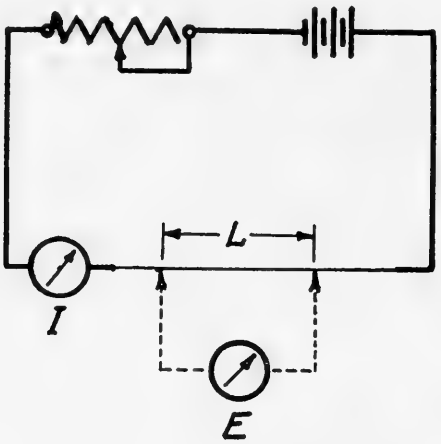

FIG. 278.—Circuit illustrating how Ohm's law may be used to determine the resistance by measuring the voltage drop across any known length L of a conductor of uniform area.

This law gives the magnitude of the current in a conductor of cross section A sq. cm., length L cm., and resistivity ρ ohm-cm. when a potential difference of $(V_2 - V_1)$ volts exist between the ends of the conductor.

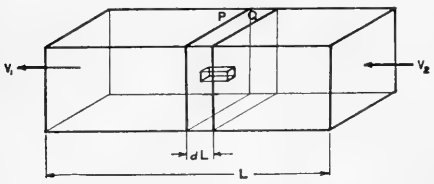

FIG. 279—Homogeneous parallelopiped. Normal cross sections P and Q are equipotential surfaces.

Differential Form of Ohm's Law

Ohm's law can be used to give the value of current which flows between two normal cross sections such as Q and P at an infinitesimal distance dL apart. (Figure 279.) It is assumed that the value of the potential is the same at any point on a cross section normal to the axis of the parallelopiped; i.e., the normal cross sections are assumed to be equipotential surfaces. If a difference of potential dV exists between the equipotentials Q and P, Ohm's law states that

$$I = -\frac{A}{\rho} \cdot \frac{dV}{dL}$$

This equation gives the current which flows through the whole cross section, i.e., through A sq. cm. The current through one square centimeter is

$$i = -\frac{1}{\rho} \cdot \frac{dV}{dL}$$

If the distance dL is not measured in the direction of current flow, Equation 3 must be modified. In this case,

$$i = -\frac{1}{\rho} \cdot \frac{\partial V}{\partial L} \tag{2}$$

where i is the current per square centimeter of area normal to L and $\frac{\partial V}{\partial L}$ is the rate of change of potential in the direction of L. In particular,

$$i_x = -\frac{1}{\rho}\frac{\partial V}{\partial x};\ i_y = -\frac{1}{\rho}\frac{\partial V}{\partial y};\ i_z = -\frac{1}{\rho}\frac{\partial V}{\partial z}$$

where i_x, i_y and i_z are the components of current density in the directions x, y, and z respectively, and $\frac{\partial V}{\partial x}$, $\frac{\partial V}{\partial y}$, and $\frac{\partial V}{\partial z}$ are the partial derivatives of V with respect to x, y and z respectively.

Flow of Current in a Continuous Medium.—When a steady current flows through a conductor, it behaves very much like an incompressible fluid in that the total current which flows into any closed surface within the conductor is equal to the total current which flows out of that surface. In order to express this fact mathematically, it will be convenient to consider a small cube within the conductor. (Figure 280.)

x, y, and z are the coordinates of the center of the cube and dx, dy, dz are the edges of the cube.

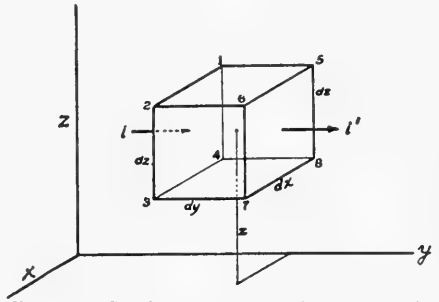

FIG. 280.—Steady state currents through a small cube.

Let $i_y dxdz$ be the total current entering the cube at the face $\overline{1234}$ and $i_y' dxdz$ be the total current leaving at the face $\overline{5678}$. Then the excess of current entering at the face $\overline{1234}$ over that leaving the face $\overline{5678}$ is

$$\Delta i_y = i_y\, dxdz - i_y'\, dxdz = (i_y - i_y')\, dxdz = \left(\frac{1}{\rho}\frac{\partial V}{\partial y} - \frac{1}{\rho}\frac{\partial V'}{\partial y}\right) dxdz$$

or

$$\Delta i_y = \frac{1}{\rho}\left(\frac{\partial V}{\partial y} - \frac{\partial V'}{\partial y}\right) dxdz$$

Also,

$$\Delta i_z = \frac{1}{\rho}\left(\frac{\partial V}{\partial z} - \frac{\partial V'}{\partial z}\right) dxdy$$

and

$$\Delta i_x = \frac{1}{\rho}\left(\frac{\partial V}{\partial x} - \frac{\partial V'}{\partial x}\right) dydz$$

If there are no sources or sinks within the cube, the total current entering the cube must equal that leaving it; hence, the sum of the currents Δi_y, Δi_z and Δi_x must equal zero. That is,

$$\frac{1}{\rho}\left(\frac{\partial V}{\partial x} - \frac{\partial V'}{\partial x}\right) dydz + \frac{1}{\rho}\left(\frac{\partial V}{\partial y} - \frac{\partial V'}{\partial y}\right) dxdz +$$

$$\frac{1}{\rho}\left(\frac{\partial V}{\partial z} - \frac{\partial V'}{\partial z}\right) dxdy = 0$$

Division of this equation by $\left(\frac{dxdydz}{\rho}\right)$ yields

$$\left(\frac{\partial V}{\partial x} - \frac{\partial V'}{\partial x}\right)\frac{1}{dx} + \left(\frac{\partial V}{\partial y} - \frac{\partial V'}{\partial y}\right)\frac{1}{dy} + \left(\frac{\partial V}{\partial z} - \frac{\partial V'}{\partial z}\right)\frac{1}{dz} = 0$$

The quantity $\left(\frac{\partial V}{\partial x} - \frac{\partial V'}{\partial x}\right)\frac{1}{dx}$ represents the average rate of change of $\frac{\partial V}{\partial x}$ in the direction of x. When dx is made to approach zero, this quantity approaches the second partial derivative of V with respect to x. That is,

$$\lim_{dx \to 0}\left(\frac{\partial V}{\partial x} - \frac{\partial V'}{\partial x}\right)\frac{1}{dx} = \frac{\partial^2 V}{\partial x^2}$$

Also

$$\lim_{dy \to 0}\left(\frac{\partial V}{\partial y} - \frac{\partial V'}{\partial y}\right)\frac{1}{dy} = \frac{\partial^2 V}{\partial y^2}$$

and

$$\lim_{dz \to 0}\left(\frac{\partial V}{\partial z} - \frac{\partial V'}{\partial z}\right)\frac{1}{dz} = \frac{\partial^2 V}{\partial z^2}$$

Hence, in the limiting case

$$\frac{\partial^2 V}{\partial x^2} + \frac{\partial^2 V}{\partial y^2} + \frac{\partial^2 V}{\partial z^2} = 0 \qquad (3)$$

This equation is known as Laplace's equation. It is frequently written in the form

$$\nabla^2 V = 0 \qquad (4)$$

where the operator ∇^2 is defined by the relation

$$\nabla^2 \equiv \frac{\partial^2}{\partial x^2} + \frac{\partial^2}{\partial y^2} + \frac{\partial^2}{\partial z^2}$$

It is clear from the derivation of this equation that whatever the shape of the conductor through which a steady current flows or whatever the particular conditions of the problem, the potential V must satisfy Equation 4. This is true everywhere except at points where there is either a source or a sink of current.* Equation 4 alone does not determine the solution of any particular problem because it expresses only one of the conditions which V must satisfy.

Furthermore, Laplace's equation (4) holds only for steady currents in isotropic, homogeneous media.

In any particular problem there are "boundary conditions" which must be satisfied. The boundary conditions require: (1) at any boundary separating two media of different resistivities, $V_1 = V_2$ where V_1 and V_2 are the potentials on opposite sides of the boundary, and (2) the normal component of the current entering the boundary through one side is equal to the normal component of the current leaving through the opposite side. That is,

$$i_n = \frac{1}{\rho_1}\frac{\partial V_1}{\partial n} = \frac{1}{\rho_2}\frac{\partial V_2}{\partial n}$$

Any solution of Laplace's equation which also satisfies the boundary conditions constitutes the unique solution of the given problem.**

Solutions of Laplace's Equation

Solutions of Equation 4 for several simple cases of current flow in media of uniform resistivity ρ will be discussed in the following paragraphs. For exploration purposes, certain portions of the earth's crust are approximately homogeneous; other portions approximate the mathematical ideal of two or three homogeneous layers of uniform resistivities; still other portions comprise, approximately, two homogeneous, semi-infinite media separated by a bounding plane (fault), etc. The flow of current through such structures may be described by a solution of Laplace's equation which satisfies the boundary conditions at all the boundaries.

Case I.—Consider a small source of current surrounded by an infinite isotropic homogeneous conductor of resistivity ρ. From considerations of symmetry, it is clear that the potential V will be a function only of the distance r from the current source.

* Points where current flows out of a conducting medium or into a conducting medium from an external source.

** For a proof that V is determined uniquely by Laplace's equation and the boundary conditions see J. H. Jeans, *The Mathematical Theory of Electricity and Magnetism* (Cambridge University Press).

If the origin of rectangular coordinates is chosen at the source,

$$r^2 = x^2 + y^2 + z^2$$

Also,

$$2r\frac{\partial r}{\partial x} = 2x \quad \text{or} \quad \frac{\partial r}{\partial x} = \frac{x}{r}$$

and

$$\frac{\partial^2 r}{\partial x^2} = \frac{r - x\left(\frac{x}{r}\right)}{r^2} = \frac{1}{r} - \frac{x^2}{r^3}$$

Furthermore,

$$\frac{\partial V}{\partial x} = \frac{\partial V}{\partial r} \cdot \frac{\partial r}{\partial x}$$

and

$$\frac{\partial^2 V}{\partial x^2} = \frac{\partial^2 V}{\partial r^2}\left(\frac{\partial r}{\partial x}\right)^2 + \frac{\partial V}{\partial r}\left(\frac{\partial^2 r}{\partial x^2}\right)$$

Hence,

$$\frac{\partial^2 V}{\partial x^2} = \frac{\partial^2 V}{\partial r^2}\frac{x^2}{r^2} + \frac{\partial V}{\partial r}\left(\frac{1}{r} - \frac{x^2}{r^3}\right)$$

Similarly,

$$\frac{\partial^2 V}{\partial y^2} = \frac{\partial^2 V}{\partial r^2}\frac{y^2}{r^2} + \frac{\partial V}{\partial r}\left(\frac{1}{r} - \frac{y^2}{r^3}\right)$$

and

$$\frac{\partial^2 V}{\partial z^2} = \frac{\partial^2 V}{\partial r^2}\frac{z^2}{r^2} + \frac{\partial V}{\partial r}\left(\frac{1}{r} - \frac{z^2}{r^3}\right)$$

Substitution of these values of $\frac{\partial^2 V}{\partial x^2}$, $\frac{\partial^2 V}{\partial y^2}$, and $\frac{\partial^2 V}{\partial z^2}$ into Equation 4 yields

$$\frac{\partial^2 V}{\partial r^2}\left[\frac{x^2 + y^2 + z^2}{r^2}\right] + \frac{\partial V}{\partial r}\left[\frac{3}{r} - \frac{x^2 + y^2 + z^2}{r^3}\right] = 0$$

or

$$\frac{\partial^2 V}{\partial r^2} + \frac{\partial V}{\partial r} \cdot \frac{2}{r} = 0$$

Since r is the only independent variable in the problem, the partial derivatives may be replaced by total derivatives. That is, the last equation may be written in the form

$$\frac{d^2 V}{dr^2} + \frac{2}{r}\frac{dV}{dr} = 0$$

This equation can be readily integrated by multiplying by r^2, thereby forming an exact differential. That is,

$$\frac{d^2 V}{dr^2} + \frac{2}{r}\frac{dV}{dr} = 0 = r^2\frac{d^2 V}{dr^2} + 2r\frac{dV}{dr}$$

and

$$\int \left(r^2 \frac{d^2V}{dr^2} + 2r \frac{dV}{dr} \right) dr = \int d \left(r^2 \frac{dV}{dr} \right) = r^2 \frac{dV}{dr} = \text{const.} = S$$

Hence,

$$\frac{dV}{dr} = \frac{S}{r^2}$$

and

$$V = -\frac{S}{r} + C$$

The values of S and C must be determined from boundary conditions of the problem. If it is assumed that the value of V at infinity is zero, C vanishes. Also, the constant S may be expressed in terms of the total current I which flows out of the source. Consider a small sphere surrounding the source. The current which flows through one sq. cm. of the surface of the sphere in an *outward* direction is

$$-\frac{1}{\rho} \frac{dV}{dr} = -\frac{1}{\rho} \frac{S}{r^2}$$

The total current is

$$I = -4\pi r^2 \left(\frac{1}{\rho} \frac{S}{r^2} \right) = -\frac{4\pi S}{\rho}$$

and

$$S = -\frac{I\rho}{4\pi}$$

Hence

$$V = \frac{I\rho}{4\pi r} \tag{5}$$

Equation 5 expresses the value of the potential at any point in an infinite isotropic homogeneous medium due to a small source of current.

It will be noticed that the solution is of the form $V = S/r$. (The particular value given for the constant: viz., $S = I\rho/4\pi$, is due to the geometric form of the electrode.) The general conclusion which can be drawn from the above analysis, therefore, is that the potential due to a small current source or sink is S/r, where S is chosen to satisfy the boundary conditions.

Practically, this condition is approximately realized in that type of electrical bore-hole exploration in which one current electrode is lowered a considerable distance into the earth while the other current electrode is fixed at a great distance from the first.

Case II.—Consider next the case of a current source located in a plane P which bounds a semi-infinite, isotropic, homogeneous conductor of resistivity ρ. (Figure 281.) The boundary conditions in this case are $V = 0$ at $r = \infty$ and $-\frac{1}{\rho}\frac{\partial V}{\partial z} = 0$ at $z = 0$. The solution of this problem is

$$V = \frac{S}{r}$$

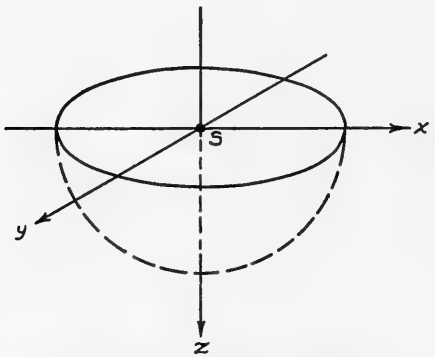

FIG. 281.—Current source S in a plane xy bounding a semi-infinite conductor.

for this solution satisfies Laplace's equation. Also, $V = 0$ when $r = \infty$ and

$$-\frac{1}{\rho}\frac{\partial V}{\partial z} = -\frac{1}{\rho}\frac{\partial}{\partial z}\left(\frac{S}{r}\right) = \frac{1}{\rho}\frac{Sz}{r^3} = 0 \text{ when } z = 0$$

The value of S in this case is not the same as that in Case I. Since the total current I flows out of a hemisphere,

$$I = -2\pi r^2 \frac{1}{\rho}\frac{\partial V}{\partial r} = \frac{2\pi S}{\rho}$$

and

$$S = \frac{I\rho}{2\pi}$$

Hence,

$$V = \frac{I\rho}{2\pi r} \tag{6}$$

By using Equation 6, it is possible to calculate the resistivity of an isotropic, homogeneous medium from the values of the potential observed at the boundary surface and the total current I flowing from the source. Suppose V is measured at a distance a and again at a distance $2a$ from

the current source. Let V_1 and V_2 be the values obtained at these two points. From Equation 6

$$V_1 = \frac{I\rho}{2\pi}\frac{1}{a} \text{ and } V_2 = \frac{I\rho}{2\pi}\frac{1}{2a}$$

In particular, if the source and the two points (a and $2a$) lie in a straight line,

$$V_1 - V_2 = \frac{I\rho}{2\pi}\left[\frac{1}{a} - \frac{1}{2a}\right] = \frac{I\rho}{4\pi a} \tag{7}$$

or

$$\rho = 4\pi a \frac{V_1 - V_2}{I}$$

In practice the conditions of this problem are approximately satisfied by placing the current or energizing electrodes at two widely spaced points and measuring the potential difference $V_1 - V_2$ between two points which are close to one of the energizing electrodes. This method is known as the uni-electrode method for measuring resistivity. †

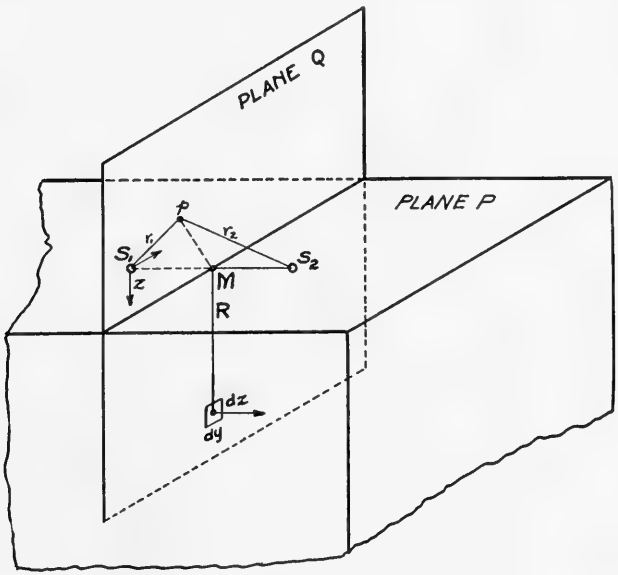

FIG. 282.—Source and sink in a delimiting plane.

Case III.—The conditions of Case II cannot be exactly satisfied in practice, because it is impractical to separate the two energizing electrodes by a sufficiently large distance. Practical measurements of resistivity, therefore, are based on the solution of a mathematical problem in which a source

† F. W. Lee, J. W. Joyce and P. Boyer, "Some Earth Resistivity Measurements," *U. S. Bur. of Mines Inform. Circ.* 6171 (1929).
L. Gilchrist, "Measurements of Resistivity by the Central Electrode Method at the Abana Mine, Northwestern Quebec, Canada," *A.I.M.E. Geophysical Prospecting*, Tech. Pub. 386 (1931).

and a sink of current are assumed to exist at a finite distance from each other. Consider the following problem. A source S_1 and a sink S_2 are located in a plane P delimiting a semi-finite, isotropic, homogeneous conductor of resistivity ρ. (See Figure 282.)

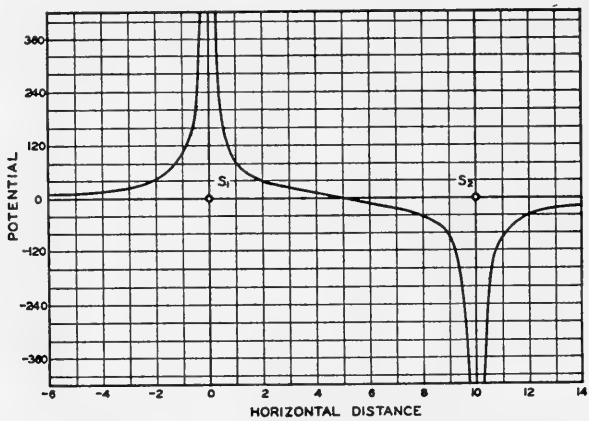

FIG. 283.—Variation of potential along line through current electrodes S_1 and S_2. (It should be noted that the potential curve is not correctly described by Equation 8 in the immediate vicinity of S_1 and S_2. It is evident from physical considerations that the potential must be finite at these points.)

The potential at any point p located at distances r_1 and r_2 from S_1 and S_2 is obtained by adding the potentials due to S_1 and S_2. The potential due to source S_1 is $V_1 = \frac{S_1}{r_1}$, and the potential due to sink S_2 is $V_2 = \frac{S_2}{r_2}$. Hence, the total potential V at p is

$$V = V_1 + V_2 = \frac{S_1}{r_1} + \frac{S_2}{r_2}$$

Since both V_1 and V_2 satisfy Equation 4, their sum satisfies Equation 4 at all points except the points where the source S_1 and the sink S_2 are located.

Also,

$$\frac{1}{\rho}\frac{\partial V}{\partial z} = 0 \text{ at } z = 0$$

If it is assumed that the total current I leaving from the source S_1 is equal to that entering the sink S_2, evaluation of the constants yields $S_1 = -S_2$ and $S_1 = \frac{I\rho}{2\pi}$ as in case II. Hence, the potential may be expressed by the equation

$$V = \frac{S_1}{r_1} + \frac{S_2}{r_2} = \frac{I\rho}{2\pi r_1} - \frac{I\rho}{2\pi r_2} = \frac{I\rho}{2\pi}\left(\frac{1}{r_1} - \frac{1}{r_2}\right) \qquad (8)$$

Equation 8 may be used to describe the distribution of potential and current in some detail. The variation of potential along the line through the electrodes S_1 and S_2 is plotted in Figure 283. Two features of this curve should be noted: (1) the large drop of potential that occurs near each electrode due to the high current densities in the immediate vicinity of the electrodes and (2) the fairly flat portion of the curve midway between the electrodes.*

The vertical section of the equipotential surfaces is shown in Figure 284 and the distribution of potential in the boundary plane containing the electrodes is shown in Figure 285.

Figure 286 shows the current per sq. cm. flowing through a vertical plane Q which intersects the line joining the two energizing electrodes at its midpoint M as a function of the ratio of the depth d to the electrode separation. Figure 287 shows the fraction of the total current which penetrates below a plane C located at a depth of d units as a function of the ratio of the depth d to the electrode separation. †

The equations needed for plotting Figures 286 and 287 may be derived as follows:

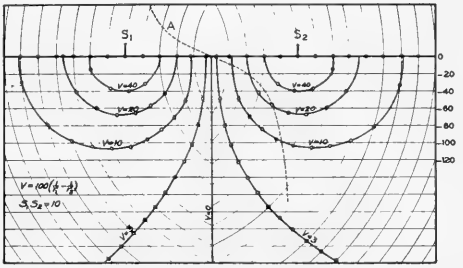

FIG. 284.—Vertical section of equipotential surfaces surrounding current electrodes S_1 and S_2. (Curve A shows the variation of potential along the surface of the ground.)

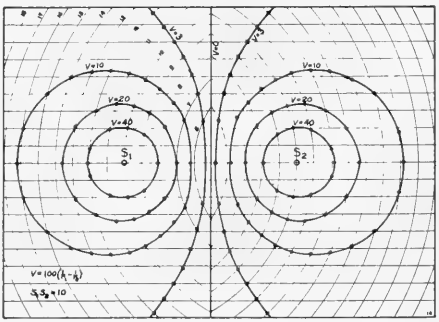

FIG. 285.—Distribution of potential in a plane P which contains a source S_1 and a sink S_2.

Let r_1 and r_2 be the distances of a point on a vertical plane Q from S_1 and S_2 respectively. Since the vertical plane Q is located midway between S_1 and S_2, the distance r_2 is equal in magnitude to the distance r_1. The current at the point (r_1, r_2) is

$$-\frac{1}{\rho}\frac{\partial V}{\partial x} = -\frac{S}{\rho}\frac{\partial}{\partial x}\left(\frac{1}{r_1} - \frac{1}{r_2}\right) = \frac{S}{\rho}\left(\frac{x}{r_1^3} - \frac{x-L}{r_2^3}\right)$$

or

$$-\frac{1}{\rho}\frac{\partial V}{\partial x} = \frac{SL}{r^3}$$

where L = distance between S_1 and S_2.

* Field work is usually planned so that the observational points (points at which the probe or potential electrodes are inserted into the ground) lie in the flat portion of the curve.

† See also W. Weaver, "Certain Applications of the Surface Potential Method," *A.I.M.E. Geophysical Prospecting*, 1929, p. 70.

From this equation the graph given in Figure 286 is readily obtained:

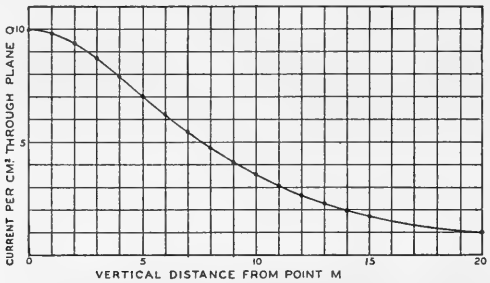

FIG. 286.—Current density versus depth in a plane Q which is normal to and midway between the energizing electrodes.

In order to calculate the fraction of the total current flowing below plane C, consider an element $dy\,dz$ of plane Q. The current flowing through this element is

$$-dy\,dz \cdot \frac{1}{\rho}\frac{\partial V}{\partial x}$$

Hence, the total current flowing below plane C is

$$I_d = -\int_d^{\infty}\int_{-\infty}^{+\infty}\frac{1}{\rho}\frac{\partial V}{\partial x}\,dy\,dz = \frac{SL}{\rho}\int_d^{\infty}\int_{-\infty}^{+\infty}\frac{dy\,dz}{r_1^3}$$

where

$$r_1^3 = \left[\left(\frac{L}{2}\right)^2 + y^2 + z^2\right]^{3/2}$$

To carry out the integration, it is convenient to make the following substitutions. Set

$$a^2 = \left(\frac{L}{2}\right)^2 + z^2$$

and set

$$y = a\tan\theta;\quad dy = a\sec^2\theta\,d\theta$$

Then

$$I_d = \frac{SL}{\rho}\int_d^{\infty}\left[\int_{-\pi/2}^{\pi/2}\frac{a\sec^2\theta\,d\theta}{a^3\sec^3\theta}\right]dz = \frac{SL}{\rho}\int_d^{\infty}\frac{2}{a^2}\,dz$$

$$= \frac{2SL}{\rho}\int_d^{\infty}\frac{dz}{(L/2)^2+z^2} = \frac{4S}{\rho}\left[\frac{\pi}{2} - \tan^{-1}\left(\frac{2d}{L}\right)\right]$$

Or on substituting the value for S and dividing through by I

$$\frac{I_d}{I} = \frac{2}{\pi}\left[\frac{\pi}{2} - \tan^{-1}\left(\frac{2d}{L}\right)\right]$$

Case IV: Layers of Different Materials.—The discussions of cases I, II, and III yielded expressions for the effective resistivity ρ of a homogeneous medium as a function of potential differences observed at the surface, distances measured along the surface (e.g., electrode separations), and the total current I passing between the energizing electrodes. In the present case (IV), a new concept appears: namely, variation of effective resistivity with depth.

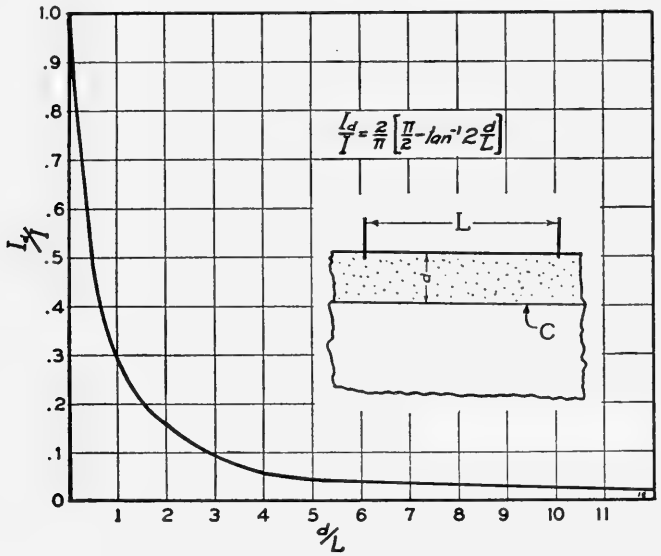

FIG. 287.—Plot of the fraction of the total current penetrating below a plane C located at a depth of d units versus the ratio of the depth d to the electrode separation L. Ratio of conductivity of upper to lower layer materials is 1:1. When the lower layer has a conductivity greater than the upper layer, the ratio I_d/I becomes smaller.

Suppose, for example, that for a given area explored by one of the methods described under Case III, it is found that the calculated values of ρ are the same for all electrode separations. Hence, if a plot of the values of the resistivity as ordinate against the values of the electrode separation as abscissa is a horizontal, straight line, one may infer that the subsurface structure is uniform. Generally, however, a resistivity graph of field data yields a complicated curve indicating that the average resistivity varies with depth below the surface. In this case, the description or deduction of subsurface conditions from the geoelectrical data may be quite difficult.

Physical considerations alone may yield useful information. Consider, for example, a semi-infinite medium of resistivity ρ_2 covered by a layer of resistivity ρ_1 and of thickness A. The source and the sink are placed at the boundary of the upper layer as shown in Figure 288. The following

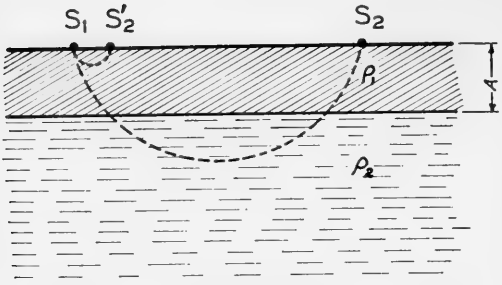

FIG. 288.—Current lines between two electrodes in a layered medium.

simple considerations indicate the type of solution to be expected: Suppose that the distance between S_1 and S'_2 is very small compared with A; only a small amount of current will flow into medium ρ_2 and the measurement of the resistivity by one of the methods described in Case III will yield a value of ρ nearly equal to ρ_1.

If, on the other hand, the electrode spacing is very large compared with the thickness A, the effect of the now relatively thin upper layer will generally be small, and the value of ρ obtained by one of the methods described in Case III will be nearly equal to ρ_2. The curve obtained on plotting ρ against $\overline{S_1S_2}$ resembles that shown in Figure 289. The region of transition AB occurs at values of $\overline{S_1S_2}$ comparable in magnitude with A.

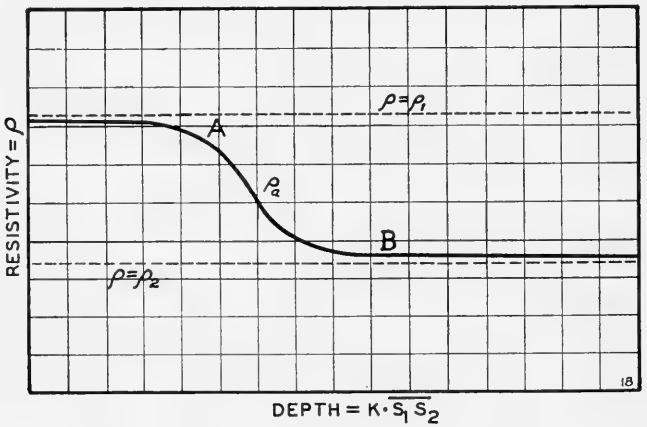

FIG. 289.—Schematic resistivity curve for two-layer structure.

Thus, in addition to enabling one to recognize a simple resistivity distribution, such considerations indicate the order of magnitude of the depth of the buried medium. It would be very difficult, however, to determine the exact depth from such physical considerations. It is much safer to refer to the exact mathematical solution of the two-layer problem.

Before considering the two-layer case, it will be of some interest to illustrate the use of the exact method by solving two simple problems by the method of images.†

† See J. A. Stratton, "Electromagnetic Theory," McGraw-Hill, 1941, p. 193.
W. R. Smythe, "Static and Dynamic Electricity," McGraw-Hill, 1939, pp. 69, 87, 283.
J. H. Jeans, "Mathematical Theory of Electricity and Magnetism," Cambridge Univ. Press, 1923, p. 200.

(1) A source of current S is placed at a distance A below a plane xy which delimits a semi-infinite medium of resistivity ρ. (Figure 290.) To obtain the solution of Laplace's equation, it will be convenient to introduce an image source S' (equal to S) at a distance A on the other side of the xy plane. It will also be convenient to assume, for the time being, that the medium of resistivity ρ extends beyond the xy plane. If S' is set equal to S, the value of the potential due to the two sources may be written

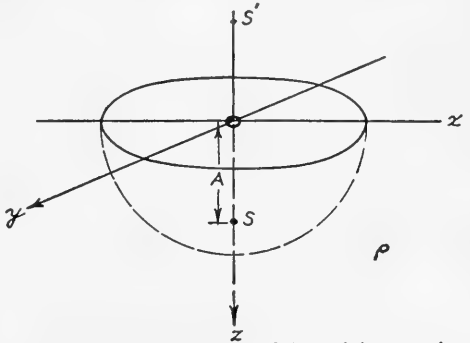

FIG. 290.—Current source S located in a semi-infinite medium of resistivity ρ at a distance A below the xy plane.

$$V = S\left\{\frac{1}{[r^2+(z-A)^2]^{1/2}} + \frac{1}{[r^2+(z+A)^2]^{1/2}}\right\} \tag{9}$$

where $r^2 = x^2 + y^2$.

This value of the potential satisfies the boundary condition that the current crossing the xy plane is zero, for

$$\left(\frac{1}{\rho}\frac{\partial V}{\partial z}\right)_{z=0} = \frac{S}{\rho}\left[\frac{(z-A)}{[r^2+(z-A)^2]^{3/2}} + \frac{(z+A)}{[r^2+(z+A)^2]^{3/2}}\right]_{z=0} = 0$$

Also, Laplace's equation $\nabla^2 V = 0$ is satisfied throughout the region below the plane xy except at S. The value of V given by the right hand side of Equation 9 does not hold for the region above the plane xy, because it makes V infinite at S'. Therefore, for the region investigated, i.e., for the region below the plane xy, Equation 9 is the required solution.

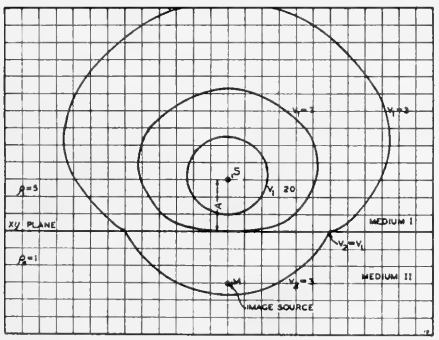

FIG. 291.—Small source of current ${}_1S$ placed at a distance A from the xy plane.

It is of interest to point out that this same procedure may be used to deduce the solution of the problem of two electrodes, a source and a sink, both buried at a distance A below a horizontal plane and thus arrive at a generalized solution for the problem treated under Case III.

(2) A plane xy separates two media having resistivities ρ_1 and ρ_2. (Figure 291.)

$$(\rho = \rho_1 \text{ for } z < 0, \quad \rho = \rho_2 \text{ for } z > 0)$$

A small source of current ${}_1S$ is placed at a distance A from the xy plane

in the negative direction. To arrive at the potential distribution, assume an image source ${}_1M$ on the other side of the plane.* The potential V_1 for the region $z < 0$ may be written

$$V_1 = \frac{{}_1S}{[r^2 + (z + A)^2]^{1/2}} + \frac{{}_1M}{[r^2 + (z - A)^2]^{1/2}} \tag{10}$$

where $r^2 = x^2 + y^2$, z is negative and A is positive.

The potential V_2 for the region $z > 0$ is a function of the distance from the source only; that is,

$$V_2 = \frac{{}_2S}{[r^2 + (z + A)^2]^{1/2}} \tag{10a}$$

where ${}_2S$ is a constant to be determined from the boundary conditions.

The boundary conditions are

$$\left.\begin{aligned} V_1 &= V_2 \\ \frac{1}{\rho_1}\frac{\partial V_1}{\partial z} &= \frac{1}{\rho_2}\frac{\partial V_2}{\partial z} \end{aligned}\right\} \text{ for } z = 0$$

If the boundary conditions are combined with Equations 10 and 10a, the following relations are obtained:

$${}_1S + {}_1M = {}_2S \tag{11}$$

and

$$\frac{1}{\rho_1}\left\{-\frac{{}_1S\,(z+A)}{[r^2 + (z+A)^2]^{1/2}} - \frac{{}_1M\,(z-A)}{[r^2 + (z-A)^2]^{1/2}}\right\}_{z=0} = \frac{1}{\rho_2}\left\{-\frac{{}_2S\,(z+A)}{[r^2 + (z+A)^2]^{1/2}}\right\}_{z=0}$$

or

$$\frac{{}_1SA}{\rho_1} - \frac{{}_1MA}{\rho_1} = \frac{{}_2SA}{\rho_2} \quad \text{or} \quad \frac{{}_1S}{\rho_1} - \frac{{}_1M}{\rho_1} = \frac{{}_2S}{\rho_2} \tag{12}$$

For Equations 11 and 12 to be true simultaneously, it is necessary that

$${}_2S = \left(\frac{2\rho_2}{\rho_1 + \rho_2}\right){}_1S \quad \text{and} \quad {}_1M = \left(\frac{\rho_2 - \rho_1}{\rho_2 + \rho_1}\right){}_1S$$

Hence, the potential may be expressed by the two equations

$$V_1 = \frac{{}_1S}{[r^2 + (z + A)^2]^{1/2}} + \left(\frac{\rho_2 - \rho_1}{\rho_2 + \rho_1}\right)\frac{{}_1S}{[r^2 + (z - A)^2]^{1/2}} \qquad z < 0$$

$$V_2 = \left(\frac{2\rho_2}{\rho_1 + \rho_2}\right)\frac{{}_1S}{[r^2 + (z + A)^2]^{1/2}} \qquad z > 0$$

The vertical cross sections of the equipotential surfaces close to ${}_1S$ are plotted in Figure 291 and their behavior is typical of what happens at the boundary of two conductors of different resistivities. In plotting these curves, values of $\rho_1 = 5$, $\rho_2 = 1$ and ${}_1S = 60$ were assumed.

* Note that in this case it is not assumed that ${}_1M$ and ${}_1S$ are equal in magnitude.

Mathematical Solution of the Two-Layer Problem

Consider a uniform layer (I) of thickness d and resistivity ρ_1 overlying a semi-infinite homogeneous medium (II) of resistivity ρ_2. This geological two-layer structure corresponds to an electrical three-layer problem, the third layer (0) being air. The "layer" of air lies above medium I and has a resistivity of $\rho_0 = \infty$. Assume that a source S_0 and a sink $-S_0$ are located at the boundary of media 0 and I. (Figure 292.)

As in case III, the solution is facilitated by considering the effects of the source and sink independently and then combining the effects. Further-

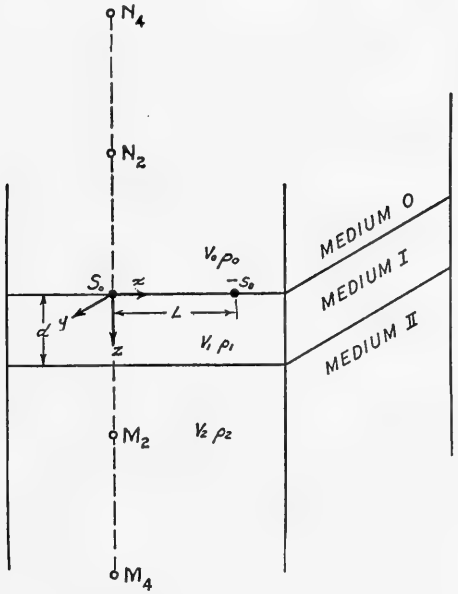

FIG. 292.—The case of three layers.

more the solution for the potential due to the sink $-S_0$ at any point on the line passing through the source and sink can be obtained from the solution for the potential due to the source S_0 by replacing x (the distance of the point from S_0) by $L - x$ where L is the distance between the source and sink. Thus the problem reduces to calculating the potential due to the source S_0. This is most readily accomplished by assuming that in addition to S_0 there exists an infinite number of images of S_0.† It will be evident from the preceding problem that the relative magnitudes of the current source and its electrical images will depend on the values of the resistivities of the media in which the images are assumed to exist. Thus the solution of the problem consists, essentially, in determining the relative magnitudes of these images.

† J. H. Jeans, *loc. cit.*

Designate the potential values in the media 0, I, and II by V_0, V_1, and V_2 respectively. Let M_2 be the electrical image of S_0 in medium II, N_2 the electrical image of M_2 in medium 0, M_4 the electrical image of N_2 in medium II and so on *ad infinitum*, all the images in medium II being denoted by M, those in medium 0 by N and the subscript denoting the distance of the image from the plane bounding media 0 and I in terms of the thickness d of the layer I as unity; i.e., each image is distant from S_0 according to

$$2d + \text{(the distance of the source, of which it is an image, from } S_0\text{)}$$

For example,

$$\begin{aligned}
\text{distance from } S_0 \text{ of } M_2 &= 2d + \text{(distance of } S_0 \text{ from } S_0\text{)} \\
&= 2d + 0 \\
\text{distance from } S_0 \text{ of } N_2 &= 2d \\
\text{distance from } S_0 \text{ of } M_4 &= 2d + \text{distance of } N_2 \text{ from } S_0 \\
&= 2d + 2d \\
&= 4d \\
&\text{etc.}
\end{aligned}$$

V_0 may be expressed as the sum of potentials due to S_0 and the images M in medium II; i.e.,

$$V_0 = \frac{S_0}{[r^2+z^2]^{1/2}} + \frac{M_2}{[r^2+(2d-z)^2]^{1/2}} + \frac{M_4}{[r^2+(4d-z)^2]^{1/2}} + \cdots$$

where $r^2 = x^2 + y^2$ and S_0, M_2, M_4, etc., are constants to be evaluated later, and z is negative.

Similarly, V_2 is the sum of the potentials due to S_0 and the images N in medium 0. V_1, however, is due to the source S_0 and to the images M and N in medium II and medium 0. Thus, the potentials in the three media are given by the equations:

$$V_0 = \frac{{}_0S_0}{[r^2+z^2]^{1/2}} + \frac{{}_0M_2}{[r^2+(2d-z)^2]^{1/2}} + \frac{{}_0M_4}{[r^2+(4d-z)^2]^{1/2}}$$

$$+ \cdots = \frac{{}_0S_0}{[r^2+z^2]^{1/2}} + \sum_{k=1}^{\infty} \frac{{}_0M_{2k}}{[r^2+(2kd-z)^2]^{1/2}}$$

with z negative.

$$V_2 = \frac{{}_2S_0}{[r^2+z^2]^{1/2}} + \frac{{}_2N_2}{[r^2+(2d+z)^2]^{1/2}} + \frac{{}_2N_4}{[r^2+(4d+z)^2]^{1/2}}$$

$$+ \cdots = \frac{{}_2S_0}{[r^2+z^2]^{1/2}} + \sum_{k=1}^{\infty} \frac{{}_2N_{2k}}{[r^2+(2kd+z)^2]^{1/2}}$$

z positive.

$$V_1 = \frac{{}_1S_0}{[r^2+z^2]^{1/2}} + \frac{{}_1M_2}{[r^2+(2d-z)^2]^{1/2}} + \frac{{}_1M_4}{[r^2+(4d-z)^2]^{1/2}} + \cdots$$

$$+ \frac{{}_1N_2}{[r^2+(2d+z)^2]^{1/2}} + \frac{{}_1N_4}{[r^2+(4d+z)^2]^{1/2}} + \cdots$$

$$= \frac{{}_1S_0}{[r^2+z^2]^{1/2}} + \sum_{k=1}^{\infty} \frac{{}_1M_{2k}}{[r^2+(2kd-z)^2]^{1/2}} + \sum_{k=1}^{\infty} \frac{{}_1N_{2k}}{[r^2+(2kd+z)^2]^{1/2}}$$

z positive.

All of these potentials satisfy Laplace's equation (4). If it can be proved that they also satisfy the boundary conditions, they will constitute the exact and unique

solution of the problem. The boundary conditions to be satisfied at the boundary of medium 0 and medium I are:

$$V_0 = V_1$$

and

$$\frac{1}{\rho_0}\frac{\partial V_0}{\partial z} = \frac{1}{\rho_1}\frac{\partial V_1}{\partial z} \text{ at } z = 0, r \text{ arbitrary}$$

Likewise at the boundary of medium I and medium II,

$$V_1 = V_2$$

and

$$\frac{1}{\rho_1}\frac{\partial V_1}{\partial z} = \frac{1}{\rho_2}\frac{\partial V_2}{\partial z} \text{ at } z = d, r \text{ arbitrary}$$

Each of these four conditions results in a number of equations involving the unknown parameters S_0, M_k, and N_k. The first condition at $z = 0$, namely $V_0 = V_1$, requires that

$$\frac{{}_0S_0}{r} + \sum_{k=1}^{\infty}\frac{{}_0M_{2k}}{[r^2+(2kd)^2]^{1/2}} = \frac{{}_1S_0}{r} + \sum_{k=1}^{\infty}\frac{{}_1M_{2k}}{[r^2+(2kd)^2]^{1/2}} + \sum_{k=1}^{\infty}\frac{{}_1N_{2k}}{[r^2+(2kd)^2]^{1/2}}$$

For this equality to hold for all values of r the corresponding terms of the summation, i.e., those having the same denominators, must be equal. This gives

$${}_0S_0 = {}_1S_0$$
$${}_0M_{2k} = {}_1M_{2k} + {}_1N_{2k} \text{ for } k = 1, 2, 3 \cdots$$

The second condition, $\frac{1}{\rho_0}\frac{\partial V_0}{\partial z} = \frac{1}{\rho_1}\frac{\partial V_1}{\partial z}$, requires that

$$\frac{1}{\rho_0}\left\{-\frac{{}_0S_0\,z}{[r^2+z^2]^{3/2}} + \sum_{k=1}^{\infty}\frac{{}_0M_{2k}\,(2kd-z)}{[r^2+(2kd-z)^2]^{3/2}}\right\}_{z=0} = \frac{1}{\rho_1}\left\{-\frac{{}_1S_0\,z}{[r^2+z^2]^{3/2}}\right.$$
$$\left. + \sum_{k=1}^{\infty}\frac{{}_1M_{2k}\,(2kd-z)}{[r^2+(2kd-z)^2]^{3/2}} - \sum_{k=1}^{\infty}\frac{{}_1N_{2k}\,(2kd+z)}{[r^2+(2kd+z)^2]^{3/2}}\right\}_{z=0}$$

or

$$\frac{1}{\rho_0}\sum_{k=1}^{\infty}\frac{{}_0M_{2k}\,(2kd)}{[r^2+(2kd)^2]^{3/2}} = \frac{1}{\rho_1}\left\{\sum_{k=1}^{\infty}\frac{{}_1M_{2k}\,(2kd)}{[r^2+(2kd)^2]^{3/2}} - \sum_{k=1}^{\infty}\frac{{}_1N_{2k}\,(2kd)}{[r^2+(2kd)^2]^{1/2}}\right\}$$

The corresponding terms in both members of the equation have the same denominators; hence

$$\frac{1}{\rho_0}\,{}_0M_{2k} = \frac{1}{\rho_1}\,{}_1M_{2k} - \frac{1}{\rho_1}\,{}_1N_{2k}$$

The boundary conditions at $z = d$ yield another set of equations between the constants. The condition $V_1 = V_2$ at $z = d$ requires that

$$\frac{{}_1S_0}{[r^2+d^2]^{1/2}} + \sum_{k=1}^{\infty}\frac{{}_1M_{2k}}{[r^2+(2k-1)^2\,d^2]^{1/2}} + \sum_{k=1}^{\infty}\frac{{}_1N_{2k}}{[r^2+(2k+1)^2\,d^2]^{1/2}}$$
$$= \frac{{}_2S_0}{[r^2+d^2]^{1/2}} + \sum_{k=1}^{\infty}\frac{{}_2N_{2k}}{[r^2+(2k+1)^2\,d^2]^{1/2}}$$

Equating corresponding terms of the summation yields

$${}_1S_0 + {}_1M_2 = {}_2S_0 \text{ for } k = 1.$$

and

$${}_1M_{2k} + {}_1N_{2(k-1)} = {}_2N_{2(k-1)} \text{ for } k = 2, 3, 4 \cdots$$

The condition $\frac{1}{\rho_1}\frac{\partial V_1}{\partial z} = \frac{1}{\rho_2}\frac{\partial V_2}{\partial z}$ at $z = d$ requires that

$$\frac{1}{\rho_1}\left\{-\frac{{}_1S_0\, z}{[r^2+z^2]^{3/2}} + \sum_{k=1}^{\infty}\frac{{}_1M_{2k}\,(2kd-z)}{[r^2+(2kd-z)^2]^{3/2}} - \sum_{k=1}^{\infty}\frac{{}_1N_{2k}\,(2kd+z)}{[r^2+(2kd+z)^2]^{3/2}}\right\}_{z=d}$$
$$= \frac{1}{\rho_2}\left\{-\frac{{}_2S_0\, z}{[r^2+z^2]^{3/2}} - \sum_{k=1}^{\infty}\frac{{}_2N_{2k}\,(2kd+z)}{[r^2+(2kd+z)^2]^{3/2}}\right\}_{z=d}$$

or

$$\frac{1}{\rho_1}\left\{\frac{{}_1S_0\, d}{[r^2+d^2]^{3/2}} - \sum_{k=1}^{\infty}\frac{{}_1M_{2k}\,(2k-1)\,d}{[r^2+(2k-1)^2\,d^2]^{3/2}} + \sum_{k=1}^{\infty}\frac{{}_1N_{2k}\,(2k+1)\,d}{[r^2+(2k+1)^2\,d^2]^{3/2}}\right\}$$
$$= \frac{1}{\rho_2}\left\{\frac{{}_2S_0\, d}{[r^2+d^2]^{3/2}} + \sum_{k=1}^{\infty}\frac{{}_2N_{2k}\,(2k+1)\,d}{[r^2+(2k+1)^2\,d^2]^{3/2}}\right\}$$

Equating corresponding terms of the summation yields

$$\frac{{}_1S_0}{\rho_1} - \frac{{}_1M_2}{\rho_1} = \frac{{}_2S_0}{\rho_2} \text{ for } k = 1.$$

and

$$\frac{1}{\rho_1}\{-(2k-1)\,d\,{}_1M_{2k} + (2k-1)\,d\,{}_1N_{2(k-1)}\} = \frac{1}{\rho_2}(2k-1)\,d\,{}_2N_{2(k-1)}$$

or

$$-\frac{{}_1M_{2k}}{\rho_1} + \frac{{}_1N_{2(k-1)}}{\rho_1} = \frac{{}_2N_{2(k-1)}}{\rho_2} \text{ for } k = 2, 3, 4 \cdots$$

Thus, the boundary conditions have yielded the following relations between the constants S_0, M_k and N_k:

(a) ${}_0S_0 = {}_1S_0$

(b) ${}_0M_{2k} = {}_1M_{2k} + {}_1N_{2k}$ for $k = 1, 2, 3 \cdots$

(c) $\frac{{}_0M_{2k}}{\rho_0} = \frac{{}_1M_{2k}}{\rho_1} - \frac{{}_1N_{2k}}{\rho_1}$ for $k = 1, 2, 3 \cdots$

(d) ${}_1S_0 + {}_1M_2 = {}_2S_0$

(e) ${}_1M_{2k} + {}_1N_{2(k-1)} = {}_2N_{2(k-1)}$ for $k = 2, 3, 4 \cdots$

(f) $\frac{{}_1S_0}{\rho_1} - \frac{{}_1M_2}{\rho_1} = \frac{{}_2S_0}{\rho_2}$

(g) $-\frac{{}_1M_{2k}}{\rho_1} + \frac{{}_1N_{2(k-1)}}{\rho_1} = \frac{{}_2N_{2(k-1)}}{\rho_2}$ for $k = 2, 3, 4 \cdots$

On combining Equations (b) and (c), we obtain

$${}_0M_{2k} = \left(\frac{2\rho_0}{\rho_0+\rho_1}\right){}_1M_{2k} \text{ and } {}_1N_{2k} = \left(\frac{\rho_0-\rho_1}{\rho_0+\rho_1}\right){}_1M_{2k}$$

From Equations (e) and (g), we obtain

$${}_2N_{2(k-1)} = \left(\frac{2\rho_2}{\rho_1+\rho_2}\right){}_1N_{2(k-1)} \text{ and } {}_1M_{2k} = \left(\frac{\rho_2-\rho_1}{\rho_2+\rho_1}\right){}_1N_{2(k-1)}$$

From Equations (d) and (f), we obtain

$${}_2S_0 = \left(\frac{2\rho_2}{\rho_2+\rho_1}\right){}_1S_0 \text{ and } {}_1M_2 = \left(\frac{\rho_2-\rho_1}{\rho_2+\rho_1}\right){}_1S_0$$

Let

$$Q_1 = \frac{\rho_0-\rho_1}{\rho_0+\rho_1} \text{ and } Q_2 = \frac{\rho_2-\rho_1}{\rho_2+\rho_1}$$

Then

$$\frac{2\rho_0}{\rho_0+\rho_1} = 1+Q_1, \quad \frac{2\rho_2}{\rho_2+\rho_1} = 1+Q_2$$

and

$$
\begin{aligned}
{}_0M_{2k} &= (1+Q_1)\ {}_1M_{2k} \text{ for } k=1,2,3\cdots\\
{}_1N_{2k} &= Q_1\ {}_1M_{2k} \text{ for } k=1,2,3\cdots\\
{}_2N_{2(k-1)} &= (1+Q_2)\ {}_1N_{2(k-1)} \text{ for } k=2,3,4\cdots\\
{}_1M_{2k} &= Q_2\ {}_1N_{2(k-1)} \text{ for } k=2,3,4\cdots\\
{}_1M_2 &= Q_2\ {}_1S_0\\
{}_2S_0 &= (1+Q_2)\ {}_1S_0
\end{aligned}
$$

Also,

$${}_1S_0 = {}_0S_0$$

These equations may be expressed in terms of one parameter S_0 as follows:

$${}_1N_{2k} = Q_1\ {}_1M_{2k} = Q_1 Q_2\ {}_1N_{2(k-1)} = Q_1^2 Q_2\ {}_1M_{2(k-1)} = (Q_1 Q_2)^2\ {}_1N_{2(k-2)}$$

or

$${}_1N_{2k} = (Q_1 Q_2)^n\ {}_1N_{2(k-n)}$$

In particular, for $k-n=1$ or $n=k-1$

$${}_1N_{2k} = (Q_1 Q_2)^{k-1}\ {}_1N_2 = Q_1 (Q_1 Q_2)^{k-1}\ {}_1M_2 = (Q_1 Q_2)^k\ {}_1S_0 = (Q_1 Q_2)^k\ {}_0S_0$$

Also,

$$
\begin{aligned}
{}_1M_{2k} &= \frac{{}_1N_{2k}}{Q_1} = \frac{(Q_1 Q_2)^k}{Q_1}\ {}_0S_0 = Q_1^{k-1} Q_1^k\ {}_0S_0\\
{}_0M_{2k} &= (1+Q_1)\ {}_1M_{2k} = (1+Q_1)\ (Q_1^{k-1} Q_2^k)\ {}_0S_0\\
{}_2N_{2k} &= (1+Q_2)\ {}_1N_{2k} = (1+Q_2)\ (Q_1 Q_2)^k\ {}_0S_0\\
{}_2S_0 &= (1+Q_2)\ {}_0S_0
\end{aligned}
$$

It remains now to find ${}_0S_0$ itself. Consider a very small sphere surrounding the real source of current S_0 or ${}_0S_0$. The total current is the sum of two currents: namely, I_0 which flows into medium 0 through a hemisphere and I_1 which flows into medium I also through a hemisphere. If the radius r_1 of the sphere is negligible relative to d, all terms except the first may be neglected in the expressions for V_0 and V_1. That is,

$$V_0 = \frac{{}_0S_0}{(r^2+z^2)^{1/2}} = \frac{{}_0S_0}{r_1}$$

and

$$V_1 = \frac{{}_1S_0}{[r^2+z^2]^{1/2}} = \frac{{}_0S_0}{r_1}$$

where r_1 = radius of sphere $= (r^2+z^2)^{1/2}$

The current flowing into medium 0 is

$$I_0 = -\frac{1}{\rho_0}\frac{\partial V_0}{\partial r_1} \cdot 2\pi r_1^2 = 2\pi\ {}_0S_0$$

while the current flowing into medium I is

$$I_1 = -\frac{1}{\rho_1}\frac{\partial V_1}{\partial r_1} \cdot 2\pi r_1^2 = 2\pi\ {}_0S_0$$

The total current is thus

$$I = I_0 + I_1 = 2\pi \left(\frac{1}{\rho_0} + \frac{1}{\rho_1}\right) {}_0S_0$$

so that

$${}_0S_0 = \frac{I}{2\pi} \frac{1}{\left(\frac{1}{\rho_0} + \frac{1}{\rho_1}\right)}$$

or

$${}_0S_0 = \frac{I}{4\pi}\rho_1 (1+Q_1)$$

All the potentials can now be written in terms of I, Q_1, and Q_2. We shall only

make use of the expression for V_0. Evidently,

$$V_0 = \frac{{}_0S_0}{[r^2+z^2]^{\frac{1}{2}}} + \sum_{k=1}^{\infty} \frac{{}_0M_{2k}}{[r^2+(2kd-z)^2]^{\frac{1}{2}}}$$

$$= \frac{{}_0S_0}{[r^2+z^2]^{\frac{1}{2}}} + \sum_{k=1}^{\infty} \frac{(1+Q_1)\,Q_1^{k-1}\,Q_2^{k}\,{}_0S_0}{[r^2+(2kd-z)^2]^{\frac{1}{2}}}$$

$$= \frac{I}{4\pi}\,\rho_1\,(1+Q_1)\left[\frac{1}{[r^2+z^2]^{\frac{1}{2}}} + \sum_{k=1}^{\infty} \frac{(1+Q_1)\,Q_1^{k-1}\,Q_2^{k}}{[r^2+(2kd-z)^2]^{\frac{1}{2}}}\right]$$

In particular, at the boundary between layers 0 and I ($z=0$)

$$V_0 = \frac{I}{4\pi}\,\rho_1\,(1+Q_1)\left[\frac{1}{r} + \sum_{k=1}^{\infty} \frac{(1+Q_1)\,Q_1^{k-1}\,Q_2^{k}}{[r^2+(2kd)^2]^{\frac{1}{2}}}\right] \tag{13}$$

Equation 13 is the general solution for the potential produced by the current source S_0 at the boundary separating layers 0 and I.

When medium 0 is air, $\rho_0 = \infty$. Also,

$$Q_1 = \frac{\rho_0-\rho_1}{\rho_0+\rho_1} = \frac{1-\frac{\rho_1}{\rho_0}}{1+\frac{\rho_1}{\rho_0}} = \frac{1-\frac{\rho_1}{\infty}}{1+\frac{\rho_1}{\infty}} = 1$$

Hence, V_0 can be written as follows:

$$V_0 = \frac{I}{2\pi}\,\rho_1\left[\frac{1}{r} + 2\sum_{k=1}^{\infty} \frac{Q_2^{k}}{[r^2+(2kd)^2]^{\frac{1}{2}}}\right]$$

or

$$V_0 = \frac{I}{2\pi}\,\frac{\rho_1}{r}\left\{1+2\sum_{k=1}^{\infty} \frac{Q_2^{k}}{\left[1+\left(\frac{2d}{r}\right)^2 k^2\right]^{\frac{1}{2}}}\right\} \tag{14}$$

Equation 14 expresses the potential at any point on the surface of the ground due to a current source S_0.*

If a sink of strength $-S_0$ is now added at a distance $x=L$ where x is measured along the line passing through the source and sink (Figure 292), the potential V_0' produced by the sink at any point on the x axis is:

$$V_0' = \frac{-I\rho_1}{2\pi}\left\{\frac{1}{L-x} + 2\sum_{k=1}^{\infty} \frac{Q_2^{k}}{[(L-x)^2+4k^2d^2]^{\frac{1}{2}}}\right\} \tag{15}$$

The total potential produced by the source and sink is obtained by adding V_0 and V_0'.

In the Roman tables, values of $W = \sum_{k=1}^{\infty} Q^k \left\{\frac{1}{k} - \frac{1}{\sqrt{k^2+a^2}}\right\}$ are given for the arguments Q and a.

* For calculations involving this formula it is convenient to use the tables given by Irwin Roman in an article entitled "How to Compute Tables for Determining Electrical Resistivity of Underlying Beds and Their Application to Geophysical Problems." (Technical Paper 502 U. S. Department of Commerce.)

The use of these tables is facilitated by noting that

$$W = \sum Q^k \left\{ \frac{1}{k} - \frac{1}{\sqrt{k^2 + a^2}} \right\} = \sum \frac{Q^k}{a} \left\{ \frac{1}{\frac{k}{a}} - \frac{1}{\sqrt{1 + \left(\frac{k}{a}\right)^2}} \right\}$$

or

$$\sum \frac{Q^k}{a} \left\{ \frac{1}{\sqrt{1 + \left(\frac{k}{a}\right)^2}} \right\} = \sum \frac{Q^k}{k} - W = -\log (1 - Q^k) - W$$

Whence

$$\sum_{k=1}^{\infty} \frac{Q^k}{\sqrt{1 + \frac{k^2}{a^2}}} = -a \log (1 - Q^k) - a W$$

The left-hand member of this equation is identical with the expression

$$\sum_{k=1}^{\infty} \frac{Q_2{}^k}{\left[1 + \left(\frac{2d}{r}\right)^2 k^2\right]^{1/2}}$$

appearing in Equation 14 provided one sets $a = \frac{r}{2d}$

For most calculations only the difference in potential between two points is used and the logarithmic term will enter the equations as an additive constant independent of r. Hence, the logarithmic term can always be dropped, because the potential is not unique to an additive constant.

The potential V at any point on the x axis is

$$V = \frac{I\rho_1}{2\pi} \left\{ \frac{1}{x} - \frac{1}{L - x} + 2 \sum_{k=1}^{\infty} \frac{Q_2{}^k}{[x^2 + 4k^2d^2]^{1/2}} - 2 \sum_{k=1}^{\infty} \frac{Q_2{}^k}{[(L - x)^2 + 4k^2d^2]^{1/2}} \right\} \quad (16)$$

where I = current leaving the source at S_0 (Figure 292).

ρ_1 = resistivity of overburden.

ρ_2 = resistivity of subsurface layer.

$Q_2 = \frac{\rho_2 - \rho_1}{\rho_2 + \rho_1}$

x = distance between S_0 and the point on the surface at which the potential is V.

L = separation of energizing electrodes (S_0 and $-S_0$).

d = thickness of overburden.

Application to Wenner Electrode Configuration.—The Wenner configuration consists of four electrodes mounted in a straight line along the surface of the ground at distances 0, a, $2a$, and $3a$ respectively. If the power is applied between the outer two electrodes, the expression for the potential produced at either of the two inner electrodes may be obtained from Equation 16 by replacing L by $3a$. That is,

$$V = \frac{I\rho_1}{2\pi} \left\{ \frac{1}{x} - \frac{1}{3a - x} + 2 \sum_{k=1}^{\infty} \frac{Q_2{}^k}{[x^2 + 4k^2d^2]^{1/2}} - 2 \sum_{k=1}^{\infty} \frac{Q_2{}^k}{[(3a - x)^2 + 4k^2d^2]^{1/2}} \right\}$$

The potential difference between the two inner potential electrodes is found by substituting $x = a$ and then $x = 2a$ into the above formula and

forming the difference of the two resulting equations. That is,

$$E = V_a - V_{2a} = \frac{I\rho_1}{2\pi}\left\{\frac{1}{a} - \frac{1}{2a} + 2\sum_{k=1}^{\infty}\frac{Q_2{}^k}{[a^2+4k^2d^2]^{\frac{1}{2}}} - 2\sum_{k=1}^{\infty}\frac{Q_2{}^k}{[4a^2+4k^2d^2]^{\frac{1}{2}}}\right.$$

$$\left. - \frac{1}{2a} + \frac{1}{a} - 2\sum_{k=1}^{\infty}\frac{Q_2{}^k}{[4a^2+4k^2d^2]^{\frac{1}{2}}} + 2\sum_{k=1}^{\infty}\frac{Q_2{}^k}{[a^2+4k^2d^2]^{\frac{1}{2}}}\right\}$$

or

$$E = \frac{I\rho_1}{2\pi}\left\{\frac{1}{a} + 4\sum_{k=1}^{\infty}\frac{Q_2{}^k}{[a^2+4k^2d^2]^{\frac{1}{2}}} - 2\sum_{k=1}^{\infty}\frac{Q_2{}^k}{[a^2+k^2d^2]^{\frac{1}{2}}}\right\} \quad (17)$$

Equation 17 is the generalized formula which applies when the geological structure consists of a semi-infinite medium of resistivity ρ_2 overlain by a homogeneous overburden of resistivity ρ_1.

In particular, if $\rho_1 = \rho_2 = \rho_a$, $Q_2 = 0$, and

$$E = \frac{I\rho_a}{2\pi a}$$

or

$$\rho_a = 2\pi a\frac{E}{I} \quad (18)$$

Equation 18 is known as Wenner's formula.* Evidently this formula gives an average resistivity ρ_a for the area under investigation in terms of measurable quantities (E/I and a). The average or apparent resistivity ρ_a is a mean or weighted value of the resistivity which is equal to the actual resistivity only if the ground is isotropic and homogeneous.

In interpreting experimental data obtained with a Wenner configuration of electrodes, the conventional procedure is to plot the average resistivity calculated from Equation 18 as a function of the electrode separation.** For an ideal two-layer case, the curve has the equation

$$\rho_a = 2\pi a\frac{E}{I} = a\rho_1\left\{\frac{1}{a} + 4\sum_{k=1}^{\infty}\frac{Q_2{}^k}{[a^2+4k^2d^2]^{\frac{1}{2}}} - 2\sum_{k=1}^{\infty}\frac{Q_2{}^k}{[a^2+k^2d^2]^{\frac{1}{2}}}\right\}$$

or

$$\frac{\rho_a}{\rho_1} = \left\{1 + 4\sum_{k=1}^{\infty}\frac{Q_2{}^k}{\left[1+4k^2\left(\frac{d}{a}\right)^2\right]^{\frac{1}{2}}} - 2\sum_{k=1}^{\infty}\frac{Q_2{}^k}{\left[1+k^2\left(\frac{d}{a}\right)^2\right]^{\frac{1}{2}}}\right\} \quad (19)$$

* Equation 18 may also be obtained by computing the potential difference between the two potential electrodes from Equation 8.

** In investigations not employing the Wenner configuration, Equation 18 does not obtain. However, it is always possible to plot the average resistivity as a function of the electrode separation by deriving an equation which expresses the apparent resistivity ρ_a as a function of measurable quantities (E/I and electrode separations). (Compare p. 518.)

The quantities ρ_a and ρ_1 can be obtained from measurements taken at the surface, since ρ_a is equal to ρ_1 for $a << d$ (electrode separation small relative to the thickness of the overburden).

Tagg's Graphical Method.—Figure 293 represents a two-layer structure comprising a bed of resistivity ρ_1 and thickness d overlying a medium of resistivity ρ_2 and infinite extent.† A Wenner electrode configuration for measuring the apparent resistivity is shown schematically in the upper portion of the figure.

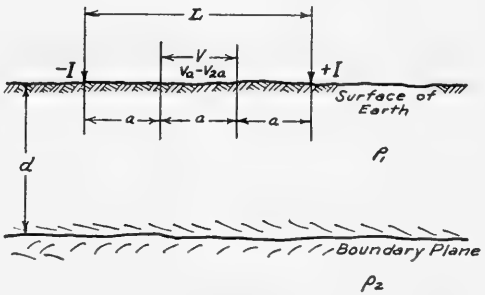

FIG. 293.—Wenner configuration applied to a two-layer structure.

The depth d to the lower formation is obtained by making use of Equation 19 and the relation $Q_2 = \dfrac{\rho_2 - \rho_1}{\rho_2 + \rho_1} = \dfrac{1 - \rho_1/\rho_2}{1 + \rho_1/\rho_2}$. It is clear that the two "unknowns" in Equation 19 are Q_2 and d/a. Also, it follows from the relation $Q_2 = \dfrac{1 - \rho_1/\rho_2}{1 + \rho_1/\rho_2}$ that Q_2 depends only on the ratio ρ_1/ρ_2. Also, Q_2 can only take on values between + 1 and − 1, corresponding to the values between the extreme conditions $\rho_1 << \rho_2$ and $\rho_1 >> \rho_2$ respectively.

The computed values of ρ_1/ρ_2 corresponding to various assumed values of Q_2 are given in Table 16, where $\dfrac{\rho_1}{\rho_2} = \dfrac{1 - Q_2}{1 + Q_2}$.

It is possible to calculate the ratio of the average resistivity to the resistivity in the upper stratum, ρ_a/ρ_1, by *assuming* various values for Q_2 and the ratio d/a. (Compare Equation 19.) This is done most conveniently by a graphical method. When Q_2 is positive, i.e., when ρ_2 is greater than ρ_1, it is convenient to use the ratio of the conductivities σ_a/σ_1, instead of ρ_a/ρ_1. (σ_a is the apparent conductivity and is equal to $1/\rho_a$, while σ_1 is the conductivity of the upper stratum and is equal to $1/\rho_1$.)

This follows from Equation 19

$$\frac{\rho_a}{\rho_1} = 1 + 4S$$

where

$$S = \sum_{k=1}^{\infty} \left\{ \frac{{Q_2}^k}{\left[1 + 4k^2\left(\frac{d}{a}\right)^2\right]^{1/2}} - \frac{{Q_2}^k}{\left[4 + 4k^2\left(\frac{d}{a}\right)^2\right]^{1/2}} \right\}$$

† G. F. Tagg, "Interpretation of Resistivity Measurements," *A.I.M.E. Geophysical Prospecting*, 1934, pp. 135-145.

TABLE 16.

COMPUTED VALUES OF ρ_1/ρ_2 CORRESPONDING TO VARIOUS ASSUMED VALUES OF Q_2†

Q_2	ρ_1/ρ_2	Q_2	ρ_1/ρ_2
1.0	1/∞	— 1.0	∞
0.9	1/19	— 0.9	19
0.8	1/9	— 0.8	9
0.7	1/5.67	— 0.7	5.67
0.6	1/4	— 0.6	4
0.5	1/3	— 0.5	3
0.4	1/2.33	— 0.4	2.33
0.3	1/1.86	— 0.3	1.86
0.2	1/1.5	— 0.2	1.5
0.1	1/1.22	— 0.1	1.22
0.0	1/1	0.0	1

When Q_2 is positive $(0 \leq Q_2 \leq 1)$ then $S \geq 0$ and therefore

$$\frac{\rho_a}{\rho_1} \geq 1 \quad \text{or} \quad 0 \leq \frac{\sigma_a}{\sigma_1} \leq 1.$$

When Q_2 is negative $(Q_2 \leq 0$ and $0 \leq |Q_2| \leq 1)$ then

$$S \leq 0 \text{ and } 0 \leq |S| \leq \tfrac{1}{4} \qquad \text{and}$$

therefore

$$0 \leq \frac{\rho_a}{\rho_1} \leq 1.$$

Families of curves showing the relationship between σ_a/σ_1 and d/a when Q_2 is positive and the relationship between ρ_a/ρ_1 and d/a when Q_2 is negative, for a given set of conditions, are shown in Figure 294.

In the practical case the apparent resistivity, ρ_a, as a function of the electrode separation, a, is known from measurements and application of Equation 18, while the surface resistivity, ρ_1, is obtained from similar measurements with small electrode separations. The procedure then in determining depth is almost the reverse of that for determining the sample $\frac{\rho_a}{\rho_1}$ curves as described above. That is, the $\frac{\rho_a}{\rho_1}$ vs. d/a curves for various Q_2's were determined by assuming values for Q_2 and d/a. In the practical case,

† Tagg, *A.I.M.E. Geophysical Prospecting*, Vol. 110, 1934.

the ratio for each a is known and Q_2 corresponding to various d/a ratios can be read from the curves. Since the electrode separation, a, is known for each set of values, we have corresponding values of Q_2 and d for each $\frac{\rho_a}{\rho_1}$

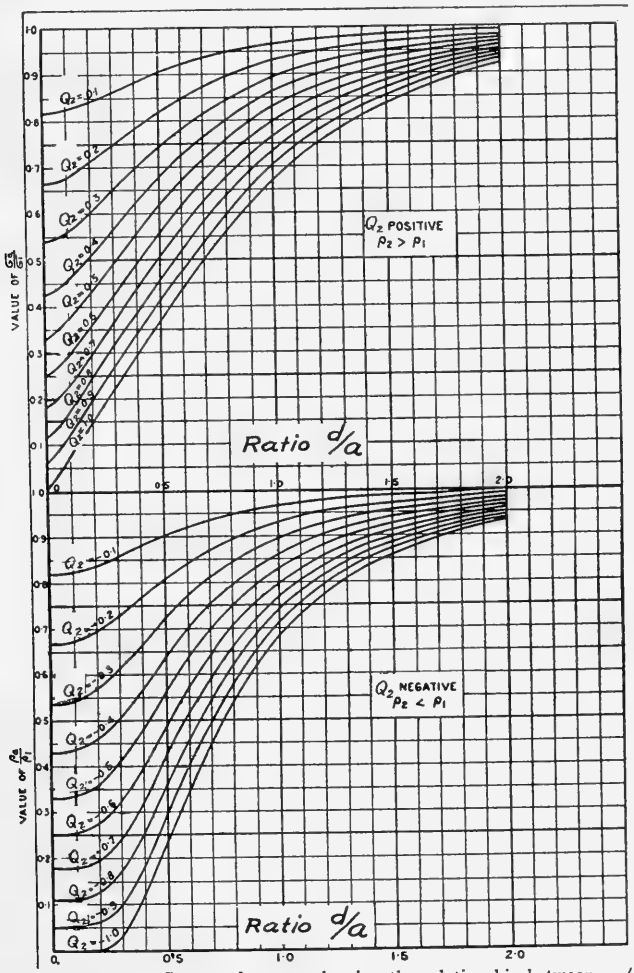

FIG. 294.—Computed curves showing the relationship between σ_a/σ_1, ρ_a/ρ_1, and d/a for various values of Q_2. (Tagg, *A.I.M.E. Geophysical Prospecting*, 1934.)

ratio. Q_2 vs. d can then be plotted for each $\frac{\rho_a}{\rho_1}$ ratio, or for each electrode spacing a.

The use of these curves for determining the depth to a horizontal stratum will be illustrated for data taken from an experimental survey conducted

by Tagg † in Gloucestershire, England. The surface material is limestone overlain by about six inches of loam; the depth of the limestone varies from 50 to 266 feet, and underneath the limestone is either sand or clay.

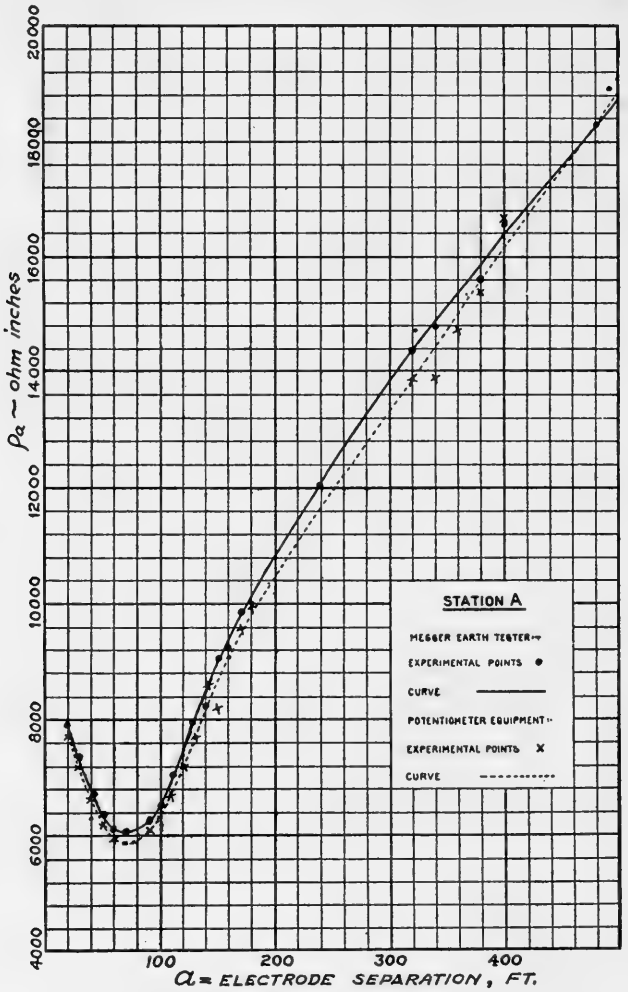

FIG. 295.—Experimental values of the apparent resistivity as a function of electrode separation. Solid curve is experimental curve obtained with Megger Earth Tester and broken curve is experimental curve obtained with potentiometer equipment. (Tagg, *A.I.M.E. Geophysical Prospecting,* 1934.)

The sites chosen were practically level. The resistivity ρ_1 of the surface limestone was obtained from measurements at electrode intervals to 70 feet. The averaged value was 6703 ohm-inches. The apparent resistivity ρ_a is shown plotted as a function of the electrode separation in Figure 295.

† Tagg, *loc. cit.*

A series of values of the apparent resistivity corresponding to several values of the electrode separation is read off the experimental curve. The apparent resistivities are then divided by the surface resistivity ρ_1 to determine the ratios ρ_a/ρ_1. Because the values of the ratio ρ_a/ρ_1 are greater than unity, the reciprocal ratios σ_a/σ_1 are also formed. (Table 17.)

The values of d/a and Q_2 corresponding to each of the values of the ratio σ_a/σ_1 given in Table 17 are now read off Figure 294. The values thus obtained are shown in Table 18.

The next step in determining the depth consists in plotting a series of curves of Q_2 as a function of d, one curve for each value of σ_a/σ_1, —i.e.

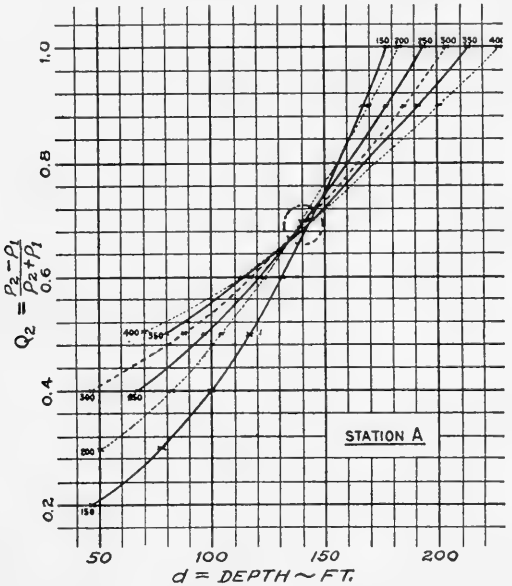

FIG. 296.—Curves showing the reflection factor Q_2 vs. the depth d for various values of σ_a/σ_1. (Tagg, *A.I.M.E. Geophysical Prospecting*, 1934.)

one curve for each electrode interval. These are shown in Figure 296. The six curves intersect within the dotted circle, and the center has the coordinates $d = 142$ and $Q_2 = 0.0702$; that is, the intersection of the curves gives 142 feet as the value of the depth and 0.0702 as the value of the reflection factor Q_2.

Also, it is of interest to point out that when Q_2 and ρ_1 are known, the resistivity ρ_2 of the lower formation can be determined from the relation

$$Q_2 = \frac{\rho_2 - \rho_1}{\rho_2 + \rho_1}$$

or

$$\rho_2 = \frac{\rho_1 (1 + Q_2)}{1 - Q_2}$$

TABLE 17

RATIO OF THE RESISTIVITIES AT VARIOUS ELECTRODE SEPARATIONS†

Electrode Separation, Feet	Apparent Resistivity, Ohm-inches	Ratio, ρ_a/ρ_1	Ratio, σ_a/σ_1
150	8,960	1.338	0.748
200	10,740	1.601	0.625
250	12,320	1.840	0.544
300	13,860	2.068	0.483
350	15,220	2.270	0.441
400	16,480	2.460	0.407

† Tagg, *loc. cit.*

Substitution of the values given above for ρ_1 and Q_2 into the last relation yields

$$\rho_2 = \frac{6703\ (1.0702)}{0.298} = 38300 \text{ ohm-inches.}$$

Resume.—The preceding sections have been concerned chiefly with the mathematical relationships governing the current flow in the subsurface. Generally, however, a rigid mathematical treatment of resistivity data obtained from measurements made at the surface of the earth is not possible because many variable factors affect the apparent resistivity.

The measured values are influenced chiefly by two mutually dependent phenomena: first, the actual path of the current flow, and second, the surface potentials at the points where the potential electrodes make contact with the surface of the earth. The current path is dependent chiefly upon the distance between the current electrodes and the relative conductivities of the strata constituting the subsurface. Although small portions of the current spread out to great distances in all directions in the earth, a considerable portion is confined to the subsurface volume included between the two current electrodes. Furthermore, only a relatively small amount of the current flows along the uppermost surface of the ground, and the potentials measured in the resistivity methods are only those created by this current flow at the surface.

The relative magnitudes of the effects produced by these factors are discussed below.

TABLE 18

VALUES OF Q_2 AT VARIOUS ELECTRODE SEPARATIONS †

Value of Q_2	150 Ft.		200 Ft.		250 Ft.		300 Ft.		350 Ft.		400 Ft.	
	$\sigma_a/\sigma_1 = 0.748$		$\sigma_a/\sigma_1 = 0.625$		$\sigma_a/\sigma_1 = 0.544$		$\sigma_a/\sigma_1 = 0.483$		$\sigma_a/\sigma_1 = 0.441$		$\sigma_a/\sigma_1 = 0.407$	
	d/a	d°	d/a	d	d/a	d	d/a	d	d/a	d	d/a	d
1.0	1.19	179	0.915	183	0.770	193	0.675	202	0.61	214	0.560	224
0.9	1.12	168	0.850	170	0.705	176	0.610	183	0.545	191	0.500	200
0.8	1.045	157	0.775	155	0.640	160	0.545	163	0.485	170	0.435	174
0.7	0.96	144	0.700	140	0.565	141	0.478	143	0.41	144	0.36	144
0.6	0.87	130.5	0.620	124	0.485	121	0.390	117	0.325	114	0.28	112
0.5	0.785	118	0.525	105	0.39	97.5	0.295	74	0.226	78	0.17	68
0.4	0.66	99	0.42	84	0.27	67.5	0.16	40	0.06	21		
0.3	0.525	79	0.26	52	0.03	7.5						
0.2	0.315	47										
0.1												

° d is obtained by multiplying d/a by a.

† Tagg, *A.I.M.E. Geophysical Prospecting*, 1934.

MEASUREMENTS OF NEAR-SURFACE INHOMOGENEITIES

In any geophysical method it is necessary that the anomalies in the measured physical property be of sufficient magnitude to manifest themselves in an unequivocal manner, despite any irrelevant variables which may be included in the measurements. In measurements of potentials, the effect of a near-surface disturbing factor increases rapidly with the depth of measurement. Very small lateral variations in the conductivity of the ground near the surface will produce effects comparable to those produced by structural variations of large magnitude at some depth below the surface. The lateral variations may be demonstrated by maintaining the current electrodes in a fixed position and measuring the E/I ratios as the potential electrodes are moved to different locations. Frequently the individual readings deviate fifty per cent or more from the computed theoretical values. Structural changes, however, seldom cause a variation in the computed resistivity value of more than a few per cent, except in unusual cases. It is evident, therefore, that the near-surface variations tend to mask the absolute resistivity variations that are associated with changes in the path of current flow caused by subsurface structural changes.

The greatest lateral variations occur in the aerated layer and are associated primarily with ground water movements. Local zones of higher resistivity are usually associated with descending fresh water movement. The more highly conductive areas are usually found in regions where ascending solutions and concentration of mineralization occur—due to surface evaporation—and in regions where local moisture content is increased by surface or near-surface impoundment of rain or drainage water. These conditions often manifest themselves visibly by alkali beds and changes in vegetation. Frequently, however, visual inspection fails to account for certain shallow anomalies, and therefore it is necessary to conduct the field work in a manner which will permit differentiating between the near-surface and the "deep" variations.

Lateral Investigations.—Lateral investigations are usually conducted to determine lateral variations associated with fault zones, contacts of different formations, variations in depth to "marker" beds, etc. Lateral resistivity measurements generally are carried out by moving the electrode configuration as a unit along a traverse line that crosses the area. The variations in resistivity are plotted against the traverse distance.*

The manner in which near-surface inhomogeneities affect the apparent resistivity values as the electrodes move over the area may be illustrated by referring to Figure 297. Positions of the electrodes are shown with reference to a zone of relatively high conductivity. The energizing or power electrodes are designated by 1 and 4. The electrode configuration shown is the conventional Wenner arrangement, wherein the separation between adjacent electrodes is equal. The lines of current (not shown in

* Measurements of this type are often termed "constant depth" traverses.

the sketches) are concentrated in the zone of high conductivity and the equipotentials are distorted so as to be displaced away from this zone.

Referring to diagram *A*, as the electrode configuration approaches the zone of high conductivity, the distortion of the equipotentials away from the conductor decreases the potential difference between 2 and 3. Hence, because the apparent resistivity is proportional to $(V_2 - V_3)/I$, the

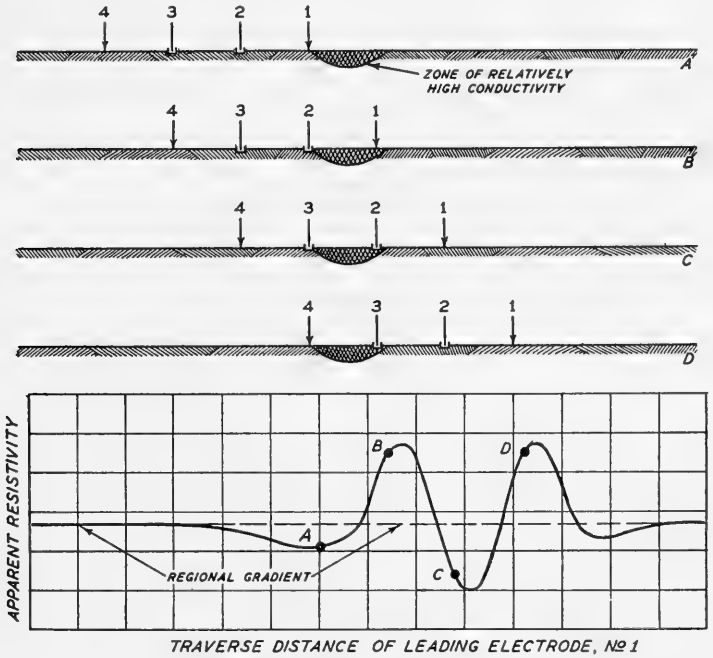

FIG. 297.—Lateral investigations and near-surface effects.

apparent resistivity is diminished with respect to the value it would have in the absence of the conductor. (Compare the resistivity-distance curve in the lower portion of the figure.) For the electrode positions shown in sketch *B*, the potential drop between 1 and 2 is very small due to the short circuiting effect of the conductor. Hence, the potential between 2 and 3 is large and the apparent resistivity has a maximum value. At the electrode positions shown in *C*, the potential difference is measured across the conductor and hence is very small. Thus for this position of the potential electrodes, the apparent resistivity is a minimum. In diagram *D*, the relative positions of the potential electrodes are the same as in *B*. Hence, the apparent resistivity again reaches a maximum. As the configuration continues its movement, the curve at first decreases slightly and then coincides with the normal regional resistivity profile.* This type of anomaly

* The *normal regional resistivity* profile or the *regional resistivity* profile is a smoothed-out plot of resistivity versus distance for a given region. The best fitting line through the regional resistivity profile is sometimes called the *regional gradient.*

is typical for the movement of such an electrode configuration across a zone of relatively high conductivity. It is the usual anomaly encountered in conjunction with fault zones and other conductive zones of relatively narrow width. By like reasoning it can be seen that a zone of lower conductivity would give an inverted type of curve having the same general characteristics.

An unsymmetrical electrode configuration which is suitable for lateral investigations is illustrated in Figure 298. In this configuration, the potential electrodes 2 and 3 are closer to power electrode 1 than to power electrode 4. The distance between electrodes 3 and 1 is about one-third that between 3 and 4. This configuration has the advantage that the surface effect at one of the energizing electrodes is minimized. Thus, the predominant resistivity variation occurs adjacent the energizing electrode which is near the potential electrodes.

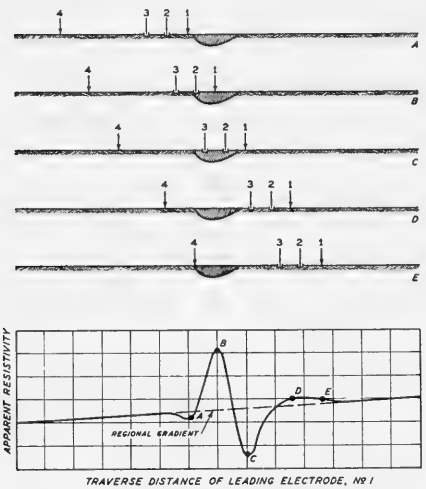

FIG. 298.—Unsymmetrical electrode configuration for lateral exploration.

Movement of this configuration across the zone of better conductivity will give the type of anomaly indicated in the lower part of the figure. The greatest deflection occurs when the electrode 1 crosses the zone of better conductivity. A much smaller anomaly is produced when electrode 4 crosses the zone.

It will be shown later that if electrodes 1, 2, and 3 are maintained stationary and if the depth of measurement is varied by moving only electrode 4, a vertical depth exploration may be made with a minimum surface effect. Hence, this type of unsymmetrical electrode configuration furnishes the basis for a surface correction method useful in vertical exploration.

Figure 299 shows a regional resistivity profile plotted from data obtained with the unsymmetrical electrode configuration shown in Figure

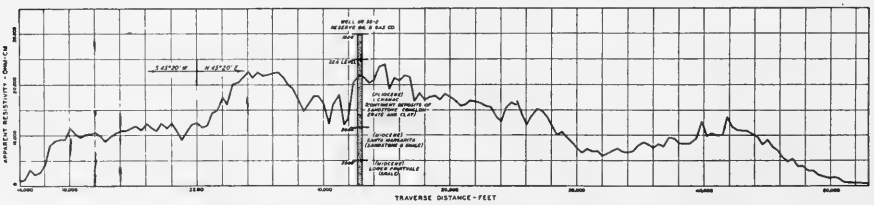

FIG. 299.—Resistivity profile in Tejon Ranch Area, San Joaquin Valley, California.

298. The separation of the energizing electrodes was 2400 feet and the entire configuration was moved as a unit, with readings made each 400 feet along the traverse.

Vertical Investigations.—Vertical depth investigations are oftentimes conducted by moving the electrodes symmetrically outward from a central point along a straight line. Figure 300 illustrates the anomaly usually obtained when the zone of better conductivity is located asymmetrically with reference to such electrode movement. The center of the electrode configuration, usually designated as the station, is located as illustrated in the figure, and electrodes 1 and 2 move outwardly in one direction from this central point of reference while electrodes 3 and 4 move outwardly in equal increments of distance in the opposite direction. If the subsurface is homogeneous, with the exception of the zone of high conductivity, movement of electrodes 3 and 4 outwardly will not produce any appreciable change in the apparent resistivity. Therefore, the present analysis may be confined to the movement of electrodes 1 and 2. As these electrodes move outward, the apparent resistivity at first decreases a small amount, then rises sharply. (Compare the resistivity-distance curve in the lower portion of the figure.) After reaching a maximum value, the resistivity gradually decreases and finally takes on the normal value it would have in the absence of the conductor.

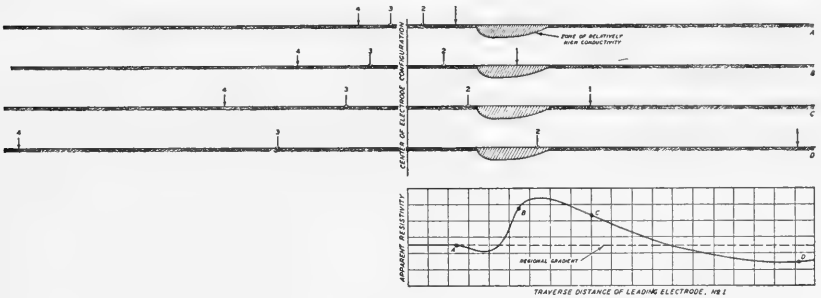

FIG. 300.—Vertical investigations and near-surface effects.

It is clear that near-surface inhomogeneities existing along the traverse to the left of the center of the configuration would yield a similar resistivity-distance curve due to the movement of electrodes 3 and 4. Evidently, it is difficult to determine the near-surface correction from data obtained with this type of electrode movement, because the near-surface disturbances may occur on either or both sides of the center point.

Investigations of Asymmetrical Subsurface Inhomogeneities.—The problem of ascertaining the subsurface structure when the subsurface inhomogeneities are asymmetrical has been attacked by numerous methods. One of the first methods for detecting anomalies produced by asym-

metrical inhomogeneities is due to F. H. Brown.† Brown's apparatus consisted essentially of a differentially wound receiver and three electrodes. The electrodes were mounted in a straight line with the "central" electrode midway between the two exploring electrodes. One winding of the receiver was connected to the central electrode and one of the exploring electrodes, and the other winding was connected to the central electrode and the other exploring electrode. This method operated on the principle of causing current to traverse different depths of the earth forming one circuit, and at the same time causing current to flow through the other earth circuit. The relative strengths of the two currents could be compared audibly by means of the differential coil in the receiver.

Schlumberger ‡ utilized equipotential studies around the power electrode to determine inhomogeneities. A non-symmetrical distribution of subsurface current flow was indicated by a distortion of the equipotential lines.

Lee§ has proposed a method wherein the ground is "partitioned," preferably into symmetrical parts, with the station center at the midpoint as in the Brown arrangement. Measurements are made on each side of the midpoint for the purpose of comparing one side with the other. The comparison may be made of the computed resistivity values or any function of these values, such as measured potentials, currents, or resistances. This arrangement measures the resultant effect produced by local zones of anomalous conductivity and dip of structure.

The potential ratio methods generally utilize a central electrode as a reference point. Zuschlag†† illustrates and describes one method for comparing electrical potentials about the midpoint of the electrode configuration. Methods of this type indicate a non-symmetry of position, but they do not isolate the near-surface effect or locate the region of its occurrence along the traverse line of measurement.

Experimental results show that the potential electrodes are subject to a far greater disturbance as a result of near-surface effects than the power, or energizing, electrodes. Hence, the near-surface effects can be minimized by employing an electrode system wherein the two potential electrodes remain in a fixed position, while the two power electrodes move outward. This condition is illustrated in Figure 313f.

An accentuation of near-surface effects occurs when the electrode movement is such that the power electrodes remain stationary and the potential electrodes move. It is this accentuation of near-surface effects which so greatly handicaps the potential ratio methods and other methods wherein only the potential electrodes are moved.

---

† F. H. Brown, "Electrical Apparatus for Determining the Location of Metallic Ores," U. S. Patent 817,749, issued April 17, 1906.

‡ C. Schlumberger, "Process for Determining the Nature of the Subsoil by the Aid of Electricity," U. S. Patent 1,163,468, issued Dec. 7, 1915.

§ F. W. Lee, "Method of Conducting Geological Survey," U. S. Patent 1,951,760, issued Mar. 20, 1934.

†† T. Zuschlag, "Electrical Prospecting," U. S. Patent 1,951,387, issued Mar. 20, 1934.

Double - Depth Investigations. — The differentiation of the near-surface effects from the deeper structural effects can oftentimes be accomplished by comparing measurements at two different depths of penetration.

Double-depth investigations may be divided into two general groups: (a) lateral exploration and (b) vertical exploration. Illustrations of both types will be given to indicate the general principles involved in the field technique. Various other modifications will occur to the reader.

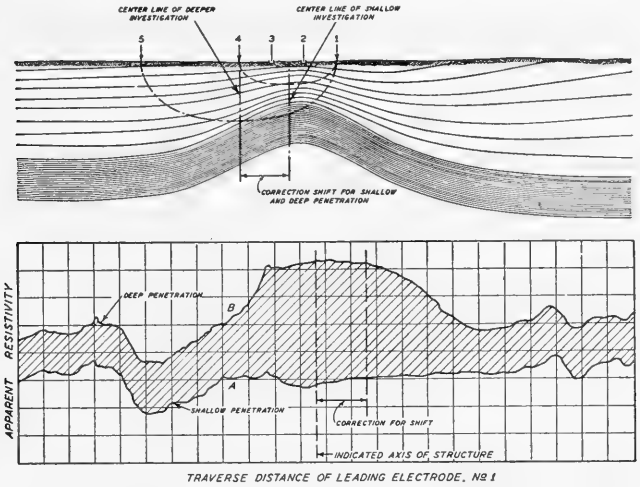

Fig. 301.—Illustration of surface corrections in the lateral exploration method.

Lateral Exploration

The operating principle of the lateral exploration method will be evident from a consideration of Figure 301. An electrode system comprising electrodes 1, 2, 3, and 4 is moved as a unit along a traverse line. The separation between power electrodes 1 and 4 is only sufficient to give an effective penetration which includes the upper near-surface beds. A third energizing electrode 5 trails the electrode system (consisting of 1, 2, 3, and 4) at a constant distance which depends on the desired depth of effective penetration into the deeper lying beds. Two sets of resistivity measurements are made for each position of the electrodes: In one, the energizing current flows between electrodes 1 and 4; in the other, the energizing current flows between electrodes 1 and 5.

The apparent resistivity data are plotted with the resistivity values as ordinates and the traverse positions of the leading power electrode as abscissas. (Lower portion of Figure 301.) Curve *A* corresponds to the case that the energizing current flows between electrodes 1 and 4, and curve *B* to the case that 1 and 5 are the energizing electrodes. In this particular area, the curves show that the shallow material affecting the

measurements at the small separations has a lower resistivity than the deeper lying material which affects the measurements at the large separations.

The curves also exhibit a general similarity, because the potential electrodes occupy the same surface positions in both the shallow and the deep measurements. If the current penetrates the earth uniformly, the effective zone of measurement for the symmetrical shallow electrode configuration will lie approximately midway between electrodes 1 and 4. For the deep investigations, the effective zone of penetration lies approximately midway between electrodes 1 and 5, but due to the unsymmetrical electrode arrangement the zone of effective measurement is shifted toward the potential electrodes. Hence, in comparing the shallow and deep investigations it is necessary to make a shift correction. The amount of this shift will depend on: (a) electrode configuration, (b) the relative conductivities of the deep and shallow zones, and (c) the changes in dip or thickness of section between the two zones.

The data utilized in the interpretation are obtained by making the shift correction and subtracting corresponding ordinates of the two resistivity curves.

Vertical Exploration

The operating principle of the vertical exploration method will be evident from Figure 302. The electrodes are placed along the traverse line with the potential electrodes 2 and 3 positioned at certain fixed distances, usually one and four units, from the stationary energizing electrode. The moving energizing electrode † is started a distance of about four and one-half units from the stationary energizing electrode. The unit length depends upon the desired depth of measurement and the relative conductivities of the strata in the area. The zone of investigation increases in depth as the energizing electrode 4 moves out. (Figure 302A.)

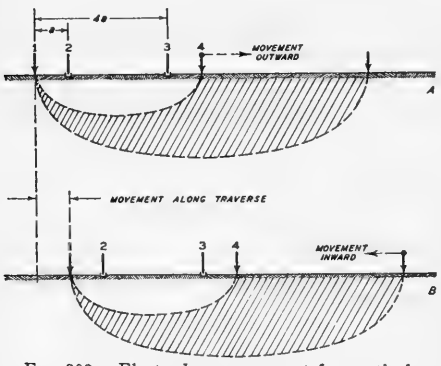

FIG. 302.—Electrode arrangement for vertical exploration.

If direct current or very low frequency alternating current is employed, the data recorded during this movement of the electrode are the values of the potential, current, and electrode separation.

Upon completion of the series of measurements, the entire electrode configuration is moved forward along the traverse line about 1000 feet. Recordings are then made of the potential, current, and electrode spacing as the moving electrode proceeds inwardly. (Fig-

† J. J. Jakosky, "Method and Apparatus for Electrical Exploration of the Subsurface," U. S. Patent 2,192,404, issued March 5, 1940.

ure 302B.) Upon completion of this series of measurements, the entire configuration is again moved another 1000 feet forward along the traverse line, and the entire procedure repeated. The technique of making two series of measurements (outward and inward) at one location constitutes the occupation of one station. As explained later, the stations are spaced to allow an overlap of about three stations in order to facilitate proper evaluation of near-surface effects.†

The potential-current ratios for each station are now reduced by an appropriate formula * and are plotted with resistivity as ordinate and electrode separation as abscissa. The near-surface resistivity anomalies appear when the moving energizing electrode traverses the inhomogeneities. Hence, the anomalies are present at the same traverse point on all of the overlapping curves,** and the initial step in the interpretation process is to "match" or "correlate" each of the apparent resistivity curves at its respective traverse location.

The correlation of four overlapping stations located on a short section of traverse line in the Permian basin near Lovington, New Mexico, is shown in Figure 303.*** The irregularities produced in the resistivity profile by the near-surface inhomogeneities are quite pronounced. Prominent anomalies which occur on all of the curves at the same traverse location are marked at *A*, *B*, and *C*. Many minor anomalies will be seen by more detailed study of the curves.

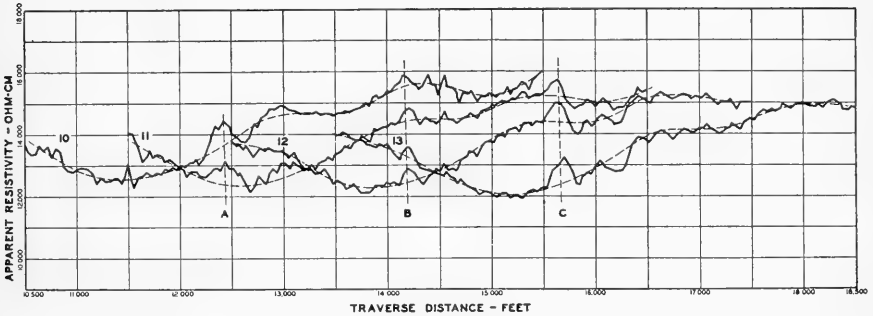

FIG. 303.—Correlation of four overlapping stations on a traverse line.

Generally the shallow near-surface effects are very apparent due to their abruptness and short lateral extent. Oftentimes, however, near-surface effects exist over a considerable distance and are not easily differentiated from the deeper effects.

† J. J. Jakosky, "Method and Apparatus for the Electrical Exploration of the Subsurface." U. S. Patent 2,211,125, Aug. 13, 1940.

* See p. 518.

** The *shapes* of corresponding near-surface anomalies which occur in curves of overlapping stations are generally not identical.

*** In practice the individual station curves are not replotted as was done for this illustration, but are matched by using a light box and superposing the curves at their proper traverse separations.

The dotted curves of Figure 303 are the diagnostic curves utilized in the interpretation. These curves are obtained by "smoothing-out" the observed data so as to minimize the near-surface variations. (Experience is required in drawing the best-fitting "smoothed-out" curve.)

Alternative Configuration.—A useful modification of the electrode system described above is obtained by placing the stationary current electrode midway between the stationary potential electrodes. With this arrangement, the electrical fields produced at the potential electrodes by the fixed current electrode are the same, provided the earth between the two power electrodes is homogeneous. Hence, variations in the measured potential difference depend only on the relative position of the moving power electrode. This arrangement also has a greater sensitivity than the arrangement previously described wherein both power electrodes are located outside the potential electrodes.

Dip Determination at a Single Station.—Determination of the dip at single stations may often be accomplished by comparing the curves obtained from measurements made in three or more directions from the station hub.† The measurements are usually made by a tri-directional system, as illustrated in Figure 304. The three lines of measurement are laid out at 120° angles, with the corresponding points of measurement on each line being equidistant from the station hub. Current is passed into the ground between electrodes I_A and I_B, then between I_A and I_C, and and then between I_B and I_C, the points of measurement moving progressively outward as the depth of penetration is increased. It will be recognized that this procedure is a combination of lateral and vertical investigation.

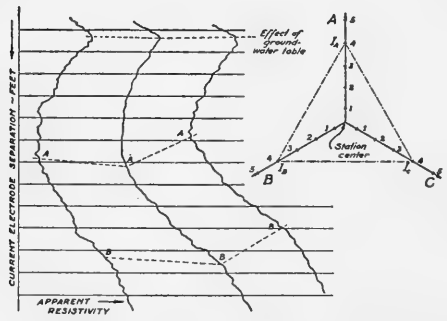

FIG. 304.—Tri-directional system of measurement for determining dip at a single station.

The subsurface distribution of current can be predicted by one of two types of measurement: (a) potential measurements at a given spacing from the energizing electrodes or (b) electromagnetometer measurements wherein the strength of the magnetic field associated with the subsurface current flow is measured at the hub.

Analysis of the multi-directional measurements is usually done by some form of curve correlation procedure. The curves for each line of

† J. J. Jakosky, "Methods of Determining Underground Structure," U. S. Patent No. 2,138,818, Dec. 6, 1938.
J. J. Jakosky and C. H. Wilson, "Electrical Mapping of Oil Structures," *Mining and Metallurgy*, May 1936, pp. 231-237.
J. J. Jakosky and C. H. Wilson, "Prospecting for Oil Structure by Electrical Methods," *The Petroleum Engineer*, Feb. 1937, pp. 143-149.

measurement are plotted as shown in the figure and are correlated by the method outlined on p. 509.

ANALYSIS OF RESISTIVITY DATA

Various interpretative procedures have been developed for inferring the subsurface structure from resistivity data. The *mathematical methods* have been discussed by Tagg, Roman, † Hummel, ‡ Watson § and others. †† The method of Tagg has already been considered. Apart from the mathematical methods, the interpretative procedures commonly employed may be classified into three groups: (1) rule of thumb or visual interpretation; (2) curve correlation methods which often can be applied successfully in many cases of complex structure where the more basic mathematical analysis would be either impractical or impossible; (3) small scale experiments.

Workers in electrical geophysics are divided into two general schools of thought regarding the technique of interpretation. The mathematically-minded school holds that the "rule of thumb" methods are not sufficiently precise or scientific, while the self-styled "practical" school holds that the mathematical parameters cannot be evaluated with sufficient accuracy under normal field conditions to justify the assumptions necessary for a rigid mathematical basis of interpretation. This school bases its interpretation upon visual inspection of the depth-resistivity or traverse-resistivity curves, and upon the experimentally proven fact that the major trend breaks may be caused by changes in the subsurface.

As in most controversies of this nature, both schools are correct in their contentions under certain conditions. Experience is essential for correct interpretation of the electrical data.

Rule of Thumb Theorems for Determining Effective Depth of Measurement.—In an attempt to simplify the calculations necessary to interpret field data, many empirical rules have been devised. The literature of electrical prospecting contains numerous illustrations of the application of such rules to actual problems. Many of these rule theorems are valid for the particular problems for which they were derived. However, the blind application of such rules to general exploration problems usually results in errors because the conditions under which the empirical

† Irwin Roman, "How to Compute Tables for Determining Electrical Resistivity of Underlying Beds and their Application to Geophysical Problems," U. S. Bur. of Mines, Tech. Pub. 502; "Some Interpretations of Earth Resistivity Data," *A.I.M.E. Geophysical Prospecting,* 1934, pp. 183-201.

‡ J. N. Hummel, "Theoretical Study of Apparent Resistivity," *A.I.M.E. Geophysical Prospecting,* 1937, Tech. Pub. 496; "A Theoretical Study of Apparent Resistivity in Surface Potential Methods," *A.I.M.E. Geophysical Prospecting,* Tech. Pub. 418, 1931.

§ R. J. Watson, "A Contribution to the Theory of the Interpretation of Resistivity Measurements Obtained from Surface Potential Observations," *A.I.M.E. Geophysical Prospecting,* Tech. Pub. 518, 1934.

†† D. O. Ehrenburg and R. J. Watson, "Mathematical Theory of Electrical Flow in the Stratified Media," *A.I.M.E. Geophysical Prospecting,* Tech. Pub. 400, 1931.

S. Stefanesto, in collaboration with C. and M. Schlumberger, "Sur la Distribution Electrique Potentielle Autour D'Une Prise de Terre Ponctuelle Dans un Terrain A Couches Horizontales, Homogenes et Isotropes," *Le Journal de Physique et le Radium,* Vol. 1, 1930, p. 132.

C. L. Pekeris, "Direct Method of Interpretation in Resistivity Prospecting," *Geophysics,* Vol. V, No. 1, January, 1940, pp. 31-42.

rules were developed may not obtain in the particular area under investigation. Two of the many "short cuts" in interpretation will be discussed here.

Many literature references contain discussions of the "potential bowl" theory. † The apparent validity of this method of interpretation derives from the following considerations. In an isotropic, homogeneous medium, all points equidistant from the current electrode lie on an equipotential surface. Hence, the potential at a point P, at any fixed distance along the surface of the ground from the current source S_1, will define the surface trace of the particular equipotential hemisphere having a radius r_s equal to the distance PS_1. (Figure 305.) It is assumed that any subsurface condition which may alter the potential value at any point a distance r_s from the point S_1 will cause a like change in the surface potential measured between P and S_1. In other words, the equipotential bowl is assumed to be a rigid, non-distorted surface; and if this were true, the depth of investigation d would be equal to the distance r_s.

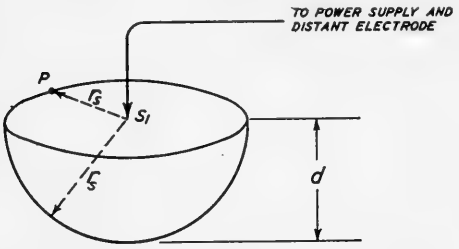

FIG. 305.—Assumed equipotential bowl surrounding electrode S_1.

Obviously, this equipotential bowl theory must be modified to correct for the distortion of the equipotential surface caused by the effect of the distant power electrode, and also for the distortion of the equipotential surface caused by the subsurface inhomogeneities, including the effect of the distortion due to the layer whose depth is to be determined. In extreme cases (where an excellent conductor exists at depth) the depth of investigation may be greater than the surface radius of the equipotential bowl, while in other cases where high resistivity materials exist at depth it may even be less than $\frac{1}{5}$ of the bowl radius. With these limitations it is obvious that the theory must be applied with extreme caution.

Empirical formulas relating the electrode spacing at the surface of the ground with the depth to an underlying stratum have also been derived for the Wenner electrode arrangement. (Figure 306.) Again it is assumed that the equipotential surfaces about the two power electrodes are undistorted hemispheres and that the depth of measurement is equal to the distance a; i.e., the effective depth of measurement is assumed to be one-third the separation of the energizing electrodes.

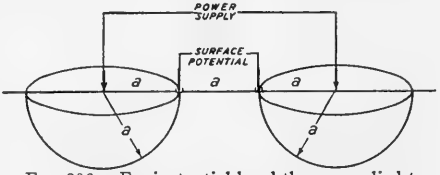

FIG. 306.—Equipotential bowl theory applied to the Wenner configuration.

† See, for example, A. S. Eve and D. A. Keys, *Applied Geophysics* (Cambr. Univ. Press), 1938, pp. 95-97.

Generally, the empirical "short cuts" just discussed are in error, because they neglect the ever present distortion of the potential bowls surrounding the source and sink of the current. For instance, in areas where the resistivity increases with depth, the effective path of current flow is always materially less than the $\frac{1}{3}$ value cited for the Wenner configuration.† Usually the depth of measurement varies from about $\frac{1}{4}$ to $\frac{1}{6}$ the distance between the power electrodes. Moreover, the depth of measurement usually is not a constant fraction of the distance between the power electrodes; instead, it depends on such factors as the relative conductivities of the component layers constituting the subsurface and the lateral variations in conductivity. In general, therefore, the depth of penetration is dependent upon many factors, only one of which is the separation and configuration of the electrodes.

Interpretation by Curve Correlation.—This method of interpretation is based upon the fact that in an area of extended flat structures, any given multi-layer structure composed of layers of different conductivity usually produces a characteristic type of resistivity curve.‡ The general shape of this curve is dependent upon the relative thickness, conductivity, and sequence of the layers or components included in the measurements. It has been found that each area usually has its own characteristic type of curve. This curve will differ from that of another area if the subsurface structure differs so as to produce electrical variations when the depth of current penetration changes.

Extensive field work has shown that in favorable cases a characteristic pattern in one portion of the curve may often be followed through a series of stations even though variations in thickness occur in portions of the geologic section. In one application of the method for subsurface structural mapping, a certain group of markers within a given depth interval is correlated.*

The measurements are made to include a given depth interval by starting with the power electrodes at some fixed distance apart and increasing their separation until the desired depth interval has been measured. The similarity of the pattern at various stations in an area will depend on the lateral uniformity of the subsurface layers. In areas where rapid lateral changes are predominant, such as in the lenticular and overlapped structures which prevail in the San Joaquin valley of California, the curves will vary rapidly in character; under such conditions, it will be found that curve to curve correlation will be difficult even

† H. M. Evjen, "Depth Factors and Resolving Power of Electrical Measurements," *Geophysics*, 1938, pp. 78-95.

‡ J. J. Jakosky, C. H. Wilson and J. W. Daly, "Geophysical Examination of Meteor Crater, Arizona," *A.I.M.E. Geophysical Prospecting*, 1933, pp. 63-97.
J. J. Jakosky, "Continuous Electrical Profiling," *Geophysics*, Vol. 3, No. 2, Mar. 1938.

* Correlations may be carried out even when the upper sedimentary beds overlying the group vary in thickness, because the variation usually is not sufficient to mask the characteristics of the curve due to the lower part of the section.

when the stations are placed close together. In areas where sufficient resistivity depth variations occur and where the lithology is fairly uniform, with resultant small variations in the characteristics of the curves, reliable correlations often may be made between stations which are many thousands of feet apart. The latter condition prevails in many parts of the Mid-Continent area and in the Permian basin area of New Mexico and Texas.

To correlate curves, the field data for each station are plotted with the resistivity values as abscissas and the separations of the current electrodes as ordinates on a separate sheet of transparent cross-section paper. Corrections for surface effects are made as illustrated in Figure 303. The corrected curves corresponding to the various stations are then matched over a light box, i.e., correlated as a unit. The interpreter first correlates the curves for the first two stations at one end of the traverse and then proceeds to successive stations. The correlation of four curves is shown

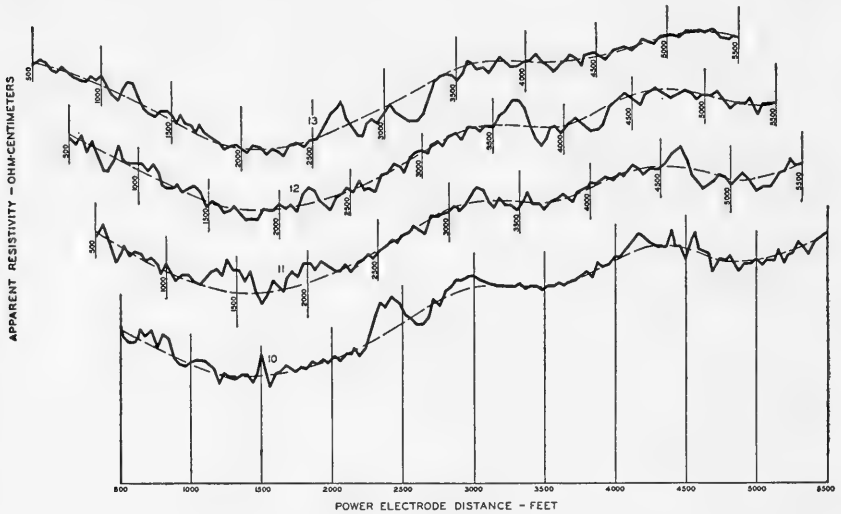

Fig. 307.—Correlation of resistivity curves from four adjacent stations along a traverse line.

in Figure 307. Before evaluating the subsurface interval between stations, it is necessary (a) to correct for variations in surface topography and elevation, and (b) to determine the effective depth of measurement.

The topography along the traverse is taken by transit and stadia rod, preferably during the initial laying-out of the traverse line, and the elevations of the electrode locations are reduced to a mean datum plane.

The effective depth of measurement varies with the area and electrode configuration used and can seldom be predicted or calculated from known theoretical relationships. Usually it is determined by control data taken from geologic logs of wells in the area. When work is done in areas where proper well control is not available, a penetration factor is assumed, the

magnitude of which is based on experience under similar geological and electrical conditions. In these cases, the results should be considered as qualitative until proper control is available.

Small Scale Experiments.—In small scale experiments designed to determine the effects of ore bodies, conductors (model conductors) of various shapes are immersed in tanks partially filled with water of appropriate conductivity. The model ore bodies may be made by covering any convenient material with copper foil. The tank should be relatively large and should have dimensions about ten times the maximum dimension of the model object contained in the tank.

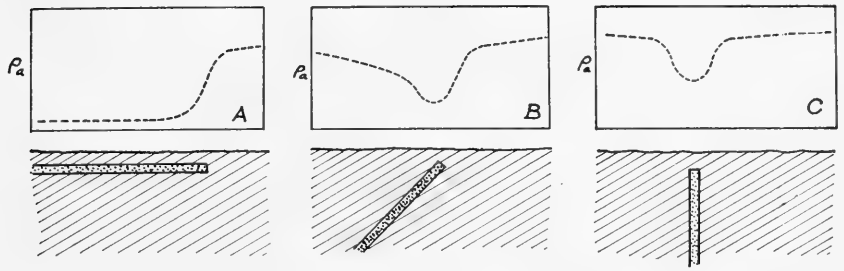

FIG. 308.—Type anomalies produced by model formations of various dips. Resistivity values obtained by moving a fixed Wenner configuration of electrodes normal to the strike.

Extensive experimental work has been done with small scale models. † A few general types of anomalies characteristic of model formations are shown in Figures 308 and 309 taken from tests by Clyde H. Wilson.

Representative results of tank tests to determine the zone of influence in a Wenner electrode configuration are shown in Figure 309. In these tests a glass partition, oriented at right angles to the line of electrodes, was moved in a direction along the line of electrodes.* Curve No. 1 was obtained for the higher partition, and curve No. 2 for the lower partition. The results show that the zone of influence is associated with the distorted potential bowl surrounding each of the energizing electrodes. The peaks of the curves shift farther away from the power electrodes at the greater depth. The results indicate that a distorted potential bowl exists around each source and sink (the power electrodes) and the actual potential as measured is the resultant of the effects in the vicinity of each.

This phenomenon explains the limited resolving power of the Wenner

† M. King Hubbert, "Theory of Scale Models as Applied to the Study of Geologic Structures," *Bull. Geological Society of America*, 1937, Vol. 48, pp. 1459-1520.
M. King Hubbert, *A.I.M.E. Geophysical Prospecting*, 1934.
C. A. Heiland, *Colorado School of Mines Bulletin*, 1929-1930.
J. H. Swartz, "Resistivity Measurements upon Artificial Beds," *U. S. Bureau of Mines, Information Circular* 6445, Feb. 1931.

* It will be seen of course that movement of the partition will produce the same result as would be obtained if the partition were to remain stationary and the electrodes moved in a fixed configuration. For experimental tests, movement of the partition is more convenient and far more rapid.

configuration because the results are dependent upon the sum of the effects in the vicinity of the two energizing electrodes. If, for example, a deep investigation were attempted and the energizing electrodes spaced 20,000 feet apart, the two effective zones of measurement probably would be from 10,000 to 15,000 feet apart. At these great distances, many changes could occur, especially in areas of steeply dipping structures.

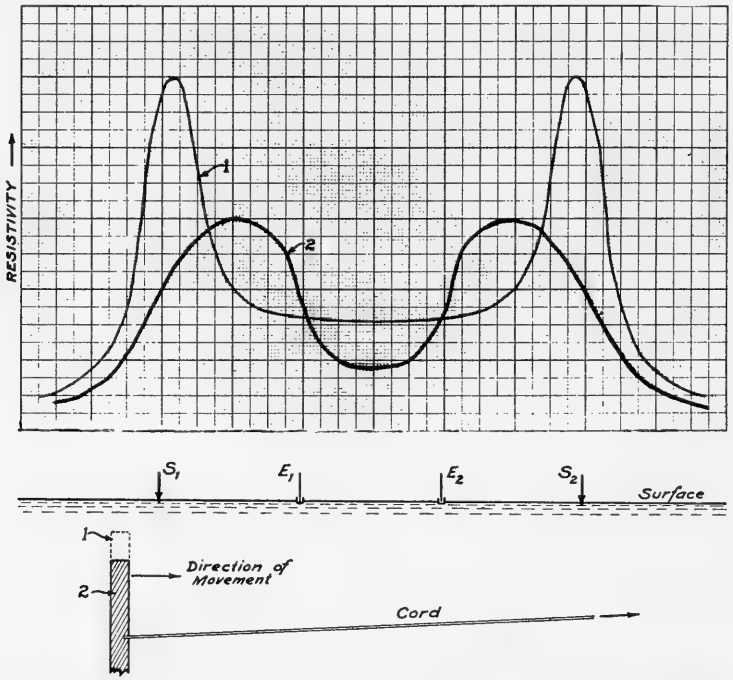

Fig. 309.—Resistivity variations over high resistance partition, using Wenner configuration.

The instruments employed for small scale investigations may be those used for the large field studies provided they have a sufficiently large scale range to enable the observer to read the very low current (usually 1 to 10 milliamperes) and the relatively high potentials (usually over 100 millivolts) encountered in the small scale investigations.

Small scale, non-polarizing electrodes may be constructed by using small diameter glass tubing. The bottom of the tube is plugged with a short saturated roll of chamois skin. The tube is filled with copper sulphate solution in which a bare copper wire is partially immersed. Ordinary electrodes may be made from small diameter graphite (lead-pencil carbons) or carbon rods similar to those employed for brushes in small motors. Chemically active electrodes, such as iron or copper, should be avoided. Finally, the electrodes should not extend into the conducting

material of the tank to a distance greater than one per cent of the minimum electrode separation employed in the investigations.

Tank or small scale experiments may supply considerable information which will be indicative of the results to be expected in field work. However, the tank experiments usually do not yield the same curve characteristics obtained in field work. This may be due to the absence of polarization and related phenomena at the interface of strata in the small scale tests. It is evident, therefore, that considerable care must be taken in using tank results as an aid in interpretation.

FACTORS TO BE CONSIDERED IN INTERPRETATION

1. Depth of Measurement and "Detectability."—In all geophysical investigations in which it is desired to map a certain formation or structural marker with reference to a horizontal datum plane, the most accurate

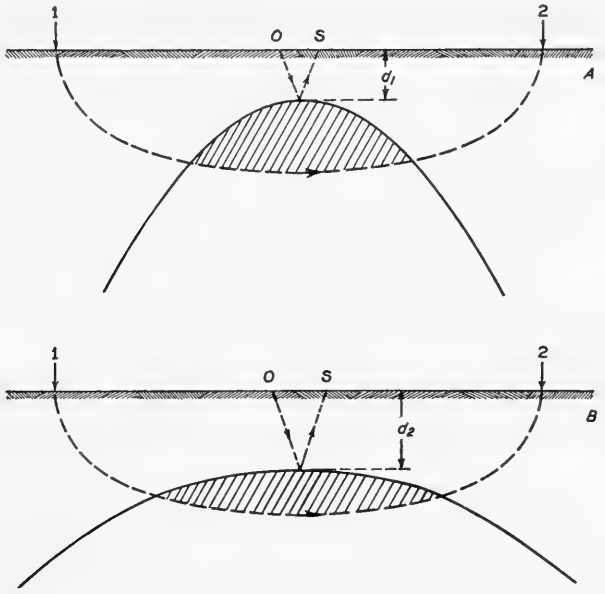

FIG. 310.—Sketch illustrating concepts of depth of penetration and detectability.

results will be obtained when the variation of the diagnostic quantity measured at the surface is proportional to the depth of the marker. In the electrical methods, however, the magnitude of the diagnostic variable does not depend solely on the vertical depth of the marker. This will be evident from a consideration of Figure 310. Part *A* of the figure illustrates a small, relatively steep, dipping structure. To produce a detectable variation in the resistivity value, it is necessary that the structure comprise a certain portion of the subsurface included in the measurements. The effect of the structure is a weighted or mass effect, depending

primarily upon the effective volume included in the zone of measurement rather than upon depth. Part *B* shows a flat lying structure, the weighted or mass effect of which is equivalent to that of part *A*. Thus, both types of structure give comparable electrical anomalies, despite the fact that their reliefs are different. Analysis of resistivity data, therefore, must proceed from the viewpoint of a weighted average, rather than from the viewpoint of a direct measurement.*

2. Variations in Effective Penetration.—The effective depth of current penetration is dependent to a large extent on the relative conductivities of the strata which constitute the volume included in the path of current flow. The ratio of the effective depth of penetration to the distance between the two power electrodes is termed the "penetration factor." This factor usually is not constant in any one area or even for any one station but varies with changes in the ratio of the conductivities of the near surface and the deeper strata.

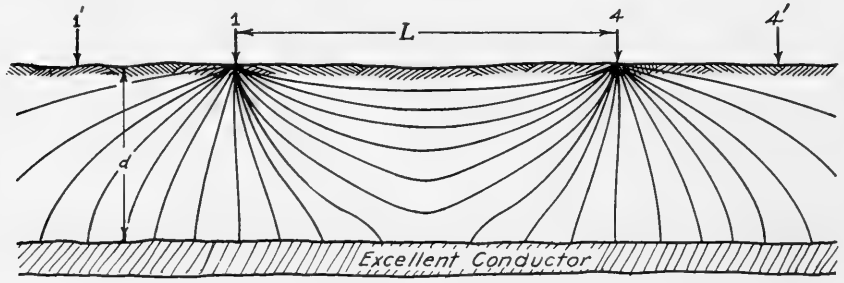

FIG. 311.—Sketch illustrating current paths for a structure comprising a layer of high resistivity underlain by a good conductor.

The reason for the changes in the penetration factor will be evident from the simplified diagram given in Figure 311. The diagram shows a layer of high resistivity underlain by an excellent conductor. † At electrode separations less than *d*, the effects of the good conducting layer is small and the penetration factor is relatively small. The highest penetration factor will be obtained when the distance *L* is slightly more than *2d*, due to the bending down of the current lines toward the good conductor. As the electrode separation is made greater than the distance *2d*, the current lines tend to be confined within the highly conducting layer and the penetration factor decreases again.

3. Anisotropic Media.—In many cases, the formations investigated by the resistivity methods possess a marked electrical anisotropy which influences the data obtained in surface measurements. Theoretical inves-

* The other potential methods, gravitational and magnetic, also depend on mass or weighted effects.

† See also, Warren Weaver, "Certain Applications of the Surface Potential Method," *A.I.M.E. Geophysical Prospecting*, 1929, p. 68.

tigations on the propagation of electric current in anisotropic media have been reported by Schlumberger and Leonardon† and by Maillet and Doll.‡ It is well known that in stratified rocks electric current is propagated more easily along the strike than in a direction perpendicular to the strike. This phenomenon may be treated quantitatively by introducing a coefficient of anisotropy λ defined by the relation

$$\lambda = \sqrt{\frac{r_t}{r_l}}$$

where r_t denotes the resistivity along the strike, "transverse resistivity," and r_l the resistivity perpendicular to the direction of the beds, "longitudinal resistivity."

Figure 312 shows a cross section of an equipotential surface on a vertical plane that is perpendicular to the bedding plane and passes through a point source of current 0 located in a homogeneous medium. If the medium is isotropic as well as homogeneous, the equipotential surfaces surrounding the current source 0 are spheres. (Compare p. 508.) If the medium is anisotropic and homogeneous, the equipotential surfaces surrounding 0 are ellipsoids of revolution around an axis through 0 perpendicular to the strike. It may be shown that the ratio of the semi-axes of the ellipse ($0A/0B$) is equal to the coefficient of anisotropy λ.

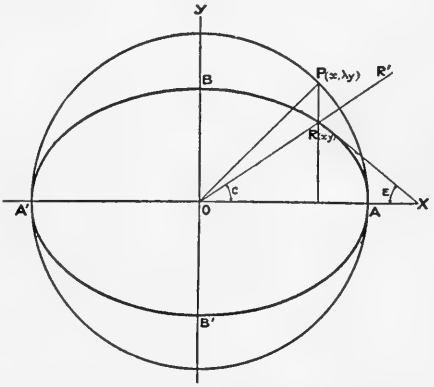

Fig. 312. — Cross section of equipotential surface by a vertical plane passing through a point source of current 0 located in a homogeneous, horizontal stratum. (After Schlumberger and Leonardon, *A.I.M.E. Geophysical Prospecting*, 1934.)

The ellipticity of the equipotential surfaces in anisotropic media has important consequences as regards the interpretation of resistivity data. One of these consequences, the so-called paradox of anisotropy, is that in the case of a stratified formation tilted vertically, the observed, *apparent* transverse resistivity is smaller than the observed, *apparent* longitudinal resistivity, while the inverse proposition holds for the true resistivities. Another consequence is that formulas derived for a stratified medium comprising several parallel, homogeneous, isotropic layers hold for a medium comprising anisotropic layers provided the resistivity of each layer is set equal to $\sqrt{r_l r_t}$, where r_l and r_t denote the longitudinal and transverse resistivities of the layer

† C. and M. Schlumberger and E. G. Leonardon, "Some Observations Concerning Electrical Measurements in Anisotropic Media, and their Interpretation," *A.I.M.E. Geophysical Prospecting*, 1934, pp. 159-181.

‡ R. Maillet and H. G. Doll, "Sur un théorème relatif aux milieux électriquement anisotropes, et ses applications à la prospection électrique en courant continu," *Ergänzungshefte für angewandte Geophysik*, Vol. 3, No. 1, 1932.

respectively, and the thickness of each layer is set equal to λd where d denotes the actual thickness of the layer and λ its coefficient of anisotropy. Evidently from a physical viewpoint these consequences affect the interpretation of resistivity data in that the values of the apparent resistivity must be modified to take into account the anisotropy of the formations being investigated.

FIELD PROCEDURE AND EQUIPMENT

Electrode Configurations for Measuring Resistivities.—Various electrode spacings and configurations may be employed in resistivity measurements.† As a general rule, the configurations employed are chosen because of their symmetrical arrangement which allows simplification of formulas. The literature, with special reference to many professional-type papers, is replete with various configurations which reputedly are superior to all other configurations. There is no theoretical basis for judging one configuration superior to another. In practice, however, it has been found that certain configurations, used in conjunction with the proper field technique, may permit better evaluations of certain factors that introduce errors. Briefly stated, these undesirable factors are introduced chiefly by: (1) near-surface effects, (2) variations in depth of current penetration, (3) lateral changes in geology.

The electrode configuration employed should preferably be such that the maximum flow of current will take place in the depth range desired in the measurement. Also, the potential electrodes should be so positioned with respect to the current electrodes that they receive the maximum influence from the subsurface flow of current.

Obviously, an electrode arrangement wherein the current electrodes are very close together will be very ineffectual for deep subsurface investigations, because the percentage of current penetrating to the desired depth range will be small and its variations will not be measurable at the surface. In practice, the separation between the current electrodes usually should be from three to six times the desired depth of measurement. The optimum value for any given electrode configuration must be determined experimentally for any given area.

The location of the potential electrodes is important, because if the potential electrodes are positioned too near the current electrodes, they will be predominately influenced by shallow effects. As the distance between the potential and the current electrodes is increased, the deeper zones have a greater effect on the measurement, but at the same time the observed potentials become smaller and the effects of near-surface variations become proportionally greater. Usually, the best "detectability"

† H. M. Evjen, "Electrical Method of Geophysical Exploration," U. S. Patent No. 2,172,557, Sept. 12, 1939.
J. J. Jakosky, "Method and Apparatus for Electrical Exploration of Subsurfaces," U. S. Patent No. 2,174,343, Sept. 26, 1939; "Electrical Exploration of Subsurfaces," U. S. Patent No. 2,256,742, Sept. 23, 1941.
R. G. Piety, "Method of Surface Prospecting," U. S. Patent No. 2,390,270, Dec. 4, 1945.

is obtained when the separation between the potential and the current electrodes is from one-third to one-half the desired depth of investigation. In areas where the lateral variations in resistivity are relatively small, it is usually advantageous to employ the larger separations. In all cases, however, the particular characteristics of the area under investigation must be taken into account.

One of the chief reasons for the indifferent results obtained in many electrical resistivity investigations has been the blind application of a fixed configuration to areas in which the relative conductivities of the upper and deeper materials make that configuration unsuitable.

The more widely employed electrode arrangements are illustrated in the following sketches. † Whatever configuration is employed, the relation between the resistivity and the observed quantities (E/I and electrode separation) may be obtained by using Equation 8 twice.

The technique of applying Equation 8 will be illustrated for the Wenner electrode configuration. The formulas for the other electrode arrangements shown in Figure 313 may be derived in a similar manner.

Wenner Configuration‡ (Figure 313a)

The four electrodes are arranged in a straight line, the current electrodes being separated by a fixed distance, $3a$, while the potential electrodes are situated at points distant a and $2a$ from the source respectively. The potential at P due to the source and sink is obtained by substituting a for r_1 and $2a$ for r_2 in Equation 8. That is,

$$V_P = \frac{I\rho_a}{2\pi}\left(\frac{1}{a} - \frac{1}{2a}\right)$$

The potential at R due to the source and sink is obtained by substituting $2a$ for r_1 and a for r_2. That is,

$$V_R = \frac{I\rho_a}{2\pi}\left(\frac{1}{2a} - \frac{1}{a}\right)$$

Hence, the potential difference between the two points is

$$V_P - V_R = \frac{I\rho_a}{2\pi}\left[\left(\frac{1}{a} - \frac{1}{2a}\right) - \left(\frac{1}{2a} - \frac{1}{a}\right)\right] = \frac{I\rho_a}{2\pi a}$$

and

$$\rho_a = 2\pi a\left(\frac{V_P - V_R}{I}\right)$$

It is of interest to point out that theoretically Wenner's formula holds

† See also J. N. Hummel, "A Theoretical Study of Apparent Resistivity in Surface Potential Methods," *A.I.M.E. Geophysical Prospecting*, 1932, p. 392.

‡ Frank Wenner, "A Method of Measuring Earth Resistivity," *Bull. U.S. Bureau of Standards*, Vol. 12, 1916.

H. Gish and W. J. Rooney, "Measurements of the Resistivity of Large Volumes of Undisturbed Earth," *Terr. Mag.* 30, 1925, pp. 161-188.

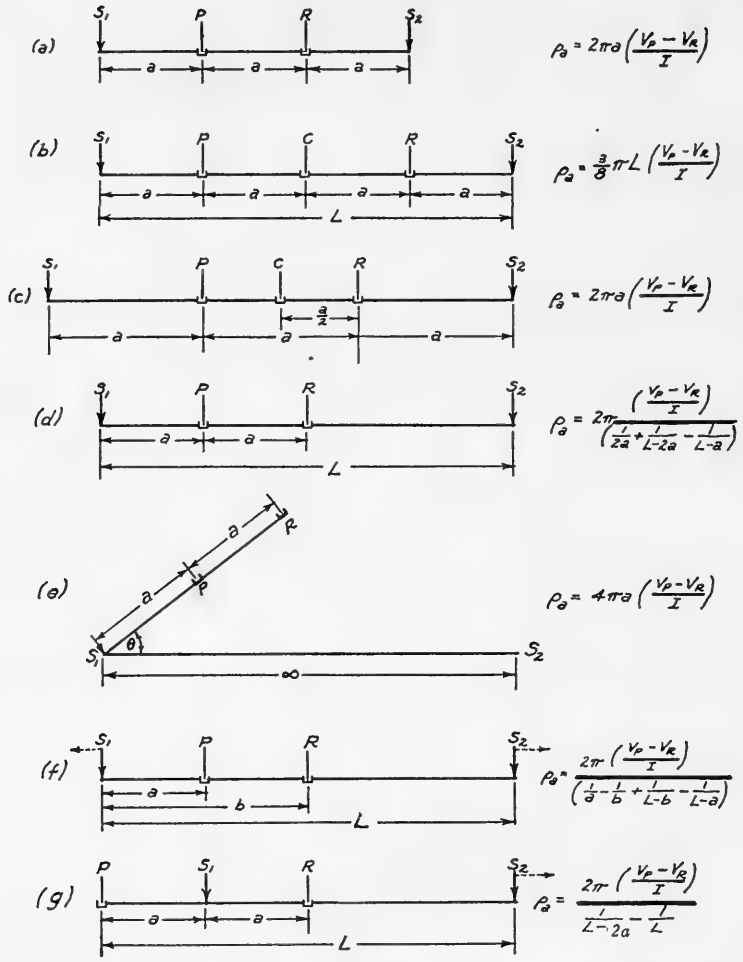

FIG. 313.

(*a*) Wenner configuration
(*b*) Five-electrode method using four equal spacings
(*c*) Lee partitioning method
(*d*) Unsymmetrical method: energizing electrodes separated by a finite distance
(*e*) Unsymmetrical method: one energizing electrode at infinity
(*f*) Method employing moving current electrodes
(*g*) Method employing one moving current electrode and one fixed current electrode positioned midway between the potential electrodes.

irrespective of whether the potential electrodes are inside or outside of the current electrodes.† Practically, however, there is a decided decrease in detectability when the current electrodes are placed inside of the potential electrodes.

† R. J. Watson, "Interpretation of Resistivity Measurements," *A.I.M.E. Geophysical Prospecting*, Tech. Pub. 518, pp. 6-7.

Five-Electrode Method Using Four Equal Spacings (Figure 313b)

$$\rho_a = \frac{3}{8}\pi L\left(\frac{V_P - V_R}{I}\right) = \frac{3}{2}\pi a\left(\frac{V_P - V_R}{I}\right)$$

$$= \frac{3}{4}\pi L\left(\frac{V_P - V_C}{I}\right) = \frac{3}{4}\pi L\left(\frac{V_C - V_R}{I}\right)$$

$$= 3\pi a\left(\frac{V_P - V_C}{I}\right) = 3\pi a\left(\frac{V_C - V_R}{I}\right)$$

Lee Partitioning Method (Figure 313c)

$$\rho_a = 4\pi a\left(\frac{V_P - V_C}{I}\right) = 4\pi a\left(\frac{V_C - V_R}{I}\right)$$

$$= 2\pi a\left(\frac{V_P - V_R}{I}\right)$$

Unsymmetrical Method: Energizing Electrodes Separated by a Finite Distance (Figure 313d)

$$V_P - V_R = \frac{I\rho_a}{2\pi}\left(\frac{1}{a} - \frac{1}{L-a}\right) - \frac{I\rho_a}{2\pi}\left(\frac{1}{2a} - \frac{1}{L-2a}\right)$$

or

$$\rho_a = \frac{2\pi\left(\frac{V_P - V_R}{I}\right)}{\frac{1}{2a} + \frac{1}{L-2a} - \frac{1}{L-a}}$$

Unsymmetrical Method: One Energizing Electrode at an Infinite (Distance Figure 313e)

The power electrode S_2 is assumed to be at infinity. (In practice, this assumption is justified when the separation S_1S_2 is 5 to 10 times that of the farthest potential electrode from S_1.)

$$V_P - V_R = \frac{I\rho_a}{2\pi} \cdot \frac{1}{a} - \frac{I\rho_a}{2\pi} \cdot \frac{1}{2a}$$

or

$$\rho_a = 4\pi a\,\frac{V_P - V_R}{I}$$

At sufficiently great spacings of the power electrodes, S_1 and S_2, the angle θ may take on any value and the formula will be correct. If the distance S_1S_2 is not much greater than S_1R, however, the effect of S_2 may not be neglected, and the formula must be modified.

Method Employing Moving Current Electrodes (Figure 313f)

$$\rho_a = \frac{2\pi\left(\frac{V_P - V_R}{I}\right)}{\frac{1}{a} - \frac{1}{b} + \frac{1}{L-b} - \frac{1}{L-a}}$$

If S_1 is fixed and S_2 moves, L, $L-a$, and $L-b$ are variable quantities, and a and b are constants. If S_2 is fixed and S_1 moves, L, a, and b are variable quantities, and $L-a$ and $L-b$ are constants.

Method Employing One Moving Current Electrode and One Fixed Current Electrode Positioned Midway Between the Potential Electrodes (Figure 313g)

$$\rho_a = \frac{2\pi\left(\frac{V_P - V_R}{I}\right)}{\frac{1}{L-2a} - \frac{1}{L}}$$

Electrodes.—In conductive methods of electrical prospecting, contact with the earth is made by electrodes imbedded or driven into the ground. The investigation of lateral or depth variations in a given area is accomplished by means of a series of measurements made at different positions or spacings of the electrodes. Usually the electrodes are moved along a traverse line. The movement may be in uniform increments of distance (intermittent readings) or at a continuous rate of progression (continuous recording). The type and design of the electrodes depend on the electrical method employed and on field conditions.

Electrodes may be divided into two general classes: (a) non-polarizing electrodes and (b) polarizing electrodes constructed of base metals.*

Non-Polarizing Electrodes

As far as practical application to geophysical work is concerned, the only type of electrode which does not change its properties appreciably with the passing of small quantities of current consists of a porous cup which contains a rod or sheet of metal and a saturated solution of a salt of the metal. In this type of electrode the metal will go into solution or will be precipitated, depending upon the direction of the current. The electrochemical process is reversible, and the chemical relationships do

* Attempts have been made to employ simple electrodes constructed of chemically inactive materials, in order to avoid the inconveniences attached to employing the usual type of non-polarizing electrode. For example, investigations have been made of carbon and graphite electrodes, as well as electrodes constructed of base metals plated with platinum, iridium, gold, silver, etc. Due to their relatively small electrochemical activity, these materials produce smaller electrolytic potentials at the electrode. They do not, however, have any advantages over the base metals, with regard to polarization phenomena associated with the flow of current.

not change with the passage of a moderate amount of current. Electrodes of this type do not completely eliminate electrolytic or contact potential phenomena,† because there must be a contact between the electrolyte seeping through the porous cup and the earth. However, contact potential effects between the two electrolytes, the electrolyte or natural moisture in the earth and the electrolyte of the electrode, is very much smaller than the contact potentials between a metal and the earth electrolyte.*

A non-polarizing electrode of simple design is shown in Figure 314. The hollow bakelite tube functions as a convenient handle and also acts as a reservoir for the saturated copper sulphate ($CuSO_4$) solution. The solution is added by removing the expanding rubber stopper at the top of the hollow bakelite tube handle. Contact with the solution is made by means of a pure copper bar, $\frac{1}{8}'' \times \frac{3}{4}''$ in cross section, with the lower end doubled back to give a larger surface area in the solution and hence a lower contact resistance.

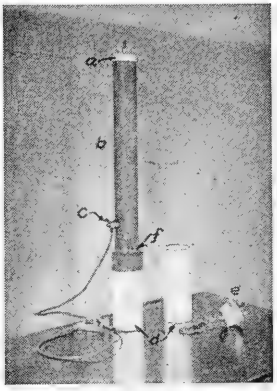

FIG. 314.—Simple non-polarizing electrode.
a—Expansion stopper and cap
b—Handle and reservoir
c—Terminal
d—Porous cup
e—Expanding stopper and guard chain
f—Rubber sleeve

Electrodes of the non-polarizing type have two chief disadvantages in field operation: (a) Precautions must be taken to insure that the materials used are chemically pure and that the materials and electrolyte of one electrode do not differ from those of the other electrode. (b) The electrodes are fragile and cannot be subjected to rough treatment.

In using non-polarizing electrodes, it is necessary to make a small hole in the ground, usually by means of a small hand or garden trowel. The porous cup portion is placed in the hole. A small quantity of water or dilute salt solution should be poured around the electrode and the earth lightly tamped to give better electrical contact.**

These operating details make the use of non-polarizing electrodes in field work rather tedious. This is especially marked in those methods wherein the potential electrodes must be moved rapidly from one set-up to another. Attempts have been made, therefore, to eliminate the use of non-polarizing electrodes by appropriate field technique and design of equipment. Various types of commutating arrangements have been devised to minimize the effects of spurious potentials at the potential electrodes. These will be described later in conjunction with the commutator methods.

† Atsushi Matsubara, "Method of Prospecting Underground Ore Bodies," U. S. Patent No. 2,153,636, April 11, 1939.
Glen Peterson, "Method of Geophysical Prospecting," U. S. Patent No. 2,190,324, Feb. 13, 1940.

* The electrolytic or contact potential between two electrolytes is usually negligible in commercial work.

** The procedure described in this sentence is frequently termed "wetting down."

Metal Stake Electrodes

Stake electrodes may be made from any type of structural or bar metal available. Angle-, H- or T-section iron bars, pipes, round and square rods, etc., have all been used by various workers. For practical use, however, it has been found that square steel rod is most satisfactory. Steel, although costing slightly more, will outlast ordinary cold rolled iron many times, and its longer field life more than offsets its initially higher cost. The initial electrode length is preferably 36 to 40 inches. The electrodes are made preferably from ¾" square rod, which is sharpened at one end.

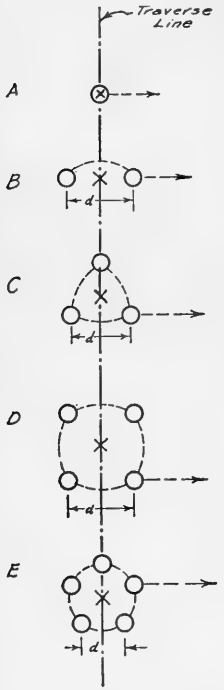

FIG. 315. — Recommended arrangements for stake electrodes. (*d* is depth the electrodes are imbedded in the ground.)

A—Single electrode placed at point of measurement, marked *x*.

B—Two electrodes placed on each side of point of measurement.

C—Three electrodes arranged in equilateral triangle with point of measurement at center.

D—Four electrodes arranged in square with point of measurement at center.

E—Five electrodes, or more, arranged on circle, with point of measurement at center.

The electrodes are driven into the ground to a depth sufficient to contact the moist layer immediately underneath the surface. This depth will vary with local conditions but usually will be from two to twelve inches below the surface. In areas where moist earth cannot be contacted within that depth of the surface, the electrode resistance will be relatively high, and more than one electrode may be necessary. The number of electrodes is governed by the voltage drop which can be tolerated in the energizing circuit. Obviously, an increased contact resistance in the energizing circuit necessitates high voltages to create a sufficient flow of current.

As a general rule, from 85% to 95% of the total potential drop in the circuit takes place in the immediate vicinity of the grounded electrode contacts. In dry earth it is often necessary to reduce the contact resistance by "wetting down" or by employing more than one electrode. Contact with the ground is a typical point contact between the irregular earth particles and the smooth electrode surface. Point contacts of this type develop notoriously high resistances. A lower effective resistance between the electrode and the ground may be obtained by using (a) a larger extended contact area or (b) an electrolyte which fills the interstices between the electrode surface and the earth's particles and thereby increases the contact area. If an electrolyte is used, "wetting down" solutions may be carried in ordinary canvas water bags, such as are employed extensively for desert travel. About one-half pint of saturated salt solution per electrode is usually sufficient.

Location of Multi-Point Electrodes.—A single stake electrode should be driven into the earth at the

desired point of measurement as shown at *A* in Figure 315. When two electrodes are employed, it is advisable to place them as shown at *B*. The individual electrodes should be separated a distance approximately equal to the depth to which they are driven into the ground; as previously mentioned, this depth will vary with the local conditions. If three electrodes are necessary to give the desired current flow, the measuring point should be approximately at the center of an equilateral triangle formed by the electrodes, as shown at *C*. Other electrode arrangements are illustrated at *D* and *E*. In each case an attempt is made to have the electrodes approximate a large extended circular electrode, because a circular arrangement of electrodes produces a minimum distortion of the current lines for a given voltage drop.

Multi-point electrodes are connected electrically by means of "jumpers" made from short pieces of the same wire used for field lines. It is convenient to use jumpers which are made of lengths of wire approximately three feet long and provided with clips at each end and at the center. A jumper of this type will connect three electrodes. The contact clips are the conventional heavy-duty battery clips, which are employed for storage battery charging. A clip which has strong spring-actuated jaws is preferable.

The electrodes are driven into the ground with heavy hammers and are removed from the ground upon completion of a given set of measurements by a special type of stake-puller, or by hammering the side of the electrode to loosen it.

The field work is greatly speeded up if two full sets of stakes are employed for each moving electrode. Two electrode men are stationed along the line of movement of the moving electrode. While one set of electrodes is being utilized in the measurement, one electrode man will move and drive in his set of electrodes at the station to be read next. With an arrangement of this type, the speed of operation in the field depends upon the spacing between electrodes and the energy of the instrument man. Even in areas of fairly rough terrain, electrode moves may be made in time intervals of two to five minutes.

Power-Driven Electrodes.—For the type of electrical measurement where considerable current must be passed into the ground, the electrodes should have a length sufficient to penetrate the dry near-surface layer of soil. The surface layer during the dry season generally contains less than one per cent moisture. When the per cent of moisture versus depth is plotted, a sharp increase in the moisture content usually occurs at a certain depth, varying from a few inches to 10 feet. In most areas this depth will correspond fairly closely to the depth at which the diurnal temperature changes are small, usually from two to four feet below the surface. The metal electrodes should penetrate into this zone of higher moisture content because its electrical conductivity may be many hundreds of times greater than that of the immediate surface layer. (See resistivity-moisture relationships, as shown in Figure 264.)

Long metal electrodes of this type can be driven most advantageously by a gasoline or air power hammer, of the general type shown in Figure 316. After the measurements have been completed, the electrode is withdrawn by means of a hollow-stem hydraulic jack, of the general type illustrated in Figure 317.

FIG. 316.—Driving long electrodes with power-driven hammer. A, gasoline hammer; B, 6-foot, tapered steel electrode; C, spare electrodes; D, hydraulic jack for withdrawing electrode; E, folding "A" frame for supporting hammer; F, reel carrying insulated wire; G, loud speaker for short wave radio communication. (Courtesy of Union Oil Company of California.)

The electrodes are preferably of mild tempered alloy steel, and approximately six feet long. The upper end should be about 1 inch in diameter, tapering uniformly to about 5/8 inch above the point at the lower end. The tapered electrode gives much better contact with the ground, and can be removed more easily.

Mobile Stake Electrodes

Various procedures have been tried for obtaining readings at closer electrode spacings without increasing unduly the time required for a series of measurements. In areas of fairly even topography and moderately hard surface materials, success has been obtained with an intermittent type of electrode mounted upon a light truck. By means of a gear drive

connected to a power take-off on the truck motor, a steel rod 1½ inches in diameter is forced into the ground to a depth of penetration which depends on contact conditions and varies from one foot to three feet. Upon completion of the measurement, the power is reversed and the rod is withdrawn from the earth. The truck is then moved forward to the next point of measurement and the procedure repeated. The reel which contains the field wire is mounted upon the truck, and the wire is auto-

FIG. 317.—Removing steel electrodes after completing electrical measurements. A, hollow-stem hydraulic jack; B, electrode; C, spare electrodes; D, plunger pump; E, electrode clamp. (Courtesy of Union Oil Company of California.)

matically played-out as the truck moves forward. Contact is maintained by means of a suitable slip ring on the reel. The first measurement is made at some predetermined electrode separation, and subsequent measurements are made at uniform increments of distance. This type of arrangement has proved to be somewhat faster than the stake method described above.

The points where contact is to be made are usually measured and marked on the ground by means of stakes (pieces of lath 12 inches long) on which are written the traverse distance. (Because the resistivity formulas for calculating resistivity values include "distance," it is necessary to measure the electrode separations with considerable accuracy.)

Continuous Contact Electrodes

To minimize the time and labor necessary for closely spaced intermittent readings, a mobile continuous contact electrode has been developed. † The mobile electrode obviates the necessity of driving electrodes into the ground at each predetermined electrode position and of surveying-in the various stations. Also, because the electrode is always in contact with the ground, oscillographs may be employed for continuous recording of the potential and current.

The electrode is a small tractor which moves forward at a constant speed which is determined by a governor on the engine. (Figure 318.)

FIG. 318.—Continuous mobile electrode. *a*, reel of flexible insulated wire; *b*, measuring sheave wheel; *c*, steel tractor wheel; *d*, steel contact stakes; *e*, guide for reeling-in cable; *f*, weighted flanged wheels; *g*, contact ring which actuates measuring signal system. (Courtesy of International Geophysics, Inc.)

The uniform movement of the tractor allows accurate control of the time of current flow. The rear wheels of the tractor have a steel rim to which short steel stakes are bolted. The stakes are approximately ten inches long in order to make good contact with the subsoil. Usually four stakes on each wheel are in continuous contact with the ground. The tractor is equipped with special low-gear ratios. A large reel holding about 20,000 feet of heavy insulated wire is mounted on the tractor as shown in Figure 318. A carriage, mounted on top of the reel, supports a measuring sheave wheel and wire spooling device. The measuring sheave is connected to a relay signalling system mounted on the tractor. The relay system automatically transmits to the recording truck the exact footage

† J. J. Jakosky, "Method and Apparatus for Electrical Exploration of the Subsurface," U. S. Patent 2,105,247, issued Jan. 11, 1938; Canadian Patent 374,475, issued June 14, 1938; other U. S. and foreign patents pending.

traversed by this mobile electrode, and this footage, at intervals of ten feet, is recorded on the chart simultaneously with the potential and current values.

A carrier current telephone system is provided to allow communication between the operator of the tractor and the operator of the recording truck. With a potential difference between the electrodes of approximately 2000 volts, an electric current of 1.5 to 5 amperes usually can be maintained. Similar continuous type measurements may be made in submerged areas by using small power-driven cruisers or boats as the moving electrode.

The mobile electrode has greatly increased the effectiveness of electrical methods of prospecting. Usually, when the intermittent type hand-driven stake electrodes are used, three to five hours are required for a series of readings at a station, which consists of measurements made at intervals of every fifty feet along a 5000 foot traverse movement. With the mobile type of electrode these same readings may be made in approximately fifteen minutes. The mobility of the moving electrode has been found to be very good, even in areas of extremely "tough going." The mobile electrode usually requires two operators, one for driving the tractor and maintaining telephonic communication and the other for handling the reel and measuring equipment.

The continuous contact electrode is employed most conveniently in areas where the surface conductivity is fairly high and the surface is not too rocky. In areas where the surface is rocky, the contact will be irregular.

Semi-Continuous Electrode System

A semi-continuous electrode system is illustrated in Figure 319. This system has operating characteristics intermediate between the intermittent stake electrode method and the continuous contact mobile electrode method. The reel contains approximately 10,000 feet of wire and is mounted on a shaft supported by two large steel wheels. These wheels have a diameter of approximately 30 inches and are similar to those used on concrete "buggies." A small hand crank, connected by means of a sprocket chain drive, is employed for reeling-in the wire at the completion of a run. As will be seen from the diagram of connections, the stationary end of the reel is connected to a commutator. The commutator has a single brush contact connected to a transformer. The other terminal of the transformer is connected to the two insulated handles for contacting the electrodes. The secondary of the transformer is connected to a double-pole, double-throw, key switch. In one position, the switch closes a buzzer circuit which is employed for signalling the instrument truck. In the reverse position, the switch closes a telephone circuit which includes a hand-set for voice communication.

Three electrodes, or sets of electrodes, *A*, *B*, and *C*, are placed along

the traverse line at the desired distance apart. By means of insulated handles, provided with spring contact clips, electrode men stationed at 2 and 3 connect the electrodes *A* and *B*, respectively, with the lead wires. The flexible lead wires connecting the reel terminal box with the electrode handles are of equal length, and this length is approximately the distance which the electrodes are to be placed along the traverse line. The operator stationed at 1 slowly moves the reel forward; after a certain distance has

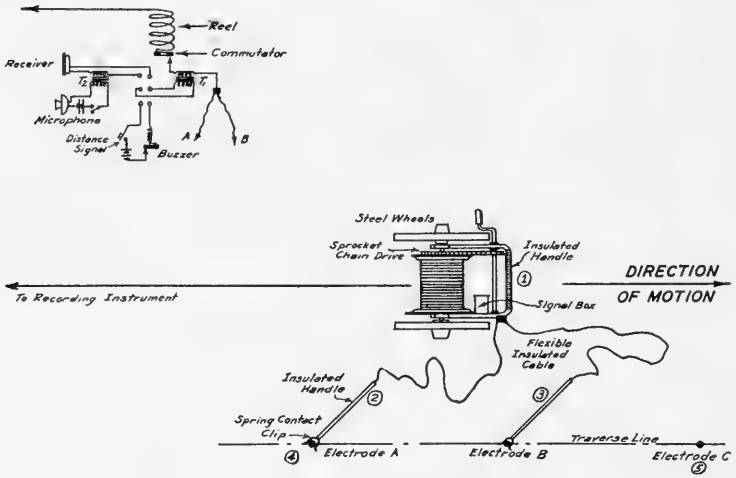

Fig. 319.—Electrical connections for semi-continous electrode system. (Courtesy of International Geophysics, Inc.)

been traversed, the flexible wire connecting the rear electrode *A* becomes taut and continuous movement forward of the reel pulls the clip from the electrode. At this time the operator stationed at 2 walks past the operator at 3 and makes contact with the next electrode *C*. The operator stationed at 4 removes electrode *A* from the ground and drives it into the ground on the traverse line beyond electrode *C*, at the desired spacing. As the reel continues to move forward, electrode *B* will automatically become disconnected, and the same procedure is repeated. By this procedure, one ground electrode, then two, then one again, and so on, are always connected to the recording equipment.

This system of semi-continuous electrode movement necessitates continuous recording equipment similar to that employed for the continuous contact mobile electrode. The position of the reel is signalled to the recording truck by the operator stationed at 1 who closes a key switch each time the reel comes abreast of an electrode. These signals are recorded at the instrument truck in a manner similar to that employed for the continuous moving electrode. The method requires at least five operators for satisfactory operation. In areas of rough terrain, an additional operator may be required for handling the reel. With sufficient

personnel, the use of this electrode is almost as rapid as that of the mobile electrode.

Insulated Wire for Field Use.—A stranded conductor covered with bare rubber insulation is preferred. Cloth braid and other protective coatings for the rubber have not proved satisfactory, principally because the cloth abrades very fast when the wire is drawn across rocks and through brush. In addition, when cloth braid is used, it is difficult to detect breaks in the conductor.

A single conductor of No. 16 American wire gauge is satisfactory for short lines. One wire of this size on the market consists of 13 strands of hard drawn copper, each of which has a diameter of 0.0142 inches and is covered with a thirty per cent rubber insulation of approximately 3/64 inch thickness. For the longer high voltage energizing circuits in which the voltage may rise to 2000 volts or more, it is recommended that a single conductor No. 14 American wire gauge, consisting of 19 strands of 0.0142 inch hard drawn copper with 5/64 inch thirty per cent rubber insulation, be employed. This wire has an estimated tensile strength of approximately 190 pounds. The estimated break-down voltage for the 5/64 rubber insulation is 24,000 volts, while for the 3/64 inch rubber insulation it is approximately 15,000 volts.

During field work in which the conductor is subjected to considerable strain, a single conductor having twelve strands of 0.0126 inch tinned steel and 14 strands of 0.0126 inch tinned copper, bunch stranded with 2-inch pitch, has proved highly satisfactory. This conductor is covered with a 5/64 inch thick, thirty per cent rubber insulation and has a tensile strength of 350 to 400 pounds.

In dry areas where potentials of less than 100 volts are used, standard flexible fixture wire may be employed for the potential and energizing circuit leads. Fixture wire is usually No. 18 or No. 16 gauge stranded copper, covered with 1/64 inch rubber composition insulation and a cotton weatherproof, pitch-impregnated braid. This wire will stand a tensile pull of approximately thirty to fifty pounds.

Wire Splices

Several precautions should be observed when making splices for repairing breaks in the line wire. A layer of self-vulcanizing rubber tape, covered with a layer of friction tape, should be employed. The usual width of friction tape is approximately three-quarters of an inch. It is advisable to split the tape to a width of approximately one-fourth to three-eighths of an inch. Prior to making measurements, all splices and field wire should be tested for line leakage. This can usually be accomplished in the field by disconnecting the ends of the wire from their respective electrodes and applying an overload voltage to the lines.

Reels

Many different types of reels are employed for handling the field wires. For shallow investigations, the length of lines usually does not exceed about five hundred feet, and it is often convenient to place all of

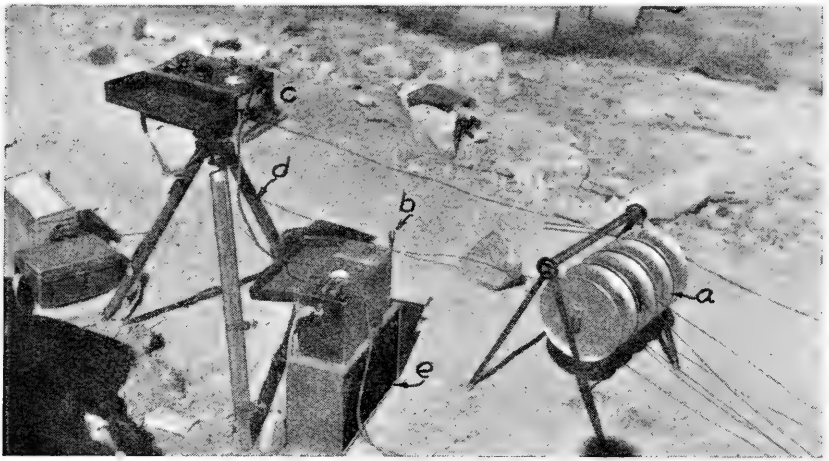

FIG. 320.—Equipment for shallow resistivity measurements. a, potential and energizing reels, mounted on common shaft; *b*, hand cranked commutator system and milliammeter; *c*, potentiometer; *d*, tripod; *e*, battery box.

the reels on a common stationary shaft and locate the shaft near the instrument. (Figure 320.) The potential and energizing lines are then carried out from this central reel system. This method, however, suffers a disadvantage where long lines are necessary, due primarily to two factors: (a) high inductive coupling between the potential and power circuits and (b) undue strain on the lines as they are dragged over the surface of the ground.

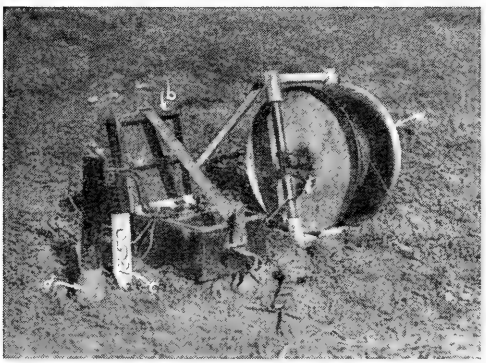

FIG. 321.—Equipment set-up at end of potential line. *a*, reel; *b*, portable field telephone and buzzer signal; *c*, stake marking traverse distance; *d*, non-polarizing electrode. (Courtesy of International Geophysics, Inc.)

For deeper investigations, it is advisable to employ separate reels, preferably of the hand type illustrated in Figure 321. These hand reels hold from 1500 to 2000 feet of 5/32-inch to 3/16-inch diameter wire and weigh approximately 55 pounds when loaded. The flanges of the reel have a diameter of 18 inches and are spun from No.

8 gauge sheet aluminum or No. 12 gauge sheet steel. The flanges are separated by a core and are mounted 5 inches apart on a steel axle, one end of which is extended and bent to form a crank. An "A" frame built of 1-inch seamless, welded, steel tubing is used for supporting the reel. The upper portion of the frame serves as a handle for carrying the reel. The core consists of a 5-inch piece of 3-inch diameter Shelby steel tubing. The inside end of the wire passes through an insulating bushing in the flange

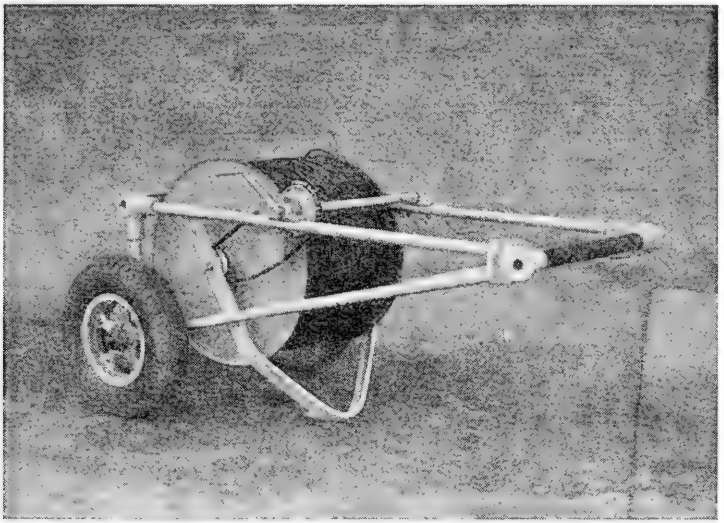

FIG. 322.—Mobile reel for handling field lines. (Courtesy of International Geophysics, Inc.)

and connects to a well-insulated terminal block. This terminal is connected to the electrode by means of a short flexible lead provided with a spring contact.

For deep subsurface investigations requiring long lines, the reel illustrated in Figure 322 is very satisfactory. This reel has flanges 20 inches in diameter which are separated by a piece of 6-inch diameter tubing 20 inches long. The pneumatic tires are the conventional type employed for concrete wheelbarrows and other industrial uses: namely, 4-ply, 4 inch x 8 inch I. D. These reels hold from 5500 to 6000 feet of the 3/16-inch diameter wire. The frames are made of 1¼-inch welded steel tubing. Roller bearings are employed for mounting the reel and the wheels. These reels weigh approximately 350 pounds when loaded, but can be handled by one man in areas of fairly even terrain.

Figure 323 shows the method of moving the reel between readings. In this view, the stakes for the next reading position have been driven and are ready for the reelman. An assistant is removing the previously used set of stakes and will have them in position at the next set-up.

FIG. 323.—Mobile reel in operation. *a*, small portable telephone; *b*, steel electrodes; *c*, flexible connectors; *d*, previously used set of electrodes. (Courtesy of International Geophysics, Inc.)

Handling Field Lines

The lines are laid out by connecting the end of the wires to the proper terminals of the measuring instruments. The wire should be anchored on a convenient wood stake to prevent disturbing the instruments when the wire is pulled. Usually one potential wire and one energizing wire will extend outward in each direction from the instruments. The potential and power lines should be separated 15 feet or more, in order to minimize mutual inductive effects and leakage between circuits.

After testing for line leakage and continuity of circuits, the initial reading may be made. The reels must then be moved consecutively to the various points of measurement. On reaching each of these points, the reelman drives in the required electrodes, carefully connecting each electrode with the reel, and then signals the instrument operator. Upon completion of the reading, the instrument operator signals the reelman and telephones the number, usually the distance in feet, of the next station. The reelman then removes the electrodes from the ground and proceeds to the next station, and the process is repeated.

Proper precautions must be taken to prevent the reelman from setting up at the wrong point. It is usually a good plan for the instrument

operator to give the next point of reading before the reelman leaves, and for the reelman to give his location to the operator before a reading is made at the new point. Abnormal readings or trends in the recorded values should be noted and checked by additional field measurements, if necessary. Careful field work is a prerequisite to proper interpretation. The instrument operator, or preferably a computer, should calculate and plot the values obtained for each point as the field work progresses. In this manner abnormal readings can be detected and checked without undue delay. Although the various steps appear somewhat involved, the operations may be conducted in a rapid manner.

Instruments and Methods.—In the majority of the conductive electrical methods, the quantity measured is the potential created at the surface of the ground for some particular electrode arrangement. Obviously, a great many different types of measurement may be made; hence, a large ramification of methods, apparatuses, and field procedures exists. Limited space prevents a full treatment of the possible field procedures.

The methods discussed below are described because of their commercial use and because they are illustrative of certain general principles of operation. The descriptions are not intended to cover all possible modifications of any of the methods. Instead, an attempt has been made to incorporate in the description of the different methods, various ramifications of instrumental technique. Thus, in the simple volt-ammeter method which is described first, a potentiometer employing a null-point type of measurement is described. It is obvious that other accurate methods of measuring potentials could be employed.

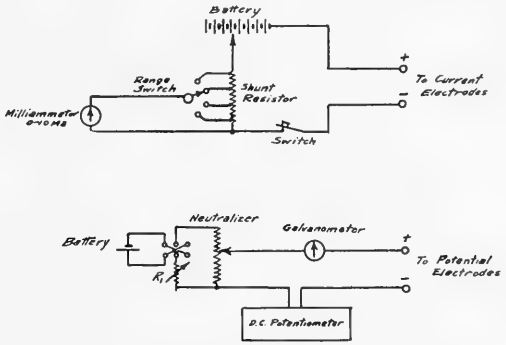

FIG. 324.—Apparatus for simple volt-ammeter resistivity measurements.

Simple Volt-Ammeter Method

A schematic diagram of the electrical connections is shown in Figure 324. Power is usually furnished by a bank of 22½ volt, heavy duty "B" batteries, such as used for radio plate supply. For average areas the potential need seldom be greater than 180 volts, while in dry desert areas potentials of 300 to 400 volts are often necessary. The batteries should

be placed near the operator, who obtains the desired energizing current flow by connecting an insulated clip to the proper battery terminal. The energizing current is measured by a D.C. milliammeter having a range of 0-10 milliamperes and a shunt switch with multiplying ratios of 5, 10, and 100. A foot-controlled, sturdy contactor switch should be provided for opening and closing the circuit. The current electrodes for energizing the ground may be of the iron stake type.

The potentials are measured by means of a D.C. potentiometer having a range of 0-1000 millivolts. The potentiometer should be provided with a double-acting, closed circuit switch or push-button control. The galvanometer should be of the high resistance type, preferably 1000 ohms resistance, and should have a current sensitivity of at least 0.005 milliamperes per scale division. A convenient zero adjustment to bring the galvanometer needle to mechanical zero balance facilitates readings. The potential difference existing between the two potential electrodes due to natural earth potentials is neutralized or reduced to zero before each reading by means of a neutralizer or auxiliary potentiometer. This potentiometer is energized by a 1½-volt dry cell. A reversing switch allows the polarity of the impressed potential to be changed so as to oppose the polarity of the natural ground potentials. A resistor R_1 is employed to reduce the potential impressed across the neutralizer potentiometer to about 500 millivolts. Higher potentials than this make adjustment of the neutralizer unduly critical. The potential electrodes are of the non-polarizing type.

In using this method considerable care is necessary to avoid errors introduced by: (1) the erratic and unpredictable variations in ground potentials in the potential measuring circuit, (2) the rapid decline of the energizing current due to polarization and electrolysis phenomena adjacent the current electrodes, and (3) failure to read the exact value of energizing current simultaneously with the adjustment of the potentiometer for a zero balance on the galvanometer. The effects of the ground current variations can usually be minimized by neutralizing the natural ground potentials and then immediately reading the current values for some setting of the

FIG. 325.—Simple millivolt-milliampere apparatus for resistivity measurements. *a*, potentiometer battery adjustment; *b*, high resistance galvanometer; *c*, ground current neutralizer; *d*, potentiometer dial; *e*, 0-10 milliampere meter; *f*, range switch for milliammeter giving values to 2000 milliamperes; *g*, galvanometer shunt and potentiometer switch keys.

potentiometer. As soon as the current value has been noted by the operator, he releases the foot switch, thereby breaking the current circuit, and then disconnects the potentiometer. If the galvanometer remains at balance it indicates that the natural ground potential has not varied, and the current and potential values read are the values desired. If an appreciable change in natural ground potentials has occurred, the ground potentials should again be neutralized, and the procedure repeated until check ratios of E/I are obtained.

Instruments using this principle may readily be made portable and convenient for field use. Figure 325 illustrates a successful form of apparatus. The folding legs bring the panel to a convenient height when the operator sits on a folding camp chair.

Controlled Potential Method

At depths of more than a few hundred feet, it is necessary that the electrical measurements have an accuracy greater than can be obtained with the simple volt-ammeter procedure described above. More accurate results can be obtained by bringing the potential (or current) up to some fixed value and measuring the corresponding current (or potential). Since a known potential is applied, the only reading that need be made is the current value.

In practice, it is customary to use a source of constant potential and vary the energizing current in order to obtain the set potential value.*

If, during a series of readings, it becomes advisable to change from one fixed value of the potential to another, the effect of the change as a disturbing influence may be evaluated by taking double readings for both potentials at one or more positions of the electrodes. The ratio of E/I is obtained by dividing the potential by the instantaneous value of the current required to balance this impressed potential.

The apparatus shown diagrammatically in Figure 326 has a general similarity to the apparatus for the simple volt-ampere method, and corresponding parts will not be described again. The desired potential is regulated by means of a multi-point switch S_1 connected to a resistor, across which there is a potential drop of 100 m.v. This potential drop is maintained by adjusting a resistor R_1 to give a predetermined reading on the voltmeter E_1. A closed circuit push-button key K_2 controls the sensitivity of the galvanometer. A closed-circuit, double-acting key K_3 normally allows only the neutralizer potentiometer P_1 to be connected in the circuit, thus providing the necessary means for neutralizing the natural earth potentials.

* Maintaining a constant value for the potential is preferable to keeping the current constant or bringing it to some predetermined value because, in the latter procedure, the current must first be adjusted to its desired value and then the potentiometer employed for measuring the potential must be adjusted. During the manipulation of the potentiometer the current ordinarily will have changed, partly because of polarization of the batteries supplying the current and partly because of changes in resistance in the earth in the immediate vicinity of the electrodes due to polarization.

When K_3 is depressed, a certain fixed potential, depending upon the setting of S_2, will be impressed on the circuit causing a deflection of the galvanometer. Key K_1, controlling the energizing current, is depressed simultaneously with K_3, and the energizing current is now adjusted by rotating the dial R_2 to bring the galvanometer back to balance. (The energizing current is adjusted to the proper value to create a potential equal to and opposite in polarity to the applied fixed potential.)

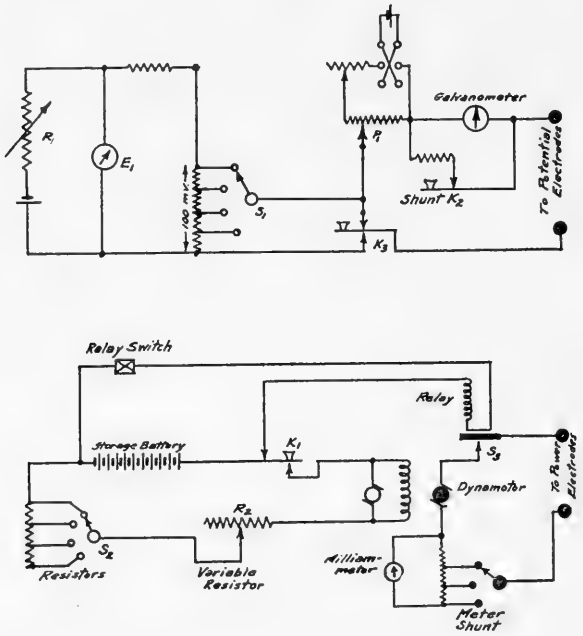

Fig. 326.—Resistivity apparatus for constant potential method.

The power is supplied by a direct current dynamotor which is connected to a storage battery through a heavy duty switch K_1. In series with the battery is a variable resistor R_2 and a bank of fixed resistors which may be tapped at various fixed values by switch S_2. The output of the dynamotor passes through a milliammeter having a range of 0-10 m.a. and a shunt having multiplying ratios 5, 10, and 100. A relay-controlled closed-circuit switch S_3 automatically breaks the circuit when the power switch K_1 is released. S_3 is made automatic in order to prevent the continued flow of current which normally would take place due to the inertia of the generator as it loses speed. The dynamotors are usually wound for 12 to 32 volts D.C. input and 500 to 1000 volts output. Full load output current should be 500 to 1000 milliamperes, intermittent service rating. By means of a tapped resistor and S_2, and the variable resistor R_2, the input current (and hence the output) may be controlled.

This constant potential method is more rapid and accurate than the volt-ammeter method. However, its use requires care on the part of the operator in reading the current at the time of galvanometer balance. In addition, the usual precautions must be taken to minimize errors due to natural ground potential variations. The rapidity with which the measurements are made, usually two to four seconds, prevents appreciable error due to ground currents except on occasional days when rapid magnetic and electrical changes occur.

Other methods have been proposed wherein the energizing current is varied.†

Apparatus for Neutralizing Natural Ground Potentials

The very large potential spacings required when working to depths in excess of 1000 feet cause considerable difficulty due to the natural ground currents.* These currents produce irregular and varying uni-directional potentials which cannot be separated from the potentials created by the flow of the D.C. energizing current. Various methods have been proposed for eliminating or minimizing the effects of these ground potentials. Perhaps the best known of these methods is the one developed by Gish and Rooney.

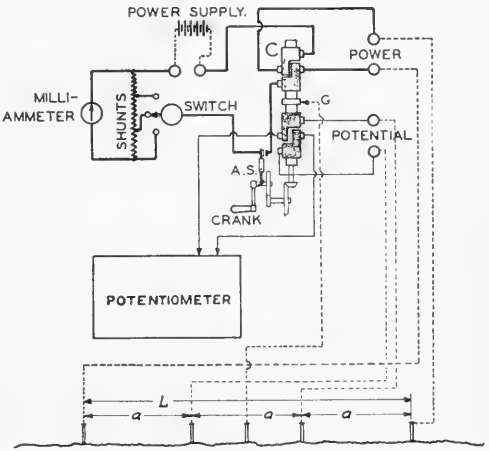

Fig. 327.—Diagram of Gish-Rooney double commutator method.

The Gish-Rooney‡ apparatus (Figure 327) employs a double commutating system so designed that the potential and current systems are reversed in synchronism. The power, which is supplied by suitable "B" batteries, passes through a direct-current milliammeter and into the commutating system. The polarity of the current is reversed periodically by the commutator at a frequency depending upon the speed of rotation—usually about 20-30 reversals per second. A second commutator mounted on the same rotating

† H. M. Evjen, "Electrical Method of Geophysical Exploration," U. S. Patent No. 2,169,685, Aug. 15, 1939.
T. S. West and C. C. Beacham, "Method of Electrical Geophysical Prospecting and Apparatus for Practicing Said Method," U. S. Patent No. 2,217,780, Oct. 15, 1940.
J. J. Jakosky, "Method of Determining Underground Structures," U. S. Patent No. 2,250,024, July 22, 1941.
F. W. Lee, "Electric Impedisivity or Resistivity Measuring," U. S. Patent No. 2,277,701, Mar. 31, 1942.
* O. H. Gish, "The Natural Electric Currents in the Earth," *Scientific Monthly*, July 1936, pp. 47-57.
O. H. Gish, "Electrical Messages from the Earth, their Reception and Interpretation," *Journal of the Washington Academy of Sciences*, Vol. 26, No. 7, July 15, 1936.
‡ W. J. Rooney and O. H. Gish, "Results of Earth-Resistivity Surveys near Watheroo, Western Australia and at Ebro, Spain," *Terr. Mag.* 32, pp. 49-63 (1927).

shaft as the power commutator is used for reversing the potential periodically. This commutator changes the alternating potential created by the commutated energizing current to a pulsating uni-directional potential which can be measured by a standard direct-current potentiometer.

The double commutator system eliminates the variable ground currents from the measurements, because any difference in a uni-directional potential existing between the two inner electrodes is automatically nullified due to the rapid reversals.

The commutator may be either hand-cranked or motor-driven. A motor-driven commutator maintains constant speed which permits more accurate work and also eliminates the services of an assistant. Between the two commutators is a guard or slip-ring which is grounded as shown in the wiring diagram in order to prevent leakage from the current commutator to the potential commutator.*

Precautions must be taken to prevent stray or leakage currents from influencing the potential readings. In addition, the lines and reels connected to the instrument should be laid in a manner which will minimize induction effects. Although direct current is secured from the power batteries, the "make" and "break" of this direct current, while being changed into a periodically reversed current, creates bad transient effects. These are usually minimized by having the power circuit "make" a short time interval before, and "break" a short time interval after the potential circuit. When this procedure is used, steady-state conditions exist during the time interval in which measurements are made.

The previously described constant potential system may be incorporated in the commutator method, with a resultant increase in general overall accuracy and speed of reading due to the fact that variations in ground potentials are removed by the commutator.

Photographic Method for Minimizing Effects of Ground Currents. —The current can be passed into the ground at predetermined time intervals, and the reoccurring pattern may be viewed with any of the conventional type oscillographic equipment. For field use, the cathode ray oscilloscope has been found particularly suitable. For this use an oscilloscope, with suitable amplification, is incorporated into the resistivity measuring instrument. The ground potentials are fed into an amplifier and then impressed across one pair of deflection plates. The energizing current is passed through deflection coils that have their axes at right angles to the potential deflection plates. The slope of the path of the resultant pattern depends upon the relative magnitudes of potential and current, and the instrumental constants.

Due to the persistence of vision, accurate measurements of slope may be made with pulses arriving as slow as one per second.

By use of suitable panchromatic film and a wide aperature (fast) lens,

* Constructional details for this equipment are available at the Carnegie Institution of Terrestrial Magnetism, Washington, D. C.

a photographic record of the pattern for each electrode position may be obtained. The exposure should be such as to give only a faint trace for each sweep of the beam. By recording a series of sweeps, the true slope is accurately shown by the record. Varying natural ground potentials merely cause a shift in the starting point of the trace, and do not affect the slope of the recorded patterns.

Alternating Current Methods

Various alternating current methods are employed for earth resistivity measurements.† As indicated earlier, the characteristic feature of these methods is the use of an alternating current power supply instead of a direct or commutated current supply.

Medium Frequency Alternating Current Method.—Power for energizing the ground for this work is obtained by alternators driven by a small gasoline engine or a D.C. converter which operates on storage battery power. Frequencies in excess of 50 cycles per second are undesirable due to errors introduced by phase shift, etc.

The output terminals of the alternator are connected to the primary of an input transformer. The secondary of this transformer is tapped in order that the secondary impedance may be matched to the electrode-circuit impedance. By means of a multi-point switch and the field rheostat of the alternator, the energizing current may be controlled as desired. The alternating current potentials are measured by means of a vacuum tube voltmeter. The required sensitivity is determined by the electrode configuration used and the power available for the current circuit.

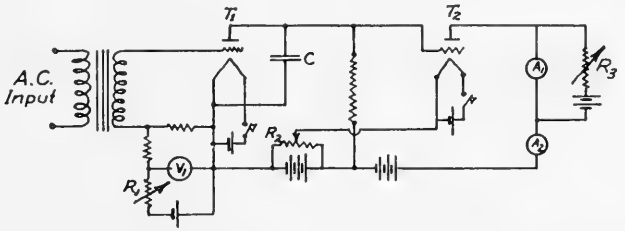

Fig. 328.—Circuit diagram of vacuum tube voltmeter for measuring alternating current potentials.

Vacuum Tube Voltmeter

The vacuum tube voltmeter shown in Figures 328 and 329, consists of a detector tube T_1 used to rectify the A.C. signal and a stage of direct coupled amplification which amplifies the D.C. output from the first stage. Calibration is dependent upon

† L. F. Athy and H. R. Prescott, "Method of Electrical Prospecting," U. S. Patent No. 2,172,271, Sept. 5, 1939.
P. W. Klipsch and S. S. West, "Electrical Prospecting with Alternating Current," U. S. Patent No. 2,231,013, Feb. 11, 1941.
P. W. Klipsch, "Method of Electrical Prospecting," U. S. Patent No. 2,293,024, Aug. 11, 1942.

maintaining the proper grid voltages on the tubes. In the first stage, the grid voltage is maintained by adjustment of R_1 to give a predetermined voltage, read on V_1. The variable resistor R_2 is used to adjust the total plate current of T_2 (read on milliammeter A_2) to its proper value with no A.C. signal input. The rheostat R_3 is then adjusted to bring the milliammeter A_1 to a zero position so that this meter can be used to read the changes in plate current of the tube T_2, which are caused by the A.C. signal input. By proper calibration the meter A_1 can be made to read the volts (or millivolts) input to the voltmeter directly.

FIG. 329.—Vacuum tube A.C. voltmeter.

Low Frequency Alternating Current Methods.—The use of very low frequency alternating current (1 to 10 cycles per second) greatly minimizes the mutual inductance between the current and potential circuits and the phase shift effects which occur when the higher frequencies are used. The ordinary low frequency alternator is not practical for field use because of its large size.

Ambronn† utilizes harmonic current variations from a rotating resistor to produce the desired low frequency alternating current. The frequency depends entirely upon the rotational speed of the resistor and may have any desired value.

A low frequency harmonic power method is illustrated in Figure 330. The power supply, which may be any suitable D.C. source, such as storage batteries or an engine-driven generator, is connected across a commutator. The commutator comprises 100 or more segments which are connected to a closed ring of resistors. A rotating arm carries a contact brush at each

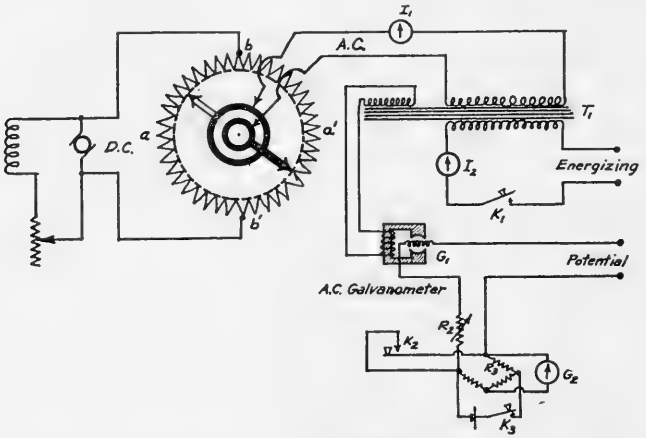

FIG. 330.—Electrical circuit for low frequency harmonic power method.

† Richard Ambronn, "Improvements in Process of and Devices for Electrically Exploring the Ground by Means of Alternating Currents of Very Low Frequency," British Patent 308,256, issued June 11, 1930.

end and connects the input winding of transformer T_1 to different segments of the commutator. (The commutator arm may be rotated by a gear train connected to the D.C. generator.) When the contact arms are at positions *a-a'*, no potential difference is impressed across the transformer; at positions *b-b'*, the full load voltage is impressed. Hence, the potential impressed across the transformer varies from zero to a maximum and passes through a complete A.C. cycle for each complete revolution of the rotating arm.

The voltage between the potential electrodes may be measured by the previously described vacuum tube voltmeter or by a sensitive alternating current galvanometer or millivoltmeter. The power supplied to the energizing circuit is measured by the milliammeter I_2 which is equipped with appropriate shunts. If an alternating current galvanometer or millivoltmeter is employed, the potential measuring circuit is current-operated (the current being measured in terms of fractions of a microampere), and a correction must be made for variations in the resistance of the circuit. This can be accomplished by two methods: (a) measuring the actual resistance of the circuit for each set-up of the potential electrodes or (b) selecting some arbitrary circuit resistance, e.g., 1000 ohms, and thereafter always adjusting the potential circuit to this value before each reading. The latter procedure simplifies the field operations and the computations.

The circuit shown in Figure 330 illustrates a conventional bridge which may be utilized for the type (b) method of operation. Adjustment of the potential circuit is made by depressing the closed-circuit key K_2, closing K_3, and then adjusting R_2 until the galvanometer G_2 indicates a balanced circuit. Flexibility of the equipment for use in different areas is obtained by making the resistor R_3 adjustable, with values of 500, 1000, and 2000 ohms. The lowest value is used in damp or wet areas; the mean value is used in areas where average surface conditions obtain; and the highest value is used in dry desert areas. Best sensitivity will be obtained by always operating at the lowest value possible in any given area. Should it be deemed advisable to change values during the progress of a survey, the data may all be converted to a common basis by correcting for the circuit resistance changes.

Methods for the Direct Measurement of the Ratio E/I.—In the methods described thus far, separate measurements are made of the voltage and current simultaneously. However, only the ratio E/I is needed for calculating the apparent resistivity, and it is advantageous to use instruments which measure this ratio directly because only one reading need be taken, with a resultant increase in speed and accuracy.

Many types of direct ratio reading instruments have been proposed. Of these, the Megger is the best known at present, although its use in geophysical measurements is limited, due to its inherently poor sensitivity.

The Megger

The Megger is a trade name applied to a type of instrument ordinarily employed for testing electrical insulation resistance and ground resistance. A modification of this instrument, the "Megger Ground Tester," may be used for shallow subsurface investigations.

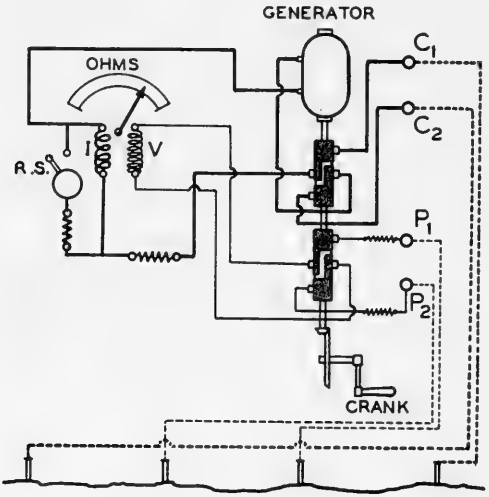

FIG. 331.—Diagram of connections for Megger circuit.

The Megger Ground Tester † is illustrated diagrammatically in Figure 331. Turning the crank rotates a small direct-current generator. The output from this generator passes first through the current coil or ammeter element of an ohmmeter; the current then goes to a commutator mounted on the same shaft as the generator and is changed into commutated current of about 50 cycles per second. The current binding posts C_1 and C_2 are connected to the two energizing stakes. The two potential stakes are connected to the potential binding posts P_1 and P_2. The potential drop across these two stakes is measured by passing the current picked up by them through a second commutator, run synchronously with the first, which converts the current back into a uni-directional flow. The current then goes to the potential coil, or voltmeter element, of the ohmmeter.

The current coil and the potential coil of the ohmmeter are mounted on a common spindle (not shown in the sketch). The mounting is such that the torques exerted by the current and potential coil on the moving element of the ohmmeter oppose one another. Hence, the deflection of the ohmmeter element is proportional to the quotient of the potential divided by the current, and the scale of the Megger may be calibrated to read volts divided by amperes, i.e., ohms, directly. The instrument therefore indicates the effective *resistance* between terminals P_1 and P_2.

Before calculating apparent resistivity values, various corrections must be applied to the E/I quotient. A small but appreciable current flows in the so-called potential

† B. Low, S. F. Kelly, W. B. Creagmile, "Applying the Megger Ground Tester in Electrical Exploration," *A.I.M.E. Geophysical Prospecting*, 1932, pp. 114-125.

circuit of the Megger, and this flow of current causes a potential drop due to electrode and circuit resistances. Corrections for these resistances are made by calibration. For one instrument, the following relationships were obtained:

TABLE 19

CALIBRATION DATA FOR MEGGER INSTRUMENT

Range in Ohms.	N Normal Resistance of Potential Circuit.	C Calibration Resistance.	Permissible Variation in Resistance for		
			1%	2%	3% error
0-3,000	150,000	2,000	500-3500	0-5000	0-6500
0- 300	50,000	1,000	500-1500	0-2000	0-2500
0- 30	20,000	400	200- 600	0- 800	0-1000
0- 3	10,000	300	200- 400	0- 500	0- 600

Normal resistance of potential circuit includes calibration resistance. Calibration resistance is the resistance assumed for the electrode stakes P_1 and P_2 in calibrating the instrument. Permissible variation means that the total resistance of the two electrodes must lie within the figures given for the error in the reading not to exceed the percentage indicated.

The procedure for correcting the electrode resistance is as follows:

P_1 and P_2 = actual resistances at potential stakes.

Actual resistance in potential circuit $= N + P_1 + P_2 - C$.

If $P_1 + P_2 = C$, the reading is correct.

If $P_1 + P_2$ is less than C, the reading is too high.

If $P_1 + P_2$ is greater than C, the reading is too low.

The correction factor is $\frac{N + P_1 + P_2 - C}{N} = F$

True resistance = Observed reading x F

% error $= \frac{F - 1}{F} \times 100$

Finally the corrected values of the *resistance* E/I may be changed to apparent resistivity values by the various formulas previously derived for the different electrode configurations wherein two current stakes and two potential electrodes are used.

RATIO INSTRUMENT

A very convenient vacuum tube instrument† for determining the ratio E/I possesses excellent flexibility, sensitivity, and ease of operation. Use is made of the linear relationship between the applied plate potential and the amplitude of the current in an oscillating vacuum tube circuit. In the usual geophysical application of the instrument, variations in the energizing current produce variations in the potential applied to the plate of an oscillating triode tube. These variations in plate potential cause corresponding variations in the oscillating current. The oscillating current is rectified and flows through a calibrated potentiometer. The potential drop across the potentiometer varies with the oscillatory current which, in turn, varies with the energizing current.

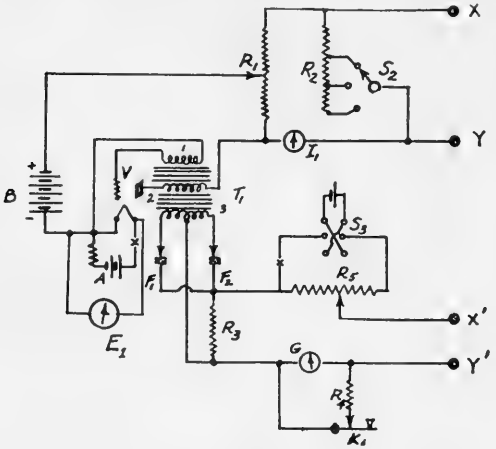

FIG. 332.—Circuit diagram for vacuum tube ratio instrument.

A schematic wiring diagram of the instrument is shown in Figure 332. The energizing electrodes and the power supply are connected to terminals X and Y which are connected to a heavy wire potentiometer R_1. A multipoint switch S_2 and resistor R_2 provide shunts for higher current ratings. The current through R_1 is indicated by the milliammeter I_1. The vacuum triode V is connected as an oscillator through transformer T_1. The potential applied to the plate of this oscillator is that of the battery B plus the potential drop across a desired part of the potentiometer R_1. Transformer T_1 must be of the shielded type, with special precautions taken to prevent leakage between the energizing current circuit which is connected to windings 1 and 2 and the potential circuit which is connected to winding 3.

Winding 3 of the transformer is connected to a full wave rectifier (of the copper-oxide type), and the rectified output passes through R_3. The drop across R_3 furnishes the potential for balancing against the E.M.F. existing between the two potential electrodes which are connected to the terminals X' and Y' of the diagram. The potentiometer R_5, with its small battery and reversing switch S_3, is used: (1) to neutralize the natural ground potentials and the potential drop across R_3 due to minimum plate current flow of the oscillator and (2) to compensate for the drift (usually negligible) of the oscillator output. The sensitivity of the galvanometer G is increased by depressing the closed circuit switch K_1 which removes the shunt R_4 from the galvanometer circuit.

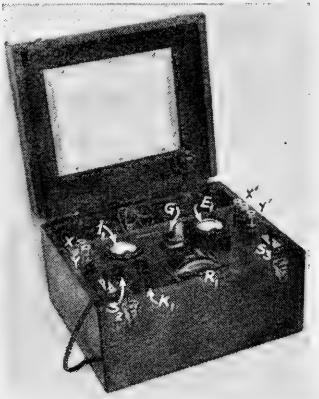

FIG. 333.—Vacuum tube ratio instrument. X and Y, current terminals; X' and Y', potential terminals; S_3, neutralizer reversing switch; E_1, filament and plate voltmeter; I_1, current meter; G, galvanometer; S_2, range switch for I_1.

† J. J. Jakosky, "Method and Apparatus for Electrical Exploration of the Subsurface," U. S. Patents 2,162,086; 2,162,087, issued June 13, 1939; "Method and Apparatus for Electrical Exploration of the Subsurface," Canadian Patent 374,475, issued June 14, 1938.

A photographic view of the instrument is shown in Figure 333. The panel controls are marked with the same designations used in the wiring diagram. Operation of the instrument is simple and rapid: (a) The desired current range is selected by means of the shunt switch S_2;* (b) the potentiometer R_5 is adjusted to neutralize the potentials existing in the potential electrode circuit; (c) the energizing circuit is closed, and the potentiometer R_1 is adjusted to give a null reading or balance on the galvanometer G. The reading of the calibrated potentiometer R_1 for null reading of G is the desired E/I ratio.

The instrument may be used with direct, commutated, or alternating current. In the latter two cases, an alternating current galvanometer, preferably of the rectifier type, is employed.

Potential Gradient Methods.—The theory of these methods is analogous to that of the gradient methods in gravimetric and magnetic explorations. Successful utilization of the gradient of the electrical potential would allow the field data to be presented in such a manner that those conductors which are better than the regional average could be plotted as positive gradients while conductors which are lower than the regional average could be plotted as negative gradients. (The contact between formations of different electrical conductivities would produce an inflection or zero gradient in the gradient profiles.) Furthermore, if it could be assumed that there is no distortion of the equipotential bowls surrounding an energizing electrode, the depth to a formation boundary would be indicated as the distance of the point of zero gradient from the energizing electrode. In practice it is found that this distance is a fraction of the potential bowl radius. This fraction is unfortunately not a constant but varies with different resistivities of the two layers.

In actual field application, these methods are subject to the same limitations as the resistivity methods, and the simple interpretation of the field data is applicable only in very limited cases.

Ratiometer Methods

In the ratiometer methods, potential drop ratio measurements are made with the aid of a modified bridge circuit.† A potential drop ratio compensator ‡ developed by Th. Zuschlag and called a "Racom" is illustrated schematically in Figure 334.

A source of power is connected to the current electrodes S and S', the electrode S' being located at such a distance that only the potential distribution due to electrode S need be considered. The bridge circuit makes contact with the ground at three points A, B, and C. The two ratio arms AD and DC contain variable known resistances R_1 and R_2 and the fixed contact resistances R_A and R_C of the electrodes A

* The current range used depends on the resistivity and the contact conditions in the area where the measurements are being conducted.

† C. Schlumberger, U. S. Patent 1,163,468.
H. Lundberg, "Potential Method for Elektrisk Malmletning," *Jernkontorets Ann.* 1919; see also *A.I.M.E. Geophysical Prospecting*, p. 50, 1932.
J. G. Königsberger, *Zeit für Geophysik*, 1930, Vol. 6.
A. Broughton Edge, British Patent Application 19120/30; see also Broughton Edge and Laby, *Geophysical Prospecting*, pp. 50-56 (Cambr. Univ. Press, 1931).

‡ H. Lundberg and Th. Zuschlag, "A New Development in Electrical Prospecting," *A.I.M.E. Geophysical Prospecting*, 1932, pp. 47-62.

and C. When the bridge is balanced, i.e., zero deflection of the indicating instrument T, the following relation holds:

$$\frac{E_{AB}}{E_{BC}} = \frac{R_A + R_1}{R_C + R_2}$$

In this equation, the resistances R_A and R_C are unknown. Hence, a *compensation process* is introduced in order to obtain an expression for the potential drop ratio in terms of measurable quantities.

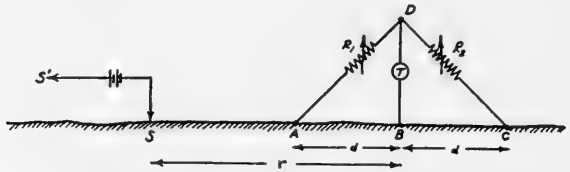

FIG. 334.—Potential drop ratio compensator. (After Lundberg and Zuschlag, *A.I.M.E. Geophysical Prospecting*, 1932.)

Suppose R_1 is arbitrarily changed to R_1', thus destroying the bridge balance. The bridge may be brought back to balance by adjusting R_2 to R_2'. The condition for balance becomes

$$\frac{E_{AB}}{E_{BC}} = \frac{R_A + R_1'}{R_C + R_2'}$$

On combining this equation with the last equation, we obtain

$$\frac{E_{AB}}{E_{BC}} = \frac{R_1' - R_1}{R_2' - R_2}$$

Although the contact resistances are eliminated from the final expression for the potential drop ratio, reliable results will be obtained only when contact resistances are negligible. This is true because the contact resistance is not a constant but is dependent on current flow and other factors which may change during a measurement.

The apparent resistivity at any station is proportioned to the product of the observed potential drop ratio and the resistivity of the surface layer.

The instrument described above is not suitable for use with alternating fields. A more recent form of the compensator is said to permit large phase adjustments and cover a wide range of contact resistances.

Low Frequency Potential Gradient Instruments

Many other potential gradient instruments have been developed† which utilize low frequency alternating current for energizing the ground. When low frequency energizing is used, the relatively detailed phase determinations that are required in the 500 and 250 cycle Ratiometers or Racoms are unnecessary, and depth penetration is increased. The circuit employed in a majority of these instruments corresponds to that of a simple alternating current bridge. Usually the zero instrument for indicating balance is a sensitive oscillograph galvanometer used with an amplifier.

As with other potential gradient instruments, depths to formation boundaries are indicated by zero gradients only if the layers are horizontal.

† For example, see C. A. Heiland, "Improvements in Geophysical Equipment for Foundation and Ground Water Research," presented at the A.I.M.E. meeting, New York City, February, 1937; "Method and Apparatus for Electrical Prospecting," U. S. Patent 2,189,377, issued Feb. 6, 1940.

Ground Current Compensation by Auxiliary Circuit.—As a general rule, the ground currents flow over large areas and show an approximately regional distribution. Advantage often may be taken of this fact to minimize ground potential variations in the measuring circuit. † A typical arrangement is illustrated schematically in Figure 335. Two potentiometers P_1 and P_2 which are mounted on the same control shaft C are connected to the three potential electrodes 3, 4, and 5. Electrodes 3 and 4 are so placed, with reference to the energizing electrode 1, that they are on the same equipotential line when energizing current flows in the power circuit. Electrodes 3 and 4 are spaced relatively close to 1 (usually less than $\frac{1}{5}$ the total separation of the energizing electrodes) so that no significant shift of the equipotential line will take place when the energizing electrode 2 is moved. The spacing between 4 and 5 is some known

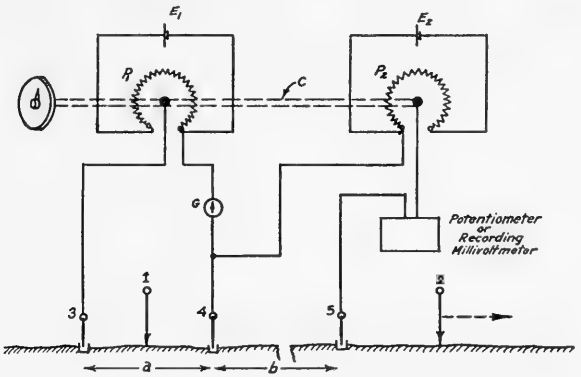

Fig. 335.—Auxiliary circuit for neutralizing variations in ground currents.

multiple of that between 3 and 4. The potentials E_2 and E_1 are in the same ratio as the electrode separations between 3 and 4 and between 4 and 5. Thus, if distance b is three times a, $E_2 = \frac{1}{3} E_1$. The distance b must be greater than a in order to minimize the effect produced by the movement of electrode 2 on the potential difference between 3 and 4.

Continuous adjustment of P_1, to keep the galvanometer G at balance, will automatically introduce a proportional neutralizing potential into the circuit containing P_2. Because the energizing current predominately affects the potential difference between 4 and 5, the readings in that circuit are employed for making the resistivity calculations. If desired, automatic compensation may be employed by means of a vacuum tube control wherein the potential difference between 3 and 4 is applied to

† J. J. Jakosky, "Method and Apparatus for Electrical Exploration of the Subsurface," U. S. Patent 2,162,087, issued June 13, 1939.

the grid of the control tube, and the correspondingly varying output across a resistor in the plate circuit is connected to electrodes 4 and 5.

Continuous Recording Apparatus. — When continuous recording apparatus is used, the values of potential, current, and electrode movement are recorded photographically on a moving film. Upon completion of the run, the record is developed and the values of potential and current are scaled from the record and substituted into appropriate resistivity formulas for the particular electrode spacing employed. Graphs are then made of the apparent resistivity values at various electrode separations, ordinarily at regular intervals of about 50 feet, versus the traverse distance.

A portion of a typical field record which shows instantaneous values of potential E and corresponding values of the current I is given in Figure 336. The vertical lines mark each ten-foot movement of the mobile electrode.

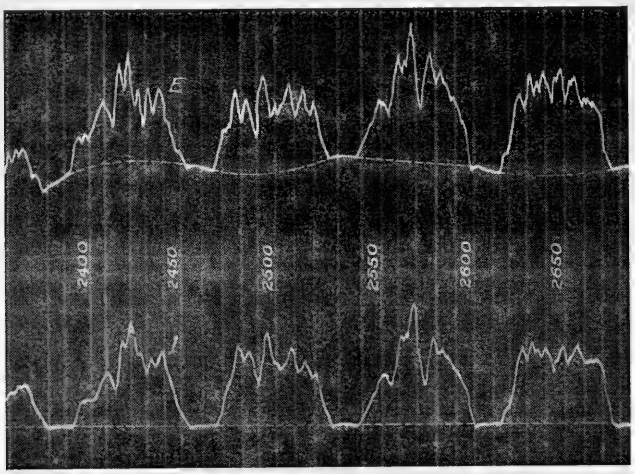

FIG. 336.—Typical record showing instantaneous values of potential E and corresponding values of the current I.

The current for energizing the ground is a uni-directional pulse having a controlled time interval † to govern polarization. During the intervals of time when the energizing current is off, the potential recorded is that created by the natural ground currents. Variations in natural ground potentials are shown by a curve which connects points obtained when the energizing circuit is open.

A view of the complete equipment for continuous profiling is shown in Figure 337.‡ Cabinet 1 contains controls for the recording camera, the potential and current galvanometers, and a carrier-current relay-

† J. J. Jakosky, "Method for Determining Underground Structure," U. S. Patent 2,015,401, issued Sept. 24, 1935.

‡ J. J. Jakosky, "Continuous Electrical Profiling," *Geophysics*, March 1938, pp. 130-153.

actuated measuring light; cabinet 2 contains the power control panel, the field rheostat for the generator, ratio instrument, etc.; cabinet 3 contains the direct current amplifier for the ground potentials; cabinet 4 contains telephone and signal apparatus, for communication between mobile and stationary electrode operators. The generators have a 2000 volt 2 ampere rating and may be connected in series or parallel. The control 11 governs the speed of the truck motor; the latter drives the generators through a conventional power take-off.

The recording camera, which is similar in design to the camera described below for seismic work, employs two recording traces and the distance measuring lines, as shown in Figure 336.

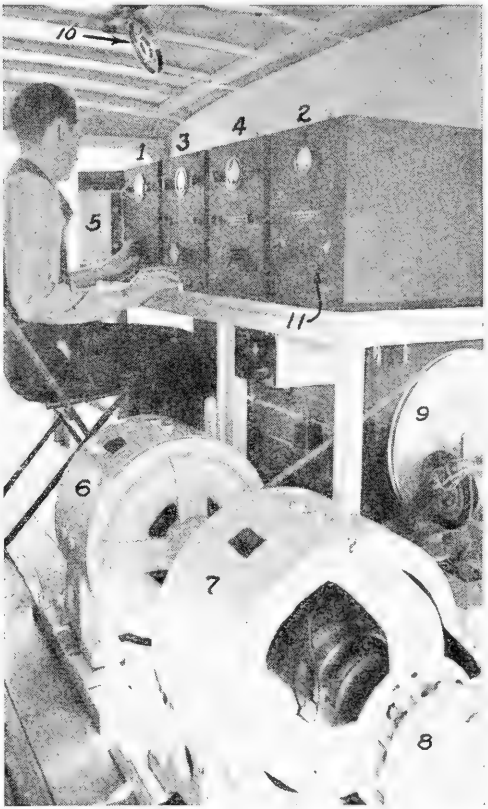

FIG. 337.—Complete equipment for continuous profiling: (1) control cabinet for recording equipment, (2) power control apparatus, (3) direct current amplifier for earth potentials, (4) communication, (5) recording camera, (6) and (7) high voltage direct current generators, (8) excitor, (9) commutator for pulse frequency, (10) microphone for communication with mobile electrode, (11) throttle control for truck engine driving the generators. (Courtesy International Geophysics, Inc.)

Transient Method.—When a *varying* current is caused to flow in the subsurface between grounded current electrodes, magnetic and electric fields varying with time are produced at the surface. These fields induce voltages in the potential or measuring circuit, which are added to the earth-conductivity voltages.

Consider, for example, that the electrode configuration comprises four electrodes with the two potential electrodes located on the *extension* of an imaginary line through the current electrodes.† Let $A(t)$ denote the transient voltage measured at the potential electrodes due to one ampere of direct current suddenly applied between the current electrodes and let $A'(t)$ denote the derivative of $A(t)$ with respect to time. ($A(t)$ and $A'(t)$ are simply the voltage oscillograms that are obtained during

† Gifford White, "Application of Rapid Current Surges to Electric Transient Prospecting, *A.I.M.E. Geophysical Prospecting*, Tech. Pub. 1216, 1940.

the measurements in surveys by the transient method.) It may be shown that if either of these functions is known the voltage due to any other driving current, however arbitrary, may be computed. That is, a single measurement of $A(t)$ or $A'(t)$ is sufficient to compute the response that would be observed for any other applied current surge, provided only that the surge is sufficiently short.*

In an early application of this method † it was desired to record the transient characteristics obtained when a direct current was established through a path, a portion of which included the area under investigation. For a single layer, a direct current transient will have a time constant ‡

$$T = \frac{Ah}{R}$$

where A is a constant, h the depth of the layer, and R the resistance of the layer.

Blau postulated that if more than one layer were present the build-up time for the first layer would be relatively unaffected, and each subsequent layer would contribute a transient whose duration would be proportional to its thickness. The various transient effects would therefore be superposed on one another and would produce a composite transient composed of "ripples." The various ripples would thus be indicative of particular subterranean strata. It was futher postulated that a thin layer would create a short ripple on the transient curve while a thick layer would create a long ripple.** Lateral changes in the thickness of any stratum would be indicated by corresponding changes in the time interval of the ripples observed at different locations.

Because the transient methods†† utilize a surge of current into the ground, studies may be made of both the time constant and the ratio of

---

* It may be shown also that the ordinary direct-current resistivity is equal to the area of the $A(t)$ oscillogram, measured by a planimeter or other means, divided by the total electric charge Q of the surge. This is true irrespective of the slowness or rapidity of the surge. Hence, by employing a surge generator to supply power and a ballistic type of meter to integrate the amplified voltage transient, readings can be taken rapidly and accurately without using calibrated potentiometers, non-polarizing electrodes, or photographic recordings.

† L. W. Blau, "Method and Apparatus for Geophysical Exploration," U. S. Patent 1,911,137, issued May 23, 1933.

L. W. Blau and L. Statham, "Apparatus for Recording Earth Current Transients," U. S. Patent 2,079,103, issued May 4, 1937.

‡ Franz Ollendorff, "Elektromagnetische Ausgleichsvorgänge in Geschichtetem Erdreich," *Archiv Für Elektro-Technik*, Vol. 23, No. 3, pp. 261-278, 1930.

** The data would be plotted with the time duration of the ripple as ordinate and the distance on the surface from the point of reference as the abscissa, just as in seismic work where the times of arrival are plotted against distance from the point of reference.

†† G. E. White, "Electrical Transient Prospecting," U. S. Patent No. 2,251,537, Aug. 5, 1941; "Geophysical Prospecting," U. S. Patent No. 2,291,596, July 28, 1942.

P. W. Klipsch, "Mixing Circuit for Electrical Prospecting," U. S. Patent No. 2,251,549, Aug. 5, 1941.

T. Zuschlag, "Apparatus for Geophysical Prospecting," U. S. Patent No. 2,278,506, April 7, 1942.

S. J. G. Pirson, "Method and Apparatus for Geoelectrical Exploration," U. S. Patent No. 2,319,764, May 18, 1943.

E/I. A paper by Karcher and McDermott† gave the results of experimental work in determining time constants and resistivities using a fixed current electrode spread and outlined the general limitations of the work. A subsequent paper by Statham‡ described a modified configuration utilizing two current circuits so positioned that their effects nullified each other.

Investigations using alternating current of rectangular or other non-sinusoidal wave form were described by West.§ In this work, the two detecting electrodes were placed in line with, but outside of, the current electrodes. The changes in wave form caused by anomalous subsurface structures were determined by a null method in which the surface poten-

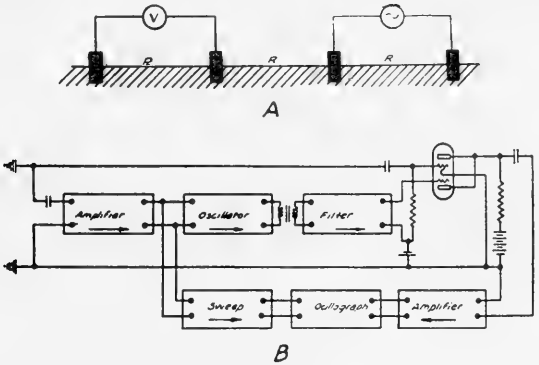

Fig. 338.—Electrode and apparatus for transient prospecting studies. *A* shows the electrode configuration with the detecting electrodes at the left and the current electrodes at the right. *R* is usually 1000 feet. *B* shows the detecting and analyzing circuit, which is represented in diagram *A* as a simple voltmeter. Arrows indicate direction of control or current propagation. (West, *Geophysics.*)

tial transient was balanced against an electromotive force produced by passing the output of an oscillator through an adjustable network. The electrical apparatus used by West is shown schematically in Figure 338. Numerous other applications of non-sinusoidal wave form currents have been made in recent years.*

Studies were conducted by Hawley** to determine the characteristics of the transients associated with the flow of current when a source of constant voltage is suddenly applied between two electrodes imbedded in the ground. In particular, detailed studies were made of: (a) the

† J. C. Karcher and E. McDermott, "Deep Electrical Prospecting," *A.A.P.G. Bull.*, vol. 19, Jan. 1935, pp. 65-77.

‡ L. Statham, "Electric Earth Transients in Geophysical Prospecting," *Geophysics,* vol. 1, No. 2, Feb. 1936, pp. 271-277.

§ S. S. West, "Electrical Prospecting with Non-Sinusoidal Alternating Currents," *Geophysics,* vol. 3, No. 4, October 1938, pp. 306-314.

* S. S. West, "Method of Subsurface Prospecting," U. S. Patent No. 2,237,643, April 8, 1941.
P. W. Klipsch and S. Bilinsky, "Electrical Prospecting," U. S. Patent No. 2,243,428, May 27, 1941.
K. H. Evjen, "Method and Apparatus for Making Geological Explorations," U. S. Patent No. 2,294,395, Sept. 1, 1942.
J. P. Minton, "Electrical Prospecting," U. S. Patent No. 2,304,739, Dec. 8, 1942.
W. B. Lewis, "Frequency Converter System for Geophysical Prospecting," U. S. Patent No. 2,342,676, Feb. 29, 1944.

** Paul F. Hawley, "Transients in Electrical Prospecting," *Geophysics,* vol. 3, No. 3, July 1938, pp. 247-257.

transient in the current circuit and (b) the potential transient in the circuit which includes the potential electrodes. The chief purpose of the investigations was to determine whether the transients contained ripples which were associated with anomalous subsurface structural conditions.

By using a camera of the high speed revolving drum type to photograph the spot of light produced by a cathode-ray oscillograph tube, Hawley showed that the current build-up time in the energizing circuit varied from 30 microseconds for a 12,000 foot spread to 4.5 microseconds for a 3,000 foot spread. The voltage transient surge showed an almost instantaneous rise to its maximum value, followed by an exponential decrease. The voltage and current transients are typical of inductive, highly damped circuits. The work did not show the presence of any ripples on any of the curves, even with recording speeds sufficiently great to reveal ripples having a duration of only 10 microseconds.

In the present utilization of the transient methods, the original concept of the presence of ripples and their diagnostic value apparently has been abandoned, and interpretation is based on fundamental resistivity relationships. The spread of current through a bed of high resistivity is much faster than that through a bed of low resistivity. As a result, the current transient in a medium of high resistivity is steeper (less time interval) than that in a medium of low resistivity. The time constant and the shape of the wave therefore furnish a means for determining the relative resistivities of the materials included within the effective path of current flow. Two typical transient curves are shown in Figure 339.† The electrode and apparatus arrangement are essentially the same as that illustrated in Figure 338.

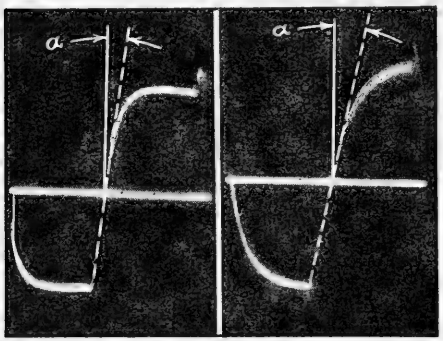

(*a*) (*b*)

FIG. 339.—Typical transient curves for (*a*) material of high resistivity and (*b*) material of low resistivity. (After Steinmann, *The Oil and Gas Journal.*)

As previously mentioned, the photographic or oscillographic method for measuring the wave form of reoccuring phenomena has an advantage in eliminating the effects of extraneous disturbances. For this work Klipsch ‡ stops down the recording camera lens until each single sweep of the oscillograph ray gives a faint image. The wave is repeated a sufficient number of times

† K. W. Steinmann, "Use of the Transient and Soil Analysis Methods in the Search for Oil," *The Oil and Gas Journal,* July 27, 1939, pp. 85-87.

‡ P. W. Klipsch, "Recent Developments in Eltran Prospecting," *Geophysics,* Oct. 1939, Vol. IV, No. 4, pp. 283-291.

to build up a well exposed negative. If no extraneous potentials are present, the reoccurring wave pattern will produce a sharp, dense wave image, while if undesirable potentials are present (caused by earth currents, stray or line leakage, induction, etc.), the picture of the wave form will be a less distinct pattern, with the greatest exposure along the path of the reoccurring wave form. Analysis is based upon the more dense wave pattern thereby minimizing the effects of extraneous non-cyclic potentials.

A manual method of measuring the characteristics of the transient has been developed wherein the distortion of the wave form produced by the shallow surface layers is determined by employing an auxiliary circuit to transform the incoming potential to an easily recognized form (straight line) and measuring the additional distortion required. †

Studies have been made by various investigators to determine the relative merits of the transient and the direct-current steady-state resistivity measurements. The steady-state measurements usually give more reproduceable results, due to the absence of inductive and current redistribution effects necessarily present with the use of transients. Figure 340 shows

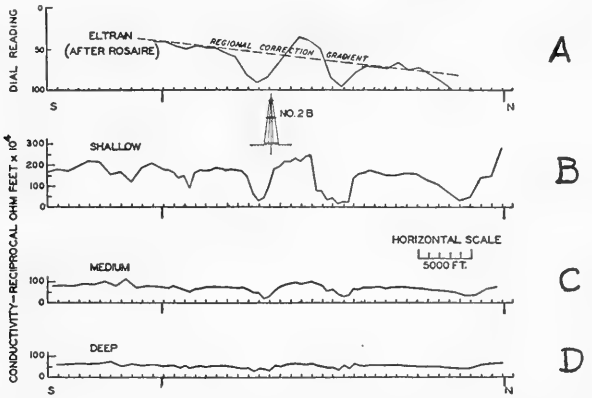

Fig. 340.—Comparison of a transient and a direct-current resistivity survey in Louisiana. *A*, transient data; *B, C, D*, direct current resistivity data for shallow, medium, and deep penetrations, respectively. (Blondeau, *Geophysics.*)

the comparison obtained by Blondeau ‡ between a transient and a direct-current resistivity survey in Louisiana. Curve *A* shows the transient results, while curves *B, C,* and *D* show the direct-current resistivity results at increasingly greater depths of penetration. The electrode configuration for curve *B* gave a current penetration of approximately 200 feet, which compares favorably with the results obtained by the transient method in curve *A*. The electrode spacing employed for the Eltran work would

† R. Saibara, S. Bilinsky and W. G. McLarry, "Exploration by Incremented Wave Distortion," U. S. Patent 2,177,346, issued Oct. 24, 1939.

‡ E. E. Blondeau, "Shallow Resistivity Survey at South Elton, Louisiana," *Geophysics,* Oct. 1939, Vol. IV, No. 4, pp. 271-278.

have given a much greater current penetration than any employed for the steady-state work if the penetration of the transient current were comparable to the steady-state current. Blondeau concludes that "the large observed variations in near surface resistivity can hardly be attributed to mineralization emanating upward over structure; and that the number of anomalies found is so great that their direct association with deep structure is highly improbable."

Seismic-Electric Effect.—Seismic-electric effect† is the name given to the possible phenomenon of the earth resistivity varying with elastic deformation. This effect has been proposed as an entirely new method of picking up seismic energy.‡ Various experiments have led to a controversy rather than elucidation of the nature of such an effect. That there is a variation in resistivity under an elastic disturbance is undeniable, but the cause has been assigned to varying electro-chemical conditions at the electrode surfaces,§ to the so-called varying volume polarization, and to a variation in specific resistivity.

APPLICATIONS OF ELECTRIC METHODS

The fields of applications of geoelectrical methods may be classified as follows: (1) prospecting for highly conductive materials; (2) structural investigations, which include prospecting for placer deposits, water supply problems, civil engineering construction problems, and oil structural mapping.

Prospecting for Highly Conductive Materials.—This application includes prospecting for certain veins, lodes, and dikes. Results obtained in vein deposit investigations will be discussed here.*

Vein Deposits

Geophysical methods are of special significance in the initial evaluation of a prospect, because they yield important data regarding subsurface conditions before purchasing or opening the property.

Prospecting for ore bodies should be done with the viewpoint that a great majority of the properties examined will be abandoned. This viewpoint implies that the risk in examining geophysically and geologically a large number of prospects is less than that in attempting to find an ore body by extensive development work on one property. The soundness of

† R. R. Thompson, "Seismic Electric Effect," *Geophysics,* Vol. I, No. 3, October, 1936, p. 327; Vol. IV, No. 2, March, 1939, p. 102.

‡ L. W. Blau and Louis Statham, "Method and Apparatus for Seismic Electric Prospecting," U. S. Patent 2,054,067, September 15, 1936.

§ St. V. Thyssen, J. N. Hummel and O. Rülke, "Die Ursachen das Seismisch-Elektrischen Effektes," Z. Geophs. 13, 1937, 112-119; "Ueber das Wessen des Seismische-Elektrischen Effektes," Beit. Angew. Geophys., 7, 1938, pp. 209-217.

* A general discussion of the applicability of geoelectrical methods in this field is given in the chapter entitled Geologic and Economic Background of Exploration Geophysics.

this concept may be illustrated by a practical case of a prospect in Sonora, Mexico. †

In a region characterized by extremely steep topography which is broken in many places by vertical cliffs, a 25-foot, copper-bearing ledge

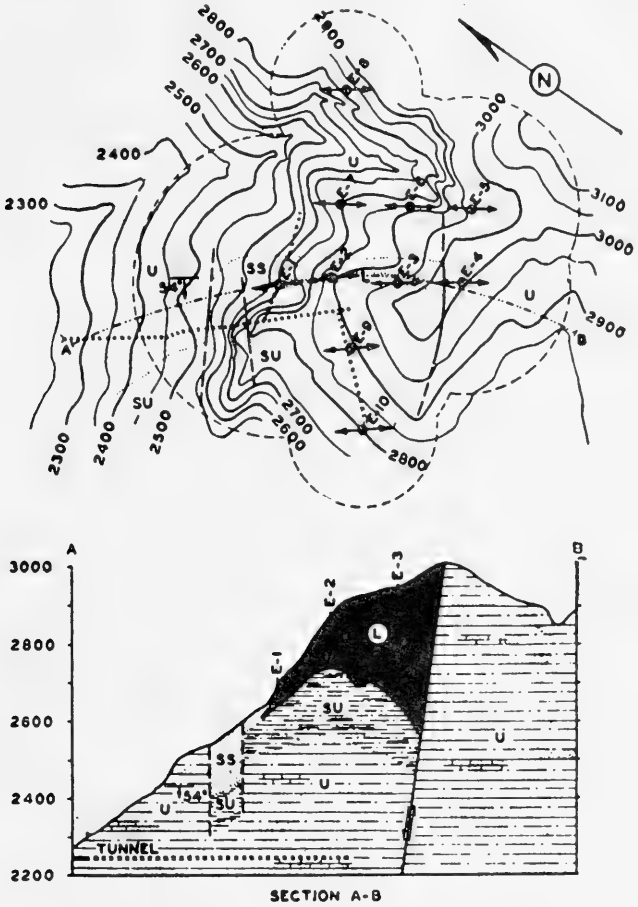

FIG. 341.—Cross section inferred from geophysical survey.
L—ledge
U—undifferentiated sediments
SU—silicified undifferentiated sediments
SS—sandstone
E—electrical stations
Electrical stations and topographic contours shown in upper portion of figure. (*Canad. Mining Journal.*)

is exposed at the surface for a distance of 500 feet. (See upper part of Figure 341.) To the south, it is cut off by a fault having considerable displacement. To the north, it was traced to station *E*-1, where it is covered by talus and detritus.

† J. J. Jakosky, "Geophysical Examination of Prospects," *Canad. Mining Journal,* Jan. 1934.

The surrounding country rock is composed chiefly of an old series of sediments, portions of which had been highly silicified. These rocks in all probability are of pre-Cambrian age.

Prior to the geophysical investigations, a tunnel was driven 770 feet parallel to, and west of the ledge outcrop in an effort to cut the ledge at the 2250 foot elevation. Because ore was not encountered, the mine operators believed that the vein might dip farther to the west. A cross cut was driven westward for 310 feet, and failing to encounter the vein, an eastward cross cut was driven for 300 feet. At this stage of the development program, the geophysical work was employed.

The cross section in the lower portion of the figure is drawn from the results of the geophysical survey and shows the depth to which the ledge extends and its relation to the surrounding rock and structure. The limited amount of sulphide ore disclosed by the geophysical survey made the property of doubtful value due to high shipping and operating costs.

Lateral Extension and Depth of Ore Body.—The application of geophysical work over known mineralized areas, where some development has already been done, allows important information to be obtained relative to the lateral extension of known ore bodies. Should the measurements indicate the possible extension of such bodies, it is economical to use a few well-placed drill holes to check values. In many instances it has been found that where the geoelectrical work shows fairly constant magnitudes, the commercial values found in the drill holes may, for purposes of preliminary estimates, be used for estimating the deposit. Occasionally, the geophysical work is of value in indicating the nature of the deposit and may throw light on whether the deposit is of primary or secondary origin.

The most familiar geoelectrical result is that obtained over a highly conductive ore body of the sulphide type. When an electric current is passed through an area containing a conductive ore body, a decided change in values will be noted when in the vicinity of the ore body. A typical example is illustrated in Figure 342, which shows the general surface conditions and the locations of the resistivity stations. The oxidized portion of a mineralized fracture zone between the diabase and the diorite porphyry outcropped at *A*. This vein showed good values in copper but was too narrow for economical mining, and no assurance could be had that commercial quantities of sulphide ores would be found at depth. A geoelectrical study of the area gave the results shown by the curves on the left of the figure. Because of the lower resistivity of the diabase, curve *B* starts with a lower initial value than either *A* or *C*. Because of the relatively low conductivity of the diorite porphyry, curve *C* has a higher initial apparent resistivity value than curves *A* or *B*, and maintains this higher value over the entire range of measurement. Under the geologic conditions existing in this district, it appeared most logical to assume

that the drops in the resistivity profiles were due to the presence of a sulphide zone at a depth of about 300 feet.* Hence, diamond drilling was recommended and the hole shown in the figure penetrated a body of sulphides with high copper and silver values.

The use of this general technique may be illustrated by a survey in Inyo County, California.† Previous history showed that lead-zinc sulphide ore occurred in the limestone, adjacent to a limestone-monzonite contact. This contact initially was discovered at four outcrops over a distance of about a mile. Between outcrops the contact was covered with fill material. This type of sulphide is a good electrical conductor and can be located by determining the subsurface zones of better electrical conductivity. Recon-

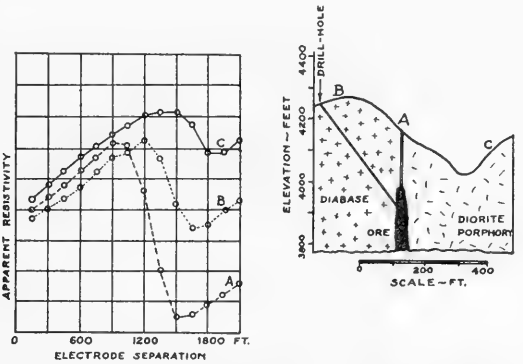

FIG. 342.—Variations of apparent resistivity on a traverse across a highly conductive ore body. (*Canad. Min. Journal.*)

naissance measurements were made along the indicated line of contact, using an inductive method. This was followed by detailed resistivity measurements to map the zones of better electrical conductivity. Two main zones of higher conductivity were mapped, one near an old tunnel. Later, a cross-cut to the contact encountered ore, consisting chiefly of lead sulphide replacements, and the large oxidized ore bodies adjacent to them, which now have been mined continuously since 1940.‡ The development work was extended to cut the second conductive zone, which was at a depth of about 300 feet below the surface. This zone proved to be high-grade sulphides, nearly underlying an old oxidized ore body previously mined and abandoned.

Prospecting for Placer Deposits.§—This work may be illustrated

* Based on a depth of penetration of approximately 0.3 the current electrode separation.

† J. J. Jakosky, "Operating Principles of Inductive Geophysical Processes," *A.I.M.E. Geophysical Prospecting*, 1929.

‡ Personal communication from H. E. Olund, U. S. Bureau of Mines, to S. E. Stein, Oct. 4, 1948, regarding the American Metals Co. property at Darwin, Calif.

§ J. J. Jakosky and C. H. Wilson, "Examining a Placer by Geophysical Methods," *Engineering and Mining Journal*, February, 1934.

J. J. Jakosky and C. H. Wilson, "Geophysical Studies in Placer and Water Supply Problems," *A.I.M.E. Geophysical Prospecting*, Tech. Pub. 515, 1933.

by a description of a survey conducted in Trinity County, California. The property consisted of 10,000 acres of gravels which, on the surface and in occasional test pits, panned uniformly in gold. The problem was first to select, by a geological study and by preliminary geophysical work,

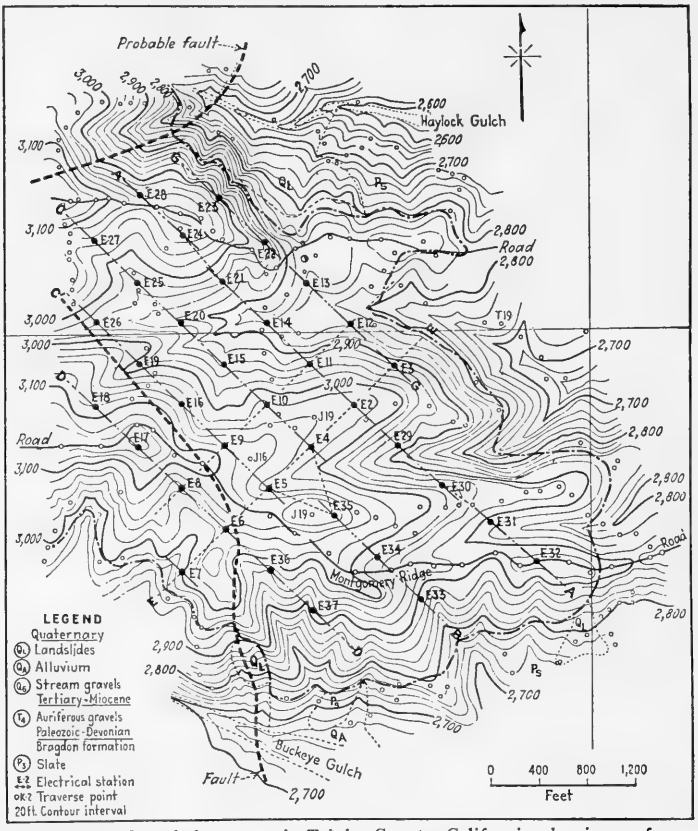

FIG. 343.—Map of placer area in Trinity County, California, showing surface geology and topography. (*Engineering and Mining Journal*, Feb. 1934.)

what part of the total acreage should first be studied; then, by detailed geological and geophysical work on that restricted acreage, to outline the gravels, give their depth, the contour of bedrock and attitude of bedrock surface, and if possible, locate the likely areas for gold concentration.* As a result of the survey, recommendations for further development and exploration were to be made.

After careful geological reconnaissance of the whole property, between 500 and 600 acres were selected for detailed work. The lateral extent of the gravels, the areal geology, and the topography of this area were

*The likely areas for gold concentration would be indicated by "black sand" concentrations.

first determined by alidade and plane table and were then plotted in detail, as shown in Figure 343.

Magnetic measurements of the vertical intensity were made at 242 stations over the area, at intervals from 300 to 400 feet. Magnetic equipment for this work was the conventional Schmidt-type field balance. A study of the geological and magnetic maps did not allow a unique interpretation either as regards major concentration zones of the "black sands" or of bedrock conditions. Hence, the magnetic and geological work was supplemented with electrical studies.

Electrical resistivity measurements were made at 37 stations distributed at regular intervals. Proper spacing of stations is a matter of experience and is governed by the local geologic and topographic conditions. In this instance, most of the stations were located at 600-foot intervals along traverses having a northeast-southwest direction. In the southwestern portion, however, the stations were placed at 800-foot intervals, because location of the gravel contact was known on three sides from the surface evidence, and closer spacing was unnecessary. Resistivity measurements were made with the constant potential apparatus and the five-electrode configuration previously described. Three curves were plotted for each station. All electrical curves showed the variation in apparent resistivity from the surface to an indicated depth of 600 feet. The first or main curve showed the variation in apparent resistivity along the traverse line. The two auxiliary resistivity curves showed the variations in two directions from the station and were used for evaluating topographic and near-surface effects.

Because of the difference in resistivity between the gravels and the more compact formations, such as the bedrock, the boundary or contact between the two materials at depth is indicated on the curves by a change in trend. The depth to bedrock at each station was determined by Tagg's method (p. 491) and correlation of curves (p. 509) using known geological conditions encountered in exploratory openings and projection of outcrops as control. By correlating the computed depths with the surface trace of the gravel-bedrock contact and with the surface elevation shown by the topographic survey, it was possible to plot subsurface bedrock contours.* The maximum thickness of gravels on this property was found to be about 300 feet.

The results of the electrical survey are illustrated in Figure 344 which shows cross sections of the deposit along the traverse lines. From these sections, the approximate total yardage of gravels was calculated. A striking feature of these sections is the evidence of faulting in the bedrock. In particular, sections *D-D, F-F,* and *E-E* indicate an escarpment in the bedrock of more than 100 feet average vertical displacement. Prior to the geophysical work, this faulting had not been suspected, because the

* The depth to bedrock given by electrical work is an average or effective depth over an area having dimensions comparable to the depth of penetration.

trace of the fault was covered by alluvium over practically the whole property. After discovery of the fault by geophysical methods, its trace was found in a gulch at one point where erosion had slightly exposed it.

The knowledge of this escarpment materially affected plans for hydraulic mining. Before the geophysical survey was made, the mining company had perfected plans for beginning hydraulic operations in the northeast part of the area, because surface topography indicated that the bedrock most likely sloped toward this gulch. When the results of the geophysical work were known, the operations at that point were abandoned, and plans were made for work in the southern part of the area.

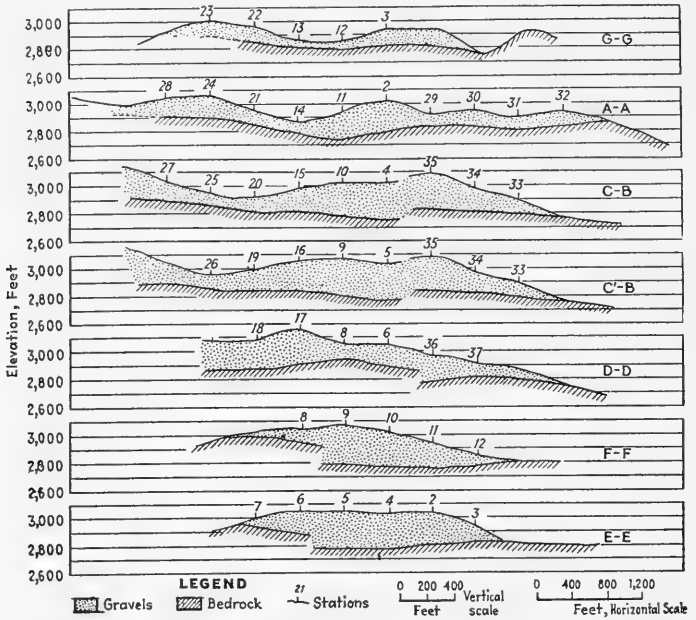

FIG. 344.—Cross sections of placer deposit along traverse lines. (*Engineering and Mining Journal*, Feb. 1934.)

The complete bedrock contours predicted on the basis of the data obtained in the geophysical investigations are shown in Figure 345.

Water Supply Problems.†—As regards the application of geophysical work to water supply, the geological considerations are somewhat similar to those involved in placer investigations. In general, the problems may be divided into two classes: (1) the determination of the existence of a permanent subsurface water table either in fill material (gravels, sands, etc.) or more consolidated rock; (2) the determination of subsurface structure that would affect ground water accumulations. In water supply investigations, as in other problems, the geophysical work is facilitated by direct correlation of the geophysical data with well logs.

† J. J. Jakosky and C. H. Wilson, "Geophysical Studies in Placer and Water Supply Problems," *A.I.M.E. Geophysical Prospecting*, Tech. Pub. 515, February, 1934.

Geophysical investigations for several different types of water supply problems are illustrated by descriptions of the following actual surveys.

In connection with some experiments * at the University of Arizona, water supply investigations were carried out on the Santa Rita Range

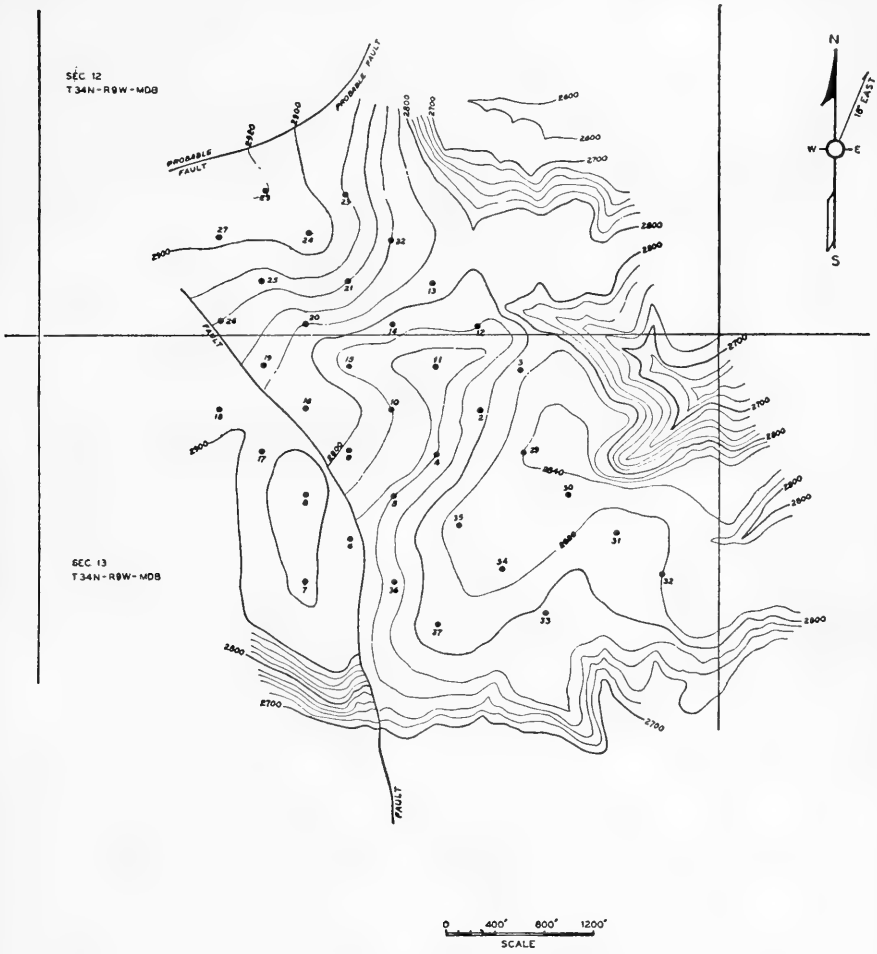

Fig. 345.—Bedrock contours on placer property in Trinity County, California. (*A.I.M.E. Geophysical Prospecting*, Tech. Pub. 515, 1934.)

Reserve at the northern end of the Santa Rita Mountains, southeast of Tucson, Arizona. The investigations were conducted in adjacent canyons or washes; namely, Saw Mill canyon, in which a small supply of water was already developed through a well to the bedrock, and in Florida

* Arranged by Dr. G. M. Butler, Dean of the College of Mines and Engineering, University of Arizona, Tucson.

canyon. The two areas have somewhat similar surface geologic and topographic features. The object of the geophysical work in the Florida canyon area was a determination of the depth and contour of the bedrock across the canyon and the electrical characteristics of the overlying fill material in order to establish the presence, or absence, of a water supply comparable to the known supply in Saw Mill canyon.

Resistivity measurements in both areas produced results of the type shown in Figure 346. The curves showed inflections corresponding to

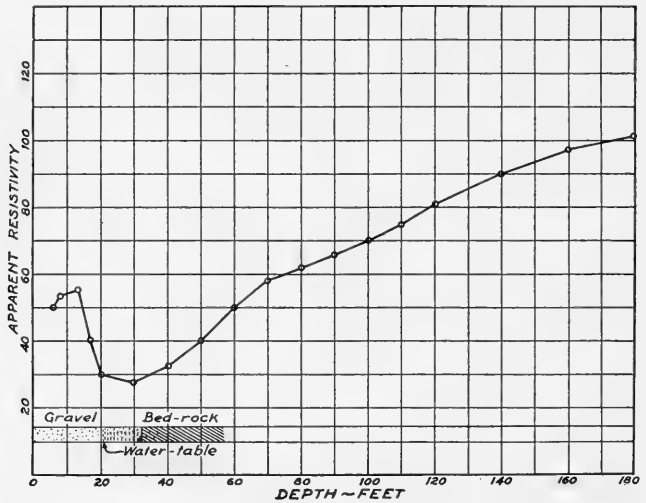

FIG. 346.—Curve showing effects of water-level and bedrock on resistivity. (*A.I.M.E. Geophysical Prospecting*, Tech. Pub. 515, 1934.)

(1) change from dry fill and stream wash to wet fill and top of water horizon and (2) change from fill material to the underlying bedrock. At this station the geophysical work placed the depth to the water level at 20 feet and the depth to bedrock at 29 feet. Direct measurement in an adjacent drill hole gave the water level as 20 feet; the depth to bedrock, 26 feet.

A combination of structural work and direct location of water table is illustrated by a survey conducted near Yuma, Arizona, for a mining company. The presence of a permanent water table in this area was known. The problem was to locate the nearest point to the mine at which a well would intersect the permanent water table in porous alluvium above the impervious bedrock which sloped downward from the foothills. Figure 347 summarizes the general results secured by the electrical survey. A well drilled near station 10 encountered the water table as predicted by curve correlation. According to the mine management, the well is capable of producing in excess of 500 gallons per minute.

In 1931 a municipality in Southern California was threatened with litigation by a group of land owners near the mouth of a river on which

upstream development by the city was removing considerable water from the surface and subsurface stream flow.

It was the contention of the land owners that removal of the water from the subsurface channel would allow infiltration of sea water from the ocean which would be detrimental to their crops. The city claimed that a natural subsurface rock barrier existed across the narrow portion of the river valley and that this would effectively halt any damaging influx of sea water.

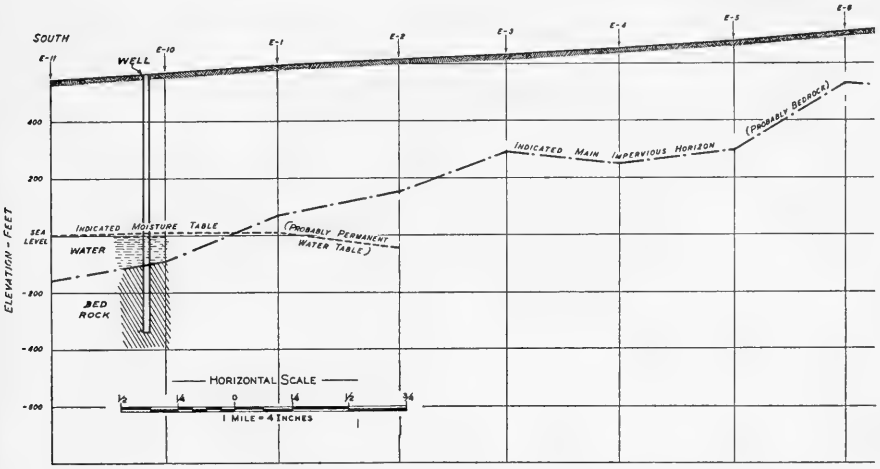

FIG. 347.—Location of water table and development of water supply, Yuma, Arizona.

It was necessary to obtain data on the depth to bedrock and character of the subsurface contour of an old stream channel. The most obvious method was to secure data allowing the plotting of a subsurface contour map. These data could be obtained by a drilling program, or by employment of a geophysical survey over the area. The latter was chosen, and at 50 selected stations covering the area, geoelectrical data were obtained showing depth to bedrock, and depth to the boundary of coarse gravel, and finer silt and clay. These "electrical logs" were obtained at a small fraction of the cost that would have been required for ordinary drilling. In addition, magnetic work over the area as a part of the survey disclosed evidence on the character of the probable subsurface conditions underlying the stream valley.

This survey also illustrates the use of electrical methods in determining distribution of pervious and impervious materials. Figure 348 shows a typical profile of the subsurface conditions as disclosed by the geophysical work. The upper soil and clays are relatively impervious, while the lower gravels are very pervious and allow flow of a subterranean stream during the dryer portion of the year.

A good example of the use of electrical prospecting for locating a fault zone is described by Hawley.† The complete survey consisted of two parts, viz., a constant depth survey (utilizing constant electrode spacing) and depth profiles (moving electrodes outwardly and symmetrically from the fixed center). In both cases the Wenner configuration was used. The comparison of results of the two parts and the problems in interpretation make the article a good reference.

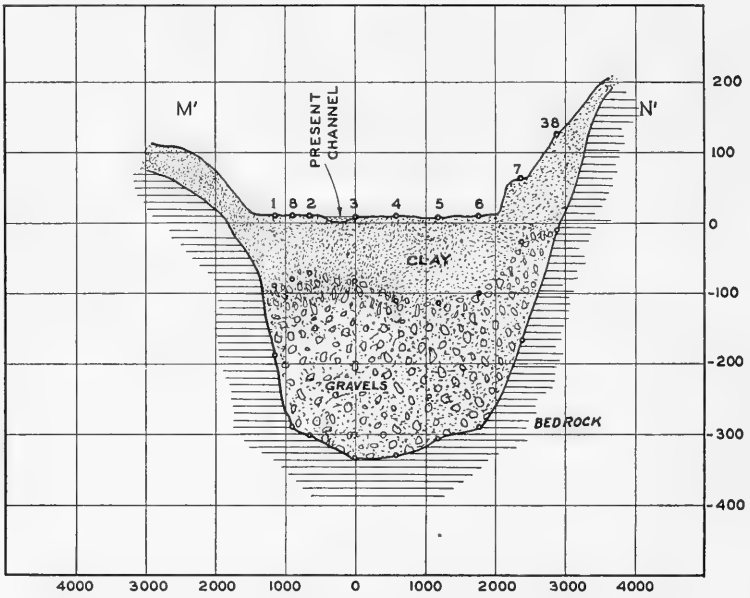

FIG. 348.—Bedrock contours and typical subsurface profile, Santa Ynez River, California. (*The Mining Journal*, Jan. 15, 1931.)

Civil Engineering Construction Problems.—Geophysical investigations are of especial value in the following engineering construction problems: (1) examination and location of dam and reservoir sites; (2) location of water wells; (3) examination and location of aqueduct and pipe line routes; (4) location of rock and gravel quarries; and (5) tunnel construction.

The application of geoelectrical methods will be illustrated by descriptions of two representative surveys: (1) a survey conducted at the Fort Peck Dam and Reservoir, Montana, and (2) a survey conducted in the vicinity of the Gillespie Dam on the Gila River near Phoenix, Arizona.

Fort Peck Dam

The primary purposes of the Fort Peck geophysical investigations were to determine: (1) the major structural features of the sedimentary rocks underlying the dam and reservoir sites, with special reference to the loca-

† Paul F. Hawley, "Fault Location by Electrical Prospecting—an Example," *Geophysics*, Vol. VIII, No. 4, October, 1943, pp. 391-403.

tion of fault zones or other structural conditions that would influence the location or construction of the proposed dam; (2) the thickness of overburden and fill materials overlying the shale bedrock at the dam site and the thickness of fill materials in the topographic depressions along the reservoir rims; (3) depth to and subsurface contour of the top of the Bearpaw shale (bedrock) at the dam site and along the reservoir rims; and (4) depths to and elevations of ground water levels in the proposed dam abutments and in the reservoir rims.

A generalized stratigraphic section of the area is shown in the right-hand portion of Figure 349. The surface is usually covered with clay which is oftentimes sandy. Beneath this clay layer is found glacial drift containing small or large boulders in a matrix of varying proportions of sand, clay, and small gravel. Underneath the glacial drift is a layer of clay, also often of a sandy nature. Beneath this clay layer there

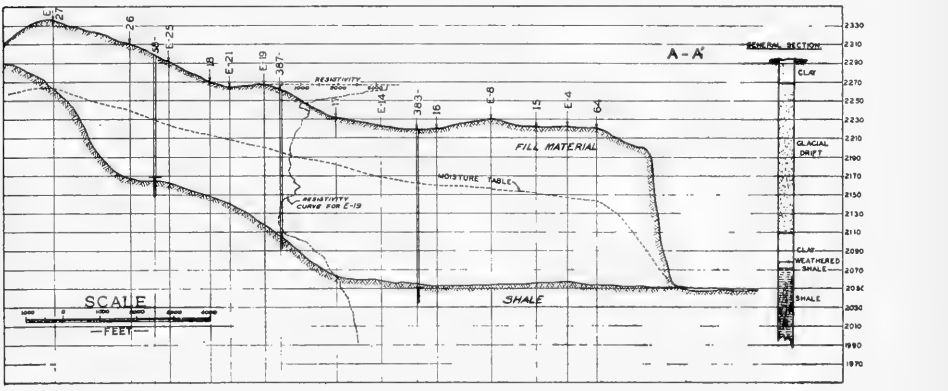

FIG. 349.—Geophysically-indicated structure and moisture table, and general stratigraphic section of west abutment of Fort Peck Dam.

occurs a weathered shale layer which is impregnated with water having a high percentage of dissolved minerals. The weathered shale layer is of relatively small thickness. As the depth increases, the weathered layer gradually merges into firm shale bedrock. The weathered shale and the firm shale layers constitute the upper portion of the Bearpaw shale. For purposes of dam site construction, the geophysical interpretation was directed toward determining the bottom of the weathered shale layer, rather than the theoretical "top" of the Bearpaw formation.

The typical stratigraphic section just described varies to a certain extent throughout the area, and in some cases there is a fairly distinct contact between the glacial drift and the shale formations, with no intervening clay, sand, or appreciable weathered shale formation.

Typical results of the geophysical studies conducted on the west abutment are shown graphically in Figure 349 and the survey may be summarized as follows:

Structure

At the dam site, the correlation of isolated outcrops with the geophysical studies at the various geophysical stations indicates that the Bearpaw shale is quite uniform and that it dips slightly to the east, in conformity with the recognized regional dip. The geophysical work disclosed no evidence of abnormal structural conditions, such as major folding or faulting on the west abutment. Localized faulting is evidenced by small displacements of seams in the shale (six inches or less). However, as most of the exposures are on steep slopes, many of these minor displacements are probably due to hill-side "creep."

Bedrock Contours and Profiles

The bedrock contour map plotted from the geophysical data indicates that the overburden-shale contact is comparatively flat over a large central area, but dips steeply to the east in the western part of the area. There is some evidence that this flat central area may represent a bedrock valley or bench underlying the ridge. This indicated subsurface depression might possibly have existed as a pre-glacial drainage channel. The uniform attitude of the contact underneath this portion of the west abutment ridge is probably a unique and local condition. Geophysical results on other parts of the area indicate that the shale surface is quite irregular.

Ground-Water Table

The geophysically-indicated moisture table in the west abutment area is shown in the profile. This moisture table marks the approximate location of the transition zone between the relatively dry near-surface material and the moisture-impregnated deeper material.

Comparison of Geophysical Results with Logs of Core Holes

To provide a basis for correlation of the electrical bedrock determinations, preliminary studies were conducted at existing core hole locations for which logs were available. As a consequence of these preliminary studies, direct correlation could be made between the electrically indicated depth to firm shale and the depth as indicated by drillers' logs. The electrical studies were then utilized to extend the depth determinations into adjacent areas.

The close check between the electrical determinations and drill hole results is shown on Profile *A-A'* on which subsequently determined bedrock depths are plotted for drill holes 58, 387, and 383.

Gillespie Dam

The survey* conducted on the Gila River is an example of the use of the electrical method to investigate complex local geology at the site of the

* For permission to publish this material, the author is indebted to Raymond A. Hill, Supervising Engineer of Quinton, Code and Hill; Leeds and Barnard, Engineers, Consolidated, Los Angeles; Salt River Valley Water Users Association, Phoenix, Arizona.

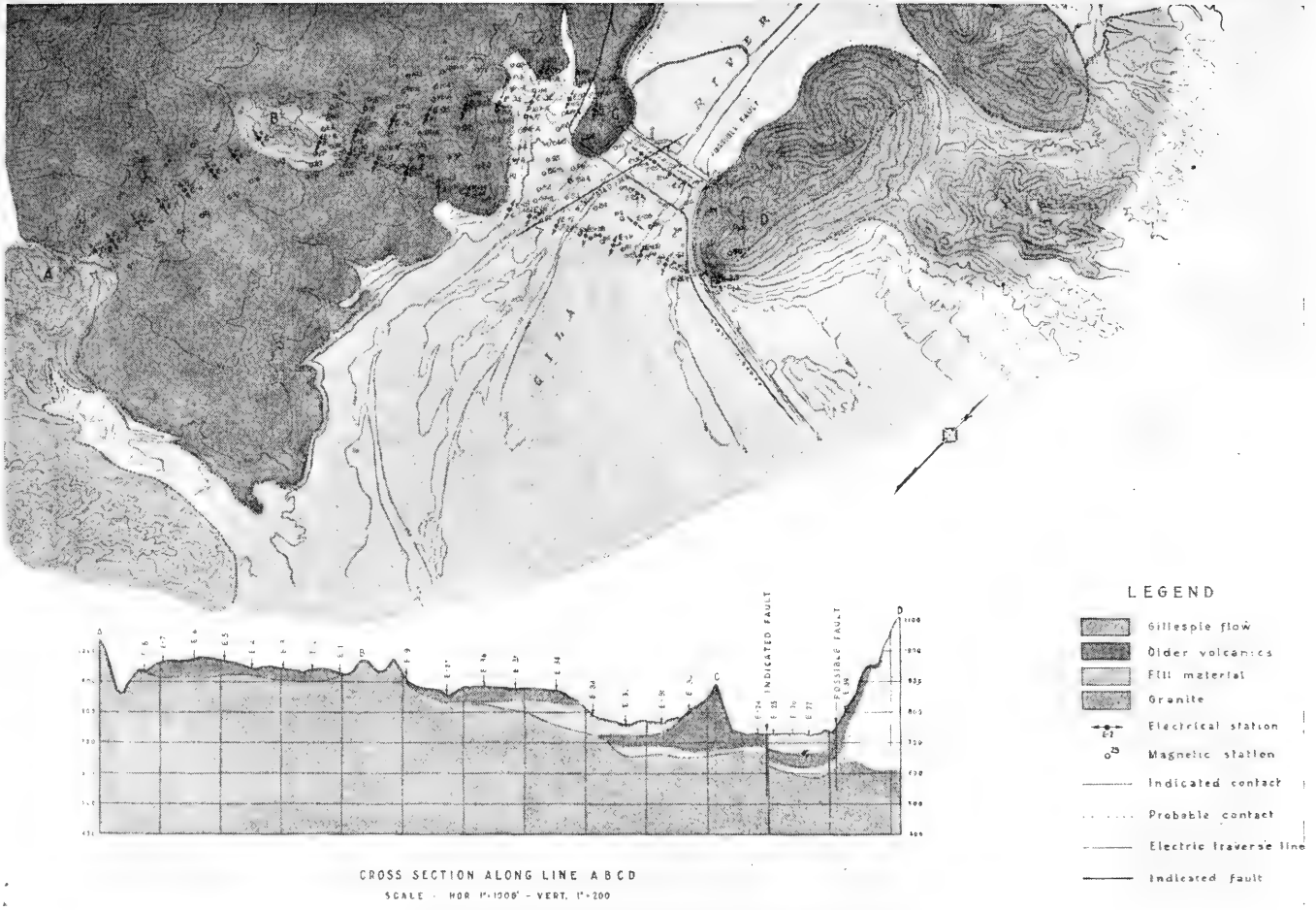

FIG. 350.—Geophysical results, Gillespie Dam, Gila River, Arizona.

Gillespie Dam. Figure 350 shows a portion of the area covered and a typical cross section obtained during the survey.

The Gila River flows between high lava abutments situated in Gillespie Gap, a natural pass formed by the Gila Mountains to the west and the Buckeye Hills to the east. The present course of the river is controlled by the high granitic peaks of the Buckeye Hills on the east and a flow of late Tertiary lava, known as the "Gillespie Flow" on the west. The Gila River channel, both ancient and present, is filled with a series of volcanic flows and various phases of flood plain detritus deposited by the river.

The granitic rocks and cropping on the east and west of the dam abutments and underlying the area of the "gap" form the boundaries which limit the flow of subsurface water. Above the granite, in order from oldest to youngest, lies a series of relatively more porous formations: (1) older volcanic rocks forming the dam abutments, (2) older flood-plain material, (3) younger volcanic rocks, (4) younger flood-plain material, and (5) recent alluvium.

The general purpose of the investigation was to determine the distribution and structural relationship of the above-named formations with particular attention to the effect they might have on subsurface flow of water. Specifically, it was desired to determine the location and cause of leakage that was taking place around the dam.

A study of the areal geology indicated that possible subsurface water flow was limited to two gaps bounded by the outcropping granite rocks: (1) that between the points where later were placed the geophysical stations *E*-1 and *E*-8, and (2) that extending from station *E*-9 eastward across the present channel of the Gila River to the granitic outcrop on the east abutment. The geophysical study was confined, therefore, to a study of subsurface conditions of these two locations.

The results of the geophysical studies are shown in Figure 350 by the cross section.

Cross section ABCD: From stations *E*-1 to *E*-8 the geophysical work indicated that the lava capping is relatively thin and that no appreciable amount of porous material such as gravel or alluvium lies between the lava and the underlying granite. From stations *E*-9 to *E*-23 a much more complicated subsurface condition was indicated. The most important structural features are the presence of the fault paralleling the stream channel and the presence of porous materials below the lava which forms the dam abutments.

The examination comprised geological, geoelectrical, and geomagnetic studies. As a result of the work it appears that the leakage occurred through the subsurface underneath the dam. The leakage probably occurred through a layer of porous material which is indicated to underlie the lava flow upon which the dam is built.

Structural Investigations

Structural Survey in East Vacuum Area, New Mexico

This survey was conducted during 1938 and is of particular interest because drilling subsequent to the survey has provided a good opportunity to evaluate the work.* Although complete structural information has not yet become avaliable, the present information shows a remarkably close agreement between the structure predicted from the geoelectrical survey and the structure as indicated by well log correlation. The accuracy of the geoelectrical work is evidenced by: (1) close agreement between

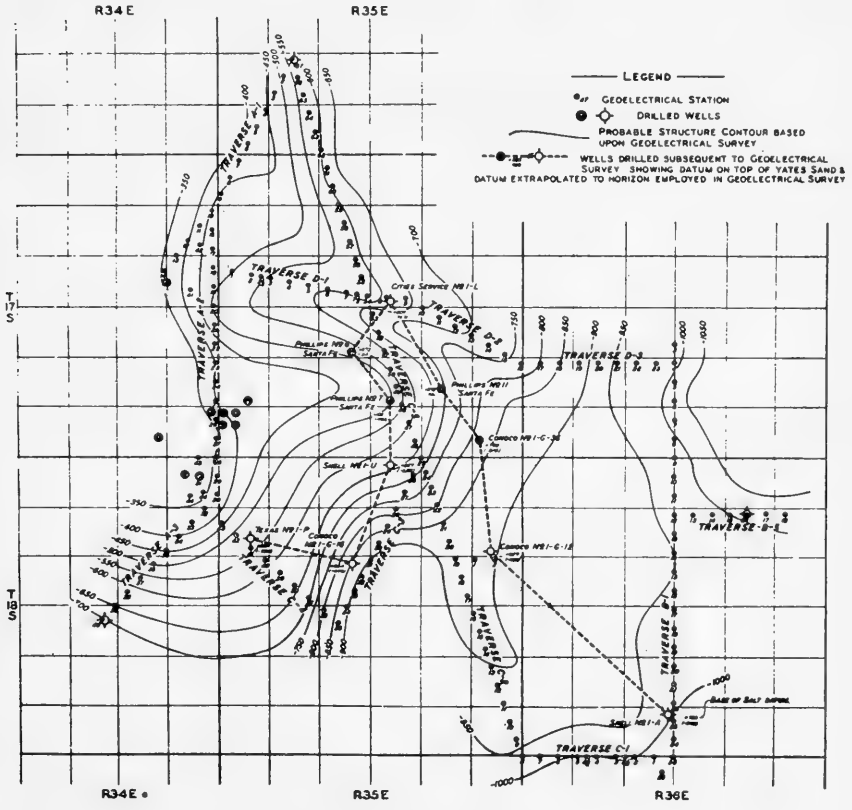

FIG. 351.—Structure contour map based on geophysical studies. (East Vacuum Area, Lea County, New Mexico.)

the proved boundaries of the oil pool and the probable boundary as predicted by structure contours plotted from the geoelectrical data, and (2) close agreement between the geoelectrical and the well log subsurface datums at the ten well locations for which information is available.

* The interpretation of the geophysical data utilized the method of curve correlation described on p. 509.

The accompanying figures illustrate (a) the results of the geoelectrical survey and (b) a comparison of these results with available data obtained from subsequent drilling. Figure 351 is a portion of the geoelectrical structure contour map. The group of ten representative wells for which well log information was available are connected by a discontinuous line. At each well location, the well log elevation of the top of the Yates sand is shown opposite the well symbol. The bracketed figure represents an extrapolation of the Yates sand datum to the deeper horizon employed in the geoelectrical correlations. This bracketed figure is directly comparable, therefore, to the subsurface values that may be interpolated from the geoelectrical structure contour map.

This comparison is better illustrated by Figure 352 which shows the subsurface values plotted on a discontinuous profile between the wells shown in Figure 351.

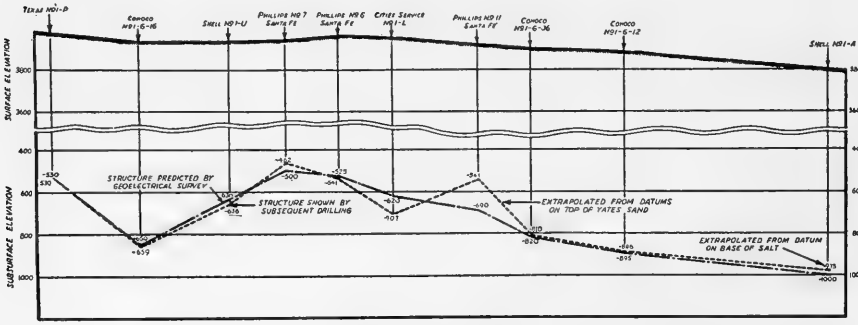

FIG. 352.—Structure profiles showing comparison of geoelectrical survey results with results of subsequent drilling. (East Vacuum Area, Lea County, New Mexico.)

The survey covered a total area of approximately 200 square miles and required approximately six months for completion.* Subsurface geoelectrical determinations were made over an approximate depth range of 3000 to 5000 feet, at 350 separate stations.

The geoelectrical survey results were submitted in terms of structure contours and profiles showing the average structural trend in the section included between the top of the Yates sand and the top of the White lime. Because of the generally greater reliability of the deeper geological marks, greater weight was attached to the geoelectrical correlation of the lower part of the measured section.

The available well log data are for the top of the Yates sand which occurs at a somewhat shallower horizon than that employed in the geoelectrical work. To facilitate the comparisons illustrated in the accompanying figures, it was necessary therefore to extrapolate from the Yates sand values, and also to interpolate the geoelectrical values from the nearest geoelectrical station to the location of the check well.

* A portion of the results only are shown in Figure 351.

Of especial interest in connection with this work are: (1) the substantiation of the indicated structurally low ground to the northeast of the Phillips No. 6-Santa Fe Location and (2) substantiation of the low and relatively flat structure between the Conoco No. 1-G-12 and the Shell No. 1-A wells in the southeastern part of the area.

The indication of low structure in the latter case is particularly significant inasmuch as it disproved the theory of a possible connection between the Monument Structure to the southeast and the East Vacuum pool. The Shell No. 1-A well is reputed to have been drilled as a result of recommendations based upon a seismic survey in this vicinity. This area is particularly difficult for seismic operations due to two factors: (a) irregular velocities in the near-surface beds, and (b) large variations in thickness of the anhydrite zone overlying the limestone.

FIG. 353.—Aerial photograph of Meteor Crater, Arizona. (*A.I.M.E. Geophysical Prospecting,* Technical Paper, 1932.)

Structural Investigation of Meteor Crater

Meteor Crater (Figure 353) lies in the high plateau of northern Arizona.† It is a natural wonder whose origin and age have been discussed for many years. Data from geologic and topographic surveys have shown that in both geologic and topographic effects the crater is unusually symmetrical for so large a structural feature.

† J. J. Jakosky, C. H. Wilson, J. W. Daly, "Geophysical Examination of Meteor Crater, Arizona," *A.I.M.E. Geophysical Prospecting,* 1932, pp. 63-97.

The dips of the strata vary somewhat around the rim and the elevations of corresponding horizons also vary, mainly because of the effect of the numerous near-radial faults. These faults are rather symmetrically distributed around the crater and are very similar in character. Displacements of the beds by these faults may amount to 85 feet in a vertical direction. In addition to the faulting which now shows in the rim of the crater, the rim rocks have suffered considerable fracturing. The main geological features of the bottom of the crater are the extent and distribution of quaternary fill material, which consists essentially of the talus slopes extending from the crater floors up the inside slope of the rim, and the very fine sandy material covering the location of the playa lake and the lake beds below. The distribution of talus is also fairly uniform around the crater rim, being less extensive on the northwest side of the crater where, correspondingly, the fine fill material extends farther out toward the rim.

The chief purpose of the geophysical work was to determine the subsurface conditions in the crater and the possible occurrence of any large body of meteoritic material.

Electrical Survey.—The geoelectrical studies were conducted with a low frequency alternating current resistivity apparatus. One current electrode remained at a fixed position within the crater. The other current electrode and the two intermediate potential electrodes moved progressively outward as the depth of investigation was increased, the lines of measurement being radial with respect to the center of the crater.

A center point selected within the crater was used as a hub or reference point. Resistivity studies were made at stations distributed circumferentially around the crater as follows: (1) 1000 feet from the center point and entirely within the crater proper; (2) 1500 feet from the center on the inside slopes of the crater rim; (3) 2000 feet from the center and on the crater rim; (4) additional studies at points within and outside of the crater at several stations selected after the first section had been completed and a general idea obtained as to depth of bedrock in the crater. Spacing between stations was selected to give sufficient overlap to allow proper mapping of the subsurface structure. The orientations of the traverses were: (a) along lines radially from the center and (b) along lines (chord lines) at right angles to (a). On both radial and chord lines studies were made to effective depths of 1800 feet.

Brief Summary of Results

Due to the symmetry of the crater, the resistivity curves all exhibit similar characteristics. (Figure 354.) Final interpretation of the data was based chiefly upon direct curve correlation. From the geophysical results a subsurface structural map was prepared showing probable thicknesses of fill material, bedrock contours, etc. This is shown by the cross section of Figure 355.

The electrical survey gave indications of the presence of an area of higher conductivity in the southwest quadrant of the crater between the center and the rim. The main portion of the relatively conductive material lies at an effective depth of approximately 700 feet. A careful study of the

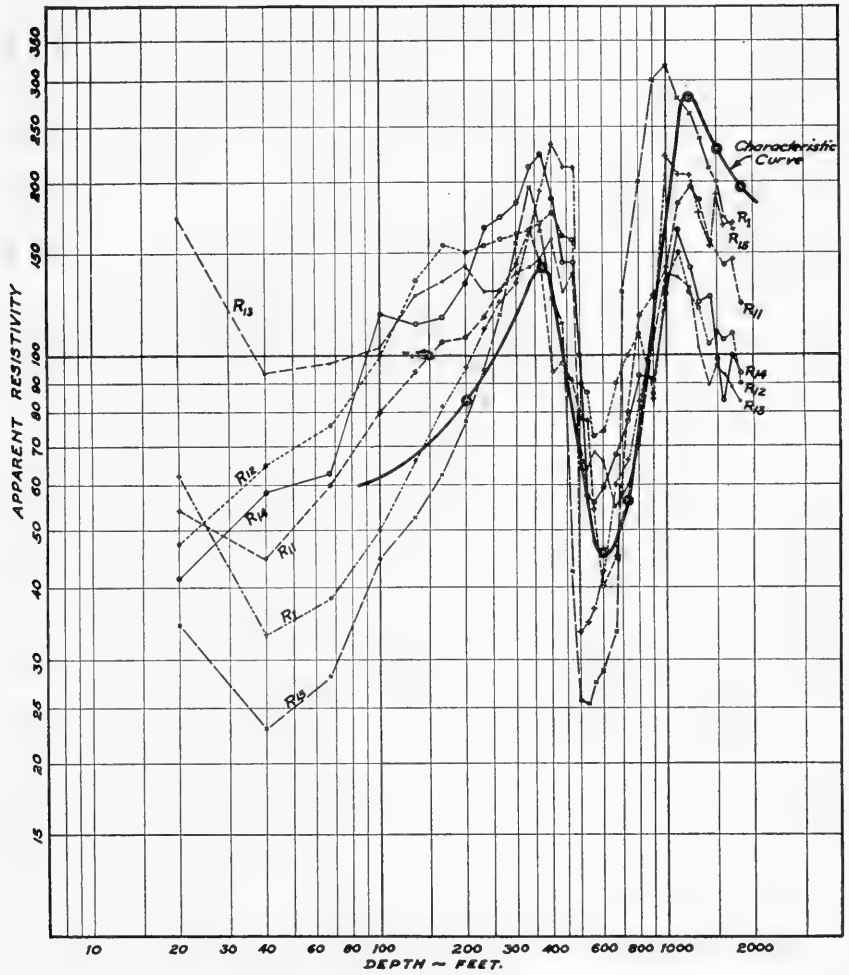

Fig. 354.—Calculated resistivity curves and characteristic curve, Meteor Crater, Arizona. (*A.I.M.E. Geophysical Prospecting*, Technical Paper, 1932.)

original and altered materials found in the area indicates that this zone of higher conductivity is not due entirely to fill material or structural condition. The conclusions are that this area contains material of metallic character. The material is probably a fragmental zone having its greatest length in a general northeast-southwest direction. Subsequent to the geophysical

work two holes were drilled to a depth of 600 feet and both encountered heavy zones of broken meteoritic iron from about 450 feet down. †

Detailed Resistivity Mapping of the Wilmar Gravel Deposit.*— The detail to which a gravel deposit can be mapped by fixed depth resistivity traverses is shown by work at the Wilmar gravel deposit, near Wilmar, Minnesota, reported by S. W. Wilcox.‡ The small abandoned sand pit

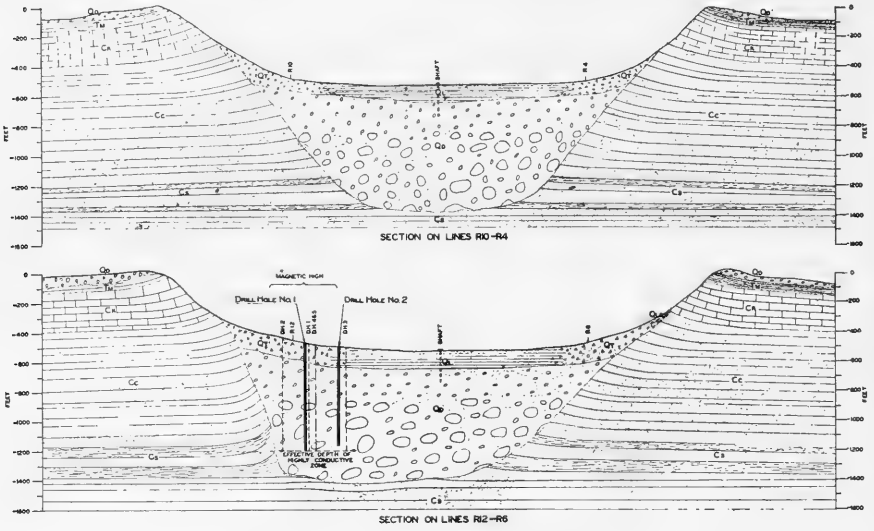

Fig. 355.—Probable geologic sections, Meteor Crater.

Q_D—Debris
Q_T—Landslides
Q_L—Lake beds
T_M—Moencopic sandstone
C_K—Kaibab limestone
C_C—Coconino sandstone
C_S—Supai formation

(*A.I.M.E. Geophysical Prospecting,* Technical Paper, 1932.)

located in the upper left of Figure 356 furnished the clue for the geophysical exploration of the locality.

Four fixed depth traverses were run, spaced 100 feet apart, using a 20-foot constant electrode spacing to secure the data for drawing the equi-resistivity contours to outline the deposit. Logs of the test holes put down in the area investigated are included in Figure 356. Test hole No. 7 showed no sand or gravel and thus served to establish one limit of the gravel body. It appears that the area within the 1000 ohm-foot contour contains substantially all that remains of an ancient stream channel gravel

† C. H. Wilson, "Drilling Proves Existence of Meteoric Mass," *The Mining Journal,* April 30, 1932.

* Dart Wantland, personal communication.

‡ S. W. Wilcox, "Sand and Gravel Prospecting by the Earth Resistivity Method," *Geophysics,* Vol. IX, No. 1, January, 1944.

deposit. The prospect contains an estimated 35,000 yards of sand and gravel.

The time required to map the entire project by the resistivity method was less than that needed to put down one such hole as No. 2 to a depth of about 18 feet. The observer and one helper made the geophysical survey in two days in the field. After the drill hole control was established, the resistivity depth measurements were used to determine the amount of overburden stripping necessary and the thickness of the gravel.

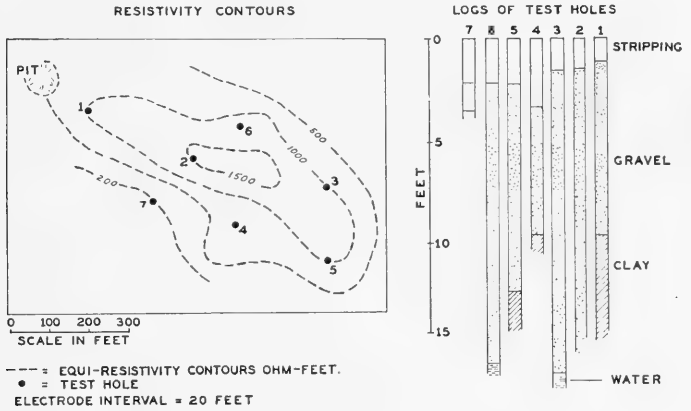

FIG. 356.—Resistivity contour map, Wilmar Gravel Project, Wilmar, Minn. (After S. W. Wilcox.)

The conventional method of mapping gravel deposits for engineering projects is to auger or test pit the likely locations. This technique yields many negative results, especially in the glaciated areas of the United States, where the geologic criteria for the occurrence of gravel are often misleading. In such areas, gravel and sand are usually costly and critical items in highway building. Under these conditions the resistivity method provides a very economical and rapid means of prospecting for gravel.

Resistivity Surveys of Riprap Deposits near Fremont Butte, Colorado.†—Resistivity investigations were made during April, 1948, at the Fremont Butte "quartzite" deposit in northeastern Colorado. The rock in this locality is petrographically a silicified sandstone, although not a true quartzite. It was sufficiently hard to be considered as potential riprap for two proposed dams by the U. S. Bureau of Reclamation in the Missouri River Basin.

The objectives of the geophysical work were as follows: (1) to check the resistivity method against existing drill holes, for determining the depth and thickness of the silicified rock and locating its boundaries; (2) to define the extent of the rock in a part of the deposit where no drilling had been done; and (3) to determine the speed and cost of resistivity work as compared with drilling for exploring such riprap sources.

† Dart Wantland, personal communication.

As shown in Figure 357 this deposit consists of a narrow outcrop of silicified sandstone which varies in width from 25 to 150 feet. The outcrop extends for a distance of about 1½ mile in a broad arc. The thickness of the rock varies from 1½ to over 20 feet, as shown by the outcrop and core drilling.

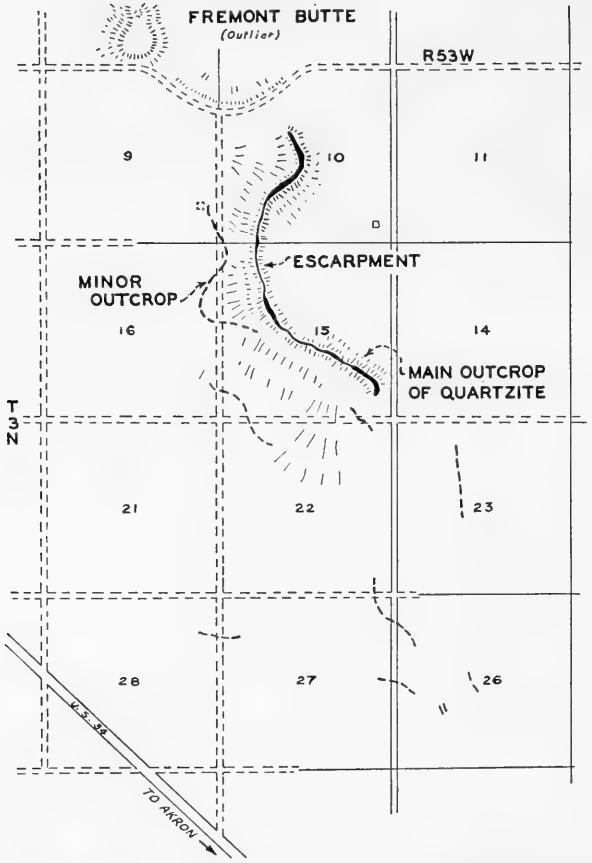

Fig. 357.—Location map, Fremont Butte quartzite deposit. (Courtesy of United States Department of the Interior, Bureau of Reclamation.)

As in the case of similar deposits in western and central Kansas and adjacent parts of Nebraska, the origin of this silicified sandstone deposit is uncertain.† There is evidence, however, that the outcrops are remnants of silicified portions of old braided stream channels. The sinuous course of the main outcrop and of numerous lesser outcrops in the general area supports this theory. The fact that the sandstone bodies as outlined by drilling and resistivity studies appear to be lenticular in cross-section, with

† J. C. Frye and A. Swineford, "Silicified Rock in the Ogallala Formation," *State Geol. Sur. Kans., Bull. 64*, part 2, July, 1946 (Lawrence, Kans.).

definite boundaries as if deposited in stream channels, likewise suggests such an origin. These features are significant in estimating yardage, as the continuity of the rock laterally and in thickness cannot be safely assumed except over short distances or between closely spaced control points.

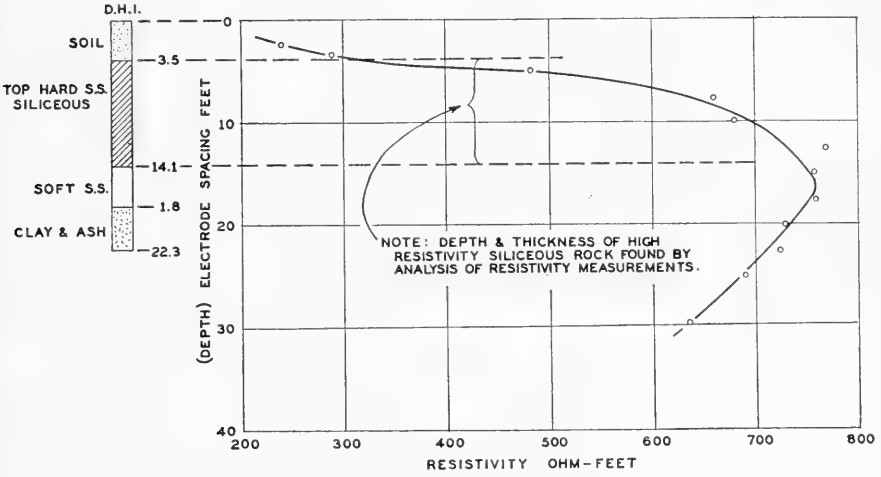

Fig. 358.—Resistivity Depth Curve No. 1, near Drill Hole 1, Fremont Butte, Colorado. (Courtesy of U. S. Department of the Interior, Bureau of Reclamation.)

The applicability of the resistivity method to the problem is based on the fact that the resistivity of the silicified sandstone is some 5 to 6 times greater than that of the material surrounding it.

The field program at Fremont Butte consisted of resistivity depth measurements at the 8 core drill holes to secure control data for determin-

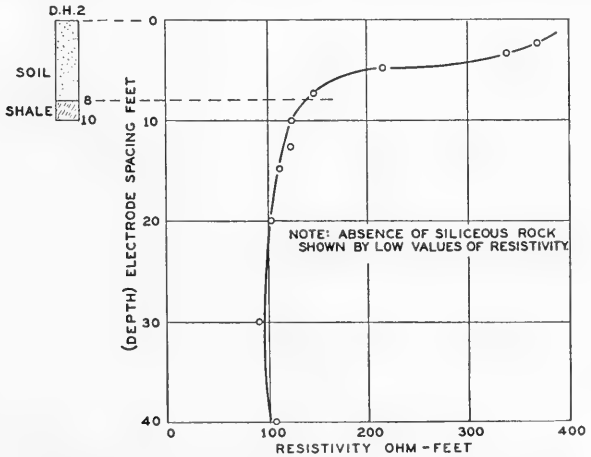

Fig. 359.—Resistivity depth curve No. 2, near Drill Hole 2, Fremont Butte, Colorado. (Courtesy of U. S. Department of the Interior, Bureau of Reclamation.)

ing the thickness and the width of the rock deposit. The resulting resistivity depth curves were compared with the drill logs as shown in Figures 358 and 359. It was found that where the silicified sandstone was present the resistivity values were high, ranging from 400 to 700 ohm-feet. (Figure 358.) Where no rock was present, the resistivity was low, with values of about 50 to 200 ohm-feet, characteristic of the soil, clay, sand and shale of the area.

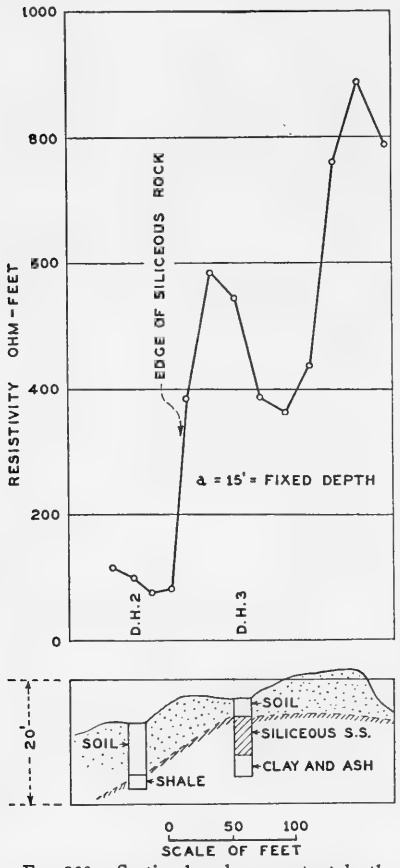

FIG. 360.—Section based on constant-depth resistivity traverse and drilling. Presence of siliceous rock shown by high resistivity values. (Courtesy of U. S. Department of Interior, Bureau of Reclamation.)

Fixed depth resistivity traverses were run between drill holes to check the location of the edge of the rock layer. As evidenced by Figure 360, it was possible to find the termination of the rock body quite accurately even when it was covered by overburden.

The interpretation of the resistivity data was made by visual inspection of the depth curves and traverses. In 8 days of field work, with a four-man crew, 13 resistivity depth curves and 7 lines of constant-depth traverse were run, the latter covering about 1000 lineal feet. It was found that 4 resistivity depth curves to an electrode separation of 50 feet could be conveniently measured in an 8-hour day, allowing travel time to and from headquarters. One constant-depth traverse 250 feet long, with readings at 10-foot intervals, required about the same time as one depth curve. The 13 depth stations and 7 traverse lines constitute 20 units of geophysical work. It is estimated that the cost of one unit is about $50.

The tests demonstrated that, under the typical conditions existing at the Fremont Butte deposit, resistivity depth curves were directly comparable to and as conclusive as drilling, in determining the presence or absence of silicified rock. The resistivity depth measurements provided quantitative data on the depth and thickness of the rock layer. Such measurements were also an index of its character, for in general high values of resistivity indicate better quality rock. The constant-depth traverses clearly outlined the edges of the rock body.

A comparison may be made of the speed of resistivity exploration with

drilling. If it can be assumed that two core holes can be drilled per day to a depth of 50 feet (such silicified rock is often hard drilling), resistivity depth measurements are twice as fast, since four 50-foot-spacing depth curves were run per day.

For the location of the covered boundaries of the rock layer the resistivity procedure has a considerable advantage. It can be assumed that it requires 3 drill holes as a minimum to locate the boundary of the rock. At the rate of 2 holes per day, 1½ days work would be necessary for one boundary determination. With the resistivity traverse this could be done in one-fourth of a day, or 6 times as rapidly.

Supplemental geophysical investigations and additional drilling were done at Fremont Butte during July and August, 1948, to secure data for an accurate estimate of the yardage of rock in the entire deposit. In 9 days, 21 resistivity depth curves were measured and approximately 1100 feet of constant-depth traverse were run. In the supplemental program, resistivity depth measurements were first made at selected sites to determine the approximate thickness of the rock zone, and, as before, constant-depth traverses were run back from the outcrop to establish the width of the deposit. Core drill locations were then selected on the basis of the geophysical findings at those places where it would be most advantageous to know the exact thickness of the rock and its quality, and which at the same time would give the best control for further resistivity tests. Useless drilling in the barren areas was minimized by use of the resistivity work.

The procedure of supplementing and guiding the selection of drill locations secured the information required for estimating the yardage in the shortest possible time and with the minimum number of drill holes. For example, the first drilling at the Fremont Butte area (December, 1947) consisted of 9 core holes. The test resistivity survey was carried on in April, 1948, as described above. These two programs explored about 2,000 feet of outcrop in the southern end of the deposit. The supplemental program required only 15 drill holes to investigate over 4,000 feet of outcrop or about twice as much as was covered in the original work.

As a result of the investigations it was estimated that approximately 147,000 cubic yards of silicified sandstone (in place) were available at the Fremont Butte deposit. The figure was considered accurate within 10 per cent, indicating quantities of from 130,000 to 160,000 yards.

During the 1948 field season the resistivity method was used in connection with drilling to map 5 other potential riprap deposits. Including the Fremont Butte area, it is estimated that a total of over 800,000 cubic yards of silicified rock was mapped.

CHAPTER VI

ELECTRICAL METHODS: *Electromagnetic*

The electromagnetic methods measure directly the magnetic field associated with the flow of current in the subsurface. The subsurface current may be created by either of two techniques: (1) *conductively,* by flow between two electrodes so positioned that the normal path of subsurface current flow will include the area under investigation (either direct or alternating current of any frequency may be employed for the energizing current); or (2) *inductively,* by creating an alternating magnetic field at the surface of the ground.

The distribution of the current in the subsurface may be determined by either of two techniques: (1) by *magnetometric* methods which measure directly the strength and/or the direction of the magnetic field associated with the flow of subsurface current. The subsurface current may be either direct or low frequency alternating current. (2) By *inductive* methods wherein a coil or large loop is positioned at the surface of the ground. The measurements are conducted to determine one or more of the following conditions: total induced E.M.F., from which the strength of the alternating magnetic field may be calculated; induced E.M.F. in two directions at right angles to each other, and their phase relationships; or direction to the effective path of subsurface flow of current.

PHYSICAL PRINCIPLES

Magnetic Field Associated with Electric Current.—An electric current flowing in a conductor produces a magnetic field which radiates outwardly from the conductor in closed magnetic circuits. The lines of magnetic force surrounding an infinitely long, linear conductor are shown in Figure 361. The direction of the field is given by the familiar right hand rule: namely, if the thumb of the right hand indicates the direction in which the current is flowing, the lines of force circle the conductor in the direction of the fingers of the closed hand.

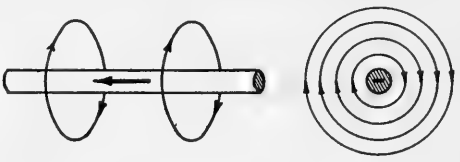

FIG. 361.—Lines of magnetic force due to current flowing in a linear conductor. *A*, side view; *B*, cross sectional view. (Minus sign indicates that current is flowing into the paper.)

Ampere's Law

The magnitude or strength of the magnetic field surrounding a current-carrying conductor may be obtained from Ampere's law. This law describes the magnetic field due to a conductor element of length dl at an external point P. Referring to Figure 362, the field at P is:

$$dH = \frac{i\,dl \sin\theta}{r^2} \tag{1}$$

where

dH = magnetic field
I = current
dl = length of current element
r = distance between dl and P
θ = angle between dl and r

Furthermore, the magnetic field is perpendicular to the plane determined by r and dl.

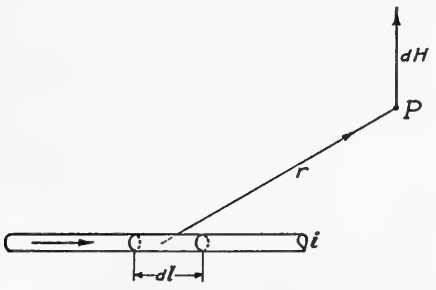

FIG. 362.—Sketch illustrating geometric relation between field dH at P and current I flowing in current element of length dl. (From Ampere's law dH is perpendicular to the plane formed by dl and r.)

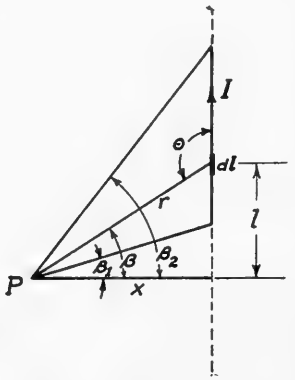

FIG. 363. — Sketch illustrating the geometric relations between the quantities I, dl, etc., which enter into the computation of the magnetic field at a point P.

Ampere's law governs the magnetic field of direct current and alternating current. If the current flowing in the conductor is an alternating current, the magnetic field surrounding the conductor is an alternating field which has the same frequency as the current, and is in phase with it.

Equation 1 may be used to determine the resultant or total magnetic field due to a current flowing in any conductor or group of conductors, provided the integration with respect to l and r can be carried out. In particular, Equation 1 may be applied, in a rather simple manner, for determining the magnetic field produced by a linear flow of current. Referring to Figure 363, it is desired to calculate the magnetic field H at a point P due to the current I flowing in the direction indicated. From Equation 1 the field due to an element of conductor of length dl is

$$dH = \frac{I\,dl \sin\theta}{r^2}$$

An inspection of the figure shows that $\sin\theta = \cos\beta$. Hence,

$$dH = \frac{I\,dl\cos\beta}{r^2}$$

If x is the perpendicular distance from the point P to the conductor l,

$$r = x\sec\beta$$

$$l = x\tan\beta$$

$$dl = x\sec^2\beta\,d\beta$$

Substitution of these values of r and dl into the expression for dH yields

$$dH = \frac{I\,x\sec^2\beta\,d\beta\cos\beta}{x^2\sec^2\beta}$$

and

$$H = \int_{\beta_1}^{\beta_2} \frac{I\cos\beta\,d\beta}{x}$$

On carrying out the integration, one obtains

$$H = \frac{I}{x}(\sin\beta_2 - \sin\beta_1) \qquad (2)$$

If the wire is very long compared to x, β_2 approaches $+\pi/2$ and β_1 approaches $-\pi/2$. Equation 2 approaches the familiar form for the field about an infinite wire: namely,

$$H = \frac{2I}{x} \qquad (2a)$$

Equation 2a shows that the field surrounding a linear conductor may be represented by concentric circles, as was illustrated in Figure 361.

Conductive Methods

Magnetic Field Produced at the Earth's Surface by Subsurface Current.—When current is conductively supplied to the earth a magnetic field will be set up, and a portion of the field will exist at the surface of the earth. Since the current distribution in the earth will be influenced by the geologic structure, the magnetic field set up by the current will likewise be influenced and measurements of this magnetic field or quantities which depend on this field give an indication of the subsurface geology.

For a given electrode spacing the greatest flow of current is along the path of greatest effective conductivity. As applied to mineral prospecting, the effective conductivity of a sulphide zone is much greater than that of the surrounding medium, and the mineralized zone may therefore be located by studying the magnetic field at the surface of the ground and by finding the path along which the current flow is greater. When

applied to structural mapping, the path of effective current flow is calculated from the magnetic measurements and variations in the depth of this path or "marker bed" versus electrode spacing or position and is plotted for various points or stations in the area under investigation.

Theoretical Relationships

The calculation of the magnetic field at the surface for the case where the earth is *homogeneous* and *non-magnetic* can be carried out readily, provided the following assumptions are made: (1) the current penetrates the earth in all directions radially from the source; (2) the current enters the sink radially in all directions from the earth; (3) the magnetic effects of the current leaving the source and the current entering the sink may be evaluated separately, and their separate effects combined vectorially; (4) the magnetic effect of the current leaving the source, or entering the sink, may be computed by evaluating the effect (differential) due to a cone of solid angle dw and intergrating throughout the semi-infinite space occupied by the homogeneous earth; (5) the magnetic field due to the total current in an infinitesimal frustum of a cone is the same as that due to a current which flows along the axis and is equal in magnitude to the total current in the frustrum.

In Figure 364, the xy plane corresponds to the earth's surface and the origin of coordinates to the current source. I denotes the current leaving the source. x denotes the distance between the current source and a point P on the x axis.

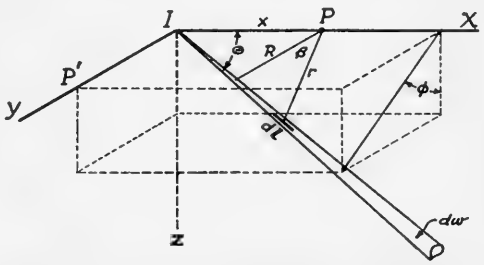

FIG. 364.—Sketch illustrating geometric quantities used in evaluating the field produced at a point P by a current I entering the earth at the origin of coordinates.

In order to determine the resultant magnetic field at P, it is convenient to calculate first the field produced at P by the current flowing in a solid angle dw. The axis l of the cone of revolution defining the solid angle makes an angle θ with the x axis. The perpendicular distance between the axis l of the cone and the point P is denoted by R. The current i passing through the cone is related to the current I leaving the source by the equation

$$i = \frac{I}{2\pi} dw$$

Let dl denote the length of a differential element and r denote the distance between dl and the point P. Also, let (dl, r) denote the angle between dl and r. From Ampere's law, the magnitude of the magnetic

field at P due to the current element dl is given by the equation

$$dH = i\,\frac{dl \sin (dl,r)}{r^2} = i\,\frac{dl \cos \beta}{r^2}$$

or

$$dH = \frac{I}{2\pi} \cdot \frac{dw\, dl \cos \beta}{r^2}$$

Also, the field dH is perpendicular to the plane passing through dl and r.

Due to the fact that the cones radiate from the source into the earth in all directions, the upward and downward vertical components of the fields produced by the cones cancel each other; that is, the resultant field at any point on the earth's surface (xy plane) is parallel to the xy plane. Also, the resultant field is perpendicular to any radius through the current source; that is, at a point such as P the resultant field is perpendicular to x and parallel to the y axis.* Hence, the calculation of the total field at P reduces to a calculation of the y component.

The y component of the field due to the element dl is

$$dH_y = \frac{I}{2\pi}\,\frac{dw\, dl \cos \beta \cos \phi}{r^2}$$

where ϕ is the angle between the y axis and the perpendicular to the plane passing through dl and r.** The last equation may be written in a more convenient form by making use of the following relations:

$$dw = \sin \theta\, d\theta\, d\phi$$

$$r = R \sec \beta$$

$$R = x \sin \theta$$

$$l = R \tan \beta$$

$$dl = R \sec^2 \beta\, d\beta = \frac{r^2 d\beta}{R} = \frac{r^2 d\beta}{x \sin \theta}$$

Whence

$$dH_y = \frac{I}{2\pi x}\, d\theta \cos \phi\, d\phi \cos \beta\, d\beta$$

or

$$H_y = \frac{I}{2\pi x} \int_0^{\pi} d\theta \int_{-\pi/2}^{\pi/2} \cos \phi\, d\phi \int_{\theta-\pi/2}^{\pi/2} \cos \beta\, d\beta$$

But

$$\int_{\theta-\pi/2}^{\pi/2} \cos \beta\, d\beta = 1 - \sin (\theta - \pi/2) = 1 + \cos \theta$$

---

* At a point such as P', the field is parallel to the x axis.

** It is evident from elementary geometry that ϕ is also the angle between the plane passing through dl and r and the xz plane.

Therefore,

$$H_y = \frac{I}{2\pi x}\int_0^{\pi}(1+\cos\theta)\,d\theta\int_{-\pi/2}^{\pi/2}\cos\phi\,d\phi$$

or

$$H_y = \frac{I}{x} \tag{3}$$

Equation 3 specifies the field produced at the surface of the earth by current flowing from a point source into homogeneous, non-magnetic earth.*

The field at P due to current flowing into a sink located on the x axis at a distance L from the source is $\frac{I}{L-x}$. This field has the same direction as the field produced by current leaving the source. Hence, the total magnetic field at the point P is:

$$H_y = H = \frac{I}{x} + \frac{I}{L-x} = I\left(\frac{1}{x}+\frac{1}{L-x}\right) \tag{4}$$

In this equation the value of H is given in gauss provided I is expressed in electromagnetic units (absolute amperes) and x and L in centimeters.

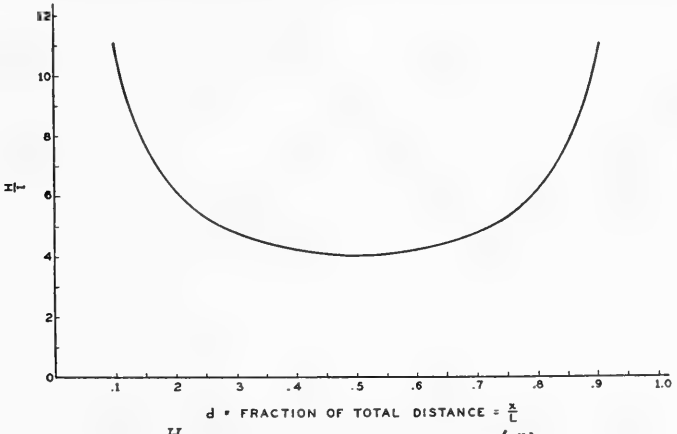

FIG. 365.—Plot of $\frac{H}{I}$ versus fraction of the total distance $\left(\frac{x}{L}\right)$ along a traverse between electrodes.

Equation 4 specifies the magnetic field at the surface due to current flow in homogeneous, non-magnetic earth. (This result does not take into account anomalous surface effects, magnetic effects produced by the return conductor connecting the current electrodes, or the natural magnetic field of the earth.)

Figure 365 is a plot of Equation 4 in which the value of H per unit

* It is of some interest to point out that the same result would be obtained if the current flowed in a straight line vertically downward from the current source.

current is plotted against the distance from an electrode (x) as a fraction of the total separation (L).

If the area under investigation is not homogeneous, the magnetic field produced at the surface of the earth is not given by the simple formula derived above. When direct current or very low frequency energizing current is employed, the magnetic effects observed at the surface of the earth depend on the current paths, and these in turn depend on the relative conductivities of the materials constituting the subsurface. For example, if the subsurface consists of several layers having different conductivities, the effective depth of current penetration and the current paths will depend principally on the values of the conductivities and on the separation of the energizing electrodes. Thus, precisely as in the resistivity methods, variation of the electrode separation permits depth control.

The resolving power of the method however is greater than that of the resistivity methods. This increased resolving power is due largely to the following factors:

(1) The near-surface effects are minimized since a considerable portion of the electromagnetic field being measured is due to the deeper current flow. In the resistivity methods, the only potentials that are effective or measured are those at the surface of the earth.

(2) Near-surface effects diminish, due to the increased flow of current to greater depths as the electrode spacing is increased.

(3) Because the electromagnetic field strength decreases inversely as the distance and the sine of the angle, the current flowing beneath the point of measurement has a much greater effect than current flowing to each side and farther removed from the instrument.

Theoretically, it is possible to calculate the magnetic effects produced by layered media in a manner similar to that used in the preceding section by taking into account the curvature of the current paths. Practically, however, recourse is usually had to an empirical interpretative technique wherein observed electromagnetic anomalies are considered as diagnostic with respect to subsurface inhomogeneities. That is, interpretation is nearly always based on anomalous conditions as indicated by deviations of the field strength from the theoretically normal values. In this respect the electromagnetic data are interpreted by the same technique employed in interpretation of resistivity data. Curves are usually plotted showing the observed *field strength* per unit current versus: (1) *electrode spacing,* (2) *traverse distance* at a constant energizing electrode spacing, or (3) *magnetometer position,* with reference to the distance to the two fixed electrodes.

The third technique results in the most advantageous field procedure where the relative depths to a marker bed or contact are to be mapped. The electrode spacing is chosen to give the maximum effective current flow within the general depth range being mapped. A curve is then plotted for this electrode spacing, as shown in Figure 365. When the effective current

flow is deeper than that for the homogeneous condition, the magnetic field strength will lie along a curve lower in value; and if the effective current flow is shallower than that of the homogeneous condition, the magnetic field strength will be greater than the homogeneous curve values. By plotting a family of such curves, the relative depths to the marker or contact may be determined rapidly.

LOCATION OF SUBSURFACE CURRENT FLOW BY FIELD STRENGTH MEASUREMENTS

Methods for measuring the field created by current flowing through the earth between grounded electrodes are conveniently classified into two groups: namely, (1) methods using direct current energizing and (2) methods using alternating current energizing. The chief practical difference between these groups is the apparatus used to detect or measure the field strength. The usual detecting device in the first group (steady-state field) may be a magnetometer or fluxmeter which measures the magnetic field strength directly. The usual detector in the second group is a search coil which measures the field strength indirectly by means of the E.M.F. induced in it by the alternating field.

Field Strength Measurements Using D.C. Energizing.—The most direct method of studying the distribution of current is to employ a sensitive magnetometer for measuring the strength of the horizontal component of the magnetic field created by a direct current flowing through the subsurface. The voltage requirements will vary from 200 to 900 volts, depending upon the near-surface conductivity, and the current required will vary from 1.0 to 50 amperes, depending upon the depth of investigation. The greater the current employed in the measurements, the less the sensitivity requirements of the magnetometer and the less the disturbance errors introduced by diurnal variations in the earth's magnetic field. A suitable indicating or recording ammeter and voltmeter should be provided for determining the value of current flowing in the subsurface at the instant the magnetometer reading is made.

Energizing Apparatus

Current is applied to the ground between two electrodes connected with a suitable power supply. The separation of the two energizing electrodes may be held constant where lateral studies are to be made, or it may be varied to increasingly greater separations to obtain increasingly greater effective depths of penetration for vertical structural studies. For deep structural studies, a 100-horsepower gasoline engine direct connected to a 1000-volt, 50-ampere DC generator may be employed. A truck-mounted power supply of this type is shown in Figure 366.

The general layout of equipment and field lines is illustrated in Figure

FIG. 366.—Power supply for deep electrical investigations. (Courtesy of Union Oil Company of California.)

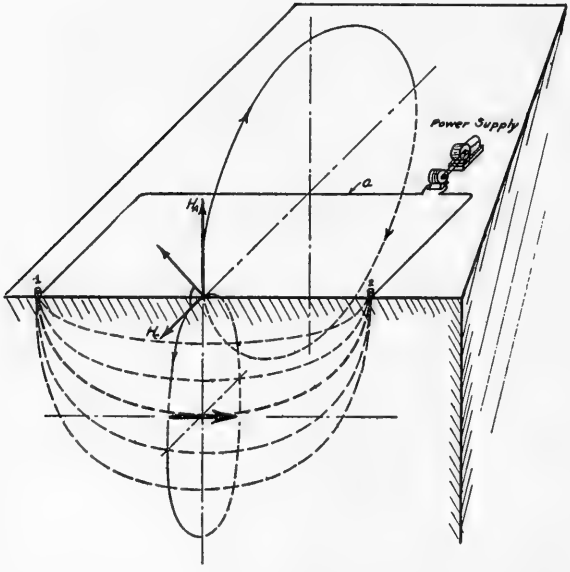

FIG. 367.—Magnetometric method of conductive exploration. H_A, field surrounding the surface wire a; H_C, field surrounding the subsurface flow of current; 1 and 2, energizing electrodes. (Courtesy of International Geophysics, Inc.)

367.† The field wires should be No. 14 stranded copper, or larger, and the electrodes should be of the multiple stake type well "wetted down" to minimize losses.

The area to be studied lies between the two grounded terminals or electrodes. The longer the legs of the "U," that is, the further away the portion of the cable parallel to the line of the electrodes, the less is the effect of the primary current flowing in the surface cable. The legs of the "U" preferably should be once or twice the depth to be worked, and measurements should not be made nearer the legs of the "U," or the electrodes, than about half the depth. The magnetometer is placed on line with the two energizing electrodes 1 and 2. At this position, the field strength measuring apparatus is then subjected to two artificially created fields: (a) the essentially vertical magnetic field H_A created by the flow of current through the energizing wire *a*, and (b) the complex field (represented as a single field H_C) created by the flow of current in the subsurface.

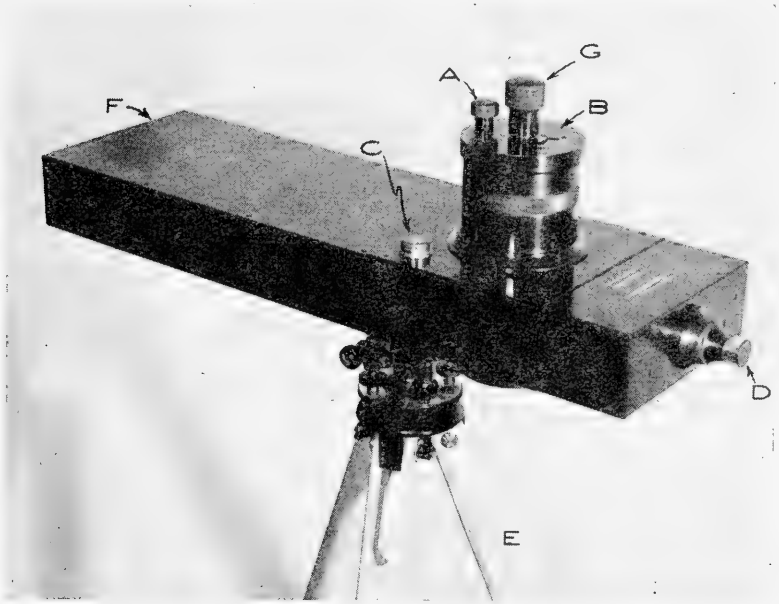

FIG. 368.—Horizontal component magnetometer: A, torsion head; B, torsion scale; C, level; D, telescope; E, tripod; F, scale, with sky mirror (not shown); G, clamp knob. (Courtesy of Union Oil Company of California.)

Measuring Apparatus

The measuring apparatus is designed or oriented to respond primarily to the horizontal component H_C of the field.

Magnetometer (Suspension Type).—One type of magnetometer

† J. J. Jakosky, "Method and Apparatus for Determining Underground Structure," U. S. Patent 1,906,271, issued May 2, 1933.

employed for shallow work of about 1000-foot depth is illustrated in Figure 368. This magnetometer is of the suspension type with a torsion head at the top of the instrument for orientation. The initial and final readings (with energizing current off, on and off) are made by means of scale and telescope. The instrument has a sensitivity of about 2 gammas per scale division.

Magnetometer (Flux Type).—An improved, more sensitive type of magnetometer is illustrated in Figure 369. This equipment comprises essentially a Permalloy-core flux coil connected to a sensitive flux meter. A

FIG. 369.—Magnetometer, flux type. A, flux coil; A', alignment sight; B, potentiometer and batteries for galvanometer lamp; C, flux meter; D, light shield and cover for scale and control panel.

potentiometer and a reversing switch bring the light beam to the proper scale position, and also compensate for thermo-electric and other spurious potentials. The instrument illustrated has a higher sensitivity of 0.61 gammas per scale division, and a lower sensitivity of 1.93 gammas per scale division. The lower sensitivity is obtained by reading the first reflection of the light beam from the galvanometer, while the higher sensitivity is obtained from the multiple reflected beam.

Field Procedure

In practice, the field procedure comprises the following steps: (1) After initial adjustment of the instrument, the magnetometer operator records the scale reading of the instrument. (2) The direct current power then is applied to the ground and the operator records the new reading of the instrument. (3) The power flow is interrupted

and the operator again records the scale reading of the instrument. (4) The power is reversed and again passed into the ground and the scale reading recorded. (5) The power flow is again interrupted and the normal scale reading of the instrument recorded. The scale deflection is computed by taking the arithmetical difference between the averages for power-on and power-off. The observed magnetic field strength is equal to the product of the scale deflection by the calibration constant. Usually, the magnetic reading is expressed as the quotient of the field strength divided by the current used in energizing the ground at that set-up, i.e., field strength per unit current.

In practice, the measurements are made by passing the current into the ground in a series of pulses and measuring the compensated earth's field during the off-current portion of the cycle and the total field (the compensated earth's field plus the electromagnetic field created by flow of the current) during the on-current portion of the cycle. The on and off portions of the cycle are made long enough to allow steady-state conditions to be reached during the measurement and short enough to allow the off-current portion of the cycle to act as a control in correcting for the earth's magnetic field variations. A generator supplies a series of intermittent current pulses to the two stake electrodes at a frequency of about one pulse per second. The current circuit is broken automatically by means of a high voltage relay operated by the energizing current. The output current is controlled by means of a commutator brush system.

The field strength may be plotted versus electrode separation, traverse distance, or magnetometer position, as desired.

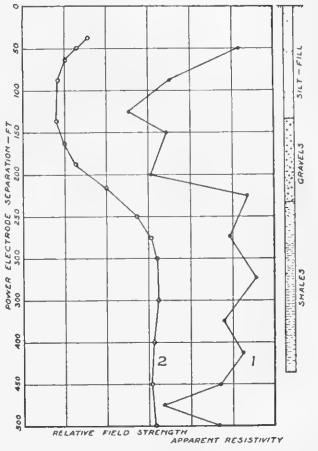

FIG. 370.—Magnetometric and resistivity curves to determine bedrock. (1) Wenner configuration resistivity measurements, (2) magnetometric measurements.

Figure 370 is a comparison of magnetometric and surface resistivity data obtained in an investigation of shallow subsurface structure. The elimination of near-surface effects no doubt accounts for the more consistent data obtained with the magnetometric method.

Field Strength Measurements Using A.C. Energizing Means.—Current is applied to the ground between two electrodes connected with an alternating current power supply. The general layout of field lines is similar to that shown in Figure 367. However, the power supply in this case may be much smaller and driven by a portable gasoline engine. An alternator with a capacity of 500 watts will furnish sufficient power for a 200 cycle supply, while approximately 1000 to 2000 watts should be provided for a 25 to 50 cycle supply.

Figure 371 shows a graph of mutual impedance as a function of frequency for a conductively energized, homogeneous earth.* The plot has been made of $\frac{|Z|}{\rho}$ as a function of $\frac{f}{\rho}$, with an electrode spacing of 1000 feet. $|Z|$ is expressed in ohms, resistivity ρ in ohm-centimeters, and frequency f in sec^{-1}.

* S. S. West, "Mutual Impedance of Collinear Grounded Wires," *Geophysics*, Vol. VIII, No. 2, April, 1943, p. 161.

Note the asymptotic behavior of $|Z|$ as the frequency becomes very large or very small, and the minimum of impedance at about 10^5 cycles.

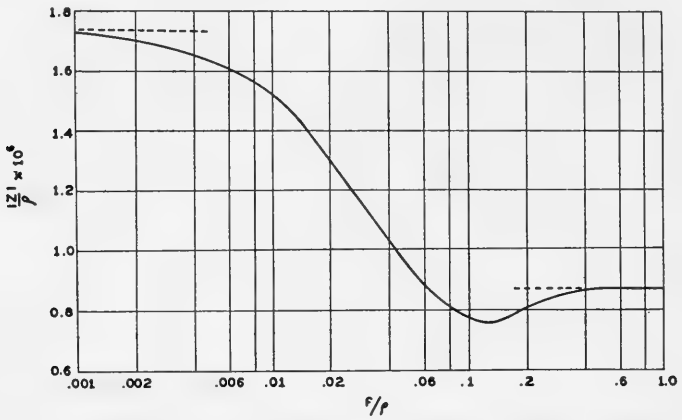

FIG. 371.—Mutual impedance/resistivity as a function of frequency/resistivity for a homogeneous earth. (*Geophysics*, VIII, 2, p. 161.)

INDUCTIVE MEASUREMENTS

Search Coil Measuring Apparatus

The term search coil, as used here, applies to a stationary coil comprising one or more turns of wire wound in any shape, usually circular or rectangular. The physical dimensions of the coil preferably are such as to allow it to be readily portable. The terminals of the coil are connected to a potential measuring device. This type of search coil can be used in magnetic field strength measurements only when the earth is energized with a varying current, e.g., an alternating current.

The operation of a stationary search coil depends on the fact that when an alternating current is caused to flow through the earth, an alternating magnetic field is produced whose magnitude and direction depend on: (1) strength of the energizing current, (2) orientation between the plane of the search coil and the line joining the energizing electrodes, and (3) the subsurface materials and structure.

The alternating magnetic field induces an E.M.F. in the search coil, and data on the magnitude of the induced E.M.F. at a series of stations in a given area are diagnostic with respect to the paths of current flow in the subsurface. The magnitude of the induced E.M.F. is given by the equation:

$$E = -\frac{d\phi}{dt} \tag{5}$$

where ϕ is the normal component of the magnetic flux threading or cutting the coil.

Consider, for example, that an alternating current flows in the earth

between two surface electrodes, with the surface conductor and power supply arranged as shown in Figure 367. Assume, as before, that the earth is homogeneous and non-magnetic. Under these conditions, the subsurface distribution of a very low frequency alternating current will be substantially the same as that of a direct current. The E.M.F. induced in a vertical coil or loop whose plane includes the line joining the energizing stake electrodes can be calculated readily, provided the area of the loop is small relative to the separation of the electrodes so that the magnetic field H may be considered as constant over the area embraced by the coil. Let A denote the area of the loop and let N denote the number of turns of wire in the loop.

Neglecting the field due to the surface or return conductor, the field at a point x on the line joining the two electrodes is given by Equation 4. That is,

$$H = I\left(\frac{1}{x} + \frac{1}{L-x}\right)$$

This field is perpendicular to the line joining the electrodes. Hence, the magnetic flux cutting the loop is normal to the loop and is given by the relation

$$\phi = \mu NHA = \mu NIA\left(\frac{1}{x} + \frac{1}{L-x}\right)$$

where μ is the effective magnetic permeability of the subsurface. If, as is frequently the case, μ may be set equal to unity, the expression for ϕ becomes:

$$\phi = NIA\left(\frac{1}{x} + \frac{1}{L-x}\right)$$

The induced E.M.F. is given by Equation 5. That is,

$$E = -\frac{d\phi}{dt} = -NA\left(\frac{1}{x} + \frac{1}{L-x}\right)\frac{dI}{dt}$$

This equation gives the induced E.M.F. in electromagnetic units when I is expressed in electromagnetic units, A in square centimeters, x in centimeters, and L in centimeters.

In practical units, the last relation becomes

$$E = -\frac{3.05}{10^8} NA\left(\frac{1}{x} + \frac{1}{L-x}\right)\frac{dI}{dt} \qquad (6)$$

where E is given in volts, I in amperes, A in square feet, x in feet and L in feet.

Numerical Illustration.—A low frequency alternating current is applied to the ground by means of two stake electrodes separated by a distance of 100 feet. Suppose

that the current has a maximum value of 10 amperes and a frequency of 5 cycles per second. That is,

$$I = 10 \cos 2\pi \cdot 5t$$

and

$$\frac{dI}{dt} = -100\pi \sin 10\pi t$$

Assume that the coil has 1000 turns and an area of 5 square feet and assume also that the coil is located midway between the stake electrodes.

Substitution of the assumed values into Equation 6 yields

$$E = -\frac{3.05}{10^8} \cdot 1000 \cdot 5 \left(\frac{1}{50} + \frac{1}{50}\right)\left(-100\pi \sin 10\pi t\right)$$

$$= .00192 \sin 10\pi t$$

or

$$E_{max} = .00192 \text{ volts} = 1.92 \text{ millivolts}$$

Field Procedure.—Field strength measurements with search coils are conducted by measuring the potential generated in the coil at various locations in the area. The induced alternating potentials usually are measured by use of a calibrated constant gain amplifier and vacuum tube voltmeter. A fixed or systematic orientation of the coil, with respect to the energizing electrodes, must be employed throughout the measurements. The simple procedure usually employed is to maintain the coil so its plane is vertical and oriented parallel to the straight line joining the two energizing electrodes.

Limitations of A.C. Energizing Methods

From the preceding numerical example it will be seen that the voltage induced in a search coil is extremely small when a low frequency is employed for energizing the ground. If a higher frequency energizing current is employed, the induced voltage in the search coil will be proportionally increased, but the effective depth of penetration decreases because the subsurface distribution of current will be altered due to self inductance. That is, the alternating current flowing into the earth induces a voltage in the earth in such a direction as to oppose the flow of the current. The effect of this induced voltage is greatest at a depth where the normal current is small and hence the potential gradient is also small. This results in a crowding of the current towards the surface.

Evjen† gives the current penetration for different frequencies as follows:

f	d	
(cycles/sec)	Km.	Ft.
0	∞	∞
1	1	3300
4	.5	1650
100	.25	825
1000	.025	83

† H. M. Evjen, "Electrical Methods in Geophysical Exploration," *Geologie en Mijnbouw* (Jaargang No. 1) pp. 2-8, January, 1939.

where d is the asymptotic value of the depth of current penetration (the depth to which one-half of the total current penetrates) as the electrode spacing is increased.*

Thus, the indicated optimum frequency which should be employed when working to a depth of 3300 feet is one cycle per second, but it is impractical to obtain sufficient induced power at this frequency to use the method. On the other hand, a more useable frequency, such as one hundred cycles per second, will have an indicated depth of penetration of only 825 feet. Hence, methods employing alternating current having an appreciable frequency are believed generally to have little economic value except for shallow investigations.

LOCATION OF CURRENT FLOW IN SHALLOW CONDUCTORS BY DIRECTIONAL SEARCH COILS

Instead of measuring the strength of a given component of the varying magnetic field associated with the flow of alternating current, the path of the subsurface current flow may be located by use of directional or direction-finding coils. This procedure utilizes a similar technique to that employed in radio direction finding. A directional search coil, with its necessary orientation and amplifying accessories, is readily portable and allows rapid manipulation for reconnaissance surveys.

Operating Principles of Directional Coils.—To obtain the most accurate determination of the direction of the resultant field, the per cent change in the magnitude of the E.M.F. for a small change in orientation angle must be as large as possible. This condition may be expressed by the relation

$$\frac{1}{E}\frac{dE}{d\theta} = \text{maximum}$$

where E is the induced E.M.F. and θ is the angle made by the direction of the magnetic field with the normal to the plane of the coil. But

$$E = -\frac{d\phi}{dt}$$

$$= -\frac{d}{dt}(NAH\cos\theta) = -NA\frac{dH}{dt}\cos\theta$$

and

$$\frac{dE}{d\theta} = NA\frac{dH}{dt}\sin\theta$$

Hence,

$$\frac{1}{E}\frac{dE}{d\theta} = \tan\theta$$

* The Evjen table affords only a general survey, because the penetration for a particular frequency is dependent upon the materials constituting the subsurface.

Evidently, $\frac{1}{E}\frac{dE}{d\theta}$ is a maximum for θ equal to 90°. That is, the direction of the resultant field is determined most accurately by rotating the coil until its plane is parallel to the magnetic field.

Figure 8 Curve

The magnitude of the induced voltage is often shown graphically by the so-called figure 8 curve. (Figure 372.)† This curve shows the relative value of the induced voltage in the loop as a function of the angle that the loop makes with the magnetic field for the case that the magnetic field is horizontal. When the coil is in the position AA' perpendicular to the direction of the field, the magnetic flux through the coil and consequently the induced voltage is a maximum. As the coil is rotated further, the flux through the coil decreases until at position DD' the coil is parallel to the field and the induced voltage is a minimum. If the rotation of the coil is continued the direction of the flux through the coil will reverse, thereby producing a reversal of phase of the induced voltage.

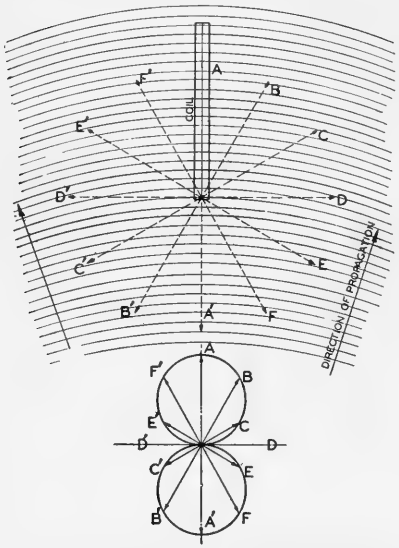

FIG. 372.—Plan view of a direction-finding coil in a uniform field. "Figure-eight curve." (*Proceedings, Institute of Radio Engineers.*)

Field Apparatus.‡—The complete direction-finding apparatus consists of a direction-finding coil, mounting head, tripod, amplifier (for audio-frequency range) or detector and amplifier set (for higher frequencies), and a pair of headphones or a vacuum tube voltmeter.

One type of direction-finding apparatus is illustrated in Figure 373. The mounting head on which the direction-finding coil is pivoted is provided with a sighting arrangement (similar to gun peep-sights) whereby the axis of rotation of the coil may be aligned quickly with the center of the energizing coil. A graduated vertical arc is attached to the pivoted plate holding the direction-finding coil. The vertical-angle index mark and level-bubble arc are attached to the movable arm, which is adjusted by a thumbscrew.

The head rotates on a vertical axis and the azimuth angle may be read on a graduated scale. The entire assembly is mounted on a ball-and-socket

† J. J. Jakosky, "Electrical Prospecting," *Proc. Institute of Radio Engineers,* Vol. 16, No. 10, Oct. 1928.

‡ J. J. Jakosky, "Operating Principles of Inductive Geophysical Processes," *A.I.M.E. Geophysical Prospecting,* 1929, pp. 138-176.

plate. The direction-finding coil is electrically connected to the vacuum-tube set-box which contains a detector (so arranged that it functions as an audio-frequency amplifying stage when using low-frequency coils) and a two-stage tuned transformer-coupled audio-frequency amplifier. The entire apparatus, consisting of heterodyne control dial, controls and batteries, is contained in a waterproof aluminum box 4½ by 4½ by 17

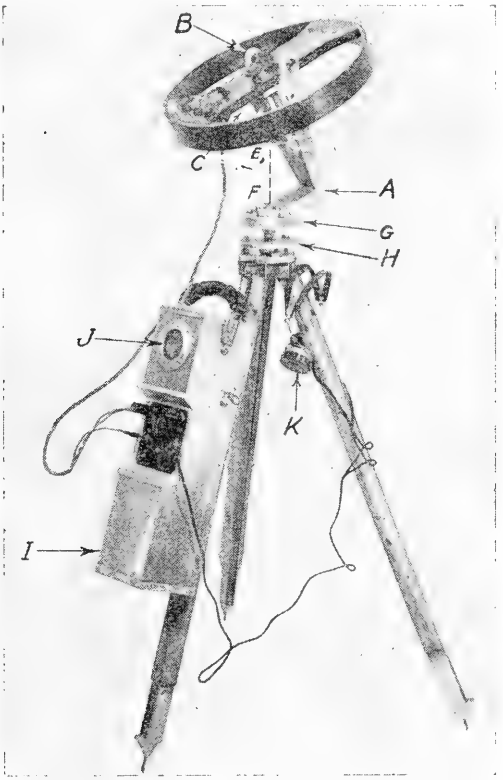

FIG. 373.—Electromagnetic direction-finding apparatus for high frequencies. *A*, mounting head; *B*, alignment sights; *C*, graduated arc for reading vertical angle; *EF*, vertical rotation axis; *G*, azimuth scale; *H*, ball and socket plate; *I*, battery compartment; *J*, voltmeter; *K*, headphones. (*A.I.M.E. Geophysical Prospecting*, 1929.)

inches. A double-range voltmeter is placed behind a waterproof "port-hole" by means of which filament and plate voltages may be read. The control knobs are placed on a recessed panel for protection against mechanical injury. Conventional type headphones are provided so that the operator can detect the point of minimum signal strength when determining the direction of the resultant field. The same mounting head and set-box are used for both low and high frequency work.

A schematic wiring diagram for high and low frequency apparatus is shown in Figure 374. When the high frequency coil is used, the detector is of the oscillating type in order to provide a heterodyne signal for audibility and increased sensitivity. For low frequency work, the detector

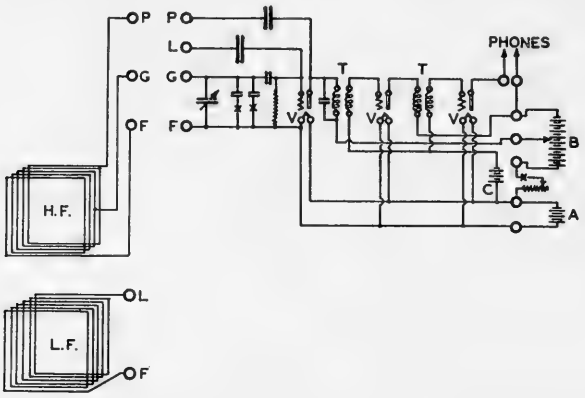

FIG. 374.—Wiring diagram for electromagnetic direction-finding apparatus.

tube functions merely as an audio-frequency amplifying tube. If desired, pentode tubes can be employed in the amplifying stages for greater amplification.

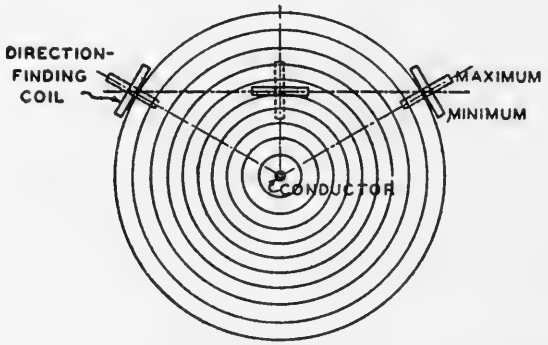

FIG. 375.—Field surrounding a simple conductor in a homogeneous medium. (*A.I.M.E. Geophysical Prospecting*, Technical Paper 134, 1928.)

Applicability of Directional Coils: Field Surrounding a Simple Conductor in a Homogeneous Medium.—The field surrounding a small diameter conductor in a homogeneous medium will travel outward from it in the form of concentric circles or envelopes, as depicted in Figure

375.† The speed of propagation will depend upon the conductivity of the medium surrounding the conductor; in air this speed will be that of light (300,000,000 meters per second), while in a highly conductive material such as sea water, the speed may be only a few meters per second. A direction-finding coil pivoted with its axis of revolution parallel to the conductor will give the maximum signal response when the coil is perpendicular to a tangent to the wave front. A minimum signal will be obtained when the coil is parallel to the tangent. This is illustrated for three positions in Figure 375. Under such conditions the direction-finding coil would become a simple means of locating a subsurface conductor by triangulation. In practice, it will be found that the field surrounding the conductor is distorted by: (1) irregular shape or configuration of the ore body or conductive zone; (2) inhomogeneity of the conductive medium surrounding the major zone of current flow; and (3) distortion of the wave front as the electromagnetic wave emerges from the ground.

Distortion of Wave Front

Because the velocity of propagation of an electromagnetic wave varies with the dielectric properties of the medium through which it passes, there is a resultant distortion of the wave front as it emerges from the ground. In practice, therefore, the wave front traveling outward from the current-carrying zone is not a true circle, and the conductor cannot be located by a simple triangulation process.

The velocity of an electromagnetic wave may be expressed in terms of its velocity in vacuum by the relationship:

$$V = \frac{V_o}{\sqrt{\mu\epsilon K}} + K'$$

where

V = velocity in medium of given properties
V_o = velocity in vacuum (300,000,000 meters per second)
μ = magnetic permeability of material
ϵ = specific inductive capacity of material
K and K' = constants which vary with frequency, etc.

If this formula is applied to a conductor of infinite conductivity ($\sigma = \infty$) the wave would have a limiting velocity equal to zero (since K is a function of σ) and its energy would be almost completely dissipated by generation of eddy currents. A small portion of the energy will be reradiated. This result indicates that a highly conductive ore body will absorb a considerable portion of the energy and reradiate (in the form of a secondary field) a smaller portion.

† J. J. Jakosky, "Fundamental Factors Underlying Electrical Methods of Geophysical Prospecting," *Eng. and Min. Journal*, Feb. 11-18, 1928.

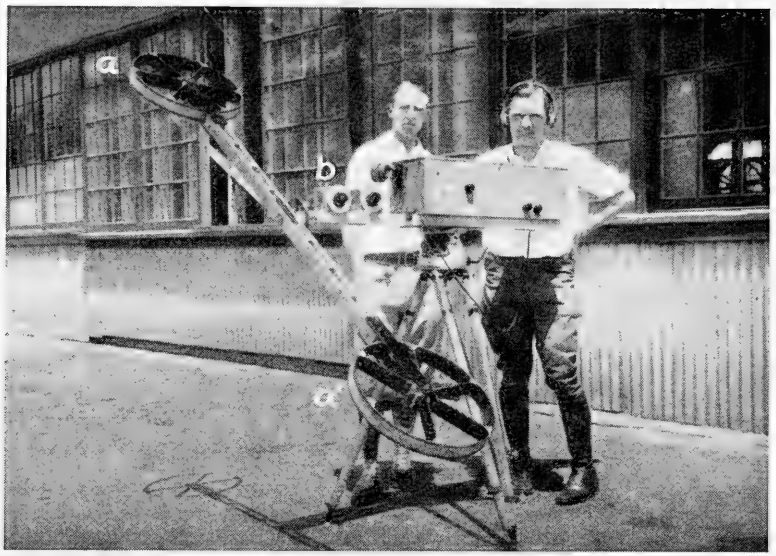

FIG. 376.—Apparatus for measuring angle of electromagnetic wave front. *a* and *a'*, two identical coils; *b*, shielded tuning condensers; *c*, shielded amplifier and phase compensator.

Experimental verification of the distortion of the wave front has been carried out by means of the apparatus illustrated in Figure 376. This apparatus comprised a shielded, antenna-compensated receiver and a double coil antenna rotatably mounted on a 6-foot arm. A graduated arc and vernier were attached to the arm for reading the position of the coils for zero signal input. The two coils had substantially identical electrical characteristics and were connected to a winding of a shielded differential transformer. The secondary of the transformer was connected to the input circuit of an amplifier and detector. In carrying out the measurements, the apparatus was so placed that the axis of rotation of the coil support was parallel to the axis of the conductor. The arm was then rotated until a minimum signal was heard, at which angle the two coils were symmetrically disposed with respect to the wave front.

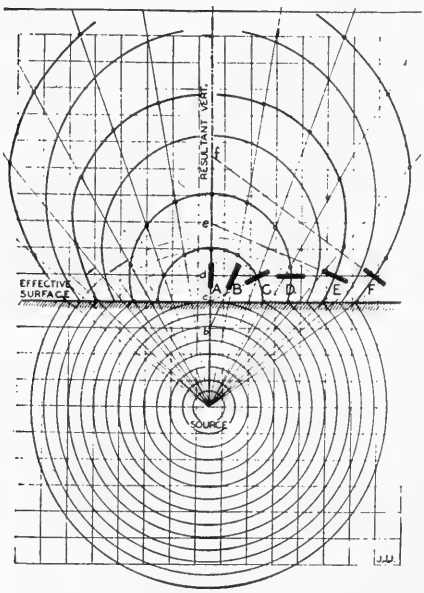

FIG. 377. — Distortion of electromagnetic waves in traveling from earth to air. (*Eng. and Min. Journal*, Feb. 11-18, 1928.)

Figure 377 is a schematic plot of the wave front for an electromagnetic wave emerging from average dry ground. Immediately above a highly conductive body, the arm connecting the two coils is downward and toward the conductor. As readings are taken to either side of the vertical, however, the direction is not toward the conductor, and empirical corrections must be made, as will be described later.

Contacting Ore Body.—In a modification of the electromagnetic process, developed at the University of Arizona,† one terminal of the current supply is connected with the ore body directly. The chief use of this method is in tracing out the extensions of known ore bodies. One energizing electrode is located to make contact with one portion of an ore body (usually an outcropping or working face) and the other electrode is located at a considerable distance from the first contact. If the ore body is shallow, medium high frequencies may be employed for this work.

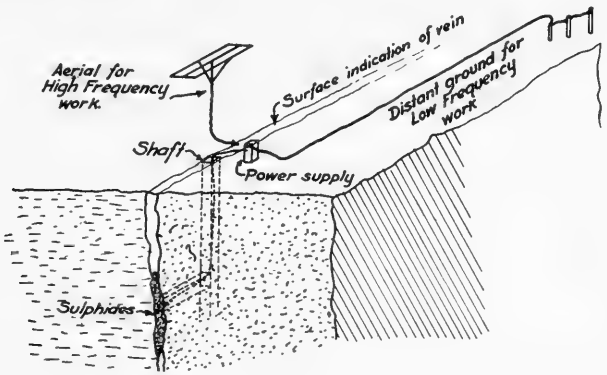

FIG. 378.—Diagram of connections for contacting method.

A schematic diagram of connections for this apparatus is shown in Figure 378. If radio frequencies are used, the ore body must be very shallow. The "antenna" should be of a proper size to allow efficient operation at or near its fundamental or a harmonic thereof.

A direction-finding apparatus similar to that illustrated in Figure 376 is employed for determining the location of the underground conductive zone. Both the dip (angle measured from the vertical) and the strike (azimuth angle) readings are made in determining the location of the body. When using radio frequencies, it will be found oftentimes that the strike readings are more reliable and give better indications of the presence of a conductive zone than the dip readings. When a vertical antenna is employed the strike readings normally should all be toward the antenna, unless an extension of the ore body exists, in which case there will be very definite deviations of the strike.

† D. G. Chilson, "Process of and Device for Locating Ore," U. S. Patent 1,491,900, issued April 29, 1924.

A simple modification of this method which permits its use for deeper lying ore bodies employs a medium frequency alternator for supplying the excitation energy. The equipotential lines are traced out with the aid of two probing electrodes connected with a pair of sensitive headphones or an audio-frequency amplifier and phones. The two probes are on the same equipotential line when no signal is heard in the headphones. Short exploring lines (100 feet or so) should be used to minimize inductive effects.

This same technique is employed for location of buried pipe lines. A contact is made with the pipe at a known location, and the other electrode placed as far away as practical, and in the probable direction of the pipe line. The concentration of current in the pipe will allow its location by use of suitable direction-finding coils.

INDUCTIVELY ENERGIZED METHODS

Inductive methods comprise those techniques wherein the earth is energized inductively by an alternating magnetic field, and measurements are made of parameters which are associated with the secondary magnetic field at the earth's surface produced by induced currents in the subsurface.

When an alternating current is supplied to an insulated loop or coil placed near the surface of the earth, the magnetic field set up by the coil (energizing coil) will cut into the earth and induce a complexity of varying voltages in the materials constituting the subsurface. These induced voltages will in turn set up currents in the earth with a resulting potential distribution at the surface and a redistribution of the magnetic field at the surface.

The effective electromagnetic field existing at the surface of the earth is the resultant of the primary field created by the energizing coil and the secondary fields due to the induced currents in the subsurface and in any other conductors in the vicinity of the energizing coil. Hence, any property of this electromagnetic field is diagnostic, theoretically at least, with respect to the subsurface distribution of current. The parameters most commonly measured or plotted are: contours of equal magnetic flux, phase of the electric or magnetic field, magnitude of vertical or horizontal component of the magnetic field, magnitude or direction of the resultant magnetic field.

The inductive methods are subject to an infinite variety of modifications as is attested by the diversity of inventions governing improvements on these methods. There are many advantages in the use of the inductive methods, chief of which are: (1) by use of electromagnetic means the ground may be energized and/or the subsurface distribution of current determined without the use of electrodes or other direct contact with the ground, (2) at low frequencies the near-surface effects are minimized,

and (3) inductive type methods are relatively rapid for reconnaissance work.

Detailed descriptions of the many modifications of these methods will not be given, but an attempt has been made to describe certain of the methods to illustrate general principles of operation and theory.

The theoretical considerations of electromagnetic exploration are usually based upon Maxwell's equations for the electromagnetic field.† An alternate solution is through the use of Hertzian vectors, which are particularly applicable when a dipole is used for energizing the ground. For a full discussion of this treatment, reference should be had to articles by Horton‡ and Wolf.§

Slichter has solved the inverse boundary value problem to which the reader is referred.†† The problem consisted in determining the variation with depth of the conductivity and dielectric constant from a knowledge of the (measured) electromagnetic field due to a prescribed oscillatory source, at the surface of a semi-infinite medium (earth). The method of attack started with the use of Maxwell's field equations, in cylindrical coordinates for convenience.

The following discussion will be limited to the application of the various techniques to exploration problems.

PHYSICAL PRINCIPLES

The present electromagnetic methods employing inductive energizing means are limited essentially to investigations at fairly shallow depths (of the order of a few hundred feet under favorable conditions). From a practical viewpoint, therefore, the inductive methods are chiefly useful for the location of ore bodies lying near the surface when covered with a thin overburden.

In general, the effect that an ore body will have on the measurements will depend on the size of the body, its relative electrical resistivity, the frequency of the energizing current, and the type and relative resistivity of the overburden.

The larger the effective length of the ore body the greater will be its effect on the magnetic field and consequently the easier will be its detection. The resistivity of the ore body relative to the surrounding earth is also important; the larger the ratio of resistivities the greater will be the effect of the ore body. Furthermore, it is important to realize that the relative resistivities may vary with the frequency used. (In particular,

† J. A. Stratton, "Electromagnetic Theory," McGraw-Hill, 1941.
W. R. Smythe, "Static and Dynamic Electricity," McGraw-Hill, 1939.
‡ C. W. Horton, "On the Use of Electromagnetic Waves in Geophysical Prospecting," *Geophysics*, XI, 4, p. 505.
§ A. Wolf, "Electric Field of an Oscillating Dipole on the Surface of a Two Layer Earth," *Geophysics*, XI, 4, p. 518.
†† L. B. Slichter, "An Inverse Boundary Value Problem in Electrodynamics," *Physics*, Vol. 4, No. 12, December, 1933.

the resistivities of *disseminated* ores may depend markedly on the frequencies employed.)*

The frequency of the energizing current and the type of overburden largely govern the maximum depth at which an ore body can be detected. The theoretical formula for the E.M.F. induced in a small diameter ore body by an energizing coil is stated to be: †

$$E_0 = 2\pi f M_1 I e^{-2\pi d\sqrt{\frac{f\mu}{\rho}}} \tag{7}$$

where E_0 is the induced E.M.F.; f is the frequency of the current in the energizing coil; M_1 the mutual inductance between the energizing coil and the conductor; I the current in the energizing coil; μ the permeability and ρ the resistivity of the overburden.**

The electromotive force E_0 produces an alternating current I_0 in the ore body. The alternating magnetic field of the current I_0, in turn, induces in the search coil an electromotive force E_s whose magnitude depends on the current I_0, the frequency of the current I_0 which is the same as the frequency of the energizing circuit, the mutual inductance between the search coil and the ore body, etc. That is,

$$E_s = 2\pi f M_s I_0 e^{-2\pi d\sqrt{\frac{f\mu}{\rho}}}$$

Hence, the net result is that the overburden exerts a *shielding effect* which varies approximately as the square of the frequency in the energizing circuit.***

The mutual inductance between the energizing coil and the conductor also is dependent upon the orientation of the coil with respect to the conductor. In methods where direction-finding coils are employed for detection of the subsurface conductive zone, the plane of the energizing coil is usually maintained in a vertical position and oriented so that it will be parallel to the probable direction of the subsurface conductive zone. Vertical coils of this type usually are circular or square and as large as may be conveniently handled in the field work, usually sixty to one-hundred square feet in area. Their small area is offset by use of many turns of wire, the number of turns depending upon the power and frequency of the energizing

* A disseminated ore may be considered as composed of small, electrically conductive particles distributed in a matrix; as a rule this matrix is calcite, quartz, or similar material and has a high electrical resistance. A small electrostatic capacity exists between the conducting particles constituting the disseminated ore. From an electrical viewpoint, therefore, a disseminated ore may be considered as a resistance shunted by a capacity.

† A. B. Broughton Edge and Laby, *Geophysical Prospecting*, p. 293 (Cambr. Univ. Press, 1931).

** In applying this formula to the E.M.F. induced in an ore body, it is assumed that the material surrounding the ore body has the same values of ρ and μ as the overburden.

*** From a physical viewpoint, it is readily recognized that the shielding effect is due to the absorption of the magnetic energy by eddy currents in the overburden.

system. The coil should be tuned to the frequency, or a harmonic, of the energizing power.

Field Due to a Circular Loop at a Point on the Axis of the Loop.—The field due to a circular circuit of one turn at a point P (Figure 379) on the axis of the circle at a distance x from the center may be calculated readily as follows: †

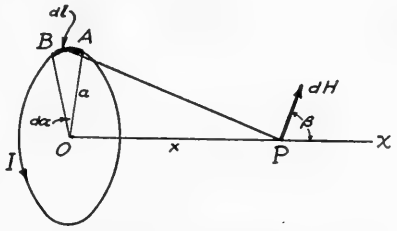

FIG. 379.—Sketch illustrating field dH due to the current element dl.

Consider first the field dH due to the current element AB. From Ampere's law (Equation 1),

$$dH = \frac{Idl \sin \theta}{r^2}$$

where $dl = AB$ and θ equals the angle between dl and r. This field is perpendicular to dl and r. Hence, $\sin \theta = 1$. Also, from the geometry of the figure, $dl = a\, da$. Hence,

$$dH = \frac{Ia\, da}{r^2}$$

From symmetry the resultant field is along the x axis and is equal to

$$H = \frac{Ia}{r^2}\left[\int_0^{2\pi} da\right] \cos \beta = \frac{2\pi Ia^2}{r^3}$$

or

$$H = \frac{2\pi Ia^2}{(a^2 + x^2)^{3/2}} \tag{8}$$

It is obvious that if the circular circuit has N turns, the last formula would become

$$H = \frac{2\pi NIa^2}{(a^2 + x^2)^{3/2}} \tag{8a}$$

Mutual Inductance Between Parallel Coils.—The mutual inductance M between two electrical circuits is equal to the magnetic flux

† L. Page and N. I. Adams, *Principles of Electricity*, p. 247 (Van Nostrand Company, 1931).

associated with one circuit due to unit current in the other. That is,

$$M = \frac{\text{magnetic flux in secondary circuit}}{\text{current in primary circuit}} = \frac{\text{magnetic flux in primary circuit}}{\text{current in secondary circuit}}$$

or

$$M = \frac{\phi}{I} \tag{9}$$

where ϕ denotes the magnetic flux in one circuit due to a current I in the other.

M is a constant for any two circuits and depends on the geometrical configurations and orientations of the circuits and the magnetic properties of the media surrounding them.

The approximate value of the mutual inductance between two parallel coaxial circles, one of which has a radius b small compared to the radius a of the other, is readily calculated. The field at the center P of the smaller coil due to the current I in the larger coil is given by Equation 8. That is,

$$H = \frac{2\pi I a^2}{(a^2 + x^2)^{3/2}}$$

where $x = OP$. Because b is assumed to be small compared to a, the field H is approximately constant over the entire cross section of the smaller coil. Therefore, the magnetic flux through the smaller coil is

$$\phi = \pi b^2 \mu H = \frac{2\pi^2 \mu a^2 b^2 I}{(a^2 + x^2)^{3/2}}$$

where μ is the magnetic permeability of the medium surrounding the coils. But from Equation 9, the mutual inductance is equal to the magnetic flux of induction divided by the current. Hence,

$$M = \frac{2\pi^2 \mu a^2 b^2}{(a^2 + x^2)^{3/2}} \tag{10}$$

If the coils have N_1 turns and N_2 turns respectively, the last equation becomes

$$M = \frac{2\pi^2 \mu a^2 b^2}{(a^2 + x^2)^{3/2}} N_1 N_2 \tag{10a}$$

The mutual inductance M is an important quantity in the analysis of inductive processes because the magnitude of the induced E.M.F. in a secondary circuit due to an alternating current in the primary circuit is directly proportional to M. That is,

$$E = -\frac{d\phi}{dt}$$

or

$$E = -M \frac{dI}{dt} \tag{11}$$

The application of Equation 11 in inductive prospecting will be indicated in the following section.

General Characteristics of Induced Fields.—Certain general ideas relative to the type of magnetic field to be expected when currents are induced in conducting masses buried in the earth may be obtained from a consideration of the interaction between the two coils P and S shown in Figure 380. †

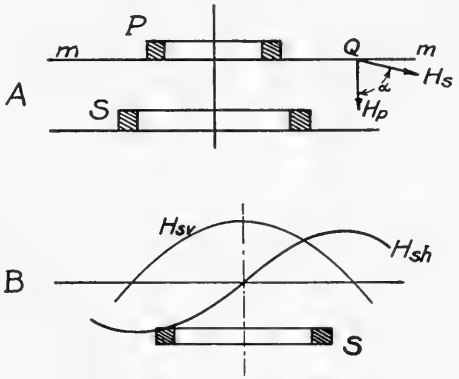

FIG. 380.—A, sketch illustrating resultant magnetic fields H_p and H_s due to the primary and secondary coils P and S. B, curve H_{sv} shows the general shape of the vertical component of the magnetic field due to the induced current in the secondary coil and curve H_{hs} shows the general shape of the horizontal component. (After Peters and Bardeen, Bulletin of the Univ. of Wisconsin, Engineering Experiment Station Series No. 71.)

An alternating current $I_p = I_{pm} \cos wt$ is sent through the primary circuit P. This current induces an E.M.F. in the secondary circuit whose magnitude is given by Equation 11; that is,

$$E = -M \frac{dI_p}{dt} = wMI_{pm} \sin wt$$

where M is the mutual inductance between the two circuits.

The electromotive force E causes a current I_s to flow in the secondary circuit. If the capacity of the secondary circuit is small, the impedance is $R_s^2 + wL_s^2$, where R_s denotes the resistance and L_s the inductance of this circuit, and the current is:

$$I_s = \frac{wMI_{pm} \sin (wt - \beta)}{\sqrt{R_s^2 + w^2L_s^2}}$$

where

$$\tan \beta = \frac{wL_s}{R_s} \quad \text{or} \quad \beta = \tan^{-1} \frac{wL_s}{R_s}$$

The expression for I_s can be put into a more conventional form by making use of the trigonometric relation

$$\tan^{-1} \frac{wL_s}{R_s} = \frac{\pi}{2} - \tan^{-1} \frac{R_s}{wL_s}$$

or

$$\beta = \frac{\pi}{2} - \theta$$

† L. J. Peters and J. Bardeen, "The Solution of Some Theoretical Problems which Arise in Electrical Methods of Geophysical Exploration" (Bulletin of the Univ. of Wisconsin, Engineering Experiment Station Series No. 71).

where

$$\tan \theta = \frac{R_s}{wL_s} \tag{12}$$

On replacing β by its equivalent in terms of θ, we obtain

$$\sin (wt - \beta) = \sin (wt - \frac{\pi}{2} + \theta) = -\cos (wt + \theta)$$

and

$$I_s = -\frac{wMI_{pm} \cos (wt + \theta)}{\sqrt{R_s^2 + w^2 L_s^2}} \tag{13}$$

On comparing Equation 13 and the expression for the primary current, it is apparent that the time phase angle between the secondary and primary currents is $\pi + \theta$.

At any point such as Q on the plane mm (Figure 380), the magnetic flux density due to the secondary current is given by the relation

$$H_s = -\frac{f_s wMI_{pm}}{\sqrt{R_s^2 + w^2 L_s^2}} \cos (wt + \theta) \tag{14}$$

where f_s is a function of the geometry of the system, the location of the point Q, and the permeability of the medium surrounding the secondary coil. The magnetic flux density due to the primary current is given by the relation

$$H_p = f_p I_{pm} \cos wt \tag{15}$$

where f_p is a function of the geometry of the system, etc.

At a particular instant of time, therefore, the fields at Q may be represented by vectors H_p and H_s as shown in Figure 380. These vectors are displaced in space by an angle α and in time phase by an angle $\pi + \theta$. Hence, *in general,* they will combine to give a rotating vector for the resultant field, and the tip of the rotating vector will trace an ellipse.*

In certain special cases, however, θ is approximately equal to zero so that the time phase angle between the secondary and primary fields is approximately 180°. For such cases, the major axis of the ellipse is much larger than the minor axis and the resultant field at any point may be represented without appreciable error by a vector which is constant in direction rather than by a rotating vector.

Consider, for example, a mineralized, highly conductive subsurface zone and assume that with respect to inductive phenomena this mineralized zone is equivalent to a coil. The resistance R_s of the mineralized zone will be small, while the inductance L_s will not, and it may be shown that $\tan \theta = R_s/wL_s$ approaches zero; that is, θ is approximately equal to zero.

* The mathematical analysis proving that two fields which differ in time phase and "space phase" combine to produce an elliptically polarized field is given on p. 614.

The time phase angle between the primary and secondary fields is therefore approximately equal to 180°, and the direction of the resultant field is substantially constant or fixed. Thus, if a direction-finding loop were revolved about an axis parallel to this fixed direction, no signal would be heard in the headphones, because the field would always be parallel to the plane of the coil.

Usually, electrical prospecting methods which utilize inductive pick-up include appropriate electrical equipment either for evaluating the elliptical polarization properties of the magnetic field (e.g., double coil method) or for minimizing the effects of the elliptical polarization at the detector. However, some methods (e.g., Conklin horizontal loop method) involve balancing the effects of two coils without regard to the elliptical polarization properties of the resultant magnetic field. The latter methods will be discussed first.

A study of the propagation of electromagnetic waves in the earth (inductive energizing) was made by Haycock, Madsen, and Hurst † in the form of a careful summary of the relevant experiments performed by numerous workers up to the present (1949). A resume of the advantages and disadvantages of the various frequencies is included in that study.

The use of radio waves wherein the transmission of radio stations was utilized was investigated by Silverman and Sheffet.‡ Penetration is discussed and attenuation graphs of various frequencies are included.

HORIZONTAL LOOP METHODS

Conklin§ was probably the first investigator to energize the ground successfully by passing alternating current through a large, horizontal, insulated loop or coil laid on the surface of the ground.

Considerable work has been done by subsequent investigators both in the United States and abroad,†† using modified equipment.

Magnetic Field Due to a Square Coil.—When current is passed through a large coil lying in a horizontal plane, the magnetic field produced within the coil by this current will be vertical; i.e., perpendicular to the plane of the coil. The *magnitude* of the magnetic field may be evaluated as follows: Referring to Figure 381, which represents a square coil carrying a current I, it is desired to compute the magnetic field at a point situated at a distance x from the side AB and a distance y from the side BC. The field due to the side AB is given by Equation 2. That is,

$$H_{AB} = \frac{I}{x}(\sin \beta_2 - \sin \beta_1)$$

† O. C. Haycock, E. C. Madsen, and S. R. Hurst, "Propagation of Electromagnetic Waves in Earth," *Geophysics*, Vol. XIV, No. 2, April, 1949, pp. 162-171.

‡ D. Silverman and D. Sheffet, "Note on the Transmission of Radio Waves Through the Earth," *Geophysics*, Vol. VII, No. 4, Oct., 1942, pp. 406-413.

§ H. R. Conklin, "Method and Apparatus for Determining Subterraneous Conductors," U. S. Patent 1,241,197, issued Sept. 25, 1917.

†† See, for example, Hans Lundberg, "Recent Results in Electrical Prospecting for Ore, *A.I.M.E. Geophysical Prospecting*, 1929, p. 87.

But

$$\sin \beta_2 = \frac{y}{\sqrt{x^2 + y^2}}$$

and

$$\sin \beta_1 = -\frac{a - y}{\sqrt{(a - y)^2 + x^2}}$$

Hence

$$H_{AB} = \frac{I}{x}\left(\frac{y}{\sqrt{x^2 + y^2}} + \frac{a - y}{\sqrt{(a - y)^2 + x^2}}\right)$$

Similarly

$$H_{BC} = \frac{I}{y}\left(\frac{a - x}{\sqrt{(a - x)^2 + y^2}} + \frac{x}{\sqrt{y^2 + x^2}}\right)$$

$$H_{CD} = \frac{I}{a - x}\left(\frac{a - y}{\sqrt{(a - y)^2 + (a - x)^2}} + \frac{y}{\sqrt{(a - x)^2 + y^2}}\right)$$

$$H_{DA} = \frac{I}{a - y}\left(\frac{x}{\sqrt{(a - y)^2 + x^2}} + \frac{a - x}{\sqrt{(a - x)^2 + (a - y)^2}}\right)$$

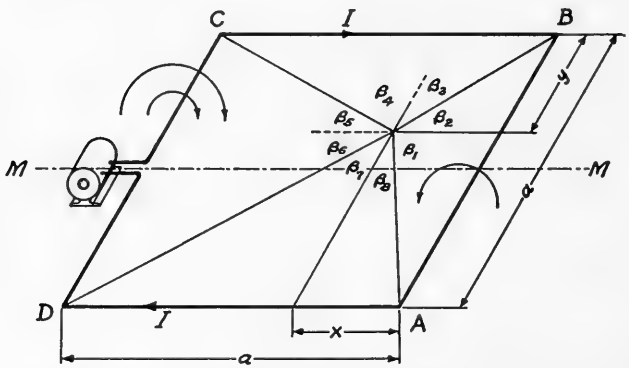

FIG. 381.—Sketch illustrating the geometric relations between the quantities I, a, etc., which enter into the computation of the magnetic field at a point having the coordinates x and y.

If it is assumed that the current I flows in the direction of the arrow, the fields H_{AB} to H_{AD} in the figure are all directed into the paper (away from the reader). Hence, the resultant field at P is

$$H = H_{AB} + H_{BC} + H_{CD} + H_{DA}$$

On substituting the values for H_{AB}, H_{BC}, etc., and rearranging terms one obtains

$$H = I\left\{\frac{\sqrt{x^2+y^2}}{xy} + \frac{\sqrt{(a-y)^2+x^2}}{x\,(a-y)} + \frac{\sqrt{(a-x)^2+y^2}}{y\,(a-x)} + \frac{\sqrt{(a-y)^2+(a-x)^2}}{(a-x)\,(a-y)}\right\} \tag{16}$$

Equation 16 specifies the magnitude of the field at any point situated at a distance x from the side AB and a distance y from the side CB.

The value of the field at various points along a line parallel to DA ($y =$ constant) may be obtained by assigning a series of values to x. In particular, the value of H along the line MM ($y = a/2$) is obtained by substituting this value of y into Equation 16.

$$H_{y=a/2} = \frac{2I}{a}\left\{\frac{\sqrt{4x^2+a^2}}{x} + \frac{\sqrt{4\,(a-x)^2+a^2}}{a-x}\right\} \tag{16a}$$

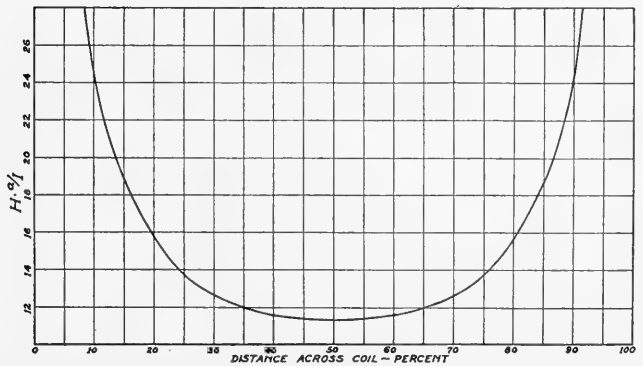

FIG. 382.—Plot showing variation of Ha/I at various distances along a profile inside a square coil of side a.

A graph of Equation 16a is shown in Figure 382. It will be noticed that a relatively small variation of H occurs for the values of a between $0.25a$ and $0.75a$, and the field measurements are usually made within this range.

Field Operations.—The ground is energized by passing alternating current through a large single turn loop of insulated wire laid on the surface of the ground, in the form of an approximate square or rectangle. Usually the current is generated by a gasoline-driven alternator and has a magnitude of 5 to 20 amperes, and for shallow investigations, a frequency of 500 to 1000 cycles per second. The size of the ground loop varies with the nature of the problem, usually being from 1000 to 2500 feet on a side.

The observational technique consists in determining contours of equal

magnetic flux anomaly. These isanomalic contours may be determined by using two search coils or loops which are opposingly connected. Each coil contains about 500 turns of fine wire wound on a four- to six-foot frame. The work can be carried out by the usual field procedure of mapping the location of points of equal magnetic strength, i.e., by leaving one coil at a station and then moving the second coil until a position is found where the induced potential between the two coils is a minimum; these two locations are marked and transferred to a plot of the area. The first coil is now moved along the traverse line beyond the second coil to the next null point of reading and the process repeated. In an alternate procedure, the second coil is moved to the position initially occupied by the first coil, and the first coil is moved forward to search for a new null point.

Precautions must be taken to have the two search coils as nearly identical electrically and magnetically as possible. The comparing circuit and amplifier should be well shielded and placed midway in the shielded two-circuit conductor connecting the two search coils. Proper electrical balance of the two coils can be readily checked during the progress of the survey by placing one coil exactly over the other. If their outputs are connected in opposition, no signal should be noted in the headphones or vacuum tube voltmeter.

The location of these points of equal magnetic flux is usually accomplished by keeping both coils in a horizontal position. In one field procedure, two operators are usually required, each one "wearing" a coil. The coil is suspended in a horizontal position by means of cross-straps which hang over the shoulders of the operator. The coil should be about waist high to allow the operator freedom in walking.

The method is relatively simple in application, and changes in the energizing current usually do not affect the comparisons. The chief limitation of this method is the fact that measurements are practically confined within the central portion of the area bounded by the large energizing ground loop. Within this area, the primary field (that created by the flow of energizing current through the coil) has its maximum value and the secondary field (that created by the flow of induced current) is superimposed on the primary field. Since the primary field is usually many thousands of times stronger than the secondary field associated with a subsurface conductive zone, it is often difficult (except when good conductive bodies lie close to the surface) to make reliable measurements which will show such small variations in the total or resultant field.

Other balancing techniques may be employed. If desired, the relative field strengths at two different points may be determined by keeping one coil horizontal and then tilting the other coil until the signal is at a minimum. † This technique necessitates that the tilted coil be the one located

† Karl Sundberg, "Method and Device for Detecting and Locating Ores in an Electromagnetic Way," U. S. Patent 1,678,489, issued July 24, 1928.

in the more intense field. Instead of tilting one coil, a variable potentiometer or a tap switch may be used to vary its output and the relative field strengths may be calculated from the relative settings of the potentiometer or the number of turns in the coil.

Other noteworthy references on both empirical and theoretical aspects of electromagnetic prospecting are given below.†

Absorption Method. — A modification of the electromagnetic method previously described employs a balance system ‡ which is essentially a differential transformer in which the inductance of the loop or exploring coil is measured by an impedance bridge or differential transformer. (Figure 383.) When a current of constant frequency is supplied by the alternator and proper balance obtained, a zero null or minimum signal will be heard in the headphones. If, now, the coil is moved over an area having a greater or smaller conductivity than that corresponding to the initial balance, the inductance of the coil will be changed resulting in an unbalanced condition, and a signal will be heard in the phone.

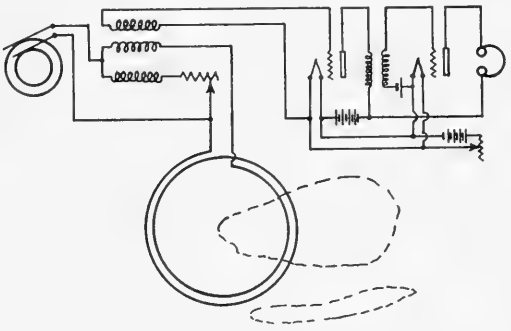

Fig. 383.—Diagram of connections for absorption method. (After Carlson and Hanson, U. S. Patent 1,325,554.)

This type of equipment, or a modification thereof, is oftentimes useful for the location of buried metal objects within a few feet of the surface. By making the coil from 1 to 5 feet in diameter and taking particular care to balance out capacity and other undesirable feed-back currents, a simple outfit can be made for the location of pipe lines, "buried treasures," etc., which occur within a few inches or a foot or two from the surface. In operation, the exploring coil is carried approximately 6 inches from the ground and the observer slowly walks over the area to

† A. S. Eve, "Absorption of Electromagnetic Induction and Radiation by Rocks," *A.I.M.E. Tech. Pub. 316* (1930).

A. S. Eve, D. A. Keys, and F. W. Lee, "The Penetration of Rock by Electromagnetic Waves at Audio Frequencies," *Proc. I.R.E. 17, 2072* (Nov., 1929).

J. W. Joyce, "Electromagnetic Absorption by Rocks," *U. S. Bur. of Mines Tech. Paper 497* (1931).

C. B. Feldman, "The Optical Behavior of the Ground for Short Radio Waves," *Proc. I.R.E. 18* (June, 1933), 764.

R. L. Smith-Rose, "Electrical Measurements in Soil with Alternating Currents," *Jour. of Inst. of Elect. Engrs.* (London), August, 1934, 221-237.

R. L. Smith-Rose and J. S. McPetrie, "The Attenuation of Ultra-Short Radio Waves Due to the Resistance of the Earth," *Proc. Phys. Soc. 43* (London), Sept., 1931, 592-620.

F. E. Terman, "Radio Engineer's Handbook," 708-709 (McGraw-Hill, New York, 1943).

C. A. Heiland, "Geophysical Exploration," pp. 310-314, 657-667 (Prentice-Hall, New York, 1940).

L. Kerwin, "Use of Broadcast Band in Geologic Mapping," *Jour. of Applied Physics,* 18 (April, 1947), 407.

‡ W. L. Carlson and E. C. Hanson, "Means for Locating Ore Bodies by Audio-Frequency Currents," U. S. Patent 1,325,554, issued Dec. 23, 1919.

be explored. The dimensions of the body to be located have a direct bearing on the depth at which they may be detected. As a general rule the conductive body should have at least two dimensions equal to or greater than the depth at which it is located from the coil. For instance, if the coil is held 6 inches above the surface of the ground and the body is buried one foot below the surface, the conducting body should have two dimensions 1½ feet by 1½ feet.

Method for Mapping Materials of Anomalous Magnetic Permeability.—Sundberg † has proposed a method for detecting magnetic materials which utilizes a magnetic field created by passing *direct* current through a coil or loop laid on the surface of the ground. This *constant* field, being vertically polarized, will cause a change in the intensity and direction of the magnetic field normally present in a magnetized subsurface body. By means of a sufficiently sensitive instrument for measuring magnetic field strength, the location and extent of the anomalous magnetic bodies may be determined.

It will be noted that fundamentally this is not a method of mapping the subsurface distribution of current, but primarily one of mapping materials of greater magnetic permeability than the surrounding earth.

Methods for Surveying an Area by Determining the Polarization Ellipse.—As indicated previously, the magnetic field at the surface of the earth is the resultant of the primary field due to the energizing coil and the secondary fields due to various induced currents.

To simplify the mathematical analysis the various secondary fields will be treated as one field. The vector representing this resultant secondary field and the vector representing the primary field will generally be displaced in space by some angle, α say, and in time phase by some other angle, for example $\pi + \theta$. (Compare p. 608.) Hence, the resultant of the primary and secondary fields is of the type known as an elliptically polarized field. The vector representation of an elliptically polarized field is a rotating vector whose tip periodically traces out an ellipse and whose length at any instant is proportional to the magnitude of the field at that instant.*

The production of a resultant elliptically polarized field by two fields which are out of phase may be shown mathematically as follows: Assume that at a point P the primary field is in the x direction and the secondary

† K. Sundberg, "Method and Apparatus for Magnetic Prospecting," U. S. Patent 1,748,659, issued Feb. 25, 1930.

* Consider for example, that the resultant magnetic field at any instant is given by the equation $H = H_0 \sin(wt - \phi)$ where H_0, w, and ϕ are constants and t denotes time. Assign a series of values to t; for example, $t = 0, \frac{\pi}{4w}, \frac{\pi}{2w}, \frac{3\pi}{4w}, \frac{\pi}{w}, \frac{5\pi}{4w}, \frac{3\pi}{2w}, \frac{7\pi}{4w}, \frac{2\pi}{w}$ and compute the corresponding values of H. Then draw vectors whose lengths are proportional to H and whose directions make angles, $-\phi$, $(\pi/4w - \phi)$, $(\pi/2w - \phi)$, etc., with some arbitrary axis. The envelope of the tips of these vectors will be found to be an ellipse.

field is in the y direction.* Assume also that the two fields have the same frequency ($w/2\pi$) and that they have a time phase difference of $\pi + \theta$. Corresponding to these assumptions, the primary and secondary fields are given by the relations:

$$X = X_0 \cos wt$$

$$Y = -Y_0 \cos (wt + \theta)$$

where X is the field component in the x direction and Y the component in the y direction, and X_0 and Y_0 the amplitudes, i.e., the maximum values of X and Y.

These two equations are the parametric equations of an ellipse as will be evident from the following analysis. On eliminating the parameter t between the two equations and simplifying, one obtains

$$\frac{Y^2}{Y_0^2 \sin^2 \theta} + \frac{2XY \cos \theta}{X_0 Y_0 \sin^2 \theta} + \frac{X^2}{X_0^2 \sin^2 \theta} = 1 \qquad (17)$$

Equation 17 is of the form

$$AY^2 + 2BXY + CX^2 = 1$$

where

$$A = 1/Y_0^2 \sin^2 \theta$$

$$B = \cos \theta / X_0 Y_0 \sin^2 \theta$$

$$C = 1/Y_0^2 \sin^2 \theta$$

Hence (17) is the equation of an ellipse.**

The analysis given in the above paragraphs treated a special case of two fields oriented in space at right angles to one another. However, it can be shown that irrespective of the number of secondary fields and irrespective of their amplitudes, phases and directions, the resultant of the primary and secondary fields may be represented by a single vector whose tip periodically traces out an ellipse. †

Determinations of the ratio of the major to the minor axis of the ellipse at various stations in a given area will frequently give valuable information on subsurface irregularities in conductivity. Such determinations are conveniently accomplished by the double coil method.

---

* Note that this assumption corresponds to assuming that $\alpha = \pi/2$.

** It is readily verified that Equation 17 degenerates into the equation of a straight line when $\theta = 0$. For on setting $\theta = 0$ in Equation 17 one obtains

$$\frac{Y^2}{Y_0^2} + \frac{2XY}{X_0 Y_0} + \frac{X^2}{X_0^2} = 0$$

or

$$(X_0 Y + X Y_0)^2 = 0$$

and

$$X_0 Y + X Y_0 = 0$$

which is the equation of a straight line.

† A. B. Broughton Edge and T. H. Laby, *Geophysical Prospecting*, p. 278 (Cambr. Univ. Press. 1931).

Double Coil Method

The double coil phase measuring system employs a large horizontal loop for energizing the earth. The Bieler-Watson detecting method† consists essentially of two coils permanently fixed at right angles to each other and connected in opposition through an amplifier and telephones. The larger or vertical coil is wound with a fixed number of turns of fine wire and is connected in parallel with a condenser of suitable value for tuning the coil to the frequency of the alternator. The smaller or horizontal coil is tuned by the same condenser and is connected to a compound multipoint switch in such manner that its number of turns may be varied. The amplifier and headphones are connected in series with one of the coils.

To determine the resultant or total magnetic field at any station, the larger coil is mounted in an approximately vertical plane and oriented in the desired direction. The apparatus is then rocked backwards and forwards slowly and the number of turns in the horizontal coil is varied by

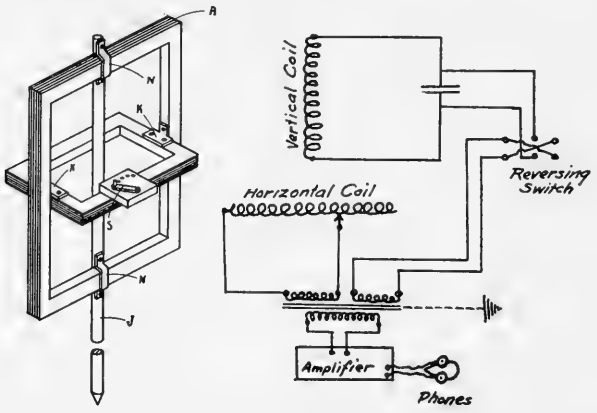

FIG. 384.—Double coil method for determining components of the elliptical electromagnetic field.

the multipoint switch until the null point or minimum signal is obtained when the double frame is vertical. The number of turns in the horizontal coil necessary to obtain this balance is noted.

If the axes of the coils are parallel to the axes of the ellipse, only one such reading is necessary, as will be evident from the following considerations:

Consider for simplicity that the horizontal coil is perpendicular to the major axis of the ellipse and the vertical coil is perpendicular to its minor axis. The induced E.M.F. of the horizontal coil (Figure 384) is altered by varying the number of turns until it balances the induced E.M.F. in

† E. S. Bieler and H. G. Watson, "Apparatus for Use in Discovering Ore Bodies," U. S. Patent 1,794,666, issued Dec. 12, 1927.

the tuned vertical coil. (A reversing switch is provided for obtaining the opposed phase relationship.) The number of turns in the horizontal coil is a measure of the field threading the vertical coil. Thus, when the plane of the ellipse is parallel to that of the vertical coil, the number of turns in the secondary coil is proportional to the ratio of the minor to the major axis of the ellipse.

In practice, two separate readings are taken at each station, instead of spending the necessary time required in determining the plane of the ellipse. That is, after a balance has been obtained for one orientation, the apparatus is rotated through 90° about the vertical axis and another balance reading is made. The two readings (number of turns) are then compounded vectorially to obtain a resultant whose magnitude is proportional to the ratio of the minor to the major axis of the ellipse.

Electrical Characteristics of Apparatus.—The amplifier and coupling transformer should be well shielded electromagnetically and electrostatically. Undesirable coupling between circuits can be minimized most successfully by feeding the output of the horizontal and the vertical coils into separate peak-tuned input windings of the transformer. These windings are connected so their fluxes oppose and, when balanced, give zero induced potential in the secondary coil. An electrostatic shield should be provided between the two primary windings and the secondary winding.

The alternator supplying power for energizing the loop should be of good design to produce as pure a sine wave as possible in order to minimize harmonics. Also, an input filter should be provided in the amplifier to remove harmonics, because in circuits of this type proper null point balance can not be obtained unless the higher harmonics are well suppressed.

Field Procedure.—The initial step in the survey is the layout of the large horizontal loop for energizing the area under investigation. The loop should extend well beyond the limits of the area in order to minimize the effects of a non-uniform field near the loop itself. If terrain conditions permit, a square or rectangular loop is usually the most desirable. Inside the loop, a regular gridwork or pattern of observation points where the readings are to be made is surveyed. If a square loop is used, the observation points are preferably laid out by intersecting lines parallel to the sides of the loop. These points of observation are to be plotted on the map.

If the energizing loop is laid in flat country, the magnetic field within the loop (primary field) is substantially vertical at all of the observation points, provided these are not too close to the cable. The magnetic field due to induced currents, however, will usually have a horizontal component at the surface. Hence, the resultant magnetic field at the surface is usually elliptically polarized, and the ratio of the major to the minor axis at a series of stations will give a measure of the magnitude, direction, and relative phase of the secondary field. For example, if measurements are taken near a large conducting body, a large out-of-phase secondary field will occur and this will give rise to a relatively large minor axis in the representative ellipse.† On the other hand, if the secondary field is zero or if it lags or leads the primary field by 180°, the minor axis of the ellipse vanishes.

Double Coil Method for Measuring Phase and Amplitude

Hedstrom‡ has developed the apparatus shown in Figure 385. The apparatus comprises two coils, each having approximately 1200 turns on a

† A. B. Broughton Edge and T. H. Laby, *loc. cit.*, p. 60,

‡ H. Hedstrom, "Phase Measurements in Electrical Prospecting," *A.I.M.E. Geophysical Prospecting*, Tech. Pub. 827, 1937,

circular 3-foot frame, connected to an alternating current bridge curcuit. A three-stage amplifier and headphones are used for null determinations. The phase relationship between the fields affecting the two coils may be

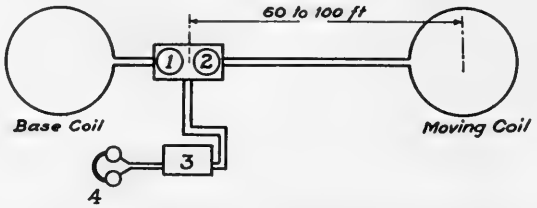

FIG. 385.—Turam method for mapping lines of equipotential, phase and amplitude. 1, amplitude control; 2, phase control; 3, audio-frequency amplifier; 4, headphones. (Hedstrom, *A.I.M.E. Geophysical Prospecting*, Tech. Pub. 827.)

determined by changing the inductance or capacity in one leg of the bridge, while the ratio of field strengths may be determined by use of the conventional potentiometer method.

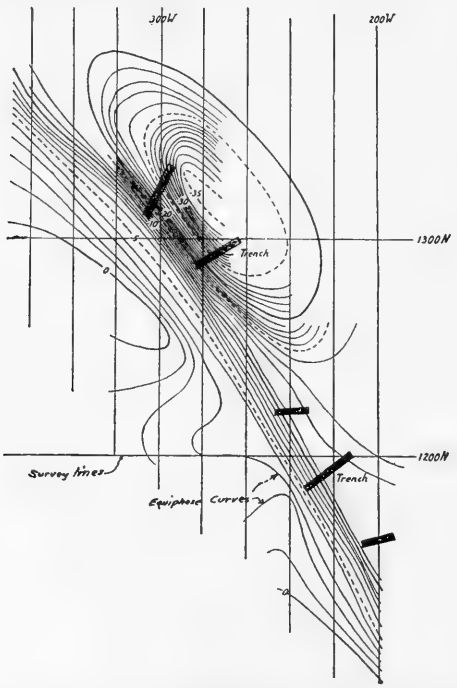

FIG. 386.—Equiphase curves in electromagnetic field over ore body. (Hedstrom, *A.I.M.E. Geophysical Prospecting*, Tech. Pub. 827.)

Interpretation is based upon phase differences and ratio of field strengths. The results usually are plotted as contours comprising equi-phase curves or equi-field-strength curves. (Figure 386.)

METHODS WHEREIN THE EFFECTS OF THE PRIMARY FIELD ARE MINIMIZED

There are many methods by which the field from the surface energizing system may be minimized at the detecting coil. Theoretically, this can be accomplished with a conductive energizing system utilizing two grounded electrodes. For this work, a direction-finding coil is used, and its axis of rotation is on the extension of the imaginary line connecting the two current or energizing electrodes. When in this position very little of the primary field from the surface wire is picked up by the coil. On the other hand, the position of the coil allows it to pick up the secondary field from the subsurface conductive zone.

The terminals of the detector coil are connected to a detector and a two stage audio-frequency amplifier for the higher frequencies, or a three stage amplifier for the lower frequencies. The out-put of the amplifier is connected to a vacuum tube voltmeter. By keeping the amplification constant relatively simple field work will often show the presence of a shallow conductor. Under such conditions, it will be found that the maximum signal

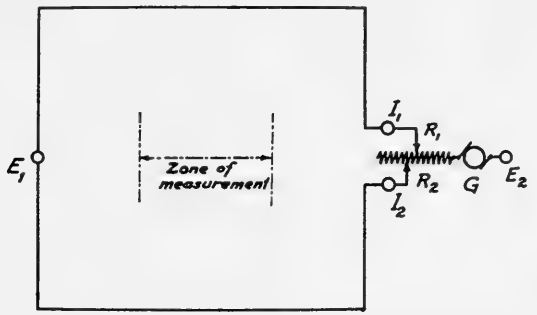

FIG. 387.—Conductive method of energizing the subsurface. E_1 and E_2, electrodes; R_1 and R_2, resistors for controlling current; G, generator; I_1 and I_2, line ammeters.

will be obtained when the detecting coil is held in a vertical position, and is located vertically over the subsurface conductor. The method, however, is not generally recommended due to the difficulties encountered by phase-shift, and the unknown distribution of the primary current between electrodes.

Another method,† applicable to the higher frequencies only and hence of limited use, consists in setting up a primary high frequency electromagnetic field polarized about a linear axis. The direction of the secondary field produced by the induced current in a conductive body is determined at points on the linear axis. The direction-finding apparatus is similar to that described and shown in Figure 376. The energizing apparatus may be of the simple Hartley oscillator type. The method works fairly well at depths not exceeding 25 to 150 feet in dry desert countries where long vein conductors are encountered.

† J. J. Jakosky, "Method and Apparatus for Locating Conductive Bodies," U. S. Patent 1,792,910, issued Feb. 17, 1931.

In another modification of this method, the surface wires are laid out as a divided conductor in the form of a rectangle or square as shown in Figure 387. If measurements are to be made along a line midway between the wires, the rheostats R_1 and R_2 are adjusted to give equal current flow in the two branches of the current. The primary fields from the two surface wires effectively neutralize each other, and the vector direction and magnitude measured by the detecting coil are chiefly due to the secondary field set up by the current flowing in the subsurface. Obviously, a disadvantage of the method is the necessity of laying the two surface lines. For general reconnaissance work only one line or "U" may be laid, although interpretation of the vector data is more difficult. This same divided conductor system for energizing the ground has also been employed successfully when magnetometric methods of measurement are used for measuring the magnetic field associated with the flow of direct current.

METHODS EMPLOYING A VERTICAL COIL ENERGIZING SYSTEM

The most widely employed electromagnetic equipment utilizes a vertical coil for energizing the ground. The vertical coil is especially suitable for energizing conductive zones which are vertical or which have a steep dip, such as veins, etc. This type of equipment permits more rapid field work than the large horizontal loop type. Also, the results may be interpreted more conveniently. The vertical type coils are usually energized with medium to high frequency alternating current because of their relatively small size.

Energizing Equipment.—A vertical type energizing system of the "high frequency" type is shown in Figure 388. This system operates at frequencies from 30 kc. (30,000 cycles per second) to 50 kc. The cross pieces for supporting the coil are each 10 feet in length, and when set up, the coil dimensions are approximately 7 feet by 7 feet. The coil is mounted on a tripod so that it may be leveled and oriented easily. Bakelite, or other insulating supports, must be provided for holding the turns of the coil in place. (The number of turns depends on the spacing and frequency.) Formulas for proper design of this coil will be found in text books on radio and high frequency phenomena. †

The vacuum tube circuit and the batteries for both plate and filament supply are contained in a hard oak case. Shoulder straps and carrying handles are provided for convenient handling of the outfit. To provide the 450 volt plate supply, ten "B" batteries, of medium-duty type (45 volts each) are connected in series. No. 6 dry cell batteries are connected in series to provide the filament supply.

† J. H. Morecroft, *Principles of Radio Communication* (John Wiley and Sons).
F. E. Terman, "Radio Engineering" (McGraw-Hill).

Power may also be obtained from a specially designed 500-cycle 75-watt hand-cranked alternator, an interior view of which is shown in Figure 389. Two handles are provided for cranking. These are connected to a gear driving the alternator. The alternator turns over at a speed of 4000 r.p.m., and the cranks rotate at a speed of approximately 100

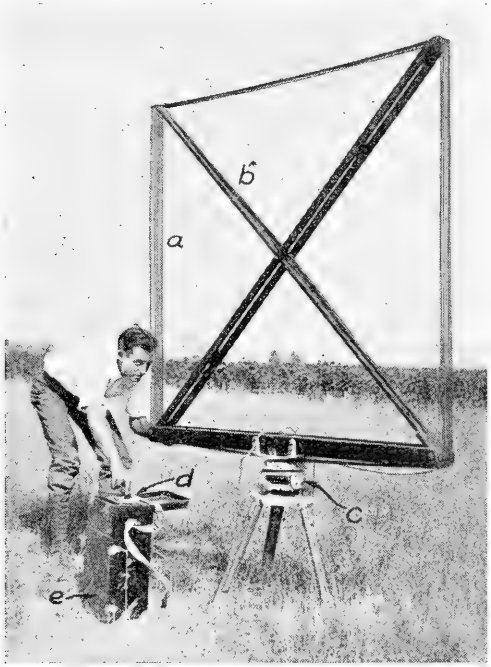

FIG. 388.—High frequency energizing system in operation: *a*, high frequency coil; *b*, folding coil support; *c*, tripod head allows rotation about vertical axis; *d*, high frequency oscillator; *e*, battery compartment.

r.p.m. Ball bearings which are provided throughout facilitate the cranking required to generate the necessary power. Approximately 50 watts input is required for operation of the high frequency apparatus. Direct current for the field of the alternator is supplied from three No. 6 dry cells. The entire apparatus is contained in a steel waterproof case.

Figure 390 gives the wiring diagram for the oscillator when using alternating current for supplying power. The output of the two tubes shown is practically the same as would be obtained from one tube when direct current is employed for plate supply.

Medium Frequency System

Power for exciting the coil may be obtained from a suitable medium frequency (100-500 cycles) alternator or from a conventional vacuum tube oscillator. A rotating type alternator or a thyratron inverter tube† may also be used.

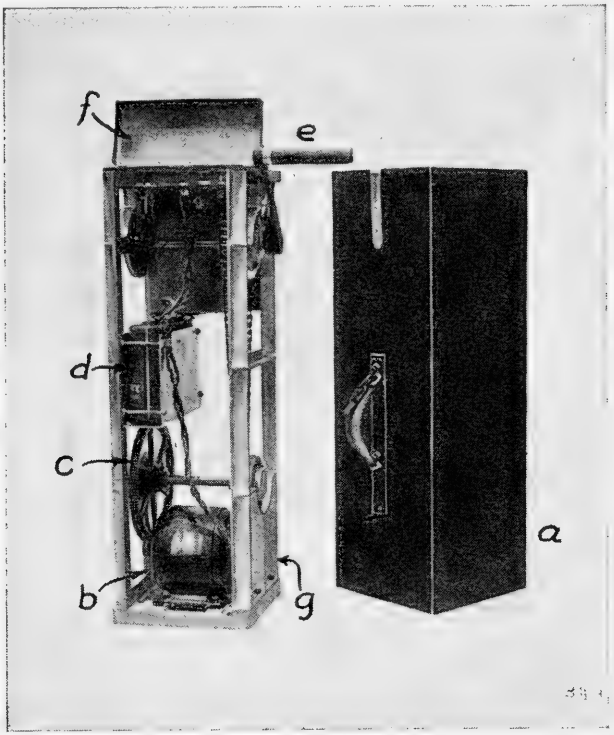

FIG. 389.—Alternator and its waterproof case. *a*, waterproof case; *b*, 500-cycle alternator; *c*, driving gear; *d*, dry cells for field of alternator; *e*, crank; *f*, waterproof lid covering control panel; *g*, cast aluminum frame.

For lower frequencies, that is, under about 25 cycles per second, it is not practical to use either vacuum tube oscillators or rotating alternators for the generation of a usable amount of power with portable equipment. This is because of the large weight and bulk of the equipment necessary to handle these low frequencies, due chiefly to the large amount of iron required in the magnetic circuits. Where these extreme low frequencies are desired, it is necessary to use a suitable commutator for inverting a direct current supply. This type of equipment has been described earlier.

Figure 391 shows a medium frequency energizing coil consisting of 50

† K. Henney, *Electron Tubes in Industry* (McGraw-Hill); also *Industrial Electronics Reference Book* (John Wiley and Sons Co.), 1948.

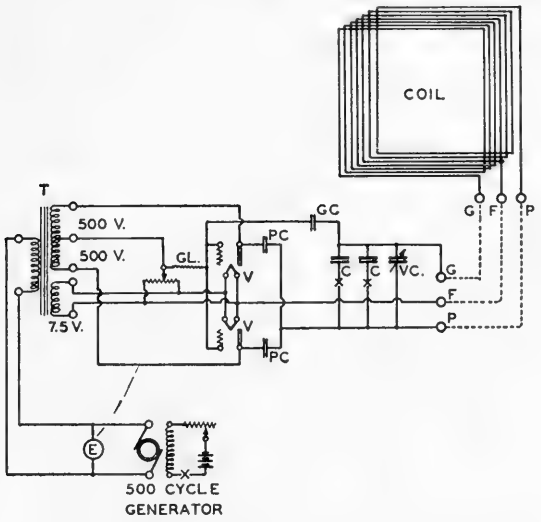

FIG. 390.—Wiring diagram for high frequency inductive equipment using 500-cycle generator for filament and plate supply. *C*, fixed condensers; *VC*, variable condensers; *T*, input transformer; *E*, voltmeter.

FIG. 391.—Vertical energizing coil in position. *a*, medium frequency energizing coil; *b*, impedance matching transformer with tuning condensers; *c*, hand-cranked alternator.

turns of rubber-insulated stranded wire bound together into a single cable to facilitate handling. The flag seen in the illustration is placed at the electrical center of the coil and is used for proper alignment of the direction-finding coils. The energizing coil should be oriented substantially parallel to the strike of the vein system. Any convenient means may be employed for supporting the cable during operation. In the work illustrated, two 15-foot 3-inch x 2-inch hardwood supports were employed, properly guyed at each end. The coil had dimensions of approximately 15 feet by 45 feet. An alternator of the type shown in Figure 389 may be used for exciting the coil where work is done at shallow depths. For deeper work, it is preferable to employ a gasoline engine-driven alternator of at least 1000 watts output.

Field Operations for Vertical Energizing Coil Method.—If the area under investigation is homogeneous, the electromagnetic field produced at the surface by the vertical coil will be polarized in a substantially horizontal direction, provided the other fields acting at the surface are negligible relative to that of the energizing coil.†. Hence, when a direction-finding coil is placed in such a position that its axis of rotation lies in the plane of the energizing coil, the minimum signal will be obtained when the two coils are at right angles to each other, i.e., when the direction-finding coil is horizontal and the energizing coil is vertical. On the other hand, a maximum signal will be obtained when the direction-finding coil is in the same plane as the energizing coil.

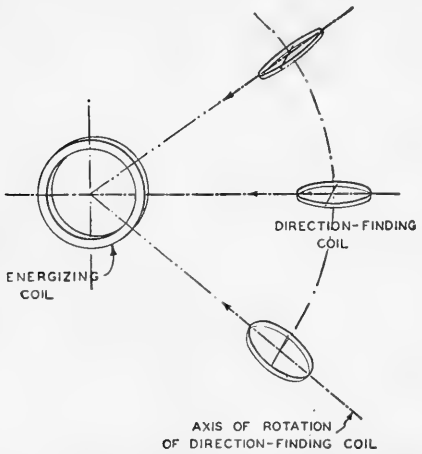

FIG. 392.—Sketch illustrating possible relative orientations of direction-finding coil and energizing coil for minimum signal. (*A.I.M.E. Geophysical Prospecting,* Technical Paper 134.)

Referring to Figure 392, it will be noticed that the axis of rotation for the direction-finding coil is horizontal *only* when the direction-finding coil is at the same elevation as the energizing coil. Initial setting up of the inductive energizing and direction-finding equipment therefore involves two operations: (1) proper alignment of the energizing coil so that its plane is always vertical and passes through the axis of rotation of the receiving coil, and (2) alignment of the direction-finding coil so that its axis of rotation passes through the center of the energizing coil. To allow this second step to be done accurately and quickly, alignment sights and a ball-socket joint are provided on the head of the direction-finding coil, as described previously.

† J. J. Jakosky, "Method and Apparatus for Locating Unknown Conductive Bodies," U. S. Patent 1,811,547, issued June 23, 1931.

When the equipment has been set up with the energizing coil vertical and "pointing toward" the direction-finding coil, the operator of the direction-finding coil knows that if he obtains any angle or dip other than zero (measuring from the vertical) and a strike not pointing toward the energizing coil, some disturbing influence is present. This disturbing influence may be another field caused by induced current flowing in an underground conductive mass.

Orientation of Search Coil Under Influence of Primary and Secondary Fields

If the direction-finding coil is cut by two electromagnetic fields which are in phase and of the same frequency, the position of the coil for maximum or minimum signal strength will be determined by a single resultant of the two fields. For example, if one field is horizontal and the other field is tilted so that it makes an angle of 60° with the horizontal, the direction-finding coil, under proper conditions, "points" somewhere between these two vectors, the exact direction depending on the relative strengths of the two fields and their phase relationship. If the fields were of equal strength, and in phase, the resultant vector would lie equidistant between them.

The elementary conditions prevailing in actual operation are illustrated in Figure 393 which is a plan view of a conductor of considerable length and small diameter placed so as to be in the field of the energizing coil. The direction-finding coil now has two fields linking it.

At position *C* (lower right-hand part of the figure) the component fields would exert the following effects. Since the energizing coil is vertical, the primary magnetic field will tend to cause the direction-finding coil to give the loudest signal when it, too, is vertical. However, for proper in phase conditions, the field surrounding the subsurface conductor will tend to produce the loudest signal when in the position shown by the resultant vector. If the direction-finding coil is moved to the position *F,* which is directly above the conductor, both the primary and the secondary fields will induce the loudest signal in the coil. As the coil is moved beyond the vertical position, the direction of the dip angle changes as shown by the vectors *G, H,* etc. Thus, it can be seen that as a traverse is taken across a conductor through which an induced current is flowing, a series of dips will be obtained on the direction-finding coil.

For purposes of illustration, assume that a series of readings is being taken on a circular traverse across the surface of the ground above the conductor, as shown in the plan view. As the distance from the conductor increases, the secondary field vectors are not sufficiently strong to give a noticeable deflection to the angle of the direction-finding coil. The resultant direction for all practical purposes is vertical, or a zero dip. As the direction-finding coil is moved along the traverse toward the conductor, the dip angle becomes increasingly larger until a maximum dip is reached,

after which it decreases until a zero dip angle is obtained when vertically over the conductor. As the readings are continued beyond a point over the conductor, the same condition results, except that the dips are in the opposite direction. This is illustrated by the arrows in the diagram marked "dips across conductor," and by the dip curve.

The illustration shows a circular traverse for the direction-finding coil. The distance between the two coils is constant; hence, the primary field has a constant intensity, and the change in the resultant angle is due only

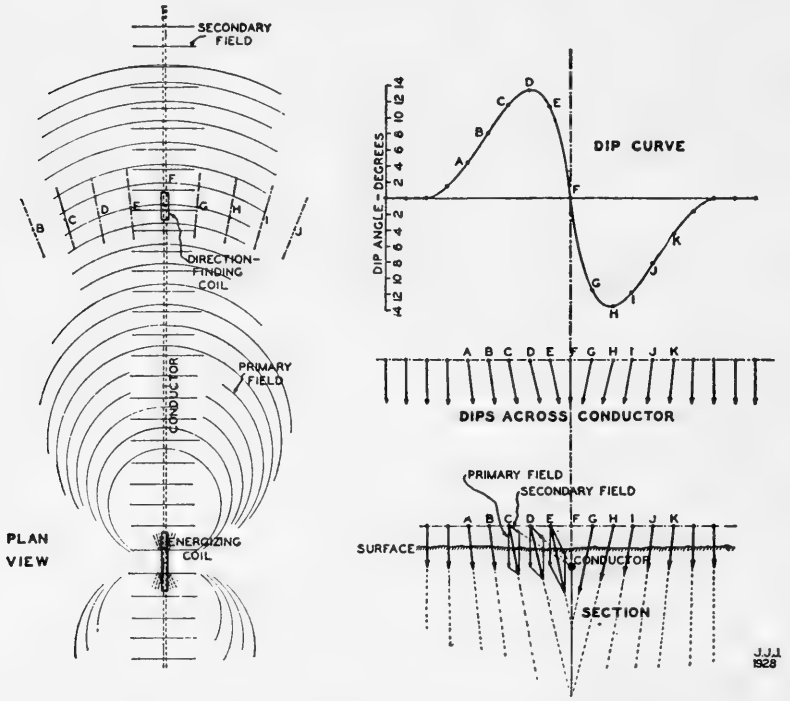

FIG. 393.—Plan view of a linear conductor situated in the magnetic field of the energizing coil. (*A.I.M.E. Geophysical Prospecting*, Tech. Paper 134.)

to variation in intensity of the secondary field and its change in emergence angle. In practice, however, the traverses are taken along straight lines perpendicular to the conductor. (The relatively great distance between energizing and direction-finding coils allows this to be done without any appreciable error.)

When working over a conductor of considerable length and uniform depth, the ratio of primary to secondary field varies with the distance between the direction-finding and the energizing apparatus. This is usually due to the smaller attenuation of the induced current when traveling along the conductor as compared to the attenuation of the primary field. As a result, the secondary field vector may be relatively large at considerable

distances from the energizer, while when very close to the energizer it may be completely masked by the strong primary field.

Since it is necessary that a certain minimum ratio exist between the field strengths of the primary and secondary fields in order that a readable dip angle may be obtained, it is evident that the deeper a conductive ore body lies, the longer must be its effective length for optimum operating conditions. After a given power input has been reached, increasing the power of the energizing system in order to impart more energy to the current induced in the conductor will not change conditions materially, inasmuch as the primary field is increased in proportion. At all times, however, enough power must be supplied to the earth to penetrate to the desired depth and induce currents of such magnitude that the magnetic fields of the induced currents travel through the overburden and reach the surface with sufficient intensity for producing a detectable effect on the direction-finding apparatus.

A high frequency energizer with an output of about 10 watts will be found to have an effective depth range of 25 to 50 feet in dry desert countries when working on favorable type conductors, i.e., a vein or other elongated conductive mineralized zone. If the 500-cycle apparatus is used, a good practical rule, in ordinary work where the mineralized zones are imbedded in damp areas or under water level, has been to employ power supply of at least three watts per foot of depth; i.e., when working to a depth of 100 feet, the energizing coil should supply a power output of at least 300 to 350 watts. It should be noted that due to the low power factor of the coil, a high volt-ampere product may be necessary to obtain this power output, unless proper means (such as a resonating condenser) are employed for power-factor correction.

Interpretation of Data.—Owing to the distortion of the primary field or improper alignment of energizing and receiving equipment, it often happens that a small (usually less than 10 degrees) "dip" or improper strike direction is obtained. These are called phantom dips or strikes and are readily recognized by the experienced operator. Such dips are frequently obtained when the energizing and direction-finding coils are located on a ridge, in a narrow valley or canyon, or at the edge of a deep cut or precipice. Usually the greater the distance between the energizing and the direction-finding coils, the greater is the wave-front distortion. The lower the frequency employed, however, the less becomes the distortion both of the primary and the secondary fields, and the distortion may usually be neglected at frequencies of 1000 cycles or less.

Because this topographic effect increases when higher frequencies are employed, the use of radio frequencies will yield "indications" over many ridges, or valleys, and all electrical inhomogeneities existing close to the surface; such "indications" are, of course, of little value in indicating the structural conditions at depth and they must be carefully evaluated by proper

planning of the field work. Shifting the position of the energizing coil will usually differentiate between topographic and subsurface conductor effects. Thus, in any area where "indications" are mapped, they should be checked by moving the energizer to a substantially different location and repeating the measurements. Although the high frequency methods are convenient and rapid for reconnaissance work, their "indications" must be checked by the low frequency or direct current methods having greater penetrating power, in order to differentiate between a surface effect and a subsurface conductive zone effect.

Strike Angle of Detector Coil

The azimuth angle or direction of the direction-finding coil when in a vertical plane is called the "strike" and represents the resultant direction of the fields cutting the direction-finding coil with reference to a horizontal plane or plan projection. The relative positions of the energizing

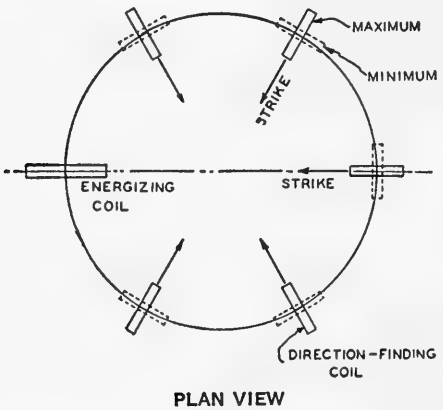

FIG. 394.—Relative positions of energizing and direction-finding coils for maximum and minimum signals. (*A.I.M.E. Geophysical Prospecting*, Tech. Pub. 134.)

coil and the direction-finding coil for maximum and minimum signals are shown in Figure 394. It will be noticed that the strike of the direction-finding coil is toward the energizing coil only when it lies in the plane of the energizing coil. When the direction-finding coil is not in the plane of the energizing coil, the directions for strike are as indicated. Thus, if the apparatus is mounted so as to "point" toward the direction-finding apparatus, the receiving operator knows that any strike other than toward the energizing equipment is caused by some distorting influence. This disturbing factor may be a distortion of the primary field wave front

or a secondary field created by an induced current flowing in an underground conductor.

Much information can be obtained by careful study of the dip and strike curves obtained in properly conducted field work. Because the conditions met with in field practice are varied and complex, care and experience are required in making final interpretations. Due to the greater distortion of the high frequencies, considerable caution must be employed in attempting to draw final conclusions from such work when not supported by supplemental data obtained from the application of other methods.

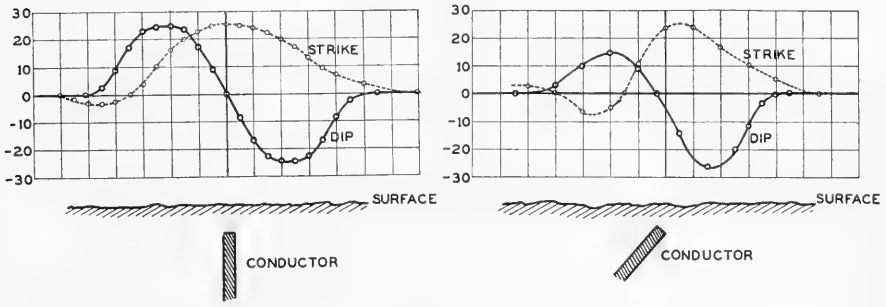

Fig. 395.—Dip and strike relationships over an experimental ore body.

Figure 395 shows the dip and strike relationships over an experimental ore body which consisted of a conductive sheet (copper-covered wood panel) buried in moist sand. The left-hand portion of the figure shows the symmetrical dip angles obtained when the conductor is vertical. Placing the conductor at an angle of approximately 40° from the vertical gives the unsymmetrical dip curve shown in the right-hand portion of the illustration. The strike curve reaches its maximum value in the general vicinity of the point where zero dip is obtained. The relationship between the position for maximum values of strike and minimum or zero dip angles is complicated because it depends on the direction of current flow in the conductor, the general distribution of current in the subsurface around the conductor, and the phase relationships between the current flow in the conductor and the primary field. However, because the dip curve passes through zero over the effective electrical axis of the conductor, it serves as a general means for determining the plan location of this axis. The general direction of dip of the conductor may also be predicted from the dip curve, because the smallest angle of dip will usually be obtained on the hanging-wall side. Various empirical methods have been developed for determining the depth of the effective conductive zone. †

† J. J. Jakosky, "Electrical Prospecting," *Proc. Institute of Radio Engineers,*" Vol. 16, No. 10, October 1928, pp. 1305-1355.

SURVEYS USING VERTICAL COIL ENERGIZING AND RADIO FREQUENCIES

A portion of a map of a typical electrical survey is illustrated in Figure 396, which shows data obtained in a survey conducted in Inyo County, California. The high frequency "indications" in the plan view are tied-in by the usual surveying methods to known property corners, bench marks, and other features to allow later location of the indication should the

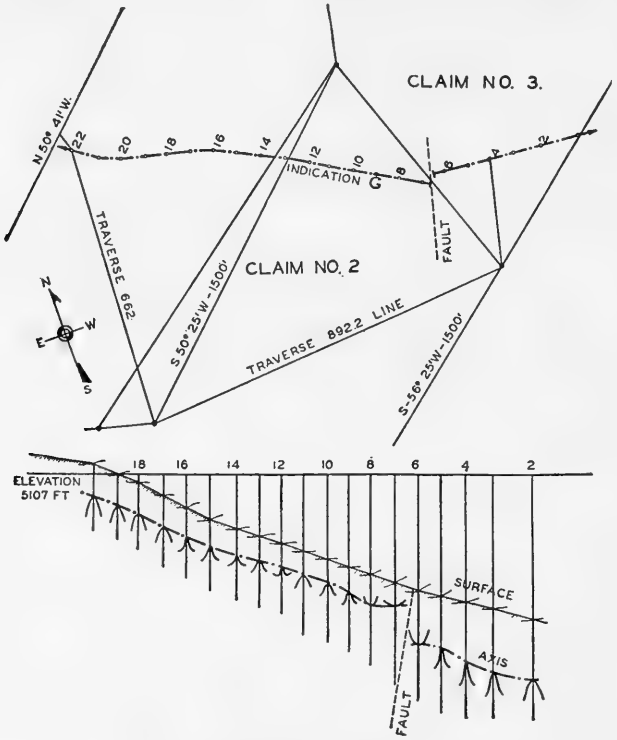

FIG. 396.—Geoelectrical map, Inyo County, California. (*I.R.E.*, Vol. 16, No. 10, Oct. 1928.)

electrical survey stakes be removed. The approximate depth of the conductor is obtained by plotting correction curves for traverses taken at intervals along the indication. † By drawing a curve through the indicated depths at each of these traverses, the indicated electrical axis of the conductor is located. The correction curves for each traverse are shown in the figure. The curves shown are drawn by imagining the traverses as being rotated 90 degrees to allow the curves to be plotted in the plane of the paper. The reversal of the index curves at the fault and the displacement of the conductor are very noticeable.

An interesting example of the continuity of a mineralized zone may be

† J. J. Jakosky, *loc. cit.*

seen in Figure 397. This indication was located during a high frequency electromagnetic survey of a property in Des Meloizes Township, Quebec, Canada. This indication was checked over a distance of 2000 feet between drill hole No. 1 and No. 8, and it is reported that the drill holes cut a wide zone of sulphide mineralization. The conductor is a dipping sheet

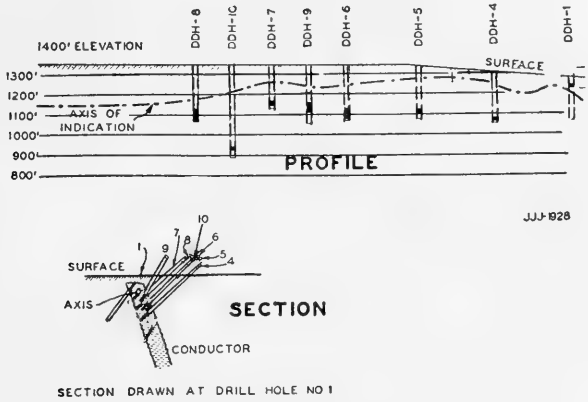

FIG. 397.—Drill results on a shallow high frequency indication. (*A.I.M.E. Geophysical Prospecting*, Tech. Pub. 134.)

vein. The "axis" of the conductive zone was determined by use of the correction curve. This axis lies close to the top of the conductor because of the poor penetrating power of the high frequencies and also because the near-surface flow of induced current has a much greater effect than that flowing in the lower portions.

ELECTRICAL METHODS

UNITED STATES PATENTS*

17,844	Frank S. Chapman. "Method of Detecting Presence and Approximate Location of Metallic Masses."
274,882	Issued Mar. 27, 1883. Fred H. Brown. "Apparatus for Detecting Mineral Ores."
277,087	Issued May 8, 1883. Cromwell F. Varley. "Electric Divining Rod."
293,518	Issued Feb. 12, 1884. Jerome Prince. "Means for Electrically Locating and Following Veins of Metal in the Earth."
308,908	Issued Dec. 9, 1884. August P. Lighthill. "Means for Electrically Locating Mineral Veins."
367,422	Issued Aug. 2, 1887. Lemuel Mellett. "Electrical Ore Detector."
367,541	Issued Aug. 2, 1887. Lemuel Mellett. "Electric Ore-Indicator."
380,842	Issued April 10, 1888. John R. Williamson and William W. Hickies. "Apparatus for Examining Ores."
412,924	Issued Oct. 15, 1889. Jesse F. Kester. "Electrical Metal Detector."
438,041	Issued Oct. 7, 1890. Robert L. Watkins. "Metal and Circuit Detector."
446,730	Issued Feb. 17, 1891. Fred Harvey Brown. "Induction Coil."
645,910	Issued Mar. 20, 1900. Fred Harvey Brown. "Process of Locating Metallic Minerals or Buried Treasures."

* In addition to those mentioned in text.

672,309 Issued Apr. 16, 1901. Fred Harvey Brown. "Process of Locating Metallic Minerals."
681,654 Issued Aug. 27, 1901. A. F. McClatchey. "Electric Prospecting Apparatus."
686,632 Issued Nov. 12, 1901. A. F. McClatchey. "Apparatus for Locating Minerals, Metals, Ores, Etc."
689,849 Issued Dec. 31, 1901. Fred Harvey Brown. "Apparatus for Detecting and Locating Metallic Ores, Minerals, Etc."
714,775 Issued Dec. 2, 1902. Fred Harvey Brown. "Electrical Process of Locating Running Water in the Earth."
727,077 Issued May 5, 1903. Fred Harvey Brown. "Apparatus for Locating Metals, Minerals, Buried Treasures, etc., without Digging."
736,411 Issued Aug. 18, 1903. George I. Leonard. "Method of Locating Minerals."
792,025 Issued June 13, 1905. John Hamilton, Jr. "Means for Protecting Electric Circuits."
817,736 Issued April 10, 1906. Leo Daft and Alfred Williams. "Apparatus for Detecting and Localizing Mineral Deposits."
840,018 Issued Jan. 1, 1907. Max Von Schultz. "Apparatus for Searching of Sunken Bodies."
841,188 Issued Jan. 15, 1907. Adolf Schmidt. "Device for Detecting Subterranean Waters."
1,045,572 Issued Nov. 26, 1912. Nils D. Levin. "Switch and Connecting Device for Electric Conductors."
1,045,575 Issued Nov. 26, 1912. Heinrich Lowy. "Method of Locating Subterranean Strata."
1,092,065 Issued Mar. 31, 1914. Heinrich Lowy. "Method for Ascertaining the Nature of Subterranean Strata."
1,126,027 Issued Jan. 26, 1915. Max Jullig. "Apparatus for Detecting Pipe-Leads or Other Metallic Masses Embedded in Masonry."
1,163,469 Issued Dec. 7, 1915. Conrad Schlumberger. "Location of Ores in the Subsoil."
1,212,763 Issued Jan. 16, 1917. Frank J. Gregory. "Device for Locating Concealed Conductors."
1,237,559 Issued Aug. 21, 1917. Shiro Sano. "Balancer."
1,241,197 Issued Sept. 25, 1917. Harry R. Conklin. "Method & Apparatus for Determining Subterraneous Conductors."
1,241,963 Issued Oct. 2, 1917. Edward H. Grove. "Electrical Means for Locating Concealed Pipes."
1,248,380 Issued Nov. 27, 1917. Rupert Nelson. "Method of and Apparatus for Detecting the Presence of Ore Deposits in the Earth."
1,287,251 Issued Dec. 10, 1918. William S. Darley. "Method for Locating Concealed Conductors."
1,297,929 Issued Mar. 18, 1919. John B. Taylor. "Differentially-Connected Exploring Coils."
1,325,554 Issued Dec. 23, 1919. Wendell L. Carlson and Earl C. Hanson. "Means for Locating Ore Bodies by Audio-Frequency Currents."
1,334,118 Issued Mar. 16, 1920. Chester W. Rice. "System for Amplification of Small Currents."
1,419,674 Issued June 13, 1922. Harry W. Hitchcock. "Electrical Measuring Apparatus."
1,461,492 Issued July 10, 1923. John F. Moody. "Electrical Testing Instrument."
1,465,352 Issued Aug. 21, 1923. George G. Dobson. "Electrical Testing System."
1,471,383 Issued Oct. 23, 1923. Alva B. Clark. "Method of and Means for Measuring Unbalance."
1,475,240 Issued Nov. 27, 1923. Harold S. Osborne. "Low-Frequency Measuring Device."
1,491,900 Issued April 29, 1924. Daniel G. Chilson. "Process of and Device for Locating Ore."
1,492,300 Issued Apr. 29, 1924. Heinrich Lowy. "Means for Electroaviatic Proof and Measuring of the Distance of Electric Conductive Bodies."
1,496,786 Issued June 10, 1924. William J. Shackelton. "Portable Impedance Bridge."
1,501,576 Issued July 15, 1924. Donald F. Whiting. "Electrical Testing System."
1,507,016 Issued Sept. 2, 1924. Lee de Forest. "Radiosignaling System."

1,507,017 Issued Sept. 2, 1924. Lee de Forest. "Wireless Telegraph and Telephone System."
1,526,391 Issued Feb. 17, 1925. Edward S. Stewart. "Testing Apparatus."
1,573,337 Issued Feb. 16, 1926. Harold J. Vennes. "Electrical Bridge."
1,537,360 Issued May 12, 1925. H. T. F. Lundberg and H. J. J. Nathorst. "Ore Detector."
1,545,672 Issued July 14, 1925. Charles D. McArthur. "Static Discharger for Automobile Trucks."
1,553,742 Issued Sept. 15, 1925. Oscar R. Blatter. "Storage Battery."
1,564,940 Issued Dec. 8, 1925. Frank Spencer Chapman. "Method of Detecting the Presence and Approximate Location of Metallic Masses."
1,569,325 Issued Jan. 12, 1926. August Leib. "Radio Direction Finder."
1,585,591 Issued May 18, 1926. Heinrich Lowy. "Means for Electric Proof of the Distance of Electrically Conductive Bodies."
1,596,942 Issued Aug. 24, 1926. Harry Nyquist and Harry A. Etheridge, Jr. "Measuring Transmission Phase Shift."
1,645,618 Issued Oct. 18, 1927. Harry Nyquist. "Method and Apparatus for Measuring Transmission Delay."
1,647,236 Issued Nov. 1, 1927. Maurice B. Long. "Electrical Testing System."
1,652,227 Issued Dec. 13, 1927. Theodor Zuschlag. "Method of Investigating the Nature of Subterranean Strata."
1,660,405 Issued Feb. 28, 1928. Herman A. Affel. "High-Frequency Measuring System."
1,660,774 Issued Feb. 28, 1928. M. Vos and K. Sundberg. "Method for Electrical Searching of Ore."
1,665,662 Issued Apr. 10, 1928. Cecil E. Godkin. "Electromagnetic Detecting Device."
1,669,400 Issued May 8, 1928. Charles E. Vawter. "Impedance Meter."
1,672,328 Issued June 5, 1928. William A. Loth. "Method of Electromagnetic Underground Prospecting."
1,673,249 Issued June 12, 1928. F. A. Kolster. "Loop Antenna."
1,676,779 Issued July 10, 1928. Shirl Herr. "Device for Underground Prospecting."
1,676,847 Issued July 10, 1928. Theodor Zuschlag. "Method and Apparatus for Exploring Subterranean Strata."
1,678,489 Issued July 24, 1928. Karl Sundberg. "Method and Device for Detecting and Locating Ores in an Electromagnetic Way."
1,679,095 Issued July 31, 1928. Greenleaf Whittier Pickard. "Closed Tuned Coil of Loop Aerial."
1,679,339 Issued July 31, 1928. Shirl Herr. "Hidden-Metal Detector."
1,684,397 Issued Sept. 18, 1928. Francis A. Hubbard. "Electrical Testing."
1,692,530 Issued Nov. 20, 1928. Theodor Zuschlag. "Method and Apparatus for Locating Ore Bodies."
1,692,849 Issued Nov. 27, 1928. Max Mason. "Method of Determining the Nature of Subsoil."
1,695,032 Issued Dec. 11, 1928. William J. Shackelton. "Impedance-Measuring Bridge."
1,705,561 Issued Mar. 19, 1929. Paul G. Edwards and Harold W. Herrington. "Electrical Testing System."
1,708,386 Issued Apr. 9, 1929. Norbert Gella. "Electrical Prospecting Device."
1,718,352 Issued June 25, 1929. Edward H. Guilford. "Method of Locating Underground Conductive Bodies."
1,718,497 Issued June 25, 1929. Byron W. St. Clair. "Telemetric System."
1,719,786 Issued July 2, 1929. Conrad Schlumberger. "Method for the Location of Oil-Bearing Formation."
1,724,794 Issued Aug. 13, 1929. W. W. Davis. "Method of Detecting Ore Deposits."
1,727,388 Issued Sept. 10, 1929. Herman A. Affel. "High-Frequency Measuring System."
1,732,311 Issued Oct. 22, 1929. Harry Nyquist. "Method and Apparatus for Testing Networks."
1,733,585 Issued Oct. 29, 1929. Joseph W. Dehn. "Method of Testing and Test Set."
1,743,386 Issued Jan. 14, 1930. Christian Paulson. "Electrical Testing Apparatus."
1,744,566 Issued Jan. 21, 1930. Everett V. Mott, Lewis H. Rovere and David H. Rowland. "Ground Resistance Test Set."

1,766,378 Issued June 24, 1930. Edward H. Guilford. "Method of Locating Unknown Conductive Bodies."
1,775,502 Issued Sept. 9, 1930. Manfred Schleicher, Dieter Albrecht, Wilhelm Gaarz and Georg Keinath. "Apparatus for Measuring Earth Resistances."
1,775,686 Issued Sept. 16, 1930. Joseph W. Milnor. "Measuring Resistance of Ground Connections."
1,791,933 Issued Feb. 10, 1931. Emil E. Mueser. "Electrical Prospecting."
1,792,910 Issued Feb. 17, 1931. John J. Jakosky. "Method and Apparatus for Locating Conductive Bodies."
1,794,666 Issued Mar. 3, 1931. E. S. Bieler & H. G. Watson. "Apparatus for Use in Discovering and Determining Ore Bodies."
1,797,545 Issued Mar. 24, 1931. William B. Churcher. "Vehicle Wheel."
1,803,405 Issued May 5, 1931. Norman H. Ricker. Electromagnetic Method of Underground Exploration."
1,805,900 Issued May 19, 1931. R. Ambronn. "Method of Exploring the Subsoil."
1,808,397 Issued June 2, 1931. L. C. Billotte, Revere & E. Lipson. "Method and Apparatus for Locating Deposits of Oil, Gas and other Dielectric Subterranean Bodies."
1,811,547 Issued June 23, 1931. John J. Jakosky. "Method and Apparatus for Locating Unknown Conductive Bodies."
1,812,392 Issued June 30, 1931. T. Zuschlag. "Method of and Apparatus for Locating Terrestrial Conducting Bodies."
1,813,845 Issued July 7, 1931. Oliver H. Gish. "Apparatus for the Study of the Earth's Crust."
1,816,958 Issued Aug. 4, 1931. Alva B. Clark & Fred H. Best. "Transmission Measuring System."
1,818,331 Issued Aug. 11, 1931. John J. Jakosky. "Method for Determining the Character of Ore Bodies."
1,820,953 Issued Sept. 1, 1931. K. Sundberg and E. D. Lindblom. "Method and Apparatus for Subsoil Investigating."
1,826,736 Issued Oct. 13, 1931. Alder F. Connery and Ronald S. Wisehart. "Alternating Current Balance Indicator."
1,832,969 Issued Nov. 24, 1931. Paul G. Edwards and Harold W. Herrington. "Testing System."
1,838,371 Issued Dec. 29, 1931. Ralph W. Deardorff. "Electromagnetic Wave Explorer."
1,839,732 Issued Jan. 5, 1932. C. H. Beal and C. E. Miller. "Process for Determining the Location of Substances having a Different Electrical Conductivity from Surrounding Media."
1,840,635 Issued Jan. 12, 1932. Henry C. Parker. "Electrical Measuring Instrument."
1,841,376 Issued Jan. 19, 1932. Charles R. Nichols and Samuel H. Williston. "Electrical Prospecting."
1,841,975 Issued Jan. 19, 1932. Charles R. Nichols and Samuel H. Williston. "Electrical Prospecting."
1,841,976 Issued Jan. 19, 1932. C. R. Nichols and S. H. Williston. "Electrical Prospecting."
1,841,977 Issued Jan. 19, 1932. C. R. Nichols and S. H. Williston. "Electrical Prospecting."
1,842,361 Issued Jan. 19, 1932. C. R. Nichols and S. H. Williston. "Electrical Prospecting."
1,842,362 Issued Jan. 19, 1932. C. R. Nichols and S. H. Williston. "Electrical Prospecting."
1,843,407 Issued Feb. 2, 1932. Karl Sundberg. "Underground Strata Prospecting."
1,847,127 Issued Mar. 1, 1932. Hans Mayer. "Electrical Testing System."
1,848,134 Issued Mar. 8, 1932. Kenneth B. Lambert. "Electrical Testing System."
1,859,005 Issued May 17, 1932. Norman H. Ricker. "Means and Method of Observing and Measuring Electromagnetic Fields."
1,861,052 Issued May 31, 1932. William Dubilier. "Variometer."
1,863,542 Issued June 14, 1932. Charles R. Nichols and Samuel H. Williston. "Electrical Prospecting."
1,864,024 Issued June 21, 1932. Heinrich Lowy. "Method of Exploring Ground."
1,876,324 Issued Sept. 6, 1932. Stephen W. Borden. "Ground Resistance Meter."

1,878,109 Issued Sept. 20, 1932. James D'Argaville Clark. "Means for Determining the Moisture Content and Quality of Materials."
1,882,113 Issued Oct. 11, 1932. Stephen W. Borden. "Earth Electrode Meter."
1,884,364 Issued Oct. 25, 1932. Karl Sundberg. "Method of Mapping Subsurface Structures."
1,884,419 Issued Oct. 25, 1932. Charles F. Wagner. "Means for Simulating Mutual Impedance."
1,884,496 Issued Oct. 25, 1932. Theodor Zuschlag. "Electrical Prospecting Apparatus."
1,887,915 Issued Nov. 15, 1932. Stephen W. Borden. "Earth Ohmmeter."
1,893,311 Issued Jan. 3, 1933. Thomas S. West. "Process of Locating Buried Pipe Lines, Etc."
1,897,688 Issued Feb. 14, 1933. Richard Ambronn. "Method of and Apparatus for Electric Earth Exploration."
1,902,265 Issued Mar. 21, 1933. Frank Rieber. "Electrical Prospecting System."
1,906,271 Issued May 2, 1933. John J. Jakosky. "Method and Apparatus for Determining Underground Structure."
1,910,021 Issued May 23, 1933. Buell B. Legg. "Soil Testing Apparatus."
1,910,820 Issued May 23, 1933. Glenn E. Blinn. "Detector for Hidden Metal."
1,910,418 Issued May 23, 1933. Theodor Zuschlag. "Determination of Electrical Characteristics of Electrical Conductors."
1,910,709 Issued May 23, 1933. Magne Mortenson. "Electrode for Geophysical Surveys."
1,912,036 Issued May 30, 1933. Erik H. Hedstrom and Theodor Zuschlag. "Method of Determining the Direction of Alternating Ground Fields."
1,917,417 Issued July 11, 1933. Theodor Zuschlag. "Method and Apparatus for Measuring Alternating Electromotive Forces and Impedances."
1,919,215 Issued July 25, 1933. Ross Gunn. "Thunderstorm or Electric Field and Potential Indicator."
1,919,538 Issued July 25, 1933. Guy A. Stone. "Process and Apparatus for Making Electrical Measurements."
1,926,212 Issued Sept. 12, 1933. C. R. Nichols and S. H. Williston. "Electrical Prospecting."
1,931,223 Issued Oct. 17, 1933. Thomas R. Harrison. "Potentiometer Instrument."
1,934,079 Issued Nov. 7, 1933. Hans T. F. Lundberg and Folke H. Kihlstedt. "Electrical Prospecting."
1,934,447 Issued Nov. 7, 1933. Norman H. Ricker. "Means and Method of Electrical Prospecting."
1,936,796 Issued Nov. 28, 1933. J. W. Legg. "Testing Device."
1,938,534 Issued Dec. 5, 1933. Leo J. Peters. "Method and Apparatus for Electrical Prospecting."
1,938,535 Issued Dec. 5, 1933. Leo J. Peters. "Method of and Apparatus for Electrical Prospecting."
1,940,340 Issued Dec. 19, 1933. Theodor Zuschlag. "Electrical Prospecting.
1,944,315 Issued Jan. 23, 1934. James K. Clapp. "Electric System and Method."
1,945,283 Issued Jan. 30, 1934. Harold S. Loomis. "Resilient Tire Construction for Track Circuit Shunting."
1,951,386 Issued Mar. 20, 1934. Theodor Zuschlag. "Electrical Prospecting."
1,951,716 Issued Mar. 20, 1934. Russel H. Varian. "Apparatus for Geophysical Exploration."
1,957,477 Issued May 8, 1934. L. Alan Sharp and James Fullman. "Detector."
1,960,027 Issued May 22, 1934. Norman H. Ricker. "Method of Electrical Prospecting."
1,960,028 Issued May 22, 1934. Norman H. Ricker. "Means of Electrical Prospecting."
1,964,141 Issued June 26, 1934. Harold A. Rhodes and Frank A. Cowan. "Impedance Measuring Circuits."
1,966,105 Issued July 10, 1934. Johann B. Ostermeier. "Method of and Apparatus for Searching for Ores."
1,971,310 Issued Aug. 21, 1934. Alfred W. Barber. "Measuring Reactance."
1,976,154 Issued Oct. 9, 1934. Herbert Walters. "Ground Contact for Vehicles."
1,978,440 Issued Oct. 30, 1934. Edgar R. Shepard. "Electrical Measuring Device."
1,997,163 Issued April 9, 1935. Theodor Zuschlag. "Electrical Prospecting."

1,997,164 Issued Apr. 9, 1935. Theodor Zuschlag. "Electrical Characteristics of Conductors."
2,012,479 Issued Aug. 27, 1935. G. U. Planta. "Device for Detecting Metals, etc."
2,034,447 Issued Mar. 17, 1936. Marcel Schlumberger. "Method for Electrically Prospecting the Undersoil."
2,035,943 Issued Mar. 31, 1936. Arthur Broughton Edge. "Determining the Nature of the Subsoil."
2,036,193 Issued Apr. 7, 1936. James Boyd and Burt E. Moritz, Jr. "Measuring Earth Resistance."
2,046,436 Issued July 7, 1936. George Wascheck. "Ground Impedance Measurement."
2,062,630 Issued Dec. 1, 1936. Theodor Zuschlag. "Method and Apparatus for Electrical Prospecting."
2,066,135 Issued Dec. 29, 1936. Randolph H., William M., and Mayer Barret. "Electrical Apparatus for Locating Bodies having Anomalous Electrical Admittances."
2,066,561 Issued Jan. 5, 1937. Gerhard R. Fisher. "Metalloscope."
2,077,707 Issued April 20, 1937. B. S. Melton. "Electromagnetic Prospecting."
2,094,116 Issued Sept. 28, 1937. A. E. Bowen. "Earth Resistivity Measurement."
2,104,440 Issued Jan. 4, 1938. L. W. Blau and L. Statham. "Method of Geophysical Prospecting by the Comparison of Steady State Potentials."
2,108,463 Issued Feb. 15, 1938. Theodor Zuschlag. "Apparatus for Electrical Prospecting."
2,113,749 Issued April 12, 1938. Louis Statham. "Method and Apparatus for Comparing Electrical Transients."
2,117,390 Issued May 17, 1938. Theodor Zuschlag. "Compensation of Alternating Current Fluctuations."
2,124,825 Issued July 26, 1938. Ludwig Machts and Bernard Rehder. "Process and Apparatus for the Indirect Determination of Earth and Air Electrical Conditions."
2,137,650 Issued Nov. 22, 1938. John J. Jakosky. "Apparatus for Electrical Exploration of Subsurface."
2,141,590 Issued Dec. 27, 1938. E. E. Blondeau. "Resistivity Meter."
2,147,643 Issued Feb. 21, 1939. Oscar E. Dudley. "System for Geological Explorations."
2,150,517 Issued Mar. 14, 1939. David S. Muzzey, Jr. "Electrical Exploration Method."
2,153,636 Issued Apr. 11, 1939. Atsushi Matsubara. "Method of Prospecting Underground Ore Bodies."
2,160,356 Issued May 30, 1939. Harry A. Fore and Albert K. Edgerton. "Geophysical Instrument."
2,160,824 Issued June 6, 1939. Ludwig W. Blau and Louis Statham. "Electrical Earth Transients in Geophysical Prospecting."
2,162,147 Issued June 13, 1939. Samuel S. West. "Means and Method of Electrical Prospecting."
2,165,214 Issued July 11, 1939. L. W. Blau and W. B. Lewis. "Geophysical Prospecting with Short Electromagnetic Waves."
2,167,950 Issued Aug. 1, 1939. John Jay Jakosky. "Method and Apparatus for Electrical Exploration of Subsurface."
2,172,271 Issued Sept. 5, 1939. Lawrence F. Athy and Harold R. Prescott. "Method of Electrical Prospecting."
2,172,688 Issued Sept. 12, 1939. W. M. Barret. "Electrical Apparatus and Method for Geologic Studies."
2,172,778 Issued Sept. 12, 1939. W. J. Taylor, Jr. "Method and Apparatus for Geological Exploration."
2,174,343 Issued Sept. 26, 1939. John Jay Jakosky. "Method and Apparatus for Electrical Exploration of Subsurface."
2,176,758 Issued Oct. 17, 1939. Stephan W. Borden. "Earth Resistance Meter."
2,176,760 Issued Oct. 17, 1939. Stephan W. Borden. "Electrode Bridge."
2,190,320 Issued Feb. 13, 1940. Gennady Potapenko. "Method of Determining the Presence of Oil."
2,190,321 Issued Feb. 13, 1940. Gennady Potapenko. "Method and Apparatus for Geophysical Prospecting."

2,190,322 Issued Feb. 13, 1940. Gennady Potapenko. "Method of Geophysical Prospecting.

2,190,323 Issued Feb. 13, 1940. Gennady Potapenko and D. Folland. "Method and Apparatus for Geophysical Prospecting."

2,190,324 Issued Feb. 13, 1940. Glen Peterson. "Method of Geophysical Prospecting."

2,200,096 Issued May 7, 1940. E. E. Rosaire and S. S. West. "Geophysical Exploration by Time-Variant Electric Currents."

2,201,256 Issued May 21, 1940. W. M. Barret. "Electrical Apparatus and Method for Locating Minerals."

2,202,369 Issued May 28, 1940. L. W. Blau and L. Statham. "Electrical Earth Transients in Geophysical Prospecting."

2,203,729 Issued June 11, 1940. J. J. Jakosky and P. B. Lyons. "Method and Apparatus for Use in Determining the Geologic Nature and Characteristics of a Formation Traversed by a Borehole."

2,204,436 Issued June 11, 1940. D. S. Muzzey, Jr. "Commutation System."

2,207,060 Issued July 9, 1940. J. J. Jakosky. "Method and Apparatus for Electrical Exploration of the Subsurface."

2,230,803 Issued Feb. 4, 1941. P. W. Klipsch, S. S. West, S. Bilinsky, and W. G. McLarry. "Wave Synthesizing Network."

2,231,013 Issued Feb. 11, 1941. P. W. Klipsch and S. S. West. "Electrical Prospecting with Alternating Current."

2,231,048 Issued Feb. 11, 1941. C. C. Beacham. "Process or Method of Geophysical Prospecting."

2,234,956 Issued Mar. 18, 1941. S. Bilinsky. "Exploration with Electrical Impulses."

2,241,623 Issued May 13, 1941. D. Silverman and P. F. Hawley. "Electrical Surveying."

2,249,328 Issued July 15, 1941. E. E. Rosaire. "Calibration Means."

2,250,703 Issued July 29, 1941. W. J. Crites and W. C. Rodgers. "Apparatus for Locating Casing Seats."

Re 21914 Issued Sept. 30, 1941. D. S. Muzzey, Jr., "Communication System."

2,270,325 Issued Jan. 20, 1942. N. W. Matthews. "Auxiliary Electrode for Ground Resistance Measurement."

2,274,903 Issued Mar. 3, 1942. S. Krasnow and J. M. S. Kaufman. "Electrical Prospecting Apparatus."

2,276,974 Issued Mar. 17, 1942. G. M. Howard. "Method of and Means for Determining the Velocity of Propagation of Waves through Subsurface Formations."

2,288,310 Issued June 30, 1942. T. Zuschlag. "Apparatus for Geoelectric and Seismic Investigations."

2,314,597 Issued Mar. 23, 1943. S. R. Phelan. "Methods of Making Geophysical Surveys."

2,314,874 Issued Mar. 30, 1943. H. M. Evjen. "Reversing Switch."

2,335,024 Issued Nov. 23, 1943. J. M. Pearson. "Method and Apparatus for Making Corrosion Studies."

2,337,352 Issued Dec. 21, 1943. C. B. Sitterson, Jr., and T. M. Berry. "Metal Detector."

2,337,962 Issued Dec. 28, 1943. J. F. Atkinson. "Method and Apparatus for Determining Resistance of Ground Connections."

2,342,627 Issued Feb. 29, 1944. K. H. Evjen and H. M. Evjen. "Apparatus for Making Geophysical Explorations."

2,342,628-2,342,629 Issued Feb. 29, 1944. H. M. Evjen and W. B. Lewis. "Coupling Circuit."

2,343,140 H. M. Evjen.

2,344,672 H. Blasier.

2,345,608 F. W. Lee.

2,351,201 R. Gillis.

2,354,535 G. Muffly.

2,362,372 Issued Nov. 7, 1944. E. S. Halfmann. "Apparatus for Measuring Alternating Current in the Conductors and/or in the Sheaths of Electric Cables."

2,375,022 Issued May 1, 1945. G. V. Morris and R. Adler. "Instrument for Testing Ground Resistance."

2,375,775-2,375,777, inc. Issued May 15, 1945. H. M. Evjen. "Electrical Prospecting System."

2,375,778 Issued May 15, 1945. H. M. Evjen. "Apparatus for Making Geophysical Explorations."
2,376,659 Issued May 22, 1945. H. Chireix. "Apparatus for Detecting Underground Objects."
2,378,440 Issued June 19, 1945. G. N. Scott. "Process and Means for Measuring Soil Resistivity and Certain Electrical Characteristics Associated with a Buried Pipe Line."
2,382,093 Issued Aug. 14, 1945. S. R. Phelan. "Method for Making Geophysical Surveys."
2,382,743 Issued Aug. 14, 1945. C. J. Penther and F. B. Rolfson. "Electromagnetic Apparatus for Pipe-Line Surveys."
2,383,855 Issued Aug. 28, 1945. C. W. Hansell. "Potential Ratio-Controlled Amplifier."
2,389,432 Issued Nov. 20, 1945. C. W. Hansell. "Communication System by Pulses Through the Earth."
2,393,717 Issued Jan. 29, 1946. D. M. Speaker. "Electronic Surgical Metal Body Locator."
2,407,363 Issued Sept. 10, 1946. W. H. Bussey. "Electrical Apparatus."
2,413,788 Issued Jan. 7, 1947. W. E. Sargeant and H. B. Hoeper. "Amplifier for Small Voltages."
2,417,609 Issued Mar. 18, 1947. D. S. Muzzey Jr. and R. D. Miller. "Electronic Commutator."
2,419,833 Issued April 27, 1947. H. E. Grimes. "Antenna Arrangement for Induction Communication System."
2,426,918 Issued Sept. 2, 1947. W. M. Barret. "Method for Electromagnetic-Wave Investigations of Earth Formations."
2,428,360 Issued Oct. 7, 1947. E. N. Dingley, Jr. "Electrical Guidance System for Surface Vessels."
2,437,134 Issued Mar. 2, 1948. A. L. Smith. "Electrode Assembly for Moisture Meters."
2,437,455 Issued Mar. 9, 1948. S. Berman. "Locator."
2,437,697 Issued Mar. 16, 1948. L. Kalom. "Electrical Probe."
2,440,693 Issued May 4, 1948. F. W. Lee. "Method for Determining the Subterranean Extension of Geologic Bodies."
2,442,805 Issued June 8, 1948. W. E. Gibson. "Metal Locator."
2,447,444 Issued Aug. 17, 1948. P. M. Waite. "Ground Stake."
2,449,313 Issued Sept. 14, 1948. A. H. Naef. "Ground Connecting Device."
2,454,911 Issued Nov. 30, 1948. D. H. Clewell. "Geological Exploration System."

CHAPTER VII

SEISMIC METHODS

The constant search for knowledge by those investigating the natural phenomenon of earthquakes led to the discovery of the fundamental principles which have been applied to the seismic method of geophysical exploration. Several large accidental explosions caused seismic waves to be initiated within the earth's crust. These were recorded by stationary seismographs set up for earthquake wave observations, and thus the first effects of artificial earth shocks were recognized by seismologists. From these early seismograms information was obtained on the velocity and the frequencies of seismic waves. These waves were of relatively shallow penetration into the earth's crust as compared with earthquake waves.

Earthquake-recording seismographs have been in use for approximately 100 years recording the natural tremors of the earth. However, most of the advancements in these earth studies have been made within the last forty years. And it was not until 1924 that seismic methods of geophysical prospecting became an acceptable tool of the exploration geologist. Improvements in both instrumentation and field technique followed rapidly from that date, though the fundamental principles of earthquake seismology remained the basis of the application of seismic methods to exploration. Only the details of instrument construction and operational technique have changed. Most of these changes were necessary because the frequencies of artificially initiated elastic waves within the outermost crust of the earth are many times greater than those of natural earthquake waves which penetrate to much greater depths and travel long distances.

The study of earthquake seismology has revealed much about the physical interior of our planet. Analyses of travel-times of earthquake waves have indicated that various concentric shells of materials of quite different elastic properties make up the interior of the earth. In a similar manner, analyses of the travel-times of artificially-produced shock waves observed for local and relatively shallow penetration of the earth's crust reveal the presence of materials of various elastic properties. This information, when studied together with the local geology, often leads to informative conclusions as to the subterranean distribution of geological formations characterized by the different elastic properties.

Relation Between Seismic Prospecting and Seismology

Seismology is that science which deals with natural earthquakes and related phenomena. This includes theories of causes of earthquakes, such

as elastic rebound; instrumentation to record the passing of earthquake waves; computation of the space paths of earthquake waves; depth of foci; locations of epicenters; nature of displacements of the various wave motions; study of earthquake wave amplitudes and frequencies of vibration; velocities of the various waves through certain portions of our planet; and study of earthquake damage. Even the possibility of predicting earthquakes probably belongs to this branch of science. If this subject falls under the scope of seismology, then precautions against earthquakes may also be closely related to seismology. However, it is now recognized by most seismologists that the element of time in prediction does not in itself afford protection against earthquakes. Since destructive earthquakes may occur at any time, the best protection lies in the building of structures sufficiently strong to withstand, with a considerable safety factor, the heaviest known shocks for any given area.

Briefly, the major cause of earthquakes is thought to be the disruptive adjustments produced by a sudden yielding to stresses built up within the earth's crust. These stresses may cause new fractures, faults, or sudden displacements along existing fault planes. Previous to the occurrence of an earthquake, slow movements of earth crustal blocks on opposite sides of a fault plane may cause elastic deformation within the rocks until such a point is reached that the strength of the rocks cannot withstand the strain any longer. At this point relief seems to occur either by rupture of the rocks or by sudden slippage adjustment along fault planes. In either case great energy is released in the form of an elastic disturbance which propagates outward in all directions from the focus of the earthquake.

Seismological stations are usually located in a network or pattern suitable for the study of the occurrence of earthquakes in a certain region under investigation. Several different types of earthquake waves are recorded on the seismograms. These waves are recognizable because each is characterized by a unique velocity, a different wave path, or a unique direction of vibration with respect to the direction of wave propagation. In the general analysis of the seismograms only the longitudinal and the transverse waves are considered. However, there are two types of waves which are often observed in the case of the more distant earthquakes. These have been named, after the investigators who first analyzed and described them, Love and Rayleigh waves. The Love wave is a unique type of transverse wave which vibrates in the boundary of a formation, while the Rayleigh wave is a combination of a longitudinal and transverse wave which vibrates in a plane perpendicular to the surface and parallel to the direction of propagation.

Theoretically several kinds of transverse waves may be demonstrated to exist in addition to those mentioned. These waves originate at geological or physical boundaries but are of minor interest to the seismologist because they are seldom recognized on the seismogram. Indications have been published showing that computed travel-time curves for once- and twice-

reflected earthquake waves fit certain observed events on seismograms. Reflected paths as computed from these data fit the conditions of the layered structure of the interior of the earth as determined from the refracted travel-time curves for earthquake waves.

The main events shown on an earthquake seismogram for a shock originating at a long distance are the onsets of the longitudinal refracted wave, the refracted transverse wave, and the surface waves. When the data from a sufficient number of stationary seismological stations are available, a travel-time curve may be constructed, using the known distances between the stations and the measured times of arrival. Analysis of such a curve makes possible inferences as to the path of the seismic wave within the earth's interior, depth of penetration and velocities of the waves along the paths.

Earthquakes may be classified according to depth of foci, i.e., deep and shallow focus earthquakes. They are also often classified as to distance, i.e., local and distant. Seismologists have learned much about the shallow focus type, but beyond the proof that deep focus earthquakes occur, little is known about the nature of their origin.

In seismic exploration, the artificial earthquakes are generated by various mechanical or explosive means. Some of the methods used to initiate a shock wave are: a heavy mechanical blow at the surface of the earth or at the bottom of a shallow hole; the explosion of a charge of dynamite buried at sufficient depth to obtain the desired propagation; or several charges exploded simultaneously in air above the ground.

For studies of the response of the ground or structures to continuous vibration at various frequencies, a mechanical method, utilizing a motor-driven shaking device whose operation depends on the rotation of a heavy eccentric mass around an axle, is sometimes employed.

Just one type of wave is utilized in applied seismology, as compared to the several wave motions employed in earthquake studies. Only the longitudinal wave is observed because of two factors. First, the distances involved are extremely short; therefore, the longitudinal and the transverse waves arrive so close together that they are recorded on the seismogram almost superimposed. The transverse wave onset is lost in the train of motion following the arrival of the longitudinal wave. Also, since only the vertical component of vibration is usually observed, the transverse components of the waves are greatly minimized.

Longitudinal waves traveling three different paths are observed from artificial shocks†: these paths are (1) surface longitudinal; (2) refracted longitudinal, and (3) reflected longitudinal. The only direct wave observed is probably recorded by the up-hole seismometer, which is placed at the surface very near the shot hole to measure the time necessary for the shock wave to travel directly from the point of detonation to the ground surface. The first onsets on the seismograms are for the most part refracted waves.

† C. Y. Fu, "Studies in Seismic Waves," *Geophysics*, Vol. XI, No. 1, Jan., 1946.

The reflected longitudinal waves are recognized as subsequent events on the seismograms.

As in earthquake seismology, two quantities are usually measured in applied seismology, i.e., time and distance. Amplitude and frequency characteristics are used in a qualitative manner in the correlation of events on various seismograms. In natural earthquake studies, the amplitude and frequencies are used to some extent in a quantitative manner as a means of recognition of various wave phases recorded. Velocities, depths of penetration, and space wave paths may be computed from the measured times and distances. The penetration, wave paths, and velocities depend upon the contrast in elastic properties of the adjacent geologic media through which the waves pass. In this manner, inferences may be made as to the distribution and attitude of subterranean geological units. These may be interpreted in terms of geological structure or the presence of specific masses distinguished from the surrounding media by the contrast of their elastic properties.

Seismology

Early instruments are illustrated in Figures 398 and 399. These illustrations show typical earthquake seismographs (instruments for detecting and recording the arrival of earthquake waves.)* Figure 398 shows a vertical seismograph which is critically damped by electromagnetic means and employs electrical recording. This seismograph, constructed by Galitzin in 1908, differs only in arrangement and size of parts from the typical seismograph employed in exploration at present.**

Most modern seismographs are designed to record the seismogram on a moving strip of photographic paper. Oscillatory currents are generated by the relative motion between the seismometer frame and the inertia reactor. Figures 400, 401, 402, and 403 are illustrations of modern stationary earthquake-recording seismograph equipment. This equipment represents an improvement in both mechanical stability and fidelity in recording the actual motion of the ground as compared with earlier models. An illustration of the push-pull principle of the variable reluctance transducer as used in these modern instruments is given by Figure 404. The amplitude of the trace on the photographic record is ordinarily about 200 times greater than

* Descriptions of seismological instruments and records commonly contain the following technical terms: seismometer, seismograph, and seismogram. A *seismometer* is a device for measuring vibrations due to earthquakes. A *seismograph* is a seismometer equipped with an indicator (mechanical, optical, or electrical) for recording a quantity which depends on the vibration or relative motion of the instrument. The quantity recorded is usually a function of the displacement, velocity, or acceleration. A *seismogram* is the record, for example photographic record, made by a seismograph.

** A detailed description of the principal types of seismographs employed in seismological observatories is given in "Selection, Installation, and Operation of Seismographs" by H. E. McComb, U. S. Department of Commerce, *Special Pub. No. 206.*

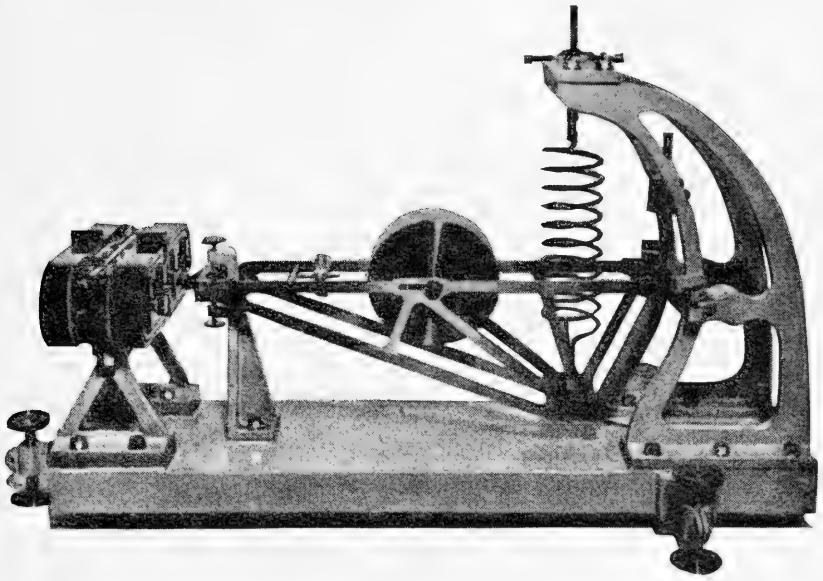

FIG. 398.—Critically damped vertical seismograph employing electrical recording. (Reproduced from Galitzin's *Seismometrie.*)

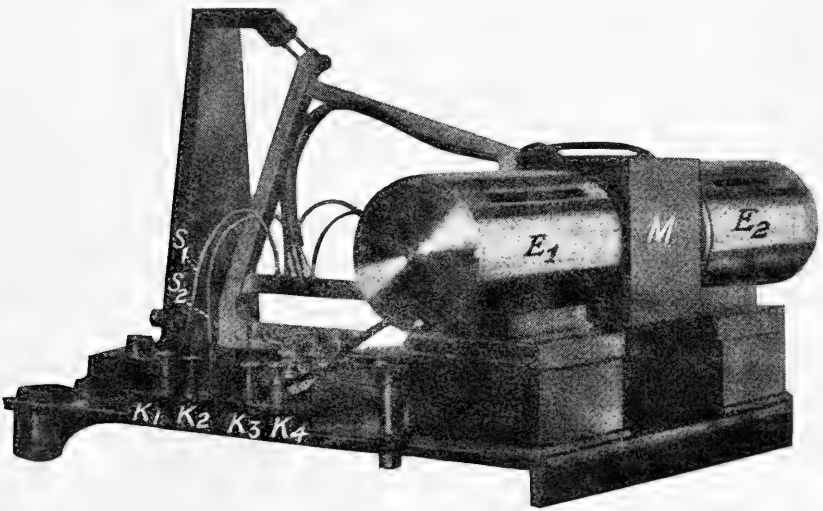

FIG. 399.—L. Grumach's seismometer. (Inductive type.) M = mass to which two coils are attached. (The coils vibrate freely in the field of the electromagnets E_1 and E_2, their axes being parallel to the direction of vibration.) S_1 and S_2 are silver strips, 0.02 mm. thick, which connect the binding posts K_1 and K_2 with the lead to the coils. K_3 and K_4 are the binding posts for the lead to the fixed electromagnet E_1. (Reproduced from Gutenberg's *Grundlagen der Erdbebenkunde*, Vol. 12, 1927. Published by Gebrüder Borntraeger, Berlin.)

the corresponding amplitude of the earth's motion. In some installations, where electrical amplification is employed, the magnification may be as great as 100,000 times.

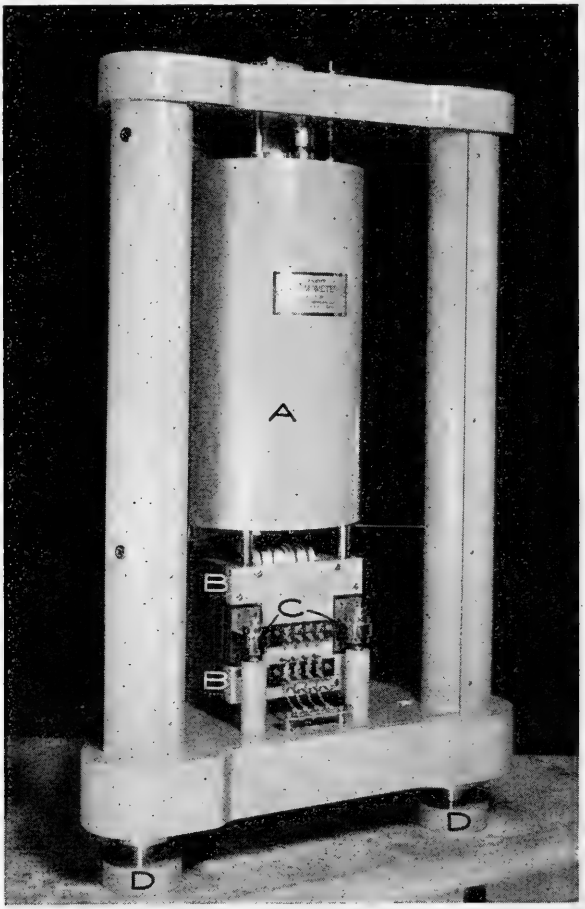

FIG. 400.—Vertical component variable reluctance electromagnetic seismometer. A, inertia mass containing spring suspension; B, transducer; C, adjusting nuts; D, leveling screw. (Courtesy of Hugo Benioff, California Institute of Technology.)

Figure 405 is a schematic representation of an earthquake record or seismogram. Some of the more prominent waves or "phases," as they are usually called, have been designated on the records by the letters *P*, *S*, *L*, and *M*. The various types of waves, i.e., the various "phases," are propagated with different velocities, depending upon their mode of vibration and the character of the medium through which they travel.

In the primary or *P* waves, the vibrations of the earth particles are

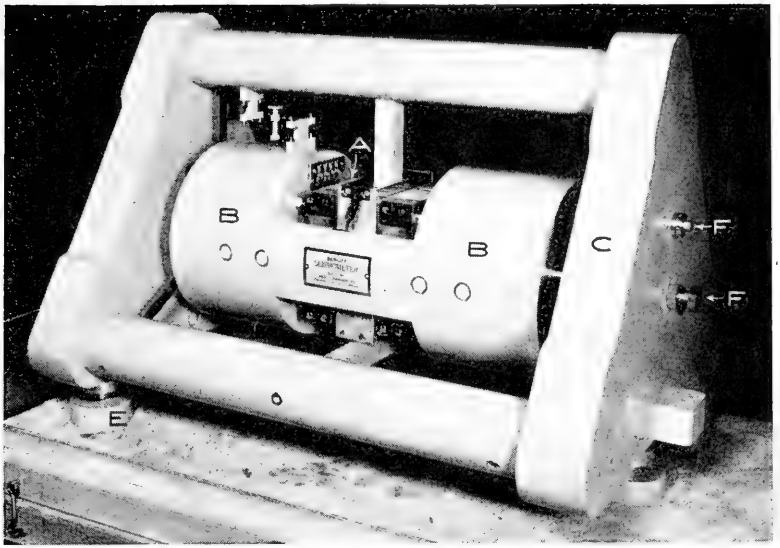

FIG. 401.—Horizontal component variable reluctance seismometer. A, transducer; B, inertia mass; C, frame; E, leveling screw; F, adjustments. (Courtesy of Hugo Benioff, California Institute of Technology.)

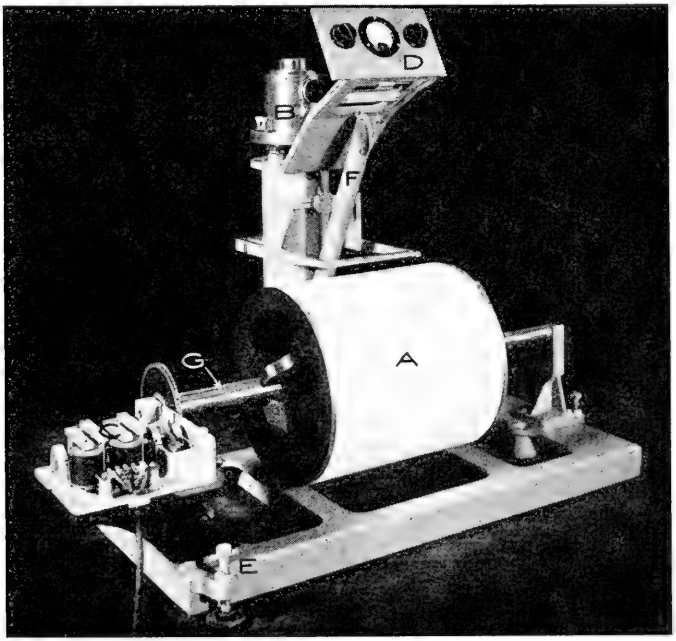

FIG. 402.—Short period galvanometer recorder. A, drum carrying photographic paper; B, short period galvanometer; C, synchronous motor drive; D, control panel; E, leveling screw; F, lamp housing; G, helical screw for transverse movement of drum. (Courtesy of Hugo Benioff, California Institute of Technology.)

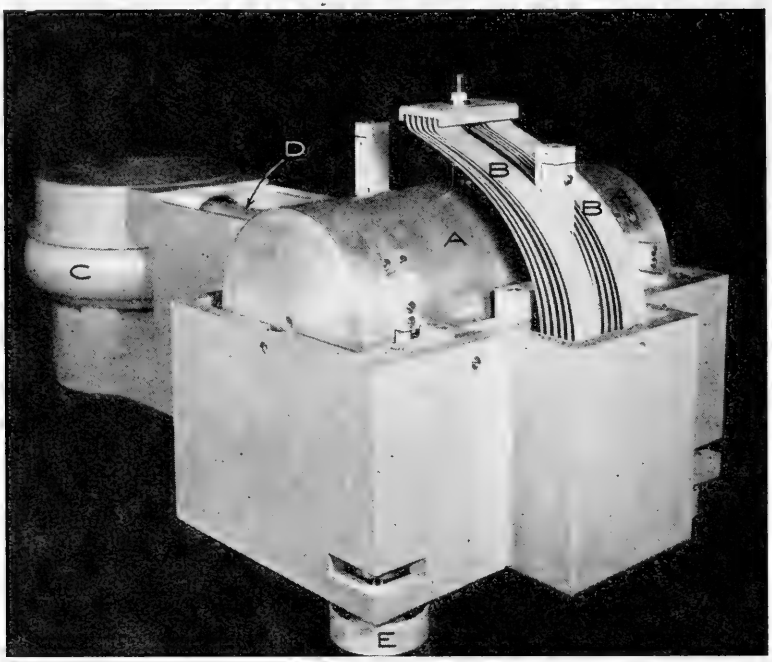

FIG. 403.—Vertical component moving conductor seismometer. Cover removed showing springs and inertia reactor. A, inertia mass; B, spring suspension; C, magnet; D, arm carrying conductor; E, leveling screw. (Courtesy of Hugo Benioff, California Institute of Technology.)

longitudinal, i.e., in the direction of propagation. In the secondary, or *S* waves, the vibrations are at right angles to the direction of propagation, and are termed transverse waves. Although the *P* and *S* waves traverse the same path, they arrive at a seismological station at different times, because the velocity of the longitudinal (*P*) wave is greater than that of the transverse (*S*) wave. The complex "surface" or *L* waves travel at a still slower speed; hence, in general, they arrive later than the *P* and *S* waves.

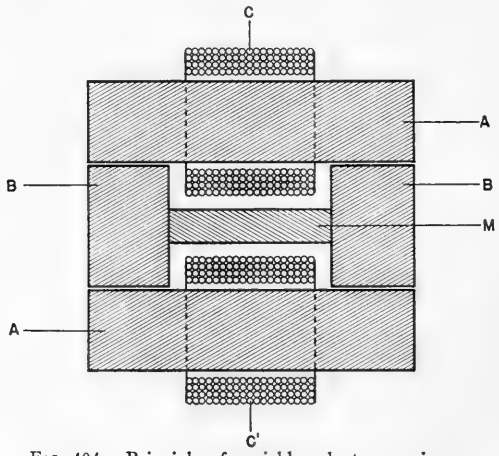

FIG. 404.—Principle of variable reluctance seismometer. A, armature carrying coils; B, pole pieces of magnet; M, permanent magnet; C and C', coils. (Courtesy of Hugo Benioff, California Institute of Technology.)

The earth is continually undergoing slight vibration as is seen in the extreme left-hand portion of Figure 405. The first sharp displacement of

this wave-like line, at *P*, represents the beginning of a larger disturbance or vibration. The amplitude of the disturbance is small and the period of oscillation is fairly short. Also, the motion is very irregular indicating that additional impulses arrive at irregular intervals. The record shows that a few minutes after this first motion, at the point marked *S*, there begins another type of motion. This motion has a somewhat larger amplitude and about the same period as, or a greater period than, the first disturbance. Following the initial large amplitude the motion becomes quite irregular indicating, as before, the arrival of additional impulses.

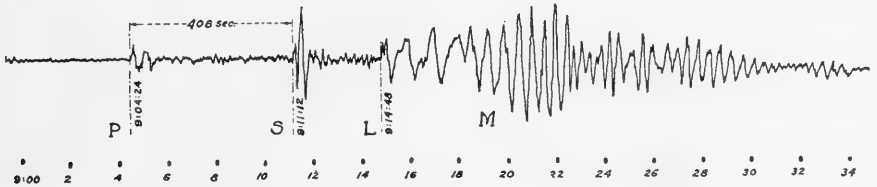

FIG. 405.—Schematic representation of an earthquake seismogram.

A short time later, at the point marked *L*, a different type of motion begins. The amplitude of this motion is relatively large and the period relatively long. This portion of the disturbance is followed by a complex vibration *M* of even greater amplitude and somewhat shorter period. These two parts of the motion are referred to as the principal portion. In the final portion, the amplitude is greatly decreased and the period is somewhat lengthened.

The maximum displacement of the ground usually amounts to a fraction of a millimeter during light shocks. In destructive earthquakes, however, the maximum acceleration often exceeds two hundred millimeters per second per second and has been known to exceed 10,000 millimeters per second per second.*

Figure 406 shows the travel-times for the *P*, *S*, and *L* waves for various distances.** The *S* wave travels faster than the *L* wave and the apparent speed increases with distance, due to penetration of the wave into zones of higher velocity. Likewise, the *P* wave travels faster than the *S* wave and its speed also increases with depth down to the core of the earth.

* It is of interest to contrast these displacements with the earth motion corresponding to a readily detectable reflection in the reflection shooting type of seismic prospecting. The amplitude of the motion at the seismometer due to the reflected wave may be a *few millionths* of a millimeter, while the acceleration may be a *few thousandths* of a millimeter per second per second. (Compare D. H. Gardner, "Measurement of Relative Ground Motion in Reflection Recording," *Geophysics*, vol. 3, No. 1, 1938, p. 40.)

** Essentially similar time-distance curves are obtained everywhere on the earth's surface. This fact attests to the uniformity of the earth's structure.

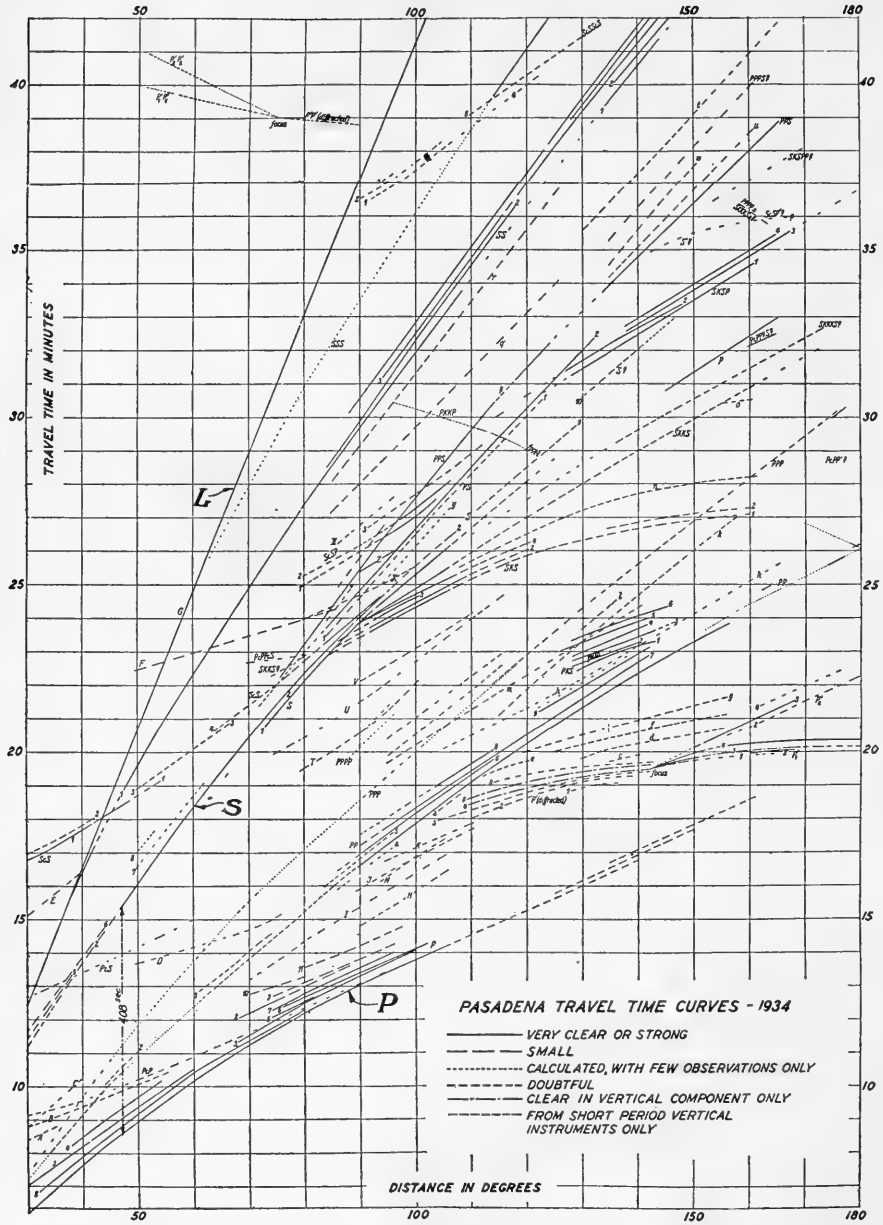

FIG. 406.—Observed earthquake travel-time curves at Pasadena, California. *P*, primary or longitudinal waves; *S*, secondary or transverse waves; *L*, complex surface waves. (Gutenberg and Richter, *Gerland's Beiträge zur Geophysik.*)

The method employed at seismological stations to determine the focus of an earthquake will be evident from Figures 405 and 406. In Figure 405, the *P* wave is recorded at 4 minutes and 24 seconds past 9 A.M., and the *S* wave at 11 minutes and 12 seconds past 9 A.M. The *S* wave, therefore, requires 6 minutes and 48 seconds longer than the *P* wave to reach the recording station. From Figure 406 it is seen that a difference of 6 minutes and 48 seconds (408 seconds) between the *P* and *S* curves corresponds approximately to 46.9 degrees or 5100 kilometers. Therefore, the earthquake must have occurred at about this distance from the Pasadena station at which the record shown in Figure 405 was obtained.

One of the most interesting applications of earthquake seismology is the investigation of the structure of the earth at great depths. Time-distance curves and tables derived from comprehensive and reliable data obtained at a great number of seismological stations have shown that over most of the earth the outer crust of the earth consists, essentially, of two layers, an upper granitic layer approximately seven and one-half miles thick and a lower basaltic layer approximately fifteen miles thick.† Below the basaltic layer, there is a layer some two thousand miles thick. Underneath the latter there lies a central core through which the primary waves pass with a velocity only two-thirds as great as the velocity just outside the core. The central core does not transmit the secondary waves, as is shown by their disappearance at large distances from the epicenter. (An *epicenter* is the point or area on the earth's surface vertically above the focus or point of origin of an earthquake.) This disappearance of the secondary waves has been taken to indicate that the central core is probably fluid or plastic.

A more detailed discussion of earthquake seismology will be found, for example, in B. Gutenberg's "Handbuch der Geophysik," Volume 4; G. W. Walker's "Modern Seismology"; or Galitzin's "Seismometrie." Of most recent interest is the book by Macelwane.*

Operating Principles of Seismic Prospecting.—General seismic prospecting makes use of artificially produced elastic waves which are the same as the longitudinal waves studied in earthquake seismology, except that they have a higher frequency of vibration. Travel-time curves are computed from prospect field seismograms in much the same way that travel-time curves are computed for earthquake waves. Characteristic features of seismic prospecting methods, however, are: (a) the location of the artificial "earthquake" and its instant of occurrence are known precisely; (b) far more sensitive instruments are used to detect the vibrations; and (c) more accurate time measurements must be made than are necessary in earthquake studies.

In seismology, the instrument used to receive and record the disturbances is called a seismograph. (Compare p. 642.) In seismic prospecting, however, it is customary to distinguish between the recording

† Charles Davison, Article on Earthquakes, *Encyclopaedia Britannica*, 14th Edition, 1929.
* J. B. Macelwane, "Introduction to Theoretical Seismology," John Wiley & Sons, New York, 1936.

instrument and the instrument which receives the seismic energy and transforms it into some other type of energy that can be recorded.*

Two methods, described as reflection and refraction shooting, are employed in seismic prospecting.** In both methods a sudden, artificial disturbance is produced at the shot-point station—for example, by exploding a charge of dynamite. When the dynamite is exploded, the earth is set in motion like a miniature earthquake and the motion of the surface of the earth is detected and recorded at several seismometer stations located at known distances from the shot-point station. In addition to the observations of the times of arrival at various seismometer stations, an accurate record is obtained of the instant of explosion of the shots.

The basic difference between the two methods lies in the character (refracted or reflected) of the waves whose times of arrival are utilized. In the refraction method, travel-time data are obtained for those artificially produced elastic waves which have been *refracted* at boundaries separating media of different elastic constants or density in such manner that portions of the wave paths in the subsurface are approximately parallel to the refracting boundaries. In the reflection method, observations are made of the times of arrival of the artificially produced elastic waves which have been *reflected* from subsurface horizons.

In addition to measuring travel-times of different types of waves, the reflection and refraction methods differ in numerous practical and theoretical details. In the refraction method, only the times of the first motions at the seismometers generally are used; in the reflection method, on the other hand, the times of later motions are of chief importance.

By knowing the travel-times (intervals between occurrence of explosion and arrivals of the elastic waves at various seismometer stations) and the distances between the source of explosion and the seismometers, it is possible, in many cases, to calculate the depths and dips of the refracting boundaries (refraction shooting) or reflecting horizons (reflection shooting).

A modification of the refraction method, known as fan shooting, is used to find structures, e.g., salt domes having an elastic wave velocity markedly different from that of the surrounding materials. In this method, the travel-times for paths of equal lengths are compared.

Physical Principles.—A disturbance of equilibrium conditions produced by a *sudden stress* at any point in an unbounded elastic solid will cause two types of elastic waves to be propagated: (a) *longitudinal* or compressional waves, i.e., waves in which the particles vibrate in a direc-

* There is no consistent terminology in seismic prospecting for the device which converts seismic energy into some other type of energy that can be recorded. The term seismometer will be employed throughout this chapter. This term is commonly used even though it is not strictly correct, because, as previously stated, a seismometer is a device for *measuring* seismic motion.

** The reflection method, however, is at present much more extensively employed than the refraction method.

tion parallel to the line of propagation, and (b) *transverse* or shear waves, i.e., waves in which the motion of the particles is at right angles to the direction of propagation. When the disturbance is an explosion—the usual case in seismic prospecting—the shear produced in the elastic medium is small compared to the change in volume; hence, in this case, most of the wave energy will be propagated in the form of longitudinal or compressional waves.

If the elastic solid is bounded, as is true of the earth, a third type of wave is produced. These waves travel along the surface and are called surface waves. Such waves are generated either by shear or change in volume close to the surface—this is the more important mode of origin—or when elastic waves reach the surface.

The sudden stress generally utilized in seismic prospecting is the explosion of a charge of dynamite. The explosion of a charge buried in the ground produces a strain in the walls of the cavity or hole in which the charge is placed due to the enormous pressure of the expanding gas. This strain is transmitted to the surrounding layers and propagated outward through the earth as elastic waves, chiefly longitudinal and surface waves. The longitudinal waves are classified conveniently into two types: (a) *direct* waves which travel in approximately straight lines from the shot-hole to the various seismometer stations and (b) waves which are *reflected* and *refracted* at various subsurface boundaries before reaching the seismometer stations. The *paths* traversed by the second type of longitudinal waves are determined by the wave velocities in the media constituting the subsurface and by the shapes of the boundaries between the media.

Distribution of Energy in Reflected and Refracted Waves

In an unbounded isotropic homogeneous medium, the energy radiates uniformly in all directions from the source, and the decrease in energy due to absorption depends only on the distance.* In the case of seismic waves traveling through the earth, however, the longitudinal waves spreading out from the shot-hole encounter boundaries separating media of different elastic constants or density, and the energy of the impinging waves is distributed among the several waves produced at these boundaries.

When a longitudinal wave is incident on a boundary separating media of different elastic constants or density, the energy of this wave is generally distributed among four new waves, a longitudinal and a transverse wave in each of the media.

Formulas for computing the relative amounts of energy transferred to these four waves have been given by Knott,† and formulas for computing relative amplitudes have been given by Zoeppritz.‡

* The absorption of energy is due to internal friction.

† C. G. Knott, "Reflexion and Refraction of Elastic Waves, with Seismological Applications," *Philosophical Magazine*, Vol. 48, July, 1899, p. 64.

‡ K. Zoeppritz, "Ueber Erdbebenwellen VIIb," *Nachrichten der Königlichen Gesellschaft der Wissenschaften zu Göttingen*, mathematische-physikalische Klasse, 1919, p. 57.

Both the energy and the amplitude equations are derived on the assumption that the velocities in the two layers differ by finite amounts so that the boundary corresponds to a substantially abrupt discontinuity.*

Amplitude of the Waves.—The densities of the two media will be denoted by d_1 and d_2 respectively and the following notation will be used for the different waves.

Wave	*Index*	*Velocity*	*Medium*
Incident longitudinal	o	V_1	1
Reflected longitudinal	l	V_1	1
Reflected transverse	t	v_1	1
Refracted longitudinal	L	V_2	2
Refracted transverse	T	v_2	2

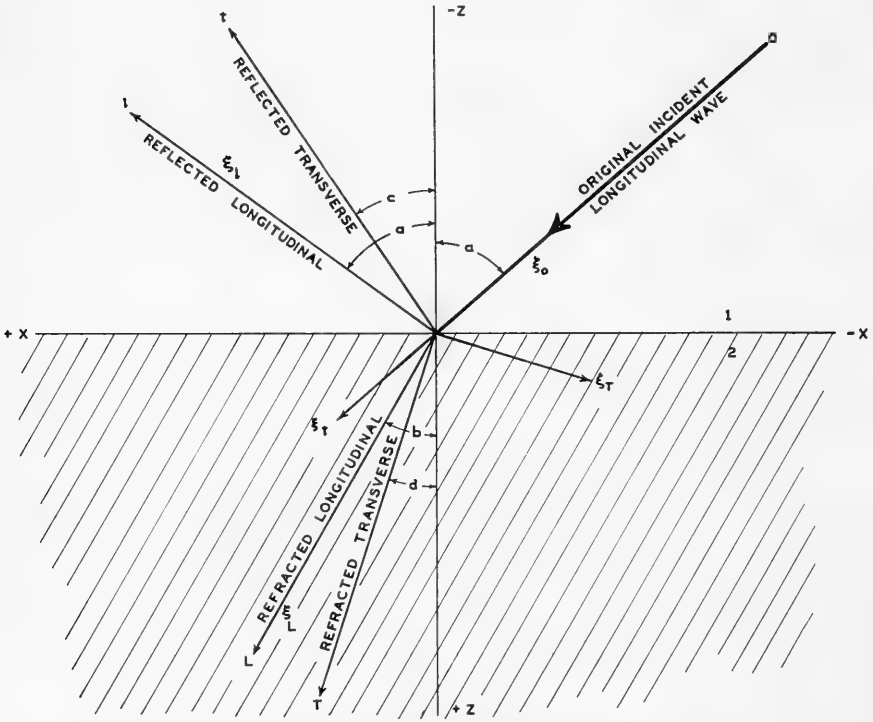

FIG. 407.—Sketch illustrating angles made by wave rays and displacements with the normal at the boundary between media 1 and 2.

The positive axis of z is in the plane of the paper and is parallel to the normal at the boundary directed from medium 1 to medium 2, and the positive axis of x is in the plane of the paper and is directed toward the left. (Figure 407.) The positive direction of displacement of the waves is assumed to be the direction from medium 1 towards medium 2.

* It is important to note that a continuous gradual change, such as that produced by increase of pressure with depth, generally will not produce detectable reflections.

The angles made by the rays with the normal are related by the equation:

$$\sin a : \sin b : \sin c : \sin d = V_1 : V_2 : v_1 : v_2$$

When the motion is a simple harmonic one, the displacement ξ at a time τ can be expressed by an equation of the form:

$$\xi = Me^{pi\,[\tau - (x \sin a + z \cos a)/V]}$$

where M is the amplitude, $(x \sin a + z \cos a)/V$ is the phase lag, p is equal to 2π times the frequency and i as usual denotes the square root of minus 1. The phase lag is obtained by substituting an appropriate value for the "initial" time θ in the equation of the wave front:

$$x \sin a + z \cos a = V\theta$$

The resultant displacements ξ of the several waves and their component displacements u and w in the x and z directions respectively may be written as follows, provided it is assumed that the incident longitudinal wave and the four waves produced at the boundary between media 1 and 2 are plane waves in the plane of the paper. (Figure 407):

$$\left.\begin{aligned}
\xi_0 &= M_0 e^{pi\,[\tau - (x \sin a + z \cos a)/V_1]} & u_0 &= \xi_0 \sin a \\
& & w_0 &= \xi_0 \cos a \\
\xi_I &= M_I e^{pi\,[\tau - (x \sin a - z \cos a)/V_1]} & u_I &= +\xi_I \sin a \\
& & w_I &= -\xi_I \cos a \\
\xi_t &= M_t e^{pi\,[\tau - (x \sin c - z \cos c)/v_1]} & u_t &= \xi_t \cos c \\
& & w_t &= \xi_t \sin c \\
\xi_L &= M_L e^{pi\,[\tau - (x \sin b + z \cos b)/V_2]} & u_L &= \xi_L \sin b \\
& & w_L &= \xi_L \cos b \\
\xi_T &= M_T e^{pi\,[\tau - (x \sin d + z \cos d)/v_2]} & u_T &= -\xi_T \cos d \\
& & w_T &= \xi_T \sin d
\end{aligned}\right\} \quad (1)$$

The component displacements given by the system of equations (1) must satisfy two equations of the form

$$(V^2 - v^2)\frac{\partial \nabla}{\partial x} + v^2 \nabla^2 u = \frac{\partial^2 u}{\partial t^2}$$

where

$$\nabla = \frac{\partial u}{\partial x} + \frac{\partial w}{\partial z} \text{ and } \nabla^2 = \frac{\partial^2 u}{\partial x^2} + \frac{\partial^2 w}{\partial z^2}$$

In addition, the following boundary conditions must be satisfied: The sum of the components of the displacement on both sides of the boundary must be the same and the sum of the normal and the tangential components of stress must be the same. That is,

$$\sum (\overline{u_1}) = \sum (\overline{u_2}) \quad (2)$$

$$\sum (\overline{w_1}) = \sum (\overline{w_2}) \quad (2a)$$

$$\sum d_1 v_1^2 \left(\overline{\frac{\partial u_1}{\partial z} + \frac{\partial w_1}{\partial x}}\right) = \sum d_2 v_2^2 \left(\overline{\frac{\partial u_2}{\partial z} + \frac{\partial w_2}{\partial x}}\right) \quad (3)$$

$$\sum\left\{ d_1 V_1^2 \overline{\nabla_1} - 2d_1 v_1^2 \left(\overline{\frac{\partial u_1}{\partial x}}\right)\right\} = \sum\left\{ d_2 V_2^2 \overline{\nabla_2} - 2d_2 v_2^2 \left(\overline{\frac{\partial u_2}{\partial x}}\right)\right\} \quad (3a)$$

where the bar above the various components and operators denotes values taken at the boundary.

On substituting the values given by the system of equations (1) into the boundary conditions, one obtains

$$\overline{u_0 + u_1 + u_t} = \overline{u_L + u_T}$$

$$\overline{w_0 + w_1 + w_t} = \overline{w_L + w_T}$$

$$d_1 v_1^2 \left\{ \left(\overline{\frac{\partial u_0}{\partial z} + \frac{\partial w_0}{\partial x}}\right) + \left(\overline{\frac{\partial u_1}{\partial z} + \frac{\partial w_1}{\partial x}}\right) + \left(\overline{\frac{\partial u_t}{\partial z} + \frac{\partial w_t}{\partial x}}\right)\right\} = d_2 v_2^2 \left\{ \left(\overline{\frac{\partial u_L}{\partial z} + \frac{\partial w_L}{\partial x}}\right) + \left(\overline{\frac{\partial u_T}{\partial z} + \frac{\partial w_T}{\partial x}}\right)\right\}$$

$$d_1 V_1^2 \left\{ \left(\overline{\frac{\partial u_0}{\partial x} + \frac{\partial w_0}{\partial z}}\right) + \left(\overline{\frac{\partial u_1}{\partial x} + \frac{\partial w_1}{\partial z}}\right) + \left(\overline{\frac{\partial u_t}{\partial x} + \frac{\partial w_t}{\partial z}}\right)\right\} -$$

$$2d_1 v_1^2 \left(\overline{\frac{\partial u_0}{\partial x} + \frac{\partial u_1}{\partial x} + \frac{\partial u_t}{\partial x}}\right) = d_2 V_2^2 \left\{ \left(\overline{\frac{\partial u_L}{\partial x} + \frac{\partial w_L}{\partial z}}\right) + \left(\overline{\frac{\partial u_T}{\partial x} + \frac{\partial w_T}{\partial z}}\right)\right\}$$

$$- 2d_2 v_2^2 \left(\overline{\frac{\partial u_L}{\partial x} + \frac{\partial u_T}{\partial x}}\right)$$

The boundary conditions (2) and (2a) can thus be written in the form:

$$M_0 \sin a + M_1 \sin a + M_t \cos c = M_L \sin b - M_T \cos d$$

$$M_0 \cos a - M_1 \cos a + M_t \sin c = M_L \cos b + M_T \sin d$$

The boundary condition (3) becomes:

$$d_1 v_1^2 \left\{ \left(-\frac{\cos a}{V_1} M_0 \sin a - \frac{\sin a}{V_1} M_0 \cos a \right) + \left(\frac{\cos a}{V_1} M_1 \sin a + \frac{\sin a}{V_1} M_1 \cos a \right) \right.$$

$$\left. + \left(\frac{\cos c}{v_1} M_t \cos c - \frac{\sin c}{v_1} M_t \sin c \right)\right\} = d_2 v_2^2 \left\{ \left(-\frac{\cos b}{V_2} M_L \sin b \right.\right.$$

$$\left.\left. - \frac{\sin b}{V_2} M_L \cos b \right) + \left(\frac{\cos d}{v_2} M_T \cos d - \frac{\sin d}{v_2} M_T \sin d \right)\right\}$$

On simplifying, one obtains

$$-\frac{d_1 v_1^2 M_0 \sin 2a}{V_1} + \frac{d_1 v_1^2 M_1 \sin 2a}{V_1} + \frac{d_1 v_1^2 M_t \cos 2c}{v_1} = -\frac{d_2 v_2^2 M_L \sin 2b}{V_2}$$

$$+ \frac{d_2 v_2^2 M_T \cos 2d}{v_2}$$

or

$$- M_0 \sin 2a + M_1 \sin 2a + \frac{V_1}{v_1} M_t \cos 2c = -\frac{d_2}{d_1} \frac{v_2^2}{v_1^2} \frac{V_1}{V_2} M_L \sin 2b +$$

$$\frac{d_2}{d_1} \frac{v_2^2}{v_1^2} \frac{V_1}{v_2} M_T \cos 2d$$

On setting,

$$\frac{V_1}{v_1} = F;\ \frac{d_2}{d_1}\frac{v_2^2}{v_1^2}\frac{V_1}{V_2} = G;\ \frac{d_2}{d_1}\frac{v_2^2}{v_1^2}\frac{V_1}{v_2} = J$$

the boundary condition (3) becomes:

$$-M_o \sin 2a + M_i \sin 2a + FM_i \cos 2c = -GM_L \sin 2b + JM_T \cos 2d$$

The boundary condition (3a) can be written in the form:

$$d_1 V_1^2 \left\{ \left(-\frac{\sin a}{V_1} M_o \sin a - \frac{\cos a}{V_1} M_o \cos a \right) + \left(-\frac{\sin a}{V_1} M_i \sin a - \frac{\cos a}{V_1} M_i \cos a \right) \right.$$

$$\left. - \left(\frac{\sin c}{v_1} M_i \cos c - \frac{\cos c}{v_1} M_i \sin c \right) \right\} - 2d_1 v_1^2 \left(-\frac{\sin a}{V_1} M_o \sin a - \frac{\sin a}{V_1} M_i \sin a - \right.$$

$$\left. \frac{\sin c}{v_1} M_i \cos c \right) = d_2 V_2^2 \left\{ \left(-\frac{\sin b}{V_2} M_L \sin b - \frac{\cos b}{V_2} M_L \cos b \right) + \right.$$

$$\left. \left(\frac{\sin d}{v_2} M_T \cos d - \frac{\cos d}{v_2} M_T \sin d \right) \right\} - 2d_2 v_2^2 \left\{ -\frac{\sin b}{V_2} M_L \sin b + \frac{\sin d}{v_2} M_T \cos d \right\}$$

On simplifying in several steps, one obtains

$$-d_1 V_1 M_o - d_1 V_1 M_i + 2d_1 \frac{v_1^2}{V_1} M_o \sin^2 a + 2d_1 \frac{v_1^2}{V_1} M_i \sin^2 a$$

$$+ 2d_1 v_1 M_i \sin c \cos c = -d_2 V_2 M_L + 2d_2 \frac{v_2^2}{V_2} M_L \sin^2 b - 2d_2 v_2 M_T \sin d \cos d$$

or

$$-d_1 V_1 M_o \left(1 - 2\frac{v_1^2}{V_1^2} \sin^2 a \right) - d_1 V_1 M_i \left(1 - 2\frac{v_1^2}{V_1^2} \sin^2 a \right) + d_1 v_1 M_i \sin 2c$$

$$= -d_2 V_2 M_L \left(1 - 2\frac{v_2^2}{V_2^2} \sin^2 b - d_2 V_2 M_T \sin 2d \right)$$

or since $\dfrac{\sin^2 a}{\sin^2 c} = \dfrac{V_1^2}{v_1^2}$

$$-d_1 V_1 M_o (1 - 2\sin^2 c) - d_1 V_1 M_i (1 - 2\sin^2 c) + d_1 v_1 M_i \sin 2c$$

$$= -d_2 V_2 M_L (1 - 2\sin^2 d) - d_2 v_2 M_T \sin 2d$$

or

$$-d_1 V_1 M_o \cos 2c - d_1 V_1 M_1 \cos 2c + d_1 v_1 M_i \sin 2c$$

$$= -d_2 V_2 M_L \cos 2d - d_2 v_2 M_T \sin 2d$$

or

$$-M_o \cos 2c - M_i \cos 2c + HM_i \sin 2c = -IM_L \cos 2d - KM_T \sin 2d$$

where

$$H = \frac{v_1}{V_1} \qquad I = \frac{d_2}{d_1}\frac{V_2}{V_1} \qquad K = \frac{d_2}{d_1}\frac{v_2}{V_1}$$

Summarizing the results just obtained, the four boundary conditions are:

$$\left.\begin{aligned} &M_0 \sin a + M_1 \sin a + M_1 \cos c - M_L \sin b + M_T \cos d = 0 \\ &M_0 \cos a - M_1 \cos a + M_1 \sin c - M_L \cos b - M_T \sin d = 0 \\ &-M_0 \sin 2a + M_1 \sin 2a + FM_1 \cos 2c + GM_L \sin 2b - JM_T \cos 2d = 0 \\ &-M_0 \cos 2c - M_1 \cos 2c + HM_1 \sin 2c + IM_L \cos 2d + KM_T \sin 2d = 0 \end{aligned}\right\} \quad (4)$$

The 4 boundary conditions and the relation previously stated between the angles and the velocities ($\sin a : \sin b : \sin c : \sin d = V_1 : V_2 : v_1 : v_2$) allow us to calculate the ratios of the amplitudes of the 4 waves produced at the boundary to the amplitude of the incident longitudinal wave for any angle of incidence a.

When the distances between the point of disturbance and the seismometer stations are small relative to the depths of the subsurface boundaries, the reflected and refracted waves strike the surface of the earth almost vertically. In this case, all the angles in the system (4) are approximately zero, and it follows from the second and fourth equations of this system that

$$\frac{M_1}{M_0} = \frac{I-1}{I+1}, \quad \frac{M_L}{M_0} = \frac{2}{I+1} \qquad \text{where } I = \frac{d_2 V_2}{d_1 V_1}$$

If, for example, the densities in the two media are equal ($d_2 = d_1$) and if $V_0 = 2V_1$, $I = 2$ and $\frac{M_1}{M_0} = \frac{1}{3}$.

Energy of the Waves.†—The formulas for the energies as given by Knott utilize the following abbreviations:

C = cotangent of angle of incidence of longitudinal wave in layer 1.
C' = cotangent of angle of refraction of longitudinal wave in layer 2.
γ = cotangent of angle of reflection of transverse wave in layer 1.
γ' = cotangent of angle of refraction of transverse wave in layer 2.
n = modulus of rigidity of layer 1.
n' = modulus of rigidity of layer 2.
A = energy factor of incident longitudinal wave.
A_1 = energy factor of reflected longitudinal wave.
A' = energy factor of refracted longitudinal wave.
B_1 = energy factor of reflected transverse wave.
B' = energy factor of refracted transverse wave.

$$X = A + A_1 \qquad Y = A - A_1 \quad (5)$$

Knott showed that the quantities just defined are related by the following equations:

$$\left.\begin{aligned} &B_1 + CY = B' + C'A' \\ &\gamma B_1 + X = -\gamma' B' + A' \\ &-2\gamma B_1 + (\gamma^2 - 1) X = 2\frac{n'}{n}\gamma' B' + \frac{n'}{n}(\gamma'^2 - 1) A' \\ &(\gamma^2 - 1) B_1 - 2CY = \frac{n'}{n}(\gamma'^2 - 1) B' - 2\frac{n'}{n} C'A' \end{aligned}\right\} \quad (6)$$

The systems of equations (5) and (6) determine the values of A_1, A', B_1, and B' as a function of A, C, C', γ, γ', n, and n'.

If, as before, the densities in the layers are denoted by d_1 and d_2, the energy equation may be written in the form:

$$Cd_1A^2 = Cd_1A_1^2 + \gamma d_1 B_1^2 + C'd_2A'^2 + \gamma' d_2 B'^2$$

† This section is taken largely from a paper by B. Gutenberg, H. O. Wood, and J. P. Buwalda, "Experiments Testing Seismograph Methods," *Bulletin of the Seismological Society of America*, Vol. 22, 1922, pp. 185-246.

1922

where the left-hand member represents the energy of the incident longitudinal wave and the right-hand member the energies of the reflected and refracted waves. Furthermore, if the energy of the incident longitudinal wave be denoted by E_0, the energy of the refracted longitudinal wave by E_L, and the energy of the reflected longitudinal wave by E_l,

$$\frac{E_L}{E_0} = \frac{C'd_2A'^2}{Cd_1A^2} \quad \text{and} \quad \frac{E_l}{E_0} = \frac{Cd_1A_1^2}{Cd_1A^2} = \frac{A_1^2}{A^2} \tag{7}$$

Obviously, if the ratios $\frac{A'}{A}$ and $\frac{A_1}{A}$ of the energy factors and the ratio $\frac{d_1}{d_2}$ of the densities are known, Equations 7 may be used to obtain the ratio of the energy of the refracted wave to that of the incident wave $\left(\frac{E_L}{E_0}\right)$ and the ratio of the energy of the reflected wave to that of the incident wave $\left(\frac{E_l}{E_0}\right)$. But for a given value of the angle of incidence, the ratio of the energy factors can be expressed as a function of the velocities and the moduli of rigidity by solving the systems of equations (5) and (6). Furthermore, if the ratio of the velocities and the ratio of the densities are specified, the ratio of the moduli of rigidity are determined. (Compare p. 658, Equation 9.) Hence, for a particular angle of incidence, the only data necessary to determine the quotients $\frac{E_L}{E_0}$ and $\frac{E_l}{E_0}$ are (1) the ratio of the velocities and (2) the ratio of the densities.

In particular, if the densities of the two layers are the same and if the velocities have the ratios

$$V_1 : V_2 : v_1 : v_2 = 1.82 : 2.05 : 1.00 : 1.31$$

the following results are obtained.

The reflected longitudinal wave receives 4 per cent of the energy of the incident wave when the latter arrives at the surface normally ($a = 0$). As the angle of incidence increases, the energy of the reflected longitudinal wave at first decreases until at a value equal to approximately 15° it reaches a minimum value of 0.2 per cent of the incident energy. Thereafter the per cent energy is small until $a = 60°$. For values of a greater than 62½° (the *critical angle* for the longitudinal wave), the reflected longitudinal wave receives more than two-thirds of the energy.* For values of a less than the critical angle 62½°, the refracted longitudinal wave carries by far the greater part of the energy. (The transverse wave, largely because of the minuteness of the energy which it represents in field operations, is not generally considered in seismic prospecting and will be neglected in the present treatment.)

If it is assumed as before that the longitudinal wave strikes the surface almost vertically, it may be shown that the systems of equations (6) and (7) become

$$\frac{A_1}{A} = \frac{I-1}{I+1} \qquad \frac{A'}{A} = \frac{V_2}{V_1}\frac{2}{(I+1)}$$

and

$$\frac{E_l}{E_0} = \frac{(I-1)^2}{(I+1)^2} \qquad \frac{E_L}{E_0} = \frac{4I}{(I+1)^2}$$

Also, if $I = 2$,

$$\frac{E_l}{E_0} = \frac{1}{9}$$

On comparing this result with that obtained for the amplitudes on p. 656, one verifies the well-known fact that the energy is proportional to the square of the amplitude.

* The critical angle is defined by the relation: $a_{\text{critical}} \equiv \sin^{-1}\frac{V_1}{V_2}$

Velocities of Elastic Waves and Elastic Constants.—The elastic wave velocities of any medium depend on the elastic constants and density of that medium.* In the case of a homogeneous isotropic solid, the elastic properties are described by two moduli of elasticity. The two moduli most frequently used are: the compressibility k and rigidity n, or Lamé's constants λ and μ, or Young's modulus E and Poisson's ratio σ.† These sets of moduli are not independent of each other. Thus

$$k = \lambda + \frac{2}{3}\mu = \frac{E}{3(1-2\sigma)}, \lambda = k - \frac{2}{3}n = \frac{\sigma E}{(1+\sigma)(1-2\sigma)}$$

$$E = \frac{\mu(3\lambda+2\mu)}{\lambda+\mu} = \frac{9kn}{3k+n} \tag{8}$$

$$n = \mu = \frac{E}{2(1+\sigma)} \qquad \sigma = \frac{\lambda}{2(\lambda+\mu)} = \frac{3k-2n}{6k+2n}$$

A comprehensive investigation of the elastic constants was the research program sponsored by the Harvard University Committee for Geophysical Research.‡ The investigations included static and dynamic laboratory measurements of elastic constants and field measurements of the wave velocities in rock bodies from which the laboratory specimens were taken.§

The velocities of longitudinal and transverse waves in an isotropic homogeneous solid are related to the elastic constants and the density by the equations:††

$$V = \sqrt{\frac{E(1-\sigma)}{d(1+\sigma)(1-2\sigma)}} = \sqrt{\frac{\lambda+2\mu}{d}} = \sqrt{\frac{k+4/3\,n}{d}} \tag{9}$$

$$v = \sqrt{\frac{E}{d}\left[\frac{1}{2(1+\sigma)}\right]} = \sqrt{\frac{\mu}{d}} = \sqrt{\frac{n}{d}} \tag{9a}$$

where d denotes the density, V the velocity of the longitudinal wave, and v the velocity of the transverse wave.

The elastic constant E varies over a wide range while σ is very nearly

* The expression elastic constants of a medium refers to the strains produced in the medium by the application of stresses.

† Compare A. B. Broughton Edge and T. H. Laby, *Geophysical Prospecting*, pp. 330-331 (Cambr. Univ. Press, 1931).

‡ L. Don Leet, *Practical Seismology and Seismic Prospecting* (Appleton Century, 1938) p. 94.

§ W. A. Zisman, "Young's Modulus and Poisson's Ratio with Reference to Geophysical Applications," *Proc. Nat. Acad. Sci.*, 19, pp. 653-665, 1933; "Compressibility and Anistropy of Rocks at and near the Earth's Surface," *Proc. Nat. Acad. Sci.*, 19, pp. 666-679, 1933; "An Improved Apparatus for the Measurement of Poisson's Ratio," *Rev. of Sci. Inst.*, 4, pp. 342-344, 1933; "Comparison of the Statically and Seismologically Determined Elastic Constants of Rocks," *Proc. Nat. Acad. Sci.*, 19, pp. 680-686, 1933.

John M. Ide, "Some Dynamic Methods for the Determination of Young's Modulus," *Rev. of Sci. Inst.*, 6, pp. 296-298, 1935; "The Elastic Properties of Rocks: A Correlation of Theory and Experiment," *Proc. Nat. Acad. Sci.*, 22, pp. 482-496, 1936; "Comparison of Statically and Dynamically Determined Young's Modulus of Rocks," *Proc. Nat. Acad. Sci.*, 22, pp. 81-92, 1936.

L. D. Leet, "Velocity of Elastic Waves in Granite and Norite," *Physics*, 4, pp. 375-385, 1933.

F. Birch and R. R. Law, "The Measurement of Compressibility at High Temperature and High Pressures," *Bull. Geol. Soc. America*, 46, pp. 1219-1250, 1935.

F. Birch and R. B. Dow, "Compressibility of Glasses and Rocks at High Temperatures and Pressures," *Bull. Geol. Soc. America*, 47, pp. 1235-1255, 1936.

†† Broughton Edge and Laby, *loc. cit.*

¼ for materials having good elastic properties.* Hence, the velocities of the elastic waves depend almost entirely upon the ratio of the Young's modulus to the density of the material. Also, it is evident from Equations 9 and 9a that the velocity of the longitudinal wave is greater than that of the transverse wave.**

The velocities of longitudinal waves in various materials found in the earth's crust are summarized in Table 20.*** The table shows that the value of the velocity for a given material varies over a considerable range. This occurs because the composition, porosity, and water content affect the wave velocity appreciably. § In addition, the experimental results show that the velocity varies markedly with the depth of the formation.

The variations in velocity which are most commonly encountered may be summarized as follows: (1) Within a single layer of homogeneous material, the velocity generally increases slowly with depth. (2) The velocity is usually greater in deeper layers, although many exceptions to this rule exist. (3) In many regions, the increase of velocity with depth is approximately linear.

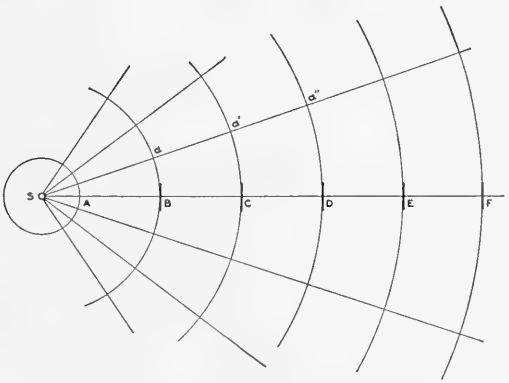

FIG. 408.—Sketch illustrating the propagation of elastic disturbances in an elastic medium.

Seismic Wave Paths.—For simplicity consider that the waves originate at a point source located in a homogeneous isotropic medium. The elastic disturbances which travel outwardly from this source are spheres with the source as center. (Figure 408.) Any one of these spheres is a wave front, i.e., a surface such that all points on it are vibrating in

* A great many deposits found in strata close to the surface of the earth are poorly consolidated. Hence, their elastic properties are not very good and their σ value may be much less than ¼.

** For the rocks composing the earth's crust, this ratio is found to be of the order of 1.6.

*** A table giving the longitudinal and transverse wave velocities, densities, and Young's moduli for laboratory specimens is given by A. Sieberg, *Geologische, physikalische und angewandte Erdbebenkunde* (Gustav Fischer, Jena, 1923), p. 171.

§ Gutenberg, Wood, Buwalda, *loc. cit.*, p. 213.

TABLE 20

APPROXIMATE RANGE OF VELOCITIES OF LONGITUDINAL WAVES FOR REPRESENTATIVE MATERIALS FOUND IN THE EARTH'S CRUST

A. *Classification According to Material*

Material	*Velocity**	
	Ft./Sec.	*M./Sec.*
Weathered surface material	1,000— 2,000	305— 610
Gravel, rubble, or sand (dry)	1,500— 3,000	468— 915
Sand (wet)	2,000— 6,000	610— 1,830
Clay	3,000— 9,000	915— 2,750
Water (depending on temperature and salt content)	4,700— 5,500	1,430— 1,680
Sea water	4,800— 5,000	1,460— 1,530
Sandstone	6,000—13,000	1,830— 3,970
Shale	9,000—14,000	2,750— 4,270
Chalk	6,000—13,000	1,830— 3,970
Limestone	7,000—20,000	2,140— 6,100
Salt	14,000—17,000	4,270— 5,190
Granite	15,000—19,000	4,580— 5,800
Metamorphic rocks	10,000—23,000	3,050— 7,020
Ice	12,050	

B. *Classification According to Geologic Age*

Age	*Type of Rock*	*Velocity*	
		Ft./Sec.	*M./Sec.*
Quaternary	Sediments (various degrees of consolidation)	1,000— 7,500	305— 2,290
Tertiary	Consolidated Sediments	5,000—14,000	1,530— 4,270
Mesozoic	Consolidated Sediments	6,000—19,500	1,830— 5,950
Paleozoic	Consolidated Sediments	6,500—19,500	1,980— 5,950
Archeozoic	Various	12,500—23,000	3,810— 7,020

C. *Classification According to Depth* †

	0—2000 ft. (0—600 M.) Ft./Sec.	2000—3000 ft. (600—900 M.) Ft./Sec.	3000—4000 ft (900—1200 M.) Ft./Sec.
Devonian	13,300	13,400	13,500
Pennsylvanian	9,500	11,200	11,700
Permian	8,500	10,000	.....
Cretaceous	7,400	9,300	10,700
Eocene	7,100	9,000	10,100
Pleistocene-to-Oligocene	6,500	7,200	8,100

* The higher values in a given range are usually obtained at depth.

† Data from B. B. Weatherby and L. Y. Faust, *Bull. Amer. Assoc. Petrol. Geologists*, 19 (1935) 1.

phase. Obviously, at large distances from the source, small portions of the wave front will approximate a plane. (Compare wave front *F* of Figure 408.)

The normal to the wave front at any instant is called the *wave ray*, or the *ray*. Rays, for example, *aa'* and *aa'a''* of Figure 408 are generally used as a convenient tool for describing the paths of elastic waves. A ray, such as *aa'a''...*, has a number of important properties, chief of which is that the travel time along such a path from the source to any point on the path is the "least" time in which energy of the type considered can travel from the source to the point.*

Propagation of Seismic Waves

In using the seismograph as a prospecting tool, it is customary to generate a seismic signal by detonating a charge of dynamite in a shallow borehole. The exploding dynamite constitutes a very intense point source of energy. Accordingly, the compressive displacements of the earth in the immediate vicinity of the charge exceed the range of linear elasticity of earth materials. The region of proportionality between stress and strain is exceeded. In many cases this results in fracturing and permanent set which accounts for the large dissipation of energy into forms other than elastic wave radiation. As the disturbance moves out from the explosion, the amplitudes decrease because of geometrical spreading of the spherical front, and finally come within the range of linear elasticity. From this point on, efficient propagation of the elastic wave ensues and the general theory of elastic wave propagation, which assumes proportionality between stress and strain, is applicable.

The wave form of the impulse at this point of linearity will vary considerably with the physical characteristics of the material surrounding the shot point. In some cases where ideal conditions exist this impulse may be as short as 0.02 seconds, while in other cases it may be spread out into a wave train a tenth of a second or more in length. Examples of this have been discussed by J. Sharpe.†

This impulse, which first arrives in the region of linear displacements, is further modified by the transmission and reflection characteristics of the earth strata. The original spectral distribution of energy in the linear impulse is subject to considerable variation, depending on the particular locality. In general, however, its energy is spread out over a relatively wide band of frequencies, from a few cycles to many thousand cycles per second. As the impulse travels through the earth, the higher frequencies are lost more rapidly than the lower frequencies. There are several mechanisms responsible for this change in amplitude versus frequency: (1)

* It should be pointed out, however, that the entire energy reaching a given point need not travel along the wave ray.

† J. Sharpe, *Geophysics*, Vol. 7, 1942, p. 311.

adsorption due to the viscous nature of earth materials which results in an exponential decrease in amplitude proportional to the square of the frequency (i.e., the amplitude falls off as e^{-af^2x} where a is an arbitrary constant, f is frequency, and x is distance traveled by the wave); (2) solid friction absorption† in which the amplitude falls off as e^{-afx}; and (3) scattering which also produces an exponential decrease in amplitude according to either the first or the second power of frequency or both. Born‡ has shown that below 150 cycles per second viscous absorption is probably unimportant. In seismic prospecting solid friction absorption is probably the main cause of attenuation, although the quantitative effect of attenuation by scattering has not been evaluated thoroughly. If the scattering is produced by small inhomogeneities,§ much less than a wavelength in size, the scattering is of the familiar Rayleigh type, and the loss in amplitude is of the same nature as for viscous absorption: viz.: e^{-bf^2x}, where b is another arbitrary constant. However, there are larger inhomogeneities existing in the earth that are of the same order of magnitude as the wavelength, and here it is probable that the scattering is of the diffraction type and proportional to the frequency rather than to the square of the frequency. Thus, as far as the decrease in the amplitude of the main wave front is concerned, diffraction scattering is indistinguishable from the attenuation caused by solid friction absorption. Scattering will, of course, add to the difficulty of detecting reflections, since it will diffuse random energy back to the surface, which tends to mask the reflected signals.

In addition to the above-described phenomena, all of which tend to discriminate against the higher frequencies, it is also probable that a low frequency discrimination exists for reflected waves due to the fact that when the sedimentary strata are thin compared to the wavelength,†† the reflection coefficient becomes considerably smaller than that calculated for thick beds having a given contrast in specific acoustic resistance. This is a result of the interference of the two reflections from the top and bottom of the bed in question. This interference can be either constructive or destructive when the bed is of the order of a quarter wavelength or more in thickness,‡‡ but for smaller thicknesses the interference is believed to be such that the reflection coefficient falls off more or less directly with frequency. This, of course, is a form of diffraction scattering.

Thus a stratified earth appears to be homogeneous to the long wavelengths; the low frequency energy is not reflected and is returned to the surface only by refraction. As far as reflected seismic energy is concerned, the earth appears as a wide pass "filter." The peak frequency of this "filter" shifts to lower frequencies as the depth of the reflecting bed is increased, because x, the distance traveled by the wave, is in the exponent of the term involving absorption and scattering. This shifts the high

† W. T. Born, *Geophysics*, Vol. 6, p. 132 (1941).
‡ W. T. Born, *loc. cit.*
§ D. H. Clewell and R. F. Simon, *Geophysics* (to be published).
†† D. H. Clewell and R. F. Simon, *loc. cit.*
‡‡ Stewart and Lindsay, *Acoustics*, p. 100 (D. Van Nostrand, 1930).

frequency cut-off to lower frequency as the depth increases, but the low frequency cut-off is believed to be substantially independent of depth, since it is controlled by a reflection coefficient rather than by distance of travel. In prospecting to depths of the order of 10,000 feet or less, the highest amplitude frequencies generally lie between 25 to 80 cycles per second. The wavelengths of the seismic waves can be computed readily from $f\lambda = v$, where f is frequency, λ is wavelength, and v is velocity. The velocity will run from as low as 2000 feet per second or less in the surface zones to as high as 15,000 or 20,000 feet per second in deep or hard formations. Velocities around 8,000 or 10,000 feet per second are quite common, and frequencies of 40 or 50 c.p.s. correspond to wavelengths of the order of 200 feet.

In the conventional application of the seismograph it is customary to use filters in the recording channels which eliminate some of the frequencies in the complex wave arriving at the surface of the earth. This practice is necessary in the visual analysis of records to discriminate against a variety of unwanted signals which would otherwise make it difficult or impossible to recognize reflection signals. It also means that the reflections as viewed on the seismograms tend to have dominant frequencies in the pass band of the filter and do not always show as marked a decrease in frequency with depth as would be expected.

Many attempts have been made to measure the *dispersion* of seismic waves: i.e., variation of velocity with frequency. At present there is no evidence that any appreciable dispersion exists except in the immediate vicinity of the explosive charge where there is non-linearity between stress and strain. The absence of dispersion is very important to seismic prospecting, since it enables the earth to propagate a pulse without any undue change in its length. In a dispersive medium, the various frequencies composing a pulse separate from one another and lengthen the pulse to such an extent that a definite arrival time cannot be determined.

Later in the chapter, in connection with Figure 512, experimental data are given relative to wave attenuation and frequency effects.

Refraction and Reflection of Seismic Waves

The terms *refraction* and *reflection* were used in connection with optical theory long before much was known about seismic waves. However, it has been found that the fundamental principles controlling the wave propagation of both light and seismic waves are very similar. For a review of these principles, the reader is referred to any standard treatise on geometrical optics.

The simplest meaning of the term *refracted waves* is that such waves have undergone a change in the direction of propagation. This change in direction occurs when waves cross a boundary at an angle less than 90 degrees separating media of different elastic properties. When an elastic

wave ray is propagated in a direction normal to such a boundary, no change in direction occurs.

The basic law of refraction is usually referred to as Snell's Law. This law was discovered experimentally, but it actually is a consequence of Fermat's principle, which states that a given ray follows a particular path so that it travels from a given point to a second point in a minimum amount of time. If the given point is in a medium characterized by a propagation velocity different from the medium containing the second point, then the ray path between these two points will not be a straight line. As a consequence of this principle we have Snell's law of refraction, which states that refraction or bending of the ray path occurs when traversing a boundary between media of different velocities such that (a) the incident ray and the refracted ray lie in the same plane and (b) the sine of the angle of incidence in the first medium is to the sine of the angle of refraction in the second medium as the velocity in the first medium is to the velocity in the second medium. These relationships have been expressed mathematically below.

Another useful principle in the study of wave propagation is that of Huygens. It states that in an isotropic medium each point on a wave front may be considered as a source of new waves with spherical wave fronts. The ensuing wave front then becomes the envelope of all wave fronts, which may be considered the surface tangent to the new spherical wave fronts at any given instant of time.

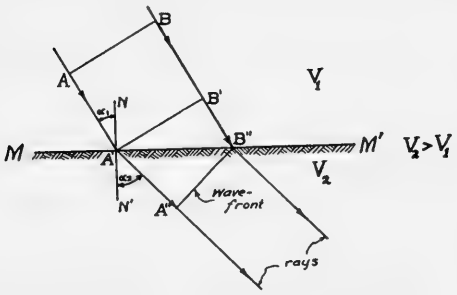

FIG. 409.—Sketch illustrating the refraction of a plane wave $A'B'$ at a boundary MM'.

The law of refraction may be proved directly by use of ray paths.† Referring to Figure 409, MM' is a horizontal boundary separating two homogeneous media in which the elastic wave velocities are V_1 and V_2, respectively. $A'B'$ is a trace of a plane wave front which is perpendicular to the plane of the paper. α_1 is the angle between the ray AA' and the normal NN' to the boundary, and α_2 is the corresponding angle in the second medium. Let t be the time required for the wave to travel from B' to B''. Then, the distance $\overline{B'B''}$ equals tV_1. In this same interval of time the wave will travel a distance $\overline{A'A''}$ in the second medium where A'' is the point corresponding to A' on the wave front at this later time. The distance $\overline{A'A''}$ is equal to the product

† A proof of the laws of reflection and refraction utilizing *Huygen's construction* may be found in any standard text on optics. See, for example, R. A. Houston, *A Treatise on Light*, 5th Edition, pp. 127-128 (Longmans, Green and Co., London) 1928.

of t and the velocity in the second medium; that is,

$$\overline{A'A''} = tV_2$$

Hence

$$\frac{\overline{A'A''}}{V_2} = \frac{\overline{B'B''}}{V_1}$$

Elementary trigonometry shows that

$$\overline{A'A''} = \overline{A'B''} \sin a_2$$

and

$$\overline{B'B''} = \overline{A'B''} \sin a_1$$

so that

$$\frac{\sin a_2}{\sin a_1} = \frac{V_2}{V_1} \text{ or } \frac{\sin a_1}{V_1} = \frac{\sin a_2}{V_2} \tag{10}$$

which is the relation desired.

Reflection or the turning back of the seismic wave occurs when it encounters a boundary separating media of different seismic velocities. The energy of the reflected wave and its phase relative to the initial wave encountering the boundary depend upon degree of contrast of the elastic properties of the two media separated by the surface of discontinuity.

The law of reflection states (a) that the incident ray and the reflected ray lie in the same plane and (b) that the angle of incidence (angle between the incident ray and the normal to the reflecting surface) equals the angle of reflection (angle between the reflected ray and the normal to the reflecting surface.)

Critical Angle of Incidence

From a consideration of Snell's law we find a unique case where the angle of refraction is 90 degrees and the corresponding sine is numerically equal to unity. By definition the angle of the incident ray which results in a refracted angle equal to 90 degrees is called the *critical angle of incidence.*

Consider now the case of two strata separated by a horizontal boundary at a depth h. (Figure 410.) Let the velocity of the elastic wave in the upper stratum be V_1 and that in the lower stratum be V_2 and assume that V_2 is greater than V_1 by a finite amount.

In the general case, a ray starting at the source 0 and reaching the boundary at the point B will produce a reflected ray BS and a refracted ray BP. The ray BS which is reflected back into the first

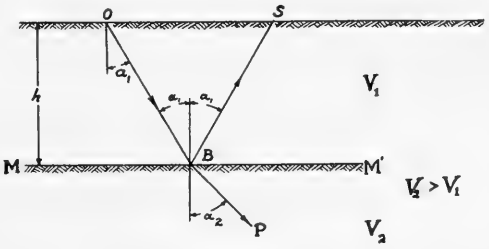

FIG. 410.—Sketch illustrating refraction and reflection of rays at a horizontal boundary.

medium makes an angle a_1 with the normal. The ray BP which is refracted into the second medium makes an angle a_2 with the normal such that a_2 is related to a_1 by Snell's law (Equation 10); that is,

$$\sin a_1 = \frac{V_1}{V_2} \sin a_2$$

In certain cases, namely, when a_1 exceeds a certain critical value, no refracted ray will be produced. This will be evident from the following consideration. For values of a_1 such that $\sin a_1$ is greater than $\frac{V_1}{V_2}$, Equation 10 cannot be satisfied, and hence no refracted ray such as BS can be produced because $\sin a_2$ would have to be greater than 1. (Physically, this means that the incident ray $0B$ is totally reflected for all values of a_1 greater than the critical angle $\sin^{-1} \frac{V_1}{V_2}$.)

The particular case of interest in refraction work occurs when a_1 *approaches the critical value* $\sin^{-1} \frac{V_1}{V_2}$. In this case, a_2 is almost 90° and the refracted ray travels approximately parallel to the boundary.

Travel-Time Curves for a Subsurface Section Consisting of Two Horizontal Layers.—Figure 411 represents a subsurface section consisting of two horizontal strata which are homogeneous and isotropic and have longitudinal wave velocities V_1 and V_2 respectively. Assume that the velocities V_1 and V_2 increase *slightly* with depth. Assume also that V_1 and V_2 differ by a finite amount so that the boundary NN' corresponds to an abrupt discontinuity in velocity. 0 represents the *shot-point** and S_k a seismometer station located at a distance x_k from 0.

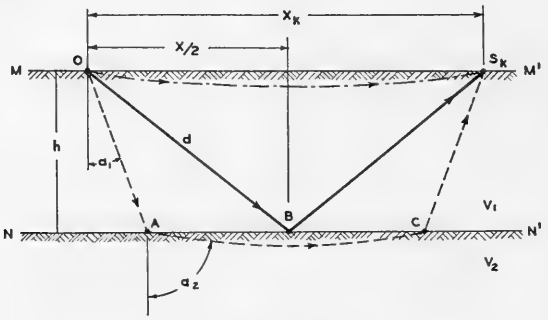

FIG. 411.—Ray paths in a subsurface section consisting of two horizontal strata.

* In seismic prospecting the charge usually is imbedded at some depth from the surface. Hence, it generally is necessary to differentiate between the actual location of the charge, i.e., the bottom of the shot-hole, and the shot-point which is a point on the surface vertically above the charge. In the present illustration, however, the charge is assumed to be located at the surface. Hence, the shot-point and the bottom of the shot-hole are identical in this case.

Following the explosion at 0, surface waves and three types of longitudinal waves (direct, reflected, and refracted) are received at S_k provided x_k is sufficiently great. The surface wave travels along the surface. The direct wave traverses the path $0S_k$, the reflected wave the path $0BS_k$, and the refracted wave the path $0ACS_k$. The travel-time curves for the three longitudinal waves may be determined as follows:

The length of the curved path $0S_k$ is approximately equal to x_k, because the curvature of the path is due solely to the slight increase of velocity with depth. Hence, the *travel-time* T_k required by the direct wave to traverse the distance $0S_k = x_k$ is equal to the quotient of the horizontal distance x_k divided by the velocity V_1. That is,

$$T_k = \frac{x_k}{V_1} \text{ and } x_k = T_k V_1$$

The equation of the *travel-time curve* of the direct wave may be obtained from the last equation by replacing x_k by x and T_k by T, where x denotes the distance between the shot-point 0 and any one of several seismometers located in a straight line through 0 and T denotes the travel-time over the distance x. Thus, the equation of the travel-time curve is

$$T = \frac{x}{V_1} \tag{11}$$

The curve is therefore a straight line which passes through the origin and has a slope of magnitude $\frac{1}{V_1}$ (Figure 412.)

From the geometry of Figure 411, it is seen that the distance from the point 0 to the point of reflection B is

$$0B = \sqrt{\left(\frac{x}{2}\right)^2 + h^2} = \sqrt{\frac{x^2}{4} + h^2}$$

$$= \sqrt{\frac{x^2 + 4h^2}{4}} = \tfrac{1}{2}\sqrt{x^2 + 4h^2}$$

when the interface between medium 1 and 2 is parallel to the surface, a condition of symmetry exists and the distance $0B = BS_k$, the total travel distance of the reflection is then $0B + BS_k$.

$$0B + BS_k = \sqrt{x^2 + 4h^2}$$

Since the distance $0B + BS_k$ is also equal to TV_1, we find that

$$T = \frac{\sqrt{x^2 + 4h^2}}{V_1}$$

This is the equation for a rectangular hyperbola, as plotted in Figure 412.

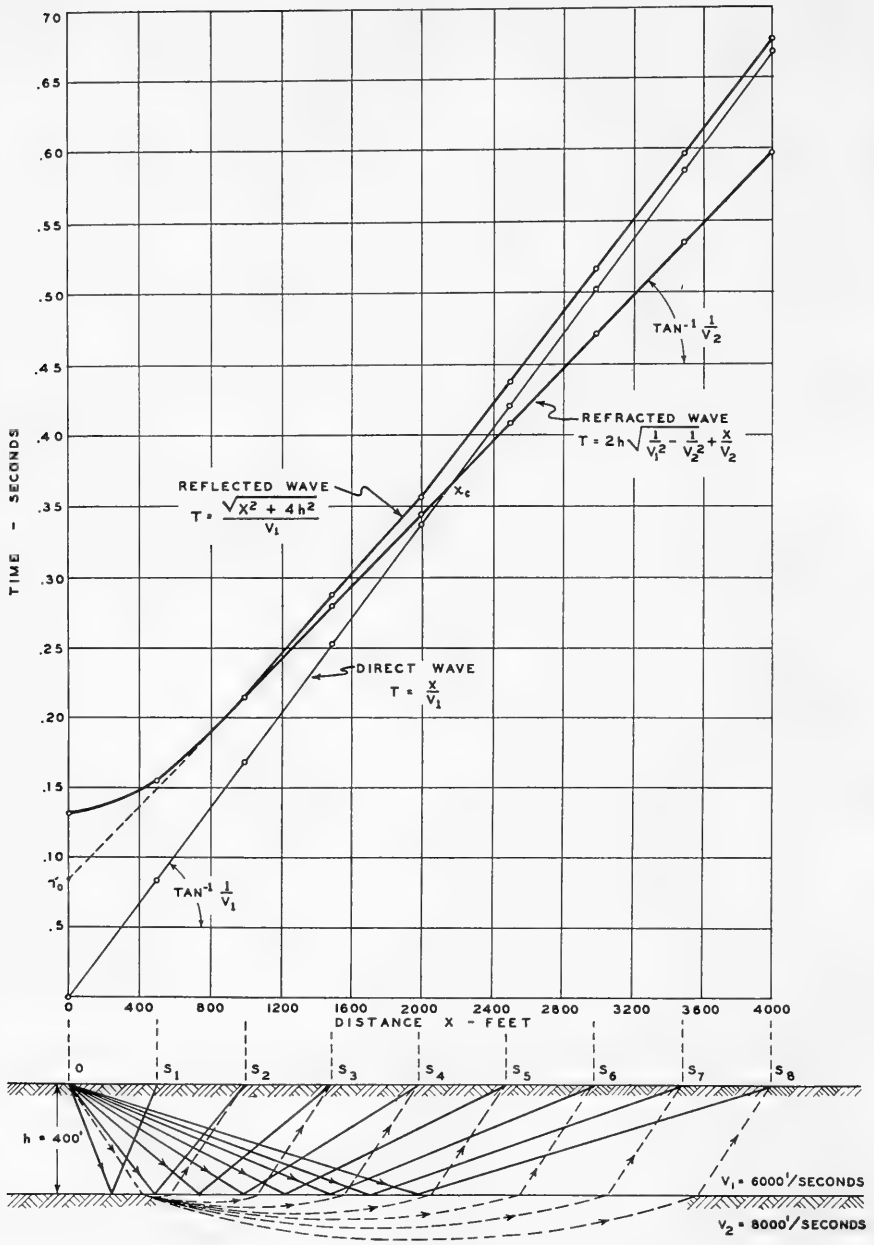

FIG. 412.—Travel-time curves for a subsurface section consisting of two horizontal strata.

The travel-time of the wave which is refracted near the critical angle, and therefore travels in the lower stratum along a path which is approximately parallel to the boundary, is obtained by adding the travel-times in the upper and lower strata. The travel-times in the two strata are $\frac{0A + CS_k}{V_1}$ and $\frac{AC}{V_2}$, respectively. It is evident from Figure 411 that $0A = CS_k = \frac{h}{\cos a_1}$; also, $AC = x_k - 2h \tan a_1$. Hence, the travel-time for the path $0ACS_k$ is

$$T_k = \frac{2h}{V_1 \cos a_1} + \frac{x_k - 2h \tan a_1}{V_2}$$

The equation of the *travel-time curve* is

$$T = \frac{2h}{V_1 \cos a_1} + \frac{x - 2h \tan a_1}{V_2}$$

where T and x denote travel-time and horizontal distance respectively.

The last equation may be simplified by replacing the trigonometric functions by their equivalents in terms of the velocities. It follows from the critical condition $\left(\sin a_1 = \frac{V_1}{V_2}\right)$ that

$$\cos a_1 = \sqrt{1 - \left(\frac{V_1}{V_2}\right)^2}$$

and

$$\tan a_1 = \frac{V_1}{V_2 \cos a_1}$$

Hence

$$T = 2h \sqrt{\frac{1}{V_1^2} - \frac{1}{V_2^2}} + \frac{x}{V_2} \qquad (12)$$

The travel-time curve for the refracted wave is therefore a straight line having a slope of magnitude $\frac{1}{V_2}$. (Figure 412.)

Some disagreement exists among investigators employing seismic methods as to whether the refracted wave travels along the slightly curved path shown in Figure 411 or along the interface itself (straight line path).† A vertical gradient in velocity would produce a curved path. However, it is not necessary to assume a vertical velocity gradient below the upper layer to explain the emergence of a refracted wave at the surface. Even though no such gradient existed, the refracted wave would be detected at the surface. The wave may be transmitted by the propagation of a strain set up at the lower boundary of the upper layer. See, for example, G. Joos and J.

† See O. v. Schmidt, "Ueber Kopfwellen in der Seismik," *Zeitschrift für Geophysik XV*, 1939, p. 141; "Ueber Knallwellenausbreitung in Flussigkeiten und festern Körpern," *Zeitschrift für technische Physik, 12*, 1938, p. 554.

Teltow, "Zur Deutung der Knallwellenausbreitung an der Trennschicht zweier Medien," *Physikalische Zeitschrift*, vol. 40, 1939, pp. 289-293.

REFLECTION METHOD

The characteristic feature of the reflection method is the measurement of the travel-times of longitudinal waves which have been reflected at subsurface boundaries separating media of different elastic wave velocities. From measurements of reflection times it is usually possible to determine the depths and dips of reflecting horizons and the velocities of the seismic waves.

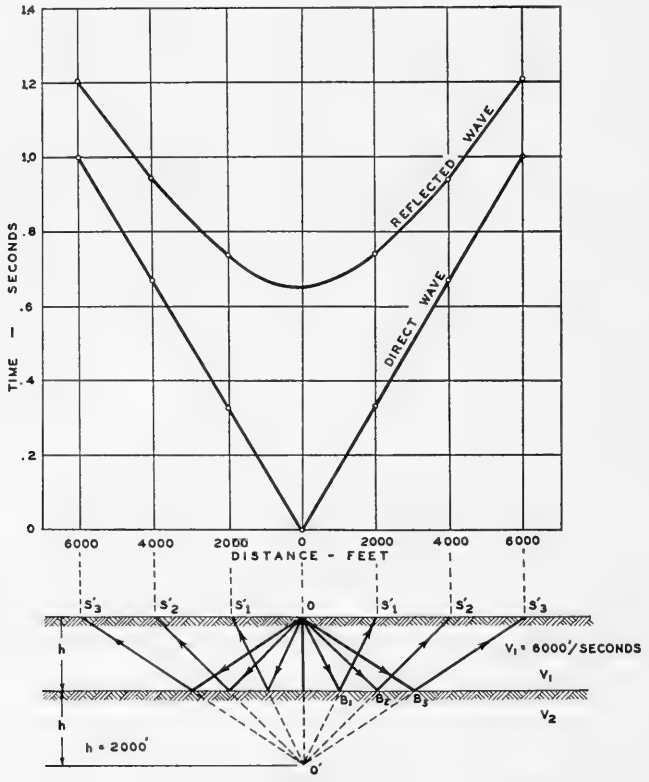

FIG. 413.—Ray paths and travel-time curves for rays reflected from a horizontal surface.

Basis of Reflection Method.—For the purpose of forming an elementary concept of the reflection method, and because of its simplicity, we may consider first the case of two horizontal homogeneous and isotropic media. (In practice this situation is seldom if ever met.) From this assumption it follows that the ray paths are straight lines. Making use of the analogy of geometrical optics, these paths may be conveniently handled

by utilizing the concept of images.† In Figure 413 the image of the shot-point 0 is located at 0′. The ray path $0B_kS_k$, where S_k is the position of any seismometer, is equivalent to the path $0'B_kS_k$, which is straight and in a medium of constant velocity V_1. The response at the seismometers is entirely unchanged by the substitution of an image shot-point.

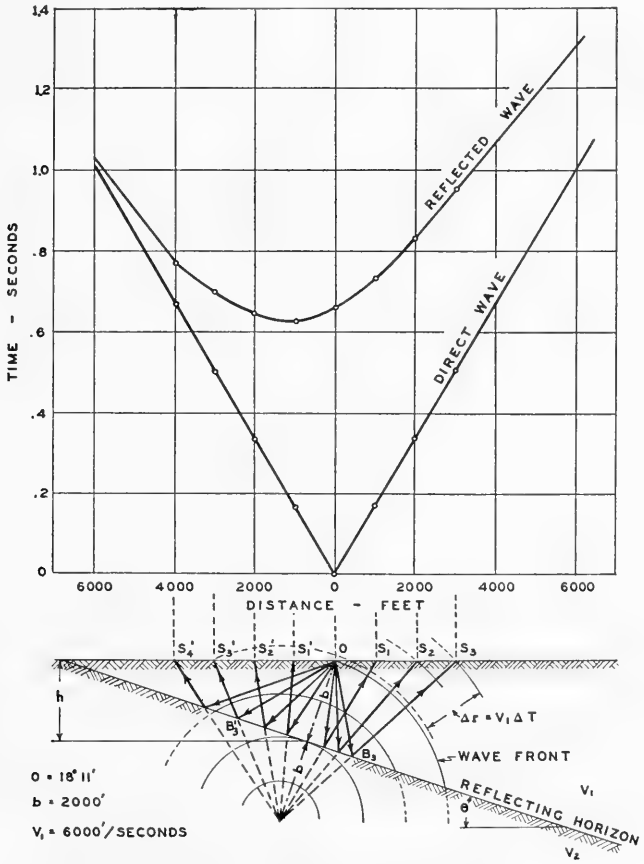

Fig. 414.—Ray paths and travel-time curves for rays reflected from a sloping surface.

In the case of a sloping interface between the two strata (Figure 414), the image shot-point is located at 0′, where $00' = 2b$. The movement of the wave emanating from 0′ is indicated by a succession of arcs of circles, whose origin is at 0′. Each arc designates the position of a particular phase of the wave at a particular time, and therefore each arc constitutes a portion of a *wave front*.

† See also Z. Specht, "Problems of Inclined Layers in Seismic Reflection Methods," *A.I.M.E. Geophysical Prospecting*, Tech. Pub. 1177, April, 1940.

If the seismometers having the same subscript (Figure 414) are located symmetrically with respect to 0, it is evident that due to tilting of the reflecting horizon, the distance $0B_3S_3$ is greater than $0B_3'S_3'$ so that when a given wave front reaches the point S_3', the wave front is still short of point S_3 by a distance Δr. This distance is therefore the difference, ΔT, of the reflection times at points S_3 and S_3' multiplied by the wave velocity of the upper stratum; i.e.,

$$\Delta r = V_1 \Delta T$$

The difference ΔT of the reflection times at two seismometers symmetrically disposed with respect to the shot-point is frequently termed the "move-out" or "step-out" for reasons which will be apparent when viewing the field reflection record. ΔT is a measure of dipping of strata when depth and velocity are known.* It is further evident that when the seismometers are located symmetrically with respect to the shot-point, ΔT increases both with degree of dip and *spread length*.**

The travel-time is calculated conveniently by introducing images both of the shot-point 0 and the seismometer station S. In Figure 415, MM represents a trace of the earth's surface, NN a trace of the upper surface of the dipping formation, and $M'M'$ the image of MM in NN. As before, 0 is the shot-point and S the seismometer station. The perpendiculars to the lower formation from 0 and S will be called b and b' respectively. $0'$ and S' are the images of 0 and S in NN; their positions are fixed by extending the perpendiculars b and b' as shown. $0''$ is a point vertically above $0'$. The point of reflection B is the intersection of the diagonals $0S'$ and $0'S$; thus, the path of the reflected wave is $0BS$. Designate the distance $0S$ by x, and the angle made by NN with the horizontal, i.e., the dip, by θ. Evidently,

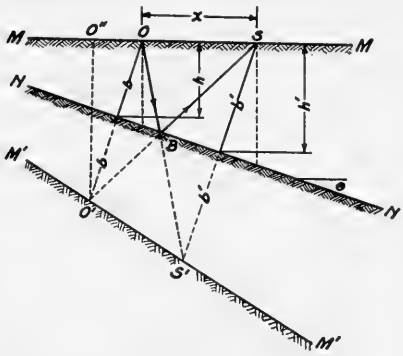

FIG. 415.—Sketch for computing travel-time of rays reflected from an inclined layer NN.

$$b' = b + x \sin \theta$$

$$00'' = 2b \sin \theta$$

$$0'0'' = 2b \cos \theta$$

* Throughout this treatment, the term ΔT will be used to designate differences of reflection time on traces of the same record, irrespective of the disposition with respect to the shot-point of the seismometers producing the traces.

** The term *spread* refers to the disposition of seismometers and shot-point on the surface. The *spread length* is the distance between the end seismometers of a spread.

The distance $0B$ equals $0'B$ so that $0BS$ equals $0'BS$. $0'BS$ is the hypotenuse of the right triangle $0''0'S$; hence

$$(0'BS)^2 = (0'0'')^2 + (0''0S)^2 = 4b^2 + x^2 + 4xb \sin\theta$$

Thus the length of the reflected ray path is

$$0BS = 0'BS = \sqrt{4b^2 + x^2 + 4xb \sin\theta}$$

Let V_1 denote the velocity in the upper bed, then the travel-time T to a seismometer located down-dip from the shot-point is:

$$T = \frac{\sqrt{4b^2 + x^2 + 4xb \sin\theta}}{V_1} \tag{13}$$

If the seismometer is located up-dip from the shot-point, the angle θ entering into Equation 13 is replaced by $-\theta$. Hence, the travel-time T' to a seismometer located up-dip from the shot-point is:

$$T' = \frac{\sqrt{4b^2 + x^2 - 4xb \sin\theta}}{V_1} \tag{13a}$$

Since three unknowns (V_1, b, and θ appear in Equations 13 and 13a, a set of three reflection times from three seismometers located at different distances from the shot-point would suffice to determine the dip, depth, and velocity for a reflecting bed.* In the general practical procedure, however, it is not customary to evaluate the velocity with each dip-depth determination. Instead, the velocity is investigated separately, as discussed in a later section.

The difference in the reflection times to the two seismometers located on either side of 0 is:

$$\Delta T = T - T' = \frac{\sqrt{4b^2 + x^2}}{V_1}\left\{\sqrt{1 + \frac{4xb \sin\theta}{4b^2 + x^2}} - \sqrt{1 - \frac{4xb \sin\theta}{4b^2 + x^2}}\right\} \tag{14}$$

A tabulation of the ΔT values corresponding to a fixed value of the dip θ and various values of the depth h is given in Table 21.

TABLE 21

VALUES OF ΔT COMPUTED FROM EQUATION 14

x	$h = 1{,}000$ ft. $b = 1{,}015.43$ ft. $V = 6{,}250$ ft./sec.	$h = 5{,}000$ ft. $b = 5{,}077.15$ ft. $V = 7{,}250$ ft./sec.	$h = 10{,}000$ ft. $b = 10{,}154.30$ ft. $V = 8{,}250$ ft./sec.	$h = 15{,}000$ ft. $b = 15{,}321.45$ ft. $V = 9{,}250$ ft./sec.
100 ft.	$\Delta T = .0056$ sec.	.0048 sec.	.0042 sec.	.0037 sec.
500	.0270	.0240	.0210	.0188
1,000	.0499	.0477	.0420	.0374
2,000	.0795	.0940	.0838	.0749

Legend:

dip $= \theta = 10°$

$h = b \cos\theta$

* This is true because the spread was assumed in the direction of maximum dip. Otherwise four reflection times would be required.

The table is computed for various values of the vertical distance h between the surface of the earth and the point of incidence of the normal ray at the reflecting horizon. It is evident from Figure 415 that h and b are related by the equation $h = b \cos \theta$. The velocity values approximate those encountered in certain parts of California and the Gulf Coast region. The table shows the *order of magnitude* to be expected in observed time differences ΔT.

Dip Calculation Using the Reflection Method

In order to investigate the wave propagation in the layered upper portion of the earth's crust, generally consisting of sedimentary beds, we may generalize the situation in the following manner. Let the subsurface medium be divided into a number of horizontal layers, each with a constant seismic velocity. This situation is illustrated by Figure 416 where the uppermost layer is given the index (1) and the successive layers are numbered 2, 3, 4, etc. Let the velocities V_1, V_2, V_3, V_4, etc. be constant within each layer and different from layer to layer.

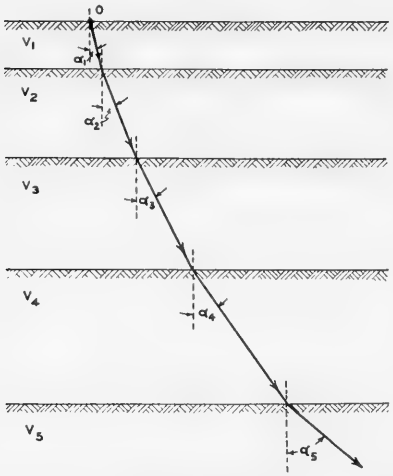

FIG. 416.—Path of refracted wave through horizontal layers.

Let a ray start downward from the surface at a vertical angle a_1, from the perpendicular. At each boundary it will be refracted according to the law of refraction:

$$\frac{\sin a_2}{\sin a_1} = \frac{V_2}{V_1} \; ; \; \frac{\sin a_3}{\sin a_2} = \frac{V_3}{V_2} \; ; \; \frac{\sin a_4}{\sin a_3} = \frac{V_4}{V_3} \; ; \text{ etc.} \qquad (15)$$

By multiplying successive ratios it is found that the vertical angle for any layer (n) is given by

$$\sin a_n = \frac{V_n}{V_1} \sin a_1. \qquad (16)$$

The thickness of the layers may be reduced and their number increased to any desired extent without affecting the law of refraction. In the limiting case, the thickness of the layers may be allowed to approach zero, with an infinitesimal change of velocity between each layer. The limiting case, therefore, is a continuous distribution of velocity with depth. The vertical

angle α at any depth, is given by the equation

$$\sin \alpha = \frac{V}{V_1} \sin \alpha_1 \qquad (17)$$

where V is a continuous mathematical function of the depth Z.

Curved Ray Paths.—The ray path may be considered as having a gradually changing slope. For the case of a continuous increase in velocity with depth, the ray path will be curved with the concave side upward, as illustrated by Figure 417.

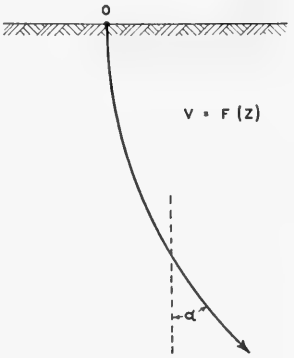

FIG. 417.—Continuous slope of ray path.

Dip Shooting—Two Dimensional Case

Where bedding planes between materials of different elastic properties are present, reflected waves will return to the surface. These waves will be propagated according to the same laws as the downward-moving incident wave, subject to the condition at the reflecting interface that the angle of reflection equals the angle of incidence.

One ray path of particular interest is that one which returns to the source of the elastic impulse. From geometrical optics we know that the direction of propagation of a ray may be reversed without changing its path. Hence a ray incident on a reflecting interface at an angle of ninety degrees will retrace its original path back to its source. In the case of seismic prospecting this source will be the shot-point. The path of such a ray is illustrated in Figure 418.

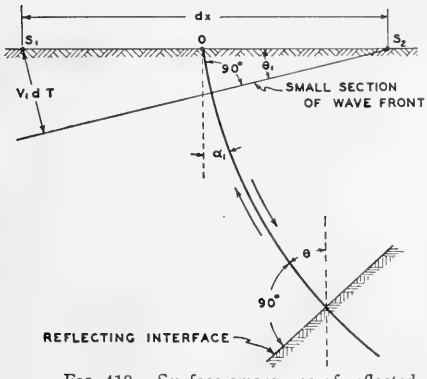

FIG. 418.—Surface emergence of reflected wave in neighborhood of shot-hole.

In an isotropic medium the wave front surfaces are orthogonal to the ray paths. A small section of the reflected wave front is shown arriving in the vicinity of the shot-point in Figure 418. Consider the arrival of the wave at two seismometers, S_1 and S_2, placed symmetrically with respect to the shot-point, 0, and separated by a small distance, dx. Let T represent the round trip or arrival time of the reflected wave at the surface of the ground and then dT will be the small difference in arrival times at the two seismometers. Since the wave surface is inclined at an angle θ_1 in the uppermost layer, the wave front moves forward a distance ($dx \sin \theta_1$) between successive arrival times at

the two seismometers. If the seismic wave velocity in layer 1 is represented by the symbol V_1, then the time difference dT is

$$dT = \frac{dx \sin \theta_1}{V_1} \tag{18}$$

since by geometry $\theta_1 = \alpha_1$, we may write

$$\sin \alpha_1 = V_1 \frac{dT}{dx} \tag{19}$$

From Figure 418 it is seen that the angle of dip θ of the reflecting interface is the same as the vertical angle of the reflected ray at the point of reflection, a fact which is true only of the reflected ray which reverses its path.

Using Equation 17 we may write for this particular situation:

$$\sin \theta = \frac{V}{V_1} \sin \alpha_1 \tag{20}$$

hence

$$\sin \theta = V \frac{dT}{dx} \tag{21}$$

where V is the wave velocity at the reflecting point.

Because of the fact that the reflecting interface is at a finite depth, the wave surface is curved, and therefore the quantity dT/dx is a function of the distance from the shot-point. In the region around the shot-point the wave front is very nearly spherical. The slope of the wave at the shot-point may be obtained in practice by measuring the time-difference, dT, as the amount of time required for the reflected wave front to pass from one end seismometer to the seismometer at the other end of a spread of instruments spaced so that the shot-point is centrally located. This quantity dT, often referred to in practice as the step-out time of a reflection, is not taken directly from the outside pair of seismometers alone. Its numerical value, usually in milliseconds, is estimated from a consideration of the reflection arrival-times of the wave at each of the instruments in the seismometer spread. Where a straight line of uniform slope cannot be drawn through the arrival-times on the record, the greatest weight generally is given to those arrival-times farthest from the center.

It is to be noted that this so-called step-out time determined for a reflection in this manner gives the direction of the dip, the down-dip being in the direction of the latest arrival-time. If the shot-point is placed at any other position than the center of the spread, the direction of the dip may be computed from the step-out time only by the use of the velocities within the media between the surface and the reflecting interface. Another practical advantage of this method of shooting (with the shot-point centrally located with respect to the seismometer spread) is that theoretically the reflected amplitude is greater in the vicinity of the shot-point.

Dip Shooting—Three Dimensional Case

In the foregoing discussion it was tacitly assumed that the seismometers were placed in a line of direction of the true dip. Thus in Figure 419, the plane of the paper represents the plane of incidence and the reflecting interface is perpendicular to it. The slope of the reflected wave is a vector, and its direction does not in general coincide with the direction of the line of seismometers in field practice. Furthermore, being a vector in two dimensions, it requires the measurement of two components to determine its direction and magnitude. To do this, two lines of instruments are set up, intersecting at the shot-point. The most accurate and easily computed arrangement of the seismometers is a right-angled cross, with the shot-point directly below the crossing point of the two spreads.

Let the lines of the cross of seismometers be the x and the y axes, and let the z axis represent depth. The origin of the coordinates then represents the shot-point.

In Figure 419 is illustrated a small triangular section of the wave surface an instant before arriving at the origin. A small pyramid is formed with its apex at the origin, its base representing a small area of the surface and the lengths of its edges being equal to the increments dx, dy, and dz. Let dp be a perpendicular to the wave surface from the origin.

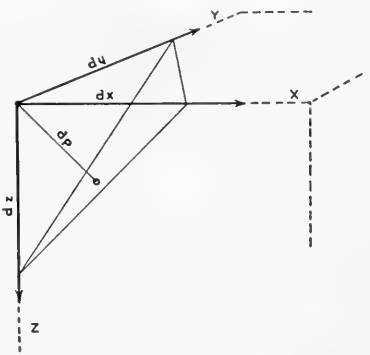

FIG. 419.—Triangular section of reflected wave front near origin.

The wave normal dp forms three angles with the coordinate axes. The cosines of these angles are known as directional cosines in analytical geometry and are customarily given the notation l, m, and n.

Thus,
$$dp = l\ dx = m\ dy = n\ dz \tag{22}$$

The wave moves forward a distance dp in time dT, where

$$dp = V_1 dT \tag{23}$$

Equating (22) and (23) and solving for l and m,

$$l = V_1 \frac{dT}{dx}$$

$$m = V_1 \frac{dT}{dy} \tag{24}$$

Since T is a function of both x and y, partial derivative notation must be used.

$$\left.\begin{aligned} l &= V_1 \frac{\partial T}{\partial x} \\ m &= V_1 \frac{\partial T}{\partial y} \end{aligned}\right\} \tag{25}$$

Now the slope, or emergence angle, of the wave front is given by

$$a_1 = \cos^{-1} n \tag{26}$$

or $$a_1 = \sin^{-1}\sqrt{1 - n^2}$$

since $$l^2 + m^2 + n^2 = 1$$

then $$\sin a_1 = \sqrt{l^2 + m^2} \tag{27}$$

Substituting Equations 25 into 27

$$\sin a_1 = V_1 \sqrt{\left(\frac{\partial T}{\partial x}\right)^2 + \left(\frac{\partial T}{\partial x}\right)^2} \tag{28}$$

The equation of the wave surface at the origin is

$$lx + my + nz = 0 \tag{29}$$

and the intersection of the wave front with the surface, $Z = 0$, is the line

$$lx + my = 0 \tag{30}$$

The direction of the dip of the wave is in the direction of motion of the wave and hence is at right angles to the direction of this line of intersection. Let the angle between the direction of the dip and the x axis be designated by ψ. Now

$$\tan \psi = -\frac{1}{-\frac{dy}{dx}} = \frac{dx}{dy} \tag{31}$$

From (30) $$\tan \psi = \frac{m}{l}$$

Hence $$\tan \psi = \frac{\frac{\partial T}{\partial y}}{\frac{\partial T}{\partial x}} \tag{32}$$

From Equations 28 and 32 it follows that the sin a_1 is a vector whose components are $V_1 \frac{\partial T}{\partial x}$ and $V_1 \frac{\partial T}{\partial y}$.

Thus the true direction and magnitude of the dip of the wave front can be computed and plotted as the vector resultant of the components of the sines of the emergence angles recorded by spreads crossing at right angles.

Figure 420 illustrates the method of plotting these results in the usual form of geological dip and strike symbols in horizontal plan. It also may be noted that the direction of the resultant of the components of the emergence angle corresponds to the true direction of the dip and strike of the reflecting interface.

It has been shown by Equation 17 that at any point of its path, a given ray forms an angle with the vertical conforming to the equation

$$\sin \alpha = \frac{V}{V_1} \sin \alpha_1 \qquad (17)$$

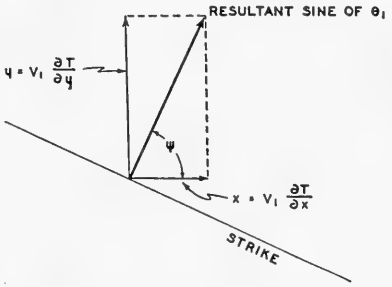

FIG. 420.—Vector magnitude of sine and direction of the dip of emerging wave front.

We may determine the numerical value of α_1 as the resultant of its measured components. Since the ray path in question is the so-called "normal ray," i.e., that ray which reverses its path, it follows that at the point of reflection the angle of incidence α is equal to the dip of the reflecting interface θ. Making use of Equation 17 and substituting θ for α, we may write the expression for the dip θ of the reflecting interface

$$\sin \theta = \frac{V}{V_1} \sin \alpha_1 \qquad (20)$$

Having determined the direction and magnitude of the dip of the reflecting interface by measurements at the surface of the ground, the next process is to find the position of the dip of the interface in space.

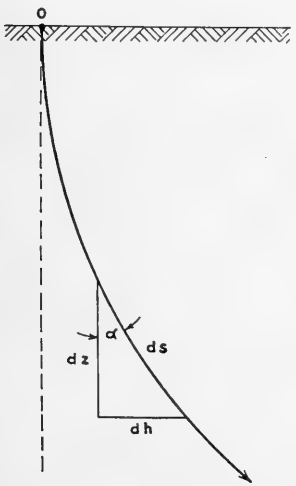

FIG. 421.—Component elements of wave path.

For the purpose of simplification, let the horizontal distance measured in the plane of incidence be given the coordinate h. Let the constant parameter $\frac{\sin \alpha_1}{V_1}$ be designated as p. Then from Equation 17

$$\sin \alpha = pV \qquad (33)$$

In Figure 421 is shown an element ds of the ray path with component elements dh and dz.

The wave moves the distance ds in the increment of time dt.

$$ds = V\,dt \qquad (34)$$

Equation 33 contains the differential equation of the ray

$$\frac{dh}{dz} = \tan \alpha \tag{35}$$

or

$$\frac{dh}{dz} = \frac{pV}{\sqrt{1-(pV)^2}} \tag{36}$$

If the ray meets a reflecting interface at the depth Z, the corresponding horizontal distance, H, is obtained by integrating Equation 36.

$$H = \int_0^H dh$$

or

$$H = \int_0^Z \frac{pV\,dz}{\sqrt{1-(pV)^2}} \tag{37}$$

Returning to Figure 421, it is seen that

$$\frac{dz}{ds} = \cos \alpha$$

This equation is the differential equation of motion of the wave by making use of Equations 34 and 33.

$$\frac{dt}{dz} = \frac{1}{V \cos \alpha} = \frac{1}{V\sqrt{1-(pV)^2}} \tag{38}$$

The reflection time T to the origin is twice the travel-time to the reflecting interface and is obtained by integrating Equation 38.

$$T = \int_0^T dt$$

or

$$T = 2\int_0^Z \frac{dz}{V\sqrt{1-(pV)^2}} \tag{39}$$

When V is a known function of Z, the integrations can be performed and Equations 37 and 39 are sufficient to determine H and Z from the measured values of T and p. H and Z cannot in general be expressed explicitly in terms of T and p. Even in those cases in which the velocity-depth function, $V = F(Z)$, can be expressed in simple enough form to

make an explicit calculation possible, the process of making this computation for each reflection is too cumbersome to be practical in the routine of seismograph work. To facilitate the speed of computation of the dip θ, the horizontal distance H, and the vertical distance Z, various forms of computing charts, slide rules, and machines have been developed which make use of these fundamental Equations 37 and 39.†

Basic Assumptions

A completely rigorous calculation of each reflection requires a thorough knowledge of the wave velocities in the media between the reflecting beds and the surface. Since the chief purpose of reflection shooting is to obtain a subsurface map of geological structure without the expense of drilling numerous deep holes, wherein exact measurements could be made, the velocity data necessary for a rigorous calculation are rarely known in detail. In some cases velocity data are obtainable from a few scattered points, such as deep wells, which far too often were drilled entirely outside the immediate area of the contemplated reflection survey. In a majority of cases, the velocity data used are approximations or estimates based on the best available data or background experience.

As a result of the experience gained in collecting a relatively large amount of velocity data from many areas where measurements have been taken, two very significant generalizations have been made: (1) the velocity increases generally with depth, and (2) the lateral variations of seismic velocity, though present, may be assumed to be small. Thus it is usual to neglect the lateral velocity variation and to use the same velocity-depth function throughout any one area. This assumption greatly simplifies the computation of reflection data. The theoretical obstacles to the computation of these data would be great indeed if the seismic velocity must be described by three spacial coordinates instead of only one.

Most modern computing methods are based upon these assumptions, which is equivalent to saying that the same velocity expression can be used for all angles of reflecting beds and for all shot-points in any one area.

Continuous Velocity-Depth Functions.—In order to make use of the basic equations 37 and 39 it is necessary to obtain a knowledge of the seismic wave velocity in the area to be prospected. There are several methods of ascertaining this data. The most accurate method is well-shooting, but if no wells are available the velocity may be measured by use of either the refraction or reflection methods. These measurements will be treated under separate headings. The determination of vertical velocities from reflection seismograph observations is discussed by Gardner,‡ utilizing specially grouped arrangements of shot-points and detectors to minimize the errors in measurement.

† The development of these equations has been prepared largely from the work of R. W. Raitt in 1935. A similar analysis is given by Haskell and Widess, *Geophysics*, Vol. 5, No. 2, April, 1940.

‡ L. W. Gardner, "Vertical Velocities from Reflection Shooting," *Geophysics*, Vol. XII, No. 2, April, 1947, pp. 221-228.

A large amount of velocity-depth data have been made available to the geophysicist by cooperative well-shooting among the various geophysical operators. A study of these measured velocity data reveals that it is impractical to attempt to predict a quantitative value for the variation of velocity with depth. It is necessary, therefore, to obtain this value from measurements made in the area or to estimate it from prior measurements made under similar geological conditions in the nearest possible vicinity.

The simplest relationship of the variation of seismic velocity and depth is obviously a linear increase of velocity with increasing depth. It is indeed fortunate that, in practice, it has been found that the velocity-depth data in many areas closely approximate this simple linear relationship. Perhaps next to this relationship in simplicity is the variation of the velocity proportional to the travel-time along the vertical *(Z)* axis. This linear time law also has been found to approximate a large number of sets of measured data. From a mathematical point of view the linear time law has some advantages over the linear depth law, but the simplicity of the form of the wave paths and wave fronts of the linear depth law offsets some of these advantages in practice.

By the direct method of least squares, the linear time relationship can be closely fitted to the experimentally measured data, whereas this is not the case with the linear depth relationship. A practical method of fitting the linear depth law to the measured data is prosecuted by using two chosen points on the experimentally measured curve to calculate a second theoretical curve. The resulting curve will intersect the experimental curve at the chosen points, but in general it will not coincide with it. By choosing other values of the slope constant, new theoretical curves may be computed which may more closely fit the observed data. By this method of successive approximations, a curve may be finally computed which fits the observed data quite closely. Obviously this method is an indirect one and involves considerable smoothing of the observed curves. The desirability of this smoothing seems to be somewhat debatable. However, in special cases, it appears that the smoothing of the observed data is justified by the fact that the observed data are based upon approximations which lie within the limits of the smoothing effects.

In some cases the measured increase of velocity data fits a parabolic increase of velocity. There is little doubt that there are many mathematical relationships which will fit the observed data for various areas, but the three variations of (1) lineal increase with depth, (2) lineal increase with time, and (3) parabolic increase with depth, are the most practical to use, if a good approximation to the measured data can be procured.

If a satisfactory fit to the velocity data cannot be obtained with a simple analytical expression, the theoretical considerations in such cases are more difficult. But such a situation is not hopeless. If it is not convenient to express a velocity-depth function in an analytical form, it is not necessary to do so, because the computations can be carried out graphically with a

purely empirical distribution of velocity with depth, though such a process may become somewhat burdensome.

The use of simple mathematical relationships between the velocity and time or depth Z gives a very convenient means of extrapolating data to depths greater than that of actual velocity measurements, an ever-present necessity since the velocity data are often not available at depths from which reflections can be consistently obtained.

Linear Increase of Velocity with Depth

In the case when the seismic velocity is proportional to the depth, the basic equations 37 and 39 can be integrated to obtain the time, T, and the horizontal displacement H. The velocity at any point may be written then as function of the first power of the depth Z.

$$V = V_1 + aZ \tag{40}$$

Considering the first Equation 37, we may transform it by the substitution

$$dz = \frac{dV}{a}$$

$$H = \frac{1}{ap} \int_{pV_1}^{pV} \frac{pV\, d(pV)}{\sqrt{1-(pV)^2}} \tag{41}$$

This is a standard integral form readily found in integrating handbooks, and the solution is

$$H = \frac{1}{ap}\left(\sqrt{1-(pV_1)^2} - \sqrt{1-(pV)^2} \right) \tag{42}$$

Since V is a known function of Z, Equation 42 gives H as a function of p and Z.

Similarly by the substitution, $dz = \frac{dV}{a}$, Equation 39 may be converted into the standard form:

$$T = \frac{2}{a} \int_{pV_1}^{pV} \frac{d(pV)}{pV\sqrt{1-(pV)^2}} \tag{43}$$

which, on being integrated, gives:

$$T = \frac{2}{a}\left[\cosh^{-1}\left(\frac{1}{pV_1}\right) - \cosh^{-1}\left(\frac{1}{pV}\right)\right] \tag{44}$$

where $\cosh^{-1}\left(\frac{1}{x}\right) = \operatorname{sech}^{-1} x = \log\left(\frac{1}{x} + \frac{\sqrt{1-x^2}}{x}\right)$

The desired equation for the surface of constant reflection time is obtained by eliminating p from Equations 42 and 44.

From Equation 44

$$\frac{1}{pV_1} = \cosh\left(\cosh^{-1}\frac{1}{pV} + \frac{aT}{2}\right) \tag{45}$$

$$= \frac{1}{pV}\cosh\frac{aT}{2} + \sqrt{\frac{1}{(pV)^2} - 1}\,\sinh\left(\frac{aT}{2}\right)$$

where $\cosh(x+y) = \cosh x \cosh y + \sinh x \sinh y$

and $$\sinh\left[\cosh^{-1}\frac{1}{pV}\right] = \sqrt{\left(\frac{1}{pV}\right)^2 - 1}$$

Multiplying by pV:

$$\frac{V}{V_1} = 1 + \frac{aZ}{V_1} = \cosh\frac{aT}{2} + \sqrt{1-(pV)^2}\sinh\frac{aT}{2} \tag{46}$$

From this equation: $$pV_1 = \frac{pV}{\cosh\frac{aT}{2} + \sqrt{1-(pV)^2}\sinh\frac{aT}{2}} \tag{47}$$

and $$\sqrt{1-(pV_1)^2} = \frac{\sqrt{1-(pV)^2}\cosh\frac{aT}{2} + \sinh\frac{aT}{2}}{\cosh\frac{aT}{2} + \sqrt{1-(pV)^2}\sinh\frac{aT}{2}} \tag{48}$$

now: $$H = \frac{1}{ap}\left(\sqrt{1-(pV_1)^2} - \sqrt{1-(pV)^2}\right) \tag{42}$$

Substituting Equation 48 into Equation 42:

$$H = \frac{1}{ap}\,\frac{(pV)^2\sinh\frac{aT}{2}}{\cosh\frac{aT}{2} + \sqrt{1-(pV)^2}\sinh\frac{aT}{2}} \tag{49}$$

or, from Equation 46: $$H = \frac{pV_1V}{a}\sinh\frac{aT}{2} \tag{50}$$

$$H^2 = \left(\frac{V_1}{a}\right)^2 (pV)^2\sinh^2\frac{aT}{2} \tag{51}$$

From Equation 46:

$$\left[Z - \frac{V_1}{a}\left(\cosh\frac{aT}{2} - 1\right)\right]^2 = \left(\frac{V_1}{a}\right)^2 [1-(pV)^2]\sinh^2\frac{aT}{2} \tag{52}$$

adding Equations 51 and 52:

$$H^2 + \left[Z - \frac{V_1}{a}\left(\cosh\frac{aT}{2} - 1\right)\right]^2 = \left(\frac{V_1}{a}\right)^2 \sinh^2\frac{aT}{2} \tag{53}$$

Equation 53 is the locus of a circle of radius $\left[\frac{V_1}{a} \sinh \frac{aT}{2}\right]$ whose center is at the depth $\frac{V_1}{a}\left(\cosh \frac{aT}{2} - 1\right)$.

As a result of carrying out the integration of Equations 37 and 39 by using the type of velocity-depth function, $V = V_1 + aZ$, and rearranging the result, it is found that a reflected wave, recorded at the shot-point at time T comes from a bed which is tangent to a sphere of radius $\left[\frac{V_1}{a} \sinh \frac{aT}{2}\right]$, whose center is at a depth $\left[\frac{V_1}{a}\left(\cosh \frac{aT}{2} - 1\right)\right]$, below the datum surface.†

This condition is illustrated by Figure 422, giving the position of the reflecting interface by the coordinates H and Z, in the plane of the incident ray.

From this result it is obvious that a computation method for reflection data may be carried out by the use of the so-called *wave front chart,* which depicts ray paths and wave fronts radiating from a shot-point. Figure 423 illustrates one of these wave front charts.

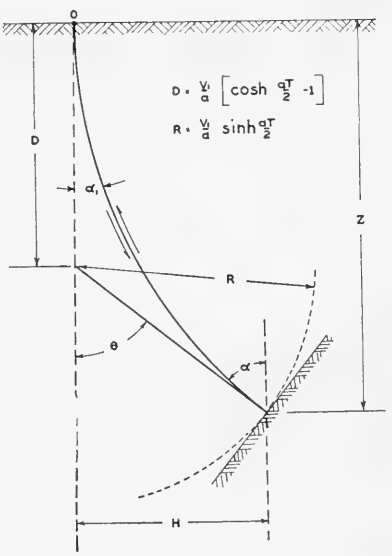

FIG. 422.—Position of reflecting interface in the plane of the angle of incidence.

A wave front chart may be visualized as representing a vertical section through the plane of incidence with the origin at the shot-point. These two sets of curves then represent the ray paths and the successive positions of the wave front surface as it moves forward through the earth. Since the time of reflection is twice the travel-time to the reflecting bed, and the chart gives the time of reflection, the apparent velocity observed on the chart is one-half of the actual wave velocity. The vertical depth and the horizontal distance are represented on the chart by cartesian coordinates. For each observed pair of values of T and $\sin \alpha_1$ obtained from reflection seismograms, one pair of values of H and Z, which give the position of the reflection, can be read from the chart. The chart can be regarded as the superposition of two orthogonal sets of curves, one the cartesian system of constant H and Z, the other the plotted system of constant T and $\sin \alpha_1$. Coincident points in the two systems give solutions of Equations 37 and 39 and hence the desired positions of the reflecting interfaces.

† A derivation of this result is found in L. L. Nettleton's "Geophysical Prospecting for Oil," p. 355, McGraw-Hill, New York, 1940.

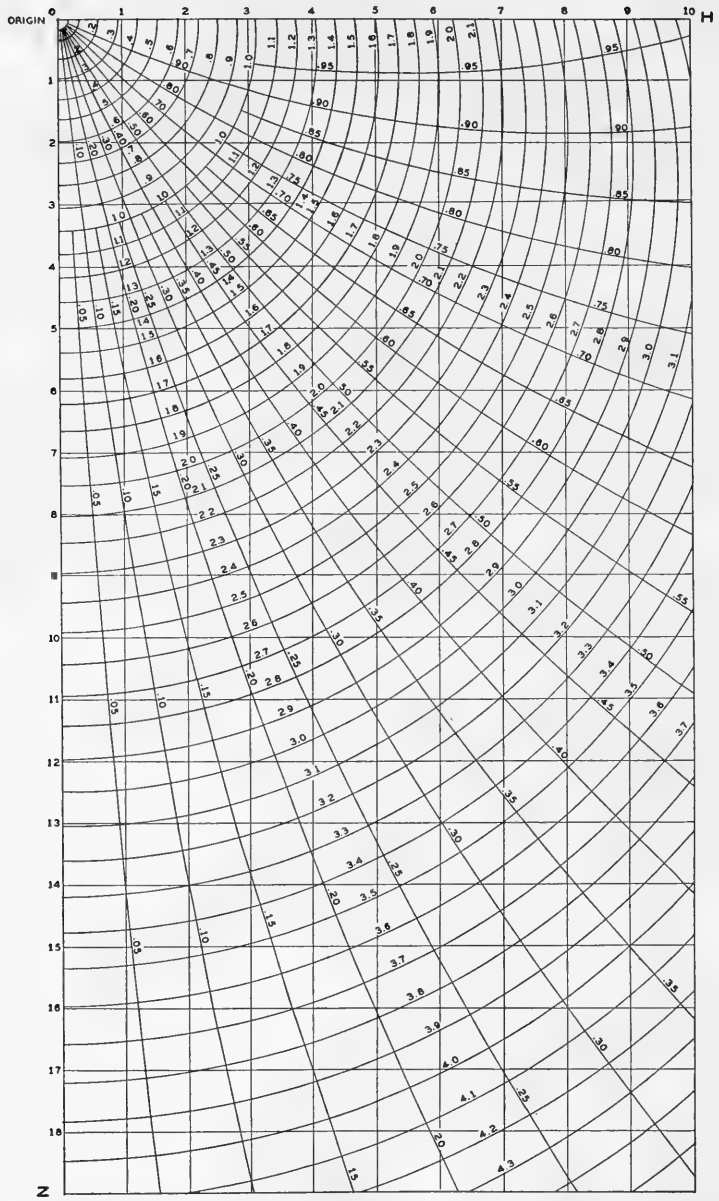

FIG. 423.—Wave Front Chart. The coordinates along the H and Z axes represent thousands of feet. The wave fronts are labeled with the reflection time corresponding to the time required in seconds for the wave to reach the respective position in space and return to the surface. The normal ray paths are labeled with values of the sine of the emergence angles for respective normal ray paths. (Courtesy of Geophysical Engineering Corp.)

It has been shown that the angle of dip of the reflecting interface is given by

$$\sin\theta = V\frac{\sin\alpha_1}{V_1} \tag{20}$$

When the depth of the interface has been determined, the velocity at that depth may be obtained from the velocity-depth function $V = V_1 + aZ$, and the angle of dip can be computed from Equation 20. In practice this process is reduced to one step by the use of a chart from which θ may be read when $\sin\alpha_1$ and the depth Z are known. When this is done, all of the data necessary to completely describe the position and orientation of the reflecting interface are known.

Computation Charts

It has been shown that if the quantities p and T of a reflection are measured at the shot-point, a complete solution for the position and attitude of the reflecting interface is given by the three Equations 37, 39 and 20. In the application of these equations to any arbitrary velocity-depth function, the integrations would probably have to be carried out by graphical or numerical methods. A description of these procedures may be found in any textbook of advanced calculus.

In dealing with a non-linear velocity-depth function the results cannot be expressed in a form in which H and Z can be separately expressed in terms of the measured values of p and T. Fortunately, however, it has been found that in the majority of cases the velocity-depth function can be satisfactorily described as a simple linear increase of velocity, V, with depth, Z. With this type of mathematical function for the velocity, the integrations of Equations 37 and 39 have been given as Equations 42 and 44.

From an inspection of Figure 422 (page 685) it can be seen that the depth is given by $Z = D + R\cos\theta$,

$$\text{or } Z = \frac{V_1}{a}\left[\cosh\frac{aT}{2} - 1 + \cos\theta\sinh\frac{aT}{2}\cdot\right] \tag{54}$$

This equation can be reduced to the more convenient expression,

$$Z = \frac{V_1}{a}\left[\, e^{\frac{aT}{2}} - 1 - (1-\cos\theta)\sinh\frac{aT}{2}\right] \tag{55}$$

The horizontal distance is given by

$$H = R\sin\theta \quad \text{or} \quad H = \frac{V_1}{a}\sin\theta\sinh\frac{aT}{2} \tag{56}$$

It is noted that the solution of these two equations requires knowledge of

the dip (θ), which can be computed from the emergence angle θ_1, with the use of

$$\tan\frac{\theta}{2} = \left[\tan\frac{\theta_1}{2}\right] e^{\frac{aT}{2}} \qquad (57)^*$$

The above expressions 55, 56 and 57 are rigorous for all values of T and θ. Furthermore, these equations may be readily utilized in the preparation of computation charts for rapid reading of the desired quantities H, Z and θ.

For practical reasons computation charts making use of curves which are complicated or difficult to construct should be avoided. It is desirable to form the charts, if possible, with straight lines and/or circular arcs, because of the ease and accuracy with which these may be drawn.

Depth Z Chart.—A chart formed of straight lines only, which can be used for determination of depths, is suggested by Equation 55. In this chart

*It has been shown (Equations 20 and 33) that for a reflection recorded at the shot-point the dip angle θ and the emergence angle θ_1 are related to the ray parameter p by the equations

$$\begin{aligned} \sin\theta_1 &= pV_1 \\ \sin\theta &= pV \end{aligned} \qquad (33)$$

Hence

$$\cos\theta_1 = \sqrt{1-(pV_1)^2}$$
$$\cos\theta = \sqrt{1-(pV)^2}$$

From Equation 48 we may write

$$\cos\theta_1 = \sqrt{1-(pV_1)^2} = \frac{\cos\theta\cosh\frac{aT}{2} + \sinh\frac{aT}{2}}{\cosh\frac{aT}{2} + \cos\theta\sinh\frac{aT}{2}}$$

and

$$\frac{1-\cos\theta_1}{1+\cos\theta_1} = \frac{1-\cos\theta}{1+\cos\theta}\cdot\frac{\cosh\frac{aT}{2} - \sinh\frac{aT}{2}}{\cosh\frac{aT}{2} + \sinh\frac{aT}{2}} = \frac{1-\cos\theta}{1+\cos\theta}\,e^{-aT}$$

where

$$\cosh\frac{aT}{2} = \frac{e^{\frac{aT}{2}} - e^{\frac{-aT}{2}}}{2} \text{ and } \sinh\frac{aT}{2} = \frac{e^{\frac{aT}{2}} + e^{\frac{-aT}{2}}}{2}$$

Since

$$\sqrt{\frac{1-\cos\theta}{1+\cos\theta}} = \tan\frac{\theta}{2}$$

then

$$\tan\frac{\theta}{2} = e^{\frac{aT}{2}}\tan\frac{\theta_1}{2}$$

which is Equation 57, the theoretical basis for the construction of the dip chart.

abscissae are depth (Z) and the ordinates are $(1 - \cos\theta)$. All reflections of time (T) lie on a straight line of (negative) slope, $-\left(\frac{V_1}{a}\sinh\frac{aT}{2}\right)$, intersecting the Z axis at the depth $Z = \frac{V_1}{a}\left(e^{\frac{aT}{2}} - 1\right)$.* The chart con-

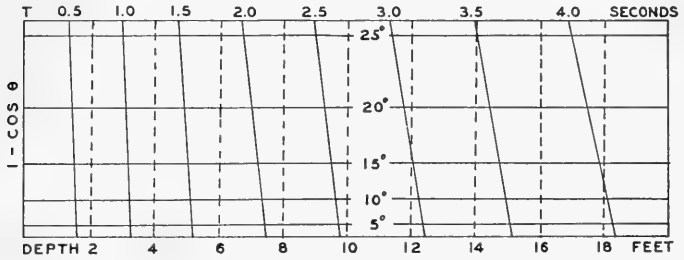

Fig. 424.—Depth chart.

sists of a family of such constant T lines plotted at one-hundredth second intervals, making possible the estimation of time to one millisecond. A second family of horizontal lines is drawn corresponding to values of θ at intervals of one degree. The ordinates of these lines are the corresponding values of $(1 - \cos\theta)$. A chart of this type is shown in Figure 424.

Dip (θ) Chart.—Equation 57 is readily utilized in a chart for converting observed reflection time, (T) and the emergence angle, (θ_1), into dip, (θ), of the reflecting interface. Let the abscissae of this chart represent $\tan\frac{\theta_1}{2}$, while the ordinates represent $e^{\frac{-aT}{2}}$. Fixed values of these abscissae chosen to represent convenient values of $\sin\theta_1$ are shown as vertical lines, while the horizontal lines show the ordinates, $e^{\frac{-aT}{2}}$, for convenient intervals. Radial lines through the origin represent computed dip, θ, and their slope is such that at the ordinate, $T = 0$, the angle of dip shall equal the emergence angle as read from the chart. In the case where the scales of both ordinate and abscissae are chosen to be equal, it will be found that the radial lines representing θ will each make an angle $\left(\frac{\theta}{2}\right)$ with the vertical axis. For increased accuracy in reading the chart it will be found desirable to use a larger scale for abscissae than for the ordinates. This

* Rewrite Equation 55 as follows:

$$\frac{Z - \left[\frac{V_1}{a}\left(e^{\frac{aT}{2}} - 1\right)\right]}{1 - \cos\theta} = -\frac{V_1}{a}\sinh\frac{aT}{2},$$ yielding straight line graphs for each value of T, with Z and $(1 - \cos\theta)$ as variables.

will have the effect of stretching out the chart horizontally and the θ lines will make a larger angle with the vertical, the increase being greatest for small angles where it is most desirable. This type of chart is shown in Figure 425.

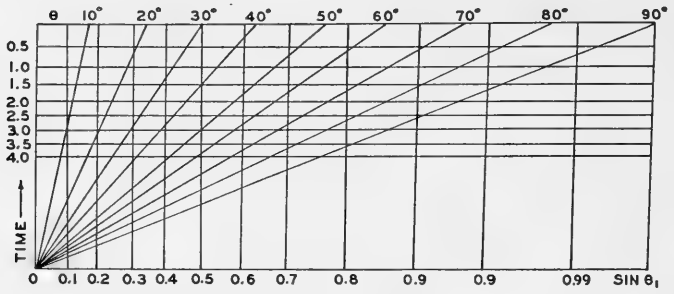

FIG. 425.—Dip chart.

Horizontal Distance (H) Chart.—Horizontal distances can be quickly read from a chart constructed from Equation 56. Circles of radius $\frac{V_1}{a} \sinh \frac{aT}{2}$ are drawn with centers at the origin. Radial lines making angles with the horizontal axis equal to convenient values of θ are also drawn. Horizontal distances corresponding to observed values of θ and T are read as ordinates. A sample of this type of chart is shown in Figure 426.

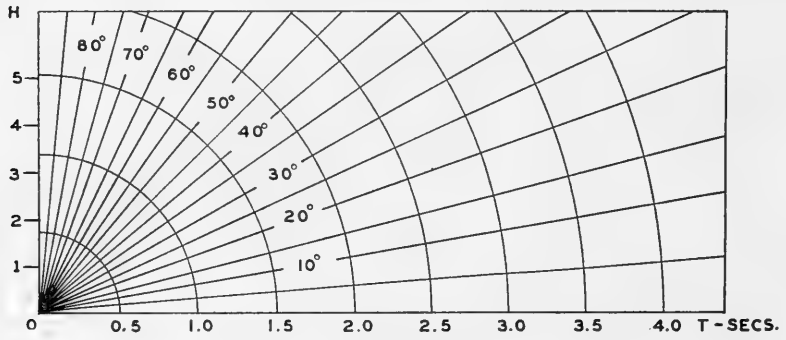

FIG. 426.—Horizontal distance chart.

Illustration of Two-Component Dip Shooting

There are a number of methods for applying the reflection technique to dip shooting. Differing chiefly in details of application and computation, all these methods obtain much the same results under the same basic assumptions.

Two field seismograms obtained by shooting two symmetrical split

spreads with reference to the same shot-point are shown in Figure 427. One instrument set-up was in the north-south and the other in the east-west direction. The top trace of the north-south seismogram was in the south direction, while the top trace of the east-west seismogram was to the east. These records were obtained on level terrain south of the city of Los Angeles at an elevation of 115 feet above sea level. A charge of 12½ pounds was placed at a depth of 95 feet to obtain the record in the north-south direction; however only 4½ pounds were placed at a depth of 85 feet to obtain the seismogram in the east-west direction. The recorded amplitudes of the traces of the records are not dissimilar, in spite of the large difference in the amounts of explosive. Both shots were placed well below the top of the water table and below the weathered layer. The difference in amplitude is small due to the action of the automatic volume control in the amplifiers.

The records were taken in an area of relatively flat-lying formations, which fact is indicated by the small move-out times of the recorded reflections. The length of spread used was 1020 feet, which in general is much too short for the mapping of flat dips. An instrument spread of 2000 or 3000 feet would have been better for accurate determination of dip. However, the problem under investigation involved the possibility of changes in dip within relatively short distances. The shorter spread was chosen for this reason.

Time has been measured on these seismograms from the instant the shock wave reached the up-hole seismometer recorded by the second trace. By reckoning time from this instant to the instant of a recorded reflection, we find the time necessary for the wave to travel from the bottom of the hole to the reflecting interface and back to the equivalent elevation of the bottom of the shot hole. Since the shot was placed twenty or more feet below the low-velocity layer, there is no correction to be applied to the time for the presence of this layer. The shot detonation was recorded by a second set of seismic equipment of different frequency response characteristics. The times of two seismograms, recorded independently, were compared by reference to the up-hole time measurements on the respective seismograms.

The thickness and velocity of the low-velocity layer in this area are uniform. The correction in the north-south direction was (plus) one millisecond, and in the east-west direction (minus) two milliseconds. These corrections were estimated by use of a least square table of the first break differences similar to that illustrated by Table 22, page 727. A rather high frequency disturbance on some of the traces was attributed to the operation of machinery in a nearby factory.

The reflections are marked across the records. The figures at the top of the seismogram represent the reflection time, and those on the bottom represent the uncorrected move-outs for the reflections. Experience of interpreters of seismic data, especially during review or re-interpretation,

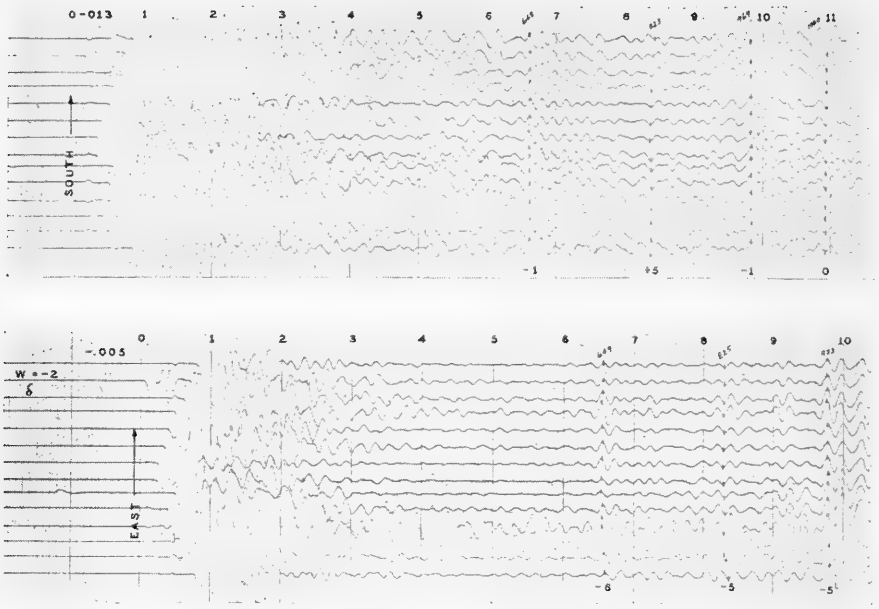

FIG. 427.—Two component seismograms recorded at right angles from one shot-point,

indicates that pencil marks placed on the records make objectivity in the restudy of the seismograms practically impossible. By not marking the reflections, as is customarily done, this handicap to anyone restudying the records is removed.

Reflection Grade. — After the seismograms have been studied for reflections and the individual reflections graded, the recorded data are transferred from the seismograms to the computing form (see Figure 428). Columns 1 and 2 contain the grade or quality of the reflection. The grade designation depends somewhat on the experience and objectives of the grader. It is usually possible to give four different grades, which may be designated A, B, C and D, or G, F, P and VP, meaning *good, fair, poor* and *very poor*. As stated in a subsequent section, the grade should be based on more than just the appearance of the reflection. It should consider filtering, the degree of mixing, the quality of the weathered correction, the possibility of wave interference, etc., and should give an approximate idea of the reliability of the final plotted result.

Time Measurements.—Columns 3 to 9 contain the reflection times and move-outs of the same reflections recorded at three different instrument set-ups from the same shot-point, all corrected to datum elevation. In the case at hand, i.e., the simple two-component recording, three of these

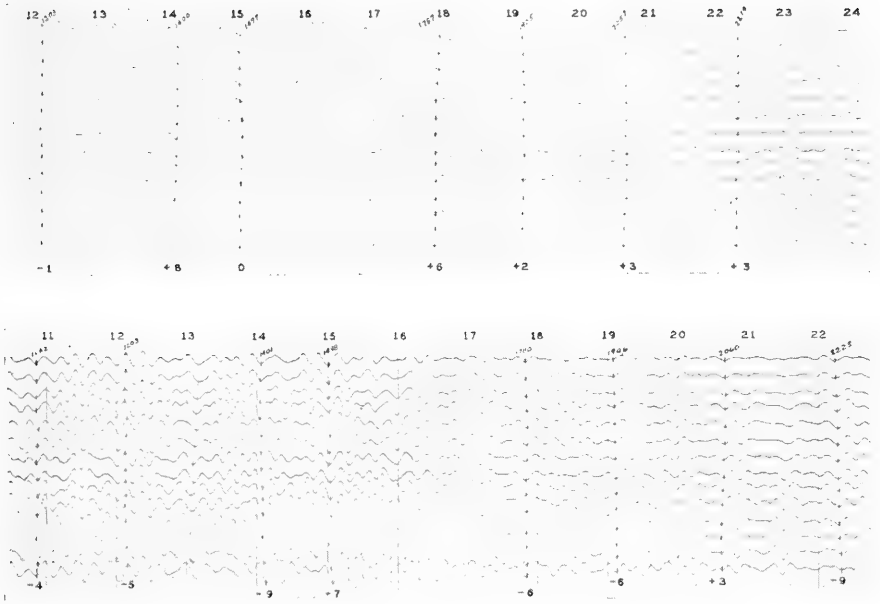

Los Angeles County, California. (Courtesy of Geophysical Engineering Corporation.)

columns are not used. The capital (T) designates the reflection time in milliseconds and small (t) designates the move-out time difference in milliseconds. The subscripts refer to the spread positions shown in a free-hand sketch in the upper left of the computing form. At the head of each pair of columns the bearing of the spread is written, the direction always being from the last towards the first seismometer on the seismogram (in this case from No. 14 to No. 1 seismometer).

Designation of the direction of the component dip is by the algebraic sign preceding the move-out figure, the plus sign being used to show that the emergence angle dips in the direction of trace number one. In other words, subtracting the time of the bottom trace from that of the top one will give the algebraic sign of the move-out time when using this convention.

Columns 10 and 11 contain the sines of the component emergence angles, *alpha* representing in-line and *beta* the cross component. These are calculated by multiplying the move-out times by the ratio of the datum velocity (V_1) to the effective spread length.

$$\sin \alpha = \frac{t_1 V_1}{S_1} \tag{58}$$

$$\sin \beta = \frac{t_2 V_1}{S_2} \tag{59}$$

GEOPHYSICAL ENGINEERING CORPORATION

170 EAST ORANGE GROVE AVENUE
PASADENA 3, CALIFORNIA

PROSPECT BANDINI STATION T1
PROFILE B-B' DATE 3-23-38
CHIEF OF PARTY R.W. RAITT
COMPUTER H.A. ACKERMAN
REMARKS V = 5960 + 0.60Z

LOCATION 80 FT. NORTH, 2600 FT. WEST

DATUM SEA LEVEL W_1 +1 W_2 -2 W_3 - t - D 95/85 d ... $S_{1,2}$ 1020' S_3 ... CIRCUIT ∝ ELEVATION 115

GRADE		SOUTH T_1	SOUTH t_1	EAST T_2	EAST t_2	T_3	t_3	t_u	sin ∝	sin β	T_u	sin Θ	Bearing	Z	Z+ΔZ (ΔZ=-25)	Hor.	Θ	Cross Θ	PROFILE Dip	PROFILE Hor.	AVERAGES sin ∝	AVERAGES sin β	AVERAGES sin Θ	AVERAGES Bearing	AVERAGES Z	AVERAGES H	AVERAGES Dip
B	B	648	0	649	-8				0	.047	649	.047	W	2125	2100	125	3½°	3½°	0°	0							
B	B	823	+6	825	-7				.035	.041	824	.054	S50°W	2790	2765	160	4°	3°	2½°	125							
B	B	969	0	973	-7				0	.041	971	.041	W	3350	3325	160	3½°	3½°	0°	0							
B	B	1080	+1	1082	-6				.006	.035	1081	.035	S80°W	3800	3775	160	3°	2½°	½°	25	.010	.041	.044	S78°W	3000	160	3½°
B	B	1203	0	1203	-7				0	.041	1203	.041	W	4310	4285	250	3½°	3½°	0°	0							
B	B	1400	+9	1401	-11				.053	.064	1401	.083	S51°W	5175	5150	600	8°	5½°	4½°	325							
B	B	1497	+1	1498	-9				.006	.053	1498	.054	S84°W	5625	5600	470	5½°	5°	½°	50	.020	.053	.059	S75°W	5010	310	5°
C	B	1787	+7	1780	-8				.041	.047	1783	.062	S49°W	7000	6975	525	6°	4°	4½°	425							
C	B	1905	+3	1906	-8				.018	.047	1906	.050	S70°W	7660	7635	630	6½°	5°	2°	200							
C	C	2057	+4	2060	+1				.023	.006	2059	.024	S14°E	8490	8465	260	2½°	1°	2°	260							
C	C	2219	+4	2223	-11				.023	.064	2221	.068	S70°W	9490	9465	1025	8½°	7½°	2½°	300	.026	.041	.051	S44°W	8130	560	5½°

FIG. 428.—Computing form.

These equations are the same as Equation 21 with the exception that the derivative $\frac{dT}{dx}$ is replaced by the expressions $\frac{t_1}{S_1}$ and $\frac{t_2}{S_2}$. A very small error is involved in this assumption, but it may be completely neglected in most practical cases.

It should be noted that the value of V_1 to be used in Equations 58 and 59 is the value which gives the best fit of the velocity-depth data to the equation,

$$V = V_1 + aZ \tag{40}$$

over the area being surveyed. It may differ somewhat from the observed unweathered velocity. The calculated emergence angle is thus really an effective value used as a computing aid in finding the solution for the reflecting bed. If the locally observed unweathered velocity is used, the true emergence angle will be given, but this will generally give an incorrect solution when used in the computing charts.

Average Reflection Time.—Column 12 contains the average of the reflection times of the same reflection observed at the different instrument set-ups. As slightly different times are usually observed due to residual error, an average gives a more accurate result. This average is weighted according to the quality and recording situations of the separate records.

Vector Resolution.—In columns 13 and 14 the vector resultants of the components sin α and sin β are tabulated, in terms of the sine of the emergence angle, θ_1, and the bearing of the dip.

Depth, Horizontal Distance and Dip.—Using the data in columns 12 and 13, the values of depth Z, horizontal distance H, and dip θ, are read from charts described as Figures 424, 426, and 425 respectively. Since the depth Z is read with respect to datum, column 16 is provided to record the depth below sea level in this case.

The cross dip, θ, is obtained by using the value of sin β and T_M and represents a component of the dip at right angles to the direction of the profile. In this case the dip is toward the west. In columns 20 and 21 are recorded the components of the dip and the horizontal distance parallel to the profile. Here the profile dip is toward the south. These values are obtained from the charts and values of sin α and T_M. In using these data, it should be remembered that in general this information is from a point not directly beneath the profile, but usually off-set from it.

Where the dips are small it is permissible to assume that the dips projected into the vertical plane of the profile represent the structure along the profile. If the dips are large and the profile forms a considerable angle with the bearing of the dip, then a large error is involved in the location of the dip by projecting into the vertical plane of the profile. *In such cases the actual position of the reflecting beds is so far from the plotted profile*

section that this method of showing the geologic structure may be more misleading than informative.

Average Dip and Strike.—In many areas of gently dipping beds, the reflections are so numerous that they cannot be shown as dips and strikes on a horizontal plan map without great confusion, due to their superposition. Also, in such regions very small errors in the component move-out times cause large errors in the resolved direction of the dip.

To improve this situation, the remaining seven columns of the computing form are designed to facilitate the computing of average values for certain vertical zones within which the reflecting strata have proven to be very nearly parallel. These zones may be chosen between certain depths or between geologic marker beds, usually after enough data has been obtained to reveal at least a qualitative picture of the geologic structure.

The values of sin α and of sin β in each group are averaged separately, different weights being given according to the quality of the reflections. As a rough basis for weighting, a grade A reflection is given a weight of 4, grade B a weight of 3, grade C a weight of 2 and grade D a weight of 1. Averaged components obtained in this manner are then resolved in the usual way and computed as individual reflections, with the difference that the depths are not computed, but averaged. The horizontal distances are then computed for an average depth in each zone.

These averaged values may now be plotted on a plan map with increased accuracy and decreased confusion. It is advantageous to plot separate zones on individual maps for greater simplicity of interpretation. These maps are a valuable aid in contouring theoretical surfaces (phantoms) within the averaged zones.

End Shots

In choosing a computing procedure it is natural to build a routine around a specific type of operation. In the case of the method just described, the normal set-up is the split or symmetrical instrument spread with reference to the shot-point. This is believed to be the best type of set-up under most conditions, but not infrequently in the course of field work situations are met which require the use of end shots. An end shot as referred to here is an instrument set-up in which the shot-point is placed outside the spread of seismometers, usually in the projection of the line of seismometers and not more than a few hundred feet from the nearest seismometer.

In practical work no computing system can be inflexibly geared to a single type of set-up, because inevitably abnormal situations arise and must be solved. Therefore the theory of interpretation developed should be capable of very wide adaptability so that almost any conceivable situation may be freed of perplexing difficulties. It is not possible to discuss in advance all of the variety of abnormal set-ups which may be encountered,

but a few of the more important will be discussed as a means of indicating the methods of solution for others. For example, following this discussion of end-shots, the problem of cross-spreads which are not at right angles will be treated.

The computation of end shots may be carried out by the construction of a set of charts based on a specific length of spread, shot-point to detector distance, and on the condition that $V = V_1 + aZ$. The labor of such an undertaking would be greater than that involved in the construction of the charts for split spreads and would be limited to a specific set-up. A simpler method of procedure is found in reducing the observed value of the reflection and move-out times of an end shot to the effective values which would have been observed in a split spread set-up.

This may be accomplished by use of a so-called "normal move-out" function which gives the value of the move-outs observed from horizontal reflecting interfaces as a function of spread length, distance from the shot-point and time of the reflection. Any given reflection obtained from an end shot may be corrected by subtracting from the observed move-out the normal move-out increment of time computed for that particular set-up. This correction is rigorous only for horizontal reflecting beds, but the error is small for dips up to 15 or 20 degrees, beyond which the correction is seldom used.

In cases where a certain type of end-shot must be used frequently, the corrections may be plotted for ready reference in the form of a normal move-out curve. The basic equation used for this computation gives the reflection time for a horizontal bed of depth Z as a function of distance x from the shot-point to the center of the spread.

$$T = \frac{2}{a} \cosh^{-1} \left\{ 1 + \left(\frac{aZ}{V_1}\right)^2 + \left(\frac{ax}{2V_1}\right)^2 \left[2\left(1 + \frac{aZ}{V_1}\right)\right]^{-1} \right\} \tag{60}$$

From this equation it can be shown by differentiation that the observed move-out time for an end shot of spread length S (center of spread a distance x from the shot-point) is

$$\Delta T = \frac{Sax}{2V_1^2} e^{\frac{-aT}{2}} \left\{ \sinh \frac{aT}{2} \right\}^{-1} \tag{61}$$

The time T used in this equation represents the reflection time to the shot-point. Since the shot point is usually not far from the nearest seismometer, the error involved in using this seismometer to obtain T for computing purposes is usually negligible. However, if the spread is a long distance from the shot-point, the normal move-out correction cannot utilize the reflection time to the shot-point, and a more complicated expression using the reflection time to the center of the spread is necessary.

$$\Delta T = \frac{Sax}{2V_1^2}\left\{\sinh\frac{aT}{2}\cosh\frac{aT}{2}\right\}^{-1} + \sinh\frac{aT}{2}\sqrt{\sinh^2\left(\frac{aT}{2}\right) - \left(\frac{ax}{2V_1}\right)^2} \tag{62}$$

Application of this correction to the observed move-out time gives the move-out that would be obtained by a conventional split-spread placed symmetrically about a shot-point midway between the actual shot-point and the center of the end-shot spread.

Reduction of the observed reflection time T to the effective split-spread time T_s is obtained by the application of the following equation:

$$T_s = \frac{2}{a}\log_e\left[\cosh\left\{\frac{aT}{2}\right\} + \sqrt{\sinh^2\left(\frac{aT}{2}\right) - \left(\frac{ax}{2V_1}\right)^2}\ \right] \tag{63}$$

By using the corrected values of the reflection and move-out times, the results may be calculated in the conventional manner as given for split-spreads, and the positions of the reflection may be plotted with reference to a point midway between the shot-point location and the center of the end-spread.

Cross Spreads Not at Right Angles.—The conventional vector resolution of the trigonometric functions of the cross components of dip requires that the two component set-ups be placed at right angles. Occasionally a set-up location will be found in which this cannot be done, but the seismometers can be set up at an angle that differs from 90° by an angle ϕ. This situation may be treated by correcting one of the observed move-out times to a normal move-out for a right-angle position for the measured component.

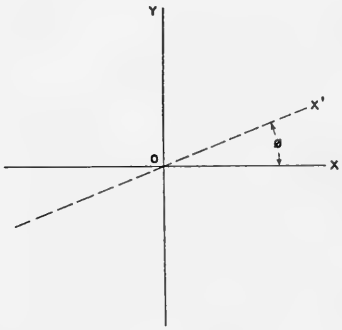

FIG. 429.—Rotation of spread.

Consider the X and Y axes to represent the normal spread directions. Let the X' axis represent the abnormal spread direction making an angle ϕ with the normal X-axis, as shown in Figure 429.

The reflection time T is a function of x and y. Therefore,

$$\frac{\partial T}{\partial x'} = \frac{\partial T}{\partial x}\frac{\partial x}{\partial x'} + \frac{\partial T}{\partial y}\frac{\partial y}{\partial x'} \tag{64}$$

or

$$\frac{\partial T}{\partial x'} = \frac{\partial T}{\partial x}\cos\phi + \frac{\partial T}{\partial y}\sin\phi \tag{65}$$

Replacing the derivatives by the measured move-out times and spread

lengths, we have

$$\frac{\Delta T'}{S'} = \frac{\Delta T_x}{S_x}\cos\phi + \frac{\Delta T_y}{S_y}\sin\phi \ * \qquad (66)$$

Solving this expression for the desired $\Delta T_x/S_x$

$$\frac{\Delta T_x}{S_x} = \left\{\frac{\Delta T'}{S'} - \left(\frac{\Delta T_y}{S_y}\sin\phi\right)\right\}\left[\cos\phi\right]^{-1} \qquad (67)$$

or

$$\frac{\Delta T_x}{S_x} = \frac{\Delta T'}{S'}\sec\phi - \frac{\Delta T_y}{S_y}\tan\phi \qquad (68)$$

This corrected value is used in the conventional manner of computation in which the components are at right angles to each other.

This transformation is not limited to the use described above but can readily be applied to other problems. For instance, it can be used to calculate the move-out time for any direction if the two component move-outs are known.

The Recorded Reflection

The problem of primary importance in the study of the reflection seismogram is to recognize reflections on the records. The ability to distinguish the reflected impulses from all other impulses is acquired to a certain degree by practice and a knowledge of the various wave properties and paths.

From a physical point of view, probably the simplest analogy to a seismic reflection is the understanding of an echo in the study of sound in air. For example, one hears a sound from a source as the sound waves pass his position, the sound wave continuing its path until it strikes a wall and is turned back. As this "turned-back" sound wave passes the observer, he hears the sound for the second time, as an echo. In the case of reflection recording, the seismometer corresponds to the listener, picking up the passing of the seismic waves through the movement of the ground from their source and again when the reflected seismic wave returns to the ground surface after being reflected from certain subterranean strata. A means of observing the length of time required for the seismic wave to travel the round trip from the origin to the reflecting strata and back to the seismometer is provided by recording the effects on the seismometer on a strip of moving photographic material.

This would be simple indeed except for the fact that the origin of the seismic wave is not a single impulse, but consists of a complex train of impulses which follow the initial one. To the resulting recorded events appearing on the seismogram have been applied such terms as *surface waves, direct waves, refracted waves, diffracted waves, transverse waves, sustained*

* The subscripts x and y refer to the directions X and Y along which the particular ΔT and spread S are measured.

strata vibration, sustained vibration at the shot-point, reverberations and *disturbances* (not attributable to the origin of the initial impulse). All of these impulses actuate the seismometer and the problem becomes one of recognizing the true reflection from the complexity of impulses with which it is associated. These complications arise from the intricate natures of the subterranean wave-transmitting media and of the initiation of the impulse. The separation of the reflection from this background of the recorded disturbances is accomplished by a study of relative time and amplitude. The property of relative time is accentuated by the arrangement of detecting seismometers, and the property of amplitude is accentuated by the overall design and vibratory frequency response of the recording equipment.

When the subsurface under investigation consists of more than two strata, the penetration of the rays to the deeper strata must be considered. At each interface the radiating wave is divested of energy, a part of which appears as a reflected longitudinal wave and is detected by the seismometer on the ground surface. The seismometer is therefore activated by a series of reflected waves from successively deeper interfaces.*

It might be expected that superposition of other energies (surface waves, direct waves, transverse waves, refracted waves, sustained strata vibration, reverberations and disturbances not attributable to the shot) on the reflected energy would outweigh the effect of the reflected wave, thereby preventing reliable recording of the reflections. To the dismay of the seismologist, this situation is sometimes approached in practice. However the non-useful energy produced by the shot can be avoided to a large degree by present-day instrumental and field techniques. Interfering energy from sources other than the shot-point is generally maintained below a "noise-level" (the background of the record), so that confusion with reflected energy from this source occurs only in the case of a disturbance of unexpectedly large amplitude. This factor is eliminated conclusively by comparison of two or more seismograms secured from the same shot-point. In field practice it has been found that seismic records are usually reproducible in close detail as far as energy from the shot is concerned, because successive shots under essentially similar conditions in the shot-hole will yield substantially similar seismograms.

The presence of rough surface topography is frequently a source of error in seismic mapping. Widess† describes various aspects of the problem and indicates methods of solution for different topographic effects.

If a single seismometer were utilized to determine movement of the

* Secondary reflections may occur and show up on the record. Secondary reflections may be due to waves which have undergone multiple reflection before striking the seismometers. Generally, multiple reflection, or reverberation, between two strata is very seldom detectable because the energy imparted to a seismometer by a wave which has undergone multiple reflection is small relative to the other energy which the seismometer is receiving at the same time. Another class of secondary reflections, however, is sometimes noticeable: namely, that corresponding to reflection of direct waves from the base of the low velocity layer or from the ground surface.

† M. B. Widess, "Effect of Surface Topography on Seismic Mapping," *Geophysics*, Vol. XI, No. 3, July, 1946, pp. 362-372.

ground following a shot, it would generally be quite difficult to distinguish with surety the reflected waves from the spurious energies recorded on the seismogram. The visual identification of the reflection is made possible by the method of simultaneously recording the motion of the ground over a relatively large section or area. This is accomplished by using as many as 12 to 48 separate detecting stations and recording the activation of all the stations simultaneously on the same photographic record. In this manner the statistical data on the emerging wave fronts are effectively sampled at the instant they pass each of the detecting seismometers. The refracted and surface waves which pass the seismometers are usually identified by their speed through the field of receivers, which corresponds to the seismic velocity of their respective media, whereas the reflected waves may be identified by the very high apparent speed with which they move through the field of receivers. In the case of relatively horizontal strata this speed of the reflected wave usually exceeds any known seismic velocity in the vicinity. For example, a reflected wave from a horizontal reflecting strata would arrive throughout a horizontal area in the neighborhood of the shot-point at virtually the same time. This would impart the same movement of the ground almost instantaneously to all seismometers in the field, and as a consequence all oscillograph trace records of the reflected waves would be similar with respect to time, relative amplitude, phase relationship and wave form. In other words, a similar event would be recorded independently by all instrument traces on the seismogram. The alignment of these similar wave forms across the seismogram is usually referred to as the *line-up* of the reflection. The time difference as estimated across the record is referred to as ΔT, or the "move-out" or "step-out" time.

Therefore, in a study of records, similar wave forms which appear in permissible "line-up" patterns will be identified visually as reflections. Prominent reflections are selected, or marked at corresponding points or phases* down the traces as shown in Figures 430 and 431.

From a knowledge of the average velocity in the region under prospect and the disposition of the seismometers with respect to the shot-point, the interpreter of the field records can determine the range of difference of times which may be expected for reflections from beds at any depth and dip. The time-distance relation for reflection indicates the nature of the patterns or so-called "line-ups" which are possible for reflections. For a *split spread,* i.e., seismometers located in line with and on opposite sides of the shot-point, the pattern or "line-up" is of the form indicated in Figure 430; with increasing depth the "line-up" approaches a straight line, i.e., curves drawn through troughs or peaks corresponding to the same reflection on the various traces approximate straight lines. Actually, it is seldom necessary to refer to velocity or spread length to recognize

* The term "phase" is used here in the conventional sense of any particular time in the history of a wave, rather than in the more limited meaning, p. 644, of the onset of a new type of wave on earthquake seismograms.

the reflections because the difference in reflection times between successive traces usually is small.

The theory of computation for dip shooting has been given in a preceding section. The computation of data in correlation shooting is essentially a special case in which the reflections, individually, persist over considerable area, usually with relatively small dip. This problem is treated in the following section.

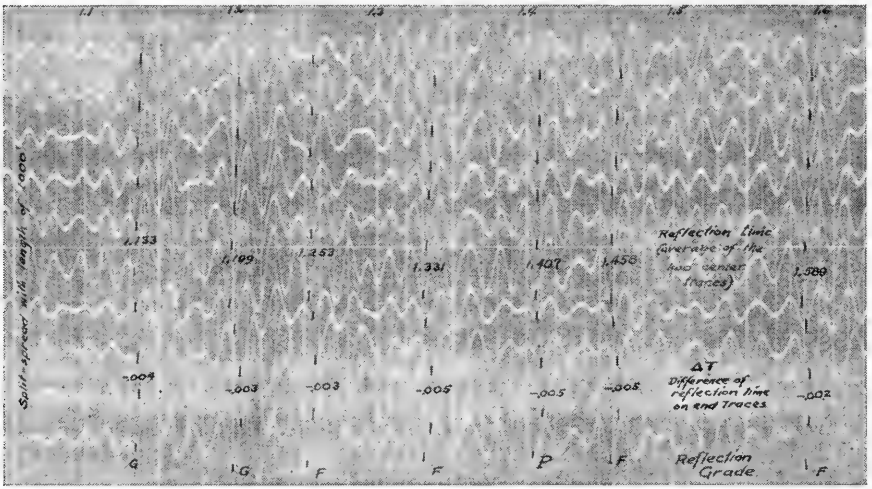

FIG. 430.—Typical dip record. ΔT is the difference in reflection times to the two end seismometers. Note 0.005 sec. lag between bottom two traces due to change of conditions in low velocity layer. (Courtesy of Western Geophysical Company.)

Reflection Correlation Shooting

Although the character of a reflection furnishes no definite information regarding the composition of the constituent layers of the subsurface, it is often observed that certain strata yield a similar and sometimes distinctive reflection throughout certain areas. In these cases, therefore, it is possible to trace and map specific geologic strata without dip information. Such mapping is done by character correlation, i.e., selecting corresponding phases of those reflections which have substantially similar wave forms on records obtained at two or more separate seismometer spreads.

Under the general heading of correlation shooting may be placed four type classifications of seismic work. These may be enumerated as pulse correlation, spot reflection correlation, correlation of a reflection with a definite geological marker bed, and refraction correlations.

Pulse Correlation.—*Pulse correlation* is an extension of the process used to recognize a reflection on a single seismogram to include all seismograms obtained in a given area. A single-pulse continuous correlation is

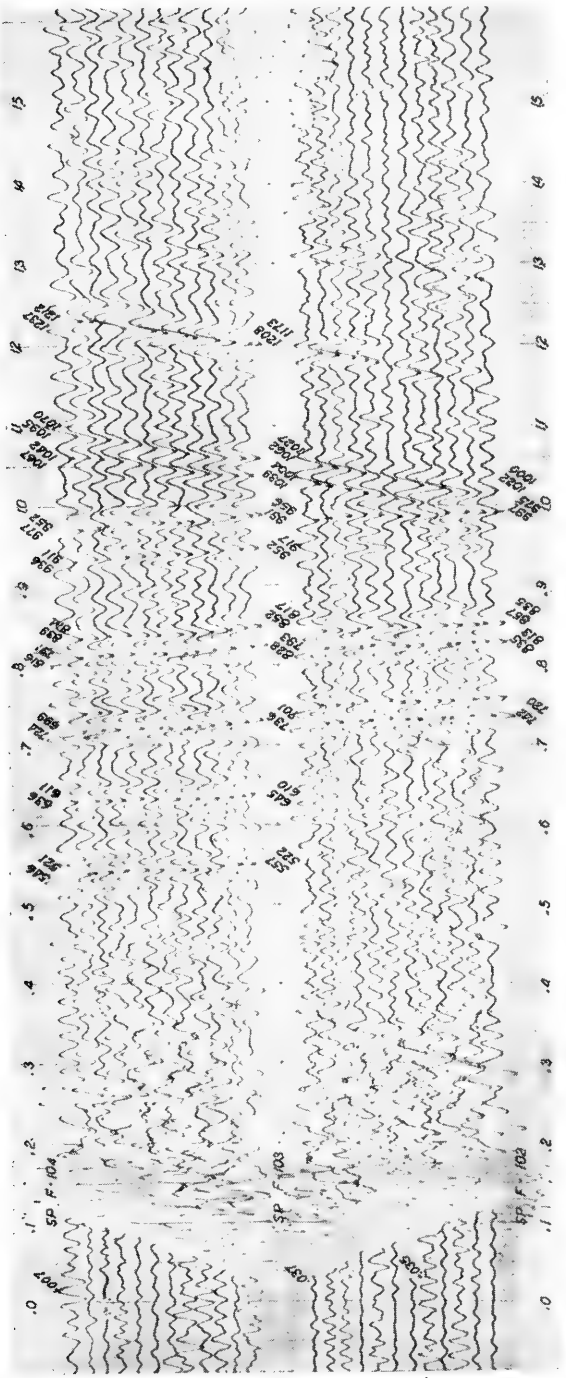

FIG. 431.—A seismogram taken across a synclinal structure, thus showing dips in opposite directions on the same record. The change in dip is indicated during the time interval of 0.8 and 1.2 seconds. (Courtesy of National Geophysical Company, Inc.)

based primarily on reflection time. This process corresponds to running relative elevations on a continuous surface by following along that surface. It has been stated that the recognition of a reflection on a seismogram is based on the correlation of time, wave form, amplitude, etc., among the individual traces of a recorded event throughout the field of seismometers of a particular instrument set-up. By expanding the field of seismometers using a method of overlapping these fields for adjacent stations, the recognized correlation of events on one station may be extended to a second station, then to a third, to a fourth, etc. Under favorable conditions this expansion may be extended to any number of stations. In this manner a single pulse from a persistent reflecting interface may be recognized and its reflection time plotted over an extensive area. This method of correlation is sometimes spoken of as *continuous profiling.*

Since the reflection time is directly proportional to the distance traveled by the reflected wave, these times may be converted into distances and consequently a subsurface set of contours on a particular reflecting interface may be drawn for an area covered by continuous pulse correlation.

A modification of pulse correlation is sometimes used when a persisting pulse cannot be carried throughout an area. Under this condition it is often possible to make single pulse correlations over limited areas only, but usually when one reflected pulse disappears from seismograms of adjacent stations, other correlatable pulses from different reflecting interfaces will be found on the seismograms. By attempting correlations of the various pulses, overlap of the discontinuous correlations often will be obtained. When this has been accomplished, a theoretical surface may be inferred which is more or less parallel to the aggregate of all the correlated interfaces of a particular zone.

Extreme care must be used in inferring such theoretical surfaces, making certain that these surfaces do not pass through known geologic features such as unconformities, stratigraphic overlaps, faults, etc.

Continuous pulse correlation is usually good in most of Oklahoma, West Texas, and parts of Kansas and California. In these areas, the strata dip very gently, seldom more than two or three degrees. Gently dipping strata are not always a sufficient condition for reliable pulse correlation, so that in some cases dip-shooting must be used. It is becoming common practice to utilize both dip computations and correlations wherever possible. The simultaneous use of dip and correlation methods provides essentially two independent types of delineation of subterranean geologic structure. Combination of these two methods usually gives more satisfactory results than can be had by the use of either one or the other separately.

Spot Correlation.—*Spot correlation* is based on character, event sequence, and relative time of reflected events on the seismogram. This type of correlation also corresponds to securing elevations on a particular subterranean surface, but by a slightly different procedure than that used for

continuous pulse correlation, which requires continuous following along the surface in question. Spot reflection correlation may be compared to obtaining elevations by means of an aneroid barometer, and the stations may be relatively large distances apart. Each observation is independent of any other, and the reflections from a certain interface or group of interfaces are recognized and correlated from station to station by wave form, amplitude character, sequence of reflected wave events, and general magnitude of the time for reflection. There is an analogy between this type of correlation and that accomplished by the paleontologist when he recognizes a certain geologic horizon by the presence of a specific fossil fauna.

In regions where competent strata exist over large areas (as, for example, the Denver or Julesburg Basin, containing uniform geological formations of wide areal extent such as the Dakota Sandstone, Madison Limestone, etc.) reflections from certain interfaces seem to persist over extensive areas, and spot correlation shooting is good. However, in areas where relatively incompetent strata occur and to which the term *lenticularity* is frequently applied by the geologist, reflections of definite character do not seem to persist from interfaces extending over large areas, and spot correlations become impossible. Considerable parts of California and the Gulf Coast exhibit this condition. When such areas are explored by seismic methods, recourse usually is made to reflection dip shooting or modified pulse correlation work.

Geological Correlation.—The correlation of reflections with definite geological marker beds can best be made in conjunction with seismic velocity surveys of bore holes. In this manner the reflections can be precisely correlated with or relative to geological marker beds. It is quite common practice for geophysicists to place the reflection record along the "time" coordinate of the seismic velocity survey graph, with the well log along the "depth" coordinate. The reflection times can thus be correlated by inspection with the geologic well log.

An observation often commented on by geophysicists and geologists is that, while excellent correlatable reflections occur over relatively large areas, these reflections are not found to represent any known or recognizable geological horizon marker. For example, excellent reflections often seem to originate from interfaces within what the geologist would describe as a massive stratum of uniform character. During the early period of reflection work this fact caused some suspicions among geologists as to whether the reflection seismograph always mapped geologic structure. The success of the reflection seismograph as a powerful tool for mapping buried geologic structure is based on the condition that the interfaces of discontinuity of the elastic properties of the strata coincide or are parallel to the bedding of the geological formations. Practice has demonstrated this assumption to be sufficiently accurate to give useful and trustworthy estimates of geologic structure. However, it does not necessarily follow that

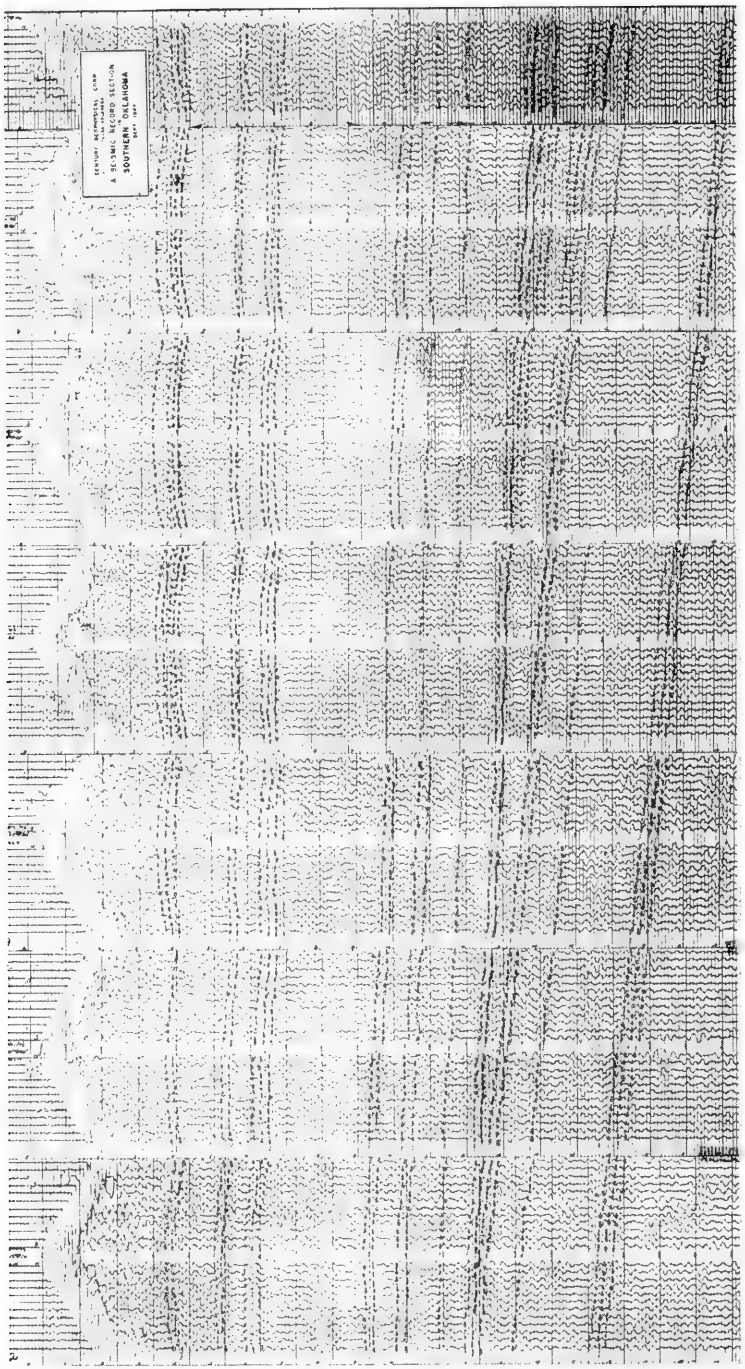

FIG. 432.—A seismic record section in Southern Oklahoma. Compare the curved line-ups of early reflections with those from deeper horizons. (Courtesy of Century Geophysical Corporation.)

all interfaces giving reflections are parallel or coincide with bedding or apparent layering of formations.

Mineralogical replacements and lenticular masses within igneous rocks have been found to give seismic reflections. It may follow that similar conditions in sedimentary formations may also give reflections.

Figure 432, a seismic record section in southern Oklahoma, is a demonstration of reflection correlation whereby a possible stratigraphic oil trap is indicated.

Reflections which correlate with each other from station to station, but do not seem to correspond with any known geologic marker, often are in agreement with the resistivity and/or self-potential correlation on electric well logs.†

Requirements for dip shooting are more severe. A 500-foot spread length is generally much too short. The actual value of the spread length to be used in any area depends on the values observed for ΔT in that area, because the value of ΔT must be appreciably greater than the magnitude of probable error.** (See also the tabulation of ΔT versus spread length for a typical case, page 673.)

In correlation shooting, the identification of the same phase of a reflection is of paramount importance; in dip shooting, the ΔT values corresponding to the reflections under investigation are of paramount importance. As far as type of spread is concerned, in correlation shooting the unidirectional spread is favored, while in dip shooting more use is made of split spreads and continuous profiling.

The dip spread is applicable for correlation shooting, even though short correlation spreads are inapplicable for dip shooting. That this condition is fortunate may be inferred from previous considerations; that is, generally where correlation shooting is used, the dip is so small that accurate dip data could not be obtained without prohibitively long spreads. However, in regions where dip shooting is utilized, correlations quite frequently appear and are plotted. If dip data contradict correlation data, whether dip or correlation or both are to be used rests on the following consideration: Because the reflection time interval for dip determination is obtained on a single record, it is inherently more accurate than reflection time intervals which are recorded on separate records at different shot-points. However, when correlations are carried over shot-points separated by large distances, the difference of reflection time is increased, and this permits increased accuracy. The balance of advantage must also be governed by the reliability of correlations and

† Personal communication from E. J. Handley, geophysicist, Century Geophysical Corporation.

** The accuracy of the travel-time values is of the order of 0.001 sec. at its best and therefore values of ΔT of larger magnitude than this are required. Important inherent deterrents to an accuracy in the ΔT value greater than 0.001 sec. are: general irregularities in the subsurface such as lenticular structure or lateral stratigraphic variation; erratic characteristics of the reflecting horizon; inaccuracies in the correction for the low velocity layer; etc.

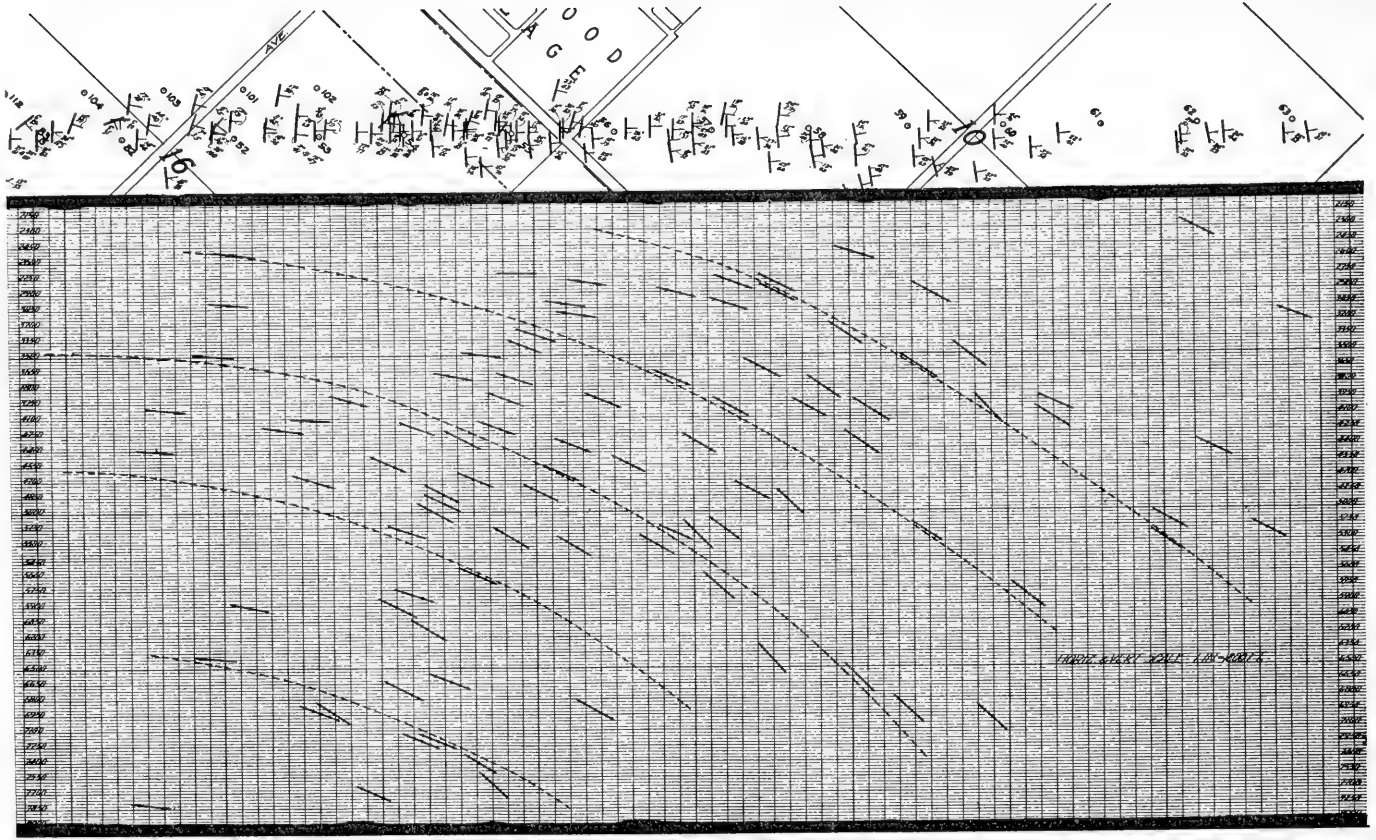

FIG. 433.—Dip shooting results plotted in vertical section and horizontal plane taken from survey in Los Angeles Basin, near Lakewood. Small figures near dips plotted in horizontal plane indicate depth to nearest 100 feet, and dips are given in degrees. (Courtesy of Geophysical Engineering Corporation.)

the possibility that if correlation is carried too far, small intermediate structural features may be overlooked.

An illustration of dip shooting together with a vertical projection of the dips into a horizontal plane is given by Figure 433.

Often the cross section is not used; instead, tabulations of reflection times and depths for each persistent reflecting stratum are maintained separately. These depths are mapped directly, the data being associated directly with the shot-point.

Methods of continuous profiling which have already been treated under dip shooting may in part be used with correlation shooting and their discussion will not be repeated at this time.

Illustrations of Correlation Shooting

An example of field correlation records is shown. These records are not typical in that they constitute better records than obtained in a normal run, and they are used only to illustrate the method of correlation.

The set of correlation records shown in Figure 434 was secured in the vicinity of St. John, Kansas. A symmetric split spread of total length equal to 270 feet was used. The low velocity zone correction was determined only for the two nearest seismometer stations and, correspondingly, reflection time was picked only on the two center traces. Depths below sea level and correlation grades are given at the bottom of the record and the horizon label at the top.

It will be noted that not all reflections are picked. This procedure is customary in correlation shooting where only those beds which persist are of value, particularly when a sufficient number of such beds are present. The characteristics of each reflection are carefully studied, particularly the sequence of phases between neighboring reflections. The presence of these phases in succeeding records is the type of correlation evidence sought.

These records show the possible quality of correlation carried across long distances as the two shot-points were separated by over three miles. The correlating bed labeled A stands isolated and yet can be correlated with certainty due to persistent and distinctive character. This reflection is from the anhydrite layer. Reflections labeled T_1 and T_2 represent the Topeka strata, which again reveal excellent persistency in character.

Treatment of Three-Dimensional Problems

Equivalent Time Horizons and Equivalent Rays. — The three-dimensional structure may be studied with relative ease by introducing the concept of *equivalent time horizons.* Consider a reflecting horizon whose slope at all points is continuous and assume that from every point on the horizon a normal ray is drawn to the ground surface. If the velocity varies with depth only and if the extent of folding of the horizon is limited to such a degree that no rays cross, a one to one correspondence is estab-

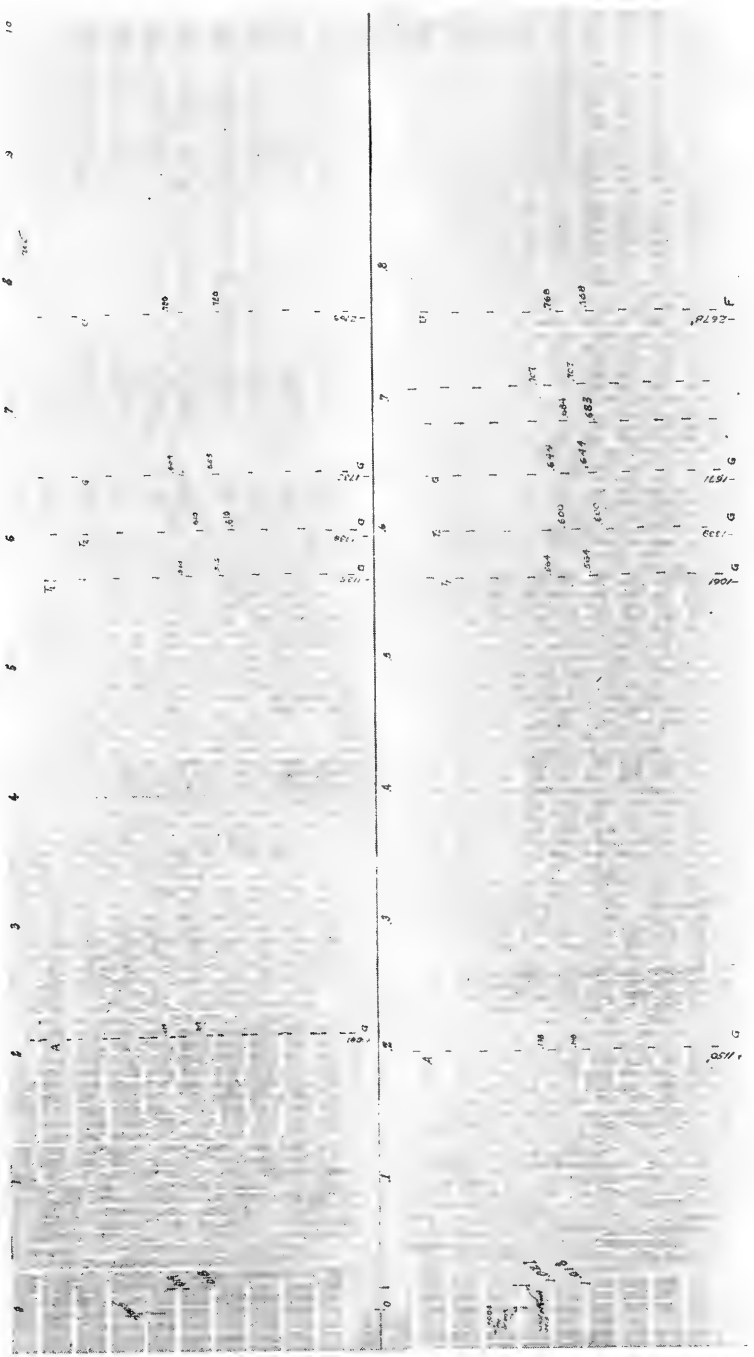

FIG. 434.—Correlation records secured near St. John, Kansas. (Courtesy of Western Geophysical Co.)

lished by the rays between points on the reflecting horizon and points on the ground surface. (Figure 435.) (That is, the reflecting point is associated with a surface point midway between the shot-point 0 and the station S.) Designate by T the reflection time along a normal ray from any point in the medium to the reflecting horizon and back to that point. T is a function of depth and lateral position in the medium. The function is continuous, and at the ground surface it gives the reflection time which would be recorded if the actual rays were normal rays.

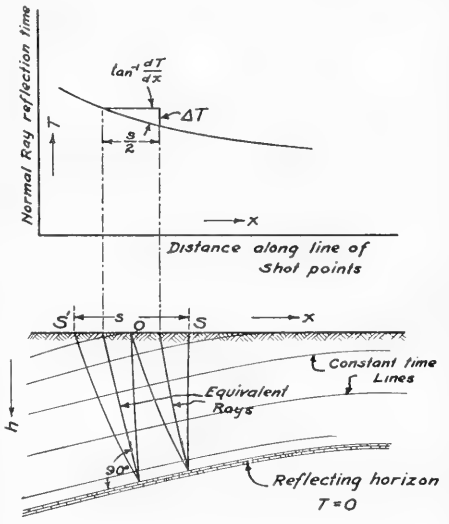

FIG. 435.—Reflection time along equivalent or normal rays.

When the distance from seismometer to shot-point is short compared to the distance from shot-point to reflecting bed, the travel-time along the ray path from shot-point 0 to seismometer S is very approximately equal to the travel-time along the *equivalent ray*: namely, that normal ray which strikes the ground surface at a point midway between shot-point and seismometer. For short symmetrical split spreads, therefore, the ray system to the end seismometers may be replaced by two equivalent rays each impinging on the surface at a distance of $s/4$ from the shot-point, where s is the length of total spread.

When seismometers and shot-points lie on a line, not necessarily along maximum dip,* the recorded reflection times would be given by an arrival-time curve such as shown in Figure 435, where each *observed* reflection time is plotted against a value of x, x being the distance from an arbitrary point on the line between 0 and a point midway between the shot-point and the seismometer station at which that reflection is recorded. Furthermore, the slope dT/dX at any point on this travel-time curve is equal approximately to the difference ΔT in the reflection times to two seismometers such as S' and S divided by half the spread length; or

$$\Delta T = \frac{s}{2}\frac{dT}{dx} \text{ (approximately)} \qquad (69)$$

An equivalent time horizon, from which reflection time gradients in any direction can be determined directly, may be obtained by plotting the values of the reflection time along the normal rays at the points of inter-

* Compare following section entitled "Vector Composition of Reflection Time Gradients."

section of the rays with the ground surface and drawing a smooth curve through the plotted points.

Vector Composition of Reflection Time Gradients.—In general the direction of the true dip of the underground strata is seldom known before the shooting, and therefore the instrument spread will be found oriented obliquely with respect to the true dip of the reflecting bed. The resulting problem of dealing with components of dip as related to the ΔT obtained with spreads oriented at an angle to the true dip is somewhat involved when exact solutions are desired. The problem may be simplified by proceeding with computations on the assumption that the component of dip of the reflection bed in the direction of the spread is related to the ΔT recorded at that spread by the equations derived for spreads along the direction of the true dip of reflecting bed.

A more exact solution can be obtained as follows: At a given point on the ground surface, a spread in the direction of maximum gradient of reflection time will be oriented along true dip, while a spread in the direction of zero gradient or constant reflection time will be oriented along strike. Furthermore, because the gradient of any scalar quantity is a vector, the component of the time gradient in any direction is obtained by the usual procedure for resolving vectors. Hence, if the maximum gradient of the reflection time at a point P on the ground surface is $(dT/dx)_{P\,\max}$, and is directed, for example, due north, the magnitude of the gradient at a bearing ϕ is:

$$\left(\frac{dT}{dx}\right)_{P,\max} \cos \phi$$

The vector property of the time gradient is applied in the following manner. Draw two lines radiating from point 0, each in the direction in which the time gradient was determined from dip reflection shooting. (Figure 436.) Choose a convenient unit of length and mark off lengths equal to the magnitude of the corresponding time gradient. Strike off normals to the vectors at their tips. The intersection of these normals establishes the point of the maximum gradient vector; that is, the length of the vector delimited by the point 0 and the intersection of the normals is proportional to the magnitude of the maximum gradient and its direction is parallel to that of the maximum gradient. The magnitude and direction of true dip is thus obtained from the determination of values of ΔT in two directions.

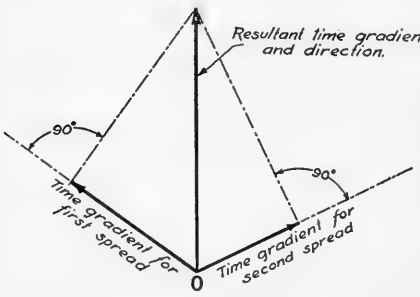

FIG. 436.—Composition for maximum reflection time gradient.

The most effective relative orientation of spreads for determination of true dip is one in which the spreads are at right angles to each other. In this case, the magnitude of the maximum gradient is equal to the square root of the sum of the squares of the component gradients, and its direction makes an angle with the direction of one of the spreads which is proportional to the inverse tangent, or cotangent, of the ratio of the component gradients.

After the magnitude and direction of the maximum gradient have been obtained, the gradient is expressed in terms of ΔT by means of Equation 69. The ΔT thus found is then inserted in Equation 21.

$$\sin\theta = \frac{\Delta T}{S} V \tag{70}$$

where $\dfrac{\Delta T}{S} = \dfrac{dT}{dx}$ of Equation 21.

It is customary to locate shot-points along a straight line ("shot-point line") in order to gain approximately a vertical cross-sectional view of the geologic strata. When *cross dip,* i.e., dip normal to the shot-point line, is small or constant, a close approach to a vertical section may be obtained. Because dip data along a line may be treated more readily than data in scattered directions, stress is sometimes given to *line spreads,* and *cross spreads* at some of the shot-points on the shot-point line are omitted.

Rigorous interpretation of dips over a prospect can be achieved by time gradients. In dip shooting, time gradients alone are determined and the process of preparing an equivalent time horizon is similar to that of preparing a contour map from a knowledge of dip only; that is, an equivalent time horizon is obtained by running time phantoms incorporating the time gradients. The time maps would be converted to space maps by measuring maximum time gradients and applying the equation (70) already established for true dip.

In general, however, the data from seismograms are converted into space coordinates long before a space map is drawn up in order that direct space information on a prospect may be furnished during the course of the survey.

The usual procedure is to utilize the time gradients determined along the line spread as though they were maximum gradients and to plot space coordinates computed from these time gradients on a vertical section through the shot-point line. The degree of approximation implicit in a vertical section of this sort depends on the magnitude of cross dip and its change along the section.

From geometric considerations, it is apparent that because the tangent of dip is a gradient of depth, the tangent of true dip of a sloping plane is related to the tangents of the component dips in exactly the manner that the maximum time gradient is related to its components.

Hence, the approximation introduced by using time gradients in the direction of the spread to determine the component of dip in that direction is subject to an error of the same degree as that by which the true dip as a function of ΔT *for a given reflection time* deviates from a linear function.

In these considerations it is assumed that the seismometer spread distance is sufficiently short so that equivalent rays may be used. When this is not the case a correction should be considered.

The Low Velocity Layer.—In practically all areas, a layer occurs at the surface of the earth which is unconsolidated, and often heterogeneous in character, and transmits waves at low velocity. The thickness of the layer may vary from almost zero to several hundred feet; however, the most common thickness is from about 25 feet to 100 feet.

In literature on seismic prospecting, the term "weathered" is frequently applied to this layer although this is a misnomer in that the layer may not necessarily exhibit a weathering condition. Furthermore, the term "weathered layer" as used by seismic investigators differs in meaning from the well established term "zone of weathering" used by geologists. The terms, low velocity, aerated and unconsolidated layer, are also used.

Of importance to seismic prospecting is the low velocity property of this layer; most commonly between 1500 and 2500 ft./sec., in contrast to velocities of about 6,000 ft./sec. and more in the deeper layers. The term "low velocity layer," therefore, has found increasing favor and will be used here.* The low velocity layer may consist of more than a single layer, and it is customary to define this layer simply as one having a velocity less than about 5,000 ft./sec.—or less than any other velocity when occasion arises.

Special attention must always be directed to the low velocity layer in seismic prospecting because the usual heterogeneous character of this layer would lead to inaccurate results if the anomalous velocity in this layer were not taken into account. The layer plays but a small part in the subsurface section despite its relatively large effect on travel-time data and must be taken into account before the data can be analyzed.

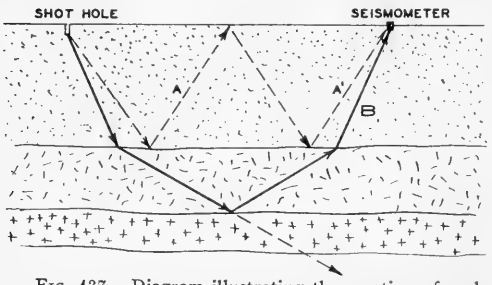

FIG. 437.—Diagram illustrating the creation of multiple reflections (A) when the shot-point is placed near the surface.

Figure 437 illustrates a theoretical effect that may be ob-

* To avoid excessive repetition of the terms *velocity of the low velocity layer* and *vertical travel-time in the low velocity layer,* these terms will be designated by V_u and t_u respectively, and the symbols will be used.

The subscript u may stand for *unconsolidated* or for *upper layer. Consolidated* is here used in the sense of unaerated; that is, a condition in which large interstices, if any, between grains are filled by water or by cementation.

tained when the shot-point is placed in the low velocity layer, at or near the surface of the ground.

The shot wave traveling downward in all directions will encounter the boundary between low velocity surface layer (1) and the underlying higher velocity layer (2). Because of the physical discontinuity between these two layers, a considerable portion of the energy is reflected at the top of the underlying layer. This reflected energy *A* traveling upward may be again reflected when it hits the surface-air interface of the upper layer, and travels back downward towards the lower interface, where the process is repeated, thus giving rise to an indefinite number of reflections or reverberations *A, A'*, etc. This reverberation will tend to mask the desired reflection *B,* and the seismometer will continue to be disturbed for a prolonged period of time by a series of shallow reflections, depending upon the acoustic properties, form, and dimensions of the low velocity layer. This undesirable condition can be greatly minimized by placing the shot-point below the low-velocity boundary, whereby more of the shot energy will go into the lower layer directly to produce stronger reflections from the deeper strata.

The source of knowledge on the low velocity layer is confined almost entirely to experiences in seismic prospecting. Research has not given a clear explanation of the low velocities found in this zone in terms of the observed properties of the layer. However, calculations for velocities for soil and air mixtures have demonstrated low velocities of the magnitudes observed in practice.† Velocities as low as 550 to 1600 feet per second have been measured in the uppermost part of this zone. In most cases the bottom of the low velocity layer is closely associated with the top of the ground water table. This layer is also characterized by generally poor seismic wave transmission qualities, and for this reason the shots are usually placed below or near the bottom of the zone. Explosives detonated below the low velocity layer produce more efficient and effective origins for seismic waves than shots placed within the low velocity zone.

The difference in velocity between the low velocity zone and the rocks below it seems to be related to the porosity or unfilled voids present. An increase in porosity of unconsolidated materials when the pore space is filled with air decreases the modulus of elasticity and the wave velocity of the material. However in the case where the pore space is filled with moisture, the modulus of elasticity of porous material is increased. This is probably the situation at the top of the permanent water table, which usually marks the bottom of the low velocity layer. Associated with the increase of the modulus of elasticity, an improvement in the wave transmission quality is noted. In field procedures, wherever possible, practical use is made of this improvement by placing the explosive charges below the water table. The increase of water content in unconsolidated materials does not have a parallel effect in the case of consolidated geological units such as sand-

† O. C. Lester, *A.A.P.G. Bull.*, Vol. 16, No. 12, pp. 1230-1234, Dec., 1932.

stones, limestones, schists and relatively porous igneous rocks. An increase in water content of these rocks seems to be associated with a decrease in velocity; however, this decrease is not as appreciable as the increase of velocity in the case of water-saturated unconsolidated rocks. The effect of water saturation of rocks on seismic velocity is obviously complex.

Evaluating Effects of Low Velocity Layer.—In general practice the so-called "weathering" problem is handled by one of two methods. In one method, the effect of the low velocity layer is eliminated by actually making all the seismic observations below this layer or zone. The second method may be described as a process of low velocity shooting, in which the velocity and the thickness of the layer or zone are measured.

In the first method, making the observations below the low velocity layer, the shot-point and the seismometers are placed at or below the contact between the low and the higher velocity layers.† Under these conditions there is no delay due to the presence of the low velocity layer. Somewhat better mechanical coupling between the seismometers and the earth is obtained, and thus more efficient detection of earth displacements may be realized. The most serious difficulties in using this technique are the numerous drill holes necessary for the seismometers, and the retrieving of instruments from the drill holes after the observations have been made.

In the second method, that of low velocity shooting, results are obtained much more rapidly and economically, but they may not be as precise. The accuracy is usually sufficient for normal commercial operations, and we can express our computations in three general ways, all giving substantially equivalent results. First, the low-speed layer may be theoretically replaced with materials of the same seismic velocity as that which underlies this layer. Second, by calculation, it is possible to reduce the observed times to correspond to a situation in which both the shot-point and the seismometers are placed at the bottom of the low velocity layer. Third, all observations may be reduced to a theoretical reference plane or datum level, as is sometimes done in surveying. This reduction is obtained by calculating what the observed times would be if both the detecting seismometers and the shock charge were placed on the datum plane of a given elevation.

A study of the surface or low-velocity layer reveals that in general three conditions exist: (1) the properties of the zone may be relatively constant over a considerable area; (2) the velocity and thickness of this layer may be approximately the same at the shot hole and along the profile of seismometers, but considerable difference may exist between shot-point locations: i.e., the velocity and thickness may vary considerably in an area to be surveyed but not perceptibly beneath a single instrument set-up; (3) the variations of the low-speed zone may be perceptible beneath a single instrument set-up.

† B. McCollum, "Method and Apparatus for Studying Geologic Structure," U. S. Patent 1,676,619, July 10, 1928.

Therefore an acceptable method of correcting for the delay of the seismic waves in passing through the low velocity layer should give proper results under all the above-mentioned conditions.

Errors in the application of the so-called "weathering correction" affect the seismic results in two general ways. The calculated depths to the reflection surfaces are only as accurate as the correction used, other factors being equal. In reflection correlation work, errors in this correction may lead to erroneous correlations of reflected impulses recorded from adjacent shot-points. Another problem arises when the proper impulses are correlated and the depth computations are affected by unknown thickening or thinning of the surface or low velocity layer. Another way in which errors in the correction may influence the seismic results is found in the dip computations. In areas of extremely low relief structures, errors in the application of the low velocity data may completely mask the changes due to structure. In areas where insufficient low velocity layer data are obtained, the errors may be of the same order of magnitude as the measured step-out time caused by the inclinations or attitudes of the reflecting interfaces. It therefore follows that, when using the reflection method to investigate areas in which the attitudes of the geological beds are of the order of zero to three degrees from the horizontal, extreme care must be used in obtaining measured data on the surface low velocity layer.

Time Corrections for Low Velocity Layer.—For the sake of simplicity the following discussion will refer all computations of depth and reflection time to the base of the low velocity layer. Data reduced in this manner may be referred to any other datum merely by adding algebraically the interval between the bottom of the low velocity layer and the elevation of the desired reference datum.

For a shot at depth H, the time to be deducted from the observed reflection time to eliminate the effect of the low velocity layer and to refer the time to the *base of the low velocity layer* is:

$$t_u' = \frac{U_0 - H}{V_{u,0}} + \frac{U_s}{V_{u,s}} \quad \text{for } H < U_0$$

$$t_u' = \frac{U_s}{V_{u,s}} - \frac{H - U_0}{V_c} \quad \text{for H} > U_0 \tag{71}$$

where H is the depth of the shot

U_0 is the thickness of the low velocity layer at the shot-point

U_s is the thickness of the low velocity layer at the seismometer

$V_{u,0}$ is the velocity of the low velocity layer at the shot-point

$V_{u,s}$ is the velocity of the low velocity layer at the seismometer

V_c is the velocity of the consolidated section immediately below the low velocity layer

To obtain a mean *datum point* between shot-point and seismometer, the elevation of the base of the low velocity layer to be used is:

$$E_u = \frac{E_0 + E_s}{2} - \frac{U_0 + U_s}{2} \tag{72}$$

where E_0 = elevation of shot-point above mean datum
E_s = elevation of seismometer above mean datum

The problem of determining the *travel-time* in the low velocity layer is one for which the refraction method is well adapted and for which the reflection method is inapplicable. A method essentially the same as that already described for a two-layer section, page 666 is used. However, the *velocity* in the low velocity layer cannot be determined accurately from the slope of the direct wave travel-time curve for short distances, because the velocity in the low velocity layer is not constant in the vertical direction.

The most accurate direct determination of the average velocity of the low velocity zone is obtained by so-called *up-hole shooting*: several light shots are discharged at varying depths in a shot-hole and the first-break times are recorded with the aid of a single seismometer placed at the shot-point.* The depth versus first-break time curve will indicate the thickness of the low velocity zone and the travel-time in this zone. (Figure 438.) (The thickness of the low velocity zone may also be obtained by electrical resistivity measurements. The electrical method is especially advantageous in that the thickness can be determined accurately at several points with relative rapidity.)

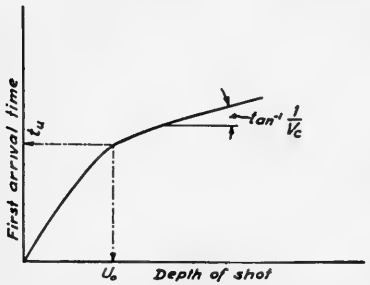

Fig. 438.—Low velocity layer diagram from up-hole shooting. t_u = vertical travel-time through low velocity layer; U_o = thickness of low velocity layer.

The use of this type of curve would dispose of the low velocity layer problem were it not for the fact that the low velocity layer is seldom uniform, even over the length of a spread. A difference of several milliseconds in the vertical travel-time in the low velocity zone is sometimes present between seismometers separated by only a few feet. It is impractical to drill holes below every seismometer in order to secure complete low velocity zone data and therefore some approximation must be made. As stated in the last paragraph, the vertical travel-time but not the velocity in the low velocity layer can be obtained accurately by the refraction method. However, because the depth U_0 of the low velocity layer and the average vertical velocity V_u in this layer may both vary from point to point along the surface, an estimate of the variation of each must

* *Up-hole shooting* or *coming up the hole* at a new location is frequently employed to determine the best depth for shooting.

depend on trend of data obtained from scattered up-hole shooting in a given region.

Figure 439 shows the ray paths for reflected waves and the paths for first-break or first arrival-times. The shot usually is placed below the low

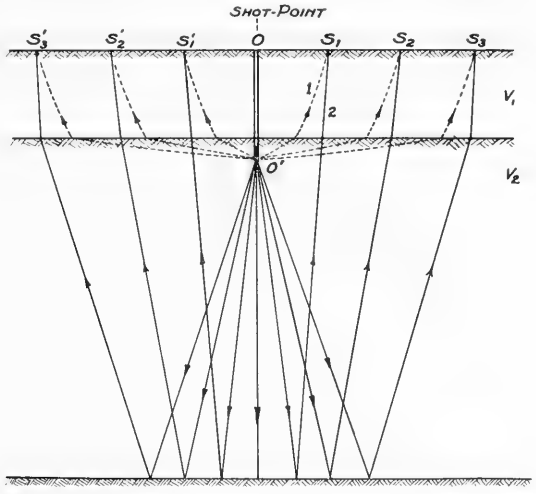

FIG. 439.—Ray paths for reflected and refracted rays. 1, first arrival ray paths; 2, reflected ray paths.

velocity layer. For the present investigation, it will be assumed that the shot is placed at a short distance below the base of the low velocity zone and that the ray paths for first arrival waves are essentially horizontal in that part of the paths which is in the consolidated zone, i.e., below the low velocity layer. Figure 440 shows the corresponding low velocity zone refraction diagram, where first arrival-times are plotted versus distance from shot-point. The slope of the best-fitting straight line through these points is the reciprocal of the velocity V_c in the top of the consolidated section.

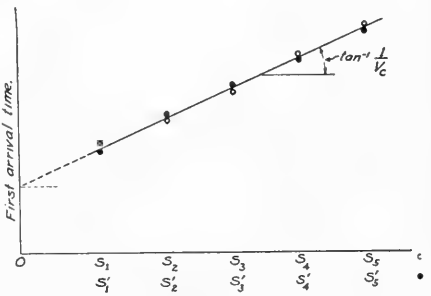

FIG. 440.—Low velocity layer refraction diagram.

Treating the velocity V_u in the low velocity layer as though it were constant in the vertical direction, the angle of the first arrival ray at the surface is given approximately by the critical angle equation

$$\sin \theta_k = \frac{V_{u,k}}{V_c}$$

where $V_{u,k}$ is the average vertical velocity between the base of the low

velocity layer and the kth seismometer. The first arrival-time to the kth seismometer is derived in the same manner as was Equation 12. That is,

$$t_k = \frac{\overline{0S_k} - U_k \tan\theta_k}{V_c} + \frac{U_k}{V_{u,k}\cos\theta_k}$$

where $\overline{0S}_k$ is the horizontal distance from the shot-point to the kth seismometer. But from the critical angle relation,

$$\cos\theta_k = \sqrt{1 - \left(\frac{V_{u,k}}{V_c}\right)^2} \quad \text{and} \quad \tan\theta_k = \frac{V_{u,k}}{V_c\cos\theta_k}$$

$$t_k = \frac{\overline{0S}_k}{V_c} + \frac{U_k}{V_{u,k}}\sqrt{1 - \left(\frac{V_{u,k}}{V_c}\right)^2} \tag{73}$$

Referring to the approximately vertical direction assumed by those rays in the low velocity layer which are of importance, it is desired to determine the vertical travel-time $t_{u,k}$ through the low velocity layer, where

$$t_{u,k} \equiv \frac{U_k}{V_{u,k}} \tag{74}$$

On solving Equation 73 for U_k, one obtains

$$U_k = \frac{\left(t_k - \frac{\overline{0S}_k}{V_c}\right) V_{u,k}}{\sqrt{1 - \left(\frac{V_{u,k}}{V_c}\right)^2}}$$

Hence

$$t_{u,k} = \frac{t_k - \frac{\overline{0S}_k}{V_c}}{\sqrt{1 - \left(\frac{V_{u,k}}{V_c}\right)^2}} \tag{75}$$

Because, in general, the effect of $V_{u,k}$ in this equation is only about 5% or less in the practical case, it is sufficient to assume that $V_{u,k}$ may be replaced by the V_u found from up-hole shooting at the shot-point.

It is seldom felt justified to expend the effort in up-hole shooting at every shot-point in a prospect for low velocity layer data alone. Instead, a seismometer is left at the shot-point in routine set-ups and is used to record the shot-hole time. (See fifth trace of Figure 441.) This *shot-point seismometer* acts as a rough gauge of the change in V_u from point to point and is used in conjunction with the low velocity layer refraction diagram.

The correction for variation in velocity or thickness of low velocity zone is particularly important when the difference in reflection times due to dip of reflecting strata is to be determined. This time difference ΔT is itself a comparatively small quantity; hence, it frequently is of the

same order of magnitude as the variations in the quantity t_u corresponding to the various seismometers of the same spread. The difference in travel-times through the low velocity zone to any two seismometers (Δt_u) is obtained by subtracting two terms of the form given by Equation 75. To avoid introducing the velocity V_c in the evaluation of Δt_u, the distances from the two seismometers to the shot-point are made equal; also,

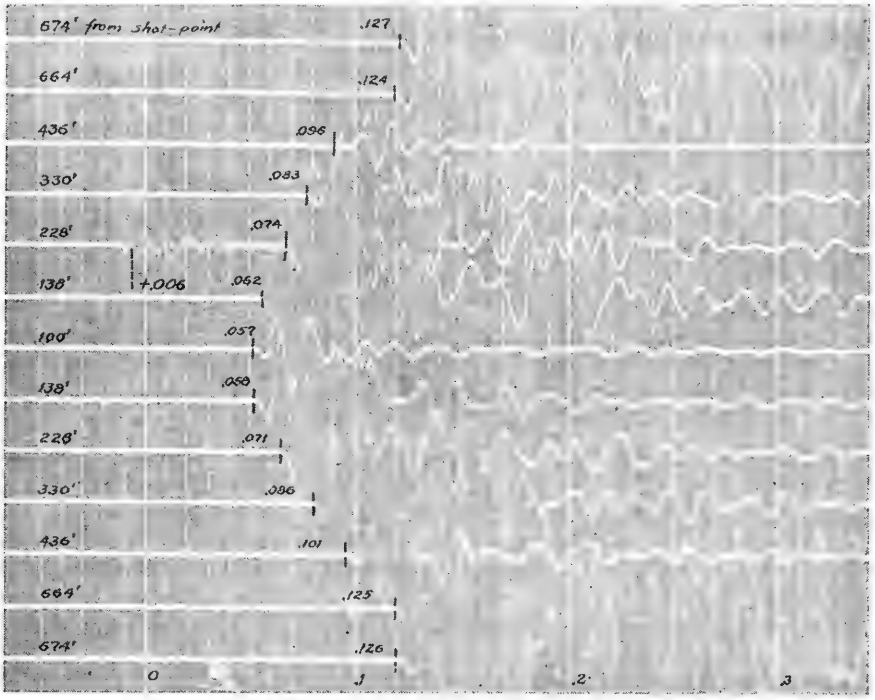

FIG. 441.—Low velocity layer refraction record. (Courtesy of Western Geophysical Co.)

the radical term can easily be reduced to unity within the general degree of accuracy.* Hence, the differential low velocity layer correction is

$$\Delta t_u = t_k - t_{-k}$$

where t_k and t_{-k} are the first arrival-times at the seismometer stations "k" and "$-k$" respectively. The first arrival-times of a record are thus used directly to obtain the correction which must be applied to the dip time difference ΔT to compensate for variations in the low velocity layer.

* Setting the radical term equal to unity is equivalent to assuming that the critical angle is 90° or that the waves travel through the low velocity zone in a vertical direction.

An example of a low velocity zone refraction record is shown in Figure 441. This record illustrates a type which is especially designed for an accurate determination of the ΔT correction for extreme points of the spread. At each end of the spread two seismometers separated by only a few feet are used to obtain the first arrival-times. This form is sometimes used when more than one seismometer feeds the end traces of a dip record* and the condition of the low velocity layer at each seismometer is to be determined. The record shows that the magnitude of the velocity V_c is approximately 8200 ft./sec. (Compare Figure 442.)

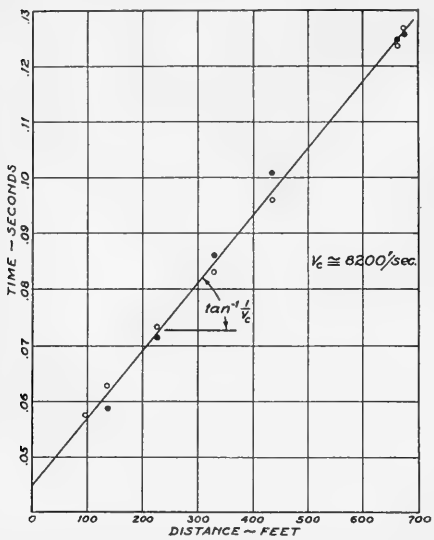

FIG. 442.—Refraction diagram corresponding to Figure 441. Open circles correspond to arrival-times at seismometers located on one side of the shot-point and solid circles correspond to arrival-times at seismometers located on the other side of the shot-point. The irregularity of the low velocity layer is indicated by the scattered character of the points.

It will be recalled that relations between dip time difference ΔT and the magnitude of dip were obtained on the basis of seismometer stations at the same elevation. Consequently, when the base of the low velocity layer is at different elevations at the seismometer stations, one must apply an elevation correction, ΔT_{El}, to the dip time difference ΔT. This correction, ΔT_{El}, is equal to the difference of elevation divided by the velocity V_c in the consolidated zone. The problem again arises as to variation of thickness H of the low velocity layer over the length of the spread and may be handled by scattered up-hole shooting, as already mentioned.

The treatment of the low velocity layer has presumed a constant value for the velocity V_c in the consolidated zone, the assumption being based precisely upon the consolidated nature of the lower zone. Although generally uniform, V_c does vary over the length of a spread in some regions. A test of the constancy of this velocity may be attained by employing so-called checking shot-points placed on a line normal to and passing through the center of the spread, as will be evident from the following considerations: The difference Δt_u of first arrival-times to symmetrically located seismometer stations depends on the low velocity layer conditions alone only if the velocity V_c in the consolidated zone is constant; hence, a test of the constancy of V_c consists in observing how constant the difference Δt_u remains for successive shot-points placed in the prescribed manner, preferably on opposite sides of the first shot-point.

The pattern or "line-up" of a reflection will be modified by the low

* See section on Multiple Detectors, p. 853.

velocity layer from that which would be expected from purely geometric considerations of reflected rays. The "line-up" in fact is largely determined by the low velocity zone in those cases where split spreads are used for mapping of deep beds.

Furthermore, the reflection pattern must be examined not only with a view to identifying reflections but also with a view to reading reflection time differences accurately on the records. This is the case because the evaluation of the reflection time difference is usually based on the trend of several traces adjacent the end traces, as well as the end traces themselves.

Time Corrections for End Shots, Low Velocity Layer.—The foregoing corrections can be applied equally well to any set-up in which the seismometers are placed in symmetrical pairs and the shot-point lies in the plane of symmetry. However, it is often desired to record with end-shots, or instrument set-ups in which the shot-point is placed outside the spread of the seismometers, usually not more than two or three hundred feet from the nearest seismometer. In this case the reflection time is taken at the nearest instrument to the shot-point; the shot-point distance is generally small enough so that this time may be considered approximately equal to the reflection time which would have been recorded at the shot-point. Correction of the reflection time for the delay in the low velocity layer is made exactly as in the case of symmetrical spreads about the shot-point. However, the step-out time correction of t is a little more difficult. Applying Equation 75 and assuming the number of seismometers to be n, with the nearest seismometer at a distance X_1 and the most distant seismometer at the distance X_n from the shot-point, we may write Equation 76 as an expression of the difference in vertical travel time $(\tau_1 - \tau_n)$ through the low velocity layer at the respective positions of seismometers number 1 and n.

$$\tau_1 - \tau_n = \frac{(t_1 - t_n) - \dfrac{X_1 - X_n}{V_c}}{\sqrt{1 - \left(\dfrac{V_u}{V_c}\right)^2}} \tag{76}$$

This expression involves the additional term, $(X_1 - X_n)/V_c$ introduced by the set-up asymmetry. Obviously small uncertainties in V_c will introduce a large percentage of error in the determination of $(\tau_1 - \tau_n)$. This difficulty is eliminated by shooting at the other end of the set-up, at a depth and distance sufficient to insure that the refracted waves will penetrate below the low velocity layer. In this case

$$\tau_1 - \tau_n = \frac{(t'_1 - t'_n) - \dfrac{X'_1 - X'_n}{V_c}}{\sqrt{1 - \left(\dfrac{V_u}{V_c}\right)^2}} \tag{77}$$

the second observations being designated by primes. Since

$$X'_1 - X'_n = -(X_1 - X_n)$$

$$\tau_1 - \tau_n = \frac{(t_1 - t_n) + (t'_1 - t'_n)}{2\sqrt{1 - \left(\frac{V_u}{V_c}\right)^2}} \tag{78}$$

and the desired correction is obtained almost independently of any knowledge of the underlying higher velocity zone, V_c. This method of measuring the correction is often more accurate than that given by Equation 75. Care should be taken that penetration to the underlying zone V_c is obtained, and if possible, shot-points should be located at equal distances from the ends of the instrument spread and the shots placed at relatively the same depth, in order that the same penetration will be achieved at each shot.

This system may be applied to split spreads by shooting shot-points at each end of the split spread. For isolated shot-points this would require the drilling and shooting of two extra shot holes. Though the two extra shot holes need not be as deep as the one from which the reflections are recorded, this extra work would consume considerable time. In the case of continuous profile work on the reflecting interface, adequate information on the low velocity layer is obtained more or less as a by-product of the continuous profiling. It therefore becomes obvious that the thoroughness of the application of the correction for the delay due to the presence of the low velocity layer is often a concession on the part of accuracy to the time and money available for securing data in the field.

In general the accuracy required need not be greater than that necessary to obtain pertinent and reliable information on the subsurface geological structure. For example, if the attitudes of the geological markers need be expressed in feet per mile rather than degrees of dip because of extremely low relief of the geologic structure, then great accuracy is needed in applying the correction for the low velocity zone. On the other hand, if the dip of the subsurface beds exceeds 10 or 15 degrees, the accuracy in the application of the correction need not be so great.

Method of Differences.—The method of differences has been found useful in estimating the thickness of the low velocity layer when a great difference in velocity occurs at its lower boundary. This method was first used in the solution of two-layer refraction problems measuring the thickness of overburden lying on an irregular bedrock surface.† Because of its simplicity and ease of application the method has met with considerable favor. It makes use of the refracted travel times recorded from shot-points placed at both ends of the line of seismometers.

In refraction work the shock origins are in shallow holes in the overburden, while in reflection work these origins are usually at or near the

† A. B. Edge and T. H. Laby, *Principles and Practices of Geophysical Prospecting*, pp. 339-341, Cambridge University Press (1931).

boundary between the low velocity layer and the high-speed consolidated material. This variation requires a slight modification of the system to make it applicable for measuring the thickness of the surface layer at each seismometer location.

Consider a shock wave origin at the point P, Figure 443. The wave thus generated reaches the point Q with a velocity V_c and emerges at the point C, traveling from Q to C with the velocity V_u. The time T_{PQC} for the wave to travel from P to C by this path may be expressed

$$T_{PQC} = \frac{PQ}{V_c} + \frac{W_c}{V_u} \tag{79}$$

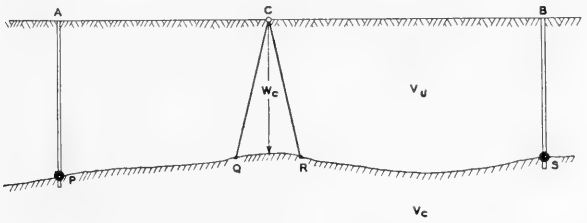

FIG. 443.—Method of differences.

where W_c is the thickness of the low velocity layer at the seismometer station C. W_c may be taken as a first approximation of that portion of the ray path QC or RC through the low velocity layer, because of the near-vertical incidence associated with the high contrast in velocities (V_u as compared with V_c).

Similarly, for a shock wave origin at the point S, T_{SRC} may be expressed

$$T_{SRC} = \frac{SR}{V_c} + \frac{W_c}{V_u} \tag{80}$$

Adding Equations 79 and 80 and solving for W_c

$$W_c = \frac{1}{2}\left(T_{PQC} + T_{SRC} - \frac{PS}{V_c} \right) V_u \tag{81}$$

After W_c has been estimated by Equation 81, then the order of the magnitude of the distance, QR, which was neglected in placing $PQ + SR = PS$, may be approximated by the expression

$$QR = 2W_c \frac{V_c}{V_u} \tag{82}$$

i.e., $\tan^{-1} \dfrac{W_c}{QR/2} \cong \sin^{-1} \dfrac{W_c}{QR/2} = \sin^{-1} \dfrac{V_u}{V_c}$

and a corresponding correction applied to the distance PS in making a second approximation of W_c. The quantity $\dfrac{PS}{V_c}$ may be checked experimentally by recording the travel times at both points A and B.

It is to be noted that the value of W_c obtained by Equation 81 depends directly on the value of V_u, and therefore uncertainties in the unconsolidated layer velocity will introduce corresponding errors in the determination of the thickness of the low velocity layer. A check on the value of V_u may be secured by frequent direct measurements by shooting a charge at various depths and recording the travel time to the surface. See Figure 438. When the time is plotted as a function of depth, the velocities are obtained from the reciprocal slopes of the time depth curve. Often these plots show a sharp break at the bottom of the low velocity layer as shown by Figure 438.

At other locations the time-depth plots will show a gradual transition rather than a sharp discontinuity of the velocity at the base of the low velocity zone. This is shown in Figure 444. In this case an average value of the velocity used is equal to the depth at which the velocity first reaches V_c, divided by the travel-time to that depth.

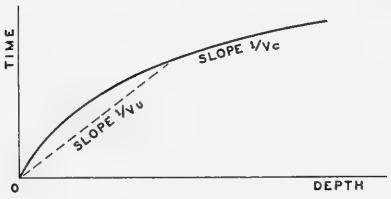

FIG. 444.—Graph showing velocity increasing with depth.

In practice a continuous check of the value of V_u is maintained by a study of the up-hole times recorded at each shot. This procedure also gives information as to whether or not the explosive charge has floated up the hole and serves as a means of explaining certain types of seismograms obtained in field practice.

The value of V_c has been found to vary within certain limits. This velocity can be checked by a study of the travel-time distance plot of the instrument spreads. However, upon an inspection of Equation 81 it will be noted that small uncertainties in the value of V_c do not result in large percentage errors in the value of W_c, the thickness of the low velocity layer at station C.

Some systems of computation do not make use of the thickness of the low velocity layer, but instead make the correction for the delay in the low velocity layer by use of the time T_{Wc}, the time necessary for the wave to pass through this layer. An expression for this quantity T_{Wc} may be written from inspection of Equation 81.

$$\frac{W_c}{V_u} = T_{Wc} = \frac{1}{2}\left(T_{PQC} + T_{SRC} - \frac{PS}{V_c} \right) \tag{83}$$

In making corrections for the delay caused by the presence of the low velocity layer, it should always be borne in mind that the wave paths of the P-wave and the reflected waves through the low velocity layer are different. This fact constitutes an inherent source of error when the low velocity correction is made from the P-wave alone. Although a reliable correction can usually be made, there are occasions, particularly when the low velocity layer is thick and the ray paths have a large angle with the vertical, when the uncertainty is large.

Application of Least Squares to ΔT.—After the delay of the reflected wave in the low-velocity layer and the elevation corrections have been applied to each recording trace of the seismogram, the next procedure is to establish the value of the step-out time ΔT to be used in the computation of the dip of the reflecting interface.

All necessary calculations could be made by the use of the step-out time of the two outside traces alone, or the data from any other pair of seismometers could be separately computed. When this is done, it is generally found that the results using different pairs recording the same reflection differ somewhat because of experimental errors of the individual traces.

It is desirable to obtain the best possible final result by averaging separate pairs of the step-out time measurements. It is also recognized that the percentage of probable error of the more distant traces is less than the corresponding errors of those traces which are nearer to the center of a split spread. Thus, it is obvious that more weight should be given to the outside pairs of traces, other conditions being equal, in obtaining the averaged value for ΔT.

The theory of least squares dictates that the weight to be given to any one measurement, when averaging it with other similar measurements, is inversely proportional to the probable error of the measurement.

Since the desired result is the ratio of the step-out ΔT to the spread S, if each trace has the same probability of error as any other trace, then the probable error in any one measurement of $\Delta T/S$ will be inversely proportional to S, and the weight of the measurement, λ, will be proportional to the square of S. Applying this to an actual case of 12-trace record in which the instrument interval is uniform over the entire length of the spread, let t_1 be the outside step-out time, t_2 the step-out time of the next inside pair, etc. Let the distance S be expressed in terms of trace intervals. The averaging can be conveniently done in tabular form, as in Table 22.

TABLE 22

t	S	λ	$t\lambda/S$
0.013	11	121	0.143
0.008	9	81	0.072
0.009	7	49	0.063
0.004	5	25	0.020
0.003	3	9	0.009
0.000	1	1	0.000
Totals		286	0.307

The weighted average of t/S is the total of the fourth column divided by the total weights in the third column. The weighted average step-out time for the total spread is obtained by multiplying this figure by 11, the spread length in units of trace intervals.

$$\text{Average } t = 0.307/286 \cdot 11 = 0.0118 \text{ sec.}$$

Some computing methods treat the low velocity correction or the delay by obtaining an average of the differences of the symmetrical traces, using the above method and thus finding an average correction for the instrument spread. Then an average is obtained for the uncorrected step-outs and the average correction applied to this figure.

Some argument has been presented suggesting that these methods of averaging by least squares are too mechanical in that they allow equal consideration to all traces, while field experience indicates that often some seismogram traces give anomalous results because of peculiar soil conditions, local noise, high background, etc., and therefore should not be equally considered. It is sometimes argued that by a glance at a reflection seismogram, giving consideration to the recording quality of each trace, an experienced interpreter can make a mental estimate of the effective average step-out time which may be more real than the laboriously calculated value.

Velocity Shooting

All methods of computation of reflection data which present the results in the form of depth or dip require the knowledge of the seismic wave velocity through the underground strata. The sources of this velocity information are well velocity surveys, reflection computations and refraction work. These sources are named in order of importance and reliability.

Reflection Method

It was observed in the treatment of reflected ray paths through a section consisting of two layers (p. 666) that velocity could be determined directly from reflection times recorded at the end seismometers of a spread. However, this method requires a large spread length. A step in refinement is to utilize reflection times recorded on each trace, to plot the times against distance between shot-point and seismometer, and to obtain an average value of velocity from the slope of the best fitting curve through the data.

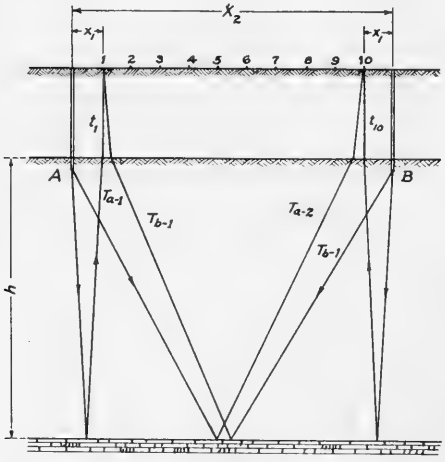

FIG. 445.—Determining average velocity by reflection method.

Consider Figure 445, a simplified section showing reflection ray paths from shot-points A and B to seismometers 1 and 10, the spread lying between these two seismometers. Separate records are of course obtained for each shot-point. It is assumed that the reflecting bed and the base of the low velocity layer are horizontal, and that the velocity V of the

medium included between the low velocity layer and the reflecting bed is substantially constant.

The time of travel for the first ray corrected to the base of the low velocity layer is given on page 667; that is

$$T_{a-1} - t_1 = \frac{\sqrt{x_1^2 + 4h^2}}{V}$$

where T_{a-1} is the time recorded at seismometer number 1 from shot-point A and t_1 is a correction time factor (equal approximately to the vertical travel-time through the low velocity layer below seismometer 1 less the time of travel from the shot to the base of the low velocity zone). Evidently this equation may also be written in the form:

$$V^2 = \frac{x_1^2 + 4h^2}{(T_{a-1} - t_1)^2} \tag{84}$$

If, therefore, one were to plot † the square of the quantity reflection time T_{a-k} less the correction time factor t_k versus the square of the distance x_k from shot-point to seismometer, the resulting points should fall on a straight line having a slope $1/V^2$ and an intercept $4h^2/V^2$. (Here, as usual, k applies to the kth seismometer.)

This procedure is followed: the distance x is measured from that shot-point for which the record was obtained, the data from both shot-points being plotted on the same graph. The effect of low velocity travel-times, which would be prominent if only one shot-point were used, is largely cancelled when the double arrangement of shot-points is used. Similarly, the effect of the dip of the stratum and of the base of the low velocity layer in the direction of the spread is largely cancelled. Nevertheless, for accuracy of final data it is important that, so far as is feasible, an area be chosen for velocity shooting in which these strata, particularly the low velocity stratum, are substantially horizontal.

To obtain useful accuracy it is often necessary to employ such extremely long spreads that they cannot be reached by the usual cables or covered adequately by the usual number of seismometers. In this event, spreads are shot in tandem, i.e., the length to be covered is traversed in steps, wherein successive spreads are begun where previous ones stopped, and one trace is left in common in order that accurate tie-in between records be available. For such long spreads it is necessary first to determine whether some of the reflecting horizons persist over the full length of the spread.

Refraction Method

In the refraction method, refracted waves through the sediments are recorded at various distances from the shot-point. Care must be taken in locating the refraction shooting so that the line of profile is substantially in the line of the strike of the sedimentary layers. This is important

† See also C. H. Green, "Velocity Determinations by Means of Reflection Profiles," *Geophysics*, Vol. 3, No. 4, p. 295, October, 1938.

because success of the method demands that the velocity discontinuities, if present, be horizontal beneath the observations. The ideal situation would be encountered when working over areas where the strata are parallel to the surface. Reasons for this will become obvious from a study of refraction shooting methods, which are covered in a subsequent section.

The velocity depth function is calculated by making a Herglotz-Bateman-Weichert integration of the measured time-distance function.

The slope $\left(\frac{dT}{dx}\right)$ of the time-distance curve is the reciprocal of the apparent velocity $1/V$. Under the condition of horizontal stratification of the velocity discontinuities, the apparent velocity V_p is equal to the velocity of the seismic wave corresponding to the depth of deepest penetration (Z_p) of the ray recorded at a distance (X_p). If (V_p) is the velocity at distance (X_p), the depth of deepest penetration, (Z_p), is given by the integral.

$$Z_p = \frac{1}{\pi}\int_0^{X_p} \cosh^{-1}\frac{V_p}{V_1}dx \tag{85}$$

This integration can be carried out with the use of Simpson's rule or other methods of numerical integration. In the general case the mathematical difficulties are somewhat formidable in obtaining an expression for the velocity distribution. However, in the special case where velocity distribution is of the type $V = V_1 + aZ$, it is relatively simple to fit the time-distance curve. In this case of a linear velocity increase with depth, the travel time-distance function has the form:

$$T = 2/a \quad \sinh^{-1}\left(\frac{aX}{2V_1}\right) \tag{86}$$

If the observed refraction travel-time distance curve can be fitted to this function, then the values of the constants a and V_1 may be directly determined.

In cases where the refraction travel-time distance curve cannot be fitted to this expression 86 for T, the integration 85 must first be carried out, then a velocity distribution function found to fit the calculated values of Z and the measured values of V.

In California, where there are considerable thicknesses of rather similar sediments, good fits of the travel-time curve to Equation 86 have been obtained. Subsequent to this early refraction work, well velocity surveys have indicated that the values of a and V_1 established by refraction work were essentially correct within the first order of magnitude.

Experience in shooting long refraction profiles in California indicates that this method is rather impractical for the investigation of depths below 4,000 feet, because of the long distances necessary, between shot-point and receiving stations, to obtain the required penetration. A distance of

approximately five miles is necessary to obtain sufficient data on penetration of 4,000 feet.

Using the simple analytical velocity-depth function found by fitting the travel-time curve to Equation 86, it is easy to compute data for depths well below the deepest point at which refraction velocity information is available. This requires the assumption that the linear increase of velocity with depth gives the best available extrapolation of data to these depths. In this case the computations of very deep reflections are to be regarded as predictions subject to correction if a later measurement of velocities at greater depths shows the extrapolation to be in error.

The low velocity layer has a similar effect on both refraction and reflection data and the corrections are of the same nature, except that during refraction shots the rays travel a much greater distance through this layer.

Both the reflection and refraction methods give way to a far more accurate method, i.e., to the direct measurement of seismic velocity by the method designated as seismic velocity well surveying.

Well Surveying Method

In this method, a seismometer is lowered into the well by an insulated conducting cable.† First arrival-times are measured for waves from shots which are fired from a shot-point located at the surface and near the well. This method utilizes direct waves and measures depths directly, thereby securing accurate velocity data.

The well seismometer is of special construction, being designed to withstand the high pressures encountered at the bottom of deep wells. Cylindrical and of small diameter, the seismometer is built to minimize the risk that it will be mired in the settled mud at the bottom of the hole and to permit entrance in narrow casing. The cable supporting the seismometer must be strong, well insulated electrically, and accurately measurable in length during operation. Fortunately, such cables are available in the equipment of electrical logging firms. The length of cable under tension is accurately known and a continuous reading of depth of seismometer is supplied by the cable trucks.

Data on the low velocity zone are obtained at the well by up-hole shooting. A surface seismometer at the shot-point serves as a check on depth of shot and a distant surface seismometer is used to check time-break during well velocity determination.

Figure 446 shows the results obtained on shooting two wells in the San Joaquin Valley, California.* The interval velocity is decidedly erratic.

---

† See also H. M. Rutherford, "Reflection Methods in Seismic Prospecting," *A.I.M.E. Geophysical Prospecting*, 1934, pp. 395-396.

* These results cannot be taken as typical of the Valley. It will be noted also that the velocity $V = 6{,}000 + 0.5h$ which was attributed to many regions of California differs from the values shown here. The variation of velocities between these two wells only one mile apart indicates the need for frequent velocity adjustments, if the seismic mapping is to represent a particular prospect accurately.

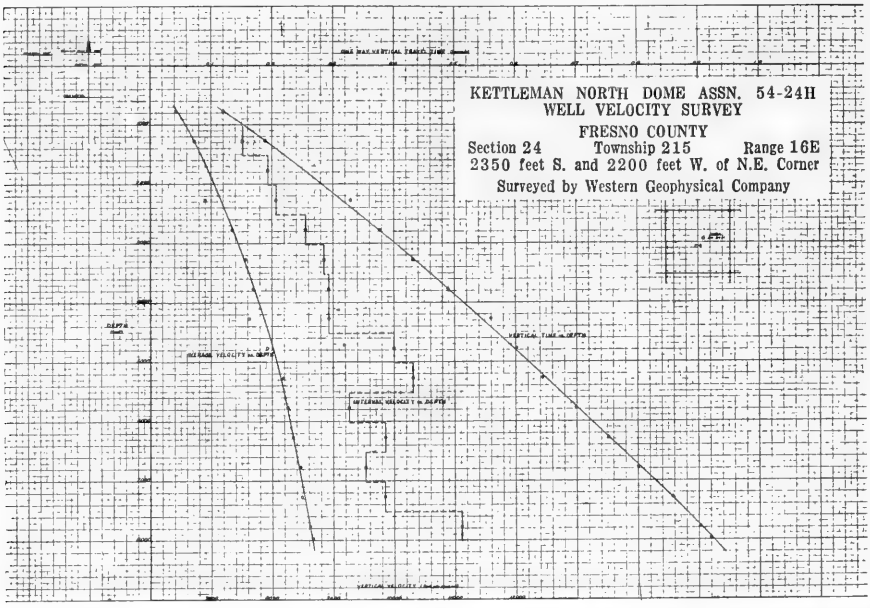

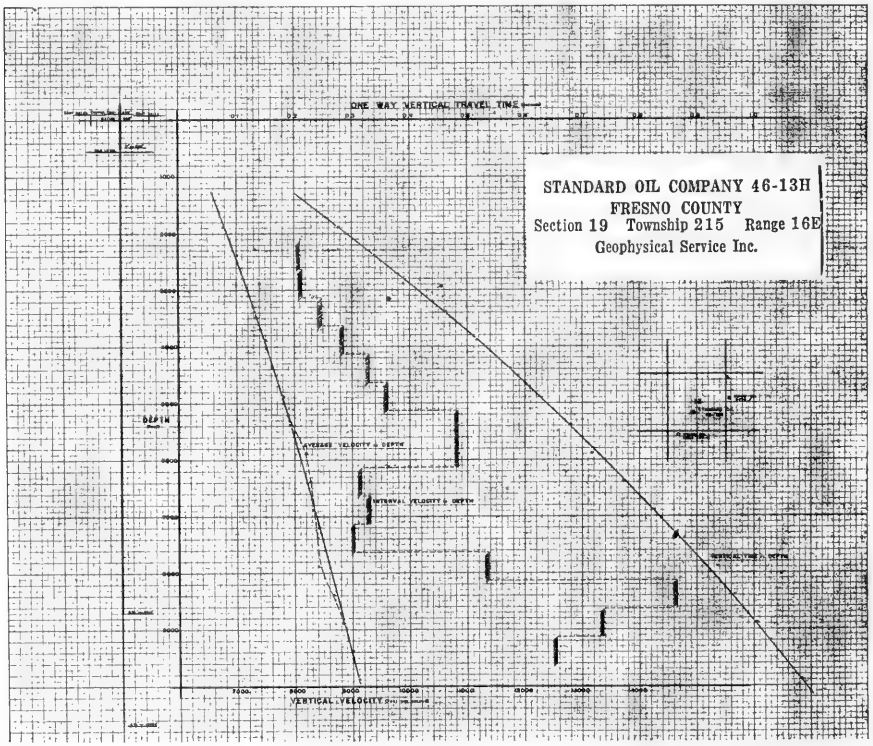

FIG. 446.—Results of well shooting of two wells about one mile apart, San Joaquin Valley, Calif.

The presence of low velocity strata is confirmed by the two wells and a correlation of these strata is noted. The interval velocities were determined from the difference of time over a depth difference of 500 feet. A considerably more accurate determination of interval velocity would be possible if the two times at the ends of the interval could be determined simultaneously. Multiple seismometers separated by a constant interval of cable are designed to realize this accuracy.† (When no special seismometers are available for well shooting but an abandoned well can be located in the area under investigation, it is possible to obtain information about the increase of the velocity with depth by shooting small charges—for shallow depths a cap is sufficient—at different depths and using a seismometer very close to the well as a detector.)

It is sometimes desired to determine the velocity V at any depth by the use of a curve such as Figure 459 which shows the average velocity $\overline{V}$ as a function of depth. The velocity V is assumed to be a continuous function of the depth. By the definition of average velocity (the average with respect to time is used throughout this chapter), one has

$$\overline{V} = \frac{h}{\int_0^h \frac{dh}{V}} \tag{87}$$

On differentiation, one obtains

$$\frac{d\overline{V}}{dh} = \frac{\overline{V}}{h}\left\{1 - \frac{\overline{V}}{V}\right\} \tag{88}$$

or

$$V = \frac{\overline{V}^2}{\overline{V} - h\frac{d\overline{V}}{dh}} \tag{89}$$

The velocity at any depth is thus obtained from a knowledge of the average velocity to that depth and the rate of change of the average velocity at that depth.

In an interpretation of well shot data, Dix‡ corrects for lateral variations in velocity which are usually found in shooting a number of wells. The variations have been accounted for and the wells tied together by tilting the linear distribution of velocity with depth in the proper way.

Curvature of the Reflecting Interface

Ray path and dip equations have been treated thus far on the basis of a plane reflecting horizon. The effect of curvature in the reflecting horizon, however, can be significant.*

† H. Salvatori, U. S. Patent 2,137,985. Issued July 9, 1937.

‡ C. H. Dix, "The Interpretation of Well Shot Data," *Geophysics*, Vol. XI, No. 4, October, 1946, pp. 457-461.

* For example, the reflecting bed could be so severely distorted that for a given shot-point the spread would be actuated by several reflecting portions scattered over the bed, a condition of multiple reflections.

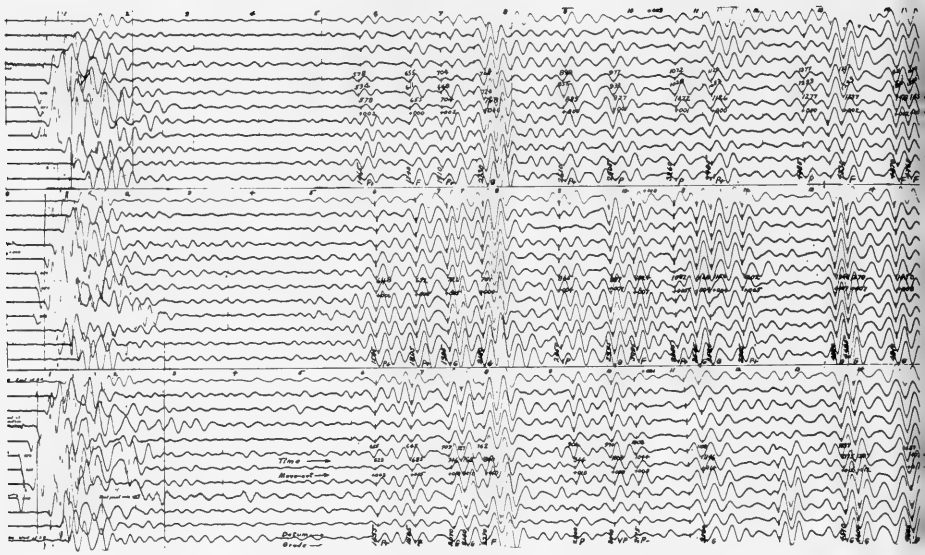

FIG. 447.—Records from three collinear shot-

The effect of spread length, i.e., the spread length correction, may be evaluated by using curved wave fronts. Furthermore, the spread is assumed sufficiently short that the wave front striking the spread approximates an arc of a circle of radius ρ. Specifically, it is assumed that the reflected rays impinging on the end seismometers of the spread originate in a portion of the reflecting horizon which is sufficiently small that it may be regarded as approximately spherical in shape.

It is a well-known law of geometrical optics that when a wave is reflected from a curved surface, the radii of curvature, ρ_i and ρ_r, of the incident and reflected wave fronts are related to the radius of curvature of the reflecting surface, ρ_s, by the equation

$$\frac{1}{\rho_i} + \frac{1}{\rho_r} = \frac{2}{\rho_s}$$

In using the equation, convex upward curvature will be reckoned positive and convex downward curvature negative. Let the path length from the origin to the point of reflection be $l/2$, then the radius, ρ_i is $-l/2$. (The effect of refraction on curvature of the wave front is neglected.) The reflected wave starts back with a radius of curvature

$$\rho_r = \frac{1}{\frac{2}{\rho_s} + \frac{1}{\frac{l}{2}}} = \frac{\rho_s l}{2(l + \rho_s)}$$

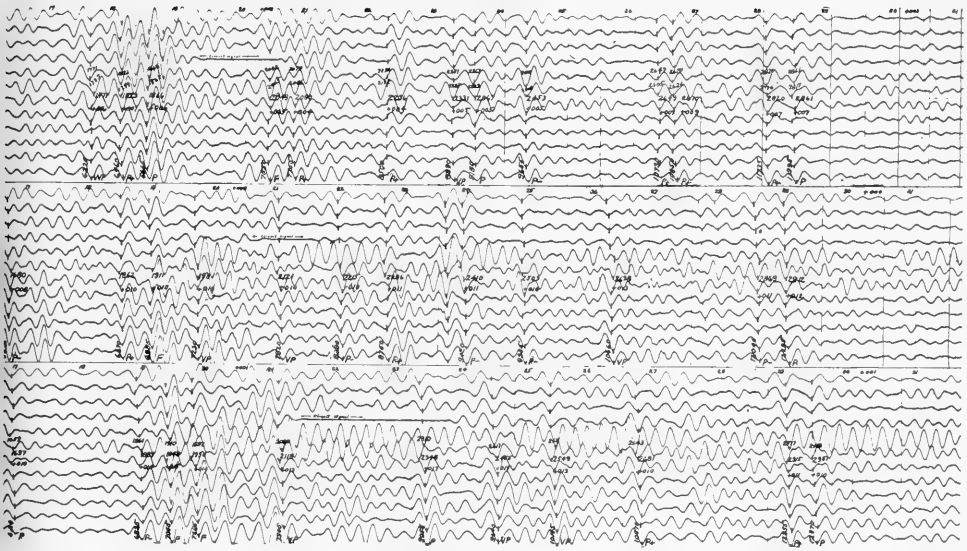

points. (Courtesy of Western Geophysical Co.)

The radius of curvature of the reflected wave when it arrives back at the origin is ρ, where $\rho = \frac{l}{2} + \rho_r$

or

$$\rho = \frac{l}{2} \frac{1 + 2\,\frac{\rho_s}{l}}{1 + \frac{\rho_s}{l}} \tag{90}$$

The effect of curvature of the reflecting surface amounts to changing the curvature of the arriving wave front according to this equation. Because the effect of the ρ term on computation equations is small, the change due to curvature of the reflecting horizon will, in general, be even smaller, provided that the spread is not excessive and that the condition of multiple reflections does not obtain.

Variations in Dip Shooting.—Dip shooting is flexible and permits of a multitude of variations depending upon geologic section, operating conditions, and economic considerations.

An excellent reference in which several standard reflection computing techniques are applied to steep-dip seismic data has been prepared by Rice.† The velocity was assumed to be a parabolic function of depth. A study is made of the overall effect of applying these methods to the computation of a specific steep-dip asymmetric structural profile.

† R. B. Rice, "A Discussion of Steep-dip Seismic Computing Methods," *Geophysics*, Vol. XIV, No. 2, April, 1949, pp. 109-122.

Continuous Seismic Profiling

A technique which has recently gained widespread application is the method of "continuous profiling." In this method the seismometer stations are spaced uniformly along the entire length of a prospect line, being offset a constant distance from the line of shot-points. Shot-points are evenly spaced and intercept a constant number of seismometers. Figure 448 shows a specific arrangement where ten seismometers are used.*

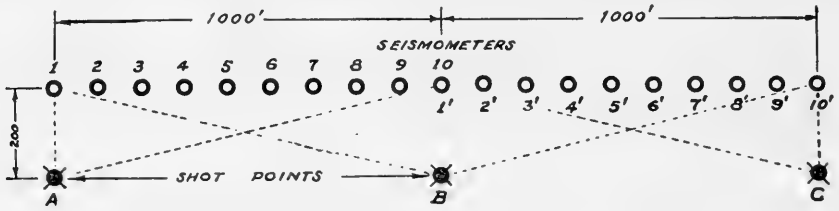

FIG. 448.—Spread for continuous profiling. (Salvatori, *Geophysics.*)

From shot-point *A,* shots are fired to give the first record which comprises traces from seismometer stations 1 through 10; for the second record, the seismometers are left in place and a shot is fired at shot-point *B*. The seismometers are then deposited in stations 1′ through 10′ and shot-points *B* and *C* are used in succession. Thereafter the entire procedure is repeated for the next interval which starts at *C,* and so on.

A section showing the paths of the reflected rays corresponding to the record for shot-point *A* is shown in Figure 449. Reflecting points on the

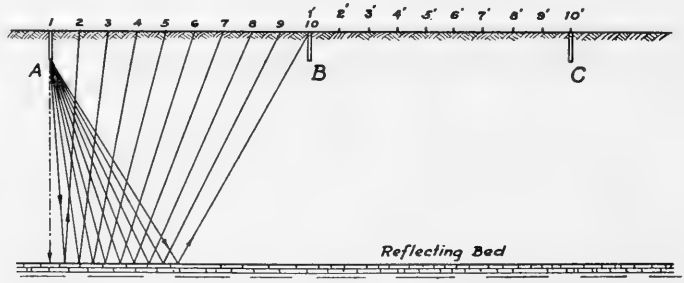

FIG. 449.—Reflected ray paths in continuous profiling; seismometers at 1 . . . 10 and 1′. . . 10′; shot-points at *A, B, C.*

reflecting bed are spaced evenly at a distance equal to approximately half the seismometer separation, and, from the sequence of shots and spreads, it is evident that the entire length of reflecting bed is covered to this detail. Moreover, the ray path traversed from shot-point *A* to seismometer 10 has virtually the same reflecting point as the ray path from shot-point *B* to seismometer 1. These ray paths would therefore

* See "Mapping Faults by the Reflection Method," Henry Salvatori, *Geophysics* 2, No. 4, October, 1937.

lead to the same reflection times were it not for the difference in the thickness of the low velocity layer at the two seismometers and the difference in the depth of shots. Because these differences can be determined, a positive correlation can be effected from the first to the second record. Furthermore, when seismometers are transferred to the opposite side of shot-point B for the third record, the single seismometer opposite shot-point B is undisturbed. Consequently, the traces corresponding to this seismometer furnish another positive correlation from the second to the third records.

Instead of making a correction on one of the records for the difference in traveltimes for the ray paths A-10 and B-1, use may be made of an overall correction ΔT_1 without regard to the various sources that contribute to the correction. Thus,

$$t_{A\text{-}10} = t_{B\text{-}1} + \Delta T_1$$

Next, one adds the same correction to $t_{B\text{-}9}$ and $t_{B\text{-}2}'$ and averages these values.

The next step is the tie-in between the two profiles, shot from B in both directions. On the two corresponding records one finds two values for $t_{B\text{-}9}$ and $t_{B\text{-}2}'$. In general, the corresponding values differ by a few thousandths of a second, probably due to repeated shooting in the same hole with consequent changes in elastic properties of the rocks at the bottom of the hole and to instrumental errors. These times are corrected by a value Δt_2 to make the average time for the two seismometers on both profiles the same. Now one adds the same correction to $t_{B\text{-}10}'$ and repeats the whole process for the next shot-point. In this way it is possible to correlate the records with little more than an occasional check on the shot-hole time (time that it takes the wave to travel from the bottom of the shot-hole to the surface). The times are then translated into terms of depths with the aid of data obtained in well-shooting.

Other methods of continuous profiling are sometimes used. The term itself applies only to a "continuous coverage" on a reflecting bed. Several advantages are apparent for the method of continuous profiling. First, the reflection points are uniformly spaced, thereby permitting most efficient correlation as well as fault investigation. (Compare p. 738.) Second, the common tie-in from record to record eliminates errors due to differences in shot-hole depth or in the timing system, thereby allowing positive correlations. Third, by use of up-hole shooting, good corrections for the low velocity layer in dip determination may be obtained. Fourth, the long distance from the shot-point to the extreme seismometer of the accompanying spread may permit adequate velocity determination. (Compare Figure 445.)

Several disadvantages of the method are often cited to offset these advantages. First, the close spacing of shot-points and seismometers greatly increases the expense of the work. Second, the method is rather inflexible, requiring continuity in seismometer line despite obstructions which may be encountered. Third, the common tie-in from record to record increases the tendency of the computer to force correlation, which may lead to error.

In continuous profiling it is theoretically impossible to differentiate between correlation data and strictly dip, or ΔT, data because the series

of records placed side by side in proper sequence may be viewed simply as one record and the corresponding actual ray paths may be treated by equivalent ray paths. Reflections can be picked not only over the traces constituting a single record but over those traces of other records for which the reflection seems reliable.

The continuous profiling method outlined above is sometimes modified in such a way that symmetrical spreads are involved—an arrangement which requires double the number of shot-points for the same spread length. Here the entire length from *A* to *C* (Figure 448) is covered by the available set of seismometers and only half the seismometers are transferred for successive spread changes.* Each shot-point then need be used but once. This method of overlapping seismometers is gaining favor because the dip is more readily computed for symmetrical spreads than for uni-directional spreads.

Continuous profiling by symmetrical spreads as described in the last paragraph is sometimes modified to achieve a compromise between quality of correlation and speed of progress in mapping a prospect. Instead of a complete overlap, shot-points are separated by a distance greater than half the spread length and the seismometer stations nearest a shot-point are used only in conjunction with that shot-point. The common tie-in between records is lost but the gap on the reflecting bed between successive spreads may be kept sufficiently short that correlation is reliable.

Fault Mapping †

The most common method of investigating faults by seismic prospecting is a *negative* one in that fault areas are generally first detected on a shot-point line when an area of poor reflections is encountered. If parallel lines also reveal similar gaps on the cross sections and if these gaps can be aligned, the fault may be delineated. An examination must be made for assurance that it is not an anomalous cause such as unfavorable surface conditions which is responsible for the poor results.

Reflections from a fault plane are helpful when available. Usually, however, reflections are not recorded from a fault plane for reasons which will be evident from the following considerations. Wave energy is reflected from a fault plane only at points where two beds of different elastic constants or density come into sharp contact. Generally, however, the displacement of the beds at the fault is relatively small, and there are many portions of the fault plane along which either the same beds or

* Referring to Figure 448, the first shot-point would be *B*, the second *C*, and so on. The disposition of the 10 seismometers supplying the traces for the first record would be symmetrical about *B* and would cover the distance between *A* and *C*. An odd number of seismometers and traces, however, is best adapted for this spread in order that one seismometer appear opposite the shot-point.

† Henry Salvatori, "Mapping Faults by the Reflection Method," *Geophysics*, Vol. 2, No. 4, October, 1937, pp. 342-356.

M. C. Kelsey, "Studies in Fault Detection with the Reflection Seismograph," *Geophysics*, Vol. XIV, No. 1, pp. 21-28, January, 1949.

A. Wolf, "Seismic Method of Locating Faults," U. S. Patent No. 2,449,921, September, 1948.

different beds of approximately similar characteristics are in contact. Hence, even when the plane of faulting is very sharp, it will rarely act as a good reflector of wave energy over an appreciable section.

A correlation showing a vertical displacement is the best kind of evidence when supported, of course, by general dip information in the region, but such evidence is not often found. Sometimes reflections indicating the fault drag are detected.

Correlations do, however, supply important negative evidence, particularly when the records have been obtained by the continuous profiling method. If correlations for several reflections cease roughly on a vertical or sloping line, as depicted on a cross section, and continue again at a certain distance beyond this line, strong evidence of a fault zone in that interval is obtained, the dip of the zone roughly indicating the hade in the plane of the cross section. This method, though strikingly effective on paper, cannot always be depended upon because of its negative character; also, correlations must be reliable and persist for several strata, and the zone of fracture must not be too extensive.*

Mapping of Structure by Angular Divergence or Interval Change Method

This method is based on the premise that a change of interval between two or more reflections recorded over an area is an indication of structure in that the geological section is normally thinner over the crest of a structure than in the surrounding area. †

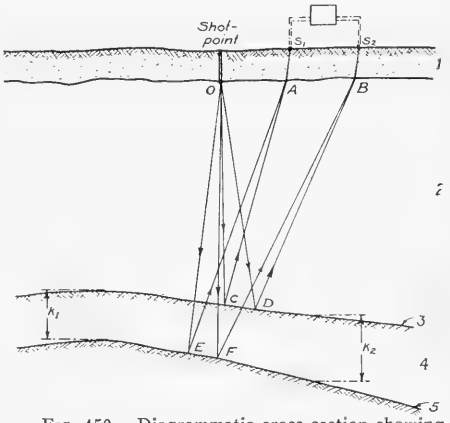

Fig. 450.—Diagrammatic cross section showing rays reflected from various reflecting horizons located above an anticlinal structure. (After McCollum, U. S. Patent 2,118,441.)

The principles utilized in the method are best explained by referring to Figures 450, 451, and 452. Figure 450 shows a schematic geological cross section through an anticlinal structure and the ray paths of rays which originate at a shot-point 0 and are reflected from the surfaces of layers 3 and 5 to the seismometers S_1 and S_2.** The low velocity or aerated layer 1 is variable in thickness and in physical characteristics. Layer 2 consists of consolidated rock having elastic properties which are different from those of layer 1. Layer 3 is rock having elastic properties which are different from those of layer 2. Layer 4 has the same general character as

* The methods of refraction shooting and continuous electrical profiling often offer a more convenient method of locating shallow faults.

† E. V. McCollum, "Method of Making Geological Explorations," U. S. Patent 2,118,441. Issued May 24, 1938.

E. V. McCollum and L. F. Athy, "Geophysical Method of Determining Geological Structures." U. S. Patent 2,118,442. Issued May 24, 1938.

E. V. McCollum and G. C. McGhee, "Method of Making Dip Determinations of Geological Strata," U. S. Patent 2,001,429. Issued May 14, 1935.

** In this analysis it will be assumed that ray paths can be approximated with sufficient accuracy by straight lines, an assumption justified only for relatively gentle dips.

layer 2, and layer 5 has the same general character as layer 3. Layer 6 (not shown) is rock which has a porosity such that petroleum may be trapped within it.

The shapes of beds 3 and 5 illustrate a geological condition usually realized: viz., the deeper beds exhibit more closure or steeper dip. Such beds are said to diverge from each other "off the structural feature." Thus, K_1 is the interval "on the structure" and K_2 is the interval at a point "off the structure."

The times of arrival of the rays traversing the various paths are shown on the seismogram. (Figure 451.) Trace 23 is the trace produced by the oscillograph connected to seismometer S_1. Point 40 on trace 23 represents the instant of arrival at S_1 of the ray traveling along $0AS_1$; point 41 represents the instant of arrival of the ray traveling along path $0CAS_1$; point 42 represents the instant of arrival of the ray traveling along path $0EAS_1$.

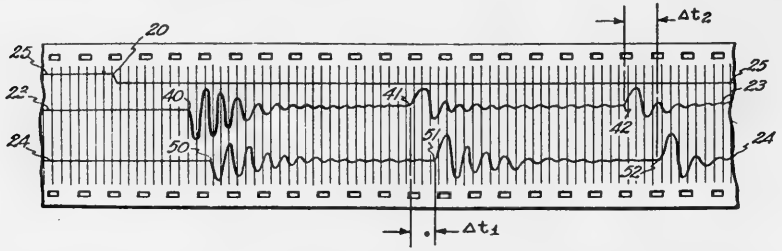

FIG. 451.—Theoretical seismogram showing traces produced by oscillographs connected with seismometers S_1 and S_2 of Figure 450. (McCollum, U. S. Patent 2,118,441.)

Point 20 on trace 25 represents the instant of explosion.

Trace 24 is the trace of the oscillograph connected to seismometer S_2. Point 50 represents the instant of arrival of the ray traveling along the path $0BS_2$. Point 51 represents the instant of arrival of the ray traveling along the path $0DBS_2$. Point 52 represents the instant of arrival of the ray traveling along the path $0FBS_2$.

The observed time intervals used for mapping the structure are ΔT_1 which is the difference between points 41 and 51 on traces 23 and 24 and ΔT_2 which is the difference between points 42 and 52 on traces 23 and 24. It will be noted that these time intervals are independent of time of origin represented at point 20.

The *normal* value of $(\Delta T_2 - \Delta T_1)$ for a given pair of reflecting horizons may be obtained by averaging a large number of observed values of $(\Delta T_2 - \Delta T_1)$ obtained at random over the area being explored.

In all portions of an area in which there is no angular divergence or in which the geological formations are parallel, the value of $(\Delta T_2 - \Delta T_1)$ is a constant for all seismograms for which the same size spreads were used. If the quantity $(\Delta T_2 - \Delta T_1)$ is not constant, it is indicative of angular divergence. In particular, if the observed $(\Delta T_2 - \Delta T_1)$ is greater than the normal value for the area, the direction in which the more distant seismometer is positioned from the shot-point is the direction of angular divergence from the shot-point. If the observed $(\Delta T_2 - \Delta T_1)$ is less than the normal value for the area, the direction of angular divergence is reversed.

Evidently, it is possible to plot arrows with lengths proportional to the divergence on maps and thus determine the differences in intervals.

Moreover, it is possible to evaluate the angle of divergence α between layer 1 and layer 2 in terms of measurable quantities. To calculate α, it is convenient to use the constructions shown in Figure 452. x_1 equals the distance $0S_1$ and x_2 equals the distance $0S_2$. L_1 corresponds to layer 3 and L_2 to layer 5. H_1 is the perpendicular distance from 0 to plane L_1 and H_2 is the perpendicular distance from 0 to plane L_2. ϕ_1 is the dip of layer L_1 and ϕ_2 the dip of layer L_2.

I_1 is the image of the shot-point 0 in plane L_1 and I_2 is the image of 0 in the plane L_2.

In triangle $0I_1S_1$ the angle S_10I_1 is equal to $90 + \phi_1$, the distance $0I_1 = 2H_1$, and the distance $I_1S_1 = 0CS_1 = V_1T_1$. (The velocity is assumed to vary with depth only and V_1 is defined as the "equivalent" or "average" vertical velocity to depth H_1. T_1 is the time interval between point 41 and 20 on the seismogram.) From the cosine law

$$V_1^2T_1^2 = x_1^2 + 4H_1^2 + 4H_1x_1 \sin \phi_1 \tag{91}$$

Similarly, from triangle $0I_1S_2$

$$V_1^2T_2^2 = x_2^2 + 4H_1^2 + 4H_1x_2 \sin \phi_1 \tag{92}$$

and from triangles $0I_2S_1$ and $0I_2S_2$

$$V_2^2T_3^2 = x_1^2 + 4H_2^2 + 4H_2x_1 \sin \phi_2 \tag{93}$$

$$V_2^2T_4^2 = x_2^2 + 4H_2^2 + 4H_2x_2 \sin \phi_2 \tag{94}$$

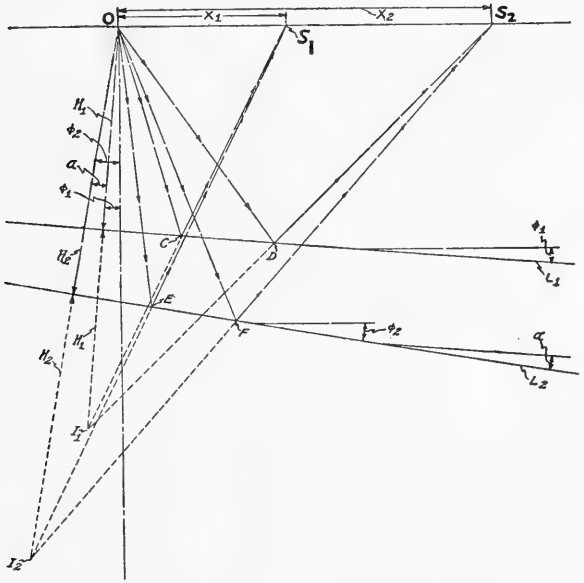

FIG. 452.—Diagrammatic sketch of ray paths corresponding to Figure 450. (McCollum, U. S. Patent 2,118,441.)

In the above equations, the quantities x_1 and x_2 are known. The quantities T_2, T_3 and T_4 are obtained from the seismogram as was T_1. (Figure 451.) The quantity V_2 is an average velocity in the material above bed 5 (L_2). Both V_1 and V_2 may be determined by methods outlined in the section on Velocity Shooting. The unknown quantities, therefore, are ϕ_1, ϕ_2, H_1 and H_2.

It is evident from Figure 452 that

$$\phi_2 - \phi_1 = \alpha \tag{95}$$

Elimination of H_1 between Equations 91 and 92 gives

$$(V_1^2T_2^2 - x_2^2 \cos^2 \phi_1)^{1/2} - x_2 \sin \phi_1 = (V_1^2T_1^2 - x_1^2 \cos^2 \phi_1)^{1/2} - x_1 \sin \phi_1$$

For the gentle dips usually treated, it is generally sufficiently accurate to replace $\cos^2 \phi_1$ by 1. On rearranging terms, the last equation becomes:

$$(x_2 - x_1) \sin \phi_1 = V_1T_2\left(1 - \frac{x_2^2}{V_1^2T_2^2}\right)^{1/2} - V_1T_1\left(1 - \frac{x_1^2}{V_1^2T_1^2}\right)^{1/2}$$

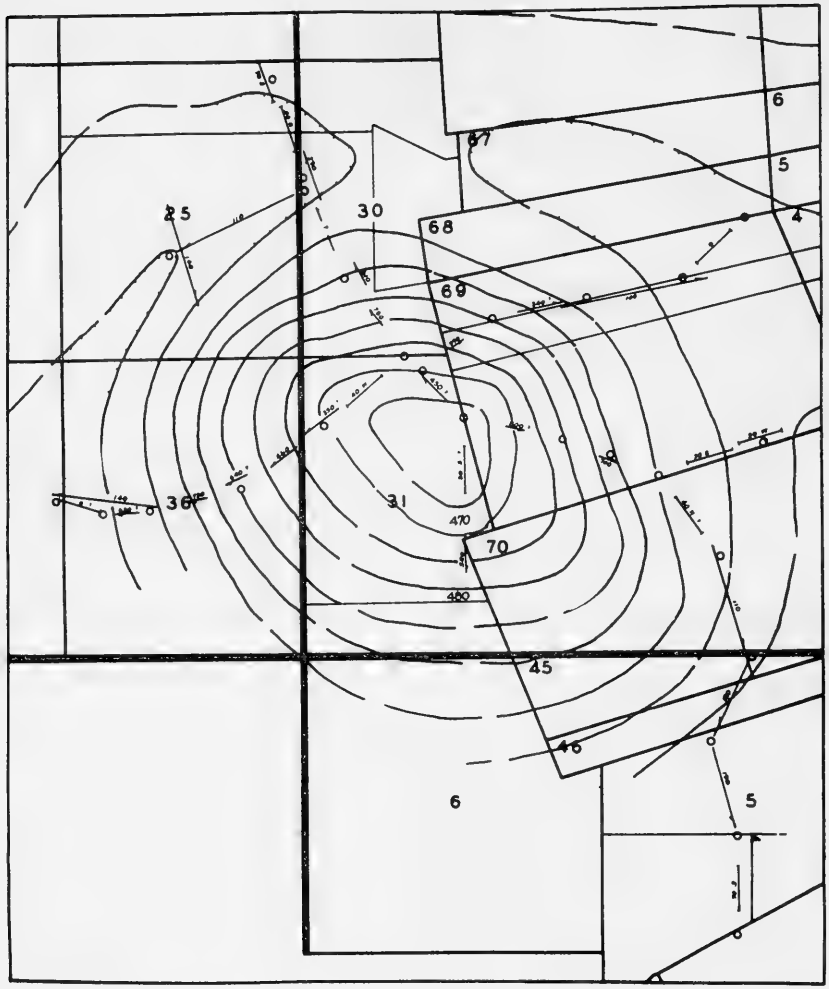

FIG. 453.—Map showing structural divergence over a salt dome. (Courtesy Continental Oil Co.)

On expanding the expressions within the parentheses on the right-hand side of this equation and neglecting all terms after the second, the equation becomes

$$(x_2 - x_1) \sin \phi_1 = V_1T_2 - V_1T_1 - \tfrac{1}{2} \frac{x_2^2}{V_1T_2} + \tfrac{1}{2} \frac{x_1^2}{V_1T_1}$$

However,

$$T_2 - T_1 = \Delta T_1$$

Also, it can be assumed without appreciable error that V_1T_2 is equal to V_1T_1. Hence,

$$\sin \phi_1 = \frac{V_1 \Delta T_1}{x_2 - x_1} - \frac{x_2 + x_1}{2V_1T_1} \tag{96}$$

Similarly, elimination of H_2 between Equations 93 and 94 leads to

$$\sin \phi_2 = \frac{V_2 \Delta T_2}{x_2 - x_1} - \frac{x_2 + x_1}{2V_2 T_3} \tag{97}$$

Furthermore, for small angles $\sin \phi_1$ and $\sin \phi_2$ are approximately equal to ϕ_1 and ϕ_2 respectively. Hence,

$$\sin \phi_2 - \sin \phi_1 = \phi_2 - \phi_1 = \alpha = \frac{V_2 \Delta T_2 - V_1 \Delta T_1}{x_2 - x_1} + \frac{x_2 + x_1}{2}\left(\frac{1}{V_1 T_1} - \frac{1}{V_2 T_3}\right) \tag{98}$$

Equation 98 expresses α as a function of measurable quantities and is therefore the relation sought. It is important to note that the values of ΔT_2 and ΔT_1 have opposite signs in Equation 98. Hence, errors due to the low velocity layer are substantially avoided.

Figure 453 is a map showing a structural divergence over an actual salt dome in Louisiana. The figures on the dip arrows indicate the amount of divergence in feet per mile in the direction of the arrow. The length of each arrow represents the spacing of 50-foot contours at the position of the arrow. The divergence was observed between beds located at approximately 3000 feet and 7000 feet; that is, the divergence was observed over an interval of approximately 4000 feet. It is evident from the map that the crest of the structure coincides closely with the center of convergence.

Grading of Reflections for Visual Correlations

The evaluation of the quality of a recorded reflection involves the following factors. (1) The consistency of wave form for every trace of a record and the consistency of the difference in reflection time for different phases of the wave: these are the primary factors by which reflections are identified and by which accuracy of dip determination may be gauged. (2) The wave form or character is judged by the degree to which it approaches the response of a seismometer to a single impulse of steep wave front. The presence of all phases of a wave without interference is some assurance that a reflected wave and not spurious energy is involved. (3) The relative amplitude of a reflection with respect to that of the waves on neighboring portions of the record determines the prominence of a reflection and is some gauge of its reliability. (4) To a certain degree, all the traces during a reflection disturbance display essentially the fundamental oscillation of the reflection as a whole. That is, despite interference of spurious energy, at least two complete cycles of the oscillation should be more or less apparent on each trace in the recording of the reflection.

Unfortunately all of these factors are not uniformly realized in reflection work. In some areas more are realized than in others, due to the variations of complexities in the reaction of the ground to the propagation of reflected waves. Experience indicates that all grades of conditions exist, from those that give good reflection results to problem areas where the standard reflection method completely fails to produce reliable data. One such problem is exemplified in parts of the Edwards Limestone area of Texas.

The grading of reflections is a practical method of attaching an empirical factor of merit or accuracy to the individual reflection. It has

been mentioned that, generally, reflections are sorted into four classifications: A, B, C and D. Grade A may correspond to good, B to fair, C to poor and D to questionable.† No general system or set of fundamentals has been widely accepted by geophysicists as a basis for grading reflections. Different bases of grading are occasionally used by the same individual, depending upon whether the area gives consistently good or consistently poor reflections.

In a general way reflection grading seems to depend on the character of the reflections obtained, together with the opinion and judgment of the observer. For example one observer may classify a reflection as good in an area difficult to prospect by seismic methods, while a second observer, working in a less difficult area, would classify the same reflection as poor according to his standard of grading.

As long as grading is done on the basis of opinion and judgment, a certain amount of confusion will exist. Fundamentally the purpose of grading is to evaluate the trustworthiness of the data. Therefore it is desirable to establish a system of grading which is based on the same fundamentals in every case and is independent as far as possible from personal opinion.

Gaby‡ has suggested an outline for a system of grading which differs from most procedures in that the evaluation of the data as a true reflection is considered together with the accuracy of the computable dip.

When the question arises as to whether a certain recorded wave group is or is not a reflection, and an attempt is made to measure this probability, the prospector might become frustrated in trying to separate the more dependable from the less reliable data. To overcome this difficulty, it is often possible by graphical analysis of the travel-time curves of the reflection to determine with certainty whether or not a recorded event is a true reflection. The grading of correlations may be made on the basis of the degree of certainty of the correlation and the agreement of reflection time of the correlatable events, without raising the question as to whether the data are real or unreal, because true reflections may or may not correlate.

As seismic work is extended into the marginal areas, the quality of the reflections will decrease and visual interpretation will become increasingly difficult. As these conditions become prevalent, more and more dependence will be placed upon instrumental interpretation employing the various methods of wave analysis, frequency patterns, and selective filtering.

Cross Section and Maps

The computed data on dip and depth of inferred strata are generally shown on cross sections or profiles which depict the dip attitude and depths in the vertical plane of shot-point and spreads. One form of section is shown in Figure 454, (the computed positions of interfaces giving reflec-

† Another classification uses the letters G, F, P, VP; G denotes good reflections, F fair, P poor, and VP very poor or doubtful.

‡ Phil P. Gaby, "Grading System for Seismic Reflections and Correlations," *Geophysics,* Vol. XII, No. 4, Oct., 1947, pp. 590-617.

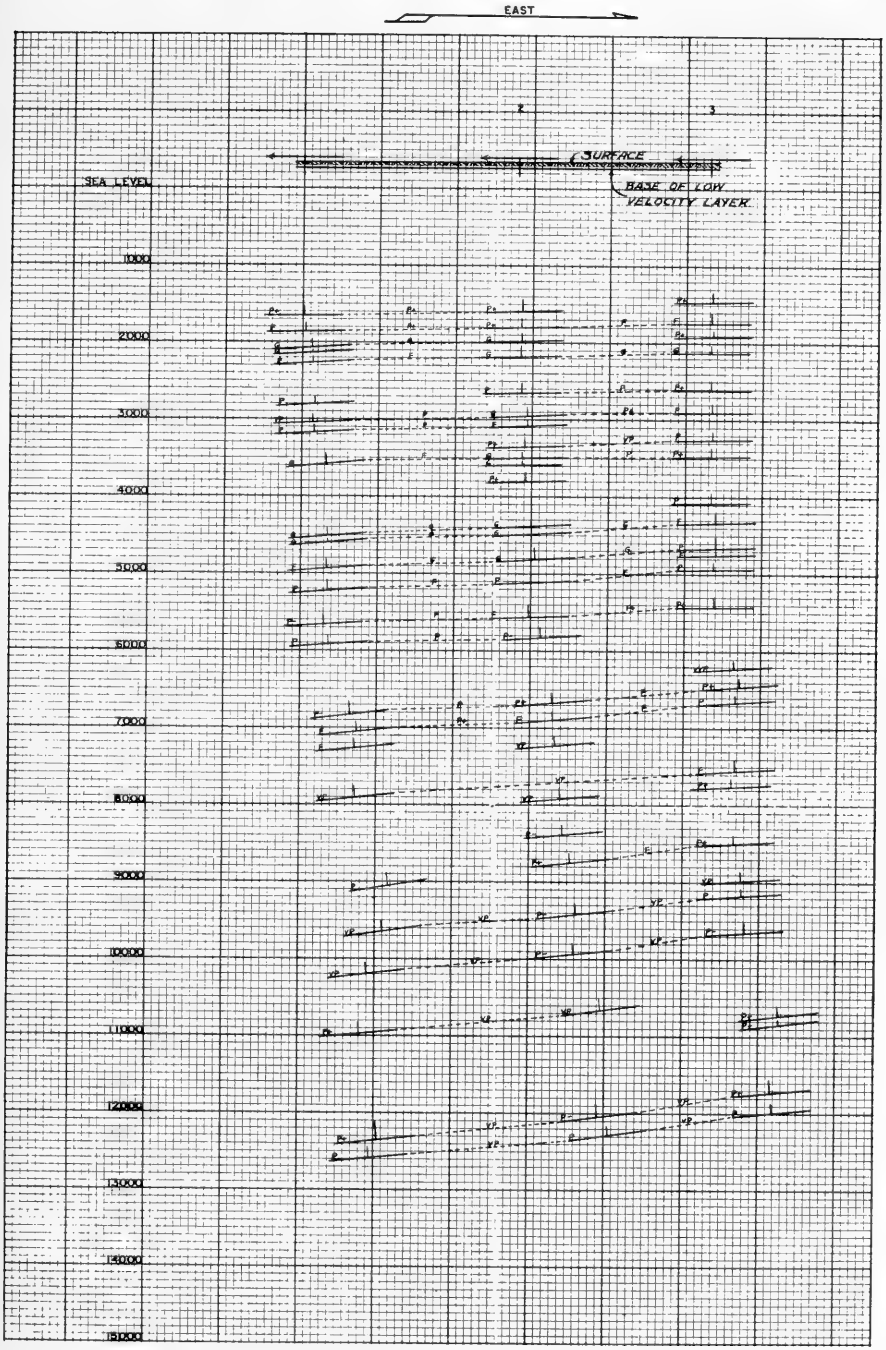

FIG. 454.—Dip section obtained from the records shown in Figure 447.

tions). Rays emanating from the shot-point are indicated only at the centers of plotted sections of the interface. Plotted depths are referred to sea level. The thickness of the low velocity layer is indicated.

The cross section represents the true dip only when the shot-point and spread line lie in the direction perpendicular to the strike of the underground strata. However, a section such as illustrated by Figure 454 does depict the dip in the direction of the section, in this case in an east-west direction, which may or may not be the direction of the true dip.

To draw a contour map of the structural relief corresponding to a horizon at a particular depth, a starting point is chosen on a section and a theoretical surface, often called a phantom or a traverse surface, is drawn from this point paralleling the dips. The phantom is extended into other sections at intersecting or tie-points until the region is covered. After a phantom has been projected parallel to the dips around any complete loop or closed horizontal traverse, it will generally be found that a misclosure in the vertical elevation of the phantom surface exists. Since misclosure may be attributed to several factors, i.e., normal experimental errors involved in the process of measurement, faulting, too large distances between stations, and a possible personal element in actual construction of the section. It is obvious that if vertical breaks in the phantom surface are to be avoided in the drawing of a set of contours on the phantom surface at the points where the closures are attempted, an adjustment must be made for these vertical misclosures.

Several methods have been developed for making closures of traverses, and anyone attempting this type of work will do well to refer to a good treatise on land surveying. In general it may be said that measurements of distances and angles are never exact quantities. This statement may also be extended to include intervals of time in the case of seismic prospecting. If these observed values are used in computing other quantities, the results are likewise inexact. And since the true value is unknown, the true error is also unknown. It is therefore essential that the geophysical interpreter have a knowledge of the various sources of error, their magnitudes, and the probable error both of the direct field measurements and of computed quantities. In order to make corrections and adjustments, the interpreter must have a knowledge of least squares for a thorough understanding of probable errors. This knowledge should also include weighted observations, weighted averages and the propagation of error. Even this is not enough to qualify a geophysical interpretation, because any interpretation of geophysical data in terms of geologic structure is likely to be in error if due consideration is not given to the known geology of the area under investigation.

For example, a geophysical interpreter unaware of the presence of a known fault of considerable displacement may erringly project a phantom surface through the faulted zone, make adjustments for vertical misclos-

ures, and draw a continuous contoured surface across the fault. This would be an unpardonable error in the eyes of most geologists.

A common method used for the adjustments of misclosures is the linear correction which is based on a constant depth adjustment per unit length of profile. Another method makes use of an adjustment proportional to the magnitude of the computed dip appearing in the profile. It is common practice to restudy a prospect when large misclosures are determined. In this manner the misclosures are established either as anomalies or as errors of accumulation.

A completed contour map in some cases requires a correction for a lateral velocity variation, because routine computations generally are based on a velocity-depth function which varies with either the depth or the reflection time. The customary correction for the lateral variation of velocity is made by obtaining products of the depth Z below the low velocity layer and the ratio $\frac{V_t}{V_z}$, where V_t is the actual average velocity in the vertical direction and V_z is the originally-employed average velocity in the vertical direction for a time T equal to $\frac{2Z}{V_z}$. The correction, although customary, is approximate, because the dip of the structure is not considered in the correction of the data. A contoured interface which gives a constant time for reflections is also helpful when studying the effect of non-vertical velocity gradients.

In areas where two components of dip are measured at each station for the purpose of resolving the components into the resultant true dip of the underground strata, horizontal plan maps are often prepared showing the location of the shot-holes and the position of the vertically projected dips into a horizontal plane. These maps are particularly valuable to geologists, who are accustomed to handling much of their measured dip and strike data in this form. An illustration of this type of map is given by the dip strike plotting on Figure 433.

One advantage of plotting of dip and strike in horizontal plan is that the computed direction of the true dip from component measurements is independent of any error in the assumed velocity depth function. Results expressed in this form are usually more accurate in areas of moderately steep dips than in areas of very flat-lying strata.

Graphical Analogue Computer

Field experience has shown that in many regions the empirical velocity data obtained from deep well shooting can be very closely fitted to the linear-increase, velocity-depth function already discussed in a former section. The assumption involved in this velocity distribution led to the development of a very simple graphical analogue computer, which is completely rigorous and will enable one to plot any seismic reflection at its proper position and attitude on a vertical section profile when the arrival time T and the move-out time t are correctly set into the machine.

This graphical machine not only saves much time in the reduction of reflection data to the vertical cross-section form, but also has the advantage of eliminating clerical errors which often creep into numerical solutions.

Figure 455 shows a plotting machine based on the relations derived from Figures 418 and 422, i.e.,

$$\tan\frac{\theta}{2} = \tan\frac{\theta_1}{2}\left[e^{\frac{aT}{2}}\right] \tag{57}$$

Where

$$\theta_1 = \sin^{-1} V_1 \frac{\Delta T}{\Delta x} \tag{99}$$

$$D = \frac{V_1}{a}\left(\cosh\frac{aT}{2} - 1\right) \tag{100}$$

$$R = \frac{V_1}{a}\sinh\frac{aT}{2} \tag{101}$$

A pivot point is arranged to move across the plotting board in a vertical direction. This mechanism is suspended by a U-shaped arm which is rigidly attached to an accurately-machined set of ways mounted on the under side of the table top. Scale D, attached to this pivot arm, is graduated in terms of T, according to Equation 100. The corrected arrival time T of the reflection to be plotted is first set on this scale, being made to correspond with a fixed reference line attached to the table top. This operation sets the pivot point at a scale depth D on the profile which is to be plotted. The θ-scale on the bottom circular segment of the plotting template is laid out in terms of the move-out t and the time T for a standard split spread length of 1200 feet. Move-outs for other spread lengths are converted to equivalent 1200-foot spread move-outs by simple proportion. This θ-scale is laid out by use of Equation 57. The time T is plotted as convenient arcs about the pivot point, and t is plotted as the curved slant lines. Values of θ are computed for each t line where it intersects each time arc. The radii of the true arcs are arbitrarily made such that the t line for a move-out of 30 milliseconds is a straight line. The other computed intersections are then laid out graphically and the t curves drawn. The second step in the plotting of a reflection is to rotate the plotting template about the pivot point, until a point on the θ-scale where the T arc intersects the t curved slant line falls on a vertical line beneath the shot-point as located on the profile.

The final step of the plotting operation is to position the slider so that its index line corresponds with T on the R-scale. The R-scale is a graphical plot of $R = \frac{V_1}{a}\sinh\frac{aT}{2}$. Using the slider as a guide, a line is then drawn corresponding to the reflection being plotted. A Z-scale corresponding to a graphical plot

$$Z = \frac{V_1}{a}\left(e^{\frac{aT}{2}} - 1\right) = D + R$$

is included on the right hand side of the plotting template so that reflections from very gently dipping interfaces may be plotted with the D-scale set on zero. The D-scale and the plotting template are easily detachable, and a separate set of these items must be made for each velocity-depth function used.

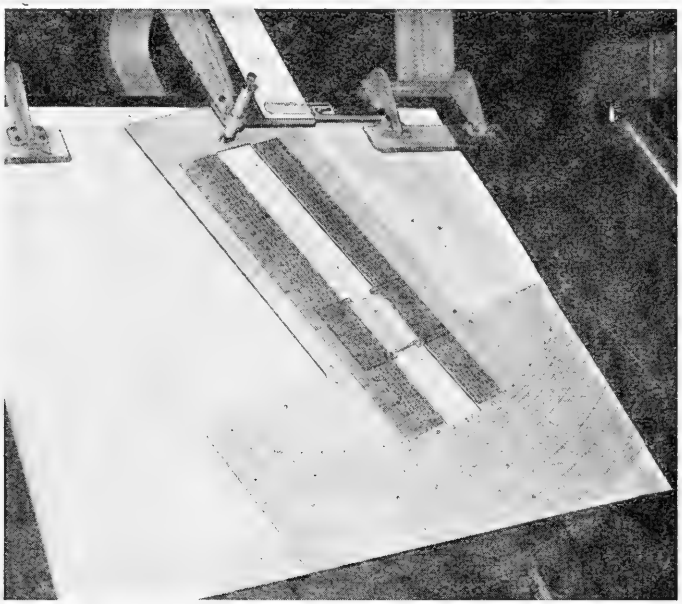

FIG. 455.—Graphical analogue computer for plotting of reflection data in vertical section, given only the corrected reflection time T and the move-out time t.

On the plotting table shown in Figure 455, the two paper finger clamps at the top of the table are operated by electrical solenoids attached to the back of the table. They are released by a foot-operated switch, leaving the operator's hands free to slide the profile paper along, and to line the pivot point upon a new shot-point. The two troughs on the sides of the table hold long rolls of profile paper. During the operation of the plotting machine the paper is rolled from one trough across the table to the other.

The D-scale ways are driven by a small reversible electric motor located on the under side of the table. This feature allows the scale to be rapidly and accurately set in the desired position for the pivot about which the template swings.

It is worth noting that the plotting system described here can be made to approximate closely many of the velocity-depth functions derived from

empirical velocity measurements made in deep bore holes. The D-scale may be calculated from the conditions given by the velocity-depth function, and then the R-scale may be obtained by subtracting the D-scale values from the empirical measured time-depth curve.

Another plotting instrument has been described by Daly,† for use in areas where the velocity may be assumed to increase linearly with depth.

REFRACTION METHOD

In the refraction method of seismic prospecting, measurements are made of the elapsed time between the shot and the arrival of the first wave trains, i.e., the "first arrivals," and successive correlatable wave trains. A series of seismometers is placed at measured distances from the shot-point, and by plotting a time-distance graph for these first arrivals (the refracted longitudinal, fastest-traveling waves) and the successive wave trains which can be correlated, changes in velocity of the wave path are shown by discontinuities or changes in slope of the graph. From the points of inflection of the graph calculations may be made to determine the depth to the boundaries separating the media of different elastic wave velocities. This information is interpreted in terms of subsurface geology.

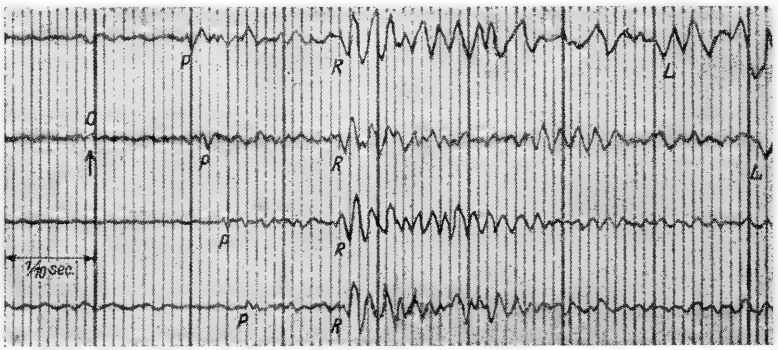

FIG. 456.—Seismogram showing the arrival of refracted waves *P*, reflected waves *R*, and surface waves *L*. The shot was 1/8 pound of 60% dynamite and was exploded at a depth of 3 feet. (Reproduced from B. Gutenberg, *Beiträge zur angewandten Geophysik*, Vol. 6, No. 2, 1936.)

Subsurface Section Consisting of Two Horizontal Layers.—The path of a refracted wave through a section consisting of two horizontal layers has already been described. (Figures 411 and 412.) A seismogram showing the arrival of refracted waves *P*, reflected waves *R*, and surface waves *L*, is given in Figure 456.

† J. W. Daly, "An Instrument for Plotting Reflection Data on the Assumption of Linear Increase of Velocity," *Geophysics*, Vol. XIII, No. 2, April, 1948, pp. 153-162.

The travel-time T for the path through two horizontal layers is given by Equation 12, that is,

$$T = 2h\sqrt{\frac{1}{V_1^2} - \frac{1}{V_2^2}} + \frac{x}{V_2} \tag{12}$$

where h denotes the depth to the boundary; V_1 the velocity in the upper stratum; V_2 the velocity in the lower stratum; and x the horizontal distance between the shot-point and a seismometer station.

If the velocity V_2 is a constant, it may be determined by measuring the slope of the straight line travel-time curve given by Equation 12 and computing its reciprocal. (Compare Figure 412.) Likewise, if the velocity V_1 is a constant, it may be evaluated from the slope of the straight line travel-curve passing through the origin, i.e., the travel-time curve corresponding to the direct wave.

Evidently, if the travel-time curve corresponding to Equation 12 were extended so as to intercept the time axis, the time intercept τ_0 would be given by the equation:

$$\tau_0 = 2h\sqrt{\frac{1}{V_1^2} - \frac{1}{V_2^2}} \tag{102}$$

Thus, if the intercept τ_0 and the velocities V_1 and V_2 are known, the thickness h of the upper stratum may be computed from the intercept formula.

The depth may also be computed from the coordinates x_c and T_c of the point of intersection of the travel-time curves corresponding to the direct wave and the refracted wave. To obtain the values x_c and T_c which satisfy the equations of both travel-time curves: namely, $T = \frac{x}{V_1}$ and $T = 2h\sqrt{\frac{1}{V_1^2} - \frac{1}{V_2^2}} + \frac{x}{V_2}$, one solves these two equations simultaneously as follows:

$$\frac{x_c}{V_1} = 2h\sqrt{\frac{1}{V_1^2} - \frac{1}{V_2^2}} + \frac{x_c}{V_2}$$

or

$$x_c = 2h\sqrt{\frac{V_2 + V_1}{V_2 - V_1}}\,; \quad h = \frac{x_c}{2}\sqrt{\frac{V_2 - V_1}{V_2 + V_1}}$$

n **Horizontal Strata.**—Referring to Figure 457, the velocities in the successive layers are $V_1, \ldots . V_{n+1}$ respectively and the thicknesses of the layers above the $(n+1)$th are: $h_1, \ldots h_n$. It was shown in a previous section that the angles made by the rays with the normals at the boundaries satisfy the equations:

$$p = \frac{\sin a_1}{V_1} = \ldots . = \frac{\sin a_k}{V_k} = \ldots . = \frac{\sin a_n}{V_n} \tag{10}$$

where p is a parameter. It can be shown that the time required by the wave in traveling from the shot-point 0 to the point A is

$$t_n = \sum_{k=1}^{n} \frac{h_k}{V_k \cos \alpha_k}$$

Furthermore, the horizontal distance from 0 to A is

$$X_n = \sum_{k=1}^{n} h_k \tan \alpha_k$$

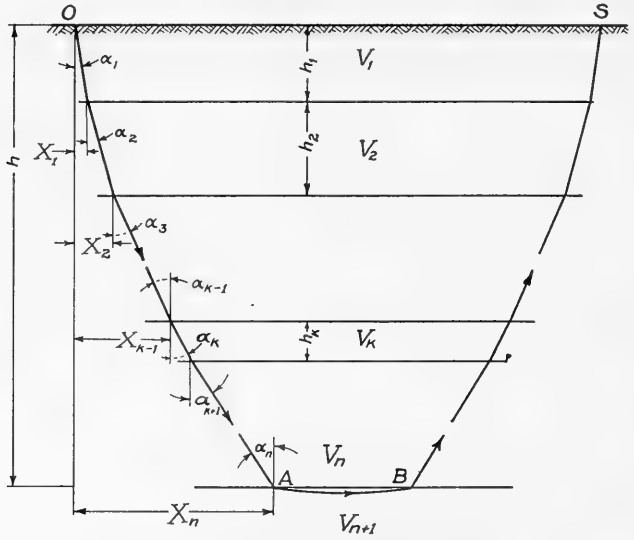

FIG. 457.—Path of a refracted ray through n horizontal layers.

The case of interest in refraction prospecting is that wherein the angle α_{n+1} has a value of 90° so that

$$p = \frac{\sin \alpha_{n+1}}{V_{n+1}} = \frac{1}{V_{n+1}}$$

and

$$\sin \alpha_k = pV_k = \frac{V_k}{V_{n+1}}$$

The total time from 0 to a point S at a distance x on the surface is obviously

$$T = 2t_n + \frac{x - 2X_n}{V_{n+1}} = \frac{x}{V_{n+1}} + 2 \sum_{k=1}^{n} h_k \left(\frac{1}{V_k \cos \alpha_k} - \frac{\tan \alpha_k}{V_{n+1}} \right)$$

$$= \frac{x}{V_{n+1}} + 2 \sum_{k=1}^{n} \frac{h_k}{V_k \cos \alpha_k} (1 - \sin^2 \alpha_k)$$

or

$$T = \frac{x}{V_{n+1}} + 2\sum_{k=1}^{n} \frac{h_k \cos a_k}{V_k} \tag{103}$$

It is evident that the travel-time curve will consist of as many segments as there are layers of different velocity, each segment corresponding to a wave path along an interface. Each segment is a straight line, and the reciprocal of the slope of each segment equals the velocity in the corresponding layer. Moreover, it is possible either from the time-intercepts or the critical distances to compute the depths to the layers.

The thicknesses of the layers may be determined successively by solving for h_n; that is, since

$$T = \frac{x}{V_{n+1}} + 2\sum_{k=1}^{n-1} \frac{h_k \cos a_k}{V_k} + \frac{2h_n \cos a_n}{V_n} ,$$

$$h_n = \frac{V_n}{\cos a_n}\left\{ \tau_{n+1} - \sum_{k=1}^{n-1} \frac{h_k \cos a_k}{V_k} \right\} \tag{104}$$

where

$$\tau_{n+1} = \frac{1}{2}\left(T - \frac{x}{V_{n+1}}\right) \tag{105}$$

is one-half the intercept time of the $(n+1)$th segment of the travel-time curve.

Numerical Illustration

Suppose the velocities and intercept-times shown in the following table have been determined from a travel-time curve.*

Layer n	V_n (ft./sec.)	T_{on} (sec.)**	τ_n (sec.)
1	5710	0	0
2	6550	.102	.051
3	7490	.252	.126
4	8320	.418	.209
5	9170	.576	.288

Let $a_{k,n}$ be the inclination in the kth layer of a ray which meets the interface between the $(n\text{-}1)$th and the nth layer at the critical angle so that

* In layer 1 the refracted wave and the direct wave are identical.

** T_{on} is the time at which the ray reaches the nth segment.

sin $\alpha_{k,n} = V_k/V_n$. With the velocities given above, sin $\alpha_{k,n}$ and cos $\alpha_{k,n}$ have the following values:

sin $\alpha_{k,n}$

k \ n	1	2	3	4	5
1	1.0000	.8718	.7623	.6863	.6227
2		1.0000	.8745	.7873	.7143
3			1.0000	.9002	.8168
4				1.0000	.9073
5					1.0000

cos $\alpha_{k,n}$

k \ n	1	2	3	4	5
1	.0000	.4899	.6472	.7273	.7825
2		.0000	.4851	.6166	.6998
3			.0000	.4355	.5769
4				.0000	.4205
5					.0000

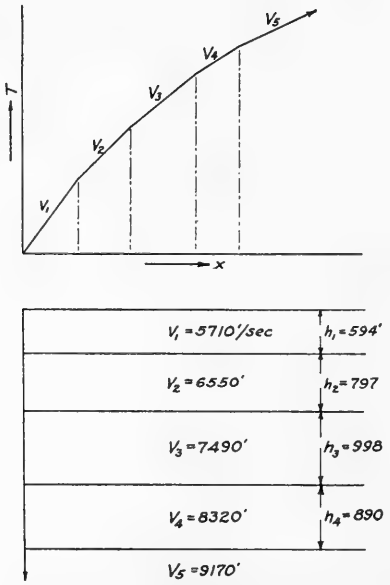

FIG. 458.—Travel-time curve for a subsurface section consisting of 5 horizontal layers.

Successive computations of the layer thicknesses proceed in the manner indicated in the table. The travel-time curve for the five-layer section is shown in Figure 458.

n	k	h_k	$\frac{h_k}{V_k}$	$\frac{h_k}{V_k}\cos\alpha_{k,n+1}$	$\sum_{k=1}^{n-1}\frac{h_k}{V_k}\cos\alpha_{k,n+1}$	$\sum_{1}^{n-1}\frac{1}{\tau_{n+1}}$	$\frac{V_n}{\cos\alpha_{n,n+1}}$	h_n	TOTAL DEPTH $=\Sigma h_n$
1	....	.....	.....	.....	.....	.051	11,655	594	594
2	1	594	.104	.067	.067	.059	13,502	797	1391
3	1	594	.104	.076	.....	.....	.....	.....	.....
	2	797	.122	.075	.151	.058	17,199	998	2389
4	1	594	.104	.081	.....	.....	.....	.....	.....
	2	797	.122	.085	.....	.....	.....	.....	.....
	3	998	.133	.077	.243	.045	19,786	890	3279

Vertical Section in Which the Velocity Increases Continuously with Depth.—When the velocity increases continuously with depth, the path of the refracted ray has the form shown in Figure 459. Due to continued refraction, the angle made by the ray with the normal at any point along its path becomes increasingly greater until at some depth H the angle becomes equal to 90°, where the ray path becomes horizontal. Thereafter, the effect produced by the continuous variation of velocity is reversed and the ray gradually swings upward and returns to the surface along a path RS which is symmetrical to the path $0R$.

To obtain the travel-time over the path $0RS$, assume that the velocity function may be written in the form $V = V(h)$ where $V(h)$ is continuous. The travel-time T and

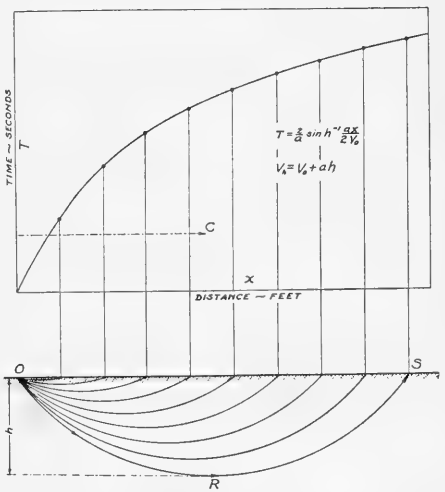

FIG. 459.—Travel-time curve for a formation in which the velocity increases linearly with depth. (Dotted line C is the locus of the centers of curvature of the ray paths.)

the horizontal distance x between the shot-point and a seismometer station may be obtained directly from the basic ray equations 37 and 39; that is,

$$T = 2t_n = 2\int_0^H \frac{dh}{V(h)\sqrt{1-p^2V^2(h)}} \tag{106}$$

and

$$x = 2X_n = 2\int_0^H \frac{pV(h)\,dh}{\sqrt{1-p^2V^2(h)}} \tag{107}$$

For the case under discussion, the parameter $p = \frac{\sin a_k}{V_k}$ has the following important properties

1. The maximum depth H is that at which $a_k = a_H = 90°$. Hence,

$$p = \frac{\sin 90°}{V_H} = \frac{1}{V_H} \tag{108}$$

That is, the parameter p is equal to the reciprocal of the velocity of the medium at the point of maximum penetration of the refracted ray.

2. The parameter p is equal to the slope of the travel-time curve corresponding to the path $0RS$. This may be proved as follows: The slope of the travel-time curve at any point is $\frac{dT}{dx}$. But $\frac{dT}{dx} = \frac{\frac{dT}{dp}}{\frac{dx}{dp}}$. Hence, the slope may be evaluated by differentiating Equations 106 and 107 with respect to the parameter p and forming the quotient.

$$\frac{dT}{dp} = 2\int_0^H \frac{pV^3(h)\,[1-p^2V^2(h)]^{-\frac{1}{2}}}{V^2(h)[1-p^2V^2(h)]}\,dh = 2p\int_0^H \frac{V(h)}{[1-p^2V^2(h)]^{\frac{3}{2}}}\,dh$$

$$\frac{dx}{dp} = 2\int_0^H \frac{V(h)\,[1-p^2V^2(h)]^{\frac{1}{2}} + p^2V^3(h)\,[1-p^2V^2(h)]^{-\frac{1}{2}}}{[1-p^2V^2(h)]}\,dh$$

$$= 2\int_0^H \frac{V(h)}{[1-p^2V^2(h)]^{\frac{3}{2}}}\,dh$$

Hence,

$$\frac{dT}{dx} = \frac{2p\int_0^H \frac{V(h)}{[1-p^2V^2(h)]^{\frac{3}{2}}}\,dh}{2\int_0^H \frac{V(h)}{[1-p^2V^2(h)]^{\frac{3}{2}}}\,dh} = p \tag{109}$$

3. The parameter p is equal to the quotient of the sine of the angle of emergence divided by the velocity at the surface of the medium. That is,

$$p = \frac{\sin a_0}{V_0}$$

where a_0 is the angle of emergence of the refracted wave and V_0 is the velocity at the surface of the medium. (Compare p. 679.)

When the velocity is a linear function ($V = V_0 + ah$), the expression for the travel-time becomes

$$T = 2\int_0^H \frac{dh}{(V_0 + ah)\sqrt{1 - p^2(V_0 + ah)^2}}$$

or

$$T = \frac{2}{a}\int_{pV_0}^1 \frac{dz}{z\sqrt{1 - z^2}} \qquad (110)^*$$

where z is defined by the equation: $z = p\ (V_0 + ah)$. On carrying out the indicated integration the expression for T becomes

$$T = -\frac{2}{a}\log_e\left[\frac{1 + \sqrt{1 - z^2}}{z}\right]_{pV_0}^1 = -\frac{2}{a}\left[\text{sech}^{-1} z\right]_{pV_0}^1$$

or

$$T = \frac{2}{a}\,\text{sech}^{-1} pV_0 \qquad (111)$$

Similarly,

$$x = \frac{2}{ap}\int_{pV_0}^1 \frac{z\,dz}{\sqrt{1 - z^2}} = -\frac{2}{ap}\left[\sqrt{1 - z^2}\right]_{pV_0}^1$$

or

$$x = \frac{2}{ap}\sqrt{1 - p^2V_0^2} \qquad (112)$$

Equations 111 and 112 are the parametric equations of the travel-time curve. The usual form of the equation of the travel-time curve may be obtained by eliminating p from equations 111 and 112. From Equation 111,

$$p = \frac{1}{V_0}\,\text{sech}\,\frac{aT}{2}$$

* The expression for the travel-time given here differs from that given on p. 683 only in the value assigned to the upper limit in the integration. The value for the upper limit used here follows directly from Equation 108.

Hence,

$$x = \frac{2V_0}{a \operatorname{sech} \frac{aT}{2}} \sqrt{1 - \operatorname{sech}^2 \left(\frac{aT}{2}\right)} = \frac{2V_0}{a \operatorname{sech} \frac{aT}{2}} \cdot \tanh \frac{aT}{2}$$

or

$$x = \frac{2V_0}{a} \sinh \frac{aT}{2} \tag{113}$$

Thus, the travel-time curve is smooth and concave downward. (Figure 459.)

Sloping Interfaces Between Strata.—While the cases of horizontal interfaces are useful in formulating ideas concerning seismic wave paths, horizontal interfaces are seldom encountered in practice. Consider, therefore, a simple two-layer problem in which the velocity in the upper layer is V_1 and the velocity in the lower layer is V_2 and assume that V_2 and V_1 differ by a finite amount. Referring to Figure 460, the *vertical depth below the shot-point* 0 is h, and the boundary dips *down* to the *right* so as to form an angle θ with the horizontal. (It is assumed that the strike of the layer is perpendicular to the plane of the figure.) x is, as usual, the distance between the shot-point and a seismometer station. 0′ is a point

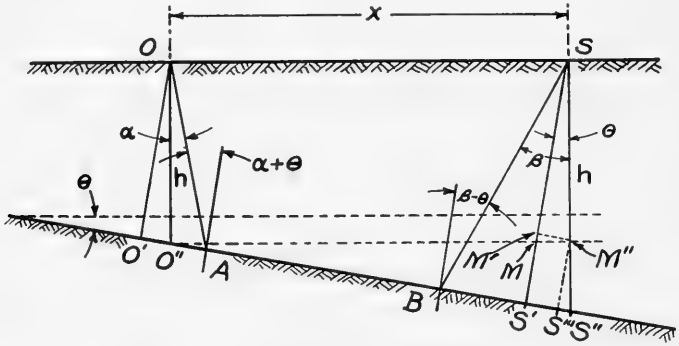

Fig. 460.—Seismic ray paths through an inclined layer.

on the bed from which a normal to the bed passes through 0; S' is the corresponding point below S; A is the point where the ray strikes the bed; and B the point where the ray leaves the bed. The angle α is the angle between the ray and the vertical at 0; β is the corresponding angle at S.

The travel-time for the path $0ABS$ is

$$T = \frac{0A + BS}{V_1} + \frac{AB}{V_2} \tag{114}$$

In triangle $00''A$,

$$\frac{0A}{h} = \frac{\sin (90 + \theta)}{\sin [90 - (\alpha + \theta)]}$$

or

$$0A = h \frac{\cos \theta}{\cos (\alpha + \theta)}$$

In triangle BSS''

$$\frac{BS}{SS''} = \frac{\sin (90 - \theta)}{\sin [90 - (\beta - \theta)]}$$

or

$$BS = SS'' \frac{\cos \theta}{\cos (\beta - \theta)}$$

But

$$SS'' = SM'' + M''S'' = h + x \tan \theta$$

Hence

$$BS = (h + x \tan \theta) \frac{\cos \theta}{\cos (\beta - \theta)}$$

Also,

$$AB = 0''S''' - 0''A - BS' - S'S'''$$

and

$$0''S''' = x \cos \theta$$

$$0''A = \frac{h \sin \alpha}{\cos (\alpha + \theta)}$$

$$BS' = BS \sin (\beta - \theta) = (h + x \tan \theta) \frac{\cos \theta \sin (\beta - \theta)}{\cos (\beta - \theta)}$$

$$S'S''' = M'M'' = h \sin \theta$$

Hence,

$$AB = x \cos \theta - \frac{h \sin \alpha}{\cos (\alpha + \theta)} - (h + x \tan \theta) \frac{\cos \theta \sin (\beta - \theta)}{\cos (\beta - \theta)} - h \sin \theta$$

If one substitutes the values of $0A$, BS and AB into Equation 114 and makes use of the relation $(\alpha + \theta) = (\beta - \theta)$ and collects similar terms, Equation 114 becomes

$$T = \frac{2h \cos \theta + x \sin \theta}{V_1 \cos (\alpha + \theta)} + \frac{x \cos \theta}{V_2} - \frac{h}{V_2 \cos (\theta + \alpha)} [\sin \alpha + \sin \theta \cos (\alpha + \theta)$$

$$+ \cos \theta \sin (\alpha + \theta)] - \frac{x \sin \theta \sin (\alpha + \theta)}{V_2 \cos (\alpha + \theta)}$$

On making use of the trigonometric identities

$$\cos (\alpha + \theta) = \cos \alpha \cos \theta - \sin \alpha \sin \theta$$

$$\sin (\alpha + \theta) = \sin \alpha \cos \theta + \cos \alpha \sin \theta$$

$$\cos^2 \theta = 1 - \sin^2 \theta$$

the expression for the travel-time T may be written in the form:

$$T = \frac{2h\cos\theta + x\sin\theta}{V_1\cos(\alpha+\theta)} - \frac{2h\cos\theta\sin(\alpha+\theta)}{V_2\cos(\alpha+\theta)} + \frac{x\cos\theta}{V_2} - \frac{x\sin\theta\sin(\alpha+\theta)}{V_2\cos(\alpha+\theta)}$$

Also, since $(\alpha+\theta)$ is the critical angle,

$$\sin(\alpha+\theta) = \frac{V_1}{V_2}$$

$$\cos(\alpha+\theta) = \sqrt{1-\left(\frac{V_1}{V_2}\right)^2}$$

Hence,

$$T = \frac{2h\cos\theta}{\sqrt{1-\left(\frac{V_1}{V_2}\right)^2}}\left(\frac{1}{V_1}-\frac{V_1}{V_2^2}\right) + \frac{x\sin\theta}{\sqrt{1-\left(\frac{V_1}{V_2}\right)^2}}\left(\frac{1}{V_1}-\frac{V_1}{V_2^2}\right) + \frac{x\cos\theta}{V_2}$$

or

$$T = 2h\cos\theta\sqrt{\frac{1}{V_1^2}-\frac{1}{V_2^2}} + x\left(\frac{\cos\theta}{V_2} + \sin\theta\sqrt{\frac{1}{V_1^2}-\frac{1}{V_2^2}}\right) \qquad (115)$$

Equation 115 is the equation of a straight line.

The travel-time curve therefore consists of two straight line segments, one corresponding to the direct wave and the other to the refracted wave. The segment corresponding to the direct wave passes through the origin and has a slope $\frac{1}{V_1}$. The segment corresponding to the refracted wave has a slope $\frac{\cos\theta}{V_2} + \sin\theta\sqrt{\frac{1}{V_1^2}-\frac{1}{V_2^2}}$ and a time intercept

$$\tau_0 = 2h\cos\theta\sqrt{\frac{1}{V_1^2}-\frac{1}{V_2^2}}.$$

If the seismometer is *up dip* from the shot-point, θ must be replaced by $-\theta$. In the usual procedure two shot-points are used, one at the up dip end of the profile and the other at the down dip end. The *vertical distance to the boundary at the down dip shot-point* will be denoted by h' and the distance between the shot-points will be denoted by L. It is evident from Figure 460 that $h' = SS'' = h + L\tan\theta$.

The travel-time curve for up dip shooting consists of two straight line segments. The first segment has a slope $1/V_1$ and passes through the point $x = L$. The second segment has a slope of magnitude $(\cos\theta/V_2 - \sin\theta\sqrt{1/V_1^2 - 1/V_2^2})$ and a time intercept with the line $x = L$ of magnitude $\tau_L = 2h'\cos\theta\sqrt{1/V_1^2 - 1/V_2^2}$.

In terms of the new variables ($h'$and L), the travel-time equations for down dip shooting and up dip shooting are:

$$T = L\left(\frac{\cos\theta}{V_2} + \sin\theta\sqrt{\frac{1}{V_1^2} - \frac{1}{V_2^2}}\right) + 2h\cos\theta\sqrt{\frac{1}{V_1^2} - \frac{1}{V_2^2}}$$

and

$$T' = L\left(\frac{\cos\theta}{V_2} - \sin\theta\sqrt{\frac{1}{V_1^2} - \frac{1}{V_2^2}}\right) + 2h'\cos\theta\sqrt{\frac{1}{V_1^2} - \frac{1}{V_2^2}}$$

respectively.

If h' is replaced by its equivalent, $h+L\tan\theta$, the expression for T' becomes identical with that for T. This is to be expected because the refracted path for up dip shooting is the same as that for down dip shooting. In practice, however, the values of V_1 obtained at the two shot-points may not be exactly the same and therefore the check times for the reversed paths may not be identical. In this case, the travel-time curves are adjusted *before* computing V_2 and θ so as to make the travel-times T and T' identical.

V_2 and θ may be obtained from the slopes of the line segments corresponding to the refracted paths. That is, V_2 and θ may be obtained from the relations

$$\frac{1}{V_2'} = \text{slope}_{\text{(down dip)}} = \frac{\cos\theta}{V_2} + \sin\theta\sqrt{\frac{1}{V_1^2} - \frac{1}{V_2^2}} \qquad (116)$$

$$\frac{1}{V_2''} = \text{slope}_{\text{(up dip)}} = \frac{\cos\theta}{V_2} - \sin\theta\sqrt{\frac{1}{V_1^2} - \frac{1}{V_2^2}} \qquad (116a)$$

The values of V_2' and V_2'' (*apparent velocities*) and V_1 are obtained from the field curve directly or from the adjusted field curve, depending on whether V_1 is the same at the two shot-points or not.

A more practical method makes use of the relationship that the sine of the angle of emergence is equal to the product of the velocity in the surface layer by the slope of the travel-time curve. This relationship may be derived from Equation 116 by making use of the relation: $\frac{V_1}{V_2} = \sin(\alpha+\theta)$. Thus

$$\text{slope}_{\text{(down dip)}} = \frac{1}{V_1}[\cos\theta\sin(\alpha+\theta) + \sin\theta\cos(\alpha+\theta)]$$

$$= \frac{1}{V_1}\sin[\theta + (\alpha+\theta)]$$

But

$$\alpha+\theta = \beta-\theta \qquad \text{and} \qquad \theta = \frac{\beta-\alpha}{2}$$

Hence

$$\text{slope}_{\text{(down dip)}} = \frac{1}{V_1} \sin \beta$$

Similarly

$$\text{slope}_{\text{(up dip)}} = \frac{1}{V_1} \sin \alpha$$

The equations just derived permit the calculation of β and α and so of θ [which is equal to $\frac{1}{2}(\beta - \alpha)$]. Also, V_2 may be obtained from the relation: $\frac{V_1}{V_2} = \sin(\alpha + \theta)$. In practice, a good approximation is $V_2 = \frac{1}{2}(V_2' + V_2'')$.

Evidently, when the values of θ, V_1, and V_2 are known, the depth h may be calculated from the intercept formula

$$\tau_0 = 2h \cos\theta \sqrt{\frac{1}{V_1^2} - \frac{1}{V_2^2}}$$

and h' may be calculated from the relation

$$h' = h + L \tan\theta$$

For successively deeper layers the calculation can proceed in a similar way; that is, formulas may be derived for the depth, dips, and velocities for the multi-layer, dipping cases by methods analogous to those already described. Another procedure favored by many investigators is to reduce the problem at each step to the two layer case. Figure 461 shows how this may be done. The dip and depth of the first interface and the velocities V_1 and V_2 are determined by the methods outlined above.*

From the slopes $\frac{1}{V_3'}$ and $\frac{1}{V_3''}$ of the third segments of the travel-time curves and the fact that the slopes are equal to the sines of the emergence angles divided by V_1, the emergence angles α and β can be found. Choose any two points S_1 and S_2 between the two shot-points. By simple trigonometry the lengths $0_1'0_2'$, $0_1'S_1'$ and $0_2'S_2'$ can be found. Also, the times along the segments $0_1'0_1''S_1''S_1'$, $0_1'0_1''0_2''0_2'$, and $0_2'0_2''S_2''S_2'$ are readily determined. For example, the total time along the path $0_10_1'\,0_1''S_1''S_1'S_1$ is read from the travel-time curve, the time along $0_1'0_1''S_1''S_1'$ is obtained by subtracting the times along the segments $0_10_1'$ and $S_1'S_1$ from the total time. This gives two points on each of the second segments of the new travel-time curve (Figure 461B) so that these two segments may be drawn. The first segments correspond to direct waves in the second layer with velocity V_2 and hence are straight lines with slope $1/V_2$ through $0_1'$ and $0_2'$ respectively. The depth, dip, and velocity are now computed as before. (It should be noted that the "depths" determined by this procedure are directed along the perpendiculars to the second boundary at

* The numerical computations are indicated on p. 763.

O_1' and O_2'.) Obviously, this process can be continued for any number of layers.

The discussion given above is restricted to ideal cases only because space does not permit coverage of field records. The solution of special cases must depend primarily on the diligence of the computer and can be learned only through experience. Usually each experienced operator eventually develops his own computing technique.

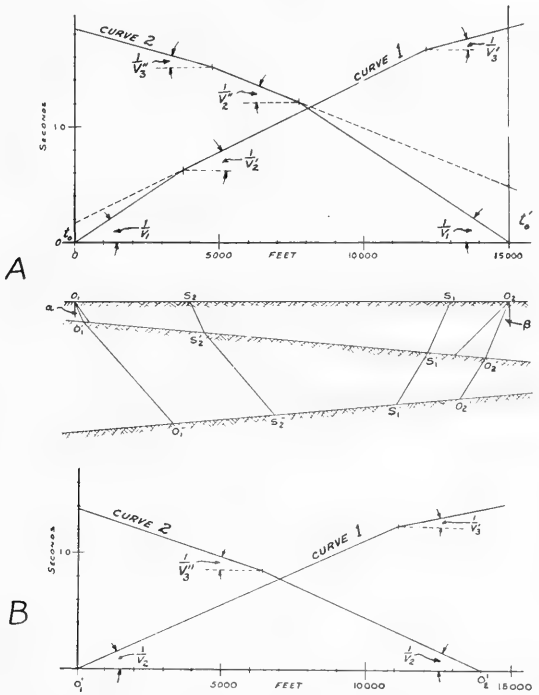

FIG. 461.—*A*, travel-time curves corresponding to a geological structure which consists of two inclined layers; *B*, computed curves obtained when the three layer case is "reduced" to a two layer case. Curve 1 is the travel-time curve for down dip shooting (shot-point at 0_1); Curve 2 is the travel-time curve for up dip shooting (shot-point at 0_2). (After W. M. Rust, Jr.)

Numerical Illustration

The values of the apparent velocities obtained from the travel-time curve are:

$$V_1 = 6000 \text{ ft./sec.}, \frac{1}{V_1} = 1.67 \times 10^{-4}$$

$$V_2' = 8250 \text{ ft./sec.}$$

$$V_2'' = 10{,}000 \text{ ft./sec.}$$

Hence,

$$\sin \alpha = \frac{V_1}{V_2'} = .727 \qquad \alpha = 46°40'$$

$$\sin \beta = \frac{V_1}{V_2''} = .600 \qquad \beta = 36°50'$$

$$\sin^{-1} \frac{V_1}{V_2} = \tfrac{1}{2} (\alpha + \beta) = 41°45'$$

$$\frac{V_1}{V_2} = .666 \qquad V_2 = 9000 \text{ ft./sec.} \qquad \frac{1}{V_2} = 1.11 \times 10^{-4}$$

$$\theta = \tfrac{1}{2} (\beta - \alpha) = 4°55' \qquad \cos \theta = .996$$

Extending the segments back to the shot-points gives

$$\tau_0 = .174 \qquad \tau_0' = .490$$

so that

$$h = \frac{\tau_0}{2 \cos \theta \sqrt{\frac{1}{V_1^2} - \frac{1}{V_2^2}}} = 700 \text{ ft.}; \quad h' = \frac{\tau_0'}{2 \cos \theta \sqrt{\frac{1}{V_1^2} - \frac{1}{V_2^2}}} = 2000 \text{ ft.}$$

From the third sections

$$V_3' = 15{,}500 \text{ ft./sec.}$$

$$V_3'' = 14{,}600 \text{ ft./sec.}$$

$$\sin \alpha_1 = \frac{V_1}{V_3'} = .387 \qquad \alpha_1 = 22°45'$$

$$\sin \beta_1 = \frac{V_1}{V_3''} = .411 \qquad \beta_1 = 24°15'$$

The times along the segments $0_1 0_1'$, $S_2 S_2'$, $S_1 S_1'$ and $0_2 0_2'$ may be computed either trigonometrically or graphically by using the values of V_1, h, h', α_1, and β_1 given above. The times are found to be 0.117, 0.191, 0.306 and 0.341 respectively. By subtracting the times along $0_1 0_1'$ and $S_1 S_1'$ from the time 1.698 along $0_1 0_1' S_1' S_1$ the time 1.275 is obtained at the distance 12,000 feet as measured along $0_1' S_1'$. The calculations of the times along $0_1' 0_2'$ and $0_1'' 0_2''$ are carried out in the same way, and the solution proceeds as already outlined.

Limitations of Outlined Calculations

By the methods just outlined, the thicknesses, dips, and velocities of the subsurface strata can be calculated when these quantities satisfy the assumptions upon which the methods of calculation are based. Strata with velocities lower than the velocities of the overlying strata or strata

which are too thin do not show up in the travel-time curves. For example, refracted waves traversing the structures *a*, *b*, *c*, and *d* (Figure 462B) have the same travel-time curve (Figure 462A) even though the geological conditions are radically different. *d*, only, can be differentiated from the others by use of a refraction shot in the reversed direction. (Figure 462B, (*c*) shows the case of an intermediate thin layer. A layer of this thickness would, in general, be detected.)

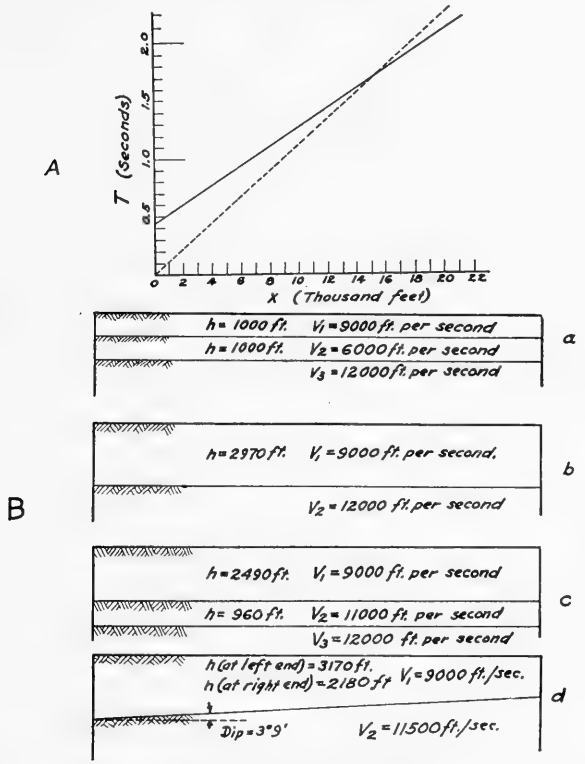

FIG. 462.—The same travel-time curve (portion *A*) is obtained for refracted waves traversing the structures *a*, *b*, *c*, *d* (portion *B*). (After W. M. Rust, Jr.)

An interesting example of the use of refracted waves other than first arrivals is the earlier work of Ewing, Crary and Rutherford† on the Atlantic Coastal Plain. By using the indications of the arrival of waves refracted through beds that were not thick enough to give first arrivals, they were able to increase the accuracy of their work and to discriminate between cases corresponding to (*a*) and (*b*) of Figure 462B.

Stated briefly, the assumptions on which refraction calculations are based are:

1. The velocities in successive strata increase as the depth increases.

† *Bulletin of the Geological Society of America*, Vol. 48 (1937) pp. 753-802.

2. The materials of the strata are such that the velocities in any direction are the same, i.e., the velocities are constant throughout each stratum.
3. The strata are sufficiently thick.
4. The boundaries between the strata are planes.

If these conditions are satisfied, the travel-time curve will consist of straight line segments having successively decreasing slopes. In practice, these conditions are rarely, if ever, satisfied. Generally the velocity increases with the depth through a single layer. Also, loose layers frequently exist under dense layers, and the velocities in the loose layers are less than the velocities in the dense layers.

Mapping Subsurface Structure from Determinations of "Delay Times."—The methods described in this section constitute a means for mapping the surface of a *marker horizon,* which exhibits gentle relief and a definite velocity increase over that of the overlying stratum.*

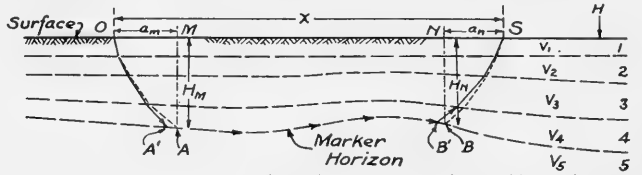

FIG. 463.—Ray path of wave following marker horizon. (After Gardner, *Geophysics.*)

Referring to Figure 463, it is assumed that the actual ray path of the refracted wave which traverses layer 5 is $0A'B'S$, where the portion of the ray path in layer 5 is here assumed to follow the interface. In addition, to facilitate calculations, it is assumed that the actual ray path $0A'B'S$ may be replaced by a hypothetical path $0ABS$ defined as that path which the waves would follow if all the beds in the neighborhood of the paths $0A'$ and $B'S$ were horizontal. Calculations based on this assumption will have only a small error if the dips are less than 10°. Let

$$a_m = 0M = \text{offset distance corresponding to } 0$$

$$a_n = NS = \text{offset distance corresponding to } S$$

The travel-time T between 0 and S is:

$$T = T_{0A'B'S} = T_{0ABS} \text{ (approximately)}$$

or

$$T = t_{0A} + t_{AB} + t_{BS}$$

where t_{0A}, t_{AB} and t_{BS} denote the travel-times along the paths $0A$, AB and BS respectively.

* With the exception of some minor changes, this section follows L. W. Gardner, "An Areal Plan of Mapping Subsurface Structure by Refraction Shooting," *Geophysics,* Vol. IV, No. 4, Oct., 1939, pp. 247-259.

Assume that the velocity V_5 in the layer whose surface constitutes the marker horizon is constant. Then

$$t_{AB} = \frac{\overline{AB}}{V_5} = \frac{x - a_m - a_n}{V_5}$$

and the expression for the travel-time T may be written in the form

$$T = \left(t_{0A} - \frac{a_m}{V_5}\right) + \left(t_{BS} - \frac{a_n}{V_5}\right) + \frac{x}{V_5} \tag{117}$$

Introduce the quantities t_m' and t_n' defined by the relations:

$$t_m' \equiv t_{0A} - \frac{a_m}{V_5} = \text{delay time at } M$$

$$t_n' \equiv t_{BS} - \frac{a_n}{V_5} = \text{delay time at } N$$

Also, set

$$b \equiv T - \frac{x}{V_5} = \text{intercept time}$$

The intercept time may also be expressed in the form:

$$b = t_m' + t_n' \tag{118}$$

Equation 118 is the basic relation of subsequent deductions. Since T, x, and V_5 are determinable from the observed data, the intercept time b may be regarded as an observed quantity.*

For a given velocity distribution in the geologic section, the delay times t_m' and t_n' are dependent only on the depths H_m and H_n respectively. Furthermore, if the velocity distribution is known, it is theoretically possible to deduce a relationship between the delay time t' and the depth H and to portray this relationship graphically. Thus, if the delay times can be determined from observed data, the corresponding depths may be read from the graph.

The relationships of delay times to depths and to offset distances may be obtained from the geometry of the hypothetical path. In Figure 464, α is the angle formed by the hypothetical wave path with the vertical at a point in the depth interval ΔH; Δa denotes an increment of offset distance; Δs is the path length in the interval ΔH. The increment of delay time corresponding to Δa will be denoted by $\Delta t'$. From the geometry of the figure,

$$\Delta H = \Delta s \cos \alpha, \qquad \Delta a = \Delta H \tan \alpha$$

and from Snell's law

$$\sin \alpha = \frac{V}{V_5}$$

* To achieve accuracy in the final results, it is of course necessary that the value of the observed travel-time be corrected for the low velocity or so-called "weathered" layer.

On combining these relations with the definition of delay time

$$\Delta t' = \frac{\Delta s}{V} - \frac{\Delta a}{V_5}$$

one obtains

$$\Delta t' = \frac{\Delta H \cos a}{V}$$

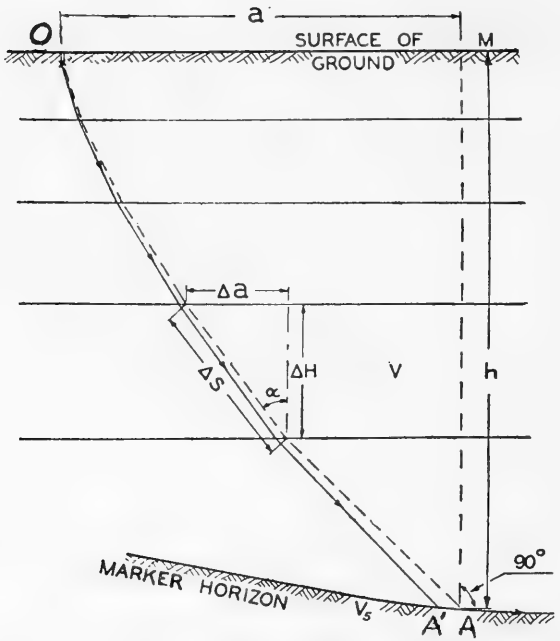

FIG. 464.—Portion of actual ray path and hypothetical ray path. (After Gardner, *Geophysics.*)

The total delay time to a given depth H of the marker horizon is

$$t' = \sum \frac{\Delta H \cos a}{V} \tag{119}$$

and the depth of the horizon is

$$H = \sum \Delta H \tag{120}$$

Equations 119 and 120 constitute a set of parametric equations from which the delay time t' corresponding to a depth H of a marker horizon can be obtained provided the quantity ΔH is known as a function of V.
Also, the total offset distance $a = \Sigma\, \Delta a$ may be written in the form

$$a = \sum \Delta H \tan a \tag{121}$$

Evidently Equations 121 and 119 are a set of parametric equations from

which the total offset distance a corresponding to a total delay time t' can be obtained.

The general types of depth vs. delay time and offset distance vs. delay time graphs frequently obtained in practice are shown in Figure 465. (The change in the slopes of these curves with increasing t' is due to increase of velocity with depth.)

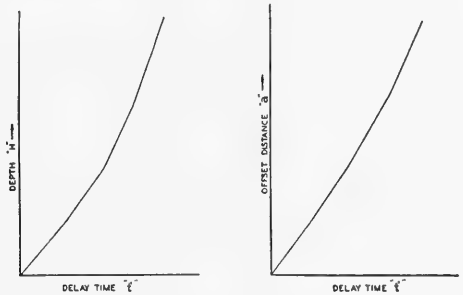

FIG. 465.—*A*, general type of depth vs. delay time graph; *B*, general type of offset distance vs. delay time graph. (Gardner, *Geophysics.*)

Correlation of Refractions

The correlation refraction method of seismic surveying is more laborious to prosecute than reflection methods. Consequently this type of prospecting is usually confined to those areas in which the conventional reflection methods fail to obtain satisfactory results.

In the application of refraction methods it is known that for the case of a multi-layered problem, there exists between the shot-point and the recording station a distance where a number of refracted energy arrivals may be observed corresponding to the seismic wave penetration of the respective layers. The basis of the refraction method of shooting is that the distance between shot-point and receiver is a measure of the wave penetration for a given vertical velocity distribution. Conversely, there is a reliable means for estimating the minimum distance required to obtain the arrival of the so-called "grazing" wave. The changes in refracted wave velocities will indicate the velocity discontinuities of the strata penetrated by the wave. The sequence and the apparent surface velocity of the refracted arrivals depend upon the depths, dips, velocities and recording distances. Conversely, given the recorded sequence and surface velocity of the refracted arrivals, and the velocities of the penetrated layers, deduction can be made of the dip and depth of the layers.†

The recording distance used for correlation refraction shooting usually is determined by the following factors: desired penetration to include layers to be investigated, economical amount of explosive energy to secure

† L. W. Gardner, "An Areal Plan of Mapping Subsurface Structure by Refraction," *Geophysics*, Vol. VII, No. 2, April, 1942.

recording, sensitivity of recording equipment, and terrain of area under investigation. This so-called "optimum distance" is established by experiment and then used as a guide for the study of a given area.

Correlation refraction shooting differs from early refraction methods in that the earlier methods were concerned only with the first arrivals on the seismogram. The instrument designs used then were for precise timing of the first arrivals, and as a consequence it was seldom that any but the first arrivals were recorded.

This early work demanded long and continuous recording distances in order to follow certain high-speed subsurface boundaries. Correlation refraction work does not make use of continuous refractions from a boundary, but depends for its effectiveness on correlation of refractions obtained from independent arrangements of shot-point and receiver stations. These correlations are made on the basis of arrival time, sequence of arrival, wave character of the recorded arrival, and horizontal velocity of the recorded impulse. In comparison with reflection correlations we have one additional criterion in refraction correlation, i.e., the recorded surface velocity of the arrivals. In practice this velocity is referred to as "move-out" or "step-out" time and is often diagnostic of a certain subsurface geologic formation.

In refraction correlation work, elevations are theoretically established on certain velocity discontinuities, and dips of these surfaces are estimated. With a sufficient number of these observations in an area, it is possible to draw a structural contour map.

The correlation of refraction methods has been applied in Russia, in the Edwards Limestone area of Texas, and experimentally in California.†

Special seismic instruments are not necessary for use in correlation refraction work. Only a slight modification of the modern reflection type of equipment, embodying an adequate amplitude control, is required to obtain sufficient separation of the various arrivals of refracted energy on the seismogram. By recording several refracted wave arrivals on a single seismogram it is possible to study the geological structure of a number of refracting layers, using only one distance between shot-point and center of instrument spread. In practice this distance usually varies from three to six miles to obtain structural information to depths from 3000 to 5000 feet. However, recording distances as long as twenty miles have been used in some cases.

Figure 466 is an illustration of a multiple-event refraction record from Crockett County, Texas, recording distance 30,250 - 33,000 feet. This is

† G. A. Gamburtsev, Izvestiya Akademii Nauk SSSR, "Seriya Geograficheskaya i Geofizicheskaya," *Bull. Acad. Sci., U.S.S.R. Serie Geogr. et Geoph.*, 1942, pp. 26-47.

L. W. Gardner, "Correlation of Refraction Shooting," *Geophysics,* Vol. XI, No. 1, Jan., 1946, pp. 59-65.

J. A. Gillin & E. D. Alcock, "The Correlation Refraction Method of Seismic Surveying," *Geophysics,* Vol. XI, No. 1, Jan., 1946, pp. 43-51.

A. J. Barthelmes, "Application of Continuous Profiling to Refraction Shooting," *Geophysics,* Vol. XI, No. 1, Jan., 1946, pp. 24-42.

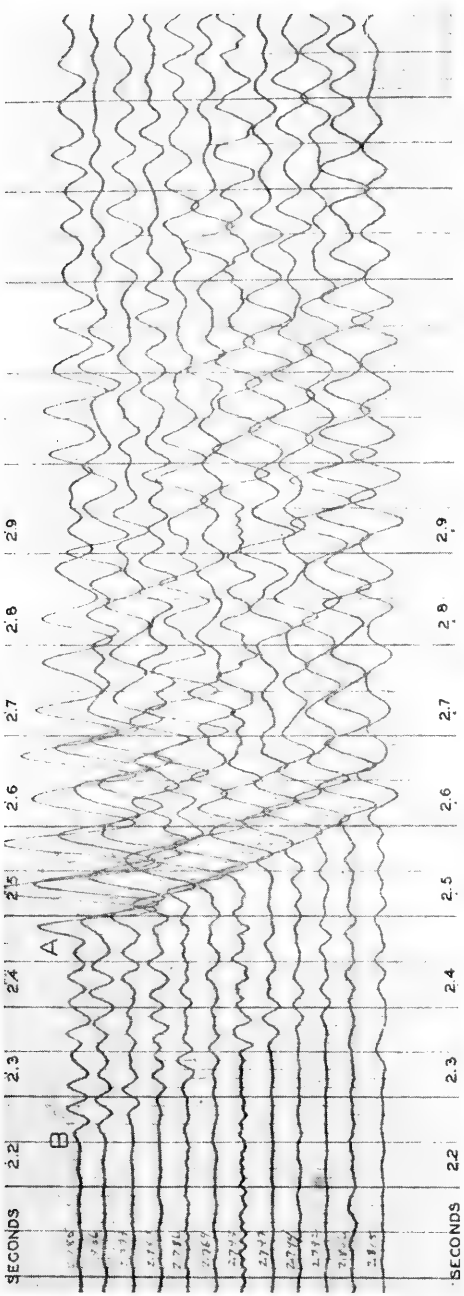

FIG. 466.—Multiple-event refraction seismogram from Crockett County, Texas, recording distance 30,250 - 33,000 feet. (Courtesy of Seismograph Service Corporation.)

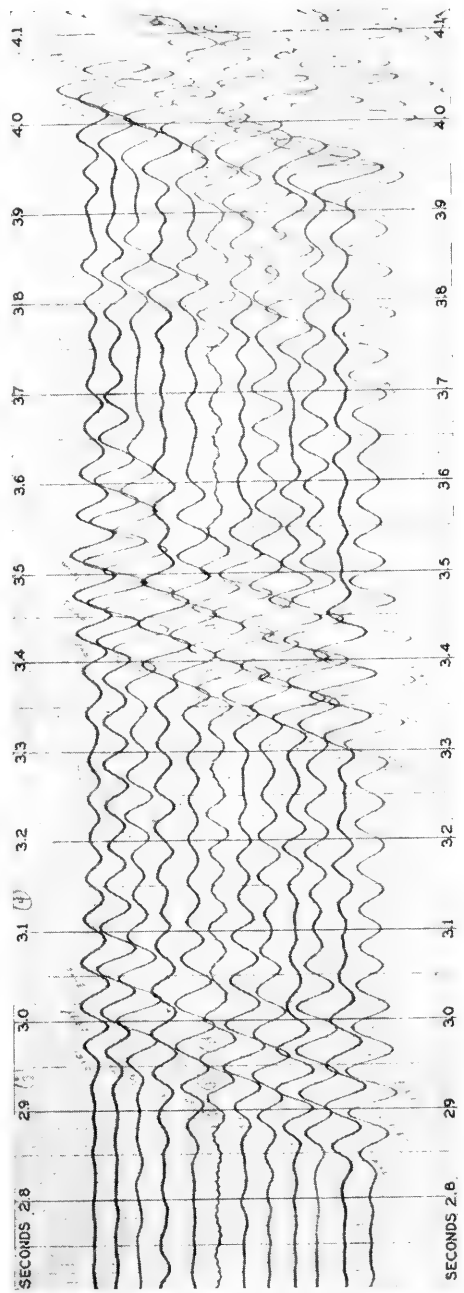

FIG. 467.—Multiple-event refraction seismogram from West Texas, recording distance 44,000 - 46,250 feet. (Courtesy of Seismograph Service Corporation.)

believed to be an example of an event from a high velocity refractor preceded by a lower amplitude arrival from a lower velocity refractor.

Figure 467 is an illustration of a multiple-event refraction record from West Texas, recording distance 44,000 - 46,250 feet. At least three outstanding refracted arrivals are present on this seismogram.

Figure 468 is an illustration of a multiple-event refraction seismogram from West Texas (same general area in which Figure 467 was obtained). This record was made with lower frequency instruments than the above. It is of interest to note that this seismogram was made with the use of only 40 pounds of dynamite buried at a depth of 90 feet and recorded at the extreme recording distance of 88,000 - 90,250 feet, or about 17 miles.

Figure 468A illustrates a type of multiple-event refraction seismogram obtained in California where no high-velocity marker beds (such as limestone formations) are known to exist in the geological column. This record was obtained from the explosion of 300 pounds of 60 per cent Vibrogel placed at a depth of 180 feet in the outcrop of the basement complex, located 21,000 feet east of the center of the instrument spread. From well logs it was known that the basement is at least 5,000 feet below the location of the instrument set-up. By placing the shot-point directly in the high-velocity material and the instrument spread above several thousand feet of sedimentary formations overlying the high-velocity basement rocks, the serious problem of securing wave penetration from the surface through the sediments to the refracting horizons was eliminated.

The first arrivals of the refracted energy of this seismogram (2.228 + .021 on trace one) are correlated with the basement complex as the refracting horizon. The later arrivals (2.884 + .021 on trace one) are correlated with corresponding refracting horizons within the sedimentary formations above the basement rocks. It is of interest to note the difference in the step-out times of the two outstanding energy arrivals: 0.078 sec. for the basement arrivals and 0.113 sec. for a layer above the basement. This step-out difference, the sequence of refracted energy arrivals and the character of the recordings are useful criteria for refraction correlation work. Also, it should be noted that the refraction from the deeper-lying basement arrived ahead of the refraction from the shallower-lying sedimentary formations, due to the higher velocity in the basement.

A test of the refraction correlations was obtained in this case by continuous recording of refraction profiles along lines radiating from the shot-points placed in the outcrop of the basement complex. It is obvious that equal arrival travel-times should be observed at identical distances and elevations for the case of horizontal stratification of the relatively constant velocity layers. When different travel times are observed at equal horizontal distances and elevations relative to the shot-point, such data may be interpreted as indicating that the refraction horizons are non-parallel with the horizontal. In this manner possible ridges and valleys in the basement complex surface may be mapped and the general geologic

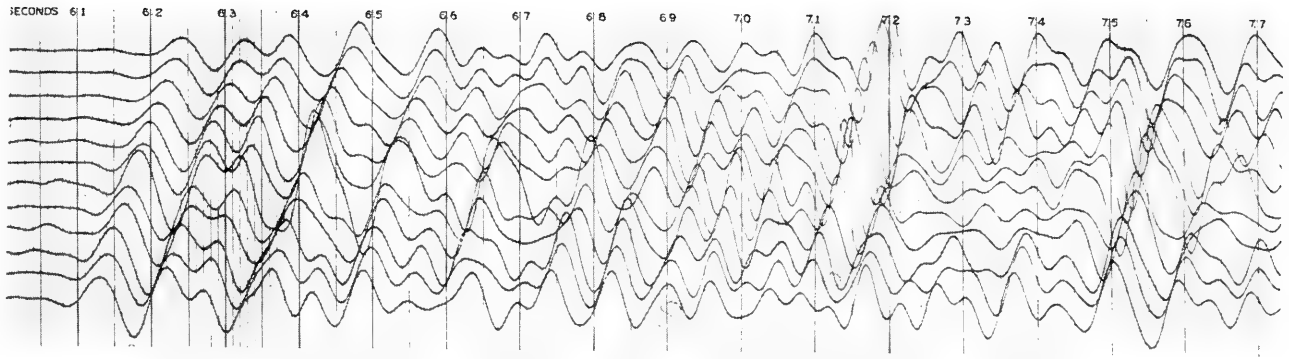

FIG. 468.—Multiple-event refraction seismogram from West Texas, recording distance 88,000 - 90,250 feet, dynamite charge 40 pounds, hole depth 90 feet. (Courtesy of Seismograph Service Corporation.)

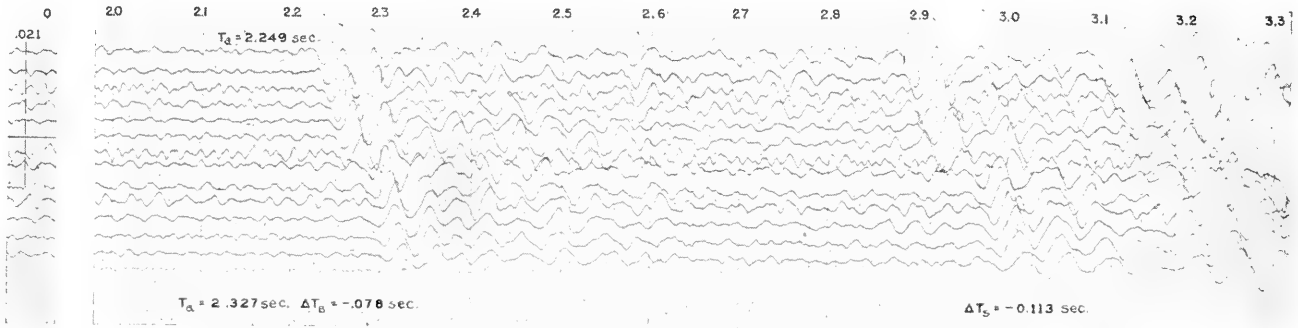

FIG. 468A.—Multiple-event refraction seismogram recorded near Arvin, Kern County, California. The explosive was placed in an outcrop of basement complex rocks, and recorded at a distance of 21,000 feet from the shot-point to the center of a 1080-foot instrument spread of 14 recording seismometers. The seismometers were distributed at 60-foot intervals, except at the center of the spread, where there was a gap of 320 feet. (Courtesy of Geophysical Engineering Corporation.)

structure of the layers above the basement rock may be deduced. This technique is useful in mapping the relative structure, but is not a method for obtaining absolute structural measurements.

Intersecting Spreads

The methods to be described here are applicable when approximate values of offset distances are known. These can be determined by computing average delay times from preliminary and subsequent field data and using the offset distance vs. delay time graph.

Consider an arrangement (ring shooting) wherein two spreads 0_1S_1 and 0_2S_2 intersect at a point M which is an approximate offset position for the two shot-points 0_1 and 0_2. (Figure 469A.) The delay times associated with the common offset position for the two spreads will be approximately equal.

The expressions for the intercept times are

$$b_1 = t_m' + t_{n_1}'$$

$$b_2 = t_m' + t_{n_2}'$$

Hence,

$$b_2 - b_1 = t_{n_2}' - t_{n_1}' \qquad (122)$$

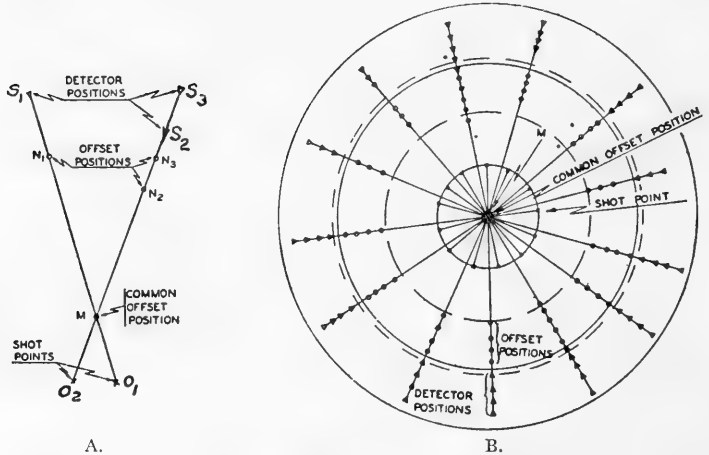

FIG. 469.—*A*, element of ring shooting arrangement; *B*, complete ring shooting arrangement. (Gardner, *Geophysics.*)

Evidently, Equation 122 can be used to calculate the difference in delay times from the *observed* intersect times b_2 and b_1. The corresponding difference in depths may be obtained from the depth vs. delay time graph.

Also, a seismometer at S_3 will have a common offset position at M with the seismometer at S_2; hence,

$$b_3 - b_2 = t_{n_3}' - t_{n_2}'$$

and the corresponding depth distance may be obtained, as before, by using the depth vs. delay time graph.

Furthermore, if a number of seismometers are placed on a relatively short line which passes through 0_2 and are orientated in an azimuth with respect to 0_2S_2, the offset positions associated with the common shot-point will be approximately coincident.

An extension of this arrangement which comprises a number of short spreads is shown in Figure 469B. The offset positions M associated with the ends of the various radial spreads lie in a small annular area. Undulations of the relative depths below the annular area can be determined by computing the delay times from the observed intercept times (Equation 122), and making use of the depth vs. delay time graph. Evidently, by arranging a number of such rings in a manner such that one or more control points from adjacent rings overlap, it is possible to combine all the data into a map showing relative depths over a large area. A triangular arrangement can also be used.

Application of Refraction Method to Salt Dome Exploration.—The velocity of seismic waves in salt domes is very much greater than that in the sedimentary materials surrounding the domes. Thus, a wave which has traveled in part through a salt dome will have a much greater average velocity than a wave traveling the same distance in a nearby area where no salt dome is present. This fact was established in 1924 and led to wide-spread use of refraction fan shooting.

Fan Shooting

In fan shooting, the seismometers are located at approximately equal distances from a shot-point. The distance is usually determined by shooting an auxiliary profile; it must be sufficiently great to insure that the waves penetrate to the desired depth. In the Gulf Coast, it is customary to use the empirical figure of one-fifth for the ratio of penetration to shot distance.*

The seismometers are so positioned with reference to the shot-point that they cover any desired portion of the 360° surrounding the shot-point. Figure 470 illustrates a common arrangement of seismometers for covering a 135° sector. After the seismometers have been positioned at known and preferably equal distances from the shot-point, a charge is exploded, and the travel-times taken by the waves to reach the various seismometers are recorded. If the waves which have traveled through any particular sector have a higher velocity than the waves which have traveled through the other sectors, a high velocity plug is indicated in that sector.

The interpretation of the results of refraction fan shooting is extremely simple, because the time differences observed are rather great.

* This relationship is similar to that prevailing in electrical work where the effective depth of current penetration is assumed to vary from about 1/3 to 1/5 of the electrode separation.

It is necessary only to plot the deviation of the travel times from the normal values. (Where it is not possible or convenient to locate all seismometers at the same distance from the shot-point, a short profile covering the interval from the shortest distance to the longest distance is shot in order to establish the normal travel-times for the various distances.)

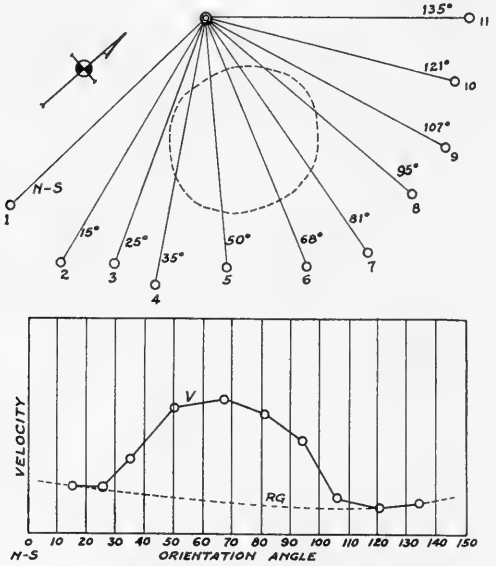

FIG. 470. — Diagrammatic sketch of fan shooting. Seismometers are placed at ends of lines 1, 2, 3, . . . 11 which radiate from the shot-point O; *V*, mean velocity; *RG*, probable regional velocity.

Figure 470 shows the shot-point at 0 and seismometers at the ends of radii 1 to 11. The lower portion of the figure schematically indicates the variation of velocity with orientation angle. (In an alternative presentation, the deviation of the travel-time from the normal value would be plotted along each radius, zero deviation being plotted on an arbitrary circle with the center at 0.)

By the use of a number of strategically located shot-points and seismometer stations, a large area can be explored fairly rapidly. If the results indicate the presence of a shallow salt dome, the position and outline of the dome can be located more accurately by additional shots approximately at right angles to the first fan.

Figure 471 shows the theoretical ray paths through a salt dome that is located 1000 feet below the surface and has a cross sectional extent of 5000 feet.

Figure 472 shows a theoretical seismogram corresponding to a seismometer *S* located a distance of 10,000 feet from the shot-point 0. It

will be observed that at the time 1.12 there is a small disturbance which corresponds to the wave traveling through the salt. The amplitude of the salt wave disturbance diminishes rapidly. At the time 1.31 a second disturbance starts. This disturbance corresponds to the normal wave through the material surrounding the dome. The difference 0.19 seconds is the deviation of the travel-time from the normal value for that distance and is called the *lead*.

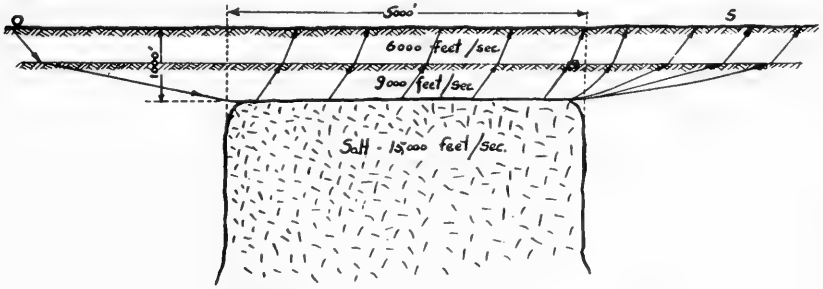

FIG. 471.—Theoretical ray paths through a cross section of a salt dome.

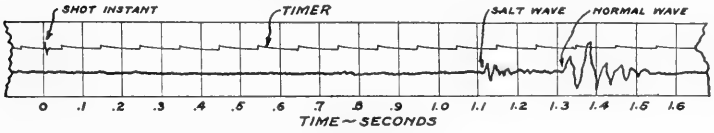

FIG. 472.—Schematic seismogram for a refraction shot across a salt dome.

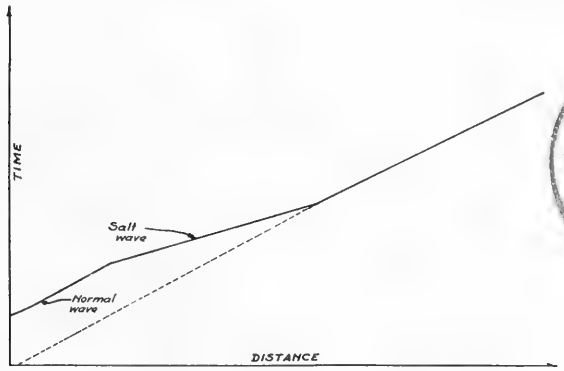

FIG. 473.—Travel-time curve for salt dome shown in Figure 471.

Figure 473 shows a schematic travel-time curve corresponding to a traverse over the dome. A portion of the lower branch of the travel-time curve corresponds to wave energy which has traveled through the salt; the remainder of the lower branch and the upper branch corresponds to energy which has traveled through the surrounding material.

A large number of comparatively shallow salt domes has been located by fan shooting. At the present time, it is believed that the numerous fan surveys carried out in the Gulf Coast have probably disclosed practically all the shallow salt domes in that region.

In addition to discovering new salt domes, fan shooting in some cases has outlined successfully regions underlain by large structural features. *

Profiling Salt Dome Boundaries

Bore Hole Method.—A method for use in bore holes has been proposed by McCollum. § The principles of the method will be evident from Figure 474 wherein 0 represents the shot-point, 7 the recorder, and 5 the seismometer. The seismometer S is adjusted to various positions in the bore hole as, for example, d_2, d_3 or d_6, by means of a hoisting winch and cable. Consider that the seismometer is stationed at d_6. The wave traversing the path $0kf_6d_6$ will reach the point d_6 in the shortest possible time. This wave will actuate the seismometer S and its exact time of arrival will be recorded by 7. Let the time of travel over the path $0kf_6d_6$ be T.

Evidently,

$$T = t_1 + t_2 + t_3$$

where t_1 is the time to traverse the path $0k$; t_2 is the time to traverse kf_6, and t_3 is the time to traverse f_6d_6. The last equation may also be written in the form

$$T = t_1 + \frac{kf_6}{V_s} + \frac{f_6d_6}{V_6}$$

where V_s is the velocity along the path kf_6 and V_6 is the velocity along the path f_6d_6.

Here t_1 and V_s may be determined from reflection travel-time data using the normal arrangement wherein both seismometer and shot-point are located at the surface of the earth.†† The velocity V_6 will depend on the path kd_6; that is, the velocities along the various paths f_5d_5, f_6d_6, etc. will, in general, be different. However, a mean value of V_5 can be determined by obtaining the travel-times T_5, T_6 and T_7 between a shot-point located at a point $0'$ on the surface near the bore hole and a seismometer positioned at d_5, d_6 and d_7 respectively.**

The position of the point k can be determined from reflection travel-time data. The position of the point d_6 is, of course, known.

---

* The theoretical basis of this type of refraction shooting has been discussed by Barton † and by Roman.‡.

† D. C. Barton, "The Seismic Method of Mapping Geologic Structure," *A.I.M.E. Geophysical Prospecting*, 1929, pp. 590-598.

‡ Irwin Roman, "Analysis of Seismic Profiles," *A.I.M.E. Geophysical Prospecting*, 1934, pp. 493-527.

§ Burton McCollum, "Seismic Method of Profiling Geologic Formations," U. S. Patent 1,923,107. Issued August 22, 1933.

†† Burton McCollum, U. S. Patents 1,724,495 and 1,724,720.

** The velocity thus determined is an average or equivalent velocity.

Hence, it is possible to determine the paths fd_6 and kf_6; that is, it is possible to determine the position of the point f_6 on the flank of the dome. The positions of the points f_4, f_5, etc., may be determined in a similar way. Thus, the method is capable of profiling the boundary surface of the subsurface geological structure.

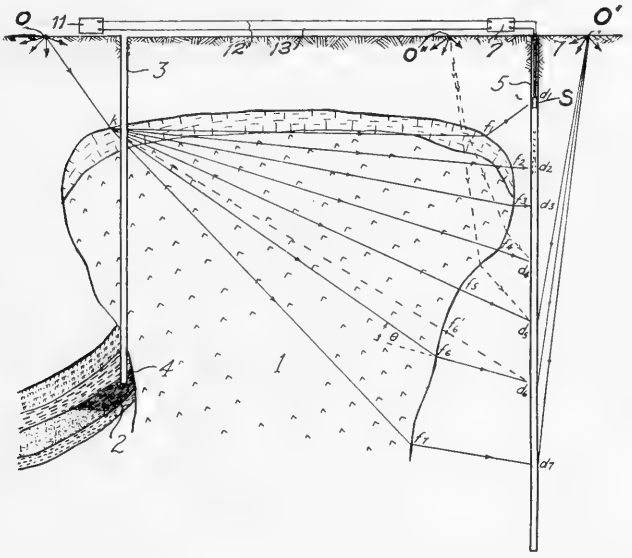

FIG. 474.—Schematic drawing illustrating a method for profiling the boundary surface of a subsurface geological structure. (After McCollum, U. S. Patent 1,923,107.)

Another method for determining the boundary of a salt dome, based upon first arrival time measurements of seismic waves from a series of shot-points, is given by Gardner.† The shot-points are distributed around the dome and received by a well detector within a deep hole flanking the dome.

INSTRUMENTS

Seismometers

Seismometers are also known as geophones, receptors, seisphones, jugs and pots. They may be classified in several ways, according to (1) the particular ground motion to which their outputs are more or less proportional, (2) whether they are tuned or untuned, (3) the component of motion to which they are chiefly responsive, such as the vertical or the horizontal component, and (4) the means for converting the ground motion (usually mechanical or electrical) into a quantity that may be recorded. The first classification, according to element ground motion, is

† L. W. Gardner, "Seismograph determination of salt dome boundary, using well detector deep on dome flank," *Geophysics*, Vol. XIV, No. 1, January, 1949, pp. 29-38.

the most universally used in exploration geophysics. This classification may be divided into:

(a) *Accelerometers,* a type of seismometer which is responsive particularly to the acceleration of the ground movement. These instruments are generally characterized by high natural periods. Mechanically, they are devices for measuring force or pressure acting on relatively fixed inertia mass.†

(b) *Velocity-type seismometers,* which measure, within certain definable limits, the rate of movement of ground with reference to a relatively fixed inertia mass. The natural periods of these instruments are intermediate in magnitude.

(c) *Displacement-type seismometers,* which react to the ground movements in such a manner that their output is proportional to the displacement or movement of the ground. Instruments of this type are generally of extremely low frequency or long period, and are usually unstable and difficult to design.

The second classification deals with seismometers which may be tuned or untuned. When the natural period of the seismometer lies within the range of the frequencies to be recorded, the instrument is *tuned;* if the natural frequency lies outside of this range, it is *untuned.*

The mechanical make-up of a seismometer usually comprises a vibratory mechanical system, of a desired frequency range or periodicity, which works in conjunction with some form of transducer or energy transfer device. It is common practice to dampen the oscillatory systems of seismometers just short of the critical stage of damping. Usually the amount of damping is referred to as a fraction of (h), such that when $h = 0$ there is no damping, and when $h = 1$ there is critical damping. The generally-used value is $h = 0.7$.

The essential parts of a seismometer are: a rugged waterproof case which rests firmly on the earth, a heavy mass or weight which is attached to the case by means of a spring or other elastic arrangement, and a movable element which transforms the movement of the heavy mass to a form of energy suitable for recording.

The arrival of seismic waves at the seismometer produces two momentary effects: (1) a displacement of the case which is in contact with the earth and (2) a displacement of the inertia reactor. That is, the seismic waves set both the case and the suspended inertia mass vibrating. The frequency of vibration of the case is approximately the same as that of the waves. The frequency of vibration of the inertia reactor depends on the natural frequency of the reactor system (mass plus suspension) as well as on the frequency of the seismic waves. In the absence of

† L. D. Statham, "Accelerometer with Electric Strain Wires," U. S. Patent 2,453,548, Nov. 9, 1948.
H. E. Webber, "Accelerometer," U. S. Patent 2,455,394, Dec. 7, 1948.
C. R. Abraham, "Means and Method of Indicating Acceleration," U. S. Patent 2,457,620, Dec. 28, 1948.
C. M. Hathaway, "Accelerometer," U. S. Patent 2,440,605, April 27, 1948.

damping, the vibration of the inertia reactor system would continue even after the seismic waves ceased arriving. For this reason, the inertia reactor of practically all seismometers is provided with some form of external damping. The damping may be mechanical, electromagnetic, or both.*

General Conditions Affecting Design.—The amplitude of the elastic wave created by the explosive or mechanical disturbance decreases with increasing distance from the source. (Compare p. 651.) In particular, the change of amplitude with depth is especially marked, and, due to this factor, high sensitivity of seismometers and high amplification are necessary. (In this connection, it should be noted that the seismometer, amplifier and recording galvanometer all act together to produce the final overall response.)

The frequencies generally encountered in seismic exploration vary with the area. In the immediate vicinity of the disturbance the waves have a wide range of frequencies with the higher frequency components constituting a major portion of the energy. Generally, the absorption is greater for the higher frequencies; hence, as the distance from the disturbance is increased, the preponderance of wave energy shifts toward the lower frequencies.

Considering the detecting system (seismometer and recording apparatus), one may note that the equipment must be so designed that the following three conditions are fulfilled: (1) The system must be sufficiently sensitive to detect and amplify the useful seismic disturbance; (2) the system must discriminate sufficiently against undesired energy to produce usable records; and (3) the system must have sufficient damping that successive seismic impulses can be recognized individually. In the matter of sensitivity, the energy output of the seismometer is of primary consideration. The seismometer must supply an impulse to the first stage of the amplifier which is sufficiently above the noise or microphone level of the first stage to allow effective amplification. (Above this level, amplifier units can be made to produce any degree of amplification desired.) The usual seismic amplifier has a gain of from 100 to 150 DB. Damping means must be present in both seismometer and amplifier units to avoid a sustained oscillation in either. Where the visual interpretation of records is employed, the frequency response of the overall system must be sufficiently narrow that both the low frequencies characteristic of ground roll and the high frequencies characteristic of wind and other disturbances are greatly attenuated. The amplifier and seismometer should be designed in such a way that their characteristics are complementary in order to obtain the desired overall response.

---

* For data on seismometer characteristics, particularly damping, see, for example, H. R. Prescott and A. P. Lipski, "System Sensitive to Vibrations," U. S. Patent 2,058,106, issued Oct. 20, 1936, and H. R. Prescott and K. C. Woodyard, "Seismophone," U. S. Patent 2,084,561, issued June 22, 1937.

Fundamental Theory of Seismometer Based on the Mechanics of a Vibrating Particle

The logical basis for the design of a seismometer to respond to the vertical component of the earth's motion is a loaded vertical spring arrangement as shown schematically by Figure 475. In actual practice the moving pendulum or inertia mass is connected to some type of transducer which develops an oscillatory voltage corresponding to the motion of the inertia mass relative to the frame. However, Figure 475 is used to illustrate only the behavior and theory of the oscillatory system, and not mechanical design.

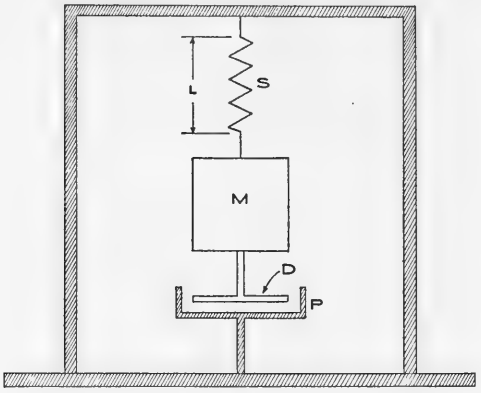

FIG. 475.—Vertical component seismometer pendulum (schematic). M—mass suspended; S—suspension spring; D—dash; P—dash pot containing viscous liquid.

Let $M =$ the mass of the pendulum
$L_o =$ length of spring unloaded
$L =$ length of spring loaded and at rest
$(L-y) =$ length of spring loaded and displaced
$F =$ force exerted by the spring per unit of extension

In this theoretical discussion the weight of the spring has been neglected; the condition of the loaded spring may be expressed by the following relationship:

$$Mg = F\,(L-L_o) \tag{123}$$

Consider the mass constrained to move along the Y axis. Assume the ordinate of the center of mass to be measured upward from the position of equilibrium. $\ddot{Z}$ is the upward acceleration of the frame caused by the motion of the earth. The upward acceleration of the mass will be given by the differential equation

$$M\ddot{y} = -Mg + F\,(L-y-L_o) - M\ddot{Z} \tag{124}$$

Substituting $F\,(L-L_o)$ for Mg and rearranging, the differential equation of motion becomes

$$\ddot{y} + \frac{F}{M}\,y + \ddot{Z} = 0 \tag{125}$$

The dots represent differentiation with respect to time as illustrated by the following:

$$\ddot{y} = \frac{d^2y}{dt^2} \quad \text{and} \quad \dot{y} = \frac{dy}{dt}$$

Equation 125 does not contain the damping term associated with the dash-pot arrangement shown by Figure 475. If this dash-pot is filled with some type of viscous oil, there will be a damping resistance to the motion of the inertia mass proportional to the velocity. The equation of motion then becomes

$$\ddot{y} + \frac{K}{M}\dot{y} + \frac{F}{M}y = -\ddot{Z} \tag{126}$$

We shall solve this equation later, but first let us discuss some definitions and make some of the more obvious observations with reference to the oscillatory system shown schematically by Figure 475. Perhaps the easiest measurement to make on this loaded spring arrangement is the period of free oscillation with no viscous liquid in the dash-pot. The period of free oscillation may be defined as the time interval between successive passages in the same direction through the rest position. For this purpose, assume that the motion of the vibrating mass is of the simple harmonic variety. This assumption, when translated into the language of the physicist, states that if there is a restoring acceleration proportional to the negative displacement, there is simple harmonic motion. The displacement (y) may then be stated by the well known formula

$$y = y_m \sin (nt + c) \tag{127}$$

This expression comes from a solution of the differential equation

$$\ddot{y} = -n^2y \tag{128}$$

To integrate, multiply both sides of this equation by $2\,dy$ which gives

$$2\,dy\,\ddot{y} = 2\,\dot{y}\,\ddot{y}\,dt = d(\dot{y})^2 = -2n^2y\,dy$$

and integrating $\dot{y}^2 = -n^2y^2 + c_1$.

To evaluate the constant of integration, consider the condition for a maximum (y_m) displacement which requires that the derivative vanish. Then

$$-n^2y_m^2 + c_1 = 0 \qquad \text{and} \qquad c_1 = n^2y_m^2$$

so that the result of the first integration is

$$\dot{y} = n\sqrt{y_m^2 - y^2}$$

Separating the variables and integrating the second time:

$$\frac{dy}{\sqrt{y_m^2 - y^2}} = n\,dt \qquad \sin^{-1}\frac{y}{y_m} = nt + c$$

Thus,

$$y = y_m \sin (nt + c) \tag{127}$$

The definition of the period (T) of the oscillatory system corresponds to a difference of 2π or 360° in the angle of Equation 127. Placing T as the symbol representing the period, then from Equation 127:

$$nT = 2\pi \qquad \text{or} \qquad n = \frac{2\pi}{T} \tag{129}$$

Replacing n in Equation 128 $\ddot{y} = -\frac{4\pi^2}{T^2} y$

Equation 128 may be used to compute the displacement for a specified acceleration. Referring to Figure 475, if there is not an outside impressed acceleration, Equation 125 may be written as

$$\ddot{y} + \frac{F}{M} y = 0 \tag{130}$$

Substituting for $\ddot{y}$ the value given by Equation 128,

$$\frac{4\pi^2}{T^2} = \frac{F}{M} \tag{131}$$

$$T = 2\pi\sqrt{\frac{M}{F}} = 2\pi\sqrt{\frac{L - L_o}{g}}$$

In the theory of the mechanics of vibrating particles, the definition of the *equivalent pendulum length* is given by

$$L_e = \frac{g}{4\pi^2} T^2 \tag{132}$$

For any oscillatory system of motion of period T, it is in general possible to compute by use of Equation 132 the length of a theoretical pendulum which would oscillate with the same frequency.

Applying this equation in our case of the loaded spring, the *equivalent pendulum length* is equal to $L - L_o$, or the elongation of the spring due to loading. From this it is evident that the arrangement shown by Figure 475 is suitable for short periods only, because long periods would make necessary the use of a very long spring. This places a practical limitation on this type of arrangement.

In the theory as developed thus far, the damping of the system has not been considered. An oscillating mass which is under the influence of an outside force (such as that due to the motion of the ground), in addition to the force tending to drive the mass to the rest position, is said to be executing a *forced vibration.* In the case of seismology the geophysicist is particularly interested in the nature of this so-called outside force. To state the matter more exactly, the geophysicist is interested in the ground motion from which this force is a consequence. Now an undamped seismometer (not under forced vibration) will for the most part vibrate at a frequency known as *free resonance* when subjected to a transient pulse. In other words, the pendulum of an undamped system will *not* follow through the motions impressed on it. It will record the instant of disturbance but will continue to vibrate after the disturbance has passed.

In seismology a usable representation of the motion of the ground must be obtained. Therefore it becomes obvious that, in so far as practical, it is necessary that the suspended mass follow the forced vibrations impressed on the seismometer rather than any free oscillatory motion inherent in the mechanism.

To eliminate the free motion of the seismometer system provision should be made for damping whereby the free motion is absorbed by doing work. In Figure 475 a dash-pot of viscous liquid is illustrated schematically for this purpose. The viscous medium is usually oil†, but the more modern damping arrangements are generally electromagnetic in nature, to avoid the varying viscosities of liquids with changes of ambient temperature. Electromagnetic damping effects are nearly independent of temperature changes.

† The relatively large temperature-viscosity variations of practically all suitable fluids necessitate a change to light oil in the colder months, and heavier, more viscous oils in the hotter months.

From a mathematical point of view it may be stated that the design is such that, in addition to the acceleration of the mass proportional to the negative displacement, there is an opposing acceleration to be added which is proportional to the velocity. As applied to a seismometer of the loaded spring type, there exists, besides the simple harmonic force of restitution, a damping resistance proportional to the velocity. The equation of motion when the frame is at rest is given by

$$\ddot{y} + \frac{K\dot{y}}{M} + \frac{F}{M}\, y = 0 \tag{133}$$

This equation represents a particle constrained to move along the Y axis as a damped linear oscillator. In order to simplify the result of obtaining solutions of this Equatior 133, we shall choose coefficients so that

$$2\,hn = \frac{K}{M}$$

and

$$n^2 = \frac{F}{M}$$

Rewriting Equation 133 using new coefficients

$$\ddot{y} + 2\,hn\dot{y} + n^2 y = 0$$

At once a solution for this differential equation may be written because of its standard form which has been discussed elsewhere† in the many treatises on the mechanics of vibrating particles and text books of differential equations.

$$y = Ae^{-at} \cos\,(wt + \beta) \tag{134}$$

Differentiating with respect to time and substituting in Equation 133 we have

$$\{2aw - 2hnw\} \sin\,(wt + \beta) + \{n^2 + a^2 - 2hna - w^2\} \cos\,(wt + \beta) = 0 \tag{135}$$

This equation is satisfied for all values of (t) if the coefficients of the sine and cosine functions vanish separately. This requires that

$$a = hn \qquad \text{and} \qquad w^2 = n^2\,(1 - h^2)$$

Thus,

$$y = Ae^{-hnt} \cos\,(wt + \beta) \tag{136}$$

is a solution of Equation 133 when $h<1$. (For $h>1$, w_o is the square root of minus a positive number, and is therefore imaginary.) Since this solution contains two *arbitrary constants, A* and β, it is therefore the complete solution. It represents the damped vibrations of the oscillator when not under forced vibration. The exponential factor indicates that the amplitude decreases with time, falling to $1/e$ of its original value in the time, $t = \frac{1}{hn}$. The frequency with damping, called the *natural* frequency (not under forced vibration) is given by

$$w = n\sqrt{1 - h^2} = \sqrt{\frac{F}{M} - \frac{K^2}{4M^2}} \tag{137}$$

† William V. Houston, *Principles of Mathematical Physics*, McGraw-Hill, 1934.
Leigh Page, *Introduction to Theoretical Physics*, Van Nostrand, 1928.

In comparing this expression with that for the free resonant frequency

$$w_o = 2\pi/T = \sqrt{F/M} \tag{131}$$

we note that the natural frequency is less than it is when there is no damping. (Note that $w = w_o$ when $h = 0$.) If we plot the displacement (y) against time, it is clear that the curve will lie between the two curves corresponding to the maximum and minimum values of the cosine for any value of t:

$$y = +Ae^{-hnt} \quad \text{and} \quad y = -Ae^{-hnt}$$

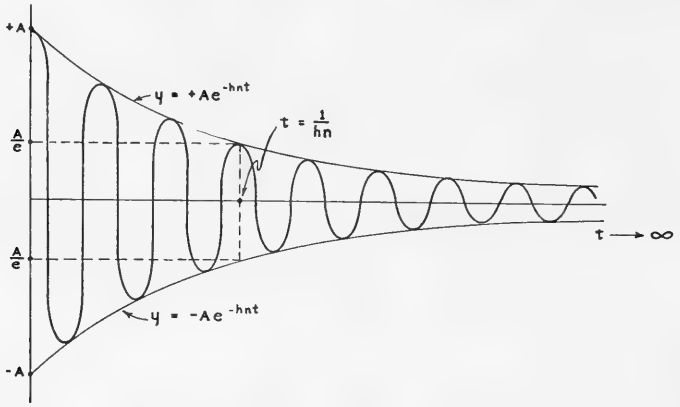

FIG. 476.—Showing damped oscillations of $y = Ae^{-hnt} \cos(wt + \beta)$.

Now consider the case when $h>1$. Then the so-called angular frequency w becomes imaginary from Equation 135. Therefore the motion will not be oscillatory, and the solution involving oscillatory trigonometric functions is not suitable as a solution of the equation of motion in the case where $h>1$. For this case we may try $y = Ae^{-at}$. Differentiating and substituting in Equation 133,

$$A\,(a^2 - 2ahn + n^2)\,e^{-at} = 0 \tag{138}$$

Equation 138 is satisfied for all values of t if

$$a = hn \pm n\sqrt{h^2 - 1}$$

Thus the complete solution of Equation 133 for the case when $h>1$ is

$$y = Ae^{-n(h+\sqrt{h^2-1})t} + Be^{-n(h-\sqrt{h^2-1})t}$$

A and B are the two arbitrary constants which may be used for the complete solution of Equation 133. In this solution, when $h>1$, the exponent is always real and negative. This means that the motion is aperiodic. If the inertia mass is pulled away from the equilibrium position and released, the damping is so great that the inertia mass never passes to the other side of the rest position, but its movement decreases exponentially to zero with time. In this case, then, when $h>1$, the system is *over-damped;* when $h = 1$, the motion is said to be *critically damped;* when $h<1$, the motion is *under-damped;* and when $h = 0$, the motion is *undamped.*

Frequency Response

Figure 477 illustrates the response of a seismometer measured in relative units plotted against the applied frequency in cycles per second.

The natural frequency of the seismometer was 6.5 cycles per second, with a constant of .727 volts /cm/ second at 250 ohms load. In conformity with theory, the outputs are a maximum in the neighborhood of the natural frequency when the seismometer is underdamped to the extent that the value of h is somewhat less than 0.7. The smaller the damping coefficient, the larger the peak output becomes. This usually corresponds to the larger

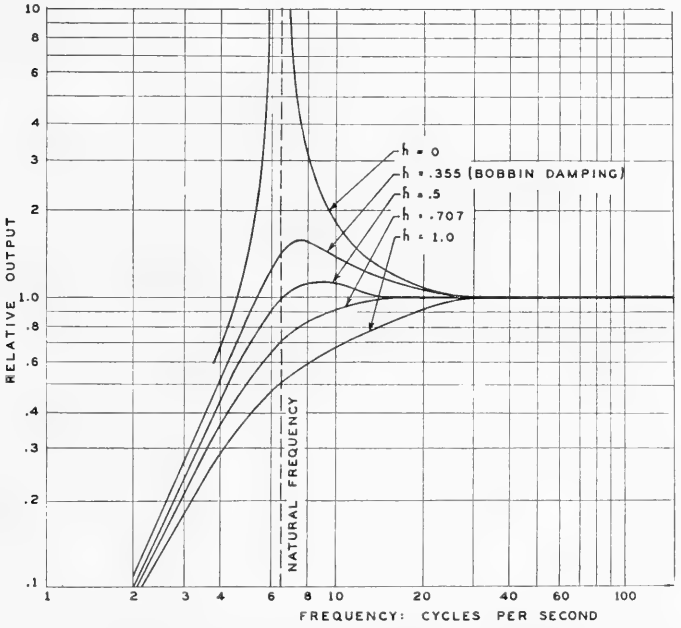

FIG. 477.—Effect of various damping coefficients on frequency response of a Type 301 seismometer. (Century Geophysical Company.)

amplitudes of the inertia mass. Another important generalization to be observed from Figure 477 is that the apparent maxima of the various curves shift to the right of the natural frequency. This indicates that the frequency of resonance increases with increasing values of the damping coefficient h. This is an important factor for consideration when designing any oscillatory system of a specified frequency response. Particular attention should be given to the character of the curve for h = about 0.7, because this is the amount of damping usually chosen for seismometers and galvanometers.

Effects of Ground Motion

The discussion just completed involving the solution of Equation 133 is perfectly general and applies to pendulums of all types, as well as galvanometers and other oscillating systems. In this theory neither friction nor mass of the spring was considered. In all cases the restoring force was assumed to be proportional to the negative displacement. The constant (n) is defined from Equation 133 as the square root of the restoring acceleration per unit displacement.

After completing the study of free vibrations of the oscillating particle, Equation 126, which describes the theoretical seismometer when disturbed by certain types of ground motion, may be studied in more detail. This equation may be written in a more familiar form

$$\ddot{y} + 2hn\dot{y} + n^2y = -\ddot{Z},$$

and now is similar to Equation 133 except for the acceleration term $(-\ddot{Z})$ which represents an outside force. A vibrating particle which is under the influence of an outside force (in addition to the force of attraction toward the rest position) is said to be executing a forced vibration. Assume that the particle is subjected to the external force H; then the equation of motion will have a term on the right-hand side such that $\ddot{Z} = \frac{H}{M}$. When $\ddot{Z}$ is a constant or is a mathematical function of time (t) only, Equation 126 may be solved by the differential treatment for equations with constant coefficients. However, if $\ddot{Z}$ is a function of both (t) and (y), the motion cannot be that of a simple forced vibration. From experience gained through working with problems of this nature, it has been found that if

$$-\ddot{Z} = a \cos wt \qquad \text{where} \quad a \equiv \frac{C}{M}$$

an approximation is obtained to the real motion of the ground caused by a buried explosion or an earthquake. It will be noted that the force, $C \cos wt$, is a simple harmonic force impressed on the system. Equation 126 now becomes

$$\ddot{y} + 2hn\dot{y} + n^2y = a \cos wt \tag{139}$$

A solution of this equation is given by

$$y = A \cos (wt - \phi) \tag{140}$$

Substituting in Equation 139 and expanding the sine and cosine of the difference,

$$[a - A\{(n^2 - w^2) \cos \phi + 2nhw \sin \phi\}] \cos wt$$
$$+ [-A (n^2 - w^2) \sin \phi + 2Anhw \cos \phi] \sin wt = 0 \tag{141}$$

This equation is satisfied for all values of (t) only if the coefficients of sin wt and cos wt are zero separately. Equating the coefficients of sin wt to zero,

$$\sin \phi = \frac{2nhw}{\sqrt{(n^2 - w^2)^2 + (2wnh)^2}}, \qquad \tan \phi = \frac{2nhw}{n^2 - w^2},$$
$$\cos \phi = \frac{n^2 - w^2}{\sqrt{(n^2 - w^2)^2 + (2wnh)^2}}, \tag{142}$$

Placing the coefficients of cos wt equal to zero,

$$A = \frac{a}{(n^2 - w^2) \cos \phi + 2nhw \sin \phi} = \frac{a}{\sqrt{(n^2 - w^2)^2 + (2wnh)^2}} \tag{143}$$

$$\text{Now} \quad y = \frac{a}{\sqrt{(n^2 - w^2)^2 + (2nhw)^2}} \cos (wt - \phi), \quad \tan \phi = \frac{2nhw}{n^2 - w^2} \tag{144}$$

This solution of Equation 139 contains no arbitrary constants; therefore it is a so-called *particular solution*. To obtain a complete solution to Equation 139, proceed in the following manner:

Let y_1 be the function of time represented by the right-hand side of Equation 136, and y_2 that represented by the right hand side of Equation 144. Then if

$$y = y_1 + y_2 \tag{145}$$

and substituting in Equation 139

$$\ddot{y}_1 + 2nh\dot{y}_1 + n^2y_1 + \ddot{y}_2 + 2nh\dot{y}_2 + n^2y_2 = a \cos wt$$

Since y_1 is a solution of Equation 133

$$\ddot{y}_1 + 2nh\dot{y}_1 + n^2y_1 = 0$$

and y_2 is a solution of Equation 139

$$\ddot{y}_2 + 2nh\dot{y}_2 + n^2y_2 = a \cos wt$$

therefore $y_1 + y_2$ is a solution of Equation 139. Since the part y_1 of this solution contains two arbitrary constants, the sum $y_1 + y_2$ is the complete solution of the differential Equation 139

$$y_1 = Ae^{-hnt} \cos (wt + \beta) \qquad \text{for } h<1 \tag{136}$$

or

$$y_1 = Ae^{-n(h+\sqrt{h^2-1})t} + Be^{-n(h-\sqrt{h^2-1})t} \qquad \text{for } h>1$$

Note that y_1 contains a damping factor which becomes smaller and smaller with time. For this reason the oscillations represented by y_1 are called the *transient terms.*

If a long time elapses in comparison with $\frac{1}{nh}$ since the beginning of the motion, then the transients will have been damped out and the oscillations will consist only of the *forced vibrations* represented by y_2 and given explicitly by Equation 144. A further study shows that these vibrations have a frequency equal to that of the impressed force but lag behind it by the phase angle ϕ. If $w<n$, then ϕ lies between 0° and 90°, whereas, if $w>n$, ϕ lies between 90° and 180°, corresponding to tan $\phi>0$ and tan $\phi<0$ respectively.

It is interesting to consider the amplitude of the steady state in this case of forced vibrations.

$$A = \frac{a}{\sqrt{(n^2 - w^2)^2 + (2nhw)^2}} \tag{143}$$

To find the frequency w_A of the impressed force for which A is a maximum we differentiate and set equal to zero.

$$\frac{dA}{dw^2} = 0$$

Thus,

$$\frac{d}{dw^2}\{(n^2 - w^2)^2 + (2nhw)^2\} = -2(n^2 - w_A^2) + 4n^2h^2 = 0$$

This gives

$$w_A^2 = n^2(1 - 2h^2) \tag{146}$$

This frequency w_A is known as the *frequency of resonance* for a damped oscillator under forced vibration. When $h^2>1/2$ there can be no *frequency of resonance* since w_A is imaginary. It can also be shown that the greater the damping factor (nh) the less the amplitude of the motion from the forced vibrations becomes.

It is sometimes convenient to measure the square of the frequency from the point of resonance. Introduce a new term (H) such that

$$H^2 = w^2 - w_A{}^2 = w^2 - n^2 + 2h^2n^2$$

then

$$A = \frac{a}{\sqrt{(2h^2n^2 - H^2)^2 + 4h^2n^2\ (H^2 + n^2 - 2h^2n^2)}}$$

$$A = \frac{a}{\sqrt{H^4 + 4h^2n^4(1 - h^2)}} \tag{147}$$

Now plot the values of the amplitude A against the square of the frequency, to obtain a curve which is symmetrical about the ordinate for which the frequency corresponds to the frequency of resonance (Figure 478).

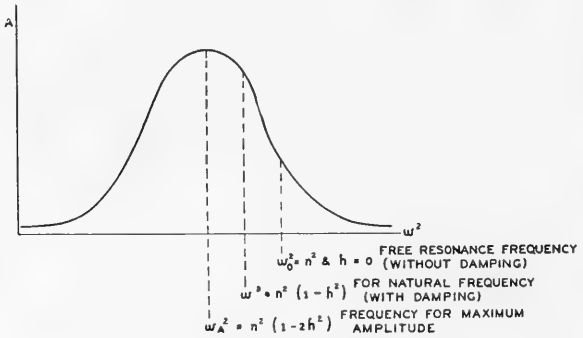

FIG. 478.—Plot of amplitude versus square of frequency, showing resonance conditions.

From a consideration of Equation 143 it may be seen that for any impressed frequency (w) the amplitude of the forced vibrations is less, the greater nh becomes. The amplitude at resonance ($H = 0$) is (from Equation 147)

$$A_{max} = \frac{a}{2n^2h\sqrt{1 - h^2}} \tag{148}$$

It is to be noted that amplitude becomes greater for small values of (nh). Mathematically the amplitude becomes infinite when the coefficient of the damping term equals zero.

Another useful expression in the study of a seismometer is the ratio of A_{max} to A, often referred to as the *sharpness of tuning*.

$$\frac{A_{max}}{A} = \sqrt{1 + \left(\frac{H^2}{2n^2h\sqrt{1 - h^2}}\right)^2} \tag{149}$$

where A represents the amplitude for a particular value of H^2. It is to be noted that the sharpness of tuning is larger for small values of the damping coefficient (nh).

The expression for the average kinetic energy due to a forced vibration may be written as follows:

$$\bar{E} = \tfrac{1}{4}\, mA^2w^2 = \tfrac{1}{4}\, \frac{ma^2w^2}{(n^2 - w^2)^2 + 4w^2h^2n^2} \tag{150}$$

Since $$\bar{E} = \frac{E_{max} + E_{min}}{2}$$

$$E_{min} = 0$$

$$E_{max} = \tfrac{1}{2}\, m\, v^2_{max}$$

and $$V_{max} = Aw$$

To find the maximum average kinetic energy, differentiate $\bar{E}$ with respect to w^2 and set the derivative equal to zero. This gives

$$w^2_e = n^2 \tag{151}$$

Therefore, it appears that the free resonant frequency without damping gives the maximum kinetic energy. Equation 150 may now be written in the following form:

$$\bar{E} = \tfrac{1}{4} \frac{ma^2}{n^2\left(\frac{n}{w} - \frac{w}{n}\right)^2 + 4n^2h^2}$$

When $w = kn$ or when $w = \frac{n}{k}$ the above equation has the same value. This is interpreted as indicating that the kinetic energy is the same for an octave above its maximum as it is for an octave below. However, the value of A is less for the higher than for the lower frequencies.

The necessary work (W) to maintain the forced vibration is that done by the force $C \cos wt$. The expression for this work may be written as

$$W = \int C \cos wt\, dy = am \int \cos wt\, dy$$

However,

$$dy = d\,[A \cos (wt - \phi)] = -Aw \sin (wt - \phi)\, dt$$

$$= -\frac{aw}{\sqrt{(n^2 - w^2)^2 + 4h^2n^2w^2}} \sin (wt - \phi)\, dt$$

$$= -\frac{aw}{\sqrt{(n^2 - w^2)^2 + 4h^2n^2w^2}} \{\cos \phi \sin wt - \sin \phi \cos wt\}\, dt$$

$$= -\frac{aw}{(n^2 - w^2)^2 + 4h^2n^2w^2} \{(n^2 - w^2) \sin wt - 2nhw \cos wt\}\, dt$$

therefore: $$W = \frac{a^2mw}{(n^2 - w^2)^2 + 4h^2n^2w^2} \int_0^t \{2hmw \cos^2 wt - (n^2 - w^2) \sin wt \cos wt\}\, dt$$

In order to avoid fluctuations occurring during the course of a single cycle, it is necessary to integrate over a whole number of periods.

Thus

$$\int_0^t \sin wt \cos wt\, dt = 0$$

$$\int_0^t \cos^2 wt\, dt = \tfrac{1}{2}\, t$$

and

$$W = \frac{ma^2w^2hn}{(n^2 - w^2)^2 + (2hnw)^2}\, t \tag{152}$$

It is of some interest in the theory of vertical load spring pendulums that the energy supplied by the applied force is equal to that necessary to overcome the damping resistance of the system. It then should follow that the value of the work (W) should also be calculable as the necessary work done against the force of damping.

$$dW = K\dot{y}\,dy$$

$$W = 2mnh \int \frac{dy}{dt}\frac{dy}{dt}\,dt$$

$$= 2mnh \int \dot{y}^2\,dt$$

where $2hn = \frac{K}{m}$ and $n^2 = \frac{F}{M}$

The kinetic energy by definition is $E = \frac{mv^2}{2}$ or for the case under consideration

$$E = m\frac{\dot{y}^2}{2}$$

Then

$$W = 4nh \int E\,dt = 4nh\,\bar{E}\,t$$

From Equation 150

$$W = \frac{ma^2w^2hnt}{(n^2 - w^2)^2 + 4h^2n^2w^2}$$

which is the expression of Equation 152.

Effects of Natural Frequency of Seismometer.—To examine the effect of the magnitude of the period of the oscillating system of a seismometer, the equation for a damped linear oscillator may be used.

$$\ddot{y} = -2nh\dot{y} - n^2y - \ddot{Z} \tag{126}$$

If the period is very great, then the coefficient (n) would be very small and the terms containing this coefficient may become unimportant. Equation 126 might reduce to an expression similar to

$$\ddot{y} = -\ddot{Z}$$

This would mean that the oscillating particle would practically duplicate the impressed motion, and the displacement of the particle would be proportional to the displacement

of the earth. However, it is impossible to construct a pendulum with so large a period that the terms containing (n) are actually negligible.

Extremely short periods would have the effect of making the terms $\ddot{y}$ and $2nh\dot{y}$ unimportant, and Equation 126 may be reduced to an expression similar to

$$y = -\frac{\ddot{Z}}{n^2}$$

This would mean that the displacement would be proportional to the acceleration of the earth, and this type of seismometer would be called an *accelerometer.* In this case (n) becomes large, therefore the displacement would become relatively small, which generally results in a low output of the instrument.

Moving Conductor Type Seismometer

The moving coil type of seismometer is probably the most common of the various designs of seismic detecting instruments. Usually this variety of seismometer makes use of the displacement (y) to cut lines of magnetic flux with a conducting coil. If we neglect phase changes, hyster-

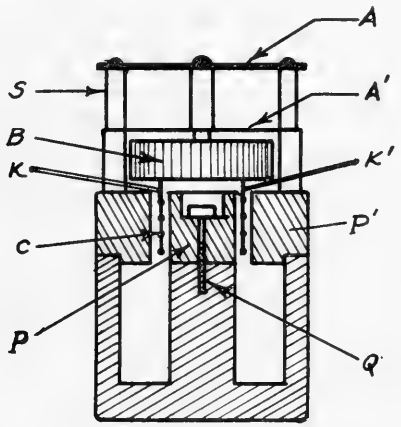

FIG. 479.—Moving coil seismometer. *A* and *A'*, suspension springs for supporting the mass *B* and the coil *C*; *K* and *K'*, flexible terminals for coil *C*; *P* and *P'*, pole pieces; *Q*, centering screw; *S*, spacer supports.

esis, eddy current effects, etc., the electromotive force developed will be proportional to the rate at which the lines of force are cut by the coil. This indicates that the electrical output of such instruments may be illustrated by the equation

$$E = -R\dot{y}$$

where E represents the E.M.F., R the proportional constant, and $\dot{y}$ the velocity of the inertia mass. Therefore, the electrical output of the moving coil

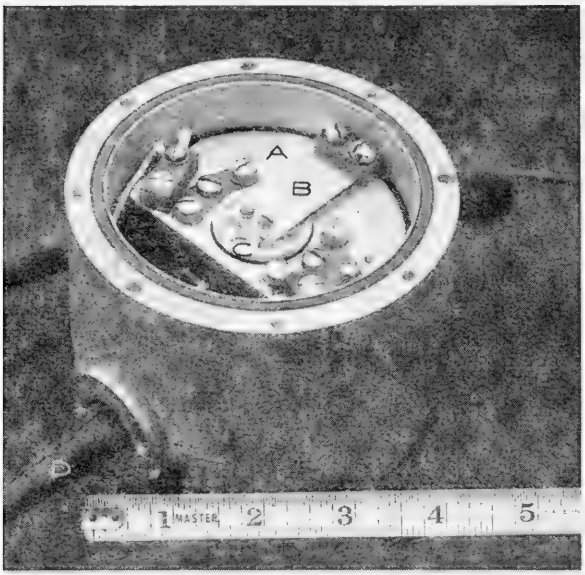

FIG. 480.—Moving coil conductor type of dynamic seismometer: (A) magnet; (B) spring; (C) bobbin on which coil is wound; (D) waterproof conductor. (Courtesy Western Geophysical Company.)

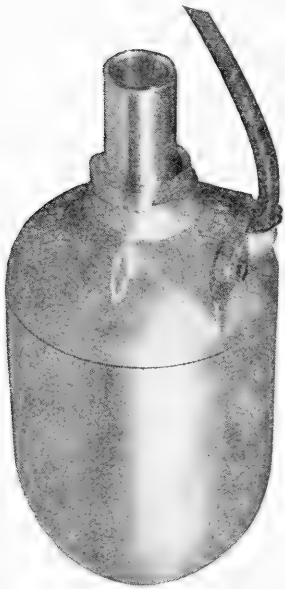

FIG. 481.—Moving coil type of geophone in waterproof case designed to be pushed into the mud. (Courtesy of Century Geophysical Corporation.)

type of seismometer would be proportional to the velocity of motion of the inertia reactor. Providing that the natural frequency of the seismometer was not too far outside the range of frequency of the impressed force, the output would be approximately proportional to the velocity of the ground motion. The electrical output of a velocity type seismometer lags behind the motion of the ground because, when the amplitude is the greatest at the end of a swing, the velocity passes through zero and changes algebraic sign. The velocity is probably greatest when the amplitude of the motion is passing through the zero or rest position.

A form of moving conductor seismometer is shown schematically by Figure 479. This instrument comprises a circular conducting coil, supported by two elastic springs, and a magnetic system rigidly attached to the case. The arrival of seismic waves produces a relative motion of the elastically supported con-

ductor coil with respect to the fixed lines of magnetic flux of the magnet system. This motion causes the conductor to cut the flux lines of force, thus inducing a current to flow in the coil. Figures 480, 481, 482, 483 and 484 illustrate modern types of electromagnetic inductance seismometers.

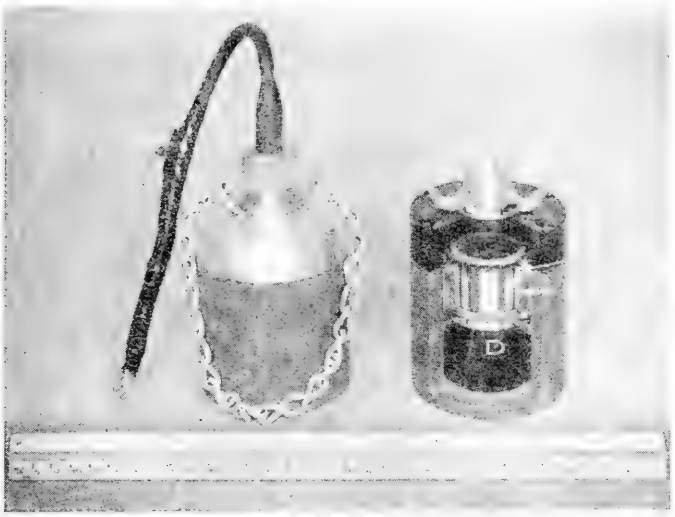

FIG. 482.—Sealed, moving-coil type seismometer with view of cut-away model. A and A′, connection clips; B, waterproof bushing; C, carrying chain; D, permanent magnet; E, armature; F, suspension spring. (Courtesy of Seismograph Service Corporation.)

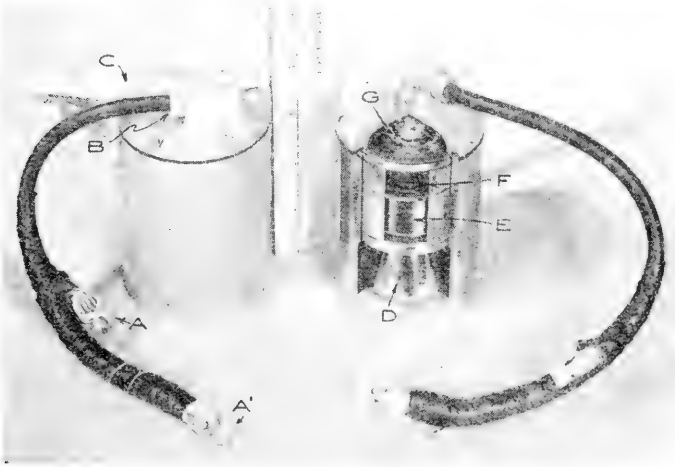

FIG. 483.—Electromagnetically damped moving-coil type geophone. A and A′, connection clips; B, waterproof bushing; C, carrying chain; D, permanent magnet; E, armature; F, suspension spring; G, shunt damping resistor. (Courtesy of Engineering Laboratories, Incorporated.)

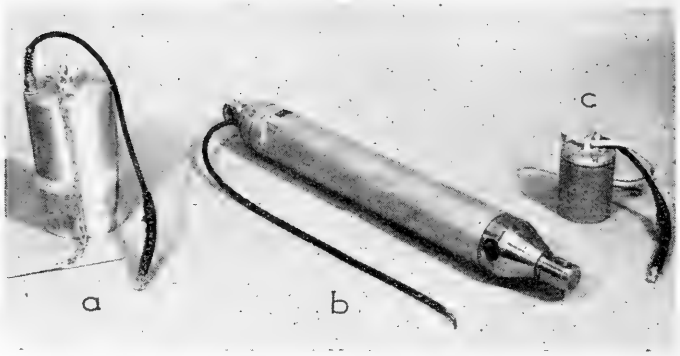

FIG. 484.—Moving coil type geophones. (a) refraction type seismometer; (b) well shooting seismometer constructed to withstand 10,000 psi for deep wells; (c) reflection type seismometer. (Courtesy of Engineering Laboratories, Inc.)

Variable Reluctance Type Seismometers

A variable reluctance type of seismometer† employing electromagnetic damping is shown by Figure 485. The schematic diagram of the magnetic

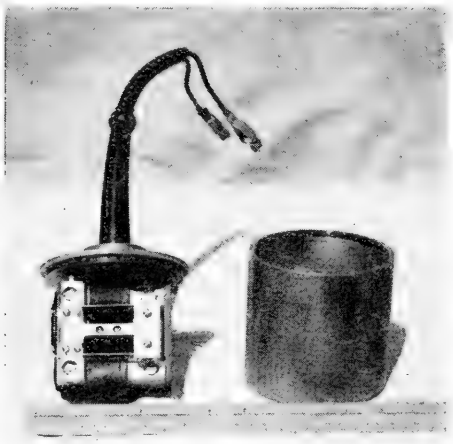

FIG. 485.—Variable-reluctance electromagnetically-damped seismometer. See Figure 486. (Courtesy of Geophysical Engineering Corporation.)

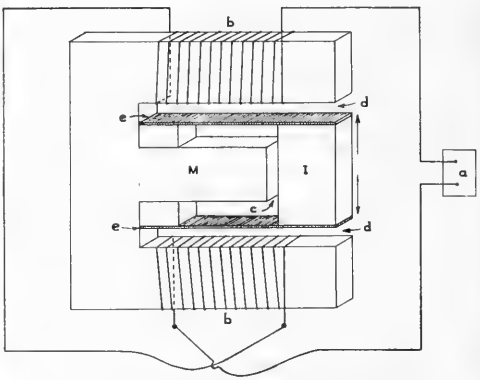

FIG. 486.—Schematic diagram of a variable reluctance type seismometer. (a) out-put terminals; (b) coils; (c) adjustable air gap; (d) working air gaps; (e) spring suspension; (I) inertia mass, which is also the permanent magnet.

circuit and mechanical arrangement are given by Figure 486.‡ The problem of obtaining good damping characteristics, calibrated period and stability for frequencies in the range between 40 and 50 cycles per second was solved in the case of this instrument design by introducing an adjustable internal air gap (*C*). This adjustable air gap places a reluctance in series with the

† J. P. Minton, "Geophysical Prospecting Apparatus," U. S. Patent 2,371,973, March 20, 1945.
‡ R. W. Raitt, "Transducing System," U. S. Patent 2,418,953, issued April 15, 1947.

magnet, which can be easily adjusted until the desired damping and frequency are obtained.

Theory of Reluctance Seismometers

The reluctance-type seismometers are those wherein the reluctance of the magnetic path is caused to vary by the relative movement of the inertia reactor with respect to the seismometer housing. Numerous instruments of this type are used for both earthquake and exploration seismology.

In one type of reluctance seismometer, two permanent magnets are supported by two springs which are attached to the case. (Figure 488.) The laminated armature is mounted in the air gap between the magnets and is rigidly connected to the case. The motion of the earth's surface during the passage of seismic waves produces a relative motion of the magnets with respect to the armature which causes an induced E.M.F. in the armature coil.

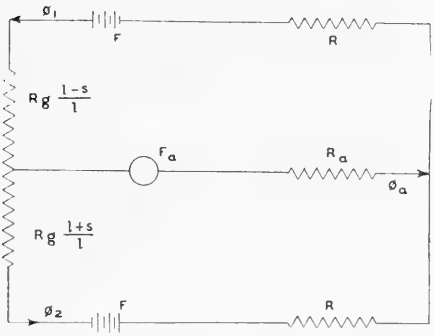

FIG. 487.—Magnetic circuit of an electromagnetic duplex reluctance seismometer. (After Scherbatskoy and Neufeld, *Geophysics.*)

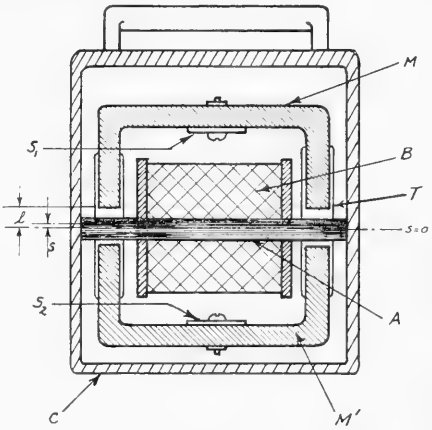

FIG. 488.—Reluctance seismometer, duplex-type. *A*, laminated armature; *B*, armature coil; *C*, aluminum case, waterproof type; *M*, permanent magnets; S_1 and S_2, suspension springs for the magnetic system (end view of springs); *T*, brass yoke.

To determine the quantities T, V, D for a reluctance type seismometer, it is convenient to refer to the equivalent magnetic circuit shown in Figure 487. The symbols denote the following quantities:†

F = magnetomotive force of each magnet.
R = reluctance of each magnet.
R_a = reluctance of the armature.
R_g = reluctance of each air gap when $s = 0$, where the reference line $s = 0$ is located midway between the magnets when they are undeflected. From symmetry R_g also equals the reluctance of the two air gaps in series above, or below, the neutral line $s = 0$.
l = one-half the vertical distance between the pole pieces of the two magnets when the magnets are undeflected.
$R_g \frac{l-s}{l}$ = reluctance of two air gaps in series above the armature corresponding to a displacement s of the reference line.

† Scherbatskoy and Neufeld, "Fundamental Relations in Seismometry," *Geophysics*, Vol. II, No. 3, July, 1937, pp. 192-198.

$R_g \dfrac{l+s}{l}$ = reluctance of two air gaps in series below the armature for a displacement s.
ϕ_1 = magnetic flux through upper magnet.
ϕ_2 = magnetic flux through lower magnet.
ϕ_a = magnetic flux through armature.
F_a = magnetomotive force created by the current in the armature coil.

The application of Kirchoff's laws to the two meshes of Figure 487 yields

$$\phi_a = \phi_1 - \phi_2$$

$$F = \phi_1 \left(R_g \frac{l-s}{l} + R \right) + \phi_a R_a$$

$$F = \phi_2 \left(R_g \frac{l+s}{l} + R \right) - \phi_a R_a$$

Whence

$$\phi_1 = \frac{F\left(R_g \dfrac{l+s}{l} + R + 2R_a\right)}{\left(R_g \dfrac{l+s}{l} + R + R_a\right)\left(R_g \dfrac{l-s}{l} + R + R_a\right) - R_a^2}$$

$$\phi_2 = \frac{F\left(R_g \dfrac{l-s}{l} + R + 2R_a\right)}{\left(R_g \dfrac{l+s}{l} + R + R_a\right)\left(R_g \dfrac{l-s}{l} + R + R_a\right) - R_a^2}$$

$$\phi_a = \frac{2FR_g \dfrac{s}{l}}{\left(R_g \dfrac{l+s}{l} + R + R_a\right)\left(R_g \dfrac{l-s}{l} + R + R_a\right) - R_a^2}$$

The total kinetic energy of the electromechanical system is given by

$$T = \tfrac{1}{2} m\dot{s}^2 + T_{e1} + T_{e2} + T_{e3} \qquad (153)$$

where

m = combined mass of magnets and springs (moving parts).
T_{e1} = energy stored in permanent magnetic field.
T_{e2} = magnetic energy due to current i induced in the armature coil.
T_{e3} = magnetic energy due to reaction of the current i on the permanent magnetic field.

If it is assumed for simplicity that the magnetic energy is contained only within the air gaps and the magnetic material and not in the space outside,

$$T_{e1} = \sum \phi^2 R \cdot \frac{10^{-7}}{8\pi}$$

or

$$T_{e1} = \left[\phi_1^2 \left(R + R_g \frac{l-s}{l} \right) + \phi_a^2 R_a + \phi_2^2 \left(R + R_g \frac{l+s}{l} \right) \right] \cdot \frac{10^{-7}}{8\pi} = T_{e1}(s) \qquad (154)^*$$

It may be shown by using Ampere's law (magnetomotive force $= 0.4\pi$ x ampere

* In setting up this equation and various subsequent equations, it is assumed that T, V, and D are expressed in joules; s in centimeters; $\dot{s}$ in centimeters per sec.; q in coulombs; $\dot{q} = i$ in amperes; m in grams x 10^{-7}; r_m in dynes sec.^{2} per cm x 10^7; C in farads; r in ohms; L in henrys; f in dynes x 10^{-7}, e in volts; F in gilberts; R in charge^2 over mass x length^2 or sec. per ohm; ϕ in maxwells.

turns $= 0.4\,\pi\,n\,i$) that the magnetic energy T_{e2} associated with the current i is given by the equation

$$T_{e2} = \frac{0.4\pi\, n\, i\, \phi_i}{8\pi} \cdot 10^{-7} \tag{155}$$

where ϕ_i, the flux created by the current i, is equal to the magnetomotive force around the magnetic circuit (Figure 487) divided by the reluctance of the circuit.

The magnetic energy T_{e3} associated with the reaction of the current i on the permanent magnetic field is given by the equation:

$$T_{e3} = \frac{ni\,\phi_a}{2} \cdot 10^{-8} \tag{156}$$

If each of the equations 154, 155 and 156 is expanded in a Maclaurin series and if all terms involving powers of s higher than the first are dropped, the *total* kinetic energy of the mechanical and electrical parts of the seismometer may be expressed by the relation

$$T = \tfrac{1}{2}\, m\dot{s}^2 + (T_{e1})_{s=0} + \left(\frac{dT_{e1}}{ds}\right)_{s=0} s + \tfrac{1}{2}\,(L_1)_{s=0}\, i^2 + \tfrac{1}{2}\left(\frac{dL_1}{ds}\right)_{s=0} i^2 s + \left(\frac{dK}{ds}\right)_{s=0} si$$

where (157)

$$L_1 \equiv \frac{n\phi_i}{i} \cdot 10^{-8} \quad \text{and} \quad K \equiv \frac{n\phi_a}{2} \cdot 10^{-8}$$

The potential energy of the system is due entirely to the mechanical part, because the electrical circuit is assumed to have no capacity; that is,

$$V = V_m = \frac{s^2}{2C_m} \tag{158}$$

where C_m is the compliance of the spring supporting the horseshoe magnets.

The total dissipation function is

$$D = \tfrac{1}{2}\, r_m \dot{s}^2 + \tfrac{1}{2}\, r i^2 \tag{159}$$

where r_m is the mechanical resistance factor (determined by the side slip between the moving horseshoes and the air) and r is the resistance of the armature coils.

The general equations of motion of the combined electrical and mechanical systems which constitute a seismometer may be obtained by using Lagrange's equations employing generalized coordinates.† In particular, most seismometers have two degrees of freedom, one corresponding to the displacement of the moving mass and the other to the flow of electrical charge or current, and the Lagrangian equations for a seismometer are:

$$\frac{d}{dt}\frac{\partial T}{\partial \dot{s}} - \frac{\partial (T-V)}{\partial s} + \frac{\partial D}{\partial \dot{s}} = f \tag{160}$$

and

$$\frac{d}{dt}\frac{\partial T}{\partial \dot{q}} - \frac{\partial (T-V)}{\partial q} + \frac{\partial D}{\partial \dot{q}} = e \tag{161}$$

The symbols T, V, D, s and $\dot{s}$ have the meanings previously indicated; d/dt denotes as usual a time derivative; q is the electrical charge; $\dot{q}$ is the time rate of change of electrical charge; f is the externally applied force; and e is the E.M.F. in the electrical circuit.

The motion of the electromechanical system constituting the seismometer is specified when the quantities representing the kinetic energy (mechanical plus magnetic), the potential energy (mechanical plus electrical) and the dissipation function (friction plus electrical heating) are substituted into the two Lagrangian equations

† A discussion of Lagrange's equations is given in many texts on theoretical mechanics. See, for example, A. Zivet and P. Field, *Introduction to Analytical Mechanics*, pp. 352-359 (Macmillan Co., New York), 1926. A more generalized discussion is given by J. H. Jeans, *Mathematical Theory of Electricity and Magnetism*, 5th Edition, pp. 489-498 (Cambr. Univ. Press, 1927).

of motion. The Lagrangian equations for various types of electric seismometers will be found in the article by Scherbatskoy and Neufeld.†

The equations of motion of the electromagnetic reluctance seismometer may be obtained by substituting the expressions for T, V, and D as given by Equations 157, 158, and 159 into the Lagrangian equations (160) and (161). In carrying out this substitution, certain terms will be zero and certain other terms will be constants which for the sake of simplicity may be set equal to zero. For example, T_e (equal to $T_{e1} + T_{e2} + T_{e3}$) is a function of s only. Hence, the derivative of T_e with respect to $\dot{s}$ vanishes; i.e.,

$$\frac{\partial T_e}{\partial \dot{s}} = 0 \tag{162}$$

Also $\frac{\partial}{\partial s}\left(\frac{dT_{e1}}{ds}\right)_{s=0}$ is a constant which may be set equal to zero, and $\frac{\partial}{\partial s}(L_1)_{s=0}$ is also a constant which may be set equal to zero. However, it will not be assumed that $\left(\frac{dK}{ds}\right)_{s=0}$ is zero, because that would be equivalent to assuming that there is no viscous drag. As a matter of convenience in notation, set

$$\left(\frac{dK}{ds}\right)_{s=0} \equiv K_m \tag{163}$$

Various derivatives of the energies with respect to the electric charge q and the current i (equal to $\dot{q}$) likewise vanish. Thus T_m equal to $\frac{1}{2}m\dot{s}^2$ is not a function of i or q and $T_e = T_{e1} + T_{e2} + T_{e3}$ is not a function of q. Hence,

$$\frac{\partial T_m}{\partial i} = \frac{\partial T_m}{\partial q} = \frac{\partial T_e}{\partial q} = 0 \tag{164}$$

Also

$$\frac{\partial T_e}{\partial \dot{q}} = \frac{\partial T_e}{\partial i} = \frac{\partial T_{e1}}{\partial i} + \frac{\partial T_{e2}}{\partial i} + \frac{\partial T_{e3}}{\partial i}$$

$$\frac{\partial T_e}{\partial i} = 0 + (L_1)_{s=0}\, i + K_m\, s \tag{165}$$

Setting

$$(L_1)_{s=0} \equiv L \tag{166}$$

$$\frac{\partial T_e}{\partial i} = Li + K_m s \tag{167}$$

Also

$$\frac{\partial V}{\partial i} = \frac{\partial V}{\partial q} = 0 \tag{168}$$

On substituting into the Lagrangian equation (160), the expressions for T (Equation 157) for V (Equation 158) and for D (Equation 159), and making use of Equations 162 and 163, the following relation is obtained:

$$\frac{d}{dt}\frac{\partial T_m}{\partial \dot{s}} + \frac{d}{dt}\frac{\partial T_e}{\partial \dot{s}} - \frac{\partial T_m}{\partial s} - \frac{\partial T_e}{\partial s} + \frac{\partial V_m}{\partial s} + \frac{\partial}{\partial \dot{s}}(D_m + D_e) = f$$

or

$$m\ddot{s} - K_m i + \frac{s}{c_m} + r_m \dot{s} = f \tag{169}$$

where $\ddot{s} \equiv \frac{d^2 s}{dt^2}$

Similarly on substituting the expressions for T, V and D and making use of Equations 164 through 168, the Lagrangian equation (161) becomes:

$$\frac{d}{dt}\frac{\partial T_m}{\partial i} + \frac{d}{dt}\frac{\partial T_e}{\partial i} - \frac{\partial T_e}{\partial q} - \frac{\partial T_m}{\partial q} + \frac{\partial V}{\partial q} + \frac{\partial (D_m + D_e)}{\partial q} = e$$

† S. A. Scherbatskoy and J. Neufeld, "Fundamental Relations in Seismometry," *Geophysics*, Vol. II, No. 3, July, 1937, pp. 192-212.

or

$$L\frac{di}{dt} + K_m\dot{s} + Ri = e \tag{170}$$

Equations 169 and 170 are the fundamental equations of motion of the mechanical and electrical parts of the seismometer. Equation 169, which describes the motion of the mechanical part, contains one term, $-K_m i$, which depends on the electrical circuit, and Equation 170, which describes the conditions in the electrical circuit, contains one term, $K_m\dot{s}$ which depends on the relative *velocity* of the moving element in the mechanical system.

It is possible to solve Equations 169 and 170 so as to obtain the current in the electrical circuit as a function of the relative velocity of the moving element in the mechanical circuit, *provided* an explicit form is assumed for the mechanical force f. This is equivalent to determining the current in the electrical circuit as a function of the velocity of the ground at the seismometer station.*

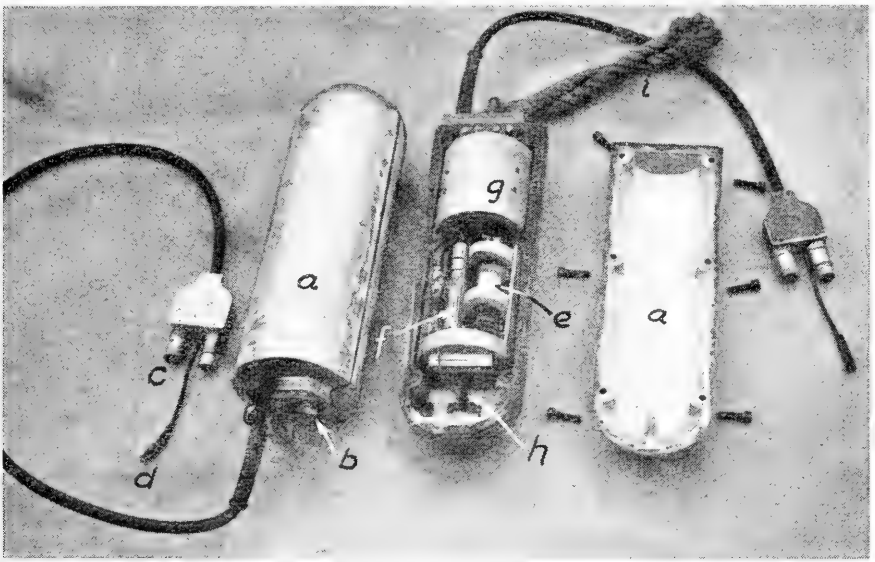

FIG. 489.—Piezoelectric type seismometer. *a*, waterproof case; *b*, clamp screw for locking instrument; *c* and *d*, double connector for filament and plate supply and pre-amplifier output; *e*, amplifier tube; *f*, grid bias battery; *g*, transformer; *h*, piezoelectric crystal; *i*, carrying rope.

Piezoelectric Seismometer

The piezoelectric seismometer† consists essentially of a crystal of anisotropic material such as quartz, tourmaline, Rochelle salt, etc., and an inertia reactor. The motion of the earth produces a relative acceleration of the inertia reactor with respect to the crystal. This relative acceleration in turn produces a potential difference between opposite faces of the crystal.

Several advantages are claimed for the piezoelectric pickup; chief of which are: (1) the seismometer does not have moving parts such as elements supported by elastic springs; (2) the voltages generated are

* The procedure for carrying out the simultaneous solution of Equations 169 and 170 is indicated by Scherbatskoy and Neufeld, *loc. cit.*

† W. P. Welch, "Accelerometer (Piezoelectric)," U. S. Patent 2,411,401, Nov. 19, 1946.

proportional to the acceleration of the ground rather than to the velocity, as in the case of the electromagnetic detector. The chief disadvantages of the piezoelectric detector are its low sensitivity and the variation of sensitivity with temperature and with moisture. The last factor makes it necessary to keep the inside of the case free of all moisture, and usually some type of desiccator is employed. The low sensitivity requires an additional stage of amplification which must be housed in the seismometer case in order to raise the signal energy above the noise level of the cable, which preferably is of the shielded type. Also, the fragility of the crystal necessitates some form of clamping device which will protect the crystal from mechanical damage during transportation.

Figure 489 shows the exterior and interior views of one type of piezoelectric seismometer. The mass acting on the crystal comprises the entire interior of the seismometer, including transformer, pre-amplifying stage, and chassis. A clamp screw is provided for locking the mechanism during transport to prevent injury to the crystal. The crystal is of composite construction having four separate crystals electrically connected in parallel, with their "Z" axes vertical. The output of the crystal is impressed across a high resistance in the grid circuit of the pre-amplifying tube.

Capacity or Electrostatic Seismometer

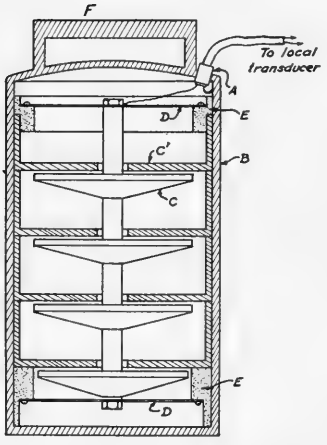

FIG. 490.—Condenser type seismometer. *A*, waterproof connector plug; *B*, case; *C* and *C'*, condenser plates; *D*, diaphragm; *E*, bakelite support ring; *F*, carrying handle.

The coupling between the mechanical and electrical systems of a capacity seismometer (Figure 490) is accomplished by means of a condenser so designed that the displacement of the earth's surface during the arrival of seismic waves produces a relative displacement of the plates of the condenser.† The varying capacity may be made to induce electrostatically a varying electromotive force in an auxiliary circuit.*

In one type, the varying capacity causes a current flow in a high potential tuned circuit. In another type of capacity seismometer, the change in capacity is made to vary the frequency of an oscillating circuit. This circuit is usually heterodyned

† O. S. Petty, "Seismic Apparatus and Method," U. S. Patent 2,408,478, Oct. 1, 1946.

* The relation between the time rate of change of electric charge on the condenser and the relative displacement of the condenser plates may be obtained from the Lagrangian equations in a manner similar to that outlined above for the reluctance type seismometer.

with another oscillating circuit to produce a beat frequency, which is amplified and rectified, and then recorded in the conventional manner.

Hot Wire Resistance Seismometer

The operation of the hot wire resistance seismometer depends on changes in the resistance of a hot wire (about 0.005 mm. diameter) when cooled by an air current which is produced by the motion of the inertia mass relative to the seismometer case. Because the changes in resistance depend on the motion of the air, the instrument responds to the *velocity* of the earth's surface at the seismometer station.

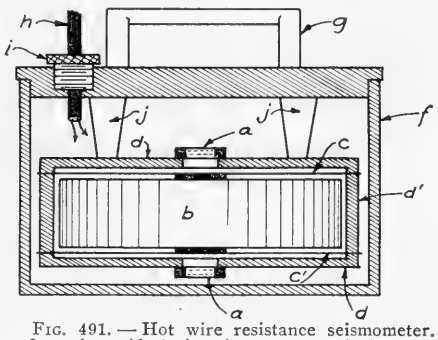

FIG. 491. — Hot wire resistance seismometer. *a*, fine wire grid; *b*, inertia mass; *c* and *c'*, upper and lower diaphragm supports; *d*, air chamber ring for diaphragms; *d'*, spacer ring; *f*, aluminum instrument case; *g*, carrying handle; *h*, cable (2 wire); *i*, water-tight lead in bushing; *j*, spacers.

An instrument of this type is illustrated schematically in Figure 491. It comprises a mass and diaphragm so mounted that they constitute a "bellows" arrangement, whereby relative motion of the mass and the case causes a movement of air past the hot wire grid. Two grids are employed, connected in series. A double diaphragm is employed to provide a good mechanical support for the mass and also to form a chamber for the oil serving as a damping medium. The milliampere current required for heating the grids is supplied by a central battery in the recording truck. By means of a transformer in series with the line to the seismometer, the variations in current are picked up and impressed on the amplifiers for recording in the conventional manner. Usually one or two stages of amplification are more than sufficient. This type of seismometer has been found to be especially suitable for the lower frequencies. (Also, it is better adapted for refraction prospecting than for reflection prospecting.)

Carbon Button Seismometer

This is one of the simplest forms of seismometers. The operation of the carbon button or carbon granule type seismometer depends on the changes of resistance which occur in carbon due to pressure variations. The resistance changes produce corresponding changes in current. Usually the carbon button is connected in series with the primary of an impedance matching transformer and a source of current (local dry cell). Variations in primary current cause corresponding variations in potential on the secondary of the transformer. The secondary is connected to the recording galvanometer. This type of seismometer is very efficient and has a high output. For shallow work it may be used without additional ampli-

fication. The carbon seismometer, however, is seldom used for deep work due to the high noise level caused by "frying" of the grains. These microphonic noises may be minimized to a certain extent by using two carbon buttons in a push-pull circuit in the primary of the transformer.

Photoelectric Seismometer

The photoelectric seismometer is a displacement type instrument wherein the relative motion of the inertia mass with respect to the seismometer case modulates the light which falls on a photoelectric cell. The instrument is shown schematically in Figure 492. The operation of the seismometer may be summarized as follows: The motion of the earth's surface produces a relative displacement of a mass, thereby actuating a pivoted mirror through a connecting link. Light rays from a small lamp are focused on the mirror by a condensing lens and are then reflected to a photoelectric cell. The output of the photoelectric cell depends on the displacement of the mass actuating the pivoted mirror.*

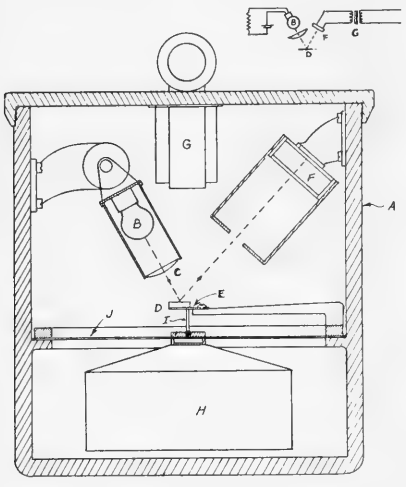

FIG. 492.—Schematic diagram of a photoelectric seismometer. *A*, case; *B*, light source; *C*, condensing lens; *D*, mirror; *E*, flexible support; *F*, photoelectric cell; *G*, impedance matching transformer between cell and line; *H*, stationary mass; *I*, connecting link between mass and mirror; *J*, diaphragm support for mass.

A seismometer of this type has certain definite advantages: namely constancy of response characteristics, negligible temperature coefficient, and a relatively high output level. One disadvantage of the instrument is the necessity for a local battery (usually placed adjacent the seismometer) or an extra pair of conductors to light the filament.

Electronic Seismometer

A seismometer with high output utilizes the mechano-electronic transducer tube,** illustrated in Figure 493. This electronic triode tube is provided with a plate shaft which extends through the center of a thin metal diaphragm. Displacement of the plate shaft changes the distance between the fixed grid and the plate, and thereby changes the plate current. The tube has a deflection sensitivity of 40 volts per degree deflection of the plate shaft, which has a minimum free cantilever resonance of 12,000 cps. By

* The cell may be connected directly to a transformer for proper impedance match.
** Radio Corporation of America mechano-electric transducer, tube No. 5734.

proper mechanical coupling to a suitable mass, an excellent seismometer is obtained. For shallow work, the output is sufficient to operate the galvanometer, without additional amplification.

The amplification factor of the mechano-electronic transducer is greater than that of the carbon-grain microphone type, and is also free of the high noise level so characteristic of the carbon-grain microphone.

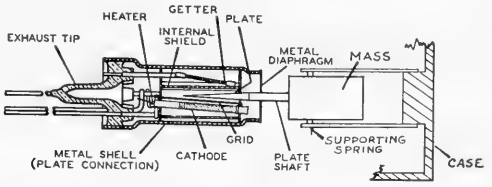

Fig. 493.—Cross-sectional view of mechano-electric transducer. (Courtesy of International Geophysics Company.)

A seismometer utilizing this transducer requires a local filament battery of 6 volts and .15 amperes. The DC source for plate potential at 300 volts and 5 milliamperes may be located at the instrument truck and transmitted to the seismometer through a two-wire cable. By suitable transformer coupling in series with each transducer, variations in the plate current will actuate the galvanometer.

Carrier Current Systems.—Various schemes have been proposed to utilize carrier frequency systems.† By having each seismometer operating on a different carrier frequency, only a simple two-conductor cable would be required between the instrument truck and the various seismometers. At the instrument truck tuned circuits would be employed to separate each of the carrier frequencies, and the amplified output of each circuit would actuate its recording galvanometer. Systems of this type have not been widely adopted, probably because the saving in cable is offset by the more complicated carrier system.

Mechanical Seismometers

At present, the mechanical seismometers are seldom used in prospecting. They are reviewed here chiefly because of their historical interest.

Type Instruments

The Schweydar instrument‡ consists of two units so designed that one unit responds to the vertical component of the earth's motion and

† E. E. Minor, "Vibration Measuring Apparatus," U. S. Patent 2,305,267, Dec. 15, 1942.

‡ W. Schweydar and H. Reich, "Künstliche elastische Bodenwellen als Hilfsmittel geologischer Forschung," *Gerland's Beiträge zur Geophysik*, 1927, 17, 121. Broughton Edge and Laby, *Geophysical Prospecting* (Cambridge Univ. Press, 1931), pp. 214-216.

the other to the horizontal component. The inertia member of the vertical component unit is supported by a vertical spring. The movement of the seismometer case relative to the inertia reactor is first magnified by a light conical lever attached to the inertia member. At the free end of the lever is a "bow and string" mechanism which revolves about a small (3 mm. diameter) spindle supported between two jewelled bearings. The mirror is mounted on the spindle. A modified arrangement which has similar mechanical amplification but eliminates the difficulty due to the bearings is shown in Figure 494.

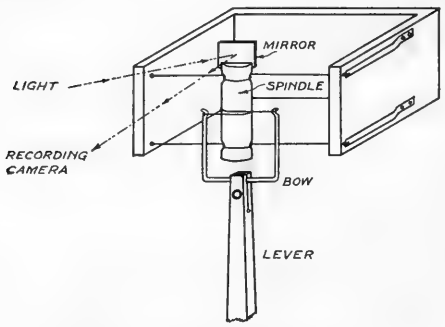

FIG. 494.—Diagram illustrating one type of mechanical and optical amplification.

The operation of the instrument may be summarized as follows. The arrival of seismic waves sets the seismometer case, and hence the bow, in motion. The movement of the bow rotates the mirror and hence causes a displacement of a beam of light which is reflected from the mirror to a photographic film in a camera located at a distance of about one meter.

A view of the Schweydar type seismograph is shown in Figure 495.

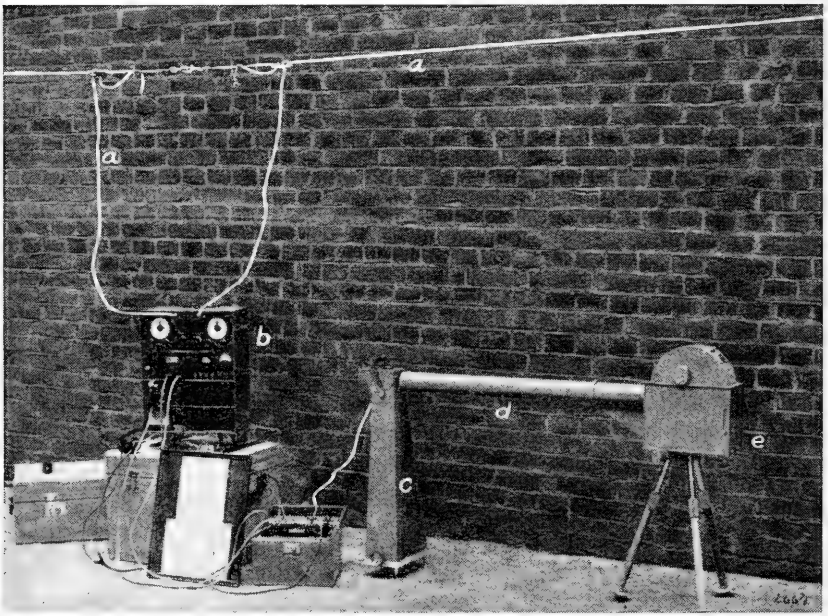

FIG. 495.—Early Askania mechanical seismograph. *a*, radio aerial; *b*, radio receiver for recording instant shot was fired; *c*, seismograph; *d*, light-tight tube for optical magnification; *e*, recording camera. (Courtesy of W. M. Rust, Jr.)

At the left of the figure is a radio for receiving the shot-time from a radio transmitter connected to the firing circuit of the charge of explosive. The mechanical seismometer is separated from the recorder by a light-tight tube in order to obtain large optical magnification. This instrument has a combined mechanical and optical amplification of over 1500.

The Taylor mechanical seismometer† was employed extensively in the Gulf Coast prior to the introduction of electric instruments. The characteristic feature of the seismometer is the provision of a thread suspension for the free end of the inertia mass. This suspension makes

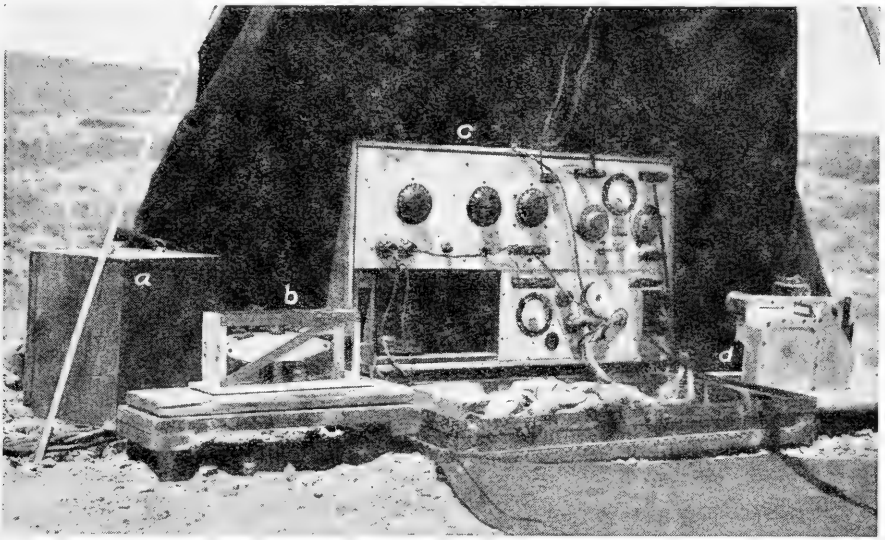

FIG. 496.—Layout of Taylor's early mechanical seismograph equipment in recording position. *a*, camera carrying case; *b*, seismometer; *c*, two-way radio; *d*, recording camera. (Courtesy of Continental Oil Co.)

possible the conversion of the vertical motion of the inertia mass into rotary motion of a mirror which is readily adaptable to registration on a photographic film. The inertia mass comprises an aluminum frame filled with some heavy metal (usually a lead compound). The mass is pivoted by the end piece of the frame and supported by a steel spring A cup partially filled with oil is provided to dampen the motion of the inertia mass when the instrument is in use. Light rays reflected from the mirror rigidly attached to the frame indicate the extent of the deflections of the inertia mass. The instrument has a combined mechanical and optical magnification exceeding 10,000.

Figure 496 shows a Taylor mechanical seismograph set up in recording position, tent open.

† H. G. Taylor, "Seismometer," U. S. Patent 1,789,055, issued Jan. 13, 1931.

Disadvantages of Mechanical Seismometers

The mechanical type seismometer requires a solid foundation, such as hard ground or a heavy wooden platform. This greatly handicaps use of the instrument, particularly in the numerous areas where marsh and open waters prevail. In addition, the single trace record necessitates many instruments placed at different locations for each shot or else many shots for a single instrument.

RECORDING EQUIPMENT FOR VISUAL ANALYSIS

The output of the seismometer, obtained by converting the energy of the seismic wave into electrical energy, is amplified, filtered and then recorded by photographic means. In addition, it is usually necessary to employ manual or automatic gain control to prevent overloading by the stronger waves and to bring out the weaker waves.

The minute currents generated by the dynamic action of the seismometer are usually transmitted through an insulated two-wire cable to the recording truck which houses the filtering, amplifying, and recording instruments.

Filtering.—The seismic wave to be recorded is a complex wave containing many different frequency components, each with varying amplitudes, rates of attenuation, and phase relationships. The predominant frequency range of the bands most useful in visual analysis is from 5 to 40 cycles per second for refracted waves, and from 20 to 100 cycles per second for reflected waves. The quality of the record for visual interpretation often may be improved by judicious selection of frequencies that are to be recorded. As an illustration, the filters and overall response range for reflection equipment are often chosen to cover the range from 40 to 75 cycles per second. The lower cut-off is preferably quite sharp, while the upper cut-off should be rather broad so as not to destroy the sharpness of the reflections. Surface disturbances caused by light winds can often be largely eliminated by attenuation of waves of frequencies above about 80 cycles per second.†

Filters are employed to obtain maximum current or voltage at certain desirable frequencies, and to reject or suppress the effects of the undesirable frequencies. Electrical literature contains many articles dealing with filter design and tuned circuits, and the reader is referred to these articles.‡

Amplification Control.—Following the strong burst of energy at the first part of a field record, the level of reflected energy will diminish down the record. The ratio of legible, reflected energy at the first and last part

† E. M. Palmer, "Seismograph Recording Apparatus," U. S. Patent 2,440,970, May 4, 1948.
W. W. Young, "Vibration Recorder," U. S. Patent 2,420,025, May 6, 1947.

‡ Reuben Lee, "Tuned Circuits and Filters," *Industrial Electronics Reference Book,* John Wiley and Sons, New York, 1948.

A typical band pass filter, which is capable of making a frequency selection in the amplifier, is described by H. R. Prescott and F. L. Searcy, "Method of Geological Exploration," U. S. Patent 2,049,727, issued Aug. 4, 1936, and by H. R. Prescott, "Method and Apparatus for Making Geophysical Explorations," U. S. Patent 2,053,841, issued Sept. 8, 1936.

of a seismometer record may be from 10^3 to 1 up to 10^4 to 1. Consequently, some variable control of the amplification or response of the recording equipment is required in order that the entire wave train be legible. Three methods of overcoming this difficulty are in use.

A simple method from the point of view of recording equipment is to shoot several shots, setting the amplifier at different levels of gain to obtain legible amplitude at successively different reflection times. An equally simple method is to use different amounts of explosive with the same level of gain. Neither of these techniques, however, is practical for commercial work, due to high explosive cost and loss of time.

A second method utilizes manual gain control. This may be accomplished by means of a gang control which simultaneously actuates a potentiometer in each amplifier. Usually one galvanometer trace will record the gain versus time on the record. A skilled operator can obtain good results with the manual type of control, by varying the gain in accordance with prior experience in the area, usually so as to maintain a relatively constant average amplitude of excursion on the galvanometer traces. For this purpose, the recording camera must be equipped with a split or double beam to allow visual observation as the recording is made.

Another method utilizes a cam-operated gain control, which is varied with time.† The time control may be a separate timing mechanism driving the cam. An alternate arrangement mechanically couples the cam with the paper feed mechanism in the camera. A somewhat more complicated arrangement utilizes an electronic trigger tube which starts the cam mechanism when the shot is fired or when the first burst of seismic energy is received. The shape of the cam is governed by the reflection characteristics of the area and the overall gain characteristics of the amplifier, filter, and galvanometer.

Another and more prevalent procedure utilizes automatic volume control or expander systems‡ which are essentially the same as those employed for radio and television reception.§ The rectified output of one of the early amplification stages is applied to a variable Mu tube or to the grid, or as a cathode follower to one of the succeeding tubes, so that the amplification is increased as the incoming signal decreases in overall gain.

The automatic control is designed to be responsive to a group of wave trains or the envelope of the waves and not to each individual peak or

† H. R. Prescott, "Method and Apparatus for Making Geological Explorations," U. S. Patent 2,158,198, issued May 16, 1939.

‡ R. G. Piety, "Automatic Volume Control for Seismograph Amplifiers," U. S. Patent 2,430,246, Nov. 4, 1947.
H. Hoover, Jr., "Seismic Amplifying System," U. S. Patent 2,430,983, Nov. 18, 1947.
J. O. Parr, Jr., "Seismic Surveying," U. S. Patent 2,424,705, July 29, 1947.
E. J. Shimek and G. M. Groenendyke, "Gain Controlling System for Seismographs," U. S. Patent 2,420,571, May 13, 1947.
R. Maillet, "Geophysical Prospecting," U. S. Patent 2,420,672, May 20, 1947.

§ Reuben Lee, "Amplifier Circuits," *Industrial Electronics Reference Book*, John Wiley and Sons, New York, 1948.
Radiotron Designers Handbook, R. C. A., 1941, Parts 1 and 2.

transient. This is usually accomplished by utilizing some form of vacuum tube time delay and time averaging circuit.†

Amplifiers.—Electrical amplification of the feeble electromotive forces generated by the seismometers is usually accomplished by means of multistage electronic amplifiers.‡ Many amplifier circuits have been designed for this purpose. However, the usual practice is to follow the general specifications necessary for a high fidelity audio-frequency transformer or resistance-coupled amplifier. From two to five stages of vacuum tube amplification are frequently employed, to have a useable gain of from 100 to 150 DB. Some form of feedback is employed for stabilization.

A majority of the amplifiers used in geophysical work are resistance coupled, with a relatively narrow-band frequency response. A good description of amplifier characteristics and their design is contained in the literature.§

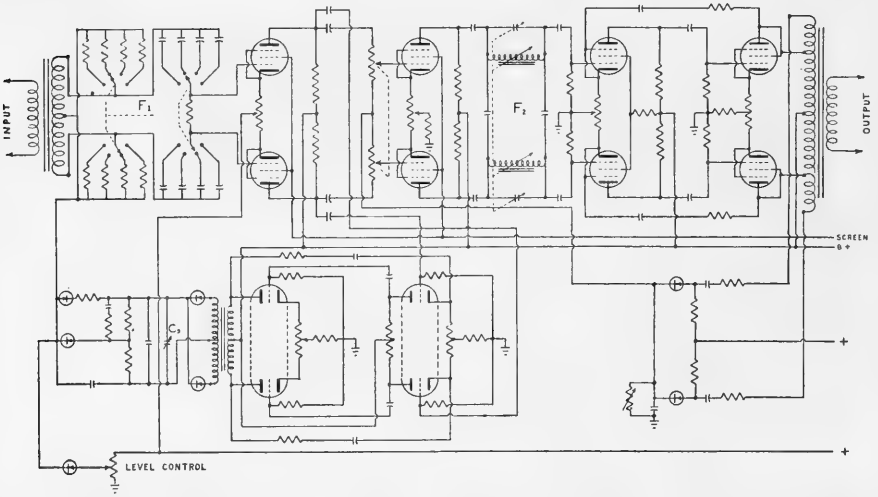

FIG. 497.—Schematic diagram of amplifier with automatic gain control. F_1, compensating high pass filter; F_2, low pass filter (step construction); C_S, variable storage condenser (step construction). (Courtesy of D. D. Dressen, Electronic Supply Corp.)

A combination type of automatic gain control and limiting amplifier is shown by schematic diagram, Figure 497. Four cascade-controlled circuits are shown in push-pull arrangement. A single ended system may be used. However, with the development of miniature tubes, the advantages of push-pull to balance out possible transients developed in gain control

† H. E. Haynes, "Gain Control System Responsive to an Average Value," U. S. Patent 2,454,169, Nov. 16, 1948.

‡ P. K. Chatterjea and C. T. Scully, "Thermionic Amplifier," U. S. Patent 2,431,306, Nov. 25, 1947.

R. H. Park, "High Gain Amplifier," U. S. Patent 2,434,223, Jan. 6, 1948.

§ L. G. Cowles, "The Narrow Band Resistance Coupled Amplifier," *Geophysics*, Vol. X, No. 3, July, 1945, and "The Resistance-Coupled Amplifier," A.I.E.E. *Transactions*, Vol. 64, 1945, June Supplement, Paper 45-69.

Valley and Wallman, "Vacuum-Tube Amplifiers," *Radiation Laboratory Series 18*, McGraw-Hill, New York, 1948.

circuits may be incorporated without the penalty of excess space or weight.

The first stage is controlled by a long time-constant circuit. A rectifier feeding an RC type of circuit builds up a direct current potential proportional to the incoming signal amplitude. A portion of this current is fed through a diode to a buss capacitor tied to the first stage grid return. The first break signals thus reduce the gain of the first stage to a low level. When the input signal from the seismometer drops appreciably, the rectified D.C. voltage also drops in value, and the voltage from the bias capacitor tends to balance out by discharging through an RC rectifier system, which reverses the original process, and increases the gain.

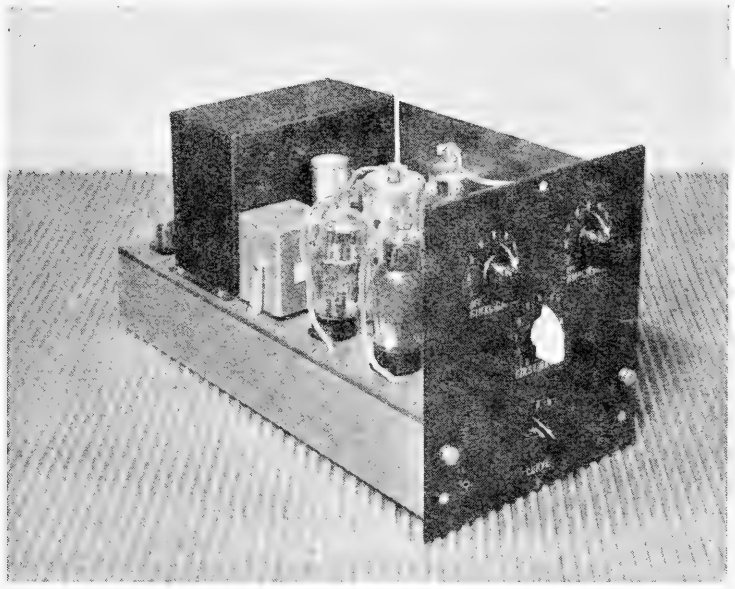

FIG. 498.—Seismic amplifier unit. (Courtesy of Western Geophysical Co.)

Maximum gain at no signal is set by the level control. Peak limiting is accomplished by rectifying the output signal and controlling the second cascade amplifier. This circuit is incorporated to limit the peak signal until the long time-constant input gain control begins to function. Soon after the first breaks arrive, the input gain control functions, and thereafter the circuit action corresponds to the well-known expander-type circuit, employing a pre-charged condenser connected to the bias circuits. This condenser discharges through an LR circuit at a time-constant commensurable to the necessary time delay for the particular area under investigation.

The output of the amplifier is applied to the galvanometer by means of a transformer to make possible the proper matching of the impedance of the output tube with that of the galvanometer.

Table 30 gives the desired operating characteristics for seismic amplifiers.

Amplifiers are of two general types of construction. Figure 498 shows a conventional type which allows rapid interchange of amplifier units, should operating difficulties develop. In another design, weight and space are conserved by mounting all amplifiers on a single chassis. An illustration

TABLE 30

GENERAL OPERATING CHARACTERISTICS OF SEISMIC AMPLIFIERS

Voltage Gain:	100-150 D.B. (Usually measured from 200 ohm input to plate of last tube.)
Frequency Response:	2 to 200 cycles per second.
Adjustable Filters:	Consisting of 1 or 2 high pass sections, and 1 low pass section controlled by selector switches on the front panel. Provision is made for choosing either 1 or 2 sections, depending upon the type of filtering desired.
Automatic Gain Control:	Operating time should be from .075 to .15 second for large ratio of signal change (such as "first breaks") and with a slower rate for small ratios which remain substantially constant regardless of the signal level or intensity, so that the reflections have time to be reproduced with their normal contrast without interference of a "fast" automatic gain control.
De-Coupled:	The amplifier should be sufficiently decoupled to permit use of any group from a common power source such as a genemotor or vibrator power supply, without "cross-talk," feed back, or coupling.
Tubes:	Should be standard radio or television tubes, non-microphonic mounted.
Power Requirements:	1.5 to 6.3 volt filaments; 6 to 12-volt motor-generator; and not to exceed 250* volts for plate supply.
Mounting:	Front panel controls, with rack mounting to allow easy interchange of amplifiers for replacement or testing. Multi-circuit connectors should be utilized for plug-in connections.
Components:	Held to rigid specifications. Transformers and inductors hermetically sealed, with multiple high-permeable and high-conductive shields to permit operation of equipment in relatively high magnetic fields such as may be encountered in vicinity of power lines. All units should be interchangeable both electrically and mechanically.

*Some designers prefer to add an extra stage of amplification, and operate at a lower plate voltage to minimize tube noises and leakage problems.

of twelve separate channel amplifiers mounted on one stainless steel chassis is given in Figure 499. All units are hermetically sealed against humidity and made to plug into a standard vacuum tube socket. When provided with standard tube prong base, a transformer or a coupling unit between amplifier stages may be pulled out and replaced in a few seconds, exactly as in changing a vacuum tube. All component parts are mounted above the chassis; only the wiring is below. Test equipment and charts are designed so that each component may be instantly checked for defects, allowing rapid trouble-shooting in the field. The design of this type of amplifier is such as to facilitate repair and upkeep rather than to withstand all field hazards. These twelve amplifiers with expander type volume control, exclusive of dry cell batteries, weigh only thirty-seven pounds. This type of portable equipment has proven satisfactory for difficult terrain conditions.

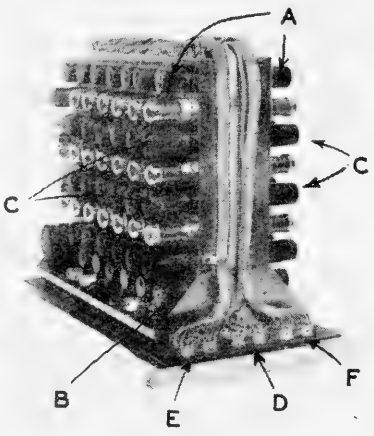

FIG. 499.—Twelve separate channel amplifiers, mounted on a single stainless steel chassis using plug-in elements. (A) input transformer; (B) output transformer; (C) interstage coupling; (D) battery plug; (E) input plug; (F) output plug. (Courtesy of Geophysical Engineering Corporation.)

Shielding.—All parts of the electrical system (seismometers, connecting cables, amplifiers, recording camera, and controls) are preferably shielded against disturbing magnetic and electrostatic fields. This is particularly advantageous when working in the vicinity of high tension power lines, street car systems, etc.* The circuits carrying the minute currents generated by the seismometers must be well insulated from the case of the seismometer and from the ground. Variable earth potentials are frequently present in the ground between the locations of the various seismometers and the recording truck. These earth potentials due to their varying magnitude may cause disturbances if picked up by the input circuit. For use in the tropics, the equipment should be protected against fungus. Metal parts should be cadmium or chrome plated.

Instrument cases, as well as the cases of the seismometers, are usually of iron or aluminum and serve both as electric shields and as mechanical protection for the instruments.

Photographic Recording.—The photographic method of recording, because of its sensitivity, reliability, and accuracy, has superseded practically

* A method of eliminating the effect of extraneous electrical disturbances, with particular reference to power line interferences, ground motions, etc., is described by K. C. Woodyard, C. A. Putnam and H. R. Prescott, "Means and Method of Making Geophysical Explorations," U. S. Patent 2,164,196, issued June 27, 1939.

all others: Recording apparatus for seismic field work should be: (1) rugged, (2) compact, (3) completely light-proof, (4) unaffected by extraneous vibrations and field transportation, (5) of sufficient recording paper capacity, (6) designed to use spools or rolls of recording paper which are commercially available, and (7) preferably equipped for visual observation of the recording traces while recording.

Galvanometers

The galvanometers are usually of the Einthoven type or of the D'Arsonval type. From a mechanical viewpoint, the Einthoven or string galvanometer is simpler than the D'Arsonval or moving coil galvanometer, but generally not as satisfactory for field work.

Einthoven or String Type.—This type of galvanometer consists of a single permanent or electro-magnet with a number of wires strung

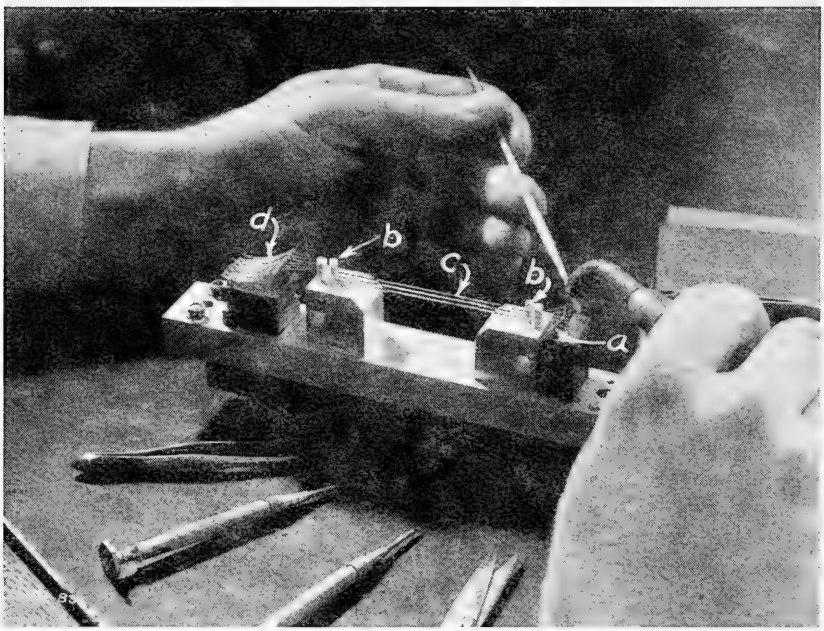

FIG. 500.—Stringing of an Einthoven galvanometer element. *a*, fixed terminals for galvanometer "strings"; *b*, ivory spacer posts; *c*, strings of fine copper wire; *d*, adjustable terminals for proper tension.

through an air gap in the magnet. Each wire carries one of the amplified seismometer outputs to be recorded. A beam of parallel light rays passing through the air gap causes the strings to cast shadows on the photographic paper. These shadows reproduce as white traces when the record is developed. The strings may be oil damped.

Certain disadvantages of the instrument may be summarized as follows: In order to obtain sufficient optical amplification of the movement of the strings, a lens of short focal length is utilized. When a large number of strings is required it may be difficult to focus all strings sharply on the record. Occasionally, when excessively strong waves are recorded, the strings collide and may tangle. The black background makes it inconvenient to mark reference points and notes on the record. The chief disadvantage of the string galvanometer arises from the fact that if more than about 10 strings are desired, the construction becomes somewhat cumbersome.

The low impedance of this type of galvanometer necessitates a matching transformer. However, for geophysical work, the low impedance is not a disadvantage, because proper transformer ratios can be employed to match the output impedance of the amplifying tube with the low input impedance of the galvanometer.

An Einthoven type of galvanometer element consisting of thirteen strings is shown in Figure 500. The individual strings consist of copper wire 0.00075 inches in diameter. They are separated from adjoining strings by means of accurately located grooves in the upright ivory posts and are soldered to batteries of connecting terminals at both ends. These terminals may be adjusted individually by set screws to obtain the desired tension in the strings after they are installed. The natural frequency of the elements is about 500 cycles per second, and the system of which they are a part gives a D.C. deflection of about 2 to 4 millimeters per microwatt at a distance of 1 meter.

Moving Coil or D'Arsonval Type.—In the D'Arsonval type galvanometer, a movable loop or coil of wire carrying the current to be recorded is suspended between the poles of a strong magnet. Light is reflected to the photographic recording paper from a small mirror attached to the coil.

Each trace on the record requires a separate galvanometer unit. Records obtained with a D'Arsonval mirror galvanometer can be distinguished from those obtained with an Einthoven string galvanometer because in the former black traces appear on a white background while in the latter white traces appear on a dark background.

Figure 501 shows a fifteen element moving coil galvanometer with the cover opened for inspection, but with only two elements in place. In galvanometers of this type the frequency is determined mainly by the torsional stiffness of the suspensions and by the moment of inertia of the coil and mirror.

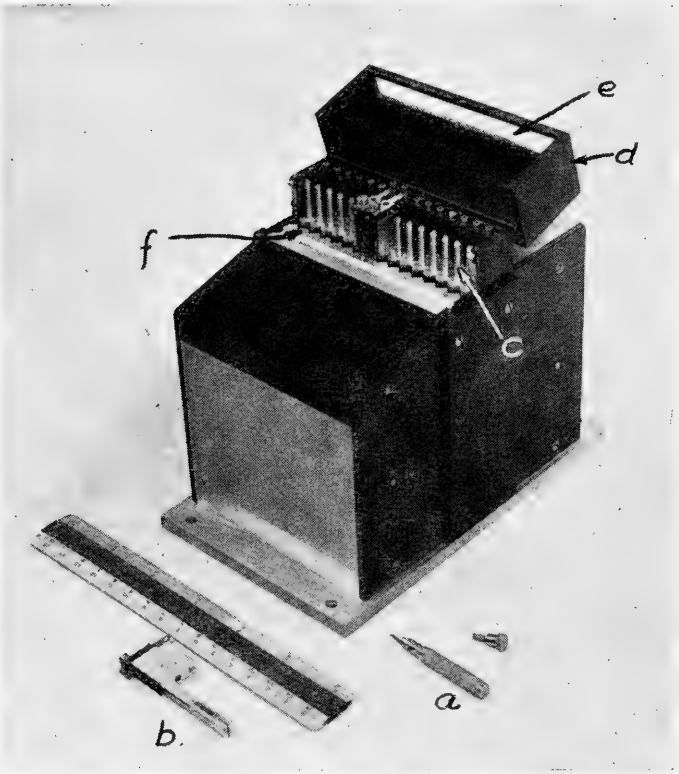

FIG. 501.—Fifteen element galvanometer, with cover open for inspection; two elements are connected. *a*, non-magnetic screw driver; *b*, single element; *c*, terminal supports for galvanometer units; *d*, dust-tight lid; *e*, plane glass window; *f*, air gap in permanent magnet for each galvanometer unit. (Courtesy of Wm. Miller.)

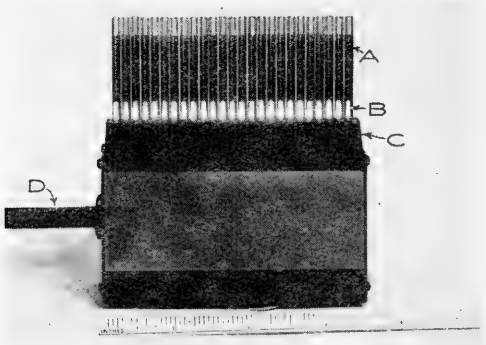

FIG. 502.—25-element galvanometer, using sealed tubular construction. A, galvanometers (25 units, each ⅛" in diameter); B, focusing mirrors; C, magnetic block; D, multi-conductor cable. (Courtesy of Century Geophysical Corporation.)

Another galvanometer used extensively in seismic recording is illustrated in Figure 502. A set of 25 hermetically-sealed plug-in galvanometers constructed of stainless steel are confined to a width of approximately 3½ inches in this design. These galvanometers are electromagnetically damped and may be constructed with natural frequencies ranging from 15 to 1500 cycles per second.

Recording Cameras for Visual Analysis of Records.—One of the several types of individual recording cameras available for seismic work is shown by Figure 503. The front panel of the camera is composed of two hinged doors. The viewing screen is permanently secured to the center of the panel. The right-hand door allows ready access to the galvanometers, while the left-hand door services the supply and re-roll magazines for photographic paper.

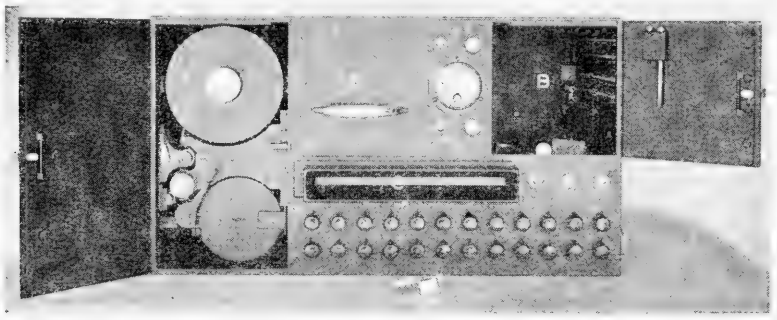

FIG. 503.—Interior view of recording oscillograph. (A) photographic paper magazine; (B) galvanometer compartment containing multi-element unit; (C) ground glass viewing screen; (D) galvanometer element consisting of coil and suspension; (E) drawer compartment containing synchronous timing system; (F) paper cutting and perforating mechanism. (Courtesy of William Miller Corporation.)

The light source is housed in a separate compartment. A beam of light passes through a diaphragm, impinges upon the focusing mirrors of the multiple galvanometer bank, and is reflected from these mirrors in individual ribbons of light, with their long dimension vertical so as to come to a focus in sharp vertical image lines at the distance of the recording paper. In front of the recording paper is placed a cylindrical lens having a length equal to the width of the recording paper, and with its axis horizontal. This lens focuses the individual galvanometer traces (vertical lines) to small bright spots on the recording paper. The lower portions of the ribbons of light reflected from the galvanometer mirrors are intercepted by a narrow reflecting mirror and are projected on the ground glass viewing screen at the front of the camera, where they may be observed while a record is being taken.

A temperature-compensated 100 c.p.s. tuning fork is mounted in a thermally insulated compartment and is equipped with either a carbon button or a vacuum tube drive. The output of the fork is amplified and

operates a small synchronous motor which rotates a thin slotted timing disc. This disc rotates at 10 revolutions per second and has 9 narrow radial slots which record as .01 seconds, and a tenth slot, wider than the others, which records .10 seconds. Light from the timing bulb shines intermittently through these slots as the disc rotates. This light is reflected from a mirror to the cylindrical lens, where it is focused as a line on the record strip. When the light shines through the wider slot, a heavier timing line is photographed, to indicate tenths of seconds.

The timing lines† can be maintained to an accuracy of better than 1 part in 2000, when 100 cycles per second is the frequency of the controlling tuning fork. For higher accuracies, temperature-compensated tuning forks of 1000 cycles per second have been used. Lower-frequency synchronous motors have been accused of hunting, thus placing a limit on the accuracy for instantaneous measurements of time. High-frequency synchronous motors probably also hunt, but the error due to this cause is less.

Unexposed recording paper, in standard rolls of approximately 200 feet and of any width for which the oscillograph is constructed, usually from 3⅝″ to 11″, is placed in the supply magazine. From there it is threaded through a paper guide and drawn into a reroll magazine. On the exit side of the reroll magazine is a steel knife for cutting off the record. This knife also closes the paper slot to make the magazine light-tight when it is removed to develop the record. The spool in the reroll magazine is driven by a constant speed, centrifugal contact governor motor. A small red glass window allows inspection of the quantity of paper in the supply magazine.

As an alternative design, the recording camera can be provided with a drive in which the paper is fed through rubberized rollers which rotate at a constant speed. Also, instead of the paper cutter mounted on the magazine, an externally-operated device is sometimes substituted which will either perforate or cut off the record, as desired by the observer.

The multiple galvanometer is carefully mounted so as to be practically shock-proof and free from disturbances by truck or other vibrations transmitted through the oscillograph case. The control switches usually are mounted on the lower edge of the front panel or on a separate panel external to the oscillograph. Because of the high recording speeds necessary for seismic work and to avoid the use of paper of too high a sensitivity, the galvanometer lamp is operated at a brightness well above its rated value. However, the lamps are so wired that their brightness is increased to the required intensity only when the drive motor is operated, which greatly prolongs their life.

Recording Papers and Photographic Developing.—The recording medium used in the photographic methods consists of a sensitized material deposited on a paper or film support. The paper should be of a good

† C. D. McClure, "Timing Device for Recorders," U. S. Patent 2,424,622, July 29, 1947.
E. W. Kammer, "Optical Time-Base Generator," U. S. Patent 2,428,369, Oct. 7, 1947.
G. W. Rusler, "Tuning Fork Construction," U. S. Patent 2,433,160, Dec. 23, 1947.

quality white stock. The film support is seldom employed in field work due chiefly to three factors: (a) greater cost; (b) developing difficulties encountered in warm weather due to separation of the sensitized emulsion from the film support; (c) greater bulk and weight. Occasionally when very high recording speeds are desired, film is used, because it usually can be obtained in a greater range of emulsion speeds than paper.

The sensitized emulsion employed for recording is a high contrast emulsion, usually of silver bromide in gelatin. This material is superior to the usual silver chloride emulsion employed in photography, because it is relatively unaffected by the processing procedure. Thus, records obtained with the silver bromide emulsion are uniform and not appreciably dependent upon the processing. †

The developer employed for processing the film should be a high contrast material, with sufficient potassium bromide to restrain fog. Practically all manufacturers of paper supply their own packaged developers. These frequently are found more satisfactory than the bulk materials, chiefly due to their convenience in use, their uniformity, and the elimination of waste and errors in weighing chemicals.

The developing time should be long enough to give a proper density in the portions of the record which have been properly exposed. The record may be examined occasionally during the development provided a safety lamp is used. The ordinary red light is seldom safe for the modern high speed recording papers. To determine the safeness of a red light, it is convenient to expose half of a test piece of the paper to the light for a few minutes and then develop and fix. Excessive fogging of the exposed portion of the test strip, as compared to the unexposed portion, will indicate that the light should be changed or moved further from the paper during the processing.

If the developing temperature is maintained at about 65° F., a more concentrated developer will usually give a more dense record. At higher temperatures, the more concentrated developer may produce less effective contrast due to the increase in fog density. The developing speed, also, is greatly dependent upon temperature; an increase to 85° F. will often cut the developing time in half, while a decrease to 50° F. may necessitate more than twice the normal developing time. The higher temperatures accentuate fog and also cause discoloration due to oxidation of the developer. For best results, the temperature should not exceed 70° F. Oftentimes, it is difficult in field work to control the developer temperature, and the best compromise is to vary the strength of the solution, i.e., use relatively strong solutions at the lower temperatures and diluted solutions at the higher temperatures. The most satisfactory method for uniform records is to employ a tank, the temperature of which is maintained constant by a surrounding water bath. Thermal insulation (cork or glass

† F. A. Tompkins, "Fundamental Photographic Processing Operations Influencing Production of Seismograph Records," *Geophysics*, 1936, Vol. 1, No. 1, pp. 107-114; "Effect of Development Time and Developer Temperature on the Production of Photographic Seismograph Records," *Geophysics*, 1936, Vol. 1, No. 3, pp. 313-318.

wool) prevents rapid temperature variations. An ice-pack in summer and a hot water bath in winter are used to adjust the temperature at the beginning of a day. Only minor attention is required thereafter to maintain it. Records are developed in accordance with time-temperature charts, with consideration given to the age of the developer.

After it has been developed, the record should be washed in a stop solution consisting of 1½ ounces of 28% acetic acid dissolved in 32 ounces of water. Fixation of the record is accomplished by immersing it in a solution of sodium thiosulphate (trade term "hypo") which removes the unexposed silver. Prepared packages of this material, with the necessary hardener, are available from all manufacturers of paper. Fixation is usually complete within three to five minutes. After sufficient fixing, the film should be immersed in a fresh water bath to insure a permanent, non-fading, and non-stained record.

Although it is often neglected, proper washing of the records is one of the important steps in the processing. The removal of soluble chemicals remaining in the paper after the fixing operation can only be accomplished by thorough washing in clean water. If it is inconvenient to supply sufficient water for each batch of records, the films should be left in the water bath until the return of the operators to headquarters. The records can then be placed in a large container (the bath tub may be convenient) with cool fresh running water and washed for about thirty minutes, and then dried.

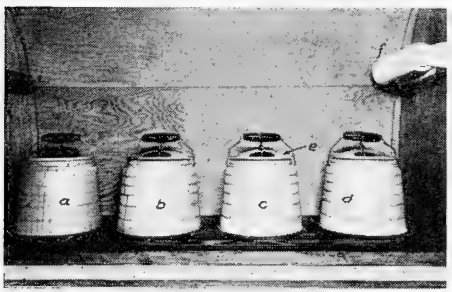

FIG. 504.—Processing assembly for photographic records. *a*, developer; *b*, stop bath; *c*, fixing bath; *d*, fresh water; *e*, rubber-sealed lids; *f*, absorbent paper toweling.

During the developing, fixing, and washing steps, the record must be carefully moved or the fluid agitated to insure uniform exposure to the solution of all parts of the record.

Caution must be exercised to prevent the stop bath and hypo from splashing or dripping into the developer. Among the best containers for solutions are glass (deep Pyrex cooking pans), glazed earthenware, or stainless steel jars. The containers should be provided with sealing lids to prevent "slopping" of the solutions when the truck is moved during the day.

Figure 504 shows a simple but effective assembly for field use where a limited number of records is to be developed. The jars are ordinary earthenware thermally-insulated jugs with large open mouth, of the type employed for food. These jars are provided with tight-fitting rubber-sealed lids that preserve the solutions and prevent splashing while the truck is in motion between set-ups. The lower ends of the jars are set into

holes in a raised base board to allow their easy removal for cleaning and filling. Absorbent paper toweling will be found a convenience.

A procedure is often used which avoids the need of a dark room, particularly in milder climates where the normal outdoor temperature is suitable for developing of records. The chemical containers are placed in a light-tight tank. The cover of the tank consists of a frame to which a hood is tightly attached, light weight leather being generally used for the hood because of its ruggedness. The hood is equipped with a sleeve through which the operator inserts one of his arms. The operator's free

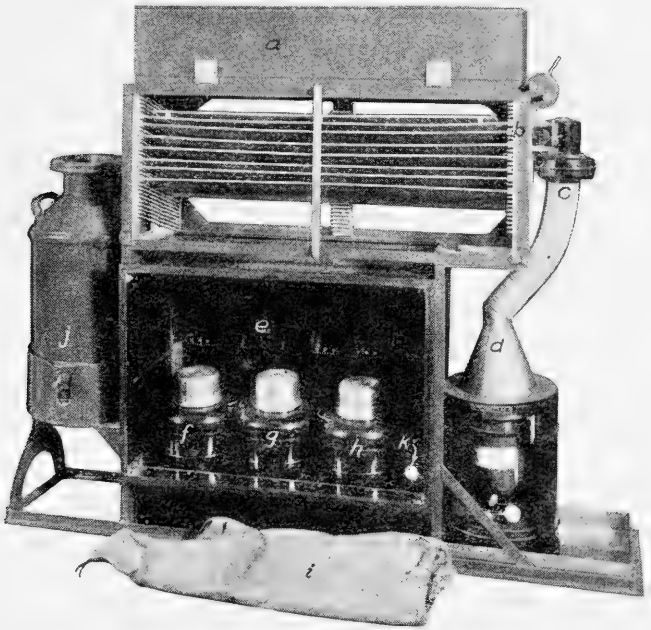

FIG. 505. — Complete photographic developing equipment. *a*, record storage compartment; *b*, drying racks; *c*, hot air circulating fan; *d*, oil-burning stove; *e*, processing compartment; *f*, developer; *g*, stop bath; *h*, fixing bath; *i*, opaque cloth cover for front of compartment; *j*, fresh water washing tank; *k*, safety light for developing. (Courtesy of Continental Oil Co.)

hand is used to clasp the sleeve tightly to avoid light leaks. The magazine is unloaded, the record developed, washed, and placed in the fixing bath before the cover is raised from the tank.

An advantage of this type of equipment is that the recording truck need not be maintained light-proof, giving the operator greater freedom of action and permitting him to attend to other matters while his subordinate proceeds with the developing.

Figure 505 shows a complete photographic developing assembly with heater, wash water can, and record rack. The heater is a modified kerosene-burning stove, with a small fan for forced hot air circulation

through the record drying compartment. This type of dryer practically eliminates the delays occasioned by cold weather and high humidity.

Three large mouthed one-gallon thermos jugs are placed in the lower cabinet. These jugs contain the developer, stop bath, and hypo solutions. A small red lamp provides a means for inspecting the developing. Over the front of the cabinet is a black opaque cloth cover which is provided with two light-tight armholes and a small red observation window. The operator conducts the developing and fixing operations by inserting his arms through the armholes. Equipment of this type will handle the records of a fast working party conveniently and allow inspection of the records at each set-up without undue loss of operating time.

INSTRUMENTAL ANALYSIS

The seismic wave arriving at the surface is a complex wave, containing many frequency components. As previously mentioned, the visual analysis of seismic records necessitates considerable filtering to remove certain components so that the frequencies passed by the filter will more clearly show the desired correlation, and also have more "eye-appeal." The characteristics of an optimum filtering system will depend upon the nature of the subsurface materials, the depth to the geological horizons of current interest, and the overall frequency response of the associated equipment. The degree of filtering is rather arbitrary or rule of thumb, and is usually determined by the crew chief on the empirical basis of obtaining records that appear to indicate the best correlation at the depth and for the other conditions believed to be of major importance at the time. If, later, exploratory interest changes: for instance, centers on a deeper horizon, it often is necessary to re-shoot the area to obtain records with the greatest "character" at that depth range. Some organizations are partially overcoming this condition by dual recording, wherein one bank of galvanometers (usually 10 or 12 traces) will record through one filter setting, while the other bank is recording through a different filter setting.

One solution to the problem of filtering lies in recording the complex seismic wave with high-fidelity equipment which will preserve the full components of the received wave motion on a reproducible record. Studies of the area may then be made as desired merely by playing back the record and varying the electrical parameters to give the desired data. The playback may involve studies of: the effects of filtering; the combination of traces under various phase relationships to achieve directional effects; the frequency analysis of the complex wave to determine its various wave components; or the frequency pattern.

A high-quality recording system such as those used for sound recording on motion picture film, magnetic wire, or tape may be employed for the recording of the seismic wave. One very important requirement in this connection is that the film or tape be moved past the scanning point at a uniform rate in order to avoid flutter or "wow," which would result in

distortion of wave shape and the introduction of spurious frequencies. Certain modifications in design are necessary to compensate for the lower frequency range of the seismic waves as compared to sound waves, but these modifications may be made without special difficulty. The following descriptions are illustrative of the instrumentation and general results to be obtained by the playback system.

Effects of Filtering.—Figure 506 illustrates a five-track variable-area recording camera which is designed to translate electrical signals into corresponding amplitude variations on a variable area film.† The camera magazine capacity is 150 feet of film, 5 inches wide. This device is provided with two film speeds, 8 or 16 inches per second. The galvanometers are coil-type, electromagnetically damped to 0.6 of critical and with a natural

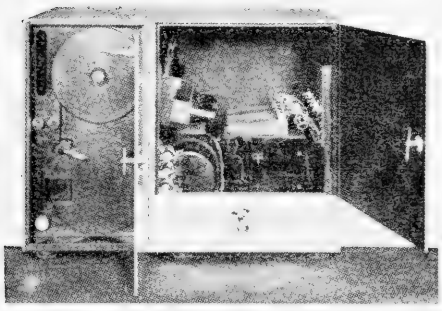

FIG. 506.—A 5-track variable area recording camera. (Courtesy of Seismograph Service Corporation.)

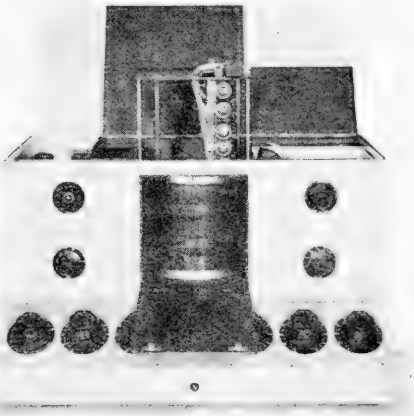

FIG. 507. — Variable area reproducer with center panel open, showing transparent drum. (Courtesy of Seismograph Service Corporation.)

frequency of 225 cycles per second. The records may be reproduced by means of a reproducer (Figure 507), consisting of an exciter lamp providing light which is passed by mirrors thru the five-track variable area film, traveling on a rotating transparent drum, to five photocells. As the film passes between the light source and the photocells, the variation in the intensity of light causes a similar variation in the photocell current which is amplified by means of a vacuum-tube amplifier. The output of the amplifier drives the recording galvanometer. At *A* in Figure 508 are shown three variable-area tracks on which are recorded the original outputs of three seismometers. At *B, C* and *D* are conventional-type seismograms recorded with different amplifier filters, showing the output of six tracks. The upper seismogram was recorded with filtering peaked at approximately 30 cycles per second; the second seismogram at approximately 50 cycles

† J. E. Hawkins, *"Method and Apparatus for Analyzing Seismographic Records,"* U. S. Patent 2,463,534, March 8, 1949.

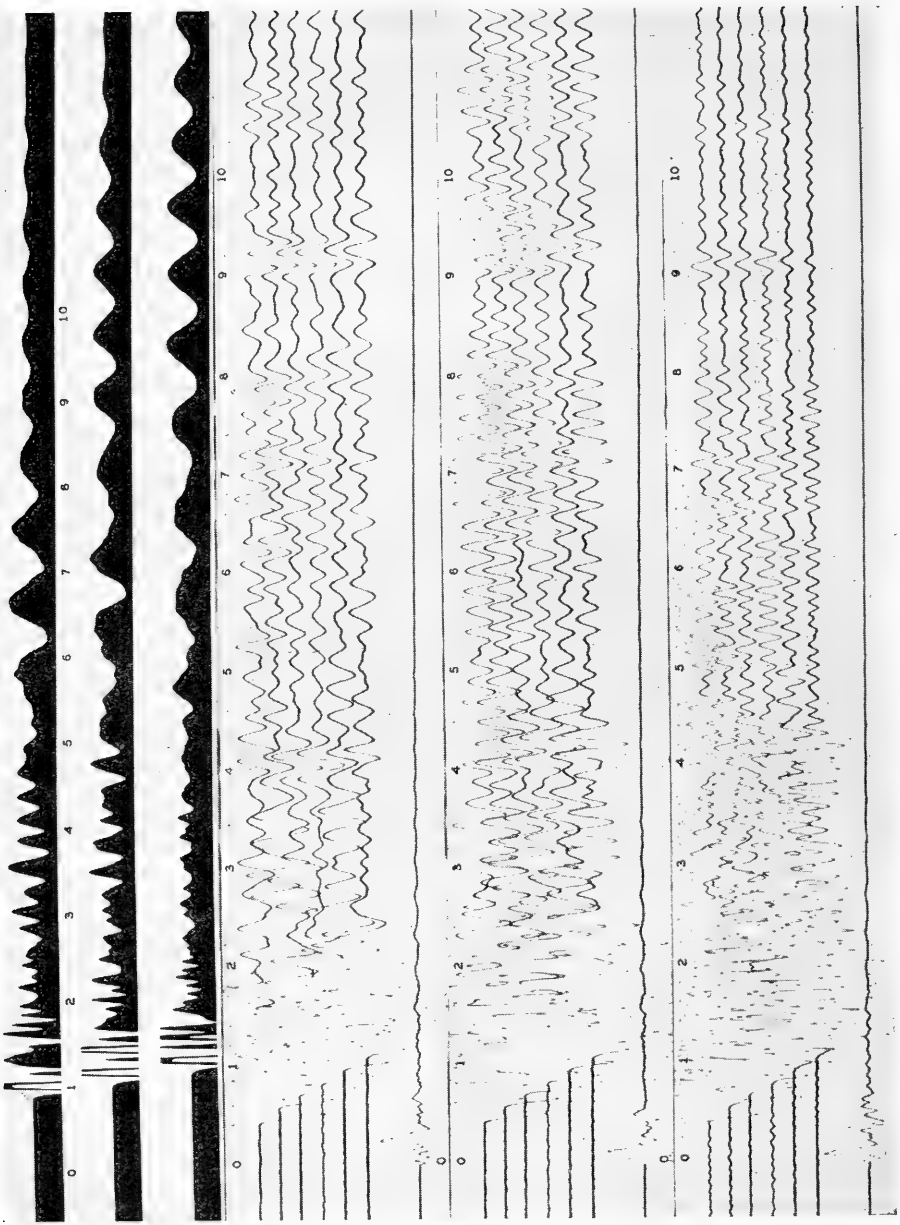

FIG. 508.—Group of four records from Montgomery County, Illinois, from the same shot-point. Top record, A, shows three tracks of a variable area earth motion record. The next three, B, C, and D, are recorded with different filtering peaked respectively at approximately 30, 50, and 70 cycles per second. This is an example of three recordings made at the same shot-point, using the same amount of explosive, depth of charge and amount of stemming in the shot-hole. (Courtesy of Seismograph Service Corporation.)

per second; and the bottom seismogram at about 70 cycles per second. This is an illustration of the effect of filtering on the recorded seismogram. The turning points of the recorded traces become progressively less sharp with decreasing peaked-frequencies of the filters.

Sonograph Equipment for Phase Effects.—This equipment† is described in detail because of its novel features and different operating

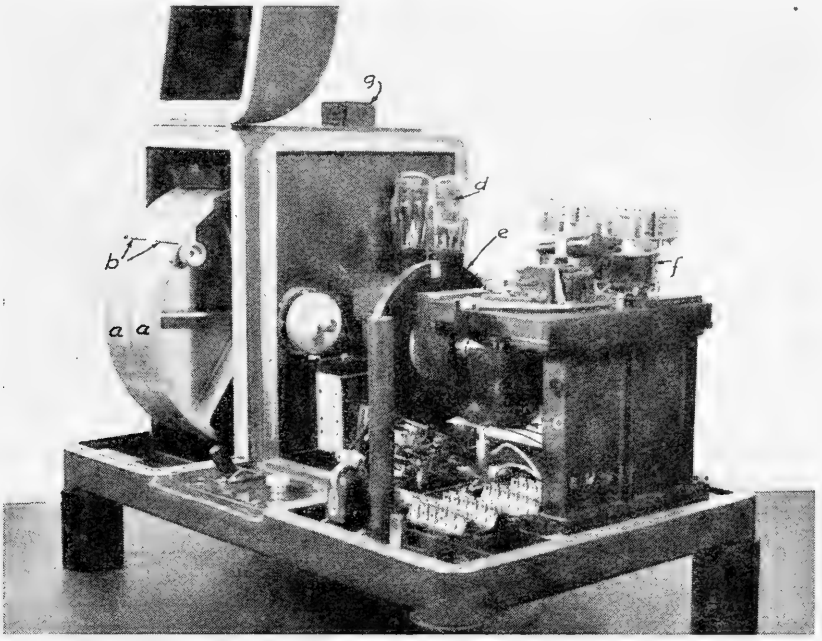

FIG. 509.—Recording oscillograph employing variable density light tracks. *a*, two film drums for 35 mm. film; *b*, clamping slots for film; *c*, motor drive; *d*, motor control tubes; *e*, commutator control for firing circuit to insure proper synchronization of firing and start of film record; *f*, relays for recording lamp circuits; *g*, housing for recording lamps. (Courtesy of Rieber Laboratories.)

principles. One characteristic feature is the elimination of the recording galvanometers. The amplified outputs of the seismometers are impressed on small overheated incandescent lamps, having special filaments capable of heating and cooling in approximate synchronism with the wave motions being recorded. Twenty such lamps are used to record twenty channels, additional lamps being employed to make records of the tuning fork motion and the shot-break. Each lamp shines through a small well-defined slit, approximately 0.010 by 0.070 inch, twelve such slits being placed side by side to record on a strip of 35 mm. positive motion-picture film.

In the twenty-trace recorder, two films are used for each shot, each

† F. Rieber, "A New Reflection System with Controlled Directional Sensitivity," *Geophysics*, Vol. 1, No. 1, Jan. 1936.

film handling ten channels. The films, each about thirty inches in length, are wrapped side by side in film-wide grooves around a drum which is driven at a uniform rate of speed by a governed motor. The speed of the motor is such that the films are driven at the rate of five inches per second. A commutator attached to this recording drum synchronizes the firing of the shot with the beginning of the record. The speed of the drum, although maintained by a governor, is checked by a stroboscopic device operated by the timing fork.

The lamps are heated by a bias battery, with their temperatures adjusted to produce a mean track density. When the amplified impulses are superposed on this bias current, the track becomes alternately darker and lighter than the mean value. Thus, a variable density record, similar to that used in motion picture sound recording, is obtained. The recording camera for this system is illustrated in Figure 509.

Figure 510 shows four Sonograph films. The left two records carry five tracks each and were made on a ten-track recorder. The right two records contain ten tracks each. Although the prime purpose of using this type of film record is to permit later analysis, a direct visual examination often may be made by comparing the wave bands. Printing all the films from a continuous profile side by side on a single sheet facilitates the correlation. If desired, records of this type may be passed through a photoelectric light intensity recorder, which yields traces similar to those obtained from the conventional galvanometer systems. Usually, however, the records are analyzed with the aid of a special device called the "analyzer."

It is the purpose of the analyzer to present the information contained in the density-modulated traces of the film in a form that can be readily interpreted. In the analyzer, the film carrying the recorded traces passes a series of narrow illuminated slots, one slot for each trace. The beam intensities are modulated by the density variations of the traces originally made in accordance with the signals derived from the geophones. A single photocell collects all light beams. The photocell output is applied to an amplifier, passed through a filter, and controls an electromagnetically-driven pen which traces the amplitude of the composite response on a paper record.

It is a basic feature of the Sonograph method to select and combine signals derived from different traces on one record. As is well known, all signals arriving from a given direction will arrive in a time sequence which can be computed on the basis of geophysical data pertaining to the particular region being explored. Time delays opposite to those occurring in this sequence are introduced between the signals derived from the different traces, and these time-corrected signals are then combined. Signals originating at one reflecting layer and received by a plurality of geophones will be in phase, while signals arriving from a different direction will be out of phase. It will be seen that the composite signal discriminates against

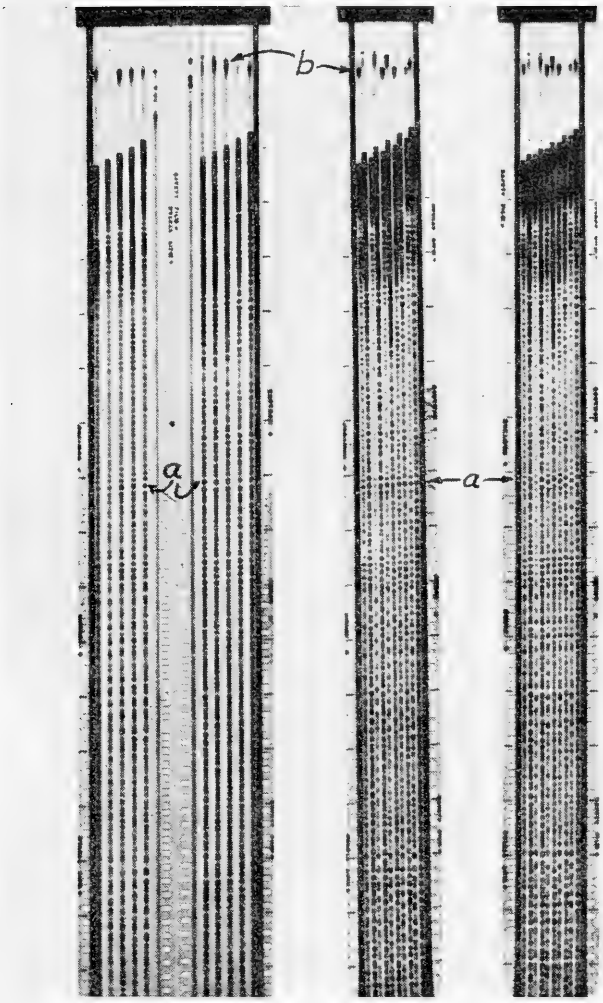

FIG. 510.—Sonograph records showing 2 five-track films and 2 ten-track films. *a*, typical correlations made by comparing light bands; *b*, shot-breaks. (Courtesy of Rieber Laboratories.)

noise as well as against signals arriving from any but the selected direction. A series of time-delays associated with another direction of wave arrival is then introduced and the composite wave for this direction studied.†

The time delays are introduced by mechanically adjusting the relative positions of the detecting slots along the time axis of the density-modulated

† Another system for determining ΔT values utilizes magnetic recording and play-back. See J. D. Eisler and J. A. Sharpe, "Recording System in Seismic Prospecting," U. S. Patent 2,394,990, Feb. 19, 1946.

F. Rieber, "Apparatus and Method for Making and Analyzing Geophysical Records" (Magnetic Recording), U. S. Patent 2,427,421, Sept. 16, 1947.

record. A mechanical drive is provided to adjust the time-delay sequence for directions spaced, for example, 4° apart, so that the operation of the machine is automatic. Figure 511 shows a composite record for the sequence of 19 discreet directions, each trace representing one direction. The east-west and north-south components are shown in the upper and lower halves of the figure, respectively. The actual angle of wave arrival for each reflection is indicated by the maximum amplitude trace. By analysis of such indicated reflections, a section map may be produced.

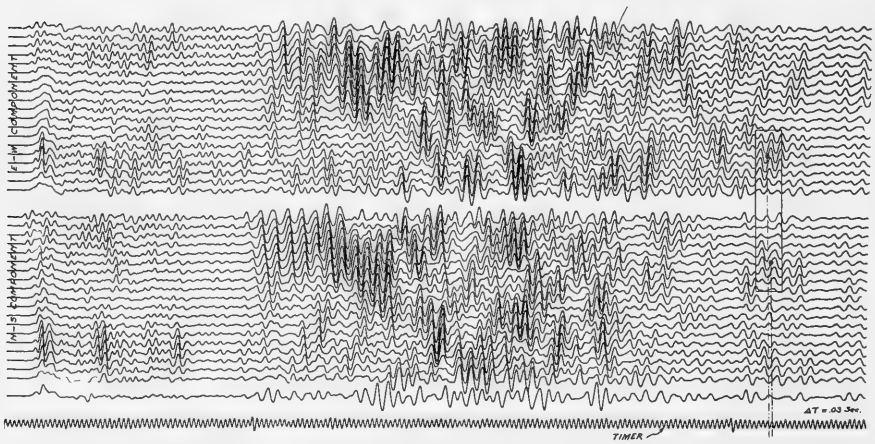

Fig. 511.—Typical record in a complex territory. For simplicity of illustration, the corresponding components of one wave group are outlined in a rectangle. Traces of maximum amplitude are marked with dots in each of the two component groups. (Courtesy of Rieber Laboratories.)

Geovision.—As an outgrowth of the experience gained with the advantages attainable from a memory-type record, Frank Rieber conceived a new approach to the problem of geophysical interpretation and devised methods which may yield an increased perception coupled with a greater speed of analysis. In this proposed method the principles of radar and television are to be utilized in conjunction with some of the accepted techniques of reflection seismography. The name "Geovision" has been applied to this proposed system for exploring geological formations and presenting the results of this exploration on a fluorescent screen where they may be inspected directly and interpreted.

Broad-band signals derived from conventional geophones are amplified in a manner not unlike that of conventional reflection seismograph equipment, but with filter characteristics attempting to preserve the signal identity while suppressing the undesirable frequency components. After passing through a corrective network, this signal energy is used to vary the filament temperature of small incandescent lamps illuminating well-defined slits. A series of these slits, corresponding to the number of geophone channels, is then focused on the surface of a photo-sensitive material.

With the photo-sensitive material passing these recording images at a constant velocity, the variations in geophone outputs within the desired band will be represented as density-modulated sound tracks quite similar in their general appearance to the earlier Sonograph records.

The drive mechanism for moving the recording material is provided with a commutator to trigger the shooting current. Suitable safety interlocks prevent the accidental discharge of the firing cap as well as accidental exposure of the recording material. The exposed film is handled throughout the entire development process by automatic controls to obtain a uniform average density for successive recordings.

The purpose of the analyzing equipment is to translate the total information contained in the memory record into a visual form more suited to interpretation.

It is proposed that by means of a photoelectric system for changing the individual variations of density of the recorded sound tracks into pulsating electrical energy, the original information will be altered to trace, on the fluorescent face of a cathode-ray tube, an image showing a cross-section of the earth under investigation. By entering known data pertaining to conditions surrounding the original field recording, with the additional faculty on the part of the examiner to vary such assumptions as the interpreter normally introduces in his analytical procedure, this image may be changed at will to indicate the effect of his introductions.

It is proposed to introduce as electrical parameters the knowledge gathered through well surveys, core samples, surface geology and the like, to obtain a more coherent picture of the geological formations under investigation. The computing equipment which produces the locating signals for the electron beam of the display tube is to perform, through successive, rapid calculations, the mathematical operations necessary to solve the interpreter's problem. Under this proposed plan the examiner will be able to vary the plane of the cross-section viewed on the screen so that it will contain information concerning dip, hade and depth relationships of the various strata.

When a series of known and assumed data has been introduced into the computing machine and a picture which seems logically related to these data has been obtained on the screen, a photograph of the image, as well as of the assumptions, will be made for future reference and comparisons to similar photographs made of adjacent investigated areas.

Frequency Analysis.—A third system utilizes a wave analysis technique whereby the complex seismic wave is broken down into its different frequency components. Analysis and interpretation are then made by correlation of these components.†

† J. J. Jakosky, method and apparatus patents pending.

Figure 512 shows the relative amplitude versus frequency of certain components of the reflections from an area near Houston, Texas. The incoming waves were recorded on 35 mm. film, and then played back through the Mirragraph wave analyzing system whereby the amplitude of each of the various frequency components could be measured. It is interesting to note the greater energy at the lower frequency range, and the gradual decrease in wave energy as the frequency increases. Of special importance are the prominent frequency bands. Some of these peaks may be partially instrumental, but the main bands are believed to be due to structure and are characteristic of the area.

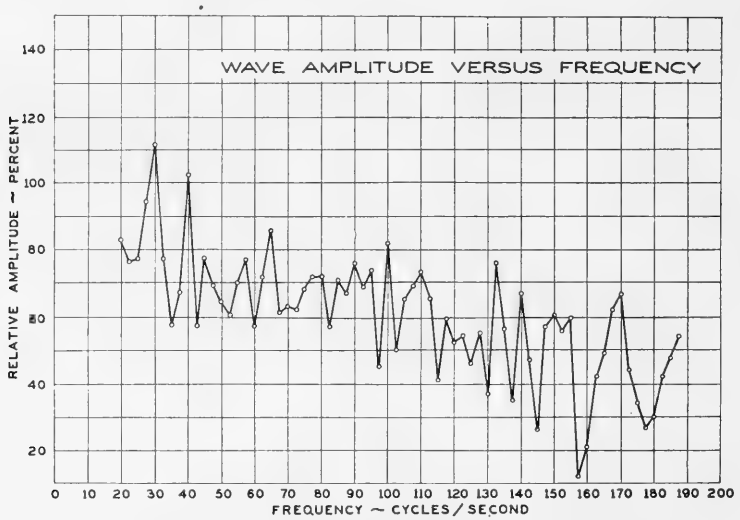

Fig. 512.—Relative amplitudes for different frequency components in the seismic wave. (Courtesy of International Geophysics Company.)

Much remains to be learned of the mechanism of energy travel from the shot-point to the seismometers. The explosion itself occurs within a few milliseconds, but the initial steepness of the wave front resulting from the explosion is modified by the characteristics of the material immediately surrounding the shot-point. The initial effect may be classified as a steep-front compressional disturbance. As this disturbance travels through the earth, its energy is partially reflected at various interfaces, some of it being absorbed by creating oscillation of certain beds. The magnitude, frequency, and persistence of these oscillations are governed by the physical properties and size of the bed and its surrounding media. There is good experimental evidence indicating that some beds vibrate at a characteristic frequency which in some cases allows their identification. Advantage may be taken of this phenomenon by frequency analysis of seismic waves recorded with true fidelity equipment.

Mirragraph.—One recording and analyzing system which is being utilized in seismic work is the Mirragraph.† This system, which was developed during the war for the study of vibration and flutter in aircraft, comprises a portable recorder, a play-back unit or reproducer, and an analyzer. The system has a flat frequency response over the range from 2 cps to 6,000 cps, and provides means for recording data in the field for later play-back and analysis by electrical methods at headquarters.

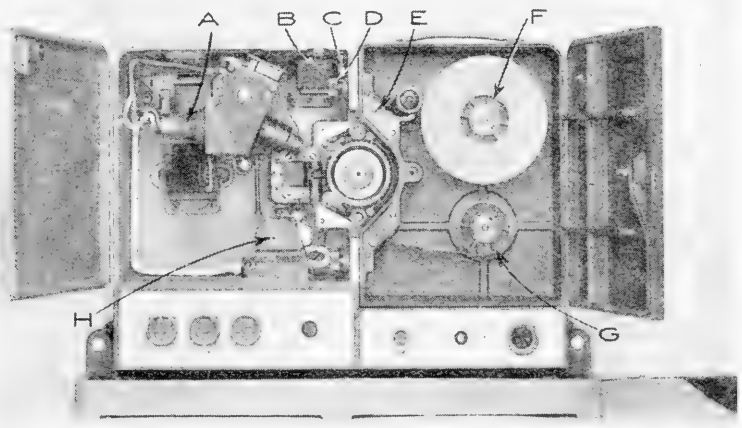

FIG. 513.—Mirragraph recorder, front view with doors open. A, slater lamp; B, footage counter; C, footage counter reset; D, magazine locking screw; E, light trap rollers; F, feed spool; G, takeup spool; H, cam gear and switch assembly. (Courtesy of Western Electric Company.)

The recorder, illustrated in Figure 513, is a thirteen-channel device which uses a light valve, similar to those employed in recording sound for motion pictures, to convert the electrical signals from the individual seismometers into photographic images on moving 35 mm. film (Figure 514). This light valve is a thirteen-ribbon Einthoven galvanometer of special design, and the records made with it are similar to oscillograph traces except that the trace width is much greater and the excursion from the zero axis is held to less than the trace width. This is necessary in order to achieve records which may be played back in the reproducer unit as variable area type records. Figure 514 illustrates a typical Mirragraph record. The bottom trace is a 1000-cycle timing track. The recorder has a motor control device which holds the speed constant to one part in 25,000.

The reproducer unit illustrated on the left of Figure 515 consists essentially of a motor drive film mechanism, an exciter lamp which illuminates all thirteen traces of the moving film record, a masking device to mask off one-half of each trace (which converts the constant width

† Trade mark, Western Electric Company.

track into a variable area track), and a bank of thirteen photo-electric cells which convert light variations through the unmasked portion of each trace into electrical signals which are the counterpart of the originally recorded signals. The two ends of a given record may be spliced together to form a loop, and the data on this loop may be played back repetitively for study and analysis. The data may be rerecorded to conventional oscillograph records and during the rerecording operation any one of several special techniques such as filtering, compositing, etc. may be employed. One model of the reproducer includes provisions for introducing discreet amounts of time displacement between the several traces during the playback.

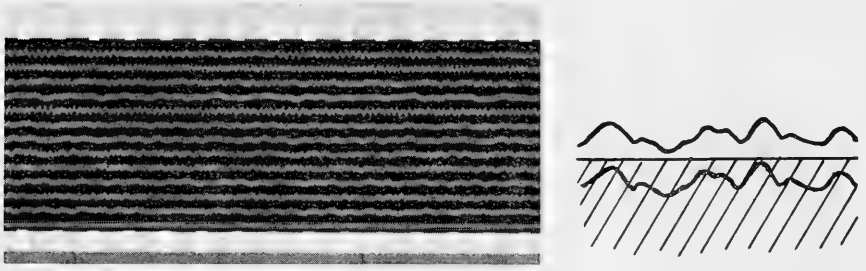

FIG. 514.—(Left) Section of Mirragraph 13-channel recording on 35 mm. film. (Right) Sketch showing enlarged variable area track obtained by masking off one-half of a constant width track. (Courtesy of Western Electric Company.)

The frequency-analyzer unit shown on the right of Figure 515 consists essentially of a crystal controlled band-pass filter of fixed width whose position in the frequency spectrum may be set at any point between 2 cps and 6,000 cps. Crystal filters of various band widths from 2 to 200 cps are available. With this instrument it is possible to make a detailed analysis of a complex signal and determine the frequency components and their relative amplitudes. The device has been well proven in connection with vibration studies, but much remains to be done in applying it to the study of transient phenomena, such as seismic reflections.

The general functions of the system as described above may also be had in the form of a multi-channel magnetic recording and reproducing unit. When using the magnetic methods for recording and reproducing low frequency signals, it is necessary to compensate for the drop in response at the low frequency end of the spectrum due to the velocity characteristics of the magnetic method. This dropping off in response, which occurs at the rate of 6 DB per octave at any given magnetic film or tape speed, can be partially compensated by recording at a low film or tape speed and reproducing at a higher speed. Carrier recording is an obvious, although not entirely satisfactory, solution, and other methods for accomplishing flat low end response are under development.

The frequency analysis of a single trace of one such record is shown in Figure 516. The top trace shows the complex wave as generated by the actual ground motion. Many of the reflections are masked by the variations in phase, amplitude, and frequency of the different reflections. By playing back the record through a narrow band-pass filter (usually 2 to 5 cycles wide) and scanning the record from the low to the higher frequency

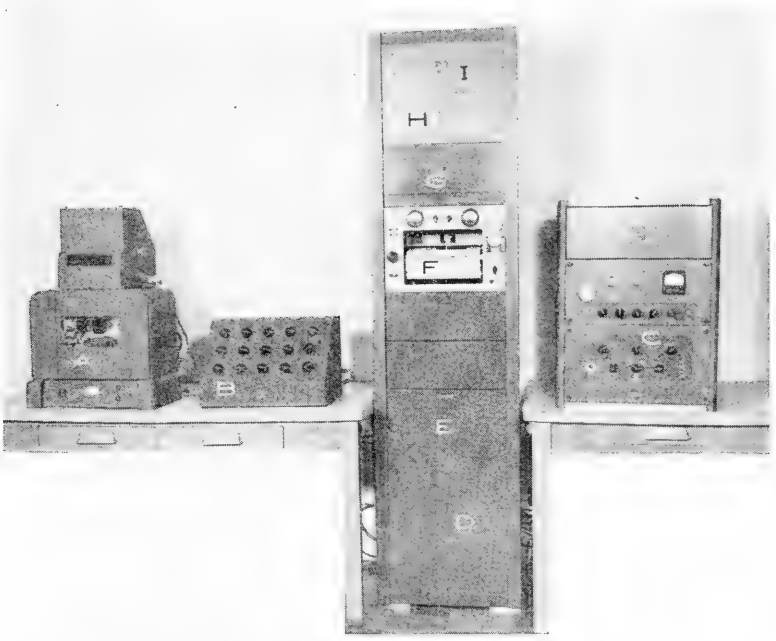

FIG. 515.—Mirragraph reproducing and analyzing equipment. A, reproducer unit; B, control unit; C, frequency analyzer; D, exciter lamp power supply; E, filament power supply; F, graphic recorder; G, control panel; H and I, plate current power supply. (Courtesy of Western Electric Company.)

limits (usually 2 to 300 cycles), the complex seismic wave may be broken down into its components. The other traces in that figure show seven of the different frequency components, their arrival times, and their relative amplitude and persistence. The higher frequency response of this particular recording is low due to the characteristics of the seismometer employed, which was peaked at about 25 cps. Later equipment employs high fidelity seismometers and amplifiers.

Detailed studies of conventional oscillograph records from many areas show changes in frequency and wave characteristics diagnostic of subsurface conditions. Although there is a general change in frequency versus depth, the frequency is influenced by factors other than mere depth below the surface. The frequency of the reflected waves seems to be governed by the characteristics of the "reflecting" bed and the character of the inter-

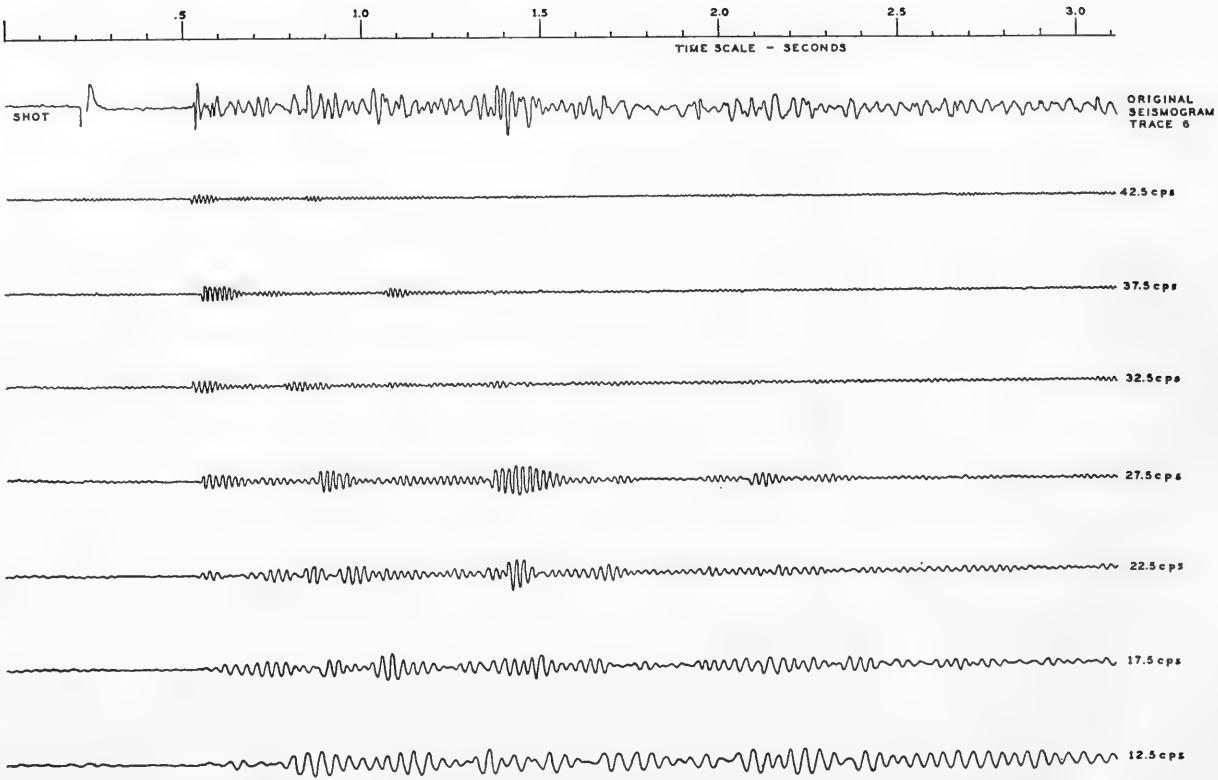

FIG. 516.—The top trace shows the original complex wave as recorded by one of the seismometers. The subsequent traces show the various frequency components and their relative arrival times. (Courtesy of International Geophysics Company.)

face. Also, the relative amplitude and time of persistence apparently vary with the physical properties of the bed and its adjacent environment. There is good experimental evidence to indicate that it is possible to identify and follow certain of these beds by frequency correlation from station to station. In areas where this is possible, it will aid in the mapping of stratigraphic traps, such as pinch-outs, lensing, changes in porosity, etc., where much oil has no doubt accumulated. In many areas trouble is encountered with reflections from successive strata or between the boundaries of a single stratum, giving rise to multiple reflections, which often cause errors in interpretation. With the frequency analysis technique such multiple reflections usually are easily recognized due to the periodic reoccurrence of the same frequency wavelet.

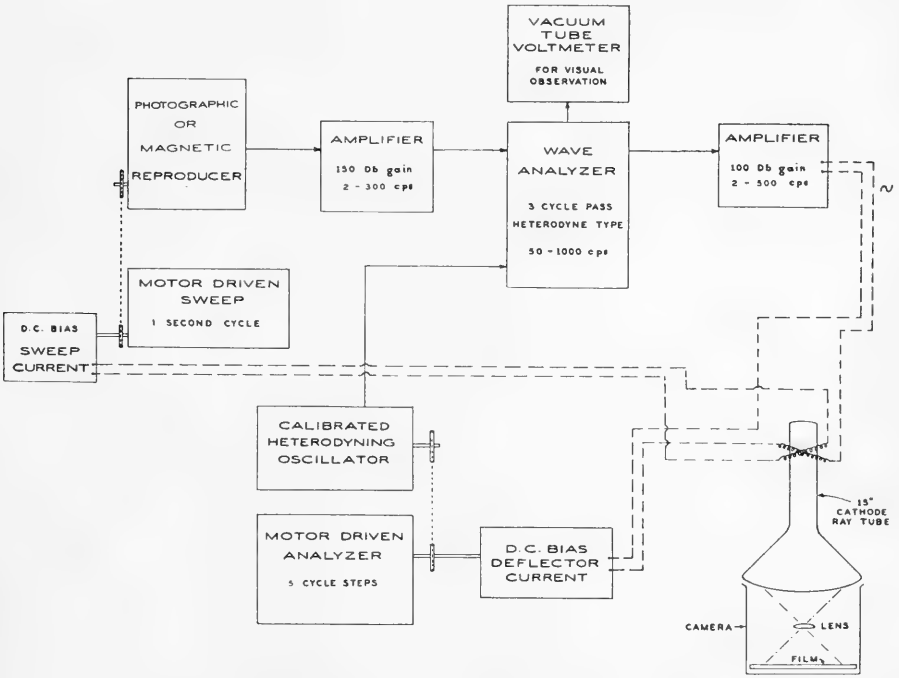

FIG. 517.—Schematic diagram for frequency analysis. (Courtesy of International Geophysics Company.)

Frequency Pattern Correlation. — Another type of instrumental analysis which offers interesting possibilities is based on the comparison of frequency patterns. In this technique the original record is played back through a relatively narrow band-pass filter. The filter is narrow enough (usually from 5 to 15 cycles pass) to give clean-cut reflection discrimination, but not sufficiently sharp to introduce undesirable distortion or delay in passing through the filter.

Generally one trace nearest the shot-point is selected for the frequency pattern studies. By comparison with the patterns of corresponding traces at the other shot-points, the structure and certain physical properties of the subsurface are revealed.

Figure 517 is a schematic diagram of one form of instrumentation employed in the frequency-pattern technique. The analysis is made in steps of 5 cycles, and usually covers the range from 2 to 500 cps. The film or magnetic tape is spliced into an endless loop and passed through the analyzer in repetitive cycles. Approximately 1.5 seconds time is required for each pass, and 100 passes are necessary to cover the desired frequency range. The total time for producing the frequency pattern is about two minutes.

A synchronous motor drives the reproducer through which the record loop is cycled. The film drive is geared to a potentiometer which supplies a D.C. bias sweep current to the cathode-ray tube, so that each sweep of the cathode ray beam across the tube corresponds to one pass of the record loop.

The output of the reproducer is passed through an amplifier and thence into a band pass filter or heterodyne type wave analyzer. The output of the filter is then amplified and actuates the vertical deflection coil of the cathode-ray tube, thereby introducing vertical displacement as the cathode-ray beam is moving horizontally across the tube. The beam is shifted downward at each successive horizontal sweep, so that a series of parallel lines is traced across the tube as the analysis proceeds. By superimposing the patterns obtained at the various stations, the relative travel times or ΔT values are indicated by the shift in the films at each station, at the best correlation.

ASSEMBLY OF EQUIPMENT FOR SEISMIC PROSPECTING

A major portion of the geophysical equipment used in commercial work is designed for mounting in trucks or other motor-propelled conveyances. Figure 518 illustrates 24-trace equipment designed to be placed in a truck or boat. Each amplifier and filter channel is incorporated into a separate panel unit. Figure 519 shows a similar type of truck equipment, with 24 recording traces, utilizing three amplifier channels per unit.

In contrast with the rather elaborate apparatus for truck mounting, extremely portable and lighter-weight equipment has been designed for use where trucks cannot operate. Simplification is the chief characteristic of such equipment. For example, one or two filter settings are usually considered sufficient, and such items as multi-recording have not appeared in portable versions. In most cases the equipment is divided into separate packages which are interconnected by plug-in cables when in use. Figure 520 illustrates portable seismograph equipment. A similar 12-trace outfit, set up at a field station, is illustrated in Figures 521 and 522. In general, results obtained with portable seismograph equipment compare very favorably with those achieved with the heavier, less portable equipment mounted in trucks or boats. The main difference in the operations is that survey

progress is usually better with the more elaborate and more sturdy truck-mounted instruments. The lighter-weight, portable type of equipment may also be transported by helicopter for work in swamps and other difficult terrain. Helicopter operations improve the time factor until approximately the same production may be obtained as with truck-carried apparatus over average terrain.

Portable seismograph equipment, like its heavier counterpart for truck mounting, must be designed to withstand fungus growths, corrosion from intense humidity, and a certain amount of field hazard in the form of

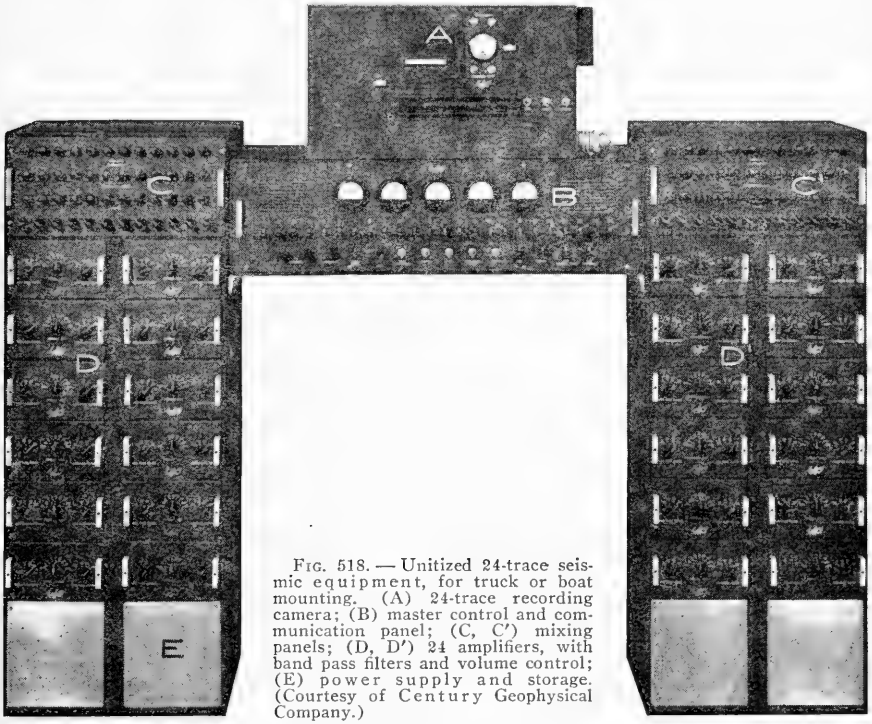

FIG. 518. — Unitized 24-trace seismic equipment, for truck or boat mounting. (A) 24-trace recording camera; (B) master control and communication panel; (C, C') mixing panels; (D, D') 24 amplifiers, with band pass filters and volume control; (E) power supply and storage. (Courtesy of Century Geophysical Company.)

accidents resulting from rough usage. The lighter weight in the portable equipment is obtained at the expense of a certain amount of ruggedness and operational completeness.

Recording Trucks and Reels.—The recording trucks shown by Figures 523 and 524 illustrate common practice as regards the instrument compartment and the arrangement of reels. In Figure 524 the reels are kept under cover when not in use, whereas in Figure 523 an arrangement is shown where the cable and reels are open to the weather. In both cases the reels are power driven. Both trucks are of the four-wheel drive type, making possible the negotiation of very difficult terrain.

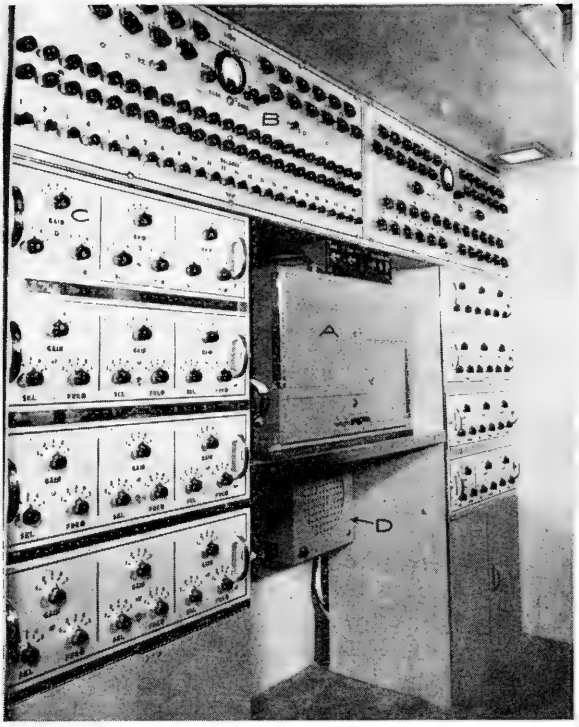

FIG. 519.—24-trace seismic recording equipment illustrating three amplifiers in unit construction. (A) 24-trace recording camera; (B) master control and communication panel; (C) three channel amplifier and filter unit; (D) communication speaker. (Courtesy of Engineering Laboratories, Incorporated.)

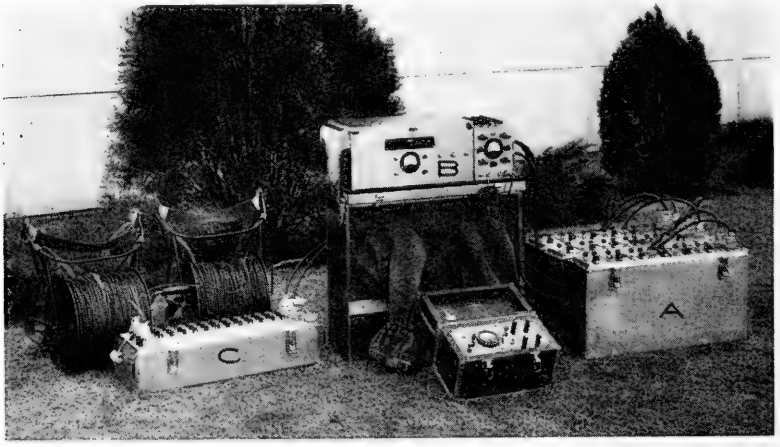

FIG. 520.—A complete set of portable seismic equipment for the recording of twelve traces. (A) amplifiers; (B) camera; (C) control and test panel. (Courtesy of Century Geophysical Corporation.)

Where climate requires, the truck, especially the roof, should be thermally insulated for work in hot summer months. Means should be provided for fan ventilation in summer and heating in winter. The truck body must be light- and dust-tight to provide the necessary dark-room facilities.

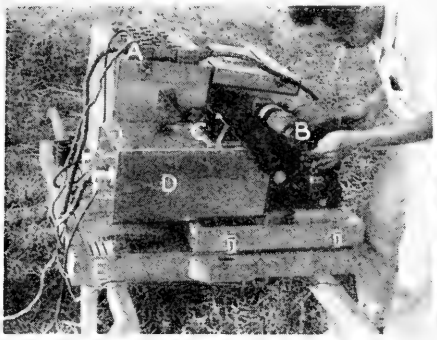

FIG. 521.—A 12-trace portable seismic outfit at a station clearing in the Philippines. (A) amplifiers; (B) camera magazines; (C) viewing window; (D) galvanometer and timing machine; (E) carrying litter. (Courtesy of Geophysical Engineering Corporation.)

FIG. 522. — Developing seismograms in daylight using portable equipment, in Philippines. (Courtesy of Geophysical Engineering Corporation.)

FIG. 523.—Instrument truck body, with power-driven reel, mounted on four-wheel drive truck. A, door to instrument compartment and dark-room; B, reel; C, seismometer storage, battery compartment, etc. (Courtesy of Century Geophysical Corporation.)

Provision must be made for carrying extra equipment, such as augers, spades, pick-axe, small tools, and emergency water and canned food rations. The recording truck must be provided with the necessary photographic paraphernalia for processing the records.

A full set of reels containing seismometer and telephone cables are fastened to the truck. The number of reels and the arrangement of cables vary considerably among operators and depend upon such factors as number of seismometers, length and type of spreads, provision for varia-

FIG. 524.—A fully-inclosed type of seismic recording truck with power-driven reels and four-wheel drive. A, door to instrument compartment; B, reel compartment; C, seismometer and other storage; D, drinking water. (Courtesy of Western Geophysical Company.)

tion in spreads, efficiency in disposing and picking up of seismometers, and preservation of cable. The number of reels varies from two to eight or more. To avoid great cable strain, the cable often is reeled-in while

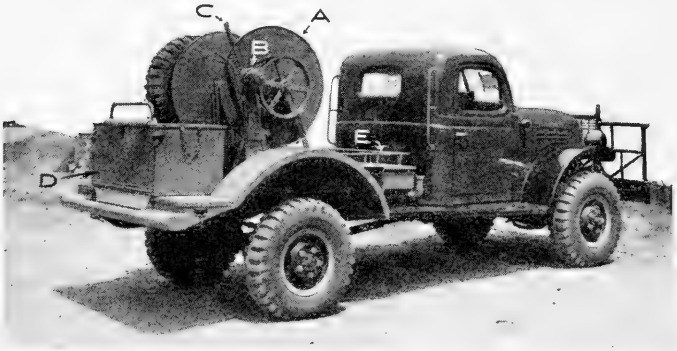

FIG. 525.—Auxiliary service truck. A, power driven reel for extra cable; B, motor drive; C, clutch and brake levers; D, box for spare seismometers; E, space for tool box, etc. (Courtesy of Griffin Tank and Welding Company.)

the truck is driven along side of the cable. In any case, at no time should cables be pulled with such force as to harm the conductors, particularly the splices and connectors.

Figure 525 shows an auxiliary service truck, which usually supplements the recording truck. It is equipped with a power-driven reel and brake

for handling the extra cable, storage box for extra seismometers and parts, and floor space directly aft of the cab for tool box, etc. Figure 526 shows a typical survey pick-up truck; one or two are used by each shooting crew. Carriers are provided for the alidade and transit tripods, a steel box for storing the instruments, "U" supports for stadia rods, and storage box for stakes, flag material, etc.

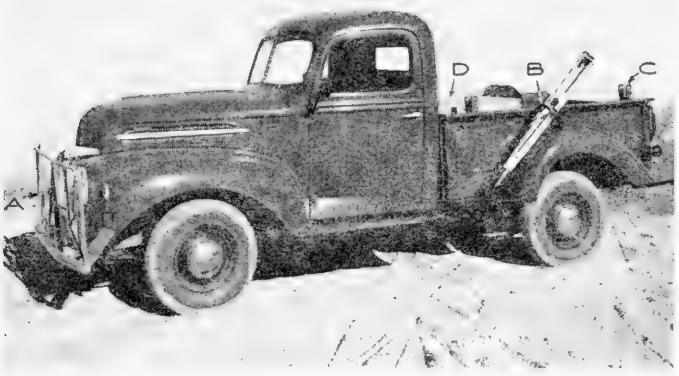

FIG. 526.—Survey pick-up truck. A, brush guard; B, support for transit and alidade tripods; C, "U" supports for stadia rods; D, steel box with lock for storage of surveying instruments. (Courtesy of Griffin Tank and Welding Service.)

Testing of Equipment.—At periodic intervals, as well as when suspicion is aroused, the following tests should be made to determine the operating characteristics of the equipment: (a) time parallax or phase relationship of the recording channels; (b) accuracy of the timing system; and (c) general circuit condition.

Phase lag between the channels can be detected by placing all of the seismometers at the same location and firing a regular reflection shot. If all channels give the same time of arrival and character of record, the equipment assembly is operating satisfactorily. If differences are recorded, tests should be conducted to determine whether the trouble is due to the location of the seismometers. This can be checked by interchanging the anomalous seismometer with one of the others. If a seismometer is faulty, it should be corrected or replaced.

The character of the record is influenced considerably by the material at and adjacent the seismometer. If differences in character occur during field operations, the anomalous seismometer should be interchanged with one of the others. If the trouble still exists, the anomalous seismometer should be replaced. Persistence of the trouble will then indicate difficulty in the amplifying, filtering, or galvanometer system of the trace.

The timing system should be checked for accuracy by comparison with a separate timing fork. The reference timing circuit should be connected

to one of the galvanometer traces to obtain a direct check with the regular timer.

Miscellaneous tests on the circuits can be conducted. An example is test for cross-feed, for assurance that energy is not being distributed over more traces than expected and thus producing artificial line-up and distorting data.

Some member of the crew should be familiar with electronic equipment and provided with the necessary test equipment and replacement parts.

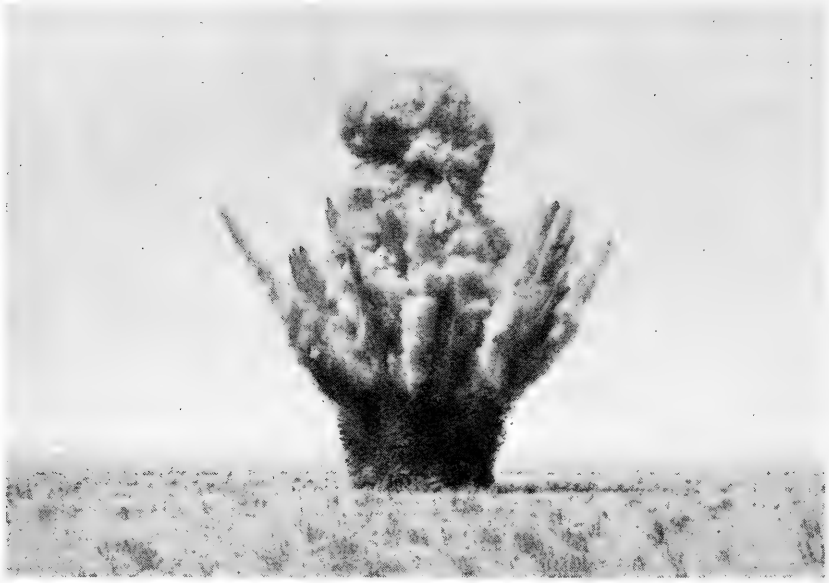

FIG. 527.—Early refraction shot.

FIELD OPERATIONS IN SEISMIC PROSPECTING

Early Refraction Shooting.—Refraction shooting was the pioneer method and it is to be expected that the early refraction apparatus and procedure were less refined than those now employed.

In the early days of refraction seismic work, the shooting was conducted on a time schedule. The clocks of the shooters and recorders were synchronized daily, and at definite prearranged times the shooter exploded the charge. Just prior to the shot-times, the various operators, each of whom had a set of seismometers, amplifiers, a recorder, and developing equipment, started the recorders and then allowed them to run for a definite length of time. After getting his record, the operator developed it and then moved to the next station, where the recorder was again set-up for the next scheduled shot. The shooter often remained in one location all day. If for any reason his first shot could not be fired on schedule, he fired it fifteen

minutes later. The instant of the shot was recorded at the point of observation by an electric signal which was transmitted from the shot-point by means of a wire.

Later, radios were introduced, each operator having a receiver and the shooter a transmitter. The shooter sent a message just before firing the shot, and the instant of explosion (shot-time) was transmitted by radio. Still later, the operator and the shooter used two-way radio communication to make sure that all instruments were in working condition before the heavy charge was fired.

The quantity of dynamite in the shot depended upon the distance; often charges of several thousand pounds were used. Originally, the shots were placed on the surface of the ground, or, after the first shot, in the crater made by preceding shots. Later the dynamite was put in holes as deep as 200 feet. A photograph of an early refraction shot is shown in Figure 527. (The resulting crater was over 20 feet deep.)

Modern Refraction and Reflection Operations.—From an operational viewpoint, refraction field procedure differs from reflection field procedure in numerous respects: viz., the refracted "first arrivals" and a few correlatable subsequent wave trains are of primary interest, to obtain time-distance curves; the size of charge (amount of dynamite) is usually much greater; the seismometer spread length and the distance of the spread from the shot-point are greater; usually the range of depth investigated is more restricted than in reflection work; and the investigations are essentially *lateral* in their scope, as compared to *vertical* for the reflection work. As the work proceeds, the configuration of shot-point and seismometer spread is moved forward in increments along a given profile line.

However, the refraction and reflection field operations and equipment have several similarities. Thus the exploration crew and the general division of duties of the crew members are similar; the field trucks used in the two types of prospecting are similar, etc. Hence, in the general description given here, refraction and reflection operations will be distinguished specifically only in the discussion of types of spread and in the methods of improving detection of reflections.

The Exploration Crew

A typical seismic party comprises a party chief, assistant party chief, permit man, surveyors, a recording truck staff, shooters, drillers, and computers. The general division of duties is given in Table 24.

The party chief* is responsible for all details of the work and arranges the schedule so that the work is done in the most efficient manner. After the party chief and the supervisor to whom he is responsible have selected the areas to be explored, the permit man secures permission from the

* In most organizations the party chief is in charge of geophysical interpretation and prospect mapping as well as field operations. In other organizations these two general functions are divided between two persons.

owners and lessees for the necessary work on the land. The permit man also makes agreements regarding the condition in which the land and fences must be left. Sometimes the final decision as to exact location of shot-holes and seismometer stations is not made until after permits are obtained. The surveyors then locate these points and mark them with stakes; the stakes are numbered and their location plotted on maps. The points are now ready for the drillers who must drill the holes to depths that have been determined from experience in the area or in similar areas. Next, the shooting and recording operations take place, preferably soon after the holes are drilled.

TABLE 24

GENERAL DIVISION OF DUTIES OF MEMBERS OF SEISMIC CREW

Party Chief	Field supervision of all operations. Interpretation of field data. Contact man between geophysical and geological departments.
Assistant Chief	Assistant to Party Chief and next in charge.
Computer	Computation of results and plotting.
Operator	Responsible for recording truck operation and in charge of crew while on field.
Assistant Operator	Assistant to operator.
Shooter	Responsible for explosives, loading, and shooting operations.
Assistant Shooter	Assistant to shooter.
Driller	Responsible for drilling of shot-points and for drilling equipment.
Assistant Driller	Assistant to driller.
Laborers	General field operations such as digging of shallow holes for seismometers, handling of cables. Helpers to drillers and shooters.
Permit Man	Right of way and shooting permits.
Surveyor	Location of seismometers and shot-holes.
Rodman	Assistant to surveyor.

The basic seismic operations are performed by two units: namely, the shooting unit and the recording unit. The procedure in the field is managed by the operator who is also responsible for the recording equipment. The recording unit consists of the recording truck and three or more men, at least one of whom, besides the operator, is sufficiently familiar with the equipment to assist in its maintenance. The shooting unit usually consists of two or more men and one truck. The head of the unit, the shooter, is responsible for his equipment, for efficient loading of the holes, and for the handling of explosives by his unit according to the legal and safety regulations.

After the seismometers of the recording truck unit are disposed and circuits checked, the recording equipment is ready for operation. By this time the shooter generally has loaded the hole with a charge at a depth

already designated by the operator. From his controls in the recording truck, the operator communicates with the shooter by telephone or radio. The shooter repeats the depth and magnitude of charge, reports that personnel, equipment, etc. are safely located, and states his readiness to fire. The final order to fire is given by the operator, who then sets the recording equipment into operation when the shooter signals back.* After the records have been developed, the operator carefully studies them in order to direct the shooter regarding depth and pounds or sticks of explosive to be used in the shots to follow. Upon completion of the shooting, the hole is suitably filled to prevent damage to crops and injury to man and cattle. Sometimes when casing is used, it is pulled later by the drilling crew. When the holes are deep, it is cheaper and more efficient to have a special crew with suitable equipment to transport, pull, and lay down casing at the shot-points.

The day's records are taken to the party headquarters and usually are computed on the following day. The first step in the interpretation of the records is to mark the shot time period and to determine "weathering" or low velocity layer data. The records are then picked for refractions or reflections. Next, the data are computed and plotted—generally on cross sections from which mapping proceeds. Subsequent field operations are outlined by the supervisor in collaboration with the party chief from studies of the current data.

A schematic layout of a reflection crew in operation, together with the path of the reflection and the record, is shown in Figure 528. The record indicates the shot-instants and the onsets of the reflections at the three reflecting horizons. For a refraction crew, the paths of the refracted rays and the refraction record would be shown; otherwise the arrangement is much the same except for distances between seismometers and between operator and shot-hole.

Transportation and Communication

The mobile equipment required for effective seismic operations is largely dependent on local conditions. Generally, the automotive equipment will comprise: recording or instrument truck, shooting truck, drill truck, water truck for drilling operations, surveyor's car, permit man's car, and party chief's car. The applicability and relative merits of standard tire equipment, dual or tandem conversion wheels, caterpillar treads, or large size marsh tires depend on the region surveyed. Even under favorable field conditions it is desirable, from the viewpoint of good mobility and minimum periods of delay, to equip the heavier trucks with four-wheel drives or dual tires. When field conditions are difficult, it is necessary to equip the heavier trucks with winches, and all explosive-carrying vehicles should be equipped with ground straps or chains.

* Sometimes the operator is provided with means to fire the shot, and patents have been granted for a device to make the shot-instant coincide with one of the time marks on the record. However, the practice of shooting by the observer is rightly criticised as dangerous for the shooting crew and chance passers-by at the shot-point.

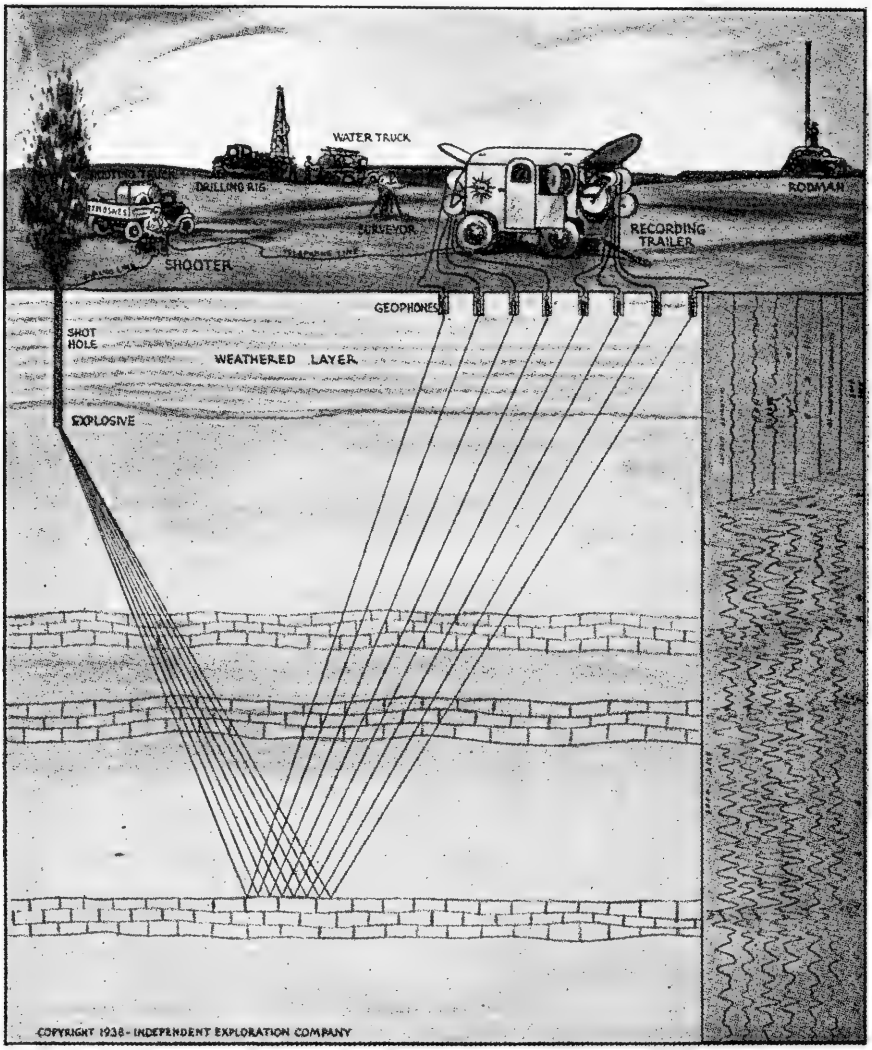

FIG. 528.—Reflection party in the field. Illustrating the path of the reflection and the record. (Courtesy of the Independent Exploration Company.)

Special types of transportation are often necessary in areas of difficult terrain. In certain sections of the bayous and swamps of the Louisiana Gulf Coast, it is convenient to travel by means of so-called "marsh-buggies." Marsh buggies are usually trucks with special wheels that provide a large supporting surface. (Figures 529 and 530.)†

In some portions of the Louisiana Gulf Coast swamps, the network of

† Harry F. Simons, "Marsh Buggy for Use in Gulf Coast Fields," *Oil and Gas Journal*, Feb. 22, 1940, p. 71.

FIG. 529.—Seismic recording truck for use in marsh and swamp areas. (Courtesy of Continental Oil Company.)

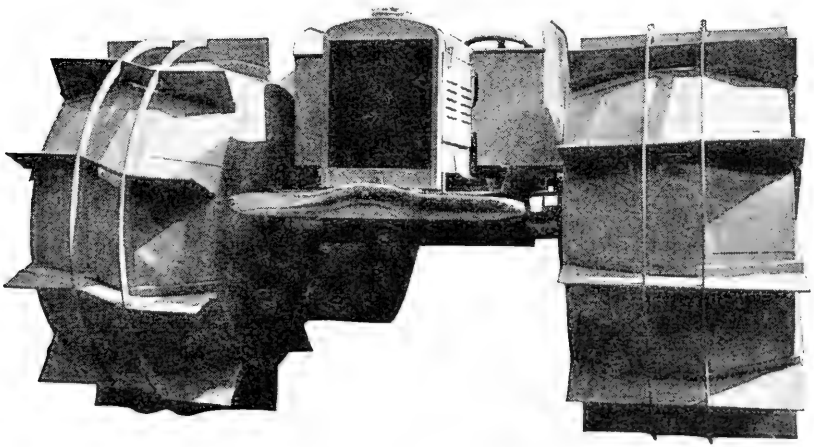

FIG. 530.—Marsh buggy. (Courtesy of Western Geophysical Company.)

streams is sufficiently close to permit the field men to reach much of the area in small power cruisers or boats. In this case the procedure is identical with the procedure on land, with the exception that the equipment is mounted in boats instead of in trucks. Special precautions must be exercised in the design of equipment in order to prevent damage due to exposure; for example, the seismometers are placed in water-tight cases.

Frequently, however, the swamp is cut up by streams which are too small to permit the use of boats and too wide to be crossed by marsh buggies. In order to avoid the necessity of transporting the amplifiers and recorders across difficult marsh by foot, a method of "remote control" is employed wherein the seismometers are located at a great distance from

FIG. 531.—Laying cables in swamp areas.

the amplifiers. Remote control work often has been done with the seismometers as much as five miles from the amplifier; in these cases, it is necessary to separate the wires enough to prevent cross-feed from one line to the next due to mutual inductance between lines. (In difficult swamps this requires a considerable amount of labor.)

Figure 531 illustrates working conditions often encountered in laying cables in swamp areas.

Recent applications of helicopter service to geophysical operations have overcome many of the obstacles encountered in swamp lands, rough terrain and in virgin country without trails or roads. Figure 532 illustrates helicopter operations in swamp areas.

In this type of operation, two helicopters are usually employed, one

for transporting personnel and supplies, and the other for moving the recording equipment, geophones and cables. When moving a short distance to another line of profile, both helicopters are used for transporting the geophone cable, one on each end. Both helicopters are employed when moving the drilling crew and equipment. To see this operation would amaze and delight some of the old-timers who remember swamp operations in the late twenties and thirties. It is a much faster operation than by marsh buggy, and production records approach those of normal automobile-equipped crews operating over poor roads. Generally the equipment is of the portable type, with a reduced crew personnel. The usual heavy-duty drill is dispensed with, and in its place is provided a light-weight drill or one of the small hydraulic units for digging shallow shot holes.

(a) (b) (c) (d)

FIG. 532.—Helicopter service applied to swamp areas in seismic prospecting. (Courtesy of Seismograph Service Corporation.)
(a) Helicopter with basket underneath for carrying equipment and supplies.
(b) Helicopter pulling geophone cables.
(c) Portable drilling unit in operation.
(d) Helicopter carrying disassembled portable drill, ready to take off for next drilling location.

Amount and Depth of Explosive

For economic reasons the charge of dynamite is made as small as consistent with adequate refraction or reflection energy.* Especially in reflection shooting, other reasons also may dictate this rule. With increasing charge, the useful wave energy does not rise proportionately to the magnitude of charge, due to increased mechanical pulverization of the earth in the vicinity of the shot-hole. Also, the energy of the surface waves generally increases more rapidly with the amount of dynamite than does the refracted or reflected energy. The usual experience is that a charge that exceeds some certain amount has scarcely any advantage and may be a definite detriment. However, sufficient dynamite must be shot so that adequate amplitude of ground movement due to reflection or refraction energy is produced at the seismometers. It also is essential that the reflection or refraction energy be greater than the extraneous energy in the recorded band of useful frequency. In certain special cases simultaneous explosion

* See pages 857 to 863 for detailed discussion of explosives and their characteristics.

in several closely spaced shot-points have been used to achieve sufficient energy. (See section on Multiple Shot-points.) This procedure is seldom employed because very small charges are difficult to load, causing time delays.

The depth of the shot is determined by the character of the subsection and must be below the low velocity, or so-called weathered zone, because absorption of energy is very great in the low velocity zone. The base of this zone frequently coincides with the top of the water table. A preliminary idea of the necessary depth for shot-holes in a new area can be obtained, therefore, from local water well records. When the medium immediately below the low velocity zone is stratified, it is preferable to seek out that stratum which yields highest efficiency of transmission of energy and to load the explosive at that depth. Shale usually transmits the shot energy more efficiently than sand or unconsolidated material, while the less porous rocks are still more effective.

The usual procedure for ascertaining the optimum shooting depth in a new area is: (1) to determine the depth of the low velocity zone from shallow refraction shooting, (2) to shoot light shots up-hole to obtain an up-hole low velocity diagram, (3) to shoot at various depths to obtain sample records. The drilled hole depth must exceed the depth of the bottom of the low velocity zone by an amount sufficient to insure that the top of the dynamite string is below the base of this zone and that the area of shattering is within the "consolidated" zone. Additional leeway is given when doubt exists as to the exact thickness of the low velocity zone.

Sufficient head of water must be maintained above the charge in order to keep the explosive from expending an excess of its energy up the hole. (The shooting truck usually carries a tank of water for this purpose.) Sometimes the subsurface water will maintain a sufficient head that no extra water need be added to the hole.

An outline of optimum shot-point procedure for efficiency, safety and quality of data is presented by Williams,† together with a review of some of the characteristics of seismic explosives.

Seismometer Disturbance

The seismometers are generally buried in shallow holes or pits which are dug either with a post-hole auger or with spades. The depth of the hole should be at least sufficiently great to allow the top of the instrument to be flush with the ground in order to minimize wind disturbances.

The recent trend in reflection shooting is toward a large number of recording channels and the use of several seismometers on each channel. This has necessitated the use of numerous seismometers and has given an impetus to placing the seismometers on the surface of the ground to conserve time and labor. When the seismometers are to be placed on the surface

† F. J. Williams, "Notes on Shot-point Procedure," *Geophysics,* Vol. XI, No. 4, Oct., 1946, pp. 443-456.

of the ground, their cases are usually designed with a flat extended bottom and streamlined upper portion. The surface of the ground is usually scraped to remove loose material, and the seismometer is then firmly seated or pressed in place.

If possible, the seismometers should be placed on firm ground and at a reasonable distance from trees, telegraph poles, irrigating ditches, pipe lines, concrete roads, and other structures that may transmit vibration to the nearby earth. Field men in the vicinity of the seismometers should remain motionless while the record is being made. In windy weather, trees, wheat, high grass, etc. often prove troublesome as they are a source of noise or vibration.

Extraneous vibrations are especially troublesome in the case of reflection prospecting. The higher the noise level in any particular location, the higher must be the energy level of the reflections in order to give a usable reflection record. This necessitates larger charges of explosive than would otherwise be necessary or even advisable. Conditions are comparable to radio reception: the incoming signal must be of a higher energy level than the static and local interference. Under conditions of high noise level, increased amplification usually does more harm than good. In areas of heavy traffic, or other disturbing factors, the operator must make his records during periods of minimum disturbance. In some cases airplane noise has proven to be a particularly disturbing factor. The operator should never give the signal for firing if any of the galvanometer traces is unduly disturbed or if interference is expected, as from approaching cars, trains, airplanes, etc. Oftentimes, the difference between usable and useless records depends upon the vigilance and ingenuity of the operator.

Seismometer Spreads

The character of the records and the nature of the information which may be obtained is dependent to a large extent on the relative positions of the seismometers and shot-point. The type, length, and orientation of the seismometer spread are determined by such miscellaneous and often unrelated factors as magnitude and direction of strata dip, presence of particular geological features, character of low velocity layer, accessibility, disturbance energy, availability of permits, economic considerations, and degree of required accuracy, i.e., whether reconnaissance or detail shooting. Furthermore, in reflection shooting, the type, length and orientation of the spread are determined to a large extent by the quality of reflections, as shown by sample records.

General classes of individual seismometer spreads used in reflection shooting include the split spread, the symmetrical offset spread, the uni-directional spread, the two-hole spread, the offset uni-directional spread and the right-angle spread. (Figure 533.)

The split and uni-directional spreads indicated in this figure are used particularly when, due to limitation of accessibility or simply to greater

ease of disposition of seismometers, the seismometers and shot-points are required to be on the same line. When the uni-directional spread has shot-points at *both* ends, it is usually called the "two-hole" spread.

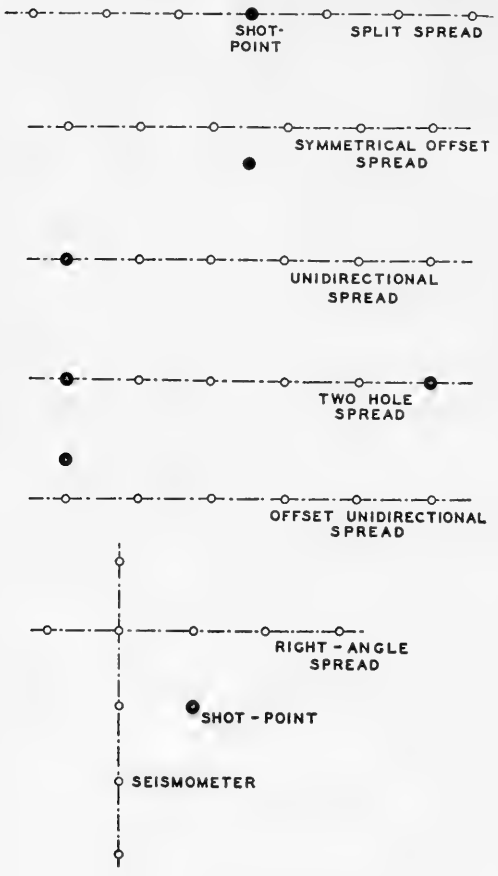

FIG. 533.—Types of seismometer spreads.

The symmetric offset spread† is used to avoid the long gap between the seismometers nearest the shot-point. The effect of the offset spread is to displace reflection points on the strata along the cross dip, but in general this may be made sufficiently small to be negligible. The right-angle spread is designed to obtain line and cross dips simultaneously. The number of seismometers used in this spread is usually greater than that used in the spreads described previously.

For dip shooting, the symmetric rather than uni-directional spreads are preferred but sometimes the uni-directional spread must be used for a variety of reasons: such as, inaccessibility and when, due to excessive shot-point disturbances, the seismometer nearest to the shot-point must be located a great distance from that point, too far to solve the problem properly by offsetting the spread laterally. (See "open" spreads, p. 853.)

In correlation shooting, the uni-directional spread is the most efficient when very short spreads are desired (p. 707). Continuous seismic profiling‡ is another frequent application of uni-directional spreads (p. 736). (Velocity shooting (p. 728) is a special application of this type of spread.)

Also, in reflection shooting, spreads are sometimes shot in various combinations under certain circumstances. For example, when using equipment with relatively few traces, such as six, it may be advantageous

† Henry Salvatori, "Apparatus for Seismic Surveying," U. S. Patent 2,117,364, issued Dec. 24, 1936.

‡ L. F. Athy and E. V. McCollum, "Method of Making Geophysical Exploration," U. S. Patent 2,336,053, Dec. 7, 1943.

to place all the seismometers on one side of the shot-point for the first spread and then move to the other side for the second spread—a single equivalent long split spread will effectively be obtained. The reverse of this procedure is sometimes used when a single symmetrical disposition of seismometers at one shot-point serves also for shots from adjacent shot-points, the process being repeated for each disposition of seismometers. Here more than one set of dip data is obtained per seismometer disposition, and both "close" and "open" spreads are supplied. (See following section.)

Relation Between Surface Waves and Spread.—The ground surface waves usually have a velocity of about 1000 ft./sec.* The relative magnitudes of the surface wave velocity and the wave velocities of the deeper beds may be important in that they may govern the choice between "close" and "open" spreads in reflection shooting. In the "close" spread, seismometers are deployed near the shot-point. This spread is used where depth of investigation is sufficient to allow the reflections in question to arrive after cessation of the surface wave. In the "open" spread, seismometers are deployed far from the shot-point so that reflections are received prior to arrival of the surface wave. The consideration of "close" and "open" spreads is required only when the disturbance from the surface wave is prominent enough to require attention.

Field Methods for Improving Detection of Reflections

Multiple Detection

Where difficulty has been encountered in obtaining good reflections, it has become almost a general custom to use several seismometers in series or parallel instead of a single seismometer. This practice is called "multiple detection."† A group of seismometers which are connected in series feeds a single channel of the recording equipment and is represented by one recording trace. Usually there are two distinct advantages in such a

* van den Bouwhuijsen has investigated the velocity of surface waves by placing seismometers in very short spreads between 5 m. and 100 m. from the shot-point. He found that the time-distance curve of these waves is not linear. The slope of the curve at the origin corresponds closely to a velocity of 330 m./sec. The slope then decreases and finally attains a limiting value denoting a constant velocity. The final value of the apparent velocity in many regions is about 500 m./sec. It appears that the velocity at the surface is equal to the velocity of sound in air and that in the near-surface the air in the pore space plays a major part in the determination of the velocity of the longitudinal waves, while with increasing depth and decreasing porosity the bulk of the material which forms the upper layers becomes of greater importance in determining the velocity. In the experiments under discussion, where the top deposits were alluvial quartz sands, a definite break in the time-distance curve was observed, corresponding to a depth of about 10 m. The velocity of the second bed was of the order of 1200 m./sec.

† H. G. Taylor, "Method of Recording Seismic Waves," U. S. Patent 1,799,398, issued April 7, 1931.

method. First, the energy received by the channel is increased considerably. Second, the ratio of useful to extraneous energy recorded by the group generally is increased. The latter condition is realized because vertical waves strike the seismometers on the surface fairly well in phase whereas extraneous energy, such as the surface wave, will in general strike the seismometers in different phases at any given instant; that is, a discrimination is created in favor of vertical waves by a group of seismometers placed on a horizontal plane. Where reflected waves from strongly dipping beds are involved, however, the discriminatory powers of the seismometers may be a disadvantage unless the seismometers in each group are closely spaced or the line of seismometers is oriented in the direction of strike of the reflecting beds. Another disadvantage of multiple detection is that the time of arrival recorded by a channel fed by several seismometers often is not as sharp as that recorded by a single seismometer because, in general, the times of arrival will differ slightly for each seismometer, resulting in a "smoothing-out" of the wave characteristics.

It often has been found true that if records of seismometers placed a short distance apart, 2 feet for example, are appreciably dissimilar, the use of multiple detection is helpful; whereas, if they are similar, benefit is seldom obtained because the separation of the seismometers is relatively unimportant.

Overlapping Seismometer Output

Another proposed aid to the detection of reflections is an artifice known by the various titles: "composite," "inter-locking," "diversity," "overlapping," etc. recording. † In this type of recording, each seismometer output feeds two or more traces of the record in some specified manner. The seismic energy is thus overlapped across more than one trace and a particular seismometer cannot be associated with a given trace alone. The reason for using overlapping may be two-fold. First, for a given total number of seismometers, it permits a greater number of seismometers to operate in series and thereby increases the discrimination in favor of reflected waves (provided that the reflecting beds are not excessively steep). Second, reflections can be followed more readily across a record, because the difference between adjacent traces is less.

The procedure of overlapping is dangerous when carried too far, as will be evident from the following considerations. Spurious energy is usually disclosed by dissimilarities in traces. Hence a diminution of dissimilarities due to overlapping may yield a pattern or "line-up" which is due to spurious energy rather than reflections. Any overlapping at all, in fact, is condemned by some operators for this reason, while others approve its use to a limited and definitely controlled degree.

† Henry Salvatori, "Apparatus for Determining Subsurface Geological Formations," U. S Patent 2,064,385, issued Dec. 15, 1936.

Variable Directional Discrimination

A method utilizing both the discriminating property of multiple detection and an extension of the overlapping principle is involved in some of the instrumental methods of interpretation.† (See page 825.)

Multiple Shot-Points

Beyond a certain maximum charge for a given shot-point the ratio of useful to extraneous response begins to decrease. (Compare p. 849.) Hence if the relative reflected energy of the "maximum" charge is inadequate, more than one shot-point may be utilized, the charges in all shot-holes being fired simultaneously in as far as uniformity in detonation is possible. The effect of multiple shot-points is very much the same as that of multiple seismometers. Besides increased energy, therefore, there is also a discriminating effect which favors waves from an approximately vertical direction.

Considerable experimental work has been done by the author, with quite interesting results, using a multiplicity of small charges, spaced uniformly within a circular pattern, and placed on the surface of the ground. The charges are fired simultaneously. When the diameter of the disc approximates the depth to the bottom of the low-velocity zone, the wave front is sufficiently flat to give good records under a majority of conditions. This procedure is helpful in glacial fill and similar areas.

FIELD OF APPLICATION OF SEISMIC METHODS

Refraction techniques are employed wherever lateral structural studies may be advantageous. They are also used for determining the depths of one or more well-marked shallow boundaries, such as the low velocity layer, the water table, or the gravel beds in placer mining. Refraction profile methods are also useful in studies of soil dynamics designed to determine the suitability of soil for dam and building purposes, highways, etc.; the required thickness of concrete highways; the bearing capacity and depth of upper and lower beds, etc.‡ Fan shooting is most useful for finding shallow structures with quite definite velocity anomalies, for example, shallow salt domes and gravel deposits.

The reflection method has an advantage where depth is a factor, and generally is the only practicable method for depths in excess of about 5,000 feet. The method gives most accurate results when the low velocity layer is uniform and the structures under investigation have uniform and gentle relief. In broad areas where correlation is good, faults can be determined. The reflection method has not proved satisfactory in

† F. Rieber, "A New Reflection System with Controlled Directional Sensitivity," *Geophysics*, Vol. 1, No. 1, Jan. 1936. "Visual Presentation of Elastic Wave Patterns Under Various Structural Conditions," *Geophysics*, Vol. 1, No. 2, July 1936. "Application of the Geo-Sonograph to Petroleum Exploration," *Petroleum Engineer*, Feb. 1937. "Complex Reflection Patterns and their Geologic Sources," *Geophysics*, Vol. 2, No. 2, March, 1937.

‡ Compare R. K. Bernhard, "Geophysical Study of Soil Dynamics," *A.I.M.E. Geophysical Prospecting*, Tech. Pub. No. 834, Feb. 1938.

regions where the upper low velocity layer does not permit effective transmission of energy, where extraneous energy is excessive, and where the subsurface section is too complex to permit of an analysis, such as in severely fractured zones.

With time, as the more likely and readily investigated regions are explored, reflection shooting will be forced into greater refinements. The reflection shooting of the future will require greater depth of penetration, greater accuracy in detecting the low relief structural features previously overlooked, and more effective analysis to interpret data from complex structural and stratigraphic conditions, such as overlaps, stratigraphic traps, etc.

GENERATION OF SEISMIC WAVES

Various methods are utilized in seismic exploration work for initiating elastic waves. The methods may be classified as (1) mechanical and (2) explosive. (Within their depth ranges, essentially similar seismograms are obtained from either source.)

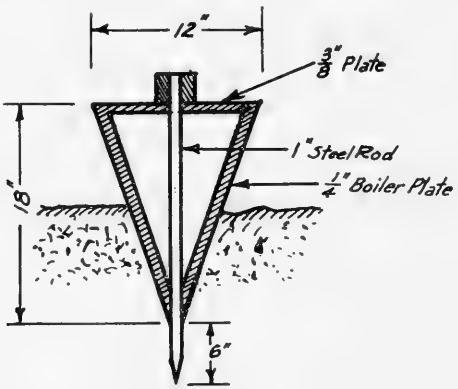

Fig. 534.—Impact stake suitable for shallow seismic investigations.

Generation of Seismic Waves by Mechanical Means.—Mechanical methods are occasionally employed for shallow mining and bedrock investigations, chiefly to avoid the danger and liabilities incident to the use of the more convenient and efficient explosive methods.

Mechanical methods are usually of the impact type, utilizing a heavy weight dropped from a known height or the blow of a heavy sledge. For general bedrock determinations and similar shallow studies, a ten-pound sledge and an impact stake of the type shown in Figure 534 may be employed. The purpose of the large surface of the stake is to provide a means for relatively efficient transmission of energy from the hammer to the soil. In regions where rocks outcrop, the impact stake may be omitted and the blow delivered directly to the surface of the rock.

The time at which the impact occurs is usually obtained by placing a seismometer fairly close to the impact stake. This seismometer is connected to one of the recording galvanometers.

A discussion of seismic experiments utilizing falling weights will be found in the literature.† Also, L. G. Howell, C. H. Kean, and R. R. Thompson have described an electrodynamic ground shaker capable of initiating continuous seismic waves of moderately high frequencies and single frequencies over a range of 20 to 1400 cycles.‡ (The use of an oscillator for generating seismic waves was described by Fessenden as early as 1914.)

Generation of Seismic Waves by Explosives.—Elastic earth waves of sufficient amplitude for deep investigations are initiated by the detonation of a charge of explosive. The characteristics of the waves depend on the properties of the earth formations in the vicinity of the explosive, the degree of confinement of the explosive charge, and the weight and type of explosive. Detailed theoretical studies of the desirable properties of explosives for this and similar purposes have been reported, but only certain factors of practical import for geophysical exploration need be considered here.

Types of Explosives

An explosive is a chemical compound or mixture of chemical compounds (usually in liquid or solid form, or both) which is capable of changing rapidly into simpler chemical compounds, largely of a gaseous nature, which occupy a much greater volume under standard conditions than the original material. This change is accompanied by a great evolution of heat. The useful or destructive effect of explosives is dependent upon the pressure developed by the sudden release of gases at high temperature and pressure, and the work done by these gases on the surrounding media.

Commercial blasting explosives may be grouped into two general classes: namely, high explosives, including dynamite and gelatin dynamites, and low explosives, i.e., explosives of the black powder type.

The explosive decomposition of high explosives is believed to proceed on a wave front along the explosive column at a high velocity, and is known as detonation. Low explosives burn or deflagrate and the decomposition proceeds inwardly from the surfaces of the individual particles. The difference in the observed effects produced by black powder and dynamite is due to the difference in rate of evolution of hot gas upon explosion, this being much less rapid for low explosives than for high explosives. Black powder is little used for seismic prospecting and only the high explosives need be considered here.

The most important types of commercial high explosives are: (1) the

† See, for example, V. G. Gabriel, "Some Experiments in Seismic Prospecting," *Ergänzungs-Hefte für angewandte Geophysik*, Vol. 2, 1931, pp. 122-130.

‡ *Geophysics*, Vol. IV, No. 3, 1939; Vol. V, No. 1, 1940.

straight nitroglycerin dynamites, (2) the ammonia dynamites, and (3) the gelatin dynamites, which may be subdivided as (3-a) ammonia gelatin dynamites and (3-b) semi-gelatin dynamites.†

The straight nitroglycerin dynamites form the standards with which high explosives are compared for strength. They should contain the actual amount of commercial nitroglycerin designated as their percentage strength. In addition to nitroglycerin these explosives contain an "active base" of absorbent carbonaceous material and an oxidizing salt, such as sodium nitrate. The straight nitroglycerin dynamites are extremely sensitive to propagation and find little use except where this property is specifically required, as for example, in ditch blasting by the propagated method.

Ammonia dynamites (also known as "extra dynamites") contain less nitroglycerin, grade for grade, than the straight nitroglycerin dynamites. Ammonium nitrate is substituted for part of the nitroglycerin in amounts sufficient to give them the same strength as the corresponding grades of the straight nitroglycerin dynamites.

Gelatin dynamites are manufactured using a colloidal solution of nitrocellulose in nitroglycerin instead of the nitroglycerin alone. Gelatin dynamites are dense, plastic, and highly water-resistant, and are the principal explosives used in seismic shooting. They are classified into three general types: namely, straight gelatins, in which the nitroglycerin-nitrocellulose colloid is the explosive ingredient, ammonia gelatins in which ammonium nitrate is substituted for part of the colloid, and the semi-gelatins. At the present time ammonia gelatins and semi-gelatins are employed almost universally for industrial blasting in this country, but all three types of gelatin dynamites are used in geophysical prospecting.

For relatively shallow seismic work, the ammonia gelatins and semi-gelatins have been found satisfactory and are recommended because they are usually sold at a lower price than the straight gelatins. While their resistances to water are not as good as that of the straight gelatins, they are still good enough for general use. In addition the ammonia gelatins are capable of being detonated by commercial electric blasting caps under moderately high heads of water. Special grades of 60% ammonia gelatin or 60% semi-gelatin are available for seismograph use and because these grades are usually furnished with features such as extra heavy wrapping, special hardness and toughness, etc., to adapt them for seismic shooting, they are to be recommended instead of the 60% ammonia gelatin ordinarily used in industrial blasting.

For the more severe conditions where explosives must be detonated under very high heads of water or where "sleeper" charges must remain in the ground for a long time, the explosives manufacturers have developed special modifications of the 60% gelatin. These gelatins are especially formulated by the manufacturers so that they will detonate with electric blasting caps under very high hydraulic pressure, even after immersion for considerable periods of time.

In addition to the 60% gelatin grades described, other gelatin grades have found some use in seismic shooting.‡ Modifications of 80% straight gelatin and 100% blasting gelatin have been developed for seismograph work, but their use has been limited. The lower strength gelatins down to

† N. G. Johnson and G. H. Smith, "Explosives for Seismic Prospecting," *Geophysics*, June, 1936, pp. 228-238.

‡ H. E. Nash and J. M. Martin, *Geophysics*, June, 1936.

30% also have been used successfully. However, the 60% straight, ammonia, and semi-gelatin grades seem to be the most popular, and certainly most of the intensive development work has been done on these grades by the manufacturers to make them suitable for seismograph use. Because of this, and because the 60% gelatin grades represent about the maximum explosives value per dollar over the entire range of gelatin strengths available, they are to be recommended for seismic prospecting.

An explosive to be suitable for seismic work should have the following characteristics: high explosive power, effective detonation under pressure, suitable plasticity, rigid packing, high density, and stable physical properties.

It is held by some that the rate of detonation of an explosive is of great importance in seismograph work, but this matter is probably controversial. Little is known of actual rates of detonation developed by charges of gelatin under the conditions of use in seismograph work. The rate of detonation may be a separate factor, but it is probably subordinate to other factors, such as the size, shape, and location of the charge, and the ability of the charge to detonate completely.

Various brands and sizes of seismograph explosives are offered by the different explosives companies, and the representatives of the manufacturers should be consulted before selection of the explosive to be used for an area.†

Electric Blasting Caps

Efficient operations in modern seismic technique require electrically fired blasting caps. Because in most firing systems the electric blasting cap becomes an integral part of the seismograph circuit, it is important that the operator have some understanding of the construction and functioning of an electric blasting cap. The caps offered by different manufacturers may be radically different in the details of their construction; however, the following general description is illustrative of the principles employed in all electric blasting caps.‡

Essentially, an electric blasting cap consists of a waterproof metal shell containing a charge of explosive material and a means of detonating this material by an electric current. The caps are equipped with insulated leg wires of various lengths. The explosive charge in the cap usually consists of a "base charge" of a highly efficient detonating material and one or more other explosive components referred to collectively as the "priming charge." A fine resistance wire, known as a "bridge wire," is in intimate contact with the priming charge and this wire is in circuit with the two insulated leg wires.

† W. R. Farren and H. H. White, "Recent Developments in Explosives for Seismic Prospecting," *Geophysics*, Mar. 1937, pp. 114-119.

‡ G. F. Rolland and H. H. White, "Developments of Essential Characteristics in Electric Blasting Caps for Seismic Prospecting," *Geophysics*, March, 1937, pp. 119-126.
F. R. Seavey, "Explosives," U. S. Patent 2,415,045, Jan. 28, 1947.
L. A. Burrows, "Blasting Cap," U. S. Patent 2,427,899, Sept. 23, 1947.
E. K. Lefren, "Electric Blasting Cap," U. S. Patent 2,428,884, Oct. 14, 1947.
D. D. Huyett, "Electric Explosion Initiator," U. S. Patent 2,431,871, Dec. 2, 1947.

Figure 535 illustrates one of the most common types of construction employed in electric blasting caps.

Whereas electric blasting caps are commonly referred to as "instantaneous" caps, this term is inaccurate because the caps require measurable intervals of time for their operation. In industrial blasting this is of little or no interest to the consumer, but in seismic work even the very short time intervals involved become important.

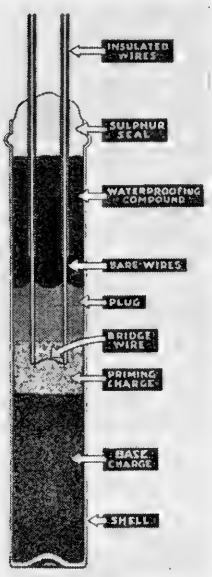

FIG. 535.—Section showing the construction of a typical electric blasting cap.

When an electric current is caused to flow in the circuit of an electric blasting cap, heat is generated by conduction losses (I^2R losses) in the bridge wire. This heat is conducted or radiated to the priming charge. If a very low current is applied, the heat generated may be insufficient to raise the temperature of the priming charge sufficiently to initiate its decomposition. A current of 0.3 amperes usually is the minimum that will detonate a commercial cap. When sufficient current is passed through the bridge wire, it raises the temperature of the priming charge and starts decomposition. The decomposition of the priming charge progresses from "burning" to "detonation" very rapidly and detonates the base charge, which in turn detonates the dynamite.

The time elapsing between the application of an electric current to the cap and the explosion depends in part on the type of cap used, but chiefly upon the magnitude of current. Figure 536 illustrates the firing characteristics of two general types of electric blasting caps and shows the relationship between current and time of detonation.

The time elapsing between the detonation of an electric blasting cap and the initiation of detonation in the charge of dynamite or gelatin is extremely short, and because it is far below the limits of accuracy of seismograph records, it may be neglected. For all practical purposes, the time of detonation of the cap may be accepted as the time of the explosion of the dynamite charge. In early seismic work the time-break was obtained from the breakage of a wire wrapped either around the dynamite charge or around a second cap connected in series with the cap used to detonate the charge. These methods have been largely supplanted by the single cap method, in which the time-break is determined from the interruption of the firing current occasioned by the breaking of the bridge wire circuit when the explosion occurs.† This method of determining the

† G. H. Loving and G. H. Smith, "Explosives and Electric Blasting Caps for Geophysical Prospecting," *Journal S.P.G.*, Vol. 6, 1935, pp. 1-27.
H. R. Prescott and F. L. Searcy, "Method of Making Geophysical Explorations," U. S. Patent 2,046,843, issued July 7, 1936.

time-break is satisfactory provided the interruption of the firing current and the detonation of the cap are simultaneous. This is not always true, however, of all caps. In general, two types of electric blasting caps are offered by explosives manufacturers for seismograph use. One is the type of cap used in industrial blasting. Typical firing characteristics of this "regular" type of firing cap are illustrated in Figure 536 by curves No. 1 and No. 1-A. For current values of about two amperes or less, the rupture of the bridge wire is simultaneous with the detonation of the cap. Above this current value, however, the interruption of the bridge wire

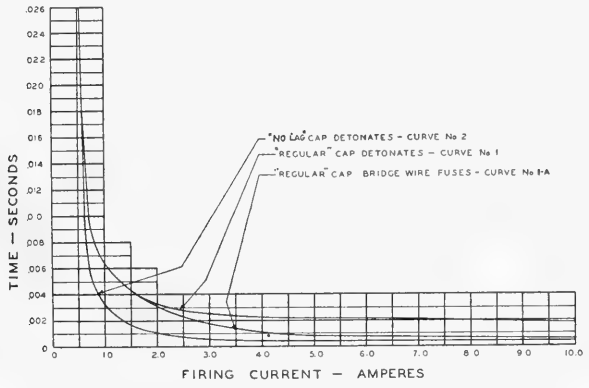

Fig. 536.—Curves showing firing characteristics of the typical "Regular" electric blasting caps (industrial type) and special "No-Lag" seismograph caps.

circuit precedes the detonation of the cap by a time interval dependent on the firing current employed. These "regular" electric blasting caps are widely used for seismograph work and are found entirely satisfactory where low firing currents are used or where firing conditions are such that a correction can be made for the time lag between the breaking of the bridge wire and the detonation of the cap.

There are circuits, however, in which these conditions cannot be maintained, and some explosives manufacturers furnish caps in which the interruption of the cap current is practically simultaneous with the explosion of the cap regardless of the firing current used. In these caps the bridge wire does not fuse and is therefore not ruptured until the cap explodes. In general, the "no-lag" caps fire more rapidly at any current than do the "regular" caps. Typical firing characteristics of these special seismograph caps are illustrated in Figure 536, curve No. 2.

Electric blasting caps are usually furnished in two strengths: the No. 6 and No. 8 grades. When fulminate of mercury was the universally used detonating material these strengths were well defined, the No. 6 caps

containing one gram of detonating material and the No. 8 caps containing two grams. At the present time, however, the different manufacturers use a wide variety of cap compositions. Nearly all of the No. 6 caps now offered are materially higher in detonating efficiency than the original No. 6 fulminate cap. No. 6 caps constitute a great majority of the caps used for seismograph shooting and are amply strong for most work. The present-day No. 8 caps are more efficient than the fulminate No. 8 caps and offer an additional margin of safety where seismograph shooting is carried out in deep holes. In addition to the regular No. 6 and No. 8 electric blasting caps in both standard and waterproof construction, there are available special electric blasting caps which offer both an increased waterproofing characteristic and a strength greatly exceeding No. 8 caps in detonating efficiency. Such caps have been found advantageous under extremely severe shooting conditions. Some of these caps embody the "no-lag" feature.

Important properties of electric blasting caps may be summarized as follows: no time lag between rupture of firing circuit and detonation of cap; sufficient detonating strength to initiate the explosion under the conditions of use; and the various physical characteristics, such as waterproofing, efficient protective shunting and a method of packaging such that the wires can be "strung out" without excessive kinking or inconvenience. The electric blasting caps offered by the various manufacturers are furnished under various brand names and come in a variety of wire lengths. The manufacturers' representatives should be consulted for further particulars on any given brand. Handle caps with caution. Never attempt to open a cap; forcing the wires or rough handling may cause it to explode.

Primacord detonating fuse consists of an explosive core contained within a waterproof textile covering. Relatively insensitive to flame, shock, friction, and impact, it must be detonated by a blasting cap. It will not deteriorate within reasonable time periods. Its explosive wave travels at approximately 20,350 feet per second.

Primacord is used in seismic work chiefly to eliminate high voltage hazards when shooting near power lines. The blasting cap should be attached to the Primacord by means of a special union made for this purpose. The charge is made up by running the Primacord through the explosive cartridge or cartridges and tying a knot at the bottom in order that the Primacord cannot pull back through the charge, or by lacing the Primacord through the charge.

The essential factors governing the assembly of a charge with Primacord are as follows. The end of the Primacord should be cut square; this end must be dry, and must have the "business" end of the blasting cap seated firmly against it. The Primacord should be in contact with the

explosive and must be securely fastened in the charge, particularly when it is used to lower the charge in the shot hole. The joint between the Primacord and the blasting cap should be about 20 feet down the shot hole.

Electric Firing. — The electric firing current may be supplied to the caps either by battery or by blasting machine. Unless a specially-constructed "blaster" is used, a blasting machine is considered relatively safer because certain definite movements are necessary to generate the current required for the firing circuit. With batteries, current can be conducted to the firing circuit simply by making contact between this circuit and the battery terminals. However "blasters" are designed with safety switches, practically eliminating the objections to the use of batteries.

The following general rules should be observed: Leads should not be attached to blaster until ready for firing. Immediately after firing, leads should be disconnected from blaster, shorted, and stretched out on the ground. Blasters should be handled by the shooter only.

Loading Procedure.—The charge is usually covered with water or mud to a depth of from 10 to 100 feet or more in order to couple the energy of the explosion to the earth in an effective manner. When shooting in an air-filled hole a large percentage of the acoustic energy is wasted in the high velocity gases which issue from the hole upon detonation. The presence of the water tends to effect a more favorable acoustic impedance match between the explosive and the earth.†

Few general rules can be given concerning the best depth for the shot in seismic prospecting. Normally, the shot should be deep enough to avoid surface cracking. Likewise, it generally should be below the low velocity layer.‡ (Compare p. 849.) In a particular area it may be found that best results are obtained when the shot is fired within the same stratum at all shot-holes—which stratum this is can only be determined by experiment. For the sake of accuracy in computing, it may be preferred to keep the bottoms of the holes at as nearly constant an elevation above sea level as field operating conditions will permit.

Various methods are used for placing the electric blasting caps in the cartridges of explosive. The cap may be inserted in a hole punched with a wooden or bronze punch, either in the end or obliquely in the side of the cartridge. The cap should be well seated at the bottom of the hole, which should not be punched to a greater diameter than is necessary to clear the cap. The explosive should be molded by hand over and around the cap. This aids in making a good mechanical assembly and also retards

† D. H. Clewell and R. F. Simon, *Geophysics* (to be published).
‡ J. L. Bisch, "Means for Positioning Explosives in Bore Hole," U. S. Patent 2,433,543, Oct. 30, 1947.

the access of water to the explosive immediately surrounding the cap. Occasionally, it is desirable to use tape for the further protection of the cartridge at this point.

Where more than one cartridge is to be loaded into a shot-hole, it is desirable to assemble the several cartridges into a unit to facilitate handling and loading. Some of the explosive companies have developed and incorporated in their products special screw-thread or quick-locking ends for

FIG. 537.—Screw thread cartridges for assembly into a single stick of explosive. (A), cartridge; (B), screw thread.

assembling cartridges. These generally offer a quick and simple means of assembling a coupled column of explosives.† Figure 537 shows one type of screw-thread cartridge.

The cap wires should be secured to the charge in a manner that will prevent strain at the point where the wires enter the cap. The assembly also should be such as to prevent strain or pull on the cap wires where they enter the cartridge. The wires may be looped or hitched around the cartridge, sharp bends or kinks being avoided. (Figure 538.) In shallow

† W. F. Smith, "Connecting Means for Explosive Cartridges," U. S. Patent 2,429,079, Oct. 14, 1947.

L. B. Counterman, "Explosive Cartridge Unit," U. S. Patent 2,425,176, Aug. 5, 1947.

clear holes the charge is lowered by the cap wires and care is taken to avoid damaging the wires during loading. After loading into a dry hole, it is desirable to confine the charge by filling the hole with water to a level well above the top of the charge. Figure 539 shows an approved procedure for loading shot-holes.

FIG. 538.—Method of assembly to prevent strain on cap wires. A, cartridge of explosives; B, cap wires; C, half hitch loop to take strain.

Safety Practices in Loading Procedure.*—Charges should not be made up prior to loading in the shot hole.

Caps must not be removed from the magazine until the charge has been made up and is ready for lowering. The shooter should then take the cap, attach it to the charge, and immediately lower the charge to the predetermined depth in the hole. The leads should then be taken to the blasting box. When personnel and equipment are safely located, the leads may be attached. The shooter should give three safety checks to the operator before firing, and must not fire until authority is received from the operator.

Magazine doors should be closed at all times except when removing explosives.

---

*The author is indebted to A. G. Munro, Aetna Life Insurance Company, Los Angeles, Calif., for many suggestions regarding safety practices.

Loading Poles.—A spear pole often is employed for placing the charge at the bottom of a hole filled with drilling mud or water.† The procedure is illustrated in Figure 540. The charge is held on to the spear by keeping the wires under tension. The poles are usually 15 feet in length and are provided with link couplings to give the required depth of place-

FIG. 539.—Approved procedure for loading shot holes. A, explosive; B, cap wires; C, loading poles; D, hose for filling hole with water; E, shooting truck with water tank; F, radio antenna. (Courtesy of Standard Oil of New Jersey.)

ment. When the charge has been pushed to the bottom of the hole the tension on the wires is released. A jerk on the pole then frees the spear and leaves the charge in place. Figure 541 shows a form of locking link for connecting the lengths of pole together.

When loading charges into holes which are two hundred feet or more in depth or where caving and "sluffing" of the wall are common, a weighted brass "spoon" is operated by a steel cable and winch. (Figure 542.) The charge is held in the spoon by two or three loose loops of wire which will allow it to slide off easily when the tension is released on the firing wires. The tubing above the spoon is filled with lead and the total weight is from 400 to 500 pounds. Using this method of loading, a charge may be pushed

† O. W. Lundblad, "Lowering Device," U. S. Patent 2,420,182, May 6, 1947.

FIG. 540. — Method of loading explosives in a medium depth hole for seismic work. *a*, explosive cartridge; *b*, firing wires; *c*, spear or "schnozzle"; *d*, loading pole; *e*, extensions with link couplings. (Courtesy of United Geophysical Company.)

through "bridges" of material. The time required for loading deep holes is greatly decreased over that required for loading by use of hand poles.

Another method of loading deep holes uses a device similar to the "spoon," except that the charge is pushed to the desired depth by a weight. However, experience has shown that it is easier to pull the charge down than to push it. To accomplish this, a heavy wire is securely attached to the explosive column and bent into a hook at the bottom of the column. This hook is inserted into a recess in the weight. Thus the force is applied at the bottom of the column, and as the weight is lowered into the hole the explosive charge is pulled to the desired depth. When the weight is raised the charge is left behind.

The character of the record is influenced by the depth and size of shot. Each area behaves somewhat differently and the sound of the explosion frequently is indicative of the shot characteristics. Generally, a muffled or dull

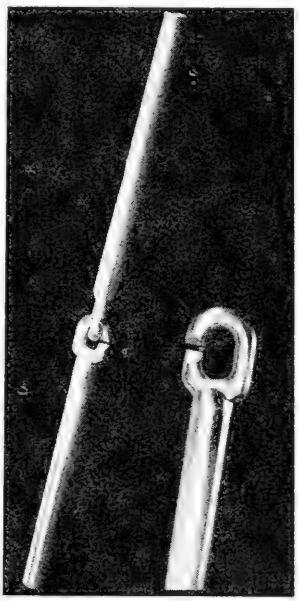

FIG. 541. — Aluminum link-connectors for loading-poles. (Courtesy of Century Geophysical Company.)

explosion sound indicates poor energy transmission and the generation of low frequency waves. An explosion which has a sharp crack or snap usually produces a record of higher frequency waves and is the most efficient for energy transmission. Few general rules can be given for the size and placement of the charge. All this must be worked out empirically for each area and sometimes even for each hole.

FIG. 542.—Loading deep seismic holes by use of weighted winch lines. *a*, explosive cartridge; *b*, weighted tube; *c*, winch; *d*, hand control on winch. (Courtesy of United Geophysical Company.)

The shooting truck often is equipped with a water tank of about 500 gallons capacity, dynamite box, cap box, shooting poles and rack, a water pump, and also a power winch for loading deep holes. Figure 543 shows a truck of this type, and the shot-point geyser following a shot.

This picture illustrates the violation of three safety rules. (1) The magazine doors should be opened only during the short period of time required to remove the necessary explosive for loading the hole. They should not be open during the shooting operation. (2) The explosives should be at least 100 feet from the shot-hole. The truck should be removed to a safe distance. (3) Empty dynamite boxes should not be left on the ground.

Figure 544 shows a powder magazine trailer and cap magazine. The trailer will hold 3,000 pounds of dynamite and the magazine 500 caps. The

inside surfaces of both the trailer and the magazine are lagged with a double thickness of one-inch oak, the grain of the wood in each layer being laid at right angles. Spuds are provided at all four corners of the trailer;

FIG. 543.—Shooting truck and shot-point geyser. *a*, water tank; *b*, explosive compartments.

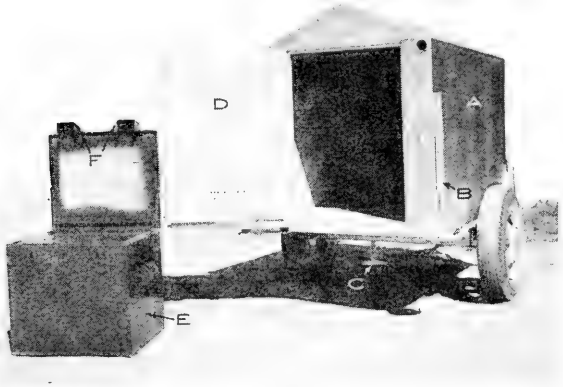

FIG. 544. — Powder magazine trailer and cap magazine. A, trailer; B, spuds, retracted; C, spud, in position; D, double oak planking; E, cap magazine; F, lock shield. (Courtesy of Griffin Tank and Welding Service.)

they are retracted when the trailer is being handled. A hole in the bottom of the magazine allows it to be bolted or anchored to prevent theft. Heavy sheet-iron shields are placed over the padlocks to protect the locks from tampering.

Some states prohibit the hauling of explosives in trailers. Local regulations should be checked carefully before transporting explosives.

Safe Use of Explosives

Improper or careless handling of explosives is the direct cause of a great majority of the accidents which have occurred in seismic service. Because of the wide range of activities and the various types of equipment and material handled, the geophysical industry must be prepared to cope with practically every type of hazard.†

Hanahan‡ calls attention to these precautions in handling and use of explosives:

The safe shooting of a hole involves the proper selection of its location. The surveyor should consider the proximity of the hole to public highways, buildings, radio transmitters and above all to power lines.

The condition of the explosive must be considered for safe and efficient handling.

Care must be taken to guard against premature explosions due to stray or static electricity, or to stray electric current when aluminum poles are used in cased holes. For this reason wooden loading poles are preferred by many operators.

Usually there will be found in each case of dynamite an instruction folder containing a list of "Don'ts" or safety rules. Each carton of electric blasting caps also contains a similar folder applying to caps. Every crew member having occasion to handle dynamite or caps or to be near the shot-hole or firing circuit should be required to familiarize himself with these safety rules and to re-read them at frequent intervals. These rules have been set up as the result of exhaustive studies of accidents from explosives, and their strict and literal observance is recommended. One of the most important precautions is to maintain a large separation in distance between the caps and dynamite, except for the single charge being prepared.

Wherever possible, wooden tools should be used. When metal parts are necessary for mechanical strength, bronze or other non-sparking metal must be used. Steel and iron should never be used, both because they can strike sparks and because they introduce a greater hazard from impact and friction than do the other materials mentioned.

There are on the market several explosives of a type differing radically from the usual varieties of commercial explosives. For some of these explosives, claim is made that they are much less sensitive to flame, impact, and friction than are dynamite and gelatin, and that these properties contribute to the safety of shooting operations where they are used. It must

† P. M. Hanahan, "Explosive Accidents on Geophysical Crews," *Geophysics*, Vol. 13, No. 3, July, 1948.
G. M. Kintz, "Informal discussion of explosive hazards on seismograph crews," *Geophysics*, Vol. 11, 1946.
‡ P. M. Hanahan, *ibid*, p. 421-426.

be borne in mind, however, that these products are designed to explode, and that under suitable circumstances they will do so.

Numerous protective devices for use in blasting have been developed recently, to be employed as part of the circuit, blasting caps, igniters, or primers.†

The following rules have been found helpful in minimizing accidents:

Trucks shall not carry more explosives than can be accommodated in the magazines. Portable magazines are available and should be utilized wherever permanent storage facilities cannot be provided. Not over three persons shall ride in the explosives-carrying truck.

Charges should not be made up prior to loading in shot hole.

Caps and dynamite shall remain in magazines until ready for use. Old dynamite should be used first. (It may be necessary to re-stow the magazine when receiving delivery.) Dynamite should not be exposed to direct rays of the sun for any long period. A complete and accurate inventory should be maintained of explosives used and on hand.

Personnel and equipment should maintain a minimum distance of 100′ from the shot hole while firing. Charges must not be prepared by other than a competent shooter.

The firing line should not be longer than ½ the distance from the shot-hole to a high tension power line. Extreme caution must be used in firing blast phone shots.

More than one charge should never be made up at any one time. Never have more than *one* firing line in use.

After firing, firing leads shall be immediately removed from blasting machine, shorted, and stretched out on ground. Firing lines or sleeper charges should be shorted and completely concealed, to prevent inquisitive persons from finding the leads and conducting experiments. Method of concealing firing line is illustrated in Figure 545.

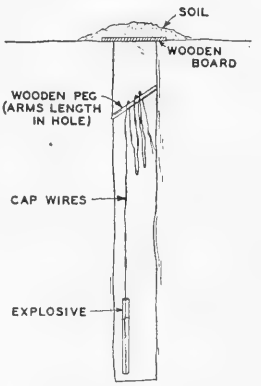

Fig. 545.—Safe practice in loading.

Misfire or delayed detonation should be given very careful consideration. One hour should elapse before the hole is reloaded. Never remove a misfire from the shot hole.

No smoking must be allowed when handling explosives.

No relaxation therefore should be permitted in the safety precautions while explosives are being used.

Carelessness seems not to be due primarily to failure on the part of the man responsible to appreciate the hazards involved, but rather to be an

† J. V. Hammond and D. J. Keenan, "Blasting Unit and Short-Circuiting Device," U. S. Patent 2,407,605, Sept. 10, 1946.
H. J. Rolfes, "Means for Safeguarding Electric Igniters of Blasting Detonators Against Accidental Firing," U. S. Patent 2,408,124, Sept. 24, 1946.
H. B. Humphrey, "Safety Primer for Blasting," U. S. Patent 2,425,741, Aug. 19, 1947.
B. L. Lubelsky and R. E. Hartline, "Protective Device for Blasting Circuits," U. S. Patent 2,428,334, Sept. 30, 1947.

example of the old adage "familiarity breeds contempt." Constant vigilance is necessary on the part of those in charge to maintain proper control of storage, transportation, and field operations where explosives are used.

DRILLING EQUIPMENT FOR SEISMIC OPERATIONS

Types of Drills.—Drills for seismograph shot holes are of two general types: (1) the rotary drill and (2) the churn drill.

The rotary drill has the cutting bit attached to the lower end of a string of hollow drill pipe. This pipe is rotated and simultaneously forced or fed downward by the drill, thus imparting rotation and pressure to the cutting bit. Water or mud fluid is pumped down through the pipe to wash the cuttings up out of the hole. The rotary drill is used almost universally for all classes of seismograph shot hole drilling.

The churn drill, on the other hand, uses a reciprocating chopping bit, which the drill repeatedly picks up and drops with a soft* rope. At frequent intervals the cuttings produced by the bit are cleaned out of the hole with a bailer. The churn drill is rarely used, and then only in some areas where large underground cavities tend to hamper the return flow of the circulating fluid used in rotary methods. Because of its relative unimportance in seismic work, no further exposition of the churn drill is given.

Rotary Drills

There are two general types of rotary drills used in seismograph work, one having hydraulic feed and the other mechanical feed. Their difference is in the method employed for applying the downward pressure, or feed, to the hollow drill pipe. Both types provide a means for rotating the pipe, and both make provision for circulating fluid down through the pipe or drill rods, thus washing the cuttings away from the bit and conveying them up to the surface in the annular space between the wall of the hole and the string of drill rods.

Hydraulic Feed Type Drill

The hydraulic-feed portable drilling unit for seismic shot-hole drilling is a modification of the standard diamond core drill used for mineral exploration and engineering test boring. Figure 546 shows the general arrangement of a portable hydraulic-feed seismograph drill. The truck engine is the source of power for driving the rotary mechanism, the hydraulic feed, the hoist or draw works, and the mud pump. A split-shaft type of power take-off is installed in the motor truck directly behind the truck transmission. This power take-off provides a means for disconnecting the drive to the rear truck wheels and utilizing all of the power from the truck engine for driving the drill machine. The essential components of

* Hemp or manila, with considerable stretch or spring which imparts the snap or impact to the bit at the bottom of the stroke.

the drill assembly are indicated in Figure 546. Figure 547 is a photograph of the same drill.

The mechanism for imparting the rotation and the feed to the drill pipe is illustrated in Figure 548. The drive rod (L) is a steel tube through which the drill pipe (Q) passes. The outside of this drive rod is either fluted or hexagonal in cross section so that it is free to travel vertically through the drive rod bushing (M) at the same time that it is being rotated by this bushing. The rotation of the drive rod bushing is derived from the beveled gearing indicated at (N). The drill pipe is attached to the drive rod by means of the chuck (A). The chuck is usually located at the bottom of the drive rod, as indicated; but on some drill assemblies the

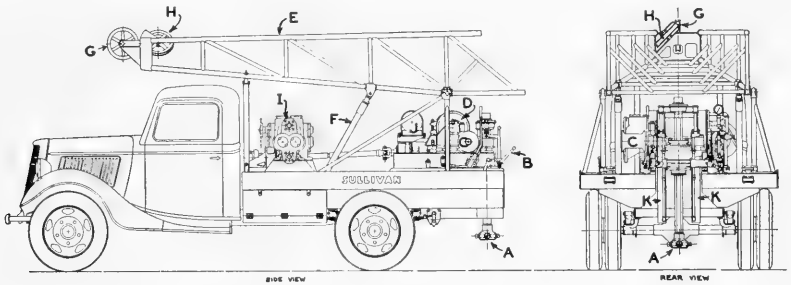

FIG. 546.—General arrangement of a portable hydraulic-feed seismograph drill. (Courtesy of Joy Manufacturing Company.)

A. Drill chuck
B. Operating controls
C. Cat head
D. Hoisting drum
E. Mast
F. Hydraulic mast raising cylinders
G. Sheave for hoisting rope
H. Sheave for cat line
I. Mud pump
J. Hydraulic oil tank
K. Hydraulic feed cylinders

chuck is at the top of the drive rod instead of at the bottom. The drill pipe is attached to or released from the drive rod by tightening or loosening the set screws (O).

On some drill assemblies the hand-operated set screw type chuck is replaced by a semi-automatic or fully automatic chuck, mounted on the top of the drive rod and operated either hydraulically or mechanically. This type of chuck permits chucking or unchucking the drill pipe without stopping its rotation and thus saves some time and labor.

The drive rod is fed downward, thus applying pressure on the bit at the bottom of the string of pipe by means of two hydraulic rams (K) which are attached to the drive rod by the yoke (P). The length of travel of this hydraulic feed is usually 30″. After each 30″ advance, the set screws in the chuck are loosened, the hydraulic feed reversed to raise the chuck to its top position, the set screws are again tightened, and the process is repeated.

The entire hydraulic system operates on a closed circuit using a light hydraulic oil as the fluid, and it is completely independent of the mud pump circuit. The system includes the hydraulic pump (usually a vane type

pump), the oil storage tank, the pressure release valves, and the control valves for operating the various hydraulic features of the drill. To feed the rods downward the oil under pressure is introduced at the top of the two

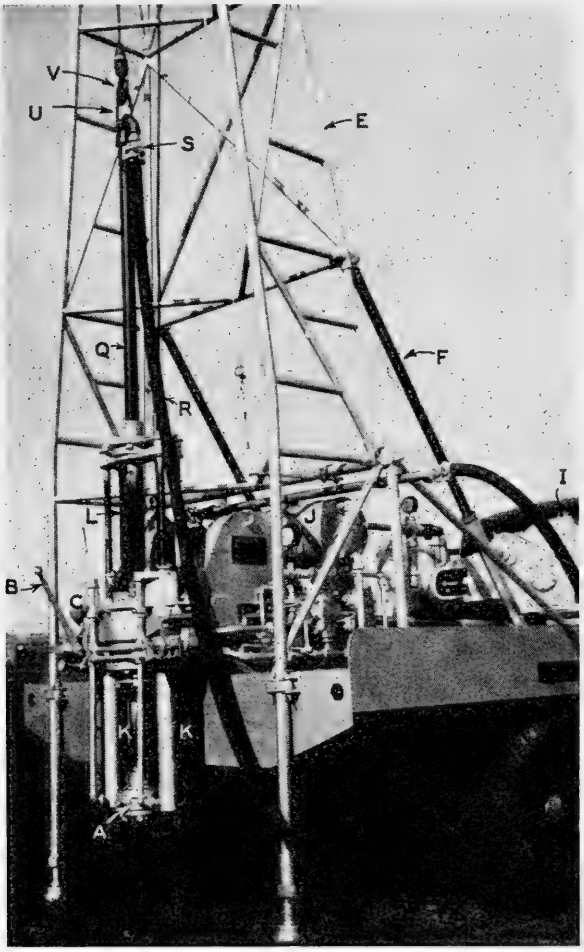

FIG. 547.—Hydraulic feed type drill, (A) drill chuck; (B) operating controls; (C) cat head; (E) mast; (F) hydraulic mast raising cylinders; (I) mud pump; (J) hydraulic oil tank; (K) hydraulic feed cylinder; (L) drive rod; (Q) drill pipe; (R) swivel hose; (S) water swivel; (U) hoisting bail; (V) safety hook. (Courtesy of Joy Manufacturing Company.)

feed cylinders (K), the drive rod (L) is fed downward, and the oil in the bottom of the cylinders below the pistons (T) flows back to the hydraulic oil storage tank (J) at atmospheric pressure. When the process is reversed, the tops of the cylinders are vented to the oil tank, the oil under pressure

introduced below the pistons, and the feed of the drive rod is upward. The upward and downward feed or travel of the drive rod does not interfere with and is entirely independent of its rotation.

Where the ground to be drilled is comparatively soft and little pressure on the bit is required to secure a satisfactory rate of penetration, a Kelly or grief stem can be used to impart rotation to the drill rod. This is a hollow

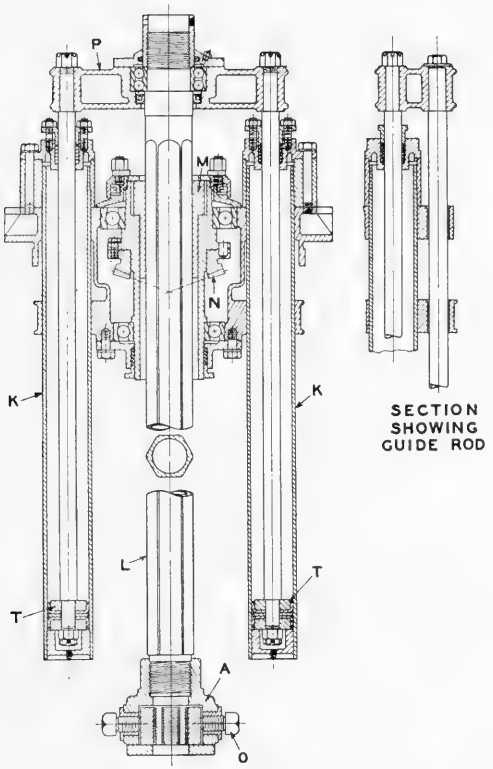

FIG. 548.—Mechanism for imparting rotation and feed to drill pipe of hydraulic feed type drill; (A) drill chuck; (K) hydraulic feed cylinders; (L) drive rod; (M) drive rod bushing; (N) beveled gearing; (O) set screw; (P) yoke.

steel rod approximately 14 feet long, the outside of which is either square or round with external splines extending its entire length (Figure 549-N). It is screwed to the top of the drill pipe and passes through a Kelly drive bushing attached to the top of the drive rod on the drill. The drive bushing fits the square sides of a square Kelly or the splines in a splined Kelly, and its rotation rotates the Kelly but at the same time permits it to slide downward as the hole is advanced.* In soft drilling, the weight of the Kelly and

* Use caution when working in the vicinity of the rotating Kelly to prevent loose clothing from being caught.

the rods is sufficient to provide the necessary pressure on the bit. If hard ground conditions are encountered, the drive rod can also be equipped with a chuck in addition to the drive bushing so that hydraulic pressure can be applied to the Kelly if needed.

Figure 547 shows the mast or derrick raised to its vertical position after the drill has arrived at the location for the hole. The Kelly or the drill pipe (Q) is in position in the drive rod (L) and is connected to the swivel hose (R) by means of the water swivel (S). The water swivel (Figure 549-K) is a hollow packed joint that provides the connection between the swivel hose, which does not rotate, and the Kelly or drill pipe, which does rotate. The swivel is equipped with a bail (U) for hoisting or lowering the drill pipe with the hoisting drum or draw works. The wire rope from the hoisting drum passes over the sheave wheel mounted in the top of the mast and is attached to the bail of the water swivel or the bail in the hoisting plug by means of a safety hook (V). After each 10-foot advance in the depth of the hole the water swivel is disconnected, and a new 10-foot piece of pipe is picked up with the hoisting plug (Figure 549-L) and screwed in place.* The hoisting plug is then removed and the water swivel again attached to the top of the new rod. When disconnecting or connecting the rods or Kelly, the string of rods remaining in the hole is suspended either from the drill chuck (A) or from a safety clamp set on the ground (Figure 549-M). Do not allow the tools to rest on bottom for more than a few minutes, without being rotated to circulate the mud; the tools may become stuck, because the rock cuttings settle fast when the mud is not circulating.

The mast or derrick is usually about 25 feet high, which allows sufficient height above the top of the drive rod for a 10-foot section of drill rod or the 14-foot Kelly plus the length of the water swivel, the length of the safety hook, and an additional two or three feet for spudding or reciprocating the rod string. At the top of the mast is mounted the sheave wheel (G, Figure 551) for guiding the wire line from the hoist. This sheave wheel is placed so that the pull in the hoisting rope will be directly in line with the center of the hole being drilled. If the drill is equipped with a cathead (*C*, Figure 547), a second sheave wheel is mounted in the top of the mast for guiding the soft line (manila rope). The cathead is frequently used for picking up each new rod, as it is added to the rod string, rather than using the hoisting line for this purpose.

The mud pump (*I*, Figure 547) is usually a two-cylinder, double acting, reciprocating-type pump with 4″-diameter pistons and a 5″ stroke. It is equipped with abrasion-resistant valves, valve seats, cylinder liners and piston rods. The suction hose connected to the pump intake has a check or foot valve on the other end. This foot valve is submerged in the mud sump or pit, which may be merely a shallow hole or trench dug in the ground adjacent to the hole being drilled. However, better practice is to use a "two-

* Pipe wrenches are not recommended for "break-out" purposes. Use the special wrenches provided, to minimize chances of personal injury.

YELLOW STRIPE "N" ROD

FISH TAIL BITS—HARD METAL FACED

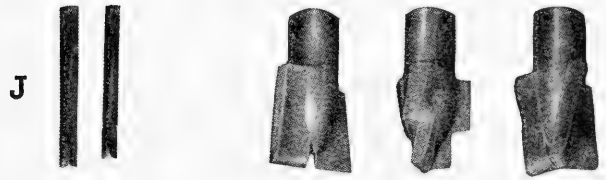

Forged Fish Tail Bits—
Hard Metal Faced

2 Wing 6 Wing Pilot 3 Wing
Cast Steel Fish Tail Bits—Hard Metal Faced

GRIEF STEMS OR KELLYS

SAFETY CLAMP

WATER SWIVEL

HOISTING PLUG

FIG. 549.

hole" sump, which may be made by positioning a screen or board in a mud ditch, to allow the cuttings to settle out. This procedure will minimize the abrasive materials carried into the pump intake. Figure 550 illustrates the general arrangement.

The mud fluid is pumped from the pit up through the suction hose and discharged into the swivel hose, and then passes through the water swivel, down through the rod string, and out through the drill bit. This fluid washes the cuttings away from the bit in the bottom of the hole and carries them in suspension to the surface, where the mud flows back to the pit through a

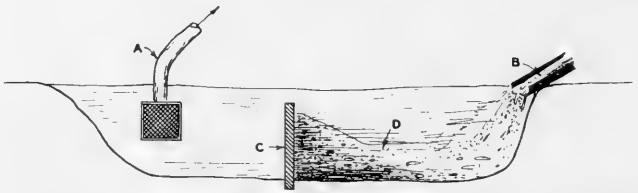

FIG. 550.—Preferred arrangement for mud pit. A, suction hose, pump intake; B, mud wash coming out of hole; C, baffle board; D, rock cuttings and sludge, to be shoveled out as required.

small trench (Figure 550). The cuttings settle in the trench or the sump and are shoveled out intermittently as they accumulate. Sometimes a heavy mud fluid or aquagell is circulated to maintain the walls of the drill hole when drilling through caving materials, thus avoiding the necessity of casing the hole.

Mechanical Feed Type Drills

In the mechanical feed or chain pull-down rotary drill, the downward pressure or feed on the drill rods or Kelly is accomplished by means of power-driven chains instead of with the hydraulic rams. Figure 551 shows the general arrangement and Figure 552 some of the details of the chain pull-down or mechanically-fed drill. The Kelly (A) is rotated by means of a small rotary table (B) which corresponds to the drive rod in the hydraulic-type drill. The two long feed chains (C) are driven by sprockets (D) mounted on either side of this rotary table. One end of each pull-down chain is attached to a combination yoke and swivel (E) at the top of the Kelly, and the other end of each chain is attached to a wire rope (F) that passes up over a guide sheave (G) at the top of the mast and back down to the top of the same combination yoke and swivel, so that each length of feed chain with its guide cable forms a complete endless loop. When the clutch driving the feed chain sprockets is released, the combination swivel and yoke can be raised or lowered with the hoist or draw works with the wire line (H) attached to the bail (I) on the swivel, as indicated in Figure 551.

Figure 552 shows the mud fluid coming up out of the hole and flowing through the trench to the sump located just to the left of the picture.

Both the hydraulic feed and the mechanical pull-down type of drill are equipped with multiple-speed transmissions and clutches. The transmissions provide different speeds for the rotation of the drill rods, for the speed of the mud pump, for the rate of the feed, and for the speed of the hoisting drum. The clutches permit the connecting or disconnecting of each of these drives.

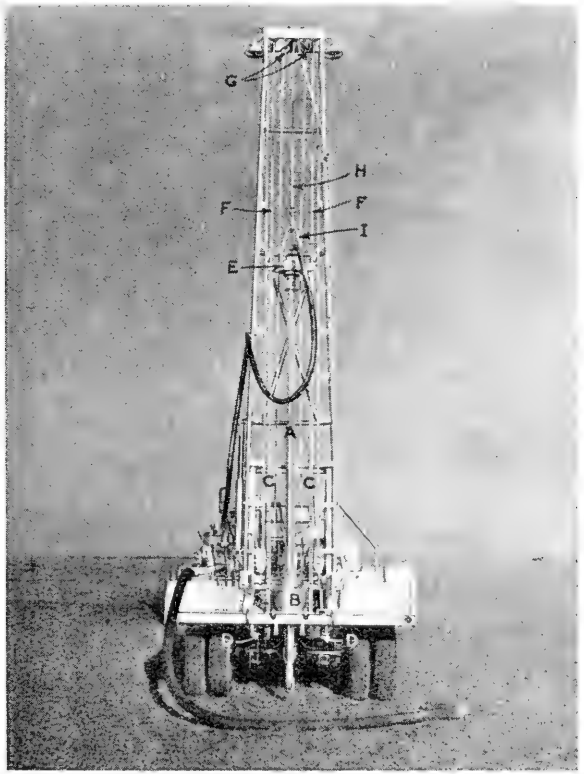

FIG. 551.—Mechanical feed type drill. (A) drive rod or Kelly; (B) rotary table; (C) feed chains; (D) sprockets; (E) combination yoke and swivel; (F) wire rope; (G) guide sheave; (H) wire line; (I) swivel bail. (Courtesy of Mayhew Machine Company.)

All drills make provision for setting casing where this is necessary. On the hydraulic feed type machine the entire drive-rod assembly is retracted forward from the hole on slide rails far enough to provide ample room for setting or recovering casing. On the mechanical feed drill the opening through the rotary table is usually large enough to set casing through the table.

Drill Rods and Bits.—The hollow drill rods or drill pipe ordinarily used for seismograph drilling are the size "N" (2⅜" outside diameter) external flush rods in exact 10-foot lengths. (Figure 549-I.)†

Numerous types of bits are used in seismograph drilling, depending upon the hardness of the ground being penetrated and the diameter of the hole. The most common type of bit is the ordinary fish tail or drag bit (Figure 549-J). These drag bits are available with either two, three, four or six

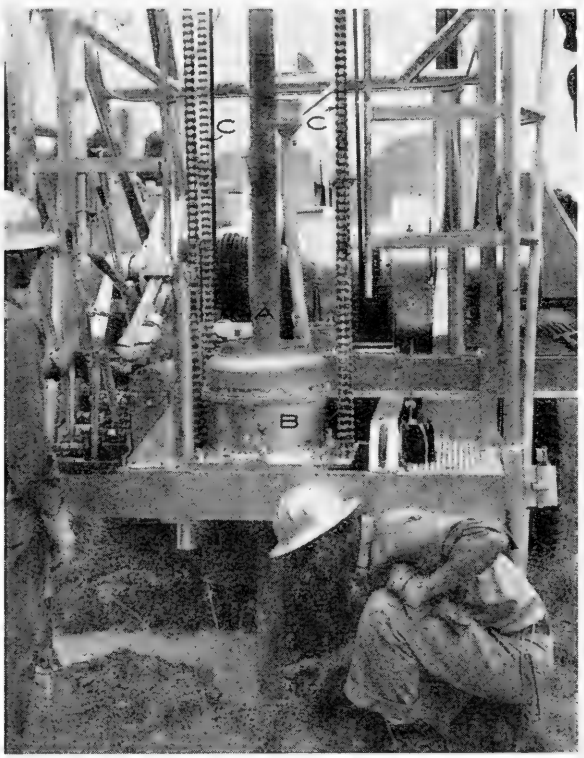

FIG. 552.—Mud pump of mechanical feed type drill, (A) drive rod or Kelly; (B) rotary table; (C) feed chains.

wings. The cutting edge of each wing is faced with tungsten carbide alloy, producing a very hard wear-resistant edge. In soft drilling the two-wing fishtail is the fastest cutting. With increasing ground hardness, it is customary to use bits with more wings or cutting edges. There are openings through all of these bits to permit the required circulation of water or mud

† For detailed dimensions of these rods and couplings, see U. S. Department of Commerce, Bureau of Standards, Publication *CS-17-30* on Commercial Standards.

fluid to clean the cutting edges of the bit, to wash the cuttings away from the bottom of the hole and convey them to the surface. Where formations are very hard, the cone type rock bit is used. (Figure 553.)

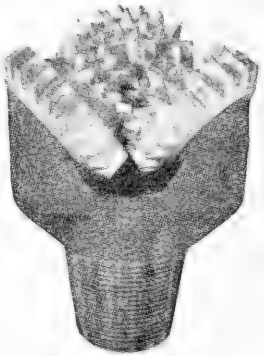

Fig. 553.—Cone type rock bit. (Courtesy of Hughes Tool Co.)

Sizes of Drills. — Seismograph drills are available in different sizes or weights. Each size has advantages under different operating conditions. Where good transportation is available, the drilling is in hard formations, and a high pressure is required on the cutting bit in order to secure rapid and economical progress, a heavy drill is required. In soft formations and in swampy areas, extremely light-weight drills are used. Some can be carried to the drilling location by man power and operated either by hand power or by light-weight air-cooled gasoline engines. Such units are illustrated in Figures 554, 555, and 556. These units can be disassembled so that the maximum weight of any piece is approximately 100 pounds. The pump illustrated is the Mayno type and the engines are 5-horsepower size, with total weight of 260 pounds.

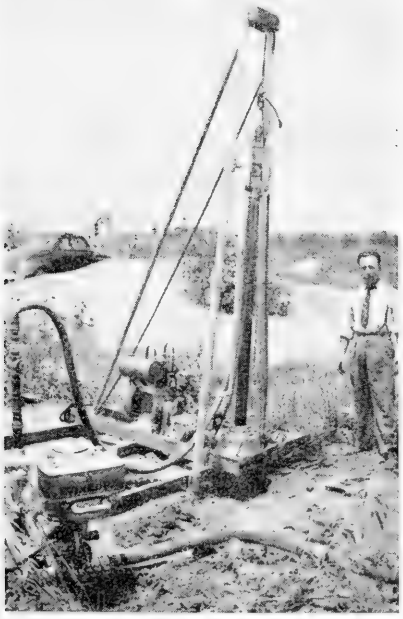

Fig. 554.—Light-weight seismograph drill. (Courtesy of Geophysical Service, Inc.)

Where larger diameter deep holes are required and the additional weight is no disadvantage, a size 4½″ x 6″ mud pump is preferable to the 4″ x 5″ size.

When speed of operation is not the prime consideration, portable drills are well adapted to shallow core drilling, seismograph shot-hole and water well drilling to depths of not over 300 feet. These units are particularly useful in areas where terrain and road conditions require extreme portability. The average time needed for a crew to assemble a unit is about 30 minutes, and the knock-down time about 20 minutes. The total weight of the rig shown in Figure 555 is approximately 800 pounds. This unit may be mounted on a half-ton truck with power take-off for drilling power.

Figure 556 shows a portable drill with gasoline-electric motor rotary

table drive and separate gasoline-driven water pump. The total weight of the "stretcher" component is about 50 pounds.

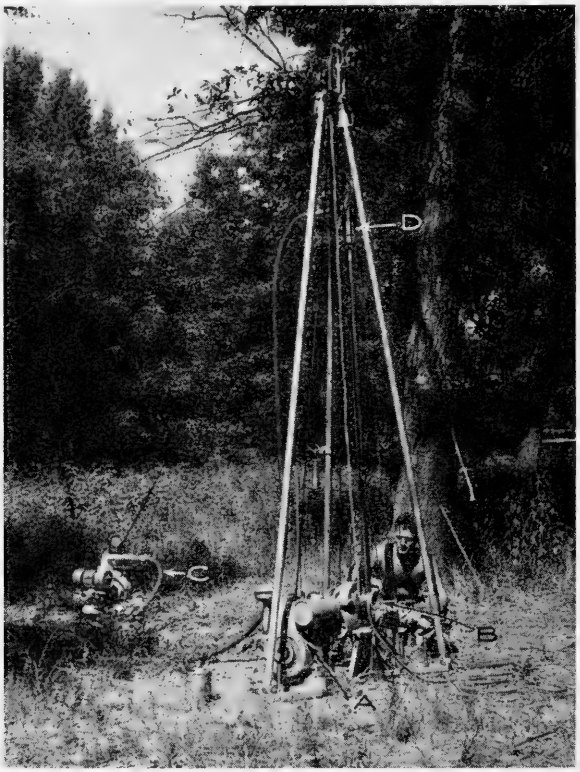

FIG. 555.—Portable drill for shallow drilling. A, engine driving rotary table; B, cathead; C, mud hose; D, swivel head. (Courtesy of Engineering Laboratories, Inc.)

Water Truck

Each standard drilling machine is served by a separate water supply truck. Occasionally when the holes are drilled on a closely spaced pattern, or when the distance for hauling water is short, it is possible for one water truck to serve two drill rigs, but this is the exception. In many areas where the location of the source of water is at some distance from the area being drilled, it is necessary to employ two water trucks for each drill unit.

Figure 557 shows a typical truck-mounted water tank assembly. In addition to the 500-gallon water tank there is also provided a small sturdy "A" frame with guide sheave mounted at the rear. A power winch (not shown) is mounted behind the truck cab and below the water tank. The

FIG. 556.—Portable drill with gasoline-electric motor drive to rotary table. A, gasoline engine direct-connected to generator; B, electric motor driving rotary table; C, rotary table; D, gasoline engine direct-connected to mud pump; E, Kelly; F, mud hose; G, swivel. (Courtesy of Seismograph Service Corporation.)

FIG. 557.—Water truck. A, 500-gal. water tank; B, "A" frame hoist; C, sheave wheel; D, guide sheave; E, roller; F, guide sheave; G, guide sheaves for winch line; H, auxiliary 30-gal. gasoline tank; I, storage box; J, drinking-water can, with large top opening for ice and cleaning; K, vertical guard posts, for extra lengths of 10′ drill pipe; L, luggage rail, for supplies; M, suction hose. (Courtesy of Griffin Tank and Welding Company.)

winch is driven from the truck engine by means of a side outlet power take-off assembly installed in the truck. The winch line passes under the truck bed and comes out between the guide sheaves (D) and the roller (E) at the rear. The winch line, threaded around the guide sheave (F) and up over the "A" frame sheave (C), is used for pulling casing from holes after they have been shot in areas where casing is required. There are also guide sheaves (G) at each rear corner of the truck, as the winch line is useful for pulling this truck or the drill truck over short stretches of wet or swampy ground or on sandy roads.

Between the spare tire and the water tank is a 30-gallon auxiliary gasoline tank. On the left side of the water tank is a storage box for carrying aquagell or other special mud additives. A drinking water can is mounted directly in front of this mud box. There is space between the vertical guard posts on either side of the truck bed to carry extra pieces of 10-foot drill rod. The water tank itself is built with a luggage rail around the top for tying down extra supplies on long hauls. The suction hose usually has one end connected to the tank. The other end is inserted in a special pipe compartment where it is carried when moving.

There are several methods used for filling the water tanks. One is to equip the water truck with a small rotary-type water pump driven by a power take-off from the truck engine. A second is to equip the water trucks with a single-cylinder, double-acting, reciprocating-type plunger pump driven by a power take-off from the truck engine and also arranged so that it can be operated by hand.

A third method is to use a separate portable gasoline-engine-driven pumping unit, light enough to be carried by one man. This is a light-weight centrifugal pump directly connected to a single cylinder gasoline engine. This method is used when the source of the water is more than eighteen or twenty feet below the lowest elevation that the water truck can reach, making it impossible to lift the water by direct suction. The portable pumping unit is carried down close to the water level where the water can be lifted by direct suction, and is discharged under pressure up through a hose line into the water tank.

A fourth method is to have the water tank made air-tight so it can be filled by means of a vacuum drawn from the intake manifold on the truck engine. This method makes it possible to create a vacuum in the tank while the truck is traveling to the location of the water supply, so that upon arrival at the water source the tank can be very quickly filled by the vacuum already created. A float-operated valve should be mounted on top of the tank to break the vacuum when the tank is full, so that water cannot be drawn into the engine intake manifold. In freezing weather the exhaust from the engine is circulated around this float valve assembly to insure its proper functioning. The quick full-opening valve at the rear has an air-tight rubber seat.

Drilling Crew Performance

The drill crew consists of three men: a driller, a helper, and a water-truck driver. When the truck driver is not actually hauling water, he assists the other two members of the crew at the drill. The truck driver frequently can have the water sump already dug and filled with water before the drill arrives at the location of the next hole.

In soft formations, such as clay and shale, it is often possible to drill a 60-foot hole in twenty or thirty minutes net drilling time. The time required for moving from one hole location to the next varies with the distance between holes, the topography of the country, the condition of the roads, and the obstacles encountered, such as swamps, forests, fences and detours around weak bridges. After the drill truck has reached the location, it takes only five or ten minutes before drilling starts if the mud pit or sump has been prepared and filled with water.

The diameter of the hole required for seismic shooting varies from 3″ to 6″. The size is determined by the hardness of the ground, the diameter of the explosive being used, and whether or not casing is required. Under average medium ground conditions it is not unusual for a crew to drill six holes per day in one eight-hour shift. Exceptional daily performances of ten to fourteen holes 60 feet in depth have been reported. Where deeper holes are required and the drilling is more difficult, a performance of one hole per day may be considered satisfactory.

The drilling equipment in some cases is all owned and operated by the organization making the seismograph survey. In other cases, the equipment is supplied by an independent drilling contractor. These contractors are usually employed on a per drill per month basis. On a one shift per day operation where the contractor provides the drill unit and the water truck, furnishes a three-man crew, and supplies gasoline, lubrication, insurance, and supervision, the rate per drill per month varies from $1,700 to $2,200 (1949).

The actual cost per foot of hole drilled varies between wide limits. It depends upon the hardness and character of the ground, the distance between the hole locations, the size of the hole being drilled, the type of drilling equipment being used, the morale, efficiency and experience of the drill crew, and the supervision provided. Direct operating expenditures include costs for labor, fuel, lubrication, bits, normal replacements and supplies, and can average as low as 12 cents or 15 cents per foot under favorable circumstances. On the other hand, these direct costs may average 60 to 75 cents per foot, if boulders or loose gravel are encountered, the holes are sparsely spaced, the roads are bad, the water supply is inaccessible, or casing is required to keep the hole open.

The initial cost of the drilling machine, including the motor truck, the complete drill assembly with mud pump, Kelly, drill rods, suction and swivel hose, bits and small tools, will vary from $8,000 to $15,000, depending upon the size of the unit. The cost of the water truck will vary from

$3,000 to $5,000, depending upon the type of truck, the size of the tank, and auxiliary items.

In addition to the truck-mounted drilling machine and the water truck, the following operating equipment and tools are recommended for average daylight operation.*

OPERATING EQUIPMENT

1—lightweight water swivel with size "N" pin connection
1—ball bearing type hoisting plug with "N" pin connection
200 ft. of 10′ lengths size "N" seismograph type drill rods
6—3″ fishtail bits
6—3½″ fishtail bits
6—4″ fishtail bits
2—4⅜″ fishtail bits
1—75′ length ½″ 6 x 37 extra pliable plow steel hoisting rope with safety hook
1—20′ length of 2½″ wire inserted suction hose with foot valve and connections
1—25′ length 1¼″ wire-wound swivel hose with connections at both ends

For **KELLY OPERATION** the following additional equipment is needed:

1—14′ length size "N" Kelly
1—top chuck assembly
1—Kelly drive plate assembly
1—L. H. bushing for water swivel to replace the R. H. bushing
1—5′ length "N" drill rod

TOOLS

1—18″ rigid pipe wrench
2—24″ rigid pipe wrenches
1—36″ rigid pipe wrench
1—12″ crescent adjustable wrench
1— 8″ crescent adjustable wrench
3—Cold chisels, ¼″, ½″, ¾″
1—¾″ x 24″ carpenter's wrecking bar
2—pipe tongs, 1″ to 6″ pipe
1—vise, 5″ jaws, with fittings for mounting on drill truck
1—hacksaw with six blades
3—12″ files—flat smooth, half round second cut, round smooth
1—hand oil can, 1 pt. size
2—#2 round point shovels
1—long handle single bit axe
1—7½″ pick with handle
1—wire brush
1—set mud pump liner and seat pullers
5 lbs. drill rod wicking

The additional cost of these tools, drill rods and operating fittings is approximately $1,200.

* Tin hats and hard toe shoes should be provided. Also investigate local safety and working regulations.

AIR SHOOTING

For many years efforts have been made to eliminate the drilling of shot holes for the dynamite charges. Drilling is expensive, due to the high initial outlay for drills and heavy truck equipment. Labor costs are high due to the personnel required for drilling, hauling water, setting casing in many areas, etc. In numerous cases exploration has been abandoned because the shot-points were inaccessible to the heavy rigs, or because of lack of water or the difficulty of drilling through till and boulder material.

Other methods for producing the elastic waves have been sought, and air shooting has been advocated for a number of years. One of the early suggestions for this technique was made by McCollum†, who desired to create a source of continuous sound which would have a long radius of curvature, i.e., the wave front would be substantially parallel to the surface when it strikes the ground. This was accomplished by placing the source at a considerable elevation above the surface of the earth, using kites or airplanes.

During 1942 tests to determine the efficacy of exploding dynamite charges above the surface of the earth were reported by Russian geophysicists.‡ The tests were made in salt dome exploration in the Kazak Republic. Best results were claimed when the dynamite charge was positioned at a height of 5 to 7 feet above the surface of the ground. The quantity of explosive was found to be 15 to 20 times greater than that required for the shot hole drilled to the bottom of the low velocity layer.

The records obtained when the explosive was positioned above ground were comparable in appearance to those obtained when the charge was placed in a drill hole. Air shots were made over many different types of surface rocks and conditions, and in all cases satisfactory seismograms were reported to have been obtained. During 1943 further work was done in the Turkmen Republic. There the explosive was placed only 1.5 feet above ground. The terrain in this area comprises quicksands which are impassable to automotive equipment. It was believed that the cost of the extra dynamite required for air shooting was more than offset by the greater speed of field operations and the lower operating cost per month.

Developments in the United States

Considerable work in developing the air shooting technique has been done in the United States by Dr. Thomas C. Poulter, under the facilities of the Southwest Research Institute and the Stanford Research Institute. During the seismic survey of the Ross Shelf ice in the Antarctic§, Poulter found that excellent reflections were consistently obtained with the dyna-

† B. McCollum, "Method and Apparatus for Studying Geologic Contours," U. S. Patent 1,675,121, June 26, 1928.

‡ A. A. Tsvetaev, "Testing the Application of Air Explosions in Seismic Reflection Exploration," *Applied Geophysics,* No. 1, 1945, p. 82-87, Organ of Federal United Geophysical Trust; Scientific Research Institution of Applied Geophysics; People's Commissariat of Petroleum, U.S.S.R. (Also reviewed in *Geophysics,* Vol. XIII, No. 3, July, 1948.)

§ Second Byrd Antarctic expedition, 1933-35.

mite charges positioned above the surface of the snow. These tests showed that there was very little absorption by the uncompacted snow layer if the amplitude was very low. Under this condition probably 95 per cent of the energy was transmitted, whereas if the shot energy was confined to a small area, resulting in high amplitude, probably 95 per cent of the energy was absorbed over the same path. Generally, in penetrating the low-velocity layer, the larger the particle size, the greater may be the amplitude before the absorption becomes excessive. For a mixture of particle sizes, the absorption covers a wider amplitude range, but in all cases, if the amplitude of the wave motion is sufficiently low, the transfer of seismic wave energy from one medium to another will be relatively efficient.

When all of the explosive is concentrated at a point and buried just beneath the top surface in the unconsolidated low velocity layer, the wave front has the form of a short radius bubble with very high energy per unit of area, and much of the energy is absorbed in useless work. The useful seismic energy is produced largely by that part of the explosion energy which (1) is directed substantially downward, and (2) does not produce stresses greater than the elastic limit of the material surrounding the bore hole.

If the point explosive is placed in the more consolidated strata beneath the low velocity layer, much greater unit stresses can be utilized, with an increased percentage of the shot energy being converted into useful seismic energy.

Many investigators have tried to devise means of developing a sudden downward force upon the surface of the ground, but in most cases, just as is true for the explosion in a shot hole, the area of application is so small that the required amplitude is far in excess of the elastic limit of the material. By employing a horizontal pattern of small explosive charges, distributed over a relatively large area, a wave of low intensity per unit area is created, and an increased portion of its total energy will be directed downward, because the force is applied to the surface of the ground by means of the air pressure wave. Since the force exerted by such a wave can only be normal to the surface, the seismic wave initiated under the pattern of charges is directed almost entirely downward. The total downward force is calculated at about 2,000,000 pounds upon the surface of the ground for each pound of total explosive used in a properly distributed pattern.

Thus a seismic wave of high total energy is produced in the ground, but since it is distributed over such a large area, the amplitude is low enough to be readily transmitted by the low velocity layer. Although the edge effect around the periphery of this flat wave front tends to develop an appreciable curvature, the dimensions of the initially flat portion of the wave front are such that it retains much of its directive character while in transit through the low velocity layer.

As shown in Figure 559, the charges are mounted on adjustable stakes, consisting of a steel rod driven into the ground over which is placed a steel tube with a clamp screw to secure the charge at any desired height. Welded into the top end of this tube is a ¾-inch diameter pin over which is placed the expendable support for the charge. This support can be a paper tube or a wooden block with a hole in one end to fit the pin forming the top of

FIG. 559.—Method of positioning explosive for air shooting. A, steel stake driven into ground; B, steel tube, adjustable as to height; C, expendable block; D, explosive stick; E, firing wires.

the stake. The explosive is held by this expendable support, which is replaced with each shot.*

Several different forms of explosive patterns have been found effective with this method, including a modification of the Munroe shaped charge which was developed into such an effective weapon of war. A flat disc charge composed of an explosive having a high detonation rate, with or without some sort of backing material, produces a very effective flat wave front. Charges having a diameter of 10 to 12 inches and a thickness of ⅜

* This is a rather unusual use of explosives, and there are potential hazards involved which are peculiar to the detonating of charges above ground. Every precaution should be carefully observed. In particular, personnel and equipment should be at a safe distance or behind barriers for protection against flying particles, etc. The set-up should be sufficiently removed from buildings, power lines, cattle, tanks, etc., to prevent damage from the air blast.

to 1 inch have given excellent results. A backing material such as one inch of sand on top of such a charge reduces the quantity of explosive required by about one-third. Flat charges should be placed on a heavy cardboard or beaverboard platform attached to a block of wood or a paper tube which will fit onto the top of the stake to keep the explosive at a minimum distance

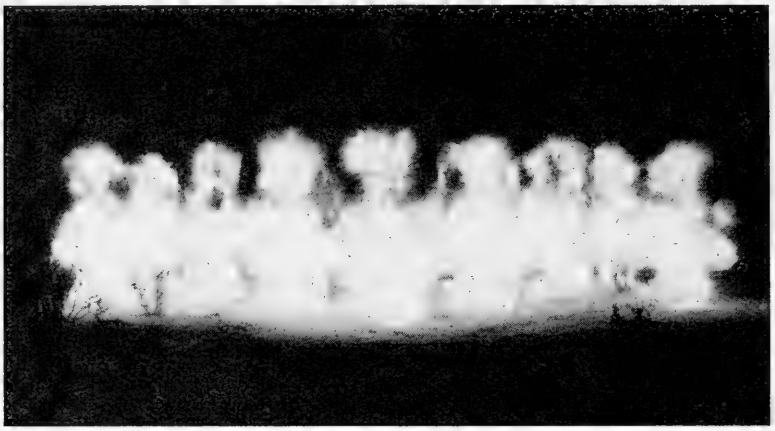

FIG. 560.—A twelve charge pattern of two pound charges using a spacing of 15 feet between charges. (Courtesy of Stanford Research Institute.)

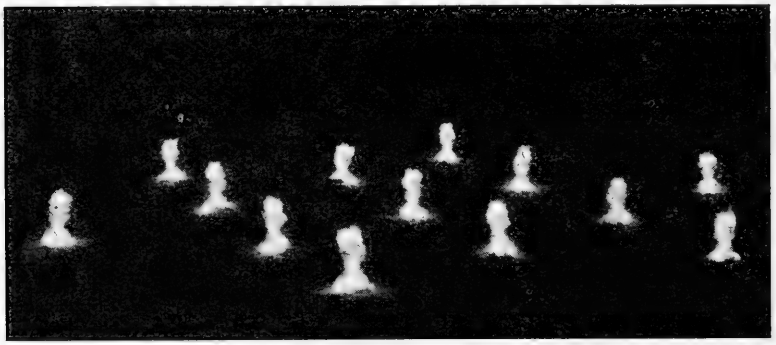

FIG. 561.—A thirteen-charge, six-pointed star pattern photographed from an elevation of 200 feet above ground. The spacing is 60 feet. (Courtesy of Stanford Research Institute.)

of 4 or 5 inches from the top of the stake. The cap should be placed at the center of the charge.

An equally effective charge in producing a flat wave front directed vertically downward is a cylindrical charge having a length-to-diameter ratio of six to one or greater, mounted in a vertical position, and with the cap in the middle or in the top end of the stick. This charge can be mounted on a wooden spike on top of the stake. This is a very convenient type of charge

to use, since the standard sticks of explosive commercially available provide a wide range of sizes of charges. Charges of this type ranging in size from one-third of a pound to 20 pounds have been effectively used.

The arrangement and spacing of the charges in the pattern is a function of the area being surveyed and will vary from a few charges arranged in a straight row to a triangularly spaced pattern of 7 or 13 charges. Figures 560 and 561 illustrate some of the patterns which have been used. The spacings likewise will vary from ten feet to more than seventy feet.

The separate shock waves merge into a single large flat wave of sufficiently low energy per unit area. Because of the velocity at which these wave fronts travel, it is necessary that all of the charges be detonated simultaneously. This is accomplished by connecting the caps in series.

A condenser-discharge type of blasting machine serves very well, or a conventional blasting machine can be used by connecting an 80-microfarad condenser across the generator (not across the terminals of the blasting machine, because the residual charge on a condenser so connected is apt to fire the next charge as soon as the condenser is connected).

Any arrangement of an offset shot-point can be used in which the distance from the shot-point to the closest geophone is great enough to permit all the desired reflections to arrive 0.3 to 0.4 second ahead of the air wave. The first arrivals are of sufficiently low energy so that a pre-set suppresser circuit is not necessary, and a properly designed automatic gain control will give the desired uniformity in amplitude. If the system includes a pre-set suppresser or mixer operated by the first arrivals, it will usually be necessary to increase the sensitivity of this circuit. A seismometer placed on the ground beneath one of the charges will provide a satisfactory time break.

Due to the absence of high frequencies as a result of this method of initiating the seismic wave, an increased band width filter setting can be used.

The air-shooting technique does not produce sufficient ground roll to damage ordinary structures, and only the airborne blast effects need be considered. Due to the horizontal spacing of the charges, the risks involved are greatly reduced. By far the most likely harm to building structures is the breakage of windows. Although any real damage is visible and limited to a relatively short range, the noise, of course, can be heard for a long distance.

Multiple Reflections

The phenomenon of multiple reflections is of common occurrence in nearly all forms of wave energy, and is most familiar in light when two mirrors are placed substantially parallel to each other. Since much of the phenomena of geometrical optics manifests itself in seismic prospecting, it seems most reasonable that multiple reflections are to be expected, and

the interpreter of seismic data should keep in mind the possibility *(and probability)* that multiple reflections may be present on the record.†

There are many examples of multiple reflections in the literature of general earthquake seismology, as refracted waves are reflected once or more by the surface of the earth. Very seldom, however, have illustrations been published of multiple reflections in seismic exploration. Perhaps this is due to the fact that they have not been recognized by the interpreter, or, if recognized, have been discarded as anomalous due to their abnormally steep dips.

In order to illustrate the general theory, we may consider two simple cases of multiple reflections: (1) between a shallow reflecting bed and the surface of the earth, and (2) between two reflecting beds. Each of these two cases may be solved by the theory of images.

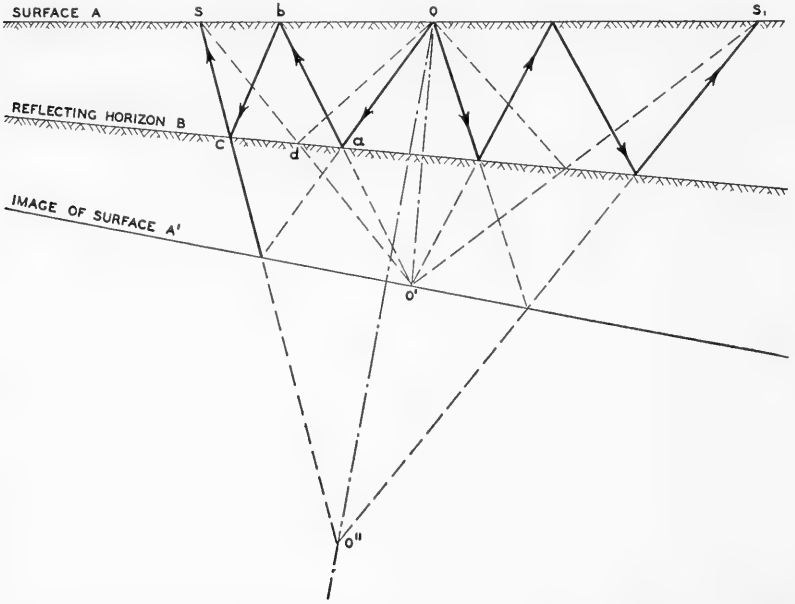

FIG. 562.—Multiple reflections between surface of the earth and a reflecting horizon.

Figure 562 illustrates a simple case of a multiple reflection occurring between the surface of the earth A and a reflecting horizon B. The mirror image of A, with respect to B, is the plane A'. In this figure, O represents the origin or shot-point, located on the surface of the earth. Using the theory of images, we can locate the image of O, which will be O' with respect to the reflecting horizon B. O'' is the image of O with respect to

† An excellent symposium on multiple reflections is given in *Geophysics*, Vol. XIII, No. 1, January, 1948, with papers by T. P. Ellsworth, C. H. Johnson, John Sloat, Frank Ittner, Joseph C. Waterman, Beno Gutenberg, C. Y. Fu, C. H. Dix, O. C. Lester, Dean Walling, C. H. Dresbach, and Raul F. Hansen.

the surface A'. Using the points O, O', and O'', we may draw the path of the rays which leave the origin O and arrive at the seismometers S and S_1, which may be considered to represent the outside seismometers of a split spread.

The reflection which appears to come from the imaginary image O'' is actually reflected twice from the real reflecting horizon B and once from the surface A. It travels the path $OabcS$, while a true reflection from bed B will travel the path OdS. Such being the case, the multiple reflection should have the following relationships to the single reflection from the real reflecting horizon: (1) nearly double the reflection time (for the seismometer placed very close to the shot point, when the reflecting horizon is substantially parallel to the surface), (2) approximately twice the correct angle of dip or ΔT value, and (3) an average velocity equal to that in the interval between the surface A and the reflecting horizon B, irrespective of the higher velocity which usually exists at the depth which would correspond to the reflection time from the image surface A'.

Theoretically we should expect many cases of multiple reflections between the surface and the shallow reflecting beds. Actually, however, such reflections have seldom been observed in land operations. Lester describes experimental work conducted in an attempt to obtain evidence of energy reflected from the surface. "No sign of a surface reflection was seen on any of the records."† Various theories have been advanced to explain this fact, such as, that the surfaces used were not sufficiently smooth to produce good reflections, or that the velocity boundary between air and the surface of the earth is not the sharp boundary to be expected, considering the relative densities of the air and the earth materials. "It has been shown that velocities of less than that of sound in air are measurable in very-near-surface earth materials. Though such velocities increase with depth at a rapid rate through the so-called seismic weathered layer, it is not unusual to find that depths of 50 to more than 100 feet are penetrated before encountering unweathered ground velocities of approximately 5,000 feet per second."‡

It has been found, however, that the base of the low velocity or "weathering" zone reflects a large percentage of the incident energy. Velocities in the "weathering" zone often range from 1,000 to 2,000 feet per second. At the base of this zone there is a discontinuity and the velocity may increase abruptly to 5,000 or more feet per second. Using normal values for density, we can expect a coefficient of reflection at this discontinuity of from 35 to 75 per cent. Quite often multiple reflections occur under these conditions, especially between the base of "weathering" and a shallow basement or other reflecting horizon.

In other words, the gradual change in velocity from the surface down through the earth prevents the air-surface interface from acting as a reflect-

† O. C. Lester, Jr., "Discussion of Multiple Reflections," *Geophysics*, XIII, No. 1, January, 1948.

‡ O. C. Lester, *ibid.*

ing horizon. The validity of this explanation is favored by the fact that multiple reflections are often obtained between the air-water interface and the ocean bottom, in offshore seismic work. Here there is a sharp change in velocity between the surface of the water and the air above it.

An analysis of Figure 468-A will show that the placing of dynamite below the low velocity or weathered zone serves to minimize the possibility of these shallow multiple reflections, while at the same time much more energy is transmitted to the higher velocity horizons.

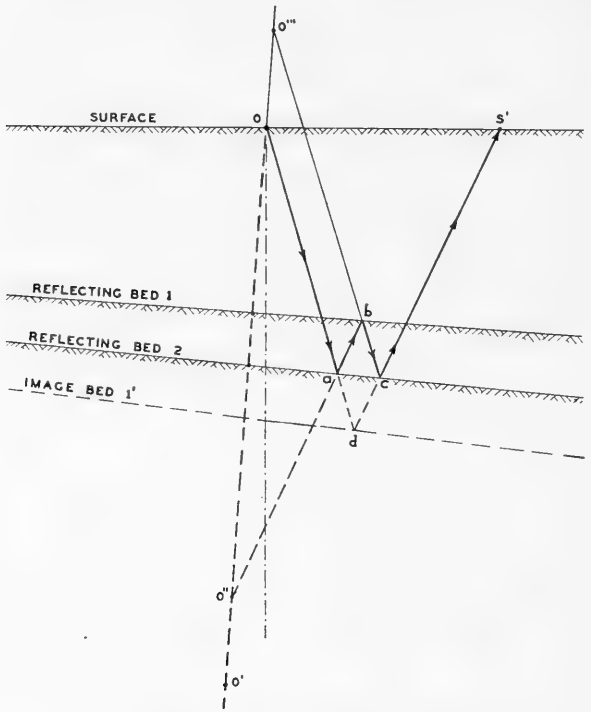

FIG. 563.—Multiple reflections between two reflecting beds.

Figure 563 illustrates the general conditions where multiple reflections may occur between two reflecting horizons substantially parallel, located below the low velocity layer. In this figure the shot-point again is located at the surface of the ground. Reflecting beds 1 and 2 are illustrated. The image of bed 1 with respect to bed 2 is shown as bed 1′. When the angle between the beds is not too great, O' may be considered as the image of O with respect to the image bed 1′; and O'' may be considered as the image of O with respect to the reflecting bed 2; while O''' is the image of O'', with respect to the reflecting bed 1. Using the real and the imaginary origins, the paths of the rays may be drawn. A multiple reflection between

beds 1 and 2 will travel the path $OabcS'$. From the record, the time for a multiple reflection occurring between bed 1 and bed 2 will delineate the image bed 1′, having a reflection time equal to that of bed 2, plus the difference in the reflection times of the two actual reflecting beds. The apparent path of travel being $OadcS_1$ this may be expressed mathematically as follows:

$$T_1 = T_2 + (T_2 - T_1)$$

wherein T_1 is the time for the reflection which came from the image bed 1′, T_2 is the reflecting time for bed 2, and T_1 is the reflecting time for bed 1, the shallower bed.

The apparent velocity of the multiple reflection will be influenced more or less by the true velocity between beds 1 and 2, and will not exhibit the higher velocities that would normally be expected if the wave traveled to the deeper horizon occupied by the image bed 1′. If the distance between beds 1 and 2 is an appreciable part of the total travel path, then the velocity between beds 1 and 2 may influence the overall velocity to a measurable amount.

There are no easily applied rules for positively identifying multiple reflections between the deeper lying beds. Generally, the subsurface conditions are complicated, and do not bear the simple relationships which were enumerated for the two previous cases. The condition is further complicated in those areas where many reflections are obtained, because then it is difficult to separate, by visual inspection, the true and the multiple reflections.

Often multiple reflections will be apparent when dip cross-sections are plotted, and some discordant dips are obtained which usually have greater dip than the true dip at the depth indicated. Another general test is to plot a time-depth graph for the reflections. Usually a smooth curve may be drawn through these points to show the relationship of velocity with depth. This curve is similar to that obtained by refraction shooting. Since multiple reflections do not follow the same time-depth relationships of true reflections, they will depart from the curve, and normally give values of time, for a given indicated depth, greater than the curve.

Multiple Reflections in Air Shooting.—In the Antarctic, T. C. Poulter conducted a study of reverberation records between the air-snow interface at the surface and the bottom of an ice flow. The height of the ice-snow above sea level was accurately known. The velocity in this solidified snow was accurately measured and found to be 12,050 feet per second. This mass of ice and snow was floating in two thousand feet of water, the depth of which was determined by direct measurements and sonic depth gear on the boats. This solidified but porous snow was flooded to sea level with salt water and the velocity in the flooded portion was accurately determined at 4,980 feet per second. The water temperature was constant to plus or minus one-half degree the year around. Under these favorable

experimental conditions it was found that, for charges buried to or just below sea level, as many as eight successive reflections were obtained with but little intervening reflection energy. When air-shooting was employed, it was found that not more than two reflections were obtained.

To further illustrate how air-shooting may minimize multiple reflections, two seismograms are shown in Figure 564. These records were taken in the Benedum Area, Upton County, Texas. A general examination of the records shows a smaller number of more sharply defined energies on the air shot than on the hole shot, but more particularly, the almost complete absence of apparent reflections on the air charge record beyond the basement reflection which occurs between 1.9 and 2.0 seconds.

Note the reflection which occurs at 2.376(Y) on the hole shot, but which is absent on the air shot. If this is inspected to determine the possibility of its being a first reverberation, the original reflection would have to be at 1.175 seconds and there is one at 1.176(X). If it were a second reverberation, there would have to be a first reverberation at 1.580 and a reflection at 0.778, and these do not exist. There is, therefore, a possibility that this is a first reverberation from the reflection at 1.175.

Now, examine the reflections at 2.160(3). For this to be a first reverberation there would have to be a reflection at 1.074, and none exists. For it to be a second reverberation, there would have to be a first reverberation at 1.462(2), and a reflection at .740(1), and both of these are definite possibilities. The reflection is picked at .735 instead of .740, and a strong energy and phase shift starts at approximately 1.462. Other examples are on the record.

Experience in seismic work indicates that reverberations or multiple reflections occur commonly between the near surface and some early, good reflecting interface. The most frequently observed reverberations appear to arrive from igneous layers of basalt, etc., interbedded with the sediments. Oftentimes between the near surface and a shallow basement, in interpreting such a reverberation as a reflection, a shift is produced which is more than twice as great as a real reflection, while the second reverberation produces a shift in excess of three times that which would be caused by the actual dip of the horizon. Since the reverberations occurring between the surface and some early reflecting horizon are in the region of lowest velocity, the displacement of the reverberation on the record is appreciably in excess of the two- or three-fold actual displacement of the reflecting horizon.

The fact that the reflections shown on these records have an energy apparently greater in the reverberation than in the initial reflection is not surprising, since most of the random energy has disappeared by the time that the reverberation arrives and the overall amplification or gain control has been vastly increased.

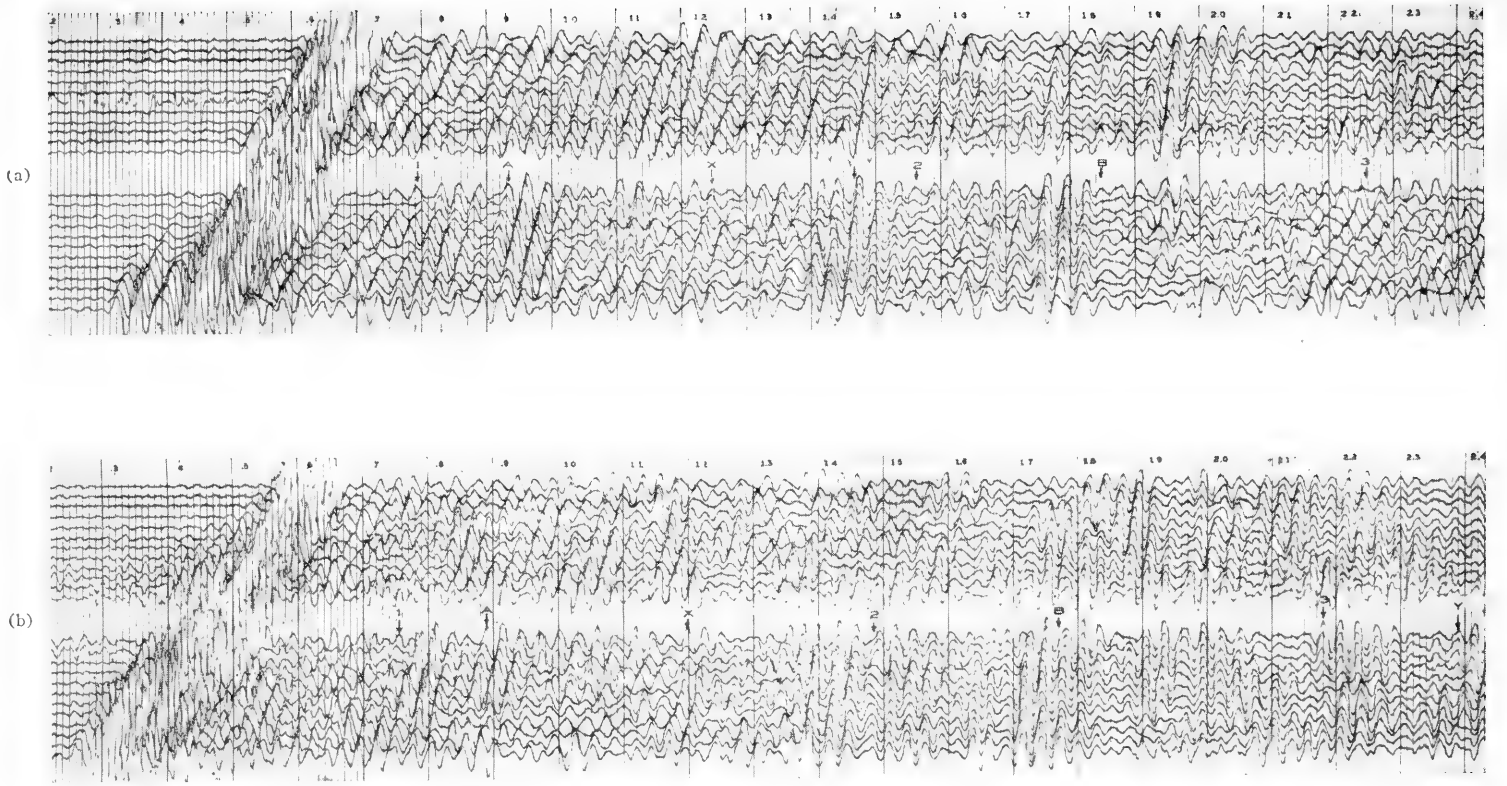

FIG. 564.—Comparison recordings, seismograms made at the same location: (a) recorded from blast in air, (b) recorded from blast in shot-hole at a depth of 162 feet. (Courtesy of Republic Exploration Company, furnished by Institute of Inventive Research.)

OFFSHORE SEISMOGRAPH OPERATIONS

Seismograph operations offshore involve some novel and spectacular features, but they are basically very similar to operations on land. Because of the greater variety of activities involved, water operations are more elaborate and costly. However, the changes necessary to adapt land equipment and methods to water work are relatively simple. Some of the aspects will be discussed under the headings of instrumentation, shot generation, surveying, interpretation, and operations.

Instrumentation.—As regards seismic wave transmission, the behavior of water in many respects is much the same as that of rock. Hence the geophone may be submerged anywhere in the water or placed on the solid bottom. The instruments commonly used on land may also be used in water work, due provision being made to prevent water reaching vital parts. The electrical output of most land type seismometers is proportional to the velocity of the ground or water motion, at frequencies above the natural frequency of the geophone. Suitable pressure-sensitive units may also be used in place of velocity-type geophones. However, their use to date (1949) is not widespread.

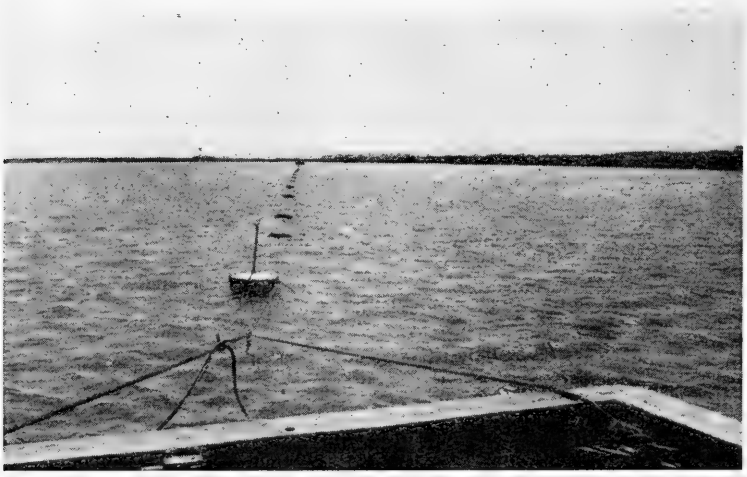

FIG. 565.—Seismometer spread in offshore seismograph operations as viewed from stern of boat. (Courtesy of United Geophysical Company.)

In some earlier water operations, geophones were individually placed on bottom from a surface boat. A heavy iron base or grill was provided to insure the geophone's coming to rest in a vertical position. In some cases geophones were "poled" into soft mud bottoms.

In most current operations, the geophones are fastened integrally into the cable system, and the entire assembly of cables and geophones is towed or dragged as a unit by the recording boat. Figure 565 shows such an

assembly of geophones and cables held taut by two boats ready for the shot. Some of the cable assemblies are designed for dragging on bottom, and the geophones are mounted in watertight housings at fixed intervals along the cable.† The geophone is usually mounted in a system of gimbals, with brushes and slip rings for electrical connection, allowing the unit to orient itself freely in a vertical position within the waterproof housing. The cable is usually built in sections, with waterproof fittings for connecting into the geophone housings. This construction allows relatively easy replacement in case of damage to or failure of a section of cable. The cable ordinarily consists of a steel center cable for strength, several pairs of insulated electrical conductors, and a protective rubber or plastic insulating covering. The entire assembly is quite heavy and bulky and is best handled on a large power-driven reel.

In a variation of this system, the geophone is mounted in or on a wood or cork buoy,‡ and floats upward a short distance from the cable lying on bottom. Electrical connection is made through a pigtail cable which enters a waterproof fitting on the main cable.

The bottom-dragging cable works best in relatively shallow water, and over bottoms which are not too rocky. If the bottom is very rough with numerous shell or rock outcrops, or if the water is deep, a floating geophone cable system may be used to advantage. The floating-type cable consists of a center steel cable, for strength, from which geophones are suspended at intervals, and to which the insulated electrical conductors are fastened. The entire system is suspended at intervals from floating rubber bladders or metal can buoys. It is towed and kept in position by a boat at each end. There is no limit to the depth of water in which the system may be used, since it is completely floating.

The geophones are mounted on paravanes or planing boards which (1) keep the geophone in a vertical orientation, (2) serve as a baffle or mechanical filter element in reducing noise, (3) keep the geophones submerged and in a stable condition while being towed, and (4) provide optimum coupling with the motion of the water by reducing the mean density of the assembly to a value near that of water. The geophone assemblies are suspended by rubber shock cords about ten feet below the surface of the water.

The recording equipment is usually installed in the boat which is used to tow or drag the cable assembly. This equipment is generally the conventional assembly of land seismograph instruments. Some minor precautions may be necessary to avoid the effects of dampness and salt-water leakage. It is convenient to have the amplifiers provided with relays which temporarily bypass low pass filters, in order that the very high frequency water-transmitted "first breaks" can be sharply recorded. These data are

† J. W. Flude, "Apparatus for Making Geophysical Surveys Under Water," U. S. Patent 2,423,591, July 8, 1947.

‡ R. A. Peterson, "Submersible Seismometer System," U. S. Patent 2,449,085, Sept. 14, 1948.

convenient during interpretation, for determining the exact location of the shot with respect to the geophone spread.

Water Shooting.—Firing of shots is usually much easier and more rapid than in land operations, since shot holes obviously are unnecessary. The explosives are usually detonated at shallow depths in the water. Regular seismograph dynamites may be used, but for reasons of economy ammonium nitrate types of explosives are commonly employed. The explosive is packed in reasonably water-tight wrapping, often as a 50-pound cartridge. Figure 566 shows some of these charges on the deck of the

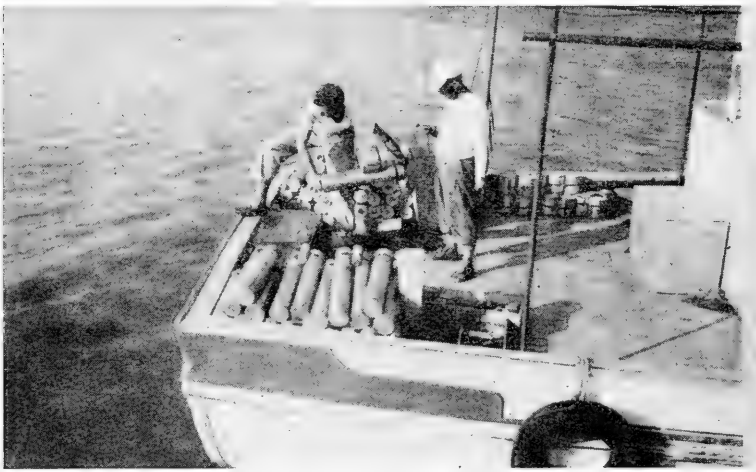

FIG. 566.—Powder technician preparing to drop a 50-pound explosive charge into water. (Courtesy of United Geophysical Company.)

shooting boat. Since several tons of explosives may be used during a day's run, it is important to have the explosives packaged in single large containers for easy handling.

When the explosive is detonated at an appreciable depth below the surface, there is oscillation of the gas bubble resulting from the explosion.† The passage of the initial shock wave imparts a high outward velocity to the water surrounding the explosive. Because of this acquired momentum the water continues to expand rapidly outwards for a considerable time, even after the pressure in the gas sphere falls to values below the normal hydrostatic pressure in the water. Eventually the outward expansion is brought to a stop and the water begins to move rapidly inward, compressing the low pressure gas sphere. Because of convergence the water picks up velocity rapidly and compresses the gas to a small volume and high pressure. At equilibrium, the maximum pressure is reached, the gas bubble again begins to expand with explosive violence, and a second shock wave

† Robert H. Cole, *Underwater Explosions,* Princeton University Press, 1948.

is generated. This subsequent shock is much lower in intensity than the original shock but is of considerably longer duration and carries appreciable energy, especially in the lower frequency components of the energy spectrum. The entire process is then repeated as the gas bubble expands and collapses a second time. The process may repeat two or three times, sending out a weaker shock wave each time. For typical seismograph shots the period of repetition is .3 or .4 of a second, and a confusing duplication of reflections may result because of the multiple generation of pressure pulses.

In practice the gas bubble oscillation is avoided by detonating the shot so near the surface of the water that the gas bubble breaks the surface on the first excursion, and the inrushing water forces the gas and spray of water upwards in a spectacular vertical jet or plume.† Figure 567 shows a water and gas plume several hundred feet high.

FIG. 567.—Water Shot. The inrushing water forces the gas and a spray of water several hundred feet high in a spectacular vertical jet or plume. (Courtesy of United Geophysical Company.)

A typical shooting depth is 5 feet below the surface for a 50-pound explosive charge. This depth is sufficiently shallow to prevent generation of multiple pulses. The charge and one end of the firing cable are ordinarily tied to an inflated rubber balloon and thrown overboard. The shooting boat pulls away to a safe distance and the shooter detonates the charge. The shot instant usually is transmitted by radio to the recording boat.

Most offshore seismograph work is done by the reflection method, using continuous, dip, or correlation shooting. In some cases the shot is detonated at a point offset from the center of the spread. In other cases,

† R. L. Lay, "Repeated P-Waves in Seismic Exploration of Water-Covered Areas," *Geophysics*, Vol. X, No. 4, Oct., 1945, pp. 467-471.

two shooting boats are used in line with, but off some distance from, each end of the geophone spread.

Along the California coast, state regulations require that explosives be jetted into the bottom where the water depth is less than 100 feet. This regulation is based on the assumption that less damage is done in killing fish by buried shots. Special jetting spoons have been developed to rapidly jet and bury charges in the bottom sediments from a surface jetting boat.

Surveying.—One of the most troublesome problems in offshore seismograph work is the accurate surveying of the geophone spread and shot locations. Within sight of the shore, sextant shots may be used for loca-

FIG. 568.—A marine seismic fleet consisting of two survey boats, a shooting boat and a recording boat. These boats are (SF-1) radar-equipped; note radar antennae and reflectors. (Courtesy of American Exploration Company.)

tions if adequate known targets are present on shore; or locations may be determined by triangulation from shore stations. As the distance offshore becomes greater, or when fog or haze is prevalent, other survey methods are necessary. A combination of running on course by gyro-compass bearings or by a system of back-sighting, together with distance measurements with a wire line machine, can be used. However, as distances from shore become of the order of 20 or 30 miles or more, it is nearly essential to use some electronic means of surveying.* Certain of these methods are limited to line-of-sight operating conditions; hence the antennas or reflectors must be mounted as high above the surface as possible in order to overcome limitations caused by the earth's curvature. (See Figure 568.) The target stations are often boats anchored at known positions rather than land stations.

* See page 905 for description of radio location systems.

In some instances the electronic surveying gear is located on a surveying boat which precedes the recording boat and marks locations in advance with anchored balloons or other markers. In other cases the gear is mounted on the recording boat, which navigates to predetermined sets of radial or hyperbolic coordinate readings. This latter method eliminates the need for the survey boat and balloon markers. A gyro-compass is valuable for getting the proper bearing as well as location. The shot location with respect to the geophone spread is often determined from the high-frequency water-transmitted "first breaks."

Agocs† has recommended a method for determining the lateral distance from shot to recorders, the depth to bottom, and the time break on seismic records obtained at sea, using direct "first arrivals" through the water, and first and second reflections. The method was later extended to apply to sloping sea bottoms.‡

Interpretation for Water Shooting.—Interpretation procedure and problems in water shooting are quite similar to those in land shooting. Reflection times are reduced to either the water surface elevation or a bottom datum. Weathering corrections are often neglected, since it is usually difficult and expensive in water operations to obtain accurate weathering data. The use of "first break" times is complicated by the fact that energy travels both through the water and through the bottom sediments. In cases where these two arrival times can be separately determined, the water-transmitted breaks can be used to determine relative distances of geophones, and the bottom-transmitted breaks furnish information concerning relative velocities in the bottom rocks. The latter in general carry much less high-frequency energy than the former. By use of dual channel recording with suitable frequency characteristics, the separation of the two events is facilitated. High fidelity recording, with later frequency analysis, will clearly show the two events.

The air-water interface at the surface of the water acts as a nearly perfect reflector of seismic waves. The water-bottom interface also in many cases acts as a fair reflector. Particularly in water more than 200 or 300 feet deep, multiple reflections between the surface and bottom may be prominent enough on the seismograms to obscure reflections from the deeper reflecting horizons. The multiple reflections may usually be identified, as described on pages 891 to 895. In shallow water multiple reflections are usually not bothersome.

In areas of steep dips with rough or irregular bottom topography and rock outcrops, a number of extraneous events with high time moveouts may be observed on the seismograms. It is usually difficult to determine the exact origin of these events, but they appear to represent waves traveling horizontally along or near the water-bottom boundary, with a velocity

† W. B. Agocs, "A method of determining the true break on deep sea seismic records from the water sound arrivals," *Geophysics*, Vol. IX, No. 2, April, 1944, pp. 163-174.

‡ W. B. Agocs, "Sea bottom slope determination from water sound arrivals," *Geophysics*, Vol. XIV, No. 2, April, 1949, pp. 123-132.

close to that of sound in water. These waves appear to be reflected from irregularities on or near the bottom, and return to the geophone spread to be recorded as apparent reflections with very great moveout times.

The phenomena described above are mentioned as features peculiar to water shooting. They are not typical of usual water seismic operations. Generally speaking, the quality of records in water shooting is comparable to that of land records. Records varying from excellent to very poor or useless are obtained in different regions. The noise level due to relative motion of the water and geophone spreads may be somewhat higher than typical noise levels on land. In some cases heavier dynamite charges are necessary to compensate for this difference, to give a better signal noise-level ratio.

FIG. 569.—Type of boat suitable for offshore operations. (Courtesy of United Geophysical Company.)

Operations on Water.—Seismograph operations on water generally lend themselves to high speed and large production. Usually the cable system is dragged along the line of profile, and shots are fired at the desired intervals. The geophones are at rest at the time of shooting, but the recording boat may keep advancing slowly in order to maintain steerageway, playing out slack cable which is pulled aboard again after the shot. Surveying is a rapid and relatively simple matter, especially with suitable electronic equipment. The shooting boat progresses with the recording boat and can fire shots as rapidly as required. In some operations the shooting boat is dispensed with, and the shot is released from the recording boat along a guiding line to a paravane near the desired shot location. The shot is detonated through a trailing firing line from the recording boat.

Production depends to a considerable extent on weather conditions.

On calm days, between 200 and 300 profiles may be obtained. Two or three days may then be lost due to bad weather, or occasionally to breakdown of equipment. The overall cost of water seismic operations may vary from $20,000 to $75,000 per month, depending on the type of operation. Because of high production the unit cost per profile is often comparable to or less than that of land operations.

During the interval from 1945 to 1950 a variety of war-surplus boats has been used in offshore seismograph operations, including sub-chasers, air-sea rescue boats, and mine sweepers. (See Figure 569.) Various types of fishing boats are also widely used. The total number of boats per crew may vary from 1 to 7, depending on the requirements of the operation. Operating crews may comprise from 10 to 40 men. The crew usually stays out for a period of ten days. Good management and coordination are required for smooth and efficient operation and satisfied personnel. Numerous supply problems, including food, provisions, water and fuel, require constant attention. Close attention must also be paid to weather conditions to insure safety of the men and equipment.

RADIO SURVEYING TECHNIQUES

During World War II a tremendous amount of research and developmental effort went into radar and related electronic techniques. After the war, military security measures were lifted, and many geophysicists returned to their former jobs equipped with new skills acquired in government-sponsored research and military service. Applications of these techniques to problems in geophysics were soon recognized.

Radar and associated radio navigation aids have been applied to geophysical field work for the purpose of quickly locating observation stations in unmapped land areas and offshore operations. Much of the military equipment was not directly suited to this work, but since some of this equipment became available after the war to geophysical workers, it was used as a stop-gap until more suitable apparatus could be designed and constructed. At the present time many laboratories are in the process of developing radio survey gear for geophysical applications. It is too early in this program to forecast what form these new developments may finally take. Probably no one type of equipment will meet adequately all of the varying needs of the different geophysical surveying operations. Radio surveying techniques are described in the literature† and only a general outline of the basic operating principles and the general limitations of the systems will be given.‡

Radio navigation systems can be divided into two basic classes, i.e., pulsed systems and c.w. (continuous wave) systems. The pulsed systems include Radar, Ratran, and Shoran. The c.w. systems include Lorac and Raydist. Basically the pulsed systems have the advantage that they gen-

† *Radiation Laboratory Series*, by M.I.T. Staff, McGraw-Hill, 1947.
‡ Eugene A. Slusser, "Radio Location in Oil Prospecting," *Electronics*, August, 1949.

erally give unique solutions to the problems without reference to a record of the portion of the traverse followed to the unknown point. In other words, this solution does not depend on any previous recording of information. The c.w. systems require that two or more stations be in continuous communication and that the results be integrated or accumulated at one station. This is somewhat analogous to the difference between navigation by astronomical fixes and navigation by dead reckoning. In the first case the unknown position is determined independently of any other observations. In the second case, to determine position it is necessary to keep a continuous log of the course, including speed and direction. The courses and the distances traversed must be computed vectorally in order to determine the location of a new position.

The pulse system consists of sending out a sudden burst of radio frequency energy and measuring the time for a reflection to return from a marker target or from a beacon or transpounder station. If the distance is measured from two points of known location in this manner, or the distance and azimuth are measured to any known point, then the position of the observer may be established by simple trigonometry or arithmetic.

In the c.w. system an interference pattern of radio waves is set up by two or more transmitter stations at known locations. This is accomplished by transmitting on the same frequency. The mobile station observer then counts and records the number of standing wave patterns which he crosses by means of an accumulating phase meter. In this way the observer may keep track of his course and position relative to the starting point in terms of standing wave patterns. If the observer moves as much as one-half of a wave length during the time when there is a loss of communication between units, an error will be introduced into the counting system. This error cannot be removed from the system without resetting the phase meter dials at a known location.

A disadvantage of the pulse system is that it requires a wide spectral band width in order to give accurate results. This means that pulsed systems, to have an accuracy of the order of 50 feet or better, must be operated in the v.h.f. (very high frequencies) or microwave region of the radio spectrum in order to conserve valuable space for communications in the lower portion of the radio spectrum. When these high frequencies are used, operation is confined to the line of sight conditions. This usually limits the range of the equipment to the horizon distance which is dependent upon the particular antenna heights. In the c.w. system with its narrow band width, it is practical to operate at lower frequencies, and as a consequence the range of the apparatus will not be limited to the horizon distance. Also the longer wave lengths follow the curvature of the earth.

Navigational Radar.—Radar equipment operating in the 3 cm. and 10 cm. bands has been used for offshore surveying. The general operating principle of radar has long been known to geophysicists. Like the reflection seismograph, radar is an echo ranging device, but unlike the seismograph,

it operates in an almost perfect physical medium where the velocity is practically constant and the attenuation is relatively low. The high velocity of radio frequency energy in the atmosphere (300,000,000 meters per second) makes possible the almost instantaneous observation of a tremendous number of reflections. In fact one of the principal disadvantages of typical radar, when applied to accurate survey work, is that too much data are generally obtained. This presents a difficulty and sometimes an uncertainty in the recognition of reflections from specific marker targets.

Exploration geophysicists have been employing radar for surveying offshore locations along the Gulf Coast. Most of these radar systems use what is known as the p.p.i. (plan position indicator) type of presentation. The antenna is slowly rotated, thus directing the sending and receiving of the radio beam. The instantaneous direction of this antenna is synchronized with that of the outward radial sweep on the cathode ray tube used for observation. This cathode ray beam sweeps from the center of the cathode ray tube toward its circumference at a uniform rate, and the beam is blanked out on returning from the circumference to the center. Echoes from objects reflecting radio waves appear as bright spots on the radial trace of the cathode ray beam, so that the net result is the production of a crude map of all the echoes received with the radar station located in the center of the cathode ray tube screen. Superimposed on this small scale map are range or distance markers which appear as concentric circles with the radar station at their center. The radii of these circles represent distance from the radar station, and thus the distance to any point on the map may be read directly. Such a system would be ideal if only echoes from the desired land markers appeared on the cathode ray tube screen. Unfortunately, echoes from many water waves,† land masses, structures and desired targets all appear on the screen as a confusing clutter. Furthermore, as the ship carrying the radar moves along its course, some targets cease to give reflections and others appear on the screen, so that often it is a difficult problem to locate land marks with the certainty needed for horizontal survey control. To avoid this dilemma certain land markers are often flagged with artificial reflectors, thus making up a type of triangulation shore network. This arrangement is helpful in most cases, but generally there are so many reflections presented on the screen that a unique solution is seldom possible for determining accurate locations. The navigation radar is excellent for the purpose for which it was designed, that is, for detecting and locating other vessels and obstacles in fog or darkness and for determining position relative to land markers on shore. The operational range is limited to line-of-sight, which may be up to 15 miles, depending upon terrain conditions and height of station. Within this distance, an accuracy of $\pm$ 25 to 100 feet may be obtained. This system is most satisfactory for ship to near-shore use.

† W. F. Gerdes and R. C. Johnson, "Industrial Radar for Hurricane Tracking," *Science,* Vol. 110, Oct. 7, 1949.

Radar Beacons Pulse Systems.—A marked improvement in the application of conventional reflection radar for survey purposes is found in the radar beacons or transpounder systems, one type uses a pulse method and the other a continuous wave phase or standing wave pattern.

In one pulse method, termed the Shoran, a pulse coming from the single moving station triggers two separated fixed beacon stations and they in turn retransmit to a receiver aboard the moving station. The time intervals representing the pulses from the two fixed beacons are indicated. The moving transmitter and the two beacons each operate on a different frequency, in the range of 220 to 310 mc. (megacycles). At these frequencies, the range is limited to line-of-sight. Aboard ship this range is about 15 to 20 miles, while from an aircraft flying at 1,000 feet elevation it may be 40 miles. At these distances, the accuracy is ± 25 to 75 feet. In both the Shoran and the Ratran systems auxiliary equipment can be provided whereby the pilot can be guided to fly a given course by means of a PDI (pilot direction indicator) for the Shoran, and a PLI (pilot location indicator) for the Ratran.

Since the two beacons are at known point locations, the position of the mobile station can be determined by direct intersection, without measuring angles. The resolution of these data comes from a solution of a triangulation problem; given, the fixed distances between two stationary beacons and the measured distances from the mobile or master station (location unknown). This is an advantageous feature over the radar, because radio distances can be measured much more accurately than azimuth angles. A further advantage of the beacon system is that lower frequencies can be used, because the narrow beams for angle measurements are not required and simple compact antennae may be used. Moreover, the required transmitter power for two-way beacon systems is less than that necessary for the operation of reflection radar. This comes from the fact that in beacon transmitter work the necessary power is proportional to the square of the distance, whereas in the case of reflected radar signals the required power is proportional to the fourth power of the distance.

The Shoran system† is a typical example of a method which has been successfully used in geophysical location surveying. This system originally was developed for precision aerial bombing during World War II. The navigator in an aircraft determines his position to an accuracy of 25 feet by measuring the range to two fixed beacon locations on the ground. The equipment of the airborne station weighs approximately 250 pounds installed and requires about 1.2 kilowatts of power. The fixed ground station equipment weighs nearly 1200 pounds installed and requires 1.6 kilowatts of power.

The Shoran method has found a ready application in the survey control for flying magnetometer and for base control in photographic mapping

† Edgar B. Stern, Jr., "Shoran Radar," *Oil and Gas Journal*, July, 1948, p. 70-74.
Carl I. Aslakson, "Can the Velocity of Propagation of Radio Waves be Measured by Shoran?", *Transactions, Amer. Geoph. Union*, Aug., 1949.

from aircraft. Here the full range of the equipment can be utilized because of the great height of the aircraft above the ground. Shoran has also been successfully used for offshore surface control.

For geophysical operations a simple and more portable apparatus for Shoran type of work is now under field test. This equipment in its present form is especially designed for mobile use on land. Because of the horizon limitation, it is seldom practical to operate over distances greater than 15 or 20 miles. For this type of service the bulky high-power transmitters of regular Shoran equipment are not necessary. A compact, low-power, experimental system of this sort has given approximately the same accuracy as the regular Shoran equipment up to distances of 10 or 20 miles. The equipment of the master and the beacon stations each weighs about 25 pounds and each requires about 100 watts power. This portable system will probably find considerable application in future geophysical land and near-shore operations. When good base maps are not available, it is believed that the services of this equipment would prove extremely valuable.

Experimental work has demonstrated that the attenuation between stations may not be too great at the high frequencies required and that satisfactory results can be obtained at short ranges through considerable dense foliage growths and other small obstacles to the direct line of sight.

The Ratran is a radar triangulation system, and determines position by using ranges from two fixed beacon points. Aboard the moving station are carried two radar transmitters; each operates at a different frequency and triggers one of the beacon stations. Location of the moving station is computed with reference to the base-line connecting the two fixed stations.

C.W. Phase Systems. — Several c.w. systems offer considerable promise for off-shore location surveying. Although there may be considerable differences in the techniques involved in these systems, they all will probably depend basically on setting up a standing radio wave pattern between two or more fixed transmitters. The distances may then be measured by counting wave lengths and comparing phase relationships. The Decca system developed in England during World War II for aircraft navigation was probably the first system of this type used.

The Lorac (Long Range Accuracy System) is one of the better-known methods for determining the location of a mobile unit by comparing the phase relationship between two pairs of received signals. In this system, two c.w. transmitters are located at known points, and operate on the same fixed frequency. For any given distance apart of the two fixed stations, a chart may be plotted showing lines of constant carrier frequency phase difference. This is of a hyperbolic pattern. The indicating instrument in the mobile station measures the phase difference between the two fixed stations, and each 360 degree change in phase is called a *lane*. To establish position on any hyperbola of the chart it is necessary only to count the number of lanes when traveling from a known point. If a fix or position is desired, a second pair of transmitters is necessary, to allow a second set

of intersecting hyperbola to be plotted. In practice, two phase meter indicators are used aboard the mobile station to give the intersection of the two sets of hyperbolas.

The basic Lorac system requires six frequencies. A recent modification, the type-A Lorac, uses only four frequencies, so chosen that they occupy but two channels. The system uses four receivers and four transmitters.

The accuracy of the Lorac system depends upon the frequency. When operating in the 2000 kc band, a distance determination of ± 25.00 feet is possible. Two important characteristics of the system may be mentioned: (1) a slight shift in phase can be tolerated, which obviates the necessity of precise phase synchronization, and (2) the system can accommodate any number of users.

The Raydist† is another system based on phase measurement. The indicators may be located either in the mobile unit or at a fixed station. The equipment may be operated either as a simple range system or as an intersecting hyperbolic system.

For determining location along a given hyperbola, four transmitters and four receivers are required. Receivers R_1 and R_2 are preferably mounted aboard the mobile unit, with transmitter T_1. T_2 and R_3 are located at one fixed beacon station; while T_3, T_4 and R_4 are at another fixed beacon station. The frequency of T_1 differs from T_4 by an audio note, and the waves from both are heterodyned at a shore station R_3. This beat note modulates transmitter T_2, which signal is received by R_2. The phase difference of this signal depends upon the relative distance between T_4 to R_3 and T_1 to R_3. Since the distance of T_4 and R_3 remains fixed, the phase therefore depends upon the distance from the moving transmitter T_1 to R_3. A similar heterodyned note is received at R_4 from transmitters T_1 and T_4, and it is transmitted by T_3 to the receiver R_1. Likewise, the phase at R_4 depends upon the distance separating R_4 from T_1. An indication of the phase relationship between the two sets of receivers is obtained by feeding the output of R_1 into the rotor, and the output of R_2 into the stator winding of a synchro. A revolution counter geared to the synchro records the number of lanes traversed from any given point. In order to obtain a fix, a duplicate set of equipment is employed.

A more simple range Raydist system has been developed, using a c.w. transmitter and receiver at the fixed station and a similar transmitter and receiver aboard the mobile station. At each receiver a heterodyned note is produced between the distant transmitter and the adjacent transmitter. This beat note is then transmitted to the other receiver by means of a third transmitter, and is compared in phase with the locally produced signal. Distance of travel of the mobile unit is determined by recording the number of phase changes encountered from the known point of starting.

When listening to these beat frequencies, the rate of movement of the

† C. J. Deegan, "A Method of Surveying by Use of Radio Waves," *The Oil and Gas Journal*, July 7, 1949, pp. 69-91.

mobile station toward or away from the fixed station is indicated by the change in heterodyne frequency due to the well-known Doppler effect. The Raydist system permits only one user at a time, but improvements now appear possible whereby about 12 units may be used jointly, by allocating a different carrier frequency to each mobile unit, and filtering out the undesirable heterodyned signals. With the Raydist system operational accuracies of ± 25 feet may be obtained at ranges of 50 miles.

RESPONSIBILITY IN EXPLORATION

The primary thinking initiating any exploration program should be geological. The technical execution of the program rests primarily with the geophysicist. As the work progresses and the field data become available, interpretation must be based upon the best geological and geophysical probabilities. Here close teamwork between the geophysicist and the geologist is required. In many instances there has not been proper integration of the geological and the geophysical effort. A full exchange of information and ideas between the geologist and the geophysicist is essential for the most successful work. Although this section deals primarily with seismic prospecting, the same direction, cooperation, and integration are necessary in any geophysical program employing any technique. The fundamental problem is the interpretation of the geophysical observations in terms of economic geology.

The purpose of the exploration program is the discovery of new reserves, and one of the essentials in exploration is the skillful employment of technical personnel and capital. The more intelligently these resources of technology and capital are used, the more assurance there can be of success.

We often hear of dry holes drilled on seismic prospects which did not check with the initial interpretation. These are usually termed "busts" and the blame is placed on the geophysicist, where it should rest if he failed to gather the field data properly and to reduce it to the correct physical parameters. However in most instances the actual responsibility belongs to the geologist who fails to make a critical analysis of all the geological factors which may affect the interpretation as it proceeds from the physical parameters to the probable subsurface geology.* Many dry holes could be avoided if the geologist assumed his full responsibility in the exploration program. The history of exploration is replete with cases where dry holes furnished the basis for discoveries by another operator who took advantage of the error made by his less alert competitor.

To further the success of any exploration program, there is a general procedure which may be followed. It may logically be divided into five

* For discussion of such factors, the reader is referred to the excellent volume on case histories prepared under the able chairmanship of Henry C. Cortes: "Geophysical Case Histories," Society of Exploration Geophysicists, Vol. 1, 1948

stages: I, preparation; II, briefing; III, execution; IV, integration; and V, review.

I. The period of preparation includes a thorough study of all the available information on the geology of the district; an investigation of the availability and price of acreage; and an analysis of previous geophysical work in the area. If these are favorable, the next step is the selection of favorable prospects, and a careful analysis of these prospects to evaluate the physical and legal problems involved in carrying out the field work. The results of subsequent work can be no better than the prospects selected. And no matter how good the prospects, the program will fail unless a geophysical unit with good equipment, and skilled and cooperative personnel is employed.

II. The briefing stage consists of thoroughly acquainting the key geophysical personnel with the necessary geologic background of the prospect and its particular geologic problems. All maps and data should be graded as to reliability. The physical problems, including areas to be held back for bad weather, trespass problems, and the location of field headquarters should be thoroughly discussed. The field technique should be approved by both the geologist and the geophysicist after considering the previous factors.

III. The execution stage is of critical importance. Activities of the geophysical crew must be followed in detail so that maximum efficiency can be secured for the expenditure involved. Frequent consultation and full cooperation between the geologist and the geophysicist are absolutely essential during prosecution of the field program. The importance of this cooperation cannot be overemphasized. Lack of proper direction and liaison may doom the effort to failure.

IV. The integration stage is reached as the geophysical field reports, maps and data are submitted. This information must be reviewed, analyzed, and given its proper weight in the overall geologic setting by the geologist responsible for the work. Decisions must be reached for the subsequent field operations. Upon completion of the field work, the final analysis is made and a recommendation for action is necessary.

V. Finally, the data must be thoroughly reviewed following subsequent drilling, or, periodically, in the light of new geologic information which may become available. This process is continuous and never-ending. The basic data is usually in the geophysical records, but cannot always be correctly interpreted until additional geologic information is available. The geologist-geophysicist team must constantly rework the files of completed geophysical work if maximum advantage is to be secured from the money spent for exploration.

The procedure outlined here is neither new nor unique. There is no universal panacea for problems of exploration, nor is there any royal road to oil-finding. Nevertheless, if the general procedure suggested here is followed, optimum results are most likely to be obtained.

GENERAL OUTLINE FOR PLANNING SEISMIC EXPLORATION.

I. **Preparation** (prior to selection of method and employment of geophysical crew).

1. Check availability and price of acreage. Currently, the attractive acreage may be leased, but the lease may be short term or in the hands of an owner with whom a deal can be worked out.
2. Find out results of previous exploration work in the area, especially geophysical. Determine particularly which method has yielded best results and the extent of its use; check the completeness of the earlier geological and geophysical work.

   A. If seismograph appears to be the logical tool, find out whether refraction or reflection method can be better used.
   B. If reflection method appears to offer more promise, determine the best technique to use, i.e., correlation, continuous profiling, or dip shooting.
   C. From the probable geology and the previous history of the area, determine formations from which reflections or refractions can be expected.

3. Thoroughly investigate the geology of the area to be explored.

   A. Check cuttings, scout tickets, drillers' logs and electric logs for oil or gas showings in all wells in area.
   B. Check all correlations, particularly those to which geophysical work may be tied and those critical to the prospect.
   C. Determine intervals of convergence or divergence, unconformities, facies changes and possible faulting.
   D. Construct subsurface structure maps, preferably near and conformable to potential seismic reflecting or refracting horizons.
   E. Construct such isopach maps or cross sections as appear useful.
   F. Review carefully and in detail the literature of the area. This calls for an exhaustive search.
   G. Examine files for all possible previous geological or geophysical work in the area, including surface, core drill, old subsurface, seismograph, gravity, electrical and magnetic work. Analyze, evaluate and integrate this work into the subsurface studies.

4. Determine who drilled test wells in the vicinity of likely prospects, and when and why they were drilled. Oil fields are often found on prospects which have been condemned. Determine significance of these test wells.
5. Secure outlines of blocks of land previously acquired in the area and determine, if possible, the reason for acquisition.
6. After a critical analysis of all the above information, list all prospects developed, grading them according to promise based on all available information.
7. Secure available road maps, topographic maps, and aerial photos in vicinity of prospects to determine whether and how prospects can best be worked.
8. Investigate type and cost of equipment required for the work, the relative cost of various geophysical techniques and probable relative value of the data.
9. Investigate previous geophysical work of competitors in the area to determine how thoroughly prospects selected may have been worked, when, and by what method.
10. Attempt to secure services of a well-equipped, well-managed crew experienced in the area. Be certain that party will be adequately supervised by the contractor. Be sure you know interpretation facilities and experience. Results can be no better than interpretation.
11. Investigate permit costs and difficulties.
12. In foreign work, investigate the regulations pertaining to the transporting of men and equipment into and out of that country.

II. **Briefing** (Some of this responsibility may be assumed by geophysical department or coordinator if such facilities are available.)

When the most promising geophysical method has been decided upon and contracted for, arrange a conference with supervisor and party chief to:

1. Select headquarters of crew where minimum time will be lost in driving to and from work area. However, in selecting headquarters, consider morale of crew. Somewhat longer driving distance may be repaid in higher production if morale of crew is high.
2. Furnish all literature on area in which prospects are located. Brief the geophysicists on regional geology and geology of local prospects. Advise them of probable unconformities, intervals of convergence or divergence, facies changes, suspected faults. Be certain the man actually doing interpretation knows these things. Give him your theories.
3. Provide maps showing location of prospect areas, location of wells critical to the prospects and the geology of the area. Furnish electric, radioactive and/or sample logs with correlations of wells to which they are expected to tie. Grade and qualify all well data as to accuracy and reliability. If accurate correlations cannot be furnished, explain why.
4. Decide on method of shooting to be employed, whether refraction or reflection, correlation or continuous line, dip shooting, three dimensional control. Consider possibility of air shooting.
5. Lay out preliminary lines, making full use of the geophysicists' suggestions and recommendations. Lay out lines so that areas of possible reverse dip can be quickly confirmed or denied. Lines generally should be laid out normal to the strike. Consider the road network, but avoid roads in areas in which much work has been done by others. This may not be too important in difficult areas, but it may increase the problems of interpretation.
6. Furnish the geophysical crew with road maps, topographic maps and aerial photos of prospect areas.
7. Arrange to go into the field, if necessary, to determine what portions of prospects can be held back for inclement weather or season.
8. Advise the geophysicist the desired formations or zones from which to obtain reflections or refractions, and why. Certain important events may be brought out at the expense of less important ones. Shoot two or more records.
9. Check shot hole drilling difficulties. Often two or more drills may be economically advantageous.
10. Educate the field parties in the proper safe operating practices (truck driving, drilling, dynamite storage and transporting, shot-hole loading and firing, etc.). Assign an assistant to party chief to observe that all regulations are being followed. Party chief will be held responsible for safety of crew and equipment.

III. **Execution** (Part of responsibility can be assumed by geophysical department or coordinator if such facilities are available.)

1. Be certain that work assignments are sufficient, with careful planning to secure maximum efficiency of crew. Consult continuously with supervisor and party chief on their suggestions for assignments.
2. Maintain frequent contact with crew during work by telephone and trips to field.
3. Obtain progress maps for all horizons weekly. Plot your own progress map.
4. Obtain a weekly progress report, summarizing the work of all units of crew to be certain that each is being utilized to the best economic advantage.
5. Check costs continuously to see if an increase or decrease in personnel will reduce costs per unit area. Check particularly costs of items chargeable to your client.

6. If field shutdowns are frequent, determine cause and take steps to remedy situation.
7. Examine records frequently for quality. Carefully examine all sections for conformation of dips.
8. If records are poor, consult with party chief and supervisor to determine reason. If not the result of poor equipment, improper technique, weathering or surface conditions, poor records are very significant because they usually have geologic reason. A no-record (NR) hole or a lack of continuity in records may be of utmost importance if due to some geological condition, such as a fault zone, etc.
9. Discuss method of weathering and elevation corrections. Determine whether corrections are being made to sufficient depth. Estimate the limit of error in work.
10. Determine whether all possible reflections or refractions are being obtained, by judicious use of filtering, etc.
11. Assist in securing velocity surveys from wells in the area.
12. Remember that there are very few areas in which there has been much exploration activity where the roads have not been thoroughly worked by numerous crews. Therefore, if you expect to find anything new, get off the roads unless you are in areas of difficult transportation.

IV. **Integration** (after reports are submitted by the geophysicists)

1. Recontour the maps, using all available geologic data. Apply data to beds above and below. Velocities may be off. Reflections have no labels. Carefully examine all maps made on phantoms.
2. Construct isopach maps of all critical intervals, particularly from the shallowest to deepest reflections, to avoid anomalies resulting from weathering. The use of uncorrected time values often is preferable. Such maps may suggest areas for further work or erroneous structural interpretations.
3. Carefully examine cross sections for continuity and to see where dips fail to conform. If dips do not conform, possible explanations should be considered. Be certain dips have been migrated in steep dip areas.
4. Read the geophysical report carefully. Look for qualifications therein. Keep an open mind because your preconceived ideas of the subsurface might be wrong. Be willing to accept new, unique, and unconventional ideas.
5. Appraise the reliability of the work; analyze the results carefully to determine whether or not more work is necessary. Then assign the geophysical records their value in the overall geologic setting. Be certain *all* useful data on records have been utilized.
6. Make a recommendation for future exploration based on a careful integrated analysis of the geology and the geophysical work.
7. Select areas of interest in which additional work may be desirable.

V. **Review**

1. If prospect has been drilled, review the geophysical work in light of information furnished by drilling of the test well, whether productive or dry. If there are discrepancies, attempt to reconcile them in order to clarify the geologic picture.
2. Request review of seismic data if such action appears desirable.
3. Post all current well data and geology on the geophysical maps. If reinterpretation of the geophysical data appears desirable, request the necessary geophysical assistance. All data should be reviewed whenever new information becomes available.
4. The construction of a composite map showing the geophysical profiles or contours and the geology as developed by wells, etc., may be of considerable benefit.

5. When additional velocity surveys are available which differ appreciably from the original values used in interpretation, request the geophysicist to review previous data to determine effects upon structure.
6. Remember that the past history of exploration work proves conclusively that many undiscovered oil fields repose peacefully in old files, awaiting discovery. Such files offer a fertile field for good prospects.

This review process cannot be overemphasized. The basic data are usually on the seismic records but cannot always be correctly interpreted until additional geologic information is available. The geologist-geophysicist team must constantly review the files of completed seismic work if maximum advantage is to be secured from money spent for exploration.

SPECIAL APPLICATIONS OF SEISMIC METHODS

Shallow Exploration

The preceding text has treated seismic exploration as applied to the search for oil structures. There are also many problems in the fields of civil engineering and engineering geology which are amenable to the geophysical approach. These problems may be classified under the heading of shallow geophysical prospecting, because the sought-for deposits or the geological conditions involved are near-surface features. The distinguishing condition of this type of geophysical exploration is the very small depth involved—from tens to a few hundreds of feet only, in contrast to the usual thousands of feet in seismic exploration for oil structures.

Finding the depth to bed rock at a dam site is, for all practical purposes, merely a solution of the "weathering" problem with a different application. Standard geophysical field equipment can be used with little or no modification and with only minor variations in the field procedure. The major change required is in the point of view of the geophysicist. He must become accustomed to thinking in terms of localized near-surface geologic problems rather than deeper basin-wide structures.

In many cases a surprisingly small amount of geophysical field work will solve completely or aid materially in the solution of various problems which confront the engineering geologist in the examination and selection of dam sites and in other phases of his work. Examples are the location of an intrusive dike not visible on the surface or the comparison of depth to bed rock at various sites. Likewise a knowledge of the extent of a strategically-located gravel deposit, which can often be obtained by geophysics, is of great value to the materials engineer who is searching for a source of concrete aggregate.

Questions of a geologic nature which can be answered by geophysical studies may be quite critical in determining the feasibility of a project. In one such case, the depth to bed rock and the course of a buried glacial gorge were determined by seismic refraction work. It was found that the bed rock was relatively shallow and that water impounded in the reservoir behind a proposed dam would *not* be bypassed through the gorge and around the dam, as had been feared.

The engineering and geological data needed to solve such problems may, in many cases, be secured by geophysical investigations at less expense and more quickly than by other means, such as drilling, test pits, trenching, hand auger holes, etc.

Geophysical work in connection with geological engineering problems has been carried on for some years by several federal and state governmental agencies. These include the U.S. Bureau of Reclamation, the Corps of Engineers, the U.S. Bureau of Mines, the U.S. Geological Survey, and the U.S. Bureau of Roads, as well as a number of state geological surveys and highway departments. Similar use of refraction profiles was made in the investigations conducted in connection with the atomic bomb tests of 1946, to obtain information on the subsurface structure of Bikini Atoll. For this work, naval depth charges were fired on the lagoon bottom along four lines across the atoll, and the refractions were picked up by water-coupled seismometers.† Similar exploration has been done by many consulting geophysicists and by institutions of higher education having courses in exploration geophysics. It is pertinent that this field of engineering geophysics is in its infancy.

Instruments and Methods.—The geophysical instruments employed in shallow prospecting are essentially those used in oil and mining exploration. With but minor exceptions, no instrumental changes are required, since the same physical quantities and variations are measured. The techniques of application are practically identical, except that the station spacing and the areas covered are smaller in engineering geophysics than in petroleum geophysics.

The equipment generally comprises a 6- to 12-trace camera, for shallow refraction shooting, with film speeds of about 15 to 20 inches per second. Automatic gain control and filtering are seldom advantageous. Standard geophones are satisfactory, but the natural periods should be about 10 cps. Portable equipment is desirable, with daylight loading and developing facilities.

Drills are not required, as the shot holes are dug with a shovel or hand auger. Powder charges are small, usually from ½ to 2 pounds of dynamite. In some cases, the blasting cap alone or a hammer blow will furnish sufficient energy to produce a good useable record.

The spread lengths are generally from 200 to 1500 feet, with seismometers spaced 25 to 150 feet apart. The stations are spaced as required, usually about equal to the depth of investigation. Refraction profiles are generally run across the area, and interpretation is based upon breaks in the travel-time curves.

The accuracy of this type of refraction work is generally ± 5 per cent of the depths obtained by drilling. The crew personnel usually comprises

† M. B. Dorbin, B. Perkins, Jr., and B. L. Snavely, "Subsurface Constitution of Bikini Atoll as Indicated by a Seismic-Refraction Survey," *Bulletin of the Geological Society of America,* Vol. 60, May, 1949.

a geophysicist, an observer, a surveyor and one or two helpers. Computation of records is usually done in the evening. The speed of the work varies with terrain and other working conditions, but generally averages 4 to 10 stations or 2 to 4 spreads per working day. The cost of a crew is from $2,500 to $4,000 for a 20-working-day month (1949 base price). A geologist or mining engineer familiar with the area usually can render valuable aid in planning the work and in the interpretation of the geophysical data in terms of the economic geology.

Del Norte Dam Site, Colorado

A seismic refraction survey of the Del Norte Dam Site was made under the direction of E. L. Current, of the United States Bureau of Reclamation, in October, 1943.†

The details of this survey illustrate some of the numerous factors which must be considered by the geologist and the geophysicist in the exploration of dam sites, and they are presented for that reason.

The site is located at the town of Del Norte on the western edge of the San Luis Valley. The axis of the proposed dam cuts across the edge

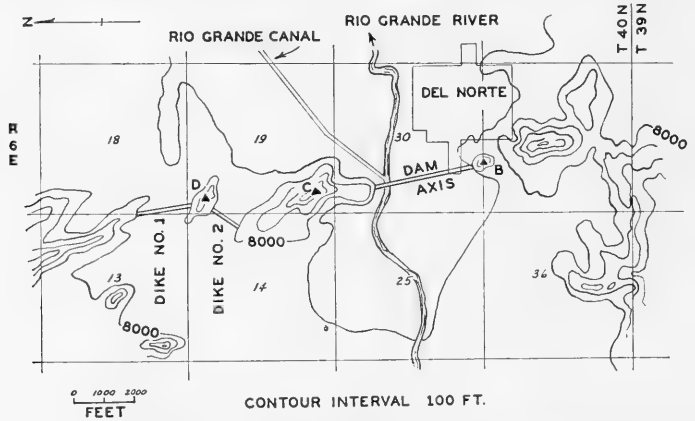

Fig. 570.—Map of Del Norte Dam Site, Rio Grande County, Colorado. (Courtesy U. S. Department of Interior, Bureau of Reclamation.)

of the town itself. Details of the location are shown in Figure 570. An earth dam with a crest length of 4,400 feet was proposed, to impound one million acre-feet of water. Two dike sections approximately 1,000 and 2,000 feet long respectively were involved, in addition to the main dam, which would require a total of some 10.6 million yards for the entire project.

Geology.—The dam site and the reservoir area cover rocks of Miocene age, represented by the Sheep Mountain and Conejos formations.

† E. L. Current, "Report on Geophysical Survey of the Del Norte Dam Site, San Luis Valley Project, Upper Rio Grande Basin," Oct., 1943. (Files of Geology Section, U. S. Bureau of Reclamation, Denver, Colorado.)

At the dam site, the Sheep Mountain formation is an andesite or andesite-latite flow which overlies andesite-basalt breccias and agglomerates of the Conejos formation. The andesite flows dip 10 to 15 degrees to the east, with occasional irregularities where the dip is to the southeast or to the northeast.

These two formations both form steep cliffs which extend to the flood plane of the river in some cases. In places the lower sections are covered by talus material and by alluvial fans. The Rio Grande River has eroded through the flows and breccias to a depth of about 150 feet. The valley floor is generally covered with 3 to 6 feet of loam, but numerous gravel deposits are visible. Beneath the topsoil, the valley fill is made up of well-rounded, moderately clean gravels, sand, and cobbles separated by lenses of clay.

Reservoir Area.—The reservoir area is enclosed by andesites and breccias which in general dip away from the reservoir basin. The andesites are fairly dense and show not more than the usual amount of jointing common for such rocks. The breccias are often interbedded with andesite flows and show little jointing or fracturing. Seepage losses should be small, as the andesites and breccias are usually well blanketed.

Left Abutment (Looking Downstream).—The left abutment is a steep cliff, the lower portion composed of a hard, coarse, tight breccia. The upper section, which is probably above the maximum flow line, is fairly dense, hard andesite. Both types of rock should be adequate for the dam proposed.

Right Abutment.—The right abutment is also a steep cliff of andesite which overlies a section of breccias. The latter are exposed on the west side of the ridge which forms the abutment. The andesite probably extends ± 50 feet beneath the flood plane of the river to the north. Beyond this point the abutment rock is breccia. Both of these rock types should prove sufficiently tight and stable.

Foundation Area.—The foundation area is a breccia, or andesite-latite, or possibly a combination of both. It is overlain by about 150 feet of sand gravels, cobbles and clay. The foundation rock is tight and stable enough for a dam. The water table is very near the water surface of the river at the dam site. The seismic wave velocity in the saturated overburden was 6,900 feet per second, which is higher than usual for such material. This may indicate that some of the overburden may be stable enough to be left in place. It appears to be sufficiently free-draining so that at least that portion of it at the downstream toe of the dam would not have to be removed. Drilling would be necessary to establish the presence or absence of clay or ash lenses, and the stability of the overburden.

Spillway and Outlet Diversion Tunnels.—The low saddle on the left abutment should be considered for the spillway location. Here a spillway would rest on hard andesite, but it should be lined. The only stripping necessary would be the removal of the surface weathered zone of about 5 feet.

From a geological standpoint the outlet tunnel could be placed on either side of the river. The rocks of both abutments should prove suitable for tunneling.

Dike No. 1.—The abutments of this dike section are fairly hard andesite, and the foundation rock is probably breccia. The overburden has a maximum thickness of ± 84 feet and consists of light gravels, sands and silts.

Dike No. 2.—This dike section is similar to the other except that the left abutment is a breccia. The overburden is similar but shallower, ± 55 feet.

Construction Materials

Impervious embankment material is plentiful. Graded gravels, sands and silts 3 to 6 feet deep cover the valley floor, while deeper deposits (± 15 feet) are to be found on the terraces above the flood plane.

Free draining material (gravels and cobbles) can be found in the river channel beneath the top soil. The terrace area between the main river and the Rio Grande Canal to the east of the dam site should also be considered. Here gravels underlie only 2 to 3 feet of the top soil, and the deposits should be satisfactory for aggregate. They are within one mile of the site of the dam.

Riprap can be quarried from any of the adjacent andesite or breccia hills.

Results of Seismic Survey

The maximum depth to the bed rock of andesite or breccia was 136 feet, as determined by seismic refraction traverses at the Del Norte Dam Site. However, bedrock may be deeper than this near the center of the present flood plane, which was not accessible for geophysical work. Depths to bedrock were also determined in the dike sections. The maximum depth at Section No. 1 was 84 feet and at Section No. 2, 55 feet. The geology and the geophysical depth points are shown in the two cross-sections which form one continuous line in Figures 571 and 572.

It is of note that no drill control was available to check the bedrock depths predicted. They appear to be reasonable, although even one drill hole would have removed any uncertainty in this respect. The geophysical survey is therefore of a reconnaissance nature, although velocity determinations in the exposed outcrops of bedrock material in work of this kind are often useful for control.

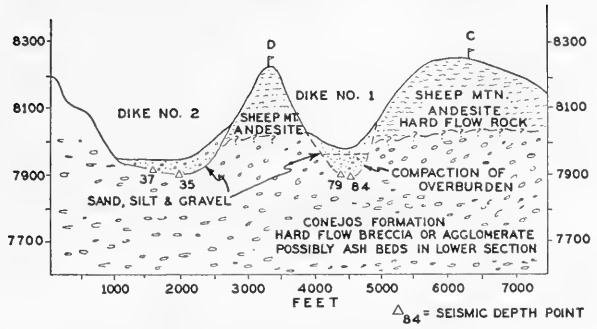

Fig. 571.—Profile, Del Norte Dam Site, Dike Section. (Courtesy of U. S. Department of Interior, Bureau of Reclamation.)

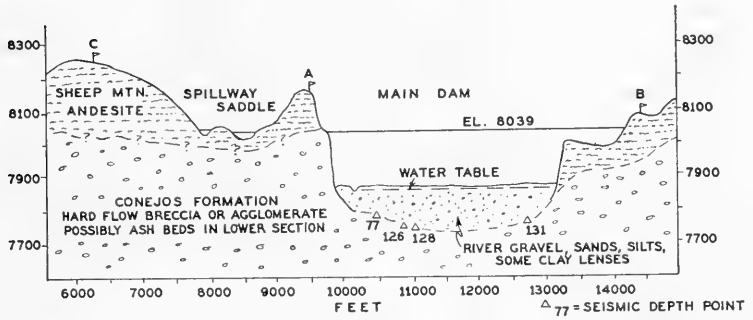

Fig. 572.—Profile, Del Norte Dam Site, Main Dam. (Courtesy of U. S. Department of Interior, Bureau of Reclamation.)

Reconnaissance Geophysical Survey of Three Alternate Dam Sites, on the Smoky Hill River, Kansas

A reconnaissance survey with the seismic refraction method was made by John Baird, of the U.S. Bureau of Reclamation, in November, 1941, covering 3 proposed dam sites on the Smoky Hill River in western Kansas. The geophysical work was strictly of reconnaissance nature, as no drilling was done with which to correlate and verify the seismic determinations of bedrock depth. The exploration made it possible, however, to compare the 3 sites at a minimum cost and in a very short time, which is advantageous in the planning stages of river basin development.

The dam sites investigated were located in Grove and Logan Counties, Kansas, about 23 miles from the town of Oakley. One site lay at Elkader, and was called the Elkader Site. The second site, below Elkader, was known as the Elkader Alternate No. 2 Dam Site. The third site, 7½ miles downstream from Elkader, was designated as the Pyramids Dam Site.

Geology.—The general area is part of the typical uplands of western Kansas, having a considerable thickness of Tertiary beds at the surface.

These are characterized by the "mortar beds" which are often aquifers.

The Smoky Hill River has its origin in eastern Colorado and flows eastward. In this part of Kansas it has cut a wide valley through the Tertiary cover down to the underlying Cretaceous Niobrara chalk formation. This allows the ground water in the Tertiary sediments to form numerous springs along the river. Since the area is one of limited and intermittent rainfall, these springs form the only firm and permanent water source for the streams.

The bedrock at the three sites was the Niobrara formation, which here consisted of blue-gray massive chalk beds and alternating shaly chalk horizons. The overburden at the sites varied from a sandy loam at higher elevations along the proposed axes to sand and gravel in the river bottoms. The stream itself was wide and slow-moving, indicative of old age and aggradation of the channel. The river bed was from 150 to 200 feet wide at the sites studied.

Geophysical Results

Elkader Dam Site.—The results of the bedrock depth determinations by the seismic refraction method are shown in the profile in Figure 573, from which the surface elevations and bedrock depths may be deter-

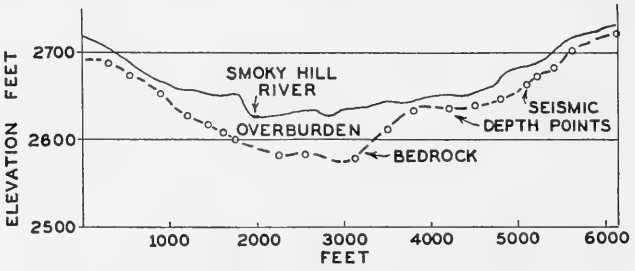

Fig. 573.—Profile, Elkader Dam Axis. (Courtesy U. S. Department of Interior, Bureau of Reclamation.)

mined for points along the proposed axis. The depth points plotted along the bedrock line were geophysically determined, and the rock line was drawn between them in what appeared to be the most logical manner.

The profile shows that the bedrock surface was covered by a relatively thin overburden near the abutments which became thicker in the river valley bottom. The maximum depth of 60 feet was reached at a point 3,100 feet from the left abutment. Across the valley the depth varied from this maximum to 35 feet.

Elkader Alternate No. 2 Dam Site.—The bedrock profile along the proposed axis at this site is shown in Figure 574. It appears that the overburden thickness is somewhat greater than at the Elkader site, as it varies from 57 to 70 feet. As evident from a comparison of Figures 573 and 574, the conditions at the abutments at the two sites are very similar.

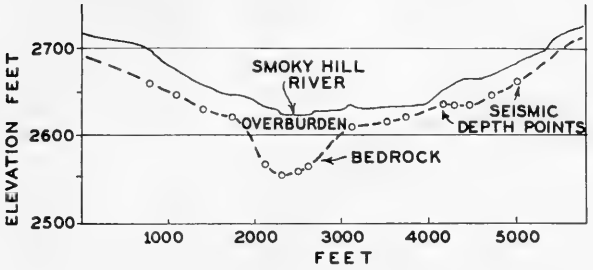

Fig. 574.—Profile, Elkader Alternate No. 2 Dam Axis. (Courtesy U. S. Department of Interior, Bureau of Reclamation.)

Pyramids Dam Site.—The geophysical results at this site are shown in Figure 575, which brings out that the average depth to bedrock is considerably greater than at the Elkader site. The maximum depth found was 72 feet. The most important difference between the Pyramids and the Elkader sites is the 10-foot greater overburden thickness at the abutments in the former.

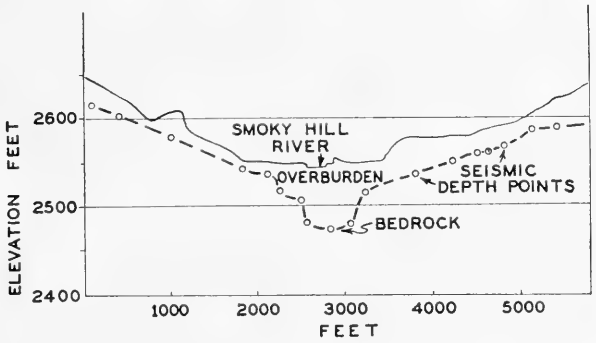

Fig. 575.—Profile, Pyramids Dam Axis. (Courtesy U. S. Department of Interior, Bureau of Reclamation.)

Differences in the depth to bedrock are the only basis of comparison of the three sites derived from the geophysical survey. The Elkader site therefore would be the most desirable, since the bedrock was at a minimum depth.

Exploration of a Buried Channel, Cedar Bluff Dam Site, Ellis County, Kansas

Geophysical investigations of a buried channel at the Cedar Bluff Dam Site, Ellis County, Kansas were made in September, 1948, using the seismic refraction method. The Cedar Bluff Dam on the Smoky Hill River is one of the units of the Missouri Basin Project, U.S. Bureau of Reclamation.

The purpose of the geophysical work was to trace the subsurface course of an old buried channel which cut across the proposed axis of the dam on

the left abutment. Evidence of the existence of this so-called preglacial channel had been found by core drilling. Where the channel crossed the axis of the proposed dam, it was about 1,000 feet wide and some 60 feet

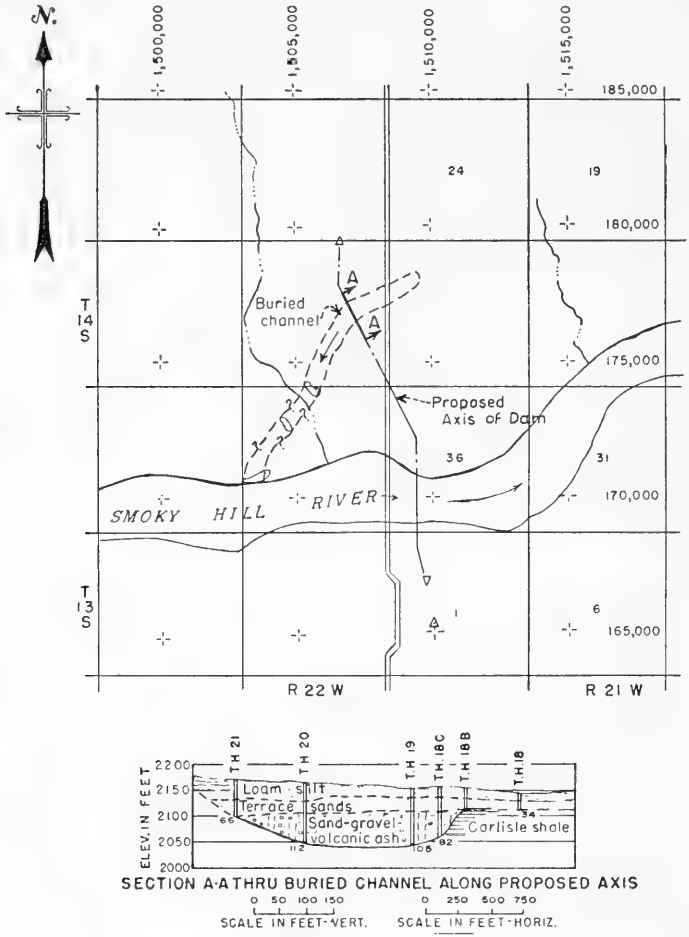

Fig. 576.—Cedar Bluff Dam Site, Ellis County, Kansas. (Courtesy Dart Wantland, U. S. Department of the Interior, Bureau of Reclamation.)

deep in the shale bedrock surface. Bedrock in the channel itself was at a depth of about 110 feet. These features are shown on the location map and cross-section of Figure 576.

An examination of the core-drill logs from holes drilled along the axis

and the results of special pumping tests indicated that the channel was filled with rather pervious material consisting of volcanic ash, sand, gravel, and some clay. It was feared that the buried channel, after crossing the axis from the west or upstream direction, might turn sharply to the south and follow along the downstream toe of the proposed dam, thus creating a potentially serious condition by providing a short leakage path for water from the reservoir.

Twenty seismic spreads were completed in 13 days, and about 90 bedrock depth measurements were made. An area approximately 3,500 feet long by 2,500 feet wide was covered in sufficient detail that the shale bedrock and the buried channel could be shown by contours. The desired information was obtained more quickly and at less expense than would have been possible by drilling. A seismic bedrock depth point costs about $30, as compared to an estimated cost of over $3 per foot for core drilling; the average depth of the core holes would be over 75 feet.

The depth to bedrock from existing core holes was used as control for the interpretation of the geophysical measurements. Where seismic depth points were in the vicinity of these drill holes, it was found that the calculated depth to the shale checked with the depth obtained from drilling within about 5 per cent.

As the work progressed, it became apparent that the supposed old channel was simply an erosion feature on bedrock, or a buried drainage, and that its preglacial origin was uncertain. The bedrock contours showed that the course of this drainage was in a northeast-southwest direction where it crossed the proposed axis and that it drained into the Smoky Hill River from the northeast. The seismic studies indicated definitely that the channel does not have an outlet near the downstream toe of the dam. Therefore it could not provide a leakage path for water from the reservoir.

The map of the shale bedrock surface, contoured on an interval of 10 feet, was comparable in degree of detail to the usual surface topographic map. It gave a subsurface topographic picture of bedrock. This suggests that with some drill control the seismic-refraction method can be used to provide information on the configuration of bedrock at dam sites, so that the proposed axes can be located in relation to bedrock topography in much the same manner as they are fitted to surface topography.

Investigations of Soil Dynamics

Analysis of the dynamic constants of soil furnishes useful information for determining load-bearing capacity. In the past, foundation and load-bearing studies had been principally conducted by static load methods, which are relatively expensive and oftentimes inadequate or misleading in their results. The dynamic methods usually can be applied more economically to obtain data on the load-bearing capacity of the soil as well as its behavior under vibrations such as are produced by earthquakes.

To determine dynamic constants, the site under investigation is sub-

jected to alternating mechanical forces by use of a special type of oscillator.† The soil is set vibrating in forced and damped oscillations, having any desired frequency and amplitude, by adjusting the frequency of alternation and the magnitude of the applied forces. Furthermore, by employing seismographs to record the motion of the soil, various characteristics of the motion are measured and the data thus obtained are used to draw inferences on the bearing capacity, composition, natural period, and compressibility of the soil.

Operating Principles

The oscillator for producing the artificial vibrations usually comprises two discs or cylinders revolving in opposite directions and provided with eccentric loading. (Figure 577.) The magnitude of the centrifugal

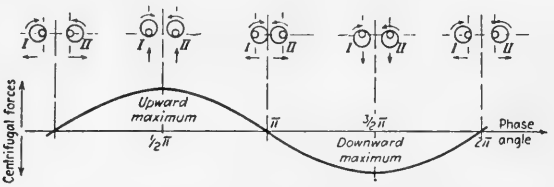

FIG. 577.—Oscillator for producing artificial vibrations. (Bernhard, *A.I.M.E. Geophysical Prospecting*, Tech. Pub. 834.)

forces produced by the rotation of the discs depends on the eccentricity of the loading, and the frequency of alternation of the forces depends upon the speed of rotation. Usually, the horizontal centrifugal forces are neutralized and only the vertical forces are utilized in the studies.

The dynamic properties of the soil may be determined by measuring: (a) the amplitude of the soil motion at the oscillator; (b) the amplitude of the soil motion at various distances from the oscillator and at various depths; (c) the time phase difference between the applied (oscillator) forces and the vibration on or in the soil; (d) the settlement of the oscillator on the soil; and (e) the natural period of the site.

The soil motion characteristics enumerated above are related to the magnitude and frequency of alternation of the exciting forces. To simplify the analysis, the following assumptions will be made:‡ (1) The oscillator is a small mass vibrating on the surface of a semi-infinite elastic medium. (2) Vertical forces only are effective. (3) The damping is proportional to the speed of propagation of the disturbance. (4) The deformation of the soil varies linearly with load and settlement.

---

† R. K. Bernhard, "Geophysical Study of Soil Dynamics," *A.I.M.E. Geophysical Prospecting*, Tech. Pub. 834, Feb. 1938.

‡ Bernhard, *loc. cit.* See also, A. Hertwig, G. Angenheister, R. Koehler, and A. Ramspeck, "Application of Dynamic Soil Investigation," *Trans. German Soc. Research in Soil Mechanics* (Degebo) (1936) No. 4.

Corresponding to these assumptions, the equation of motion of the vibrating element is :†

$$m\frac{d^2x}{dt^2} + K\frac{dx}{dt} + cx = P\sin\omega t$$

where m = mass of vibrating element = mass of oscillator plus a small amount of soil directly under the oscillator.
x = amplitude of vibration.
t = time.
K = coefficient of friction.
c = elastic coefficient (force in pounds required to deflect the system one inch).
ω = frequency of oscillator.
$P\sin\omega t$ = centrifugal force of rotating disc oscillator.

The maximum amplitude a of the disturbance is given by the equation:

$$a = \frac{P}{m\sqrt{(\omega_0{}^2 - \omega^2)^2 + 4\delta^2\omega^2}}$$

where ω_0 = natural frequency of the vibrating element

$$\delta = \text{damping} = \frac{K}{2m}$$

The phase difference ϕ between the exciting force and the amplitude of the motion is given by the relation

$$\tan\phi = \frac{2\delta\omega}{\omega_0{}^2 - \omega^2}$$

The resonance point of the soil adjacent the oscillator may be determined by measuring the amplitude of the motion—as recorded by a seismograph located near the oscillator—for various frequencies, i.e., for various values of ω and by plotting an amplitude versus frequency curve. The *resonance frequency* may also be determined by measuring the settling or movement of the oscillator for various frequencies of the oscillator and plotting a settlement versus frequency curve.

The empirically established correspondence between natural frequency and bearing capacity or allowable soil pressure is given in Table 25.

The soil adjacent the oscillator will be set into vibration at its *natural* or *resonance* frequency for a particular value of the oscillator frequency. However, this soil, as well as the remainder of the soil constituting the elastic medium, will undergo *forced* vibrations for any frequency of the oscillator.

Corresponding phases of the waves impinging on two seismometers located at different distances from the oscillator arrive at different times. Hence, the velocity of the wave in the soil under investigation can be

† cf. p. 788.

determined by measuring the time phase difference of two corresponding maxima or minima, the velocity being obtained from the relationship:

$$V = \frac{T_2 - T_1}{x_2 - x_1}$$

where T_1 and T_2 are the times for corresponding maxima or minima on the traces and x_1 and x_2 are the distances from the seismometers to the oscillator. The correspondence between wave velocity and allowable soil pressure is also shown in Table 25.

Oscillators of this type may also be employed for shallow structural investigations to determine depths to bedrock, dip of contact, etc., by the techniques utilized in general refraction studies.

TABLE 25

CORRESPONDENCE BETWEEN WAVE VELOCITY, NATURAL FREQUENCY AND ALLOWABLE SOIL PRESSURE†

Test No.	Formation of Soil	Phase Speed, Miles per Hr. (Frequency 20 to 25 Cycles per Sec.)	Natural Frequency, Cycles per Sec.	Allowable Soil Pressure, Lb. per Sq. In.
1	10 ft. marshland on sand	180	4.0	0
2	Very fine sand	245	19.3	14
3	Tertiary clay, moist	290	21.8	
4	Clay sand	310	20.7	
5	Medium sand, moist	310	21.8	28
6	Jura clay, moist	335		
7	Old sand and cinder	355		
8	Medium sand in water	355		28
9	Medium sand, dry	355	22.0	28
10	Argillaceous sand	380	22.6	36
11	Gravel with stones	400	23.5	36
12	Clay, moist	420	23.5	
13	Marl boulder	420	23.8	42
14	Fine sand with 30 per cent medium sand	420	24.2	
15	Clay sand with lime inclusions	445	25.3	
16	Medium sand, undisturbed	490		57
17	Marl	490	25.7	57
18	Keuper sandstone, soft	560		
19	Diluvial loess, dry	580	23.5	
20	Gravel under 12 ft. sand cover	730		64
21	Gravel, dense	940	30.0	64
22	Sandstone, disintegrated	1120	32.0	⅔ of the allowable compression strength
23	Keuper sandstone, medium hardness	1450		
24	Sandstone, undisturbed	2450		

Investigations of Pressures on Rock Pillars of Underground Mines.—A sonic method for determining the pressure on pillars in underground mines has been proposed which requires, first, laboratory determinations of the variation of the velocity of sound with pressure in samples of rocks taken from mine pillars and, second,

† Bernhard, *A.I.M.E. Geophysical Prospecting*, Tech. Pub. 834.

measurements of the velocity of sound in the mine pillars from which the laboratory samples were taken. From a knowledge of the velocity of sound in a particular rock as a function of pressure (laboratory measurement) and the velocity of sound in an underground pillar composed of the same rock (mine measurement), the pressure on the underground rock pillar can be inferred. †

A direct and relatively simple method for measuring the variation of elastic wave velocity with pressure utilizes rocks cut in the form of rectangular prisms. Known amounts of pressure are applied to the ends of the rock specimen by means of a mechanical press. The prism of known dimensions and density is caused to vibrate in one of its fundamental modes of vibration and the frequency of vibration is determined. The elastic wave velocity for any pressure can be computed from well-known relationships expressing the velocity as a function of frequency, density, and geometrical dimensions. For example, if the prism is supported at its ends and if the driving force is applied at the center of the prism so as to cause the prism to vibrate as a unit with its two points of support as nodal points, the elastic wave velocity V of the prism material is given by the relation

$$V = \frac{2\sqrt{12}\,L^2 f}{\pi t}$$

where L is the length of the column, f the frequency of vibration, and t the thickness of the column.

Earthquake Insurance.—The appalling loss of life and the damage to property caused by earthquakes has led the governments of several countries, notably the United States, Japan and Germany, to institute investigations of methods of minimizing this damage.* Studies of the damage produced during the San Francisco earthquake of 1906, the Santa Barbara earthquake of 1925, and the Long Beach earthquake of 1933, have shown that the damage was due largely to the collapse of poorly constructed structures not designed to withstand earthquake forces and to fires which could not be controlled because of the failure of water supplies. These studies, therefore, indicated that one very important method of minimizing the damage is to construct buildings in earthquake areas which are as earthquake-resistant as feasible.‡ From an engineering design viewpoint, this is accomplished by so constructing the building that it will not be markedly affected by the natural frequency of vibration common to earthquakes in the area.

An important economic problem associated with earthquakes concerns insurance. Logically, earthquake insurance rates for buildings in a given area should vary according to their susceptibility to earthquake damage. For example, if the natural period** of vibration of a building is the same as the ground period set up by most earthquakes in the area in which the

† L. Obert, "Measurement of Pressures on Rock Pillars in Underground Mines," U. S. Bureau of Mines, Report of Investigations 3444, April, 1939.

* It has been estimated that during the last two centuries on the average some thirty thousand persons were killed each year by earthquake phenomena.

‡ M. H. Gilmore, "Earthquake Investigations," *Geophysics*, Vol. II, No. 3, July, 1937, pp. 253-264.

** It will be recalled that the period of a vibration is equal to the reciprocal of the frequency.

building is located, a dangerous condition of resonance may be anticipated during the earthquake and the insurance premium correspondingly should be high. Furthermore, it is reasonable to expect that if the periods of the ground, the building, and the earthquake are approximately equal, a more dangerous resonance may be set up in the structure than would be the case if these periods were substantially different.

An evaluation of the earthquake-resistant properties of a particular building or structure requires, therefore, a knowledge of: (1) the dominant or most common periods of the earthquake waves in the area, (2) the natural period of the ground on which the building is located, and (3) the natural period of vibration of the building.

The first of the above factors can be deduced from a statistical analysis of earthquake records obtained at permanent seismological stations. Thus, Professor B. Gutenberg deduced from an analysis of numerous records that the following earthquake wave periods are most common in California: 0.2 to 0.3 sec., 0.5 to 0.6 sec. and 1.0 sec. The second factor (natural period of the ground) may be determined by an application of seismic methods, as described in the section on soil dynamics investigations. The third factor (natural period of vibration of the building) can be determined by putting controlled vibrations into the building. The oscillator used for this purpose is of the type previously described, except that much smaller energy is necessary. The natural frequency of the structure under test is determined by plotting a frequency-amplitude curve for the building and noting the frequency corresponding to maximum amplitude.*

To check buildings for damage, their periods must be redetermined after a severe earthquake. If the period has increased appreciably, the building probably has suffered considerable structural damage which may not be apparent always from a visual inspection of plaster or masonry cracks.

SEISMIC METHODS

UNITED STATES PATENTS

859,123	Issued July 2, 1907. Johann Schütte. "Instrument for Recording and Measuring Vibrations."
1,095,022	Issued April 28, 1914. Thomas O'Brien. "Seismograph."
1,194,376	Issued Aug. 15, 1916. H. J. Furber, Jr. "Apparatus for Ascertaining the Relative Locations of Distant Points."
1,227,114	Issued May 22, 1917. George A. Campbell. "Electrical Receiving, Translating, or Repeating Circuit."
1,240,328	Issued Sept. 18, 1917. Reginald A. Fessenden. "Method and Apparatus for Locating Ore Bodies."
1,406,445	Issued Feb. 14, 1922. C. A. Culver. "Photographic Receiving Apparatus."
1,451,080	Issued April 10, 1923. Ludger Mintrop. "Field Seismograph."
1,552,186	Issued Sept. 1, 1925. John A. Anderson. "Seismometer."
1,578,998	Issued Mar. 30, 1926. John J. Jakosky. "Shot-Firing System."
1,599,538	Issued Sept. 14, 1926. Ludger Mintrop. "Geological Testing Method."

* Governmental agencies have measured the natural periods of several hundred buildings and many water towers and dams.

1,669,135 Issued May 8, 1928. Karl Ludwig Kithil. "Seismo-Vibrometer."
1,672,495 Issued June 5, 1928. Burton McCollum. "Method and Apparatus for Determining the Contour of Subterranean Strata."
1,672,892 Issued June 12, 1928. Karl Ludwig Kithil. "Seismo-Vibrator."
1,706,066 Issued Mar. 19, 1929. J. C. Karcher. "Method and Apparatus for Locating Geological Formations."
1,743,358 Issued Jan. 14, 1930. J. G. Koenigsberger. "Method of Locating Salt or Rock Layers."
1,774,379 Issued Aug. 26, 1930. J. H. Jones. "Seismograph and Applicable to Other Measuring Instruments."
1,782,445 Issued Nov. 1930. Frank Rieber. "System and Method for Geophysical Exploration."
1,784,415 Issued Dec. 9, 1930. Hugo Benioff. "Electrical Recording Seismograph."
1,784,439 Issued Dec. 9, 1930. Harvey C. Hayes. "Method for Making Subterranean Surveys."
1,790,080 Issued Jan. 27, 1931. A. N. Stanton. "Method of Seismological Research."
1,814,444 Issued July 14, 1931. Harvey C. Hayes. "Geophysical Method and Apparatus."
1,825,554 Issued Sept. 29, 1931. Guy A. Rupp & Walter O. Snelling. "Seismometer."
1,827,371 Issued Oct. 13, 1931. Frank Rieber. "Method & Means for Geological Explorations."
1,832,901 Issued Nov. 24, 1931. H. C. Harrison. "Measurement of Mechanical Impedance."
1,842,968 Issued Jan. 26, 1932. Sepp Horvath. "Seismograph."
1,843,725 Issued Feb. 2, 1932. John C. Karcher. "Determination of Subsurface Formations."
1,848,490 Issued Mar. 8, 1932. A. M. Nicolson. "Stress Measuring."
1,864,214 Issued June 21, 1932. O. Scott Petty. "Instrument for Detecting Vibrations."
1,869,828 Issued Aug. 2, 1932. James E. Shrader. "Device for Measuring and Recording Vibrations in Three Directions Simultaneously."
1,872,504 Issued Aug. 16, 1932. Cullen R. Rogers. "Electrical Geological Disturbance Detector."
1,878,029 Issued Sept. 20, 1932. Orley H. Truman. "Underground Exploration Method."
1,880,425 Issued Oct. 4, 1932. Paul B. Flanders. "Measurement of Mechanical Impedance."
1,899,970 Issued Mar. 7, 1933. Burton McCollum. "Seismic Method of Profiling Geologic Formations."
1,909,205 Issued May 16, 1933. Burton McCollum. "Seismic Method of Profiling Geologic Formations."
1,919,917 Issued July 25, 1933. Orley H. Truman. "Geophysical Exploration Method."
1,923,088 Issued Aug. 22, 1933. Harvey C. Hayes. "Vibration Detector."
1,936,321 Issued Nov. 21, 1933. Richard Ambronn. "Process of and Device for Detecting and Measuring Minimum Accelerations."
1,943,725 Issued Jan. 16, 1934. Oscar E. Dudley and Con Lucid. "Method of Creating Artificial Seismic Waves."
1,959,004 Issued May 15, 1934. John E. Owen. "Method for Surveying Subsurface Formations."
1,978,668 Issued Oct. 30, 1934. Kenneth E. Burg. "Method of Determining Geological Structure."
1,983,483 Issued Dec. 4, 1934. Franz J. G. Neumann and Werner R. Haubold. "Apparatus for Making Geophysical Measurements."
1,998,412 Issued April 15, 1935. Harold R. Prescott. "Method of Making Geological Explorations."
2,003,780 Issued June 4, 1935. William T. Born. "Seismic Surveying."
2,008,857 Issued July 23, 1935. Paul B. Flanders. "Mechanical Impedance Meter."
2,018,737 Issued Oct. 29, 1935. John E. Owen. "Seismic Surveying."
2,018,756 Issued Oct. 29, 1935. Ludwig W. Blau, Morris M. Slotnick & Louis Statham. "Compound Seismograph."
2,021,943 Issued Nov. 26, 1935. Burton McCollum. "Seismic Method for Profiling Geologic Formations."

2,024,921 Issued Dec. 17, 1935. William G. Green. "Method of Determining Slope of Subsurface Rock Beds."
2,028,286 Issued Jan. 21, 1936. Earle W. Johnson. "Seismic Surveying."
2,046,104 Issued June 30, 1936. L. W. Blau & L. Statham. "Method and Apparatus for Seismic Prospecting."
2,049,236 Issued July 28, 1936. Benjamin B. Weatherby. "Surveying Underground Structures."
2,051,153 Issued Aug. 18, 1936. Frank Rieber. "Method and Apparatus for Recording Elastic Waves."
2,054,067 Issued Sept. 15, 1936. L. W. Blau & L. Statham. "Method and Apparatus for Seismic-Electric Prospecting."
2,055,476 Issued Sept. 29, 1936. L. W. Blau. "Seismic Prospecting."
2,055,477 Issued Sept. 29, 1936. L. W. Blau. "Electrical Circuits for Seismic Prospecting."
2,055,618 Issued Sept. 29, 1936. L. W. Blau. "Tamping for Explosives."
2,058,764 Issued Oct. 27, 1936. L. W. Blau. "Reflection Shooting Procedure for the Accurate Determination of Dip."
2,059,018 Issued Oct. 27, 1936. Willard North. "Subsurface Surveying."
2,062,151 Issued Nov. 24, 1936. Benjamin B. Weatherby. "Method of Making Subsurface Determinations."
2,062,784 Issued Dec. 1, 1936. William G. Green. "Seismograph."
2,063,820 Issued Dec. 8, 1936. K. L. McHenry. "Method of Recording Seismic Waves."
2,064,451 Issued Dec. 15, 1936. Vanderveer Voorhees. "Seismic Surveying."
2,067,636 Issued Jan. 12, 1937. Carl A. Heiland. "Vibration Detector."
2,081,350 Issued May 25, 1937. L. W. Blau. "Method and Apparatus for Eliminating Low Frequencies."
2,087,120 Issued July 13, 1937. H. Salvatori, et al. "Method of Making Weathering Corrections in Seismic Surveying."
2,087,702 Issued July 20, 1937. Leo J. Peters. "Method and Means for Recording Terrestrial Waves."
2,088,588 Issued Aug. 3, 1937. Oscar E. Dudley. "System of Geological Exploration."
2,089,983 Issued Aug. 17, 1937. Norman H. Ricker. "Method and Means of Geophysical Prospecting."
2,095,676 Issued Oct. 12, 1937. H. R. Prescott. "Method of Making Geological Explorations."
2,099,536 Issued Nov. 16, 1937. J. Neufeld & S. A. Scherbatskoy. "Method and Apparatus for Seismic Prospecting."
2,099,837 Issued Nov. 23, 1937. L. W. Blau. "Seismic Reflection Method."
2,101,408 Issued Dec. 7, 1937. D. S. Muzzey, Jr. "Seismic Surveying Method."
2,111,643 Issued Mar. 22, 1938. H. Salvatori. "Seismometer."
2,117,365 Issued May 17, 1938. H. Salvatori and J. N. Walstrum. "Seismic Surveying."
2,133,484 Issued Oct. 18, 1938. S. Sherar. "Use of a Distributed Charge in Seismic Prospecting."
2,144,812 Issued Jan. 24, 1939. F. Rieber. "Method of Geophysical Exploration."
2,147,060 Issued Feb. 14, 1939. F. F. Reynolds. "Electromagnetic Wave-Pickup Instrument."
2,148,422 Issued Feb. 28, 1939. L. W. Blau. "Method of Determining the Dips of Geological Strata with Substantially Vertical Reflections."
2,148,679 Issued Feb. 28, 1939. L. W. Blau, R. R. Thompson and W. D. Mounce. "Use of High Frequencies in Measuring Changes in Electrical Impedance."
2,149,427 Issued March 7, 1939. L. Y. Faust. "Subsurface Exploration."
2,151,878 Issued Mar. 28, 1939. B. B. Weatherby. "Seismic Surveying."
2,153,920 Issued April 11, 1939. L. W. Gardner. "Seismograph Prospecting."
2,154,548 Issued April 18, 1939. B. B. Weatherby. "Seismic Surveying."
2,155,507 Issued April 25, 1939. F. Rieber. "Wave Record Analyzer."
2,156,198 Issued April 25, 1939. S. A. Scherbatskoy. "Seismic Prospecting."
2,156,259 Issued May 2, 1939. L. W. Blau. "Seismic-electric Prospecting by Means of Continued Waves."
2,156,624 Issued May 2, 1939. L. Y. Faust. "Subsurface Seismic Surveying."
2,158,198 Issued May 16, 1939. H. R. Prescott. "Method and Apparatus for Making Geological Explorations."

2,160,224 Issued May 30, 1939. J. P. Minton. "Seismic Survey."
2,161,764 Issued June 6, 1939. J. P. Minton. "Apparatus for Recording Seismic Waves."
2,161,764 Issued June 6, 1939. J. P. Minton. "Method and Means for Recording Seismic Waves."
2,164,196 Issued June 27, 1939. K. C. Woodyard, C. A. Putnam and H. R. Prescott. "Means and Method of Making Geophysical Explorations."
2,167,124 Issued July 25, 1939. J. P. Minton. "Apparatus for Recording Seismic Waves."
2,180,949 Issued Nov. 21, 1939. L. W. Blau, W. D. Mounce and W. M. Rust, Jr. "Feedover Device."
2,184,313 Issued Dec. 26, 1939. J. E. Owen. "Seismic Surveying."
2,184,953 Issued Dec. 26, 1939. A. B. Bryan. "Time Lines Recording Apparatus."
2,192,972 Issued March 12, 1940. A. I. Innes. "Seismic Surveying."
2,193,620 Issued March 12, 1940. R. T. Cloud. "Attenuator."
2,193,769 Issued March 12, 1940. J. P. Minton. "Frequency Multiplication System for Seismic Recording."
2,203,140 Issued June 4, 1940. W. G. Green. "Seismic Prospecting."
2,203,272 Issued June 4, 1940. N. R. Sparks. "Apparatus for Determining Seismic Velocities."
2,207,398 Issued July 9, 1940. F. M. Floyd. "Seismic Surveying."
2,209,100 Issued July 23, 1940. J. P. Minton. "Electrical Seismograph."
2,215,297 Issued Sept. 17, 1940. J. E. Owen. "Seismic Surveying."
2,216,452 Issued Oct. 1, 1940. J. E. Owen. "Seismic Surveying."
2,217,720 Issued Oct. 15, 1940. J. F. Anderson. "Apparatus for Solving Seismographic Problems."
2,217,806 Issued Oct. 15, 1940. G. Muffly. "Seismograph Prospecting."
2,217,828 Issued Oct. 15, 1940. R. D. Wyckoff. "Seismograph Prospecting Apparatus."
2,219,508 Issued Oct. 29, 1940. L. F. Athy and E. V. McCollum. "Method and Apparatus for Seismic Surveying."
2,229,191 Issued Jan. 21, 1941. H. C. Schaeffer and R. A. Peterson. "Method of Making Weathering Corrections."
2,230,002 Issued Jan. 28, 1941. J. P. Minton. "Method of Calibrating Field Timing Systems."
2,231,243 Issued Feb. 11, 1941. R. F. Beers. "Method of and Means for Analyzing and Determining the Geologic Strata below the Surface of the Earth."
2,231,575 Issued Feb. 11, 1941. L. W. Gardner. "Seismograph Prospecting."
2,232,613 Issued Feb. 18, 1941. P. W. Klipsch. "Seismic Prospecting."
2,238,023 Issued April 8, 1941. P. W. Klipsch. "Equalizer."
2,241,428 Issued May 13, 1941. D. Silverman. "Apparatus for Underwater Seismic Surveying."
2,243,729 Issued May 27, 1941. L. G. Ellis. "Method for Analysis of Seismographic Records."
2,243,730 Issued May 27, 1941. L. G. Ellis. "Apparatus for Analysis of Seismographic Records."
2,253,358 Issued Aug. 19, 1941. P. S. Williams. "Seismic Exploration Method."
RE 22535 E. J. Schimek.
2,257,187 Issued Sept. 30, 1941. J. E. Owen. "Seismic Surveying."
2,257,423 Issued Sept. 30, 1941. J. D. Malmqvist. "Determining the Velocity of Elastic Waves in the Ground."
2,257,859 Issued Oct. 7, 1941. E. E. Rosaire and F. M. Kannenstine. "Method and Apparatus for Recording Waves."
2,259,478 Issued Oct. 21, 1941. C. G. Morgan. "Geophysical Exploration System."
2,260,217 Issued Oct. 21, 1941. E. A. Eckhardt and G. Muffly. "Method of and Apparatus for Seismograph Prospecting."
2,261,321 Issued Nov. 4, 1941. P. S. Williams. "Seismic Exploration Method."
2,263,519 Issued Nov. 18, 1941. O. F. Ritzmann. "Seismograph Prospecting Apparatus."
2,264,098 Issued Nov. 25, 1941. L. C. Paslay. "Deflection Limiter for Galvanometers."
2,265,513 Issued Dec. 9, 1941. K. E. Burg. "Prospecting Method and Apparatus."
2,265,538 Issued Dec. 9, 1941. J. P. Minton. "Gain Control for Seismograph Amplifiers."

2,266,040 Issued Dec. 16, 1941. H. Hoover, Jr. "Geophysical Prospecting Receptor Circuits."
2,266,041 Issued Dec. 16, 1941. H. Hoover, Jr. "Geophysical Prospecting Receptor Circuits."
2,266,837 Issued Dec. 23, 1941. H. F. Wiley. "Method and Apparatus for Translating Seismic Waves."
2,267,357 Issued Dec. 23, 1941. O. F. Ritzmann. "Apparatus for and Method of Seismograph Recording."
2,267,858 Issued Dec. 30, 1941. C. H. Dix. "Method of Seismic Surveying."
2,268,130 Issued Dec. 30, 1941. M. M. Slotnick. "Method of Geophysical Investigation."
2,269,453 Issued Jan. 13, 1942. E. L. Gayhart. "Device for Detecting Displacements."
2,269,890 Issued Jan. 13, 1942. L. W. Blau. "Seismic-Electric Prospecting."
2,271,864 Issued Feb. 3, 1942. P. M. Honnell and L. W. Dickerson. "Seismic Wave Detector."
2,272,201 Issued Feb. 10, 1942. H. Hoover, Jr. "Method and Apparatus for Signaling."
2,272,984 Issued Feb. 10, 1942. O. F. Ritzmann. "Seismograph."
2,276,306 Issued March 17, 1942. H. Hoover, Jr. and H. C. Schaeffer, "System for Making Weathering Corrections."
2,276,335 Issued March 17, 1942. R. A. Peterson. "Method of Making Weathering Corrections."
2,276,423 Issued March 17, 1942. D. Silverman. "Recording System."
2,276,565 Issued March 17, 1942. M. G. Crosby. "Limiting Amplifier."
2,276,708 Issued March 17, 1942. R. D. Wyckoff. "Seismograph Amplifier."
2,276,709 Issued March 17, 1942. R. D. Wyckoff. "Apparatus for and Method of Seismograph Prospecting."
2,276,974 Issued March 17, 1942. G. M. Howard. "Method of and Means for Determining the Velocity of Propagation of Waves through Sursurface Formations."
2,277,521 Issued March 24, 1942. M. D. McCarty. "Timing Device."
2,279,191 Issued April 7, 1942. J. L. Adler. "Method and Apparatus for Seismic Surveying."
2,281,949 Issued May 5, 1942. O. F. Ritzmann. "Apparatus for Seismograph Prospecting."
2,283,200 Issued May 19, 1942. J. W. Flude. "Method and Apparatus for Subsurface Mining."
2,285,610 Issued June 9, 1942. O. S. Petty. "Method and Apparatus for Seismic Surveying."
2,286,106 Issued June 9, 1942. O. F. Ritzmann. "Apparatus for and Method of Receiving and Recording Vibrations."
2,286,170 Issued June 9, 1942. C. A. Heiland. "Selector System for Amplifiers."
2,286,386 Issued June 16, 1942. D. Silverman. "Seismometer."
2,286,567 Issued June 16, 1942. J. O. Parr, Jr. "Seismic Surveying."
2,291,779 Issued Aug. 4, 1942. W. R. Welty. "Geophysical Apparatus and Method."
2,294,627 Issued Sept. 1, 1942. J. O. Parr, Jr. "Seismic Surveying."
2,296,754 Issued Sept. 22, 1942. A. Wolf and L. G. Cowles. "Astatic Electromagnetic Vibration Detector."
2,297,319 Issued Sept. 29, 1942. J. O. Parr, Jr. "Seismic Circuits."
2,298,020 Issued Oct. 6, 1942. J. O. Parr, Jr. "Seismic Surveying."
2,301,739 Issued Nov. 10, 1942. J. P. Minton and E. M. Shook. "Gain Control for Seismograph Amplifiers."
2,302,219 Issued Nov. 17, 1942. G. W. Hostetler. "Infinite Period Seismometer."
2,303,357 Issued Dec. 1, 1942. H. Hoover, Jr. "Seismic Wave Amplifier."
2,303,358 Issued Dec. 1, 1942. H. Hoover, Jr. "Stable Seismic Wave Amplifier with Automatic Volume Control."
2,303,413 Issued Dec. 1, 1942. H. W. Washburn. "Seismometer."
2,304,738 Issued Dec. 8, 1942. M. D. McCarty. "Seismograph."
2,304,740 Issued Dec. 8, 1942. J. P. Minton. "Method for Recording Seismic Waves."
2,304,901 Issued Dec. 15, 1942. J. D. Eisler. "Timing Device."
2,305,383 Issued Dec. 15, 1942. H. Hoover, Jr., C. G. Morgan and N. J. Christie. "Geophysical Exploration System."
2,305,543 Issued Dec. 15, 1942. M. D. McCarty. "Expander for Electrical Seismographs."

2,306,224 M. Artzt.
2,306,456-8 Issued Dec. 29, 1942. W. H. Mayne. "Measuring and Recording Apparatus."
2,306,991 Issued Dec. 29, 1942. G. M. Groenendyke. "Automatic Volume Control."
2,307,790 Issued Jan. 12, 1943. H. Hoover, Jr. "Automatic Amplitude Control System."
2,307,791 Issued Jan. 12, 1943. H. Hoover, Jr. "Seismic Exploration System."
2,307,792 Issued Jan. 12, 1943. H. Hoover, Jr. "Seismometer."
2,309,560 Issued Jan. 26, 1943. W. R. Welty. "Method and Apparatus for Measuring and Recording Vibrational Effects."
2,309,817 Issued Feb. 2, 1943. L. F. Athy and E. V. McCollum. "Method of Making Geophysical Explorations."
2,311,079 Issued Feb. 16, 1943. J. O. Parr, Jr. "Transducer."
2,312,642 Issued March 2, 1943. A. J. Herzenberg. "Seismic Exploration Method."
2,312,934 Issued March 2, 1943. E. M. Shook. "Gain Control for Seismograph Amplifiers."
2,313,091 Issued March 9, 1943. D. S. Reener. "Seismic Recording."
2,316,354 Issued April 13, 1943. B. E. Moritz, Jr. "Gain Control."
2,317,334 Issued April 20, 1943. E. J. Shimek. "Master Control for Electric Seismographs."
2,318,248 Issued May 4, 1943. J. P. Minton. "Phase Meter."
2,318,624 Issued May 11, 1943. O. S. Petty and J. O. Parr, Jr. "Automatic Volume Control for Recorder Amplifiers."
2,318,795 Issued May 11, 1943. L. J. Peters. "Seismograph Amplifier System."
2,319,626 Issued May 18, 1943. L. C. Paslay. "Signal Controlled Amplifier."
2,321,341 Issued June 8, 1943. B. B. Weatherby and W. T. Born. "Seismic Surveying."
2,321,450 Issued June 8, 1943. L. F. Athy and E. V. McCollum. "Seismic Surveying."
2,323,211 Issued June 29, 1943. F. J. Faltico. "Method and Apparatus for Automatic Gain Control."
2,324,816 Issued July 20, 1943. W. T. Born. "Seismic Surveying."
2,325,199 Issued July 27, 1943. J. P. Woods. "Method and Apparatus for Seismic Exploration."
2,328,222 Issued Aug. 31, 1943. M. D. McCarty. "Geophone."
2,329,558 Issued Sept. 14, 1943. S. A. Scherbatskoy. "Automatic Volume Control."
2,329,570 Issued Sept. 14, 1943. R. Wellenstein, W. Holle and M. Schumacher. "Device for Regulating the Sensitivity of Signal Receiving Apparatus."
2,329,721 Issued Sept. 21, 1943. H. Hoover, Jr., C. G. Morgan and N. J. Christie. "Geophysical Exploration System."
2,330,216 Issued Sept. 28, 1943. H. Hoover, Jr. and M. Swan. "Apparatus for Seismic Prospecting."
2,331,080 Issued Oct. 5, 1943. O. S. Petty. "Method of Seismic Reflection Surveying."
2,331,363 Issued Oct. 12, 1943. H. W. Washburn. "Seismic Prospecting System."
2,331,624 Issued Oct. 12, 1943. J. O. Parr, Jr. "Method of and Apparatus for Seismic Surveying."
2,331,904 Issued Oct. 19, 1943. G. V. A. Gustafsson and J. D. Malmqvist. "Geophysical Instrument."
2,332,536 Issued Oct. 26, 1943. K. H. F. Schlegel. "Electrical Circuit Control Device."
2,336,198 Issued Dec. 7, 1943. C. C. Stotz. "Apparatus for Seismic Prospecting."
2,336,206 Issued Dec. 7, 1943. J. P. Woods. "Seismograph Amplitude Control."
2,345,288 Issued March 27, 1944. W. E. Pugh. "Method of Seismic Prospecting."
2,346,369 J. D. Eisler.
2,347,702 Issued May 2, 1944. H. B. Maris. "Device for Measuring Extremely Small Angles."
2,348,225 Issued May 9, 1944. O. S. Petty. "Magnetic Seismometer."
2,348,401 Issued May 9, 1944. L. Manzanera. "Apparatus for Recording Wave Form Signals."
2,348,409 Issued May 9, 1944. J. O. Parr, Jr. "Seismic Surveying."
2,348,411 Issued May 9, 1944. O. S. Petty. "Method for Correlating Seismographic Curves."
2,349,186 Issued May 16, 1944. E. Merten, "Sensitivity Control for Seismic Recording."
2,350,803 Issued June 6, 1944. R. D. Newcomb. "Automatic Volume Control."
2,351,456 Issued June 13, 1944. N. H. Ricker. "Seismic Surveying."
2,352,494 Issued June 27, 1944. J. O. Parr, Jr. "Seismic Surveying."

2,352,869 Issued July 4, 1944. J. F. Tolk. "Seismic Surveying."
2,354,420 Issued July 11, 1944. J. P. Minton. "Contractor - Expander for Electric Seismographs."
2,354,548 Issued July 25, 1944. N. H. Ricker. "Seismic Prospecting."
2,354,659 W. O. Bazhaw and J. O. Parr, Jr.
2,355,826 J. A. Sharpe.
2,360,507 Issued Oct. 17, 1944. J. P. Minton. "Apparatus for Recording Seismic Waves."
2,361,648 Issued Oct. 31, 1944. O. S. Petty. "Seismic Surveying."
2,363,985 Issued Nov. 28, 1944. W. Moser. "Automatic Volume Control Device."
2,364,655 Issued Dec. 12, 1944. H. H. Pratley. "Geophysical Exploration."
2,364,755 Issued Dec. 12, 1944. O. F. Ritzmann. "Apparatus for Seismograph Prospecting."
2,365,289 Issued Dec. 19, 1944. O. S. Petty. "Seismic Surveying."
2,366,043 Issued Dec. 26, 1944. W. D. Mounce. "Automatic Gain Adjusting Device for Reflection Seismographs."
2,367,049 Issued Jan. 19, 1945. O. S. Petty. "Automatic Volume Control for Recorder Amplifiers."
2,370,483 Issued Feb. 27, 1945. G. Muffly. "Amplifier."
2,372,056 Issued March 20, 1945. R. A. Broding. "Method and Apparatus for Recording Seismic Waves."
2,373,180 Issued April 10, 1945. F. J. Faltico. "Automatic Volume Control Circuit."
2,374,204 Issued April 24, 1945. H. Hoover, Jr. "Apparatus for Recording Seismic Waves."
2,375,283 Issued May 8, 1945. R. T. Cloud. "Amplification Control in Seismic Surveying."
2,375,433 Issued May 8, 1945. J. P. Minton. "Seismograph."
2,375,570 Issued May 8, 1945. E. McDermott. "Seismic Detector System."
2,376,195 Issued May 15, 1945. S. A. Scherbatskoy. "Amplifying Apparatus."
2,378,925 Issued June 26, 1945. E. E. Hoskins and R. M. Moore. "Seismic Prospecting System."
2,383,571 Issued Aug. 28, 1945. E. M. Shook. "Gain Control for Seismograph Amplifiers."
2,383,855 Issued Aug. 28, 1945. C. W. Hansell. "Potential Ratio-Controlled Amplifier."
2,384,393 Issued Sept. 4, 1945. J. O. Parr, Jr. "Stabilizer for Automatic Volume Control Circuits."
2,384,529 Issued Sept. 11, 1945. V. W. Breitenstein. "Magnetic Instrument."
2,387,845 Issued Oct. 30, 1945. W. R. Harry. "Electroacoustic Transducer."
2,388,303 Issued Nov. 6, 1945. H. M. Wise. "Elastic Measuring Scale."
2,388,703 Issued Nov. 13, 1945. R. A. Peterson. "Geological Prospecting System."
2,388,848 Issued Nov. 13, 1945. W. C. Howe. "Magnetic Shielding for Transformers and the Like."
2,390,187 Issued Dec. 4, 1945. J. A. Sharpe. "Seismic Surveying."
2,390,322 Issued Dec. 4, 1945. J. O. Parr, Jr. "Seismic Surveying."
2,390,328 Issued Dec. 4, 1945. R. J. Roberts. "Directional Seismograph Pickup."
2,392,758 Issued Jan. 1, 1946. J. P. Minton and R. A. Broding. "Method and Apparatus for Recording Seismic Waves."
2,394,990 Issued Feb. 12, 1946. J. D. Eisler and J. A. Sharpe. "Recording System in Seismic Surveying."
2,395,289 Issued Feb. 19, 1946. J. Neufeld. "Method and Apparatus for Seismic Prospecting."
2,395,427 Issued Feb. 26, 1946. O. S. Petty. "Seismic Prospecting."
2,395,481 Issued Feb. 26, 1946. H. Hoover, Jr. "Seismic Exploration System."
2,396,691 Issued March 19, 1946. R. R. Galbreath. "Condenser Transmitter - Amplifier System."
2,400,245 Issued May 14, 1946. W. H. Mayne. "Seismic Surveying."
2,400,522 Issued May 21, 1946. H. Hoover, Jr. "Range Finder."
2,401,411 Issued June 4, 1946. S. F. Carlisle, Jr. and A. B. Mundel. "Frequency Response Testing System."
2,403,974 Issued July 16, 1946. W. D. Goodale, Jr., B. F. Lewis and W. H. Martin. "System for Locating the Source of an Explosion Wave."
2,404,391 Issued July 23, 1946. W. P. Mason. "Prismatic and High Power Compressional-Wave Radiator and Receiver."

2,404,786 Issued July 30, 1946. L. G. Bostwick. "Moisture Control in an Electro-mechanical Device."
2,405,226 Issued Aug. 6, 1946. W. P. Mason. "Low Frequency Projector or Hydrophone."
2,405,227 Issued Aug. 6, 1946. W. P. Mason. "Geometrical Instrument."
2,406,014 Issued Aug. 20, 1946. W. R. Harry. "System for Locating the Source of an Explosion Wave."
2,406,391 Issued Aug. 27, 1946. W. P. Mason. "Compressional Wave Directional, Prismatic, and Focusing System."
2,407,363 Issued Sept. 10, 1946. W. H. Bussey. "Electrical Apparatus."
2,407,662 Issued Sept. 17, 1946. H. M. Hart. "Method and Apparatus for Submarine Signaling."
2,408,001 Issued Sept. 24, 1946. E. J. Shimek and W. B. Hemphill. "Gain-Control System for Seismic Amplifiers."
2,408,125 Issued Sept. 24, 1946. H. J. Rolfes. "Means of Safeguarding Electric Igniters of Blasting Detonators against Accidental Firing."
2,408,189 Issued Sept. 24, 1946. A. W. Baker. "Waterproof Explosive Cartridge."
2,416,321 Issued Feb. 25, 1947. E. T. Jones. "Automatic Volume Control in Voice Frequency Circuits."
2,417,077 Issued March 11, 1947. H. Hoover, Jr. "Seismometer."
2,418,953 Issued April 15, 1947. R. W. Raitt. "Transducing System."
2,420,025 Issued May 6, 1947. W. W. Young. "Vibration Recorder."
2,420,868 Issued May 20, 1947. M. G. Crosby. "Diversity Combining Circuit."
2,423,970 Issued July 15, 1947. L. W. Gardner. "Geophone Polarity Indicator."
2,424,724 Issued July 29, 1947. J. F. Folk. "Position-Dampened Seismometer."
2,428,168 Issued Sept. 30, 1947. G. B. Loper. "Seismic-Wave Detector."
2,431,307 Issued Nov. 25, 1947. P. K. Chatterjea and C. T. Scully. "Thermionic Valve Amplifier."
2,431,600 Issued Nov. 25, 1947. A. Wolf. "Seismic Exploration with Control of Directional Sensitivity."
2,435,903 Issued Feb. 10, 1948. O. F. Ritzmann. "Method and Apparatus for Exhibiting Seismograph Signals."
2,438,217 Issued March 23, 1948. C. H. Johnson. "Method for Elimination of Periodic Stray Signals from Seismic Signals."
2,438,526 Issued March 30, 1948. C. H. Waterman. "System for Determining the Direction of a Source of Sound."
2,438,755 Issued March 30, 1948. E. W. Larsen. "Vibrating Apparatus."
2,438,756 Issued March 30, 1948. E. W. Larsen. "Vibrating Apparatus."
2,440,971 Issued May 4, 1948. E. M. Palmer. "Seismograph Recording Apparatus."
2,444,676 Issued July 6, 1948. F. W. Roberts and R. C. Curtis. "Sound Recording and Reproducing Control System."
2,445,014 Issued July 13, 1948. L. Wolff. "Vibratory Mechanical System."
2,446,195 Issued August 8, 1948. S. L. Shive. "Tester for Electrical Shieldings."
2,446,818 Issued August 10, 1948. S. Flam. "Vibrator."
2,448,812 Issued Sept. 7, 1948. J. Lemire. "Electric Timing Motor."
2,449,921 Issued Sept. 21, 1948. A. Wolf. "Seismic Method of Locating Faults."
2,450,352 Issued Sept. 28, 1948. R. G. Piety. "Seismic Wave Correction Means and Method."
2,450,366 Issued Sept. 28, 1948. J. D. Williams. "Apparatus and Method of Seismographic Exploration Shooting."
2,456,401 Issued Dec. 14, 1948. R. P. Gilmore. "Interference Eliminator for Seismic Recording Systems."
2,457,214 Issued Dec. 28, 1948. H. G. Doll and G. K. Miller. "Recording Device."
2,457,712 Issued Dec. 28, 1948. H. F. Olson and J. Preston. "Method and Apparatus for Noise Control of Reproduced Sound."
2,461,005 Issued February 8, 1949. G. C. Southworth. "Ultra High Frequency Transmission."
2,462,764 Issued February 22, 1949. W. J. O'Brien. "Navigation System."
2,463,474 Issued March 1, 1949. H. G. Busignies. "Air Navigation System."
2,463,476 Issued March 1, 1949. H. G. Busignies. "Radio Navigation System."
2,461,187 Issued February 8, 1949. W. Steinmann. "Direction Finding Apparatus."
2,461,213 Issued February 8, 1949. W. D. Herschberger. "Distance Measuring Device."

CHAPTER VIII

CHEMICAL METHODS

Geochemical Prospecting for Petroleum

Geochemical prospecting methods are based on the premise that the lighter and smaller molecule hydrocarbons which make up gas and oil accumulations slowly migrate upward from the deposits to the surface of the earth. In practice, samples of soil or soil air are collected at relatively shallow depths in a systematic manner over an area to be investigated. The samples are analyzed for hydrocarbons and from the distribution patterns obtained, significant conclusions concerning the possible presence of petroleum accumulation may be drawn. This method, then, unlike geophysical methods which locate structure with which oil and gas may be associated, attempts to localize the oil or gas accumulation itself.

In addition to the hydrocarbons themselves, other constituents, both organic and inorganic, have been found to be present in the soil over petroleum accumulations and these materials are believed to result directly from hydrocarbon migration.

The first method of searching for oil and gas fields involved the search for visible gas and oil seepages. The success of this early method is proven by the fact that of 141 salt domes discovered prior to 1936, 35 owe their discovery to the detection of these gas and oil seepages.†

In view of the fact that oil and gas, in sufficient quantities to enable detection by the naked eye, can migrate to the surface of the earth, it was logical to assume that microscopic seeps over gas and oil fields would be much more numerous. The first systematic attempt to search for microscopic seepages as indicators of gas and oil deposits was made by G. Laubmeyer in 1929. This investigator described methods for collecting samples of soil air from systematically located bore holes and analyzing these samples for traces of methane. The results of his work indicated that the soil air over a producing area is richer in methane than is the soil air over a barren area.

In 1932, a group of Russian investigators, headed by Sokoloff, became engaged in similar work. Sokoloff and co-workers improved Laubmeyer's sampling technique and found heavier gaseous constituents as well as methane.

The conclusions of the Russian investigators substantiated those of Laubmeyer in that they, too, reported that maximum hydrocarbon concentrations occur in the center of the region overlying the subsurface accumulation, with minimum values over the surrounding barren area.

† George Sawtelle, "Salt Dome Statistics," *Gulf Coast Oil Fields*, A.A.P.G. Publication, pp. 109-118, 1936.

In 1936, Americans became interested in this new approach to petroleum prospecting. Instead of collecting samples of the soil air in the field, however, a technique was developed whereby samples of the soil itself were collected and analyzed for hydrocarbons. Saturated hydrocarbons even heavier than those reported by the Russians were extracted from the soil samples. An important advantage of this technique is the fact that samples may be collected under practically all conditions, while with the techniques which require pumping the gas from the bore hole itself, it is impossible to collect samples in water-covered or in arid areas.

During the migration of hydrocarbon gases from a petroleum deposit, the formations penetrated are believed to be modified chemically. Further, at the surface of the earth, where the hydrocarbons come in contact with oxygen and sunlight, it is believed that the gases are converted to heavier materials such as waxes and liquids. Thus a geochemical exploration technique has been devised whereby samples are collected from the top few inches of soil and analyzed for their wax-like materials. Concentration distribution patterns are often obtained which agree with those resulting from the analysis of the deeper samples for saturated hydrocarbons.

Another method is based on the fact that there are present in shallow soils certain inorganic materials which fluoresce under ultra-violet light. Proponents of this method believe that these materials are associated with petroleum accumulation at depth. Still another method is based on the observation that the growth of certain bacteria is accelerated in the presence of hydrocarbons. Therefore, this method is applied by collecting shallow samples at depths of approximately six inches and making bacterial counts on these samples.

In addition to the foregoing methods, determinations are made for various minerals present in soils. These are also believed to be indicators of petroleum at depth.

Physical Principles.—All geochemical methods are based on the assumption that the lighter components of an oil or gas deposit flow continuously, although at a very slow rate, from the reservoir, through the various overlying strata, into the atmosphere. The exact mechanism of migration is unknown. Undoubtedly, diffusion plays the most important role, with effusion and permeation being involved to a lesser extent. Whatever the mechanism, the phenomenon becomes readily conceivable when it is considered that diffusion can take place through metals,† fused silica,‡ various glasses,§ and other solids normally regarded as impervious.

† W. R. Ham, "Diffusion of Hydrogen Through Platinum and Nickel and Through Double Layers of These Metals," *Jour. Chem. Physics*, Vol. 1, pp. 476-481, 1933.

‡ E. O. Braaten and G. F. Clark, "The Diffusion of Helium Through Fused Silica," *Jour. Am. Chem. Soc.*, Vol. 57, pp. 2714-2717, 1935.

§ William D. Urry, "The Permeability of Various Glasses to Helium," *Jour. Am. Chem. Soc.*, Vol. 54, pp. 3887-3901, 1932.

Gas Analysis Methods

The gas analysis methods include those techniques which involve the collection of soil air samples *in situ* and the analysis of these samples for the minute concentrations of hydrocarbons present. The introduction and development of these techniques are due principally to Laubmeyer and to Sokoloff and co-workers.

Sampling and Analysis.—Briefly, Laubmeyer's technique† consists in digging bore holes one to two meters deep, closing these holes with a special seal, consisting of a lid provided with two concentric cylinders of large radius and a piece of tubing to which a stopcock is attached, and allowing twenty-four to forty-eight hours for the composition of the enclosed air to reach equilibrium. A sample of the air is then extracted for analysis. Laubmeyer points out that the hydrocarbon content of the soil air sample, collected in this manner, consists principally of methane, since hydrocarbons heavier than air would not tend to diffuse into the bore hole. The gas is brought in contact with a heated platinum filament and the hydrocarbons, in the presence of air, are burned. This reaction raises the temperature of the filament which in turn increases its resistance. The change in resistance is a measure of the hydrocarbon concentration.

In the Russian technique, a hole of suitable depth (10 to 30 feet) is dug by means of a hand auger so that its upper half has a larger diameter than its lower half. The shoulder of the hole is then wetted, tamped, coated with clay, and sealed from the atmosphere by means of a bell-shaped sampling container. Next, the atmospheric gases are pumped out of the enclosure by means of a vacuum pump and the soil gases are allowed to seep into the enclosure and are collected in a suitable container by displacement of water.

Two methods of gas analysis were developed by the Russians, one for use in the field and the second for use in the laboratory. In the case of the former, the sample is passed through a caustic solution to remove the carbon dioxide present and then through a combustion chamber which oxidizes the hydrocarbons. The carbon dioxide formed on oxidation is measured by allowing the gas to bubble through a barium hydroxide solution and noting the volume necessary to produce the first observable turbidity. This volume is compared with the volume required when carbon dioxide in known concentration is bubbled through the same apparatus. This method gives a measure of the total hydrocarbon content of the sample without regard to the types of hydrocarbons present.

In the laboratory, a more refined apparatus is used.‡ After freeing the gas sample of carbon dioxide, water vapor, and basic constituents such as

† G. Laubmeyer, "A New Geophysical Prospecting Method, Especially for Deposits of Hydrocarbons," *Petroleum,* Vol. 29, No. 18, pp. 1-4, 1933.

‡ V. A. Sokoloff, "Methods of Exploration for Natural Gas," *Monograph,* 1932.

V. A. Sokoloff, "Summary of the Experimental Work of the Gas Survey," *Neftyanoye Khozyaystvo,* Vol. 27, No. 5, pp. 28-34, 1935.

V. A. Sokoloff, "Methods of Interpretation of the Gas Survey," *Neftyanoye Khozyaystvo,* Vol. 17, No. 5, pp. 18-23, 1936.

ammonia, the sample is circulated through a trap immersed in liquid air. At this temperature, methane and ethane are not condensable and therefore pass through the trap and are converted to carbon dioxide and water by combustion. The carbon dioxide is collected and by means of a McLeod gauge its pressure is determined. This is called the *light fraction* and is expressed in per cent by volume of sample analyzed.

The condensable portion of the sample, called the *heavy fraction,* is directly measured with a McLeod gauge and is believed to consist of a mixture of complex hydrocarbons and their derivatives. The heavy fraction is calculated and expressed in per cent by volume of sample analyzed.

In conducting surveys, the analytical values are found to range from less than .0005 per cent to about .03 per cent by volume.

Results of Gas Surveys.—The Russian workers, as well as Laubmeyer, reported hydrocarbon distribution patterns in which the greater

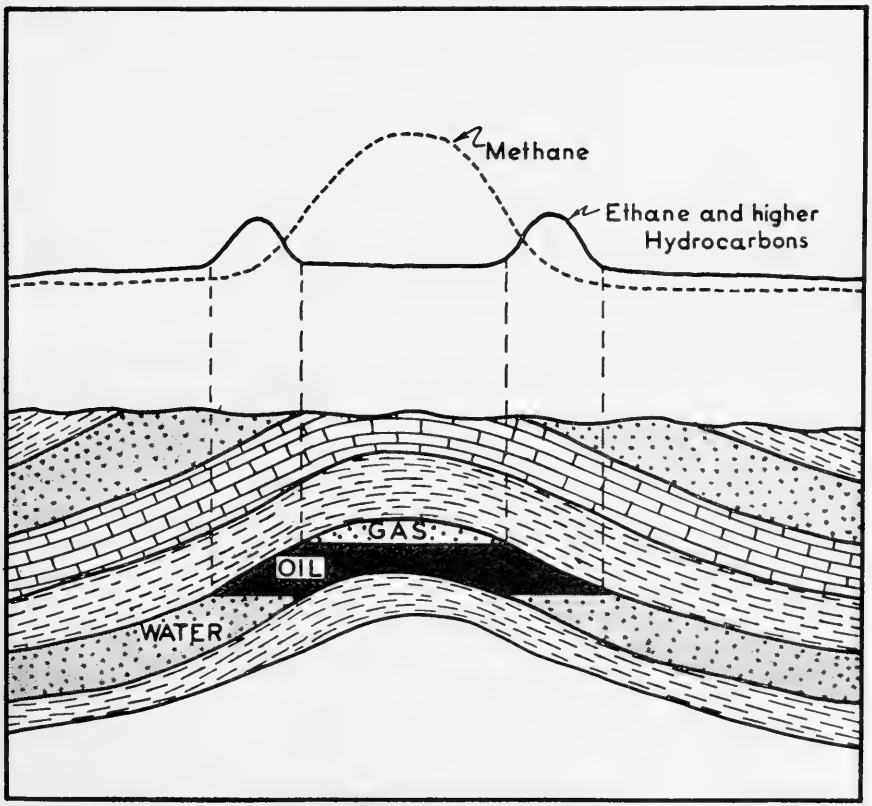

FIG. 578.—Idealized profiles showing significant hydrocarbon patterns as reported by Russians. (Howard, *Oil and Gas Journal.*)

concentrations of hydrocarbons occur in the soil air over productive zones, with relatively lower values over barren areas.

Figure 578 illustrates, ideally, the significant hydrocarbon distribution patterns as reported by Russian workers. High concentrations of methane are observed in the soil air over gas accumulations, while high concentrations of the heavy fraction are noted over the oil accumulations. Low concentrations are found in the soil gas over barren areas.

Theoretical Interpretation of Gas Analysis Anomalies.—The development of interpretative technique by the Russian investigators has proceeded along the lines of attempting: (a) to deduce theoretical curves characteristic of petroliferous and gaseous deposits at various depths below the surface and (b) to solve the inverse problem: viz., infer the depth of the deposits from the observed anomaly curve.

Antonov † has published an article in which he assumes that diffusion takes place through a homogeneous overburden. In the stationary state, the diffusion equation reduces to Laplace's equation which may be written in the form:

$$\frac{\partial^2 M}{\partial x^2} + \frac{\partial^2 M}{\partial y^2} + \frac{\partial^2 M}{\partial z^2} = 0$$

where M is the concentration or partial pressure of the hydrocarbon gas. Typical boundary conditions used by Antonov are: (a) the region below the source is completely impervious and (b) no diffusion takes place through the surface of the earth into the air. The validity of such boundary conditions is not self-evident.

In addition to this theoretical technique, the Russian investigators employ various empirical techniques derived from extensive investigations over many oil and gas fields. For example, investigations of various deposits have shown that the percentage of heavy hydrocarbons increases over an oil horizon and the percentage of methane generally increases over a gas deposit.‡ The ratio of the light to the heavy hydrocarbon content is assumed therefore to furnish a useful diagnostic variable.

The Emanometric Method. — Another technique, known as the *emanometric* or *geodynamic* method, should be classified with gas analysis methods. This technique§ endeavors to measure the absolute rate of emanation per unit area of the earth surface of one or more diagnostic gases and to recognize a commercial oil or gas accumulation by near-surface measurements. Ethane is considered the most diagnostic constituent and, over a square foot of area, the emanation of this gas is calculated to be 5.2 cu. mm. per 24 hours measured under normal conditions of temperature and pressure.

In conducting a survey, selective adsorbent tubes are placed over a measured and confined surface of the ground for a specified period of time, usually of the order of twenty-four hours. After the exposure time is completed, the adsorber tubes or "emanometers" are sealed and taken to the laboratory for the next steps which include degassing, fractionation, distillation, identification, and quantitative measurement of the diagnostic gases. After correcting the data for topography and ground water percolation, there remains the anomaly map, which is the leakage configuration

† P. L. Antonov, "Contribution to the Theory of Gas Surveying," *Neft. Khoz.* 26, No. 5, pp. 19-23 (1934).

‡ B. N. Victoroff, "Interpretation of the Nature of a Gas Survey," *Neft. Khoz.*, Sept., 1934.

§ Sylvain J. Pirson, "Emanometric Oil and Gas Prospecting," *The Petroleum Engineer,* January, 1946.

believed to be due to confined pressure sources of oil and gas pools, but which must be subjected to further reduction for climatic, seasonal, and atmospheric effects; for nature of soils and in particular for soil permeability; and finally, for deep geologic effects. Once the reduction of the various influences have been taken care of, the residual map is the anomaly map representing the diffusion zone from oil or gas fields.

Soil Analysis Methods

The development of soil analysis techniques is due primarily to American investigators. These methods may be classified into: (1) those techniques which involve the extraction and measurement of the volatile, saturated hydrocarbons in the soil; and (2) those which involve the determination of one or more constituents that are present in the soil in larger than normal quantities through secondary enrichment. Among the materials determined are organic wax-like and liquid materials, fluorescent materials, and inorganic compounds such as carbonates, sulfates, and chlorides.

Soil Analysis for Volatile Hydrocarbons.—The modification of the Russian technique was introduced by Rosaire and Horvitz who began their investigations in 1936. This approach is based on the thought that during the upward migration of the hydrocarbons from the oil deposit, there is present a strong tendency for their adsorption and occlusion by the soil particles. It was anticipated that analysis of the soil itself for these entrained constituents would yield substantially greater concentrations than would result from the analysis of the interstitial air.

While the soil gas methods depend upon a large and undetermined quantity of soil from the interstices of which the air sample is drawn, the soil analysis method has apparently yielded satisfactory results with samples as small as fifty grams.† In the collection of gas samples in the field by the methods previously described, insurmountable difficulties are encountered which limit proper sampling to restricted areas. For example, satisfactory soil air samples cannot be obtained *in situ* from cohesive clays, in alluvial gravel deposits, in sand hills because of intensive aeration, in regions with a high ground water level.‡

Sampling.—Sample locations are first surveyed over the area to be investigated (Figure 579). Care must be taken to locate the stations at considerable distances from roads, pipe-lines, drilling wells, and other sources of possible contamination. The bore hole may be dug with bucket-type hand augers, or with mechanical drilling equipment. In either case, lubricants should be avoided. When the desired depth is reached, a sample is brought to the surface, placed in a pint glass jar, and securely sealed (Figure 580). The sample jars are carefully labeled as to station number,

† Leo Horvitz, "On Geochemical Prospecting," *Geophysics*, Vol. 4, No. 3, pp. 210-225, July, 1939.

‡ V. A. Sokoloff, Monograph published in U.S.S.R., 1932.

depth, and name of prospect, and delivered to the analytical laboratory. Samples are usually taken at depths ranging from eight to twelve feet and if possible at even greater depths, the actual depth chosen depending largely upon the area under investigation. Whenever possible, the samples are collected at the various locations from a constant depth below the surface. In this way, all samples are taken from a zone of fairly uniform aeration.

In carrying out broad reconnaissance surveys in search of large features, use is made of all available roads. Samples are first taken about one-fourth to one-half mile apart, sufficiently to one side of the road to avoid possible

FIG. 579.—Stations are located by means of an alidade and plane table.

FIG. 580.—Sample being removed from auger and placed in pint glass jar. (Courtesy of Horvitz Research Laboratories, Houston, Texas.)

contamination. In this manner, large areas can be prospected within a relatively short period of time. If the analytical data indicate a hydrocarbon anomaly of interest, additional samples are taken to produce a more dense and uniform sampling pattern in the interesting areas.

In the case of areas where anomalies can be expected to cover approximately 500 acres, a sample density of 1 to 80 acres is usually sufficient for reconnaissance. In the case of accumulations of small areal extent, such as on the flanks of piercement type domes, where the accumulations may be only several hundred feet wide, samples are often taken as close as 200 feet apart.

Analytical Technique.—In using the earlier analytical technique,† the jar containing the soil sample is attached directly to the analytical

† Leo Horvitz, "On Geochemical Prospecting," *Geophysics*, Vol. 4, No. 3, pp. 210-225, July 1939.

apparatus. The pressure in the sample jar is reduced, thereby eliminating interstitial soil air, and the adsorbed constituents are liberated in gaseous form by heating at 100° C. for about 45 minutes. Since the pressure within the sample jar is less than atmospheric, the sample temperature never reaches 100° C. Under these mild conditions, decomposition of organic matter to produce methane is prevented. After freeing the liberated gases of contaminating constituents normally present in the soil, they are separated into various fractions by employing refrigerants at different temperatures. In this early work, the extracted hydrocarbons ranged from methane through butane.

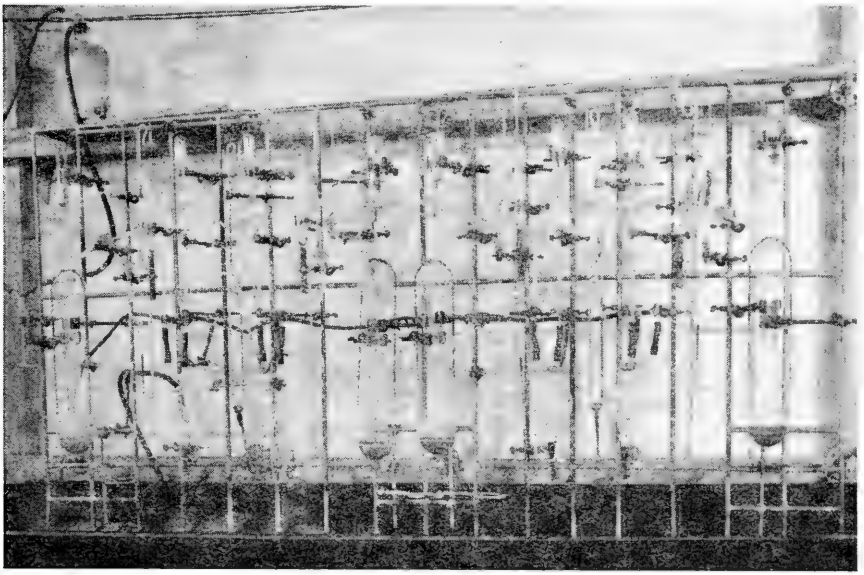

FIG. 581.—Bank of four extraction units for removing hydrocarbon gases from soil samples. Sample flasks, potassium hydroxide chambers and gas collecting tubes may be observed. (Courtesy of Horvitz Research Laboratories.)

More recently, Horvitz† reported improved methods for extracting and analyzing the hydrocarbons in soil. In some oil-bearing areas, the quantities of hydrocarbons obtained when using the earlier technique were too low for satisfactory correlation. It was found that heat alone was not sufficient to remove the adsorbed and occluded gases. Investigation indicated that heating the samples in the presence of an aqueous solution of an acid, such as hydrochloric or phosphoric, increased considerably the efficiency of extraction, yielding much larger quantities of significant constituents. By this technique, the hydrocarbons are practically entirely removed from the soil in one treatment without increasing the temperature.

† Leo Horvitz, "Chemistry in Exploration for Petroleum," paper presented before the Petroleum Division, American Chemical Society, St. Louis meeting, April 7-11, 1941.

The gas extraction is carried out in an apparatus separate from that used for analysis. Briefly, about 100 to 150 grams of sample are placed in a 500 cc. flask and the pressure is reduced to about 60 mm. If no reaction occurs upon adding several cc. of acid, indicating that the carbonate content of the sample is low, an additional 25 cc. portion of acid is added. If the carbonate content of the sample is high, a vigorous reaction will occur

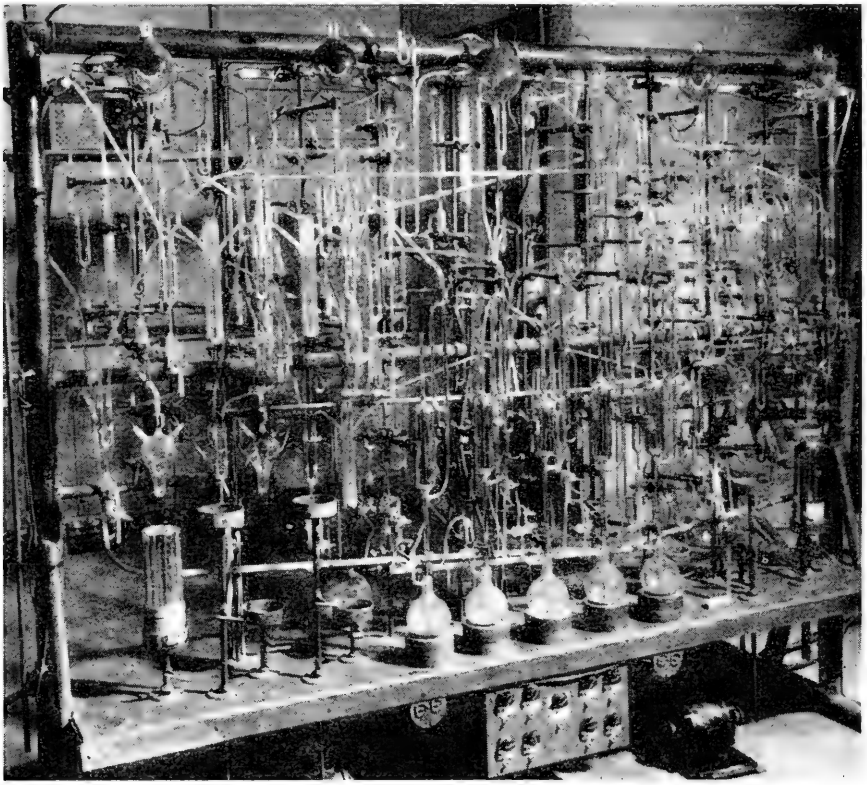

FIG. 582.—Gas analysis units showing gas purifying train, special traps for separating hydrocarbon fractions, combustion chambers, McLeod gauges used for measuring small quantities of gases, and auxiliary equipment. (Courtesy of Horvitz Research Laboratories.)

upon the addition of the first portion of acid. The carbon dioxide evolved is rapidly removed by opening the flask to a chamber containing potassium hydroxide solution and shaking the latter. The procedure is repeated until the carbonates are decomposed. An excess of 25 cc. of acid is then added. The flask containing the sample is now immersed in boiling water and heated for 30 minutes. The gas sample is then displaced into the potassium hydroxide flask where the volume of the sample is determined. It is next displaced from there into a previously evacuated tube.

The tube containing the extracted gases is attached to the analytical apparatus and, after passing through potassium hydroxide solution, concentrated sulfuric acid, ascarite and phosphoric anhydride, the gas enters the analytical apparatus proper, the pressure of which has previously been reduced to about 10^{-5} mm. of mercury.

The technique for carrying out the analysis of the extracted gases involves the combination of low-temperature fractionation and combustion methods. The routine analysis has been standardized to include three separate fractions. *The first* includes that portion of the gaseous mixture which is non-condensable at the temperature of liquid nitrogen (−196°C.) and consists mainly of air, methane, and hydrogen. *The second fraction* includes that portion of the mixture which is not retained at a temperature of −145°C., but is condensable at the temperature of liquid nitrogen. *The last fraction* is made up of the volatile soil constituents which are retained at −145°C. The middle fraction contains the ethane, propane, and butane which may be evolved from the sample, while the last fraction is made up of pentane and heavier hydrocarbons. The methane is determined by combustion of the non-condensable mixture over a glowing platinum wire. The water and carbon dioxide thus produced are collected and measured. The water, in excess of that required to account for all the carbon dioxide as methane, is calculated as hydrogen. The quantities of the other fractions, heavier than methane, are determined by first measuring the initial volumes present and then measuring the carbon dioxide resulting from combustion with purified air. The increase in the final volume is used as a measure of the quantities of these fractions initially present, the ethane-propane-butane fraction being calculated as propane, while the heaviest fraction is calculated as hexane.

Since the total volume of the gas sample initially prepared is known, and since the various parts of the analytical apparatus are calibrated, permitting the calculation of the volumes of gas used for the different determinations, the volumes of the various constituents are readily determined. The weights of the different fractions are calculated from the gas laws and the final results expressed in parts per billion by weight (dry basis) of the soil sample.

The following equation, applicable to methane, illustrates the method used in calculating the final results.

$$\text{Methane (parts per billion by weight)} = V \cdot 10^9 \cdot \frac{V_1}{V_2} \cdot \frac{.000714}{\text{Weight dry sample}}$$

V = Total volume of gas sample in cubic centimeters.
V_1 = Volume, in cubic centimeters, of carbon dioxide produced upon combustion of methane fraction.
V_2 = Volume, in cubic centimeters, of portion of gas sample used for methane determination.
.000714 = Weight, in grams, of 1 cubic centimeter of methane.

Weight dry sample = Weight, in grams, of original sample used in analysis corrected for moisture content which is determined with a separate portion of the original sample.

Results of Hydrocarbon Soil Surveys.—The reported results of several surveys are in apparent disagreement with the observations of Laubmeyer and Sokoloff. Instead of a distribution pattern in which the

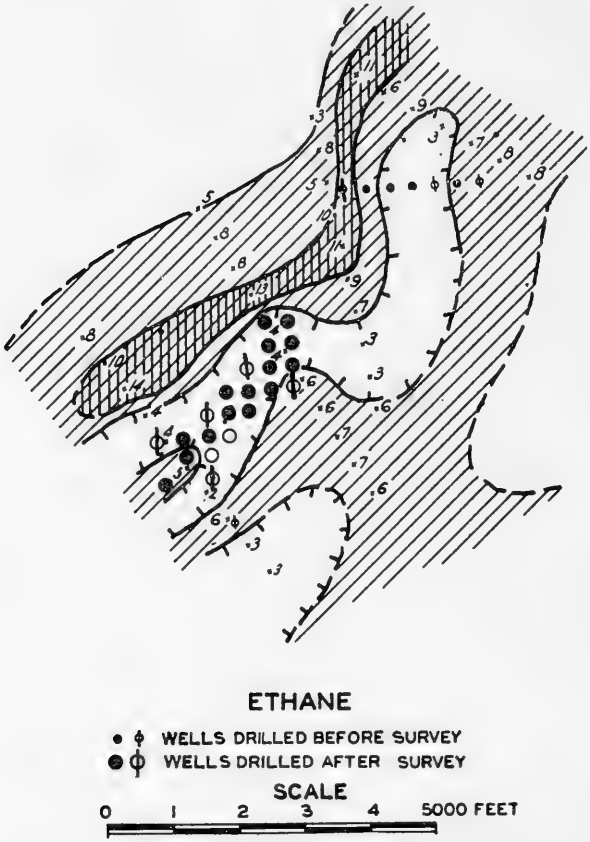

FIG. 583.—Soil analysis for ethane and propane. Station interval is 500 feet. (Horvitz, *Geophysics*, Vol. 10, No. 4.)

higher concentrations of hydrocarbons occur in the soils over the center of the productive areas, it was found that the higher concentrations are present in shallow soils around the edges of the productive areas producing the so-called "halo" pattern.

Upon re-examination of the reports of the Russian investigators, it was found that their data, in several instances, also indicated high concen-

trations at the edges of the producing areas.† One or two cases were noted by these workers‡ but explained away to their satisfaction, leaving their original conclusions unchanged.

One explanation of the observed soil survey patterns has been proposed by Rosaire§ who suggests that the "halo" pattern results from shallow mineralization produced by the deposition of minerals from ground waters during their upward migration. This mineralization produces a less permeable zone immediately over the structure, so that subsequent migration of hydrocarbons would result in relatively greater concentrations around the edges, rather than over the center. He substantiates his view by pointing out that drilling rates are lower for wells over structures than for those in the immediately surrounding territory. The existence of electrical†† and refraction anomalies over structures further supports his theory.

The application of soil analysis to stratigraphic prospecting is illustrated in Figure 583, which shows the ethane and propane values obtained by analysis of subsurface samples collected over a producing sand lens located in South Texas.

An example of the type of data‡‡ obtained by the acid extraction technique is shown in Figure 584, which gives the results of a reconnaissance survey over the Heidelberg area, Jasper County, Mississippi. In this survey analysis was made of 364 samples collected at depths of 12 feet. The station locations together with the total hydrocarbon values (methane plus ethane and heavier hydrocarbons) are shown on the map. The field development at the time the survey was started is shown by the well symbols. In order to ascertain the background values, data were obtained over an area extending four to six miles east, west, and south of the then known producing limits.

The following groups of values (expressed in parts per billion by weight) are enclosed by the various contour lines: 50-99; 100-199; 200-399; 400-799; and 800 and above. In order to display the variations in hydrocarbon concentration over the area sampled, various degrees of shading have been used; the darker the shading, the higher the concentration. Values below 50 parts per billion by weight are in the unshaded areas; values from 50-99 parts per billion are in the areas with the lightest shading; values from 100-199 parts per billion are in the medium shaded areas; and values of 200 parts per billion and above are in the zones with the heaviest shading.

The areas of low hydrocarbon concentration which are bordered by relatively high values are considered by Horvitz to be the favorable areas. The outer limits of the anomalous area are marked by the band of high hydrocarbon concentration which starts in Section 21, T. 1 N., R. 13 E.,

† E. E. Rosaire, *Geophysics*, Vol. 4, No. 4, pp. 300-304, 1939.
‡ V. A. Sokoloff, *Neftyanoye Khozyaystvo*, Vol. 27, No. 5, pp. 28-34, 1935.
§ E. E. Rosaire, "Shallow Stratigraphic Variations over Gulf Coast Structures," *Geophysics*, Vol. 3, No. 3, pp. 96-115, 1938.
†† See Figures 299, 351, 352.
‡‡ Leo Horvitz, *Geophysics*, Vol. 10, No. 4, pp. 487, 493, 1945.

and passes through Sections 27 and 34 of T. 1 N.-R. 13 E., then through Sections 2, 3, 10, 9, 8, 5, and 6 of T. 10 N., R. 10 W., and continues through Sections 1 and 2 of T. 10 N., R. 11 W. and into Section 33, T. 1 N., R. 12 E. The survey was not extended sufficiently to the north and northwest to determine the edges of the anomaly in these directions. An interesting feature of these data is the band of extremely high hydrocarbon concentrations which covers most of Section 36, T. 1 N., R. 12 E. and part of Section 31, T. 1 N., R. 13 E. This band of high values separates the main anomaly into two sub-anomalies.

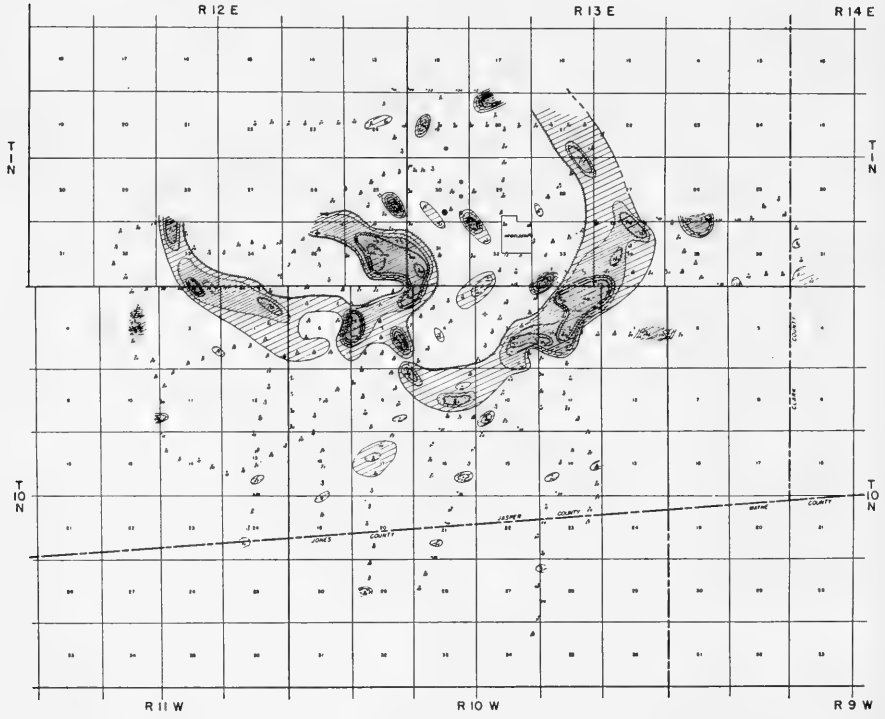

FIG. 584.—Geochemical survey of the Heidelberg Area, Jasper County, Mississippi. Well symbols show field development at start of survey, May 28, 1944. (Horvitz, *Geophysics*, October, 1945.)

Outside of the anomalous area are occasional values which are higher than the background values (below 50 parts per billion). Of 25 such values, 15 are in the first contour interval (50-99 parts per billion); five are in the next higher interval (100-199); four are in the third interval (200-399); and one is in the highest interval. Of significance is the fact that only 15% of the values in the background area attained 50 parts per billion or more, while in the anomalous area, 38% of the values are 50 parts per billion or more. Of the 16 extremely high values (800 parts per billion and above), only one is outside of the anomalous area.

A uniform grid was not used in conducting this survey. Instead, advantage was taken of the network of roads which covers the area, thus permitting the sampling of a large region within a relatively short period of time. A uniform grid may have produced a more outstanding pattern. This procedure could not be followed because of the limited time available for conducting this survey.

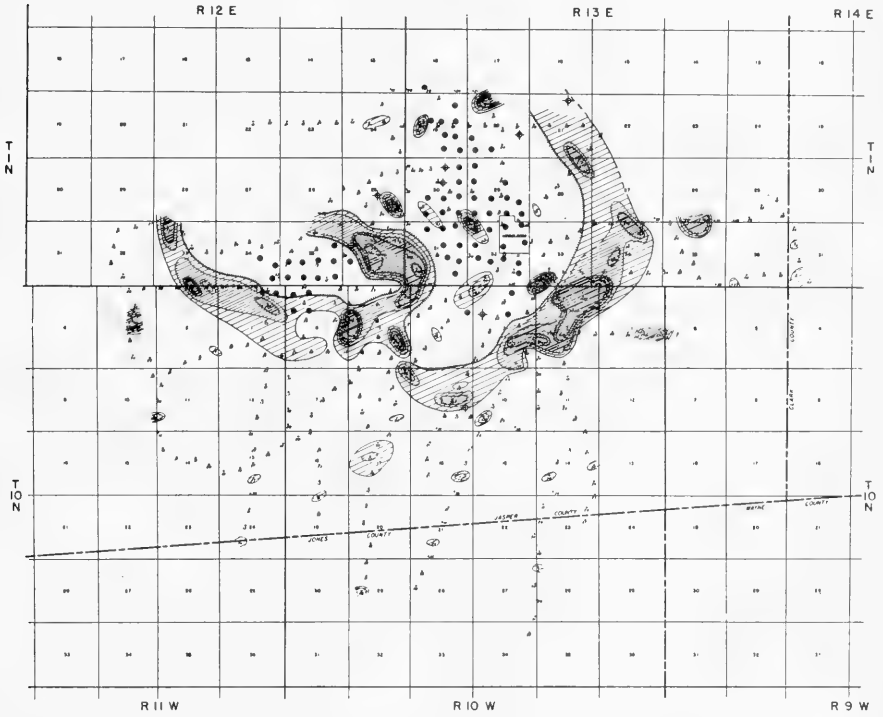

Fig. 585.—Geochemical survey of the Heidelberg Area, Jasper County, Mississippi. Field Development as of March 20, 1945, is indicated by well symbols. (Horvitz, *Geophysics,* October, 1945.)

Figure 585 shows the development of the Heidelberg Oil Field as of March 20, 1945. It is apparent that the geochemical data predicted the development rather well.

Soil Analysis for the Non-Volatile Constituents.—Close to the surface of the earth, mixtures of liquid and solid materials are present in appreciable quantities, and significant concentration patterns are often indicated by their determination. The concentration of these liquid and waxy materials decreases very rapidly with depth; therefore samples are usually collected from the top few inches of soil. Great care must be exercised to avoid sampling in plowed or otherwise disturbed areas. After drying, the samples are pulverized and sifted to remove vegetation. About

50 grams of each sample are extracted with a solvent such as carbon tetrachloride in standard Soxhlet extraction apparatus. After removing the solvent, the residue, composed of the organic solids and liquids, is weighed on an analytical balance. When samples are taken from the top one-half inch of soil, the waxes are predominant, while below this depth, the liquid fraction predominates. The sensitive analytical techniques used in the determination of the volatile hydrocarbons are not required here due to the fact that appreciable quantities of waxy and liquid materials are present in near-surface soils ranging from 20-30 parts per million by weight to several hundred parts per million by weight.

The wax values are calculated from the following equation:

$$\text{Parts per million of soil wax} = 10^6 \cdot \frac{\text{grams of soil wax extracted}}{\text{grams of pulverized sample analyzed}}$$

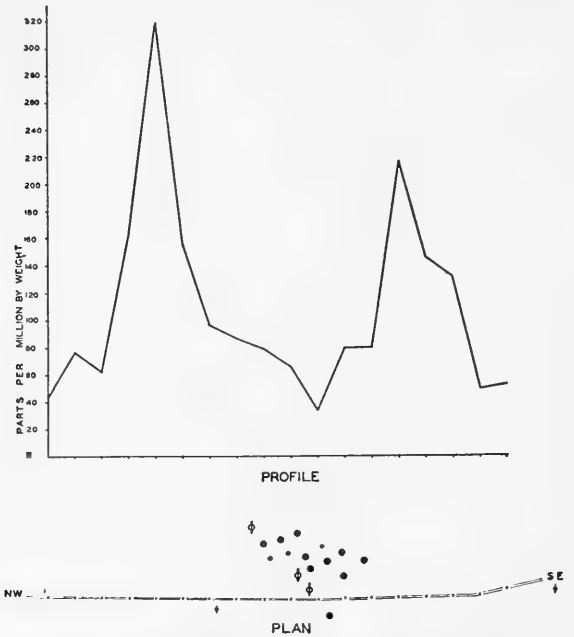

Fig. 586.—Soil wax survey. Station interval 1,000 feet indicated along profile. Small symbols indicate wells drilled before and large symbols indicate wells completed after the soil survey. (Horvitz, *Geophysics*, July, 1939.)

Figure 586 shows the results obtained with samples collected at depths of one-half inch along a profile crossing a producing field in South Texas. It will be noted that, as for the case of volatile soil hydrocarbons, the highest wax values are associated with the edges of the producing area.

McDermott† reports the presence of waxes and liquids in near-surface soils and finds a close relationship between these materials and petroleum accumulations at depth. In profiles crossing the East Texas Field, he reports the highest concentrations to be associated with the edge of the producing area.

Ransone‡ describes the discovery of the Hardy Oil Field, Jones County, Texas, which resulted from a reconnaissance geochemical survey covering most of northeast Jones County. The area surveyed included six producing areas, over all but two of which geochemical anomalies were found. In addition, four anomalies were found which, at the time the survey was made, were not associated with known petroleum accumulation. One of these anomalies now has been proved to be associated with the Hardy Field. It is of interest to note that this field is believed to be of the stratigraphic trap type.

In carrying out the geochemical survey, soil samples were collected at depths of 7 feet and analyzed for a constituent, the composition of which is not disclosed but which is considered to be present in the soil as a result of the upward passage of hydrocarbon gases.

The geochemical data obtained around the Hardy Field, together with the wells that have been drilled in the area, are shown in Figure 587.

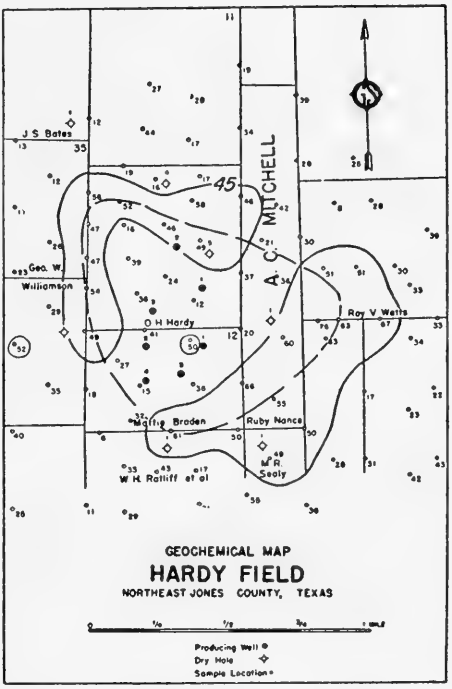

FIG. 587.—Geochemical survey of the Hardy Field. Data were originally obtained and map prepared prior to drilling of discovery well. (Ransone, *Geophysics*, July, 1947.)

The fluorographic method, developed by Ferguson and described by Campbell,§ involves exposing soil samples to ultra-violet light and recording the emitted light on a light-sensitive medium. The densities of the recorded sample images are measured by a transmission photometer. The fluorescent intensities of the samples are readily derived from the photometer readings, since the densities of the images are directly proportional to the fluorescent intensities of the corresponding samples.

† Eugene McDermott, "Concentrations of Hydrocarbons in the Earth," *Geophysics*, Vol. 4, No. 3, pp. 195-209, July, 1939.

‡ W. R. Ransone, "The Hardy Oil Field, Jones County, Texas," *Geophysics*, Vol. 12, No. 3, pp. 384-392, July, 1947.

§ Orton E. Campbell, "The Fluorographic Method of Petroleum Exploration," *World Petroleum*, March, 1946.

Reconnaissance surveys are made on a quarter mile grid pattern, while detail mapping requires that samples be taken at intervals of one-eighth and one-sixteenth mile. Samples of one ounce (by volume) are taken with an earth auger at depths of two feet. Since their fluorescent intensities do not vary, samples may be taken at different times and under varying conditions.

The high fluorescent intensities are found sometimes over the accumulation and sometimes around the edges of the accumulation.

Figure 588 shows the results of a fluorescent survey made of the Griffin Pool, Jones County, Texas, and illustrates the results obtained over an accumulation trapped by porosity variations in a lime reef formation. This anomaly is a so-called fluorescent minimum.

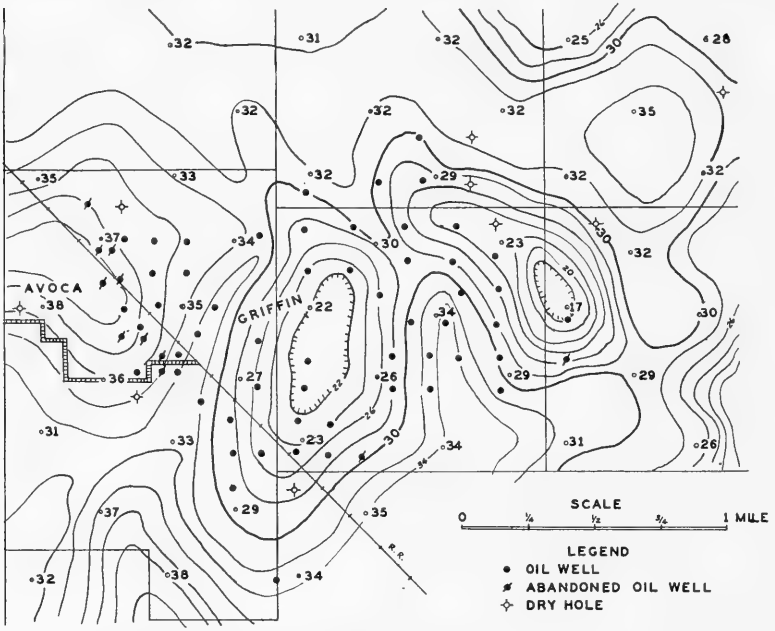

Fig. 588.—Fluorescent Survey of the Griffin Pool, Jones County, Texas. (Campbell, *World Petroleum*, March, 1946.)

Radioactivity measurements are reported† to be of value in determining the probable limits of production after the discovery well has been completed. In practice, a four-inch hole is bored to about three feet or to a depth insuring the formation of an adequate shoulder. The hole is extended another foot with a three-inch auger, after which a special packer is set at the shoulder so as to seal off the lower section of the hole from above.

† R. A. Stothart, "Radioactivity Determinations Set Production Delimitations," *The Oil Weekly*, January 4, 1943.

The closed portion is then exhausted through a vacuum pump, and the collector at the end of a small hose placed on the bottom of the sampling hole. When the hole has reached a condition of equilibrium, as indicated by a gauge on the suction line, the sample is collected, the packer removed, and the next station sampled in like manner. The radon concentrations are determined by means of an electroscope and, after plotting the values, the crest of the curve of emanation is determined. It is along this crest that the most favorable wells are expected. Successful extension work has been reported for Hunton lime areas in Oklahoma and many areas in the Texas Gulf Coast.

Based on the escape of hydrocarbons from a petroleum accumulation, Tripp† suggests another approach to the search for oil. The technique involves the determination of the concentration of radioactive minerals in the zone of maximum colloidicity and simultaneous determination of the mineral wax content. Tripp states that the concurrence of anomalies in both properties has been experimentally demonstrated to be related to the occurrence of petroleum at depth. The experience background has been obtained in areas believed to be ideal with respect to soil and climate conditions.

Costs.—The expense of conducting a geochemical survey depends upon the type of method employed. In general, the surveys which involve the collection of samples from about eight to twelve feet and report determinations for the volatile hydrocarbons cost approximately fifteen cents per acre in the case of reconnaissance and twenty-five to fifty cents per acre for detail surveys. On an individual sample basis, the analysis charge is about $15 and the cost of collection averages about $7.50 per sample. In employing the methods which involve the analysis of near-surface samples, the costs range from about $5 to $10 per sample for collection and analysis.

The average cost of a geochemical survey is usually less than one-half the cost of a seismic survey and approaches the cost of a gravity meter survey.

Application of Geochemical Prospecting Methods. — The direct approach afforded by the use of geochemical methods in prospecting for oil and gas and their relatively low cost suggest reconnaissance surveying as an important application. Localized areas which show favorable indications may then be detailed by the more expensive seismograph to determine if structure is associated with the geochemical anomalies. Although used to a limited extent in reconnaissance work, geochemical methods are more frequently employed to obtain data for correlation with information already available from the use of other methods such as the seismograph, gravity meter, or subsurface geology.

† R. Maurice Tripp, "Geophysical Principles for Determining Subsurface Conditions," *The Oil Weekly*, June 9, 1947.

The greatest potential value of geochemical methods lies in their possible application to the search for stratigraphic traps. However, their use for this purpose will have to await wider acceptance by the oil industry, which will not come until sufficient statistical evidence is available to show that the chemical methods can assist materially in the search for oil. As more is learned concerning the mechanisms through which geochemical anomalies are produced and as improvements continue to be made in the quality of the collected data and their interpretation, the place of geochemistry among the established methods of prospecting may eventually be assured.

Geochemical Prospecting for Ore

The application of geochemical techniques to the location of hidden ore deposits is a relatively recent development.† The method is founded on the assumption that many ore deposits, either at the time of their formation or at some later time, emitted traces of the components of the ore or solutions that had permeated the environment of the ore. Traces of the metals may thus be found in the overlying or surrounding soils, or in the ground or surface waters at a considerable distance from the ore. The metal content of the plants in the area of metal dispersion may also be influenced.

Surface Waters.—When investigating a new area, the average concentration of heavy metals in the surface waters of the area as a whole is first determined. The search is then continued to determine whether any unusually high concentrations are to be found locally. For reconnaissance testing, diphenyl thiocarbazone, an organic dye which forms colored compounds with sixteen metallic elements, is of considerable value. A concentration of less than one part per million of zinc, copper, lead, silver, gold, mercury, and other metals can be detected with this reagent. Separation of these metals, in the field test, is impracticable and unnecessary, as the chief purpose of the water testing is to provide a background for more detailed studies as to the kind and extent of mineralization in the area. By observing the relative intensities of colors developed by the reaction of the dye with the dissolved metals, and by following the colors upstream, the source of the metals in question can generally be located.

Soils.—Geochemical anomalies, that is, abnormally high concentrations of some particular element in the soil or the soil materials, are quite commonly associated with mineralized bedrock. The anomalies may fan out both horizontally and vertically from the mineralized source area. A series of such anomalies, related to underlying mineralized material, is called a *dispersion halo*. Having determined the origin, kind, shape, and extent of a dispersion halo, it is then often possible to deduce its spatial relation to an ore body.

† This discussion is based largely on an address entitled "Geochemical Prospecting for Ore," delivered by V. P. Sokoloff at the annual meeting of the Colorado Mining Association, Denver, Colorado, February 7, 1948.

Figure 589 shows three general types of dispersion halos which may be found under various conditions. These develop in a climate where the soil-forming processes are not especially intense and where the ores are not particularly deep below the surface. This is especially true of metals of low solubility like molybdenum, tungsten, tin, and lead. Halos of this type can be outlined by making a series of field tests on samples taken in a grid pattern. The resulting map, on correlation with geologic data, may be sufficient to warrant more expensive sampling in depth or drilling. This method has been used successfully in Russia† to locate economically

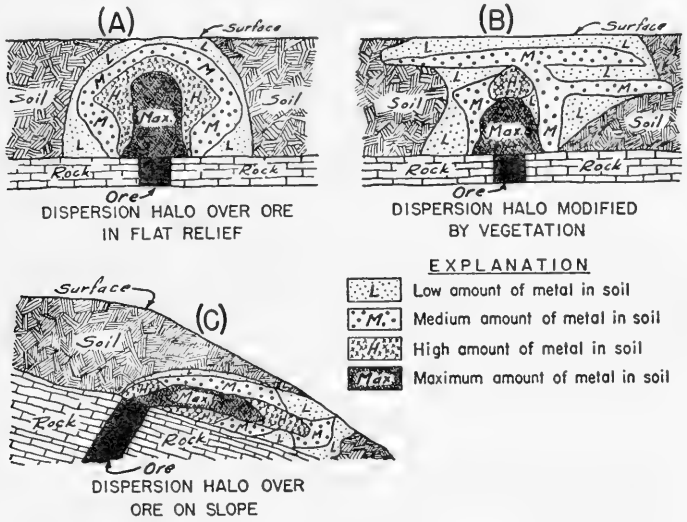

FIG. 589.—Typical dispersion halos formed under various conditions. (A) ideal case; (B) disturbing effect of vegetation; (C) disturbing effect of slope. (Courtesy of V. P. Sokoloff, "Geochemical Prospecting for Ore," *ibid.*)

important ore bodies. According to the Russian literature, this method is most successful in areas where residual soils are of only moderate thickness; and for certain metals occurring in minerals that are fairly resistant to weathering. Prospecting for complex or for buried halos would be difficult.

Once the probability of geochemical anomalies has been established, the problem then involves: (1) the selection of indicator elements for which tests are to be made; (2) sampling procedures; (3) chemical tests; and (4) interpretation of results.

The indicator element does not necessarily have to be the same element the prospector is seeking in the ore. Above some oxidized lead-zinc deposits, for example, determinations of sulphate in the soil are fully as useful in

† E. A. Sergeev, "Fisico-Himicheskii Metod Poiskov Rudnyh Saleshei," Materially Vsesoiuznogo Nauchno-Issledovatelnogo Geologicheskogo Institute. Geofisica-Sbornik 9-10: 3-54. (Geochemical Method in Prospecting for Ore Deposits.)

outlining the dispersion halos as determinations of the metals themselves. In dealing with ores containing several metals, the choice of the indicator metal is determined entirely by environment and the judgment of the prospector.

The sampling procedure followed also depends upon the particular problem and environment. The Russian geochemists usually have sampled the soil on a close grid pattern and at fixed intervals in depth.

A large number of testing procedures adapted for field use are known. They include color reactions between traces of metals and organic dyes, spectrographic analyses, electric potential measurements, flame tests, and others. In general, the color tests appear to be the most rapid and satisfactory. Since prospecting in the field requires a very large number of tests, rapidity and qualitative sensitivity of the test are preferred to quantitative accuracy. In outlining the dispersion halos, determination of the relative amounts of the indicator metal in the samples is sufficient, and the results may be expressed as "high," "medium," and "low" rather than by actual numbers. By following this procedure, from 40 to 200 tests per day can be made by a single chemist, whereas a quantitative analysis of the same number of samples in the laboratory would require weeks or months.

A map showing chemical anomalies, plotted with reasonable accuracy, is the final result of any geochemical prospecting job. Interpretation of such a map is rarely possible without correlation with the geologic features. However, it is conceivable that in areas of thick residual soils, geochemical prospecting alone may locate ores at much lower cost than other prospecting methods.

Plants.—The interest in plants, in connection with ore prospecting, has been motivated chiefly by three observations. (1) Certain species of plants have a specific requirement for certain metals and may not develop in the absence of these metals. Such species are regarded as *indicator plants*. The so-called "zinc flora," for example, is a group of species, chiefly grasses and sedges that develop best on soils high in zinc. (2) By means of their roots, plants sample a large mass of soil, and some of them concentrate certain metals, chiefly in their tissues. Thus unusually high concentrations of metals in the soil, water, and rock in which the plants grow may be expressed by a high concentration of those metals in the plant material. Zinc, nickel, copper, and cobalt are stored chiefly in the plant leaves. Lead, arsenic, and some others, on the other hand, are believed to be concentrated chiefly in the roots. Once such accumulator plants have been recognized, the presence and even the boundaries of a geochemical anomaly may be established by analysis under favorable conditions. (3) The presence of unusually high amounts of certain metals in the soil, water, or rock may cause injuries or abnormalities in the plants, although the plants themselves may be neither indicators nor accumulators of the element in ques-

tion. Thus from a study of these plant symptoms, information may be obtained concerning the presence of certain metals in the area.

Although plant chemistry studies show promise of increasing their value in locating ore bodies, they have not progressed to the point attained by soil and water studies.

Geochemical Well Logging

Geochemical well logging involves the analysis of cuttings or drilling fluids, primarily for hydrocarbons. Various inorganic constituents, such as chlorides, sulphates, and carbonates, may also be determined. The data obtained by the various techniques used are very helpful in locating potential producing horizons, and in many instances to predict in advance of the drill the probability of encountering a petroleum accumulation.

Methods Using Well Cuttings

Hydrocarbon Logging.—The techniques† used for extraction and analysis of hydrocarbons from well cuttings are the same as those described in connection with geochemical exploration.

The hydrocarbon values are plotted and, based on their order of magnitude and patterns they produce, interpretations are made. Logs of wells located toward the center of an accumulation show low hydrocarbon concentrations in the upper part of the well, but at some distance above the accumulation a definite increase is obtained. From this point on, the values gradually increase until the deposit is reached, when *maximum values* are obtained. After passing the first accumulation, the values rapidly decrease to normal unless another deposit is being approached, in which case the same pattern obtained above the first accumulation will be repeated. Logs of wells located at the edge of an accumulation show higher values in the upper part of the well than do centrally located wells. In such cases, the values increase gradually until the accumulation is reached. Logs of nonproductive wells that are located at considerable distance, laterally, from a petroleum accumulation show low hydrocarbon concentrations throughout.

For the case of producing wells, the length of the section immediately above the deposit over which significantly high values are obtained depends upon the nature of the deposit. The higher the gravity of the accumulation, the greater is the distance to the point above the deposit where the first abrupt increase in concentration is observed.

The relative quantities of the ethane-propane-butane, pentane, and heavier hydrocarbons present serve as an index to the type of accumulation. Approximately equal quantities of these constituents are found in the case of gas-condensate accumulations. In the case of oil accumulations, the pentane and heavier hydrocarbons predominate.

† Leo Horvitz, "Well Logging Methods Conference," *Bulletin No. 93 of the Agricultural and Mechanical College of Texas,* March 11-15, 1946. See also W. R. Ransone, "Geochemical Well Logging," *Geophysics,* Vol. 6, No. 3, pp. 287-293, July, 1941.

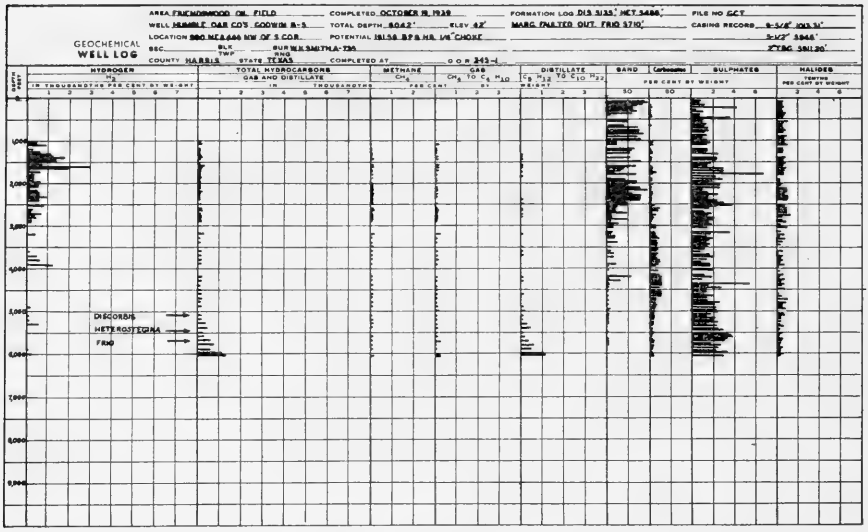

FIG. 590.—Geochemical log, producing well, Friendswood Oil Field, Harris County, Texas. (Rosaire, A.A.P.G., Vol. 24, No. 8, August, 1940.)

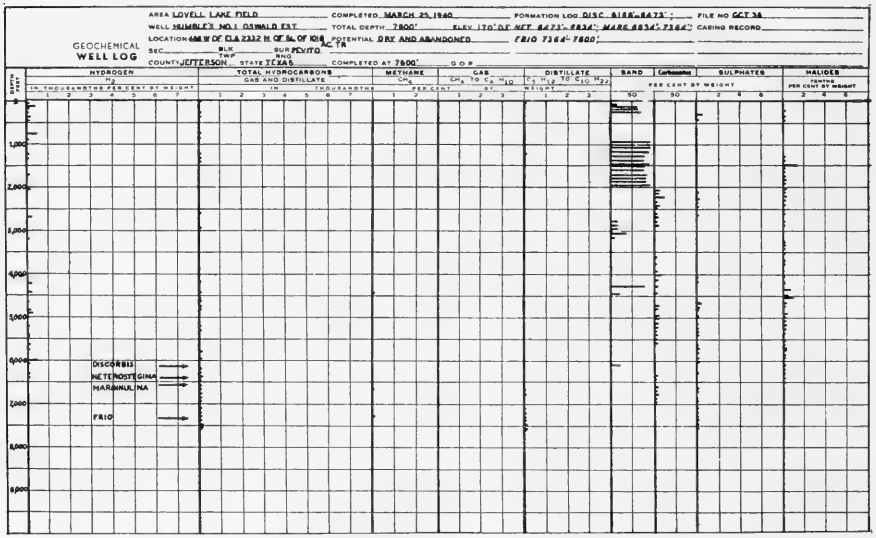

FIG. 591.—Geochemical log, dry hole, about 3,500 feet outside (present) limits of production. (Rosaire, A.A.P.G., Vol. 24, No. 8, August, 1940.)

Figure 590 shows the geochemical well log of a producing well in the Friendswood oil field. The oil is of approximately 40° Bé gravity. The total hydrocarbons began to attain significantly high values at about 5,300 feet and yielded the highest value at about 6,040 feet, from which depth

the producing zone is reached. It will be noted that the predominating fraction is that of the pentane and heavier hydrocarbons.

Figure 591 is a geochemical log of a dry hole located only 3,500 feet from production in the Lovell Lake oil field. It is seen that the various constituents are present in very small quantities, suggesting that the geochemical effects produced by a petroleum accumulation extend laterally for only short distances; i.e., the migration of hydrocarbons is substantially upward.

It will be noted that other constituents, in addition to the hydrocarbons, have been plotted on the logs. These inorganic constituents are of use for correlation purposes only.

Fluorologging.—A logging technique has been described† which is based on the principle that the rocks overlying an oil accumulation are characterized by anomalously high fluorescent intensities. This technique, known as *Fluorologging,* involves the preparation of logs by plotting the fluorescent intensity of well cuttings against depth. A geologic section overlying an oil accumulation will show a considerably higher average fluorescent intensity than a section penetrated in barren territory. A porous rock recovered from the subsurface which shows a value of 1.25 fluorescent units or more is considered to be from a commercial zone.

Two logs are usually plotted for a well, showing: (1) the "fixed fluorescence" which represents the fluorescence of a formation after any oil or gas present is flushed out; and (2) the "free fluorescence," which represents the fluorescent intensities of the free oil and gas in well samples. From these data, predictions can be made as to whether the well will encounter a petroleum accumulation. Also, commercial zones which have been passed up during drilling can be located.

Mud Analysis Logging.—The mud analysis logging system‡ continuously analyzes and records the oil and gas content of mud returns from wells being drilled by the rotary method. Oil or gas detected in the returning drilling fluid indicates oil or gas in the formation penetrated by the bit. Another useful phase of the system plots, in detail, drilling speed as a function of depth, see page 1093.

For the purpose of detecting oil in the drilling mud, ultra-violet light is used. The apparatus is capable of detecting quantities as small as one part of oil in a hundred thousand parts of mud. The mud samples are treated to remove any excessive viscosity and gel strength before they are viewed in the detection apparatus. The oil in the samples appears as small fluorescent spots under the ultra-violet light. By observing a fluorescent spot through a magnifier, and then switching to visible light, it is possible to distinguish crude oil from other oils or greases that may accidentally get into the mud. Crude oil from a previous show that has already been

† O. E. Campbell, "Principle Uses of Fluorologs," *The Oil Weekly,* December 30, 1946.
‡ Robert E. Souther, "Application of Mud Analysis Logging," *Geophysics,* Vol. 10, No. 1, pp. 76-90, January, 1945.

circulated is distinguished from a new show by virtue of the fact that new oil fluoresces more brightly than that which has been circulated.

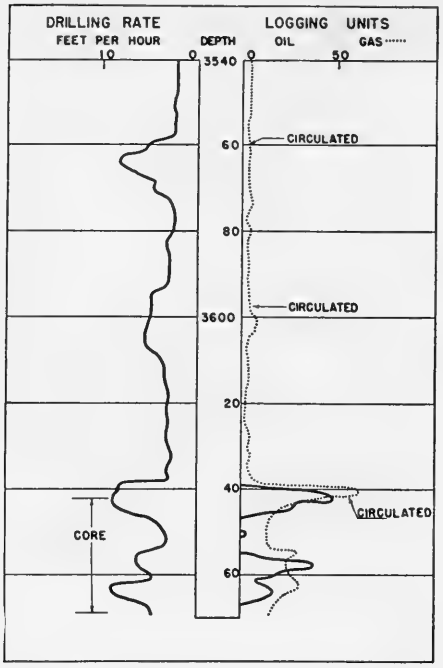

FIG. 592.—Mud analysis log of a West Texas discovery well. The well was completed in the deeper of the two oil zones logged. (Souther, *Geophysics.*)

In determining the gas content, a portion of the returning mud is first passed through a trap where the gas is removed. Air, which is constantly drawn through the trap by means of a motor-drawn vacuum pump, then carries the gas through a flexible hose to the analyzer, where it passes in turn through a filter, a humidifier, a flow meter, and a "hot wire" gas detector.

The results of the oil and gas analyses are correlated with depth by means of a special instrument which indicates the depth of the bit at all times. All of the information is assembled in the form of a log which shows curves for rate of penetration, oil content and gas content.

Figure 592 illustrates the application of mud analysis logging in West Texas, as used to supplement the electrical logs.

GEOCHEMICAL METHODS

UNITED STATES PATENTS

1,843,878 Issued Feb. 2, 1932. Gunther Laubmeyer. "Method of and Apparatus for Detecting the Presence of Profitable Deposits in the Earth."

2,103,187 Issued Dec. 21, 1937. August Gustav and Adolf Schröter. "Method for Detecting Small Quantities of Gas."

2,112,845 Issued April 5, 1938. Lynn G. Howell. "Apparatus for Locating Hydrocarbon Deposits in the Earth."

2,141,261 Issued Dec. 27, 1938. Joseph Baldwin Clark. "Method and Apparatus for Collecting Soil Gas Samples."

2,158,980 Issued May 16, 1939. Nils Brundin. "Method of Locating Metals and Minerals in the Ground."

2,165,214 Issued July 11, 1939. Ludwig W. Blau and William B. Lewis. "Geophysical Prospecting with Short Electromagnetic Waves."

2,165,440 Issued July 11, 1939. George S. Bays. "Gas Mapping."

2,170,435 Issued Aug. 22, 1939. William J. Sweeney. "Gas Analysis Apparatus."

2,174,349 Issued Sept. 26, 1939. John B. Littlefield. "Gas Analysis."

2,177,139 Issued Oct. 24, 1939. Leo Horvitz. "Gas Separation."

2,183,964 Issued Dec. 19, 1939. Leo Horvitz. "Method of Exploration for Buried Deposits."

2,192,525 Issued March 5, 1940. Esme E. Rosaire and Leo Horvitz. "Geophysical Prospecting Method."

2,198,619 Issued April 30, 1940. Leo Horvitz. "Geochemical Exploration."
2,210,546 Issued August 6, 1940. Gerald L. Hassler. "Soil Gas Sampling Device and Method."
2,212,211 Issued August 20, 1940. August H. Pfund. "Apparatus for Detecting and Measuring Heteroatomic Gases."
2,212,681 Issued Aug. 27, 1940. Thomas H. Dunn. "Soil Gas Analysis."
2,213,138 Issued Aug. 27, 1940. John T. Hayward. "Method and Apparatus for Detecting Oil in Well Drilling."
2,213,904 Issued Sept. 3, 1940. Thomas H. Dunn. "Geochemical Prospecting."
2,213,905 Issued Sept. 3, 1940. Joseph Baldwin Clark. "Geochemical Prospecting."
2,219,540 Issued Oct. 29, 1940. Benjamin Miller. "Gas Analysis Method and Apparatus."
2,223,183 Issued Nov. 26, 1940. Edward B. Peck. "Prospecting for Oil."
2,223,785 Issued Dec. 3, 1940. Gerald L. Hassler. "Gas Sampling System."
2,227,438 Issued Jan. 7, 1941. John G. Campbell. "Method of Determining the Petroleum Oil Content of Earth Samples."
2,228,223 Issued Jan. 7, 1941. George S. Bays. "Geochemical Prospecting."
2,229,884 Issued Jan. 28, 1941. Curtis R. Chalkley. "Oil and Gas Detector Apparatus."
2,230,593 Issued Feb. 4, 1941. Gerald L. Hassler. "Apparatus for Analyzing Gaseous Mixtures."
2,234,637 Issued March 11, 1941. Millard S. Taggart, Jr. "Oil Prospecting Method."
2,241,154 Issued May 6, 1941. Jacob Neufeld. "Well Surveying Method and Apparatus."
2,257,170 Issued Sept. 30, 1941. Lynn G. Howell. "Method for Locating Hydrocarbon Deposits in the Earth."
2,261,498 Issued Nov. 4, 1941. John C. Karcher. "Apparatus for Analyzing Gases."
2,261,764 Issued Nov. 4, 1941. Leo Horvitz. "Geochemical Prospecting."
2,266,556 Issued Dec. 16, 1941. Walter A. Kelly. "Method of Locating Oil Deposits."
2,269,889 Issued Jan. 13, 1942. Ludwig W. Blau. "Process for Locating Valuable Subterranean Deposits."
2,270,299 Issued Jan. 20, 1942. Leo Horvitz. "Geochemical Prospecting."
2,272,645 Issued Feb. 10, 1942. Esme E. Rosaire. "Geochemical Prospecting."
2,278,929 Issued April 7, 1942. Leo Horvitz. "Geochemical Prospecting."
2,283,650 Issued May 19, 1942. Charles M. Sanborn. "Earth Sampling Equipment."
2,284,147 Issued May 26, 1942. Henry N. Herrick. "Method and Apparatus for Soil Gas Analysis."
2,286,384 Issued June 16, 1942. Robert Thomas Sanderson. "Apparatus for Gas Analysis."
2,287,059 Issued June 23, 1942. Ralph N. Platts. "Apparatus for Obtaining Soil Samples."
2,287,101 Issued June 23, 1942. Leo Horvitz. "Means and Method for Analysis."
2,289,687 Issued July 14, 1942. R. W. Stuart. "Method and Apparatus for Logging Wells."
2,292,300 Issued Aug. 4, 1942. Robert O. Smith. "Photochemical Exploration Method."
2,294,425 Issued Sept. 1, 1942. Robert Thomas Sanderson. "Geo-Micro-Biological Prospecting."
2,297,939 Issued Oct. 6, 1942. John G. Campbell. "Method of Detecting the Penetration of an Oil-Bearing Horizon."
2,305,082 Issued Dec. 15, 1942. Claude R. Hocott. "Geochemical Prospecting."
2,305,384 Issued Dec. 15, 1942. Herbert Hoover, Jr. "Geophysical Prospecting Method."
2,310,291 Issued Feb. 9, 1943. Leo Horvitz. "Geochemical Prospecting."
2,310,318 Issued Feb. 9, 1943. Esme E. Rosaire. "Geochemical Prospecting."
2,311,151 Issued Feb. 16, 1943. John G. Campbell. "Analysis of Soil Samples for Determining Oil Content."
2,312,271 Issued Feb. 23, 1943. Robert O. Smith. "Method of Locating Subterranean Petroleum Deposits."
2,318,062 Issued May 4, 1943. Trent R. Dames. "Soil Sampler."
2,320,577 Issued June 1, 1943. Thomas H. Dunn. "Geochemical Prospecting."
2,319,734 Issued May 18, 1943. Leo Horvitz. "Geochemical Prospecting."
2,320,681 Issued June 1, 1943. Hubert H. Thompson. "Method of Analyzing Earth Formations."
2,321,293 Issued June 8, 1943. Gerald L. Hassler. "Apparatus for Measuring Pressures in Containers."

2,324,085 Issued July 13, 1943. Leo Horvitz and Esme E. Rosaire. "Geochemical Well Logging."
2,324,107 Issued July 13, 1943. Sylvain J. G. Pirson. "Method for the Geochemical Prospection of Hydrocarbon Deposits."
2,325,057 Issued July 27, 1943. Herbert Hoover, Jr. and Herbert E. Metcalf. "Means for Obtaining Soil Samples."
2,327,539 Issued Aug. 24, 1943. Edward D. McAlister. "Apparatus for Gas Analysis."
2,328,555 Issued Sept. 7, 1943. Herbert Hoover, Jr. "Well Logging Method."
2,329,824 Issued Sept. 21, 1943. John G. Campbell. "Method of Determining Suitable Areas for Oil Exploration."
2,330,021 Issued Sept. 21, 1943. M. A. Arthur. "Geochemical Prospecting."
2,330,026 Issued Sept. 21, 1943. Ludwig W. Blau. "Geochemical Prospecting."
2,330,716 Issued Sept. 28, 1943. Leo Horvitz. "Geochemical Prospecting."
2,330,717 Issued Sept. 28, 1943. Leo Horvitz. "Geochemical Prospecting."
2,330,758 Issued Sept. 28, 1943. Millard S. Taggart, Jr. "Geochemical Prospecting."
2,330,829 Issued Oct. 5, 1943. H. T. F. Lundberg and N. B. Keevil. "Method of Geophysical Exploration."
2,334,269 Issued Nov. 16, 1943. Stephen A. Kiss. "Geochemical Prospecting Method."
2,336,176 Issued Dec. 7, 1943. Leo Horvitz. "Geochemical Prospecting."
2,336,612 Issued Dec. 14, 1943. Leo Horvitz. "Geochemical Prospecting."
2,336,613 Issued Dec. 14, 1943. Leo Horvitz. "Geochemical Well Logging."
2,337,443 Issued Dec. 21, 1943, Ludwig W. Blau. "Process for Locating Valuable Subterranean Deposits."
2,337,465 Issued Dec. 21, 1943. J. J. Heigl. "Well Logging."
2,338,643 Issued Jan. 4, 1944. Leo Horvitz. "Geochemical Prospecting."
2,339,651 Issued Jan. 18, 1944. Donald S. Rearden, Earl G. Brewster and Robert Thomas Sanderson. "Geochemical Prospecting."
2,341,169 Issued Feb. 8, 1944. R. W. Wilson, A. Long, Jr. and M. T. Randolph. "Method and Apparatus for Detecting Gas in Well Drilling Fluids."
2,342,273 Issued Feb. 22, 1944. J. T. Hayward. "Method of Detecting Oil in Well Drilling."
2,343,772 Issued March 7, 1944. Leo Horvitz. "Geochemical Prospecting."
2,345,219 Issued Mar. 28, 1944. Robert Thomas Sanderson. "Geochemical Prospecting."
2,346,203 Issued April 11, 1944. W. M. Zaikowsky. "Well Logging Method."
2,346,735 Issued April 18, 1944. Patrick F. Dougherty. "Method of Detecting Petroleum Deposits."
2,348,103 Issued May 2, 1944. Arnold O. Beckman. "Method of Soil Analysis for Location of Oil Deposits."
2,349,250 Issued May 23, 1944. Richard L. Doan. "Gas Detection."
2,349,472 Issued May 23, 1944. Millard S. Taggart, Jr. "Oil Prospecting Method."
2,356,454 Issued Aug. 22, 1944. William B. Ferguson. "Method and Apparatus for Fluorography."
2,361,261 Issued Oct. 24, 1944. John G. Campbell. "Method of Detecting Penetration of an Oil-Bearing Horizon."
2,362,805 Issued Nov. 14, 1944. Richard L. Doan. "Method and Apparatus for Detecting Hydrocarbons."
2,364,898 Issued Dec. 12, 1944. Gerald L. Hassler. "Analysis Method for Geochemical Exploration."
2,364,940 Issued Dec. 12, 1944. Clarence C. Bies. "Gas Analysis and Combustion Chamber Therefor."
2,366,351 Issued Jan. 2, 1945. James L. Patton. "Measurement of the Rate of Soil Gas Evolution."
2,367,592 Issued Jan. 16, 1945. Eugene McDermott. "Method of Prospecting for Buried Deposits."
2,367,664 Issued Jan. 23, 1945. John G. Campbell and Ralph H. Fash. "Method of Petroleum Exploration."
2,369,811 Issued Feb. 20, 1945. R. W. Stuart. "Drill Mud Logging Recording System or the Like."
2,370,703 Issued Mar. 6, 1945. Wladimir M. Zaikowsky. "System for Gas Analysis."
2,370,793 Issued March 6, 1945. Leo Horvitz. "Geochemical Prospecting."
2,371,637 Issued March 20, 1945. Eugene McDermott. "Method of Prospecting for Buried Deposits."
2,374,135 Issued April 17, 1945. Edwin E. Roper. "Geochemical Surveying."

2,374,227 Issued April 24, 1945. Herbert E. Metcalf. "Geochemical Prospecting System."
2,374,937 Issued May 1, 1945. Leo Horvitz. "Geochemical Well Logging."
2,375,949 Issued May 15, 1945. Robert Thomas Sanderson. "Geochemical Prospecting."
2,376,145 Issued May 15, 1945. Leo Horvitz. "Gas Analysis."
2,376,366 Issued May 22, 1945. Reed C. Lawlor and Herbert E. Metcalf. "Geochemical Prospecting System."
2,377,082 Issued May 29, 1945. Bela Hubbard. "Geochemical Prospecting."
2,379,045 Issued June 26, 1945. Henry F. Sturgis. "Analyzing Earth Formations."
2,382,992 Issued Aug. 21, 1945. Jesse Stewart Harris. "Soil Sampling Apparatus."
2,386,832 Issued Oct. 16, 1945. Wladimir M. Zaikowsky. "Method of Obtaining Soil Gas Samples."
2,387,513 Issued Oct. 23, 1945. C. R. Hocott. "Well Logging."
2,389,706 Issued Nov. 27, 1945. Philip S. Williams and Monroe W. Kriegel. "Apparatus for Gas Analysis."
2,393,092 Issued Jan. 15, 1946. R. L. Doan. "Apparatus for Gas Analysis of Drilling Mud."
2,393,650 Issued Jan. 29, 1946. Herbert E. Metcalf. "Apparatus for Analyzing Hydrocarbons."
2,393,674 Issued Jan. 29, 1946. Wladimir M. Zaikowsky. "Apparatus for Gas Analysis."
2,394,703 Issued Feb. 12, 1946. Edward Lipson. "Soil Analysis by Radiant Energy."
2,395,014 Issued Feb. 19, 1945. Edwin E. Roper. "Geochemical Prospecting."
2,398,580 Issued April 16, 1946. F. W. Crawford. "Method of Prospecting for Hydrocarbons."
2,399,965 Issued May 7, 1946. Reinhold Weber. "Method for Determining Combustible Gases in Gas Mixtures."
2,400,046 Issued May 7, 1946. F. E. Hummel. "Mud Logging System."
2,400,420 Issued May 14, 1946. Leo Horvitz. "Geochemical Prospecting."
2,403,002 Issued July 2, 1946. H. L. Johnson. "Apparatus for Undisturbed Overburden Sampling."
2,403,631 Issued July 9, 1946. C. B. Brown. "Method for Determining the Petroleum Hydrocarbon Content of Earth Samples."
2,406,611 Issued Aug. 27, 1946. Harvey T. Kennedy. "Geochemical Prospecting Method."
2,408,964 Issued Oct. 8, 1946. W. E. Winn and Patrick F. Dougherty. "Method of Logging Wells."
2,408,965 Issued Oct. 8, 1946. W. E. Winn and Patrick F. Dougherty. "Method of Logging Wells."
2,412,237 Issued Dec. 10, 1946. H. W. Washburn and D. D. Taylor. "Mass Spectrometry."
2,412,359 Issued Dec. 10, 1946. Edwin E. Roper. "Ionic Analysis."
2,414,876 Issued Jan. 28, 1947. Leo Horvitz. "Gas Analysis."
2,414,913 Issued Jan. 28, 1947. Philip S. Williams. "Soil Gas Prospecting."
2,422,852 Issued June 24, 1947. G. L. Ratcliffe. "Process of Detecting Oil Dispersed in Well Drilling Fluids."
2,423,774 Issued July 8, 1947. J. J. Heigl. "Oil Determination."
2,427,261 Issued Sept. 9, 1947. F. W. Crawford. "Method for Analyzing Gas."
2,431,019 Issued Nov. 18, 1947. R. B. Barnes. "Multicomponent-Gas Analyzer."
2,431,487 Issued Nov. 25, 1947. D. H. Larsen. "Oil Detection in Drilling Muds."
2,437,045 Issued March 2, 1948. E. E. Roper. "Determination of Hydrocarbon Concentration in Soil Samples."
2,442,476 Issued June 1, 1948. M. S. Taggart, Jr. "Prospecting for Petroleum Deposits."
2,449,627 Issued Sept. 21, 1948. W. J. Sweeney. "Oil Prospecting Method."
2,451,885 Issued Oct. 19, 1948. R. M. Squires and N. P. Stevens. "Geophysical Prospecting."
2,459,512 Issued Jan. 18, 1949. R. H. Fash and J. G. Campbell. "Petroleum Exploration by Soil Analysis."
2,465,563 Issued March 29, 1949. A. J. Abrams. "Geophysical Prospecting Method."
2,465,564 Issued Mar. 29, 1949. A. J. Abrams. "Location of Buried Hydrocarbon Deposits."

CHAPTER IX

THERMAL METHODS

The generation and dissipation of heat governs the life history of the millions of stars distributed throughout celestial space. After the initial period of condensation of the nebula which formed our earth, when intense heat was generated, a period was ultimately reached when the internal energy of the earth was radiated more rapidly than it was generated. From this period onward the radioactive matter in the earth became an increasingly important source of heat. With any reasonable assumption regarding the distribution of radioactive material with depth, it can be shown that ¾ to ⅘ of the present total surface flow of heat is supplied by radioactivity. During the estimated 3,000 million years' life of our earth there has been a decrease in radioactivity heat generation of about 50 per cent. The internal heating of the earth has therefore reached a fairly stable phase and will continue to decline at a slower rate, i.e. exponentially with time.

The present temperature of the earth is governed by many factors.† From a geophysical viewpoint however, we are concerned chiefly with only one factor; i.e., the dissipation of heat coming from the interior of the earth. The heat from the interior must flow through the outer crust, and in so doing, it affects the temperature of the upper surface layers of the earth. This temperature will not be uniform but will vary with the thermal conductivities of the various materials in the surface and near-surface of the crust, and with their geometric distribution. From studies of these temperature variations, predictions often may be made of the nature and subsurface distribution of these materials.

Temperature measurements of the earth's outer crust can be used to furnish fundamental information relating to the origin and the history of the areas under observation. In addition, temperature measurements in favorable cases will yield valuable information regarding the zonal distribution of ores; the configuration of intrusive bodies; the contacts between sedimentary and igneous rocks, or between (different) sedimentary rocks; the location, hade, and throw of faults; the ground water distribution and local regional subsurface flow. The practical application of geothermal measurements to the solution of various problems of economic geology is usually one of two types: (a) near-surface temperature measurements, to study the lateral variations of temperature; (b) subsurface measurements

† Wm. D. Urry, "Significance of radioactivity in geophysics; thermal history of the earth," *Trans. Amer. Geophysical Union*, Vol. 30, No. 2, April, 1949.
B. Gutenberg, "Physics of the Earth," McGraw-Hill, 1939.

in drill holes, to study the vertical distribution of temperature along the drill hole. (See Chapter XI.)

Mathematical Theory of Heat Flow

As in the case of flow of electrical current through a solid medium, it is convenient to derive the differential equation for the uni-dimensional flow of heat and then generalize the equation for three-dimensional flow. Physically, uni-dimensional flow is illustrated by the flow through a sheet or slab of material having two dimensions considerably greater than the third dimension.

The theoretical discussion will be confined to a homogeneous and thermally isotropic medium.

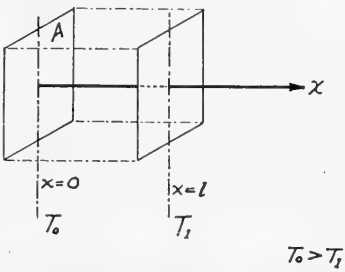

FIG. 593. — Sketch illustrating uni-dimensional heat flow in x direction.

Referring to Figure 593, assume that the planes $x = 0$ and $x = l$ are at temperatures T_0 and T_1 respectively and that $T_0 > T_1$. According to Fourier's law the quantity of heat which flows in the x direction across unit area in a time t is proportional to the product of the time and the temperature gradient.

$$q = kt\frac{T_0 - T_1}{l} \tag{1}$$

where

q = quantity of heat
t = time
l = thickness of slab
$\frac{T_0 - T_1}{l}$ = temperature gradient
k = a constant, called the thermal conductivity of the material.

k may be a function of position; in general, however it is determinate at each point, when the temperature is known for a homogeneous medium and for moderate ranges of temperature.

In differential form, the equation for uni-dimensional heat flow in the x direction is:

$$\left(\frac{\partial q}{\partial t}\right)_x = k\frac{\partial T}{\partial x} \tag{2}$$

Equation 2 states that the time rate at which heat is transported across unit area of a plane perpendicular to the x direction is equal to the product of the thermal conductivity and the thermal gradient in the x direction.

The equation for three-dimensional flow may be obtained from Equa-

tion 2 by replacing $\frac{\partial T}{\partial x}$ by the temperature gradient appropriate to three dimensions. This yields:

$$\frac{\partial q}{\partial t} = k\left(\frac{\partial T}{\partial x} + \frac{\partial T}{\partial y} + \frac{\partial T}{\partial z}\right) \tag{3}$$

This equation implies that heat flow may be represented by a vector whose x, y, and z components are, respectively:

$$k\frac{\partial T}{\partial x}, \quad k\frac{\partial T}{\partial y}, \quad k\frac{\partial T}{\partial z}$$

It is likewise apparent from the equation that the flow field, being a gradient, is everywhere perpendicular to the isothermal surfaces, T = constant.

Rate of Temperature Change

Equation 3 can be simplified by transforming it into a second order differential equation in which T is the only independent variable. To carry out this transformation, it is necessary to introduce the *specific heat*, c, of the material in which the heat flow is assumed to occur. The specific heat is defined as the quantity of heat expressed in calories required to raise a unit mass of the material by 1°C.

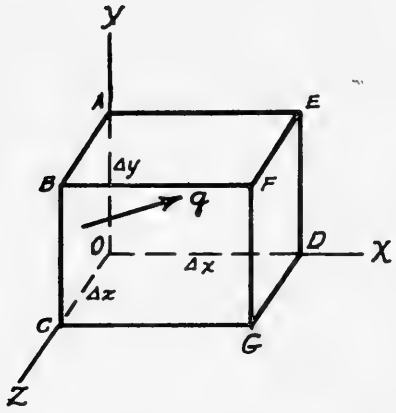

FIG. 594. — Sketch illustrating three-dimensional heat flow.

Consider a volume element having the shape of a rectangular parallelopiped and sides of lengths Δx, Δy, and Δz, located in an infinite, homogeneous, isotropic medium of density σ, specific heat c and heat conductivity k. (Figure 594). When the temperature of the volume element increases by an amount ΔT, the quantity of heat absorbed by the volume element changes by an amount equal to the product of the specific heat, the mass, and the change in temperature. Hence, the time rate of change of absorption is

$$c\sigma\,\Delta x\,\Delta y\,\Delta z\frac{\partial T}{\partial t}$$

If it is assumed that the volume element does not contain any heat sources or sinks, the rate at which heat flows into the volume element must equal the rate at which heat flows out of the volume element. The rate at which heat flows into the volume element across the face $0ABC$ is:

$$\left(\frac{\partial q}{\partial t}\right)_{\sigma} \Delta y\,\Delta z$$

From Equation 2

$$\left(\frac{\partial q}{\partial t}\right)_x \Delta y\,\Delta z = k\frac{\partial T}{\partial x}\Delta y\,\Delta z$$

For convenience, set

$$k\frac{\partial T}{\partial x} = U_x;\ k\frac{\partial T}{\partial y} = U_y;\ k\frac{\partial T}{\partial z} = U_z \tag{4}$$

In terms of the new variable, the rate of heat flow into the parallelopiped across the face $0ABC$ is:

$$U_x\,\Delta y\,\Delta z$$

The rate of heat flow out of the parallelopiped across the face $DEFG$ is:

$$\left(U_x + \frac{\partial U_x}{\partial x}\Delta x\right)\Delta y\,\Delta z$$

Therefore, the net rate of flow out of the element in the x direction is:

$$U_x\,\Delta y\,\Delta z - \left(U_x + \frac{\partial U_x}{\partial x}\Delta x\right)\Delta y\,\Delta z = -\frac{\partial U_x}{\partial x}\Delta x\,\Delta y\,\Delta z$$

Similarly, the net outward flow in the y and z directions are:

$$-\frac{\partial U_y}{\partial y}\Delta x\,\Delta y\,\Delta z \quad \text{and} \quad -\frac{\partial U_z}{\partial z}\Delta x\,\Delta y\,\Delta z$$

respectively.

The total rate of flow out of the element is:

$$-\left(\frac{\partial U_x}{\partial x} + \frac{\partial U_y}{\partial y} + \frac{\partial U_z}{\partial z}\right)\Delta x\,\Delta y\,\Delta z$$

Replacing U_x, U_y, U_z, by their equivalents from Equation 4, the total rate of flow out of the element is:

$$-k\left(\frac{\partial^2 T}{\partial x^2} + \frac{\partial^2 T}{\partial y^2} + \frac{\partial^2 T}{\partial z^2}\right)\Delta x\,\Delta y\,\Delta z$$

But the outward flow is equal in magnitude and opposite in sign to the absorption of heat in the volume element; therefore,

$$k\left(\frac{\partial^2 T}{\partial x^2} + \frac{\partial^2 T}{\partial y^2} + \frac{\partial^2 T}{\partial z^2}\right)\Delta x\,\Delta y\,\Delta z = c\,\sigma\frac{\partial T}{\partial t}\Delta x\,\Delta y\,\Delta z$$

or

$$\frac{k}{c\,\sigma}\left(\frac{\partial^2 T}{\partial x^2} + \frac{\partial^2 T}{\partial y^2} + \frac{\partial^2 T}{\partial z^2}\right) = \frac{k}{c\,\sigma}\nabla^2 T = \frac{\partial T}{\partial t} \tag{5}$$

Equation 5 states that the time rate of the change of temperature at any point in an isotropic homogeneous medium is equal to $\frac{k}{c\,\sigma}$ times the Laplacian of the temperature. Thus, the temperature distribution expressed by Equation 5 involves the specific heat, the thermal conductivity, and the density

of the material under investigation.† Hence, changes in any of these parameters result in changes in temperature and heat flow distribution. The observation of temperature changes, therefore, affords a means of mapping the contacts of rocks having different thermal coefficients and density.

Equation 5 does not cover the case of sources or sinks of heat inside the volume element. Hence, if chemical or radioactive processes play an important part in the temperature distribution in the area that is being surveyed by geothermal methods, Equation 5 should be modified to take into account such sources and sinks of heat near the geothermal stations.

For stationary flow and constant conductivity (e.g., a bar with constant temperature at its ends, having no sources or sinks within it, and where the temperature at each point is independent of the time) heat flows at a constant rate, and the analogy to other fields (e.g., Newtonian force field) is complete. In this case

$$\frac{\partial T}{\partial t} = 0 \quad \text{and} \quad \nabla^2 T = \frac{\partial^2 T}{\partial x^2} + \frac{\partial^2 T}{\partial y^2} + \frac{\partial^2 T}{\partial z^2} = 0 \tag{6}$$

An even closer analogy is that of stationary current flow wherein

$$i = \frac{dQ}{dt} = \sigma \operatorname{grad} u \qquad \text{(compare to Equation 3)}$$

$$\operatorname{div} i = \nabla^2 u = 0 \qquad \text{(compare to Equation 6)}$$

where

Q = charge
i = current density (compare to rate of flow of heat)
u = potential (compare to temperature)
σ = electrical conductivity (comparable to thermal conductivity)

As is apparent from the assumption $\frac{\partial T}{\partial t} = 0$, Laplace's equation is applicable to an earth wherein the temperature is not a function of time. Neglecting any internal sources of heat, such as radioactive elements, and neglecting further the upper part of the earth's crust which is subject to radiation from the sun, what measurably remains of the earth is then subject to application of Laplace's equation.

Assuming the earth to be a homogeneous, isotropic sphere, Laplace's equation can best be attacked with the use of spherical coordinates and the obvious assumption that the temperature is a function of the radial distance only. Making the transformation,

$$\nabla^2 T = \frac{1}{r} \frac{d^2(rT)}{dr^2} = 0 \tag{7}$$

and integrating,

$$T = A + \frac{B}{r} \tag{8}$$

† Compare also D. O. Ehrenburg, "Mathematical Theory of Heat Flow in the Earth's Crust," Univ. of Colorado Studies, Vol. 19, No. 3, May 1932.

which expresses the temperature T as a function of the radial distance r. It is apparent that the temperature increases with decreasing r, which is measured from the center of the earth as always, in spherical coordinates. The earth of course is not a homogeneous sphere, and anomalies, noted in measurements, from the theoretical temperature-depth curve must be attributed to these inhomogeneities.

Applications

Vertical Geothermal Gradients.—Variations in the thermal conductivity with depth produce corresponding variations in the thermal gradient; and such variations in the thermal gradient usually are associated with variations in the subsurface materials. Thermal measurements along a drill or bore-hole are termed *temperature logs,* and are described in Chapter XI.

Thermal surveys have been made throughout the United States and temperature logs obtained for various regions. In attempting to correlate the experimental bore-hole data to theoretical predictions, one summary† of data, taken in 400 deep wells distributed in 18 states, yielded the following results:‡ 5% of the depth-temperature curves could be classified as linear, 36% were concave to the depth axis, and 59% were convex to the depth axis. A partial explanation of the difference in the shapes of the curves lay in the change of thermal conductivity with depth. The convex curves may be explainable by (1) a decrease of thermal conductivity with depth resulting from a corresponding decrease of the moisture content of the rocks, or (2) a very thick sedimentary section well removed from the basement rocks. The concave curves may be explained by an increasing conductivity of more dense crystalline or basaltic rocks beneath a relatively thin sedimentary section; i.e., the temperature rises at an increasing rate as the better thermally-conducting basement rocks are approached. In the concave type curves the reciprocal gradients increased from 38.8 to 56.0 feet per degree Fahrenheit, while in the convex type curves they decreased from 116.3 to 67.8 feet per degree Fahrenheit.*

To obtain a type curve for any one area, it is generally necessary to average the gradients found in a survey of numerous wells. The general formulas for performing such averaging, while properly weighting the various readings, are as follows:

Let y_i = rise in temperature from a point just beneath the surface of ground to a depth x_i in well A_i.

By definition

$$b_i = \frac{y_i}{x_i} = \text{gradient in well } A_i. \tag{9}$$

The arithmetic mean of the gradient is

$$b = \frac{\sum_{i=1}^{n} b_i}{n} = \frac{\sum_{i=1}^{n} y_i/x_i}{n} \tag{10}$$

and assuming the weight of each value, b_i, is proportional to the depth

$$y_i = x_i b_i$$

† C. E. Van Orstrand, "On the Correlation of Isogeothermal Surfaces with the Rock Strata," *Trans. of the Society of Petroleum Geophysicists,* Vol. II.

‡ Assuming the data to be plotted with depth as ordinate, and temperature as abscissa.

* H. Landsberg, "On the Frequency Distribution of Geothermal Gradients," *Transactions American Geophysical Union,* August, 1946.

which gives for the weighted mean,

$$b = \frac{\sum_{i=1}^{n} y_i}{\sum_{i=1}^{n} x_i} \tag{11}$$

Equations 10 and 11 are the ones in general use.

As an example, consider the following field data and calculations.

READING NO.	DEPTH IN FT. (x_i)	TEMP. DIFF. (°F) (y_i)	$\frac{y_i}{x_i}$
1	430	8	0.01860
2	540	10	0.01850
3	860	16	0.01855
4	1075	20	0.01863
5	1350	25	0.01852
6	1885	35	0.01859
7	2150	40	0.01862
8	2425	45	0.01855
9	2700	50	0.01852
10	3230	60	0.01858
	$\sum_{i=1}^{10} x_i = 16645$	$\sum_{i=1}^{10} y_i = 309$	$\sum_{i=1}^{10} y_i/x_i = 0.1857$

Applying Equation 10 to determine the arithmetic mean of the gradients (where $n = 10$)

$$b = \frac{0.1857}{10} = 0.01857 \text{ F.°/ft.}$$

Applying Equation 11 to determine the weighted mean of the gradients,

$$b = \frac{309}{16645} = 0.01858 \text{ F.°/ft.}$$

Agassiz and Ingersoll have made temperature surveys in the deep copper mines of the Keweenaw peninsula in northern Michigan.† The results of their work gave an average gradient in that particular area of 1°C. in 59.5 meters or 1°F. in 108.5 feet. On the basis of measurements of the diffusivity of rock specimens in the region (found to be 0.0075 c.g.s.), theoretical temperature-depth curves were made which indicated that at least 30,000 years have elapsed since the last glacial epoch.

Figure 595 provides a comparison of temperature gradients in oil wells; for example, the data for the California wells yield a temperature gradient of 1°F./42 feet, approximately, and the data for the Louisiana oil well yields a gradient of approximately 1°F./100 feet.

† L. R. Ingersoll, "Geothermal Gradient Determinations in the Lake Superior Copper Mines," *Trans. Soc. Pet. Geoph.*, Vol. II, March, 1932.

Porosity and Temperature.—The graphs of Figure 596 provide a comparison of the depth-temperature† curve with the porosity-depth curves‡ of an oil well (Ransom No. 1, Syracuse, Hamilton County, Kansas). This data shows that the increase of the temperature gradient with

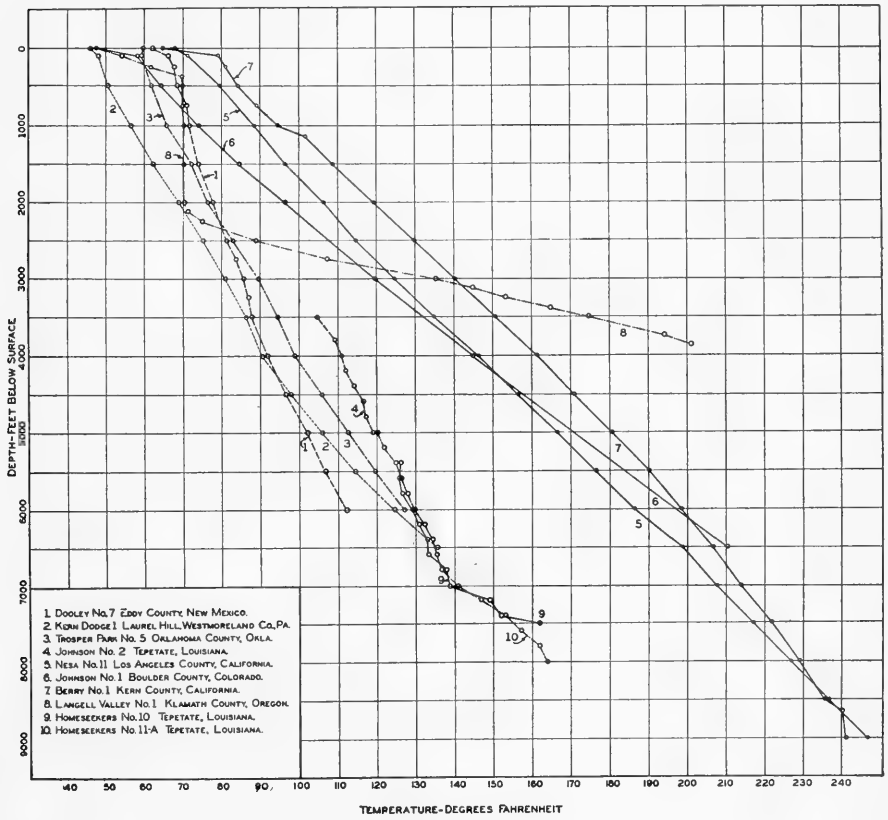

Fig. 595.—Graphs showing depth versus temperature for oil wells in various sections of the United States. (Courtesy of Howard Pyle.)

depth may be dependent upon the moisture content of the rocks.§ The product of the thermal gradient and the thermal conductivity represents the flow of heat through a vertical column of unit cross-section area in time t, (Equation 1).

$$q = kt\,\frac{\Delta T}{l}$$

† N. W. Bass, "Geologic Investigations in West Kansas," *State Geol. Survey Kansas,* Bull. 11 (1926), p. 83.

‡ W. W. Rubey, "The effect of gravitational compaction on the structure of sedimentary rocks," *Bull. A.A.P.G.,* Vol. 11, No. 6 (June, 1927), pp. 621-632.

§ C. E. Van Orstrand, "Application of Geothermics to Geology," *Bull. A.A.P.G.,* Vol. 18, 1, Jan., 1934.

Assuming no sources on sinks in the vicinity ($q = \text{constant}$), then this product must be constant for the given time t. That is,

$$\frac{q}{t} = \text{constant} = k\,\frac{\Delta T}{l}$$

Thus, as the gradient $\frac{\Delta T}{l}$ increases with depth, the conductivity k decreases with depth. But the porosity likewise diminishes with depth. So the conductivity diminishes with decreasing moisture content, and the thermal gradient varies inversely with the conductivity.

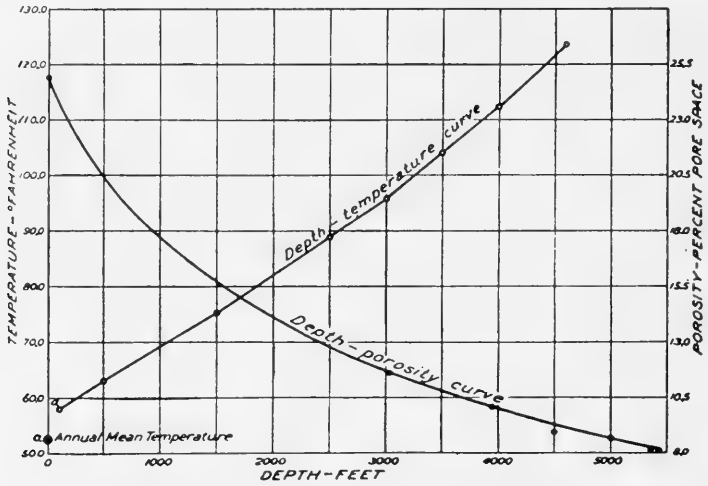

FIG. 596.—Depth-temperature curve and porosity curve. (C. E. Van Orstrand, "Some Possible Applications of Geothermics to Geology," *Bull. A.A.P.G.*, Vol. 18, No. 1, Jan., 1934.)

Areal Studies.—Thermal variations may be local or regional. Local, or small area, variations have been found over faults, salt domes, granite ridges and sand lenses. Regional, or large area, variations are of course not limited to such particularized structures and their explanations are not always readily apparent. In the north-central Oklahoma region both regional and local variations have been encountered, and their explanation may lie in a hypothesis proposed by Nevin and Sherrill† to explain the origin of certain local uplifts. In this area, there is a gradual rise in temperature over a diminishing depth to granite, i.e., over the basement highs. The highest temperatures were found over the oil fields where the granitic rocks, having higher thermal conductivities, have pushed up through the basement complex. The process of uplift proposed by Nevin and Sherrill may thus explain both local and regional temperature variations in that area.

† C. M. Nevin and R. E. Sherrill, "The nature of uplifts in North-Central Oklahoma and their local expression," *Bull. A.A.P.G.*, Vol. 13, Jan., 1929, pp. 23-30.

A similar example was presented by Darton† showing that the temperature gradients in eastern South Dakota increase as the depth to the granite or quartzite decreases.

The Salt Creek anticline‡ provides an excellent example of a local variation in which the isogeothermal surfaces are related to the structure.

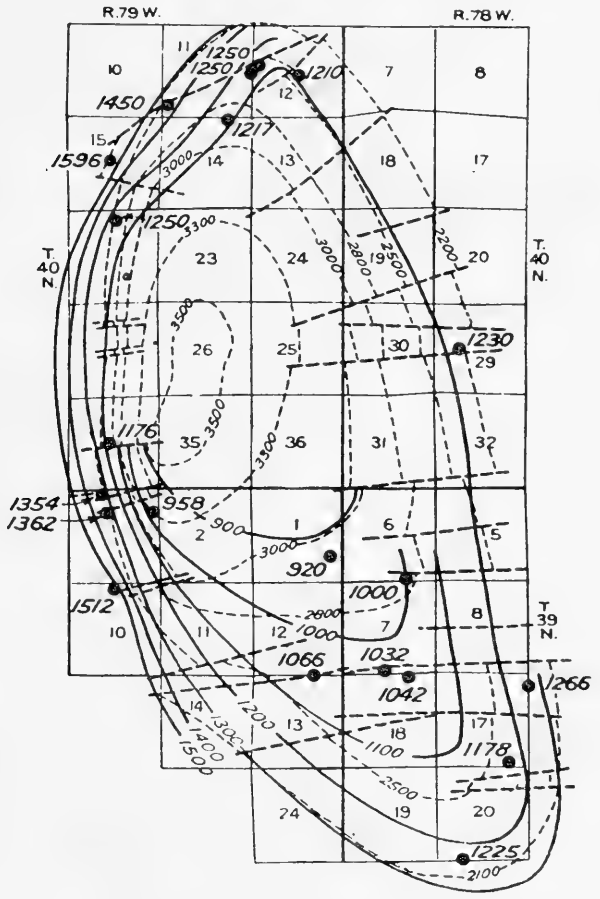

Fig. 597.—Salt Creek Dome, Natrona County, Wyoming.
(C. E. Van Orstrand, *loc. cit.*)

In Figure 597 the closed broken lines represent elevations on the "Second Wall Creek Oil Sand." Faults are represented by broken lines intersecting the structural contours. The dots represent well locations, and the accompanying numbers represent the depth at which a temperature of 80° F. was

† N. H. Darton, "Geothermal Data of the United States," *U. S. Geol. Survey Bull.* 701 (1920), p. 80.

‡ C. E. Van Orstrand, "Correlation of isogeothermal surfaces," *Trans. Soc. of Petrol. Geophys.*, Vol. II, March, 1932.

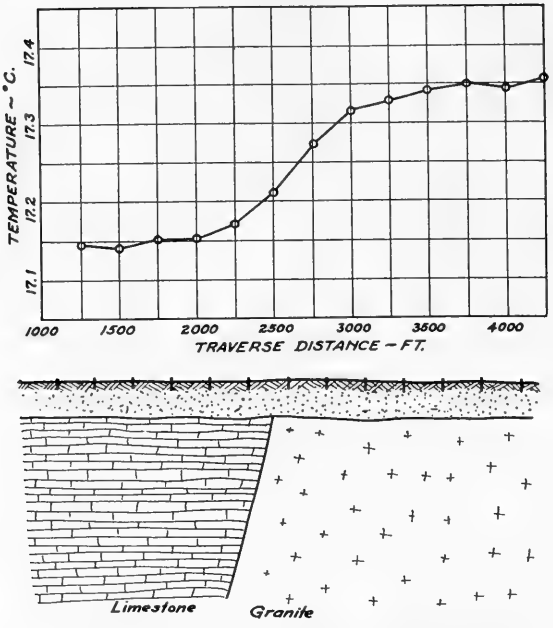

FIG. 598.—Temperature anomaly along a traverse over the contact between limestone and an intrusive granite.

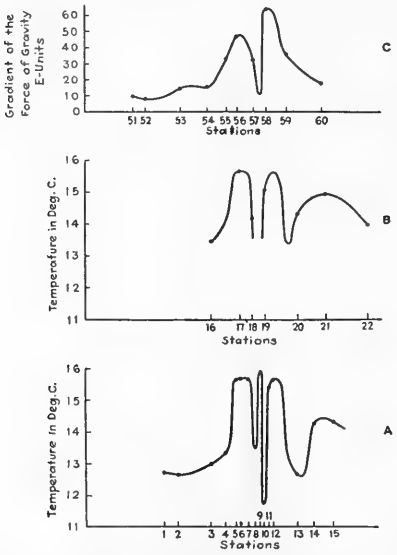

FIG. 599.—Comparison of gravity gradient and temperature anomalies over a fault. (van den Bouwhuijsen, *Eng. and Mining Journal.*)

reached. The heavy continuous lines represent contours on the 80° F. isogeothermal surface. It can be seen by inspection of the figure that the highest point on the isothermal surface corresponds very closely to the structurally highest point of the producing zone.

Similar results were obtained over the Long Beach Field in Los Angeles County, California. Isothermal surfaces exist over the producing structure, and these surfaces follow closely the upper oil-producing strata.

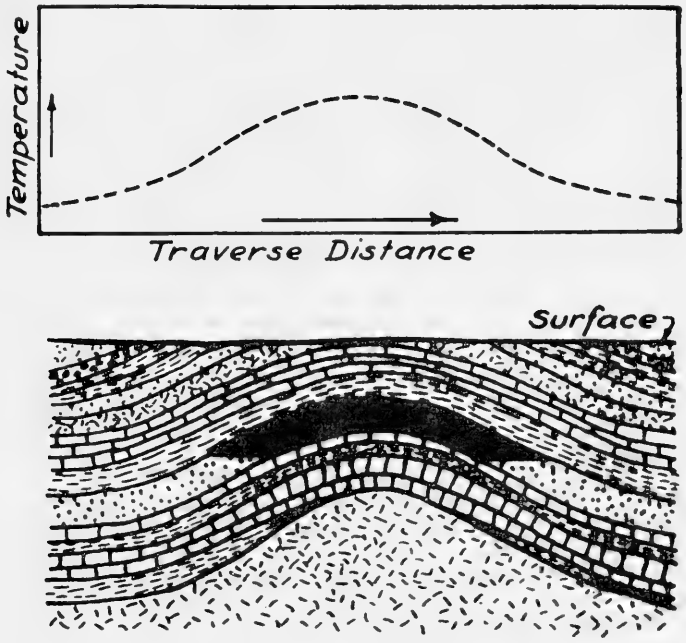

FIG. 600.—Temperature anomaly over a typical anticline.

Figure 598 shows the temperature anomaly obtained across a traverse over a contact between a limestone series and an intrusive granite. The contact is clearly shown, even though the overburden is approximately 40 feet thick. The temperature anomaly along two traverses (*A* and *B*) over a fault is shown in Figure 599. The vertical displacement along the fault is approximately 2700 feet.†

The temperature anomaly, at depth, over a typical anticlinal structure is illustrated in Figure 600. It will be noted that the curves rise in passing

† J. N. A. van den Bouwhuijsen, "The Thermocouple Proves Useful on a Geophysical Survey," *Eng. and Mining Jour.*, Vol. 135, No. 8, Aug. 1934.

over the crest of the anticline. Similar results have been obtained by several investigators.†

Periodic Heat Flow.—The radiation of the sun causes a periodic change in the flow of heat through points close to the surface of the earth. The periodicity of the change in temperature is a double one and is associated with the change in position of the sun during the day in relation to the horizon and with the change in the path of the sun during the year. These two periodic changes in temperature are called the diurnal and the annual variation, respectively.

The heat of the sun reaches the surface of the earth mostly by radiation. The conductivity of the atmosphere is very poor.* The spectrum of the sun has a peak in the yellow portion, and the absorption of this radiation in the atmosphere is smaller than that of longer wave lengths. During the night, the earth, which has a much lower temperature and therefore a spectrum with a peak far in the infra red, loses a great part of the heat received during the day; but the atmosphere absorbs a great part of this radiation and therefore acts as a protective screen against loss of radiation, and this factor, combined with the poor conductivity of the atmosphere, allows the earth in the summer to retain during the night a part of the heat received from the sun. Hence, in the summer, the outer portion of the earth's crust gains heat over a 24-hour period. In the winter, however, the losses during the night exceed the gains during the day, and the balance is negative over a 24-hour period.

During the day the temperature is a maximum between 2 and 3 p.m. and a minimum just before sunrise. The plotting of temperature against time during a 24-hour period affords a means for evaluating the gains and losses over the whole or part of the period.

The diurnal temperature variations manifest themselves only to a depth of a few feet below the surface. The depth to which the changes are measurable depends on the character of the rocks close to the surface. In solid rock formations the diurnal variations usually become imperceptible at a depth of about 3 feet. In loose sand and alluvial fill material, the variations escape measurement at a depth of 1 to 2 feet. In swamps and porous materials containing water and in areas where the water table is near the surface of the earth, the variations become imperceptible at a depth of 3 to 5 feet.

The annual variation for a given area is determined from data on

† C. E. Van Orstrand, "Normal Geothermal Gradient in the United States," *Bull. Amer. Assoc. Pet. Geol.*, Vol. 19, No. 1, Jan. 1935.

M. W. Strong, "Significance of Underground Temperatures," Proc. World Petr. Congress, Vol. 1, 1933, 124 pages, abstract, *Jour. Inst. Petr. Techn.*, Vol. 20, Feb. 1934, p. 63.

E. de Golyer, "The Significance of Certain Mexican Oil Field Temperatures," *Economic Geology*, Vol. 13, 1918, pp. 275-301.

James Fisher, L. R. Ingersoll, and H. Vivian, "Recent Geothermal Measurements in the Michigan Copper District," *A.I.M.E Geophysical Prospecting*, Tech. Pub. 481.

C. E. Van Orstrand, "Some possible applications of geothermics to geology," *A.A.P.G. Bull.*, Vol. 18, No. 1, Jan., 1934.

* The fact that the temperature of the air at higher altitude is generally lower than that at lower altitude shows that conduction of heat plays a minor part in the transport of the sun's heat to the surface of the earth.

measurements made intermittently throughout the year, or daily, at the same time of day.

The annual variation can be observed to a depth of between 75 and 100 feet, depending on the thermal properties of the rocks. The periodic variations in temperature may show local fluctuations due to changes in meteorological conditions and to differences in topography and overburden.

Below 100 feet, the temperature depends, in general, only on the flow of heat from the center of the earth.

Diurnal variations (when they have not been excluded from measurements by a sufficient depth of bore hole) are corrected for in a manner very similar to that used in correcting for the diurnal magnetic variations, (see Chapter III), or by calculation, as described in the following paragraph.

Calculation for Periodic Temperature Variations

The theory to be applied in this case rests in Equation 5, the general equation excluding internal sources or sinks.

$$\frac{k}{c\sigma}\nabla^2 T = \frac{\partial T}{\partial t} \tag{5}$$

The one-dimensional form of Equation 5 may be used without introducing any appreciable error. This implies the assumption that the surface of the earth is a plane in the region of investigation.* The surface is thus uniformly radiated, leaving the temperature a function of the depth z only.

$$\frac{k}{c\sigma}\frac{\partial^2 T}{\partial z^2} = \frac{\partial T}{\partial t} \tag{5a}$$

Since the radiation of the sun is roughly periodic, the change in heat flow through points close to the surface of the earth is likewise periodic in both diurnal and annual variations. At the surface, then, the following periodic boundary condition must be imposed.

$$T = T_0 \sin wt \quad \text{at} \quad z = 0 \tag{12}$$

Equation 5a is linear and homogeneous, and a particular solution has the form,

$$T = Ae^{\alpha t + \beta z} \tag{13}$$

which, by substitution into Equation 5a, is a solution if, and only if,

$$\alpha = \frac{k}{c\sigma}\beta^2$$

With proper substitutions,† and noting that Equation 13 is *a* particular solution, a total of four particular solutions may be written as follows:

$$T = Be^{-R}\sin(\gamma t - R) \tag{14}$$

$$T = B'e^{R}\sin(\gamma t + R) \tag{15}$$

$$T = Ce^{-R}\cos(\gamma t - R) \tag{16}$$

$$T = C'e^{R}\cos(\gamma t + R) \tag{17}$$

* In areas of rugged topography and complicated geology, precise mathematical treatment is almost impossible, and the interpreter must then depend upon his knowledge of probable subsurface geology and prior experience.

† The discussion follows that given by Ingersoll and Zobel, "Mathematical Theory of Heat Conduction," Ginn and Co.

where $$R = \frac{z}{\sqrt{k/c\sigma}}\sqrt{\frac{\gamma}{2}}$$

and $$\alpha = \pm i\gamma$$

Equations 15 and 17 demand that the temperature increase indefinitely as z increases, which is impossible. Equation 16 is excluded by the boundary conditions of Equation 12. Equation 14 satisfies 12 if

$$B = T_o \qquad \text{and} \qquad \gamma = w$$

With these substitutions, the solution of Equation 5a is

$$T = T_o e^{-\frac{z}{\sqrt{k/c\sigma}}\sqrt{\frac{w}{2}}} \sin\left(wt - \frac{z}{\sqrt{k/c\sigma}}\sqrt{\frac{w}{2}}\right) \tag{18}$$

which yields the temperature at any time t, at any depth z from the surface.

The range of temperature for any point below the surface may be calculated from the maximum variation of the temperature at the point. Since $\sin\theta = \pm 1$ for a maximum and minimum respectively,

$$R_T = 2T_o e^{-\frac{z}{\sqrt{k/c\sigma}}\sqrt{\frac{w}{2}}} = 2T_o e^{-\frac{z}{\sqrt{k/c\sigma}}\sqrt{\frac{\pi}{P}}} \tag{19}$$

where $w = \frac{2\pi}{P}$ and P is the period of the variation of the sun's radiation. From Equation 19, it can be seen that T_o is the amplitude or half range at the surface ($z = 0$).

Consider the diurnal wave as an example. Suppose, at a certain season of the year, the surface temperature of the soil $\left(\frac{k}{c\sigma} = 0.0049\right)$ varies from + 16° C. to −4° C. The surface half range value (T_o) is then $\frac{16 - (-4)}{2} = 10°$. $P = 24$ hours $= 86{,}400$ seconds. The mean surface temperature is 6°.

Use Equation 19 to determine the temperature range at 30 cm. and at one meter, as follows:

$$z = 30 \text{ cm.}: \quad R_T = 2\,(10)\, e^{\frac{-30}{\sqrt{.0049}}\sqrt{\frac{\pi}{86{,}400}}}$$
$$= 2\,(10)\,(.07) = 1.4° \text{ C.}$$
$$z = 100 \text{ cm.}: \quad R_T = 2\,(10)\, e^{-3.7}$$
$$= 2\,(10)\,(0.00016) = 0.0032° \text{ C.}$$

Lag, Velocity and Wave Length.—A maximum or minimum of temperature will occur to a given depth at the time

$$t_1 = \frac{\frac{z}{\sqrt{k/c\sigma}}\sqrt{\frac{w}{2}} + (2n+1)\frac{\pi}{2}}{w} \tag{20}$$

where odd values of n give minima, and even values, maxima.

Considering a particular (first: $n = 1$) minimum occurring at the surface ($z = 0$) when $t_1 = \frac{3\pi}{2w}$, then as x and t increase, this particular minimum is propagated into

the surface according to

$$wt - \frac{z}{\sqrt{k/c\sigma}}\sqrt{\frac{w}{2}} = \frac{3\pi}{2} \tag{21}$$

and reaches a point z within the surface at a later time ($t_1 > t_2$). This is known as the *lag* of the temperature wave, and Equation 22 gives the amount of time later at which the minimum occurs at the depth z.

$$t_1 - t_2 = t = \frac{z}{\sqrt{k/c\sigma}}\sqrt{\frac{w}{2}}\frac{1}{w} = \frac{z}{2\sqrt{k/c\sigma}}\sqrt{\frac{P}{\pi}} \tag{22}$$

A like reasoning holds for the maximum or any other phase.

From Equation 22, the lag of the temperature wave can be determined using the above data, as follows:

$$z = 30 \text{ cm.}: \qquad t = \frac{30}{2\,(.0049)^{1/2}}\sqrt{\frac{86{,}400}{\pi}}$$

$$= 34{,}860 \text{ seconds}$$

$$= 9.6 \text{ hours}$$

That is, the maximum or minimum (or any other phase) of temperature would occur at 30 cm. below the surface, approximately 9.6 hours after its occurrence at the surface.

Equation 22 likewise gives the time it takes for the wave to travel from the surface to the depth z. The apparent velocity of such a wave, which is merely the rate of travel of a given maximum or minimum (or any particular phase) is then given by

$$V = \frac{z}{t} = 2\sqrt{k/c\sigma}\sqrt{\frac{\pi}{P}} \tag{23}$$

This velocity does not express the actual speed of transmission of heat energy, which is high, since that is a complex function of many variables.

To illustrate the actual transmission of heat energy: for a good conductor, like copper, at 13° C. one calorie is transmitted through one square cm. cross-section area in one second, if the faces of the sample are at a temperature difference of 1° C. and the width between faces is one cm. This, of course, is the definition of thermal conductivity.

An expression for the wave length may be deduced from Equation 23.

$$\lambda = VP = 2\sqrt{k/c\sigma}\sqrt{\pi P} \tag{24}$$

Using the same data given above, the apparent velocity and wave length may be readily obtained from Equations 23 and 24 respectively:

$$z = 30 \text{ cm.}: \qquad V = \frac{30}{34{,}860} = 2\,(.07)\sqrt{\frac{\pi}{86{,}400}}$$

$$= 0.00086 \text{ cm./sec.}$$

$$\lambda = (0.00086)\ (86{,}400) = 2\,(.07)\ \sqrt{(\pi)\ (86{,}400)}$$

$$= 74.3 \text{ cm.}$$

From measurements of the lag, velocity or wave length, the diffusivity $\left(\text{which is } \frac{k}{c\sigma}\right)$ may be readily determined. Forbes† used this method on soils near Edinburgh.

Internal Heat Sources.—A final step in the study of earth temperatures necessitates invoking factors for internal sources and sinks of heat. Two possible heat sources will be considered briefly—radioactive and chemical. The sinks, in general, are moving subterranean waters.

Normally, the temperature of the earth at any point located below a depth subject to the periodic variations will remain constant for all practical purposes. Due to the great mass and heat capacity of the earth, temperature changes due to heat losses alone would amount to only 1° C. over a period of from 10 to 50 million years. When consideration is given to both radioactive heat sources and general heat losses, there may even be an increase in temperature of perhaps 30° C. per million years, *if* the radioactivity values at depth are of the order of the minimum values at the surface.‡ Though the percentage of radioactive material in surface rocks is minute, yet if such material is scattered throughout the earth with the same density, then the total aggregate would be sufficient to supply many times over the yearly loss of heat. In fact, the heat generated would be so great as to necessitate the assumption that the radioactive materials exist to a depth of only a few miles of the surface shell.

The other major source of possible internal heat is chemical reaction. In mining work, this source of heat may be due to oxidation or alteration of ore bodies, while in petroleum exploration it may be due to oxidation of the hydrocarbons escaping from the reservoir.

To investigate the possible effects of heat from the oxidation of petroleum, Strong§ made calculations based upon data obtained from geothermal field measurements.

Experimental work has yielded a temperature of 1.65° C. at Haverhill, Kansas, over a sand lens located at a depth of 762 meters. After making certain simplifying assumptions, it was shown that this temperature difference can be maintained by a source generating $1 \cdot 10^{-7}$ calories/cm.^{2}/sec. This quantity of heat was then compared to that obtainable from the oxidation of petroleum in its natural state.

Assuming that the sand lens, about 100 feet thick, contained a given quantity of oil and that the heat of combustion of crude oil is about 11,094 calories/gm, it was shown that to continuously generate the heat needed to maintain the 1.65° C. difference, all the oil would be oxidized in $3.2 \cdot 10^6$ years. This result is definitely not in agreement with geological facts, and so the conclusion to be drawn is that oxidation of oil, though possibly a contributing factor, is not in itself the only cause of the higher temperature values over oil fields. The explanation for these higher temperatures probably lies in the fact that the basement complex generally is at a lesser depth over structures favorable to the accumulation of oil, and the greater transmission of heat under these conditions supplements any heating which may be caused by oxidation of the hydrocarbons.

Near-Surface Temperature Variations.—A homogeneous, spherical earth surface would be an isothermal surface. Irregularities in the surface caused by topography, cause corresponding irregularities or anomalies in the temperature distribution because the isothermal surfaces are compressed underneath the valleys, and expanded over the hills and mountains. In this respect, the isothermal surfaces behave almost identically with the equipotential surfaces in electric potential fields. Calculations can be made showing probable temperature gradients for different topographic configurations.††

---

† Forbes, *Trans. Roy. Soc. Edinburgh,* 16, Pt. II (1846).

‡ Ingersoll and Zobel, *loc. cit.*

§ M. W. Strong, "Geothermal Phenomena and Geological History with Special Reference to Old Structures in Geothermal Equilibrium," *Jour. Inst. Petrol. Tech.* (London), Vol. 16 (1930), pp. 889-901.

†† Van Orstrand, *Physics,* Vol. 2, No. 3, 1932.

Field Operations

The geothermal crew usually consists of two men, the driller who drills the holes, and the instrument man who plants the thermocouples, and later takes the readings. The readings at each station should not consume more than 10 to 15 minutes. The cost of geothermal surveying is approximately twice that of magnetic surveying, on a per station basis, where the holes can be drilled with a hand auger. In more difficult areas, the cost increases with the cost of drilling.

The driller can usually drill the required holes with a hand drill. Any well-designed rotary spiral feed post-hole digger may be employed. An easily constructed hand drill for fill and surface soil may be made from a rod equipped with a suitable handle, welded to a piece of pipe. The pipe is cut off slantwise (about a 45° angle) at the end and its edge sharpened and bent slightly in the form of a spoon. When the surface deposits are hard, some kind of power-driven drill may be used.

The measuring apparatus* required for this type of work may be of two general types: thermocouple or resistance thermometers. The thermocouple equipment usually comprises a sensitive galvanometer, potentiometer, and a thermopile or thermocouple of special construction. In addition, a couple of ordinary thermos flasks and a thermometer, reading to 0.01°C., are needed.

The sensitivity of the potentiometer should be such that a difference of 0.01°C. can be measured. The best thermocouples give an E.M.F. of 40 microvolts per °C. Measurement of 0.01°C. requires a voltage sensitivity of the galvanometer of 4×10^{-7} volts when one couple is used. For a thermopile this factor is cut down according to the number of junctions of the thermopile. The thermopile or thermocouple is constructed so that the hot junction can be lowered into the hole at the end of a supporting rod, while the cold junction can be kept at a constant temperature in a thermos flask at the surface of the earth.

The use of a thermopile has the advantage that the sensitivity requirement of the galvanometer is less than that for a thermocouple. The use of a thermocouple has the following two advantages: (1) A single thermocouple usually can be mounted to fit a hole of smaller diameter than a thermopile with many junctions, and this is important because the disturbance of the temperature equilibrium of the ground by a hole increases rapidly with the diameter of the hole due to convection air currents and the exposure of the hole to direct sunlight. (2) The heat capacity of a single thermocouple can be made very small compared to that of a thermopile, which allows the hot junction to take the temperature of the rocks with which it is in contact in the shortest possible time.

* See list of patents at end of chapter.

The resistance thermometer equipment† usually comprises some form of sensitive resistance bridge, connected to a resistance thermometer. The resistance thermometer should preferably be of the lead compensated type, although the effects of temperature changes in the lead circuits may be minimized by a high ratio of thermometer/lead resistance. One type of thermometer bridge used for resistance measurements is a double slide-wire Wheatstone bridge to measure resistance from 0 to 200 ohms. Measurements accurate to 0.005 ohms are necessary, and with a good resistance element will read ± 0.010 to .015°C.

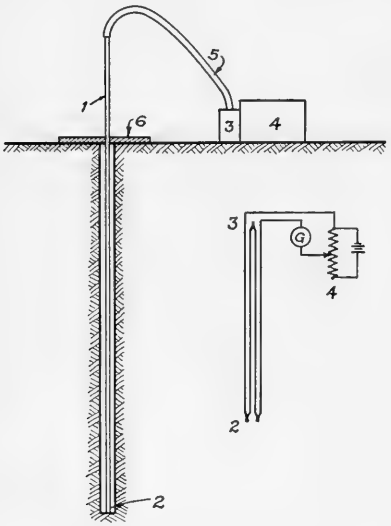

FIG. 601.—Schematic diagram of thermopile and associated apparatus in place for geothermal measurements. 1, sheath of low thermal conductivity; 2, hot junction; 3, cold junction; 4, potentiometer; 5, flexible rubber tube sheath; 6, cover plate of low thermal conductivity; *G*, galvanometer.

Figure 601 shows the arrangement of the apparatus ready for measurements.

In calibrating the galvanometer in terms of differences in temperature, the two junctions are first placed in a Dewar flask filled with water or ice to determine the zero of the potentiometer and then one junction is transferred to a flask containing water at another temperature. This is repeated for a series of temperatures and a plot is made of the potentials against the temperature differences.

Field Technique.—A preliminary series of measurements is made at different depths in the same hole to determine the depth at which the diurnal variations become imperceptible for the particular region under investigation. Anomalies in this critical depth should be discovered before a great number of observations are made at a depth insufficient to eliminate the diurnal variations. Furthermore, a determination of the minimum depth to which the holes need be drilled will tend to speed up the survey because the speed of drilling determines the speed of the observations. When the survey is made in a region where the water table is close to the surface of the earth, all holes must be drilled uniformly to the water table and measurements made at that depth.

In order that thermal equilibrium may be reached, measurements should not be made for a period of at least 24 hours after drilling.

A uniform reading and thermometer-setting procedure should be used to minimize the influence of diurnal temperature variations and other extraneous effects. The temperature measurements are made at the same

† J. J. Jakosky, R. M. Dreyer and C. H. Wilson, "Geophysical Investigations in the Tri-State Zinc and Lead Mining District," *Univ. of Kansas, Bull. 44*, Dec., 1942.

time each morning, ordinarily before the atmospheric temperature has started to increase. After completion of the readings, the thermometers are moved to another set of holes in which they are left until the next morning when measurements are again made. Generally the thermometers should be left in the hole for at least 16 to 24 hours before reading, so as to insure their reaching equilibrium with the ground temperature.

Overcast skies during part of the observations, rain, snow, wind, and other factors affecting the distribution of temperature must be taken into account for proper correlation of observations when they are extended over a considerable period of time. Consideration must be given to the effect produced by varying coefficients of absorption of the surface at different stations. For example, sand or alkali patches have different coefficients of absorption than a surface covered with vegetation. Also, one must take into account that the distribution of temperature under a clump of shade-trees may be entirely different from that in the sun.

Great care should be taken to locate points of observation as far as possible from the exposed face of an outcrop or from the edge of a deep ditch filled with water or from any point where a sudden change in elevation can be observed. The field notes should show a complete record of all these local circumstances and, if the location of a station at an unfavorable point is imperative, proper care should be taken to detect changes in the distribution of temperature due to these local conditions by staking several stations in the vicinity of the discontinuity.

For purposes of mapping and correlation, a network of traverses is surveyed, the configuration of which depends on local conditions and on the particular features of the exploration problem. When the suspected structure has a well-defined strike, the traverses may be parallel lines perpendicular to the strike, and the stations 100 to 500 feet apart, depending on the rate of change in temperature to be expected. It is good practice to start a survey with a base line on which the stations are only a short distance apart and to determine the best distance between stations from the results obtained on this traverse. The measurements on this base line are repeated from time to time as the survey progresses to determine whether the annual variation has any influence on the observations.

Special care should be taken that the connections between thermocouple and galvanometer are clean and tight. Plugs of the ordinary type generally do not meet these requirements. Care should be taken also that the thermocouple and the galvanometer are always connected in the same way. The small difference in temperature between the junctions makes it possible to introduce appreciable errors by reversing terminals. Spurious thermoelectric potentials are the greatest source of error in obtaining the field data.

The Age of the Earth.—As a point of interest, the determination of the age of the earth through geothermal methods may be mentioned.

The problem has been attacked in various ways. One method divides it into two

parts—for a non-radioactive earth, and for a radioactive earth. The results of the two parts are then combined for final calculation.† An article by Urry‡ offers excellent reference to work along this line. The problem is not simple and the calculations are laborious. The interested reader is referred to the literature for details.

TABLE 26

THERMAL CONDUCTIVITY CONSTANTS* IN C.G.S. UNITS

Material	Conductivity	Material	Conductivity
Air (0°C.)	0.00005 - 0.00006	Petroleum	0.003 - 0.004
Calcite	0.005 - 0.015	Porphyry	0.005 - 0.008
Coal	0.0003 - 0.0008	Rock Salt	0.006 - 0.007
Clay (dry)	0.002 - 0.003	Sand (very dry)	0.0008 - 0.0009
Clay (moist)	0.003 - 0.004	Sand (about 10% moisture)	0.002 - 0.003
Feldspar	0.005	Sand, Quartz (dry)	0.001 - 0.003
Gneiss	0.005 - 0.006	Sand, Quartz (moist)	0.008 - 0.009
Granite (100°C.)	0.004 - 0.008	Sandstone (dry)	0.002 - 0.003
Graphite	0.01 - 0.02	Sandstone (moist)	0.005 - 0.007
Gypsum	0.002 - 0.004	Slate	0.0047 - 0.0057
Ice	0.002 - 0.006	Snow (fresh)	0.0003 - 0.0005
Lava	0.002 - 0.005	Soil (clay or sand, slightly damp)	0.003 - 0.004
Lime	0.0003 - 0.006	Soil	0.0003 - 0.0009
Limestone	0.005 - 0.008	Water	0.0014
Marble	0.005 - 0.007		
Mica	0.0009 - 0.0018		
Paraffin	0.00023 - 0.00061		

THERMAL METHODS

UNITED STATES PATENTS

2,245,700 Issued June 17, 1941. W. D. Mounce. "Resistance Thermometer."
2,318,601 Issued May 11, 1943. F. C. Doble. "Electrical Means for Indicating Temperature Conditions."
2,365,706 Issued Dec. 26, 1944. G. Keinath. "Temperature Compensated Condition Response Measuring System."
2,375,892 Issued May 15, 1945. G. Bouyoucos. "Thermometer."
2,393,197 Issued Jan. 15, 1946. R. Scott. "Remote Reading Temperature Instrument."
2,395,192 Issued Feb. 19, 1946. R. H. Ostergren. "Resistance Thermometer."
2,396,724 Issued March 19, 1946. A. F. Spilhaus. "Bathythermograph and Sea Sampler."
2,412,564 Issued Dec. 17, 1946. F. L. Current. "Heat Measuring Apparatus."
2,437,085 Issued March 2, 1948. J. Evans. "Heat Detection Device."

† C. E. Van Orstrand, "Geothermal Methods of Estimating the Age of the Earth," *Geophysics*, Vol. V, No. 1, Jan., 1940, pp. 57-79.
‡ Wm. D. Urry, "Thermal History of the Earth," *Trans. Am. Geophys. Union*, Vol. 30, No. 2, April, 1949, pp. 171-180.
* Taken from various sources in the literature.

CHAPTER X

RADIOACTIVITY METHODS*

When Henri Becquerel discovered that a lump of pitchblende fogged his photographic plate,† he had stumbled upon a phenomenon of far-reaching implications. The subsequent researches of the Curies in France and Rutherford in England drew attention to the fact that here at last was a way in which man could learn about the subatomic particles and the forces that hold them together. The field of nuclear physics was born and grew at an ever-increasing rate.

Important geophysical implications of the new science became apparent shortly after the turn of the century. First, since the ever-present radioactive substances liberate energy in their decay, they must contribute materially to the internal heat of the earth.‡ Second, since the rate of decay can be measured with good accuracy, we can deduce the absolute age of an igneous rock by analyzing for the amounts of the decaying element and the product of the decay. The age determinations that have been particularly successful are based on the decay of uranium and thorium into lead,§ the accumulation of helium†† (dead alpha particles), and the decay of rubidium into strontium.‡‡

Throughout the first third of this century, sporadic attempts were made to use radioactivity for geophysical exploration. The work of Lind§§ in the carnotite fields of western Colorado and of Ambronn††† in Germany is probably outstanding. Almost all measurements of this era were made by gold-leaf electroscope combined with various types of ionization chambers.

The first large-scale application of radioactivity to exploration came in the late thirties, when it was discovered that logs of gamma-ray activity‡‡‡ in oil wells are very useful in stratigraphic correlation. The success of the

---

* Contribution from the Laboratory for Nuclear Science and Engineering and the Department of Geology, Massachusetts Institute of Technology.

† H. Becquerel, *"Sur les radiations émises par phosphorescence," Compt. rend. 122,* 420-1 (1896). See also *ibid.*, 1086-8.

‡ L. B. Slichter, "Cooling of the Earth," *Bull. Geol. Soc. Am. 52,* 561-600 (1941).
W. D. Urry, "Significance of Radioactivity in Geophysics—Thermal History of the Earth," *Trans. Am. Geoph. Union 30,* 171-80 (1949).

§ A. Holmes, "The Age of the Earth," Th. Nelson and Sons. London, 1937.

†† C. Goodman and R. D. Evans, "Age Measurements by Radioactivity," *Bull Geol. Soc. Am. 52,* 491-544 (1941). See also *Phys. Rev. 65,* 216-27 (1944).
P. M. Hurley and C. Goodman, "Helium Age Measurement", *Bull. Geol. Soc. Am. 54,* 305-24 (1943).

‡‡ L. H. Ahrens, "Measuring Geologic Time by the Strontium Method," *Bull. Geol. Soc. Am. 60,* 217-266 (1949).

§§ S. C. Lind and C. F. Whittemore, "The Radium-Uranium Ratio in Carnotites," *U. S. Bur. Mines Tech. Paper 88,* 29 pp. (1915).

††† R. Ambronn, "Elements of Geophysics," McGraw-Hill, New York, 1928.

‡‡‡ W. Green and R. E. Fearon, "Well Logging by Radioactivity," *Geophysics* V, 272 (1940).

gamma-ray log led to reexamination of the radioactivity of sediments† and was the principal impetus behind the unpublished radioactivity research of most major oil companies.

With the discovery of fission and the subsequent development of nuclear power (1939-42) came a renewed interest in uranium ores, and considerable attention was directed toward the methods of searching for radioactive minerals.‡ Most of the procedures described in this chapter are products of this development.

As geophysical methods go, however, radioactivity exploration is still in its infancy. Most of the theoretical analysis and the practical refinement of field technique is yet to come.

Particles and Quanta

Let us first consider the missiles by which radioactive atoms make known their decay. The projectiles may be either charged particles of matter with a definite rest mass (*alphas* or *betas*), or merely bundles of energy with zero rest mass, called *quanta* (*gamma*-rays).

The energy of these radiations is usually expressed in electron-volts (ev), or the same unit multiplied by 10^6 (Mev). One ev is the energy acquired by an electron in falling through a potential difference of one volt, and it is equal to $1.6 \cdot 10^{-12}$ ergs. There are three types of nuclear decay which interest us here:

(1) **Alpha Emission.** — A radioactive nucleus of atomic number Z and mass number A may emit a stripped helium atom (α-particle) and decay into a daughter nucleus with atomic number $(Z\text{-}2)$ and mass number $(A\text{-}4)$. No further event will take place in this particular decay if the α removes sufficient energy to leave the nucleus in the ground state. However, a weaker α may be emitted, leaving the daughter nucleus in a quantized excited state. The excited nucleus then falls to ground state by emitting its excess energy in the form of a gamma-ray. The decay of radium^{226} into radon^{222} is an example of such a process (Figure 602). The energies of α's and γ's emitted in α decay are definite and discrete, and may be thought of as a line spectrum.

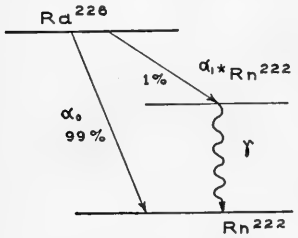

FIG. 602.—Decay scheme of radium^{226}. Energies α_0 4.79 Mev; α, 4.61 Mev; γ, 0.18 Mev.

(2) **Beta Emission.**—In another type of disintegration, a fast electron (β particle) is emitted from the nucleus, Z increases by one unit, and

† K. G. Bell, C. Goodman, and W. L. Whitehead, "Radioactivity of Sedimentary Rocks and Associated Petroleum," *Bull. Am. Assn. Pet. Geol. 24*, 1529-47 (1940).
B. Pontecorvo, "Radioactivity Analysis of Oil Well Samples," *Geophysics* VII, 90-94 (1942).
W. L. Russell, "The Total Gamma Ray Activity of Sedimentary Rocks as Indicated by Geiger Counter Determinations," *Geophysics* IX, 180-216 (1944).

‡ H. Faul, "Radioactivity Exploration with Geiger Counters," *A.I.M.E. Tech. Pub. 2460, Mining Technology*, Nov., 1948.

there is no change in A. In other words, the element changes into its next higher neighbor in the periodic table. Each beta decay is thought to be accompanied by the emission of a hypothetical particle of zero charge and very small rest mass, the neutrino.† The energy E_{max} released by the decay is divided between the β and the neutrino, so that the β may have any energy between zero and E_{max}. The approximate shape of the energy spectrum is shown in Figure 603. The spectrum is continuous, with a definite upper limit (E_{max}). The average energy is approximately $\frac{1}{3}$ E_{max}.

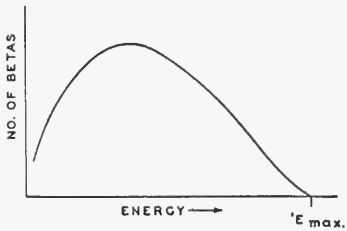

FIG. 603—Continuous spectrum of a β emitter.

(3) **K-capture.**—The most uncommon mode of decay is the capture of the innermost atomic electron (K-electron) by the nucleus, resulting in a decrease in Z by one unit, with A unchanged. For example, potassium^{40} decays to argon^{40}, its next lower neighbor in the periodic system. The K-capture is followed by x-ray emission as the atomic electrons fall into the vacated lower orbits.

A radioactive nucleus frequently has the opportunity of decaying in more than one of these ways. Again, we may use potassium as an example (Figure 604). A given nucleus of this element has an uncertain future. It may change to calcium^{40} by β-decay, or capture a K-electron and decay into argon^{40}. It is thought that the known potassium gamma-ray is emitted by the excited argon nucleus. The different types of decay are not equally likely. In the case of potassium^{40}, twice as many nuclei decay by β-emission as by K-capture, but in other nuclei the decay is much more unequally divided. For instance, bismuth^{214} (RaC, see Figure 605) prefers β-decay and transforms into polonium^{214}, 2500 times more often than into thallium^{210}, by α decay.

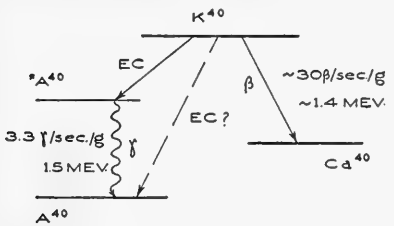

FIG. 604.—Decay scheme of potassium^{40}. Occurrence of the "silent" electron capture (E.C.) transition from K^{40} to A^{40} is now in doubt. (Modified after Ahrens and Evans, *Phys. Rev. 74*, 279, 1948.)

Absorption

The three types of radiation are all absorbed in matter, but each to a different degree. Because of their great ionizing power, alphas are the first absorbed. A sheet of paper is sufficient to stop them completely and they travel only two or three inches in air. Natural alphas have a limited range of energies: the weakest known (samarium) has an energy of 2 Mev, while the most energetic (α_2 from Po^{212} in the *Th* series) carries 10.6

† C. W. Sherwin, "The Neutrino," *Nucleonics 2*, No. 5, 16-24, May, 1948.

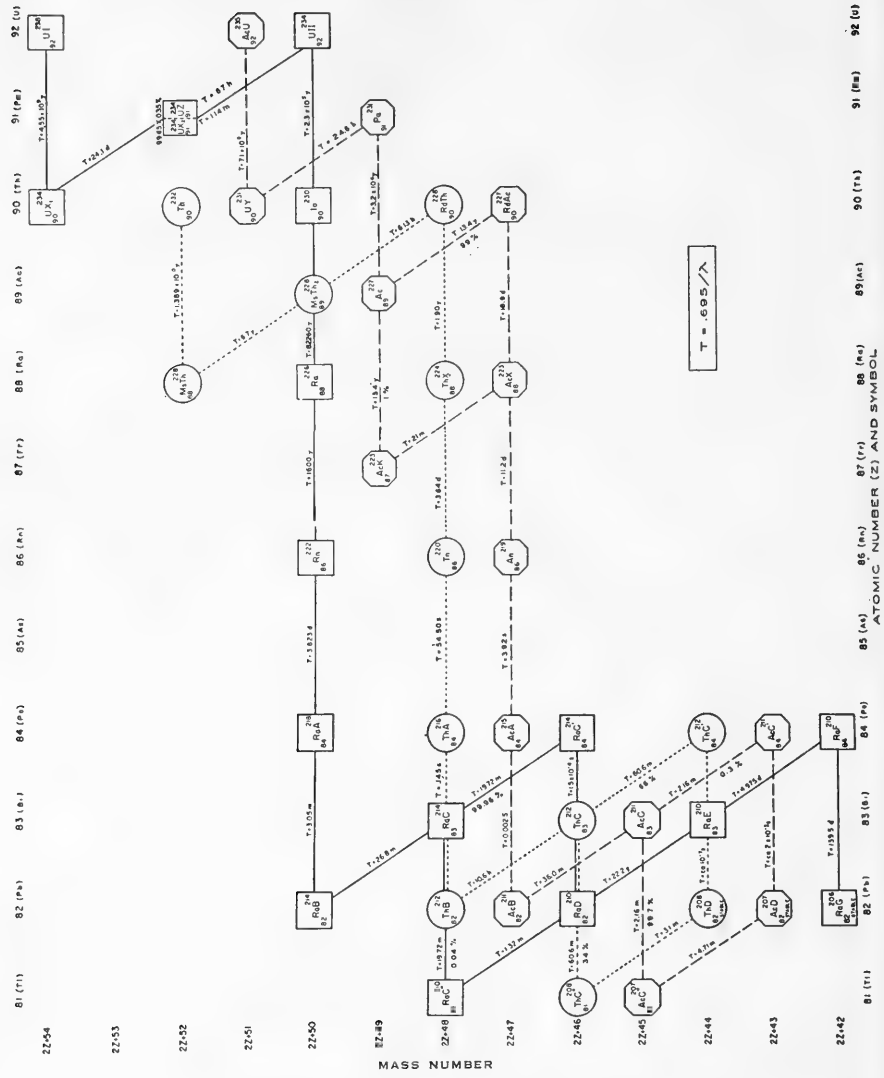

FIG. 605.—The natural radioactive series. (After R. D. Evans, *The Science and Engineering of Nuclear Power*, Vol. I, Addison-Wesley, 1947).

Mev. The range of the average energetic α in aluminum is of the order of 10^{-3} cm.

There is much greater variety in the energy (E_{max}) of known natural beta emitters, with a distribution from a few Kev to 3.1 Mev (Bi^{214} in the U series). But a beam of ½ Mev β's will be stopped almost completely by a 16-gauge sheet of aluminum.

Natural gamma-rays have energies up to 2.2 Mev. Energetic ("hard")

gammas are very penetrating, but their absorption is usually underestimated. It is well to remember that one foot of rock will absorb about 99 per cent of the gammas from the uranium series. Gamma rays are absorbed in several different ways; but photoelectric absorption and Compton scattering are particularly important in this discussion.

When a gamma ray is absorbed by the *photoelectric effect,* it transmits its energy to an electron. It effectively tears the electron away from its atom and propels it through the absorber. The photoelectron acts much like a β and is soon absorbed. Therefore, the simple absorption law

$$I = I_o e^{-\mu X}$$

describes the photoelectric absorption quite accurately. I_o and I are the initial and final γ intensities, μ is the photoelectric absorption coefficient and X is the thickness of the absorber.

The second important effect is *Compton scattering* where a γ, acting this time just like a particle, collides with an electron and bounces off, transferring some of its energy to the recoiling electron. The γ does not disappear, but continues on its way with diminished energy and in a new direction. Consequently, we may not represent this type of "absorption" by the simple exponential relation. Instead we must write

$$I = I_o \left(e^{-\pi X} + C\right)$$

where π is the Compton absorption coefficient and C is the proportion of quanta scattered back into the detector after the first Compton collision. C will be determined by the geometrical disposition of the source, absorber, and detector, as well as by the atomic number and density of the absorbing material. The analytical evaluation of C is difficult, even for simple geometries.

Photoelectric absorption increases with the fourth power of the atomic number Z, whereas Compton scattering depends only on the electron density in the absorber, or roughly the first power of Z. Therefore photoelectric absorption will predominate in heavy elements but the Compton effect will be more important for the lighter atoms. In light elements such as aluminum, for instance, almost all first interactions of 1-Mev γ's will be of the Compton type. It should be kept in mind that common rocks consist of light elements almost exclusively.

Natural Radioactive Elements

Most of the naturally occurring radioactive elements belong to three major families, each of which comprises isotopes of most of the elements on the heavy end of the periodic table. The parent elements of the three families are uranium ($_{92}U^{238}$ and $_{92}U^{235}$) and thorium ($_{90}Th^{232}$), and the daughter elements include isotopes of protoactinium, actinium, radium, francium, radon, polonium, bismuth, lead, and thallium (in order of decreasing atomic weight). The decay cascade of the three families

together with half-lives and decay constants is shown graphically in Figure 605.

The two uranium families always occur together in nature with the parent elements intimately mixed in a fixed proportion which is constant throughout the earth ($U^{235}/U^{238} = 1/139.2$). The thorium family is sometimes found with uranium, but more frequently occurs in minerals by itself. Most of the commercial ores of uranium contain no thorium whatever.

There are other naturally radioactive elements: the alkalis potassium and rubidium, the rare earths samarium and lutecium, and the heavy metal rhenium.

The radioactive isotope of potassium ($_{19}K^{40}$) comprises 0.012 per cent of all natural potassium and has a half-life of $4.5 \cdot 10^8$ years.† It emits β-rays, orbital electron capture x-rays and γ-rays, and occasionally may be the principal contributor to the radioactivity of a rock.‡ Natural potassium compounds can be quantitatively analyzed by geophysical means with great accuracy.§ The activity of common K amounts to roughly 30 betas and 3.3 gammas per second per gram. The activity of the uranium series (in equilibrium) is approximately 40,000 betas* per second per gram of U. Consequently, a very small uranium contamination may cause a large error in a potassium analysis, but the error caused by potassium in uranium and thorium analyses is usually negligible.

Rubidium receives its radioactivity from $_{37}Rb^{87}$ which has an isotopic abundance of 27.2 per cent in natural rubidium and a half-life of $5.8 \cdot 10^{10}$ years, or about 20 times the accepted age of the earth. Common Rb_2O has a specific activity approximately 10 times greater than the activity of common K_2O. The rubidium β, however, is 10 times weaker than that of potassium.** As a chemical element, rubidium is comparatively rare in nature. Its richest "ore" is lepidolite, which usually contains about 1.5 per cent Rb_2O, and lesser amounts are found in amazonite, pollucite, and some varieties of microline and muscovite.

The radioactive samarium isotope is probably $_{62}Sm^{152}$, which makes up 14.2 per cent of natural samarium. It is the only known α emitter outside of the heavy elements, but the half-life of the activity is extremely long ($1.4 \cdot 10^{11}$ years). The element itself is found only in minute quantities in samarskite, cerite, monazite, and a few other rare minerals. The lutecium activity also has a long life ($7 \cdot 10^{10}$ years) and the concentration of the

† L. H. Ahrens and R. D. Evans, "The Radioactive Decay Constants of K^{40} as Determined from the Accumulation of Ca^{40} in Ancient Minerals," *Phys. Rev.* 74, 279-86 (1948).

‡ F. E. Senftle, "The Effect of Potassium in Prospecting for Radioactive Ores," *Can. Mining Jour.*, Nov., 1948.

§ H. C. Spicer, "Gamma Ray Studies of Potassium Salts and Associated Geological Formations," *U. S. Geol. Survey Bull. 950*, 143-61 (1942-45).

R. B. Barnes and D. J. Salley, "Analysis for Potassium by its Natural Radioactivity," *Ind. and Eng. Chem., Anal. Ed., 15*, 4-7 (1943).

A. M. Gaudin and J. H. Pannell, "Radioactive Determination of Potassium in Solids," *Anal. Chem. 20*, 1154-6 (1948).

* Neglecting the weak β's of Th^{234} and Pb^{210}.

** Maximum β energies: Rb — 0.13 Mev, K — 1.3 Mev. Rb also emits weak γ rays.

radioactive isotope (Lu^{176}) is only 2.5 per cent. The element itself is very rare and usually is associated with yttrium in nature. The recently reported β activity of rhenium probably comes from $_{75}Re^{187}$ which has an isotopic abundance of 61.8 per cent. The reported half-life is immense, and the radiation very weak (approximately $3 \cdot 10^{12}$ years, 0.04 Mev). Small amounts of rhenium are found in columbite, tantalite, and wolframite.

It is clear that rubidium, samarium, lutecium, and rhenium, although interesting in themselves, are not commonly encountered in radioactivity exploration, and are therefore of little importance within the scope of this book.

Equilibrium

If we take a fixed amount of uranium that has just been purified, some of it will immediately start decaying into its first daughter element (see Figure 605) which in turn decays into its own daughter and so on down the line until the last stage is reached—a stable isotope of lead. The rate at which a radioactive element decays is frequently expressed in terms of the *half-life T,* which is the length of time required for the decay of half the atoms in a given amount. The half-life is inversely proportional to the *decay constant* λ, which is defined as the number of atoms which decay in one unit of time divided by the total number of atoms in the sample of the decaying element.

The relation between T and λ is

$$T = \frac{log_e 2}{\lambda} = \frac{.693}{\lambda}$$

As the decay cascade proceeds, the isotopes with a small λ will tend to accumulate, and those with a very large λ will decay a very short time after their birth. We can visualize the process if we imagine water running through a series of vats connected in cascade by pipes of different sizes. The water accumulates and builds up pressure in the vats with small outlet pipes, but runs right through the vats with large drains.

The concept of equilibrium becomes very important when we try to measure the amount of any particular radioactive element in a rock by measuring the rate of overall radiation. We must remember that radioactive parent and daughter are always chemically different and can therefore be separated in nature by normal geological processes. The result is the same as if one or more of our vats had sprung a leak and we could no longer be sure that the amount of flow from any particular vat to the next lower one was the same as the flow from the top vat.

Such a case arises when we measure the radiation from some of the supergene uranium minerals (carnotite, tyuyamunite, and others). One of the daughter elements of uranium is radon, a noble gas, and these minerals are sufficiently porous to permit the escape of some of the gas with the consequent loss of radiation from radon and its numerous daughter

elements (Figure 605). Therefore, if we compare the radioactivity of an impermeable mineral such as pitchblende with the radioactivity of carnotite, the carnotite will appear low even though the uranium content of the two minerals be the same. The ability of a mineral to lose radon is called the *emanating power* and may vary widely from specimen to specimen. This effect may be a serious source of error in radiological sample testing, unless the samples are treated to fix the gas in place and then stored for a few weeks to reestablish the radon equilibrium.

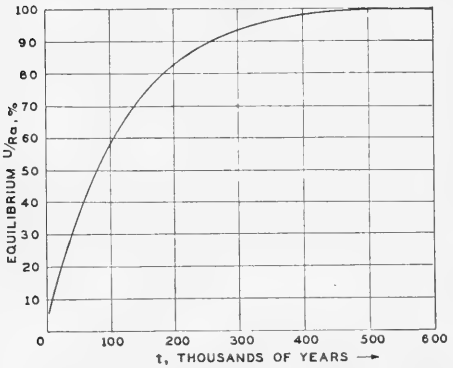

FIG. 606.—Uranium-radium equilibrium plotted as a function of time. (After A. F. Kovarik, Nat. Res. Council *Bull. 80,* 110, 1931.)

Another important ratio is that between U^{238} and radium, which is usually constant in nature. There are many instances, however, where minerals are undergoing leaching or chemical weathering which results in differential movement of the active elements. In this way the equilibrium may be disturbed faster than it can reestablish itself and anomalous assay results are obtained from radioactivity measurements. Figure 606 shows the time required to establish equilibrium between U^{238} and Ra^{226}. The question of the radium-uranium ratio in carnotites has been investigated by Lind and co-workers,† who found the ratio constant in large samples even though individual specimens showed various degrees of deviation from the average value.

Statistical Error

The decay of a radioactive nucleus is not influenced by events that preceded it nor by events which may follow. The radiations therefore are emitted at random (or "perfectly irregular") intervals.

In any random procession the number of events which occur in one unit of time is not the same as the number of events in the following unit of time, and the fractional difference between a single measurement and an average of a large number of measurements is referred to as the "statistical error." This quantity will be different for each individual measurement, and it cannot be given a definite numerical value. Instead, we must think of it in terms of probability. The absolute probable* error of a measurement is defined as

$$p = 0.6745 \quad \sqrt{N}$$

† S. C. Lind and C. F. Whittemore, "The Radium-Uranium Ratio in Carnotites," *U. S. Bur. Mines Tech. Paper 88,* 29 pp. (1915).

* The commonly used percentage probable error is the ratio of the absolute probable error and the measured quantity, expressed in per cent (see Figure 607).

where N is the total number of events recorded. We have an even chance that a measurement will differ from the average of a large number of

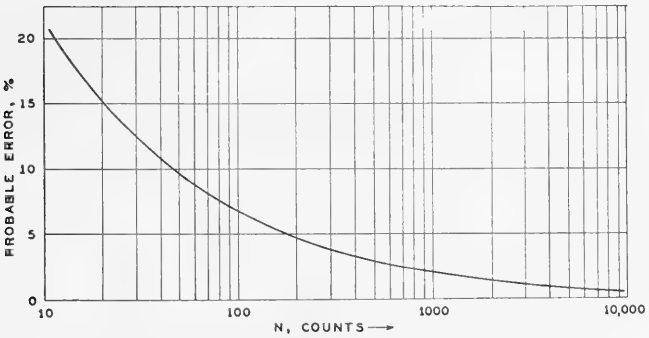

Fig. 607.—Probable error (in per cent) as a function of total number of counts recorded in one measurement.

measurements by an amount smaller than p. In other words, if we take a large number of repeated measurements with a perfect instrument, half of the readings will differ from the average by an amount smaller than p and half will differ by more than p. It is important to realize that p is a function of N only, and it does not depend on the time it took to make the measurement. The probable error therefore can be kept constant in a series of radioactivity measurements by measuring the time required to rack up a given number of counts rather than the number of counts per unit of time. This procedure is commonly used in routine testing of radioactive samples.

In some applications of radiation measurement, especially drill-hole logging as described in Chapter XI, it is convenient to use integrating instruments. These devices measure the flux of radiation through an ionization chamber or the rate at which impulses are received from a counter. The statistical error of these measurements will show itself as an irregular fluctuation of the observed quantity (see Figure 608.) Again, the magnitude of the fluctuation will depend only on the total number of ionizing events recorded in the inherent interval given by the characteristics of that particular instrument.

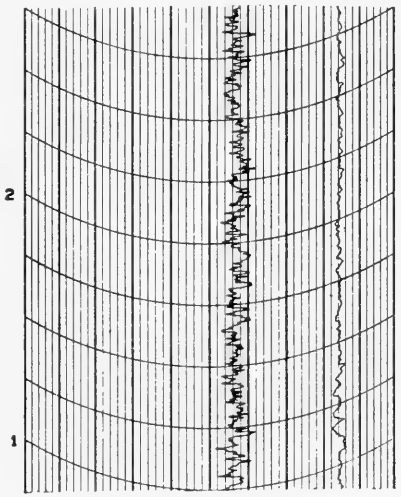

Fig. 608.—Counting-rate meter records of constant rates of 570 counts/min. (left) and 8,400 counts/min. (right). Note the difference in statistical fluctuation.

RADIATION MEASURING DEVICES

The Ionization Chamber

Radioactive particles and quanta can be detected by the ionization they produce in gases. If we set up an electric field in a suitable vessel (Figure 609) we shall sweep out most of the ions and produce an electric current which will be proportional to the amount of ionization produced by the radiation.

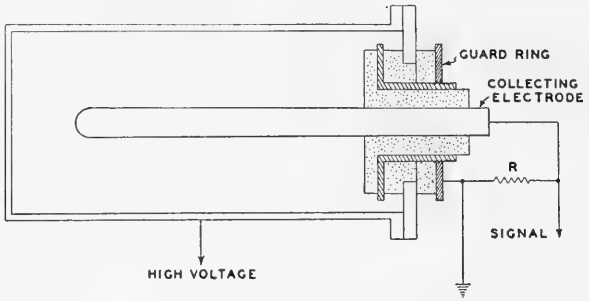

FIG. 609.—Scheme of an ionization chamber. Insulators are shown stippled.

The ionization chamber will have a certain capacitance C, usually on the order of a few micromicrofarads, and the high resistance between the electrodes will be R. The product RC is called the *time constant*. If we now charge the chamber to a voltage V_0, the charge will leak off at the rate

$$\frac{dV}{dt} = \frac{V_0}{RC}\, e^{-\frac{t}{RC}}$$

We may handle the ionization current in two different ways. First, we can make the time constant so small that the charge leaks off almost as fast as it accumulates. Each ionizing event will then produce a pulse proportional to the magnitude of the event. Pulse chambers are useful in the laboratory for α counting in a strong β-γ background. Suitable discriminating pulse amplifiers can easily distinguish the large α pulses from the ripple produced by β's and γ's.

Integrating (or direct current) chambers have a very high time constant, on the other hand, and are usually used for γ detection. They require powerful D.C. amplifiers but can be made very sensitive when filled to a high pressure. Such chambers find their greatest use in bore-hole logging.

The potential of the collecting electrode is usually negative with respect to the case, to collect positive ions. The ionization current will be greatest when the chamber is saturated, i.e., when an additional increase in voltage causes no further increase in ionization current, at a given flux of ionizing radiation. D.C. chambers are best operated at saturation (several thousand volts), but pulse chambers will work well at much lower voltages.

It is common practice to incorporate a guard ring in the insulator of ionization chambers (see Figure 609). The guard ring is usually connected to ground and has two functions. First, it provides an electrostatic shield which keeps the collecting electrode from seeing any external A.C. "antenna," such as a light bulb or an electric cord. Second, it collects all current that may leak across or through the high-voltage (outer) insulator. The collecting electrode is kept at a low potential with respect to the guard ring, so that the leakage across the inner insulator is negligible.

The Geiger-Müller Counter

In the literature† and on the market are many varieties of counter tubes. Their essential parts, however, have remained unchanged since Hans Geiger and Walther Müller announced their *Zählrohr* more than 20 years ago.‡

All the tubes have a thin center wire (anode) surrounded by a usually cylindrical cathode. The volume of the counter is filled by a gas at pressures ranging from a few centimeters to atmospheric. A wide variety of gases can be used for the purpose, but the most common mixture consists of argon with a small amount of polyatomic vapor (alcohol, amyl acetate, etc.) added to quench the discharge.

Gamma counters may have walls of glass or metal tubing, which absorbs all β's and α's. The efficiency of γ counters is very low. About one out of every 100 γ's which enter the counter actually produces a pulse-giving discharge.

Thin-wall (beta-gamma) counters (Figure 610) are sometimes made of glass 0.005 to 0.007 inch thick in the sensitive region, and will admit the more energetic betas. All-metal counters are available with an aluminum wall 0.004 inch thick (about 25 milligrams/cm^2), and will count β's of medium energy very well. Counters are also frequently provided with mica windows that can be made sufficiently thin to admit even some α particles. The thinnest windows conveniently used in the laboratory weigh about 1.5 mg/cm^2.

For α counting, however, it is usually preferable to introduce the sample into the counting volume without any intervening wall. Such counters are generally operated in the proportional region below the Geiger-Müller threshold (see Figure 611). The counter efficiency for β's and α's is very high. Almost all charged particles that penetrate into the counting volume produce a pulse.

Portable Field Instruments

Attempts have been made to use ionization chambers of various types, but the inherent instability of their D.C. amplifying circuits and their

† D. R. Corson and R. R. Wilson, "Particle and Quantum Counters," *Rev. Sci. Inst. 19,* 207-33 (1948).
S. C. Brown, "Theory and Operation of Geiger-Müller Counters," *Nucleonics, 2,* No. 6, 10-22 (June, 1948); *ibid. 3,* No. 2, 50-64 (August, 1948); *ibid. 3,* No. 4, 46-61 (October, 1948).
‡ H. Geiger and W. Müller, "Das Elektronenzählrohr," *Phys. Zeit., 29,* 839-41 (1928); *ibid. 30,* 489-93 (1929).

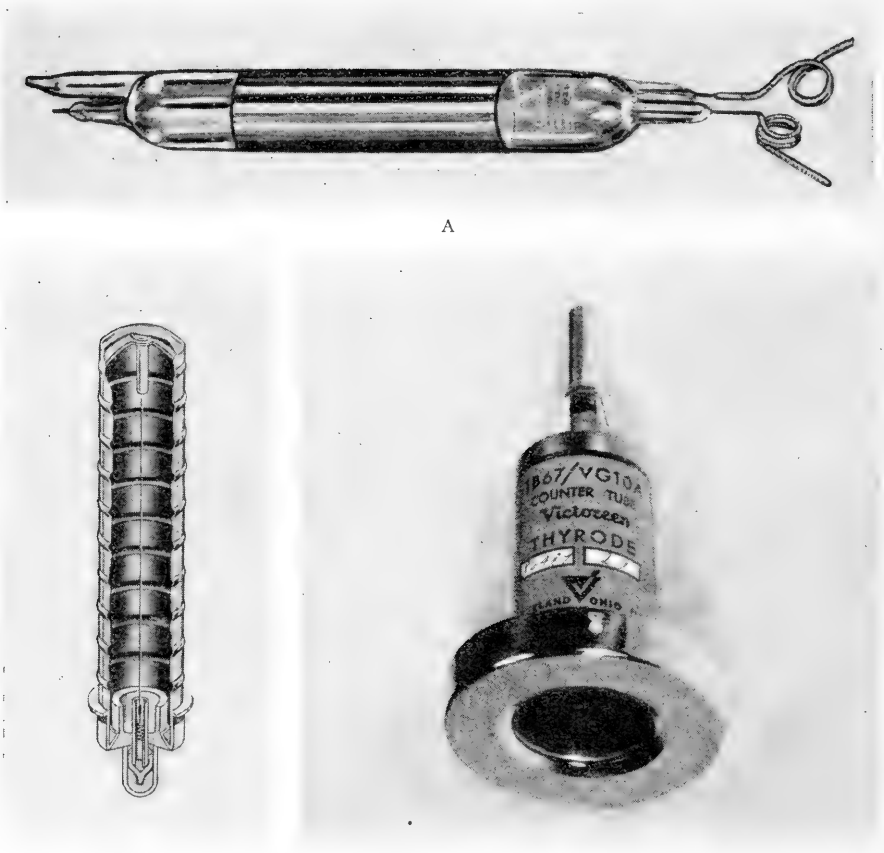

FIG. 610.—Typical thin-wall β-γ counters. (A) All glass tube with chemically silvered cathode (wall about .007 inch thick). (Courtesy of Radiation Counter Laboratories.) (B) Aluminum tube with .001-inch wall, cut away to show construction, and (C) mica window tube. (Courtesy of Victoreen Instrument Company.)

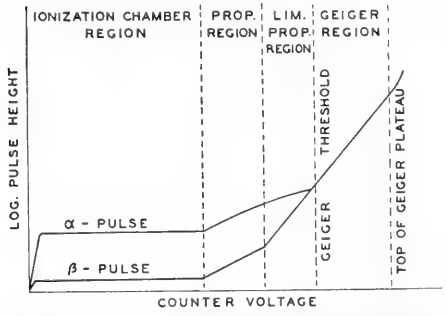

FIG. 611.—Relationship between pulse height and counter voltage. (After Montgomery and Montgomery, *J. Franklin Inst. 231,* 447, 1941.)

relatively large bulk make them less suitable for portable use than for other applications, where their superior sensitivity may be the dominant factor. Almost all portable detectors now used in the field are Geiger counters.

The simplest Geiger counter may consist of a Geiger-Müller tube, a source of high voltage and a pair of earphones. Such a counter is very simple, rugged, and

reliable, but counting the Geiger impulses by ear is very tedious and limited to low counting rates. The human ear cannot reliably follow more than about 150 to 200 random counts per minute, and the human error is great even at very low counting rates. Therefore it is desirable to eliminate the necessity of counting by ear either by amplifying and recording the Geiger pulses mechanically with an impulse register (relay-driven clock) or by integrating the current flow resulting from the passage of amplified pulses. Impulse recorders are most useful for low rates (up to about 300 counts per minute) and rate meters are usually used for higher activities.

The lowest potential conveniently used with conventional modern G-M tubes is about 800 v. Various types of vibrators and oscillators have been used to supply this voltage, but their output must necessarily be kept small to conserve battery power, and proper voltage control therefore becomes difficult. Consequently oscillator-powered high-voltage circuits are not well suited to accurate quantitative work in the field, although they are quite sufficient for rough qualitative detection (Figure 612). The pocket-type instrument shown in this figure has a vibrator-powered auditory counter. All power is supplied by two flashlight cells.

Dry cell batteries should supply the high voltage in instruments to be used in accurate surveys where good reproducibility is all-important. Small batteries are manufactured commercially in 300-volt packs. Three packs weigh about 3 lbs. 3 ozs., and occupy about 59 cubic inches. They are frequently used as a 900-volt supply for standard G-M tubes in precision instruments.

FIG. 612. — Simple Geiger-Müller counter with vibrator high-voltage supply. (Courtesy of Nuclear Instrument and Chemical Corporation.)

A cathode-coupled multivibrator circuit* (Figure 613) makes a very good "amplifier" for Geiger pulses because a small trigger pulse fed into the circuit produces a much more powerful "shaped" output pulse. The effective gain per tube is considerably higher than that obtained from a conventional amplifier, resulting in economical power drain which in turn permits the use of small batteries.

The multivibrator may be adapted to drive a commercial impulse register by using an R-F pentode (such as the 1N5) and a power amplifier tube (1T5, 1Q5, or similar) for V_1 and V_2 respectively. The register is connected at R, and a 22½ v. "C" battery provides bias to cut off the power tube. Most counting rate meters, on the other hand, use subminiature tubes (Figure 614) for V_1 and V_2, since these tubes require as little as 15 milliwatts of filament power per tube. A microammeter is then connected at R, by-passed by a high-capacity electrolytic condenser to form a storage circuit (Figure 615) which smooths out the output pulses to give a steady current proportional to the

* Also known as Schmitt's trigger circuit. For an extensive discussion of trigger circuits, see O. S. Puckle, "Time Bases," Chapter 4 (John Wiley and Sons, New York, 1943).

number of pulses per unit of time. The "C" battery is omitted when subminiature tubes are used, but provision is made to vary the coupling constants R_1 and C_1 in two or three steps so that a single instrument may have several ranges of sensitivity (Figure 616).

A great variety of small counting rate meters is available, but few of these instruments are designed for mineral exploration. For accurate surveying, the instrument should fulfill the following requirements:

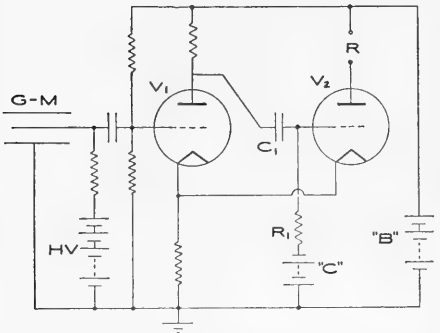

FIG. 613.—Portable Counter Circuit. Symbols: *G-M*, Geiger-Müller tube; V_1, first stage (normally on); V_2, second stage (normally off); *R*, recorder or rate meter connections; *HV*, high voltage batteries; *"B"*, *"C"*, plate and bias batteries. (Modified after O. H. Schmitt, *Jnl. Sci. Inst. 15*, 24, 1938.)

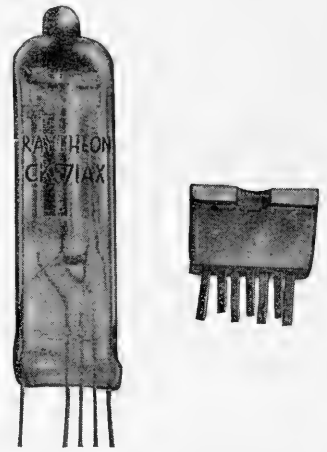

FIG. 614.—Typical subminiature pentode and socket, enlarged × 1.5. (Courtesy of Raytheon Manufacturing Co.)

a. All scales should be approximately linear, i.e., the meter reading should be directly proportional to the true counting rate. (The linearity may be checked by tapping the pulses from the G-M tube directly into a scaler and comparing the scaler count with the rate meter reading at various counting rates.)

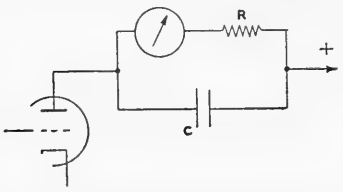

FIG. 615.—Capacity resistance type "storage" circuit used in counting-rate meter.

b. The factor between the various ranges of sensitivity should be constant. A factor of 10 is generally used. (Its constancy is again best checked with the aid of a scaler.)

c. The reading of the instrument should not vary with temperature and humidity. All high-voltage connections should be well protected against moisture, to prevent spurious "counting." Although an external probe is frequently convenient, a G-M tube built into the instrument case (with short high voltage leads) is to be preferred for work in humid surroundings, especially underground.

d. Provision should be made to check the B battery voltage easily. The reading of all counting rate meters falls off with decreasing plate voltage, and a constant check is essential if the measurement is to be reproducible. For the same reason, B batteries should be large enough to maintain voltage for at least eight hours of continuous operation.

Mobile Field Equipment

The measurement of radioactivity in drill holes and a few other applications require integrating instruments of great sensitivity, good stability

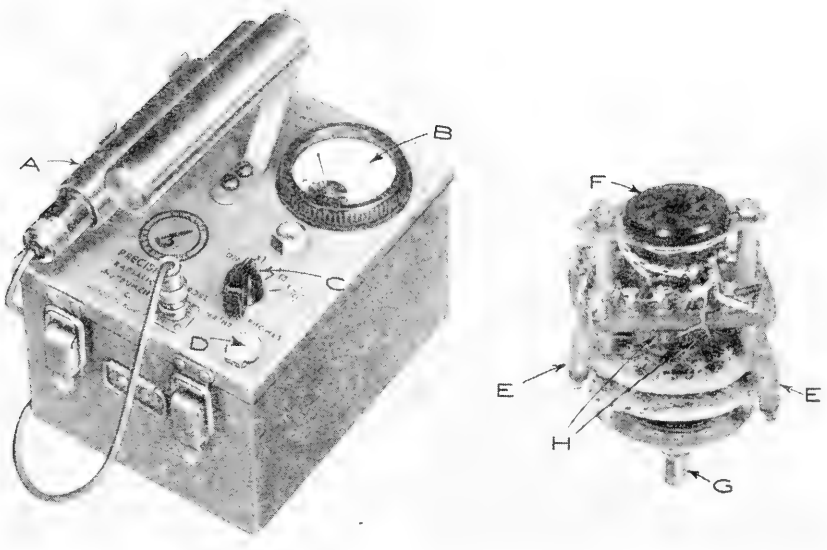

FIG. 616.—(Left) Counting rate meter with three stages of sensitivity. (A) G-M tube, (B) meter, (C) sensitivity switch, (D) phone jack for audio counting. (Right) Quick change plug-in assembly for multi-stage sensitivity counter. (E) subminiature tubes, (F) battery connector, (G) sensitivity switch, (H) R-C coupling. (Courtesy of Precision Radiation Instruments, Inc.)

FIG. 617.—Radioactivity logging equipment for diamond drill holes: (A) cable; (B) tripod support for guide sheave; (C) reel; (D) recording equipment; (E) sheave wheel; (F) tripod brace.

and quick response. Such instruments are usually provided with strip chart recording meters and are generally mounted in light trucks (Figure 617), together with the accessory equipment, storage batteries, charger, etc. Heavy-duty trucks carry the large winches required to hold the long cables necessary for oil-well logging. The winches have internal slip-rings to connect the cable to the surface instruments (Figures 664 and 665). The diamond-drill holes commonly drilled for mineral exploration are relatively shallow, and instruments for logging them are generally much lighter than their oil-well counterparts.

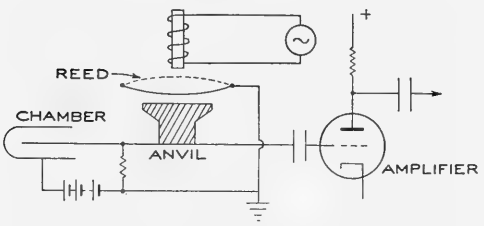

FIG. 618.—Principle of vibrating-reed electrometer.

Both high-pressure D.C. ionization chambers and special high-efficiency G-M counters are used for γ-ray logging of oil wells. The chambers are filled with argon or a mixture of argon and CO_2 at pressures up to several hundred atmospheres, and electrometers of the vibrating-reed or capacitative commutator type† are used to measure the ionization current. The combination has a very high sensitivity for γ's.

The vibrating-reed electrometer (Figure 618) is based on the principle that a small alternating current is easier to amplify than a small direct current. The A.C. is produced by impressing the small D.C. voltage on a condenser, one plate of which is made to vibrate at a frequency of several hundred cycles per second. The resulting A.C. passes through a condenser into a linear audio amplifier. After sufficient amplification it is synchronously rectified and measured.

Simple Geiger counters are not sensitive enough for the fast gamma-ray logging of oil wells (up to 100 feet/min.) but their sensitivity may be increased by increasing the effective area of their cathode, either by fabricating it from wire screen‡ or by cellular construction (Figure 619). A wire-screen cathode has a greater effective area than a solid wall and therefore emits more photoelectrons in a given gamma-ray flux. The comparable efficiency of a cellular cathode may be made several times greater than that of a simple cylinder of equivalent size.

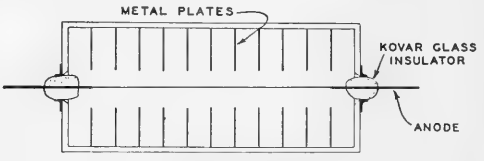

FIG. 619.—High-efficiency gamma counter with cellular cathode for increased sensitivity and faster rate of logging. (After S. C. Brown.)

The diamond-drill holes are usually too small for the ionization instruments and cellular counters. On the other hand, the holes are frequently shallow so that great logging speeds and correspondingly high sensitivity are not required. Simple G-M counters are amply sufficient for most diamond-drill-hole logging, and counters with very low sensitivity are even essential for the exploration of drill holes in uranium-bearing ore bodies.

The smallest conventional diamond-drill holes are 1.45 inches in diameter, and it may be necessary to case them before the logging probe can be lowered safely. There-

† H. Palewsky, R. K. Swank and R. Grenchik, "Design of Dynamic Condenser Electrometers," *Rev. Sci. Inst. 18*, 298-314 (1947).
S. A. Scherbatskoy, T. H. Gilmartin and G. Swift, "The Capacitative Commutator," *Rev. Sci. Inst. 18*, 415-421 (1947).

‡ W. Good, A. Kip and S. Brown, "Design of Beta-Ray and Gamma-Ray Geiger-Müller Counters," *Rev. Sci. Inst. 17*, 262-5 (1946).

fore the probe should be smaller than 1 inch overall outside diameter. Modern subminiature tubes, small high-efficiency pulse transformers, and "hearing-aid" type construction make it possible to make a probe about ⅞ inch in diameter, using a simple G-M counter tube. The light casing (1 inch inside diameter) can be set and pulled by hand down to about 200 feet. A pipe clamp is used to hold the string while sections are added.

The pulses from the G-M tube are integrated to give a continuous graph of the pulse counting rate plotted against depth in the hole. The principle of a counting rate meter is deceptively simple (Figure 615), but the detailed design is fairly difficult. The pulses coming into the circuit pile up on the condenser, and slowly leak off through the meter. If the meter reading is to have any significance, all the pulses must be equal in the amount of energy that they transmit. Geiger pulses are not all strictly alike and must be shaped before they can be metered. The shaping circuits are similar to that shown in Figure 613. The shaper must have excellent stability and sufficient power to put out a pulse large enough to deflect the meter and fast enough to trigger in time for the next pulse to be received. The speed is governed by the product of R_1C_1, which is the trigger coupling time constant (Figure 613).

The rate meter resistance (R, Figure 615) must be so small that the voltage drop across it at full meter deflection is still negligible compared to the plate voltage of the feeding tube. The two principal causes of nonlinearity in counting rate meters are insufficient speed of the shaping circuit and excessive meter resistance.

The product of the meter resistance R and capacitance C determines the magnitude of the time interval ΔT over which pulses are integrated. At a fixed counting rate, the statistical fluctuation of the needle will be proportional to $\sqrt{\Delta T}$. When a constant source of radiation is placed near a counter feeding into a rate meter, the reading will climb toward the equilibrium position at an exponentially decreasing rate. For most practical purposes the needle reaches equilibrium in the approximate time

$$T \cong 3\,RC$$

Where T is in seconds, R in ohms, and C in farads. The design of the logging instrument must be such that the probe travels only a small distance, compared to the length of the detector, in the time T.

The plate voltage supply for a counting rate meter must be free from ripple and well controlled to maintain constant amplification throughout the measurement. Frequent calibration of rate meters is essential to guard against the error arising from drift, usually caused by fluctuating plate voltage and the progressive decrease in cathode emissivity of the rate-meter vacuum tube.

Laboratory Instruments for Radioactivity Measurement

A staggering variety of detectors and accessory equipment is available to measure the radioactivity of samples in the laboratory. The principal types of equipment are described, and the reader will find additional information in the references.

Detectors.—The *pulse chamber* is primarily an instrument for counting α's. The usual shape of the chambers is broadly cylindrical with the collecting electrode in the form of a grid or plate. It is usually filled with argon, nitrogen, or air at atmospheric pressure. The chambers are so designed that the α has sufficient room to expend most of its energy in the gas. The resulting pulses are amplified electronically and counted or recorded as "pips" on a strip chart. The first stages of the linear amplifiers tend to be microphonic and must be guarded against noise and vibration.

This difficulty may be overcome with the vibrating-reed electrometer which makes an excellent nonmicrophonic pulse amplifier for very low counting rates (Figures 620 and 621). The collecting electrode is a circular grid, parallel to the sample. Only the ions formed inside the cage are collected. Most of the precise uranium and thorium measurements for the helium method of geological age determination have been made by pulse chambers. *Proportional counters* are instruments which utilize the principle of gas amplification but operate in a voltage region too low for the Geiger discharge (see Figure 611). They are usually filled with methane at atmospheric pressure and require less powerful amplifiers than the pulse chambers.

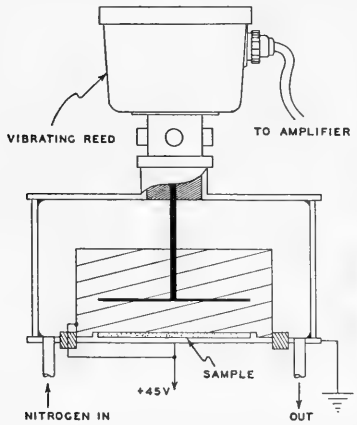

FIG. 620.—Pulse chamber for measurement of very low α activities. (Modified after Hurley.)

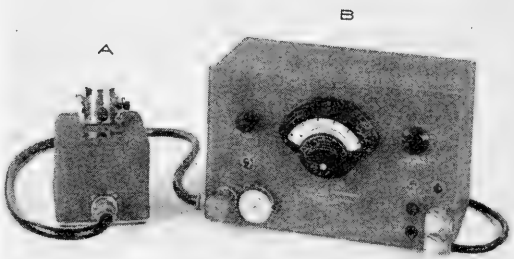

FIG. 621.—(A) vibrating-reed (housed) and (B) associated amplifying circuits. (Courtesy of Applied Physics Corporation.)

They will count β's as well as α's. With the aid of a simple discriminator it is possible to measure first the α activity of a sample and then the α and β activity by simply raising the voltage. A proportional counter with circular center wire and the associated electronic equipment are shown in Figures 622 and 623. Although the proportional counter is finding its way into geophysical research, it has not been used extensively in the past.

The *Geiger counter* is the simplest radiation detector and therefore the most commonly used in the laboratory. Depending on the construction, it will count either γ's alone of both β's and γ's, but the γ counting efficiency of mica-window β-counters can be made very small, so that they count essentially only β's. The pulses from the counter are usually recorded with a scaler that has a built-in regulated high-voltage supply for the G-M tube. The counting equipment is identical for β and γ counters.

Laboratory counters are usually shielded with a few inches of lead or iron to reduce the background radiation from softer components of cosmic rays and radioactive contamination of the laboratory.

Scintillation counters† are a new development in the field of nuclear instrumentation. Various organic and inorganic crystals emit visible and ultraviolet light when traversed by ionizing radiation. The proper crystals are transparent to their own radiation so that the light flash from each ionizing event can be picked up by an electron-multiplier phototube. The pulses from the phototube are then amplified and recorded.

Various investigators have used anthracene, naphthalene (moth flakes), scheelite, alkali halides, and other crystals in their experiments. The principal advantage of the scintillation counter is its high γ efficiency. Almost

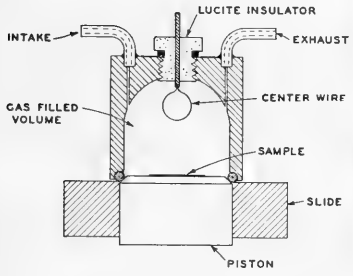

FIG. 622.—Sketch of methane-flow proportional counter with circular center wire. (Courtesy of Nuclear Measurements Corporation.)

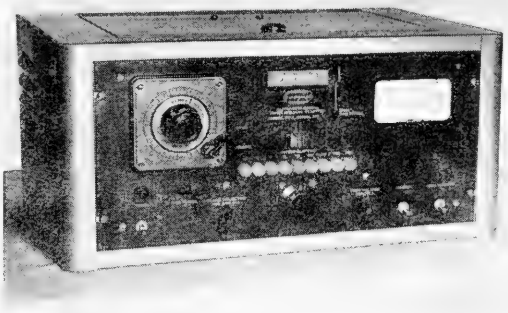

FIG. 623.—Electronic equipment (amplifier and scale of 512 scaler) for proportional center wire counter. (Courtesy of Nuclear Measurements Corporation.)

every γ passing through a relatively dense large crystal will lose a fraction of energy sufficient to produce a countable flash. The resulting pulses are much shorter than pulses from a G-M tube, and fast amplifiers with very high resolution can be used.

Photographic nuclear emulsions can be very useful in detecting ionizing radiation, particularly α particles.‡ The dense ionization of the α's produces sharp tracks that are clearly visible under the microscope. The method is particularly well adapted to the study of the α radioactivity of small grains and the detailed examination of activity in polished sections.

Auxiliary Equipment.—The *scaling circuit* is an electronic device for counting the random pulses from radiation detectors. The pulses frequently

† H. Kallman, "Quantitative Measurements with Scintillation Counters," *Phys. Rev. 75,* 623-6 (1949).
P. R. Bell, "The Use of Anthracene as a Scintillation Counter," *Phys. Rev. 73,* 1405-6 (1948). See also *AECD* 1854 and 1889, Oak Ridge Natl. Lab. (1948).
R. J. Moon, "Inorganic Crystals for the Detection of High Energy Particles and Quanta," *Phys. Rev. 73,* 1210 (1948).
‡ H. Yagoda, "Radioactive Measurements with Nuclear Emulsions," John Wiley and Son, New York (1949).

come at rates that are much too fast for any mechanical device, and their number must be reduced before they can be recorded. The basic scale-of-two circuit is shown in Figure 624.

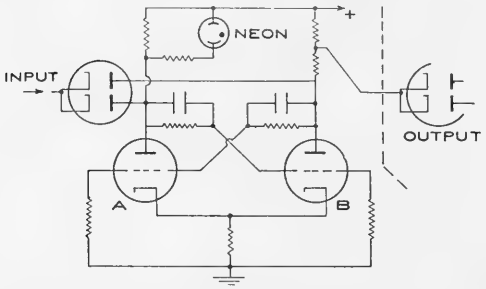

FIG. 624.—Basic scale-of-two circuit (the Eccles-Jordan version, modified by Higginbotham).

The circuit has two stable positions: when triode *A* is conducting, triode *B* cuts off, and vice versa. Let us assume that tube *A* is off. The input pulse passes through the diode to the grids of both tubes *A* and *B*. But tube *B* is already conducting, so that the pulse will have no effect on it. Triode *A*, however, will start to conduct, thus lowering the grid potential of *B* and cutting it off. The neon lamp will glow and a negative pulse will be transmitted to the diode of the next stage. But the diodes are biased to cut-off so that the negative output pulse has no effect. Nothing is transmitted to the next stage, but the glow of the neon lamp shows that the circuit "remembers" one pulse.

The second positive pulse arriving at the input affects *B*, shuts off *A*, and stops the glow of the neon bulb. A positive pulse is transmitted through the diode to the next stage. Each time the scale-of-two receives a positive pulse, it swings over, emitting alternatively negative and positive pulses. The negative pulses have no effect so that the scale effectively swallows every other pulse.

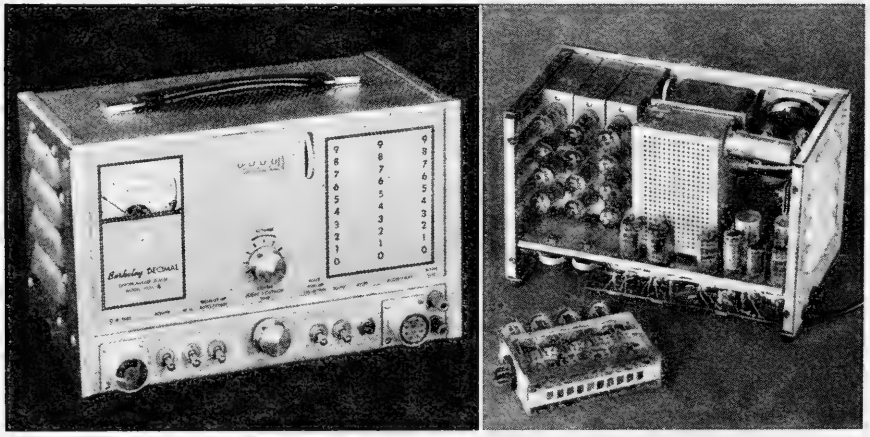

A B

FIG. 625.—A, portable decimal scaler and high voltage supply; B, internal view. (Courtesy of Berkeley Scientific Company.)

Scaling circuits frequently have six scales, with a pre-amplifier to feed the first stage and a power amplifier to actuate a mechanical pulse register after the last stage. Such an instrument will register one click for each 64 pulses received at the input end. Decimal scalers also have been developed, and are usually arranged as scales-of-1000 (Figure 625). Electronically they are more complicated than instruments based on

the scale-of-two, but their slightly higher cost is offset by the convenience of the decimal system in routine operation.

The *counting rate meters* used in the laboratory are essentially similar to the integrating instruments previously discussed. The integrating instruments do not possess the inherent precision of the scaling circuit,† and their use mostly is limited to special applications such as monitoring, automatic counting, etc., where a continuous permanent record of mean values is desired.

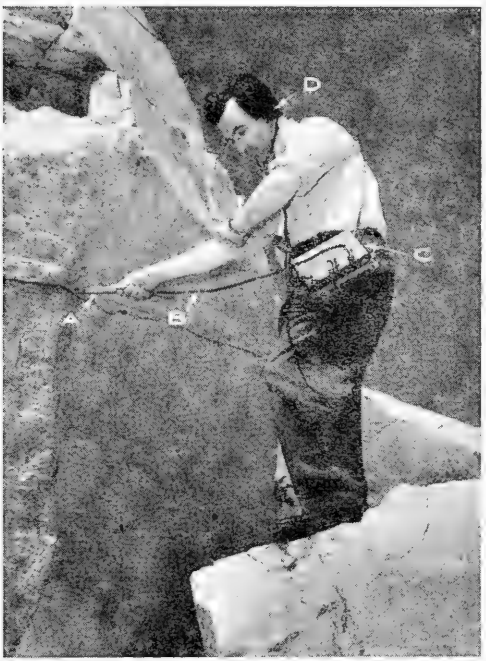

FIG. 626.—Method of measuring approximate radioactivity of rock on face of ledge. Operator notes in headphones number of clicks due to Geiger tube held close to rock. The number is counted against a stop watch on the operator's wrist. *A*, G-M tube; *B*, extension cord; *C*, counter instrument; *D*, headphones. (Courtesy of Geophysical Instrument Company.)

FIELD TECHNIQUES OF RADIOACTIVITY EXPLORATION

Reconnaissance

Fairly indiscriminate reconnaissance of outcrops may not be the most successful method of radioactivity exploration, but it is certainly the most common one (Figure 626). The best instrument for reconnaissance or "snooping" is a small G-M counter with earphones, of the general type

† A. G. Bousquet, "Counting Rate Meters Versus Scalers", *Nucleonics 4*, No. 2, 67-76 (Feb., 1949).

shown in Figures 612 and 626. A skillful operator can learn to pick up moderate changes in the counting rate without actually stopping to count the clicks, and the light weight and low cost of the "snooping" counters make them attractive to the prospector.

Traversing

Having found a geologically interesting area, it may be advisable to examine its surface radioactivity systematically. The best procedure usually is to measure the activity at a number of points, which later are surveyed and plotted to scale on a map. Radioactivity contours then may be drawn, or the data can be plotted in profiles showing radiation intensity versus traverse distance. Considerable geological information usually can be obtained from plots showing only relative radiation intensity, expressed in some arbitrary unit (e.g., counts per minute), but it is often desirable to calibrate such a map to show the actual concentration of the radioactive

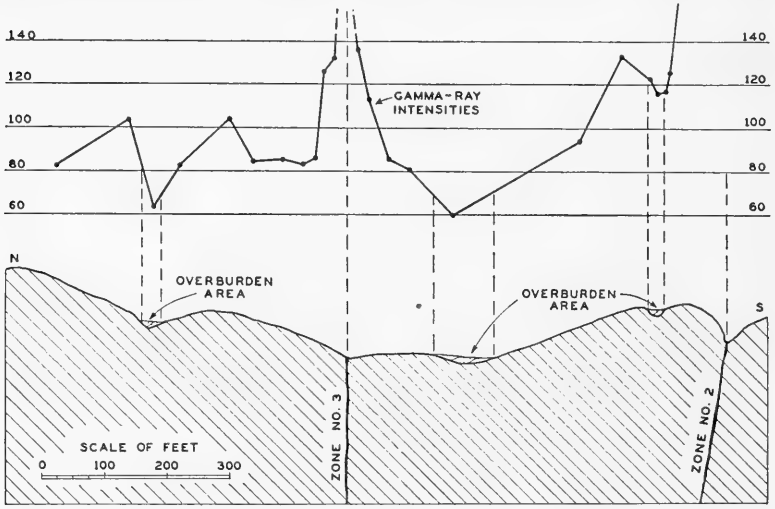

Fig. 627.—Profile of surface radioactivity across two ore zones at LaBine Point, N.W.T. (After Ridland, *Trans. A.I.M.E., 164,* 117, 1945.)

material in the surface layer of rock. The most frequently used method of calibration† involves sampling at selected points and laboratory analysis of these samples. The relative-intensity map is then used to interpolate between the sampled points, giving consideration to the surface conditions which may affect the results.

Although it is obvious that quantitative results are best obtained in areas of bare rock, traversing may be useful in regions covered with overburden or in areas where radioactive bodies may exist at shallow depths.

† A. Szalay and E. Csongor, "Determination of Radioactive Content of Rocks by Means of Geiger-Müller Counters," *Science 109,* 146-7 (1949).

Russell† showed that even in some "areas of deeply weathered residual soils the stratigraphy of the underlying formations may be mapped by plotting the area variations in the radioactivity of the weathered products," and Ridland‡ clearly recorded the No. 3 ore zone at LaBine Point, N.W.T., where a vein of pitchblende comes within 60 feet of the surface, by detecting the radiation from radon gas carried along the otherwise barren fissure above the vein. (See Figure 627.) Radon-carrying waters are found occasionally along fault zones and fissures in regions where no uranium ore is known. The radioactivity profile may show a pronounced peak over a structure of this sort if it is not buried too deeply. On the other hand, very misleading measurements may be made in regions covered by glacial drift and in the uranium mining districts, where much high-grade ore is frequently scattered about the countryside by blasting and spillage from ore trucks.

Gamma-Ray Logging

The radioactivity of sedimentary formations varies within wide limits, and a log of radioactivity vs. depth in a drill hole can be of great value for stratigraphic correlation,§ and for tracing radioactive cement. Gamma and neutron logging are described in Chapter XI.

The gamma-ray log is made by lowering a sensitive probe to the bottom of the well and recording the activity at the surface while the probe is being withdrawn. Relative radioactivity data are all that is required where the logs are used primarily for stratigraphic correlation, but in exploration for uranium absolute calibration is of the utmost importance. It is essential to know as much as possible about the actual concentration of radioactive matter in the immediate vicinity of the hole. The theoretical approach is not simple but it is possible to calibrate a probe empirically by surrounding it with radioactive material of known concentrations arranged in layers of different thickness to form a "synthetic drillhole". The material must be chosen so as to have a gamma-ray absorption coefficient similar to that of the actual rocks expected in the field.

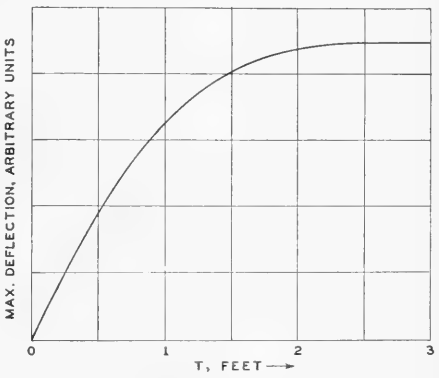

Fig. 628.—Maximum meter deflection plotted as function of thickness of a uniform horizontal bed of radioactive rock drilled vertically and logged with an 8-inch Geiger-Müller counter.

Generally, with an 8-inch G-M tube in sandstone the total indication of the counting rate meter is proportional to the absolute concentration of radioactive matter around the tube only when the radioactive layer is over 2 feet thick and laterally continuous for more than a foot or two. In thin layers of "ore" the factors of *thickness* and *grade* cannot be separated by analysis of readings taken with a single G-M tube,

† W. L. Russell, "The Total Gamma-Ray Activity of Sedimentary Rocks as Indicated by Geiger Counter Determinations," *Geophysics IX*, 180-216 (1944).

‡ G. C. Ridland, "Use of the G-M Counter in the Search for Pitchblende-Bearing Veins at Great Bear Lake, Canada," *Trans. A.I.M.E. 164*, 117 (1945).

§ W. J. Jackson and J. L. P. Campbell, "Some Practical Aspects of Radioactivity Well Logging," *Trans. A.I.M.E. 164*, 295-321, and *165*, 241-67 (1945-6).

since a 2-inch layer of 2 per cent ore will produce essentially the same effect as a 4-inch bed of 1 per cent ore. In either case, the peak meter deflection will be substantially smaller than it would be for a 2-foot layer of the same grade. The relationship of deflection versus thickness for a given grade is shown graphically in Figure 628. The curve levels off at about 2 feet. This distance will be somewhat less for shorter detectors and somewhat greater for longer ones, but it is usually impractical to make small tubes shorter than about 2 inches or longer than a foot or so. Nevertheless, approximate information on the thickness of thin radioactive beds can be obtained by logging a drill hole first with a long G-M tube and then relogging the radioactive zones with a very short tube. The relative widths of the deflection peaks will serve as an indication of the thickness of the ore beds.

Neutron Logging†

The gamma-ray logging instrument can be used for neutron logging when a source of neutrons is attached about one or two feet below the γ detector. The usual source of neutrons is a mixture of about 3 parts beryllium and one part radium bromide, intimately mixed and compressed in a small capsule. Such a source gives off about 10^7 neutrons/sec and about 10^{11} gammas/sec per gram of radium. A lead plug occupies the space between the source and the detector, to absorb the heavy γ background of the neutron source.

Most of the neutrons from the source are fast (mean energy very roughly 5 Mev). They fly out into the formation and collide with the nuclei of the atoms that make up the rock. They lose most of their energy in collisions with hydrogen and very little in elastic collisions with other nuclei. After about 25 collisions with hydrogen the neutrons are slowed down to thermal energies (about .025 ev) and diffuse through the rock until they are absorbed. A γ is emitted in most neutron capture reactions, and some of the γ's find their way into the detector.

Now if the formation contains little or no hydrogen, the neutrons will travel far before they are slowed down and absorbed. A good many of them will be absorbed near the γ detector and we shall observe a high reading on the log. When the instrument passes through formations with much hydrogen (in the form of water or hydrocarbons) the γ indication will be small, for most of the neutrons will be slowed down and absorbed in the immediate vicinity of the source and few γ's will reach the recorder.

The neutron curve is therefore useful as an indicator of the amount of hydrogen in the formation. The electrical resistivity of sedimentary rocks usually is an inverse function of their water content, and the correlation between resistivity logs and neutron curves is frequently excellent (see page 1107).

Unfortunately, the neutron log is subject to a number of errors which must be carefully considered before we attempt any interpretation. The neutron source emits about 10,000 times as many γ's as neutrons. Some of the quanta will pass into the formation and reach the detector after one or two Compton collisions. The actual number will be determined by the γ scattering and absorption properties of the rock, so that this parameter will be reflected in the neutron log.

† B. Pontecorvo, "Neutron Well Logging," *Oil and Gas Jour. 40,* No. 18, 32-3 (Sept. 11, 1941). R. E. Fearon, "Neutron Well Logging," *Nucleonics 4,* No. 6, 30-42 (June, 1949).

Neither can we ignore the natural radioactivity of the formation. Some hydrogenous rocks, notably shale, would appear as lows on the neutron curves, were it not for their high radioactivity. The γ detector does not differentiate between quanta from neutron absorption, from Compton collisions or from naturally radioactive nuclei. It records them all quite indiscriminately, and the reading from Compton quanta alone is frequently greater than the neutron effect.

The slowing down of neutrons in barite drilling mud is about as good as in pure water. Therefore the presence of mud in the immediate vicinity of the neutron source will seriously affect the measurement, and the probe should be large enough to displace most of the mud. It is important to consider carefully the probability of mud-filled caves behind the casing, lest we interpret them as porous zones filled with water or oil. Bore-hole calipering is an important adjunct. (See Chapter XI.)

LABORATORY TECHNIQUES

Direct α Counting†

The range of the natural α particles in average rock is only about 15 to 50 microns. It follows that in any measurement of α activity we deal primarily with the surface of the sample, and grain size becomes a critical parameter. The sample may be prepared as either a thin source or an "infinitely thick" source, depending on the type of measurement.

Very thin deposits of metallic uranium can be made by electrolytic deposition on a flat metal plate (usually nickel), but the preparation of thin layers from rock samples is considerably more difficult, for the maximum permissible particle size is on the order of only a few microns. One of the methods is to deposit the sources from a thin slurry made with a volatile organic solvent. Sources that are sufficiently thin to cause only slight absorption of the weakest α will give a lower counting rate than thick sources, but the conversion of the counting rate to actual specific α activity is easier for thin layers and does not necessitate accurate knowledge of the α stopping power μ in that particular material. We may define *counting efficiency* as the observed α counting rate divided by the actual rate of α disintegration within the sample. For a sample of zero thickness, the efficiency would be 50 per cent. Half the alphas would spend their energy in the gas of the chamber and be counted, while the others would imbed themselves in the sample tray and would not produce detectable ionization. As we increase the thickness of the sample, more and more of the α's are absorbed in the sample layer and the counting efficiency decreases, as shown in Figure 629. The decrease is almost rectilinear up to a sample thickness of about 5 mg/cm².

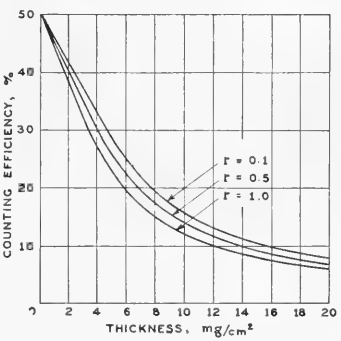

FIG. 629.—Alpha counting efficiency as a function of sample thickness for instruments of fair, good, and excellent sensitivity; r is the minimum detectable residual α range in air-cm. (After Keevil and Grasham, *loc. cit.*)

Thick sources have been used more widely in geological laboratories, for they do not present the problem of preparation, which is inherent to the thin source technique.

† R. D. Evans and C. Goodman, "Radioactivity of Rocks," *Bull. Geol. Soc. Am. 52,* 459-90 (1941).

N. B. Keevil and W. E. Grasham, "Theory of α-ray Counting from Solid Sources," *Canadian Jour. Res. 21A,* 21-36 (1943).

H. H. Nogami and P. M. Hurley, "The Absorption Factor in Counting Alpha Rays from Thick Mineral Sources," *Trans. Am. Geoph. Union 29,* 335-40 (1948).

Fine crushing is still essential, however, lest we emphasize the effect of any radioactive material which may merely coat the rock grains. "Infinitely thick" layers (about 1 mm or about 150 mg/cm²) are frequently used, for they are easily spread with a straight-edged tool. The counting rate from a thick layer is given† by

$$C = \mu\rho\,[89.4\ U + 26.6\ Th] \cdot 10^3 \text{ counts/sec/cm}^2$$

where $\mu\rho$ is the stopping power for alphas in the sample, U and Th are the contents of uranium and thorium in radioactive equilibrium with their daughter products in grams per gram, and r, the minimum detectable residual air range is assumed to be 0.5 air-cm for the α counter used. The value of $\mu\rho$ for any material follows approximately from the Bragg-Kleeman relation

$$\mu = \frac{R_o}{R} = 3.2 \cdot 10^{-4}\sqrt{W}$$

where R_o and R are the ranges of the α particle in the sample material and in air, and W is the mean atomic weight given by

$$\sqrt{W} = f_1\sqrt{W_1} + f_2\sqrt{W_2} + \ldots.$$

where the f's are weight proportions and the W's atomic weights of all the elements present in the sample.

Radon Method of Radium Detection.—The amount of radium in a rock can be determined indirectly but very accurately by the radon method, independent of any other radioactive elements that might be present. The rock is fused with sodium carbonate or any other inert flux. Fusion releases all gases from the rock (including radon). The gas passes into a large pulse chamber where the α activity is measured. The method is laborious but can be extremely sensitive.‡ A good radon chamber will detect the radon in equilibrium with as little as 10^{-13} g. of radium.

Beta Counting

The determination of relative content of radioactive material in rock samples by measurement of their β-activity has become a widespread technique in geology as well as in mineral exploration for uranium. The extensive use of the method can be largely ascribed to its relative simplicity and reliability. Beta-ray assaying with chemical control is frequently adopted when large numbers of samples are to be tested,§ and when speed is an important factor.

The usual procedure is to place a fixed volume of the finely crushed rock sample in the immediate vicinity of the sensitive region of a thin-wall or mica-window beta counter. The thickness of the sample is usually chosen to be somewhat greater than the maximum range of the most energetic β-ray emitted from the sample to be measured. In this way the recorded activity will consist almost exclusively of β's. The γ-radiation of the sample will have little effect due to the low efficiency (on the order of 1 per cent) of Geiger-Müller counters for γ-rays and the small amount of sample. Even though some mica-window counters are sufficiently delicate to admit and count the

† J. Beharrell, "Absorption of Alpha-Rays in Thick Sources," *Trans. Am. Geoph. Union 30,* 333-6 (1949).

‡ L. F. Curtiss and F. J. Davis, "A Counting Method for the Determination of Small Amounts of Radium and of Radon," *Jour. Res. Nat. Bur. Stds. 31,* 181-96 (1943), (Res. Paper *RP* 1557).

§ W. C. Peacock and W. M. Good, "An Automatic Sample Changer for Measuring Radioactive Samples," *Rev. Sci. Inst. 17,* 255-61 (1946).

more energetic α-rays, the self-absorption of α's in the sample is usually great enough to make their contribution also negligible.

For uranium, thorium, and potassium work, the choice of a proper counter is usually determined by the available amount of sample. One- or two-gram samples are best examined by mica-window counters, but larger samples can be tested with aluminum or glass thin-walled counters, which are generally much cheaper than the mica-window type. Normally only 2 - 3 g. of sample are required for a β assay. To improve the geometrical relation of counter and sample for work with low-grade materials, several thin-wall counters can be connected in parallel and placed over the sample tray, or the sample may be placed to coaxially surround the counter.† The latter method is awkward for routine operation, but has the most efficient geometry, and is generally preferred for rocks and minerals of very low β activity (the order of 0.001 per cent uranium or equivalent) when large counting intervals are used and clean-up time becomes relatively unimportant. Even under most favorable conditions, however, ultimate sensitivity of the β counter will be less than that of the more sensitive α detectors, largely because of the cosmic-ray‡ and contamination background to which all β counters are subject.

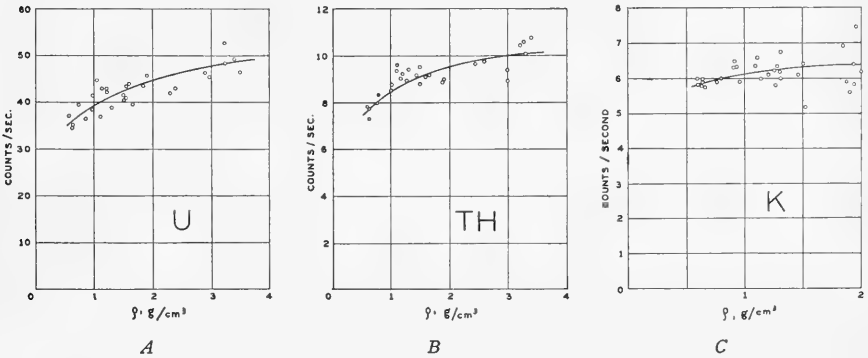

FIG. 630.—Beta counting rate plotted against apparent density of samples with constant radioactive content: *A*, 0.43 per cent U_3O_8; *B*, 0.4 per cent ThO_2; *C*, 12 per cent K_2O.

Because of the uncertainties in the energy distribution of β spectra, back-scattering, and absorption, theoretical calibration of beta counters can be only very rough. An empirical calibration is therefore essential. Beta counting of samples of known radioactive content and a statistical comparison of the beta activities of these "standard" samples to the activities of unknown samples, in general, constitute sufficient calibration, if all samples are essentially identical in their apparent density,§ and in the proportion of radioactive elements contributing to the total activity, which also implies constancy of the factors of radioactive equilibrium and emanating power. This condition may be met, to a greater or lesser extent, in various types of rocks, and the simple standard-sample calibration will give reasonably accurate results when judiciously applied.

For more accurate work with heterogeneous samples it is usually desirable to make a density correction.†† The effect of variable apparent density can be established very simply by diluting, in a given proportion, a known amount of radioactive material with

† A. M. Gaudin and J. H. Pannell, "Radioactive Determination of Potassium in Solids," *Anal. Chem. 20*, 1154-6 (1948).

‡ J. M. Jauch, "Cosmic Rays," *Nucleonics 4*, No. 4, 39-51, and No. 5, 44-58 (April, May, 1949).

§ *Apparent density* is here defined as the weight of the actual sample divided by its volume when placed under the counter.

†† H. Faul and G. R. Sullivan, "Density Correction in Beta-Ray Assaying of Rock and Mineral Samples," *Nucleonics 4*, No. 1, 53-6 (Jan., 1949).

radioactively inert minerals of various densities. We can then plot specific activity against apparent density of the various mixtures (Figure 630). Knowing the apparent densities of our unknown samples, we can now adjust their measured beta activities to any arbitrarily established "mean density" by using the curve.

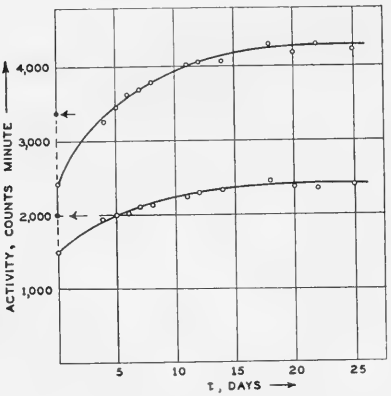

FIG. 631.—Increase in the β activity of carnotite samples after sintering. The original activity (before heating) is indicated by solid circles and arrows.

Samples containing minerals with high emanating power require additional treatment to bring back the radioactive equilibrium disturbed by loss of radon. It is necessary to render the sample impermeable in some way to stop the outward diffusion of the gas and then store the fixed sample for about two to four weeks to reestablish equilibrium. Probably the simplest way of "sealing" a sample is by sintering, i.e., heating to a temperature where the emanating mineral begins to fuse. Figure 631 shows the beta activity of two samples of carnotite that have been sintered at about 1000° C. for one hour. Heating drives off most of the radon, but the sintering lowers the emanating power to a very small value, and equilibrium reestablishes itself with time. It is interesting to note that apart from a slight discoloration, sintering produces no change visible to the naked eye in most powdered carnotite ore samples. Only rarely is it necessary to re-grind the sample after sintering. The overall loss of water which results from the sintering process must be considered in some samples, although the correction is usually very small.

Gamma Counting

Measurement of γ activity in the laboratory is a method no more difficult than β counting, but considerably less sensitive. If a large sample is available, it is usually placed coaxially around the counter, in a layer up to several inches thick. Special multiple anode G-M tubes or scintillation counters can be used on small samples. It is generally difficult to make good γ determinations on samples smaller than about 20 g.

The γ-rays from the uranium series and from potassium are fairly well known, so that theoretical calibration is possible if we know the γ counting efficiency of our detector. The empirical method of calibration is much simpler, however, in spite of the fact that the geometrical relation of the sample to the counter must be taken into account. The problem has been analyzed by Davis† and by Hushley and Dixon,‡ who present a comprehensive theoretical treatment.

Economic Applications

Probably the most important economic application of radioactivity in geophysics to date is the gamma-ray logging of wells drilled for petroleum.

† F. J. Davis, "An Improved Geiger Counter Arrangement for Determination of Radium Content," *Jour. Res. Nat. Bur. Stds. 38,* 513-518 (1947), (Res. Paper *RP* 1792).

‡ Hushley and Dixon, "The Gamma-Ray Measurement of Radium Ore Concentrates," *Can. Jour. Res. 25A,* 210-22 (1947).

The application of radioactivity measurements in the mining, exploration, and prospecting for uranium ores is obvious. The radioactivity of these ores is their principal distinguishing characteristic and serves in all phases of their handling, from first discovery, through exploration and drilling, mining, assaying, milling, and ultimate refining. The use of radioactivity methods in other fields is growing at an increasing rate.

REFERENCES FOR GENERAL READING

W. C. Elmore, "Electronics for the Nuclear Physicist," *Nucleonics 2:* No. 2, 4-17; No. 3, 16-36; No. 4, 43-55; No. 5, 50-58 (Feb.-May, 1948).

W. C. Elmore, "Electronics—Experimental Techniques," McGraw-Hill, New York (in press).

R. D. Evans, "Fundamentals of Radioactivity and its Instrumentation," *Advances in Biology and Medical Physics,* I, 151-221, Academic Press, Inc., New York, 1948.

R. D. Evans, "Fundamentals of Nuclear Physics," *Sci. and Eng. of Nuclear Power I,* Addison-Wesley, Cambridge (Mass.), 1947, Chapter I.

S. A. Korff, "Electron and Nuclear Counters," D. Van Nostrand, New York, 1946.

R. E. Lapp and H. L. Andrews, "Nuclear Radiation Physics," Prentice-Hall, New York, 1948.

Nuclear Instrument Handbook, Nucleonics 4, No. 5, 97-152 (May, 1949).

B. Rossi and H. H. Staub, "Ionization Counters and Chambers," McGraw-Hill, New York (in press).

H. D. Smyth, "Atomic Energy for Military Purposes," Princeton Univ. Press, 1945.

RADIOACTIVITY METHODS

UNITED STATES PATENTS

2,277,756 Issued March 31, 1942. D. G. C. Hare. "Method and Apparatus for Measuring Thickness."

2,304,910 Issued Dec. 15, 1942. D. G. C. Hare. "Determination of Specific Gravity of Fluids."

2,315,819 Issued April 6, 1943. C. H. Schlesman. "Method of Exploring Operating Structures."

2,316,239 Issued April 13, 1943. D. G. C. Hare. "Method and Apparatus for Determining Density of Fluids."

2,323,128 Issued June 29, 1943. D. G. C. Hare. "Method and Apparatus for Determining Liquid Level."

2,346,043 K. J. Mysels.

2,346,486 D. G. C. Hare.

2,348,810 D. G. C. Hare.

2,349,429 G. Herzog and J. H. Stein.

2,365,553 Issued Dec. 19, 1944. J. E. Hill. "Method of Analysis with Radioactive Material."

2,383,820 Issued Aug. 28, 1945. S. Rosenblum. "Apparatus and Method of Utilizing Ionizing Radiations."

2,394,703 Issued Feb. 12, 1946. E. Lipson. "Soil Analysis by Radiant Energy."

2,397,071-2,397,072 Issued March 19, 1946. D. G. C. Hare. "Radiation Detector."

2,397,073-2,397,075 Issued March 19, 1946. D. G. C. Hare and G. Herzog. "Radiation Detector."

2,397,661 Issued April 2, 1946. D. G. C. Hare. "Radiation Detector."

2,398,934 Issued April 23, 1946. D. G. C. Hare. "Radiation Detector."

2,401,723 Issued June 11, 1946. J. H. Deming. "Method and Apparatus for Locating Objects."

2,405,572 Issued Aug. 13, 1946. H. Friedman. "Radiographic Exposure Meter."

2,408,230 Issued Sept. 24, 1946. W. E. Shoupp. "Measuring Apparatus."

2,409,498 Issued Oct. 15, 1946. A. S. Keston. "Geiger-Müller Counter."

2,412,174 Issued Dec. 3, 1946. R. G. Rhoades. "Radiographic Inspection Method."

2,413,788 Issued Jan. 7, 1947. W. E. Sargeant and H. B. Hoeper. "Amplifier for Small Voltages."

2,425,533 Issued Aug. 12, 1947. G. Herzog. "Device for Measuring Wall Thickness."

2,437,935 Issued March 16, 1948. E. M. Brunner and E. S. Mardock. "Radiological Measurement of the Permeability of Porous Media."

CHAPTER XI

BORE-HOLE INVESTIGATIONS

During the past 15 years geophysical bore-hole logging has been universally accepted as one of the more important exploration tools.

It is now generally known that the measurement of certain physical properties provides a record of the formations traversed by the drill hole. This record is complete, detailed, and highly useful and may give additional information regarding the fluid and mineral content of the rocks.

It has become general practice, when a hole has been drilled, or at intervals during the drilling, to run a bore-hole survey. This recording is of immediate value for the geological correlation of the strata, and the detection and evaluation of possible productive zones or horizons. The information of the log may at the same time be supplemented by side-wall samples of the formations taken from the walls of the hole, or by cuttings taken from the circulating mud.

In common with surface exploration methods, drill or bore-hole explorations may be classified according to two principles. One basic classification is concerned with the application of an *artificial* field to the formations penetrated by the drill hole. This field may be: (a) electrical; (b) magnetic; (c) thermal; (d) seismic; or (e) neutron. The corresponding properties of the formations which may be investigated are: (a) resistivity, impedance, electrical anisotropy, and other electrical properties; (b) magnetic permeability and retentivity; (c) thermal conductivity and temperature; (d) velocity, attenuation, and absorption of seismic waves; and (e) radioactivity. The other basic classification is concerned with *natural* phenomena. These include: (a) electrochemical effects due to differences in the concentration of the fluids (electrolytes) in the hole and in the formations and electrofiltration effects due to flow of fluid through the pores of the formations; (b) magnetic anomalies associated with the formations penetrated by the bore hole; (c) variations of natural earth temperatures with depth and with the formations; (d) gravitational anomalies associated with the formations; and (e) radioactive effects (gamma ray).

The greatest commercial application and development in bore-hole investigations has been in the measurements of electrical resistivities, electrolytic and electrofiltration potentials, and the radioactive effects of neutron and gamma rays.

ELECTRICAL METHODS

In addition to the location of subsurface geological markers which are of value for correlation purposes, the proper combination of resistivity and potential measurements will oftentimes show the presence of oil sands, with particular reference to the boundary between oil and water-bearing formations. Although the electrical resistance of oil is very high, that of the formations which contain oil is not correspondingly high, due largely to the presence of connate waters in the formations. This factor, and its effect on electrical resistance, has been discussed in connection with Figure 264. However, the oil-bearing formations generally do have a measurably higher resistance than the water-bearing formations which are usually adjacent to them. Hence, a relatively high electrical resistance *may* be indicative of an oil-bearing formation.

In certain oil fields, the parameters supplied by resistivity and potential measurements are quantitative and depend on the amount of oil in the formation; hence, such measurements occasionally are useful for ascertaining the general productivity.† However, due to the fact that there is no direct relation between the quantities measured (resistivity and earth potentials) and the information desired (production in barrels per day), inferences concerning productivity are entirely empirical and are valid only for the particular field and sand for which the empirical relationships were established.*

In mining work, drill-hole measurements are often useful for determining the proximity of ore bodies and the extent of mineralization. In this application, electrical drill-hole exploration may be considered as a means of extending the diameter of the drill hole. The history of mining exploration is replete with cases where commercial ore bodies have been missed by very short distances by drill holes. A contributing factor to this condition is the crookedness or drifting of drill holes.

The electrical records are similar to the common core and sample records, and they are, for that reason, termed "electrical logs." These logs generally may be obtained without an appreciable increase in drilling time and at a small fraction of the cost of mechanical coring. Usually, a complete and continuous electrical log of a drill hole may be obtained at a cost equivalent to only a few feet of mechanical coring.

---

† M. Martin, G. H. Murray, and W. J. Gillingham, "Determination of the Potential Productivity of Oil Bearing Formations by Resistivity Measurements," *Geophysics*, July 1938, Vol. 3, No. 3, pp. 258-271.

*Production is often affected by conditions created during the drilling operations, for instance, the deposition of a mud sheath on the wall of the well opposite the oil- and gas-bearing formation. (Compare C. P. Bowie, "Hardening of Mud Sheaths in Contact with Oil, and a Suggested Method for Minimizing their Sealing Effect in Oil Wells," Bureau of Mines Report of Investigation No. 3354.)

Resistance Measurements

The Unit of Resistivity.—In electrical logging the practical unit of resistivity is the ohm-meter. The resistivity of a substance in ohm-meters is equal to the resistance in ohms of a cube of the substance if placed between two parallel conducting plates one meter square, and separated one meter. In present practice the same unit is also commonly designated ohm-meters squared per meter (ohm m^2/m). In the conventional method of plotting a resistivity log, an increase in resistivity causes an excursion to the right.

The Relation of Salinity and Temperature to Resistivity.—It will be seen later that most problems of resistivity logging involve comparisons between different resistivity measurements, such as, for instance, the resistivity of the drilling mud and the resistivity of a formation or of the interstitial water in the formation. Sometimes the resistivity of a formation water must be deduced from a knowledge of its salt content. In making such comparisons the following laws of electrolytic conduction should be borne in mind:

The conductivity of an electrolyte increases roughly in proportion to the amount of chemicals in solution. Formation waters and drilling muds usually contain several chemicals in solution, which differ in their ability to conduct electric current. It is convenient in electrical logging calculations to convert the amounts of the various electrolytes present into their equivalent weights of sodium chloride. The resulting equivalent concentration is expressed in parts per million or grains per gallon of sodium chloride.

The resistivity of an electrolyte decreases with temperature. It is frequently necessary to compare the resistivity of the drilling mud, which has been measured at surface temperatures, to that of a formation measured at a much higher temperature in a deep bore hole. Obviously the two values of resistivity cannot be compared without converting them to values which would have been observed at a common temperature. This conversion, for most drilling muds, may be made by assuming sodium chloride as the electrolyte, and calculating its change in resistivity versus temperature.†

Total Resistance Measurements.—The simplest method of measuring the electrical resistance of the formations traversed by a drill hole employs two electrodes. One electrode is lowered into the drill hole while the other electrode remains fixed at the surface of the ground or at some other convenient point.‡ Referring to Figure 632, electrode A is arranged

† Noyes and Coolidge, *Jour. Amer. Chem. Society*, 26, 134.
E. B. Millard, *Physical Chemistry for Colleges*, McGraw-Hill.

‡ C. Schlumberger, "Electrical Process and Apparatus for the Determination of the Nature of the Geological Formations Traversed by a Drill Hole," U. S. Patent 1,819,923, issued Aug. 18, 1931.

to traverse the drill hole and electrode B is fixed in position at the surface of the earth. This is termed a monoelectrode system.

The resistance may be measured by use of a conventional bridge circuit, or voltmeter and ammeter. Intermittent readings or continuous recording may be employed as desired. The bridge may be of the slide wire or switch type for intermittent readings, or of the recording type for continuous readings.

The total resistance will depend on the size of the electrodes, the resistance of the connecting cables, the effective resistance of the formations relatively near the electrodes, and the salinity of the water or mud in the drill hole.* The earth immediately adjacent to the electrodes contributes a major part of the total resistance of the current path. That is, aside from the material within a few feet of the electrode surfaces, the main mass of earth included between electrodes A and B has a relatively low, or negligible, resistance due to its large cross-sectional area. Hence, the total resistance R of the circuit may be expressed by the relationship

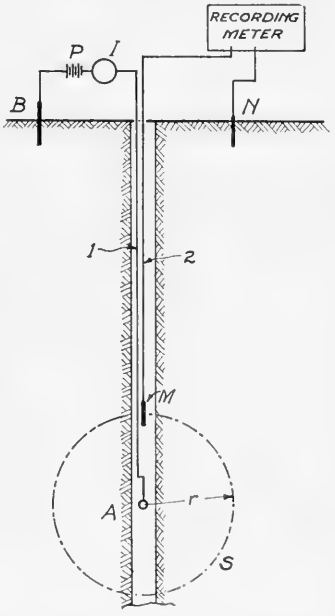

FIG. 632. — Schematic diagram of arrangement of measuring electrical resistance of formations traversed by a bore hole.

$$R = R_1 + R_2 + R_3 = (R_1 + R_2) + R_3 \qquad (1)$$

where R_1 = resistance of the cable. This resistance is measured directly and is a function of the cable length. It remains substantially constant.

R_2 = effective resistance of the electrode B. This resistance consists of the contact resistance between the electrode surface and the earth and the effective resistance of the earth material immediately adjacent to the electrode. It remains substantially constant.

R_3 = effective resistance of the electrode A. This resistance consists of the contact resistance between the electrode surface and the

* The resistivity of the mud varies over fairly wide limits. Where the drill hole penetrates strata containing materials which are readily dissolved or where saline solutions from the strata enter the bore hole, the resistivity may be as low as 0.1 ohm-cm. In drill holes where the mud is relatively free from such effects or where fresh water enters the drill hole, the resistivity may be many hundred ohm-cm. Average drilling mud which is encountered in the usual drilling well varies in value from about 1 ohm-cm. to 10 ohm-cm.

drilling mud filling the drill hole and the effective resistance of the earth material near the electrode. The contact resistance is relatively constant between electrode and drilling mud throughout the entire length of the drill hole, while the effective resistance of the earth materials near the moving electrode varies.

Since the resistances R_1 and R_2 remain relatively constant throughout the measurements, the measured total resistance R is equal to a constant resistance plus a varying resistance. The changes in the value of the resistance in the immediate vicinity of the moving electrode A may therefore be plotted as the moving electrode traverses the bore-hole.

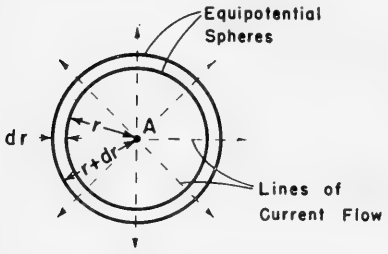

FIG. 633.—Equipotential surfaces around a point electrode.

The theoretical potential drop around a single electrode may be derived. Assume the electrode to have small dimensions so it can be treated as a point electrode, and that it is surrounded by a homogeneous and isotropic medium of infinite extent, with the bore hole of such small diameter that its effect can be neglected. Referring to Figure 633, in the vicinity of A the current will tend to flow radially outward equally in all directions, and the equipotential surfaces will be spheres centered on A.

The difference of potential dE between points located on an equipotential sphere of radius r and of potential E, and an equipotential sphere of radius $r + dr$ and of potential $E + dE$ is expressed by a form of Ohm's Law:

$$dE = I \cdot \frac{\rho dr}{4\pi r^2} \tag{2}$$

where ρ is the resistivity of the medium.

By integration, taking the absolute potential to be zero at great distances from A, the potential E at a distance r from source A is obtained:

$$E = \frac{\rho I}{4\pi r} \tag{3}$$

Equation 3 still applies to the space surrounding the electrode if r is the radial distance measured from the center of the electrode. This equation may be rewritten:

$$\frac{E}{I} = \frac{\rho}{4\pi r} \tag{4}$$

The ratio E/I, which is seen to be proportional to the resistivity ρ of the surrounding formation, may be interpreted as the resistance of a mono-electrode of radius r, and it is in fact the resistance which would be meas-

ured between electrode A and an electrode at a great distance, provided the latter electrode is of large enough dimensions that its own mono-electrode resistance is negligible.

A modification of the method employs an electrode system wherein two electrodes are lowered into the drill hole at a fixed distance apart. Variations in the total circuit resistance are due to changes in earth materials in the vicinities of both of the electrodes. For example, if the separation of the moving electrodes were such that at any depth the two electrodes were opposite two strata having different resistances, the total resistance measured would depend on both formations. Because these two variables cannot be separated where numerous anomalies occur within distances comparable to the electrode separation, it is necessary: (a) to use a small separation of the electrodes so they both will be affected by the same condition or (b) to make one of the electrodes sufficiently long (about 100 feet or more) so that it is not affected appreciably by the formations being passed.† If the electrodes are separated by too small a distance, the penetration into the strata will not be great enough to give resistance data which are sufficiently independent of variations in the size of the bore hole and the composition of the drilling mud. (The penetration is usually less than ⅓ the effective separation of the electrodes.)

In a later development of the two-electrode method,‡ an electrode system is lowered into the drill hole and measurements are made of the alternating current properties of the subsurface included between the two electrodes. The electrodes are maintained a fixed distance apart, and the entire assembly is moved in the drill hole. Measurements are preferably made with a moderate or high frequency alternating current.

Blau and Gemmer (§) utilize a similar electrode arrangement wherein an alternating current may be passed between two electrodes in the hole or between a single moving electrode and a stationary surface electrode. The variations in current which are caused by changes in the effective resistance of the strata are measured in a suitable auxiliary circuit. A modification of this method utilizes an electrical transient instead of an alternating current.††

McDermott‡‡ has utilized the single moving electrode arrangement in a bore-hole exploring method which does not require removal of the drill pipe from the bore hole before making the measurements. In this method, the drill and tubing are raised the desired distance off bottom, and an insulated conductor, on the end of which is a weighted electrode, is lowered through the inside of the drill pipe. The electrode passes out of the bit and

† J. J. Jakosky, "Electrical Method and Apparatus for Determining the Characteristics of Geologic Formations," U. S. Patent 2,140,798, issued Dec. 20, 1938.

‡ J. J. Jakosky, "Method and Apparatus for Alternating Current Investigation of Uncased Drill Holes," U. S. Patent 2,038,046, issued April 21, 1936.

§ Ludwig S. Blau and Ralph W. Gemmer, "Method and Apparatus for Logging a Well," U. S. Patent 2,037,306, issued April 14, 1936.

†† L. W. Blau and L. Statham, "Electrical Transient Well Logging," U. S. Patent 2,165,213, issued July 11, 1939.

‡‡ E. McDermott, "Method of Electrically Exploring Bore Holes," U. S. Patent 2,070,912, issued Feb. 16, 1937.

is employed for mapping the resistance changes in its vicinity. The method is essentially one of mapping short intervals of formation, after which the drilling operations are resumed. The chief intention of the invention is to avoid the necessity of removing the drill pipe and bit from the bore hole before making the survey.

Karcher† has developed a modification of the single moving electrode method which is designed for exploring bore holes continuously during the process of drilling. This method utilizes an arrangement which causes an electric current to flow through a conductor, the drill bit, and thence into the earth. Both the conductor and the drill bit are insulated from the drill pipe. From an operator's viewpoint, the method has the advantage of allowing continuous exploration of the bore hole during the drilling process and the disadvantage of necessitating a special type of insulating cable passing through the drill pipe. In addition, it is necessary that the bit be electrically insulated from the drill stem by an insulating stem or section which is mechanically capable of taking the entire drilling load. An alternate arrangement consists in insulating the entire drill stem, thereby leaving only the bit exposed for contact with the formations.

Another continuous logging method‡ has been developed wherein the measurements are made between the entire drill rod assembly, including the rotary equipment, and an electrode which is placed at a distance from the well comparable to the depth of the hole. In this system, the electrical properties of the earth included between the entire drill mechanism and the distant electrode are measured. A recording is made of the variations in electrical properties as the drill stem traverses the strata. Measurements may be made with direct or alternating current. The electrical logs show variations of an electrical property versus depth. Usually, simultaneous continuous recording is made: (a) of the fluctuating potentials associated with the cutting action of the bit and (b) of the change in electrical resistance or impedance between the drill stem and the distant electrode.

Several modifications of this method are used. In one modification the drilling is done with oil or other poorly conducting fluid, such as is utilized in many areas to avoid sealing of the producing formations and other damaging effects of drilling muds.§ Contact of the drill stem with the wall of the hole is prevented by use of the rubber protectors commonly employed during drilling operations. A second modification employs direct current for energizing the ground. The back E.M.F. due to polarization around the drill pipe provides a sufficient potential drop to cause a detectable portion of the current to travel down the drill stem and flow into the earth at a point

† John C. Karcher, "Method and Apparatus for Exploring Bore Holes," U. S. Patent 1,927,664, issued Sept. 19, 1933.

‡ J. J. Jakosky, "Method and Apparatus for Continuous Investigation of Drill Holes," U. S. Patent 2,150,169, issued March 14, 1939. Reissue 21,102, May 30, 1939.

J. J. Jakosky, "Method and Apparatus for Continuous Exploration of Bore-holes," U. S. Patent 2,153,802, issued Apr. 11, 1939.

J. J. Jakosky, "Method and Apparatus for Continuous Exploration of Bore-holes," U. S. Patent 2,181,601, issued Nov. 28, 1939.

§ J. J. Jakosky, "Method and Apparatus for Continuous Exploration of Bore Holes," U. S. Patent 2,153,802, issued April 11, 1939, and Foreign Patents.

where polarization is not effective. This point is the cutting end of the bit, where new rock is continually being exposed by the bit. The resistance variations in the circuit, therefore, are predominately those encountered by the bit.

Numerous high frequency and radio methods† have been proposed, but such methods have not come into commercial operation for deep bore hole work due chiefly to the enormous and unpredictable changes in capacity and leakage which occur when long lengths of cable are lowered into the hole. As a matter of fact, up to the present, the commercially successful methods utilize direct current or alternating current having a frequency of less than 750 cycles per second.

The *total resistance methods* are relatively simple in their practical application but suffer from one defect: Variations in the earth or mud filling the drill hole in the immediate vicinity of the moving electrode, or electrodes, will sometimes exercise an undue effect on the readings, due to the fact that the total resistance between the electrodes is confined almost entirely to the immediate vicinity of the electrodes. (Compare Fig. 283.) The drilling mud itself is relatively uniform due to the circulation during the drilling process. On the other hand, because the mud is weighted to produce a hydrostatic head in excess of the probable formation pressures, it permeates and impregnates the porous formations.* Obviously, this invasion of the mud may influence the effective resistance of the permeable formations markedly.

The variations produced by changes in the effective diameter of the bore hole constitute another disadvantage of the single electrode method wherein the electrode is not in direct contact with the formation itself. This variation is particularly pronounced when drilling with excessive mud circulation through the relatively soft formations (shales, unconsolidated sediments, etc.) frequently encountered in the Gulf Coast and California areas. When single electrode logs are run, they should be supplemented with caliper logs to show the changes in effective area of the bore hole.

There are certain advantages, however, which tend to offset the disadvantages. When the moving electrode is of small size (a few inches in length), the single moving electrode system will give much greater detail and will show the very thin formations better than the multiple moving electrode systems. In addition, the single moving electrode system utilizing a small moving electrode (or the multiple moving electrode system having a short separation between the current and the potential electrode) gives sharper structural breaks corresponding to the tops and bottoms of the resistivity variations than the measuring systems having a greater penetration. This greater detail is, of course, superposed on the non-structural variations previously mentioned.

† T. Zuschlag, "Methods of Investigating the Nature of Subterranean Strata," U. S. Patent 1,652,227, issued Dec. 13, 1927.
H. Lowy, "Methods for Ascertaining the Nature of Subterranean Strata," U. S. Patent 1,092,065, issued March 31, 1914.

* The distance of permeation is primarily a function of the differential pressure, time of contact, viscosity and sealing properties of the mud, and the permeability of the formation.

It is advantageous to have both the shallow and the relatively deep penetration curves and it is common commercial practice to furnish a logging record which shows both curves. Interpretation is based on these two resistance curves and the potential curve.

Measurements may also be made between electrodes in two uncased wells.† Broadly, this method contemplates disposing at least one electrode in each of two wells and then adjusting the levels of these electrodes until the resistance between them reaches a maximum or a minimum.

Another arrangement utilizes resistance measurements along the bedding planes of the strata.‡ This method measures the resistance between an electrode in the bore hole and another electrode spaced a considerable distance from the hole. Another modification utilizes a distant electrode and two electrodes in the hole to determine the anisotropic properties of the strata by measuring vertically and along the bedding planes, and comparing the two sets of measurements.§

Electrical logging of cased holes has been proposed by Ennis†† and Neufeld.‡‡ In this method a current is applied between casing and ground, and the record is made from a movable electrode centered in the casing.

The Normal Sonde.§§ — In order to remove almost entirely the effects of the potential drop adjacent to the moving power electrode, resistivity measurements are made over a short section of the total current path which is sufficiently distant from the moving power electrode to be unaffected by minor variations in its vicinity.

In Figure 632 is pictured a two-electrode normal sonde,* which consists of a current electrode A and a measuring electrode M, separated by a short distance r, called the spacing. Current is passed between A and an electrode B located at a distance from A; the potential difference created by the flow of current is measured between M and an electrode N, which is remote from both current electrodes and which is relatively at zero potential.** It follows that the potential difference measured is equal to the potential E

† P. F. Hawley, "Two-well Method of Electrical Logging and Apparatus Therefor," U. S. Patent 2,183,565, issued Dec. 19, 1939.

‡ J. J. Jakosky, "Electrical Method and Apparatus for Determining Characteristics of Geological Formations," U. S. Patent 2,155,133, issued April 18, 1938.

§ J. J. Jakosky, "Electrical Method and Apparatus for Determining Character of Geologic Formations," U. S. Patent 2,140,798, issued Dec. 20, 1938.

†† G. H. Ennis, "Method and Apparatus for Locating Formations in Cased Wells," U. S. Patent 2,414,194, Jan. 14, 1947.

‡‡ J. Neufeld, "Method of and Apparatus for Investigation of Cased Drill Holes," U. S. Patent 2,400,593, May 21, 1946.

§§ C. Schlumberger, "Electrical Process and Apparatus for Determination of the Nature of the Geological Formations Traversed by a Drill Hole," U. S. Patent 1,819,923, issued Aug. 18, 1931.
C. and M. Schlumberger and E. G. Leonardon, "Electrical Coring: A Method of Determining Bottom-hole Data by Electrical Measurements," *A.I.M.E. Geophysical Prospecting*, 1934, p. 237.

* In well logging practice the apparatus which is lowered into a drill hole at the end of a cable, for the purpose of taking measurements of formation characteristics, is often called an exploring device or *sonde*.

** C. Schlumberger, "Electrical Device for the Determination of Specific Resistivity," U. S. Patent 1,894,328, Jan. 17, 1933.

of electrode M. Since E is given by Equation 3 it is possible to write (still neglecting the effect of the drill hole):

$$R = 4\pi AM \cdot \frac{E}{I}$$

Since the factor $4\pi AM$ is a constant for a given electrode arrangement, it is called the coefficient of a normal sonde of spacing AM. Thus for a constant value of I there is for a given spacing a proportionality between the resistivity of the surrounding medium and the voltage measured.*

Multi-Electrode Sonde. — It may be convenient for practical reasons to have in the hole not only electrodes A and M but also electrode B or electrode N. In Figure 634 is shown the electrode arrangement actually used with certain electrical logging equipments for recording normal curves.

The Lateral Sonde.—In the lateral device (Figure 635a), the potential difference between two electrodes M and N due to the flow of current from A is measured. Since the distance separating M and N is small in comparison with the distance between A and the midpoint O of MN, the quantity measured is little different from the electrical field strength, or potential gradient, at point O. For this reason the lateral is often called a *gradient sonde*, whereas the normal is called a *potential sonde*. The distance AO is called the *spacing* of the sonde.

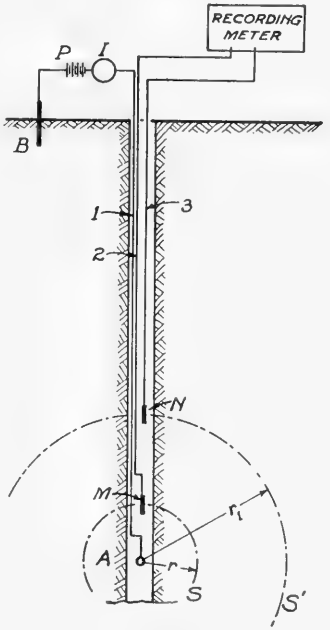

FIG. 634. — Schematic diagram of three-electrode arrangement for measuring electrical resistivities of formations traversed by a bore hole.

Recalling Equation 3 the potentials at the measuring electrodes are:

$$E\ (\text{at } N) = \frac{\rho I}{4\pi} \cdot \frac{1}{AN} \qquad E\ (\text{at } M) = \frac{\rho I}{4\pi} \cdot \frac{1}{AM}$$

and the potential difference between M and N is:

$$\Delta E = E\ (\text{at } M) - E\ (\text{at } N) = \frac{\rho I}{4\pi}\left(\frac{1}{AM} - \frac{1}{AN}\right)$$

or

$$\rho = 4\pi \cdot \frac{AM \cdot AN}{MN} \cdot \frac{\Delta E}{I} \qquad (5)$$

* It is interesting to note that, from the similarity of Equations 3 and 4, a normal sonde may be compared to a monoelectrode of radius AM. The spacing of the normal sonde is not limited by the size of the hole, however, as is the case for the radius of a monoelectrode.

The factor of proportionality $4\pi \cdot \frac{AM \cdot AN}{MN}$, which is a constant for a given electrode arrangement, is called the *coefficient* of the lateral sonde.

In Figure 635b is shown an equivalent electrode arrangement actually used in certain electrical logging equipment for recording lateral curves. In this arrangement, the positions of the current electrodes and measuring electrodes have been interchanged, resulting in what is termed the "reciprocal arrangement".*

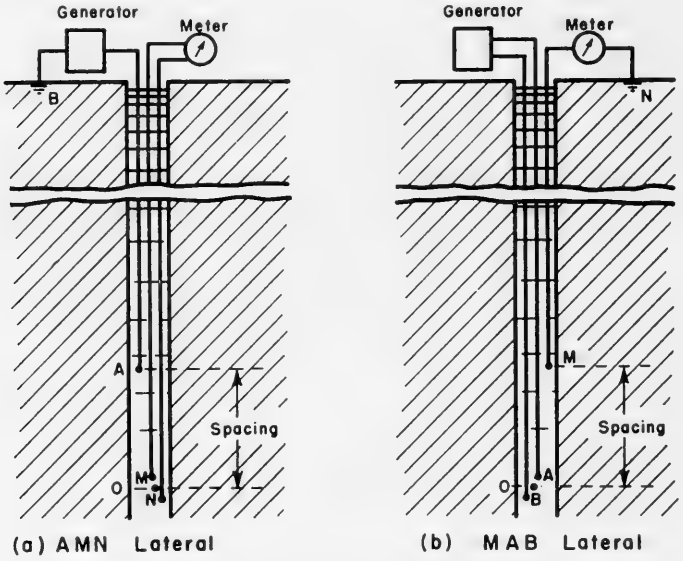

FIG. 635.—Lateral sonde (equivalent circuits).

Slichter † has proposed a method in which four electrodes are lowered into the drill hole. The electrodes are spaced a fixed distance apart, and the entire electrode system is moved as a unit along the length of the drill hole. Means are provided for employing expanding prongs or contacts whereby electrical contact may be made with the wall of the drill hole, in the event the drill hole is not filled with water. (The electrodes may consist of many fine spring wires that extend radially outward and form a circular "brush" which sweeps along the wall of the drill hole.) The method is applicable, therefore, to dry drill holes frequently encountered in mining

* This is in accordance with the "principle of reciprocity," the general validity of which has been demonstrated mathematically and experimentally and which may be stated:

Considering four electrodes, 1, 2, 3, 4, arranged in any way, the difference of potential measured between 1 and 2 due to a passage of current between 3 and 4 is equal to the difference of potential that would be measured between 3 and 4 due to the passage of the same current between 1 and 2.

† Louis B. Slichter, "Apparatus for Exploring for Ore," U. S. Patent 1,826,961, issued Oct. 13, 1931.

operations above the water table and to drill holes filled with non-conducting fluids, such as oil, etc.

The expression for the resistivity may be calculated from the fundamental relations expressing the flow of current in an infinite medium. The derivation for an arrangement in which the four electrodes lie in a line and are equidistantly spaced is as follows:

Assume that the electrodes A, M, N and B are located in a straight line and at distances of 0, a, $2a$, and $3a$, respectively, from A. Let I denote the measured current passing out of the electrode A and into the electrode B. The potential at M due to the source A and the sink B, is *

$$E_M = \frac{I\rho}{4\pi}\left(\frac{1}{a} - \frac{1}{2a}\right)$$

and the potential at N due to A and B is

$$E_N = \frac{I\rho}{4\pi}\left(\frac{1}{2a} - \frac{1}{a}\right)$$

Hence,

$$E_N - E_M = \Delta E = \frac{I\rho}{4\pi a}$$

or

$$\rho = \frac{4\pi a\,\Delta E}{I} \qquad (6)$$

It is evident from Equation 6 that the resistivity ρ may be determined from the observed values of the potential drop ΔE, the current I, and the electrode spacing a.

Huber † has described a method for obtaining two resistivity curves simultaneously. One curve shows the variations in the resistivities of the strata in the immediate vicinity of the moving current source, and the other curve shows the variations in the resistivities of the strata at an appreciable distance from the moving electrode. Thus, this method yields a direct comparison of the variations in electrical resistivity close to the bore hole where the formation may be permeated with the fluid of the bore hole, and the variations in electrical resistivity at a distance from the bore hole, the distance in question being greater than the distance of penetration of the bore-hole fluid.

Apparent Resistivity

Up to this point a homogeneous medium has been assumed, and the basic exploring devices have been described on this basis. It is obvious,

* The expression for E_M is a modified form of Equation 5, p. 473.

† F. W. Huber, "Methods of and Apparatus for Electrically Exploring Earth Formations," U. S. Patent 2,072,950, issued March 9, 1937.

however, that in an actual drill hole homogeneity is departed from in several ways. Factors which affect the distortion of the equipotential surfaces include: (1) the existence of the hole itself filled with drilling mud, and (2) the inevitable non-homogeneities in the formations, as well as (3) the existence in permeable formations, of a zone next to the hole which has been invaded by the mud filtrate.

In a heteregeneous medium, then, the exploring device measures a quantity which will be called "apparent resistivity" ρ_a and which is defined for a normal sonde:

$$\rho_a = 4\pi AM \cdot \frac{E}{I}$$

and for a lateral sonde:

$$\rho_a = 4\pi \frac{AM \cdot AN}{MN} \cdot \frac{\Delta E}{I}$$

where, as before, I is the current between electrodes A and B, E is the potential of electrode M in the case of the normal sonde, and ΔE is the difference of potential between electrodes M and N in the case of the lateral sonde.

From these definitions, if the medium surrounding the device is homogeneous and of infinite extent, the value of the apparent resistivity will be equal to the resistivity of the homogeneous medium.

The apparent resistivity is an average value involving the resistivities of all the different media surrounding the electrodes and depending on the arrangement and spacing of the device. When sufficient information is available regarding the conditions of the measurement, it is often possible to use the measured values of apparent resistivity to arrive at the true formation resistivity by means of resistivity departure curves, which will be described later.

Radius of Investigation.—The extent to which the various media surrounding the electrodes affect the value of apparent resistivity is dependent on the spacing of the electrodes, and is termed the "radius of investigation." When a very short electrode spacing is used, the mud in the hole may have a dominant effect on the value of resistivity obtained. As the spacing is increased, the effect of the formations surrounding the mud column becomes more important. For large spacings, the resistivity of the surrounding formations becomes dominant.

It is commonly assumed for simplicity, based on considerations of the potential drops in the vicinity of the M electrode, that in near-homogeneous media the radius of investigation of a normal device is equal to its AM spacing. The radius of investigation of a lateral device is taken under the same conditions as equal to its AO spacing. More precise ideas regarding the radius of investigation of a device under various conditions may be arrived at by the study of the resistivity departure curves.

For the determination of true formation resistivities, it is useful to record curves having large radii of investigation. This is particularly true in the case of permeable formations which have been deeply invaded by the mud filtrate and which therefore have, encircling the hole, a zone whose resistivity still differs from the true resistivity of the formations.

Electrode Combinations for Well Logging.—The relative positions of the electrodes in the sonde or exploring device lowered into the hole govern the type of curve obtained. Depending on the distribution of electrodes, a device may, for instance, be good for marking the thin breaks, but may not give a good representation of the thick layers. Another device which permits the determination of fluid content may not be suitable for locating formation boundaries. For this reason, it has been found best to employ several different electrode arrangements simultaneously in order that the several resistivity curves recorded may give a more complete picture of all the formations encountered in the bore hole, however different their characteristics may be. The actual electrode arrangements to be used in any area are dependent on the characteristics of the formations, peculiarities of the drilling mud, etc.

For the soft and usually less resistant formations, a sonde is employed which permits the simultaneous or alternate recording of normal curves and lateral curves of different spacings, using the same set of electrodes. The usual combination is a short normal of AM spacing between 10″ and 20″, a long normal of AM spacing between 20″ and 7′, and a lateral of AO spacing from 15′ to 30′.

One electrode arrangement used in modern electrical logging permits, with the use of six electrodes in the hole, the simultaneous recording of an S.P. curve, a 16″ short normal, a 64″ long normal, and an 18′8″ lateral curve.

Some Properties of Normal and Lateral Devices

The Normal Sonde.—Figure 636 indicates the shape of curves recorded with normal devices for the case of homogeneous resistive layers sandwiched between beds of low resistivity. The point of measurement of the readings is midway between A and M on the sonde.

It can be seen that the curves are symmetrical with respect to the center planes of the layers. This is a general feature of the normal device. As a matter of fact the same curves are recorded if M is above A, instead of A above M as indicated in the figure.

The upper part of the figure illustrates the case of a bed thicker than the spacing (bed thickness $e = 5d$, spacing $AM = 3d$, d = hole diameter). It is observed that the boundaries of the bed are not sharply indicated on the resistivity log, but tend to be rounded off owing to the influence of the drill hole. Moreover the thickness of the bed, as indicated by the distance between the two points of inflection, P and P', on the curve, is less than its actual thickness by an amount equal to the spacing. The error in picking the boundaries of thick resistive beds is small for normal curves of short spacings, and this is one reason for the recording in practice of a short normal. It should be remembered, however, that normal curves tend to show resistive beds thinner than they actually are by an amount equal to the spacing. In a similar manner they tend to show conductive beds thicker than they actually are by an amount equal to the spacing.

The lower part of the figure shows the case of a resistive layer thinner than the spacing. This case is characterized by a depression opposite the layer and two symmetrical small peaks, *c* and *d*, on each side of the depression. This feature illustrates the main disadvantage of the normal device; beds thinner than the spacing, no matter how resistive they may be, appear on the logs as being conductive.

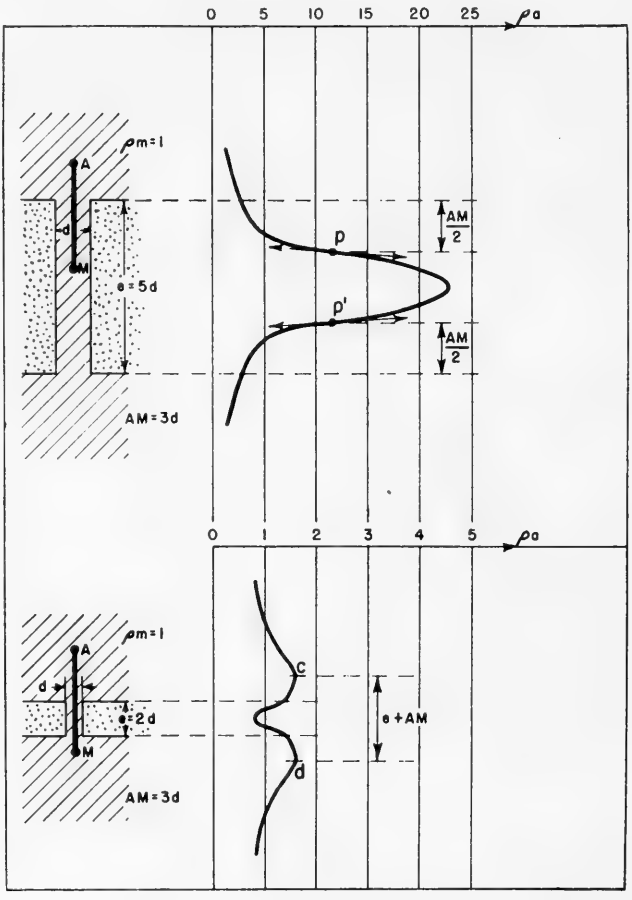

FIG. 636.—Resistivity curves for normal sonde.

The Lateral Sonde.—In Figure 637 are shown the corresponding curves for lateral devices. The point of measurement of the readings is *O*, midway between electrodes *M* and *N*.

In contrast to curves recorded with normal sondes, the lateral curves are markedly dissymmetrical with respect to the center planes of the layers, and their features are considerably more complex. As before, the transitions in the curves corresponding to formation boundaries have been rounded off by the effect of the drill hole.

As the sonde is lowered through the thicker layer indicated at the top of Figure 637, the sequence of events may be described as follows. When electrode *N* enters the

layer, a slight depression is recorded on the curve. The apparent resistivity then increases gradually until upper electrode A has entered the layer, at which time the slope of the curve becomes sharper. A maximum is reached just above the lower boundary of the bed. Below this maximum the decrease of apparent resistivity is rapid, and a value slightly greater than the resistivity of the adjacent formations is attained

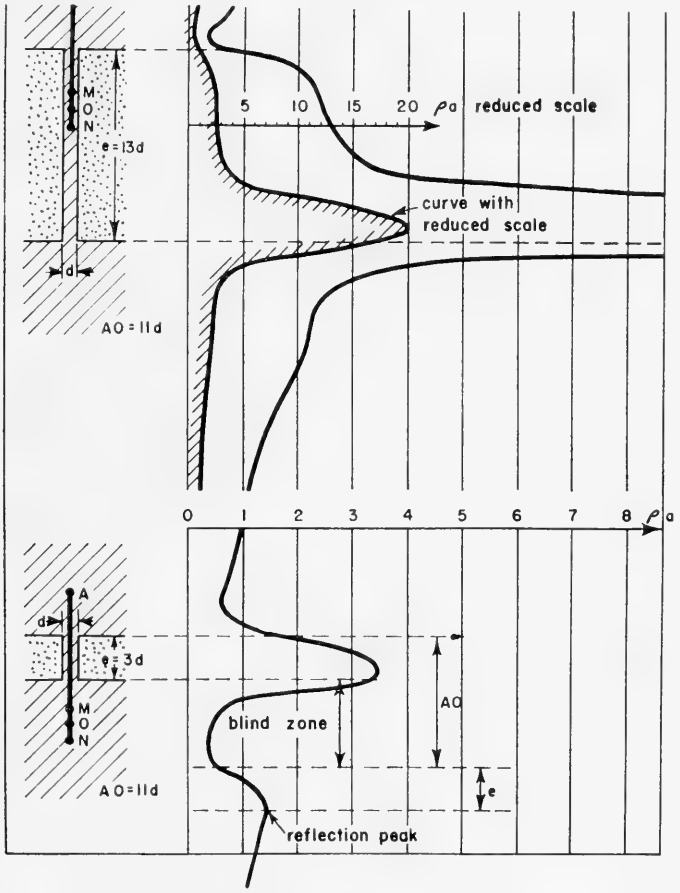

Fig. 637.—Resistivity curves for lateral sonde.

at a distance below the bottom boundary equal to the spacing. This corresponds to the moment when the upper electrode of the device passes the bottom of the layer.

It is observed, for the case of a bed thicker than the spacing, that the upper boundary of the bed is not well defined on the lateral curve and, as a whole, the bed appears as being displaced downwards. The amplitude of the shift is approximately equal to the spacing.

The lower part of Figure 637 corresponds to the case of a resistive layer thinner than the spacing. The bed is indicated by a sharp peak of comparatively low apparent resistivity. A slight depression is observed above the layer, but a more striking feature

is the presence of a zone of low resistivity below the layer, followed by a second smaller peak located at a distance below the bottom boundary of the layer equal to the spacing. This secondary peak is called a *reflection peak,* and the zone of very low apparent resistivity is called the *blind zone.* The blind zone corresponds to the interval during which the resistive streak is located between the current electrode and the measuring electrodes.

The lateral is useful for the location of thin, highly resistive streaks, although the interpretation may be difficult if several resistive streaks are close together; a lower streak located in the blind zone of an upper resistive streak may be missed, and reflection peaks may be mistaken for actual resistive streaks in the formation.

For the case of a resistive layer whose thickness is approximately the same as the spacing (critical thickness), the curve is almost completely flattened.

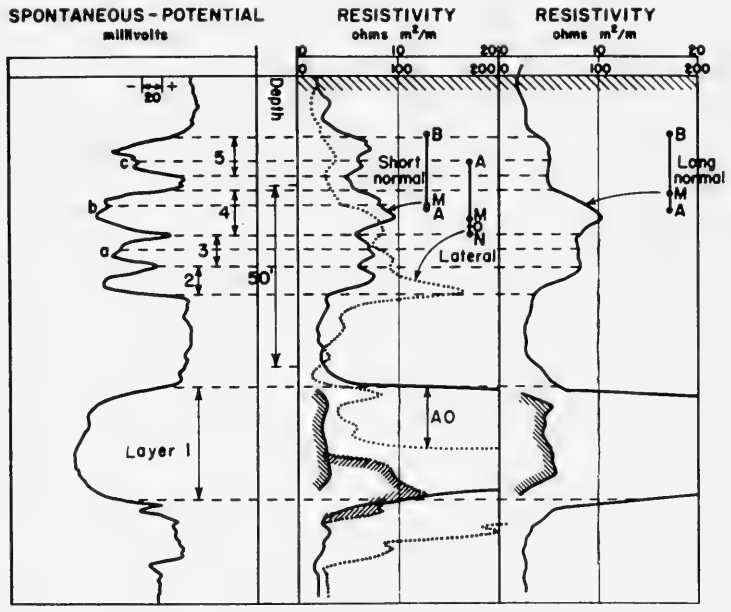

Fig. 638.—S.P., normal and lateral curves in low resistivity formations.

Similar generalizations are possible for lateral curves recorded for beds more conductive than the surrounding formations. Whether the layer is thick or thin the shape of the curve is dissymmetrical and the anomalies are spread downward, outside of the bottom boundaries. The apparent increase of thickness is roughly equal to *AO*.

Examples of Resistivity Curves.—Figures 638 and 639 offer further illustrations of the characteristics of normal and lateral curves, in the case of beds of moderate or low resistivity, which can be considered as *soft formations.* The solid curve in the middle track is a short normal of 16″ spacing. The dotted curve is a lateral of 18′ 8″ spacing. The curve in the right-hand track is a long normal of 64″ spacing. The S.P. curve is reproduced in the left-hand track. In Figure 638 the shaded curves represent recordings of the curves on reduced sensitivity (200 ohm-meters full scale) when the recording of the regular sensitivity (20 ohm-meters full scale) goes off-scale. The depth scales and sensitivity scales are not the same on the two figures.

Layer 1 of Figure 638 is a good example of the behavior of the various curves in

a thick, resistive formation. Both normal sondes give fairly symmetrical curves. The lateral curve corresponding to layer 1 is low in the top part of the bed for an interval corresponding to the spacing. The curve then sharply increases and tends to level off at a high value of apparent resistivity. The maximum is reached at a very short distance above the lower boundary of the layer, and the curve approximately regains the shale line at a distance below the base of the layer equal to the spacing.

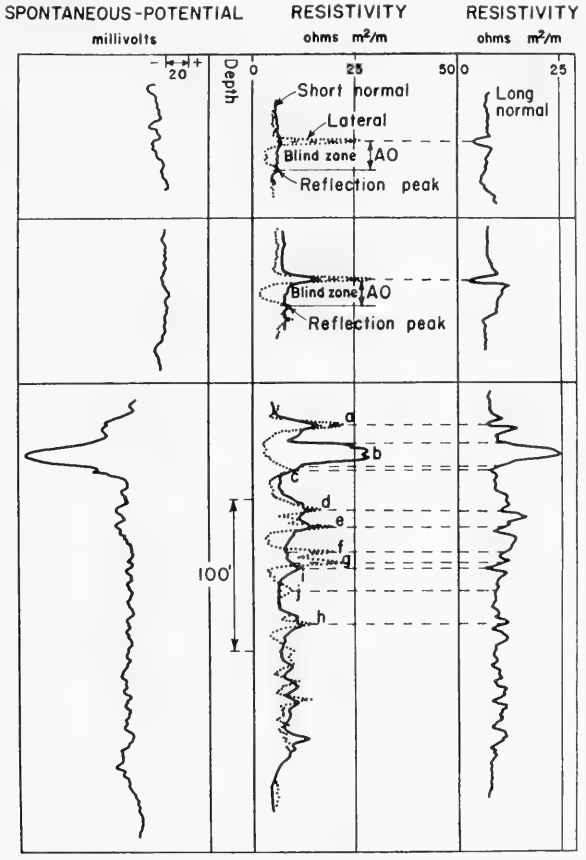

FIG. 639.—S.P., normal and lateral curves for thin resistive beds.

In the upper part of Figure 638 the S.P. log shows four main negative deflections (2, 3, 4 and 5), corresponding to four permeable layers, with some minor depressions (*a*, *b* and *c*) in the crest of the deflections indicating thin shale streaks inside these permeable layers.

The average thickness of each permeable bed is greater than the short normal spacing, and this curve makes a fair distinction between the layers, although the thin streaks *a*, *b* and *c* are poorly marked. For the long normal, however, the thickness of the permeable layers is of the same order of magnitude as the spacing of the sonde. The resulting curve is rounded and no distinction between individual beds is possible (except for layer 4 which is thicker than the others).

As for the lateral, the thickness of each bed and the distances between beds are so small in comparison with the spacing that the curve recorded approximates that which would be read opposite a single homogeneous layer with a thickness equal to the total thickness of the group and a resistivity equal to an average of the resistivities of the different beds.

Figure 639 is related to thin resistive beds located in conductive formations. In the upper part a single thin resistive bed is shown, which is indicated on the lateral by a characteristic peak and blind zone, on the long normal by a marked depression, and on the short normal by a very slight depression. The thickness of the layer is evidently slightly less than the short normal spacing.

The resistive layer of the middle part of Figure 639 is slightly thicker, as indicated by the fact that the short normal shows a peak. It is still thinner than the long normal, however.

The lower part of Figure 639 shows how the presence of a sequence of thin resistive streaks at short distances from one another may complicate the interpretation. The depression of the lateral opposite permeable layer *b* may be because it falls inside the blind zone of resistive streak *a*, or it might also be because the thickness of bed *b* is approximately equal to the lateral spacing. Lower, both normal curves show a series of depressions and kicks which could not be easily interpreted without the help of the lateral curve. The lateral shows definite peaks such as *c, e, f, g, h.* Peak *j* is obviously a reflection peak corresponding to resistive streak *g*, since they are separated by a distance *AO*. Peak *i* which is shown on the short normal, and which corresponds to a depression on the long normal, does not appear on the lateral since it is inside the blind zone of resistive streak *g*.

The Logging of Hard Formations

Features of Normal and Lateral Curves in the Logging of Hard Formations.—Figure 640 signifies, by means of a qualitatively established example, some typical indications given by normal and lateral devices opposite a thick, highly-resistive formation, such as limestone, containing porous or more conductive zones.

To understand the behavior of these curves it should be remembered that opposite a highly-resistive formation the current from electrode *A* is almost entirely confined to the bore hole; part of it flows up the hole and part down the hole, *dividing in inverse proportion to the resistance of the two paths.* The resistance of each path is determined mostly by the resistance of the mud column in the hole between the current electrode and the nearest conductive bed in that direction; once the current reaches the conductive bed it has there, depending on the thickness and the conductivity of the bed, a relatively low resistance path away from the hole.

This circumstance can be used to explain why the lateral device, which has electrodes *M* and *N* below the current electrode, records a curve which is lopsided in a downward direction. The deeper the device is into the resistive bed the greater is the proportion of the current flowing downward in the hole from electrode *A*, and therefore the greater is the potential drop in the mud measured between electrodes *M* and *N*. The apparent resistivity corresponding to this potential drop will thus be largely dependent on the size of the hole, the resistivity of the mud, and the position of the device with respect to the boundaries of the highly resistive zones.

The unsymmetrical appearance of the normal curve is explained in a similar manner for the three-electrode arrangement illustrated, in which electrodes *M* and *N* are above the current electrode. As soon as all three electrodes are inside the hard formation, the upper electrode is no longer near zero potential, as is basically assumed for the normal, and the arrangement actually measures the potential drop due to the current flowing in the mud between *M* and *N*.

It is thus seen that three-electrode devices give unsymmetrical curves in hard formations, and the direction of the lopsidedness depends on whether the measuring

electrodes are above or below the current electrodes. Along with this dissymmetry it is observed from the figure that for the lateral the positions of the minima are shifted quite noticeably downward with respect to the exact depths of the conductive layers, and for the normal a slight upward shift of the minima is also discernible. This often results in the maximum of one curve matching in depth the minimum of the other curve, a feature which can make logs recorded in actual practice seem very confusing to those not acquainted with the behavior of the devices used.

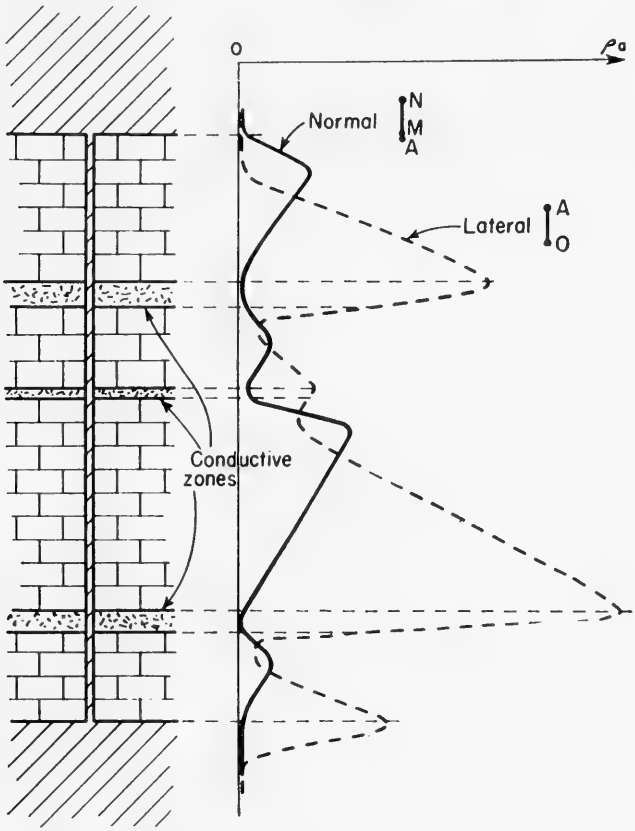

FIG. 640.—Normal and lateral curves opposite thick, highly resistive formations.

It may be further observed that the depressions read on the normal curve opposite the conductive layers are very smooth and considerably broader than the thickness of the beds, and the boundaries of the limestone formations are poorly marked so that accurate determinations are practically impossible.

If a two-electrode normal is used, or if a normal device is employed in which the upper electrode is far enough from the other two so that it is always located outside of the highly resistive bed, the curve will tend to be symmetrical, but the formation

boundaries will still be rounded and indefinite, and the apparent resistivity measured will be dependent on the distance of the device from the formation boundaries.*

The Limestone Sonde.—For the purpose of obtaining clearer and simpler logs in hard formations, the *limestone* or *hard formation* sonde was devised according to the scheme indicated in Figure 641. Four current electrodes, A and A', B and B', connected as shown in the figure by means of insulated wires of negligible resistance, are arranged so the $AB = A'B'$, and a measuring electrode M is placed in the middle of the device. The system being symmetrical, depths are measured from the middle electrode M.

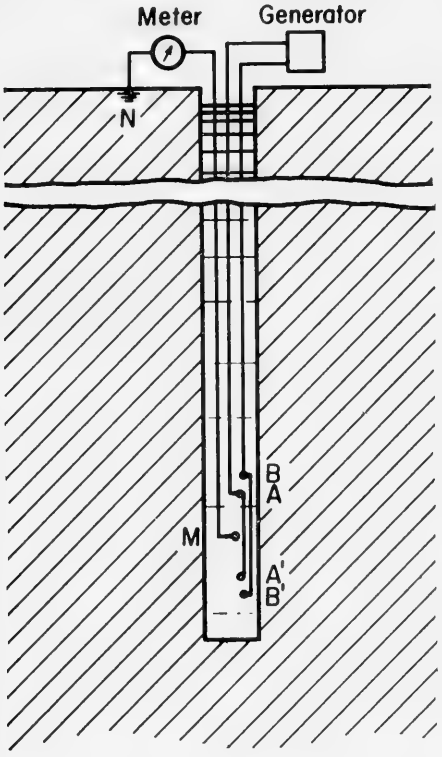

FIG. 641.—Electrode arrangement for logging the more resistive or hard formations.

The arrangement behaves as a symmetrical combination of two three-electrode sondes, which can be either two normal or two lateral sondes, depending on the relative lengths of AA' and BB'. In practice an arrangement is used in which $AM = A'M = 30''$ and $AB = A'B' = 4''$ and which therefore corresponds to a lateral combination.

If, as in the upper part of Figure 642, this device is located opposite a thick, highly-resistive layer, the flow of current is confined entirely to the space in the hole between electrodes A and B and between electrodes A' and B'. In this case no current flows from B or B', up or down the hole away from the device. It follows from Ohm's law that B and B' are at the same potential as any point at a great distance from the device, which is zero potential. Similarly, M is at the same potential as A and A', since no current flows in the space between A and A'.

The potential of electrode M is therefore equal to the potential difference between electrodes A and B (or A' and B'), and this is in turn equal to the potential drop in the mud due to the flow of current between A and B (or A' and B'). As long as all the electrodes of the device are opposite the hard, more resistant formation, this potential difference is dependent only on the hole size and the mud resistivity: if these are constant along the hard formation, a constant apparent resistivity is recorded.

If, on the other hand, as indicated in the lower part of the figure, the device is located just above a conductive streak, the presence of the streak has the same effect as a low resistance connecting adjacent portions of the device to points at zero potential. Part of the current now flows in the paths indicated by the arrows, and the potential of electrode M is correspondingly decreased. The presence of the conductive streak is thus indicated by a relatively sharp, symmetrical depression on the apparent resistivity curve.

* An interesting special case is the instance when the hole has been drilled into a resistive formation, such as a salt bed, but has not completely penetrated it. In this case practically all the current flows up the hole from the current electrode, and nearly none in a downward direction. A lateral with A above M and N would give a practically zero reading in the formation, whereas a normal with M and N above A would give a high reading corresponding to the potential drop in the mud between electrodes M and N.

Study of True Resistivities

The Resistivity Departure Curves.—It has already been pointed out that the apparent resistivity is dependent on the resistivities of all the different media in the vicinity of the electrodes and may thus differ considerably from the true resistivity of the formation being logged.

The evaluation of the fluid content of permeable beds from electrical log data requires an accurate knowledge of the true resistivity of the beds; hence it becomes

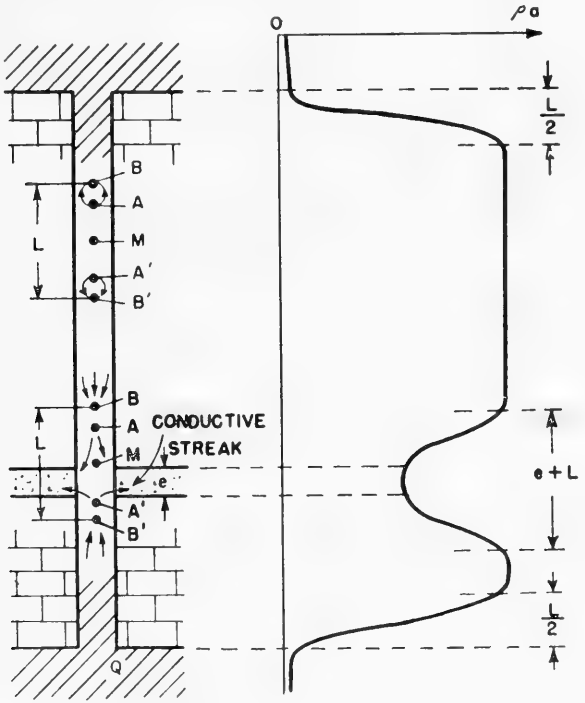

FIG. 642.—Resistivity log opposite a thick, highly resistive layer, using electrode arrangement of Figure 641.

important to have a means of determining the true resistivity of a formation. A method of arriving at the desired values, at least in favorable cases, is furnished by the resistivity departure curves.* These curves can also be used to evaluate the effect on the apparent resistivity of various factors, such as, for instance, the size of the hole or the extent of invasion.

Potential Measurements

The S.P. log, or spontaneous potential log, is a record of the naturally-occurring potentials measured in the mud at different depths in a drill hole. Usually, the S.P. log indicates an increase in potential by excursions or

* The first issue of the *Resistivity Departure Curves* was published by the Schlumberger Well Surveying Corporation in 1947. A second issue, which includes a number of additional curves and which also contains departure curves for beds of finite thickness, is being published in 1949. Detailed instructions for the use of the departure curves are given in these publications.

H. G. Doll, J. C. Legrand, E. F. Stratton, "True Resistivity Determination from the Electric Log—Its Application to Log Analysis" (A.P.I. meeting, Los Angeles, 1947).

peaks to the left of the chart. The base line corresponds in most cases to impervious beds, whereas the peaks are generally opposite permeable strata. The shape and the amplitude of the peaks may be quite different according to the formation, but *there is no definite correspondence between the magnitude of the peaks and the values of permeability.*

The importance of potential measurements is probably equal to that of resistivity measurements in commercial bore hole investigations. In some areas, e.g. in the Gulf Coast area, the potential measurements are of major importance.

In 1896 P. Bachmetjew† described an experiment which he believed indicated that potentials could be created which were due not to mineral contacts but to the motion of ground waters through subsurface sands and porous materials. These potentials were believed to be due to an effect first discovered and described by C. Quincke‡ in 1859. The first practical application of these phenomena to drill-hole exploration appears to have been made by Schlumberger,§ who received a patent for the location of permeable strata traversed by a drill hole.

The potential existing at the faces of the strata traversed by a drill hole consists, essentially, of two components: one, the potentials of electrofiltration caused by movement of the fluid either into or out of the porous formations traversed by the drill hole; and two, the electrochemical potentials created at the contact of two solutions having different concentrations of dissolved salts. Although the two effects exist simultaneously, they are best described separately.

Electrofiltration Potentials

In most drill holes, the well is filled with water or mud in sufficient quantities to exert a pressure on the walls distinctly superior to the hydrostatic head of the fluid in the rocks. This is particularly true in the numerous cases where the muds filling the holes are purposely made relatively heavy to avoid the caving-in of the hole and blowouts of gas or oil. In these cases, the penetration of the circulating mud into the pervious layers generates electrofiltration or electrokinetic potentials.

The electromotive force produced by the flow of an electrolyte through a pervious dielectric is directly proportional to the differential hydrostatic pressure and the electrical resistivity of the electrolyte and is inversely proportional to the viscosity of the electrolyte. It does not depend on the thickness of the filtering sheet nor on the radii and number of pores of the pervious medium. The magnitude of the E.M.F. produced by filtration may be expressed by the equation:††

† See article by W. M. Rust, Jr., "A Historical Review of Electrical Prospecting Methods," *Geophysics*, Vol. 3 (1938), pp. 1-6.

‡ C. Quincke, *Annalen der Physik*, Series 2, Vol. 107 (1859), pp. 1-47.

§ C. Schlumberger, "Electrical Process for the Geological Investigation of the Porous Strata Traversed by Drill Holes," U. S. Patent 1,913,293, issued June 6, 1933.

†† C. and M. Schlumberger and E. G. Leonardon, "Electrical Coring: A Method of Determining Bottom-hole Data by Electrical Measurements," *A.I.M.E. Geophysical Prospecting*, 1934, pp. 237-272.

$$E = \frac{m\, p\, \rho}{v} \tag{7}$$

where E = electromotive force; m = a constant which depends on the porous medium; ρ = resistivity of the fluid; p = the differential hydrostatic pressure; v = viscosity of the flowing electrolyte.

According to Poiseuille's† law, the quantity Q of fluid which flows through a given capillary tube at a pressure p is:

$$Q = \frac{m' p}{v} \tag{8}$$

where m' is a constant.
On combining Equations 7 and 8 one obtains

$$E = \frac{m\, \rho\, Q}{m'}$$

or

$$E = \text{constant} \cdot \rho Q \tag{9}$$

Equation 9 states that the electromotive force of filtration for a given electrolyte and pervious medium is proportional to the product of the amount of liquid which is filtered and the electrical resistivity of the liquid.

Generally, the potential opposite a surface of ingress will be negative with respect to that opposite a surface of egress. That is, in the usual case, a potential measured opposite a porous formation will be relatively negative if the bore-hole fluid is flowing into the formation, and relatively positive if the formation fluid is flowing into the hole.

The electrofiltration potentials are a minimum at the boundaries of the porous zone and a maximum in the most permeable section. The *magnitude* of the electrofiltration potential differences may be of the order of 100 to 200 millivolts over a length of a few meters.

It has been suggested that formation pressures may be determined from electrofiltration potential measurements by using Equation 7 twice.‡ To develop the relevant mathematical theory, it is convenient to write Equation 7 in the form:

$$E = k\,(H - P) \tag{10}$$

where k is a constant for a given porous medium and electrolyte; H is the pressure of the well fluid; P is the pressure of the formation fluid. If the fluid level in the well is lowered, by bailing for example, then for the new hydrostatic pressure H'

$$E' = k(H' - P)$$

Hence,

$$\frac{E}{E'} = \frac{H - P}{H' - P} \tag{11}$$

Theoretically, therefore, it is possible to determine the pressure P of the formation fluid by altering the fluid level and observing the quantities: E/E', H/H', and H or H'.

† Poiseuille, *Comptes Rendus* (1842), 18, 1167.
‡ C. and M. Schlumberger and Leonardon, *loc. cit.*, p. 262.

Potentials Due to Electrochemical Forces

Electrochemical potentials occur at the contact or boundary between two solutions of dissolved salts. For example, an electrochemical potential is created when the sweet water of a bore hole comes in contact with the salt water of a porous formation.

Figure 643 shows schematically a permeable layer, for example, a salt-water sand, situated between impervious formations such as clays or shales. The three media, the salt-water sand layer, the adjacent clay formations, and the mud, are separated by boundaries *A, B* and *C,* as indicated on the figure, and electromotive forces *a, b* and *c* of electrochemical origin exist at the corresponding boundaries. As each medium is considered fairly homogeneous, each of the electromotive forces is uniform along the corresponding boundaries.†

Laboratory experiments‡ have shown that the sum E of the electromotive forces *a, b,* and *c* generated by the electrochemical phenomenon can be represented by the formula:

$$E = K \log \frac{\rho_m}{\rho_w}$$

where ρ_w is the resistivity of the connate water contained in the layer; ρ_m the resistivity of the mud; and K a constant factor which depends on the constitution of the clay formation and the chemical composition of the fluids in contact. The sign of E changes according to whether ρ_m is greater or smaller than ρ_w. When $\rho_m = \rho_w$ the E.M.F. is equal to zero.

At boundary *A* both electrokinetic and electrochemical phenomena are present, so that the total electromotive force *a,* which occurs along this boundary, is actually equal to the algebraic sum of electromotive forces contributed by the two different phenomena.

Circulation of S.P. Current.—The three electromotive forces *a, b,* and *c,* add their effects to generate the S.P. current which follows the paths represented on Figure 643B by solid lines, each line corresponding to a line of flow. In the usual case where the pressure of the mud is higher than the formation pressure of the sand layer, and the resistivity of the mud is higher than the resistivity of the connate water, the current circulates in the direction of the arrows (from inside the bore hole towards the permeable bed).

Each current line must necessarily cross the three boundaries *A, B,* and *C.* Furthermore, that part of the current generated by each of the three E.M.F.'s, *a, b,* and *c,* follows the same path. In other words, the intensity of the current circulating in the mud of the drill hole depends only upon the algebraic sum of all the partial E.M.F.'s in the circuit, and does not depend upon the allocation of these partial E.M.F.'s to each boundary, provided that each E.M.F. is uniform everywhere on its corresponding boundary.

This combination of three electromotive forces at the boundaries, producing a current along a closed path traversing all three media, is termed a *three-link chain* E.M.F.

Along its path, the S.P. current has to force its way through a series of resistances, both in the ground and in the mud. In so doing, it produces potential differences. Along a given line of flow, the potential decreases continuously in the direction of the

† In order to simplify the explanation, boundary A, between the mud and the original fluid in the layer, is considered to coincide with the wall of the hole. The conclusions would be approximately the same for the case in practice where this boundary is located at a certain distance beyond the wall of the hole.

‡ C. and M. Schlumberger and E. G. Leonardon, "A New Contribution to Subsurface Studies by Means of Electrical Measurements in Drill Holes," *A.I.M.E. Geophysical Prospecting,* 1934, pp. 273-288.

current, as indicated by arrows, but across each boundary where an electromotive force occurs, the potential increases by an amount corresponding to the value of the electromotive force. Along a closed line of current flow, the total of the potential drops is necessarily equal to the sum of the electromotive forces encountered.

Also, since the magnitude of the current flow is constant all along its path, the potential drop varies according to the resistance of the section through which it flows. This means that the total potential drop (which is equal to the sum of the electromotive

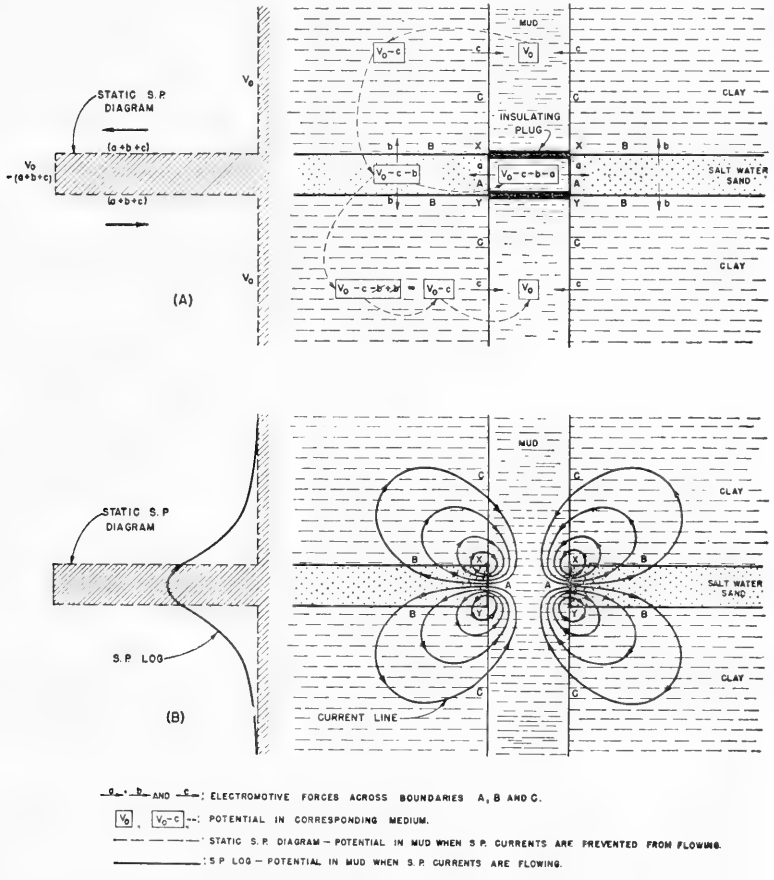

FIG. 643.—Schematic representation of potential and current distribution in and around a permeable bed. (After H. G. Doll, *A.I.M.E. Tech. Pub.* 2463, Sept., 1948.)

forces) is divided between the different formations and the mud in proportion to the resistance encountered by the current in each respective medium. Accordingly, the potential drop in the mud of the drill hole is a measure of only part of the total E.M.F., unless the electrical resistance offered by the mud is very large compared to that offered by the formations.

The Static S.P.—It is convenient to indicate the values of the electromotive forces which produce the S.P. currents, and which therefore determine the S.P. log, by an idealized representation based on the hypothetical case illustrated in Figure 643A. In

this figure it is supposed that the S.P. current is prevented from flowing by means of insulating plugs, placed in the hole to intercept the electrical continuity of the mud column at the boundaries between sand and clay.

The value of the potential within each single medium, enclosed by boundaries or plugs, would be constant. However, the potential would vary from medium to medium, the difference of the potentials in the different media being equal to the electromotive force existing at their common boundary.

In the case illustrated it can be shown that the difference of the potentials in the mud between and outside of the plugs would be equal to the total of the electromotive forces *a, b,* and *c*. If the potentials in the mud could be recorded in this idealized case, a log such as the dashed, cross-hatched curve on the left side of Figure 643A would be recorded, and the amplitude of the deflection opposite the permeable layer would be equal to the total of the electromotive forces, $a + b + c$.

Such a diagram, plotted for the case in which no current is allowed to flow, i.e., for the static case, is called a *static S.P. diagram* and is often useful in reaching a better understanding of the effect of the electromotive forces.

Factors Influencing the Shape and Amplitude of the S.P. Peaks—the S.P. Log in Soft Formations†

As shown in Figure 643B, the current circulates in the mud not only opposite the permeable formation, but also a short distance beyond its boundaries. As a result, although on the static S.P. diagram the boundaries of the permeable beds are indicated by sharp breaks, the S.P. log exhibits a more progressive change in potential, extending along the drill hole beyond the boundaries of that bed.

An analysis of the circulation of the current shows that the boundaries of the layer are located at the level of the *inflection points on the S.P. log.* This fact provides a way of determining the thickness of a bed from the S.P. log.

Moreover, since the S.P. log records only that portion of the potential drop occurring in the mud, the amplitude of the peak of the S.P. log approaches the amplitude of the static S.P. only in favorable cases, when the resistance offered to the current by the sand layer and the adjacent formations is negligible in comparison with the resistance of the mud in the bore-hole.

The shape and the amplitude of the peak on the log opposite a given bed may be influenced by the following factors: (a) the total electromotive forces involved (static S.P.); (b) the thickness of the bed; (c) the resistivity of the bed, of the surrounding formations, and of the mud; (d) the diameter of the drill hole; (e) the depth of penetration of the mud filtrate in the permeable beds; (f) the presence of impervious and conductive material, such as shale, inside the permeable bed.

The S.P. log would in addition be influenced by a lack of homogeneity of the mud; a change in salinity of the mud at a certain level would result in a base-line shift at that level. However, it has been found in practice that such changes in salinity are very seldom encountered.

The manner in which the above-mentioned factors influence the S.P. may be explained for the case of permeable beds, situated between impervious formations, the resistivity of which is less than, or of the same order as, that of the permeable beds. This case is typical of the so-called soft formations. The case of permeable zones in hard formations (limestone) is a rather specific topic which will be discussed separately.

(a) All other factors remaining the same, a change of the total E.M.F.'s affects the amplitude but does not otherwise modify the shape of the S.P. log.

In practice, the E.M.F.'s involved may vary in different bore holes, either because the salinity of the mud (or of the formations) is quite different, or to a smaller extent because the differential pressure between the mud and the formations is different. In a given hole, however, and for the same type of formations and depth, there is a definite tendency for the total E.M.F.'s to be the same for all beds of the same type.

† H. G. Doll, "The S.P. Log: Theoretical Analysis and Principles of Interpretation," *A.I.M.E. Tech. Pub.* 2463 (1948).

Permeable beds of different porosity, or with different dimension of grains, give the same E.M.F.'s, if other factors are unchanged. The E.M.F.'s are also independent of the permeability value, even down to fractions of one millidarcy.

It has been observed that the salinity and the differential pressure are not always constant for all permeable beds penetrated by a hole, especially at widely different depths or in very different formations. Fresh-water sands or very salty sands will show respectively abnormally low or large amplitude peaks. The polarity of the peak may even reverse if the water in the sand is less salty than the mud.

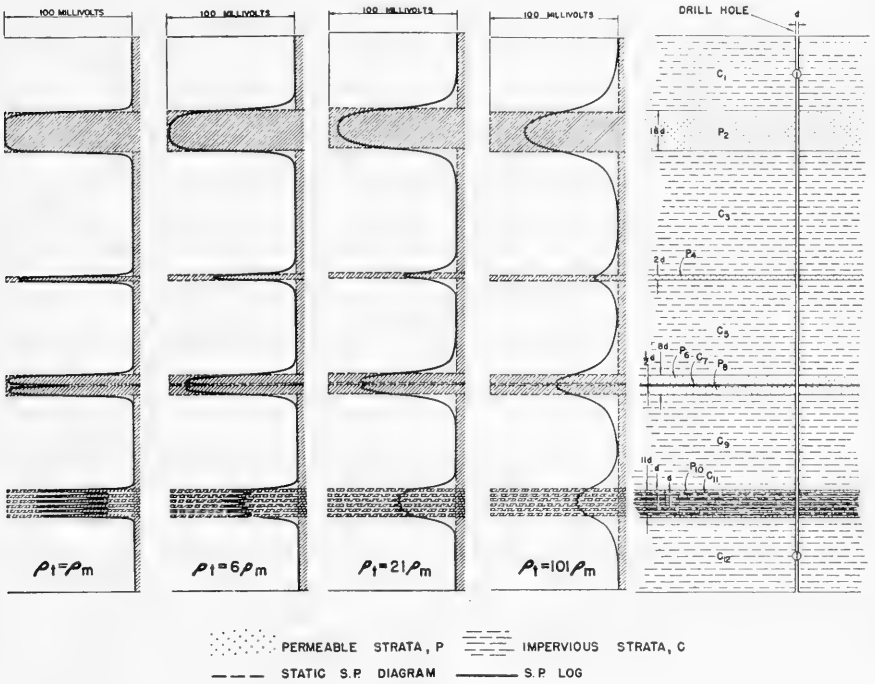

FIG. 644.—Comparison of S.P. logs for different values of $\frac{\rho_t}{\rho_m}$. (After H. G. Doll, *A.I.M.E. Tech. Pub.* 2463, Sept., 1948.)

(b) Theoretical computations and field experience have shown that the amplitude of the S.P. deflection is practically equal to the static S.P. (i.e., it gives the value of the total E.M.F.'s) when the permeable beds are very thick, and when the resistivities of the formation are approximately the same as that of the mud. Moreover, in this case the S.P. curves mark the location of the boundaries of the bed with great accuracy.

The amplitude of the deflection is less than the static S.P. for thin beds, and the smaller the bed thickness, the smaller the peak.

(c) On the other hand, when the resistivity of the formations ρ_t is higher than that of the mud ρ_m, the S.P. curves are rounded off, the boundaries are marked less accurately, and all other conditions being the same, the magnitude of the peak is less than when the ratio $\frac{\rho_t}{\rho_m}$ is close to 1.

Figure 644 shows theoretical data illustrating the influence of the thickness of bed and the resistivity of the formations. To facilitate the comparison, the value of the static S.P. has been supposed the same for all permeable beds and equal to 100 mv.

The figure shows that the static S.P. is reached only when bed thickness is equal to at least 16 times the hole diameter (about 10′ to 13′), and provided ρ_t is not higher than about 6 ρ_m (for example, 6 ohm-meters in the Gulf Coast, where ρ_m is about 1 ohm-meter on the average).

It also is indicated that the S.P. curve spreads a considerable distance outside the boundaries of the layer, when $\frac{\rho_t}{\rho_m}$ is large, and the higher ρ_t, the greater the effect.

From the preceding statements it can be seen that the mud resistivity has a predominant influence on the magnitude of the S.P. deflection: the total E.M.F.'s (static S.P.) are the sum of the electrokinetic potentials (which are proportional to the mud resistivity) and the electrochemical potentials (which are closely related to it). The salinities of connate water are usually very high, so that, if the mud is also of high salinity, the electrochemical potentials can be practically nil. Moreover, for a given static S.P., the lower the mud resistivity, the smaller is the ohmic drop in the mud. All these factors contribute therefore toward the same result, which is to minimize the S.P. deflection. In fact, it is a common observation that the S.P. logs show very minute deflections, and are even completely flat, when the bore-holes are drilled with very conductive muds. In the case of comparatively fresh connate formation water, conductive mud may give rise to reversed peaks (deflections toward the positive side) provided the conductivity is not too high. The computed curves shown in Figure 644 are for successive beds having the same or very nearly the same values of resistivity. In practice, this is not always the case, and the resistivities of the successive beds may even differ widely, as for instance when shales are interbedded with oil-bearing sands.

In such a case, the shape of the S.P. log remains approximately the same, and it should be noted particularly that the boundaries between permeable and impervious beds still correspond to the inflection points on the log. However, the S.P. curve is more rounded off in the more resistive formation than in the other one, and the inflection point is displaced toward the bottom of the peak if the peak corresponds to the more resistive formation, and vice-versa.

(d) An increase in hole diameter acts approximately like an increase in the ratio $\frac{\rho_t}{\rho_m}$. It tends to round off to a greater extent deflections on the S.P. log and to reduce the amplitude of the peaks opposite thin beds.

(e) In general the permeable beds are invaded by mud filtrate: the boundary between the mud filtrate and the liquid in the permeable formation where potentials of electrochemical nature orginate is therefore somewhere inside the permeable formation, at a certain distance from the wall of the hole. As a result, penetration of mud filtrate into the permeable bed has an effect on the S.P. log similar to an increase in hole diameter; the S.P. peaks are wider than they would be in the case of no invasion, and the amplitude of peaks corresponding to thin permeable beds located in impervious formations is smaller than for no invasion.

(f) A combination of thin layers of sand in shale or of thin layers of shale in sand constitutes what has been called a *sandwich;* such a combination can be considered as a more or less shaly sand. One such case is illustrated by Figure 644. The following points are of interest concerning the logs of sandwiches:

(1) On thick sandwiches, the average deflection is approximately proportional to the percentage of sand.

(2) The average contour corresponding to a sandwich of finite thickness is the same as for a homogeneous permeable bed of the same thickness and resistivity but for which the total E.M.F. involved would be smaller. The amplitude of the ripples around the average curve decreases very quickly when the thickness of the individual beds is decreased, and the ripples are hardly noticeable when the individual thickness of each of the sandwiched beds, both permeable and impervious, is less than one-half the diameter of the hole.

(3) The average amplitude of the peaks decreases when the resistivity of the sand increases in comparison with that of the shale.

The expression *shaly sand* has been applied above, in a general way, to interbedded thin streaks of sand and shale. There are, however, sand beds containing certain unstratified shaly material, which therefore must also come under the category of shaly sands. Whether the different shaly particles enclosed in a shaly sand are stratified or not, the material affects the S.P. curve in substantially the same way, as long as the shaly sand remains permeable; the amplitude of the S.P. log is maximum for a clean sand and it is reduced with an increased percentage of shaly material, but this amplitude does not depend on the distribution of the shaly material, provided, of course, that the average distribution is uniform.

The presence of oil in a shaly sand will increase the resistance of the permeable part of the medium. Accordingly, the amplitude of the deflection on the S.P. log can be expected to be smaller opposite an oil-bearing section than opposite a water-bearing section. Such a change in the magnitude of the peaks can be observed only for shaly sands or for clean sands of small thickness; it will not be observable for very thick clean sands.

Since many sands are shaly, it is not surprising that a change in the deflection on the S.P. log occurs when passing the oil-water contact in a sand. It is to be noted however, that this change is not necessarily diagnostic of oil, since the same effect would be obtained if the salinity of the interstitial water were reduced, or if the percentage of shale were increased.

Base Line Shifts.—Usually the S.P. is the same in front of all thick shale beds, or, in other words, there is a straight "shale line" or "base line" on the S.P. log. Experience has shown however that in certain fields there is a systematic shift of this shale line which occurs always at the same location in the geological column. In fact, in certain cases, such base line shifts constitute excellent markers.

The shift is generally due to a difference in the nature of the shales above and below the shift level. There can be a shift in the base line, however, even though the shales above and below the shift level are of the same nature. This occurs when there is a dissymmetrical sequence of formations in the ground, constituting one or more three-link chain E.M.F.'s which do not cancel out.

The S.P. Log in Hard Formations (Limestone Fields)

The case of limestone fields, or more generally the case of permeable beds in compact and highly resistive formations, is of particular interest.

The S.P. log in hard formations has a character which is often difficult to understand. It must be remembered that such formations are highly resistive except for conductive zones of two types: (1) permeable zones, whether oil-bearing or water-bearing, which are usually conductive because of their connate water of generally high salinity; and (2) shales and other conductive beds, which are of an impervious nature but contain highly conductive connate waters.

According to the nature of the electromotive forces present, the S.P. current tends to flow from the hole into the permeable zones, and from the shales into the hole. If the beds adjacent to these conductive zones were also conductive, they would furnish the return path for the S.P. currents. If the adjacent beds are highly resistive, the S.P. currents tend to be confined to the hole opposite the resistive beds, flowing via the hole between the permeable beds and the nearest conductive, impervious (shale) beds and completing the circuit, after deep penetration into the conductive beds, by flowing through a very large cross-section of the highly resistive beds.

This means that S.P. currents are flowing in the hole along the entire thickness of the resistive beds, and in so doing they produce potential differences by ohmic effect in the mud. The result is that the peaks corresponding to the permeable zones spread above and below these zones in an apparently abnormal manner, and it is impossible to determine with accuracy from the S.P. log the boundaries of the permeable zones.

Figure 645A represents schematically the case of four thin permeable zones P_3, P_7, P_9 and P_{11}, and three thick shales C_1, C_5, and C_{13}, separated from each other by thick, compact, and highly resistive beds H_2, H_4, H_6, H_8, H_{10}, and H_{12}. In order to characterize the problem more explicitly, it is assumed, taking the resistivity of the mud as equal to unity, that the resistivity of the permeable zones, as well as that of the shales,

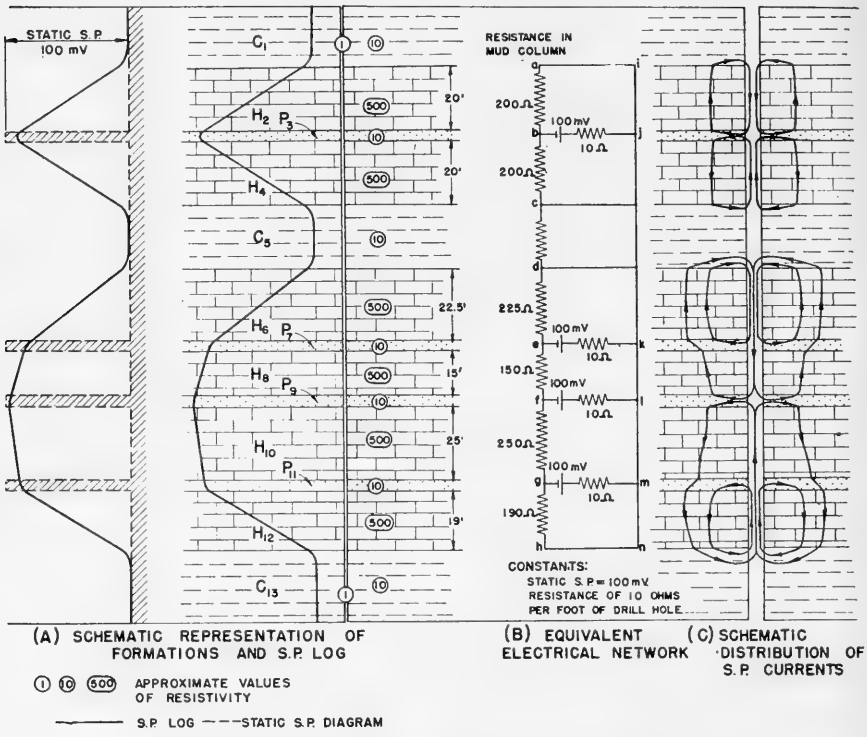

FIG. 645.—A schematic representation of S.P. phenomena in highly resistive formation. (After H. G. Doll, *A.I.M.E. Tech. Pub.* 2463, Sept., 1948.)

is approximately 10, whereas the hard formations have a relative resistivity of 500 or more. The log shown in the illustration corresponds approximately to these figures in ohm-meters.

The E.M.F.'s involved are represented by the static S.P. diagram on which the S.P. is superimposed. As can be seen, the departure of the S.P. log from the static S.P. diagram is remarkable in this case, and often a log of this type is considered abnormal.

The circulation of the S.P. currents is represented, in a schematic way, in Figure 645B. The S.P. currents, which are generated by the different E.M.F.'s, flow into the sands. They cannot traverse the adjacent hard formations through sections located close to the drill hole, because these sections are small in area and introduce large resistances which practically prevent the current from flowing. On the contrary, the S.P. current penetrates deeper than usual in the permeable beds and consequently enters the hard formations through larger cross sections. From there on, it is easier for the S.P. currents to continue their path in the hard formations without appreciable reduction in their cross section, as would be required if they were to converge quickly toward the hole. The S.P. currents flow therefore toward conductive beds through

which they can return to the mud in the hole, and then through the mud back to the permeable beds to complete their circuits. They cannot come back to the mud through other permeable beds, because they would encounter E.M.F.'s which would oppose the flow of currents in that direction. When the first conductive beds they encounter are of the permeable type, they simply cross them until they reach the more conductive and impervious beds. This is the case for the S.P. currents which penetrate the permeable bed P_9; they have to cross the permeable bed P_7 in order to reach the impervious bed C_5, or have to cross the permeable bed P_{11} in order to reach the impervious bed C_{13}.

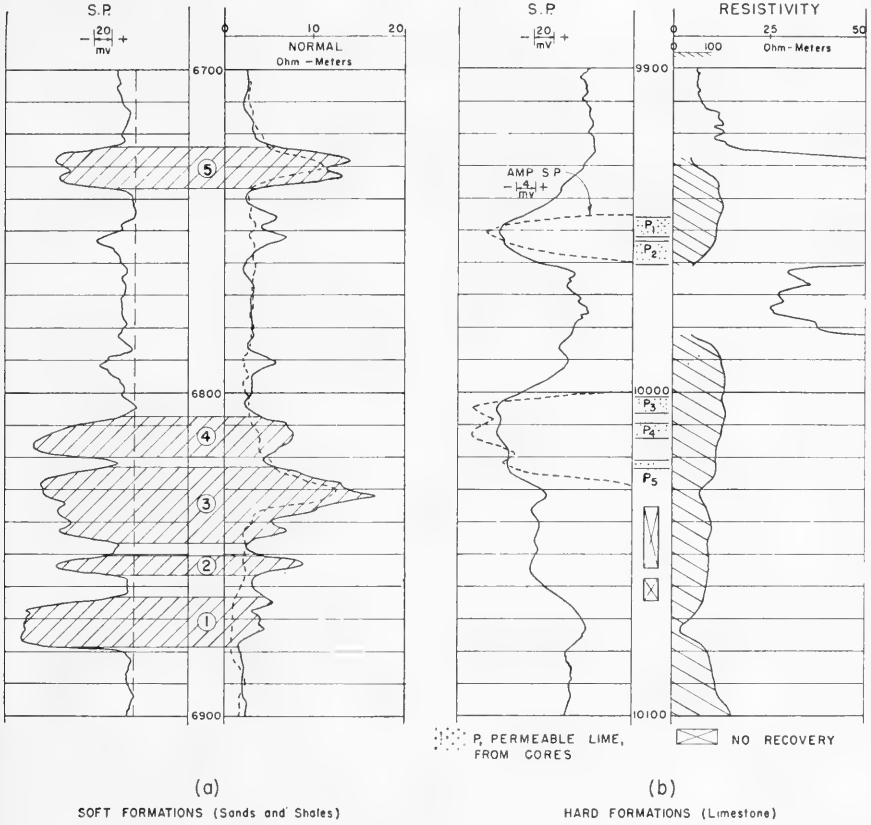

FIG. 646.—Comparisons of S.P. and resistivity logs in soft and hard formations. (After H. G. Doll, *loc. cit.*)

All along the drill hole opposite a given hard formation, the current in the mud column remains substantially the same, and so does the drop of potential per unit length of hole, thus giving a constant slope as shown by the S.P. log of Figure 645A.

At the level of each conductive bed, some S.P. current generally enters or leaves the hole; therefore the slope of the S.P. log is modified. In Figure 645A, for example, the S.P. log changes its slope at the level of the permeable bed P_7, because part of the current leaves the hole and flows into that bed.

As a general rule, the permeable beds are characterized on the S.P. log by slope changes, or curvatures, with the convexity toward the negative side of the log, and

impervious beds of low resistivity are characterized by slope changes, or curvatures, with the convexity toward the positive side of the log. Highly resistive formations correspond to substantially straight parts of the S.P. log.

Field Examples.—Figure 646 shows two typical field examples of S.P. logs and the corresponding resistivity logs.

Figure 646(a) illustrates the case of a section comprising mostly shales and sands. In front of bed 1 the greatest S.P. deflection—about 115 millivolts from the base line—is attained. It corresponds to a sand having a low resistivity; the S.P. curve is steep and the boundaries of the sand are well defined. It is likely that the magnitude of the deflection is not far from the value of the static S.P.

Although sand body 3 is of greater total thickness, the S.P. deflection is appreciably less—about 95 millivolts. This is due partly to the presence of intercalated shale beds, notably at 6830′, 6835′, and 6840′, and partly to the higher resistivity of the sand, which accounts also for a certain rounding off of the S.P. curve. A similar feature is observed in front of bed 5. Since bed 2 is very thin, its indication on the S.P. log is a sharp peak whose amplitude is definitely lower than the value of the static S.P.

In front of bed 4 the S.P. log shows an almost constant slope; the S.P. rises progressively from the base line to a maximum deflection of about 105 millivolts. This probably indicates a transition zone of shaly sand.

Figure 646(b) illustrates an S.P. log recorded in a limestone section. The permeable zones are shown by the S.P. log, but their limits are not well defined.

The two S.P. logs of Figure 646 are very different in shape, although the E.M.F.'s involved are of the same order of magnitude. The first shows steep variations of great amplitude, and the boundaries of the permeable zones, at least of those of appreciable thickness, can be determined with good accuracy. The second, on the contrary, due to the effect of the high resistivities encountered in the limestone, presents more gradual variations of the S.P., and the boundaries of the different formations, particularly of the permeable zones, are poorly indicated.

Measurement of S.P.—The recording of S.P. logs is a simple technique, as shown in Figure 647. A measuring electrode M is lowered in the hole at the end of an insulated cable. The differences of potential between an electrode N,* which, being stationary, is at a fixed potential, and electrode M, whose potential varies as it is moved along the hole, are observed by means of a recording galvanometer. A curve is recorded on which the ordinates are proportional to the depth of electrode M, and the abscissae represent the potential of electrode M with reference to electrode N.**

The drill holes in which the S.P. logs are recorded are usually filled with mud having a water base. The density of the mud is ordinarily such that at each depth the hydrostatic pressure in the hole is greater than the formation pressure; as a result, the fluid contained in the permeable beds cannot contaminate the mud. Also, the mud has been in constant circulation during the drilling operation, prior to the logging, and therefore it is homogeneous.

From the circuit shown on Figure 647, it can be seen that the recording galvanometer measures all the differences of potential appearing between electrodes M and N. However, provided proper precautions are taken, experience has shown that under usual conditions the deflections on the S.P. log correspond to phenomena occurring at the contacts between the mud and the different beds, and also at the contacts between the beds themselves. These phenomena produce an electric current, called the *S.P. current*† which uses the mud as its return path. Potential differences are created by ohmic effect.

Other sources of potential, which are not related to the formation, do not usually cause any deflection on the S.P. log; if they are present and bothersome, proper steps

* Usually placed in the mud pit, for convenience.

** In usual practice, the S.P. curve is recorded simultaneously with the resistivity curve.

† The expression *S.P. current* may seem rather illogical, as S.P. stands for *spontaneous potential;* however, as it has become common usage, it will be employed here.

are taken to overcome them. A constant difference of potential may normally appear between these two electrodes in the absence of any S.P. current. This constant difference of potential is not recorded on the S.P. log; it is counterbalanced by means of a potentiometric circuit not shown in the figure.

Accordingly, the potential of electrode *M* is actually measured on the S.P. log with reference to an arbitrary fixed potential. However, the variations of the potential, i.e., the deflections on the S.P. log, do not depend on this fixed potential. It is these variations which are a measure of the potential differences created in the mud by the S.P. current and which make it possible to characterize the formations. Under normal conditions, the excursions toward the negative characterize permeable beds, whereas excursion toward the positive characterize impervious beds.

The electrodes employed for commercial potential or porosity measurements are preferably made from a material having a low electrochemical contact potential with the mud. In practice lead is the material commonly employed. Theoretically, all electrodes lowered into bore holes should be of the non-polarizing type to minimize errors caused by electromotive forces arising from contacts between a metal and the water of the bore holes; practically, however, the error introduced by use of lead electrodes is negligible because of the homogeneity of the bore hole mud with which they are in contact.

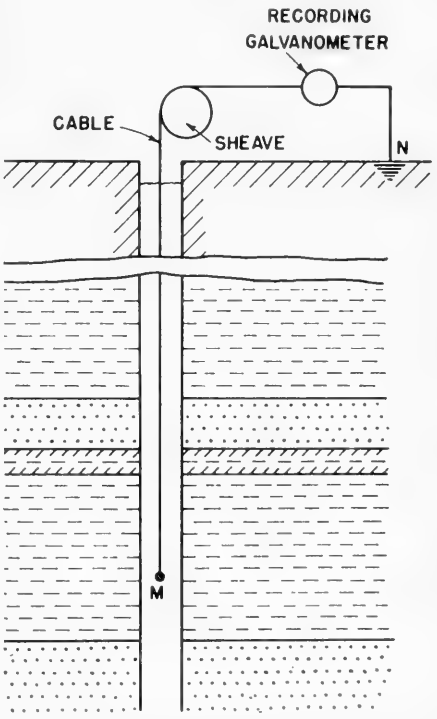

FIG. 647.—Schematic arrangement for measuring potentials in a bore hole.

An alternative method which has been proposed by Schlumberger,† but not employed commercially to a large extent, places two small or "point" electrodes within the bore hole, the electrodes being a fixed distance apart. The difference in potential between the two electrodes within the bore hole is measured and recorded at the surface of the ground. The readings obtained when employing two electrodes within the bore hole give the gradient of the potential, and it is necessary to convert this gradient to a potential difference along the bore hole. In areas where bad ground currents prevail, this method has the advantage over the method described above that it is much less affected by ground currents, due to the short distance between the electrodes. However, interpretation of the gradient curve is almost impossible due to the many thin strata encountered in the usual bore hole.

Another modification employs an extended electrode, with a small or "point" electrode spaced about 50 feet below it. Such a system is practically unaffected by extraneous ground currents and has the advantages of the two "point" electrode system. In practice, the metallic braid over the cable, if of the shielded type, will serve as the extended electrode.

---

† C. Schlumberger, "Electrical Process for the Geological Investigation of a Porous Strata Traversed by Drill Holes," U. S. Patent 1,913,293.

Various modifications of the potential method have been proposed. For instance, Hummel † proposes to measure the potentials at null-point conditions without the use of a manually-controlled or automatically-controlled potentiometer. In Hummel's method, two electrodes are usually lowered into the bore hole; one is a current electrode and the other a potential electrode. Sufficient current is passed into the well through the current electrode to balance out exactly the natural ground potentials measured between the potential electrode in the well and the other potential electrode at the surface. A record is made of the variation in current necessary to create the zero potential condition.

The effects of extraneous earth potentials may also be eliminated or minimized by use of an auxiliary potential circuit. In this arrangement, the extraneous earth potentials are fed into the measuring circuit in such a manner that they oppose or neutralize the same variations in the measuring circuit.‡

Karcher § has developed a means for measuring polarization during drilling. The polarization in question is a back E.M.F. which opposes the voltage causing the current flow and persists after the voltage is removed. The method utilizes a bit which is insulated from the remainder of the drill stem and connected electrically to a recording potentiometer at the surface of the ground. It is claimed that because the electrical properties of the earth formations are affected by their porosities, the phenomena of polarization are also affected by the porosities; consequently, a variable which depends on the polarization is diagnostic with respect to the amount of the porosity of the earth formation in question. In operation, the current is allowed to flow for some definite period, for example, one minute, during which time the resistance to ground is recorded.†† The drilling bit is then disconnected from the current supply and connected to the potential measuring device. The instantaneous reading of the potential is, therefore, the diagnostic variable which depends on the amount of polarization produced by the original current applied to the measuring circuit.

It is contemplated that the above operation would be repeated as the drilling proceeds, and means are provided for performing this operation automatically.

A means of conducting electricity through the drill stem to the bit has been developed by Hawthorne.‡‡ It should be noted that if the measurements are made while drilling is in progress these potentials are superimposed on the rapidly varying potentials generated by the bit. Measurement of the latter potentials when the entire bit and drill stem are in contact with the mud or earth has been described previously.

Complementary Application of Resistivity and S.P. Data

In the preceding description of the resistivity and the S.P. curves, interpretation was treated separately. In practice, however, the two curves supply data which is complementary for most areas or geological provinces. The interpreter therefore must consider both curves jointly. The following examples illustrate such general interpretation problems, as applied to the cases of soft formation (mostly sands and shales of low or moderate resistivity) and hard formations (mostly limestone of high resistivity).

---

† J. N. Hummel, "Process for Inspecting the Ground," U. S. Patent 2,084,143, issued June 15, 1937.

‡ J. J. Jakosky, "Method and Apparatus for Electrical Exploration of the Subsurface," U. S. Patent 2,162,086, issued June 13, 1939.

§ J. C. Karcher, "Method and Apparatus for Determining the Porosity of Rock Formations," U. S. Patent 2,085,664, issued June 29, 1937.

†† J. C. Karcher, "Method and Apparatus for Exploring Bore Holes," U. S. Patent 1,927,664, issued Sept. 10, 1933.

‡‡ David G. Hawthorne, "Apparatus for Subsurface Surveying," U. S. Patent 2,096,359, issued Oct. 19, 1937.

Soft Formations.—Figure 648 is a portion of a typical log showing the S.P. curve, A; the short normal, B; amplified short normal, C; long normal, D; and lateral curves, E; for soft formations interbedded with a harder formation.

Geological strata generally form sequences of thin sand and shale layers. The relative proportion of sand and shale is variable with the depth. The intervals where the proportion of sand is much greater than that of shale are considered as sand beds; sometimes the amount of shale is so small that the beds are practically clean sands. Conversely, the zones where the shales are predominant are termed *shale beds.*

The S.P. curve and the short normal curve give an accurate record of the boundaries of the thicker shale and sand beds, as they have just been defined; the very thin layers are shown only by minor wiggles on the curves (see, for instance, permeable beds 1, 2, and 5 in Figure 648).

Moreover, very thin hard beds in shale formations, which are rather poorly indicated or not indicated at all by the S.P. log, appear quite clearly on the short normal curve when recorded on an amplified scale, and provide, in many cases, excellent markers for correlations. (See, in particular, the shale bed 4, Figure 648).

Generally, the resistivity of the mud is much greater than that of the connate water. On the Gulf Coast, for example, the mud resistivities are confined to a range from about .5 to 2 ohm-meters, whereas the resistivity of the connate water is about .05 ohm-meter. The resistivity of the invaded zone is therefore much higher than the true resistivity of the water-bearing formation (10 to 20 ohm-meters for the former against .5 to 1 for the latter), and sometimes the resistivity of the invaded zone may be even higher than the true resistivity of oil-bearing formations (5 to 20 ohms). Therefore the resistivity measured with the short normal is greatly affected by the presence of the invaded zone, and peaks are generally obtained on the log in front of the permeable beds, even if these beds are highly conductive.* (Note Figure 646, bed number 1.) Sometimes, however, the depth of penetration of the mud into the permeable layers is small enough so that the short normal curve is very little affected and gives depressions in front of conductive layers (Figure 648, beds 1, 2, and 5).

The readings on the long normal curve are little influenced by the mud and the invaded zone, and wherever the thickness of the bed is great enough, the comparison between the short and long normal curves determines, in general, whether the true resistivity of the permeable beds is high or low. A conductive bed is indicated by a low apparent resistivity on the long normal, whereas a resistive bed gives rise to a high resistivity, sometimes higher than the reading obtained with the short normal.

In Figure 646, for example, permeable beds 3 and 5 appear as being resistive, and bed 1 as more conductive. Also in Figure 648, for instance, permeable beds 3 and 4 are resistive, whereas all the other permeable beds are conductive. These indications are confirmed in the case of thick beds, by those of the lateral sonde.

When the thickness of the bed is of the same order as the spacing of the long normal, or smaller, no reliable indication can be deduced from the normal curves as far as the value of the resistivity of the bed is concerned. The only indications in this respect are given by the lateral sonde which gives rise to short peaks in front of resistive beds and no peak in front of conductive beds.

Wherever the beds are sufficiently thick clean sands, and are less resistive or of approximately the same resistivity as the surrounding impervious formations, the magnitude of the deflections on the S.P. log are practically equal to the static S.P. When the permeable beds are more resistive than the adjacent formations, the static S.P. is attained only if the bed is very thick. In the case of thin sands, or of shaly sands, the magnitude of the S.P. peak is less than that of the static S.P.

The principles of interpretation cannot be reduced to the above simplifications in all cases. For instance, when the connate water is fresh, *the distinction between oil-bearing and water-bearing beds becomes difficult, and sometimes impossible.* Also,

* The recording of the short normal on an amplified scale has often been found quite useful for correlation purposes in the case of long flat shale sections, in which the recording in the regular sensitivity reveals very little feature.

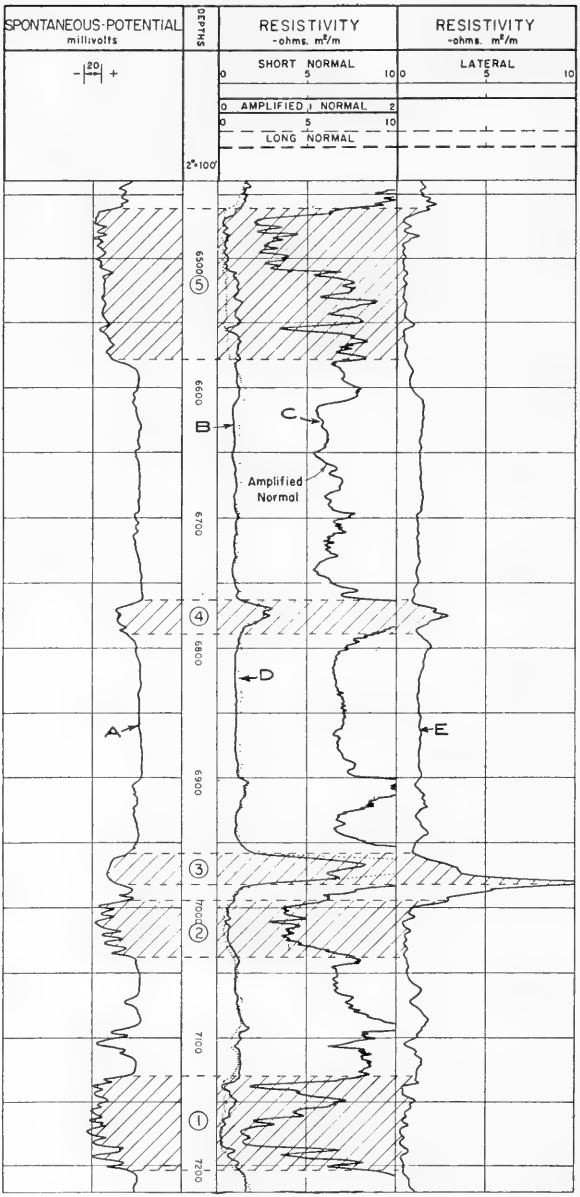

FIG. 648.—S.P. and resistivity curves for interbedded soft and hard formations. A, S.P. curve; B, short normal; C, amplified short normal; D, long normal; E, lateral curve.

sands containing a great amount of colloidal material, whether stratified or not, give rise to low resistivities, whatever the fluid content may be.

In all these difficult cases, the use of instruments for the recovery of samples from the interesting layers is particularly helpful, as will be explained later.

Hard Formations.—In hard formations the interesting zones, from the standpoint of the oil production, are those which show some porosity and permeability. These zones generally contain highly mineralized connate waters, and, even if oil-bearing, they are more conductive than the surrounding, more compact rocks. But porous and impervious layers (shales) may also exist inside these formations, and are also conductive. The problem is therefore: (1), to determine the location of the conductive zones in highly resistive formations, and (2), to find out which of these zones are permeable and which are impervious.

Conventional resistivity logs generally give a rather confusing representation of the boundaries of the layers of different resistivities in hard formations. The special device called the limestone sonde is better adapted for this purpose, and the combination of the limestone device and the S.P. log may provide, in favorable cases, a fair solution to the problem. Figure 649 is an example of a log recorded opposite a thick limestone bed containing several conductive streaks. The limestone sonde indicates these by a series of well-marked depressions. Opposite depressions 1, 3, and 6, the S.P. log shows slight inflections, with a convexity towards the negative side, which is representative of permeable zones. In front of depressions 2, 4, and 5, the S.P. log shows inflections, with convexity towards the positive side, characteristic of impervious beds. But it is clear that the indications of the logs, and particularly of the S.P. logs, are far from being as definite as in the case of soft formations; the approximate location of the interesting beds is barely suggested, and sometimes, as in the case of 7, the S.P. curve shows no response at all. No indication

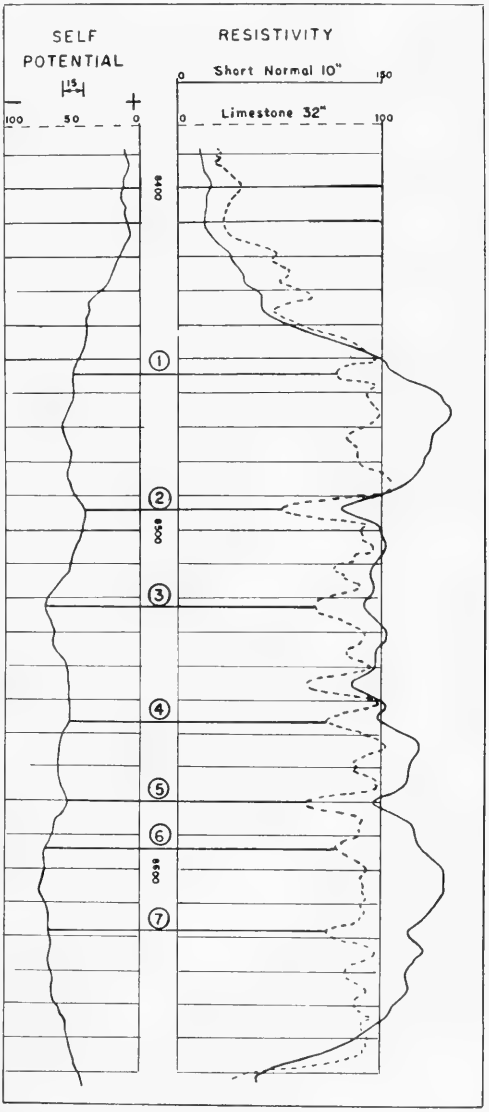

FIG. 649.—S.P. and resistivity curves opposite a limestone formation containing thin conductive streaks.

can be derived from the log in this case regarding the exact boundaries of the beds. It is furthermore impossible to determine the true resistivity of the permeable beds in hard formations, or to determine, even qualitatively, their fluid content.

Determining Fluid Content.—Efforts have been made for many years to determine the fluid content of reservoirs. In certain areas, a close analysis of the logs, and a careful consideration of all geological data (particularly the results of production tests) often will give an indication of the nature of the fluid content.† Side-wall samples are of help in problems of this nature.

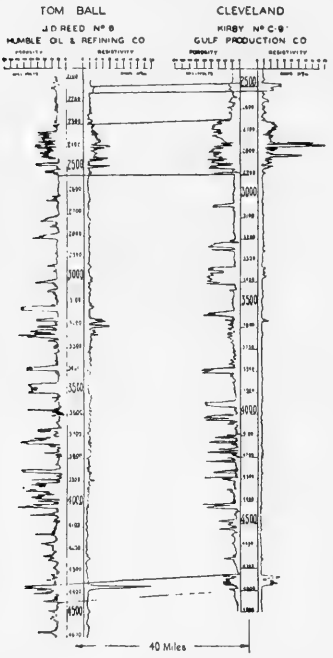

FIG. 650. — Correlations between two wells in the Tom Ball and Cleveland area along the Conroe trend. (Deussen and Leonardon. Paper presented before *A.P.I.* at the 16th Annual Meeting, Los Angeles.)

Correlation Between Wells

Where lateral continuity is prevalent, as is likely to be the case for marine deposits, the sediments are identical in texture, porosity, and salinity at the time of deposition. Although these characteristics may have undergone important modifications since the deposition, the initial similarity still remains to a large extent because most of the modifications (variation of compactness due to varying pressures, alteration of the ion content of the connate waters, etc.) are of a regional character. For example, the concentration of subsurface waters often exhibits a gradual and regular variation; this makes it possible to identify various horizons by means of isoconcentration curves covering areas of a large extent.‡ Consequently, if the electrical logs of two neighboring wells are similar or nearly identical, as is often the case, the lithology and conditions of impregnation may be assumed to be very similar. On the other hand, decided changes in the form of the diagrams indicate corresponding lateral modifications of the geological sections.

---

† M. Martin, G. H. Murray and W. T. Gillingham, "Determination of the Potential Productivity of Oil-Bearing Formation by Resistivity Measurements," *Geophysics*, Vol. III, p. 258.

G. E. Archie, "The Electrical Resistivity Log as an Aid in Determining Some Reservoir Characteristics," *A.I.M.E. Tech. Pub.* 1422.

M. R. J. Wyllie, "A Quantitative Analysis of the Electrochemical Component of the S.P. Curve," *A.I.M.E. Tech. Pub.* 2511 (1949).

M. R. J. Wyllie, "A Statistical Study of the Accuracy of Some Connate Water Resistivity Determinations Made from S.P. Log Data," A.A.P.G. meeting, St. Louis, March, 1949.

M. P. Tixier, "Electric Log Analysis in the Rocky Mountains," A.P.I. meeting, Los Angeles, 1949.

G. E. Archie, "Electrical Resistivity an Aid in Core Analysis Interpretation," *Bull. A.A.P.G.*, Vol. 31, No. 2, Feb., 1947.

H. W. Patnode, "Relationship of Drilling Mud Resistivity to Mud Filtrate Resistivity," *A.I.M.E. Tech. Pub.* 2511 (1949).

M P. Tixier, "Evaluation of Permeability from a Determination of the Resistivity Gradient on the Electric Log," A.A.P.G. meeting, St. Louis, March, 1949.

‡ L. C. Case, W. R. Berger, R. F. Fash, and H. E. Miner, *Problems of Petroleum Geology*, Part VI, published by *A.A.P.G.*, 1934.

Correlation of electrical logs of wells in widely separated areas is usually confined to the more important changes or breaks in sedimentation. Continuous correlation, bed by bed, over long distances is possible, however, if the wells are spaced closely enough to indicate the presence of overlaps and faults which destroy the continuity of the geologic formations. Figure 650 shows the correlation of a well in the Tom Ball field with one in the Cleveland field. These two wells are forty miles apart on the Conroe trend. The group of sands at the top of the Marginulina zone is very distinct in both wells and, in spite of the distance, certain detailed features are recognizable. At greater depths, in a series of alternating beds of sands and shale of a uniform distribution, a characteristic sandy horizon located just above the Textularia Hockleyensis zone is apparent. This horizon is easy to identify in both wells.

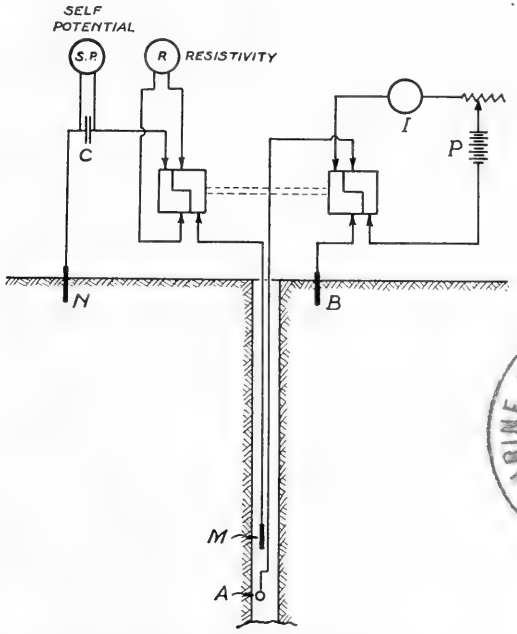

FIG. 651. — Electrical connections for simultaneous recording of self potential and resistivity by means of a double commutator. *S.P.*, self potential recorder; *C*, by-pass condenser; *R*, resistivity recorder; *A*, moving current electrode; *M*, moving potential electrode; *N* and *B*, stationary surface electrodes; *I*, current meter; *P*, power supply.

Instrumentation

Resistivity and self potential logs may be obtained simultaneously by means of the double commutator apparatus termed the *pulsator*, illustrated schematically in Figure 651. The energizing current is reversed periodically and in synchronism with the resistivity potentials which are to be measured. The direct-current self potential recording meter is unaffected by the periodically reversed energizing current. The

S.P. and the resistivity parameters are recorded on a sensitized film. The movement of the film is synchronized with the cable, so that a definite ratio exists between a unit of length on the film and a unit of length along the bore hole. For example, scales of 1″, 2″ or 5″ of film to 100 feet of cable are available. Synchronization of film and cable may be accomplished by use of two interlocking synchronized motors, one being

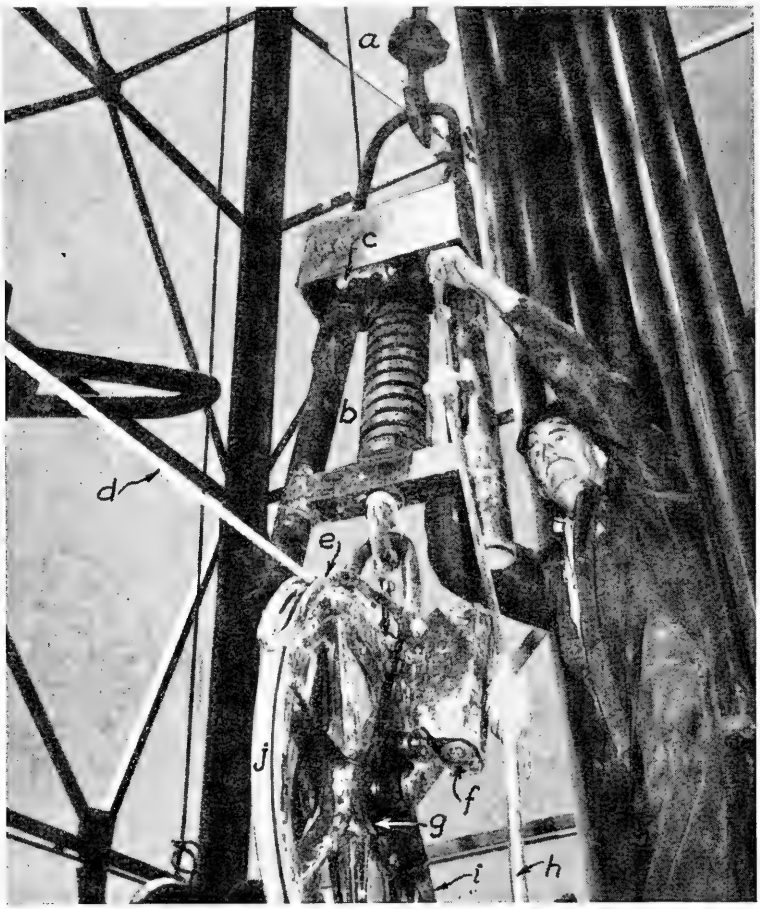

FIG. 652. — Measuring sheave wheel for electrical logging. *a*, supporting hook fastened to traveling block; *b*, weight spring; *c*, weight selsyn motor; *d*, cable to recording truck; *e*, cable guides; *f*, footage selsyn motor; *g*, selsyn drive gear; *h*, cable connections to selsyn motors; *i*, bail for tie-back chains; *j*, ground manganese steel sheave rim for measuring cable. (Courtesy of Lane-Wells Company.)

geared to a sheave or measuring wheel frictionally contacting the cable, and the other to the film drive (Figure 652). The ratio of film to cable speed is varied by changing the film-drive gears.

The S.P. and the resistivity recorders are of the general type previously described in connection with seismic exploration, with depth markers substituted in place of time markers.

An alternate type of equipment is schematically illustrated in Figure 653. An alternating current, which is generated by a vacuum tube oscillator and has a frequency of approximately 700 cycles per second, flows in the cable to the main electrode and back through the formations to the return electrode at the surface. *Impedance* measurements are made between the single electrode in the well and the surface electrode. At the same time over the same cable, it is possible to measure the D.C. self potential existing between the two electrodes. The single conductor cable therefore serves both for the D.C. and the A.C. measurements.

Measurements are made between the moving electrode *A* in the hole and the stationary surface electrode *B*. Changes in the effective resistance or impedance are recorded on the meter 1. The direct current recording meter 3 is shunted by the large condenser 2, which by-passes the alternating current. The winch and commutator are shown diagrammatically at *C*.

Numerous telemetering arrangements have been proposed for transmitting multichannel information over a single conductor.† To date these devices have not met with favor in well-logging applications because of instrumental complications. Usually the multiconductor cable is cheaper and easier to maintain than the single-conductor cable and more complicated carrier system.

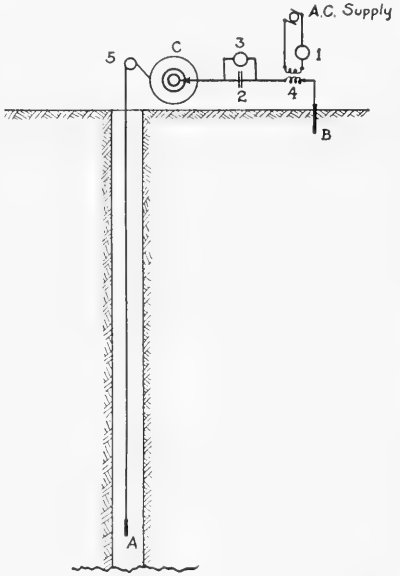

FIG. 653.—Method for simultaneous resistivity and potential logging with single moving electrode. *A*, moving electrode; *B*, stationary surface electrode; *C*, winch and commutator assembly; 1, A.C. recording meter; 2, by-pass condenser; 3, D.C. recording meter; 4, coupling transformer; 5, sheave wheel. (Halliburton Oil Well Cementing Company.)

Induction Logging

Electrical logging, using electrodes, requires electrical contact with the formations. Ordinarily this contact is made through the drilling mud in the bore-hole which usually has a water base and is therefore conductive.

However when the drill hole is empty, as may be the case when the drilling is done with cable tools, or when oil-base mud is used, electrical contact between electrodes and formation is no longer attained by conduction through the drilling fluid. Scratcher electrodes, which are forced by spring action against the wall of the bore-hole to make direct contact with the formations, are often employed. In some cases fairly satisfactory resistivity curves are recorded in this manner, but oftentimes when the

† H. W. Lensner and J. B. Singel, "A Versatile Power Line Carrier System," A.I.E.E. *Tech. Pub.* 44-34, Dec., 1943.

R. C. Cheek, "A Comparison of the Amplitude-Modulation, Frequency-Modulation, and Single-Side-Band Carrier Systems for Power-Line Carrier Transmission," A.I.E.E. *Transactions*, May, 1945, pp. 215-220.

S. Krasnow, "Method and Apparatus for Taking Physical Measurements in Bore-holes," U. S. Patent 2,421,423, June 3, 1947.

W. D. Mounce, "Logging Boreholes," U. S. Patent 2,415,364, Feb. 4, 1947.

A. Frosch, "Well Logging," U. S. Patent 2,436,563, Feb. 24, 1948.

L. Dillon, "Method and Apparatus for Logging Drill Holes," U. S. Patents 2,425,868 and 2,425,869, Aug. 19, 1947.

P. Subkow & L. Dillon, "Method and Apparatus for Logging Drill Holes," U. S. Patent 2,225,668, Dec. 24, 1940.

formations are highly resistant, the measurements are not too reliable because of poor or intermittent contact. To overcome these difficulties *induction logging* may be employed.

Induction logging does not require any direct contact between the exploring device and the mud or the formations. It would work just as well in a hole cased with a highly resistive material such as bakelite or concrete pipe. Like conventional electrical logging, however, it will not work in holes cased with metallic pipe. Induction logging has been operated successfully in water-base drilling muds, and produces a curve very similar to the conventional resistivity curve.

In this method of logging,† the formations are energized by electromagnetic induction. This energizing field is created by an alternating current flowing through a "transmitter" coil, which is one component of the exploring device. The alternating magnetic field induces eddy currents in the earth surrounding the coil. These eddy currents set up a secondary magnetic field, and induce an electromotive force in a "receiver" coil, which comprises the other component of the exploring device. If the energizing current is maintained at a constant value and frequency, the electromotive force thus induced in the receiver coil is proportional to the mutual inductance; i.e., (1) to the spacing between the two coils, and (2) to the conductivity of the earth, and consequently is inversely proportional to the earth resistivity. See pages 605 to 607 for a discussion of the factors affecting the mutual inductance between two parallel coils. A further development of inductive logging has been made using high frequencies.‡

Figure 654A shows schematically a simple induction logging system in which an energizing coil and a receiver coil are wound coaxially on a supporting insulating mandrel. The distance between the coils, designated in the figure as L, is called the *spacing* and remains constant during a run. The larger the value of L, the greater the effective penetration of the flux into the strata.

An alternating current of constant magnitude and frequency (in certain cases, of two different frequencies§) is fed to the transmitter coil from an oscillator, which is housed with the amplifier in a steel cartridge above the coil system. (See Figure 654B.)

The voltage induced in the receiver coil is amplified and then rectified into direct current for transmission through the cable to the recorder at the surface. As in conventional electrical logging, the readings are recorded continuously on film as the instrument traverses the bore hole. The point of measurement is taken to be at point O, midway between the coils.

Before entering the bore hole, the instrument is adjusted (in air) to a reading of desired value. The receiving coil actually comprises two coils: one spaced at distance L (whereby its mutual inductance with the energizing coil is affected by the resistance of the material through which the magnetic flux penetrates) and another coil of very small area and number of turns. This latter coil is positioned close enough to the energizing coil so that its coefficient of coupling is substantially constant regardless of the material surrounding the bore hole. The initial adjustment (to one side of the null

† H. G. Doll, "Introduction to Induction Logging and Application to Logging of Wells Drilled with Oil-Base Mud," A.I.M.E. meeting, San Francisco, February, 1949.

‡ J. W. Millington, "Electrical Prospecting Method and Apparatus," U. S. Patent 2,376,610, May 22, 1945; also U. S. Patent 2,398,800, April 23, 1946.

C. B. Aiken, "Electrical Logging," U. S. Patent 2,390,409, Dec. 4, 1945.

§ C. B. Bazzoni and J. W. Millington, "Electrical Prospecting Apparatus," U. S. Patent 2,408,029, Sept. 24, 1946.

point) is obtained by adjusting the second coil so that its induced E.M.F. will reduce the E.M.F. of the first coil to the desired amount. (See page 613).

The Induction Log—Sensitivity Scales.—In logging practice, the resistivity unit is the ohm-meter. The corresponding unit of conductivity is its reciprocal, the *mho per meter.*† As the usual range of formation conductivities expressed in mhos per meter

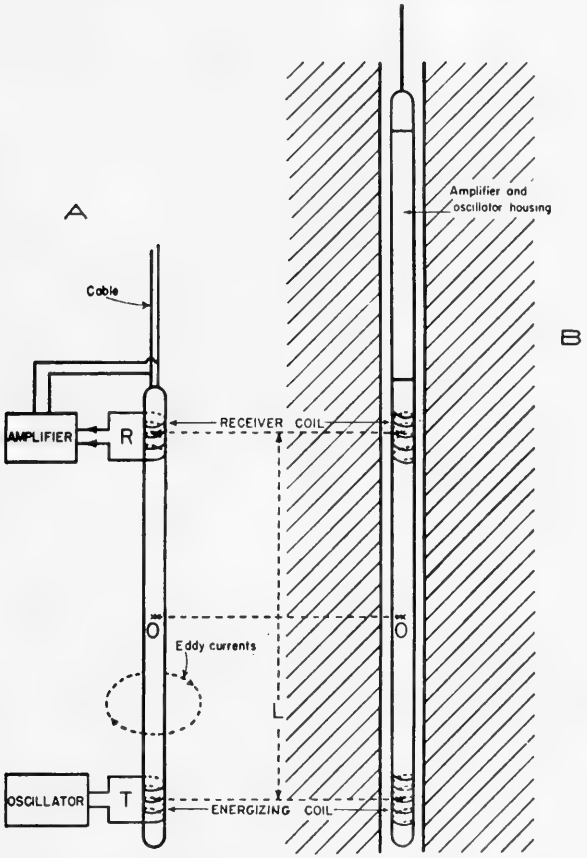

FIG. 654.—Inductive logging apparatus. A, schematic; B, general apparatus arrangement.

would involve extensive use of fractional values, it is preferred to use a smaller unit, the *millimho* per meter.

With this unit:

$$\text{Conductivity (in millimhos per meter)} = \frac{1000}{\text{Resistivity (in ohm-meters)}}$$

For illustration, a bed having a resistivity of 100 ohm-meters would thereby have a conductivity of .01 mhos per meter, or 10 millimhos per meter.

† *Mho* is *ohm* spelled backward.

In Figure 655 is shown a comparison of an induction log with the conventional electrical log in the same well. The resemblance of the induction log to the resistivity log is at once apparent.

Since for induction logging the direct-current signal coming into the recorder is proportional to the conductivity of the formation, the deflection of the trace will also be proportional to the conductivity. Zero conductivity, i.e., infinite resistivity, corresponds to zero signal, and for this case the recorded trace is made to print near the

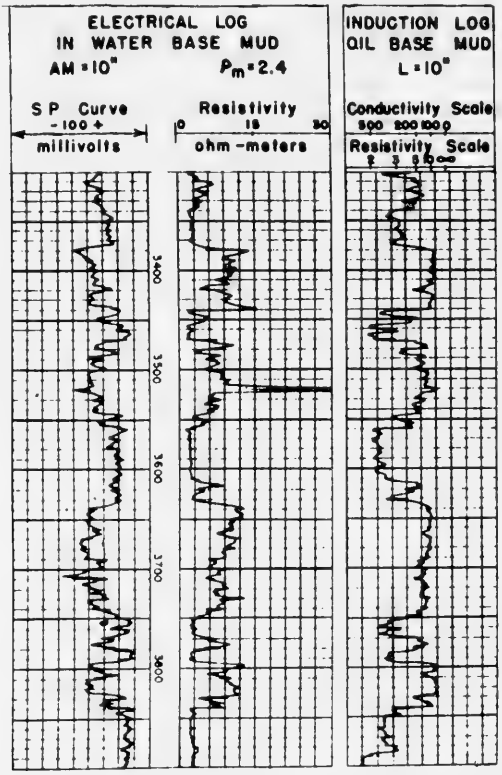

Fig. 655.—Comparison of S.P. and resistivity logs in a conductive mud, with an induction log in an oil-base insulating mud.

righthand side of the film track. Increasing conductivity causes the trace to move to the left in proportion.

The upper sensitivity scale on the induction log of Figure 655 is the conductivity scale (in millimhos per meter), which is seen to be a linear scale. The underneath sensitivity scale is the equivalent scale of resistivity in ohm-meters. The resistivity scale is of course non-linear; variations of resistivity tend to be amplified for low readings and minimized for high readings.

The proper scale for the recording of an induction log will depend on the range of conductivities (or resistivities) to be encountered. It is usual practice to keep the sensitivity low enough so that the greatest conductivities recorded will not go off-scale. However, as already pointed out, variations in resistivity in the more resistive sections

tend to be minimized on the recording, so that if more feature in the resistive sections is desired, it is necessary to make a recording through these sections using a greater sensitivity. Although a great deal of feature cannot be expected for very high resistivities, much more feature is available at low resistivities than on the conventional electric log.

Investigation Characteristics

The investigation characteristics of an induction logging sonde may be described according to the manner in which the apparent conductivity reading is affected by: (1) horizontal variations in the surrounding media; (2) vertical variations in the surrounding media.

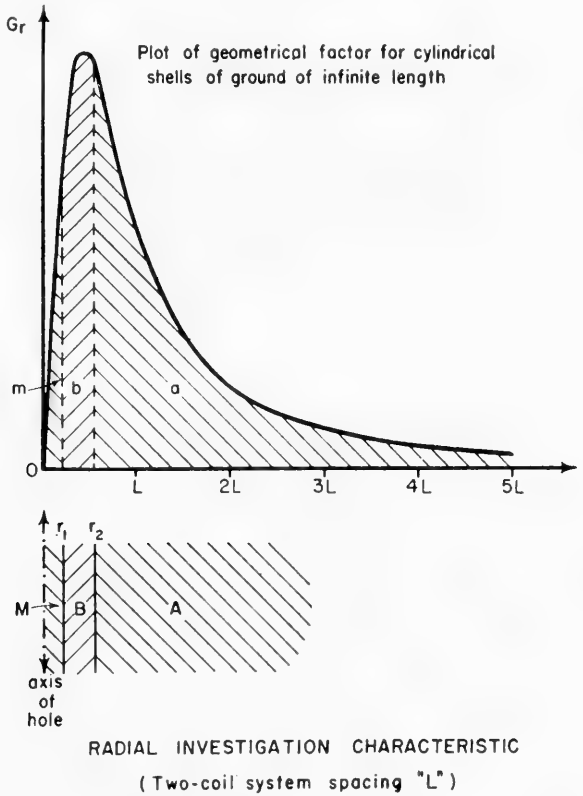

FIG. 656.—Curve showing radial characteristic of two-coil induction sonde.

The first effect is described by means of the radial investigation characteristic, the second by means of the vertical investigation characteristic.

Radial Investigation Characteristic.—Consider a very thick formation in which the conductivity does not vary with depth, but does vary with the radial distance from the axis of the hole; for example, let the formation next to the hole, invaded with mud filtrate, have one value of conductivity, whereas the formation at a distance from the hole has some different value of conductivity. The boundaries between regions of differing conductivity, in this case, are circular cylinders coaxial with the hole.

It is now convenient to consider the medium around the instrument as being divided into a series of thin cylindrical shells of equal wall thickness and coaxial with the hole. Each of these cylindrical shells will have a geometrical factor G_r, which, if the whole medium were of uniform conductivity, would represent the relative portion of the total signal contributed by that shell. Successive values of G_r may be plotted as a function of the radii of the cylindrical shells. In Figure 656 such a plot is shown for the sonde of Figure 654, consisting of one transmitter and one receiver coil. This curve is known as the *radial investigation characteristic* of the sonde.

The curve is zero at the axis of the hole, increasing rapidly to a maximum and then dropping off less sharply as the radial distance is increased. If the medium were

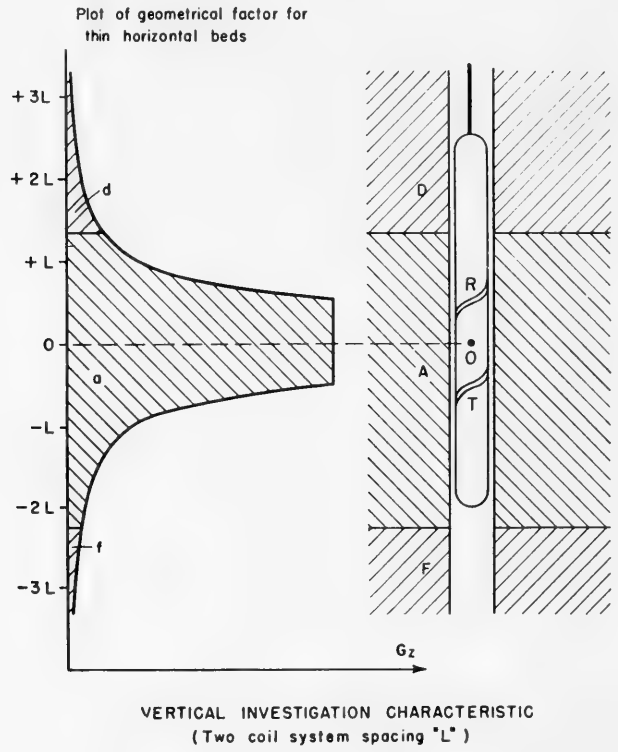

FIG. 657.—Curve showing vertical characteristic of two-coil induction sonde.

homogeneous, the amplitude of the curve would indicate the relative proportion of the signal coming from the formation at different radial distances from the instrument. The radial distance is indicated in multiples of the spacing L.

If, as is also indicated in Figure 656 for values of the radial distance between zero and r_1, the medium is the mud M, and between r_1 and r_2, the medium is an invaded zone B, and beyond r_2, the medium is the uninvaded formation A, the geometrical factors of each of these three zones will be proportional to the corresponding areas, m, b, and a, under the curve, and the relative signal response of each of these areas is the product of its geometrical factor by its conductivity.

The Vertical Investigation Characteristic.—In a similar manner, for the study of beds of finite thickness, it is convenient to think of space as being divided into a great number of horizontal layers of equal thickness. For this purpose, the conductivity of all the medium in any layer can be assumed to be constant, the relative effect of the mud and the invaded zone thus being neglected.

Successive layers have their own geometrical factors G_z, the values of which may be plotted as a function of the distance of the layer above or below the center O of the coil system, as shown for a simple two-coil sonde in Figure 657. This curve is known as the *vertical investigation characteristic.*

If, as shown in Figure 657, there is a bed of finite thickness A between two other beds D and F, the geometrical factor of each of these beds, for the indicated position of the coil system, will be proportional to the respective areas, a, d, and f under the vertical investigation characteristic. The contribution of each area to the signal will be proportional to the product of its conductivity by its geometrical factor.

It has been found that by proper combinations of additional coils, it is possible to minimize the influence of the mud column and the invaded zone, or to minimize the influence of formations adjacent the bed under study.

The sonde assembly is about 4⅛ inches in diameter, 14 feet long, and weighs 250 pounds. Rubber centralizers, up to 8 inches in diameter, are employed for centering the sonde in the bore hole.

Temperature Measurements in Bore Holes

As was shown in connection with Figure 595, the temperature in the earth increases with depth. The rate of increase of temperature with depth is known as the *geothermal gradient,* and varies with the locality and the heat conductivity of the geological formations. Because of the dependency of the geothermal gradient on the conductivity of the formations, measurements of the relative temperature gradients, at various depths of wells in which thermal equilibrium has been established, have been used for the logging of formations. The temperature gradients are in general low in formations having high heat conductivities and high if the heat conductivity is low.†

Temperature measurements offer an independent technique which frequently provides information not available from any other source. Such measurements may be used for determining the height of cement behind casing, logging the position of certain formations, and locating gas or water sands. In contrast to the electrical surveys, the presence of casing has little effect on the temperature measurements. Hence, temperature data may yield valuable information useful in the rehabilitation of declining pumping wells.

Considerable work on thermal measurements has been done by Van Orstrand,‡ Fisher,§ and others who used maximum registering thermometers of the mercury type. Considerable work has also been done with electrical thermometers.††

† M. Schlumberger, H. G. Doll, and A. A. Perebinossoff, "Temperature Measurements in Oil Wells," paper presented at meeting of Institute of Petroleum Technologists, Nov. 10, 1936.

‡ C. E. Van Orstrand, "On the Estimation of Temperatures at Moderate Depths," *Trans. Amer. Geophys. Union,* 1937, pp. 21-23.

§ J. Fisher, L. R. Ingersoll, and H. Vivian, "Recent Geothermal Measurements in Michigan Copper District," *A.I.M.E. Geophysical Prospecting,* 1934, pp. 528-536.

†† E. G. Leonardon, "Thermometric Measurements in Drill Holes," *Geophysics,* Vol. I, 1936, pp. 115-126.

The technique of intermittent readings has not been commercially applied, however, because of the length of time necessary for the well to reach thermal equilibrium and because of the relatively few points which can be read in a reasonable period of time.

Direct Temperature Measurements.—Direct temperature measurements are usually conducted with the aid of an electrical resistance thermometer which is suspended in the drill hole by a two-wire insulated cable. The thermal element of the resistance thermometer is composed of materials whose resistances change rapidly with the temperature. In commercial work, suitable materials are iron, nickel, silver, and certain alloys which have high temperature coefficients.

When employing D.C. measuring or recording methods, the apparatus consists essentially of a small size wire wound on a cylindrical tube of small diameter in a single spaced layer. Because the electrical resistance of this unit is very high, changes in the cable resistance due to temperature changes constitute a relatively small part of the total change in circuit resistance. The thermal unit may be housed in an oil-filled copper container with a small separation between the winding and the walls of the container to minimize thermal lag. Any suitable recorder may be employed. The speed at which the instrument is lowered into the drill hole will be dependent primarily upon the response speed of the thermal unit. A surveying speed of 2000 to 3000 feet per hour is usually possible. Measurements must be made going down in the hole in order to avoid disturbing the mud with its perturbing effect on temperatures. Should a second run be required, it usually is necessary to wait from 6 to 12 hours in order that the original temperature conditions may have time to reestablish themselves.

Measurements Made After Thermal Equilibrium Has Been Established

In this method, a graph is made of depth versus temperature along a drill hole which has been undisturbed for a sufficiently long time to allow the hole and surrounding formations to be in thermal equilibrium. Because of differences in thermal conductivity and temperature, the gradient will tend to be different for different formations, each gradient change corresponding to the boundary between the major thermal zones. The general form of the temperature curve after thermal equilibrium has been reached is illustrated in Figure 658.

Probably the most successful application of temperature measurements has been the location of cement behind casing. The method † depends on the heat produced by the chemical reactions involved in the "setting" of the cement. It has been found that the temperature of the cement,

† C. Schlumberger, "Thermometric Method of Locating the Top of Cement Behind a Well Casing," U. S. Patent 2,050,128, issued Aug. 4, 1936.

and of the drill hole opposite the cement, is at a maximum between twelve and forty-eight hours after cementation, depending on the conditions and the nature of the cement. Consequently, it is only necessary to make one or more continuous temperature surveys during this period. The portions of the hole showing abnormally high temperatures, as compared to the normal curve, indicate the position of the cement behind the casing. (It is desirable to avoid any circulation immediately prior to the survey in order that the thermal conditions produced by the setting of the cement will not be disturbed.)

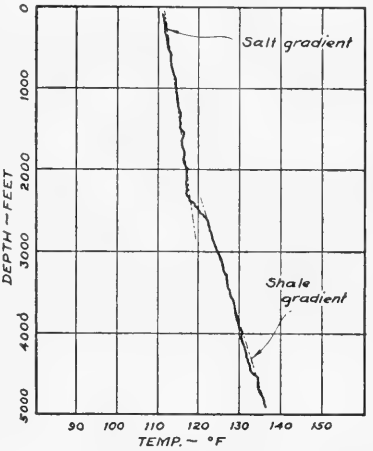

FIG. 658. — Temperature curve after thermal equilibrium has been reached. (Note change in slope at about 2300 feet.)

The temperature log is recorded photographically on film, usually at the same scale value employed for the electrical log. The log extends from a point well above the expected cement top. Above the cement the temperature will generally increase gently, with small anomalies due to the heat characteristics of different formations. When the cement top is reached there is ordinarily a very marked increase in the temperature, and the temperature anomalies due to the formations behind the cement are greatly exaggerated (Figure 659).

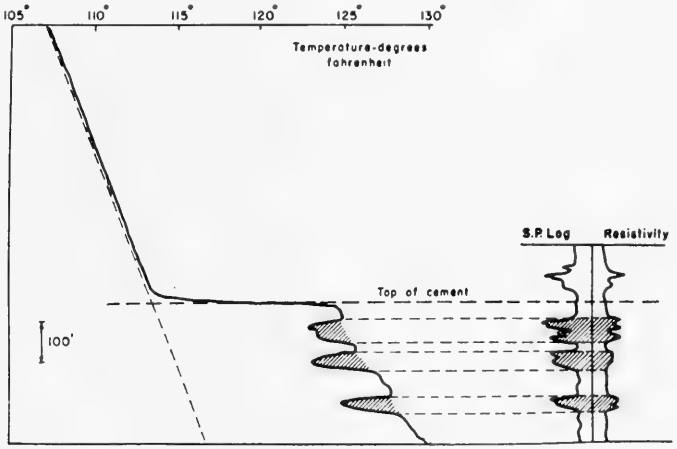

FIG. 659.—Temperature log, showing top of cemented zone.

Cement top indications are usually quite definite and can generally be pointed out as soon as the photographic record of the survey has been developed.

Measurements Made Before Thermal Equilibrium is Established

This method, which is more commonly used than the one described in the last section, utilizes the evolution or change in the thermal gradient, measurements being made before the well is in equilibrium.

In practice, the mud of the well is circulated for several hours before the survey. During this circulation, the mud from the surface is forced down through the drill pipe and returns upward between the pipe and the formations.† At the beginning of this cycle, the mud is cooler than the

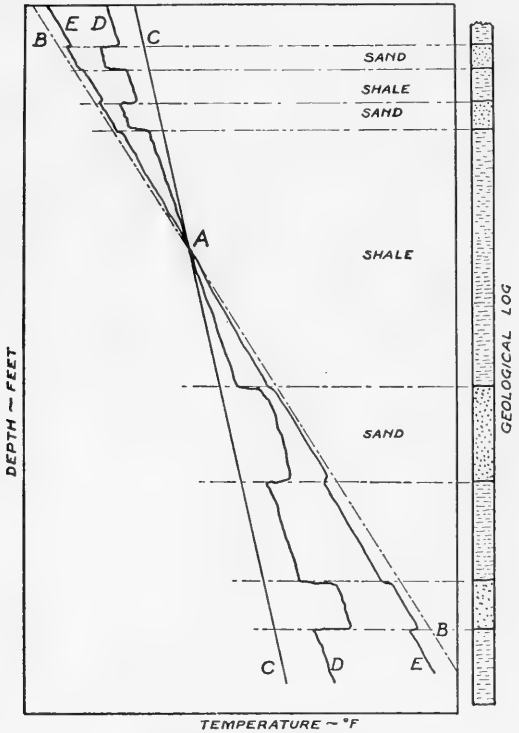

FIG. 660.—Evolution of temperature gradient. (After Leonardon, *Geophysics.*)

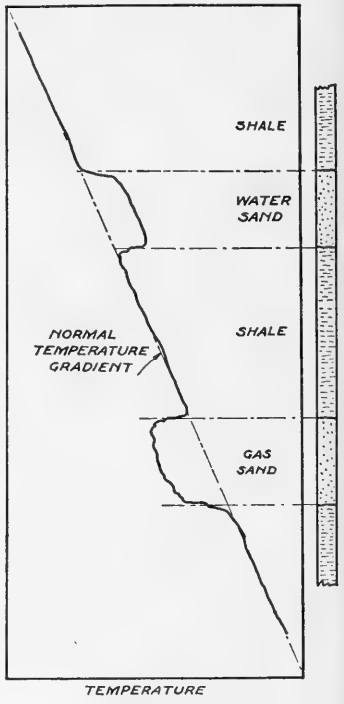

FIG. 661.—Temperature curve illustrating change in thermal gradient at gas and water sands.

normal formation temperature at the bottom of the hole and warmer than the formation temperature near the surface. During circulation, therefore, the formations near the bottom of the hole *give up* heat to the mud, and the formations near the surface *absorb* heat. Finally, when circulation is stopped, the temperature curve for the mud in the hole is approximately a straight line, having temperature values which are lower than the temperatures of the formations in the lower portion of the hole and higher

† E. G. Leonardon, "Thermometric Measurements in Drill Holes," *Geophysics,* Vol. I, 1936, pp. 115-126.

than the temperatures in the upper portion. In Figure 660, the curve *B-B* represents the true temperatures of the formations, and *C-C* the temperatures of the mud immediately after circulation. It will be noted that the curves cross at point *A* where mud temperature and formation temperature are the same.

As the mud temperature and formation temperature seek equilibrium, curve *C-C* rotates about point *A*, tending to approximate curve *B-B*. However, certain formations, due to differences in heat capacity, tend to give up or acquire heat from the well mud faster than other formations. Thus, after a given time, a curve *D-D* is produced which shows deviations from the normal trend at the locations of the sand formations. After a longer time, the temperature curve for the mud approximates curve *E-E* and finally *B-B* wherein the anomalies due to the formations have disappeared.

The operation of this temperature method of logging formations may be summarized as follows. Use is made of a suitable mud circulation, following which a number of temperature curves are recorded in order to obtain curves *C-C*, *D-D*, and *E-E*. (Curve *B-B* is seldom obtained, due to the length of time involved in allowing the formations and mud to reach their original value.)

In the interpretation of the results, use is made of the fact that most gases absorb heat during expansion. Therefore, because a certain amount of gas escapes from a sand during drilling and circulation, a gas sand will be relatively cool, and will produce a temperature drop on the temperature curves. (Figure 661.)

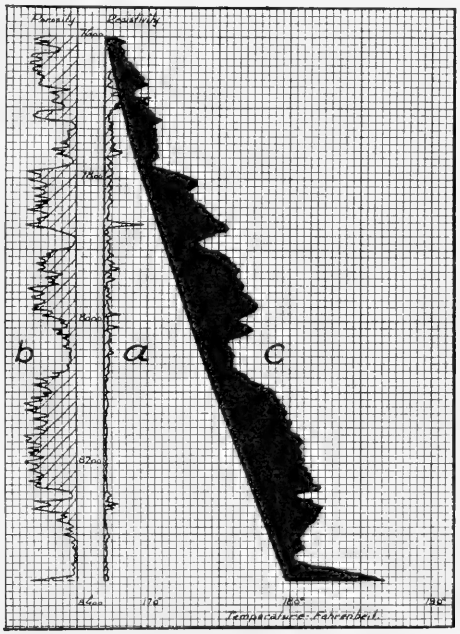

FIG. 662.—Comparison of original resistivity and porosity logs of the uncased well and a thermometric log obtained after setting of casing. (*The Petroleum Engineer*, Feb. 1937, p. 155.)

Under certain conditions temperature data are indicative of structure and hence constitute an important parameter in drill-hole logging. Such a condition is illustrated in Figure 662, which shows a graph of thermometric data obtained after casing was set, and graphs of original porosity and resistivity data obtained prior to setting of casing.

Temperature measurements may also be used to locate lost circulation.

When circulation is being lost, the mud taken by the formation is continually being replaced in the hole by the mud pumps. The temperatures measured in the hole down to the point of lost circulation would tend to be markedly cooler than the equilibrium temperature of the formations.

Below the point of lost circulation, the mud will have been stagnant in the hole for some time, and will be practically at the natural formation temperatures. A noticeable discontinuity in temperature will thus be observed at that depth.

Power Supply for Logging Operations

The characteristics and capacity of the power supply are dependent upon the type of recording and measuring equipment. When direct current, usually periodically reversed by a suitable commutator device, is employed for energizing the ground, the power supply may be a bank of storage batteries or heavy duty dry cells. Such battery supply is usually employed with the mechanical type film feed. This type of feed utilizes a measuring sheave wheel mechanically connected to the film drive mechanism.

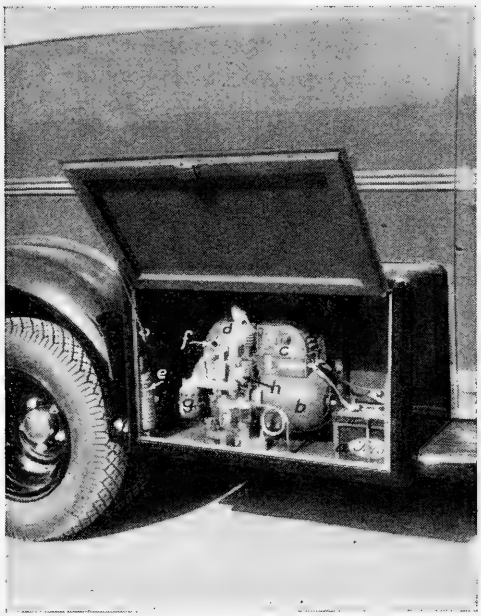

FIG. 663.—ONAN gasoline-driven alternating current power supply. *a*, storage batteries for starting; *b*, alternator; *c*, control panel and relays; *d*, two-cycle gasoline engine; *e*, demountable muffler; *f*, exhaust line; *g*, air cleaner; *h*, carburetor. (Courtesy of John C. Stick, Jr.)

When the energizing current is alternating or when the power must be transformed to different potentials, as for supplying the plate current in amplifying tubes or oscillators, some form of alternating current power supply is most desirable. Alternating current is also required if the interlocking synchronous motor system is employed between the measuring sheave wheel and the film drive. The alternating current for these purposes may be supplied by one of two convenient methods. The first method utilizes a bank of storage batteries, usually 200 ampere-hours and 32 volts, which supply direct current to a suitable rotary converter. The output of the converter is usually 110 volts at 60 cycles, which may then be transformed to any desired potential. The storage batteries are charged by rotating or vacuum rectifier equipment whenever the

truck is at its base station garage. The second method for power supply utilizes a small gasoline engine direct-connected to a 110-volt 60-cycle alternator. A 1000 watt ONAN outfit is illustrated in Figure 663. Numerous generating units of this type are available on the market. They may be obtained generally in sizes ranging from ¼ to 10 kilowatts capacity.

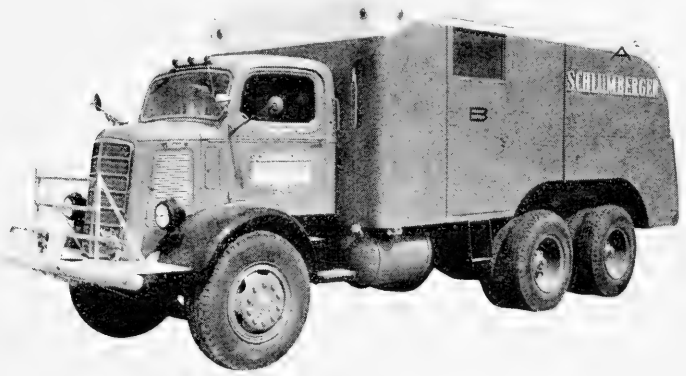

FIG. 664.—Electrical logging truck containing cable reel and instruments. A, reel compartment; B, instrument and control compartment. (Courtesy of Schlumberger Well Surveying Corporation.)

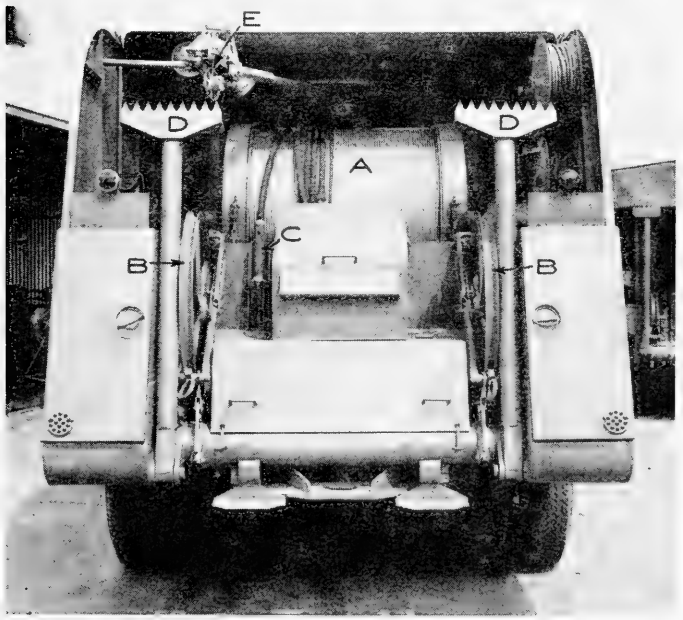

FIG. 665.—Electrical logging truck, showing reel compartment, preparatory to making set-up at well. A, cable; B, sheave wheel; C, threaded sleeve for connecting to device; D, safety stops; E, measuring sheave wheel. (Courtesy of Schlumberger Well Surveying Corporation.)

Field Equipment

Electrical logging operations are performed using trucks provided with the following equipment: various sondes, reel and cable, control panel containing the necessary circuits, the pulsator, photographic recorder, blow-out preventer, weight indicator, film-developing tanks and printers, resist-

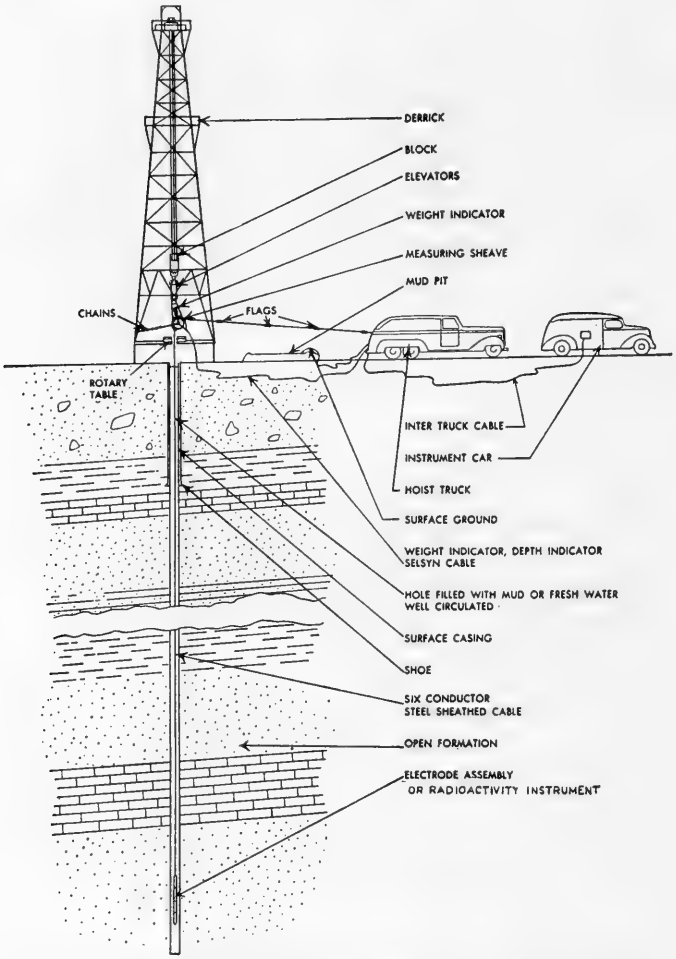

FIG. 666.—Schematic set-up for electrical logging of oil wells. (Courtesy of Lane-Wells Company.)

ivity cell for measuring the resistivity of the mud, etc. In addition they must carry a source of power. All of the equipment may be carried in one truck, as illustrated in Figures 664 and 665, or it may be divided between a hoist truck and an instrument car. The two-car set-up is shown schematically in Figure 666.

The sonde is a system of electrodes, mounted on an insulating mandrel, which is lowered into the hole on the end of the cable, to which it is connected by means of a threaded sleeve. The cable passes over a sheave located at the surface above the bore hole. In order to raise or lower the sonde in the hole, the cable is wound or unwound on a reel, set permanently on the truck and driven by a power take-off from the engine of the truck. The various electrodes of the sonde are connected by means of insulated conductors in the cable, through a slip-ring collector on the reel, to the appropriate terminals of the recording instruments.

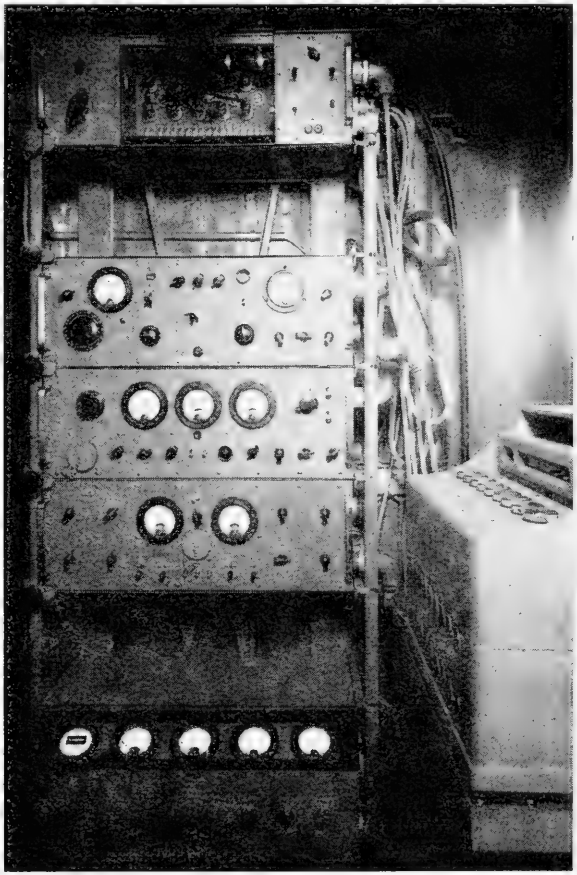

FIG. 667.—Control panels and recording camera for electrical logging of oil wells. (Courtesy of Schlumberger Oil Well Surveying Company.)

In the recorder a photographic film is exposed by narrow beams of light, reflected from each galvanometer mirror. The deflection of each beam of the film is proportional to the potential difference being recorded by that galvanometer. The circuits are adjusted so that suitable sensitivity scales for the S.P. and apparent resistivities are obtained. Figure 667 is a view of the control panels and recording camera.

The film in the recorder moves in synchronism with the movement of the sonde along the hole, so that the effect of each light beam is to trace on the film a curve,

which at a position on the film corresponding to a given depth of the sonde has an amplitude indicative of the magnitude of the S.P. or apparent resistivities measured at that depth. The film drive is usually connected by a servo-mechanism with the sheave or a measuring wheel frictionably held against the cable. By use of suitable gearing, a proper relationship is obtained between a given movement (in feet) of the cable, and a movement (in inches) of the recording paper, usually 1″ to 100′, 2″ to 100′ or 5″ to 100′. A sheave wheel feed system is illustrated in Figure 652.

Modern equipment for the electrical logging of deep wells may employ as many as six conductors, in an armored cable, connected to a nine-galvanometer recorder. This equipment is appropriate for service in the deepest holes, and can record on a single run: the S.P. curve, three resistivity curves, including as well reduced sensitivity scales for each of the resistivity curves where necessary, and an amplified recording of the short normal, if desired. For shallow wells, a four-conductor cable covered with nylon braid is often used with a nine-galvanometer or a five-galvanometer recorder.

The standard electrical logging sonde can be used in holes as small as 5″ in diameter. For smaller holes special core-hole equipment is available.

Photographic means are usually provided for developing and fixing the film immediately upon completion of the survey. The film is then dried. If required, short prints may be made of the section of immediate interest.

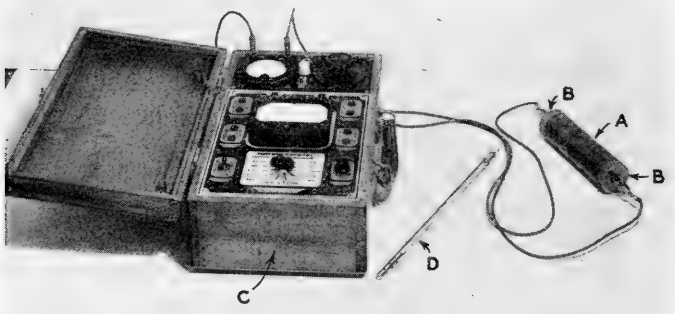

Fig. 668.—Resistivity cell for determining the specific resistance of the drilling mud. A, plastic cylinder; B, end contact plugs; C, ohm-meter; D, thermometer.

A resistance cell and thermometer should be provided for determining the specific resistance of the mud. One type of cell is illustrated in Figure 668, and comprises a plastic cylinder of known cross-sectional area, fitted with metal end contact plugs, spaced a fixed distance apart. A thermometer is immersed in a well, for measuring the cell temperature at the time the resistivity determination is made. A conventional ohm-meter may be employed for measuring the resistance of the cell. The specific resistivity of the mud may then be calculated, knowing the area of the mud and the distance between the end plugs. (See page 467.)

METHODS OF LOCATING WATER SOURCES IN A DRILL HOLE

The location of the source, or point of entrance, of formation water in oil wells is a problem of considerable economic importance in oil production. It is good engineering practice to keep the production of

water at a minimum because this reduces the pumping, treating, and disposal costs, and in addition reduces corrosion damage to casing, pump, rods, and tubing. Also, in many fields, the maintenance of reservoir pressure is dependent upon the formation water, and a minimum water production will insure a longer flowing life for many wells.†

Repair operations to stop the flow of water into a well must be preceded by a means for locating the point where the water is entering the well. Several geophysical methods have been developed for determining the depth at which water is entering the hole. Usually, proper interpretative technique, based on production experience, will show the cause of water entrance and its remedy.*

In contrast to the previously described electrical logging methods, the methods under discussion utilize means for causing the water to enter the drill hole from the formations, as well as means for locating the point of entry. Thus, for these methods, the hydrostatic pressure must be reduced by bailing, in order to allow the formations to produce into the hole.

Resistivity Methods.—In contrast to the use of resistivity methods for structural studies, this application requires that the sphere of measurement be confined substantially within the bore hole. The method of Figure 634 may be applied by reducing the lengths of r_1 and r_2 to values somewhat smaller than the radius of the bore hole.

During resistivity measurements, the hole should be conditioned with fresh water if the formation fluid is salty and with conductive salty fluid if the water source produces fresh or relatively non-conductive fluid. Immediately after the conditioning, a survey is made to verify that the column of fluid in the bore hole is of uniform resistivity. Following this, the well is bailed and a second survey made. The entire procedure (bailing and temperature surveying) is repeated until a change of resistivity, produced by the entrance of water into the well, is noted.

Early work along these lines was done by Schlumberger, Huber‡ and Elliott.§

Natural or Self Potential Method.—The spontaneous potential method utilizes the electrochemical potentials previously described. Obviously, if a well is conditioned with a fluid of different electrolytic concentration than that of the formation fluid and if water is then caused to flow into the hole from the formation, a potential will exist at the boundary between the entering fluid and the conditioning fluid.

This method uses two electrodes, situated only a short distance apart, and suspended on a cable. The parameters measured, therefore, are the potential gradients. Conditioning of the well is effected by circu-

† P. T. Amstutz, Jr., and E. A. Stephanson, "Optimum Producing Rates for Arbuckle Limestone Wells," Univ. of Kans. Research Foundation, *Bull. 1*, Sept. 1944.

* H. G. Abadie, "Method and Apparatus for Locating Leaks in Wells," U. S. Patent 2,383,455, Aug. 28, 1945.

‡ F. W. Huber, U. S. Patents 1,536,007; 1,555,800; 1,555,801; 1,555,802; and 1,555,803.

§ R. D. Elliott, U. S. Patent 1,537,919.

lating a suitable mud. For example, Ennis† has developed methods wherein the desired electrolytic concentration of the mud is produced by lowering a soluble electrolyte into the hole. The bailing process is then used to cause a flow into the well. Measurements of the electrochemical potentials are made throughout the length of the hole, before and after bailing.

Thermometric Method.—The thermometric method does not require special conditioning of the mud. The only preparation necessary is circulation. Measurements of this type are particularly adapted to dynamic wells and to wells in which there is an interchange of fluid between two formations.

In one actual case, a well was drilled to 6441 feet, with casing set at 6373 feet. When tested, the well produced no water and only a small amount of oil. A small nitroglycerine shot was then made, after which water appeared. It was believed that the shot had caused bottom water to break into the well. After standing for several days, the fluid level rose to about 2400 feet.

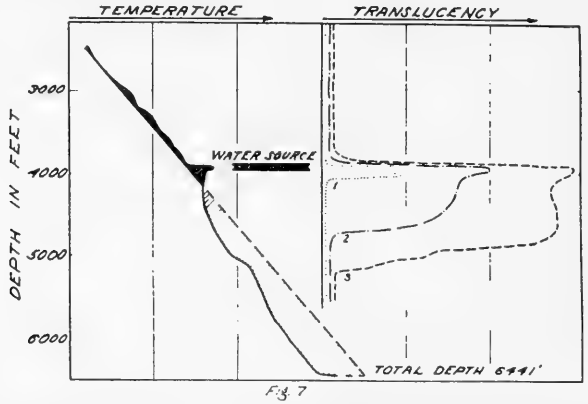

FIG. 669. — Comparison of temperature data and photoelectric data for the same well. (Courtesy of Schlumberger Oil Well Surveying Corp.)

A thermometric survey was then made. (Figure 669.) The temperature-depth curve showed an abrupt temperature change between 3913 and 3945 feet. The temperatures above the anomaly followed the normal curve, and the temperatures below the anomaly were less than the normal values. The data suggested that the temperature increase between 3913 and 3945 feet was due to entrance of water which had a slightly higher temperature than the normal temperature of the bore hole at that depth.

This water had a temperature of approximately 106° and flowed *down* the hole. Hence, it exerted a cooling effect on all formations below,

† Geo. H. Ennis, U. S. Patents 1,725,979; 1,786,196; 1,865,847; 1,889,889; 1,994,761; and 1,994,762.

because the normal temperatures of these formations are higher than 106°. This well will be discussed further in connection with the photoelectric method.

Photoelectric Method.—The photoelectric method locates water flows by measurements based on variations in the translucency of the drill-hole fluid. Usually, the static column standing in the hole will have clear fluid in the upper part. Also, formation water entering a well is more translucent than muddy water or oil. Hence, it is necessary that the well fluid in the interval to be surveyed be made opaque by suitable conditioning in order to offer a contrast with the clear formation water that will enter when the fluid level is reduced by bailing or swabbing.

Conditioning of the well is done by one of two methods. In flowing wells, it usually is necessary to stop the flow and circulate a well-mixed muddy water. This usually gives the required opaqueness. In pumping wells, the interval to be surveyed can be conditioned by the use of a special dump bailer that can be tripped either at the bottom or at any desired depth.

The instrument for measuring the translucency of the liquid in the hole is about 2″ in diameter and 30″ long and consists, essentially, of a constant source of light, which is energized by dry cells, a selenium photoelectric cell, and louvers through which the fluid circulates. As the instrument is raised or lowered in the hole, the fluid passes between two windows which define the path through which the light rays reach the selenium cell. Variations in the translucency of the mud cause variations in the amount of light reaching the photoelectric cell, with corresponding variations in the current output. The cell is connected by means of an insulated cable to a continuous recording meter at the surface. The recording film, which is moved in synchronism with the cable, uses an arrangement similar to that described for the resistivity logging method. The photoelectric log is a plot of depth versus a parameter which is proportional to the translucency of the liquid passing through the instrument.

The practical application and interpretation of the photoelectric data* may be best illustrated by actual examples. The photoelectric data shown in Figure 670 were obtained in a well in which mud was dumped throughout the open hole. A conditioning run with the instrument gave curve number 1. The linear character of the curve showed that all the fluid in the zone that was being examined was opaque and would therefore offer a contrast to any translucent formation water which might enter the drill hole in that zone. Fluid was then bailed from the well and subsequent runs (Nos. 2, 3, 4) indicated that translucent water was entering from the bottom ten feet of the exposed formation. This determination allowed the operators to confine the cementation to the water-bearing zone, thus preventing the loss of oil resulting from cementation of a portion of the oil-bearing zone.

* The analysis is comparable to that employed in the electrical resistivity drill hole methods.

Another example, Figure 669, shows the relation between thermometric measurements and photoelectric recordings on the same well. The thermometric data for this well have already been discussed. After obtaining the temperature anomaly between 3913 and 3945 feet, that section of the hole was conditioned by dumping several barrels of mud through the interval. The photoelectric instrument was then lowered into the well. A translucency versus depth graph (curve 1) obtained immediately after the conditioning run showed that 150 feet of translucent water had entered the hole. (Note that the water was entering at 3915 feet and going down.) The instrument was pulled up, and 45 minutes later it was again lowered

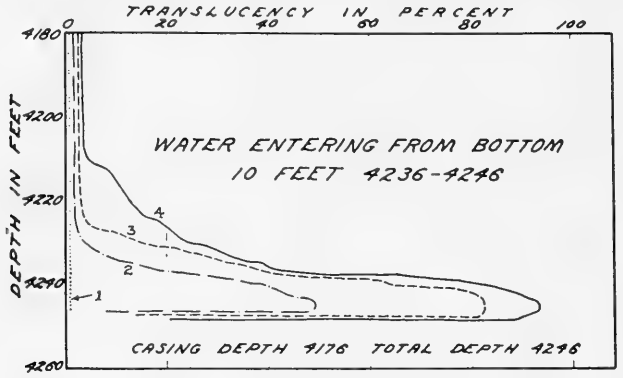

Fig. 670.—Photoelectric survey. Graph shows that water entered at bottom of well from exposed formation. 1, initial curve after conditioning well; 2, 3, 4, curves after formation water entered well. (Dale and Deleney, Personal Communication.)

through the zone (curve 2). This curve showed 500 feet of clear fluid, and hence indicated a rate of flow of at least 400 feet per hour. This quantity of water entering at 3900 feet and going down into the producing formation would soon have flooded not only this one well but also the nearby producing wells had it not been shut off by cementing.

Correlation of Oil Well Waters

An analysis of the salts of oil well waters oftentimes allows correlating the waters with regard to their origin. † Oil well waters commonly contain, in addition to various other elements, lithium, sodium, potassium, calcium, strontium, and barium. The procedure is as follows: Well waters are evaporated to dryness and the residue volatilized in a direct current carbon arc. The light emitted by the arc is photographed by a grating spectrograph.*

† M. F. Hasler, "The Spectrographic Correlation of Oil Well Waters," *Geophysics*, Vol. 2, No. 2, March 1937, pp. 127-131.

J. S. Ross and E. A. Swedenborg, "Analysis of Waters of the Salt Field Applied to Underground Problems," *A.I.M.E. Petroleum Technology*, 1928-29.

* A grating spectrograph comprises a slit, a lens, a grating, and a camera. The camera records the "spectral lines," i.e., images of the slit, characteristic of the "excited" substances—in this case, the elements present in the salts.

The statistical treatment of the data may be illustrated by a practical instance. Suppose a number of samples from each of several water zones are analyzed. Mean values are calculated from several samples of each zone. Suppose further that the mean value of the ratio of the potassium to sodium content is very different in each of the zones and the deviations from the mean are small, then this ratio is assumed to be diagnostic. It is postulated that by setting up several diagnostic factors, inferences can be drawn regarding the origin of the water zones.

THE DIPMETER

In the study of geological structures and in the selection of locations for new wells, it is important to know the angle and direction of the dip of the strata. The dip of the strata may sometimes be determined by the study of mechanical cores, cut under special conditions. Various other methods have been employed, but generally they have met with limited success.

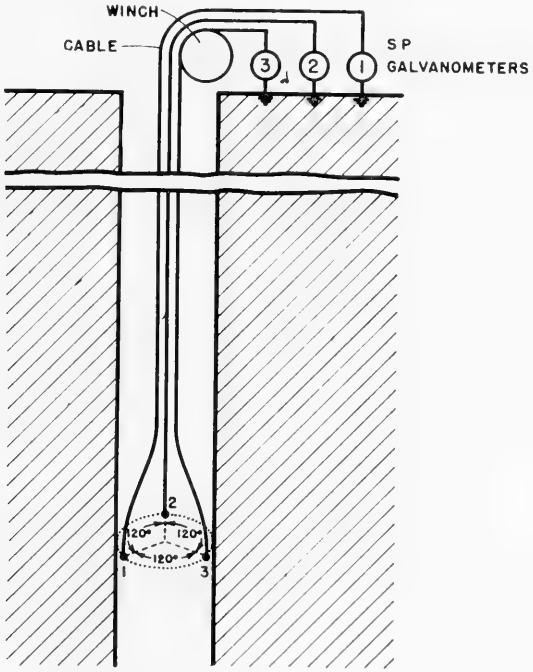

FIG. 671.—Schematic arrangement for logging the spontaneous potential on three sides of a bore hole.

Dip Determination between Wells.—Dip measurements are often obtained by correlating the electric logs of at least three wells or drill holes not in a straight line. The correlation lines passing through the same formations in the three wells define the plane of the formations. This method

is operative where there are no geological disturbances between the wells and when three correlatable logs are available.

Electrical dipmeters† utilize a somewhat similar idea, but require the use of only one well. The principle is illustrated by the electrode arrangement shown schematically in Figure 671, in which the spontaneous potential is logged simultaneously on three sides of an uncased hole. The three independent electrodes are located 120° apart in a plane perpendicular to the axis of the instrument and are mounted at a radial distance such that they are all fairly close to the wall of the hole. (Also see page 506.)

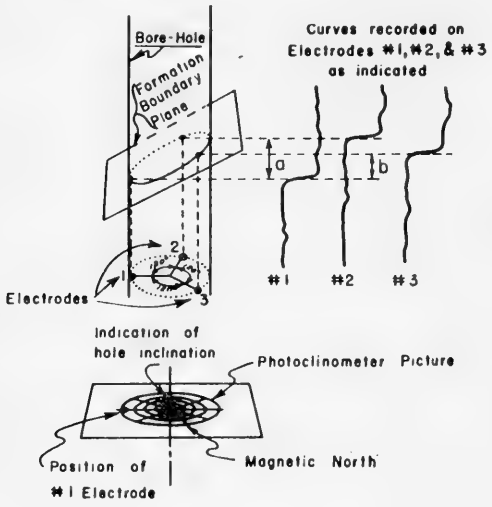

FIG. 672.—Schematic arrangement of the S.P. dipmeter.

In Figure 672, curves 1, 2, and 3 represent the S.P. curves recorded simultaneously by each of the three electrodes as the sonde traverses the bore hole. The sharp break in each curve represents the instant when the corresponding electrode crosses the formation boundary. It is noted that these breaks are not recorded at exactly the same depth on each electrode, but differ by an amount a for electrodes 1 and 2 and an amount b for electrodes 1 and 3. These variations in depth correspond to, and are a measure of, the dip of the formation boundary, and consequently of the formations themselves.

If the hole were assumed to be vertical, it would be easy, knowing the diameter of a circle through the dipmeter electrodes and the differences in depth between correlated points on the recorded curves, to calculate the angle of dip of the formations. In order to determine the direction of the dip, the orientation of the instrument must be known.

When the drill hole is not vertical, as is the general case, the problem becomes more complex, and for the correct evaluation of the angle of dip a knowledge of the inclination of the hole and of the orientation of the instrument is also necessary. The additional data required to determine completely both the amount and direction of the dip are furnished by a photoclinometer which is included as a part of the dipmeter assembly. The photoclinometer picture (bottom of Figure 673) serves two purposes: (1) a triangular marker (a) on the edge of the picture shows the position of the #1 dipmeter electrode with respect to magnetic north, i.e., indicates the orientation of the instrument; and (2) the position of the black dot (b) shows the amount and direction of inclination of the drill hole from the vertical.

† H. G. Doll, "The S.P. Dipmeter," *A.I.M.E. Tech. Pub.* 1547 (1943).
H. G. Doll, "Method and Apparatus for Determining the Dip of Strata Traversed by a Borehole," U. S. Patent 2,427,950, Sept. 23, 1947.

It may be seen that similar results may be obtained by making measurements of resistivity, or of some other formation characteristic, instead of S.P. measurements; and in some geological territories the resistivity dipmeter has definite advantages, particularly in "hard rock" areas where the S.P. curve may have little feature, but where satisfactory correlating points are available on the resistivity curve. The resistivity sonde comprises a current electrode centered in the hole, between three pairs of potential measuring electrodes, positioned on three sides of the hole. The potential difference observed between each pair of measuring electrodes, due to the flow of the current, is amplified and transmitted to the surface where it is recorded. The three curves are recorded simultaneously and, as with an S.P. dipmeter recording, the relative depths at which correlated anomalies occur on the three curves are used to determine the dip.

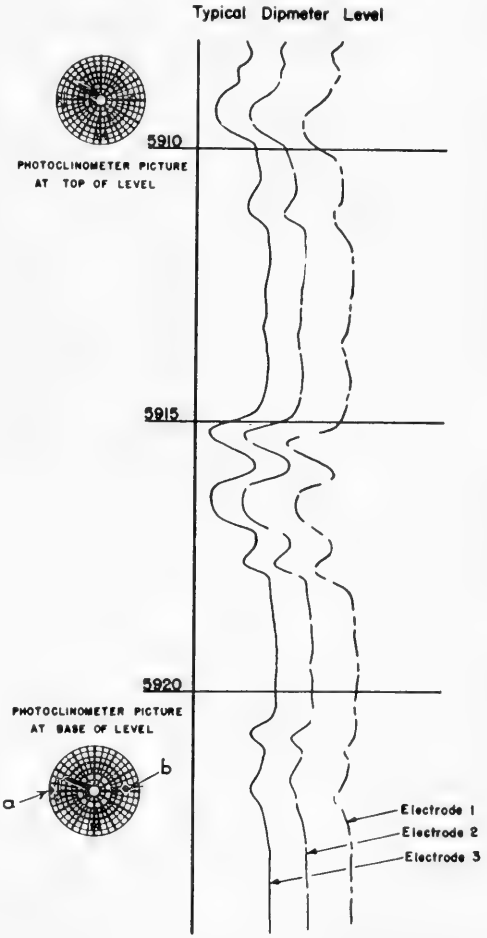

FIG. 673.—Typical S.P. dipmeter curves, showing photoclinometer pictures at top and bottom of the section.

Equipment for Dipmeter Surveys.—The hole unit assembly is about 25 feet long and weighs about 400 pounds. The dipmeter electrode unit consists of a mandrel to which are attached three hard rubber arms spaced 120° apart; in the center of each arm is one of the three pairs of recording electrodes. For an S.P. dipmeter survey, only one electrode of each pair is used; for a resistivity dipmeter survey, both are used. The corresponding electrodes of each of the three pairs are located in the same plane perpendicular to the axis of the instrument.

The hard rubber arms on which the electrodes are mounted are interchangeable and come in several sizes. The size is chosen so that the dipmeter electrodes will be positioned close to the wall of the hole. It is therefore necessary for the operator to know in advance the average size of the hole. The smallest hole in which present dipmeter equipment can be run is 6 inches in diameter. The accuracy decreases with the diameter of the bore hole.

Above the electrode unit is positioned the photoclinometer, which determines the orientation of the three S.P. or resistivity curves, and gives the drift and azimuth of the drill hole. Spring guides above and below the photoclinometer electrode assembly serve to keep the device centered in the hole and to prevent it from rotating. The same cable and truck are used as for electrical logging. The three S.P. or resistivity dipmeter curves are recorded at the surface by the standard electrical logging recorder.

Field Procedure.—Common practice is to run the dipmeter immediately following the electrical log. The levels to be examined for dip are chosen, as explained later, from the electrical log. Meanwhile, the dipmeter assembly—electrode unit, photoclinometer, and spring centering guides—has been made up to the cable and lowered into the hole.

The assembly is lowered to a point in the hole just below the first level or zone. After a short interval to allow the compass needle and the indicating ball in the photoclinometer to come to rest, a photoclinometer picture is taken. This picture is used to determine the orientation of the electrodes and the inclination of the drill hole at the base of the level. The assembly is then pulled slowly up the hole, and the three dipmeter curves are recorded to the top of the level. At that point, the dipmeter assembly is again stopped long enough to take another photoclinometer picture. If the level is unusually long, an intermediate photoclinometer picture may be taken in the middle of the level. These recordings will permit the interpreter to ascertain if the assembly has rotated excessively while being pulled up-hole.

The recording of one run over a typical S.P. dipmeter zone is shown in Figure 673. The three curves are recorded on an enlarged depth scale, and are coded as solid curve, dashed curve, or long-dash, short-dash curve, according to which pair of electrodes was used to make the recording. The photoclinometer pictures at the bottom and top of the level are also indicated.

Interpretation and Accuracy.—The accuracy of the measurements will vary according to the value of the dip angle, the sharpness of the breaks or other electrical markers in the recorded curves, the angle of drift of the bore hole, and the diameter of the dipmeter electrodes, which depends on the hole diameter. Under normal conditions, it has been found that for dip angles of 10° or greater, the accuracy is very good; between 5° and 10° reliable determinations can be made when the correlations between the curves are good and when the inclination of the hole is not too great; below 5° it is possible to give only the general direction of the dip.

Selection of the Zones of Measurement.—Experience indicates that the usefulness of a dipmeter survey depends principally upon a careful selection of the depth zones over which the measurements are made. It is important that the sections chosen include geologic or stratigraphic features which are consistent laterally for some distance and which are not greatly affected by local lensing, cross-bedding, or faulting. A good way to determine this, when possible, is to examine electrical logs of nearby wells and to select zones containing formations which repeat from well to well.

It has been found that the most satisfactory zones for dip measurements are those consisting of relatively thin beds, 2 to 10 feet thick, having sharp contacts with adjacent formations. Such zones for a resistivity dipmeter level are thin limestones or resistive sandstones interbedded with shale, or for an S.P. dipmeter level, thin sands or sandstones interbedded in shale.

On the other hand, thin shale or sandy shale beds within thick sand sections, and thin shale beds or minor resistivity variations within a massive limestone, frequently give erratic dip determinations.

Areas of Application.†—Those regions where the geologic section is primarily sand and shale, i.e., California or the Gulf Coast, are best suited for the use of the S.P. dipmeter. The spontaneous potential here in general shows sharp, well-defined anomalies at formation boundaries which give definite dip determinations. Likewise, in these areas, a series of bedding surfaces between sand and shale can usually be found at any depth in a well where a dip determination is needed.

The resistivity dipmeter, on the other hand, has proven of utility in such areas as West Texas, the Mid-Continent, and the Rocky Mountains, where the features of

† E. F. Stratton and R. G. Hamilton, "Application of Dipmeter Surveys," A.I.M.E. meeting, Tulsa, October, 1947.

the S.P. curves are often not sharp enough to permit the S.P. dipmeter to be used with safety. The numerous resistivity anomalies between, for example, shale and limestone, found in most wells in these areas provide satisfactory levels for dip determinations at almost any position in a well.

THE PHOTOCLINOMETER†

The photoclinometer is an instrument for measuring the angle a drill hole deviates from the vertical, known as the *drift,* and the direction of the deviation, known as the *azimuth.* In common with other instruments using a magnetic compass, the indications of azimuth are not reliable, inside of steel casing. The indications of drift in cased portions of the hole are valid, however, as regards the deviation of the casing from vertical.

By means of either an extension rod with weight at the lower end, or guides on the instrument case, the axis of the instrument is kept parallel to the axis of the hole. The inclination of the instrument itself is then the quantity measured.

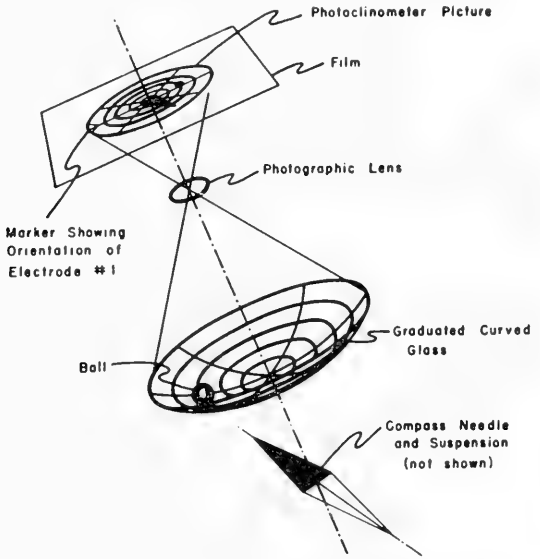

FIG. 674.—Schematic arrangement of parts of the photoclinometer.

Inside the instrument are contained the elements pictured in Figure 674. A magnetic compass is mounted on gimbal rings and gives (in uncased holes) the reference datum as to direction. A metal ball, rolling free on a graduated, spherically-curved glass, indicates by the position it seeks at rest the amount of the drift, and also by comparison with the direction of the compass needle, the azimuth. A photographic lens focuses the images of the compass needle, metal ball, and calibrated glass onto a

† A predecessor of the photoclinometer was the electromagnetic teleclinometer which determined orientations by comparing the magnetic fields of the earth and of a solenoid vertically suspended in the instrument. The measurements were made by means of an induction compass, which is essentially a rotating coil in which an E.M.F. is induced due to the magnetic field linking the coil. (C. and M. Schlumberger and E. G. Leonardon, "Electrical Coring, a Method of Determining Bottom-Hole Data by Electrical Measurements," *A.I.M.E. Tech. Pub.* No. 462, pp. 34-36.)

35 mm. photographic film, so that the resulting picture has the general appearance of Figure 675.

Since the compass needle is painted half black and half white, an image of the white end only registers on the film to indicate magnetic north. The radial lines, which are 10° apart, facilitate reading differences of azimuth.

Sometimes it is necessary, as in the case of a dipmeter survey, to know also the orientation of the instrument. For this purpose on one edge of the graduated glass a triangular marking is provided which conventionally indicates on the film the side of the instrument on which the #1 dipmeter electrode is located.

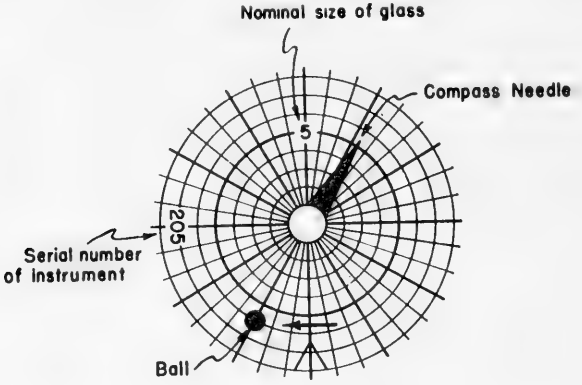

FIG. 675.—Photoclinometer picture.

The position of the ball with reference to the successive concentric circles of the graduated glass indicates the drift. Interchangeable in any given instrument are various sizes of graduated glasses: usually a glass of 5° nominal size which indicates drift angles up to 7°; a glass of 10° nominal size which indicates drift angles up to 15°; and a glass of 20° nominal size which indicates drift angles up to 27°.

Field Procedure.—Photoclinometer surveys are run on multiconductor cable of the same type used for electrical logging; it is usual to perform this operation in uncased holes after an electrical log has been run, using the same truck. It is possible to run a photoclinometer survey in conjunction with a section gauge survey on the same trip in the hole.

Referring to Figure 675, in which a 5° glass has been used, it can be seen that each successive circle is 1° apart in drift, and that the position of the center of the ball represents a drift of 6°.

In the same figure the azimuth angle measured in a clockwise direction from magnetic north to a radial line through the center of the ball is 177°. The azimuth angle with respect to true north, or true bearing, is now calculated by correcting for the declination. It is general practice to give the true bearing in degrees east or west of north or south.

Presentation of the Results.—The "horizontal footage" is the distance the hole deviates laterally, irrespective of direction, between successive stations. It is computed by the formula:

Horizontal Footage = length of interval between stations • sine of drift angle

The vertical footage is the vertical distance between successive stations corrected for shortening due to drift. Unless the drift angle of the hole is very large, this quantity differs little from the nominal vertical distance between successive stations. The vertical footage is computed by the formula:

Vertical Footage = length of interval between stations • Cosine of drift angle

The *latitude* is the distance the hole travels north or south between successive stations. Similarly, the *departure* is the distance the hole travels east or west between successive stations. The *coordinates* are the values of the latitude and departure cumulated from the casing shoe down to the depth for which the coordinates are given. The coordinates actually give the position of the hole at that depth using the position of the casing shoe as the reference point.

The coordinate data are used to construct a curve or plot of the computed course of the hole, starting from the casing shoe and going down to the bottom.

SIDE-WALL SAMPLING

The various logging records previously described indicate certain physical properties of the formation, and this information must be translated into terms dealing with the constitution of the rocks and their fluid content. It is often difficult, however, to interpret completely certain portions of the logs, since there is not always an unequivocal correspondence between the electrical measurements and the geological properties. Certain data, such as porosity, permeability, paleontological characteristics, etc. can be determined uniquely only by the analysis of actual samples taken from the formations.

Inspection of the cuttings, brought continuously to the surface by the circulation of the mud during the drilling, often is a valuable source of information, but, in general, not sufficiently complete and accurate for practical purposes. The conventional means of coring, by the rotary method, is the best way of getting the most reliable information, but coring is time-consuming and expensive, and only the horizons of most interest, chiefly reservoir rocks and certain geological markers, are cored. One big difficulty when coring is in estimating the probable depths of these horizons, and, with a reasonable margin of safety, coring through those sections only. In fact, key horizons may be passed inadvertently while the drilling is being performed. It is oftentimes considered a safer and more economical practice to proceed with the drilling, followed by electrical logging. After the electric log has been run and has indicated the exact location of the different beds, the side-wall samples are taken.

Mechanical Samplers.—Various mechanical samplers are on the market. One type is operated hydraulically by mud pressure. The instrument is mounted on the bottom of the drill stem and is run into the hole to the depth at which it is desired to secure a sample. While traversing the hole, the sampling blades remain inside the body of the tool, but when the desired point is reached, pump pressure applied at the surface pushes down on a piston which expands the blades outward and upward against the formation, and with the pumps still running, the weight of the string of drill pipe is slowly and steadily placed upon the tool. This causes the blades to penetrate the formation, forcing cores of the formation into each of the sampler tubes.

At no time during the coring operation is the drill string rotated in either direction. When the pump pressure is removed and the string raised, the blades close into

the body of the sampler, and the tool is removed from the hole with samples of the formation in the core tubes.

Another instrument has been designed especially to recover the harder formations. This instrument comprises a diamond core drill, driven by an electric motor, and is guided by a track on which it slides into the cylindrical body of the instrument. Ordinarily the drill is retracted inside the body. In drilling a core, it extends diagonally downward from the side of the instrument. Before the coring operation, the instrument is anchored in the hole at any desired depth by an anchor arm system, which is released from an initially retracted position by the rotation of the electrical motor. Then, as the cable is slackened, the anchor pushes the instrument against the side of the wall to be cored; the rotating drill is applied against the formation with a pressure furnished by the weight of the driving motor, and a core is cut. When the drilling of the core is complete, the core is broken off at its root by a percussion motion and the drill is retracted from the formation with the core inside it. Provision is made for the removal of the core from the drill and for its temporary storage in a core magazine, so that several cores can be taken during one trip in the hole.

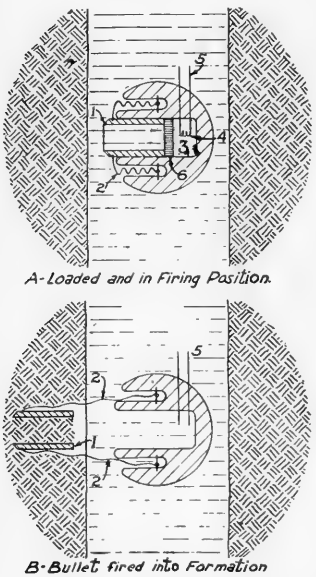

Fig. 676. — Schlumberger gun-type sample taker. 1, bullet; 2, retrieving wire; 3, explosive; 4, ignition wire; 5, firing cable; 6, removable cap.

The mechanical sample taker is about 10 feet in length, 5 inches in diameter, and weighs approximately 290 pounds. It can be run in holes from 7 inches up to 12 inches in diameter. From three to ten minutes time is required to cut a core, and as many as nine cores per run can be taken within a period of three hours or less, according to the depth and nature of the formations cored. Successful operations have been performed down to 11,000 feet. The cores obtained are ¾" in diameter and from 2" to 2¾" in length. On the average they are appreciably longer than the cores taken by the percussion-type sample taker. They are usually suitable for porosity, permeability, and other analyses. The recovery depends on the type of formation and also on the conditions of the well. The average recovery is about 80 per cent and is likely to be improved still more in the near future.

Percussion or Gun Samplers

The operating principles of the gun-type mechanical side wall sample takers† are illustrated in Figure 676. Part A shows the loaded gun in a well with the essential parts: bullet, fastening wires, powder, and igniting wire. By means of two electrical connections, a current is passed through the igniting wire, which thereupon becomes heated and ignites the explosive. The bullet is propelled into the formation as illustrated in Figure 676B. During this process, the bullet bottom cap is forced off so that the mud cake on the wall of the hole, which is collected first, passes through. The bullet is recovered by lifting the gun, which in turn pulls the bullet, with sample, from the formation by the fastening wires. A view of a

† M. Schlumberger, U. S. Patents 2,055,506, issued Sept. 19, 1936, and 2,119,361, issued May 31, 1938.
E. G. Leonardon, "Exploring Drill Holes by Sample Taking Bullets," A.I.M.E. *Pet. Tech.*, 1939.

small gun is shown in Figure 677.* The gun is fastened to the lower end of a weight or stem suspended by the logging cable.

Side-wall sample guns in present use contain 6 or 18 bullets and recently a 30-shot gun has been introduced into field use. The 18-shot is the standard gun, and actually consists of three 6-shot guns mounted in one housing.

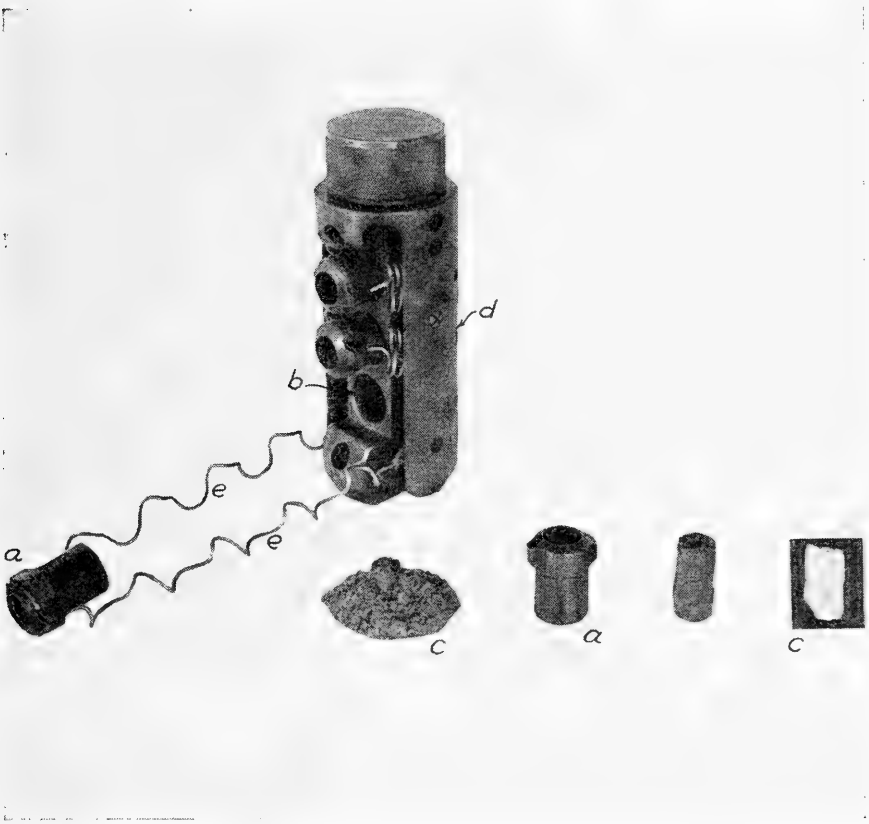

FIG. 677.—Small gun assembly. *a*, bullet; *b*, barrel; *c*, cores; *d*, body; *e*, retrieving spring. (Courtesy of Schlumberger Oil Well Surveying Corp.)

Each bullet in the gun is fired separately at one of the points to be cored. It is thus possible to recover several cores, all from different horizons, within a period of three hours or less, depending on the depth. The gun is lowered into the drill hole on the end of the same cable used to run the electrical log.

The present guns should not be used in a hole of insufficient diameter to permit the passage of the guns with the bullets fired. The very minimum permissible hole diameter is five inches, and only a 6-shot gun should be used in this case. For the use of an 18-shot gun, it is preferred that the hole be at least seven inches in diameter.

*A description of a similar gun for taking ocean-bottom samples is given by C. S. Piggot in the "News Science Bulletin," Carnegie Institution of Washington Pub., Vol. IV, No. 9, Sept. 6, 1936.

An 18-shot gun is 6′ 8½″ in length, 4¼″ in diameter, and weighs 149 pounds. A 6-shot gun is 18¾″ in length, 4″ in diameter, and weighs 31 pounds.

Field Operations

The side-wall sampling operation usually follows the electrical survey, at which time the electrical log is inspected for interesting uncored zones, and zones on which more information is desired. Then the electrical logging sonde on the cable is replaced with a side-wall sample gun, and samples secured at the points of interest indicated by the electrical logs.

By means of an electrode on the cable near the sample gun, the operator observes, on his recorder in the electrical logging truck, the S.P. of the formations through which the gun is moving. It is thus usually possible to verify the accuracy of depths and to place the gun at the exact depth corresponding to a point of the electrical log at which a core is desired. By this procedure the operator may take samples with great accuracy with respect to the formations *as they are indicated on the electrical log,* irrespective of absolute depth.

When the gun is positioned at the proper depth, it is fired by the operator. The firing of the bullet is observed by the operator as a sharp crack heard in a set of headphones or a sharp kick of a galvanometer spot in the recorder.† The operator then turns off the voltage and applies a tension to the cable to remove the sample from the formation. If the sample bullet has penetrated the formation an unusually great distance, so that it cannot be pulled loose, the wire fasteners joining the fired bullet to the gun are designed to break well before the strain on the cable becomes dangerous. In this case, the bullet is left in the wall of the hole. Nothing is left in the hole.

When the bullet is pulled loose, the operator repeats the procedure at other coring points until all the samples are taken. The gun is then pulled out of the hole and the cores are removed from the bullets, bottled, and delivered for the necessary core studies. If it is desired to use the cores for permeability analysis, the cores may be delivered intact in the bullets.

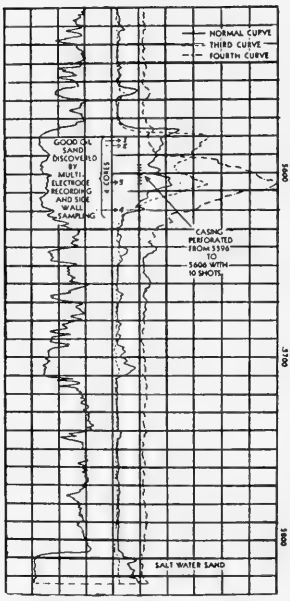

FIG. 678.—Correlations between electrical logging and side wall samples. (Courtesy of Schlumberger Well Surveying Corp.)

The Cores.—The cores taken with present guns are ¾″ in diameter and may be up to 2″ in length, depending on the recovery. The cores obtained, although relatively small, are large enough to give cuts, odors, and visual examination which will permit the confirmation of interesting zones. They can also be used, in favorable cases, for the usual porosity, permeability, and other analyses. There is, in general, no great compaction or crushing of the core, because of the construction of the bullet, or core barrel.

The fluid content of cores from porous formations is fairly representative of the original conditions prior to the penetration of the formations by the drill hole. No core, mechanical or otherwise, can escape completely the washing effect of drilling mud. The side-wall sample operations have shown, nevertheless, that, while the invasion of the permeable formation takes place, a true oil sand generally retains some of its oil, and a salt-water sand retains much of its salt, at least at a very short distance from the wall of the hole.

Efficiency and Safety.—The efficiency of the side-wall sample taker, like that of the rotary method, is not 100 per cent, but the recovery of satisfactory cores, as

† See seismo-electric effect, page 554.

compared to bullets fired, is at present about 70 per cent. In general, the 18-shot gun may be expected to return 12 to 15 cores, and this loss of a few cores is relatively unimportant because another attempt is always possible and because the method is extremely rapid. The loss of bullets in the formation by breaking the fastener wires is about 2 per cent.

Figure 678 illustrates the discovery of a new sand in an old field from the combined data provided by multi-electrode recording and side wall sampling. The normal and third curves indicate a higher resistivity in the region from 5571 to 5622 feet. The fourth curve verifies the resistivity indication in this section and indicates further that the sandy shale from 5622 to 5632 feet is also oil-bearing. Cores, taken before the casing was set, are shown. The loose sand proved to be a medium grain oil sand of the Marginulina with a very good odor. Casing was set and perforated from 5596 to 5606 feet with ten shots, resulting in an initial yield of five barrels per hour.

THE SECTION GAUGE

The hole calipering or section gauge is an instrument for measuring the effective diameter of a bore hole. As it is moved in the hole, the effective size of the hole at the depth of the instrument is logged continuously by a recorder at the surface.

The measurement of the size of a drill hole permits the computation of the hole volume and of the quantities necessary in cementing operations. It is useful in the selection of points for setting packers, and for determining the amount of gravel to be used for gravel-packing a well. Another use is for determining the effects of nitroglycerin shots and the effects of acidizing.

A most important use is the more accurate interpretation of the various types of electrical logs: the determination of the true resistivities by means of the departure curves requires a knowledge of the hole diameter. Generally, the S.P. log resembles the caliper log, because the shale sections wash away, enlarging the hole.

The operation of one type of instrument may be understood by reference to the schematic diagram of Figure 679. The measuring system of the instrument comprises three long flexible springs which belly out until they touch the sides of the bore hole. The bottom ends of the springs are fastened to a plunger which telescopes into a cavity in the upper part of the instrument. Relative distance of insertion of the plunger into the cavity depends on how much the flexible springs are constricted, which in turn depends on the size of the hole.

The position of the plunger determines the degree of inductive coupling between an energizing coil and a pick-up coil contained in the upper part of the instrument. Through the energizing coil is passed an alternating current of constant amperage. The electromotive force induced in the pick-up coil depends on the position of the plunger, and therefore on the size of the hole. The design of the coils and the plunger

is such that the voltage induced in the pick-up coil varies proportionally with the effective cross-sectional area of the hole. The voltage induced in the pick-up coil is transmitted through the cable to the surface, then rectified into direct current, and recorded as a log showing diameter versus depth.

In another type of caliper, a variable resistor is actuated by each finger, and this change is recorded at the surface as a log showing depth versus resistance, i.e., hole-diameter.†

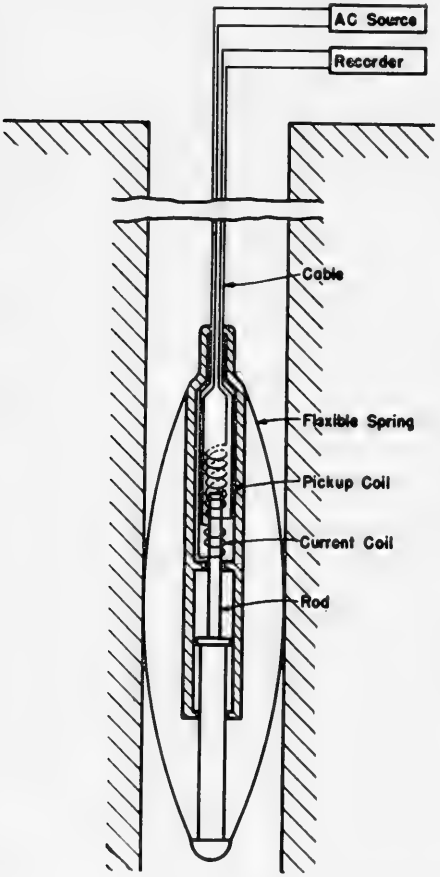

FIG. 679.—Operating principle of the bore-hole section gauge.

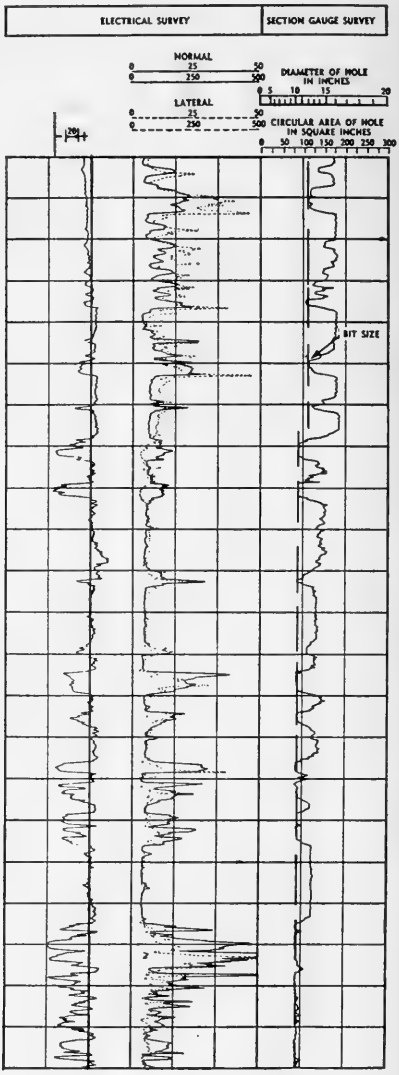

FIG. 680.—Comparison of electrical survey and section gauge survey.

The Section Gauge Log.—An example of a section gauge log is shown in Figure 680, along with the S.P. and the resistivity logs.

Section logs are generally run on a standard scale, the width of a single film

† C. P. Parsons, "Caliper Logging," *A.I.M.E. Pet. Tech.*, Vol. 151, 1943.

track corresponding to a cross-sectional hole area of 250 square inches. The recording is usually made on two film tracks, the first trace indicating hole diameters up to 25.2 inches. When this trace goes off-scale on the right side of the second film track, another trace appears which indicates larger hole sizes up to about 32 inches of diameter.

It is interesting to observe that in the figure a correlation can be made between the electrical log and the section gauge log. It is frequently observed, when the formations are not too firmly consolidated, that the shale sections will wash out, leaving an enlarged hole, whereas the hole through the sand sections is likely to more nearly maintain its gauge.

Evaluation of Hole Volume from the Section Gauge Log.—It is commonly desired to know the volume in cubic feet of the hole between specified depths in order to determine the cement required for cementing the casing. This data may be obtained by measuring the area with a planimeter, and then using the proper factors which depend upon the scale value and the depth scale of the recorded log.

Field Operations with the Section Gauge.—Section gauge measurements are performed with conventional electrical surveying trucks equipped with multiconductor cable and a photographic recorder. The length of the unit is 8′ 7″, its diameter (without springs) is 3⅝″, and its weight is 133 pounds. The maximum diameter of expansion of the springs is 36″. Before the survey, the calibration of the instrument is checked by placing a calibrating ring over the springs. The recording is generally made coming up-hole, with a surveying speed of 60 to 100 feet per minute.

Devices have been proposed by Bays† and Johnson‡ wherein the primary electrical log is automatically corrected for variations in hole diameter as determined by calipers, or for variations in well fluid resistivity by means of auxilliary conductivity electrodes.

RADIOACTIVE MARKER BULLETS

With the increasing depths of oil wells, the problem of accurate depth measurements becomes more important. The accuracy in absolute depth measurements, whether made in an open hole or a cased hole, and whether determined by a cable or a drill pipe, depends upon a number of factors, such as tension, temperature, and calibration. Errors due to these factors can be minimized by carefulness in actual measurements of depth and the application of corrections based on experience and frequent calibration or checking.

Although the accuracy of depth measurements has improved in recent years, other means may be employed to verify, for example, that a casing is perforated at a particular place with reference to a certain producing zone. Such a reference point may be a radioactive bullet shot into the formations from a sample-taker or a perforating gun.§ The bullet contains a radium salt and is therefore a compact source of gamma rays. These rays are able to pass through several inches of cement and steel, and can be detected easily by suitable equipment. The location of the radioactive marker, after casing has been set, identifies the depth of a point in the hole whose position is known with reference to the formations. That point may

† G. S. Bays, "Well Logging," U. S. Patent 2,392,357, Jan. 8, 1946.

‡ E. A. Johnson, "Method and Apparatus for Logging Wells," U. S. Patent 2,415,636, Feb. 11, 1947.

§ H. G. Doll and H. F. Schwede, "Radioactive Markers in Oil-Field Practice," A.I.M.E. *Petroleum Technology*, Vol. 174, 1948.

be correlated with the casing collars, which thereby provide another permanent set of references. As a result, regardless of absolute depth, a tool or device may later be placed in the hole at any specified short distance from these known reference points.

Apparatus.—The active part of the radioactive marker is a small brass capsule containing 1/10 milligram of radium salt. The brass pellet is placed inside a steel bullet which can be shot out of a sample-taker gun or a perforating gun.

The detector for radioactive markers consists of a casing collar locator and a radioactive marker detector sonde assembled together, to locate simultaneously the position of the radioactive markers and the position of the casing collars.

Field Operations.—Radioactive markers are usually placed immediately following the electrical survey. If side-wall samples are required, the taking of cores and the placing of radioactive markers can be accomplished during the same round trip in the hole by means of a sample-taker gun loaded partly with markers and partly with sample-taker bullets.

For each zone to be perforated, it is advisable to place three or more markers at intervals of about 50 feet over a section that straddles the zone.

During the placement of the markers an S.P. log is recorded, and the bullets are fired as the gun travels past the desired placement points. The firing of the bullet makes an indication on the log in the form of a sharp pip on the curve. (Figure 681.) The position of these pips with respect to the recorded curve determines exactly where the bullet lies in the formation. The placement of radioactive markers is a quick operation. The necessary rig time, according to the depth, may vary from one to two hours.

The later location of the radioactive markers is a separate operation, made usually after casing has been set. It ordinarily involves the detection of the markers and their correlation with the depths of the casing collars in their vicinity. The radioactive marker detector has a low sensitivity, so that the natural gamma radiation from the formation will have no measurable effect on the recording galvanometer. When the detector passes by a marker in the hole, a sharp deflection of the galvanometer occurs and a peak is recorded on a photographic record. (See location and collar log, on right side of Figure 681.)

It is important to verify that the intervals between the three or more markers placed in a zone are the same as at placement, so as to make sure that the markers have not moved. Since the positions of the radioactive markers and the positions of the casing collars are recorded simultaneously, it is evident that the positions of the collars are determined accurately with respect to the formations. The positions of these collars may then be used as reference points for the accurate placement of a perforating gun or other instrument. Like the placement of radioactive markers, the location of radioactive markers and casing collars requires little rig time.

Applications.—The use of radioactive markers is valuable where accuracy in depth measurements is important, in particular: (1) production from specific zones of an oil-bearing formation, and in known relation to any oil-gas or oil-water contact; (2) increased efficiency in placement of perforations for cement squeeze jobs or tests; and (3) testing and production from thin beds at great depths below the surface.

Radioactive markers also provide permanent and consistent reference points for all production problems throughout the life of a well, regardless of any change in the equipment at the surface.†

Paleontological Studies.—Paleontology is of course invaluable in the recognition of markers. Paleontological markers, in addition, are in

† H. G. Doll and H. F. Schwede, "Radioactive Markers in Oil Field Practice," *A.I.M.E. Tech. Pub.* 2261 (1947).

general very definite. Studies of the foraminifera of the Gulf Coast have contributed widely to an advancement of the geology of that area. In much of the Gulf Coast, however, due to the scarcity of fossils in many of the formations (especially the younger ones) and the non-fossiliferous character of other formations, the number of horizons that can be definitely identified are limited. Identification of paleontological horizons is done by microscopic examination of cores or side wall samples. These samples are obtained by coring or taking side wall samples over that section of the hole in which it is believed the studies should be made.

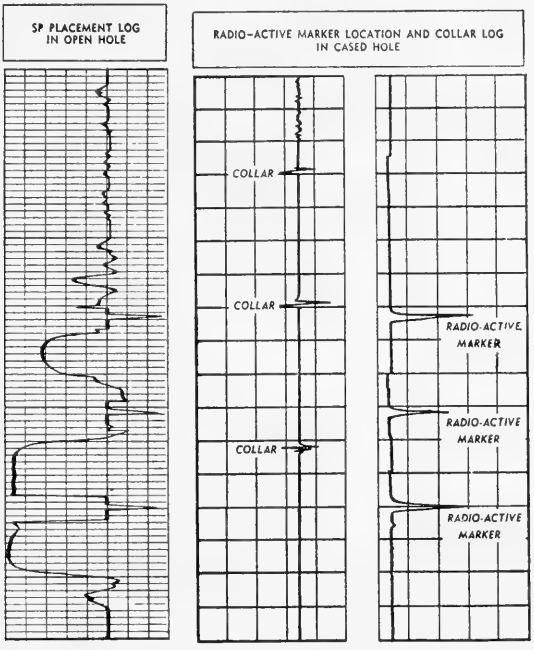

FIG. 681.—S.P. placement log in open hole, compared with radioactive marker location and collar log in cased hole.

Drill Core Measurements.—In the absence of continuous logging data, measurements are often made of the magnitudes of certain properties of drill core specimens. The magnitudes of the electrical resistivity,† fluid permeability,‡ radioactivity,§ relative mineral content,†† magnetic orientation and permeability,‡‡ fluorescence,§§

† M. W. Pullen, "Tentative Method for Making Resistivity Measurements of Drill Cores and Hard Specimens of Rocks and Ores," U. S. Bureau of Mines, Circular 6141, June, 1929.

‡ H. C. Pyle and J. S. Sherborne, "Core Analysis," *A.I.M.E. Petroleum Technology*, 1939, pp. 33-61.

§ E. Rothe and T. Kopcewicz, "Comparaison de la radioactivité des roches d'Alsace par la méthode des tubes compteurs," *Compt. Rend.* (1937), Vol. 205, pp. 165-166.

†† H. C. Pyle and J. S. Sherborne, *loc. cit.*

‡‡ H. N. Herrick, U. S. Patents 1,792,639, issued Feb. 17, 1931; 1,909,619, issued May 16, 1933; 2,104,746, issued Jan. 11, 1938.
H. N. Herrick and E. D. Lynton, U. S. Patent 2,104,752, issued Jan. 11, 1938.

§§ J. A. Radley and J. Grant, *Fluorescence Analysis in Ultra Violet Light*, D. Van Nostrand Co., Inc., New York, 1935.

and other parameters have all been utilized as a means for obtaining supplementary data for guidance of the drilling and completion operations, and for structural correlation with other wells.

An illustration of resistivity measurements on core samples is shown in Figure 682. For this work, resistivity measurements were made on the cores and plotted

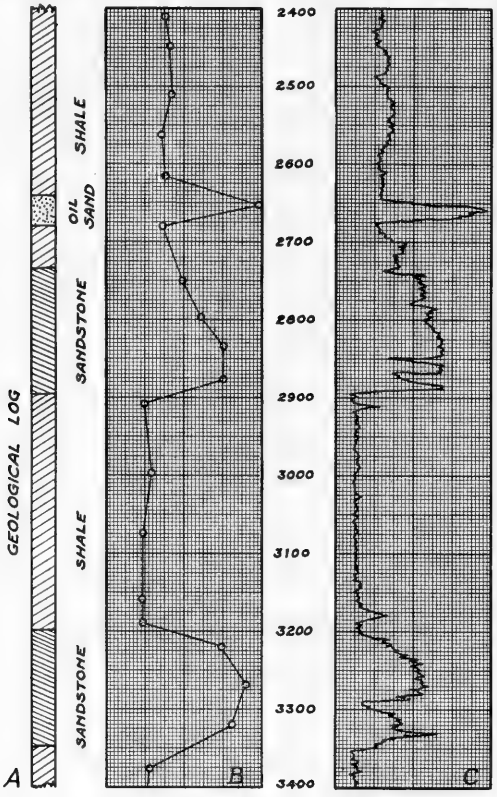

FIG. 682.—Comparison of *A*, geological log; *B*, resistivity measurements on core specimens; *C*, resistivity log in bore hole for a well in the San Joaquin Valley, California.

against depth (curve B) in conjunction with the geological log (A) determined by inspection of the cores. Upon completion of the well an electrical log was run (curve C). There is a good general agreement between the logs, although as would be expected, the core log (B) lacks the good detail shown by the electrical log (C) of the hole. This lack of detail is due largely to (a) limited number of samples measured, (b) contamination of cores by the drilling mud, and (c) loss of cores during the drilling operations.

The most satisfactory method for measurement of core specimens is the potential drop method discussed in connection with Figure 278. Electrical connection to the ends of the core specimen may be obtained by wrapping a few turns of bare wire tightly around each end at right angles to the axis of the core. Two single turn coils are employed for making connection to the core for measuring the potential drop across any convenient length *L*.

When grinding facilities are available for dressing the ends of the cores, a more rapid and convenient method is that illustrated in Figure 683.† In this arrangement, metal rings are pressed against the ends of the specimen and serve as the energizing or current electrodes. The two potential electrodes are placed coaxially with the current rings.

Another arrangement of lower accuracy but greater convenience for irregularly shaped specimens is the four-prong resistivity method illustrated in Figure 684.

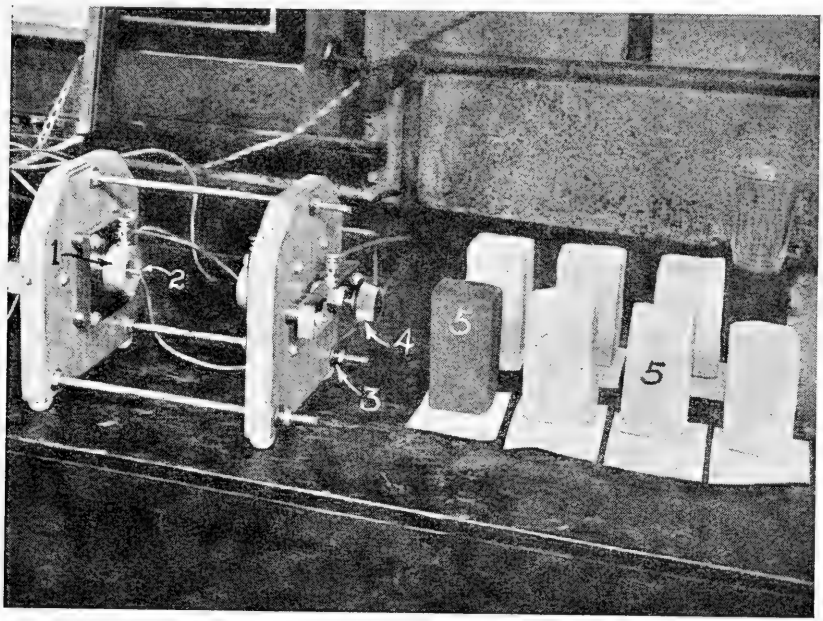

FIG. 683.—Apparatus for measuring resistivities of dressed specimens. 1, current contact ring; 2, potential contact; 3, nuts for clamping specimens between the contact rings; 4, knob for tightening potential contact; 5, test specimens.

DRILLING TIME LOGS

It has been recognized for many years that the time required for drilling a unit depth of formation varies with the nature of the formation, as well as with the mechanical characteristics of the drilling equipment. Data may be plotted showing depth versus drilling time per unit depth of penetration.

Formerly, the proper correlation between time and depth was chiefly dependent on a log made by the driller, and many errors were common. Recently, it has been the practice to use mechanically actuated recorders which are geared to the drill stem. This is usually accomplished by means of a flexible cable connected to the swivel or the traveling block, which feeds over an idler near the top of the derrick to the recording instrument.‡ Movement of the cable, as the drill is raised or lowered, produces corresponding movement of the recording paper. In some cases, a ratchet device is employed to allow for continuous forward motion of the recording paper. In other devices, the chart is

† J. J. Jakosky and R. H. Hopper, "The Effect of Moisture on the Direct Current Resistivities of Oil Sands and Rocks," *Geophysics*, Vol. 2, No. 1, January, 1937.

‡ T. C. Heistand and P. B. Nichols, "Drilling Time Data in Rotary Practice," *Oil and Gas Journal*, July 13 and 20, 1939.

J. J. Jakosky, U. S. Patents 2,150,169, 2,153,802 and Reissue 21,102.

moved at a uniform rate of speed and each vertical trip of the Kelly produces a varying pressure recording on the chart. Drilling time is proportional to the length of chart between corresponding phases of the pressure curve.

Drilling logs supply valuable information for later correlation with sample logs and electrical and thermal logs. Proper correlation with sample logs is dependent on an accurate evaluation of the time required for cuttings to reach the surface sampling box. This time varies with the effective diameter and the

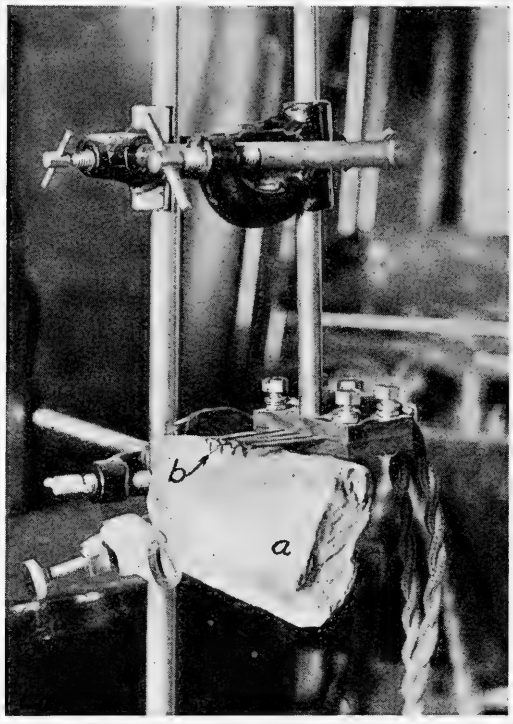

FIG. 684.—Method for determining the approximate resistivity of irregularly shaped materials. *a*, specimen; *b*, four-electrode system. (Power applied between the two outside electrodes, and potential measured between the two inner electrodes.)

depth of hole, the rate of mud circulation, and the viscosity of the mud. In a 5000-foot hole, the time lag is usually about one hour. Drilling time logs are finding increasing use in the industry, because they not only supply information which allows the operator to choose the optimum drilling technique, but they also supply a record showing time going in and out of hole, condition of bits, stand-by periods, etc.

Recent developments in mud analysis and logging electrically while drilling supplement the drilling time logs.

RADIOACTIVITY WELL-LOGGING

Radioactivity well-logging is a conspicuous example of a successful application of the physics of the nuclear atom to exploration. Two early

examples of radioactivity logging in a bore hole are found before 1909. One of these is the study of the Balfour Bore, in Fifeshire, England.† In this log, it is highly probable that the report is a measurement of radium, the only substance for which there was a good means of measurement at that time. Interesting questions are raised about these measurements because of the low values reported for black shales, which are quite contrary to expectation. Another early well log was prepared by Ambronn, who measured the natural radioactivity of well samples by a radiation method.‡ This log is unusual, in that it suggests a correlation between radioactivity and the occurrence of petroleum, a finding which is not supported by more general experience on interpretation of these logs.

Considerable added confusion, was created in this subject by a publication by Hurinuzescu,§ showing high activity of Romanian oils, Vingershoets and Maurer††,‡‡ have done the subject no good by their fantastically exaggerated claims regarding relationship between petroleum and radioactivity. At the present it may be said with the utmost assurance that there is no generally applicable principle of correlation between petroleum and radioactivity.

A very interesting early log is the one based on radium measurements, in the St. Gothard Tunnel through the Alps, before 1909. In this case, an effort§§ was made to correlate the occurrence of high temperatures with the high values of radium concentration. The earliest published gamma-ray well-log made by a continuous profiling method appeared in 1939.††† Other workers were very active at the same time, and it was not long until several more experimental papers were published.‡‡‡ The development of gamma-ray well-logging followed very rapidly. An extensive bibliography of these developments is to be found in the literature.§§§

Neutron well-logging began in 1938, and was the subject of a patent application by Fearon.†††† The public was first informed of the discovery of neutron well-logging in an article by B. Pontecorvo.‡‡‡‡ The first developed form of the neutron log was not very successful economically, because

---

† J. Joly, "Radioactivity and Geology," p. 80, Constable, London, 1909.

‡ Jahrbuch des Halle'schen Verbandes zur Erforschung der mittel deutschen Bodenschatze und ihrer Verwertung," Halle a. S., Vol. 3, No. 2, p. 45.

§ Hurinuzescu, A., "Radium," Paris, 7, 231-2, 1910 (126).

†† Vingershoets, F.I.G., "Zeitschrift des intern," *Vereins der Bohringenieure und Bohrtechniker,* Wien, 34, 538, 1926 (126).

‡‡ Maurer, R., "Zeitschrift des intern," *Vereins der Bohringenieure und Bohrtechniker,* Wien, 34, 371, 1926 (126).

§§ J. Joly, "Radioactivity and Geology," Plate IV, Constable, London, 1909.

††† Lynn G. Howell and Alex Frosch, "Gamma-Ray Well Logging," *Geophysics,* Vol. IV, No. 2, March, 1939, pp. 106-144.

‡‡‡ S. A. Scherbatskoy and G. H. Westby, "Well Logging by Radioactivity," *Oil and Gas Journal,* Feb. 22, 1940.

W. G. Green and R. E. Fearon, "Well Logging by Radioactivity," *Geophysics,* Vol. V, p. 272, 1940.

§§§ R. E. Fearon, "Radioactivity Well Logging," *Oil Weekly,* 118, 1945, pp. 33-41.

G. Hevesy, F. A. Paneth, "Radioactivity," Lawson Translation, Oxford, London, 1938, pp. 126-137, 221-239.

Blackwood, *et al,* "Atomic Physics," Wiley and Sons, 1937, pp. 235-240.

E. Rutherford, "Radiations from Radioactive Substances," Cambridge, 1930, pp. 1-37.

U. S. Patents 2,349,225, May 16, 1944, and 2,361,389, Oct. 31, 1944.

†††† "Well Logging Method and Apparatus," U. S. Patent 2,308,361, Jan. 12, 1943.

‡‡‡‡ *Oil and Gas Journal,* Sept. 11, 1941.

of large errors, both random and systematic. Improved instrumentation has corrected this difficulty.

Physics of Modern Radioactivity Logs

The gamma-ray log† recognizes the radioactive families occurring in nature and emitting gamma rays. For the most part, the families may be considered to be in radioactive equilibrium, in rocks which are old enough and have remained undisturbed long enough. A discussion of radioactive families and their radiations has been given in Chapter X. Recent evidence‡ points to a much greater significance of potassium in gamma-ray logs than had hitherto been recognized.

The size of the sample observed during gamma-ray logging depends, in each particular case, on the nature of the radiation emitter which is permanently present.§ Speed of logging, required accuracy of the measurement, and length of the section sampled at each point of the log are interrelated in a manner which depends on the statistics of the arrival of the radiation. This problem has been extensively discussed in Chapter X and in earlier publications.††

Kubitschek and Dancoff‡‡ have made extensive studies of the gamma rays of several elements, which are emitted by these elements upon absorbing a slow neutron. Their experiments show a typically rather large emission of energy by an element-capturing neutron. They find, in general, that the energy so emitted is more than twice the energy of the quanta radiated by the most energetic gamma-emitting radioelements found in the rocks. Fearon§§ and Pontecorvo††† have published descriptions of the use made of these facts in logging.‡‡‡

It is interesting to note that whereas the gamma-ray curve is fundamentally limited in regard to logging speed, no such limitation is essential to the neutron curve, which, in principle, can always be speeded up by using stronger radiation sources. Sampling of the rock by the neutron process is extensive and representative. The sample is egg-shaped§§§ rather than cylindrical, as in the case with the gamma-ray log. Examples showing the desirable qualities of the sampling obtained in neutron well-logging are given in the reference cited. As discussed in Chapter X, hydrogen is the element chiefly recognized by a neutron curve.

The neutron curve therefore may be expected to show a minimum opposite petroleum. There are many other factors which can cause a minimum, as will be seen in the section on interpretation. It is interesting to note that the neutron curve is an *atomic* detector of hydrogen, being sensi-

† See list of patents on gamma-ray logging at end of chapter.
‡ *Physics Review*, 72, 640 (1947).
§ R. E. Fearon, "Gamma Ray Well Logging," *Nucleonics* 4, 70 (1949).
†† R. E. Fearon, "Gamma Ray Well Logging," *Nucleonics* 4, 71 (1949).
R. E. Fearon, "Gamma Ray Well Logging," *Oil Weekly* 118, 36 (1945).
‡‡ Data released at April meeting, A.P.S., 1948 (to be published).
§§ R. E. Fearon, "Well Logging Method and Device," U. S. Patent 2,349,712, May 23, 1944.
††† *Loc. cit.*
‡‡‡ See end of chapter for list of patents on neutron logging.
§§§ R. E. Fearon, "Neutron Well Logging," *Nucleonics*, June, 1949.

tive to that element in whatever form or state of combination, or lack of it, it may occur. Also it may be noted that in neutron well-logging use is made of the release of the pent-up nuclear energy of the atoms of common elements. The energy received by the detector in a neutron well-logging instrument is released by the destruction of a small quantity of matter when the neutrons coalesce with a nucleus of the rock substance. The neutron curve is thus a practical modern use in the petroleum industry of the principle set forth by Einstein, that matter may be converted into energy.

Instrumentation

A typical radioactivity well-logging apparatus consists of the logging instrument, a hoist truck carrying the well cable and hoisting mechanism, and an instrument truck containing the electrical amplifying and recording equipment, as illustrated in Figure 666.

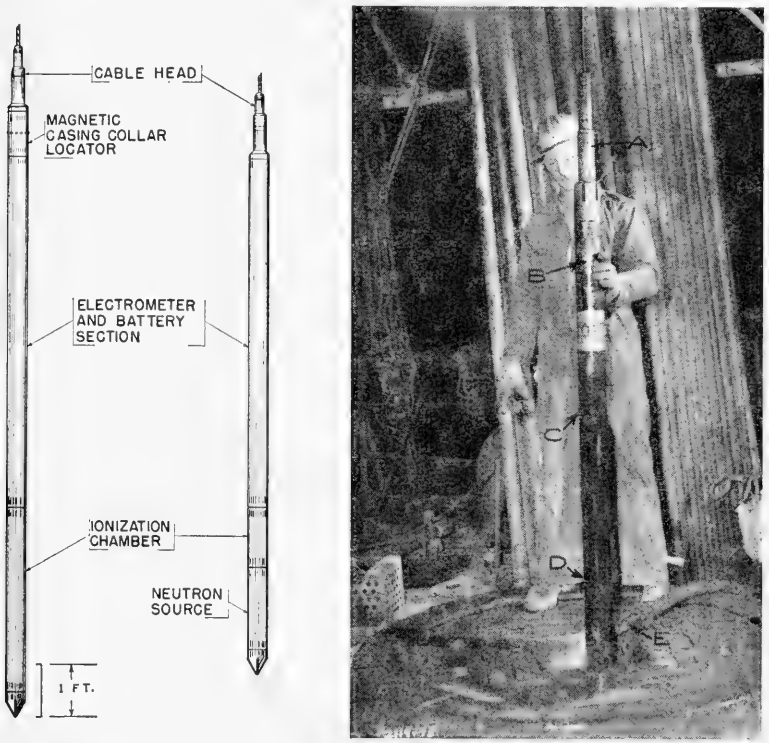

FIG. 685.—(Left) Gamma-ray and (center) neutron logging instruments. (Right) gamma-ray instrument emerging from well. A, cable head; B, magnetic casing collar locator; C, electrometer and battery section; D, ionization chamber; E, water stream for washing mud from cable and instrument. (Courtesy of Lane-Wells Company.)

The subsurface instrument is illustrated in Figure 685, and contains a detector, which continuously measures the radiation intensity as the instrument traverses the well-bore, an electrometer, which converts the weak electrical signals supplied by the

detector into a form suitable for transmission to the surface, and a set of batteries for supplying power required by the detector and electrometer.

A hoisting cable, comprising an insulated copper conductor surrounded by two layers of steel wires, wound reverse-concentric, furnishes the electrical circuit between the bore-hole instrument and the surface measuring equipment.

At the well head the cable passes over a calibrated measuring sheave, which is supported by a spring-type weight indicator. (See Figures 652 and 666.) From the sheave, the cable passes to the hoist truck which contains a hoisting drum, driven through an auxilliary transmission from the truck engine, and the necessary instruments and controls. Electrical connections from the well cable are brought out through revolving slip-rings mounted on the hoist-drum shaft, and pass through an interconnecting cable to the instrument truck.

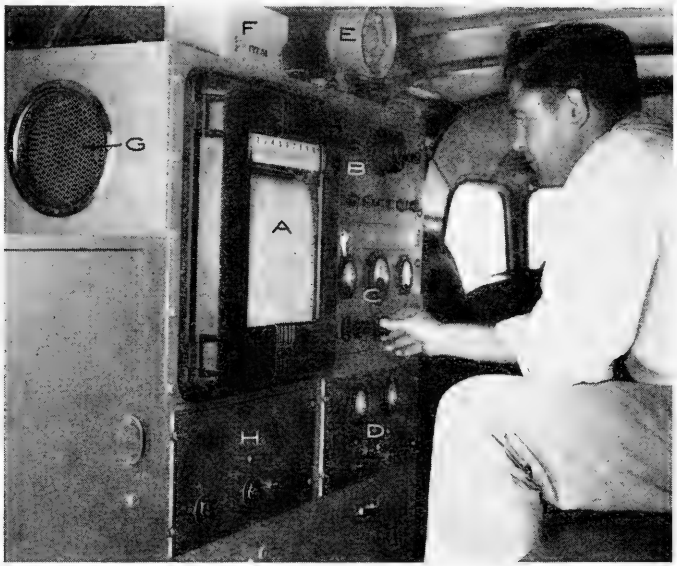

FIG. 686.—Radioactivity logging instrument truck. A, graphic recorder; B, oscilloscope panel; C, amplifier panel; D, power supply panel; E, intercommunicating loudspeaker to hoist operator; F, depth indicating odometer; G, ventilator; H, recorder control panel. (Courtesy of Lane-Wells Company.)

The instrument truck contains the surface amplifiers and the recorder as shown in Figure 686. This equipment is operated from 115-volt, 60-cycle current generated by a portable power unit carried on the hoist truck (Figure 663).

Depth indicators in both trucks are electrically driven by synchros connected to the measuring sheave. The recording chart is similarly driven in order to register the subsurface radioactivity measurements as a function of depth.

Subsurface instruments of several different types are used for gamma-ray logging and neutron logging, depending upon the well diameters, bottom hole pressures and other factors encountered in various areas. The radiation detectors employed in the most frequently-used instruments are high pressure ionization chambers, containing nitrogen, argon or other inert gases at pressures around 100 atmospheres. In the presence of gamma radiation, a small current flows between a pair of electrodes in the ionization chamber and the magnitude of this current is a measure of the intensity of the incident radiation.

Under normal gamma-ray well-logging conditions the ionization current may be of the order of 10^{-13} amperes, and changes in this current of the order of 10% are required to produce a recording pen movement of one or more inches. A pen deflection of one-tenth inch, which is about the smallest readable detail, thus may correspond to a change in ionization current as small as 10^{-15} amperes. The accurate measurement of these extremely minute direct current signals and the transmission of this data to the surface require instrumentation of rather unusual characteristics.

A continuous automatic null-balance system is employed to transmit and record

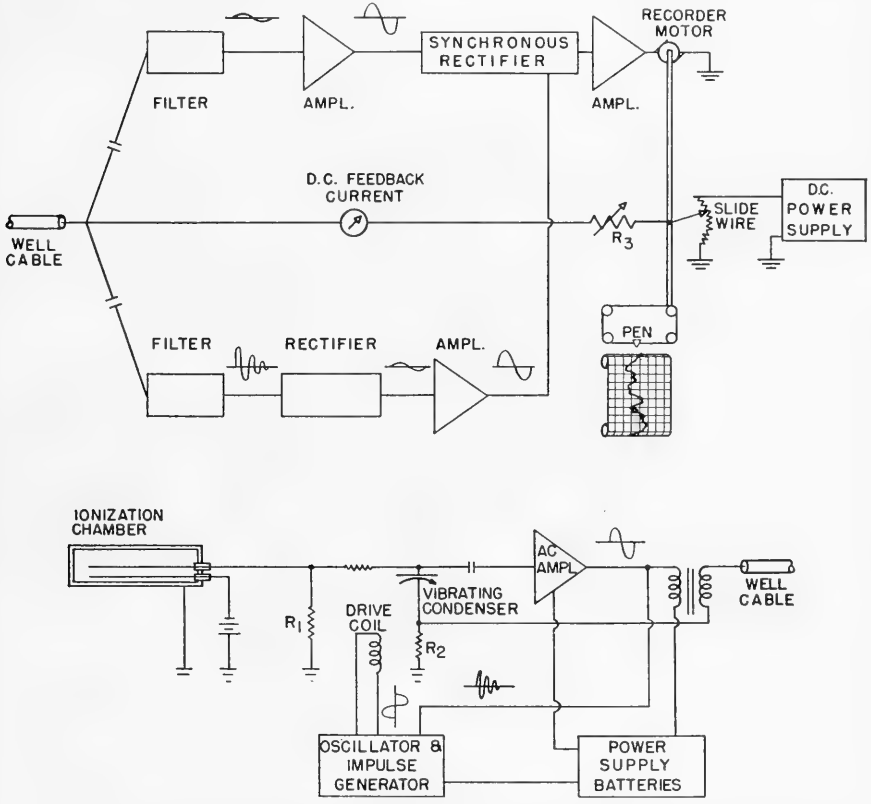

FIG. 687.—(Above) Functional schematic diagram of radioactivity well-logging system surface section. (Below) Subsurface section.

the magnitude of the ionization current. This is accomplished by the use of a "capacitative commutator" electrometer† in the subsurface instrument, together with appropriate amplifying and recording apparatus at the surface.

A block diagram of the system is shown in Figure 687. Operation of this system may best be explained by tracing the actions of the successive elements, starting with the ionization chamber.

Assuming the system to be in balance, with the recording pen at rest and the logging instrument hoisted into a region of greater radiation intensity. The minute current in the ionization chamber will increase, thus raising the potential of the upper

† See Figure 618, Chapter X.

plate of the continuously vibrating condenser to a higher value than that of the opposite plate. The action of the vibrating condenser, which can be likened to that of a condenser microphone, is such as to generate a small alternating current signal, which is amplified in the subsurface amplifier and coupled to the hoisting cable through a transformer.

Another signal, having the form of a damped oscillation, is derived from the action of a pair of contacts driven mechanically with the vibrating condenser. This phase reference signal is transmitted continuously over the same circuit to the surface.

At the surface, these signals are further amplified in frequency-selective amplifiers and combined in a synchronous rectifier to produce a direct current output. The polarity and magnitude of this direct current are representative of the magnitude and polarity of the unbalance between the potentials at the vibrating condenser. This output current is used to control the speed and direction of motion of the pen of a commercial type high-speed motor-driven recorder. (Figure 686.)

Under the conditions described above, the polarity of the current will be such as to cause the motor to drive the recording pen to the right, and simultaneously to move the contact arm on the slide-wire so that more direct current flows from the surface power supply, through the well cable to the subsurface instrument. There this increased current, flowing through R_2, raises the potential of the lower plate of the vibrating condenser. It will now be seen that the recorder motor continues to run until it has caused the potential of the lower plate of the vibrating condenser to equal that of the upper plate. When this condition has been achieved, the motor stops, since the vibrating condenser produces no alternating output signal when its plates are equipotential. The pen has now been moved to the right by an amount corresponding to the increase in radiation intensity and the system is again in balance. A decrease in radiation will cause the system to operate similarly, but in the opposite direction, since the polarity of the signals will be reversed.

The direct current transmitted down the cable to achieve and maintain balance is, in practice, many thousands of times greater than the ionization chamber current, the exact ratio being determined solely by the relationship between the resistors R_1, through which the ionization current flows, and R_2, through which the feed-back current flows. Usually, the value of R_1 is chosen about 10^{10} times larger than R_2 so that, at balance, the current transmitted down the cable to the subsurface instrument is related to the ionization current by this ratio. Since the system continuously and automatically maintains the condition of balance, the value of this feed-back current accurately represents the value of the ionization current, and, therefore, the value of the radiation intensity encountered by the ionization chamber. By virtue of operating continuously to maintain a null-balance condition, the system is essentially independent of variations of gain in the A.C. amplifiers, and of the transmission characteristics of the cable. This enables the subsurface equipment to be powered by self-contained dry batteries, even though such batteries undergo large changes when subjected to the elevated temperatures encountered in many wells.

The scale-factor of the recorder, or the amount of pen travel for a given change in radiation intensity, may be varied by adjustment of the value of the resistor R_3, through which the feed-back current flows. It will be seen that a greater travel of the slide-wire arm, and hence of the recording pen, is required to produce the same current change when this resistor is made larger.

In secondary ray logging, one example of which is the neutron curve, the instrumentation remains basically unchanged. The subsurface instruments used for this type of logging carry an emitter of radiation, consisting usually of a small capsule of radioactive material, and generally employ a smaller, less sensitive detector in order to minimize the effects of the naturally occurring variations in radioactivity. By suitable choice of the strength of the radiation source, the secondary radiation is made many times greater than the normal gamma-ray activity of the earth's strata, so that the curve produced by the neutron-logging instrument is essentially free from this effect.

The radioactivity-logging instrument is often combined with a magnetic casing-collar locator which detects the magnetic discontinuities in the steel well-casing and transmits this intelligence to the surface equipment. There a second pen, working in the margin of the recorder chart, places a mark corresponding to the depth of each casing collar. By this means the radioactivity curves, and thus the location of the strata, are tied directly to permanent depth reference markers which can be located precisely on subsequent runs of these or other well tools. Much use is made of these collar determinations in the subsequent positioning of gun perforators in order that the shots may be placed in the desired formations with accuracy.

The field techniques employed in obtaining a radioactivity log are very similar to those used in other forms of well-logging and therefore need not be detailed here. However, certain phases of the procedure which are peculiar to the measurement of radioactivity will be discussed.

Just before the subsurface instrument is lowered into the well, its sensitivity to radiation is checked and standardized by placing a standard source of radiation adjacent to the center of the detector.

The response of the system to this standard radiation is recorded in terms of inches of pen travel. After traversing the well on the downward trip, and observing the relative activity obtained, the scale sensitivity may be changed at the operator's discretion. The initial response to the standard radiation is then multiplied by the factor by which the scale has been changed. This latter figure is then a direct measure of the overall sensitivity employed in making the record, and is indicated on the log, at the beginning and end of any section logged at this value of sensitivity.

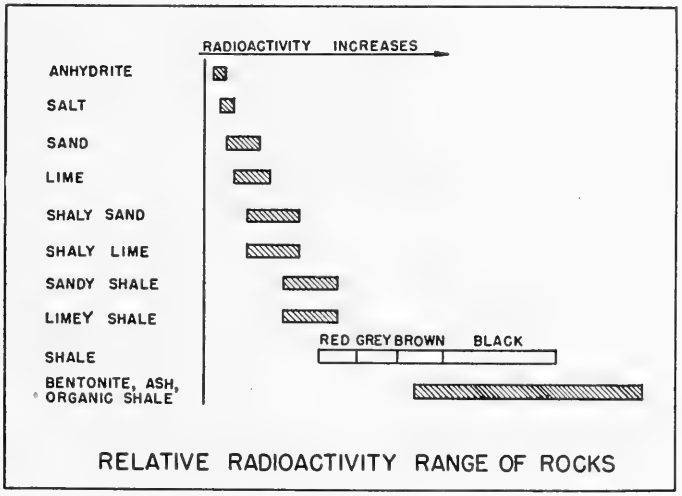

FIG. 688.
(Courtesy of Lane-Wells Company.)

Logging is always conducted during the upward trip in order to secure the most accurate depth registration, since the upward travel of the instrument with the hoisting cable in tension is generally more uniform. Logging speeds from 25 to 50 feet per minute are employed customarily, although higher speeds may be used at some sacrifice in accuracy. This is brought about by the extremely low levels of radiation intensity being observed. The total number of radiation quanta entering the detector per second is generally quite small, and a sufficient number of quanta must be observed in order to determine the intensity, or average rate, with the desired accuracy. By

proper choice of logging speed, the detector remains for a sufficient period in the vicinity of each stratum to provide an accurately reproducible record of its radioactivity. In areas where strong contrasts exist between various strata which it is desired to differentiate, the logging speed may be made relatively rapid: in other areas a slow speed may be required to obtain the accuracy necessary to differentiate between strata whose radioactive properties are nearly alike. The time constant, or overall speed of response of the system, is adjusted by the operator to suit the local conditions, and the hoisting speed is then controlled accordingly.

Gamma-Ray Curve Interpretation

The radioactivity intensity ranges of the formations commonly associated with oil-bearing structures are shown in Table 27 and Figure 688. The relative ranges shown were determined by combining the results of measurements obtained in hundreds of laboratory tests of the radioactivity of many rock samples. The relative range of radioactivity intensity of each formation is indicated by the position and length of the block in Figure 688.

TABLE 27

Lithologic Type	*No. of Samples*	*Average radioactivity in radium equivalents per gram*
Black and grayish-black shale	40	26.1
Dark to black shales, neither calcareous nor sandy	74	22.4
Shales, including sandy shales	164	16.2
Marls and limy shales, grayish-black and black	3	16.5
Sand and shale	9	13.5
Dark to black shales, not calcareous, but sandy	16	13.2
Medium to light gray shales, neither sandy nor calcareous	17	11.3
Siltstone	11	10.3
Medium to light-gray shales, not calcareous, but sandy	18	9.0
Marls and limy shales, dark	10	8.8
Sandstones, silty but not shaly	26	7.3
Shaly sandstones	40	7.0
Marls and limy shales of light shades	16	6.8
All sandstones, including shaly sandstones	131	5.3
All sandstones, excluding shaly sandstones, but including silty types	105	4.0
Sandstones free from silt and shale	76	4.1
Shale-free limestones and dolomites	64	4.1
Microcrystalline to earthy limestones and dolomites of medium to light shade	28	4.0
Medium to light shade, shale-free limestone	33	3.8
Finely to coarsely crystalline limestones and dolomites of medium to light shade	24	3.1
Medium to light shade, shale-free dolomite	21	3.1
Effect of shade in shale-free limestone and dolomite:		
A. Light gray to white	30	3.1
B. Medium shade	22	4.1
C. Dark to black	10	6.1
Estimated original permeability of sandstone before cementation:		
Very high	35	2.9
High	37	5.1
Low	40	6.6
Very low	24	7.5

(From "The Total Gamma-Ray Activity of Sedimentary Rocks as Indicated by Geiger Counter Determinations," W. L. Russell, *Geophysics,* Vol. IX, No. 2, April, 1944.)

It may be observed from this table that the average intensity values of these formations (approximately the midpoints of the ranges) permits subdivision of the formations into three general groups:

Group 1—Formations Having Low Radioactivity

Sandstone, limestone, dolomite, salt and anhydrite come under this category. In general, sandstone, limestone, and dolomite show similar, low-intensity radioactivity values and cannot be reliably distinguished from each other by their radioactivity alone. Some knowledge of local stratigraphy is therefore necessary for their reliable identification. Mixtures of limestone, dolomite, and pure sandstone are about as weak radioactively as the pure types. Porous and non-porous sandstone, limestone, and dolomite exhibit the same degree of radioactivity. There appears to be little, if any, difference between the radioactivity values of uncemented sands and those showing various degrees of cementation. The presence of interstitial water in formations appears in general to have no measurable influence on their radioactivity.

Group 2—Formations Having High Radioactivity

Shale, clay, and silt are the most common formations having a normally high order of radioactivity. Whenever these materials either contaminate, or are highly interbedded with, formations having low radioactivity, they increase the radioactivity of the zone. Thus mixtures such as shaly sand, shaly limestone, sand, shale, calcareous shale, etc., commonly show medium to high values of radioactivity.

Group 3—Formations Having Abnormally High Radioactivity

Formations possessing abnormally high values of radioactivity are black or organic marine shale, granite, bentonite, and volcanic ash. Igneous rocks in general possess very high radioactivity values. Formations in the lower radioactive groups are frequently contaminated with bentonite and volcanic ash with the result that they show increased radioactivity. Some underground waters are very highly radioactive and are capable of making mineral deposits which are very radioactive. Such ground waters rising through fault planes or fractures, or traveling through unconformities and making such deposits may cause distinct radioactive markers. (See Figure 627, Chapter X.)

Typical Response of Formations

Figure 689 is a chart which will aid in the general interpretation of radioactivity logs. The gamma-ray curve, on the left, represents typical response to a wide variety of formations. The following description is an elaboration of the brief description indicated on the figure.

Surface Formations.—The susceptibility of the gamma-ray curve to cosmic radiation and the gamma radiation from soil is indicated at the top of the curve. Although beds capable of producing oil or gas rarely occur close enough to the surface to involve the effect of cosmic rays, it is worthy of note for the few instances in which interpretation to the surface is desired.

Uncontaminated Formations.—The typical response of uncontaminated sand, lime, dolomite, salt and anhydrite is illustrated at various points on the graph. Such formations are characterized by low, relatively uniform radioactivity. Typical response patterns for relatively pure limestone and dolomite appear to be the most highly developed in practically all areas in which wells have been surveyed. Salt and anhydrite are normally very low in radioactivity and are frequently quite easily distinguished from other formations. Normal shales show reasonably constant radioactivity values throughout the log.

Contaminated or Interbedded Formations.—As the amount of shale, silt, etc., intermixed with sand, lime or dolomite increases, the gamma-ray curve shows in-

creased radioactivity values. A somewhat similar effect results when sands, limes or dolomite are highly interbedded with shale. It is important to note that shales with interbedded sandy shale and thin sand beds show higher average radioactivity values than thicker sand beds separated by thin shales. This is due primarily to the averaging effect of the ionization chamber.

FIG. 689.
(Courtesy of Lane-Wells Company.)

Clean sand or lime grading into shaly sand or lime is a frequent occurrence and presents a problem in the exact determination of the top or bottom of the clean zone. As a rule, only that part of the zone exhibiting minimum radioactivity represents the clean sand. This is subject to many exceptions, however, and an intimate knowledge of local conditions is desirable for accurate interpretation.

Formations Exhibiting Unusual Response.—As stated previously, the black, organic marine shales, e.g., the Chattanooga, most frequently show extremely high

values of radioactivity. This is true also of volcanic ash and bentonite. Horizons of unusual significance are formations classified as "radioactive sand or lime," because these high radioactivity values are frequently misinterpreted. Such formations have been found to be rather rare, but are worthy of note, especially if the horizon is a possible producer of oil or gas in the area under study. The phenomenon has been detected in both sandstone and limestone. Core analyses through zones of this kind have shown the cause to be an extreme concentration of highly radioactive contaminating material probably deposited under some unusual circumstance.

The granite or basement rock is extremely radioactive and results in very high gamma-ray curve values.

Effect of Casing

The effect of various bore-hole conditions on the gamma-ray curve is illustrated in Figure 690. While each additional string of casing effects a slight reduction in gamma-ray intensity, there may be cases where this is not always apparent. When the casing is set in shale or other more highly radioactive formations, the greatest curve shifts usually result. It is important to compare the casing record with the curve to identify such shifts and eliminate possible misinterpretations.

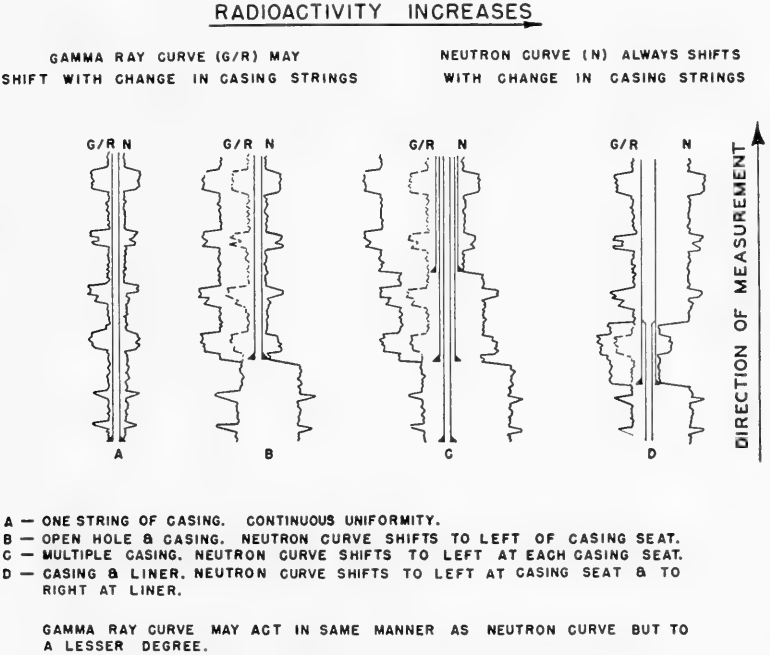

FIG. 690.—Effect of physical bore-hole conditions on gamma-ray and neutron curves. (Courtesy of Lane-Wells Company.)

The gamma-ray curve is normally not affected by the static fluid level or by changes in the type of fluid. Satisfactory gamma-ray curves can be obtained in any type of well fluid.

Neutron Curve Interpretation

The *neutron curve* is primarily a measurement of the amount of fluid surrounding the measuring instrument. The word *fluid* denotes the total amount of liquid present,

without regard to whether it is oil, gas, distillate or water, since the neutron curve responds only to the hydrogen content of fluids. This fluid may be considered to be of two types: that contained within the bore hole, and the connate or invaded fluid content of the formations.

The effective thickness of fluid surrounding the instrument normally remains constant except where there are changes in bore-hole diameter or at the fluid level. The bore-hole fluid (while permitting accurate location of such points) has negligible influence on the formation fluid response of the neutron curve. The principal effect registered on the neutron curve, therefore, is the amount of fluid present in the adjacent formation. The behavior of the curve is such that the greater the amount of fluid the lower the intensity of the curve. The neutron curve, as a result, reflects formation porosity rather than permeability.

Shales in general contain the greatest amount of total fluid since total fluid includes chemically combined as well as interstitial water. Shales therefore represent a reliable base or reference value on the neutron curve. Shale has been found to have as much as 44% total water. Sands do not contain chemically combined water, and the most porous sands often show a low neutron curve response approaching that of shale. Nonproductive limes and dolomites may contain very little, if any, actual fluid and therefore record as the highest intensity values.

Proper interpretation of the neutron curve is simplified when it is used in combination with the gamma-ray curve. (The resistivity or natural (self) potential curves of the electrical log may be used where available in place of the gamma-ray curve.) Formations which show relatively similar response on the gamma-ray curve may frequently be differentiated on the neutron curve. For example, limestone response is usually higher than sand response on the neutron curve. The presence of large amounts of silt or bentonite in certain productive sands may result in very high intensity response of the gamma curve, leading to their interpretation as normal or highly radioactive shale. The neutron curve, by showing response higher than shale, permits their proper identification as sand or lime.

Fluid content studies of sand and lime zones by the combined use of gamma-ray and neutron curves are extremely valuable. Frequently such zones may be either extremely dense or fluid-bearing throughout, or may be dense on top or at the base. It is not unusual to have a dense streak within a sand or lime body effectively creating a condition of separate reservoirs which might require completion by other than conventional means. In such cases the gamma-ray curve serves to identify the extent of the sand or lime body and the neutron curve indicates the dense and fluid-bearing zones, thus permitting proper completion measures to be applied. Many case histories have proved that the fluid zones in a productive horizon can be recompleted according to neutron curve intensity values to provide longer production life.

Under certain conditions the neutron curve has been found useful for detecting gas-fluid contacts. Dry gas sands (containing less than approximately one gallon of fluid per 1000 cubic feet of gas) normally record as highs, similar to dry, dense formations of the neutron curve. Since the fluid-bearing zones register as medium to low values, the gas-fluid contact is recorded on the log as a sharp shift to the right.

Interpretation of the neutron curve may be clarified by reference to Figure 689, which indicates the neutron curve response corresponding to typical formations. The solid, dotted, and dashed lines indicate the range of neutron curve response to be expected for formations differing widely in amount of fluid content. Particular attention is called to the zones marked "fluid". These zones show the method of identifying such porous zones. It is important to note that the neutron curve response to fluid-bearing zones of less than 2 feet in thickness may not show the pronounced throw-back experienced in thicker zones. This results from the loss of detail caused by the length of the ionization chamber and should be considered when interpreting the curve.

A second type of information supplied by the neutron curve, the accurate location of casing shoes, parted casing, liners, and fluid levels is shown in Figure 690.

As previously described, the shale value on the neutron curve remains a relatively constant base line throughout the traverse. Each additional layer of steel, such as casing or a liner surrounding the neutron instrument, reduces the curve intensity because of the shielding effect on the neutron source. Thus the entrance of the instrument into an additional string of casing or liner overlap results in a shift to the left of the entire base line. This new base line is assumed until some other physical change is encountered. When short ionization chambers are used, these physical changes can be located within one foot.

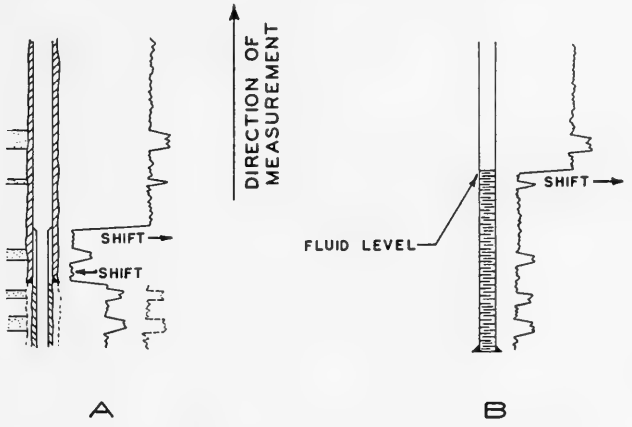

Fig. 691.—Additional effects of physical bore-hole conditions on neutron curves. (A) Neutron curve is affected by hole diameter. The curve shifts as shown for each change in hole diameter. A change in the amount of casing surrounding the instrument also causes the curve to shift as indicated. No change in bore-hole diameter: note length of shift. (B) Neutron curve is affected by well fluid-level. The curve shifts to the right at the fluid level.

The neutron curve is also useful in determining or checking fluid level, as shown in Figure 691. Being very sensitive to the amount of fluid surrounding the instrument, a drastic change such as that encountered at fluid level records as a large base line shift to the right. After the shift has taken place, however, the curve continues in a normal manner on the newly-assumed base line. If the fluid level is at a critical or interesting zone, where relative intensity comparisons of adjacent formations are desired, it is recommended that the hole be filled to a higher level and a re-traverse made to eliminate the curve shift at this point.

Comparison of Radioactivity Logs and Electrical Logs

Figures 692 and 693 show comparison plots of radioactivity and electrical logs for limestone and sandstone fields, respectively.

The close resemblance between the gamma-ray curve and the S.P. curve on the one hand and the neutron curve and the resistivity curves on the other is very striking. Although this close resemblance is usually observed, it should be pointed out that it is mainly coincidental because each of the two methods of logging measures different parameters.

The resemblance is quite useful when attempting to make correlations between wells having electric logs and those having radioactivity logs.

Applications of Radioactivity Well Logs

In the early stages of the development of this type of logging it was thought that some direct relationship might exist between natural radioactivity and petroleum. Expe-

rience to date indicates the absence of any such relationship. The logs have proved to be a very useful tool, however, and have been indirectly responsible for locating large petroleum reserves.

Prior to the development of radioactivity well-logging, it was necessary to obtain

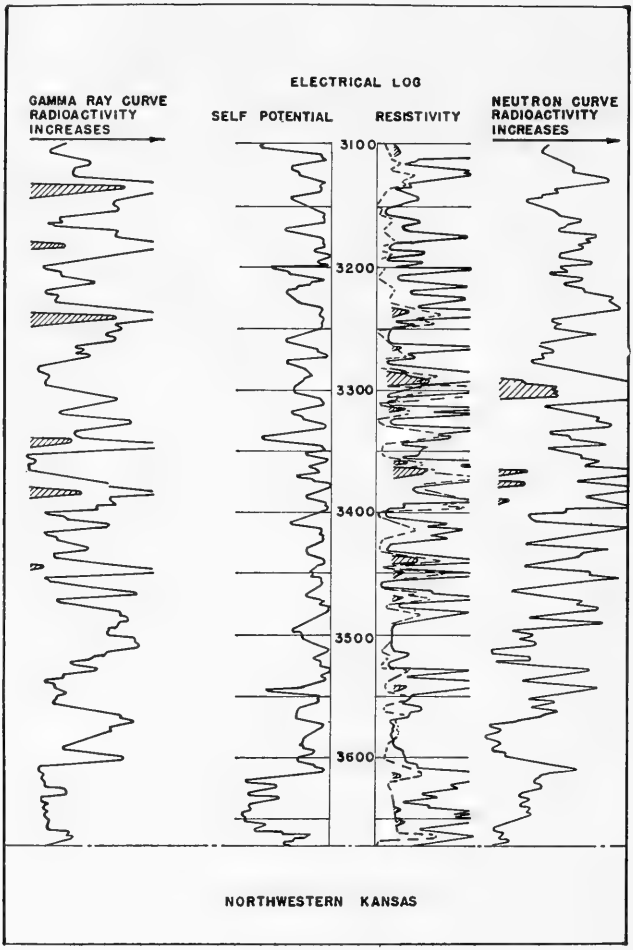

Fig. 692.
(Courtesy of Lane-Wells Company.)

all desired well information before casing was set. For this reason, completion practices have included various types of logging and sample-taking in open holes to assure complete information for subsequent operations.

Determining the Tops and Bottoms of Formations

An important part of the correct interpretation of any log is the accurate determination of the tops and bottoms of formations. This procedure requires particular attention for radioactivity well logs because of the characteristically sloping transitions

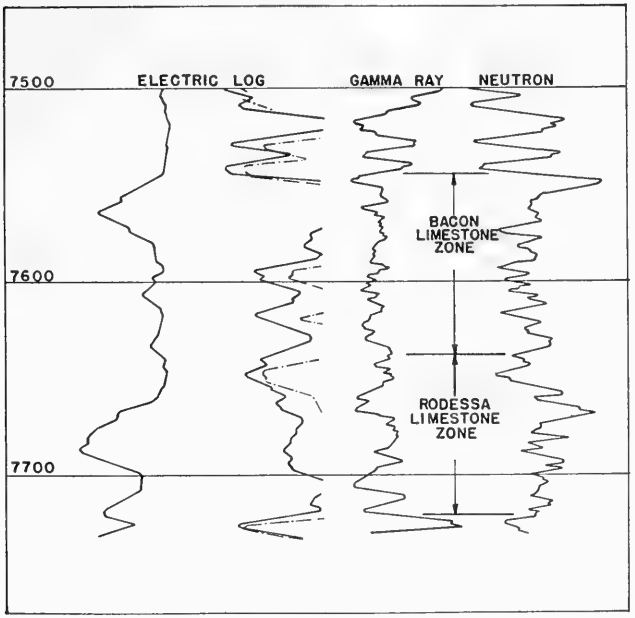

FIG. 693.
(Courtesy of Lane-Wells Company.)

which represent formation contacts. An understanding of the causes of these sloping transitions is helpful in their interpretation. The primary cause of this type of representation is the length of the measuring device. The nature of the instruments requires a measuring device approximately three feet in length for the gamma-ray curve and one foot for the neutron curve. This means that the complete zone of contact may cover as much as five feet for the former and three feet for the latter. It is obvious

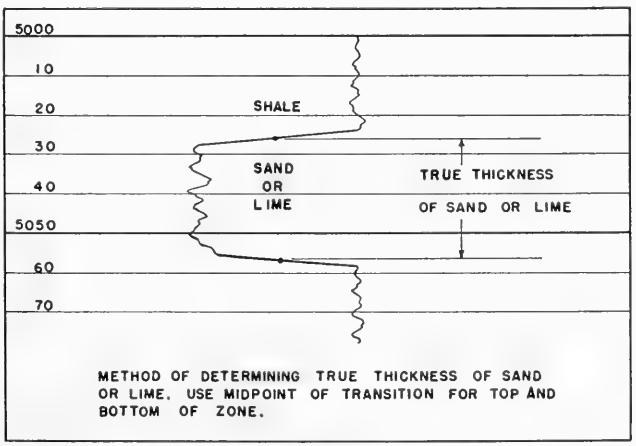

FIG. 694.
(Courtesy of Lane-Wells Company.)

that the formation breaks and details shown on the neutron curve may be sharper than those shown on the gamma-ray curve. In all cases, regardless of the magnitude of the break, the midpoint, or center of the minimum-maximum intensity value on the curve will usually indicate the formation contact. See Figure 694.† Other factors such as the lack of uniform distribution of radioactive materials may influence the sharpness with which formation contacts can be measured. Effects of this nature cannot be easily determined, but experience indicates that they generally do not materially influence the accuracy of determining formation breaks.

Cement Detection.—Gamma-ray logging may be used to locate the presence of cement behind the casing by mixing carnotite (containing about 10 per cent uranium oxide) with the cement.‡

Obtaining Stratigraphic Information

Early experience with the gamma-ray curve indicated that a reliable picture of the stratigraphy of the section covered by the log was obtainable. The location of upper, cased-off, potential producing zones presented a logical field for this type of logging, particularly where no information was available or where the available information was somewhat doubtful. The location of the top of a producing zone for bottom water shut-off, the correction of some of the earlier drillers' logs, the location of upper sands for salt water disposal, the supplying of additional information where cores were not completely recovered or were lost, the location of upper potential fresh water sands, and the location of the top and bottom of an oil-producing zone for gas-oil ratio control are all applications of this type.

Structural Studies

In most areas, one or more outstanding, easily-identified horizon markers have been found. In some instances, they are exceptionally clean sands or limes. In other cases, some highly-radioactive shale, bentonite or zone of volcanic ash is present as a persistent marker which can be located on the gamma-ray curve. In such cases surveys are run on key wells, or over selected cross-sections of the area being studied. With a few accurate points scattered over a pool, a much better idea of subsurface conditions is obtained. Figures 695 and 696 illustrate cross-sections in studies of this kind.

In Figure 695 the two marine shales of each well have been accentuated by the heavier lines and through proper correlation show the traces of the two apparent fault planes of the block. It is reasonable to assume that, with the block lying between wells C and D, another test drilled between them would find the 8040 foot sand higher in the fault block. By locating a fault through well C which is not present in well B, correlation indicates an interruption in the normal dip. The other fault is located between C and D by correlation of radioactive shales and confirmed by obvious correlation on the sands.

On many of the large ranches in West Texas, New Mexico and other areas a large number of cased water wells are scattered over the range land. Good structural markers are present in some of these wells. Gamma-ray curves have provided the information for structural studies based on these markers.

Locating Zones of Porosity

The porous limestones and sandstones usually contain fluid, and these porous zones may be located by a combination of gamma-ray and neutron curves. The gamma-ray curve defines the stratigraphic breaks in the section with limes and sands recorded as minimum values. The response of the neutron curve is proportional to the amount of hydrogen within the neutron field. The greater the amount of hydrogen within a formation, the lower the value recorded on the curve. It follows, therefore, that dense, barren horizons will be recorded on the curve as comparatively high values. Shales, because

† Note similarity with Figures 636, 643, 657 of electrical logs.

‡ L. G. Howell and A. Frosch, "Detection of Radioactive Cement in Cased Wells," A.I.M.E. *Pet. Tech.*, Vol. 136, 1940.

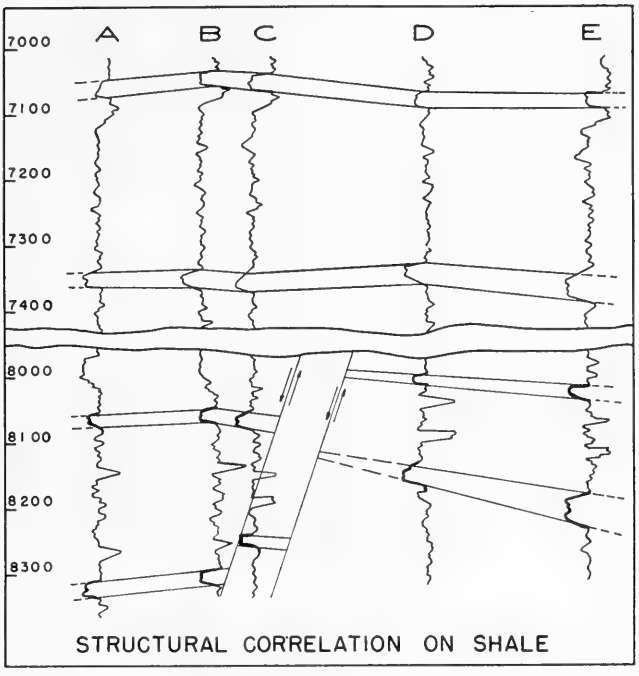

FIG. 695.
(Courtesy of Lane-Wells Company.)

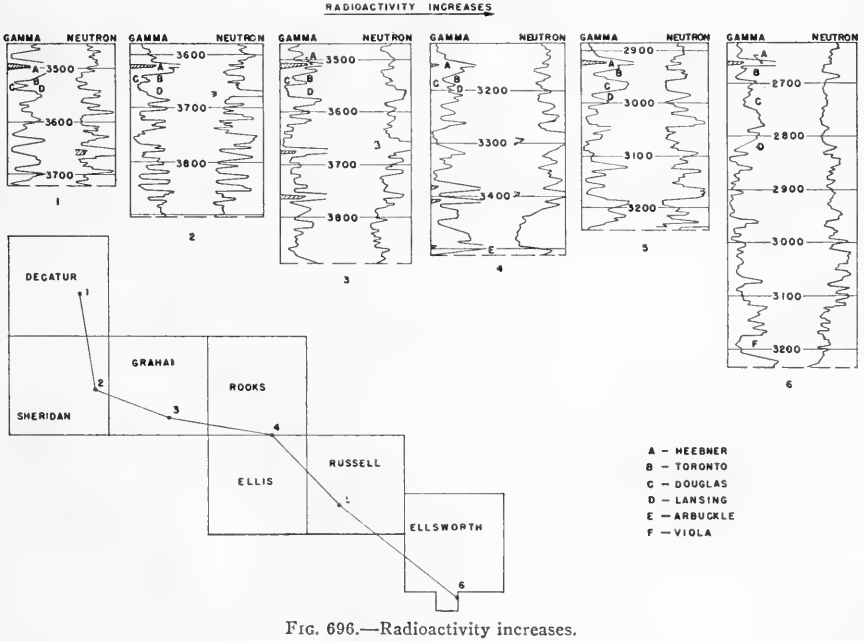

FIG. 696.—Radioactivity increases.

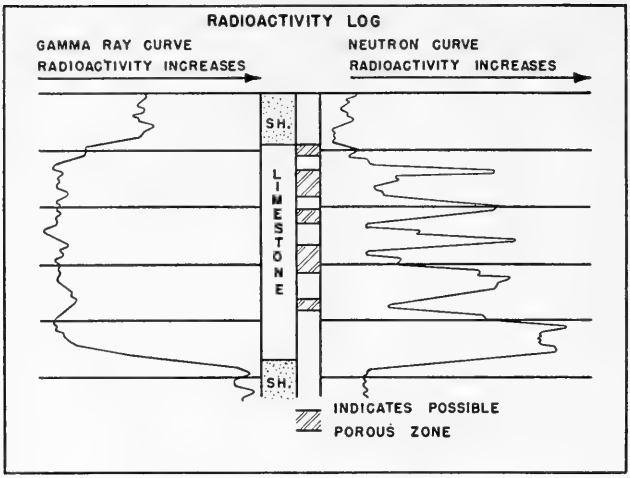

FIG. 697.—Radioactivity log. (Courtesy of Lane-Wells Company.)

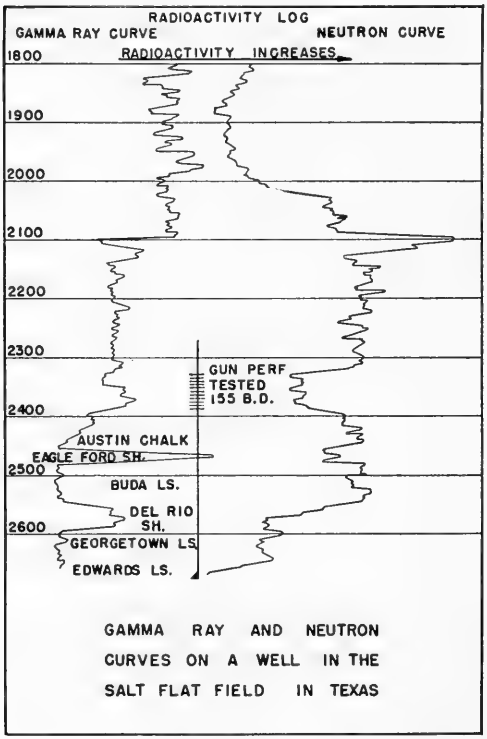

FIG. 698.
(Courtesy of Lane-Wells Company.)

of their connate water and the water of crystallization in the minerals out of which they are made, contain more hydrogen than saturated, porous limes or sands. As a result they usually are recorded as minimum values. Porous limestones and sands containing fluid are usually recorded as proportionally intermediate values somewhere between the value for shale and that for a dense formation.

Figure 697 shows a log run in a well in Kansas to locate the porous zones in the Mississippi limestone. The gamma-ray curve clearly outlines the limits of the limestone body with a shale both above and below it. The minimum values of the neutron curve indicate five porous zones within the otherwise dense limestone. These checked very closely with other available information on this particular well.

Figure 698 represents a well in the Salt Flat Field of Caldwell County, Texas. The well was almost at the depletion stage in the Edwards lime. The log was run in an attempt to locate a porous streak in the Austin Chalk. Although indications of porosity are shown on the neutron curve throughout the Austin, the only really significant zone is the one between 2320 and 2390 feet. This zone was perforated and acidized, and it became a producer.

DRILL-HOLE INVESTIGATIONS

UNITED STATES PATENTS

73,513 Issued Jan. 21, 1868. John D. Dale. "Improvement in Apparatus for Discovering the Fissures in the Sides of Wells."

270,597 Issued Jan. 16, 1883. E. F. MacGeorge. "Method of and Apparatus for Determining the Inclination of Borings."

281,772 Issued July 24, 1883. E. F. MacGeorge. "Clinometer-Compass and Apparatus for Reading its Indications."

649,636 Issued May 15, 1900. Hermann Gothan. "Apparatus for Determining Direction of Gradients of Stratified Masses."

802,071 Issued Oct. 17, 1905. William R. Bawden. "Clinometer."

821,048 Issued May 22, 1906. Hugh F. Marriott. "Means for Surveying Bore Holes."

830,730 Issued Sept. 11, 1906. Hugh F. Marriott. "Means for Surveying Bore Holes."

845,875 Issued Mar. 5, 1907. Percy Edward Lewis. "Instrument for Surveying Bore Holes."

856,990 Issued June 11, 1907. K. W. O. Schweder. "Instrument for Surveying Bore Holes."

963,242 Issued July 5, 1910. Robert Osterberg. "Measuring Instrument."

965,808 Issued July 26, 1910. Matthias Garvey. "Apparatus for Testing Drill Holes."

1,003,624 Issued Sept. 19, 1911. George J. Maas. "Instrument for Surveying Bore Holes."

1,090,673 Issued Mar. 17, 1914. Titus A. Beecher. "Method for Locating the Place and Character of a Liquid Coming from Strata in a Well."

1,090,674 Issued Mar. 17, 1914. Titus A. Beecher. "Method for Locating the Place of a Liquid Stratum in a Well."

1,133,218 Issued Mar. 23, 1915. Titus A. Beecher. "Method for Locating Liquid Strata in a Well."

1,152,701 Issued Sept. 7, 1915. Helge A. Borresen. "Device for Ascertaining the Vertical Angle and Direction of Diamond Drill Holes."

1,209,102 Issued Dec. 19, 1916. Hermann Anschütz-Kaempfe. "Apparatus for Determining Deviation of Bore Holes from the Vertical."

1,440,778 Issued Jan. 2, 1923. Walter L. Foster. "Water Indicator for Oil Wells."

1,536,007 Issued April 28, 1925. Frederick W. Huber. "Method for Locating Water-Bearing Strata in Bore Holes."

1,537,919 Issued May 12, 1925. Raymond D. Elliott. "Method of Locating the Level at which Water Enters a Well."

1,555,800 Issued Sept 29, 1925. Frederick W. Huber. "Method of Locating Water-Bearing Strata in Bore Holes."

1,555,801 Issued Sept. 29, 1925. Frederick W. Huber. "Method of Locating Water-Bearing Strata in Bore Holes."

1,555,802 Issued Sept. 29, 1925. Frederick W. Huber. "Apparatus for Locating Water-Bearing Strata in Bore Holes of Flowing Wells."

1,555,803 Issued Sept. 29, 1925. Frederick W. Huber. "Electrode Means for Conductivity Tests of Liquids in Oil Wells or other Bodies of Liquid."

1,582,184 Issued April 27, 1926. Sidney W. Mims. "Method and Means for Perforating Well Casings."

1,593,150 Issued July 20, 1926. F. L. Von Wurstemberger. "Apparatus for Determining Deflections from the Perpendicular of Bore Holes."

1,700,642 Issued Jan. 29, 1929. W. Meindersma. "Apparatus for Indicating and Determining the Point of Entrance of Fluids in Bore Holes."

1,720,325 Issued July 9, 1929. John D. Hackstaff and Labanna T. McCutcheon. "Method and Apparatus for Determining the Position of Fluid-Bearing Sands while Drilling Wells."

1,725,979 Issued Aug. 27, 1929. George H. Ennis. "Dose Distributor."

1,786,196 Issued Dec. 23, 1930. George H. Ennis. "Method and Apparatus for Determining the Location of Water Strata in Wells."

1,793,894 Issued Feb. 24, 1931. Reuben C. Baker. "Formation Direction Indicator."

1,796,547 Issued Mar. 17, 1931. Laurence E. Trout. "Apparatus for Indicating the Flow of Subsurface Fluids."

1,811,648 Issued June 23, 1931. E. E. Rosaire. "Method of Determining the Straightness of Drill Holes in the Earth."

1,819,923 Issued Aug. 18, 1931. Conrad Schlumberger. "Electrical Process and Apparatus for the Determination of the Nature of the Geological Formations Traversed by Drill Holes."

1,822,203 Issued Sept. 8, 1931. Frank M. Collins. "Indicating Means for Wells."

1,826,961 Issued Oct. 13, 1931. Louis B. Slichter. "Apparatus for Exploring for Ore."

1,845,379 Issued Feb. 16, 1932. Thomas S. West. "Process of and Apparatus for Locating Mineral Deposits in Subsurface Earth Strata."

1,865,847 Issued July 5, 1932. George H. Ennis. "Method of Locating the Point of Entry of Water into Oil Wells."

1,877,593 Issued Sept. 13, 1932. Irwin Roman. "Method and Apparatus for Surveying Bore Holes."

1,889,889 Issued Dec. 6, 1932. George H. Ennis. "Method of Testing Open Wells."

1,891,628 Issued Dec. 20, 1932. Charles R. Nichols. "Method of Determining Angle and Direction of Dip of Geological Formations."

1,894,328 Issued Jan. 17, 1933. Conrad Schlumberger. "Electrical Device for the Determination of Specific Resistivity."

1,913,293 Issued June 6, 1933. Conrad Schlumberger. "Electrical Process for the Geological Investigation of the Porous Strata Traversed by Drill Holes."

1,913,845 Issued June 13, 1933. Hallan N. March and John H. Howard. "Apparatus for Determining Deep-Well Temperatures."

1,927,664 Issued Sept. 19, 1933. John C. Karcher. "Method and Apparatus for Exploring Bore Holes."

1,970,342 Issued Aug. 14, 1934. Conrad Schlumberger. "Process for the Reconnaissance of the Geological Formations, and Especially for the Study of Porous Strata Encountered by a Bore Hole."

1,994,761 Issued Mar. 19, 1935. George H. Ennis. "Solution for Use in Testing Wells."

1,994,762 Issued Mar. 19, 1935. George H. Ennis. "Electrolyte for Use in Testing Wells."

1,995,492 Issued Mar. 26, 1935. O. E. Andrus and K. S. Willburg. "Device for Determining the Composition of Fluid Bodies in Motion and for Selectively Distributing the Flow of Portions of said Bodies to Predetermined Locations."

1,996,530 Issued April 2, 1935. Karl Sundberg and Erik Helmer Lars Hedstrom. "Method of and Apparatus for Electrical Investigation of Rock Drill Holes."

2,015,873 Issued Oct. 1, 1935. Conrad Schlumberger. "Apparatus for Sampling the Rock in Bore Holes."

2,018,080 Issued Oct. 22, 1935. Oscar Martienssen. "Method of and Device for Differentiating Between Geologic Strata Traversed by Bore Holes."
2,029,491 Issued Feb. 4, 1936. Wilfred G. Lane. "Gun Type Formation Tester."
2,029,454 Issued Feb. 4, 1936. Walter T. Wells. "Means and Method of Perforating Well Casings."
2,029,478 Issued Feb. 4, 1936. Marcus W. Haines. "Means and Method of Perforating Deep Wells."
2,029,490 Issued Feb. 4, 1936. Wilfred G. Lane. "Method and Means for Controlling Deep Well Gunfire for Perforating Casings."
2,033,562 Issued Mar. 10, 1936. Walter T. Wells. "Method for Preparing Oil Wells for Production."
2,037,306 Issued April 14, 1936. Ludwig W. Blau and Ralph W. Gemmer. "Method and Apparatus for Logging a Well."
2,038,046 Issued April 21, 1936. J. J. Jakosky. "Method and Apparatus for Alternating Current Investigation of Uncased Drill Holes."
2,050,128 Issued Aug. 4, 1936. Conrad Schlumberger. "Thermometric Method of Locating the Top of the Cement Behind a Well Casing."
2,053,967 Issued Sept. 8, 1936. E. N. Merrill and George A. Young. "Apparatus for Determining Well Temperatures."
2,070,912 Issued Feb. 16, 1937. Eugene McDermott. "Method of Electrically Exploring Bore Holes."
2,072,950 Issued Mar. 9, 1937. F. W. Huber. "Method of and Apparatus for Electrically Exploring Earth Formations."
2,076,211 Issued April 6, 1937. A. P. & G. H. Straatman. "Apparatus for Well Surveying."
2,084,143 Issued June 15, 1937. J. N. Hummel. "Process for Inspecting the Ground."
2,085,664 Issued June 29, 1937. John C. Karcher. "Method and Apparatus for Determining Porosity of Rock Formations."
2,089,216 Issued Aug. 10, 1937. Edward D. Lynton. "Apparatus for Orienting Cores."
2,096,359 Issued Oct. 19, 1937. D. G. Hawthorne. "Apparatus for Subsurface Surveying."
2,104,743 Issued Jan. 11, 1938. Henry N. Herrick. "Method of Correlating Subsurface Strata."
2,105,650 Issued Jan. 18, 1938. Donald Hering. "Core Orientation Apparatus."
2,114,056 Issued April 12, 1938. Ralph W. Lohman. "Method for Electrically Investigating Subterranean Strata."
2,131,993 Issued Oct. 4, 1938. Bruno A. Wittkuhns and Frederic M. Watkins. "Sonic Depth and Height Indicator."
2,132,807 Issued Oct. 11, 1938. W. M. Rust, Jr., et al. "Single Cable Electrical Well Logging."
2,133,786 Issued Oct. 18, 1938. J. Neufeld. "Method of and Apparatus for Determining the Dip of the Earth's Substrata."
2,140,798 Issued Dec. 20, 1938. J. J. Jakosky. "Electrical Method and Apparatus for Determining the Characteristics of Geologic Formations."
2,141,826 Issued Dec. 27, 1938. C. Schlumberger. "Method and Arrangement for the Electrical Survey of the Strata Traversed by a Bore Hole."
2,142,555 Issued Jan. 3, 1939. M. C. Bowsky and A. D. Winter. "Automatic Compensator for Geophysical Devices."
2,147,942 Issued Feb. 21, 1939. Randall Wright. "Method for Determining Directional Orientation of Materials."
2,150,169 Issued Mar. 14, 1939. J. J. Jakosky. "Method and Apparatus for Continuous Exploration of Bore Holes."
2,153,802 Issued Apr. 11, 1939. J. J. Jakosky. "Method and Apparatus for Continuous Exploration of Bore Holes."
2,155,133 Issued Apr. 18, 1939. J. J. Jakosky. "Electrical Method and Apparatus for Determining the Characteristics of Geologic Formations."
2,156,052 Issued April 25, 1939. C. W. Cooper. "Logging Device."
2,156,519 Issued May 2, 1939. C. P. Walker. "Means for Measuring the Location of Obstructions in Wells."
2,159,418 Issued May 23, 1939. E. Babcock. "Electrical Logging Apparatus."
2,161,976 Issued June 13, 1939. F. T. Robidoux. "Electrode for Well Logging."

2,165,013 Issued July 4, 1939. C. Schlumberger. "Method and Apparatus for Identifying the Nature of the Formations in a Bore Hole."
2,165,213 Issued July 11, 1939. L. W. Blau and L. Statham. "Electrical Transient Well Logging."
2,167,066 Issued July 25, 1939. D. W. Elliott. "Locating Water Strata in Oil Wells."
2,167,630 Issued July 25, 1939. C. B. Bazzoni and Jos. Razek. "Electrical Prospecting Methods and Apparatus."
2,170,857 Issued Aug. 29, 1939. R. D. Elliott. "Recording Apparatus and Method."
2,174,638 Issued Oct. 3, 1939. C. Schlumberger. "Method and Apparatus for Electrical Survey of the Formations Cut by a Bore Hole."
2,176,169 Issued Oct. 17, 1939. H. G. Doll. "Method and Arrangement for Determining the Direction and Value of the Dip of Beds Cut by a Bore Hole."
2,183,565 Issued Dec. 19, 1939. P. F. Hawley. "Two-well Method of Electrical Logging and Apparatus Therefor."
2,184,338 Issued Dec. 26, 1939. G. H. Ennis. "Method of Apparatus for Locating Water Leakages in Wells."
2,189,900 Issued Feb. 13, 1940. David G. Hawthorne & John E. Owen. "Drill Stem Circuit Tester."
2,190,686 Issued Feb. 20, 1940. L. B. Slichter. "Mineral Exploration."
2,191,119 Issued Feb. 20, 1940. Conrad Schlumberger. "Method and Apparatus for Surveying the Formations Traversed by a Bore Hole."
2,191,120 Issued Feb. 20, 1940. L. B. Slichter. "Method of Geological Survey."
2,191,121 Issued Feb. 20, 1940. L. B. Slichter. "Geological Surveying Apparatus."
2,197,493 Issued April 16, 1940. L. G. Ellis and J. W. Millington. "Electrical Prospecting Apparatus."
2,199,367 Issued April 30, 1940. L. F. Athy and H. R. Prescott. "Method of Logging Bore Holes."
2,199,705 Issued May 7, 1940. J. C. Karcher. "Apparatus for Making Electrical Surveys of Bore Holes."
2,202,656 Issued May 28, 1940. C. J. Haynes. "Well-Logging Electrode."
2,206,863 Issued July 9, 1940. R. T. Cloud. "Electrical Logging of Earth Formations."
2,206,864 Issued July 9, 1940. R. T. Cloud. "Electrical Logging of Earth Formations."
2,206,890 Issued July 9, 1940. P. F. Hawley. "Electrical Logging of Wells."
2,206,891 Issued July 9, 1940. P. F. Hawley. "Electrical Logging of Earth Formations."
2,206,892 Issued July 9, 1940. P. F. Hawley. "Electrical Logging of Earth Formations."
2,206,893 Issued July 9, 1940. P. F. Hawley. "Method and Apparatus for Logging Wells."
2,206,894 Issued July 9, 1940. D. Silverman. "Method and Apparatus for Logging Wells."
2,207,280 Issued July 9, 1940. L. F. Athy, et al. "Method of Electrical Logging."
2,207,281 Issued July 9, 1940. L. F. Athy and H. R. Prescott. "Seismic Method of Logging Bore Holes."
2,210,795 Issued Aug. 6, 1940. R. T. Cloud. "Method and Apparatus for Electrical Logging."
2,211,124 Issued Aug. 13, 1940. J. J. Jakosky. "Method for Continuously Exploring Bore Holes."
2,211,125 Issued Aug. 13, 1940. J. J. Jakosky. "Method and Apparatus for the Electrical Exploration of the Subsurface."
2,212,273 Issued Aug. 20, 1940. Oscar Martienssen. "Arrangement for Measuring the Local Specific Resistance of Bore Hole Strata."
2,212,274 Issued Aug. 20, 1940. Oscar Martienssen. "Method of Exploring the Porosity of Geologic Strata Traversed by Bore Holes."
2,214,786 Issued Sept. 17, 1940. B. P. Bishop. "Apparatus for Logging Holes while Drilling."
2,219,274 Issued Oct. 22, 1940. S. A. Scherbatskoy. "Well Survey Method and Apparatus."
2,220,070 Issued Nov. 5, 1940. C. B. Aiken. "Method of and Apparatus for Magnetically Exploring Earth Strata."
2,220,788 Issued Nov. 5, 1940. R. W. Lohman. "Method and Apparatus for Investigating Subterranean Strata by Means of Electromagnetic Measurements."

2,221,951 Issued Nov. 19, 1940. W. D. Mounce and W. M. Rust, Jr. "Making Electrical Measurements."
2,222,149 Issued Nov. 19, 1940. E. Lipson. "Method and Apparatus for Logging Wells."
2,222,182 Issued Nov. 19, 1940. W. D. Mounce and W. M. Rust, Jr. "Earth Impedance Measuring Device."
2,222,608 Issued Nov. 26, 1940. R. D. Elliott. "Electrical Surveying in Drill Holes."
2,224,635 Issued Dec. 10, 1940. E. Lipson. "Alternating Current Method and Apparatus for Logging Wells."
2,225,668 Issued Dec. 24, 1940. P. Subkow and L. Dillon. "Method and Apparatus for Logging Drill Holes."
2,229,604 Issued Jan. 21, 1941. D. Silverman. "Electrical Logging."
2,230,502 Issued Feb. 4, 1941. J. M. Pearson. "Electrical Prospecting Method and Apparatus."
2,230,999 Issued Feb. 11, 1941. H. G. Doll. "Methods of Indicating Spontaneous Potentials in Shallow Wells."
2,233,420 Issued March 4, 1941. E. G. Leonardon. "Method and Apparatus for Exploring Drill Holes."
2,236,668 Issued April 1, 1941. L. W. Blau and R. R. Thompson. "Method and Apparatus for Logging Wells."
2,239,466 Issued April 22, 1941. J. Neufeld. "Method and Apparatus for Electrical Investigation of Drill Holes."
2,242,161 Issued May 13, 1941. L. F. Athy and H. R. Prescott. "Method of Logging Drill Holes."
2,242,612 Issued May 20, 1941. E. G. Leonardon. "Method for Determining the Beds Traversed by Drill Holes."
2,245,700 Issued June 17, 1941. W. D. Mounce. "Resistance Thermometer."
2,246,460 Issued June 17, 1941. C. B. Bazzoni and J. M. Pearson. "Electrical Prospecting Apparatus."
2,247,417 Issued July 1, 1941. D. Silverman and R. W. Stuart. "Electrical Logging."
2,248,101 Issued July 8, 1941. R. W. Lohman. "Method and Apparatus for Investigating Subterranean Strata."
2,249,769 Issued July 22, 1941. E. G. Leonardon. "Electrical System for Exploring Drill Holes."
2,251,900 Issued Aug. 5, 1941. B. S. Smith. "Well Surveying."
2,253,485 Issued Aug. 19, 1941. C. B. Bazzoni and J. Razek. "Electrical Prospecting Method and Apparatus."
2,255,754 Issued Sept. 16, 1941. L. C. Beers. "Multiple Record Electrologging of Wells."
2,259,904 Issued Oct. 21, 1941. B. F. McNamee and F. Rieber. "Method and Apparatus for Logging Boreholes."
2,264,318 Issued Dec. 2, 1941. F. W. Lee. "Geophysical Surveying."
2,261,563 Issued Nov. 4, 1941. F. Rieber. "System for Measuring Earth Conductivity."
2,262,419 Issued Nov. 11, 1941. L. F. Athy and H. R. Prescott. "Method of Electromagnetic Logging."
2,264,318 Issued Dec. 2, 1941. F. W. Lee. "Geophysical Surveying."
2,265,978 Issued Dec. 16, 1941. D. E. Batchelder. "Alternating Current Electro-Logging of Well Bores."
2,266,071 Issued Dec. 16, 1941. R. G. Piety. "Well Surveying Device."
2,268,137-8 Issued Dec. 30, 1941. H. M. Evjen. "Electrical Well Logging System."
2,269,269 Issued Jan. 6, 1942. F. W. Jessen. "Well Logging."
2,271,951 Issued Feb. 3, 1942. J. M. Pearson and G. A. Smith. "Electrical Prospecting Method and Apparatus."
2,273,215 Issued Feb. 17, 1942. J. Neufeld. "Well Surveying Method and Apparatus."
2,273,363 Issued Feb. 17, 1942. E. Lipson. "Method for Electrical Investigation of Cased Drill Holes."
2,274,248 Issued Feb. 24, 1942. S. A. Scherbatskoy and J. Neufeld. "Well Surveying Method."
2,281,766 Issued May 5, 1942. P. F. Hawley. "Logging of Permeable Formations Traversed by Wells."
2,281,960 Issued May 5, 1942. V. V. Vacquier. "Apparatus for Logging Bores."
2,288,876 Issued July 7, 1942. J. C. Arnold. "Magnetic Logging."

2,288,884 Issued July 7, 1942. M. C. Bowsky. "Electrical Logging in Oil-Filled Wells."
2,288,973 Issued July 7, 1942. J. Neufeld and E. H. Cooley. "Well Surveying Method and Apparatus."
2,289,687 Issued July 14, 1942. R. W. Stuart. "Method and Apparatus for Logging Wells."
2,290,075 Issued July 14, 1942. M. Schlumberger. "Thermal Process and Device for Surveying the Beds Traversed by Drill Holes."
2,290,408 Issued July 21, 1942. W. J. Crites. "Exploration of Boreholes."
2,291,692 Issued Aug. 4, 1942. R. T. Cloud. "Magnetic Logging."
2,297,568 Issued Sept. 29, 1942. E. G. Leonardon. "Spontaneous Potential by Induction."
2,297,754 Issued Oct. 6, 1942. G. H. Ennis. "Method of Locating Strata in Wells and Electrode Apparatus Therefor."
2,301,326 Issued Nov. 10, 1942. C. E. Reistle, Jr. "Process for Obtaining Temperature Gradients in Bore Holes."
2,307,887 Issued Jan. 12, 1943. C. J. Haynes. "Rotating Contact Device."
2,310,611 Issued Feb. 9, 1943. E. E. Blondeau. "Electrical Exploration of Geologic Strata."
2,311,757 Issued Feb. 23, 1943. J. J. Jakosky. "Thermometric Method and Apparatus for Exploration of Boreholes."
2,313,384 Issued March 9, 1943. R. E. Lee. "Means for Determining the Tectonics and Nature of Subsurface Geology."
2,315,127 Issued March 30, 1943. W. D. Mounce. "Resistance Thermometer."
2,315,840 Issued April 6, 1943. W. J. Crites. "Borehole Thermometer."
2,316,942 Issued April 20, 1943. H. G. Doll. "Apparatus for Measuring Temperatures in Boreholes."
2,317,259 Issued April 20, 1943. H. G. Doll. "Device for Determining the Strata Traversed by Drill Holes."
2,317,304 Issued April 20, 1943. C. Schlumberger. "Apparatus for the Electrical Surveying of Boreholes."
2,324,103 Issued July 13, 1943. L. C. Miller. "Well Survey Apparatus."
2,333,883 Issued Nov. 9, 1943. R. G. Piety. "Well Surveying Device."
2,334,491 Issued Nov. 16, 1943. J. J. Jakosky. "Method and Apparatus for Determining the Electrical Characteristics of Geological Formations Traversed by Drill Holes."
2,337,442 Issued Dec. 21, 1943. L. W. Blau. "Well Logging."
2,340,987 Issued Feb. 8, 1944. F. T. Robidoux. "Electrical Well Caliper."
2,364,159 Issued Dec. 5, 1944. G. Muffly. "Apparatus for Electrical Bore Logging."
2,364,957 Issued Dec. 12, 1944. N. Douglas. "Electrical Surveying."
2,366,694 Issued Jan. 9, 1945. J. C. Bender. "Means and Method of Well Logging."
2,370,814 Issued March 6, 1945. J. A. Riise, Jr. "Method of Well Logging."
2,371,270 Issued March 13, 1945. A. L. Smith. "Electrical Logging of Well Bores."
2,376,168 Issued May 15, 1945. W. D. Mounce. "Well Logging."
2,388,141 Issued Oct. 30, 1945. G. G. Harrington. "Electrical Logging Apparatus."
2,388,896 Issued Nov. 13, 1945. C. B. Aiken. "Electrical Method and Apparatus for Logging Boreholes."
2,393,009 Issued Jan. 15, 1946. M. E. Chun. "Electrical Well Logging Method and Apparatus."
2,397,254 Issued March 26, 1946. G. H. Ennis. "Method and Apparatus for Electrical Coring in Cased Boreholes."
2,397,255 Issued March 26, 1946. G. H. Ennis. "Method of and Apparatus for Electrically Determining the Formation in Wells."
2,398,324 Issued April 9, 1946. B. Pontecorvo. "Well Surveying."
2,398,562 Issued April 16, 1946. W. L. Russell. "Apparatus for Well Logging."
2,398,761 Issued April 23, 1946. C. B. Aiken. "Method and Apparatus for Simultaneous Determination of Various Properties of the Subsoil."
2,398,868 Issued April 23, 1946. R. W. Stuart and D. Silverman. "Apparatus for Electrical Well Logging."
2,400,593 Issued May 21, 1946. J. Neufeld. "Method of and Apparatus for Investigation of Cased Drill Holes."
2,400,678 Issued May 21, 1946. G. E. Archie. "Method and Apparatus for Electrically Logging Wells."

2,401,371 Issued June 4, 1946. J. M. Pearson and C. R. Nichols. "Electrical Prospecting Method and Apparatus."
2,404,132 Issued July 16, 1946. J. T. Hayward. "Apparatus for Use in Logging Wells."
2,404,622 Issued July 23, 1946. R. L. Doan. "Well Logging Apparatus."
2,411,843 Issued Dec. 3, 1946. C. B. Aiken. "Compensating Means for Electrical Borehole Apparatus."
2,414,862 Issued Jan. 28, 1947. R. E. Fearon. "Well Surveying Apparatus."
2,414,899 Issued Jan. 28, 1947. W. M. Rust, Jr. "Well Logging."
2,421,423 Issued June 3, 1947. S. Krasnow. "Method and Apparatus for Taking Physical Measurements in Boreholes."
2,428,034 Issued Sept. 30, 1947. C. R. Nichols and S. H. Williston. "Electrical Prospecting Apparatus."
2,428,155 Issued Sept. 30, 1947. H. Guyod. "Method and Apparatus for Logging Boreholes."
2,433,746 Issued Dec. 30, 1947. H. G. Doll. "Method and Apparatus for Investigating Earth Formations Traversed by Boreholes."
2,436,503 Issued Feb. 24, 1948. J. Y. Cleveland. "Delayed Well Logging."
2,438,518 Issued March 30, 1948. R. G. Piety. "Circuit for Measuring Voltage of an Alternating Source."
2,441,065 Issued May 4, 1948. W. G. Green. "Apparatus for Well Logging."
2,446,303 Issued Aug. 3, 1948. J. E. Owen. "Well Logging Apparatus."
2,446,527 Issued Aug. 10, 1948. M. E. Chun and J. C. Stick, Jr. "Phase Shift Logging of Well Bores."
2,450,060 Issued Sept. 28, 1948. R. Ring. "Well Surveying Instrument."
2,455,940-2 Issued Dec. 14, 1948. M. Muskat and N. D. Coggeshall. "Method of Geophysical Exploration by Microwaves."

GAMMA-RAY LOGGING

2,275,456 Issued March 10, 1942. J. Neufeld. "Method and Apparatus for Radioactive Investigation of Drill Holes."
2,275,747-8 Issued March 10, 1942. R. E. Fearon. "Well Survey Method and Apparatus."
2,284,345 Issued May 26, 1942. C. H. Schlesman. "Method and Apparatus for Geophysical Prospecting."
2,285,840 Issued June 9, 1942. S. A. Scherbatskoy. "Well Survey Method and Apparatus."
2,288,278 Issued June 30, 1942. L. G. Howell. "Gamma-Ray Well Logging."
2,296,176 Issued Sept. 15, 1942. J. Neufeld. "Well Survey Method and Apparatus."
2,298,794 Issued Oct. 13, 1942. L. G. Howell. "Well Logging."
2,309,835 Issued Feb. 2, 1943. R. E. Fearon. "Well Logging Apparatus and Method Thereof."
2,316,361 Issued April 13, 1943. R. G. Piety. "Method and Apparatus for Surveying Wells."
2,323,484 Issued July 6, 1943. J. Neufeld. "Well Logging Method and Apparatus."
2,345,119 Issued March 28, 1944. D. G. Hare. "Subsurface Prospecting."
2,349,225 Issued May 16, 1944. S. A. Scherbatskoy, G. Swift, R. E. Fearon and J. Neufeld. "Well Logging Instrument."
2,349,712 Issued May 23, 1944. R. E. Fearon. "Well Logging Method and Device."
2,349,753 Issued May 23, 1944. B. Pontecorvo. "Method and Apparatus for Geophysical Exploration."
2,351,028 Issued June 13, 1944. R. E. Fearon. "Well Surveying Method and Apparatus."
2,358,574 Issued Sept. 19, 1944. L. G. Howell. "Gamma-Ray Well Logging."
2,365,763 Issued Dec. 26, 1944. B. J. Kalb and D. H. Wise. "Well Logging Device."
2,369,550 Issued Feb. 13, 1945. A. Frosch. "Well Logging."
2,391,093 Issued Dec. 18, 1945. L. G. Howell. "Radioactivity Well Logging."

NEUTRON LOGGING

2,220,509 Issued Nov. 5, 1940. Folkert Brons. "Process and Apparatus for Exploring Geological Strata."
2,231,577 Issued Feb. 11, 1941. D. G. C. Hare. "Locating Cement."

2,302,247 Issued Nov. 17, 1942. J. Neufeld. "Well Surveying Method and Apparatus."
2,303,688 Issued Dec. 1, 1942. R. E. Fearon. "Well Surveying Method and Apparatus."
2,303,709 Issued Dec. 1, 1942. A. J. F. Siegert. "Subsurface Prospecting."
2,308,361 Issued Jan. 12, 1943. R. E. Fearon. "Well Logging Method and Device."
2,316,329 Issued April 13, 1943. D. G. C. Hare. "Subsurface Prospecting."
2,334,262 Issued Nov. 16, 1943. D. G. C. Hare. "Sursurface Prospecting."
2,345,119 D. G. C. Hare.
2,349,712 R. E. Fearon.
2,390,433 Issued Dec. 4, 1945. R. E. Fearon. "Well Survey Method and Apparatus."
2,398,324 Issued April 9, 1946. B. Pontecorvo. "Well Surveying."
2,408,230 Issued Sept. 24, 1946. W. E. Shoupp. "Measuring Apparatus."

RADIOACTIVITY LOGGING

2,197,453 Issued April 16, 1940. G. L. Hassler. "Method of Underground Exploration."
2,219,273 Issued Oct. 22, 1940. S. A. Scherbatskoy. "Well Logging by Measurements of Radioactivity."
2,219,274 Issued Oct. 22, 1940. S. A. Scherbatskoy. "Well Survey Method and Apparatus."
2,220,205 Issued Nov. 5, 1940. S. E. Buckley. "Method of Locating Detectable Cement in a Bore Hole."
2,273,215 Issued Feb. 17, 1942. J. Neufeld. "Well Surveying Method and Apparatus."
2,289,926 Issued July 14, 1942. J. Neufeld. "Well Survey Method and Apparatus."
2,308,176 Issued Jan. 12, 1943. L. G. Howell. "Operations in Boreholes."
2,313,310 Issued March 9, 1943. J. C. Arnold. "Well Bore Radiation Logging Apparatus."
2,315,355 Issued March 30, 1943. S. A. Scherbatskoy. "Well Surveying Method and Apparatus."
2,316,576 Issued April 13, 1943. R. E. Fearon. "Well Surveying Method and Apparatus."
2,320,643 Issued June 1, 1943. J. Neufeld. "Well Surveying Method and Apparatus."
2,320,890 Issued June 1, 1943. W. L. Russell. "Method of Geophysical Prospecting."
2,320,892 Issued June 1, 1943. S. A. Scherbatskoy, and R. E. Fearon. "Method of Geophysical Prospecting."
2,321,295 Issued June 8, 1943. L. G. Howell. "Apparatus for Logging Boreholes."
2,322,634 Issued June 22, 1943. L. B. Howell and L. W. Blau. "Method and Apparatus for Logging Boreholes."
2,332,873 Issued Oct. 26, 1943. D. Silverman. "Differential Radioactivity Logging."
2,337,269 Issued Dec. 21, 1943. R. G. Piety. "Marking Device."
2,339,129 Issued Jan. 11, 1944. M. M. Albertson. "Radiological Method of Surveying Wells."
2,346,789 Issued April 18, 1944. E. E. Roper. "Well Logging."
2,349,366 Issued May 23, 1944. C. A. Moon. "Method for Geophysical Prospecting."
2,352,433 Issued June 27, 1944. G. Herzog. "Well Logging."
2,352,993 Issued July 4, 1944. M. M. Albertson. "Radiological Method of Logging Wells."
2,353,619 Issued July 11, 1944. B. Pontecorvo and G. Swift. "Geophysical Prospecting."
2,358,945 Issued Sept. 26, 1944. C. F. Teichmann. "Method of Determining the Porosity and Location of Permeable Formations in Oil Wells."
2,361,274 Issued Oct. 24, 1944. A. M. Cravath and G. L. Hassler. "Radiological Exploration System."
2,361,389 Issued Oct. 31, 1944. R. E. Fearon. "Well Survey Method and Apparatus."
2,362,164 Issued Nov. 7, 1944. D. Silverman. "Radioactivity Logging."
2,364,975 Issued Dec. 12, 1944. J. J. Heigl and L. R. Hodell. "Determining Permeability of Geological Structure."
2,368,486 Issued Jan. 30, 1945. J. J. Mullane. "Well Logging."
2,368,532 Issued Jan. 30, 1945. R. E. Fearon. "Well Surveying Method and Apparatus."
2,369,672 Issued Feb. 20, 1945. D. G. C. Hare. "Method and Apparatus for Logging Boreholes."

2,370,162 Issued Feb. 27, 1945. D. G. C. Hare. "Method and Apparatus for Logging Boreholes."
2,371,628 Issued March 20, 1945. S. Krasnow. "Method and Apparatus for Dynamic Measurement of Borehole Radioactivity."
2,374,197 Issued April 24, 1945. D. G. C. Hare. "Borehole Logging Method and Apparatus."
2,376,196 Issued May 15, 1945. S. A. Scherbatskoy. "Ionization Chamber."
2,376,821 Issued May 22, 1945. S. A. Scherbatskoy, R. E. Fearon, J. Neufeld, and G. Swift. "Well Logging Instrument."
2,378,408 Issued June 19, 1945. G. Herzog. "Method and Apparatus for Logging Boreholes."
2,381,904 Issued Aug. 14, 1945. D. G. C. Hare. "Method and Apparatus for Logging Wells."
2,382,279 Issued Aug. 14, 1945. A. Wolf and G. Herzog. "Device for Recovering a Radiation Source."
2,384,840 Issued Sept. 18, 1945. S. Krasnow and L. F. Curtiss. "Radioactivity Well Logging Method and Apparatus."
2,385,378 Issued Sept. 25, 1945. R. G. Piety. "Well Surveying."
2,385,857 Issued Oct. 2, 1945. G. Herzog. "Cushioning Device for Radiation Detectors."
2,390,931 Issued Dec. 11, 1945. R. E. Fearon. "Well Logging Method."
2,390,965 Issued Dec. 11, 1945. S. A. Scherbatskoy. "Central Electrode Support."
2,409,436 Issued Oct. 15, 1946. S. Krasnow and L. F. Curtiss. "Method and Apparatus for Direct Recording of Borehole Radioactivity."
2,416,702 Issued March 4, 1947. S. Krasnow. "Apparatus and Method for Recording Borehole Radioactivity."
2,429,577 Issued Oct. 21, 1947. R. W. French. "Method for Determining Fluid Conductance of Earth Layers."
2,433,554 Issued Dec. 30, 1947. G. Herzog. "Well Logging Apparatus."
2,436,503 Issued Feb. 24, 1948. J. Y. Cleveland. "Delayed Well Logging."
2,443,680 Issued June 22, 1948. G. Herzog. "Method of Determining the Nature of Substrata."
2,443,731 Issued June 22, 1948. G. Herzog and K. C. Crumrine. "Method and Apparatus for Logging Boreholes."
2,446,588 Issued Aug. 10, 1948. G. Herzog and A. Wolf. "Method of Determining the Permeability of Substrata."
2,450,265 Issued Sept. 28, 1948. A. Wolf. "Method of Logging Boreholes."

CHAPTER XII

PHYSICAL PRINCIPLES APPLIED TO PRODUCTION PROBLEMS

The present chapter deals with the application of sound or pressure waves for determining the distance (depth) to the fluid level and to partial obstructions in an oil well. Before considering this specific application, it is well to review briefly certain physical principles of oil recovery in wells.

Principles Underlying Oil Recovery in Wells

The fluid level in an oil well or, more specifically, the height to which liquid petroleum and/or water stands above the producing horizon, is a direct indication of the pressure exerted against the producing zone in the bore-hole.†

Under equilibrium conditions,

$$p_{bh} = hd + p_g + p_{ch} \tag{1}$$

where

p_{bh} = bottom hole pressure in pounds per sq. in.
h = height of fluid in the well in ft.
d = average fluid pressure gradient or fluid density in pounds per sq. in. per foot
p_g = weight in pounds of section of gas column one inch square from fluid level to casing head
p_{ch} = casing head pressure in pounds per sq. in.

In words, Equation 1 states that the bottom-hole pressure is equal to the pressure of the column of fluid, plus the pressure of the gas column, plus the casing-head pressure.

† T. E. Swigert and C. R. Bopp, "Experiments in Use of Back-Pressure on Oil Wells," U. S. Bureau of Mines, Tech. Paper 322, 1924.
S. F. Shaw, "Well Back-Pressure and Fluid Levels," *Oil and Gas Journal*, Nov. 22, 1928.
S. F. Shaw, "Increasing the Ultimate Recovery of Oil," *A.I.M.E. Petroleum Technology*, 1931, pp. 178-193.
C. V. Millikan and Carrol V. Sidwell, "Bottom Hole Pressures in Oil Wells," *A.I.M.E. Petroleum Technology*, 1931, pp. 194-205.
C. V. Millikan, "Reservoir and Bottom Hole Producing Pressures as a Basis for the Proration of Crude Oil," *Oil and Gas Journal*, Aug. 11, 1932.
C. E. Reistle, Jr., and E. P. Hayes, "A Study of Sub-Surface Pressures and Temperatures in Flowing Wells in the East Texas Field and the Application of These Data to Reservoir and Vertical Flow Problems," U. S. Bur. of Mines Report of Investigations, 3211, May 1933.
H. C. Miller, E. S. Burnett, and R. V. Higgins, "Oil Well Behavior Based upon Subsurface Pressures and Production Data," *A.I.M.E. Petroleum Technology*, 1937, pp. 97-109.
M. Muskat, "Use of Data on the Build-up of Bottom Hole Pressures," *A.I.M.E. Petroleum Technology*, 1937, pp. 44-48.
M. Muskat, R. D. Wyckoff, H. G. Botset, and M. W. Meres, "Flow of Gas Liquid Mixtures Through Sands," *A.I.M.E. Petroleum Technology*, 1937, pp. 69-96.
M. L. Haider, "The Productivity Index," *A.I.M.E. Petroleum Technology*, 1937, pp. 112-119.
J. J. Jakosky, "Bottom Hole Measurements in Pumping Wells," *A.I.M.E. Petroleum Technology*, Tech. Pub. 1058, 1939.

A knowledge of producing zone pressures is a prime requisite for the solution of numerous petroleum reservoir analysis and producing well problems. For the former purpose the shut-in or static pressure (zero rate of production) is generally of most importance, while for the latter, the major concern usually involves the establishment of a relation between pressure and rate of production. It is occasionally found that the determination of a shut-in pressure may not be feasible, in which event the use of an extrapolation of the pressure-production rate relationship to a zero rate of production can be resorted to.

The rate of production Q depends on the difference between the reservoir pressure p_r, and a "friction pressure" p_f, plus the bottom-hole pressure p_{bh}. At moderate rates of flow, the rate of production Q may be expressed in the form

$$Q = C\,[p_r - (p_f + p_{bh})]$$

where

Q = rate of production
C = a constant of proportionality
p_r = pressure of fluid in the formation at zero production
p_f = "friction pressure." This so-called friction pressure is a back pressure in the formation and is a measure of the resistance which the fluid must overcome while flowing through the oil sand into the hole.

If it is assumed that the "friction pressure" is proportional to the rate of production ($p_f = kQ$, where k is a constant), the equation given above for Q may be written in the form

$$Q = Cp_r - CkQ - Cp_{bh}$$

On collecting the terms involving Q, one obtains

$$Q\,(1 + Ck) = C\,(p_r - p_{bh})$$

or

$$Q = c\,(p_r - p_{bh}) \qquad (2)$$

where

$$c = \frac{C}{1 + Ck} = \text{a constant.}$$

The assumption that the pressure p_f varies linearly with the rate of production leads to a theoretical production rate that is always greater than the physical pumping rate. This is especially true at the higher rates of production where turbulent flow occurs in the vicinity of the well. Thus, at production rates approaching zero and also at high rates, where a transition takes place from stream-line to turbulent flow in the stratum adjacent the hole, Equation 2 may break down. However, in problems concerned with the theoretical maximum rates of production, it is customary to assume that the assumptions made in deriving Equation 2 are fulfilled approximately, and this convention will be followed here.

By combining Equations 1 and 2 the rate of production may be expressed as follows:

$$Q = c(p_r - hd - p_g - p_{ch}) \tag{3}$$

Equations 2 and 3 are the basic theoretical equations relating the rate of production Q with the bottom-hole pressure p_{bh} and with the fluid level h. Because p_r is assumed to be a constant, it follows from Equation 2 that a graph of the values of bottom-hole pressure p_{bh} as ordinate and rates of production Q as abscissa is approximately a straight line. Also, it is evident from Equation 3 that a graph of the values of the fluid level h versus Q is approximately a straight line. Extrapolation of this line to the Q intercept ($h = 0$) yields the *theoretical* maximum rate of production, because $h = 0$ corresponds to a minimum back pressure of the fluid in the hole.* Thus, from Equation 2

$$Q_{\max} = c(p_r - p_g - p_{ch}) \tag{4}$$

As will be illustrated later, this *theoretical* rate is ordinarily not achieved in practice, because a definite hydrostatic flow head is necessary to force the oil to flow into the pump.

The production characteristics of a well may be determined by measuring or calculating the factors in Equations 2 or 3. Equation 2 is employed when using bottom hole pressure gauges, while Equation 3 utilizes the data obtained from fluid-level measurements.

BOTTOM-HOLE PRESSURE GAUGES

The bottom-hole pressure gauges in use at the present time are usually of a self-contained, continuous recording design.† The gauges are enclosed in a suitable case and consist essentially of two parts: (a) pressure element to record the hydrostatic pressure and (b) a clock, pressure or thermal-drive chart drum. A stylus attached to the free end of the pressure element records its movement on sensitized paper or metal affixed to the chart drum. The clock-drive comprises a small spring clock mechanism capable of driving the chart for periods of 24 to 72 hours. The pressure-drive depends upon a decrease in recorded pressure to rotate the chart. The thermal-drive comprises a bimetallic temperature-actuated system which produces a small angular rotation of the chart. The operation of the latter system depends on the increase of temperature with depth.

In flowing or gas-lift wells, depth pressure measurements may conveniently be made by running the bottom-hole pressure gauge into the tubing on a wire line, without greatly interfering with the well's production. In some wells it may not be possible to

* For thick sands and fluid level below the top of the sand a mean pressure should be used.

† C. V. Millikan and C. V. Sidwell, *loc. cit.*
E. K. Parks and C. W. Gibbs, "Instruments and Equipment for Recording Subsurface Pressures," *A.I.M.E. Petroleum Technology*, 1934, pp. 42-52.
Paul G. Exline, "A Precision Gage for Subsurface Pressure Measurements," *A.P.I., Drilling and Production Practice*, 1936, p. 116.

lower the instrument beyond certain critical rates of flow, which are a function of the respective cross-sectional areas of the bomb and the tubing, the velocity of the rising column, and the specific gravity of the fluid being produced. If bottom-hole pressures are to be taken by the pressure-bomb method when a well is pumping, it is generally most expedient to attach a clock-driven gauge to the bottom of the pump. In some wells it is possible to lower a small diameter pressure gauge† on a wire line in the annular space between the tubing and the casing. This method is subject to a number of limitations such as the size of the annular space, or the presence of waxy deposits or other obstructions such as liner tops, tubing catchers, or anchors. The attachment of a gauge to the bottom of the pump necessitates removing the pump, the rods, and at times even the tubing from the well. The equipment is then run back into the hole, and the gauge records the pressure existing in the well at the depth of the pump. On conclusion of a run, the pump must be pulled a second time to recover the gauge and chart. The record shows the variations in pressure versus time during the test.

It is evident that the above procedure for the procurement of direct bottom-hole pressures in pumping wells entails considerable time and expense for pulling rods and possibly tubing, as well as loss of production during the time the well is idle. Also, the effects produced on the bottom-hole pressures by altering the pump speed or the rate of production while the gauge is in the well are not available until after the instrument is recovered. Experience with pumping wells has indicated that it is generally most expedient to determine the height of the fluid column when the well is shut in, or producing at various rates, and to translate the column weight into a corresponding bottom hole pressure. Such tests can be made more economically and without shutting down operations or pulling rods and tubing.

METHODS FOR DETERMINING FLUID LEVELS

Under certain conditions, various types of measuring lines, floats, and chalk-line systems may be employed for determining fluid heights. As a general rule, however, such methods are limited to open wells and cannot be employed successfully during pumping operations. The most practical methods for measuring fluid levels in pumping wells or wells under pressure utilize sound or pressure wave reflections.

Considerable work has been done on sound ranging,‡ sonic means of determining fluid levels, and also on sound or pressure-wave methods for locating obstructions in tubings of various kinds.§ The first practical applications of the wave method in the United States were probably made

† C. C. Olson, "Running Instruments in Annulus of Tubed Wells," *The Oil Weekly,* March 4, 1946.

‡ C. W. Rice, "Sound Wave Apparatus," U. S. Patent 1,889,614, issued Nov. 29, 1932.
R. A. Fessenden, "Method and Apparatus for Determining Distance by Echo," U. S. Patent 1,853,119, issued April 12, 1932.
P. Langevin and C. L. Florisson, "Method and Apparatus for Sounding and for Locating Submarine Obstacles by Means of Ultra-Audible Waves," U. S. Patent 1,858,931, issued May 17, 1932.
H. C. Hayes, "Method and Apparatus for Sound Ranging," U. S. Patent 1,900,015, issued March 7, 1933.
E. E. Turner, U. S. Patents 2,009,460, 2,003,160, 2,044,820, on echo methods of measuring depths, issued July 30, 1935, Mar. 10, 1936, and June 23, 1936, respectively.
R. L. Williams, "Method and Apparatus for Measuring Distances and Depths," U. S. Patent 2,015,702, issued Oct. 1, 1935.

§ Th. Vautier, "Secondary Waves Produced by an Aerial Wave," *Comptes Rendus,* June, 1925, p. 1919; "Experimental Researches on Propagation of Aerial Waves Through a Long Cylindrical Pipe"; *Annales de Physique,* Series 10, Vol. 6, pp. 311-364, 1926; Vol. 14, *Annales de Physique,* pp. 263-626, 1930.

by Batcheller† and by Stoddard* about 1900. A schematic arrangement of the apparatus is illustrated in Figure 699. The pressure wave was created by firing a pistol K, and the elapsed time between initiation n^1 of this wave and its reflection n^3 was measured on a recording chronograph, actuated

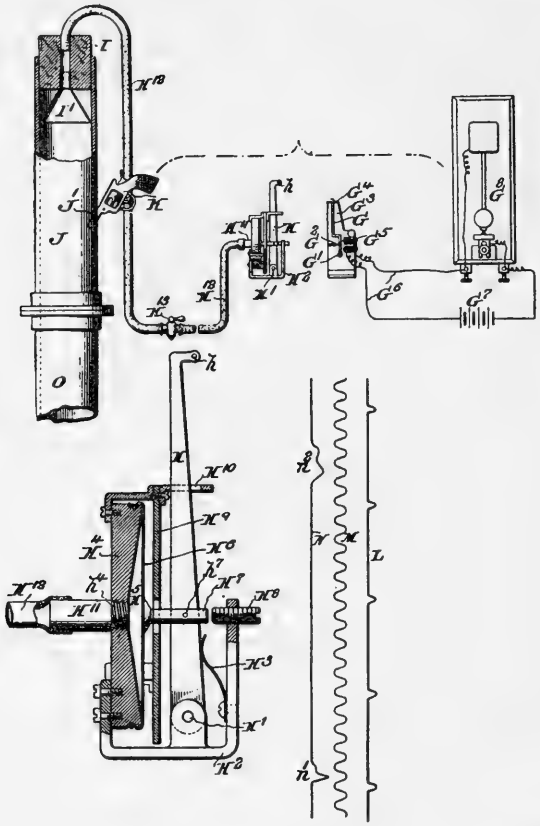

FIG. 699.—Early sound wave method of locating obstructions. (Batcheller, U. S. Patent 602,422.)

by a diaphragm H^6. The trace M of a tuning fork of known frequency was recorded on the record simultaneously to provide a means for measuring time intervals accurately.

A commercial incentive for this early work was furnished by the difficulties encountered in operation of the underground pneumatic mail and transport tubes in New York City, Philadelphia, Boston, etc. These tubes were from six to eight inches in diameter and in some cases had lengths of

† Birney C. Batcheller, "Apparatus for Locating Obstructions in Tubes," U. S. Patent 602,422, issued April 19, 1898.

* Personal communication from Chas. F. Stoddard, formerly Chief Engineer, American Pneumatic Service Company.

15 to 20 miles, with various stations along the route. The material to be transported was placed in a carrier tube and propelled to its destination by compressed air. Where the carrier became lodged between stations, it could be located by echo methods.

In applying this method in long tubes, it was found that the velocity of the wave in the tube varied with temperature, pressure, and humidity. It was noted further that where the tubes turned corners in following streets, and also where switch points or other partial obstructions were located, minor reflections were obtained, in addition to the main reflection coming from the blocked carrier. Changes in the velocity of the wave therefore were minimized by applying correction factors between these partial obstructions at known locations, or by measuring from the last recorded partial obstruction at a known location to the blocked carrier.

Sonic Method

The sonic or pressure-wave method of determining depths to fluid comprises: (1) a means for initiating the sound or pressure wave, (2) a suitable wave detecting and recording apparatus, and (3) a constant-speed recording system and/or timer.

Efforts to obtain more reliable data than those given by the original Batcheller procedure have yielded two general methods for initiating the pressure wave: (1) a method employing a pressure impulse created by the release of compressed gas from a small tank and (2) methods which employ the pressure wave initiated by a cartridge.

The first mentioned method was developed by Lehr and Wyatt.† The wave is created by releasing a small quantity of gas under pressure in a tank. The recorder attached to the casing head of the well comprises a diaphragm-driven system that actuates a mirror utilized in the photographic recording mechanism.‡ The second method creates the pressure wave by use of a cartridge, and the reflections coming from the well are detected by a microphone. The microphone may be of the electrodynamic type§ or a thermistor grid.†† The output of the microphone is amplified about 50 decibels, and then fed to a direct-writing ink recorder.

After the pressure wave has been generated, the echoes coming from the well consist of those from the tubing collars, other partial obstructions such as gas anchors, liner tops, tubing hangers, gas valves, etc., and the reflection from the fluid level. As will be seen in a later paragraph, the tubing collar reflections are useful in determining the velocity of wave propagation, and are used in calculating the depth to the fluid.

The tubing collar reflections generally are weak; to record them to the

† Paul E. Lehr and H. D. Wyatt, "Method and Apparatus for Measuring Well Depths," U. S. Patent 2,047,974, issued July 21, 1936.

‡ C. P. Walker, "Determination of Fluid Levels in Oil Wells by the Pressure Wave Echo Method," *A.I.M.E. Petroleum Technology*, 1937, pp. 33-43.

§ A. Wolf, "Acoustic Well-Depth Indicating," *World Oil*, Sept. 22, 1947.

†† J. J. Jakosky, "Bottom Hole Measurements in Pumping Wells," *A.I.M.E. Petroleum Technology*, Tech. Pub. 1058, 1939.

depth of fluid in deep wells requires either (1) careful tuning of the equipment or (2) high amplification. In one type of equipment† this may be accomplished by setting up a condition of resonance between the collar echoes coming out of the well and an oscillation that takes place in the tuning pipe between the recording instrument and the casing head. The tuning pipe is adjusted to resonance by changing its length in small increments until maximum tubing collar response is obtained. Usually the optimum frequency of the pipe will be the third harmonic of the tubing collar reflections. This is a "cut and try" procedure.

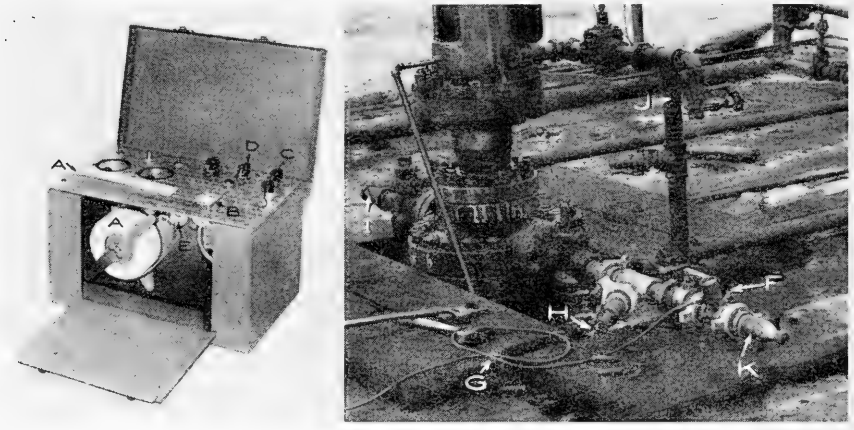

FIG. 700.—Reflectogram equipment for determining depth to fluid level. (Left) Direct-writing ink recorder. *A*, 35 mm. recording paper; *B*, ink stylus; *C*, amplification control; *D*, frequency response switch; *E*, sprocket feed for paper. (Right) Casing-head unit connected to well. *F*, microphone chamber, connected by cable, *G*, to the recorder mounted in a field car; *H*, gun for creating sound wave; *I*, gas line; *J*, oil line; *K*, microphone surge chamber. (Courtesy of International Geophysics Company.)

A second method for obtaining the tubing collar reflections‡ utilizes much greater audio amplification of the incoming signal, followed by filtering to remove the higher frequencies. Since filters are always responsive to the harmonics as well as the fundamental frequency to which they are adjusted, the recorded trace contains harmonics that often prove to be sources of error when an attempt is made to count the tubing collar reflections.

A third method utilizes a tuned recording pen or galvanometer§ which has been adjusted to cover the general frequency range of the incoming tubing collar reflections. This tuned recorder reproduces the tubing-collar frequencies and effectively suppresses the higher frequencies and well noises, thereby eliminating the source of error commonly present if the

† C. P. Walker, "Means for Measuring the Location of Obstructions in Wells," U. S. Patent 2,156,519, issued May 2, 1939.
C. P. Walker, "Pressure Wave Velocity Measuring System," U. S. Patent 2,190,141, issued Feb. 13, 1940.
‡ A. Wolf, *loc. cit.*
§ J. J. Jakosky, patents pending.

higher frequency harmonics are recorded. Unlike other low frequency recorders, this instrument has an exceptionally high and rapid response to a steep front wave like that from the fluid reflection. A view of the complete equipment is shown in Figure 700.

Operation of Wave Reflection Equipment.—The Reflectogram recorder is installed in a field car and when measurements are to be made, the car is positioned near the well and connected to the microphone by a shielded cable. The casing-head unit is connected to the well by a two-inch union and a standard gate or block valve. The distance between the casing-head and the casing unit should be as short as possible to minimize loss of reflection energy. The sound wave utilized to make these measurements is created by a specially loaded Reflectogram cartridge, which produces a low-frequency, high-energy sound pulse. When the shell is fired, the pulse enters the casing-head and travels down the annular space between the tubing and casing, being gradually dissipated and partially reflected by the various obstructions in the annulus. Small reflections are produced by tubing collars; stronger reflections are received from such larger obstructions as tubing catchers and liner tops, while the fluid surface reflects practically all of the wave energy impinging upon it, and gives a correspondingly greater reflection on the record. Production of oil and gas need not be halted during the tests. The unit is designed to withstand high pressures.

Calculating the Depth to Fluid

In most wells, each tubing collar between the casing head and the fluid will be shown as a small reflection on the tape record. The fluid level will be shown by a larger reflection. The depth to the fluid may therefore be determined by simply counting the number (to the nearest 0.5) of tubing collar reflections between the shot and the fluid-level reflection, and then multiplying this count by the average length of tubing. This method is shown in Figure 701, where 91.7 tubing-collar reflections exist between the shot and the fluid. Since the average length of tubing in this well is 30.1 feet, the depth to fluid is $30.1 \cdot 91.7 = 2760$ feet.

Occasionally, wells will be encountered with small diameter casing or other unfavorable conditions which impede the travel of the sound wave down the annulus. In such wells, the tubing-collar reflections may be weak and may therefore not be recorded entirely to the fluid level. The depths may then be determined by simple proportion. The procedure is to count the number of tubing-collar reflections to a given point as far down the record as possible, then calculating the depth of that point by multiplying the number of tubing-collar reflections by the average length of tubing. The depth to fluid will then be found by the simple proportion

$$\frac{\text{Depth to fluid}}{\text{Depth to point}} = \frac{S_f}{S_p}$$

where S_f is the length of record between the shot and the fluid reflection, and S_p is the length between the shot and the point of calculation. In like manner use may be made of the reflections from liner-top, tubing catcher, or any other partial obstruction whose accurate location or depth is known from the well records. Successful work has been done in many wells exceeding 8,000 feet in depth.

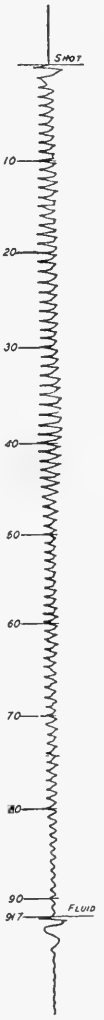

FIG. 701.—Typical reflection record without filter showing shot-point, tubing-collar reflections, and fluid reflections.

Fluid Density and Subsurface Pressures.—When wells of high productivity are pumped at rates considerably less than their potential, the fluid separates into its components when equilibrium is reached. The effects of this gravitational separation are illustrated in Figure 702. Because the pump is removing the fluid at the same rate that it is flowing into the well (the condition obtaining when equilibrium is reached and the fluid level is stationary), the fluid below the producing horizon is essentially of the same composition as that leaving the formation. In the annulus above the producing horizon, where direct flow of fluid from the formation is not taking place, a quiescent fluid condition exists. The oil-gas phase will comprise the upper portion of the fluid column, while the water phase will comprise the lower portion of the column. The degree to which this separation takes place will be chiefly dependent upon: (a) time during which equilibrium has existed and (b) the stability of the oil-water mixture in that particular well. When measurements are made in wells producing appreciable quantities of gas, the work must be conducted so as to compensate for the changes in density.

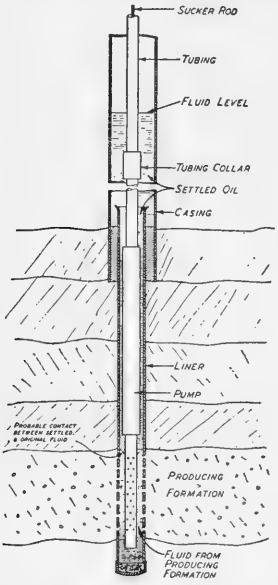

FIG. 702. — Illustration of gravitational separation of oil from fluid produced by a well. (Jakosky, *A.I.M.E. Petroleum Technology*, Tech. Pub. 1058, 1939.)

The fluid-pressure gradient in the annulus of a well depends on the producing conditions and on the effective area of the annulus. For given producing conditions, the pressure gradient in the annulus is practically constant from the top of the fluid to the perforations, if there is no change in casing size. It has been found that the gradient varies from about 0.05 to 0.4 pounds per square inch pressure per foot of depth below the fluid level, depending upon the gas-oil ratio. Often, the density decreases almost proportionally to the effective area of the annulus. The reason for this will be apparent when it is recalled that the gas-oil ratio remains relatively constant at any given rate of production. As this gas is being evolved, it bubbles up through the oil in the annulus. The smaller the area of the annulus, the greater must be the percentage of gas present, with a resultant decrease in the weight of the fluid column, i.e., its effective density. Referring to Figure 702, the density in the liner will be much less than in the upper cased part of the hole, due to the change in area of the annulus.

Determinations of the Fluid Density or Fluid-Pressure Gradient

To determine the average fluid density or fluid-pressure gradient in a well, measurements may be made of the variation in fluid level as a function

of casing-head pressure at a constant rate of production. If the rate of production is held constant, the bottom-hole pressure p_{bh} is constant. After equilibrium has been established, the rate of production is normally unaffected by the value of the casing-head pressure because the rate of production is dependent only upon the difference in pressure between the bottom-hole producing pressure and the formation pressure. That is, for any given rate of production, a change in casing-head pressure causes a corresponding change in fluid elevation and after equilibrium has been established there is no resultant change in bottom-hole pressure. Hence, for a constant rate of production, Equation 1 may be written in the form:

$$p + hd = p_{bh} = \text{constant} \tag{5}$$

where p equals $p_{ch} + p_g$.

When Equation 5 is solved for h explicitly,

$$h = \frac{p_{bh}}{d} - \frac{p}{d} = \text{height above datum plane}$$

Differentiation of the last equation with respect to p yields

$$\frac{dh}{dp} = \frac{d}{dp}\left(\frac{p_{bh}}{d}\right) - \frac{d}{dp}\left(\frac{p}{d}\right)$$

p_{bh} is constant. Hence, $\frac{d}{dp}(p_{bh}) = 0$ and the last equation becomes

$$\frac{dh}{dp} = -\frac{p_{bh}}{d^2}\frac{d}{dp}(d) - \frac{1}{d} + \frac{p}{d^2}\frac{d}{dp}(d)$$

Also, if the fluid density does not depend on the total gas pressure,

$$\frac{d}{dp}(d) = 0 \quad \text{and} \quad \frac{dh}{dp} = -\frac{1}{d}$$

or

$$d = -\frac{dp}{dh} = -\frac{d(p_{ch} + p_g)}{dh} \tag{6}$$

Equation 6 is a well known relationship for static-fluid surfaces and other equilibrium systems. The equation states that the fluid density or fluid-pressure gradient is equal to minus the slope of the total gas pressure versus fluid-level curve, provided the fluid density does not depend on the total gas pressure.*

In practice, an *average* value for the absolute magnitude of d may be

* The density might be expected to vary with gas pressure, temperature, producing gas-oil ratio, and diameter of casing—or annular spacing. Practically, it is usually observed that the fluid density is relatively constant provided the casing diameter does not vary. However, if there is a change in the size of the annulus, the fluid density changes almost proportionately to the effective areas of the annulus.

obtained by using the relation:

$$d = \frac{(p_{ch} + p_g)_2 - (p_{ch} + p_g)_1}{h_1 - h_2} \tag{7}$$

where h_1 and h_2 are the heights of the fluid corresponding to the total gas pressures $(p_{ch} + p_g)_2$ and $(p_{ch} + p_g)_1$.

It is of interest to point out that Equation 7 tacitly assumes that the total gas pressure versus fluid-level curve is a straight line, that is, the fluid density is constant throughout the well.† (This assumption is usually valid under equilibrium conditions, except near the top of the well.)

The value of p_{ch} may be read directly on a pressure gauge connected to the casing head of the well. The value of p_g may be determined by use of charts or by the formula:

$$\log_{10} p_g = \frac{Shf}{122.82\ (t + 460)} + \log_{10} p_{ch} \tag{8}$$

where S is the specific gravity of the gas in the well, h is the length of gas

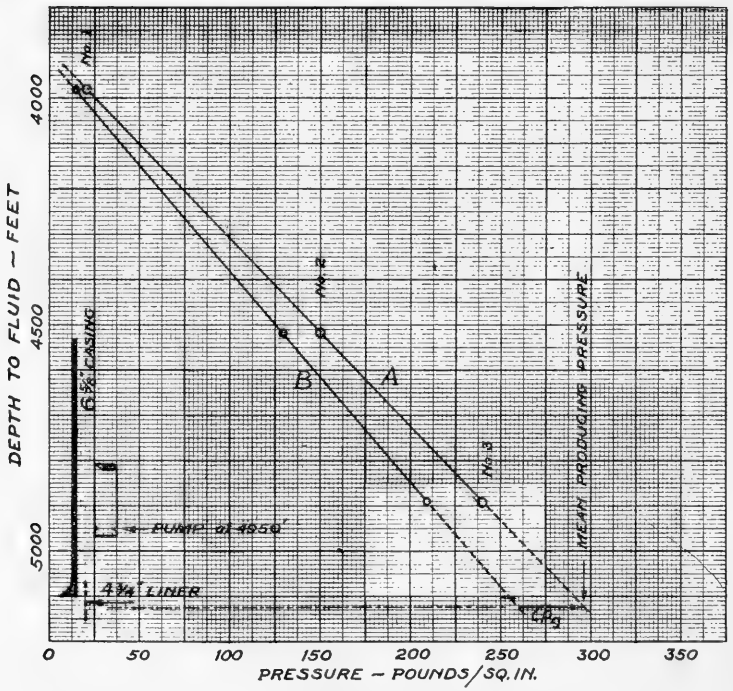

FIG. 703.—*A*, determining formation pressure (mean producing pressure) from fluid-level data obtained at a constant rate of production; *B*, determining formation pressure from measurements wherein the weight of the gas column need be evaluated only once.

† C. P. Walker, "Method of Determining Fluid Density, Fluid Pressure and Capacity of Oil Wells," U. S. Patent 2,161,733, issued June 6, 1939.

column between top of fluid and casing head, f is the deviation factor from Boyle's Law, and t is average temperature in degrees Fahrenheit.

Hence, an average value of the fluid density may be obtained by keeping the rate of production constant and determining two values of h corresponding to two values of $(p_{ch} + p_g)$.

Determination of Formation Pressure

The original bottom-hole pressure and its rate of decline as the well produces are of considerable importance. These data may be obtained by direct measurement with a subsurface pressure gauge or they may be calculated from the known relations between fluid level, casing-head pressure, and rate of production.

A plot of fluid-level data with h as ordinate and total gas pressure on the fluid as abscissa is a straight line, provided the production rate is held constant and the density does not vary with depth. Hence, the pressure at the reservoir depth, p_r, may be approximated by extrapolation. Curve A of Figure 703 shows a typical fluid-level versus gas-pressure curve. The data plotted in this curve are given in Table 28. The density of the fluid may be determined by applying Equation 7 to a small portion of the curve.

TABLE 28

TYPICAL WELL AND FLUID-LEVEL DATA

Well Data			
Total Depth	5,150′		
Casing	6⅝″ Grade D cemented at 5,100′		
Liner	80′ of 4¾″ Grade C hung at 5,150′		
Perforations	Kobe 120 mesh perforated from 5,100′ to 5,150′		
Depth to Pump Intake	4,950′		
Temperature	182° at 5,150′		
Production Data			
Oil Rate	153 B/D Gross, 2% Cut		
Gas Rate	170 M/ft. per day		
Gas Gravity	0.782		
Fluid Level Data	*Run* 1	*Run* 2	*Run* 3
Fluid Level	3,980′	4,515′	4,890′
Casing Pressure	16 lbs.	130 lbs.	209 lbs.
Total Pressure on Fluid *	21 lbs.	150 lbs.	241 lbs.
Calculations			
Pressure at Pump	258 lbs. per sq. in.		
Mean Producing Pressure	296 lbs. per sq. in.		
Fluid Gradient in Casing	0.241 lbs. per sq. in. per ft.		

* Includes casing-head pressure plus weight of gas column from fluid surface to the casing-head gauge. Weight of gas is calculated by formula

$$\log_{10} p_g = \frac{Shf}{122.82\,(t + 460)} + \log_{10} p_{ch}$$

An alternative and more rapid method requiring only one determination of the weight of the gas column is illustrated in curve *B*. As before, the production rate is maintained constant and two or more measurements are made of fluid levels versus casing-head pressure. Extrapolation of the data to the depth of the mean producing horizon gives the theoretical casing-head pressure necessary to force the fluid level down to the producing horizon. The total pressure at this depth may be obtained by adding the weight of the gas column at this depth to the extrapolated casing-head pressure. Referring to the figure, the extrapolated casing-head column was found to be 258 pounds, while the calculated weight of the gas column was 38 pounds, giving a total formation pressure of 296 pounds. (In this procedure, a direct determination of density cannot be obtained from the slope of the graph.)

PRODUCTIVITY DETERMINATIONS: WELLS WITH LOW CASING-HEAD PRESSURE

The "absolute potential" of a well is determined by conducting a series of measurements to evaluate two factors: (a) the effects of casing-head pressure and (b) the effects of rate of production. In most wells operating at low casing-head pressures, or at atmospheric pressure, the casing-head pressure plus the weight of the gas column is sufficiently low to have a negligible effect on the potential. Measurements on such low pressure wells need therefore be conducted only to determine the effects of rate of flow on the fluid height or the bottom-hole pressure.

The producing characteristics of wells with negligible casing-head pressures may be determined by obtaining bottom-hole pressure or fluid-level data at two or more stable production rates. If fluid-level measurements are made, the casing-head pressure is held constant during the measurements at each of the production rates. The data are then plotted as shown in Figure 704.

It will be noted that the pressure-rate curve must deviate from a straight line in order to fit the static reservoir pressure value. Extrapolation of the curve to the Q-intercept gives the theoretical maximum production which the well is capable of yielding, provided flow friction, water coning or other variables encountered in practice do not change the slope of the curve. †

The productivity index is determined from the slope of the pressure-rate curve and is defined as "the barrels per day of gross liquid produced per pound per square inch pressure drop at a specified subsurface datum."‡

Any condition tending to change the productive capacity of the well is indicated by a change in the productivity index or slope of the curve. §

† M. L. Haider, *loc. cit.*

‡ B. P. Kantzer and E. G. Trostel, "Oil Well Performance, Discussion and Proposed Terminology," *A.P.I., Drilling and Production Practice*, 1937.

§ T. V. Moore, *Proceedings Amer. Pet. Inst.*, 1930, 11 (4), 27.
M. L. Haider, *loc. cit.*
H. C. Miller, E. S. Burnett and R. V. Higgins, *loc. cit.*

For oil which is fully saturated with gas at initial conditions of reservoir pressure and temperature, the productivity index will decrease as the reservoir is being depleted, because of the corresponding decrease of the oil saturation in the reservoir rock and the fact that the viscosity of the reservoir liquid increases as the reservoir pressure diminishes. Other secondary effects may contribute to productivity index decline. Some

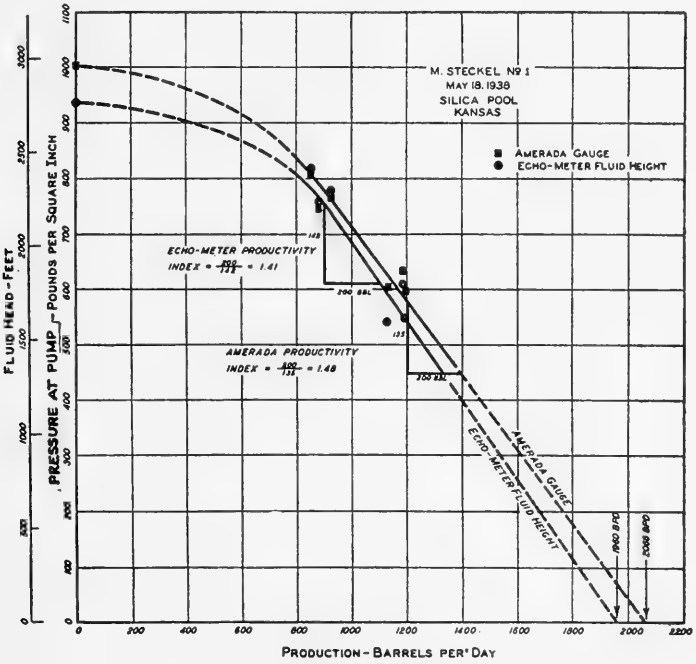

FIG. 704.—Determining productivity in wells making small quantities of gas from fluid-level or pressure-gauge data. (Jakosky, *A.I.M.E. Petroleum Technology*, Tech. Pub. 1058, 1939.)

commonly-observed effects are filling of the liner by sand, and plugging of the perforations of the sandface by calcareous or waxy deposits or fine silts. In some instances the productivity index is found to increase. This condition occurs when the reservoir fluid is undersaturated at initial conditions of reservoir pressure and temperature, since, then, the liquid viscosity decreases as the reservoir pressure declines to the saturation point. Other factors which may contribute to productivity index increases are the elimination of completion effects and the establishment of drainage channels. Periodic productivity index measurements are thus a vital necessity in keeping a close check on a well's performance. The decline of a well's potential and its pumping performance can be intelligently followed, and in many cases controlled, by the use of bottom-hole pressure or fluid-level data.

PRODUCTIVITY DETERMINATIONS: WELLS UNDER CASING-HEAD PRESSURE

The producing characteristics of wells under pressure can best be determined as follows:

The bottom-hole pressure at some given datum point—usually the average depth of the producing formation—is plotted as ordinate and the production rate as abscissa. Methods of determining total pressures at a given datum point have been described in connection with Figures 703 and 704.

The productivity of the well may be determined by making a series of measurements with varying casing-head pressures at a given production rate to determine one of the pressure datum points. The rate of production is now changed and after equilibrium is established a second series of measurements is made to determine another pressure datum point. Two or more of these pressure datum points are then plotted, and the pressure-rate curve extrapolated to zero pressure (where no back-pressure will be exerted against the producing formation) to determine the theoretical maximum production rate for the well.

Another procedure allows the productivity to be obtained with no fluid above the pump. In this procedure, the pump is operated at a given production rate and the casing-head pressure increased to a value such that the well is pumped-off. Under this condition, the pressure at the pump intake is equal to the casing-head pressure plus the weight of the column of gas. The production rate is now changed by altering the speed of the pump, and the procedure is repeated. A curve is then plotted showing the total gas pressure versus production rate, and the curve is extrapolated to zero pressure to give the theoretical potential of the well at that particular depth setting of the pump.

SOLUTION OF PUMPING PROBLEMS

Dynamic Measurements.—It is possible to determine various important characteristics of a well, such as the maximum rate of production and the reservoir pressure, etc., by dynamic measurements wherein the bottom-hole pressure or the depth to the fluid level is determined as a function of the time before equilibrium has been established. † The theory of such measurements as applied to the determination of the reservoir pressure will be illustrated for a case in which the following assumptions are made. (1) The well is open to the atmosphere so that the casing-head pressure p_{ch} is zero. (2) The weight of the gas column p_g is negligible. (3) The free area a of the open flow string is uniform. (4) The fluid-pressure gradient d is a constant, and the rate of produc-

† Morris Muskat, *A.I.M.E. Petroleum Technology*, 1937.

tion Q may be expressed by the equation

$$Q = a\frac{\partial h}{\partial t} \tag{9}$$

(5) The production is the same as that in a "dead well"; that is,

$$Q = c\,(p_r - p) \tag{2}$$

It follows from assumptions (1) and (2) and Equation 1 that the bottom-hole pressure is equal to the weight of the fluid, provided the friction drop in the well bore is negligible; that is,

$$p_{bh} = hd$$

Or if p_{bh} is set equal to p,

$$p \equiv p_{bh} = hd \tag{10}$$

On inserting this value of p into Equation 9 one obtains

$$Q = \frac{a}{d}\frac{\partial p}{\partial t} \tag{11}$$

Equating the right-hand members of Equations 2 and 11,

$$c\,(p_r - p) = \frac{a}{d}\frac{\partial p}{\partial t}$$

The last equation may be written in the form

$$\frac{dp}{p_r - p} = \frac{cd}{a}\,dt$$

or

$$p_r - p = k \cdot e^{-\frac{cd}{a}t}$$

where k is a constant which may be evaluated as follows. At $t = 0$

$$p_r - p_0 = k$$

Hence

$$p_r - p = (p_r - p_0) \cdot e^{-\frac{cd}{a}t} \tag{12}$$

In the same way, it may be shown that

$$h_r - h = (h_r - h_0) \cdot e^{-\frac{cd}{a}t} \tag{13}$$

where h_r is the equilibrium value of h and h_0 is the value of h at the instant chosen to represent $t = 0$.

Combining Equations 12 and 13,

$$\frac{p_r - p}{p_r - p_0} = \frac{h_r - h}{h_r - h_0} = e^{-\frac{cd}{a}t}$$

or

$$c = \frac{a}{td}\log_e\frac{p_r - p_0}{p_r - p} = \frac{a}{td}\log_e\frac{h_r - h_0}{h_r - h} \tag{14}$$

Equation 14 may be related to the theoretical maximum rate of production as follows. From Equation 2

$$Q_{max} = c \cdot p_r$$

Hence

$$Q_{max} = \frac{ap_r}{td} \log_e \frac{p_r - p_0}{p_r - p} = \frac{ah_r}{t} \log_e \frac{h_r - h_0}{h_r - h} \qquad (15)$$

Evidently a plot on semilogarithmic paper of $p_r - p$ or $h_r - h$ versus time should be a straight line, if the assumptions made in deriving Equation 15 are valid.

The practical use of the above analysis may be summarized as follows. Determinations are made of the bottom-hole pressure or the fluid level

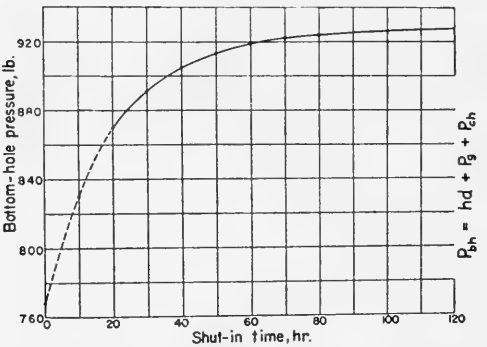

FIG. 705.—Average bottom-hole pressure rise for 20 wells in the Judkins Field, Ector County, Texas. (Muskat, *A.I.M.E. Petroleum Technology*, 1937.)

as a function of time. (Compare Figure 705.) An approximate value of the *equilibrium* bottom-hole pressure p_r is read off the curve. A plot is then made on semilogarithmic paper of $p_r - p$ versus time. (Figure 706.) If the estimated or approximate value of p_r is inaccurate, the plot (curve II, Figure 706) will deviate from a straight line. The value of p_r is then adjusted so as to make the data fall on a straight line. Thus, this method of observing the bottom-hole pressure as a function of time before equilibrium is reached yields an accurate determination of the reservoir pressure.

Maximum Pumping Efficiencies.—Fluid-level measurements supply information that will allow an operator to ascertain whether a well is pumping-off or is gas-locked. Oftentimes, it is impossible to tell by the pounding on the polished rod which condition exists in a well. Pounding due to the well being pumped-off is caused by a low fluid-level or by the

pump being set too high in the well, while the pounding due to gas-locking may occur when a high fluid level exists above the pump.

For the maximum rate of recovery, the bottom-hole pressure usually should be reduced as much as possible, and this can be achieved by maintaining the lowest practical fluid level. In actual pumping operations, it is not possible to obtain the full theoretical production rate due to the

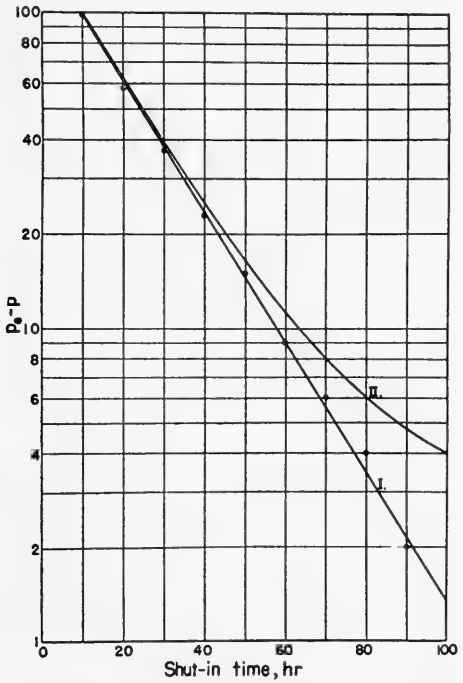

FIG. 706.—Plot of $p_r - p$ versus shut-in time. The data for this semilogarithmic plot were obtained from Figure 410. (Muskat, *A.I.M.E. Petroleum Technology.*)

hydrostatic head that must be maintained in order to feed the oil into the pump. The factors on which this head depends must be determined for each field and include viscosity of the oil, pump speed and capacity, valve design on pump intake, etc.

After making changes in pump speed or capacity, it is advisable to run a subsequent fluid-level measurement to be certain that the proper draw-down is being obtained.

OTHER APPLICATIONS OF FLUID-LEVEL MEASUREMENTS

Field Development Studies.—Shut-in reservoir-pressure data are often presented on maps showing lines of equal bottom-hole pressure, generally expressed with refer-

ence to a common depth-datum plane. Such isobars give important information regarding areas where major drainage has occurred, and thus allow the assignment of individual well production rates and the performance of development work to be done on a better engineering basis. This type of work is of considerable importance in connection with various regulatory measures and with the unit control trend of recent legislation. In those instances where individual well-fluid densities are fairly uniform, it is possible to attain the same objective by using shut-in fluid-level (static) data directly, without their prior conversion in terms of equivalent pressures. Likewise, valuable production information can often be obtained from maps showing lines of equal pumping-equilibrium fluid levels.

Gas Lift Operations.—An interesting application of fluid-level measurements in Texas concerns existing or projected gas-lift installations.† If a well is being converted from pumping or flowing to gas lift, it is convenient to be able to obtain the fluid level in the annular space in advance of the pulling job. Also, the draw-down at various producing rates will give valuable information regarding the size and location of the valves to be installed. If a flow-valve installation is made, its operation can be checked quickly and conveniently by fluid-level observations. If it is suspected that a valve is sticking, a close check of the fluid-level variation when the well begins to unload will show which valve is kicking off. Also, the correctness of valve spacings and their effective performance can be studied.

In wells where the conventional type insert valves are used, it is impossible to run a bottom-hole pressure bomb because the valves obstruct the tubing. In all gas-lift installations using flow-valves the wave reflection measurements have the additional advantage that the fluid level can be watched continually and the input pressure properly regulated without the possibility of changed flow conditions as a result of running the pressure bomb in the flow string.

Primary Pressure Control and Secondary Recovery Projects.—Periodic studies of formation pressures are the basis of any conservation program designed to secure optimum oil recovery. As a result of such studies it is often found desirable to augment the reservoir's native energy artificially by fluid injection. Such a program may be instigated when a pool has nearly reached its economic limit by conventional production procedures (secondary recovery) or during the early life of the field (primary pressure control). For the latter case, the decline of subsurface pressures will be materially lessened and consequently the flowing life prolonged. Thus depth pressures will probably be obtained most conveniently by means of bottom-hole pressure gauges, although fluid-level measurements could also be used. Once the pumping stage is reached, bottom-hole pressure information may be obtained most economically by means of the sonic procedures.

It is also necessary to check the gas-input wells periodically for fluid, to see that no condensate has accumulated in their bottoms. In a multi-zone field, gas may be injected into two or more pays from the same well. In this case the wave reflection instrument proves itself invaluable as a rapid and accurate means of measuring the depths to fluid or to bottom.

Cementing Operations.—The "squeeze" cementing technique has become a standard practice in completing and reconditioning wells whenever an undesirable water stratum is to be shut off. Such a procedure depends for its success upon the effectiveness of a protecting packer set above the stratum to be sealed off. Should any cement slurry which is forced down the tubing string under pressure escape around the packer, there is danger of contamination to the oil zone above. Also, this "leak" effectively lowers the pressure differential which would normally be applied to the face of the watered formation.

Such leaks during a cementing process can be detected by measuring progres-

† Geo. Webber, "Fluid Level Indicator Useful in East Texas," *The Oil and Gas Journal*, Dec. 19, 1938, pp. 44-50.

sively the depth to the top of the quiescent fluid which stands in the casing above the packer. If the wave reflection equipment shows a sudden change in fluid level, it indicates that some disturbance or leak has occurred, and it may be concluded that slurry is being pumped around the packer and into the casing annulus above. Such application of fluid-level measurements is a valuable one.

Water Disposal and Supply Wells.—The problem of salt water disposal is one which receives considerable attention both of legislative and engineering bodies. Oil field brines, after being separated by treatment from the pipe-line oil, must be cared for in some manner satisfactory both to the landowners and to the operator. One method of disposal is by the use of wells, either drilled expressly for such a purpose or abandoned from oil production and plugged back to some upper permeable zone. The brine is flowed into the well, by gravity or under a pressure head, and then absorbed by the porous stratum.

Productivity indices can be determined for disposal wells in the same manner as for gas-free oil wells. Potential computations will show the amount of water which can be disposed of in any given well, and comparisons of indices computed periodically will show whether or not the thief formation is salting-up. If a treatment is necessary for the brine in order to keep the disposal wells clean and functioning properly, the effectiveness of different treating processes can be studied from fluid-level data.

In Michigan and other states, salt-water producing wells are drilled to obtain their brine contents for chemical manufacturing. Here again the same applications for fluid-level measuring devices are present. Productivities, pumping problems, fluid build-up studies, and pumping efficiencies are a practical part of the brine production program.

Detection of Collapsed Casing and Leaks.—The sonic method has been found helpful in locating points where oil well casing has been ruptured above the fluid level, as such casing breaks often will cause reflections comparable to those obtained from tops of perforations.

PHYSICAL PRINCIPLES APPLIED TO PRODUCTION PROBLEMS

UNITED STATES PATENTS

17,242 Original 1,672,495 issued June 5, 1928. Reissued Mar. 19, 1929. B. McCollum. "Method & Apparatus for Determining the Contour of Subterranean Strata."

571,739 Issued Nov. 24, 1896. Francis B. Badt. "Electromagnetic Sentinel."

602,422 Issued April 19, 1898. Birney C. Batcheller. "Apparatus for Locating Obstructions in Tubes."

737,866 Issued Sept. 1, 1903. Charles F. Pike. "Indicator for Locating Sunken Metals."

793,652 Issued July 4, 1905. Reginald A. Fessenden. "Signaling by Electromagnetic Waves."

1,212,438 Issued Jan. 16, 1917. Arthur R. Bauder. "Method of and Means for Determining and Indicating the Depth of Water."

1,217,585 Issued Feb. 27, 1917. Reginald A. Fessenden. "Method for Measuring Distance."

1,335,738 Issued April 6, 1920. Yoshinao Kawakita. "System of Electrically Indicating on Board Ship the Depth of Sea Water."

1,351,356 Issued Aug. 31, 1920. William S. Tucker. "Sound-Detecting Device."

1,409,794 Issued Mar. 14, 1922. Samuel Spitz. "Method and Apparatus for Utilizing Sound Vibrations."

1,682,706 Issued Aug. 28, 1928. Max Mason. "Determination of Wave-Energy Direction."

1,776,228 Issued Sept. 16, 1930. Roscoe A. Coffman. "Starter."
1,808,709 Issued June 2, 1931. Alfred E. Blake. "Apparatus for Metering Gaseous Fluids."
1,853,119 Issued April 12, 1932. Reginald A. Fessenden. "Method and Apparatus for Determining Distance by Echo."
1,858,931 Issued May 17, 1932. Charles L. Florisson and Paul Langevin. "Method & Apparatus for Sounding & for Locating Submarine Obstacles by Means of Ultra-audible Waves."
1,860,740 Issued May 31, 1932. Harvey C. Hayes. "Oscillograph."
1,889,614 Issued Nov. 29, 1932. C. W. Rice. "Sound Wave Apparatus."
1,890,786 Issued Dec. 13, 1932. William S. Johnston. "Radio Distance or Location Finder."
1,900,015 Issued Mar. 7, 1933. Harvey C. Hayes. "Method and Apparatus for Sound Ranging."
1,923,088 Issued Aug. 22, 1933. Harvey C. Hayes. "Vibration Detector."
1,946,309 Issued Feb. 6, 1934. Roscoe A. Coffman. "Motor."
2,005,913 Issued June 25, 1935. Roscoe A. Coffman. "Motor and Motive System."
2,009,459 Issued July 30, 1935. Edwin E. Turner, Jr. "Distance and Depth Finding."
2,009,460 Issued July 30, 1935. Edwin E. Turner, Jr. "Means for Measuring Depths or Distances."
2,015,702 Issued Oct. 1, 1935. Robert Longfellow Williams. "Method and Apparatus for Measuring Distances and Depths."
2,033,160 Issued Mar. 10, 1936. Edwin E. Turner, Jr. "Method and Apparatus for Measuring Depths."
2,040,850 Issued May 19, 1936. Beverly R. Hubbard. "Method and Apparatus for the Determination of Direction of a Source of Wave Energy."
2,044,820 Issued June 23, 1936. Edwin E. Turner, Jr. "Apparatus for Measuring Depths."
2,047,974 Issued July 21, 1936. Paul E. Lehr and Harold T. Wyatt. "Method and Apparatus for Measuring Well Depths."
2,096,017 Issued Oct. 19, 1937. R. L. Williams. "Depth Sounding Apparatus."
2,134,428 Issued Oct. 25, 1938. Serge A. Scherbatskoy and Jacob Neufeld. "Apparatus for Exploring the Level of Liquid in a Bore Hole."
2,232,476 Issued Feb. 18, 1941. O. F. Ritzmann. "Method of and Apparatus for Measuring Depths in Wells."
2,281,301 Issued April 28, 1942. C. P. Walker. "Means for Determining the Location of Obstructions in Wells."
2,310,559 Issued Feb. 9, 1943. C. P. Walker. "Vibration Translating Means."
2,324,340 Issued July 13, 1943. C. P. Walker and E. E. Simmons. "Detector for Pressure Wave Translation Systems."
2,403,535 July 9, 1946. J. T. Kremer. "Well Sounding Microphone."

CHAPTER XIII

LAND TENURE, PERMIT AND TRESPASS PRACTICE; INSURANCE; PATENTS.

A general knowledge of the laws relating to trespass is extremely important to those engaged in geophysical field operations. Rarely does a field party complete its exploratory work without trespassing on the property of others. Covering, as a field party does, a very wide range of territory, with operations in states and localities in which the principal business of its concern is not located, it becomes of prime importance that the geophysical field party be instructed in certain basic principles of law relating thereto and the medium through which the employer can be protected from vexatious quarrels and litigation. Good-will of the public, and particularly of landowners, is essential to efficient geophysical prospecting with its allied leasing operations. In fact, it is only with the good-will and consent of landowners and lessees that most field operations can be carried on. It is the surface landowner's natural right to expect to be consulted before his fences are let down or fields crossed and if damage is done to his crops or other surface rights, he is entitled to just compensation for such loss. It is therefore necessary for every member of a party to be mindful at all times of the individual rights of others, not only because it pays to maintain the good-will of the public but from the legal standpoint such consideration prevents expensive and ofttimes protracted litigation.

The nature of this volume on geophysics prevents any extended discussion of the manner in which permission to enter upon lands of another is obtained or an oil and gas lease is acquired prior to making a survey. Of necessity this chapter is limited to a brief treatment of the more general procedures followed, and a consideration of principles which should serve to guide field parties when operating in various localities.

Land Tenure

There is a fundamental difference between the manner in which mineral claims and petroleum leases are acquired. This should be appreciated at the outset, since it has a bearing on the procedures followed in conducting surveys over these lands. The difference arises from the nature of the mining laws of our country, which require that mineral be discovered *in place* in order to file a valid discovery notice; the geophysical anomaly does not fulfill the requirements of discovery on the public domain. The prin-

cipal limitations affecting field work in both mining and petroleum surveys will be briefly considered.

Petroleum Lands.—Broadly speaking, most potential petroleum lands in this country are owned in fee by farmers and stock men. Our agricultural and range lands often occupy sedimentary basins underlain by great thicknesses of stratified rocks, where, of course, most of our important oil and gas fields are found. It should be borne in mind that the availability of these large tracts of privately-owned lands for geophysical prospecting and the simplicity of acquiring sub-surface rights by means of a standard lease have been two of the dominant factors contributing to the phenomenal growth of the petroleum industry in the United States. In the majority of cases the reconnaissance geophysical parties have free access to the ground before negotiations are opened by the Land Department for leasing, simply by asking for permission to go upon the land. Commonly it is not until the preliminary surveys are completed and some general knowledge of the sub-surface structure is acquired that negotiations are opened with a view to the formal leasing of certain selected tracts or acreage.

The consideration for an oil and gas lease may vary from one to many dollars per acre, depending on its location relative to producing wells and on the geological conditions. In the case of wildcat acreage usually no bonus is paid, the only consideration granted being the lessee's promise to drill a well within a given time period. It is customary to hold large blocks of leases today simply by the payment of delay rentals.

Lands of the public domain, that is, Federal lands within the limits of the various states, may usually be investigated without permission from either the State or the Federal government. Oil and gas leases on such lands are secured through the Department of the Interior under the Public Land Leasing Act of 1920, as amended.

Mining Lands.—The mining laws and regulations of the civilized countries of the world, governing the acquisition of mineral lands, can be broadly grouped under (a) the concession system, and (b) the claim system. The *concession system* provides that either the state or a private land owner may grant concessions or leases to individuals or corporations. Under the so-called *claim system,* the individual, when conforming to local regulations, has the right to locate or stake a claim in lands of public domain over certain limited areas of ground. This latter system originated during the early development of the Colorado and California mining districts.

In the United States all metalliferous deposits, such as copper, gold, lead, zinc, chromium, etc., found on lands of the public domain, may be acquired by locating claims, following the claim system. As outlined above, petroleum and gas lands situated in the public domain are acquired by leases under the concession system. No provision is made in the United States for location of mining claims upon or within privately owned lands. Only public mineral lands may be located and entered under the mining laws.

Our Federal and State mining laws are based on the Mining Act of 1872 (commonly known as the Apex Law), which holds that the right of property in mines is dependent on physical discovery and development; that is, actual discovery of mineral in place is made the source of title, and subsequent development or working is the condition of the continuance of that title. Specifically the law states:

"No location of a mining claim shall be made until the discovery of the vein or lode within the limits of the claim or location. Sufficient development work is required to disclose signs of a vein, or if possible, its general course and indications that it contains valuable minerals." These two principles constitute the basis of all our local mining laws and regulations. Therefore discovery is the very pith of the present law. Our forefathers made no allowance for the entry of the geophysicist on the scene.

Moreover, the discoverer of the top of a mineral vein or lode, usually called the *apex,* has the right to follow the vein or lode down the dip (with certain limitations) even though this takes him onto adjacent properties under other ownership. This feature of the law was framed to validate an ancient procedure long established in

some of the oldest mining camps of Europe. It has resulted in endless disputes costing many millions of dollars in litigation, because a vein or lode is rarely a simple or precisely-defined structure that may be easily followed without interruption or contortions.

Merely locating an interesting geophysical anomaly does not of course fulfill the legal requirements of discovery. Though the mining laws of Canada are patterned after ours in many respects, they differ in that a geophysical anomaly can be made the basis of discovery, and geophysical surveys may constitute part of the development work required for the continuance of title. The apex feature of the United States law poses a particularly troublesome problem with respect to geophysical prospecting.

All this tends to discourage the use of geophysics when conducting reconnaissance or exploration surveys over the public domain unless sufficient finances are available to follow the geophysical work with direct exploration, by means of a drill hole, prospect shaft, or tunnel, in order to make a physical discovery of the mineralization responsible for the anomaly. This is an important factor to consider when employing geophysics in mining exploration.†

Mining Properties: Titles and Legal Assistance

Geophysical surveys usually are conducted in connection with the geological study of a property. For many reasons almost all mine examinations, including geophysical work, are conducted under some form of option agreement. This is chiefly to protect the individual or group for whom the examination is being made if later it is decided that the property should be acquired.

Characteristically, the mining districts of the west contain a dismaying number of claim owners, each controlling a small group of claims or even a single location. They include both patented claims and mineral locations held from year to year by virtue of performing the annual assessment work. The situation may be very complicated, due to disputed titles or failure to perform annual work. Before beginning an examination of an area it is commonly necessary to consolidate various blocks or interests by obtaining options on each and every claim located in the area. In such cases legal assistance versed in the local laws should be secured on all questions pertaining to title, working bond, or escrow agreements. Many miners and prospectors have most optimistic and fanciful views about the richness and extent of the mineralization contained in their ground, including a strong conviction as to its worth. It is always best to work out in a general way the terms and manner under which the property may be acquired before spending time and money on geological or geophysical surveys of any kind. Since there is no traditional standard form of option or lease established through long use and custom, a separate deal must be worked out with each claim owner. Options should allow adequate time

† J. J. Jakosky, "The Economies of Geophysics in Mining Exploration," *A.I.M.E. Mining Transactions, 184,* Sept., 1949.

for preliminary study and sampling prior to any diamond drilling or actual exploratory development work. The following periods are recommended and should be provided for in the agreement:

(a) At least 60 to 90 days or more for preliminary geological (including geophysical) study, sampling, review of records, etc. No payment is customarily made during this period.

(b) If the preliminary option granted under (a) is exercised, usually two years or more should be allowed for diamond drilling, more detailed geological studies, and possibly underground development. Sometimes small annual payments are made during this period.

(c) Depending on the results of (b) the option may be dropped, or the property acquired in accordance with the specified terms of the agreement.

Permit and Trespass Practice

A "trespasser" has been defined as:* "One who does an unlawful act, or a lawful act in an unlawful manner, to the injury of the person or property of another; one who makes an unauthorized entry of another's property; one who goes upon the premises of another without invitation, express or implied, and does so out of curiosity, or for his own purposes or convenience, and not in the performance of any duty to such owner; one who unlawfully enters or intrudes upon another's land, or unlawfully and forcefully takes another's personal property." From this definition of a trespasser one can readily define the word "trespass," and ascertain what acts or conduct fall within the category of trespass.

The gist of the action of trespass is disturbance of possession. Unlawful intent is not necessary; therefore, the intent or motive is immaterial as regards the trespasser's liability, except in so far as it may affect the measure of damages. The fact that the trespass was wilful or malicious is material only for the purpose of obtaining punitive damages.

From the foregoing it might appear that actual damage must be suffered by the party against whom the trespass is committed, but this is not the case. A trespass may be committed without any damage being done, as the act itself of entering unlawfully upon another's property is sufficient to support a cause of action for trespass.

In all jurisdictions a cause of action arises against the trespasser for all "actual" damages suffered by the landowner, the actual damages being based upon the amount of money which would compensate him for all damages suffered at the hands of the trespasser. This would include the cost of repairing fences, compensation for lost crops, replacing the soil so that it is in the same condition as before the trespass was committed, and other damages of like nature. In many jurisdictions exemplary or punitive damages are allowed in addition to the actual damages, and in most jurisdictions the landowner would be entitled to exemplary or punitive damages, although no actual damage of a substantial nature had been suffered.

* Little vs. State, 89, Alabama Reports, p. 89. Heller vs. New York, 265, U. S. Federal Reports, 192, Vol. 63, Corpus Juris, p. 887.

Exemplary or punitive damages are given to punish the wrong-doer and to act as a deterrent to the commission of like acts in the future. The amount of actual damage which might be awarded is fairly well fixed by the ordinary rules of law and is always confined to the reasonable cost of restoring the landowner to his former estate and position, but exemplary or punitive damages may be awarded in the sound discretion of the court and for an amount which, in the opinion of the court, will accomplish the result which the court is seeking to accomplish. As a result, exemplary or punitive damages may be in a substantial amount and, having emanated from the mind of a court, it is sometimes difficult to review or obtain a reversal of that portion of the judgment.

It is a complete defense to the awarding of punitive or exemplary damages if permission is given by the landlord to the geophysical party to enter upon the property and conduct the exploration activities. As a result thereof the geophysical party should be instructed, wherever possible, to contact the landowner or the lessee of the landowner and procure his signature to an instrument, which it is suggested should read about as follows (modified as required by local conditions):

> "The undersigned is conducting geophysical field operations in this vicinity and requests permission to enter upon property, of which we understand you are the owner (or lessee), to conduct such operations.*
>
> Will you kindly permit us to enter upon the parcel of real property described as: (here insert a description of the property involved).
>
> In consideration of the granting of this permission on your part we agree to commit no nuisance on your property and to leave your property in the same condition it was in before our entry thereon."

By use of a written authorization of entry such as this the geophysical party not only avoids the possibility of expensive litigation involving exemplary or punitive damages but the good-will of the public will be maintained. In most instances the landowner will cooperate in the work on his property and oftentimes will assist in locating other owners and securing like permissions from them.

After the exploration work has been completed the field party should be instructed to replace and repair all fences, and, in general, place the property in the same condition it was in before the entry was made. An improperly repaired fence or a gate left open by the exploration party may result in the loss of cattle or other stock, and accidents happening on the highway between vehicles and stray cattle may be directly traceable

---

* The purpose of the field work, and such other information as the geophysical company may desire to give, can be explained verbally by the party chief or contact man.

to this negligence on the part of the exploration party. For instance, holes left in the surface of the earth after seismic operations may be used as a basis for damages for injury to or loss of cattle, injury to persons, and other claims of injury, some of which may be of a very fantastic nature. It should always be remembered that regardless of how fantastic the claims may be there will be found unscrupulous practitioners who thrive on such litigation. To the geophysicist not trained in legal matters the ultimate chance of recovery may seem remote, but regardless of the possibility of recovery the expense of litigation still remains, and this expense will vary in the locality in which the geophysical party is working, with a possibility that several hundred dollars may be expended in defending such an action. In addition, there will be the expense occasioned by the loss of time preparing for and defending the action.

A complete defense to the possibility of an action involving "actual" damage is the procuring of a release from the landowner after the work of replacement or repair has been completed. This form should be as short and concise as possible, as a lengthy legal document is more formidable and invariably results in "thinking it over" delays. This release may also serve as a receipt for payment of damages or trespass privileges. Proposed forms of release are set forth on pages 1149 and 1150.

In many states the laws provide that a general release does not extend to claims which the creditor does not know or suspect to exist in his favor at the time of executing the release, which, if known by him, must have materially affected his settlement with the debtor.* In the event the field party has engaged in such type of exploration work as would give rise to the possibility of claims being asserted which the landowner did not know or suspect to exist in his favor, then a provision should be placed in the general release which would acknowledge receipt of satisfaction for such claims. Most statutes of this type can be circumvented in the event there is an express provision in the release by which the creditor waives such right.

In most states permission may be obtained to do geophysical work along public highways. It is good practice to obtain such permission from the proper public official before permitting the geophysical party to conduct its exploratory work. In seismograph work the shot-holes must normally be drilled beyond the limit of the highway and where there is any question shot-holes should not be drilled without obtaining information in relation thereto, as the drilling of such holes along public highways is a bad safety practice and when so drilled should never be left open or unattended.

The public official from whom permission must be obtained will vary in the different states. As an illustration, in Louisiana and certain counties in other states, a license must be obtained from the State Highway Commission or other local authority to work on public roads. Louisiana further requires that a separate license be secured for each

* Civil Code of California, Sec. 1542.

RECEIPT AND DISCHARGE

Check No.....

KNOW ALL MEN BY THESE PRESENTS: That,

The undersigned, in consideration of the sum of $....., and other valuable consideration, in hand paid by the ....., a corporation of ....., ..., receipt of which is hereby acknowledged, do hereby acknowledge full payment, settlement and satisfaction for, and do hereby forever discharge the said .....(company)..... from any and all actions, causes of action, claims and damages of whatsoever kind, nature and character sustained by the undersigned that may have arisen by reason of, or founded upon the operation and acts of the .....(company)....., its agents, servants and employees in carrying on exploration work, tests, surveys and operations by seismograph or other methods, on, in, over, under or about the following described land, of which the undersigned declare that I/we am/are the lawful owner, situated in the County of ....., State of ....., to-wit:

.....

.....

.....

.....

Dated this ..... day of ....., 19.....

.....

.....

.....

.....

.....

.....

RECEIPT AND RELEASE

....., 19.....

RECEIVED from .....(company)..... the sum of ....DOLLARS ($.....) which ..... acknowledge to be in full settlement and discharge of a claim growing out of property damage sustained by ..... on or about ....., 19....., for which damage ..... have claimed the said .....(company)..... to be legally liable, and in consideration of said sum so paid to ....., ... hereby remise, release and forever discharge the said ....., and its employees from any and all actions, causes of action, claims and demands for, upon or by reason of any damage or loss which heretofore has been or which hereafter may be sustained by ..... in consequence of .....

.....

.....

.....

.....

.....

.....

.....

WITNESS ..... hand ..... and seal ..... the day and year first hereinabove written.

.....

Witness.....

Address.....

Witness.....

Address.....

parish in which work is done, and the District Road Commissioner of the specific parish in which work is contemplated must be advised when the work is initiated. Before the field party undertakes its work all of this information can be obtained as a general rule from the Division of Highways of the State in which the work is to be conducted. Highways which are within the incorporated limits of cities are generally supervised by municipal authorities, and in addition to obtaining the permission of the State Highway Commission a permit should be obtained from such local authorities.

It is best to secure from an attorney practicing in the locality in which the geophysical work is being done a simple form of receipt and discharge to be presented to and signed by the landowner after the geophysical party has completed its work. In the event there is no attorney available, the previously presented forms will in most cases be sufficient.

Insurance for Geophysical Operations

One of the requisites in successful geophysical operations is adequate insurance which will serve as a protection against the expenditure of substantial sums of money in defense of actions for alleged trespasses involving property damage or personal injury. Inadequate insurance or coverage is a hazard which no reputable geophysical operator should assume, yet unnecessary insurance or coverage is not only an added expense, but an economic waste.

The most common forms of liability encountered by an exploration company are: (1) injury or death of employees on and away from the premises of the company, (2) injury or death of members of the public resulting from operations on and away from the premises of the company, (3) damage to or destruction of the property of others resulting from operations on and away from the premises of the company, (4) injury or death of others and damage to property of others arising out of operation of motor vehicles owned by or operated by or for the company, (5) loss by fire, and (6) theft of equipment.

Unfortunately, insurance coverages can not be tabulated in a simple table, due to the diversity of operating methods and conditions encountered in field operations.

The insurance rates vary with the duties of the employees. For example, the base or beginning rate for an office employee may be six cents per $100.00 of salary received, while for field operators handling explosives the beginning rate may be $2.02 per $100.00 of such payroll. Generally, the rating provides for a credit or debit based upon past experience (record of accidents). The employer, therefore, over a period of time more or less makes his own rates. For this reason, it is to the employer's benefit to teach his employees to think "safety" at all times.

In all cases, careful consideration must be given to the reliability of the insuring company and the extent of its operations. For example, it is

possible in some cases to effect a saving by placing the coverages with companies operating in one state only. This plan is satisfactory provided the geophysical operations do not extend into other states. The standard form of policy limits not only the kind, but the extent of operations as well. It is therefore necessary that a policy be endorsed to cover all operations and all states. For this reason it is advisable to place the coverage with a company licensed to do business in the various states and countries where geophysical operations are contemplated during the term of the policy.

Caution must be taken to see that the coverage provided by the insurance company does not conflict with state laws. Some states, termed "monopolistic" states, require that Compensation Insurance be furnished by the respective state organizations, (State Funds, etc.)

To protect himself the operator must carry the following types of insurance:

Compensation Insurance. — Workmen's Compensation insurance covers the obligation imposed upon an employer, who is subject to the "Worker's Compensation Law" of a State, Territory of the United States and of the United States Longshoremen's and Harbor Workers' Compensation Act (with respect to off-shore operations), to pay the benefits prescribed by such law to his employee.

The form of policy issued by the standard insurance companies also provides Employer's Liability coverage, which protects the employer in those cases where the Workmen's Compensation Law is not the sole remedy at law of the employee. Appropriate state endorsements must be attached if the field operations are outside the state in which the policy is issued. In some states, individual policies are mandatory.

It is unnecessary to provide coverage for any states before the field operations are extended to them. However, an employee should never be sent to another state until the policy has been checked to determine if it covers operations in such state.

Public Liability and Property Damage Insurance. — 1. Public Liability (generally written on the contractors form for geophysical operations) covers bodily injuries to or the death of others (except employees) caused by or resulting from the ownership, maintenance or use by the employer of property, or from the operations conducted by him on or away from his premises.

2. Property Damage Liability covers damage to or destruction of property of others caused by or resulting from the ownership, maintenance or use by the employer of property, or from the operations conducted by him on and away from his premises (property owned, leased, rented, occupied or used by or in the care, custody or control of the employer or any of his employees being excluded).

Standard forms of policies are generally used when writing this form of coverage. Endorsements broadening or limiting the coverage to meet the assured's requirements should be made a part of the policy. If

there is any ambiguity or doubt as to the coverage, the assured should make certain that the policy is properly endorsed to correct this ambiguity.

Under the definition of Property Damage Liability, "property in the care, custody or control of the assured" is not covered. Unless this exclusion is modified by endorsement, the coverage does not protect the assured against a claim by the client for any damage to client's property caused by the field operations of the Geophysicist.

Some Property Damage Policies do *not* exclude blasting or explosion, but rather there may be a specific exclusion attached to the classification "Geophysical Exploration—*seismic method.*" It is essential, therefore, that the geophysical operator check to determine if there is a blasting or explosion exclusion in either the policy or the classification wording. An additional charge is made in the rate to include blasting or explosion.

Automobile Insurance. — 1. Automobile Public Liability covers bodily injury to or the death of others caused by or resulting from the ownership, operation or use of automobiles in the business of the operator, including automobiles owned by or operated for the operator.

2. Property Damage Liability covers damage to or destruction of property of others (including loss of use thereof) caused by or resulting from the ownership, operation or use of automobiles in the business of the operator, including automobiles owned by or operated for the operator.

(Policies that include coverage for:—

Motor Vehicles owned by the geophysical operator,
Motor Vehicles hired by the operator,
Motor Vehicles owned by employees or others and operated in the business of the geophysical operator

will give the geophysical operator complete protection for the Automobile exposure.)

The type of automobile (its net weight if a truck or tractor), its use and location determine the premium for the coverages. Many states have stringent "Financial Responsibility Laws" which make it imperative for the owner to carry certain forms of coverage and limits of liability. It is advisable that the limits of liability should be sufficiently large to take care of serious claims. Usually, a $25,000/50,000 Bodily Injury and a $5,000 Property Damage Policy is deemed the *minimum* limit for adequate protection. Policies in much larger amounts are frequently carried by the more prudent operators.

Patent Rights

A patent is a grant by the government to an inventor or his assignee, giving the right for a period of seventeen years from the date of the patent to exclude others from manufacturing, using or selling embodiments of a patented apparatus or product, or from practicing a method, process, or art.

Patents on methods or processes for geophysical surveying ordinarily fall under the general classification of an *art* as defined in the patent laws of the United States.

The patent laws of foreign countries vary somewhat, and no attempt will be made here to deal with such. There is no international bureau or central world office where a world-wide patent may be secured. Each country has its own patent system, and a separate application must be filed in each foreign country where protection is desired.

In the United States a patent is obtained by filing a formal *application,* which is usually followed by what is termed the *prosecution.* Prosecution includes the official examination and actions by the Patent Office Examiner, to which a response is made by the applicant's attorney, after which, if the subject matter presented and claimed is new, useful and involves invention over prior art, the Patent Office will send a formal notice of *allowance,* and upon payment of a final fee the patent will issue.

A patent application consists of (1) a *specification,* which is somewhat comparable to the usual technical article, describing and preferably illustrating at least one embodiment of the invention, (2) an *oath* and (3) a set of *claims* attached to the specification which define in general or specific language the improvement or invention which the applicant believes to be novel. The claims mark out the legal boundaries of the patent. They may be revised during the prosecution of the case as may be necessary or desirable. The majority of applications are filed through an attorney, in which case a *power of attorney* accompanies the application when it is filed.

The examining procedure is necessarily time-consuming, and there may normally be a lapse of two to four years between the *filing date* of the application (the date it is received at the patent office), and the issuance of the patent. More time may be consumed if more than one inventor files on the same patentable subject matter, in which case the Patent Office conducts an *interference* proceeding, which is equivalent to a trial to determine who was the first inventor.

Inventors may, and some do, file and prosecute their own applications, but this is not recommended, for while the inventor may be an expert on the technical phases of the subject matter, there are many legal aspects to patent law which require the experience and training of a patent attorney. Anyone interested may obtain pamphlets dealing with the patent laws, rules of practice and Patent Office procedure by writing to the Commissioner of Patents, Washington, D.C.

No rights are conferred on the inventor before the issuance of his patent. The words *patent applied for* or the equivalent, appearing on a piece of apparatus, constitute merely an unofficial notice that the inventor is seeking a patent.

A patent *expires* at the end of seventeen years after the date of its grant, and the subject matter thereof is open to use by the public.

The philosophy upon which the government grants a patent monopoly

is that, by the patent, the public is fully apprised of the invention, and after the expiration of the 17-year exclusive period, the public has the benefit of the invention. This explains why the laws are somewhat stringent as to adequacy and completeness of the disclosure in the patent specification. For this reason, the specifications of a patent constitute an excellent reference and source of information.

In the field of geophysics there has been considerable patent activity. A large number of patents have been granted on methods and apparatus. Many of these early patents have now expired, but improvements in methods and apparatus continuously form the subject matter of new patents.

In the allied arts, such as electronics, wave recording and photography, there is a vast maze of patents. Many of these are used in geophysical exploration and instrumentation. In the field of geophysics itself, the general policy among those obtaining patents has been to license the same for use upon payment of royalty or other compensation.

There have been very few situations in which any considerable number of relatively important geophysical patents were collected by any one owner.* Probably the largest single collection of related patents in the field of seismic prospecting was acquired by the Texaco Development Corporation. Texaco has made these patents available by licensing them either on a paid-up basis, depending upon the number of crews operating, or on a running royalty basis. This policy and program became generally effective after a preliminary legal skirmish in 1934.

At that time the Texas Company brought a patent infringement suit against the Sun Oil Company in the District Court of the United States for the Southern District of Texas, at Houston. This suit was based upon three patents assigned to the Texas Company.

The first was on an invention of Dr. Ludger Mintrop, of Germany, and related to a process for testing and exploring geological structures. He applied for United States Letters Patent in 1920 and was granted Patent No. 1,599,538, entitled "Geological Testing Methods," on September 14, 1926.

A second patent, obtained on an application of Dr. Burton McCollum, of Washington, D.C., related to a process and apparatus for determining the slope of subsurface rock boundaries. He filed his application in 1923, and Patent No. 1,724,495, entitled "Method and Apparatus for Determining the Slope of Subsurface Rock Boundaries," was granted on August 13, 1929.

The third patent, also obtained upon an invention of Dr. McCollum, concerned a process and apparatus for studying subsurface contours. This application was filed in 1923, and Patent No. 1,724,720, entitled "Methods and Apparatus for Studying Subsurface Contours," was granted on August 13, 1929.

Since the life of a United States Patent is seventeen years from the date of grant, these three patents have now expired, but at that time they were in effect and formed the nucleus of a large-scale program initiated by the infringement suit mentioned.

In the complaint The Texas Company alleged that it and its predecessors in title had spent large sums of money in exploiting these patents, which had proved to be very successful, and asserted that the Sun Oil Company had willfully infringed the patents. The complaint prayed for an accounting and payment of profits and damages,

* C. R. Hrdlicka, "Summary of Some Pending Patent Litigation Relating to Seismic Exploration," *Geophysics*, Vol. I, No. 1, Jan., 1936.

including treble damages, costs of litigation, and an injunction against further infringement.

The Sun Oil Company filed its answer to the complaint, denying The Texas Company's title to the Mintrop Patent No. 1,599,538 and challenging the validity of that patent on the ground that the subject matter "does not comprise any new, useful art, machine, manufacture or composition of matter or new and useful improvements thereof, and is not the statutory subject of a patent." The answer further averred that the patent was void because the description of the invention was such that a person skilled in the science could not use the patent; also, that the applicant introduced new matter into the application after it was filed, and that such new matter was substantially different from that contained in the original application. The answer even alleged fraudulent representations as to facts and results in connection with the presentation of the invention to the Patent Office. Additional and more conventional defenses were also interposed.

Substantially the same defenses were pleaded as to Patents No. 1,724,495 and No. 1,724,720, in addition to which the subject matter of these two patents was asserted to be anticipated by earlier patents obtained by the same inventor.

Evidence on the issues presented never was submitted to the Court. The case was settled on the morning it was to go to trial, the defendant having concluded to acknowledge that the Mintrop and McCollum patents were valid.

One of the provisions of the settlement was that The Texas Company would license Sun Oil and twenty odd companies which had contributed to the defense fund. At a meeting held shortly thereafter in Houston, at which a large number of seismograph operators and contractors were represented, Texas presented a form of license in compliance with the settlement and it was accepted as satisfactory.

That general form has been continued in use by the Texaco Development Corporation, a subsidiary of The Texas Company, and to date more than one hundred companies have been licensed, in addition to the licenses granted at the time of the settlement.

In 1946, after a number of the more basic patents had expired, the royalty charged by Texaco was voluntarily decreased to one-fifth of the rates originally in force.

No similar situation has arisen in the other methods of surface prospecting. An operator wishing to practice some particular type of geophysical operation has dealt individually with the owners of the various patents involved.

It is not unusual in the expeditious settling of interferences, particularly those involving more than two inventors, for the parties to agree to cross-license each other under the subject matter covered by the interference, and thereupon to settle the interference relatively rapidly on presentation of the proofs of the various parties. This affords a quick and simple manner of avoiding expensive and complex details. Instances of this type of cross-licensing, which almost invariably preserve to each party an unrestricted right to license the public without accounting to the other cross-licensees, have occurred in the field of geophysical prospecting. In one case, for example, inventions belonging to more than ten parties were involved at the same time in a number of interferences in the field of seismic recording equipment. A cross-license of the type discussed above was worked out between the parties which enabled the legal controversy to be amicably settled, whereas otherwise it is very probable that years of legal discussion and an expense which would have been a hardship on all parties concerned would have resulted.

In the older fields of geophysical work, namely, magnetic, gravimetric, surface electrical and seismic exploration and electrical well-logging, the early patents have now expired so that it is possible to carry out a great deal of exploration without involvement in questions of patent infringement. Early in the life of each geophysical method there have been issued a few relatively basic patents, followed by a large number of improvement patents as the development of the technique progresses, after which the patentable developments decreased in magnitude. However in any active field there are patentable improvements for many years, usually as long as research is carried on. An example of the growth and decline of the number of

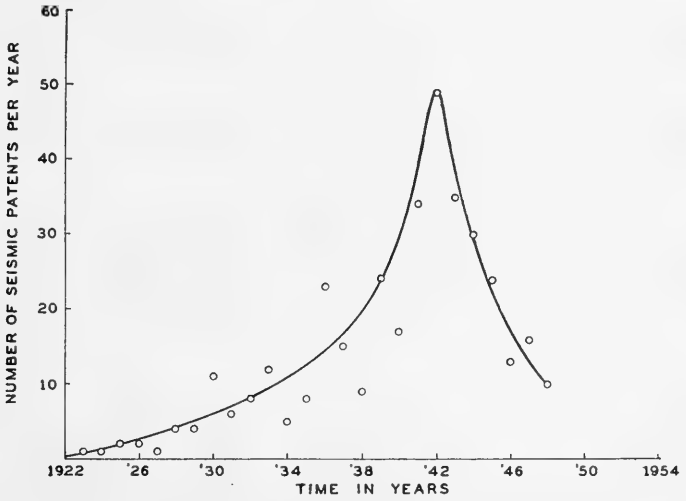

FIG. 707.

patents issued in one particular field is shown in Figure 707. It should be recognized that the inevitable time lag between application and issuance of patents makes the peak of the curve fall a number of years after the maximum in the rate of conception of these inventions. The peak shown as occurring in 1941 corresponded to a maximum in patentable inventions four or five years earlier.

The petroleum industry has long been patent-conscious. Practically everything from jarring tools to cracking processes has been patented. Wherever the traffic would tolerate it, patent royalties would be exacted, as fabulous as the value of the black gold being sought. A royalty of 33⅓% of the income from rental of patented equipment was not uncommon at a time when 10% was high in more sedate industries.

The rush for patents, and the premium demanded by those successful in obtaining a patent which proved to be a gusher, have excited numerous and hotly-contested infringement suits. The records of testimony taken and briefs written in petroleum patent litigation would constitute a large

library, and the court opinions in these cases, if collected, would make a legal encyclopedia.

Relatively few patent cases reach the United States Supreme Court, because ordinarily that court is accessible only when there are conflicting decisions in two judicial circuits on the same patent. Occasionally the Supreme Court will accept for consideration a case outside the general rule, where special public interest appears, or when members of the high court believe that the federal courts subject to their policy-fixing powers (in the form of interpretation of the law) have strayed from home.

Announcement of a Supreme Court decision in a patent case is always news in the patent world, and sometimes contains elements of surprise. The petroleum industry may claim the distinction of recently contributing such a case to the annals of American jurisprudence. This case is entitled "Halliburton Oil Well Cementing Company vs. Walker, et al.," and is reported at 329 U.S. 1, as well as at 71 U.S.P.Q. 175, and in some other publications. The patents in question were granted to Cranford P. Walker, who lost the broader claims after several years' litigation and seven different court rulings.

This case is a good primer in patent law to a point, and its facts well illustrate certain patent problems of the petroleum industry.

The patent involved (No. 2,156,519, granted May 2, 1939, and entitled "Means for Measuring the Location of Obstructions in Wells") covered a method for the measurement of the distance from the casing head to the fluid surface, and was one of several patents which Walker secured in this field.

The measurement of distance by timing the travel of a sound from its point of inception to an obstruction and its returning echo had long been known. In 1898, a patent was granted describing an apparatus whereby the noise from a gun might be injected into a tube; the returning echoes from obstructions vibrated a diaphragm, which moved a stylus to record a graph on paper. (See p. 1126.) Recognizing the need for measuring the distance to the fluid surface in deep oil wells, where it is impractical to measure depth by the old method of lowering a rope or cable, the oil industry in the 1920's began to look to the sound-echo time method as a possibility. Work was initiated by a number of investigators. Lehr and Wyatt secured a patent on measuring the distance by timing the echo of an "impulse wave" generated by a "sudden change in pressure". The Lehr and Wyatt apparatus comprised a gas cylinder with a quick-opening valve by means of which a short blast of gas could be injected into a well. It was particularly noted that the wave impulses could be recorded by use of a microphone which might include an amplifier and a device to record a picture of the wave impulses. Thus Lehr and Wyatt contrived an apparatus composed of old and well-known elements or parts in combination to measure and record the time required for a pressure wave to travel down and back from the fluid surface in an oil well.

Under certain conditions the Lehr and Wyatt apparatus and method were found to be inadequate for the reason that pressure waves do not always travel at a constant velocity. Consequently the mere measurement of the time elapsing between the initiation of the wave and the return of the echo may not allow accurate calculation of depth.

Cranford P. Walker and other early workers were acquainted with the work of Lehr and Wyatt, and soon active research work was in progress to devise a method which would be more accurate in results. It was well known in the art that the tubing string is made up of pipe sections coupled together; where the coupling joints occur,

there are collars or shoulders. Also occasionally there are more prominent projections on the tubing string known as *tubing catchers.*

In some wells the distance to the tubing catcher is known, and it was observed that the distance to the fluid surface could be measured by a simple time-distance proportion formula. (See page 1129.)

There were wells, however, in which the distance from the tubing catcher was unknown. To provide for this, Walker utilized the fact that the sections of tubing used in a given oil well are generally of equal length and consequently the shoulder joints ordinarily are at equal intervals from each other. The section lengths may vary in different wells. Walker's immediate objective was to measure the unknown distance to the tubing catcher, from which the depth to the fluid surface could be readily ascertained by the formula referred to above. Walker thereupon concluded to measure the unknown distance to the tubing catcher by observing and recording the shoulder echo waves. Multiplication of the number of shoulders as revealed by the number of echo waves times the length of an average pipe section would show the distance to the tubing catcher.

The Lehr and Wyatt instrument was capable of recording the tubing collar echoes but was not efficient, and Walker therefore added to the Lehr and Wyatt apparatus a mechanical acoustical resonator which would make the shoulder echo waves more prominent on the graph and easier to count.

The mechanical acoustical resonator was not *per se* new with Walker, but was an already well-known device. It consisted primarily of a short pipe which would receive the wave impulses from the casing head. This pipe, being one-third the length of the tubing joints, would act as a tuner adjusted to the third harmonic of the frequency of the shoulder echo waves, amplifying these waves and thereby minimizing the random echoes. Walker attached to the resonator a mechanical adjusting means so that the length of the resonator tube could be set exactly at one-third of the interval between shoulders in any particular well.

The Halliburton Oil Well Cementing Company began the use of an electrical filter apparatus which achieved results similar to Walker's mechanical device, and Walker brought suit against Halliburton in the Federal Court at Los Angeles for infringement of patent No. 2,156,591 and two other patents, the latter never reaching the Supreme Court. The District Judge held the Walker patent as to claims 1, 13, 14, 15 and 17 (the only ones in issue) valid and infringed. Halliburton appealed to the Ninth Circuit Court of Appeals. The Court of Appeals affirmed the District Court with respect to the patent under discussion, concluding that Halliburton's electrical filter was equivalent, under the patent law, to Walker's mechanical resonator. The court commented that while Halliburton's device was by no means a Chinese copy of Walker's, the court considered that the Walker patent was entitled to a liberal construction and to a fair range of equivalents.

As mentioned before, carrying a patent case from the Court of Appeals to the Supreme Court is not a matter of right in the absence of conflicting decisions, and there were none. Halliburton's counsel therefore filed a petition for *writ of certiorari* in the Supreme Court, asking for a special ruling by sufficient members of the court to call up the case for consideration on its merits. In the first instance the petition was denied, but a week later the Supreme Court accepted the case. It was briefed and argued before a court composed of an even number of judges. They were equally divided in their opinion and under such circumstances the decision by the Court of Appeals was necessarily affirmed. A petition for a re-hearing in the Supreme Court was filed and, this being finally granted, the case was ordered re-argued.

The final opinion of the Supreme Court was delivered by Mr. Justice Black with a dissent by Mr. Justice Burton. The opinion reviewed most of the facts referred to above and then addressed attention to the claims, their technical construction as patent claims, and whether these claims fulfilled the requirements of the patent law.

Revised Statute 4888, 35 U.S.C. Section 33, is important in this regard and necessary to an understanding of the case. It is therefore quoted here:

"Before any inventor or discoverer shall receive a patent for his invention or discovery he shall make application therefor, in writing, to the Commissioner of Patents, and shall file in the Patent Office a written description of the same, and of the manner and process of making, constructing, compounding, and using it, in such full, clear, concise, and exact terms as to enable any person skilled in the art or science to which it appertains, or with which it is most nearly connected, to make, construct, compound, and use the same; and in case of a machine, he shall explain the principle thereof, and the best mode in which he has contemplated applying that principle, so as to distinguish it from other inventions; and he shall particularly point out and distinctly claim the part, improvement, or combination which he claims as his invention or discovery."

Halliburton's counsel argued that the Walker claims were indefinite and did not comply with the statute, more specifically that the claims did not describe the invention but used "conveniently functional language at the exact point of novelty". The quoted phrase was taken from the Supreme Court opinion in General Electric Co. v. Wabash Electric Co., 304 U.S. 364, 371 (37 U.S.P.Q. 469).

Patent claims which are purely functional in scope are invalid. The doctrine has generally been recognized, however, that functional phrases are not objectionable if supported by adequate structural definition; thus, in claims for a combination of old elements it has become a practice to define various elements in the broad term "means", followed by a functional statement of what service is performed. Apparently such a type of claim is still recognized as lawful if the combination is broadly new. The Supreme Court frowned upon this practice in the Halliburton case, at least upon the facts in that case, wherein Walker's invention was held to be in a "field crowded almost, if not completely, to the point of exhaustion".

The Supreme Court, for the purpose of its opinion, accepted without ratifying the proposition that Walker's addition of a tuned acoustical means brought about a new patentable combination even though it advanced only a narrow step beyond Lehr and Wyatt's old combination. In construing a patent, however, it is the claims which control, each claim being for most practical purposes a separate patent grant. As a typical example for purposes of argument and analysis, claim 1 of the Walker patent was set forth. It reads as follows:

"In an apparatus for determining the location of an obstruction in a well having therein a string of assembled tubing sections interconnected with each other by coupling collars, means communicating with said well for creating a pressure impulse in said well, echo-receiving means including a pressure responsive device exposed to said well for receiving pressure impulses from the well and for measuring the lapse of time between the creation of the impulse and the arrival at said receiving means of the echo from said obstruction, and means associated with said pressure-responsive device for tuning said receiving means to the frequency of echoes from the tubing collars of said tubing sections to clearly distinguish the echoes from said couplings from each other."

The Court pointed out that some of the claims which were not in the litigation did describe the tuned acoustical pipe as an integral part of the Walker invention, showing its structure, its working arrangement, and its alleged new combination and the manner of its connection with the other parts; but that no one of the claims involved in the litigation even suggested the physical structure of the acoustical resonator. The opinion pointed out further that no one of these claims described the physical relation of the Walker addition to the old Lehr and Wyatt apparatus, and that no one of these claims described the manner in which the Walker addition would operate together with the old Lehr and Wyatt apparatus. The Court concluded: "Thus the claims failed adequately to depict the structure, mode and operation of the parts in combination."

The Court pointed out that a claim typically described the resonator and its relation with the rest of the apparatus as "means associated with said pressure-responsive device for tuning said receiving means to the frequency of echoes from the tubing collars of said tubing section to clearly distinguish the echoes of said couplings from each other." The Court criticized the language of the claim as describing the most crucial element in the "new" combination in terms of what it will do, rather than in terms of

its own physical characteristics or its arrangement in the new combination apparatus. Adopting this view, the Supreme Court held the claims in suit to be invalid.

Walker thus eventually lost the fruits of his inventive efforts insofar as a broad range of equivalents is concerned. He had left relatively narrow claims describing more or less specifically the features of his apparatus and presumably remained protected against a Chinese copy of his device. Quite obviously, however, it is possible for anyone to add a substitute for Walker's addition to the old Lehr and Wyatt apparatus.

This case will undoubtedly remain a center of controversy until further clarified, overruled or re-affirmed. It leaves the question open as to whether and under what facts a combination invention is broadly new or narrowly new. Admittedly, all of the elements in the Walker complete apparatus were separately old, and, under standards of combination invention generally recognized previous to the Halliburton decision, there had been no distinction made between combinations in general and combinations where one element was said to represent the exact point of novelty.

A general rule, at least, may be drawn from this case, namely, that if the invention is but a short step forward, the claims to be valid must particularize that step, leaving the field open to others to provide other means to achieve the same result. It does not abolish all reward to the inventor, but restricts the extent of his patent monopoly.

NAME AND PLACE INDEX

C

D

E

F

G

H

I

J

K

L

M

N

O

P

Q

R

S

W

SUBJECT INDEX

A

B

C

D

E

F

G

H

I

K

L

M

Q

R

S

T

U

V

W

Z